NUCLEAR SCIENCE ABSTRACTS

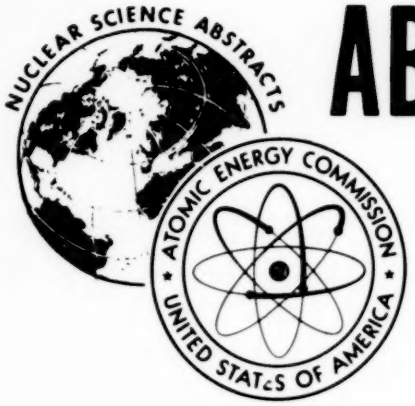

Volume 25 Number 2

Abstracts 2059-4007

January 31, 1971

UNITED STATES ATOMIC ENERGY COMMISSION
Division of Technical Information

XUM

REPORT COLLECTIONS IN THE UNITED STATES

The libraries listed below purchase and maintain microfiche collections of USAEC and foreign reports that are abstracted in *NSA*. Their collections also include *NSA* and its indexes, AEC's Technical Progress Reviews, AEC-sponsored translations, conference proceedings published by AEC, and various bibliographic tools. Most of these libraries have microfiche reader-printers or other photocopy facilities with which to reproduce enlarged copies from microfiche. Charges for reproduction services vary.

ALABAMA
Auburn, Auburn University
ALASKA
College, University of Alaska
ARIZONA
Tucson, University of Arizona
ARKANSAS
Fayetteville, University of Arkansas
CALIFORNIA
Davis, University of California
Los Angeles, University of California
COLORADO
Boulder, University of Colorado
DISTRICT OF COLUMBIA
Washington, Library of Congress (by deposit)
FLORIDA
Gainesville, University of Florida
GEORGIA
Atlanta, Georgia Institute of Technology
HAWAII
Honolulu, University of Hawaii
IDAHO
Pocatello, Idaho State University
ILLINOIS
Evanston, Northwestern University
Urbana, University of Illinois
INDIANA
Lafayette, Purdue University
IOWA
Ames, Iowa State University
KANSAS
Manhattan, Kansas State University
KENTUCKY
Lexington, University of Kentucky
Louisville, University of Louisville
LOUISIANA
Baton Rouge, Louisiana State University
New Orleans, Tulane University
MARYLAND
Baltimore, Johns Hopkins University
College Park, University of Maryland
MASSACHUSETTS
Cambridge, Massachusetts Institute of Technology
MICHIGAN
Ann Arbor, University of Michigan
MISSISSIPPI
State College, Mississippi State University
MISSOURI
Kansas City, Linda Hall Library
NEVADA
Las Vegas, University of Nevada
Reno, University of Nevada
NEW JERSEY
Princeton, Princeton University
NEW MEXICO
Albuquerque, University of New Mexico
NEW YORK
Albany, New York State Library
Buffalo, State University of New York at Buffalo
Ithaca, Cornell University
New York, Columbia University
Rochester, University of Rochester
Syracuse, Syracuse University
Troy, Rensselaer Polytechnic Institute
NORTH CAROLINA
Raleigh, North Carolina State University
OHIO
Cincinnati, University of Cincinnati
Columbus, Ohio State University
Toledo, University of Toledo
OKLAHOMA
Norman, University of Oklahoma
PENNSYLVANIA
Philadelphia, University of Pennsylvania
Pittsburgh, Carnegie Library
University Park, Pennsylvania State University
PUERTO RICO
San Juan, University of Puerto Rico
SOUTH CAROLINA
Columbia, University of South Carolina
TENNESSEE
Knoxville, University of Tennessee
Nashville, Joint University Libraries
Oak Ridge, Oak Ridge Associated Universities
TEXAS
Austin, University of Texas
College Station, Texas A & M University
Houston, Rice University
UTAH
Salt Lake City, University of Utah
VIRGINIA
Blacksburg, Virginia Polytechnic Institute
Charlottesville, University of Virginia
WASHINGTON
Pullman, Washington State University
Seattle, University of Washington
WEST VIRGINIA
Morgantown, West Virginia University
WISCONSIN
Madison, University of Wisconsin
WYOMING
Laramie, University of Wyoming

The following governmental and international organizations offer for sale USAEC reports abstracted in *Nuclear Science Abstracts*:

National Technical Information Services, U. S. Department of Commerce
Springfield, Virginia 22151
International Atomic Energy Agency, Vienna, Austria
National Lending Library, Boston Spa, England

XUM

Volume 25, Number 2, January 31, 1971

NUCLEAR SCIENCE ABSTRACTS

A semimonthly publication of the USAEC Division of Technical Information, Edward J. Brunenkant, Director, Published by the USAEC Division of Technical Information Extension, Robert L. Shannon, Extension Manager.

Nuclear Science Abstracts provides the only comprehensive abstracting and indexing coverage of international nuclear science literature. *Nuclear Science Abstracts* covers scientific and technical reports of the U. S. Atomic Energy Commission and its contractors, other U. S. Government agencies, other governments, universities, and industrial and research organizations. In addition, books, conference proceedings, individual conference papers, patents, and journal literature on a worldwide basis are abstracted and indexed. Each issue of *Nuclear Science Abstracts* includes four indexes: subject, personal author, corporate author, and report number.

The following organizations scan and abstract the nuclear science literature in their respective countries:

Atomic Energy of Canada Limited
Australian Atomic Energy Commission
Danish Atomic Energy Commission
Finnish Atomic Energy Commission
French Atomic Energy Commission
Japan Atomic Energy Bureau–Atomic Energy Research Institute
Institutt for Atomenergi (Norway)
Aktiebolaget Atomenergi (Sweden)
United Kingdom Atomic Energy Authority

Numerous organizations, societies, and publishers throughout the world provide *Nuclear Science Abstracts* with advance page-proof copy of their publications, e.g., in the United States the American Institute of Physics provides page-proof copy of its publications.

A list of the journals scanned regularly and the abbreviations used appears in Issue 1 (January 15) of each volume of *Nuclear Science Abstracts* and is supplemented in Issues 7, 13, and 19. Issue 1 of each volume also describes the scope and arrangement of the subject matter covered in *Nuclear Science Abstracts*. The subject matter covered is also described in TID-4552, *Subject Scope of Nuclear Science Abstracts*, available free from the USAEC Division of Technical Information Extension, P.O. Box 62, Oak Ridge, Tennessee 37830. An outline of the subject categories appears in the Contents of each issue.

AVAILABILITY OF PUBLICATIONS ABSTRACTED

Public availability of all U. S. Atomic Energy Commission reports is indicated in the report number indexes. The availability of other reports, when known, is also indicated. The availability of some unnumbered reports is given in the abstract.

Dissertations abstracted in *Dissertation Abstracts* and included in *Nuclear Science Abstracts* are available from University Microfilms, Inc., 315 N. First Street, Ann Arbor, Michigan 48103.

Information on the availability of the published literature and unpublished conference papers abstracted in *Nuclear Science Abstracts* can be obtained from the USAEC Division of Technical Information Extension, P.O. Box 62, Oak Ridge, Tennessee 37830.

HOW TO OBTAIN NUCLEAR SCIENCE ABSTRACTS

Nuclear Science Abstracts is available to the public on a subscription basis from the Superintendent of Documents, U. S. Government Printing Office, Washington, D. C. 20402.

For the 24 regular issues, the yearly rate is $42.00 for domestic subscribers and $52.50 for foreign subscribers. A single issue costs $1.75, domestic rates, or $2.19, foreign rates. Domestic rates apply to the United States, Canada, Mexico, and Central and South American countries except Argentina, Brazil, Guyana, French Guiana, Surinam, and British Honduras.

For a yearly subscription to the cumulative indexes, the rates are $38.00 for domestic subscribers and $47.50 for foreign subscribers.

The following cumulative indexes are available:

From Johnson Reprint Corporation, 111 Fifth Avenue, New York, N. Y. 10003:
Vols. 1–4, Subjects and Authors (1948–1950), $30.00.

From Superintendent of Documents, U. S. Government Printing Office, Washington, D. C. 20402:

Vols. 5–10, Subjects and Authors (1951–1956), $5.25.

Vols. 11–15, Subjects (1957–1961), $19.00.
Vols. 11–15, Personal Authors (1957–1961), $14.25.
Vols. 11–15, Corporate Authors (1957–1961), $2.50.

Vols. 16–20, Subjects (1962–1966), $36.00.
Vols. 16–20, Personal Authors (1962–1966), $22.50.
Vols. 16–20, Corporate Authors (1962–1966), $3.75.

Vol. 21, Subjects and Authors (1967), $16.00.
Vol. 22, Subjects and Authors (1968), $26.00.
Vol. 23, Subjects and Authors (1969), $25.75.

Cumulative Report Number Index, Vols. 1-15 Revised, $4.00.
Cumulative Report Number Index, Vols. 16-20 Revised, $5.50.
Cumulative Report Number Index, Vols. 21-23, $4.25.

Nuclear Science Abstracts is available on an exchange basis to universities, research institutions, industrial firms, and publishers of scientific information. Government agencies may obtain *NSA* free of charge. Inquiries should be directed to the USAEC Division of Technical Information Extension, P. O. Box 62, Oak Ridge, Tennessee 37830.

INDEXES TO NSA

Comprehensive indexes appear in each issue and are cumulated quarterly and annually. Multivolume cumulations have been issued as indicated above.

All documents abstracted are indexed by subjects and personal authors. Report literature is indexed also by corporate author and report number. Each of these indexes in every issue is preceded by an introduction explaining in detail the organization of the index and the principles by which it is compiled. The reader is referred to these explanations for information not found in the brief summary below.

Personal Authors

Each author's name is indexed in the form appearing on the document abstracted:

ISHIHARA, T., Accumulation of fallout ^{137}Cs in newborn infants, 23:50538
ISHIHARA, Toyokuki, Shielding effect of paraffin, water, soil, concrete, Fe, and Pb for high-energy neutrons, 23:51748

Subjects

The subject index consisting of specific materials, objects, and processes is arranged alphabetically. Modifying phrases specific to these subjects in turn are arranged alphabetically under the subjects.

MELPHALAN
  effects on proliferation of cultured antigen-stimulated spleen cells from mice, dose-response curve for, 23:50820
MEMBRANE FILTERS
  design for removal of cell-free Streptococcus faecalus from bacteria cultures in fermentation tank, 23:49996 (UCRL-18667, pp 322-9)
MENDELEVIUM
  separation from einsteinium and fermium by electrolysis, 23:49772 (UCRL-18667, pp 277-312)
  separation from sodium acetate solutions by solvent extraction using sodium amalgam, 23:49772 (UCRL-18667, pp 277-312)
  stability of divalent state of, 23:49772 (UCRL-18667, pp 277-312)

Corporate Authors

Technical report literature is indexed from the name of the organization or institution responsible for the issuance of the report.

51093 (LA-4164) FABRICATION OF BORON CARBIDE RINGS AND DISKS. Sheinberg, H.; Herrera, T.; Kostacopoulos, J. **(Los Alamos Scientific Lab., N. Mex.).** Apr. 25, 1969. Contract W-7405-eng-36. 11p. Dep. CFSTI.

is indexed as:

LOS ALAMOS SCIENTIFIC LAB., N. MEX.
  Fabrication of boron carbide rings and disks, 23:51093 (LA-4164)

Report Numbers

Technical report literature is also indexed by report numbers. This index includes information on where individual reports may be obtained. While not reports, patents and conference papers are indexed here as a matter of convenience.

JPRS-	**(Non-AEC)**	
46949	23-51587	CFSTI
48330	23-52305	CFSTI
48331	23-52451	CFSTI
48481	23-50889	CFSTI
48743	23-51034	CFSTI
49025	23-51706	CFSTI (U. S. Sales Only)
JUL-	**(German)**	
571-RG	23-52269	Dep
578-PP	23-51624	Dep. CFSTI (U. S. Sales Only)
581-FN	23-51079	Dep. CFSTI (U. S. Sales Only)
584-RG	23-52313	Dep
586-FN	23-51035	Dep. CFSTI (U. S. Sales Only)
K-		
1777	23-50987	Dep. CFSTI
1778	23-50988	Dep. CFSTI
KFK-	**(German)**	
743	23-52461	Dep
743	23-52447	For translation see EURFNR-613
781/I	23-52462	Dep
824	23-52397	Dep. CFSTI (U. S. Sales Only)

XUM

TABLE OF CONTENTS (continued)

Category	Page
PHYSICS (GENERAL) (Cont'd.)	
Kinetics (General)	305
Kinetics (Experimental)	306
Kinetics (Theoretical)	306
Production	309
Stability	310
Thermonuclear Processes	311
Wave Phenomena	312
Shielding	314
Solid-State Physics	316
Radiation Effects	316
Physical Properties	318
Moessbauer Effects and NMR	319
Theory	319
Theoretical Physics	320
PHYSICS (HIGH-ENERGY)	322
Particle Interactions and Properties (Experimental)	322
Electromagnetic	322
Weak	323
Strong (Baryon-Induced)	323
Strong (Meson-Induced)	324
Particle Interactions and Properties (Theoretical)	326
General	326
Electromagnetic	327
Weak	329
Strong (General)	330
Strong (Baryon No. = 0)	331
Strong (Baryon No. = 1)	332
Strong (Baryon No. ≥ 2)	335
Particle Invariance Principles and Symmetries	336
Field Theories	337
General	337
Quantum Field Theory	337
Gravitation and General Relativity	338
Scattering Theory	338
Particle Accelerators	339
PHYSICS (NUCLEAR)	346
Neutron Interactions with Matter	346
Nuclear Properties and Reactions, A ≤ 5	347
PHYSICS (NUCLEAR) (Cont'd.)	
Nuclear Properties and Reactions, 6 ≤ A ≤ 19	349
Nuclear Properties and Reactions, 20 ≤ A ≤ 89	352
Nuclear Properties and Reactions, A ≥ 90	358
Nuclear Theory	364
REACTOR TECHNOLOGY	370
Commercial Power Reactors	370
Operation and Economics	370
Safety and Siting	372
Power Reactor Development	374
Kinetics and Dynamics	374
Control Systems	374
Shielding	374
Cooling Systems	374
Fuels	375
Auxiliary and Emergency Systems	377
Operation and Economics	377
Safety and Siting	378
Power Conversion Systems	378
Research and Test Reactors	379
Rocket and Space Reactors	380
Process Heat and Desalination Reactors	380
Marine and Portable Power Reactors	380
Production Reactors	380
Reactor Theory	381
Kinetics	381
Experimental Applications	382
Reactor Components, Fuels, and Accessories	382
GENERAL	383
CORPORATE AUTHOR INDEX	INDEX-1
PERSONAL AUTHOR INDEX	INDEX-10
SUBJECT INDEX	INDEX-50
REPORT NUMBER INDEX	INDEX-128

TABLE OF CONTENTS

Volume 25, Number 2, January 31, 1971

Category	Page
CHEMISTRY	197
Analytical Chemistry	197
Chemical and Spectral Procedures	197
Isotope Dilution Procedures	201
Radiometric and Radiochemical Procedures	201
Activation Procedures	202
Inorganic, Organic, and Physical Chemistry	206
Chemical Properties	206
Isotope Effects and Exchange	207
Physical Chemistry	210
Radiation and Nuclear Chemistry	213
Radiation Effects	213
Radiation Processes	215
Radiolysis	217
Radioisotope Production	221
Recoil Production and Reactions	222
Radiochemistry	222
Separation Processes	222
EARTH SCIENCES	227
Geology and Hydrology	227
Meteorology	229
Mineralogy and Exploration	229
Oceanography	230
ENGINEERING	231
Nuclear Explosions	231
Facilities and Equipment	231
Heat Transfer and Fluid Flow	232
Isotope Technology	233
Materials Testing	233
Radioactive Material Handling	234
Vacuum Engineering	236
INSTRUMENTATION	237
Radiation Detection Instruments	237
General Detectors and Monitors	237
Nuclear Spectroscopic Instrumentation	240
High Energy Physics Instrumentation	241
Radiation Dosimeters	242
Radiometric Instruments	243
Miscellaneous Instruments and Components	243
Radiation Effects on Instruments and Instrument Components	244
LIFE SCIENCES	245
Biochemistry, Physiology, and Molecular Biology	245
Basic Processes	245
Metabolism, Physiology, and Toxicology	246
Radiation Effects	247
Immunology	247
Ecology	248
Genetics and Cytogenetics	249
Health Physics and Safety	250
Radioactive Contamination and Decontamination	250
Dosimetry and Monitoring	251
Radiation Protection	251
Safety Procedures	252

Category	Page
LIFE SCIENCES (Cont'd.)	
Legal Aspects	252
Medicine	252
Protective Substances	252
Radiodiagnosis	252
Radiotherapy	253
Radiation Effects on Animals	253
Invertebrates	253
Vertebrates	253
Man	254
Radiation Effects on Plants	254
Radiation Effects on Microorganisms	255
METALS, CERAMICS, AND OTHER MATERIALS	256
Metals and Alloys	256
Corrosion and Erosion	256
Preparation and Fabrication	260
Properties Evaluations	262
Structure and Phase Studies	269
Radiation Effects	272
Ceramics and Cermets	273
Corrosion and Erosion	273
Preparation and Fabrication	273
Properties Evaluations	275
Structure and Phase Studies	277
Radiation Effects	278
Plastics and Other Materials	279
PHYSICS (GENERAL)	280
Astrophysics and Cosmology	280
Cosmic Ray Exposure Ages	280
Stars	280
Quasi-Stellar, Radio, and X-Ray Sources	281
Solar Phenomena	283
Galaxies	284
Cosmology	284
Planetary Phenomena	285
Atomic and Molecular Physics	286
Atomic, Electron, Ion, and Molecular Beams and Their Reactions	286
Atomic and Molecular Properties	286
Positronium, Muonium, and Mesic Atoms and Molecules	287
Collision Phenomena	287
Atomic Theory	290
Cosmic Radiation	290
Direct Energy Conversion	290
Fluid Physics	291
Geophysics (Upper Atmosphere)	292
Low-Temperature Physics and Cryogenic Equipment	299
Superfluidity	299
Superconductivity	300
Equipment and Devices	303
Plasma and Thermonuclear Physics	303
Confinement and Heating	303
Diagnostics	304

XUM

STAFF OF NUCLEAR SCIENCE ABSTRACTS

John W. Norris
Managing Editor

Donald D. Davis
Assistant Managing Editor

David E. Bost
Production Manager

Sidney F. Lanier
Subject Heading Specialist

J. Paul Meredith
Descriptive Cataloging Specialist

Frederick E. Marsh, Jr.
Computer Index Coordinator

Clara L. Fox
Corporate Author Specialist

Helen W. White
Report Number Specialist

Section Editors

Everett J. Hoffman
Chemistry

Robert C. Kelly
Engineering; Earth Sciences; Metals, Ceramics, and Other Materials

Lee M. Thompson
General Physics

Charles E. Stuber
High Energy Physics; Instrumentation

Helen G. Donald
Life Sciences

Lawrence T. Whitehead
Nuclear Physics

James M. Jacobs
Reactor Technology

Evaluators

Thomas S. Chapman
Rose V. Jermain
John H. Mitchell
Mary H. Newman
Polly C. Summers

Abstractors

F. S. Armstrong*
Ellis R. Bedford
Mary M. Brown
Jane G. Buchanan
D. Lamar Cason
Gloria M. Caton
David C. Cunningham
James R. Dulaney
Helga B. Gerstner
Mary C. Grissom
Phyllis C. Hansen
Carolyn D. Houston
Elaine E. Huber
Rose V. Jermain
W. Hugh Kinser, Jr.
Lisbeth C. Lieberman
Betty L. McDowell
Patricia B. McEwen
Fay M. Martin
William D. Matheny
Dora H. Moneyhun
Jean F. Peckham
Henry D. Raleigh
Mona H. Raridon
Julia S. Redford
Jessie W. Rushing
Robert W. Rutkowski
Francis L. Sachs
Lila B. Smith
Anne G. Ward
Helen L. Ward
Milton O. Whitson
Juanita Wilson

*Atomic Energy of Canada, Ltd.

Charles R. Bruce
Publishing Coordinator

Communication concerning the editorial policy and content of *Nuclear Science Abstracts* should be addressed to the Managing Editor, *Nuclear Science Abstracts*, USAEC Division of Technical Information Extension, P. O. Box 62, Oak Ridge, Tennessee 37830.

Use of funds for printing this publication approved by the Director of the Bureau of the Budget, June 26, 1969.

Volume 25, Number 2 January 31, 1971

NUCLEAR SCIENCE ABSTRACTS

CHEMISTRY

Analytical Chemistry

Refer also to abstract 2356.

2059 (NYO-4700(3rd Ed.)) MANUAL OF STANDARD PROCEDURES. Harley, John H. (ed.) (New York Operations Office (AEC), N. Y. Health and Safety Lab.). Sep 1970. 554p. Dep. NTIS.

Procedures that have been tested over an extended period of time with many samples are included. The divisions within the manual are: general; data section; radiation measurements; sampling; chemical procedures; fallout methods; specifications. (P.C.H.)

2060 COMPUTERS IN ANALYTICAL CHEMISTRY. 1968 Eastern Analytical Symposium, New York, N. Y., November 13-15, 1968. Orr, Charles H.; Norris, John A. (eds.). Progress in Analytical Chemistry. Volume 4. New York; Plenum Publishing Corporation (1970). 113p. $12.50. (CONF-681138).

The information included is wide-ranging and includes applications to mass spectrometry, x-ray spectrography, NMR spectroscopy, gas chromatography, ir spectrography, the use of dedicated computers, and the multiple user laboratory. (P.C.H.)

2061 CONTEMPORARY METHODS FOR DETERMINATION OF SMALL QUANTITIES OF CERIUM. Eremin, Yu. G.; Martyshova, T. I. Zavod. Lab.; 36: 769-75(1970). (In Russian).

The literature from 1963 through 1969 was surveyed. The methods considered include gravimetric, volumetric, and photometric. Attention was also given to methods for separation of cerium from accompanying components in natural and artificial materials. (129 references). (tr-auth)

Chemical and Spectral Procedures

Refer also to abstracts 2159, 2199, 2278, 2640, 2694, and 3110.

2062 (CNEA-271) USE OF ELECTROPHORESIS IN THIN FILMS FOR CONTROL OF THE RADIOCHEMICAL PURITY OF TRACER COMPOUNDS. Baruel, J.; Marques, R. O. (Comision Nacional de Energia Atomica, Buenos Aires (Argentina)). 1970. 11p. (In Spanish). Dep. NTIS (U. S. Sales Only).

The usefulness of a thin layer electrophoresis method is discussed in order to check the radiochemical purity of labeled compounds in routine work. For that purpose a comparative study was made of the behavior of different absorbent layers of commercial origin in the separation of mixtures under the same experimental conditions. (auth)

2063 (CNEA-276) DETERMINATION OF TRACES OF HAFNIUM IN ALUMINUM-URANIUM ALLOYS. Guido, O. O.; Grahmann, H.; Amaya, C. B.; Zucal, R. (Comision Nacional de Energia Atomica, Buenos Aires (Argentina)). 1970. 14p. (In Spanish). Dep. NTIS (U. S. Sales Only).

A method was developed for the determination of trace amounts of hafnium in aluminum-uranium alloys. Previously, hafnium was concentrated and separated from the components of the alloy by extraction, in 3M HCl, by a solution of TTA in benzene and later reextracted by a solution of hydrofluoric and hydrochloric acids. The quantitative determination was carried out by emission spectrography, using a continuous feed method and a porous electrode. The reproducibility was appreciably improved by using titanium as an internal standard. The method makes it possible to determine hafnium in the range from 2 to 20 ppM with a relative standard deviation of 3% (level of confidence of 68%). (tr-auth)

2064 (DP-Report-494) THE DETERMINATION OF TOTAL CARBON IN SILICON CARBIDE COATED DRAGON FUEL PARTICLES. Project DRAGON. Siddal, R. E.; Smith, D. L. G. (Atomic Energy Establishment, Winfrith (England)). Jan 1967. 14p. Dep. NTIS.

A method is described for the determination of total carbon in uranium carbide and uranium/thorium dicarbide fuel particles coated with a triplex layer of pyrolytic carbon, silicon carbide, and pyrolytic carbon. Carbon is converted to carbon dioxide and measured gravimetrically after absorption on soda asbestos. An iron/copper flux is used and combustion is by means of an induction furnace. The 95% confidence limits of the method at the 45.92% level are ±0.12% for a single result based on 15 replicate observations. (auth)

2065 (LA-4529) DETERMINATION OF 0.01 TO 1.0 PER CENT OF TITANIUM, ZIRCONIUM, HAFNIUM, NIOBIUM, TANTALUM, MOLYBDENUM, AND TUNGSTEN IN URANIUM ALLOYS BY ATOMIC ABSORPTION SPECTROPHOTOMETRY. Gardner, R. D.; Henicksman, A. L.; Ashley, W. H. (Los Alamos Scientific Lab., N. Mex.). Oct 1970. Contract W-7405-eng-36. 6p. Dep. NTIS.

A rapid atomic absorption spectrophotometric procedure was developed for the determination of titanium, zirconium, hafnium, niobium, tantalum, molybdenum, and tungsten in uranium-matrix alloys containing 0.01 to 1% of these seven metals. The elements can be determined singly or in any simultaneous combination by analysis of a single solution. The procedure involves the dissolution of 1-g alloy samples in hydrochloric acid-hydrogen peroxide with small additions of hydrofluoric acid and nitric acid, dilution to 25-ml volume, and direct atomic absorption analysis. This very direct procedure is made possible by the fact that the uranium effectively suppresses interelement atomic absorption effects as well as enhancing the sensitivities of the individual elements. Suitable instrument settings for each element are given. The measurement coefficient of variation generally is better than 1% at the 1% (by weight) alloy level, better than 3% at the 0.1% alloy level, and except for niobium and hafnium, better than 7% at the 0.01% alloy level. (auth)

2066 (NIM-834) DETERMINATION OF NIOBIUM AND TANTALUM BY THE CHROMATOGRAPHIC METHOD. No. 41/4. Steele, T. W.; Marks, Maria H.; Stoch, H. (National Inst. for Metallurgy, Johannesburg (South Africa)). 30 Sep 1969. 6p. Dep. NTIS (U. S. Sales Only).

The sample is fused with sodium peroxide, and the niobium and tantalum are precipitated using ammonium hydroxide. The precipitate is ignited and the residue dissolved in HF. The solution is then passed through a chromatographic cellulose-powder column. Methyl ethyl ketone is used in separating the niobium from the tantalum. The tantalum is determined gravimetrically and the niobium by subtraction. (M.C.G.)

2067 (NIM-906) DETERMINATION OF URANIUM IN ORE SAMPLES BY LIQUID-LIQUID EXTRACTION AND SPECTROPHOTOMETRIC DETERMINATION. Steele, T. W.; Summerson, Col-

leen D.; Stoch, H. (National Inst. for Metallurgy, Johannesburg (South Africa)). 21 Jan 1970. 5p. Dep. NTIS (U. S. Sales Only).

Tributyl phosphate is used to extract uranium from nitric acid solution and after dibenzoyl–methane solution and pyridine are added, the absorbance of the solution is measured at 420 μm. The procedure is applicable to ore samples and aqueous solutions containing small quantities of uranium. (M.C.G.)

2068 (NLCO–1071) DIRECT READING SPECTROMETRIC METHOD USING A AgCl–LiF CARRIER TO DETERMINE IMPURITIES IN NUCLEAR-GRADE U_3O_8 SAMPLES. Pepper, C. E.; Blank, G. R.; Duff, C. E.; Pardi, A. J. (National Lead Co. of Ohio, Cincinnati). Oct 1970. Contract AT(30-1)-1156. 21p. Dep. NTIS.

A method employing a 2-meter Production Control Quantometer with a 10% AgCl–LiF (11: 1) carrier dc-arc technique is described for determining trace impurities in nuclear-grade U_3O_8 samples. Included are brief descriptions of U_3O_8 sample preparation, electrode design, preferred electrode graphite grades, carrier development, modifications made to the standard Quantometer, the use of alternate read-out systems, and the importance of temperature and humidity control. The accumulated development results of 16 years of operation, which could be beneficial to other users of direct-reading spectrometers for carrier-distillation dc-arc work, are summarized. (auth)

2069 (Y–1740) AUTOMATED QUANTOMETER DATA HANDLING SYSTEM. Bowers, G. L.; Maxson, R. C. (Union Carbide Corp., Oak Ridge, Tenn. Y-12 Plant). 25 Nov 1970. Contract W-7405-eng-26. 136p. Dep. NTIS.

Analysis by spectrographic methods requires that large volumes of data be recorded and processed; and, prior to element analysis, a time-consuming system calibration procedure must be completed. To automate the data acquisition, data analysis, and calibration procedures, a small digital computer has been interfaced to a direct-reading spectrograph (Quantometer). Development of this system has essentially eliminated several hours of menial paper work which were required to prepare the Quantometer for each day's work, thereby making the instrument useful for production analysis. Two methods of analysis were utilized at the Oak Ridge Y-12 plant: aluminum spark and uranium carrier distillation. (auth)

2070 BISMUTHIOLS AS ANALYTICAL REAGENTS. Busev, A. I.; Simonova, L. N.; Zayukova, N. D. Tr. Kom. Anal. Khim., Akad. Nauk SSSR; 17: 218-29(1969). (In Russian).

The spectrophotometric characteristics of derivatives of bismuthiol I, substituted in position 3 with naphthyl, methoxyphenyl, p-bromophenyl, benzyl, phenylethyl, benzyloxyphenyl, or 3,4-dimethoxybenzyl, as reagents for Te and Bi were studied. The naphthyl and 3,4-dimethoxybenzyl derivatives are used as reagents for the extraction-photometric determination of Te^{4+} and Bi in various substances. A critical review is given of the use of bismuthiols I and II as analytical reagents for the qualitative detection and quantitative determination of certain ions and a comparison was made with the newly synthesized derivatives. (42 references.) (Referativnyi Zh.)

2071 DETERMINATION OF MICRO-QUANTITIES OF CARBON IN METALS. Arsenijevic, Desanka; Tomasevic, Magdalena. Tehnika (Belgrade); 24: HI245-9(Oct 1969). (In Serbo-Croatian).

A conductometric method for measuring microquantities of C in metals and alloys (U, Ni, Zr, Mo, Ti, Fe–Mo, and Fe–W) is described. The specimens were heated with a flux in an induction furnace to 1000°C. The furnace was supplied with O and the CO_2 produced by oxidation of the C in the metal was passed through an aqueous solution of $Ba(OH)_2$ kept at a constant temperature by (40°C) by a thermostat. The variation in electrical conductivity of the $Ba(OH)_2$ solution was measured by a bridge-circuit, the point of balance being indicated by a cathode-ray oscilloscope. The choice of flux and the amount used depended on the metal being examined. For U, Ni, Zr, Mo, Fe–Mo, and Fe–W a flux of Fe + Sn in specified quantities was used; for Ti the flux was Fe + Cu + Sn. The aqueous solution of $Ba(OH)_2$ used to absorb the CO_2 contained additives, gelatine and 2-ethylhexanol, in specified amounts. The results were considered satisfactory with a lower limit of C determination 0.0005% and an experimental error ±10%. The determination of C in Mg was also investigated (minimum determination 0.0010%, error ±15%, flux Cu + Fe). (Metals Abstr.)

2072 PYRIDINE-2-ALDOXIME AND 6-METHYLPYRIDINE-2-ALDOXIME AS GRAVIMETRIC REAGENTS FOR ESTIMATION OF PALLADIUM(II) AND URANIUM(VI). Kumar, Narayan; Manku, G. S.; Bhat, A. N.; Jain, B. D. (Univ. of Delhi). Talanta; 17: 873-6(Sep 1970).

Pyridine-2-aldoxime (I) was found to be a sensitive reagent for the gravimetric determination of palladium(II). From chloride medium, precipitation is complete at pH 3.0 to 11.0, and in solution containing 1 N HNO_3 to pH 6.0. The compositions of the precipitates (dried at 130°) correspond to PdL_2 and $PdL_2 \cdot HNO_3$ (HL representing the reagent), respectively. PD(II) can be estimated gravimetrically in the presence of acetate, oxalate, tartrate, phosphate, fluoride, borate, perchlorate, Cu(II), Cd, Co(II), Fe(III), Ni, Zn, Pb, Bi, Sb(III), Pt(IV), Ir(IV), Ru(III), Rh(III); Os(IV) in quantities more than twice that of Pd(II), and Ag(I), Au(III), and Fe(II) even in traces cause serious interference. The yellow uranium(VI) complex with (I) is precipitated quantitatively over the pH range 3.5 to 10.0 and, after washing and drying corresponds to the composition $(C_6H_5N_2O)_2UO_2$. The uranium(VI) complex with 6-methylpyridine-2-aldoxime (II) is precipitated quantitatively over the pH range 3.0 to 10.5, and after washing and drying at 120 to 130°C corresponds to $UO_2(C_7H_7N_2O)_2$. Both (I) and (II) are suitable for the estimation of 1 to 50 mg of uranium(VI) in the presence of up to 10-fold quantities of Th(IV), La(III), and Ce(III) even when present together. Ce(IV) in quantities more than three times that of U must be reduced to Be(III). Tartrate, citrate, phosphate, Ti(IV), and Zr interfere, but acetate, oxalate, and borate do not. (auth) (UK)

2073 COLORIMETRIC DETERMINATION OF TRACES OF SELENIUM, TELLURIUM, MANGANESE, AND CERIUM. Naidu, P. P.; Gopala Rao, G. (Andhra Univ., Waltair, India). Talanta; 17: 817-22(Sep 1970).

Methods are described for the colorimetric determination of micro- and semi-micro quantities of selenium, tellurium, cerium, and manganese. The test solution in 0.35 to 3 M condensed phosphoric acid medium is oxidized with an excess of permanganate. The color intensity of the unreacted permanganate is measured at 530 nm. (auth) (UK)

2074 SPECTROSCOPIC ANALYSIS OF URANIUM. Chandola, L. Vigyan Pragati; 19: 310-11(Jul 1970). (In Hindi).

The metallurgy and properties of uranium, which is used as fuel in nuclear reactors, are described. To maintain the chain reaction in the fuel, impurities contained in uranium such as boron and cadmium, which are strong neutron absorbents, are removed. Spectrographs are used to detect impurities in uranium before the fuel rods are used in a reactor. Aluminium-coated uranium fuel rods are used in the CIRUS reactor. In the Bhabha Atomic Research Centre, India, uranium is analyzed by the modified carrier distillation technique. (INIS)

2075 PAPER CHROMATOGRAPHIC DATA FOR INORGANIC SUBSTANCES. Lederer, M.; Majani, C. (CNR, Rome). Chromatogr. Rev.; 12: 239-426(Sep 1970).

R_F values for many inorganic substances are tabulated. Data are included under the following headings: adsorption chromatography of metal ions on paper (i.e., aqueous solvents); partition chromatography of metal ions on paper (i.e., organic solvents); chromatography of metal ions on papers loaded with inorganic ion exchangers; chromatography of metal ions on papers loaded with ion-exchange resins and ion-exchange cellulose papers; chromatography of metal ions on papers impregnated with liquid ion exchangers; chromatography of metal ions on modified celluloses; and, partition and ion-exchange chromatography of anions. References are given for each of the 233 tables. Author and subject indexes are included. (J.G.B.)

2076 DETERMINATION BY X-RAY FLUORESCENCE OF CHROMIUM IN CELLULOSE. Ant-Wuorinen, O.; Visapaeae, A. (State Inst. for Tech. Research, Helsinki). Pap. Puu; 52: 525-33(1970).

A new method is proposed for determination of the chromium content in cellulose by means of x-ray fluorescence. It is especially useful for studying the mechanism of Cr sorption. One gram pellets of air-dry cellulose are pressed after mechanical disintegration and analyzed by the ratio method with an external standard sample. A scintillation counter and LiF are employed. The curved calibration line, obtained using cellulose samples containing known added amounts of Cr, was linearized by application of a correction for the effective dead-time. The error of the method, at a level of 2000 ppM Cr (= 0.2%), is ±14 ppM (= ±0.0014%). The time needed for one determination is about 3 minutes, sample preparation included. The smallest concentration still determinable is about 0.9 ppM Cr (= 0.00009%), with a counting time of 40 seconds. A study was also made of the influence exercised by absorption of the CrKαI-line by inorganic impurities in the sample. Details of the method are presented, and the results obtained are examined statistically. (auth) (Finland)

2077 DETERMINATION OF NEODYMIUM AND PRASEODYMIUM IN MISCH METAL. Mustacescu, Erica; Morait, Mar-

gareta. Metalurgia (Bucharest); 21: 520-1(Oct 1969). (In Rumanian).

The elements can be determined as chlorates, perchlorates, and nitrates. A photometric method is described using wavelengths of 740, 521, or 575 nm for Nd and 440 to 450 nm for Pr in 10% HCL–10% HNO_3 mixture at concentrations of 12.5 to 200 mg/50 cm^3. Calibration curves are given. (Metals Abstr.)

2078 CUPFERRON IN THE ANALYTICAL CHEMISTRY OF RARE EARTHS AND SCANDIUM. Das, Ajit Kumar; Banerjee, Siddheswar (Central Chemical Lab., Calcutta). Indian J. Chem.; 8: 284-9(Mar 1970).

Composition and conditions for complete precipitation and extraction of the cupferronates of trivalent rare earths and scandium have been described. If precipitated at pH 6.5 and above, the cupferronates of lighter rare earths up to gadolinium are insoluble in water, have normal composition 1:3 (metal:ligand), and can be dried at 100°, with the exception of cerium(III) cupferronate, which is stable up to 80° only. The cupferronates have been utilized for gravimetric determination of lighter rare earths after drying at 60° in a vacuum oven. The cupferronates of scandium, yttrium, and rare earths heavier than gadolinium are appreciably soluble in water, but can be precipitated completely from solutions containing large amount of ammonium salts and determined through ignition gravimetry. These cupferronates also contain more cupferron than required by normal composition, the scandium compound having the formula $NH_4Sc(C_6H_5N_2O_2)_4$. If precipitated in the presence of barium salt, scandium forms a double compound of the formula $Ba[Sc(C_6H_5N_2O_2)_4]_2$, which is insoluble in water and can be used as such for gravimetric determination of scandium. Procedures have been described for the solvent extraction of the rare earth cupferronates with isoamyl alcohol and separations have been achieved from alkaline earths and magnesium without using any masking agent, uranium using ammonium carbonate as masking agent, and many other elements using sulfosalicylic acid as masking agent. The solvent extraction procedure has been used for separation of traces of thorium, scandium, and rare earths in silicate rocks and their spectrographic determination. (auth)

2079 ON THE REACTION OF TRIVALENT AMERICIUM AND CURIUM WITH THE REAGENT ARSENAZO III. Myasoedov, B. F.; Milyukova, M. S.; Ryzhova, L. V. (Verdanskii Inst. of Geochemistry and Analytical Chemistry, Moscow). Radiochem. Radioanal. Lett.; 5: 19-23(16 Oct 1970).

The reactions of trivalent americium and curium with the reagent Arsenazo III have been investigated. The optimum pH for the spectrophotometric determination of these elements was found to be 3 to 3.5. Under such conditions, americium and curium react with Arsenazo III in ratios of 1:1 and 1:2. Complexes with a maximum of light absorption at 650 nm are formed. The apparent molar extinction coefficients of the complexes 1:2 are 82.000 ± 2.000. (auth)

2080 CATALYTIC AMALGAM METHOD FOR DETERMINING SMALL AMOUNTS OF CHROMIUM, VANADIUM, AND MOLYBDENUM IN A BRINE. Volkov, G. I.; Melnikova, S. A. Zh. Anal. Khim.; 25: 2049-50(Oct 1970). (In Russian).

Effects of small amounts of chromium, vanadium, and molybdenum on the decomposition of a sodium amalgam were studied. It was found that the amalgam test method can be used for determining chromium, vanadium, and molybdenum due to the increase of the exposure time. The sensitivity of the method is $n \times 10^{-7}$%. (auth)

2081 COULOMETRIC TITRATION OF MANGANESE(VII), CERIUM(IV), CHROMIUM(VI), AND VANADIUM(V) BY ELECTROGENERATED VANADIUM(III). Agasyan, P. K.; Basov, V. N.; Kostromin, A. I. (Moscow State Univ. Kazan State Univ., USSR). Zh. Anal. Khim.; 25: 1933-7(Oct 1970). (In Russian).

Methods were developed for the internal and external generation of V(III) in sulfate and phosphate vanadyl solutions using a generating Pb cathode. A coulometric titration was carried out on ≥0.1 mg in 20 ml of Mn(VII), Ce(IV), Cr(VI), and V(V) with the internal generation, and of Mn(VII) and Cr(VI) using the internal and external generation of V(III). (auth)

2082 USE OF N-BENZOYL-o-TOLYLHYDROXYLAMINE IN THE METHOD OF AMPEROMETRIC TITRATION. COMMUNICATION 3. AMPEROMETRIC DETERMINATION OF TITANIUM AND ZIRCONIUM. Gallai, Z. A.; Sheina, N. M.; Nifontova, N. V.; Bodyagina, V. V. (Moscow State Univ.). Zh. Anal. Khim.; 25: 1851-4(Oct 1970). (In Russian).

A method was developed for the amperometric titration of Zr(IV) with a N-benzoyl-o-tolylhydroxylamine solution in 0.5 to 2N H_2SO_4 in the presence of certain elements. The composition of the compound formed was found and its solubility in 1N H_2SO_4 was determined. Conditions were found for the amperometric titration of Ti(IV) with the reagent solution. It is possible to determine 0.40 to 7.0 mg of Ti in 8N HCl in the presence of a number of elements. The composition and the solubility of the compound formed were found. (auth)

2083 LUMINESCENCE OF NEODYMIUM AND EUROPIUM IN CERIUM DIOXIDE AND ITS USE IN ANALYSIS. Poluektov, N. S.; Smirdova, N. I.; Efryushina, N. P. (Inst. of General and Inorganic Chemistry, Odessa). Zh. Anal. Khim.; 25: 1902-5 (Oct 1970). (In Russian).

A method was developed for determining neodymium and europium as impurities in pure cerium dioxide. The method is based on recording the luminescence of the CeO_2 crystal phosphor activator by Nd and Eu. The sensitivity of the method is $6 \cdot 10^{-5}$% (Nd) and $5 \cdot 10^{-8}$% (Eu). The standard deviation of a determination is 4.2%. (auth)

2084 NEW REAGENT FOR THE PHOTOMETRIC DETERMINATION OF ZIRCONIUM AND HAFNIUM. Dedkov, Yu. M.; Ermakov, A. N.; Korsakova, N. V. (Inst. of Geochemistry and Analytical Chemistry, Moscow). Zh. Anal. Khim.; 25: 1912-17 (Oct 1970). (In Russian).

The reagent, 8-hydroxy-7-[(2-hydroxy-3,5-dinitrophenyl)-azo]-1,6-naphthalenedisulfonic acid, was used for determining zirconium and hafnium. In strongly acid media it forms complexes M:HR of 1:1 and 1:2 with the cations of these metals which can be characterized by the following values: $\epsilon_{ZrR}^{540} = 22.5 \times 10^3$, $\epsilon_{ZrR_2}^{540} = 37.3 \times 10^3$, $\epsilon_{HfR}^{545} = 22.1 \times 10^3$, $\epsilon_{HfR_2}^{520} = 40.3 \times 10^3$, $\lambda_{max}^{HR} = 496$ nm, $\lambda_{max}^{ZrR_2} = 540$ nm, $\lambda_{max}^{HfR_2} = 520$ nm. The ratio $\epsilon_{ZrR} : \epsilon_{HR}$ is 46.7; $\epsilon_{HfR_2} : \epsilon_{HR}$ is 38.6 at the working wavelength. Photometric methods for determining zirconium and hafnium in 0.1N HCl were developed. No interference is caused to the determination of 0.3 to 50 μg of Zr or 0.75 to 50 μg of Hf in 25 ml by 5,000 to 10,000-fold amounts of rare earths, Zn, Ca, Mg; 1,000 to 5,000-fold amounts of Al, Pb, Fe, In, Ba, Ni, Be, Bi; 500 to 1,000-fold amounts of Ti, Cu, V; 100 to 500-fold amounts of Cr, Mo, Th, and hydroxy acids. The method was tested on geological specimens. (auth)

2085 EXTRACTION–PHOTOMETRIC DETERMINATION OF NIOBIUM(V) WITH BENZOHYDROXAMIC ACID. Gibalo, I. M.; Voskov, V. S.; Lobanov, F. I. (Moscow State Univ.). Zh. Anal. Khim.; 25: 1918-21(Oct 1970). (In Russian).

A study was made of the formation of a niobium(V) compound with benzohydroxamic acid (BHA) in HCl solutions. Effects of the HCl and the organic reagent concentrations on the formation of the colored compound were examined. The composition of the compound was found, and the formation constants were calculated. Effects of organic solvents on the extraction of the colored compound were investigated. A study was made of the effects of Zn, Fe, Co, Ni, Mn, Cr, Mo, Zr, W, Ta and Ti on the results of the extraction–photometric determination of niobium with BHA. The method was applied to the determination of niobium in alloys. (auth)

2086 INCREASING THE SENSITIVITY AND ACCURACY OF THE LUMINESCENCE DETERMINATION OF THE RARE EARTHS BY THE METHOD OF THE PERIODICAL SCANNING OF THE SPECTRUM. Karyakin, A. V.; Anikina, L. I.; Bin, Le Viet; Belyaev, Yu. I. (Inst. of Geochemistry and Analytical Chemistry, Moscow). Zh. Anal. Khim.; 25: 1898-1901(Oct 1970). (In Russian).

The method of the periodic scanning of the spectrum increased the sensitivity of the luminescence determination of the rare earths by two orders. (auth)

2087 USE OF CHELATING REAGENTS IN THE EXTRACTION–PHOTOMETRIC DETERMINATION OF ELEMENTS WITH BASIC DYES. Zolotov, Yu. A.; Seryakova, I. V.; Vorob'eva, G. A.; Sapragonene, M. S. (Inst. of Geochemistry and Analytical Chemistry, Moscow). Zh. Anal. Khim.; 25: 1845-50(Oct 1970). (In Russian).

The use of metal acidocomplexes with chelating agents for the extraction–photometric determination of elements by means of basic dyes was investigated. It was established that colored complexes are formed in the systems Ni, Zn, or U(VI)–8-hydroxyquinoline–rhodamine 6G (butylrhodamine). These complexes can be extracted with benzene. Effects of the organic solvent and buffer solution, pH, the reagent concentration and some other factors were examined. The sensitivity of the determination of nickel, zinc, and uranium(VI) is 0.02, 0.05, and 0.2 μg/ml respectively. The absorbance of blank extracts is insignificant. (auth)

2088 COMPLEXOMETRIC DETERMINATION OF URANIUM WITH EDTA. Hodisan, T.; Crisan, I. Al. (Babes-Bolyai Univ., Cluj). Stud. Cercet. Chim.; 18: 641-50(1970). (In Rumanian).

The currently used complexometric determination of uranium involves the back titration of the excess of Complexon III (EDTA), added to a solution of tetravalent uranium; the hexavalent state is determined by high-frequency titration or by direct methods. The various reactions of uranium with EDTA are reviewed, pointing out that the literature mentions proportions of 1 : 1 and 1 : 2 for the uranyl complexonate. The study indicates that in contrast to the hexavalent uranium, U(IV) forms only the 1 : 1 complex. The metallochromic indicators described in previous studies present the disadvantage of being nonspecific; they cannot be used in the presence of other elements, and their absorption in the ultraviolet range interferes with photometric determinations. (TTT)

2089 DETERMINATION OF GADOLINIUM IN IRRADIATED GADOLINIA/MAGNESIA MIXTURES. Robins, I. H.; Hilton, D. A. (Berkeley Nuclear Labs., Eng.). Int. J. Appl. Radiat. Isotop.; 21: 619-23(Oct 1970).

A method is described whereby gadolinium is determined in irradiated gadolinia/magnesia mixtures by titrating an acetic solution of these oxides with sodium oxalate. The ^{153}Gd activity in solution is used as an internal indicator and this is measured at regular intervals throughout the titration by high resolution γ spectrometry until complete precipitation of gadolinium oxalate is obtained. The acetate ions in solution have little effect on the overall reaction and the proposed method has an accuracy and precision of the order of 0.5 per cent. (auth) (UK)

2090 POLAROGRAPHIC DETERMINATION OF TELLURIUM (IV) IN MONOETHANOLAMINE SOLUTION. Rao, A. L. J.; Puri, B. K. (Panjabi Univ., Patiala, India). Indian J. Chem.; 8: 301-2(Mar 1970).

The polarographic determination of tellurium(IV) using monoethanolamine as a base electrolyte is reported. In 0.3M of the electrolyte two waves were obtained at lower pH, and above pH 10.8 only one wave was obtained; all the waves were diffusion-controlled. The method can be employed for the micro determination of Te(IV) even in the presence of elements like Se, Cr, Mo, V, Th, Ce, Mn, Fe, and W. (auth)

2091 VALUE OF THE RECIPROCAL SLOPE OF THE CALIBRATION GRAPH AND METHODS OF CALCULATING IT IN THE INDIRECT SPECTROPHOTOMETRIC DETERMINATION OF YTTRIUM IN RARE-EARTH METALS. Ganopol'skii, V. I. Vestsi Akad. Navuk BSSR, Ser. Khim. Navuk; No. 1, 36-8(1969). (In Russian).

The indirect determination of Y in total rare-earth metals (r.e.m.) was based on the differences in atomic weight of Y and r.e.m. with similar values of molar extinction coefficient of their colored complexes with some organic reagents. A method was described for calculating the reciprocal slope of the calibration graphs, so avoiding construction of the calibration graphs. The method was based in the determination of the mean value of the apparent molar extinction coefficient for 3 or 4 compounds of r.e.m. with a given reagent. A comparison of the values of reciprocal slope for some mixtures of Y with r.e.m., obtained experimentally and by calculation, confirmed the reliability of the proposed equation. The method is recommended for the analysis of r.e.m. concentrates of diverse and complex compositions, and for the rapid monitoring of processes for the separation of r.e.m. (Referativnyi Zh.)

2092 VOLTAMMETRIC DETERMINATION OF EUROPIUM(III) USING THE LANTHANUM HEXABORIDE ELECTRODE. Curran, D. J.; Fletcher III, K. S. (Univ. of Massachusetts, Amherst). Anal. Chem.; 42: 1663-6(Nov 1970).

A study of the use of lanthanum hexaboride as a voltammetric indicating electrode for the determination of europium(III) using linear sweep voltammetry is reported. It was not possible to arrive at kinetic parameters for the europium reduction at LaB_6 because the mechanism is unknown; therefore, it was concluded that for the present the linear dependence of peak current on concentration and on the square root of the sweep rate must be viewed as empirical but useful data. (D.H.M.)

2093 NEW SENSITIVE SPECTROPHOTOMETRIC DETERMINATION OF SCANDIUM WITH 4-(2-THIAZOLYLAZO)RESORCINOL. Shimizu, T.; Momo, E. (Gunma Univ., Maebashi, Japan). Anal. Chim. Acta; 52: 146-9(Oct 1970).

A new sensitive spectrophotometric procedure for determining scandium with 4-(2-thiazolylazo)resorcinol (TAR) and its application for trace quantities of scandium in silicate rocks are reported. Beer's Law was obeyed over the concentration range 0.12 to 1.6 ppM scandium at pH 8.1 and 540 nm. The sensitivity of the reaction was 0.001 μg scandium cm^{-2} for log $I_0/I = 0.001$. The molar absorptivity of the complex was estimated to be 50,600 at 540 nm. (D.H.M.)

2094 DETERMINATION OF RARE-EARTH ELEMENTS IN ROCKS BY ISOTOPE-EXCITED X-RAY FLUORESCENCE SPECTROMETRY. Kunzendorf, H.; Wollenberg, H. A. (Danish Atomic Energy Commission, Risoe, Denmark). Nucl. Instrum. Methods; 87: 197-203(1970).

Isotope-excited x-ray fluorescence spectrometry furnishes a rapid determination of rare-earth elements in unprepared rock samples. The samples are excited by ^{241}Am γ rays, generating x-ray spectra on a multichannel pulse-height analyzer. Gaussian peaks of the Kα and Kβ x-ray energies are treated by the least-squares method to yield the fractions of La, Ce, Pr, and Nd in the samples. A calibration was established between the fractions of Ce and Nd and their abundances determined by mass spectrometry. Statistical considerations indicated that detection limits are of the order of 10 ppM. An x-ray spectrometric scan of a longitudinally sliced drill core showed a close correlation between rare-earth abundances and appropriate minerals. (auth)

2095 MASS ABSORPTION COEFFICIENTS AND QUANTITATIVE MICROANALYSIS OF REFRACTORY METAL CARBIDES. Gray, Lawrence J.; Wert, C. A. (Univ. of Illinois, Urbana). Advan. X-ray Anal.; 12: 563-80(1969). (COO-1190-580).

Consideration of variations in atomic potentials permits an estimation of the mass absorption coefficients of many elements for the characteristic emission lines of carbon, nitrogen and oxygen. The accuracy of (μ/ρ) values presented is better than 5% in most cases. These values are tested in the microanalysis of defect titanium carbides. Limitations of the theoretical correction procedures lead to the definition of a set of analysis conditions which permit carbon analysis to within 1.0% absolute. (auth)

2096 STUDIES OF SPECTROCHEMICAL ANALYSIS OF RARE EARTH ELEMENTS. V. DIRECT READING EMISSION SPECTROMETRIC DETERMINATION OF TRACE ELEMENTS IN LANTHANUM, NEODYMIUM, AND YTTRIUM BY ROTATING ELECTRODE. Osumi, Yasuaki; Kato, Akihiko; Miyake, Yoshizo (Government Industrial Research Inst., Osaka). Jap. Anal.; 19: 1404-10(Oct 1970). (In Japanese).

A direct reading emission spectrometric method by rotating electrode was applied in the presence of cesium or methanol for the quantitative determination of traces of rare earths and other elements in lanthanum oxide, neodymium oxide, and yttrium oxide. The sample (La_2O_3 5.0 g, Nd_2O_3 2.5 g, and Y_2O_3 1.0 g) is dissolved in hydrochloric acid, and the solution is evaporated. The residue thus obtained is made up to volume (100 ml) by adding cesium or methanol, and the aliquots are subjected to the emission spectrochemical determination by high voltage spark discharge (C: 0.007 $\mu F \times 2$, V: 10 kV, L: 450 μH, analytical gap 3 mm and pre-spark time 60 sec). Cesium and methanol enhance the emission intensity of the spectral line and permit the determination of microquantities of the elements within limits of detection from 1 to 45 ppM in lanthanum oxide, neodymium oxide, and yttrium oxide. (auth)

2097 SPECTROCHEMICAL ANALYSIS OF TITANIUM AND ITS ALLOY. IV. X-RAY FLUORESCENT ANALYSIS OF TITANIUM ALLOYS. Matsumura, Tetsuo; Kotani, Naomi; Goto, Takeshi (Kobe Steel Ltd., Japan). Jap. Anal.; 19: 1393-1400(Oct 1970). (In Japanese).

The x-ray fluorescent analysis of titanium alloys was investigated for the accurate determination of widely varying concentrations of many alloying elements. The analytical curves for the elements aluminum, cobalt, chromium, copper, iron, manganese, tantalum, vanadium, and zirconium were found to be linear with a standard deviation of difference of chemical and x-ray results of ±0.005 to ±0.178% for single measurement at the concentrations of 0.05 to 20.0%. However, discrepancies from the chemical analyses were found for molybdenum, palladium, and tin, and were found to be caused by an interelement effect due to x-ray absorption, which was empirically corrected by means of an equation by the use of mass absorption coefficient derived from the fundamental x-ray intensity formula. To establish the analytical curves by this correction procedure, it is not necessary to produce a great number of standards. The analysis by the method can be accomplished in approximately one-fifth to one-tenth of the time necessary for conventional wet chemical methods. (auth)

2098 TITANIUM AND ZIRCONIUM IN HYDROTHERMALLY ALTERED ROCKS FROM THE TATEYAMA JIGOKUDANI HOT SPRINGS, TOYAMA, JAPAN. Imahashi, Masayuki (Tokyo

XUM

Metropolitan Univ.). Bull. Chem. Soc. Jap.; 43: 2475-8(Aug 1970).

Hydrothermally altered rocks and muds collected from the Tateyama Jigokudani Hot Springs were analyzed for titanium and zirconium. In order to estimate the acidity of the thermal waters that contributed to these altered rocks, the concentration factor of the elements relative to SiO_2 was used for convenience. The titanium and zirconium contents of the alteration products were approximately equal to those of the fresh rocks. This seems to indicate that most of these elements remain in the rocks during the alteration under acidic conditions. The muds were characterized by high values of the concentration factors and the factors proved to be dependent on the acidity of the mud-suspending waters From the relation between the concentration factors and the pH's of the waters, the acidities of the thermal waters which attacked the altered rocks in the earlier stages were estimated. (auth)

2099 TITRIMETRIC DETERMINATION OF U(IV) ALONE AND IN MIXTURES WITH V(IV), Mn(II), Ce(III), AND Fe(II). APPLICATION TO THE ANALYSIS OF STEELS AND ALLOYS. Naidu, P. P.; Rao, G. G. (Andhra Univ., Waltair, India). Z. Anal. Chem.; 252: 7-11(1970).

A rapid and accurate method is described for potentiometric determination of uranium(IV) with permanganate at room temperature using trace amounts of ortho-phosphoric acid as a catalyst. The procedure was extended for the differential potentiometric determination of mixtures with vanadium, manganese, or cerium. The methods are easy, non-time-consuming and free from interference by a large number of foreign ions. Conditions were also developed for the differential photometric determination of uranium and iron in mixtures. Based on these procedures, a differential titrimetric procedure was developed for determination of iron(III), vanadium(V), chromium(VI), and manganese(VII) [or cerium(IV)] in a single solution at room temperature. This procedure was also tested on Bureau of Standard samples. (auth)

2100 ULTRAVIOLET SPECTROPHOTOMETRIC DETERMINATION OF GALLIUM BY THE 1-PYRROLIDINE-CARBODITHIOATE METHOD. Likussar, W.; Sagan, C.; Boltz, D. F. (Wayne State Univ., Detroit). Mikrochim. Acta; No. 4, 683-7(1970).

A new ultraviolet spectrophotometric method for the determination of gallium(III) is proposed. It is based on the formation of a stable, extractable complex using ammonium 1-pyrrolidinecarbodithioate as the reagent. Conformity to Beer's law was observed, and the optimum concentration range is 2 to 25 ppM of gallium. The molar absorptivity at 308 nm is 2.58×10^3 l mole^{-1} cm^{-1}. (auth)

2101 NON-SULFIDE SCHEME OF INORGANIC QUALITATIVE MICROANALYSIS. Prokopov, Theodore S. (Upper Iowa Coll., Fayette). Mikrochim. Acta; No. 4, 694-701(1970).

A nonsulfide scheme of inorganic qualitative microanalysis is presented with solutions of HCl, CH_3COONa, H_2SO_4, and NaOH as group reagents. Color reactions (spot tests) are also included in this scheme. The purpose of this new approach to qualitative analysis is to eliminate disagreeable odor and corrosive action of hydrogen sulfide and also to introduce complete group separations leading to more definite analytical results. It is possible to identify NH_4^+, Na^+, K^+, Mn^{2+}, Cr^{3+}, Fe^{2+}, Fe^{3+}, Sn^{2+}, Pb^{2+}, Hg^{2+}, As^{3+}, and As^{5+} among 26 cations in the original unknown sample. (auth)

2102 MICRODETERMINATION OF RHENIUM: REMOVAL OF INTERFERENCE FROM MOLYBDENUM, VANADIUM, TUNGSTEN, AND SOME OTHER ELEMENTS IN THE THIOCYANATE METHOD. Yatirajam, V.; Kakkar, L. R. (Kurukshetra Univ., Haryana, India). Mikrochim. Acta; No. 4, 708-14(1970).

Without separating the interfering elements, rhenium color is developed by a slightly modified thiocyanate-stannous chloride method. The thiocyanates are extracted into iso-amyl alcohol, the interfering elements are extracted back from the solvent with 10% KHF_2 solution and the absorbance of rhenium thiocyanate is measured. Molybdenum, vanadium, tungsten, uranium, iron, cobalt, nickel, chromium, platinum, copper, selenium, and tellurium do not interfere in amounts up to 20 mg, alone or together. Palladium, ruthenium, and osmium still interfere. (auth)

2103 TENTATIVE METHOD OF ANALYSIS FOR MOLYBDENUM CONTENT OF ATMOSPHERIC PARTICULATE MATTER. Health Lab. Sci.; 7: 149-51(Jul 1970).

The method described for the satisfactory determination of Mo depends largely on the quantitative formation of a stable Mo(V) thiocyanate complex. The complex is formed, in the presence of Fe and Cu, by reduction of Mo(VI) with stannous chloride in a solution containing potassium thiocyanate. The thiocyanate complex is extracted with methyl isobutyl ketone. The absorbance of the extract is measured in a 10-cm cell at 500 nm using methyl isobutyl ketone in the reference cell. The absorbance is a linear function of Mo concentration, at least between 0 and 15 μg of Mo/25 ml of solvent. The sensitivity is 1.1 μg of Mo/0.05 absorbance units, a concentration of 0.055 μg of Mo/m^3 of air can be measured if a 20 m^3 sample is taken for analysis. The interferences caused by Re, Pt, Pd, Rh, Se, and Te are negligible in concentrations found in ambient air. (P.C.H.)

2104 POTENTIOMETRIC STUDIES WITH A LIQUID ION-EXCHANGE LEAD-SELECTIVE ELECTRODE. Lal, Sudarshan; Christian, Gary D. (Univ. of Kentucky, Lexington). Anal. Chim. Acta; 52: 41-6(Oct 1970).

The performance of the Orion liquid ion-exchange lead-selective electrode was determined in terms of the working concentration range of lead ions, its selectivity to other ions, its response time, the effective pH range in which it can be used, and its use in potentiometric titrations. The electrode exhibits relatively high response to monovalent cations and can be used in the potentiometric titration of potassium, rubidium, cesium, thallium(I), silver(I), and ammonium ions with sodium tetraphenylboron, as well as for titrations of lead(II) with various solutions. (auth)

2105 USE OF AN X-RAY FLUORESCENCE SPECTROMETER WITH A COMPUTER. APPLICATION TO THE DETERMINATION OF AN ELEMENT IN SOLUTION AND ANALYSIS OF INDETERMINATE SHAPE SAMPLES. Florestan, J.; Bouvier, J. M. (Commissariat a l'Energie Atomique, Fontenay-aux-Roses, France). Chim. Ind., Genie Chim.; 103: 1903-10(Sep 1970). (In French).

Accurate and reproducible determination of various elements in solution by x-ray fluorescence was made by making measurements on three standard solutions and a sample solution several times. Each series of measurements gave a nonlinear computed standardization curve. The sample solution was determined according to the new curve. Uranium was determined in concentrated solutions (300 to 400 g/l). In the case of the analysis of samples of indeterminate shape where interference occurs between the various peaks, the use of a computer allows results to be obtained rapidly by using special correction formulas. (auth) (France)

Isotope Dilution Procedures

2106 RADIOCHEMICAL DETERMINATION OF TRACES OF ANTIMONY BY ISOTOPE EXCHANGE REACTION IN THE ORGANIC PHASE. Kratzer, K. (Tech. Univ., Prague). Radiochem. Radioanal. Lett.; 5: 69-74(16 Oct 1970).

A new radioanalytical method for the determination of traces of antimony (0.5 to 20 μg) has been developed. The method is based on the homogeneous exchange reaction between antimony(III) iodide and labeled antimony(III) diethyldithiocarbamate in carbon tetrachloride. (auth)

2107 DETERMINATION OF TRACE AMOUNTS OF CONTAMINANTS IN WATER BY ISOTOPE DILUTION GAS CHROMATOGRAPHY. Wasik, S. P.; Tsang, W. (National Bureau of Standards, Washington, D. C.). Anal. Chem.; 42: 1649-51(Nov 1970).

The suitability of isotope dilution gas–liquid chromatography for the analysis of water pollution samples is demonstrated in the determination of benzene in water at the ppB level. Deuterium, in the form of perdeuterated benzene, was used as the isotope and an aqueous silver nitrate column was used to determine the ratio of benzene to perdeuterated benzene. Results showed that although the benzene was only partially transferred from the carbon tetrachloride solutions to aqueous silver nitrate solution this does not interfere with the total benzene determination since all that is required is the isotope ratio. (D.H.M.)

Radiometric and Radiochemical Procedures

Refer also to abstracts 2380 and 2482.

2108 (RT/PROT-(70)14) ESTABLISHMENT OF A LABORATORY FOR THE DETERMINATION OF PLUTONIUM IN BIOLOGICAL SAMPLES: REVISION AND COMPARISON OF VARIOUS METHODS OF ANALYSIS. Testa, C.; Masi, G.; Marchionni, V. (Comitato Nazionale per l'Energia Nucleare, Rome (Italy)). 27 May 1970. 100p. (In Italian). Dep. NTIS (U. S. Sales Only).

The preparation of a radiotoxicology laboratory for determination of plutonium in biological samples is described. Some urine analysis methods were tested and a special technique that had given

XUM

good results in the presence of metabolized plutonium was selected. Rapid determinations of plutonium in nose blows and feces, to be used for inhalation intakes, are also described. The plutonium counting in contaminated wounds is obtained with special probes for alpha particles and 17-keV X rays. The features of a plutonium radiotoxicological laboratory are illustrated and the necessity to isolate it from the other laboratories is pointed out. The action and reference levels for the different biological samples and the routine results obtained are indicated. (auth)

2109 SELECTIVE DETERMINATION OF INORGANIC MERCURY IN THE PRESENCE OF ORGANOMERCURIAL COMPOUNDS IN BIOLOGICAL MATERIAL. Clarkson, T. W.; Greenwood, M. R. (Univ. of Rochester, N. Y.). Anal. Biochem.; 37: 236-43(Oct 1970).

A method was developed for the selective measurement of radioactive inorganic mercury in the presence of organomercurial compounds labeled with the ^{203}Hg isotope. This method may be used for the study of the cleavage of the carbon–mercury bond in animals injected with labeled organomercurial compounds. The principle of the method is the selective reduction of inorganic mercury by $SnCl_2$ to elemental vapor. The latter is swept from the sample by an air stream collected on a specific absorbent, Hopcalite, where the radioactivity is determined by γ scintillation counting. (auth)

2110 SEPARATION AND DETECTION OF ^{181}W AND ^{185}W FROM RADIOACTIVE FALLOUT. Suzuki, Toshio; Sotobayashi, Takeshi; Noda, Tomohiko (Niigata Univ., Japan). Jap. Anal.; 19: 1432-4(Oct 1970). (In Japanese).

Tungsten-181,185 was detected in rain samples collected on December 25, 1968 at Niigata. A recommended procedure for rapid separation of tungsten from radioactive fallout has been developed. No detectable amount of radionuclides other than tungsten can be found in a γ spectrum of the counting sample obtained through the present procedure. (auth)

2111 APPLICATION OF ABSORPTION METHOD USING THE GAMMA RADIATION WITH TWO DIFFERENT ENERGIES FOR CONTINUAL ANALYSIS. Kubicek, Petr; Mrazek, Libor (Inst. of Mining and Metallurgy, Ostrava, Czech.). Jad. Energ.; 16: 272-80(Aug 1970). (In Czech).

Influences having importance for the application of the gamma–gamma method during the continual analysis are considered. The equations for calculation of attenuation coefficients, the resolving power of the method, and its theoretical value are given. The nonlinearity of absorption curves in semilogarithmic coordinates, the change of spectrum caused by detectors, and influence of deadtime and stability of detectors are discussed. The first dynamic approximation of this method in which ten basic parameters are involved into the system of some equations are shown. Experimental results of application gamma–gamma method for analysis of coal heterogenously mixed with waste rocks are described. (auth)

2112 RAPID METHOD FOR THE DETERMINATION OF ^{210}Po AND ^{210}Pb IN SEAWATER. Shannon, L. V. (Division of Sea Fisheries, Cape Town); Orren, M. J. Anal. Chim. Acta; 52: 166-9(Oct 1970).

The levels of ^{210}Po and ^{210}Pb can be measured conveniently in small seawater samples by solvent extraction followed by α-counting and/or α-spectrometry. Although 1.5-l samples are adequate for ^{210}Po measurements, larger samples would be more satisfactory for ^{210}Pb determinations. (auth)

2113 TENTATIVE METHOD OF ANALYSIS FOR PLUTONIUM CONTENT OF ATMOSPHERIC PARTICULATE MATTER. Health Lab. Sci.; 7: 141-5(Jul 1970).

The procedure described for the determination of Pu may also be applied to the determination of ^{238}Pu, ^{239}Pu, and ^{240}Pu in air filters. The Pu is equilibrated with ^{236}Pu tracer, and isolated by coprecipitation with Ce and Y fluorides. The Pu is further purified by a double anion exchange column technique; first by absorbing from a HCl medium, the second time from a HNO_3 medium. Finally the Pu is electrodeposited onto a Pt disc. The Pu isotopes are resolved by a solid state α spectrometer. The ^{236}Pu is used to determine the chemical yield. The minimum detectable quantity of Pu is 0.015 pCi if a 1000-min counting time is used. Under practical conditions, a concentration of 0.08×10^{-3} pCi/m^3 (0.08×10^{-15} μCi/cc) can be determined with a standard error of less than ±10%. There are no interferences. The precision of the method is essentially a function of volume of air sampled, and the length of time for which the sample is counted. (P.C.H.)

2114 TENTATIVE METHOD OF ANALYSIS FOR ^{89}Sr CONTENT OF ATMOSPHERIC PARTICULATE MATTER. Health Lab. Sci.; 7: 138-40(Jul 1970).

Strontium-89 can be determined at the same time as ^{90}Sr, using the separated strontium fraction from the previously described ^{90}Sr procedure. (Health Lab. Sci.; 130-7(Jul 1970)). The ^{89}Sr content of the sample is calculated by correcting the total counting rate of the $SrCO_3$ fraction for the ^{90}Sr present and for the ^{90}Y which grows in between separation and counting. The procedure is simple chemically but requires rather complex calculations, particularly in obtaining the estimate of counting error. A minimum of 5 pCi per sample of ^{89}Sr can be determined with an error of less than ±10% the 95% confidence level under usual conditions (counter background of less than 1 cpm and a 60-min counting time). The interferences are the same as for ^{90}Sr. Because the determination of ^{89}Sr is based on the difference in total count rate in the Sr fraction and that due to ^{90}Sr and ^{90}Y, the precision and accuracy is limited by a greater error than for ^{90}Sr determination. (P.C.H.)

2115 TENTATIVE METHOD OF ANALYSIS FOR ^{90}Sr CONTENT OF ATMOSPHERIC PARTICULATE MATTER. Health Lab. Sci.; 7: 130-7(Jul 1970).

The determination of ^{90}Sr in ambient air is performed by dissolution of a filter through which a known volume of air has been passed. The required volume of air sampled is dependent on the ^{90}Sr concentration and should be large enough to obtain a statistically significant result. Sr is separated from Ca, other fission products, and natural radioactive elements. Nitric acid separations remove the Ca and most of the other interfering ions. Radium, Pb, and Ba are removed with barium chromate. Traces of other fission products are scavenged with iron hydroxide. After the ^{90}Sr + ^{90}Y equilibrium has been attained, the ^{90}Y is precipitated as the hydroxide and converted to the oxalate for counting. Sr chemical yield is determined gravimetrically as strontium carbonate. 0.5 pCi ^{90}Sr can be determined by this method with an error of less than ±10% at the 95% confidence level under usual conditions (counter background of less than 1 cpm and a 60-min count). (P.C.H.)

2116 GAMMA COUNTING OF ^{125}I USING A METAL-LOADED LIQUID SCINTILLATOR. Ashcroft, J. (Microbiological Research Establishment, Salisbury, Eng.). Anal. Biochem.; 37: 268-75(Oct 1970).

A tin-loaded liquid scintillator was used with a liquid scintillation analyzer for the routine gamma counting of iodine-125. The most suitable solution gave a counting efficiency of 55% with a background of 40 cpm, which compares favorably with sodium iodide well crystal counting of this isotope. A modified counting vial allows the sample to be kept separate from the liquid scintillator. The advantages of the method are the ease of sample preparation and the use of an automatic counting facility. (auth)

2117 RAPID METHODS FOR ESTIMATION OF CONTENT OF RADIOACTIVE CATIONS IN WATER. Haberer, K.; Stuerzer, U. Gas- Wasserfach, Wasser - Abwasser; 111: No. 1, 29-32 (1970). (In German).

Two different methods for the determination of drinking water contamination are presented. They are based on the application of ion exchange paper and AMP filters. Described are: the model, washing water and eluants, loaded filters, procedures, and investigations using AMP filters, SA-2 filters, or combinations of both. The mode of operation is described in detail. The time consumption for ^{90}Sr/^{90}Y, ^{144}Ce, and ^{137}Cs without measuring time amounts to 20 min; the yield is higher than 90%. (INIS)

Activation Procedures

Refer also to abstracts 2332, 2333, 2474, 2516, and 3527.

2118 (CONF-700322–, pp 205-20) PRECISE NONDESTRUCTIVE DETERMINATION OF SOME MAJOR ELEMENTS IN LUNAR MATERIAL BY 14-MeV NEUTRON ACTIVATION. Ehmann, William D.; Morgan, John W. (Kentucky Univ., Lexington. Dept. of Chemistry).

From Proceedings of the second Oak Ridge conference on the use of small accelerators for teaching and research, March 23–25, 1970.

Improved techniques for precise analysis of small rock samples for O, Al, Si, and Fe by 14-MeV neutron activation using a sequential irradiation–single transfer system are described. Analyses for O were made using a new multiscaling technique which minimizes errors due to inaccurate timing and to neutron beam variations during the irradiation period. For other elements, close attention was paid to the statistics of gamma-ray photopeak evaluation. The problems associated with analyzer dead time when short-lived radionuclides are measured were considered in detail. (auth)

XUM

2119 (CONF-700322–, pp 221-30) ANALYSIS OF OCEANOGRAPHIC SAMPLES BY 14-MeV NEUTRON ACTIVATION. Kuykendall, W. E. Jr.; Hoffman, B. W.; Wainerdi, R. E. (Texas Agricultural and Mechanical Univ., College Station. Activation Analysis Research Lab.).

From Proceedings of the second Oak Ridge conference on the use of small accelerators for teaching and research, March 23–25, 1970.

Equipment and procedures used for the nondestructive analysis of ocean sediment samples by 14-MeV neutron activation are discussed. A computer routine which analyzes gamma spectra on the basis of both energy and half-life is described. Results obtained when the procedures were tested on USGS standard rock samples are given along with results of analyses of selected core samples from the NSF Deep Sea Drilling Project. (auth)

2120 (CONF-700322–, pp 231-48) STUDIES IN FAST NEUTRON ACTIVATION ANALYSIS. Kenna, Bernard T. (Sandia Labs., Albuquerque, N. Mex. New Mexico Univ., Albuquerque. Dept. of Chemistry).

From Proceedings of the second Oak Ridge conference on the use of small accelerators for teaching and research, March 23–25, 1970.

The advent of the small fast neutron generators provided a capability that had not been available previously. A full neutron energy spectrum and a damaging gamma ray flux are not present as they are in a reactor. This not only limits the radiation damage experienced by a sample, but also permits greater specificity in activation analysis. In the area of radiation damage studies, one is able to determine the effect of high-energy neutrons without having to compensate for, or perform special operations to account for, the effects of epithermal or thermal neutrons and gamma rays. This, in effect, gives a truer picture of what is occurring and permits relatively simple experiments to be performed. Analytical activation analysis can be divided into the two customary areas: qualitative and quantitative. Characterization of materials by qualitative neutron activation analysis is now being used routinely. Analogous to several other analytical techniques, this method provides a rapid and generally simple way to distinguish between alloys, plastics, and other materials. Quantitative activation analysis provides a means of analyzing materials such as ceramics and determining the presence of low-Z elements such as nitrogen and oxygen which would be difficult by other means. To be sure, there are inherent problems in activation analysis, such as self-shielding and geometry, but these are not insurmountable. (auth)

2121 (CONF-700322–, pp 249-57) APPLICATION OF NEUTRON GENERATORS IN THE STEEL INDUSTRY. Wicker, E. E.; Nardozzi, M. J. (United States Steel Corp., Monroeville, Pa. Applied Research Lab.).

From Proceedings of the second Oak Ridge conference on the use of small accelerators for teaching and research, March 23–25, 1970.

A description is given of the present applications of a 14-MeV neutron generator in the Applied Research Laboratory of United States Steel Corporation. The principal use is in the determination of the oxygen content of several hundred varied samples per month. Emphasis will be placed on the operational aspects of this analytical service and the prospects for extending this application to actual steel-producing sites. A description is also given of the equipment and method used for the determination of silicon in steels and other materials. Proposed applications of activation analysis to continuous analysis of production streams are also discussed. (auth)

2122 (IAEA–122) USES OF ACTIVATION ANALYSIS IN STUDIES OF MINERAL ELEMENT METABOLISM IN MAN. Papers Given at a Panel Meeting, Teheran, Iran, 3–7 June 1968. (International Atomic Energy Agency, Vienna (Austria)). 1970. 172p. (CONF-680668).

Eleven articles are included plus one that is appended; separate abstracts were prepared for six. The remaining articles contain information on: normal values for trace elements in human tissues; mineral elements in relation to protein-calorie malnutrition and the nutritional anemias; effects of trace element deficiencies with special reference to Zn; clinical and biochemical uses of stable iodine measurements; trace elements in cardiovascular diseases, which mentions the role of radioactivity and the fact that neutron activation analysis can be used in this type study; and selected aspects of trace elements in cancer research, which mentions briefly ^{90}Sr retention. A brief bibliography of 33 key references for activation analysis is appended. (P.C.H.)

For abstracts of individual papers see: 2123–2127 and 2474.

2123 (IAEA–122, pp 1-13) THE APPLICABILITY OF NEUTRON ACTIVATION TECHNIQUES IN HUMAN METABOLIC STUDIES. Bowen, H. J. M. (Reading Univ. (England). Dept. of Chemistry).

The advantages and disadvantages of the technique of thermal neutron activation analysis are described. Applications are briefly listed, and it was concluded that the technique is unsuitable for C, H, O, and N; has no special advantage for Ca, Fe, Mg, and S; is competitive for Cl, Br, P, Na, K, Cu, Zn, Mn, and Mo; and is one of the few techniques with adequate sensitivity to detect Co, Cr, I, Se and many rare elements at their natural concentrations in human tissues. Recent in vivo studies are also mentioned. (auth)

2124 (IAEA–122, pp 15-26) THE MEDICAL ACTIVATION ANALYSIS RESEARCH PROGRAMME OF THE IAEA LABORATORY. Parr, R. M. (International Atomic Energy Agency, Vienna (Austria)).

Analyses carried out under the Agency's laboratory program in medical activation analysis commenced in 1967, including the laboratory facilities and experimental methods now in use are described. Results obtained to date are reported. The analytical scheme places greatest emphasis on nondestructive methods (i.e., without radiochemistry), and by the use of a Ge(Li) detector and a 2-parameter NaI(Tl) gamma spectrometer, presently allows the determination of up to 12 elements in unprocessed tissue samples. Projects completed or underway include an investigation into the uniformity of distribution of mineral elements in human liver, studies of tissue concentrations of trace elements in relation to malnutrition and cardiovascular diseases, and the determination of iodine in food, natural waters, and other biological materials in relation to the epidemiology of endemic goiter. (auth)

2125 (IAEA–122, pp 27-36) INVESTIGATIONS OF THERMAL AND 14-MeV NEUTRON ACTIVATION ANALYSIS IN PAKISTAN. Qaim, S. M. (Atomic Energy Centre, Lahore (Pakistan)).

From uses of activation analysis in studies of mineral element metabolism in man.

The applicability of the technique of activation analysis is briefly discussed. Experimental facilities available in Pakistan and the envisaged program of analyses of trace elements are outlined. The sensitivities of both thermal and fast neutron activation analysis for various essential elements are discussed. A survey of the activation work done in Pakistan, as regards biological materials, is also presented. (auth)

2126 (IAEA–122, pp 37-40) APPLICATIONS OF NEUTRON ACTIVATION ANALYSIS IN MEDICAL RESEARCH IN THE PHILIPPINES. De la Cruz, B. (Philippine Atomic Research Center, Diliman, Quezon City).

Neutron activation analysis, as used for determining the concentrations of trace elements in biomedical samples, could be an indispensable tool in medical research in the Philippines. The vital role that trace elements play in many biological processes is well known. As essential constituents of certain vitamins, hormones, and enzymes, they are needed for the proper functioning of all living cells. The current activities and future program of applications of neutron activation analysis in biomedical research at the Philippine Atomic Research Center are described. (auth)

2127 (IAEA–122, pp 145-8) USE OF ACTIVATION ANALYSIS IN THE STUDY OF CYSTIC FIBROSIS. Bowen, H. J. M. (Reading Univ. (England). Dept. of Chemistry).

Nondestructive neutron activation analysis has been used to determine sodium in fingernail samples from 73 healthy subjects, and from 7 patients with cystic fibrosis. The technique has adequate sensitivity but its precision is poor. It was concluded that better precision requires gamma detectors with better energy resolution than sodium iodide crystals. (auth)

2128 (LYCEN–7060) OXYGEN DETERMINATION IN SILICON BY MEANS OF ALPHA PARTICLES. Giroux, J.; Talvat, M.; Thomas, J-P.; Tousset, J. (Lyon Univ. (France). Institut de Physique Nucleaire). 6 Jul 1970. 25p. (In French). Dep. NTIS (U. S. Sales Only).

The determination of low oxygen contents in silicon by alpha activation is based on the Engelmann's method. The influence of the energy distribution on the activation curves was investigated. Some complex phenomena arising between 54 and 40 MeV explain the production profiles of ^{18}F and the other radioisotopes. Some details are given about the microanalysis of the surface oxide layers. Diffusion of oxygen or ^{18}F nuclides induced at the surface during the irradiation does not explain production of this radioisotope in the matrix. Parasitic reactions on the matrix ($Si \xrightarrow{\alpha} {}^{18}F$) are avoided by using other conditions of irradiation, the best energy range being about 35 MeV. Some results of the analysis are given. (France)

XUM

2129 (NBS-TN-532) POLLUTION ANALYSIS: A BIBLIOGRAPHY OF THE LITERATURE OF ACTIVATION ANALYSIS. Lutz, G. J. (ed.) (National Bureau of Standards, Washington, D. C.). Jun 1970. 32p. GPO $0.45.

The literature on the use of activation analysis of pollution samples is reindexed in detail with respect to element determined, matrix analyzed, and technique used for precise literature searching. An author index is included. 71 references were extracted from the matrix categories: water, air, atmosphere, foodstuffs, pesticides, particles, dusts, drugs, and soils. (P.C.H.)

2130 (NBS-TN-533) 14-MeV NEUTRON GENERATORS IN ACTIVATION ANALYSIS: A BIBLIOGRAPHY. Lutz, G. J. (ed.) (National Bureau of Standards, Washington, D. C.). Jun 1970. 91p. GPO $1.00.

Literature on the use of 14-MeV neutron generators in activation analysis is reindexed in detail with respect to element determined, matrix analyzed, and technique used for precise literature searching. An author index is included. 353 references were selected from the technique category Accelerator Sealed Tube-Neutrons. (P.C.H.)

2131 ACTIVATION ANALYSIS AT THE INSTITUTE OF APPLIED GEOPHYSICS, BRNO. Kasparec, I. (Inst. of Applied Geophysics, Brno). Geol. Pruzkum; 11: 106-8(Apr 1969). (In Czech).

The principles and methods of activation analysis and the equipment at the activation analysis laboratory are described. The laboratory is equipped with a neutron generator NA-2 (maximum yield 5×10^{10} n/sec, neutron energy up to 14.7 MeV), a 512-channel γ spectrometer NTA-512 and a two-channel pneumatic tube conveyor. (NSA of Czech.)

2132 ESTIMATION OF THE AMOUNT OF EXOGENOUS INCLUSIONS IN STEEL BY MEANS OF NEUTRON-ACTIVATION ANALYSIS. Wezranowski, E.; Kosciukova, B.; Zarzecka, E.; Radwan, M. Freiberg. Forschungsh.; B141: 153-9(1969). (In German).

Inclusions derived from furnace or ladle refractories may be identified from separated residues using radioactive material added to the furnace or ladle linings, but the method is dangerous. An investigation into the possibility of adding materials suitable for subsequent identification by neutron-activation analysis is described. La, added in the form of Mischmetal oxides, was found to be suitable and details of procedure are given. (Metals Abstr.)

2133 NEUTRON ACTIVATION STUDY OF ANCIENT PIGMENTS FROM MURALS OF CHOLULA AND TEOTIHUACAN. Ortega, R. F.; Lee, B. K. (Iowa State Univ. of Science and Tech., Ames). Archaeometry; 12: 197-203(Aug 1970).

Ten samples of pigments from the murals were activated and studied to investigate the homogeneity of the material and the trace composition of the pigments in order to establish a technique for future analysis. The methods used for irradiation, counting, and data handling are presented. Cu, Br, As, Au, Ag, Pt, and Hg were found in larger amounts than in standard rocks or ceramic materials. A reliable analysis was possible using short irradiation periods, especially for Al, V, and Ti, but the possibility of using standard rocks as standards for quantitative measurements was found to be poor. The long irradiation approach was more satisfactory but the use of standard material was still not possible except for a few elements. For future analysis it is suggested that artificial standard material should be developed for comparison. (UK)

2134 NEUTRON ACTIVATION ANALYSIS OF TRACE ELEMENTS IN SKIN. V. COPPER AND ZINC IN PSORIASIS. Molokhia, Mohamed M.; Portnoy, Benjamin (Manchester and Salford Hospital for Skin Diseases, Manchester, Eng.). Brit. J. Dermatol.; 83: 376-81(Sep 1970).

Copper and zinc levels were estimated in skin biopsies from a group of 20 psoriatic patients and compared with those of 10 normal subjects. The concentrations of zinc in psoriatic epidermis and dermis were significantly higher than normal, while those of copper were not. The levels of these two trace elements were also determined in the serum of 23 psoriatic patients and 22 normal subjects. There was a significant increase in serum copper levels in the psoriatic group. Zinc levels did not show significant variations. (auth)

2135 ACTIVATION ANALYSIS IN STOMATOLOGY. Blada, J. (Inst. of National Health, Dunajska Streda, Czech.); Toelgyessy, J. Cesk. Stomatol.; 69: 150-60(May 1969). (In Slovak).

A detailed survey is given of the use of activation analysis in stomatology for the determination of trace elements in teeth. The main advantage of activation analysis is considered to be its extreme sensitivity; it is therefore very useful for trace element determinations. Trace elements appear to play an important role in the resistance of teeth to caries. The exact mechanism of action of trace elements in this resistance is not yet clear. The use of activation analysis makes it possible to determine the concentration of trace elements in different layers and places of a tooth thus being an efficient means for the solution of many hitherto uncleared theoretical and practical problems of stomatology. The principle of the activation analysis, its sensitivity, and analytical procedures are described, and the importance of trace element determinations in teeth is pointed out. Papers published on trace element determinations in teeth samples are referred to. (NSA of Czech.)

2136 SULFUR DETERMINATION IN MOLYBDENUM BY ACTIVATION ANALYSIS BY THERMAL NEUTRONS. Fedoroff, Michel (Centre National de la Recherche Scientifique, Vitry-sur-Seine, France). Compt. Rend., Ser. C; 271: 399-402(10 Aug 1970). (In French).

Molybdenum irradiated by thermal neutrons is dissolved into successive layers. The ^{35}S radioactivity is measured in each layer after the chemical separation of sulfur by ion exchange and precipitation. A ^{35}S concentration gradient was observed up to a depth greater than 70 μm for molybdenum samples with surfaces highly etched by chlorine. This etching is nevertheless lower than that observed previously in the case of nickel, iron, copper, and zirconium. (auth) (France)

2137 DETERMINATION OF LEAD BY FAST NEUTRON INELASTIC SCATTERING INDUCED ^{204m}Pb. Filby, R. H.; Shah, K. R.; Davis, A. I. (Washington State Univ., Pullman). Radiochem. Radioanal. Lett.; 5: 9-18(16 Oct 1970).

A rapid, precise, and accurate method for the determination of lead by fast-neutron inelastic scattering induced ^{204m}Pb has been developed. The procedure consists of irradiating samples and lead standards in a high fast-neutron flux position of a reactor. Ge(Li) spectrometry is used for the instrumental measurement of ^{204m}Pb without chemical separation of lead. The method is useful for the nondestructive determination of lead in lead compounds and ores. (auth)

2138 RADIOACTIVATION DETERMINATION OF IMPURITIES IN YTTRIUM AND MOLYBDENUM BY MEANS OF EXTRACTION DISPLACEMENT CHROMATOGRAPHY. Stepanets, O. V.; Yakovlev, Yu. V.; Alimarin, I. P. (Inst. of Geochemistry and Analytical Chemistry, Moscow). Zh. Anal. Khim.; 25: 1906-11 (Oct 1970). (In Russian).

A method is proposed for the radioactivation determination of Mn, Zn, Cd, Ag, Hg, and Co in yttrium and molybdenum by means of successive displacement extraction chromatography and substoichiometric separation. The sensitivity is 10^{-6} to 10^{-4}%. (auth)

2139 RADIOACTIVATION DETERMINATION OF TANTALUM IN MINERALS AND ROCKS WITH A Ge(Li)-SPECTROMETER. Zaitsev, E. I.; Dneprovskii, I. S.; Sotskov, Yu. P.; Laptev, V. G. (Inst. of Mineralogy, Geochemistry, and Crystallochemistry of Rare Elements, Moscow). Zh. Anal. Khim.; 25: 1922-6(Oct 1970). (In Russian).

A Ge(Li)-detector with a capacity of 20 cm^3 was used for the instrumental radioactivation analysis of geological samples. Tantalum was determined in samples of rocks and minerals with a sensitivity of $n \cdot 10^{-5}$. The output is 30 to 40 samples a day. This method may be used for a highly sensitive determination of Hf, Sc, Co, Cs, and other rare elements in rocks. (auth)

2140 APPLICATION OF COMPTON-SCATTERING TECHNIQUES TO ACTIVATION ANALYSIS: A SHORT EVALUATION. Munera, H. A.; Spyrou, N. M. (Univ. of Surrey, Eng.). Nucl. Energy; 11: 148-50(Sep-Oct 1970).

The radioactive content in calcium carbonate (vaterite) crystals was measured after irradiation in the core of a reactor to a thermal dose of 5.10^{20} n/cm^2 and a fast neutron dose of 2.10^{20} n/cm^2. A Ge(Li) detector was used in conjunction with a 400-channel analyser. Because of the large number of radioisotopes present in the sample, the resulting spectra were extremely complex. Quantitative calculations in the lower energy regions were thus made difficult and, in general, problems in resolving the closely situated full energy peaks (FEP) arose, despite the good resolution of the Ge(Li) detector. To obtain results from the complex spectrum without unfolding it (either by computational or graphical means), but by using only the full energy peaks seated on the Compton scattering continuum, the possibility of employing some Compton scattering techniques was considered both theoretically and experimentally. It was concluded that, by using an anticoincidence method, some improvement was made in measurement of FEP of low energy without changing the efficiency in the counting of high-energy rays. (UK)

XUM

2141 SIMPOZIUM PO ISPOL'ZOVANIYU METODOV MECHENYKH ATOMOV DLYA SOVERSHENSTVOVANIYA TEKHNOLOGICHESKIKH PROTSESSOV PROIZVODSTVA I PRIMENIYU YADERNO-FIZICHESKIKH METODOV ANALIZA SOSTAVA VESHCHESTVA, POL'SHA-POZNAN', 12-15. XI. 1968g. (Symposium on Technological and Industrial Uses of Labeled Atoms and Applications of Nuclear-Physics Methods for Analysis of Materials, Poznan, Poland, November 12-15, 1968. Warszawa; Osrodek Informacji o Energii Jadrowej (1969). 477p. (CONF-681137).

Thirty-two papers are included on industrial uses of labeled atoms and on radiometric analysis. The methods for wear control of ship engine piston rings, analysis of coal product mixtures, corrosion studies on steel parts, studies on welding processes, determination of the effects of microquantities of wear products in a large volume of oil, determination of the final groups of polyethylene terephthalate, studies of cyclohexanol dehydration to cyclohexanone in the presence of phenol, boiler tube wear control, and control of various operations in metallurgy and metals technology and fabrication are discussed in the first chapter. Methods for neutron activation analysis using a 14-MeV neutron generator, rapid analysis of barium by beta backscattering methods, techniques of a neutron absorption method for determining fluoride content in fluoride salts and aluminum bath electrolytes, neutron activation analysis for determining Au, Pt, Mo, In, Se, F, and other elements in solutions, x-radiometric methods and apparatuses, and γ-activation methods for the determination of elements in various materials are covered in the second chapter. (R.V.J.)

2142 DETERMINATION OF CHLORINE AND VANADIUM IN GRAPHITE BY THE ACTIVATION METHOD. Frolov, V. V. Zavod. Lab.; 36: 807-9(1970). (In Russian).

An activation method using thermal neutrons is described for determining chlorine and other impurities in graphite using gamma spectrometry and a critical graphite-uranium assembly with a neutron beam of $10^8 n/cm^2 sec$. The sensitivity of the method is $\sim 5 \times 10^{-5}$ wt % Cl in the presence of $<10^{-4}$ % Mn and $<10^{-3}$ % Na. The sensitivity of the vanadium determination is 10^{-7} wt %. (tr-auth)

2143 DETERMINATION OF OXYGEN IN SILICON IN THE SUB-PART-PER-MILLION RANGE BY CHARGED-PARTICLE ACTIVATION ANALYSIS. Schweikert, Emile A.; Rook, Harry L. (Texas A and M Univ., College Station). Anal. Chem.; 42: 1525-7(Nov 1970).

Results for the determination of trace amounts of oxygen in silicon by charged particle activation analysis are presented. A nondestructive analytical method using proton, helium-3, and helium-4 activation was developed and applied on a number of silicon samples with oxygen concentrations ranging from 20 to ~0.01 ppM. Case studies, which included repeated analyses on each sample, allowed an evaluation of experimental detection limits and systematic errors for the individual nuclear reactions. The accuracy of the method was evaluated in the 1- to 10-ppM range by comparing the charged particle activation results with those obtained by infrared spectrometry. For oxygen concentrations below 0.5 ppM, repeated nondestructive determinations were carried out using different activating particles. The agreement between the results obtained shows that accurate oxygen determinations can be obtained at the sub-ppM level. (auth)

2144 NEUTRON RADIATIVE CAPTURE METHODS FOR SURFACE ELEMENTAL ANALYSIS. Trombka, J. I. (Goddard Space Flight Center, Greenbelt, Md.); Senftle, F.; Schmadebeck, R. Nucl. Instrum. Methods; 87: 37-43(1970).

Both an accelerator and a ^{252}Cf neutron source have been used to induce characteristic gamma radiation from extended soil samples. To demonstrate the method, measurements of the neutron-induced radiative capture and activation gamma rays have been made with both Ge(Li) and NaI(Tl) detectors. Because of the possible application to space flight geochemical analysis, it is believed that NaI(Tl) detectors must be used. Analytical procedures have been developed to obtain both qualitative and semiquantitative results from an interpretation of the measured NaI(Tl) pulse-height spectrum. Experiment results and the analytic procedure are presented. (auth)

2145 ACTIVATION ANALYSIS FOR DETERMINING THE CONTENT OF Ta AND Cs IN ROCKS. Lobanov, E. M.; Nurmatov, D. (Inst. of Nuclear Physics, Tashkent). Dokl. Akad. Nauk Uzb. SSR; No. 3, 17-19(1970). (In Russian).

A simplified nondestructive method for the determination of Ta and Cs in rock was developed. The specimens were crushed into powder, sealed in polyethylene tubes, irradiated for one to 4 hr, and cooled for one to 3 weeks. The drop in specimen activation using soft radiation (0.068 MeV) and hard radiation (0.5 to 1.6 MeV) in the γ spectra was measured in a single-crystal γ spectrometer with a 100-channel amplitude pulse analyzer. Data on the contents of Cs and Ta in the rocks are tabulated. (R.V.J.)

2146 SAMPLE PREPARATION FOR NEUTRON ACTIVATION ANALYSIS. DEPOSITION OF MERCURY ON A PLASTIC MATRIX. Montalvo, Joseph G. Jr.; Thibodeaux, Devron P.; Klein, Elias (Gulf South Research Inst., New Orleans). Anal. Chim. Acta; 52: 160-3(Oct 1970).

A technique is presented for concentrating non-volatile activities in liquid samples before neutron activation assay. The technique allows total recovery of non-volatile activities by recovery on a plastic medium; the efficiency of recovery of mercury(II) compounds such as the nitrate, oxide, and dithizonate, is demonstrated. (D.H.M.)

2147 STUDIES OF THE CARBON CONTENT OF STEEL AND ITS DEPTH DISTRIBUTION BY MEANS OF PROTON ACTIVATION ANALYSIS. Brune, D.; Hellborg, R. (Aktiebolaget Atomenergi, Studsvik, Sweden). Anal. Chim. Acta; 52: 109-14(Oct 1970).

The carbon content and depth distribution close to the surface in steel samples at the 0.1 to 1% level were studied, by means of proton activation in the energy range 1 to 4.5 MeV. A Van de Graaff accelerator was used, initiating the nuclear reaction $^{12}C(p,\gamma)^{13}N$ which possesses two resonances at the energies of 0.46 and 1.70 MeV. The technique is of interest in connection with carbonization of iron products. (auth)

2148 DETERMINATION OF ZIRCONIUM AND HAFNIUM IN METEORITES AND TERRESTRIAL MATERIALS BY ACTIVATION ANALYSIS. Rebagay, Teofila Velasco. Lexington, Ky.; Univ. of Kentucky (1969). 185p. University Microfilms Order No. 70-12,370.

Thesis.

A sensitive analytical technique to measure the zirconium and hafnium concentrations simultaneously in the same specimen was developed to establish abundance distribution patterns of these elements in natural materials. The procedure involved a radiochemical separation of zirconium and hafnium following neutron irradiation of the specimens. The specimens were irradiated for 7 to 10 days in a reactor core to enhance the longer-lived activities of zirconium and hafnium radioisotopes in them. A preliminary separation of zirconium and hafnium from the bulk materials, which required no individual separation of these elements from each other, was achieved through ion exchange on a strongly basic anion exchange resin. The determination of zirconium and hafnium abundance was based on the use of a lithium-drifted germanium detector for high resolution spectrometry of the induced gamma activities of these elements. Intensities of the 724-keV gamma branch from the 65-day ^{95}Zr used as zirconium indicator and the 480-keV gamma ray from the 42.5-day ^{181}Hf used as hafnium indicator measured in the specimens and standards of zirconium and hafnium irradiated in the same run were compared. An automated fast neutron activation analysis system was employed for the rapid and nondestructive determination of the chemical yield of the zirconium oxide (ZrO_2) used as carrier for both elements which was added to the specimen prior to wet chemistry. The chemical yields determined this way were in good agreement with those found using spectrophotometric methods. A total of 163 analyses for both zirconium and hafnium in natural materials were conducted. Included were the analyses of 27 chondrites, 7 achondrites, 1 troilite phase of an iron meteorite, 1 olivine phase of a stony-iron meteorite, 2 tektites, 1 eclogite, 1 oceanic basalt, and 9 standard silicate rocks. The distribution pattern of zirconium and hafnium in the three major classes of chondrites showed that the order of atomic abundances of these elements ($Si = 10^6$) was: carbonaceous chondrites > ordinary chondrites > enstatite chondrites. An average atomic abundance of 13 atoms Zr ($Si = 10^6$) and 0.19 atom Hf ($Si = 10^6$) were established for these chondritic meteorites. The calcium-rich achondrites were observed to be enriched in zirconium and hafnium relative to the chondrites while an opposite trend was noted for the calcium-poor achondrites. The average Zr/Hf ratio on a weight basis for all the stony meteorites analyzed in this work was 43, a value which is in good agreement with that reported in the literature for the earth's crust. Based on this ratio, no significant fractionation of these elements between the earth and meteorites was implied. The data on the zirconium and hafnium abundances in the selected meteoritic phases, namely, the troilite and olivine phases of an iron and stony-iron meteorite respectively, indicated that these phases were not the sites of concentration of these elements. The tektites analyzed have Zr/Hf ratios resembling sandstones. The basalt from the Mid-Atlantic Ridge resembled closely the calcium-rich achondrites. The eclogite from the Roberts Victor Mine indicated a composition closer to ultramafic than to basaltic, a characteris-

tic of the primitive material of the upper mantle suggested by a current model of the upper mantle of the earth. The data gathered for the meteorites formed a basis for a discussion of current theories of meteorite formation and nucleosynthesis of heavy elements. (Diss. Abstr. Int., B)

2149 SOME ASPECTS OF NEUTRON-ACTIVATION ANALYSIS OF SILICATE ROCKS. Vandergraaf, Tjalle Thys. University Park, Pa.; Pennsylvania State Univ. (1969). 163p. University Microfilms Order No. 70-13,897.

Thesis.

The complexity of gamma spectra obtained from irradiated silicates and other geological and extraterrestrial materials by a scintillation detector precludes the qualitative and quantitative determination of all but a few elements. Although the increased resolution of solid state detectors has reduced this problem to some extent, the inferior sensitivity of these detectors has by no means made the scintillation detector obsolete. Because of the complexity of gamma spectra, chemical separations are necessary in most cases. The number of separation steps can be reduced, however, if group separations are made. In order to bring the silicates into solution, the irradiated silicate samples are fused with lithium metaborate in graphite crucibles. Since little is known about the process that takes place during the fusion step, about the losses that occur during fusion, or about any interference of the fusion product on chemical separations, these three areas were investigated. Titrations were performed on the fusion mixture, and a structure is proposed for the boron–silicon product that was thought to be formed. The loss of elements during fusion and the effects of the fusion product on chemical separations were studied with the use of radioactive tracers. The results showed that practically all elements in the periodic table to the right of the copper–silver–gold group experienced some loss, but that there was no noticeable effect of the fusion product on precipitations in the pH range from 1 to 6 on ion exchange separations, or on extractions. A computer program was developed to eliminate from consideration the interference caused by some elements of relatively low abundance in geological materials or elements which have unfavorable nuclear properties. The computer program is then used in conjunction with the fusion process to eliminate a number of elements and thus to effect a separation. In order to solve the problem of adding flux monitors to gauge the neutron flux to which the standards and samples are exposed, intrinsic flux monitors were used. These flux monitors were in effect the matrix of the sample itself or an element in the sample that is readily activated and whose abundance in the sample was well known. This method, involving the intrinsic flux monitors, was used to determine manganese in five silicate rock samples, and the results were compared to the values obtained by more conventional methods. It was found that the values are sufficiently close and that the intrinsic flux monitor method can be used. Using a rapid chemical separation step to remove the transition metals from the bulk of the sample, and using optimum irradiation and decay times, copper was determined in five silicate samples, and, with an additional chemical separation step, lanthanum was also determined. The values obtained for these two trace elements were well within the range found for these elements in the literature, and show the validity of this approach. (Diss. Abstr.)

2150 PHOTON-ACTIVATION ANALYSIS FOR IODINE BY USING CESIUM AS THE INTERNAL-REFERENCE ELEMENT. Tsai, Hui-tuh; Kato, Toyoaki; Oka, Yoshinaga (Tohoku Univ. Sendai). Bull. Chem. Soc. Jap.; 43: 2482-6(Aug 1970).

The internal-reference method proposed previously has been applied to the determination of iodine by photonactivation analysis, using cesium as the internal-reference element. The present method is based on the measurement of the ^{126}I, ^{124}I, and ^{123}I activities produced by the neutron-emitting reactions in iodine, and on the comparison of these activities with that of ^{130}I coming from cesium by the $(\gamma,2pn)$ reaction. A lithium-drifted germanium diode with a sensitive volume of 36 cm^3 was used as the detector. The yields of various photonuclear reactions in both elements have also been examined as a function of the bremsstrahlung maximum energies up to 65 MeV. A series of synthetic mixtures of iodine–cesium with known weight ratios has been used to check the sensitivity and the accuracy of this method. It was found that amounts of iodine down to 0.2 μg under the present experimental conditions could be determined. (auth)

Inorganic, Organic, and Physical Chemistry

Chemical Properties

Refer also to abstracts 2710, 2711, 2775, 2781, and 2782.

2151 (DP-Report-569) THE PYROLYSIS OF METHANE IN A BED OF PARTICLES. Project DRAGON. Voice, Eric (Atomic Energy Establishment, Winfrith (England)). May 1967. 31p. Dep. NTIS.

From a simple observation the mode of gas flow in a fluidized-bed fuel-particle coating furnace is deduced. The probable course of methane pyrolysis and carbon deposition is then developed, and related to the nature of the product. (auth)

2152 (ORNL-4572–, pp 231-5) SPECTROPHOTOMETRIC STUDIES OF SOLUTIONS OF LANTHANIDES AND ACTINIDES. (Oak Ridge National Lab., Tenn.).

Spectrophotometric techniques are being developed to study the chemical properties of aqueous solutions, especially in comparisons of the lanthanide or actinide elements. Spectra of H_2O and D_2O were studied. The spectra of ^{34}Am were also investigated. (M.C.G.)

2153 DISSOLUTION OF PLUTONIUM IN DILUTE NITRIC ACID. Miner, F. J.; Nairn, J. H.; Berry, J. W. (Dow Chemical Co., Golden, Colo.). Ind. Eng. Chem., Prod. Res. Develop.; 8: 402-5(Dec 1969). (RFP-1070).

Rates of dissolution were determined for plutonium metal as a function of nitric acid concentration, hydrofluoric acid concentration, and temperature. The interactions of these parameters were determined, as well as the conditions that produced the maximum relative rate of dissolution. The maximum rate of dissolution occurred at approximately 3M nitric acid, a hydrofluoric acid concentration of 0.13M (the highest investigated), and any temperature between 26 and 67°C (the range investigated). The effects of temperature over this range were insignificant compared to the other two parameters investigated. The mechanism of the dissolution reaction is uncertain. (auth)

2154 DECOMPOSITION OF BROWN PEROXY COMPLEX OF PLUTONIUM(IV) IN PERCHLORIC ACID. Ghosh Mazumdar, A. S.; Natarajan, P. R.; Vaidyanathan, S. (Bhabha Atomic Research Centre, Bombay). J. Inorg. Nucl. Chem.; 32: 3363-7(Oct 1970).

A study of the formation and decomposition of the brown peroxy complex of plutonium(IV) in perchloric acid was carried out. The complex decomposes to give plutonium(III) following a first-order rate law. The rate constant for the decomposition was determined as a function of acidity and ionic strength of the medium, and a mechanism for the decomposition is proposed. The Arrhenius activation energy for the decomposition was also estimated. (auth) (UK)

2155 OXIDATION OF NEPTUNIUM(III) BY OXYGEN AND HYDROGEN PEROXIDE. Burgener, C. S.; Sullivan, J. C. (Argonne National Lab., Ill.). Inorg. Chem.; 9: 2604-5(Nov 1970).

The major product of the oxidation of Np(III) by oxygen in acidic perchlorate media was Np(IV). Production of Np(V) did not appear to be dependent on hydrogen ion concentration. Equilibrium constants were calculated from spectrophotometric measurements. The percentage of Np(V) formed in the oxidation of Np(III) by hydrogen peroxide in acidic perchlorate media is not directly proportional to increased ratio of peroxide to initial concentrations of Np(III) and Np(IV), nor is it dependent upon the mole fraction of Np(IV) originally present. Possible mechanisms of the reactions are discussed. (J.G.B.)

2156 SYSTEMS XENON HEXAFLUORIDE–TANTALUM PENTAFLUORIDE, XENON HEXAFLUORIDE–MANGANESE FLUORIDE, XENON HEXAFLUORIDE–URANIUM HEXAFLUORIDE. Aubert, Jacques; Cady, George H. (Univ. of Washington, Seattle). Inorg. Chem.; 9: 2600-2(Nov 1970).

$NXeF_6$ reacted readily at 60°C with TaF_5 to yield $2XeF_6 \cdot TaF_6$, which decomposed under vacuum at 20° to give XeF_6 and $XeF_6 \cdot TaF_5$. X-ray powder patterns were obtained. A compound which appears to be either $4XeF_6 \cdot MnF_4$ or $4XeF_6 \cdot MnF_3$ was formed when Mn was heated with Xe and F_2. The reactants Mn, XeF_6, and F_2 may also be used. No evidence for combination was found when UF_6 and XeF_6 were mixed and held together at 70 or 100°C. (J.G.B.)

2157 THORIUM(IV) ADDUCTS OF 8-QUINOLINOL AND DERIVATIVES. Abraham, John; Corsini, Alfio (McMaster Univ., Hamilton, Ont.). Anal. Chem.; 42: 1528-31(Nov 1970).

The structural nature of the thorium(IV) adduct of 8-quinolinol was investigated by [^{14}C]-8-quinolinol tracer and infrared techniques. It is concluded that the additional 8-quinolinol molecule in $Th(C_9H_6NO)_4 \cdot C_9H_7NO$ is not a weakly held lattice component but is coordinated to the thorium ion as a zwitterion through the phenolate oxygen. Adducts of several derivatives of 8-quinolinol were prepared. Substitution of appropriate substituents in the 2-

XUM

or 7-positions results in the formation of the normal tetrakis compounds. (auth)

2158 PHOTOCHEMICAL REACTIONS OF URANYL IONS WITH ORGANIC COMPOUNDS. II. THE MECHANISM OF THE PHOTO-OXIDATION OF ALCOHOLS BY URANYL IONS. Sakuraba, Shukichi; Matsushima, Ryoka (Shizuoka Univ., Hamamatsu, Japan). Bull. Chem. Soc. Jap.; 43: 2359-63(Aug 1970).

Quantum yields were measured under various conditions for the photooxidation of aliphatic alcohols by uranyl ions in aqueous solutions and kinetic treatments were made. The measurements of uranyl fluorescence quenching by the alcohols showed that a complex formation between uranyl ions and alcohol molecules prior to the photolysis is not likely to be involved. A temperature effect on the quantum yield was strong evidence for a collisional energy transfer from the excited uranyl ions to the alcohol molecules. The relative rates of the photolysis of four isomeric butyl alcohols, and the isotope effect on the photoreactivity by using alcohols labeled with deuterium, showed that the alcohol molecules are attacked on the α-hydrogen atom as a primary photochemical act. (auth)

2159 ACTINIUM POLAROGRAPHY. David, Francois (Paris Univ., Orsay, France). Compt. Rend., Ser. C; 271: 440-2(17 Aug 1970). (In French).

Radiochemical polarography was applied to actinium (^{228}Ac) in perchloric medium with pH between 1.9 and 3.1. The polarograms indicate two waves. The first is due to the reaction $M^{2+} \rightarrow M^0$; the second is probably due to the process $M^{3+} \rightarrow M^0$. This method reveals directly the formation of Ac(II). The values of the half-wave potentials are constant between pH 2.5 and 3.1. The potential of the couple Ac^{3+}/Ac^{2+} was calculated. (France)

2160 PLATINUM AND THE REFRACTORY OXIDES. III. CONSTITUTIONAL RELATIONSHIPS IN THE ALLOYS FORMED. Darling, A. S.; Selman, G. L.; Rushforth, R. Platinum Metals Rev.; 14: 124-30(Oct 1970).

Platinum reacts exothermically with aluminum, zirconium, and thorium, but is very reluctant to alloy with magnesium. It dissolves 2.2 wt % aluminum at 1500°C and 10 wt % zirconium at 1650°C. These wide solid solutions are in equilibrium with very stable intermetallic compounds, thus accounting for the severe reactions that can occur when platinum is heated in contact with alumina and zirconia. Zirconium reacts peritectically with platinum. (auth) (UK)

Isotope Effects and Exchange

2161 MATHEMATICAL ANALYSIS OF ISOTOPE EXCHANGE REACTIONS. Corio, P. L. (Mobil Research and Development Corp., Princeton, N. J.). J. Phys. Chem.; 74: 3853-60(29 Oct 1970).

A mathematical analysis of rate equations for the single-step redistribution of hydrogen and deuterium atoms among the deuterium isomers of a parent molecule containing N chemically equivalent exchangeable hydrogen atoms is presented. Assuming complete degeneracy in the specific rate constants for all exchanges, the explicit solution of the rate equations was obtained for arbitrary N in terms of a system of orthogonal polynomials. The properties of these polynomials were used to deduce important properties of the redistribution kinetics. In particular, their orthogonality may be used to transform experimental data to a representation in which the exponential decays are uncoupled. The application of the uncoupled representation to the analysis of experimental data was illustrated for the exchange among the deuterioethylenes on nickel wire, and the exchange among the deuteriobenzenes over a rare earth-exchanged zeolite. The rate equations were also solved for the case where all hydrogenations are described by the specific rate constant k_H and all deuterations by the specific rate constant k_D. The isomer distributions obtained in this circumstance are formally identical with those obtained in the absence of an isotope effect. The observed rate constant is equal to an atom fraction weighted average of the rate constants for hydrogenation and deuteration. The ratio k_H/k_D can, in principle, be determined from the observed equilibrium distribution. The analysis is strictly applicable to homogeneous reactions, but it is also applicable to heterogeneous catalytic systems for which the contact time between molecules and catalyst is long enough to ensure the establishment of isotopic equilibrium in reasonable time periods, but short enough to preclude the necessity for considering diffusion and multistep kinetics. (auth)

2162 ENTHALPIES OF ALKYLAMMONIUM IONS IN WATER, HEAVY WATER, PROPYLENE CARBONATE, AND DIMETHYL SULFOXIDE. Krishnan, C. V.; Friedman, Harold L. (State Univ. of New York, Stony Brook). J. Phys. Chem.; 74: 3900-7(29 Oct 1970).

The enthalpies of solution at infinite dilution of alkylammonium salts were measured in several solvents. Salts of R_3NH^+, $R_2NH_2^+$, RNH_3^+, and NH_4^+ were studied, with R a normal alkyl chain ranging from methyl to amyl and, in some cases, to octyl. The regularities previously reported for the behavior of alkyl chains in aprotic solvents (J. Phys. Chem., 73, 1572, 3934 (1969)) were also found in the enthalpies of transfer to PC (propylene carbonate) from DMSO. In addition, evidence was found for the strong mutual interference of the N–H . . . O hydrogen bonds involving a single nitrogen. For example, the enthalpy of transfer to PC from DMSO, after extrapolating to zero length of the R chains, was 1.64 kcal/mol for R_3NH^+ and 1.16 kcal/mol for $\frac{1}{3}RNH_3^+$. The enthalpies of transfer of the alkylammonium ions to DMSO from H_2O showed a relatively complex dependence on the length and number of R chains. This was interpreted in terms of two effects in the aqueous solutions: interference of the R chains with the N–H . . . O hydrogen bonds and mutual interference of the N–H . . . O hydrogen bonds. The latter effect was so great that the enthalpy of NH_4^+ was 5 kcal/mol higher in water than in PC. The enthalpies of transfer of RNH_3^+ to D_2O from H_2O, when analyzed as in the earlier studies of ROH and R_4N^+ solutions, tended to confirm the estimate that the structural or hydrophobic effect of alkyl groups in aqueous media is 5% larger in D_2O than in H_2O. The previously reported saturation of the structural effect was not found. (auth)

2163 PYRIDINE-N-OXIDE: VIBRATIONAL ASSIGNMENT AND THERMODYNAMIC QUANTITIES. Varsanyi, Gy.; Szoke, S.; Keresztury, G.; Gelleri, A. (Central Research Inst. for Chemistry, Budapest). Acta Chim. Acad. Sci. Hung.; 65: 73-80 (1970).

The infrared spectra of pyridine-N-oxide (indexed as pyridine-1-oxide) and of mixtures of the 2,6-dideutero- and 2,4,6-trideutero derivatives were recorded. Using Wilson's notation for benzene, the assignments of the vibrational spectra of the above molecules were made and checked against the Redlich–Teller product rule. On the basis of the molecular geometry and spectroscopic data of pyridine-N-oxide, some of its thermodynamic functions were calculated. (auth)

2164 BENZENE–DEUTEROXYL EXCHANGE OVER DEUTERATED γ-ALUMINA. DeRosset, A. J.; Padrta, F. G. (Universal Oil Products Co., Des Plaines, Ill.). J. Catal.; 19: 49-54 (Oct 1970).

The exchange reaction between benzene and a large excess of deuteroxyl on deuterated γ-alumina was investigated as a possible test reaction for evaluating the Lewis acid sites on the alumina surface. The kinetics were first order in adsorbed benzene, but approached zero order in total benzene when tested in the saturation portion of the adsorption isotherm. Preferential retention of deuterium on the alumina is attributed to an equilibrium isotope effect. This is consistent with related equilibria. The rate of the exchange was very sensitive to minor changes in the pretreatment technique probably because of the resulting small variations in surface structure and catalytic activity. This complicates use of the reaction as a probe for surface Lewis acidity. (auth)

2165 NEAR-INFRARED SPECTRA OF WATER AND HEAVY WATER AT TEMPERATURES BETWEEN 25 AND 390°. Bell, J. T.; Krohn, N. A. (Oak Ridge National Lab., Tenn.). J. Phys. Chem.; 74: 4006-7(29 Oct 1970).

The near-infrared region of the H_2O and D_2O spectra was examined at temperatures between 25 and 390°C. Changes in the transition energies and intensities of the water absorption bands were found to be linear functions of the molar concentration of water over the range 55 to 4M. (M.C.G.)

2166 INFLUENCE OF DEUTERONS ON PROTON RELAXATION TIMES IN PARAMAGNETIC SOLUTIONS. Padmavathi, G. (Andhra Univ., Waltair, India). Indian J. Pure Appl. Phys.; 6: 216-18(1968).

The influence of deuterons on proton relaxation times was studied by measurements on proton relaxation times in aqueous solutions of paramagnetic ions (1) when D_2O replaces H_2O in varying amounts and (2) in (H_2O + D_2O) mixtures of varying relative concentrations. The paramagnetic ions studied are Mn^{2+} with ^6S ground state and Ni^{2+} and Ce^{3+} with F ground states. It is observed that: (1) there is always an increase in proton relaxation time when D_2O replaces H_2O; (2) in all the three cases this increase is larger as the percentage of D_2O is increased; and (3) the relative increase is very much larger in the case of Ce^{3+} and Ni^{2+} ion solutions than in the case of Mn^{2+} ion solution. This large increase in relaxation where D_2O concentration is increased is accounted for as due to the proton exchange across hydrogen bond. The larger relative increase in the case of Ce^{3+} and Ni^{2+} ions than

that in Mn^{2+} ion may arise from the difference in the ground states of these ions. (auth)

2167 RELATIONS BETWEEN GAS CHROMATOGRAPHIC BEHAVIOR AND CHEMICAL STRUCTURE. III. THE NATURE OF INTERNAL ROTATION IN METHYL DERIVATIVES OF BENZENE. Kwa, T. L.; Boelhouwer, C. (Univ. of Amsterdam). J. Chromatogr., 52: 21-9(7 Oct 1970).

The absence of a large isotope effect in the gas chromatographic behavior of methyl derivatives of benzene indicates that the methyl rotation is not free in the investigated model compounds, but corresponds to rotation–oscillation. An incremental value in log a is found whenever one methyl group is in the ortho position with respect to another. Additional absorption bands, which are the expected overtones of methyl nonsymmetric deformations in the infrared spectra of such compounds, suggest that this "ortho-shift" effect in gas chromatography is due to perturbation of the methyl rotation–oscillation. It is suggested that the "ortho-shift" effect in gas chromatography may be exploited as an additional or a complementary technique in the investigation of configuration and conformation of isomers in organic chemistry. (auth)

2168 DEUTERIUM ISOTOPE EFFECTS IN ENZYMATIC TRANSAMINATION. Fang, Sen-maw; Rhodes, Harold J.; Blake, Martin I. (Univ. of Illinois, Chicago). Biochim. Biophys. Acta; 212: 281-7(Aug 1970).

The ionic fraction from the hydrolysate of residual cell walls of Scenedesmus obliquus grown in a medium containing 99.6% ^2H_2O was subjected to ion-exchange chromatography for the fractionation of fully deuterated L-glutamic acid. L-[2-^{2}H]-glutamic acid and L-[3,3,4,4-$^2H_4$] glutamic acid were synthesized from L-glutamic acid and L-[2,3,3,4,4-$^2H_5$] glutamic acid, respectively. A kinetic study of enzymatic transamination was conducted using the four L-glutamic acid analogs (L-glutamic acid and three deuterated analogs) as the substrates. The rate of transamination was followed by photometric measurements at 280 mμ. Maximum velocity determinations, based on the binary mechanism of the enzymatic transamination, were performed on each of the L-glutamic acid analogs. The deuterium isotope effect reflected in the rate of transamination was estimated through maximum velocity analysis. The compound with deuterium in the α-position showed an isotope effect of 1.85. A similar isotope effect was observed for the compound with deuterium in the α-, β-, and γ-carbons. The data indicate that the bond to the α-carbon and not to the β-carbon is ruptured during transamination. It is clearly demonstrated, therefore, that an α-elimination mechanism is involved in the enzymatic transamination. (auth)

2169 STUDY BY TRIPLE LABELING OF REACTIONS BETWEEN TETRAPHENYLSTIBONIUM AND ANTIMONY TRICHLORIDE. Aulagnier, D.; Chemette, H.; Martelet, C.; Tousset, J. (Institut de Physique Nucleaire, Lyon). Radiochem. Radioanal. Lett.; 5: 63-8(16 Oct 1970). (In French).

In some organic media antimony trichloride and tetraphenylstibonium hydroxide react giving a product for which the following structure is proposed: $(\Phi_4Sb-Sb_n)(OH, Cl)_{3n+1}$. The ultimate step is a compound that shows promise for fluorine extraction. (auth)

2170 INTERACTION OF TRANSITION METAL HYDRIDE COMPLEXES WITH DEUTERIUM, ETHYLENE-d_4, AND 1-BUTENE. Schunn, R. A. (E. I. du Pont de Nemours and Co., Wilmington, Del.). Inorg. Chem.; 9: 2567-72(Nov 1970).

The reactions of a series of transition metal hydride complexes with D_2, C_2D_4, and 1-butene were studied by mass spectroscopic and gas chromatographic techniques. Exchange of D_2 and C_2D_4 with the metal–hydrogen bond was observed and the degree of exchange varied with the nature of the complex. The activity of the complexes in the isomerization of 1-butene generally paralleled the activity toward exchange with C_2D_4 except in the cases of $[(C_6H_5)_2PCH_2CH_2P(C_6H_5)_2]_2RhH$ and $[(C_6H_5)_3P]_3Ir(CO)H$. Ligand–metal hydrogen transfer was observed in the D_2 and C_2D_4 exchange studies of $[(C_6H_5O)_3P]_4CoH$, $[(C_6H_5O)_3P]_3Co(CO)H$, $[(C_6H_5)_3P]_3Co(N_2)H$, $[(C_6H_5)_3P]_3RuHCl(CO)$, and $[(C_6H_5)_3P]_3RuHCl \cdot C_6H_5CH_3$. The synthesis and properties of the new metal–hydride complexes $[(CH_3)_2PCH_2CH_2P(CH_3)_2]_2CoH$, $[(C_6H_5O)_3P]_3Co(CO)H$, and $[(C_6H_5)_2PCH_2CH_2P(C_6H_5)_2]_2IrH$ are described. (auth)

2171 APPROXIMATE METHODS FOR DETERMINING THE STRUCTURE OF H_2O AND HOD USING NEAR-INFRARED SPECTROSCOPY. Luck, W. A. P.; Ditter, W. (Badische Anilin- and Soda-Fabrik AG, Ludwigshafen, Ger.). J. Phys. Chem.; 74: 3687-95(15 Oct 1970).

Approximate methods are described for determining the H-bonded state of liquid water to the critical region. It is shown that differences between spectra of solutions, and liquids in the bulk, indicate H bonds having different angles and distances. Spectra from water in solution in HF and NH_3 and in the gas-hydrate state are also presented. (auth)

2172 PREPARATION AND ACETOLYSIS OF 5-DEUTERIATED EXO-NORBORNYL BROSYLATES. Werstiuk, N. H.; MacDonald, R. R.; Ouwehand, R. W.; (and others) (McMaster Univ., Hamilton, Ont.). Tetrahedron Lett.; No. 49, 4363-6(Oct 1970).

The exo-norbornyl-5-d- and exo-norbornyl-5,5-d_2-brosylates were prepared and solvolyzed to check for nonbonded effects due to deuterium and stabilization of the norbornonium ion via hyperconjugation to the C-5 hydrogens. For calibration exo-norbornyl-6-endo-d-brosylate was also prepared and solvolyzed. Results indicate that hyperconjugation to the C-5 protons is not important in the solvolyses of 2-X-norbornyl systems and provide the first experimental evidence that hydrogen (deuteron) shifts followed by internal return to brosylate contribute negligibly to the isotope effects. A general route to previously unknown norbornyl-5-d systems and an alternative more direct route to exo-norborneol-6-endo-d are also shown. (UK)

2173 EQUILIBRIA AND PROTON TRANSFER IN THE BISULFATE–SULFATE SYSTEM. Irish, D. E.; Chen, H. (Univ. of Waterloo, Ont.). J. Phys. Chem.; 74: 3796-3801(15 Oct 1970).

Relative integrated Raman intensities were obtained from NH_4HSO_4, $KHSO_4$, and $(NH_4)_2SO_4$–HCl aqueous solutions and $KDSO_4-D_2O$ solutions. The apparent concentration quotient, Q_v, and the degree of dissociation, α, were computed at each concentration. The broadening of the 981-cm^{-1} Raman line of sulfate is directly proportional to the hydronium ion concentration. This dependence is linked to the proton transfer occurring in these systems. An overall second-order rate constant of 5.5×10^{11} sec^{-1} is implied. The spectra and the kinetics are rationalized in terms of the existence of ion pairs. (auth)

2174 EFFECT OF HYDROGEN–DEUTERIUM SUBSTITUTION ON THE ASSOCIATION OF N-METHYLACETAMIDE. Loewenstein, Henning; Lassen, Hans; Hvidt, Aase (Univ. of Copenhagen). Acta Chem. Scand.; 24: 1687-96(1970).

The self-association of N-methylacetamide (NMA-H) and of deuterated N-methylacetamide (NMA-D) dissolved in carbon tetrachloride was measured by infrared spectroscopy at three different temperatures. Assuming that the amides form chain aggregates through hydrogen bonding, values of the dimerization equilibrium constant, K_0, and of the equilibrium constant, K, for the formation of higher aggregates, were calculated. The values of K for NMA-D, ranging from 19 l $mole^{-1}$ at 50°C to 32 l $mole^{-1}$ at 25°C, were found to be 10 to 20% smaller than the corresponding values for NMA-H. This result was ascribed to a difference of 0.5 kcal $mole^{-1}$ in ΔH° for the association reaction. The experiments do not permit any quantitative estimate of the isotope effect on K_0; but since it was observed that the transition from free to associated amide with increasing concentration is steeper for NMA-H than for NMA-D, it was concluded that the ratio K_0/K is smaller for NMA-H than it is for NMA-D. (auth) (Denmark)

2175 D_0 ACIDITY FUNCTION IN DEUTERIUM SULPHATE SOLUTIONS AT 25°C. Sierra, J. (Univ. de Chile, Santiago); Ojeda, M.; Wyatt, P. A. H. J. Chem. Soc., B; No. 8, 1570-3 (1970).

The D_0 scale for $D_2SO_4-D_2O$ solutions is extended, with a special technique in which additions are made to the same spectrophotometric cell to increase the precision of the measurements, and pK_{BD^+} values are recorded for the Jorgenson and Harrter series of nitroaniline bases. Though D_0 is slightly more negative than the corresponding H_0 up to over 90% (w/w) of the acid when the comparison is made on a simple % (w/w) basis, the scales become virtually identical up to 90% when allowance is made for the different molecular weights. Small differences do however appear in the 90 to 100% region. (auth) (UK)

2176 EVIDENCE FOR PROTON TRANSFER CONCOMITANT WITH HYDRIDE EXPULSION FROM SILANES. Schowen, R. L.; Bacon, R. (Univ. of Kansas, Lawrence). Tetrahedron Lett.; No. 48, 4177-80(Oct 1970).

Measurements of second order rate constants, k_2^n, for methoxide-catalyzed methanolysis of triphenylsilane in mixtures of CH_3OH and CH_3OD (subsequently referred to as CH_3OL) are tabulated for values of n, the atom fraction of D in CH_3OL. A plot of k_2^n vs n is given. The plot shows that the reaction rate is reduced by adding deuterium and its non-linearity excludes the possibility that the normal isotope effect arises from a single proton transfer. A non-unique model of the mechanism involved is given which accounts for the measured data. It is concluded that the expulsion of free hydride ion does not occur along the main reaction pathway for basic methanolysis of silanes and that proton transfer from solvent is occurring in the transition state. (UK)

XUM

2177 RATE CONSTANTS OF EXCHANGE REACTION OF THE TYPE RI + $I^{*-} \rightleftharpoons RI^{*} + I^{-}$ IN ACETONE–WATER SOLUTION. Yamamoto, Jiro (Tottori Univ., Japan); Miyagawa, Masayoshi. Tottori Daigaku Kyoikugakubu Kenkyu Hokoku, Shizenkagaku; 20: No. 2, 45-50(Dec 1969). (In Japanese).

A study was made to determine the rate constants of the exchange reaction between alkyl iodides and iodide ion in acetone–water solution, using ^{131}I as an indicator. The following results were obtained: the rate constants decrease with the increasing carbon atoms of alkyl iodides; the rate constants of straight-chain alkyl iodides are about 50 times as large as those of the branched-chain homologs; as water in acetone–water system is increased, the rate constants fall, which indicates hydration of iodine ion; and temperature effects are observed in exchange reaction of alkyl iodides. On the basis of these data, it was found that activation energy of iodide isotopic exchange reaction is 23.6 kcal/mole in 90% acetone–10% water solution. (auth) (Japan)

2178 ISOTOPE EFFECT AND DIFFUSIVITY MEASUREMENTS IN EQUI-ATOMIC IRON–COBALT ALLOYS. Fishman, Steven Gerald. Urbana, Ill.; Univ. of Illinois (1969). 50p. University Microfilms Order No. 70-13,308.

Thesis.

Several radioactive isotopes of Fe and Co were simultaneously diffused into equi-atomic Fe–Co alloy which exhibits fcc, bcc, and CsCl-type ordered phases with decreasing temperature. Penetration profiles were obtained by standard lathe sectioning and a submicron sectioning technique described in this paper. From ln D vs 1/T plots, activation energies of 68.5 kcal and 55 kcal and frequency factors of 1.26 cm^2/sec and 0.25 cm^2/sec were obtained for diffusion of ^{59}Fe in the fcc and bcc phases, respectively. From similar plots, activation energies of 69.4 kcal and 60.0 kcal and frequency factors of 1.33 cm^2/sec and 2.00 cm^2/sec were obtained for diffusion of ^{57}Co in the fcc and bcc phases of the FeCo alloy. The average isotope effect parameters were 0.66 in the fcc phase and 0.52 in the bcc phase. It was observed that the isotope effect parameter decreased with increasing degree of order during the bcc to CsCl-type ordering transformation. Manning's theory for concentrated alloys was used to calculate correlation factors for the Fe–Co alloy. From these calculated values and experimentally measured isotope effect parameters, K was determined to be slightly larger in the fcc and bcc phases of the Fe–Co alloy than has been reported in pure Fe. (Diss. Abstr.)

2179 ACID-CATALYZED CYCLIZATION REACTIONS. IX. THE FORMATION OF OXAZOLINIUM AND THIAZOLINIUM CATIONS FROM N-ALLYL AND SUBSTITUTED N-ALLYL-AMIDES, -URETHANS, -UREAS, AND -THIOUREAS. McManus, Samuel P. (Univ. of Alabama, Huntsville); Carroll, John T.; Pittman, Charles U. Jr. J. Org. Chem.; 35: 3768-74(Nov 1970).

N-Allyl and substituted N-allylamides, -urethans, -ureas, and -thioureas were cyclized in 60 to 96% sulfuric acid to their corresponding oxazolinium and thiazolinium cations. By drowning certain of these acid solutions into base, a useful synthetic route to 2-oxazolines and 2-thiazolines was demonstrated. The formation of oxazolinium (2a-o) and thiazolinium (2p-r) cations was studied by NMR techniques. In general, the simple N-allyl derivatives were only protonated at carbonyl oxygen or thiocarbonyl sulfur when introduced into the acid media at room temperature. The cyclic ions formed upon heating. The formation of N-acylpolyethyleneimines competed with cyclization in some of these examples. N-2-methylallyl and N-2-phenylallyl derivatives cyclized immediately at room temperature. The remarkable stability of oxazolinium and thiazolinium cations was indicated by their stability towards heating in acid media and their marked resistance to H–D exchange. Oxazolinium and thiazolinium ions are more resistant to H–D exchange than are oxoniacyclopent-1-enyl and 1,3-dioxoniacyclopent-1-enyl cations. The NMR spectra of these heterocyclic ions are tabulated and discussed. The mechanism of the cyclization process is discussed in light of these findings. (auth)

2180 PRIMARY ISOTOPE EFFECTS IN HYDROGEN ATOM TRANSFER REACTIONS FROM α-HYDROXYALKYL AND MONOHYDROPYRIDYL RADICALS. Huyser, Earl S.; Kahl, Allan A. (Univ. of Kansas, Lawrence). J. Org. Chem.; 35: 3742-4(Nov 1970).

The rates of oxidation of O-d-2-butanol and N-d-3,5-dicarbethoxy-1,4-dihydro-2,6-lutidine by tert-butyl peroxide are slower than those of nondeuterated samples of these compounds. This isotope effect is ascribed to hydrogen atom transfer reactions of radicals derived from these species to the oxygen–oxygen linkage of the peroxide. No isotope effect was observed in the reactions of either acetyl peroxide or tert-butyl peracetate with the secondary alcohol or oxidation of the dihydropyridine with acetyl peroxide. A route other than hydrogen atom transfer, possibly a direct displacement or an electron transfer process, likely is operative in the reduction of the peroxide by the radicals derived from these compounds. (auth)

2181 HYDROLYSIS OF BIS(4-NITROPHENYL) CARBONATE AND THE GENERAL BASE CATALYZED HYDROLYSIS OF o-(4-NITROPHENYLENE) CARBONATE. Fife, Thomas H.; McMahon, Diane M. (Univ. of Southern California, Los Angeles). J. Org. Chem.; 35: 3699-3704(Nov 1970).

The rates of hydrolysis of o-(4-nitrophenylene) carbonate were measured in H_2O at 30°C. The values of k_{obsd} for spontaneous hydrolysis are independent of pH from pH 1 to pH 7. In this pH region a water-catalyzed reaction is occurring with a D_2O solvent isotope effect (k_{H_2O}/k_{D_2O}) of 2.35. As acid concentration is increased from 1.0 M to 5.29 M, the rate of hydrolysis decreases. This behavior is similar to that observed previously for bis(4-nitrophenyl) carbonate. Hydrolysis is catalyzed by a series of general base catalysts. A linear plot of log k_B vs the pK_a of the catalyzing base is obtained with a slope of 0.30. The point for imidazole fits well on this line with catalysts of much lower basicity including H_2O. The value of $k_{Im}^{H_2O}/k_{Im}^{D_2O}$ is 3.49, indicating proton transfer in the transition state. In contrast, nucleophilic catalysis takes place in the imidazole-catalyzed hydrolysis of bis(4-nitrophenyl) carbonate. Formation and decomposition of an intermediate could be observed in that reaction. Reasons for the mechanism change with the cyclic ester are discussed. (auth)

2182 PROTON SPIN-LATTICE RELAXATION TIME OF ANILINE-d_2 IN DEUTERATED BENZENE AND DEUTERATED ANILINE SOLUTION. Bock, S. (Univ. of Manitoba, Winnipeg); Czubryt, J.; Tomchuk E. Can. J. Chem.; 48: 2814-8(15 Sep 1970).

The proton spin–lattice relaxation time of aniline-d_2 in deuterated aniline solution was determined as a function of concentration and temperature over the temperature interval 260 to 360°K using a pulsed nuclear magnetic resonance technique. In addition the proton spin–lattice relaxation time of aniline-d_2 in deuterated benzene solution at 20°C was also determined. The activation energies of the intra- and inter-molecular relaxation rates were of similar magnitude, viz 4.5 and 4.4 kcal/mole, respectively. It was also found that at 20°C the rotational correlation time, τ_r, of the $C_6H_5NH_2$ molecule in infinitely dilute perdeutero benzene solution was approximately half that of the partially deuterated aniline molecule, viz 3.0×10^{-12} and 6.3×10^{-12} s, respectively, and that τ_r of $C_6H_5ND_2$ in infinitely dilute perdeutero aniline solution is much larger than in infinitely dilute perdeutero benzene solution and is equal to 19×10^{-12} s. (auth) (Canada)

2183 INFRARED SPECTRUM OF HDO IN AQUEOUS SOLUTIONS OF PERCHLORATES AND TETRAFLUOROBORATES. Brink, G.; Falk, M. (National Research Council of Canada, Halifax). Can. J. Chem.; 48: 3019-25(1 Oct 1970).

The OH and OD stretching bands of HDO in aqueous solutions containing the ions ClO_4^- and BF_4^- were split into two components. The high-frequency component, A, did not shift with temperature. It is interpreted as due to OH groups involved in weak OH ... ClO_4^- or OH ... BF_4^- hydrogen bonds. This interpretation is in line with the corresponding OH frequencies of other systems containing ClO_4^- ions, such as methanolic solutions and crystalline hydrates. Solvent-separated ion pairs may account for the observed cation effect on band A. The low-frequency component, B, varied with temperature almost exactly like the corresponding band of pure water. It is interpreted to be due to those OH groups which are not associated with the anion. Components A and B are not resolved in solutions of most electrolytes, because the distribution of strengths of interactions of OH groups with most anions overlaps that of OH ... O interactions between water molecules. (auth) (Canada)

2184 PROTON EXCHANGE KINETICS OF OLEFINS IN CYCLOHEXYLAMINE. Maskornick, Michael John. Berkeley, Calif.; Univ. of California (1969). 137p. University Microfilms Order No. 70-13,114.

Thesis.

Tritium exchange rates were determined for a series of vinylic protons with cesium cyclohexylamide in cyclohexylamine at 25.0°. The rates of these compounds relative to benzene are: 9,10-dihydro-9,10 ethenoanthracene-11-t, 150; bicyclo[2.2.1]hepta-2,5-diene-2-t, 10; benzene-t, (1.00); ethylene-t, 0.071; trans-3,3-dimethyl-but-1-ene-1-t, 0.016; cis-3,3-dimethylbut-1-ene-1-t, 0.0046; 3,3-dimethylbut-1-ene-2-t, 0.0013; and cis-2,2,5,5-tetramethylhex-3-ene-3-t, 0.00001. Isotope effects, as measured by k_D/k_T, were also evaluated for several of these compounds: trans-3,3-dimethylbut-1-ene-1-t, 2.72; cis-3,3-dimethylbut-1-ene-1-t, 2.02; and 3,3-dimethylbut-1-ene-2-t, 1.73. Similarly, deuterium exchange rates were measured for some allylic protons with lithium cyclohexylamide in cyclohexylamine at 50.0°. These rates relative to toluene are: toluene, (1.00); 2-methylbi-

XUM

cyclo 2.2.1 hepta-2.5-diene (methyl protons), 0.26; 2-methylbicyclo [2.2.1]hept-5-ene (methylene protons), 0.049; 2-methylbicyclo [2.2.1]hept-2-ene (methyl protons), 0.048; and 2-methylenebicyclo [2.3.1]-heptane (methylene protons), 0.012. These exchange rates, combined with the rates of isomerization of the methyl compounds to the methylene compounds, give a value of 30% for the intramolecularity of the exchange reaction. The relative rates and isotope effects of these compounds were combined with other available data in a discussion of the mechanism of proton exchange in cyclohexylamine. The importance of intramolecularity (internal return) and metal ion-ligand coordination are separately evaluated. (Diss. Abstr.)

2185 DISSECTION OF α-ISOTOPE EFFECTS ON THE SOLVOLYSIS OF BENZHYDRYL BENZOATE. Murr, B. L.; Donnelly, M. F. (Johns Hopkins Univ., Baltimore). J. Amer. Chem. Soc.; 92: 6688-90(4 Nov 1970).

The separation of the solvolytic isotope effect for benzhydryl benzoate in ethanol and an estimate of the isotope effect on ^{18}O equilibration are reported. It was found that the solvolytic isotope effect is substantially greater than the ^{18}O equilibration isotope effect. (D.H.M.)

2186 DETECTION OF A SECONDARY ISOTOPE EFFECT ON PARTITIONING OF BENZHYDRYL BENZOATE ION PAIRS. Murr, B. L.; Donnelly, M. F. (Johns Hopkins Univ., Baltimore). J. Amer. Chem. Soc.; 92: 6686-8(4 Nov 1970).

In an effort to probe the existence of partitioning isotope effects, the α-tritium isotope effect was measured on partitioning of benzyhydryl benzoate ion pairs generated from diphenyldiazomethane and benzoic acid in ethanol-O-t and in 90% acetone. The reaction entails rate-determining proton transfer from monomolecular, undissociated benzoic acid giving diazonium benzoate ion pair that loses nitrogen to form what appears to be the same benzyhydryl benzoate "ion pair or spectrum of ion pairs" as in solvolysis. It was found that there is a nil solvent isotope effect on benzhydryl benzoate ion-pair partitioning in ethanol. (D.H.M.)

2187 BASE-CATALYZED HYDROGEN–DEUTERIUM EXCHANGE IN DIENE–IRON TRICARBONYL COMPLEXES. Whitlock, Howard W. Jr.; Reich, C. R.; Markezich, R. L. (Univ. of Wisconsin, Madison). J. Amer. Chem. Soc.; 92: 6665-7(4 Nov 1970).

The treatment of electronegatively substituted diene–iron tricarbonyl complexes with deuterated alcohols at 25°C in the presence of base leads to hydrogen–deuterium exchange with the exchange limited to those hydrogen α to the Z substituent (where Z = CHO, C ≡ N, or COR). (D.H.M.)

2188 THERMODYNAMIC AND KINETIC SECONDARY ISOTOPE EFFECTS IN THE COPE REARRANGEMENT. Humski, Kresimir; Malojcic, Rajko; Borcic, Stanko; Sunko, Dionis E. (Rudjer Boskovic Inst., Zagreb). J. Amer. Chem. Soc.; 92: 6534-8(4 Nov 1970).

Secondary α-deuterium isotope effects are shown to be a nonlinear function of the location of the transition state on the reaction coordinate. Thermodynamic and kinetic deuterium isotope effects on the thermal rearrangement of 1,5-hexadienes (1a = biallyl-1,1,6,6-d_4 and 1b = biallyl-3,3,4,4-d_4) and 3,3-dicyano-2-ethyl-1-methyl-1,5-hexadienes (2a = 6-d_2 and 2b = 4-d_2) were determined. The isotope effect on the equilibrium constant for 1a ⇌ 1b (1.10/atom D) gives a measure of the isotopic fractionation factor for hydrogen between an sp^3 and sp^2 hybridized carbon where a carbon–carbon bond is cleaved. The kinetic effects on the rearrangement of 2a and 2b are shown to be the same as the thermodynamic effects on the bond-breaking side (k_H/k_D 1.1), but only a fourth as large (k_H/k_D 0.97/atom D) on the bond-making side. (auth)

2189 INFRARED SPECTRA AND STRUCTURE OF BERYLLIUM BOROHYDRIDE. Cook, T. H.; Morgan, G. L. (Univ. of Wyoming, Laramie). J. Amer. Chem. Soc.; 92: 6493-8(4 Nov 1970).

Infrared spectral assignments for beryllium borohydride vapor are made by analogy with compounds of known structure and with the aid of deuterium and ^{10}B substitution. The structure of beryllium borohydride consists of an approximate triangular arrangement of metal atoms. Each boron is bound to beryllium via a double hydrogen bridge and all four bridging hydrogens are in a plane perpendicular to the plane of the three metal atoms. Each boron has two terminal hydrogens and all four terminal hydrogens lie in the plane of the metal atoms. The molecule has C_{2v} symmetry. A gas-phase infrared study of the trimethylamine adduct of beryllium borohydride supports these conclusions and shows the nonexistence of beryllium–hydrogen terminal bonds in beryllium borohydride. (auth)

2190 LASER RAMAN AND INFRARED SPECTRA OF AMINO ACIDS AND THEIR METAL COMPLEXES. III. PROLINE AND BISPROLINATO COMPLEXES. Herlinger, Albert W.; Long, Thomas Veach (Pennsylvania State Univ., University Park). J. Amer. Chem. Soc.; 92: 6481-6(4 Nov 1970).

The laser-Raman spectra of DL-proline and L-proline in the solid state and in aqueous solutions of pH 1.0, 6.0, and 11.0 are investigated, and bands characteristic of the cationic, zwitterionic, and anionic forms of the amino acid residue are discriminated. The infrared spectra of solid DL-proline and L-proline were measured in the region between 4000 and 200 cm^{-1} and the infrared and Raman spectra of proline in D_2O solutions are also reported. Vibrational modes that principally contribute to the observed frequencies are empirically assigned on the basis of spectral changes resulting from N-deuteration and pH variation and through comparison with a Urey–Bradley force-field analysis of glycine and with the spectrum of pyrrolidine. The infrared spectra of anhydrous, monohydrato, and dihydrato forms of the bis-DL-prolinatocopper(II) complex and the dihydrate of bis-DL-prolinatonickel(II) were carefully examined in order to infer structural differences in these complexes and to detail the effects of variable hydration on their infrared spectra. Similarities in the positions of the metal–nitrogen and metal–oxygen stretching modes indicate that the trans configuration is maintained in all four complexes, and spectral features resulting from removal of the groups occupying axial coordination positions are discussed. Contrasting with this result for the DL-proline complexes, the anhydrous and hydrated forms of bis-L-prolinatocopper(II) appear to adopt cis geometries. (auth)

2191 SOLID STATE ISOTOPIC EXCHANGE IN RADIO COBALT DOPED TRISDIPYRIDYL Co(III) PERCHLORATE: EFFECT OF PRIOR HEAT TREATMENT. Mathur, P. K.; Sengupta, S. (Bhabha Atomic Research Centre, Bombay). Indian J. Chem.; 6: 608-10(Oct 1968).

Effect of prior thermal treatment of the complex on the rate of solid-state isotopic exchange during the process of hydration was studied in $^{58}Co^{2+}$-doped trisdipyridyl Co(III) perchlorate. The higher the preheating temperature the faster the subsequent exchange. A much faster rate of exchange was observed in the doped "hydrated" form of the complex (prepared from the thermally pretreated anhydrous compound) as compared with the trihydrate. Studies with mixtures of the doped trihydrate and a large excess of the inactive "hydrated" complex showed a much higher rate of exchange as compared to the trihydrate alone; but it is much lower with the inactive hydrated sample, which was stored for long periods at 30°C prior to mixing with the doped trihydrate. The results are discussed on the basis of the "variable depth electron traps" model. (auth)

2192 SELF-DIFFUSION IN LIQUIDS: H_2O, D_2O, AND Na. Murday, J. S.; Cotts, R. M. (Cornell Univ., Ithaca, N. Y.). J. Chem. Phys.; 53: 4724-5(15 Dec 1970).

The NMR spin echo technique with magnetic gradient was used to measure the self-diffusion coefficients in two isotopic forms of water H_2O and D_2O, and in molten ^{23}Na. The ratio of self-diffusion in pure heavy water to the self-diffusion in pure light water is 0.79 ± 0.02. The NMR measurements agreed with the radiotracer work within experimental error. (M.C.G.)

Physical Chemistry

Refer also to abstracts 2615, 2712, 2714, 3211, and 3534.

2193 (CONF-700403–8) INFRARED AND RAMAN SPECTRA OF TRIVALENT LANTHANIDE–DI-(2-ETHYLEXYL) PHOSPHORIC ACID SOLVENT EXTRACTION ORGANIC EQUILIBRIUM PHASES. Lloyd, Robert C.; Bostian, Harry (Mississippi Univ., University. Dept. of Chemical Engineering). [1970]. 13p.

From 8th Rare Earth Conference, Reno, Nev.

Infrared analyses and Raman polarization studies were made on organic phases of the systems: di-(2-ethylhexyl) phosphoric acid–$Re(NO_3)_3$–H_2O, where Re represents a trivalent lanthanide, either lanthanum or neodymium. These studies substantiated extraction stoichiometries suggested by semimicro material balance studies and other studies and aided in determining the structure of the extracted complexes. The principal stoichiometries suggested were: $Re^{3+}_{aq} + 3[(HDEHP)_2 \cdot H_2O]_{org} \rightleftharpoons Re[H(DEHP)_2]_{3\,org} + 3H_2O_{aq} + 3H^+_{aq}$ and $Re(NO_3)^{a+}_{b\,aq} + a[(HDEHP)_2 \cdot H_2O]_{org} \rightleftharpoons Re(NO_3)_b[H(DEHP)_2]_{a\,org} + aH_2O_{aq} + aH^+_{aq}$ where HDEHP represents di-(2-ethylhexyl) phosphoric acid, DEHP is the acid monomer less a hydrogen ion, aq refers to aqueous, org to organic, a is the charge on the rare earth nitrate complex and b represents the number of nitrate anions. The first stoichiometry was found to hold at low aqueous phase concentrations. The second stoichiometry with a =

2 and b = 1 was found to be the principal mechanism of extraction in the mid concentration range and the reaction with a = 1 and b = 2 the principal extraction stoichiometry near saturation. In addition to confirming the above stoichiometries, the infrared spectra indicated the nature of much of the bonding. The Raman polarization data showed that the nitrate groups were bound in a bidentate fashion to the rare earth. (auth)

2194 (KFK–1070) COMPLEX COMPOUNDS OF HEXAVALENT ACTINIDES WITH PYRIDINE CARBOXYLIC ACIDS. Robel, Wolfgang (Kernforschungszentrum, Karlsruhe (West Germany). Institut fuer Radiochemie). Mar 1970. 76p. (In German). Dep. NTIS (U. S. Sales Only).

The complex compounds of hexavalent actinides with picolinic acid (HAPS), 6-methylpicolinic acid (HMAPS), picolinic acid N-oxide (HAPSNO), and nicotinic acid (HNIC) were investigated. The following types of compounds were obtained: complexes with the metal–ligand ratio of 1:2: $MO_2(APS)_2$, $MO_2(APSNO)\cdot 2H_2O$, $MO_2(NIC)_2\cdot 2H_2O$ (M = U(VI), Np(VI), Pu(VI), Am(VI)); solvated complexes = $MO_2(APS)_2\cdot HL$ (HL = HAPS or 8-hydroxyquinoline derivatives); complex adducts with neutral ligands – $MO_2L_2\cdot DMSO_n$ (DMSO = dimethyl sulfoxide), n = 1 and 2, respectively where M = U(VI), Np(VI), Pu(VI), $UO_2L_2\cdot PyO$ (PyO = pyridine N-oxide). The complexes were characterized by thermogravimetric, ir, and ^{1}H-NMR spectroscopic investigations. The evaluation of photometric or potentiometric titrations showed that with all ligands, except for picolinic acid N-oxide, hydrogen complexes ($MO_2HL^{2+}:\beta_{1H}$). are formed besides the normal complexes ($MO_2L^+:\beta_1$, $MO_2L_2:\beta_2$). The following stability constants were determined: (μ = 0, 1, T = 25°C): Pu(VI)/HAPS: lg β_{1H} = 0.69 ± 0.05 and lg β_1 = 4.58 ± 0.02; Pu(VI)/HMAPS: lg β_{1H} = 0.6 ± 0.04 and lg β_1 = 2.51 ± 0.04; Pu(VI)/HNIC: lg β_{1H} = 0.98 ± 0.07 and lg β_1 = 1.73 ± 0.03; Pu(VI)/HAPSNO: lg β_1 = 3.33 ± 0.02; U(VI)/HAPS: lg β_{1H} = 1.2 ± 1.3 and lg β_1 = 4.51 ± 0.12; and U(VI)/HAPSNO: lg β_1 = 3.62 ± 0.1. (auth)

2195 (ORNL–4572–, pp 251–7) CHEMICAL ENGINEERING RESEARCH. (Oak Ridge National Lab., Tenn.).

Mass transfer of water from sol droplets in preparation of microspheres was studied. Methods are being evaluated for producing microspheres with diameters as small as 20 μ. Axial dispersion in packed columns was measured for contacting liquids with a high density difference. Development work on the stacked-clove contactor is reported. (M.C.G.)

2196 PREPARATION AND STRUCTURE PROPERTIES OF A URANYL HYDROXYFORMATE. Bideau, Michele; Bressat, Rene; Mentzen, Bernard; Navarro, Alain (Institut National des Sciences Appliquees, Villeurbanne, France). Compt. Rend., Ser. C; 271: 225-7(27 Jul 1970). (In French).

A new uranyl hydroxyformate was prepared by two methods: a water vapor reaction with uranyl diformate $UO_2(HCOO)_2\cdot H_2O$ and a water vapor and oxygen reaction with uranium(IV) formate U(HCOO). Chemical analysis indicated the formula $UO_2(OH)(HCOO)\cdot 1H_2O$ and x ray crystallography revealed a unit orthorhombic cell with the following parameters: a = 10.55 Å, b = 13.52 Å, c = 16.02 Å. The study of the molecular vibration spectra confirmed the existence of the various groups in the formula. (France)

2197 TRACER CHEMICAL STUDIES OF LAWRENCIUM. Silva, R.; Sikkeland, T.; Nurmina, M.; Ghiorso, A. (Univ. of California, Berkeley). Inorg. Nucl. Chem. Lett.; 6: 733-9(Sep 1970).

The discovery of ^{256}Lr with a half-life of 35 sec and α energies of 8.3 to 8.6 MeV made it possible to carry out tracer chemical experiments on Element 103, and the studies described were made to determine the most stable oxidation state for Lr in aqueous solution. A fast solvent-extraction procedure using methyl isobutyl ketone (MIBK) containing the chelating agent TTA as the organic phase and buffered acetate solutions as the aqueous phase was used to distinguish between the 2^+, 3^+, and 4^+ oxidation states. Ions of the different charge states formed extractable chelates over different pH ranges. Results are tabulated for ^{256}Lr in comparison with ^{255}No, and it was found that Lr extracted over the same pH range as Cf and Fm, and by analogy that the most stable species for Lr in aqueous solution is the trivalent ion. Data on other higher actinides and their rare earth analogues are also briefly discussed. (UK)

2198 ROLE OF IMPURITIES AND D_2O SUBSTITUTION ON FLUORESCENCE LIFETIMES OF URANYL SALTS. Pant, D. D.; Pant, H. C. (DSB Government Coll., Naini Tal, India). Indian J. Pure Appl. Phys.; 6: 219-22(May 1968).

Lifetimes (τ) of various uranyl salts were measured at RT (room temperature) and 80°K. The anomalies in certain data, for example, in uranyl sodium acetate and uranyl chloride, are explained to be due to the presence of other uranyl impurities. The fresh samples have longer τ and variation in τ of different uranyl salts arises due to the difference in the oscillator strength of the first electronic transition in absorption. Effects of D_2O substitution on τ of uranyl sulfate ($UO_2SO_4\cdot 3H_2O$) and potassium uranyl sulfate ($K_2UO_2SO_4\cdot 2H_2O$) were studied. While the sulfate showed an increase in τ on deuteration, no such effect was observed in potassium uranyl sulfate. The behavior is discussed on the basis of the ideas developed by G. W. Robinson and R. P. Frosch [J. Chem. Phys., 38(1963), 1187]. An increase in τ on D_2O substitution results from a smaller value of Franck–Condon overlap integral between the excited state and the ground state vibrational levels in resonance with the former, leading to a nonradiative dissipation process. In uranyl potassium sulfate where the quantum yield was unity at low temperatures, such processes were absent. The observed fact that no D_2O effect was found in such a salt appears to support the theory of Robinson and Frosch. (auth)

2199 NEW ORGANIC REAGENTS FOR NIOBIUM. Savvin, S. B.; Alimarin, I. P.; Okhanova, L. A.; Belova, T. Ya. Tr. Kom. Anal. Khim., Akad. Nauk SSSR; 17: 163-74(1969). (In Russian).

Thirty-five 3,6-bisazo derivatives of chromotropic acid, most of which contained an oo'-dihydroxyazo grouping, were synthesized, and their reactions with Nb, Zr, and Cu were studied by spectrophotometry. The color of the Nb complex was developed in N to 3N-HCl at 60 to 80° in 15 min. The best analytical characteristics were found with reagents having a symmetrical structure, e.g., chlorosulphophenol S [3,6-bis-(5-chloro-2-hydroxy-3-sulfophenylazo) chromotropic acid], or with an asymmetrical structure in which one of the substituents in the 3 or 6 position is derived from, e.g., metanilic acid. For these reagents there is a difference of 80 to 95 nm between the absorption maximum of reagent and complex, and the molar extinction coefficient of the complex range from 40,000 to 50,000. Tartrate, SO_4^{2-}, EDTA, and oxalate interfere, but Ti (100-fold excess), Al (400-fold), Zn (10-fold), and Ta (5-fold) do not. (Referativnyi Zh.)

2200 UBr_5 AND THE URANIUM(IV)–URANIUM(VI) COMPOUND $UOBr_3$,2.5DMA. Lux, Franz; Wirth, Gernoth; Bagnall, Kenneth Winfield (Technische Hochschule, Munich). Chem. Ber.; 103: 2807-13(1970). (In German).

A previous report on the preparation of uranium pentabromide could not be substantiated. The pentabromide can, however, be readily prepared by the reaction of uranium metal or uranium tetrabromide with either boiling bromine or, at room temperature, with bromine and catalytic amounts of acetonitrile. UBr_5 is isostructural with α-$PaBr_5$. In the solid state and in solution UBr_5 exhibits typical uranium(V) spectra; the solution spectrum in CH_2Cl_2/HBr is characteristic of uranium(V) in octahedral coordination (probably "$HUBr_6$"). Dissolution of UBr_5 in acetone and addition of N,N-dimethylacetamide (DMA) yields $UOBr_3\cdot 2.5$ DMA. The infrared and electronic spectra show that this compound contains both uranium(IV) and uranium(VI), the latter as the uranyl group. Apart from the actinide oxides and halides, $UOBr_3\cdot 2.5$ DMA is the first coordination compound containing an actinide element in two different oxidation states. (auth)

2201 SOLUBILITY OF XENON IN CARBON TETRACHLORIDE AND IN CHLOROFORM. Yagi, Masuo; Kondo, Kenjiro (Tohoku Univ., Sendai). Kakuriken Kenkyu Hokoku; 2: No. 2, 153-4(Dec 1969). (In Japanese).

Recently it has been found by Hamaguchi, et al., that daughter nuclides ^{133}Xe and ^{135}Xe can be extracted carrier-free from the mixed solution of ^{133}I and ^{135}I by carbon tetrachloride. From this fact, the influence of the dissolution of Xe into organic solvent cannot be neglected in the system to which Xe moderator is added, when the chemical effect of nuclear disintegration is investigated in a gas phase system. Therefore, studies were made on the solubility of Xe in carbon tetrachloride and in chloroform to obtain quantitative information on the fact described above. In both cases, the total pressure of Xe was proportional to the mole fraction of Xe in the solvent. The Henry number at room temperature was 5.75×10^4 for carbon tetrachloride and 6.84×10^4 for chloroform. From this, it was found that the solubility of Xe is slightly higher in the nonpolar solvent, carbon tetrachloride, than in the polar solvent, chloroform. The effects of degassing on solubility were not observed. (Japan)

2202 STABILITY CONSTANTS FOR PROTACTINIUM(V)–ACETYLACETONE COMPLEXES. Liljenzin, J. O. (Chalmers Univ. of Tech., Goteborg). Acta Chem. Scand.; 24: 1655-61 (1970).

The stability (K) and distribution (Λ) constants for the complexes formed between Pa(V) and acetylacetone (HAA) have been calculated from the results of solvent extraction experiments. The following species were found; PaO^{3+}, PaO_2^+ (log K_{22} = 1.05 ±

0.11), $PaO(AA)^{2+}$ (log K_{11} = 1.00 ± 0.17), $PaO_2(AA)$ (log K_{13} = −2.10 ± 0.15, log Λ_{13} = 0.02 ± 0.12), $PaO_2(AA)_2^-$ (log K_{24} = −7.77 ± 0.16), $PaO(AA)_3$ (log K_{33} = −0.38 ± 0.11, log Λ_{33} = −0.06 ± 0.30), $PaO(AA)_3 \cdot 2HAA$ (log $K_{33}\Lambda_{33}$ = 0.73 ± 0.18). (auth)

2203 STEADY-STATE CHEMICAL POTENTIAL PROFILES IN SOLID ELECTROLYTES. Choudhury, N. S.; Patterson, J. W. (Iowa State Univ., Ames). J. Electrochem. Soc.; 117: 1384-8 (Nov 1970).

Steady-state chemical potential profiles in a solid electrolyte under open-circuit and ion-blocking conditions may be obtained by balancing the steady-state flux at points inside the electrolyte. Steady-state oxygen chemical potential profiles inside a scaling layer of thoria and inside yttria-doped thoria specimens under open-circuit and ion-blocking (dc polarization) conditions are illustrated in special cases. (auth)

2204 PREPARATION AND CRYSTALLINE STRUCTURE OF THE URANIUM BARIUM SULFIDE: $BaUS_3$. Brochu, Robert; Radiou, Jean; Grandjean, Daniel (Rennes Univ., France). Compt. Rend., Ser. C; 271: 642-3(14 Sep 1970). (In French).

A new mixed sulfide $BaUS_3$ was prepared by two methods: the action of carbon sulfide on the monouranate $BaUO_4$, or by the reaction between BaS and US_2. This material crystallizes in the orthorhombic system with four bases per unit cell: a = 7.44, b = 10.38, c = 7.24 Å. The space group is Pnma. A reliability factor of 0.086 was obtained from the atomic coordinates. An effective magnetic moment of 3.20 μB was obtained by magnetic susceptibility measurements. (auth) (France)

2205 THERMOCHEMISTRY AND SOLUTION CHEMISTRY IN THE SODIUM–OXYGEN–HYDROGEN SYSTEM. Jansson, Sven A. (Westinghouse Research Labs., Pittsburgh). pp 523-60 of Corrosion By Liquid Metals. /Draley, Joseph E. (ed.). New York; Plenum Publishing Corp. (1970).

From Corrosion by Liquid Metals Conference, Philadelphia, Pa. See CONF-691007.

Thermochemical analyses are made to define the fields of existence of condensed phases and the vapor pressures of gaseous species in the sodium–oxygen–hydrogen system between 400 and 1000°K, oxygen being the most important contaminant in liquid sodium [Na(l)]. Calculated phase relations are compared with experimental data reported in the literature. The calculations showed that Na(l) and NaOH(l) could coexist at ~707°K and higher temperatures, provided that the hydrogen pressure was sufficiently high. Experimental data indicated that ~680°K was the lower limit. The deviations depend primarily on the high solubilities of NaH and Na_2O in NaOH(l). Below ~680°K the phases that may coexist with Na(l) are Na_2O(s) and NaH(s). A model is developed for solutions in Na(l). It is suggested that the solubilities of oxygen and hydrogen depend directly on the additive solubilities of solution compounds of the general type $Na_aO_bH_c$, and, therefore, on the chemical potentials for sodium, oxygen, and hydrogen. It is also proposed that solution compounds generally exist in metal solutions and that the same solubility–chemical potential relations are valid. Possible changes of the chemical potentials for oxygen and hydrogen with the concentrations of these elements in Na(l) are discussed. It is concluded that the solubilities of solution compounds need to be determined while measuring the chemical potentials of all the components. (auth)

2206 MIXED-METAL COMPLEXES BETWEEN INDIUM(III) AND URANIUM(VI) WITH MALIC, CITRIC, AND TARTARIC ACIDS. Adin, Anthony; Klotz, Paul; Newman, Leonard (Brookhaven National Lab., Upton, N. Y.). Inorg. Chem.; 9: 2499-2505 (Nov 1970).

The formation of mixed-metal complexes between indium(III) and uranium(VI) with various hydroxycarboxylic acids was studied using spectrophotometric, potentiometric, and solvent extraction methods. Over wide concentration ranges, it was found that the reactions for the formation of the indium(III) uranium(VI) malate, citrate, and tartrate mixed-metal complexes can be written $In^{III}L_2 + 0.5(U^{VI}L)_2 \xrightleftharpoons{K'_{mmc}} In^{III}U^{VI}L_2 + L$, where L is the hydroxycarboxylic acid ligand. At 25° and pH 4 values of K'_{mmc} are as follows: malate 30; citrate, 720; tartrate, 31. In order to study these reactions, it was first necessary to investigate the polymerization of indium(III) and dimerization of uranium(VI) complexes. (auth)

2207 INFRARED STUDIES OF THORIUM OXIDE SURFACES: HYDROXYL SPECTRA. Fuller, E. L. Jr.; Holmes, H. F.; Gammage, R. B. (Oak Ridge National Lab., Tenn.). J. Colloid Interface Sci.; 33: 623-7(Aug 1970).

A spectrophotometric system, capable of in situ studies over a wide range of temperature (−196 to +1000°C) and pressure (10^{-7} to 760 torr), is described. The spectra indicate that the adsorbed water is tenaciously bound in a rigid array with its orientation epitaxially dictated by the substrate. There are three preferred hydrogen-bonded species characterized by infrared bands at 3665, 3550, and 3310 cm^{-1}, in addition to the free surface hydroxyl group with a band at 3742 cm^{-1}. The latter is not observed until vacuum dehydration temperature exceeds 300°C. The heat of absorption of water is related linearly to the square root of the hydrogen bond frequency shift. The merit of observing the spectra at elevated temperatures is noted relative to the practice of interpreting room temperature spectra in terms of phenomena occurring at previously elevated temperatures. D_2O exchange studies show the tenacity of the water binding and substantiate the frequency assignments. (auth)

2208 ACETATE COMPLEXING BY TRIVALENT ACTINIDE IONS. Choppin, Gregory R.; Schneider, Joan K. (Florida State Univ., Tallahassee). J. Inorg. Nucl. Chem.; 32: 3283-8(Oct 1970).

The stability constants for the formation of the monoacetate complexes of trivalent Ce, Eu, Am, Cm, Bk, and Cf were determined by a solvent extraction technique in a 2.0 M ($NaClO_4$) ionic medium. The thermodynamic parameters of complex formation were obtained by the temperature differential method. These thermodynamic values are interpreted as supporting a model of inner sphere complexing. Both the enthalpy and entropy values are larger for the actinides than for the lanthanides, reflecting a greater degree of dehydration of the former upon complexation. (auth) (UK)

2209 DIRECT PROTON MAGNETIC RESONANCE CATION HYDRATION STUDY OF URANYL PERCHLORATE, NITRATE, CHLORIDE, AND BROMIDE IN WATER–ACETONE MIXTURES. Fratiello, Anthony; Kubo, Vicki; Lee, Robert E.; Schuster, Ronald E. (California State Coll., Los Angeles). J. Phys. Chem.; 74: 3726-30(15 Oct 1970).

A cation hydration number study was carried out for solutions of $UO_2(ClO_4)_2$, $(UO_2(NO_3)_2$, UO_2Cl_2, and UO_2Br_2 in water–acetone mixtures by the direct proton magnetic resonance (PMR) method. At temperatures below −85°C, proton exchange is slow enough to permit the observation of separate PMR signals for bulk water molecules and water molecules in the UO_2^{2+} solvation shell. In ClO_4^- solutions, UO_2^{2+} is hydrated by a maximum of four water molecules and complex formation is negligible. Bidentate complexing occurs with NO_3^- and the equilibrium quotient for the formation of the mononitrato complex is roughly an order of magnitude greater than that for the dinitrato complex. Complexing is evident in the Cl^- and Br^- solutions but spectral complexities prevented an unambiguous identification of the species. (auth)

2210 PEROVSKITE PHASES CONTAINING TETRAVALENT URANIUM. Charvillat, J. P.; Baud, G.; Besse, J. P. (Service de Chimie Minerale, Clermont-Ferrand, France). Mater. Res. Bull.; 5: 933-8(Nov 1970). (In French).

A series of lacunary ordered perovskites including tetravalent uranium of $A_2^{II}B^{II}U^{IV}O_5$ type was prepared by solid state reaction (A = Ba, Sr; B = Ba, Sr, Ca, Cd). Ba_3UO_5 was found to have two allotropic forms: an α tetragonal low-temperature form and a β cubic high-temperature form. The study of pseudo-binary α Ba_3UO_5–Sr_3UO_5 shows the existence of tetragonal, cubic, and orthorhombic crystallographic areas. (auth)

2211 ABSORPTION SPECTRUM OF AMMONIUM URANYL SULFATE. Narasimham, K. V.; Girija, M. (Defence Science Lab., Delhi). Indian J. Pure Appl. Phys.; 6: 231-5(1968).

The electronic absorption as well as the infrared absorption spectra of ammonium uranyl sulfate, $(NH_4)_2UO_2(SO_4)_2 \cdot 2H_2O$, were reinvestigated. For the electronic absorption bands, an analysis is proposed on the basis of four electronic transitions from the common ground state to the different upper states. In the analysis, besides the uranyl frequencies, frequencies of the sulfate ion and crystal lattice were obtained. In the infrared spectrum, an interpretation for some of the bands was proposed on the basis of the frequencies of the uranyl ion, sulfate ion, ammonia ion, and water of hydration. (auth)

2212 LOW FREQUENCY INFRARED AND RAMAN SPECTROSCOPIC STUDIES OF SOME URANYL COMPLEXES: THE DEFORMATION FREQUENCY OF THE URANYL ION. Bullock, J. I. (Univ. of Surrey, Eng.); Parrett, F. W. Can. J. Chem.; 48: 3095-7(1 Oct 1970).

A study of the low-frequency vibrational spectra of compounds of the type $L_2UO_2(NO_3)_2$ (L = monodentate ligand), $MUO_2(NO_3)_3$ (M = monovalent cation), and $Cs_2UO_2X_4$ (X = Cl or Br) indicated that the deformation frequency of the uranyl group occurs in the region 274 to 245 cm^{-1}, but detailed assignments of the U–O (nitrate) frequencies are not given since it was found that structurally related complexes do not necessarily give similar low frequency infrared and Raman spectra. (auth) (Canada)

XUM

2213 ENTHALPY OF FORMATION OF THORIUM TETRAFLUORIDE BY FLUORINE BOMB CALORIMETRY. Van Deventer, Erven H.; Rudzitis, Edgars; Hubbard, Ward N. (Argonne National Lab., Ill.). J. Inorg. Nucl. Chem.; 32: 3233-6(Oct 1970).

The enthalpy of formation of thorium tetrafluoride was measured by combination of the elements in a bomb calorimeter. The standard enthalpy of formation, $\Delta H_f^0(ThF_4$, monoclinic, 298.15°K), was calculated to be -504.5 ± 1.2 kcal/mole. (auth) (UK)

2214 X RAY STUDIES OF MONOAQUOTETRACARBAMIDOURANYL HALIDE NITRATES. Kuznetsov, V. G.; Ellert, G. V.; Tsapkina, I. V.; Mikhailov, Yu. N. (Inst. of General and Inorganic Chemistry, Moscow). Zh. Neorg. Khim.; 15: 2474-80(Sep 1970). (In Russian).

Monoaquotetra carbamidouranyl halide nitrates were studied roentgenographically and it is shown that unlimited solid solutions are formed in the iodide series. In the bromide series limited solid solutions were formed based on $[UO_2 \cdot 4CO(NH_2)_2H_2O](NO_3)_2$ and on the basis of a 1:1 bromide nitrate with the composition $[UO_2 \cdot 4CO(NH_2)_2H_2O]Br_{0.47} \cdot (NO_3)_{1.53}$ there is formed, apparently, an ordered phase. Two individual chloride nitrate complexes were studied. (M.C.G.)

2215 SPECTROPHOTOMETRIC STUDY OF UO_2^{2+}–SCN^- SYSTEM IN AQUEOUS AND WATER–METHANOL MEDIA. Iyer, H. Parasurama; Venkateswarlu, Ch. (Bhabha Atomic Research Centre, Bombay). Indian J. Chem.; 6: 526-7 (Sep 1968).

Simple spectrophotometric methods, viz. molar ratio, Bent and French, and Job's continuous variation were applied to the UO_2^{2+}–SCN system in aqueous and water–methanol media. Correlation of the data obtained by different methods indicated the formation of 1:1, and higher complexes in both the media. (auth)

2216 VIBRATIONAL SPECTRA OF URANYL COMPOUNDS IN SOLUTIONS. Bist, Hari D. (Indian Inst. of Tech., Kanpur, India). Indian J. Chem.; 8: 174-7(Feb 1970).

The characteristic changes in the antisymmetric stretching frequency, ν_3, of the uranyl ion in the infrared spectra of purely aqueous, acidic, and alkaline solutions of uranyl nitrate hexahydrate (UNH), and also in aqueous uranyl sulfate, chloride, and perchlorate solutions are explained on the basis of formation of known complex species. The formation of ionic species like $UO_2NO_3^+$ and $UO_2(NO_3)_3^-$ in acidic (HNO_3) solution of UNH, already known on the basis of other physico-chemical data and also shown to be responsible for the characteristic fluorescence and absorption spectra, were inferred from the peaks at 950, 985 (sh), and 1280 cm^{-1} in 50% acid concentration. The appearance of ν_3 at 950 cm^{-1} indicates that the coordination around uranyl ion in ionic complexes resembles that of lower hydrates of crystalline UNH; in the crystalline trihydrate ν_3 appears at 945 cm^{-1}. The vibrational data obtained from the studies in fluorescence, infrared, and Raman effect are discussed. (auth)

Radiation and Nuclear Chemistry

Refer also to abstracts 2497 and 2536.

2217 ACHIEVEMENTS OF THE PURE AND APPLIED RADIATION CHEMISTRY IN POLAND. Kroh, Jerzy; Hankiewicz, Ewa (Technical Univ., Lodz, Poland). Nukleonika; 14: 1241-60(1969).

A concise review of the achievements of Polish radiation chemistry and technology in the period 1958 to 1968 is presented. Studies of Polish research workers initiated at foreign centers and the ensuing theoretical and practical research conducted mainly in seven centers in Poland are considered. The theoretical and experimental data are discussed in the following sections: water and aqueous solutions, inorganic solids, simple organic systems, polymer systems (effects of radiation on polymers and radiation-induced polymerization), and radiation chemistry of foods.(272 references). (auth)

Radiation Effects

Refer also to abstracts 2120 and 2821.

2218 (CONF-700322–, pp 345-56) APPLICATIONS OF ACCELERATORS IN THE RADIATION CHEMISTRY OF POLYMERS. Stannett, V. (North Carolina State Univ., Raleigh. Dept. of Chemical Engineering).

From Proceedings of the second Oak Ridge conference on the use of small accelerators for teaching and research, March 23–25, 1970.

Although a large volume of research has been conducted on the radiation chemistry of polymers, work with accelerators has been rather neglected. This is particularly true with the smaller energy accelerators below the 1 MeV range for example. The difficulties have been mainly experimental including accurate dosimetry, accompanying heat effects and the problems of irradiating sufficient sample at the 2 mm or as thicknesses used. This is true particularly with liquids when it is often necessary to exclude air from the sample. The three areas of interest are (1) the effects of the radiolysis of polymers, these can be conveniently studied with small accelerators using thin films, (2) radiation polymerization of liquid or solid monomers (this is the most difficult experimentally in the case of liquids), and (3) graft copolymerization. Here interesting studies are possible with comparative ease using selected techniques. A number of further details of the three areas together with some recently obtained results with liquid phase polymerization are presented. (auth)

2219 (NP-18449) RELATIVE SIGNS OF PRINCIPAL ELEMENTS OF THE α-PROTON HYPERFINE COUPLING TENSOR IN NH_2CONHO. Lund, Anders; Gillbro, Thomas (Aktiebolaget Atomenergi, Studsvik (Sweden)). 1970. 8p. (LF-28). Dep. CFSTI (U. S. Sales Only). Almquist and Wiksell Gamla Brogatan 26 Stockholm, Sweden Sw Cr 10:-.

The relative signs of the proton coupling tensor of the radical NH_2CONHO formed from γ-irradiated hydroxyurea crystals were determined by comparing experimental and calculated spectra for orientations of the crystal in which $\Delta M_I = 1$ transitions were observed. It was found that the anisotropy could be explained by taking into account the contributions of the dipolar interaction between spin densities on the oxygen atom, as well as that on the nitrogen atom, and the proton. In a similar way the N–H bond distance $r_{N-H} = 1.0$ Å and effective charge of the nitrogen nucleus $Z^* = 3.7$ of the NH_2CONHO radical were found adequate to explain the anisotropy of the proton coupling in the $N_2H_4^+$ ion when the contribution from spin density on the nonadjacent nitrogen atom was included. (auth)

2220 IR-SPECTROSCOPY STUDIES OF γ-RADIATION EFFECTS ON THE CRYSTALLINITY OF POLY(VINYL ALCOHOL). Korodenko, G. D.; Karimov, S. N.; Narzullaev, B. N.; Zakharchuk, A. V. (Tadzhik State Univ., Stalinabad, USSR). Dokl. Akad. Nauk Tadzh. SSR; 13: No. 7,18-21(1970). (In Russian).

The effects of γ radiation on the submolecular structure and properties of poly(vinyl alcohol) (PVA) were studied. It was shown that γ-irradiation increased the degree of crystallinity as a result of formation of short fragments with an increased mobility which was conducive to better ordering in the material. (R.V.J.)

2221 ELECTRICAL CONDUCTIVITY OF γ-IRRADIATED SOLID MONOMERS AT LOW TEMPERATURE. Kadoi, Hajime; Tabata, Yoneho; Oshima, Keichi (Tokyo Univ.). J. Phys. Chem.; 74: 3962-8(29 Oct 1970).

The electric conductivity of solid monomers irradiated by γ rays at −196°C was measured during temperature elevation and compared with that of nonirradiated systems. For the nonirradiated systems, peaks in the current–temperature curve were observed at the transition points that were determined by x-ray diffraction and thermal analysis. Activation energies for nonirradiated systems ranged from 0.3 to 1.2 eV in the higher temperature region. At low temperatures there were pronounced differences between the irradiated and nonirradiated systems, although a negative current was observed in both cases. In nonirradiated systems this negative current might be explained as rising from the depolarization of the oriented permanent dipoles, whereas in the case of irradiated systems it might result from the annihilation of charge pairs produced by the irradiation. In the latter case, the average migration distance of the electron was estimated to be about 100 Å. (auth)

2222 INFLUENCE OF RADIOACTIVE RADIATION ON THE HETEROGENEOUS EQUILIBRIUM IN THE SYSTEM SOLID–SOLUTION. Spitsyn, V. I.; Torchenkova, E. A.; Glazkova, I. N. (Inst. for Physical Chemistry, Moscow). Monatsh. Chem.; 101: 1164-76(Jul-Aug 1970). (In German).

The electrokinetic potentials of radioactive and nonradioactive barium sulfate samples have been determined by the streaming potential method. It has been shown that depending on the method of preparation, $BaSO_4$ samples can have both positive and negative ζ-potentials. In the case of deposition in a neutral medium (Na_2SO_4) the $BaSO_4$ deposit can have a negative ζ-potential, whereas when it is prepared in an acid medium (H_2SO_4) the value of the ζ-potential is positive. The introduction of radioactive sulfur-35 into $BaSO_4$ deposit does not affect the sign of the surface charge, but changes the electrokinetic potential value. These changes depend on the radioactive isotope content in the deposit. The extremal effect was observed with specific radioactivity of 1 to 2 mCi/g. (auth)

2223 DESTRUCTION OF FOAM BY α PARTICLES. Exerowa, D.; Ivanov, D. (Inst. of Physical Chemistry, Sofia). Compt. Rend. Acad. Bulg. Sci.; 23: 547-50(1970).

Foam columns were subjected to alpha particles after appropriate waiting. Foam destruction was studied as a function of radioactive source, temperature, surfactant, and electrolyte concentration. The mechanism of destruction by alpha particles differs from the mechanism of spontaneous destruction. A pronounced specificity of the destructive action for different types of particles was observed. (R.W.R.)

2224 EPR STUDIES OF STABLE HYDROGEN ATOMS ON γ-IRRADIATED CLINOPTILOLITES CONTAINING La, Mg, AND K IONS. Papp, Ya.; Mikheikin, I. D.; Kazanskii, V. B. (Moscow Inst. of Organic Chemistry). Kinet. Katal.; 11: 812-13(May-Jun 1970). (In Russian).

Studies were made on the strongly stabilizing influence of clinoptilolites on hydrogen atoms. Specimens of clinoptilolites containing La^{3+}, Mg^{2+}, and K^+ incorporated by cation exchange were annealed in a vacuum at 400, 500, 600, and 700°C for 3 to 4 hr and γ irradiated with 10 Mrad doses at liquid nitrogen temperature. Measurements were also made on the relative concentration of hydrogen atoms (formed during γ radiation) as a function of the temperature of specimens heated before irradiation. It was found that in all three types of clinoptilolites hydrogen concentration did not change at temperatures up to 400 to 500°C. At 600°C the EPR signal diminished somewhat and completely disappeared at 700°C. (R.V.J.)

2225 ELECTRIC BREAKDOWN IN PLASTICS IRRADIATED WITH CHARGED PARTICLES. Deev, Yu. S.; Kruglyi, M. S.; Lyapidevskii, V. K.; Sergeev, V. I.; Serenkov, V. I. Plast. Massy; No. 8, 49-50(1970). (In Russian).

The tree-shaped cracks formed in poly(methyl methacrylate) after exposure to fast electrons have been attributed to radiolysis and secondary processes induced by it. It may be assumed that the space charges created by the slowing down of electrons generate internal stresses in the material by means of electrostatic interaction. This in turn causes the formation of trajectories with greatly reduced mechanical and electric strength and with a short half-life. The mobility of the molecules of the polymer is greatly reduced in the vitreous state, resulting in low relaxation rates; under such conditions the time of life of the trajectory may become sufficiently long to create a discharge. The proposed mechanism allows prediction of the behavior of organic glasses with respect to the tree-shaped fissuring process on the basis of the physical and mechanical properties of the material. (TTT)

2226 COMPARISON OF ISOMERIC TRANSITION-ACTIVATED ^{80}Br REACTIONS IN $CH_4-{}^{80m}BrBr$ AND $CH_4-H^{80m}Br$ SYSTEMS. Yagi, M.; Kondo, K. (Tohoku Univ., Sendai). Radiochem. Radioanal. Lett.; 5: 75-81(16 Oct 1970).

The reactions of isomeric transition-activated ^{80}Br with gaseous CH_4 have been compared in the $CH_4-{}^{80m}BrBr$ and $CH_4-H^{80m}Br$ systems. As a result, a tremendous difference was observed between $CH_3{}^{80}Br$ yields in the two systems. That is, the $CH_3{}^{80}Br$ yield at zero mole fraction of the additive in the $CH_4-{}^{80m}BrBr$ system was much higher than the yield in the $CH_4-H^{80m}Br$ system. The difference can be understood to be caused principally by the initial kinetic energies acquired by the Coulomb repulsion in different ^{80m}Br source molecules. (auth)

2227 AQUOLUMINESCENCE: AN ALTERNATIVE MODE OF RELEASE OF ENERGY STORED IN γ-IRRADIATED CRYSTALS. Arnikar, H. J.; Damle, P. S.; Chaure, B. D. (Univ. of Poona). Radiochem. Radioanal. Lett.; 5: 25-8(16 Oct 1970).

The emission of light during the dissolution of an irradiated salt is reported for the first time and it is proposed to name this glow "aquoluminescence." The method for releasing the stored energy was achieved by destroying the crystal lattice and thus setting free the trapped electrons. The irradiated salt (NaF, NaCl, KCl, NaBr, and KBr) is dissolved in water, the crystal structure breaks down completely, and all the ions as well as the released electrons become hydrated. It was found that the recombination of the hydrated electrons with the parent atoms is accompanied by the emission of a faint bluish-green glow that is visible in total darkness. This method also provides an easy means of generating hydrated electrons. (P.C.H.)

2228 NEW PROCEDURE FOR PURIFYING WATER FOR RADIATION CHEMISTRY. Sasse, Ronald A. (Army Ballistic Research Labs., Aberdeen Proving Ground, Md.). Health Phys.; 19: 675-9(Nov 1970).

The radioinduced chain reaction $H\cdot + H_2O_2 \rightarrow OH\cdot + H_2O$, $OH\cdot + H_2 \rightarrow H_2O + H\cdot$ serves as the basis for this procedure which is a convenient substitute for the radiation–photolysis method routinely used in radiation chemistry. Water is γ-irradiated to oxidize impurities; the chain reaction is invoked by saturation with hydrogen and irradiating again, thereby destroying the hydrogen peroxide. Values obtained for $G(H_2)$ and $G(H_2O_2)$ by this method were identical to those obtained by the radiation–photolysis procedure. (J.G.B.)

2229 FREE RADICALS IN gamma-IRRADIATED DISODIUM SUCCINATE. PART I. MONOCLINICAL CRYSTALS. Vyas, H. M.; Janecka, J.; Fujimoto, M. (Univ. of Guelph, Ont.). Can. J. Chem.; 48: 2804-8(15 Sep 1970).

Crystals of disodium succinate have two distinct modifications, monoclinic and triclinic. These were recognized by electron spin resonance (ESR) studies of the free radicals produced by γ irradiation. In the monoclinic crystals, ESR spectra and radiation processes appear similar to those observed in γ- (or x-) irradiated succinic acid. In monoclinic crystals irradiated at 77°K, two types of radicals coexist. They were identified as $^-O_2CCH_2$-$CH_2\dot{C}O_2^{2-}$, together with a distorted conformation of the radical $^-O_2C(\dot{C}HCH_2)^*CO_2^-$. On warming to room temperature the former species disappears while the latter changes irreversibly to a stable conformation $^-O_2C\dot{C}HCH_2CO_2^-$. (auth) (Canada)

2230 FREE RADICALS IN gamma-IRRADIATED DISODIUM SUCCINATE. PART II. TRICLINICAL CRYSTALS. Fujimoto, M.; Seddon, W. A. (Atomic Energy of Canada Ltd., Chalk River, Ont.). Can. J. Chem.; 48: 2809-13(15 Sep 1970). (AECL-3649).

Electron spin resonance spectra and radiation processes in γ-irradiated triclinic crystals of disodium succinate are more complex than those observed in monoclinic crystals. At 77°K, three species coexist, $^-O_2CCH_2CH_2\dot{C}O_2^{2-}$ (1), a distorted conformation of the radical $^-O_2C(\dot{C}HCH_2)^*CO_2^-$ (2), and an unidentified radical X. On warming to room temperature, 1 and X disappear, while 2 changes to a more stable conformation $^-O_2C\dot{C}HCH_2CO_2^-$ (3). In addition the species CO_2^- (4), and $^-O_2C\dot{C}HCH_3$ (5) were produced. On further warming to 40°C, species 4 disappeared while at the same time species 3 increased in intensity. Radical 5 remained unaffected. Possible mechanisms and comparisons with monoclinic crystals are discussed. (auth) (Canada)

2231 IN-FIELD BEHAVIOR OF AND CUMULATIVE EFFECTS ON CERTAIN ELECTRODES IN A GAMMA FIELD. Kubota, Hisashi (Oak Ridge National Lab., Tenn.). Anal. Chem.; 42: 1593-6(Nov 1970).

The effect of a gamma radiation field on the response of the saturated calomel, glass, fluoride specific, and nitrate specific electrodes was studied. All four electrodes gave reliable readings in gamma-radiation fields as high as 15,000 rad/min. The calomel electrode was unaffected by cumulative dose up to 10^8 rad. The glass electrode was somewhat affected by large dose to give readings to the high pH direction. The potential response of the fluoride electrode shifted in one instance; however, the Nernstian slope remained unaffected. As a result, the affected electrode did not lose its effectiveness as long as calibrations were made periodically with standard solutions. The nitrate electrode began to give erratic readings as the cumulative dose approached 10^7 rad. Replacing the internal standard by fresh solution restored this electrode. The radiation stability of any internal reference solution is a prime factor that governs the behavior of an electrode in a radiation field. The calomel and glass electrodes were stable in solutions of high alpha activity at least up to dose of 10^8 rad. (auth)

2232 CHEMILUMINESCENCES OF AQUEOUS Tl^I SOLUTIONS PRODUCED BY IRRADIATION WITH 8.5-keV X RAYS. Steffen, G.; Sommermeyer, K. (Univ., Freiburg i. B.). Biophysik, 6: 123-36(1969). (In German).

The luminescence of aqueous solutions of Tl^+ during irradiation with 8.5-keV x rays was investigated. In particular the Tl^+-luminescence in neutral solutions, acid solutions, alkaline solutions, and solutions containing various concentrations of NaCl, was studied. On varying the pH the luminescence yield passed a maximum on the acid side as well as on the alkaline side (at pH = 3.4 respectively pH = 12). Compared with neutral solutions the luminescence yield was increased by a factor 2 to 3 at these pH values. By adding 1 M NaCl to neutral Tl^+-solutions the luminescence yield was enhanced by a factor five, however in relation to pH no further increase was observed, but only quenching of the luminescence at low and high pH. The luminescence originates from the formation of Tl^{++} by the reaction of e_{aq} with Tl^{2+} formed by oxidation of Tl^+ by OH. However, Tl^{2+} is not formed directly by $Tl^+ + OH \rightarrow Tl^{++} + OH^-$ but via dissociation of the intermediate Tl^+OH after a delay $>10^{-7}$ sec. The increase of the luminescence yield in acid solutions is explained by the reaction $Tl^+OH + H^+ \rightarrow Tl^{2+} + H_2O$ and in alkaline solutions by the reaction $Tl^+OH + OH^- \rightarrow Tl^{2+} + O^{2-} + H_2O$. In alkaline solutions the luminescence spectrum

shifts to longer wavelengths; it was concluded that this spectrum is attributed to $Tl^{+*}O^{2-}$. Evidently the reaction of Tl^+Cl^- and Tl^+Cl_2 —with OH leads to formation of $Tl^{2+}Cl^-$ and $Tl^{2+}Cl_2^{2-}$ without any efficient delay. (auth)

2233 LUMINESCENCE OF AQUEOUS Tl^1-SOLUTIONS AFTER IRRADIATION WITH PULSES OF 10 MeV ELECTRONS. Steffen, G. (Univ., Freiburg i. B.); Cercek, B. Biophysik, 6: 137-44(1969).

The luminescence of deaerated aqueous Tl_2SO_4 solutions after irradiation with 50- and 500-nsec pulses of 10-MeV electrons was investigated for doses of 100 and 1000 rad per pulse, respectively. The effect of the pH of solutions and of the scavenging of e^-_{aq} and OH radicals on the luminescence was studied. The luminescence in neutral and acid solutions is due to: the de-excitation of Tl^{++*}_{aq} produced during the pulse of radiation (probably by optical excitation); and the chemoluminescence in which the excitation of Tl^+_{aq} is produced via the sequence of reactions $Tl^+_{aq} + OH \rightarrow Tl^{++}_{aq} + OH^-$ followed by $Tl^{++}_{aq} + e^-_{aq} \rightarrow Tl^{+*}_{aq}$. From the decay of the luminescence obtained with low doses of radiation the half-life of the Tl^{++}_{aq} emission was calculated to be $T_{\frac{1}{2}} = 4.2 \times 10^{-7}$ sec. The time-characteristics and the total yield of the chemoluminescence per pulse are pH dependent; thus, 3 μsec after the pulse the intensity of the luminescence is strongly enhanced by increasing the H^+_{aq} concentration. The pH dependence of the luminescence and of the optical absorption spectra of the transients suggests that the OH radicals react with Tl^+_{aq} ions to yield first the long-lived $TlOH^+_{aq}$ intermediate which is converted by a fast reaction with H^+_{aq} to Tl^{2+}_{aq}. The emission of the Tl^{+*}_{aq}, especially that of the Tl^{++}_{aq} produced during the pulse of radiation, is in alkaline solutions progressively quenched by increasing concentrations of the OH^-_{aq} ions. There is concomitantly a bathochromic shift of the chemoluminescence; the maximum of the emission being at 465 nm. The total yield of the chemoluminescence per pulse in a 10^{-4} M OH^-_{aq} solution is about three times that in a neutral solution; the yield is strongly enhanced by increasing the OH^-_{aq} concentration. The chemoluminescence in alkaline solutions is likely to be due to the $Tl^{+*}O^{2-}_{aq}$ specie produced via the sequence of reactions $Tl^+_{aq} OH + OH^-_{aq} \rightarrow Tl^{2+}O^{2-}_{aq} + H_2O$ and $Tl^+_{aq} + O^-_{aq} \rightarrow Tl^{2+}O^{2-}_{aq}$ followed by $Tl^{2+}O^{2-}_{aq} + e^-_{aq} \rightarrow Tl^{+*}O^{2-}_{aq}$. (auth)

2234 PARACRYSTALLINE STRUCTURE OF POLYMER-CRYSTAL LATTICE DISTORTION INDUCED BY ELECTRON IRRADIATION. Nagasawa, Toshio (National Bureau of Standards, Washington, D. C.); Kobayashi, Keinosuke. J. Appl. Phys.; 41: 4276-84(Oct 1970).

From Meeting of the American Physical Society, Los Angeles, Calif., and Dallas, Tex. See CONF-691222; CONF-700329.

The melting temperature of polyethylene crystals decreases and the lattice constants (both a and b) and lattice distortion increase, but the macroscopic volume of the specimen does not change with electron irradiation. From these results a model of a deformed lattice structure with point defects produced by irradiation is proposed. Calculations indicate that the anisotropy of a polymer crystal (difference between the elastic modulus along the molecular axis and perpendicular to the axis) increases the range of the distortion in a crystal caused by a defect. The presence of lattice distortion in electron irradiated polymer single crystals produces observable features in the Moiré patterns obtained from the crystals. (auth)

2235 SHAPE OF THERMOLUMINESCENCE GLOW PEAKS IN MOLECULAR SOLIDS. Butterfield, A. W.; Ericson, L. G. (Univ. of Adelaide). Mol. Cryst. Liquid Cryst.; 11: 145-54 (Sep 1970).

Existing physical models predicting the profile of thermoluminescence glow peaks are critically examined and extensions of these models are tested against experimental data for one glow peak from the organic solid hexamine. It is pointed out that gross departures of the experimental data from the Randall and Wilkins curve must lead to the rejection of models based on the annealing of isolated centers such as self-trapped excitons. All reasonable departures from this model introduce the concept of retrapping and so are applicable to a physical situation involving electrons and positive holes trapped in physically separated centers. A simple test for departure from the Randall and Wilkins model was found in the comparison of experimental activation energies derived from the initial rise of the luminescence intensity with those given by other methods based on peak shifts or peak widths. (auth) (UK)

2236 KINETICS OF ISOTHERMAL ANNEALING OF GAMMA-IRRADIATION DAMAGE IN CRYSTALLINE LEAD NITRATE. Mohanty, S. R.; Nair, S. M. K. (Utkal Univ., Bhubaneswar, India). Indian J. Chem.; 8: 158-61(Feb 1970).

The annealing of γ-irradiation damage in crystalline lead nitrate at different temperatures in the range 140 to 230°C is a combination of a first-order process affecting a small proportion of the fragments and a second-order process, with a higher energy of activation, governing the behavior of the remainder. The mean values of the proportions of the original nitrite, which recombine by the first and the second order mechanisms, are respectively 12.7 and 87.3%. As expected, these values are independent of temperature. (auth)

Radiation Processes

2237 (N–70–32826) RADIATION-INDUCED PREPARATION OF METALS FROM THEIR AQUEOUS SALT SOLUTIONS. Philipp, Warren H.; Marsik, Stanley J. (National Aeronautics and Space Administration, Cleveland, Ohio. Lewis Research Center). Jul 1970. 14p. (NASA-TN-D–5880; E–5623). NTIS.

Eleven metals (copper, zinc, cadmium, thallium, tin, lead, antimony, nickel, cobalt, iron, and palladium) were prepared from their aqueous salt solutions by irradiation with 2-MeV electrons. In the more successful attempts, the metal yields nG(M) (atoms per 100 eV multiplied by the valence change n) averaged about 2. The yields are interpreted in terms of the radical scavenging mechanism and the chemistry of the metal system involved. (auth) (STAR)

2238 IMPROVEMENT OF WOOD BY PLASTIC IMPREGNATION. Lunde, Gulbrand (Central Inst. for Industrial Research, Oslo). Kjemi; 30: No. 8, 20-2(24 Sep 1970). (In Norwegian).

The improvement of the properties of wood as a structural material by impregnation with a plastic monomer and subsequent polymerization, principally radiation-induced, but also catalytic, is discussed. The choice of monomers and the suitability of native Norwegian woods for such treatment are briefly mentioned. The application of ^{60}Co irradiation is described and also the use of electron beams for surface treatment. Some present and possible future applications of plastic-impregnated wood are discussed. (Norway)

2239 RADIATION-INDUCED ISOMERIZATION OF [2,2,1]-BICYCLOHEPTADIENE (NORBORNADIENE) TO [2,2,1,$0^{2,6}$,$0^{3,5}$]-QUADRICYCLOHEPTANE (QUADRICYCLENE) IN CYCLOHEXANE SOLUTIONS. van Ingen, J. W. F.; van Tieghem, C. H. C.; Cramer, W. A. (Interuniversitair Reactor Instituut, Delft, Netherlands). J. Chem. Phys.; 53: 3665-74(1 Nov 1970).

Radioinduced isomerization of norbornadiene (NBD) into quadricyclene (Q) was studied in cyclohexane solutions. From the effects of charge and radical scavengers it could be concluded that at low NBD concentrations isomerization is initiated by a reaction of NBD with electrons and probably proceeds via singlet excited NBD. Low yields of Q show that this is not an efficient process. At higher NBD concentrations the isomerization becomes more efficient, indicating that other reactions may begin to contribute. Selfquenching of NBD* also becomes important at higher concentrations. In the presence of SF_6, electron transfer from NBD^- to this second solute occurs. Enhanced isomerization yields are observed in the presence of benzene, toluene, and acetophenone. Scavenger studies indicate that triplet-excited states of these solutes contribute to this increase in G(isom). They are formed by charge transfer from cyclohexane positive ions to the aromatic additives followed by neutralization. Complex formation between triplet-excited aromatic molecules and NBD is suggested to be an essential step in the isomerization reaction. (auth)

2240 GAMMA-RAYS INDUCED GRAFT COPOLYMERIZATION OF POLY(ETHYLENE TEREPHTHALATE) WITH ACRYLIC AND METHACRYLIC ACIDS. PART I. THE EFFECT OF RADIATION AND GRAFTING CONDITIONS. MECHANISM OF THE REACTION. Robalewski, Andrzej M.; Stolarczyk, Lech W. (Inst. of Nuclear Research, Warsaw). Nukleonika; 15: 55-68 (1970).

The efficiency of grafting polyethylene terephthalate (PETP) with acrylic and methacrylic acids, which depends on the conditions of polymer irradiation in a gamma source, has been tested as well as the efficiency of the grafting reaction in aqueous solutions of the monomers. It has also been found that during exposition in an oxygen atmosphere peroxide bonds able to initiate the copolymerization reaction are formed. (auth)

2241 EFFECT OF THE TYPE OF POLYETHYLENE ON THE GRAFTING OF STYRENE ON POLYETHYLENE. II. GRAFTING INITIATED BY PRE-IRRADIATION IN AIR AND BY CHEMICAL INITIATORS. Ranogajec, F.; Dvornik, I.; Dobo, J. (Inst. Ruder Boskovic, Zagreb. Research Inst. for Plastics, Budapest). Eur. Polym. J.; 6: 1179-85(Aug 1970).

Low and high density polyethylenes were irradiated in a cobalt-60 source in air at a low dose rate. Differences in behavior in grafting were observed. The form of the kinetic curves, the tem-

perature effect, and the effects of the foil thickness suggest that there are different grafting mechanisms depending on the type of polyethylene. It was concluded that the grafting reaction is initiated by peroxides in low density polyethylene and by free radicals in high density polyethylene. When graft copolymerization was initiated by chemical initiators such as azoisobutyronitrile and benzoyl peroxide, in all cases higher grafting rate was obtained for low density polyethylene. It is assumed that chain transfer to branched low density polyethylene is much more effective than that to linear polyethylene. Thicker foils were grafted at a higher rate in low density polyethylene. The thickness effect often observed in polyethylene grafting must be mainly ascribed to structural differences, affecting the termination rate constant. (auth)

2242 EFFECT OF THE TYPE OF POLYETHYLENE ON THE GRAFTING OF STYRENE ON POLYETHYLENE. I. DIRECT RADIATION GRAFTING AND GRAFTING BY PRE-IRRADIATION IN VACUO. Ranogajec, F.; Dvornik, I.; Dobo, J. (Inst. Ruder Boskovic, Zagreb. Research Inst. for Plastics, Budapest). Eur. Polym. J.; 6: 1169-77(Aug 1970).

The influence of the type of polyethylene on the rate and yield of grafting of styrene was studied by using simultaneous irradiation with γ rays and also pre-irradiation in vacuo. By both methods, the grafting yield was found to be higher in high density polyethylene, except at low temperature with thick samples. The effects of the foil thickness were the same for both methods: the grafting yield generally increased with increase in foil thickness. It was assumed that the advantageous effect of higher crystallinity and of greater thickness on the grafting rate can be explained by the greater rigidity of the polymeric matrix. This causes a lower degree of swelling, a greater gel effect, and perhaps a better utilization of the radicals. In these cases, the structure of the polyethylene affects kinetic parameters, mainly the termination rate constant. During grafting, probably through the mechanical action of the growing and swelling chains, some free radicals trapped in the crystalline regions may become accessible for grafting. The creation of new grafting sites was not excluded. A rise in temperature diminished the rigidity of the matrix: the overall grafting rate decreased and the effects of crystallinity and of sample thickness became less marked. By further increase of the rigidity of the matrix, the pressure exerted by the growing and swelling chains was incapable of loosening the structure. The grafting became limited by the structure; only low grafting yields and rates could be obtained. This was the case with high density polyethylene at low temperature, where the grafting yield decreased steeply with thickness. As could be expected, a rise in temperature had, in this case, the opposite effect on the rate: grafting was favored at higher temperatures. (auth)

2243 RADIATION CURING OF COATING. Hirose, Kazutoyo (Dainippon Ink Inst. of Chemical Research, Urawa, Japan). Shikizai Kyokaishi; 43: 168-78(Apr 1970). (In Japanese).

Advances in the paint industry are divided into two factors; namely, the improvement of paints and of painting techniques and drying-hardening techniques. In the latter factor, the radiation curing by electron beams is attracting increasing interest because of rapid painting and drying. This trend is accentuated by the recent development of the high-output low-price accelerators of low-energy electrons. The practical utilization of radiation curing in the paint industry is thus expected in the near future. The following are described: the present state of radiation curing; the principle and feature of the technique; low-energy accelerators; the mechanism of radiation curing; the paints used for radiation curing, including monomers, unsaturated polyester resin, and acrylic polymers; the influence of dose rate; the application as paints; and the future prospects. (Japan)

2244 RADIATION INDUCED GRAFT TERPOLYMERIZATION OF POLY(ETHYLENE TEREPHTHALATE). PART I. RADIOLYSIS OF THE POLYESTER AND GRAFTING KINETICS. Stolarczyk, Lech W.; Achmatowicz-Szmarjke, Teresa (Inst. of Nuclear Research, Warsaw). Nukleonika; 15: 97-106(1970).

The radiolysis of poly(ethylene terephthalate) was carried out and the radiolytic yields of hydrogen gas and those of terminal carboxyl groups were estimated. The kinetics of graft terpolymerization of the polyester in aqueous solution of acryl- or methacrylamide and unsaturated dicarboxylic acids performed simultaneously in the course of irradiation was investigated. The radical mechanism of the processes involved is proposed. (auth)

2245 TEMPERATURE EFFECTS IN THE GAMMA-INITIATED POLYMERIZATION OF STYRENE. Sood, S. P.; Hodgins, J. W. (Univ. of Hawaii, Hilo. McMaster Univ., Hamilton, Ont.). J. Polym. Sci., Part B; 8: 529-30(Aug 1970).

The effects of temperature on γ-radioinduced reactions of styrene carried out to complete polymerization were investigated. Sigmoid conversion curves were obtained for polymerization carried out at 50, 74, and 89°C for dose rates of 0.09, 0.21, and 0.64 megarads per hour (of 1.3 MeV γ radiation). At about 10% conversion and 74°C the polymerization rate (R_p) and the average degree of polymerization (D_p) began to be less dependent upon dose rate. At 109°C, R_p and D_p are independent of dose rate. (J.G.B.)

2246 ROLE OF HYDROGEN ATOMS IN FREE RADICAL SITE MIGRATION. Horan, P. K.; Snipes, W. Int. J. Radiat. Biol.; 17: 201-3(1970).

Experiments are described, which were carried out on hexachlorethane, checked by infra-red spectroscopy for freedom from OH and CH bonds. The samples were sealed in a quartz tube under 1 atmosphere of nitrogen and irradiation was carried out with 6.5-MeV electrons from a linear accelerator at a dose rate of 1 MR/min at room temperature. Subsequently EPR spectra showed that site migration could occur by a process that does not involve hydrogen atoms. (UK)

2247 RADIATION-INDUCED REACTIONS WITH CELLULOSE. VIII. EFFECT OF ADDITIVES ON COPOLYMERIZATION WITH STYRENE USING THE SIMULTANEOUS TECHNIQUE. Dilli, S.; Garnett, J. L. (Univ. of New South Wales, Kensington, Australia). Aust. J. Chem.; 23: 1767-77(Sep 1970).

The effects of additives on the grafting of styrene to cellulose was studied for the system cellulose–styrene–methanol irradiated in air at dose-rates ranging from 0.045 to 0.77 Mrad/hr in a cobalt-60 facility. The additives included glycol, acetic acid, ethyl acetate, chloroform, acetone, aniline, benzaldehyde, hydroquinone, thiourea, thiophene, pyridine, benzene, naphthalene, pyrene, phenanthrene, durene, hexamethylbenzene, stilbene, acridine, and fluoro-, chloro- and bromobenzene. At a low concentration (10^{-2} M) of the non-aromatic additives, a reduction in grafting yields was observed whereas at a higher concentration (10^{-1} M) of the same additives sensitization was common. Radical scavengers such as hydroquinone and thiourea suppressed grafting provided their concentration in the grafting solution was sufficiently high. With the aromatic additives, little change in grafting yields was observed except for anthracene and acridine. Possible reaction mechanisms are discussed. Preliminary studies are also reported for the effects on grafting of chemically bound lignin and non-cellulosic material present in the trunk polymer. (auth) (Australia)

2248 CRYSTAL STRUCTURE OF THE COMPOUNDS U_2N_2X AND Th_2N_2X WITH X = Sb, Te, AND Bi. Benz, Robert (Los Alamos Scientific Lab., N. Mex.); Zachariasen, W. H. Acta Crystallogr., Sect. B; 26: 823-7(1970).

The compounds U_2N_2Sb, U_2N_2Bi, U_2N_2Te, Th_2N_2Sb, Th_2N_2Bi, and Th_2N_2Te were prepared and found, from x-ray diffraction powder patterns, to form body-centered tetragonal crystals (space group I4/mmm). Data on unit-cell parameters are tabulated. The atomic positions are 2Sb, 2Bi or 2Te in (000) $(\frac{1}{2}\frac{1}{2}\frac{1}{2})$ and 4 metal atoms in (000) $(\frac{1}{2}\frac{1}{2}\frac{1}{2}) \pm (00u)$. The probable positions of the 4N atoms are (000) $(\frac{1}{2}\frac{1}{2}\frac{1}{2}) \pm (\frac{1}{2}0\frac{1}{4})$. Nitrogen in the Th_2N_2Sb crystal lattice can be replaced to an appreciable extent by oxygen. Saturated with oxygen, the compound has a composition given by the formula $Th_2(N_xO_{1-x})_2Sb$ and the lattice parameters $a_0 = 4.041 \pm 0.001$ and $c_0 = 12.84 \pm 0.01$ Å. Oxygen solubility and its effect on lattice parameters is considerably less in Th_2N_2Bi and is not at all perceptible in the remaining four compounds. (auth)

2249 PREVENTION OF STRESS RUPTURE FORMATION OF THERMOPLASTICS BY RADIATION CROSS-LINKING. Langbein, W.; Fischer, H. (Deutsches Kunststoff-Institut, Darmstadt, Ger.). Kunststoffe; 60: 256-61(1970). (In German).

The stress-rupture formation in plastic parts which are simultaneously exposed to aggressive media and stresses has an essential practical signification. This susceptibility could be reduced by high-energy radiation because irradiation cross-links some important plastics and increases their molecular weight. High-pressure and low-pressure polyethylene, isotactic polypropylene, polystyrene, 6,6-polyamide, and hard and soft PVC were irradiated with 1 MeV electrons at 14°C in dose range 1 to 110 MRad/hr. An increase in stress-rupture stability was obtained only in the case of polyethylene and to a smaller extent in polystyrene. At 5 MRad the durability was increased by factors of 1000 to 10,000, at 20 MRad practically unlimited durability was obtained. The irradiation costs were approximately 1 Pfg/kg and MRad for Van de Graaff accelerators. The loading capacity was increased by a time factor of 10 to 20 at 5 MRad and 30 to 1500 at 20 MRad according to the stress-rupture test. The improvement in stress-rupture stability was better for highly oriented polyethylene than for less oriented ones. Relative thick samples can be irradiated in air using high dose rates with negligible oxidative degradation effects. (INIS)

XUM

2250 RADIATION CHLORINATION OF POLYMERS. Dzhagatspanyan, R. V.; Korolev, B. M. Vysokomol. Soedin., Ser. A; 12: 1809-16(Aug 1970). (In Russian).

The analysis of results on diffusion kinetics of radiation chlorination of powdered polyethylene and polypropylene shows that inhomogeneity of the chlorination mainly resulted from chlorination of the amorphous regions and may be increased owing to the diffusion character of the process. (auth)

2251 SELECTED PAPERS IN HIGH-POLYMER PHYSICS. Meeting of the American Physical Society, 29–31 December 1969, Los Angeles, California, 23–26 March 1970, Dallas, Texas. J. Appl. Phys.; 41: 4248-4378(Oct 1970). (CONF-691222; CONF-700329).

Nineteen papers were presented as part of the program of the Division of High-Polymer Physics. Separate abstracts were prepared for two of the papers. (D.H.M.)

For abstracts of individual papers see: 2234 and 2252.

2252 POLYOXYMETHYLENE CRYSTALS GROWN WITHIN IRRADIATED TRIOXANE CRYSTALS. Colson, James P.; Reneker, Darrell H. (National Bureau of Standards, Washington, D. C.). J. Appl. Phys.; 41: 4296-4313(Oct 1970).

From Meeting of the American Physical Society, Los Angeles, Calif., and Dallas, Tex. See CONF-691222; CONF-700329.

The morphological development of polyoxymethylene crystals polymerized from and grown within trioxane crystals was observed following irradiation of the trioxane with alpha particles and a subsequent heat treatment. A novel method of sample preparation enabled the morphology to be observed in detail and resulted in the discovery of new forms of polyoxymethylene crystals as well as an improved description of previously reported forms. A solid–gas–solid crystal growth mechanism was postulated to account for the predominantly acicular habit of the polyoxymethylene crystals. (auth)

2253 RADIATION-INDUCED POLYMERIZATION OF TRIOXANE. Rao, M. H.; Rao, K. N. (Bhabha Atomic Research Centre, Bombay). J. Polym. Sci., Part B; 8: 643-4(Sep 1970).

Studies on the γ-radioinduced polymerization of trioxane showed that it is possible to get reproducible data and also complete conversion of the monomer into the polymer due to the removal of impurities, presumably water, by molecular sieves. It was clearly established that the impurities play an important role in the ionic polymerization even in the solid state. (P.C.H.)

2254 PREPARATION OF WOOD-PLASTIC COMBINATIONS ON THE BASIS OF UNSATURATED POLYESTER RESINS. II. EFFECT OF TEMPERATURE. Pesek, Miroslav; Pultar, Frantisek; Jarkovsky, Jaroslav (Inst. for Research, Production, and Uses of Radioisotopes, Prague). Jad. Energ.; 16: 261-9 (Aug 1970).

Attention was devoted to the possibility of increasing the styrene content in the impregnation mixture by irradiation at elevated temperature. The styrene conversion and hardness of wood-plastic combinations were measured after irradiation in relation to radiation dose. Under higher temperature, the polymerization proceeded more quickly and so it was observed that with a 70% styrene content in a polyester resin, the complete polymerization of monomer mixture occurred at 80°C, with as low a dose as 1 Mrad. The wood-plastic combinations can be prepared from polyesters by different combined procedures. Two kinds of two-stage processes are described. In the first one, impregnated wood was first irradiated with low doses of radiation and than postcured at 80°C. Another procedure allowing a low radiation dose is a combined method of curing by means of high energy radiation and chemical initiators of polymerization. Similar results were obtained when using different kinds of wood and various types of polyester resins. It was found that dyes affect radiation polymerization of polyester resins. Therefore the effect of dyes on radiation polymerization of polyester resins in beech wood was studied. (auth)

2255 ARYLATION OF NITROBENZENE INDUCED BY γ-RADIATION. Knight, J. A. (Georgia Inst. of Tech., Atlanta). Radiat. Res.; 44: 50-8(Oct 1970). (ORO–3519-4).

Phenylation and nitrophenylation take place during γ radiolysis of nitrobenzene to produce the three isomeric nitrobiphenyls and the six isomeric dinitrobiphenyls (one nitro group per phenyl ring), respectively. For the radiolytic phenylation and nitrophenylation, all positions of nitrobenzene are attacked and ortho-para substitution is favored over meta substitution. This is in general agreement with the free radical arylation of aromatic compounds. Relative reactivities for the radiolytic phenylation of nitrobenzene were obtained, and the radiolytic phenylating intermediates show less ortho-para selectivity than the phenyl radical. The relative reactivities for the radiolytic phenylation were not in quantitative agreement with the relative reactivities reported for the free radical phenylation of nitrobenzene. The results of irradiations of nitrobenzene with DPPH scavenger show that both the scavenged and non-scavenged precursors for the formation of the nitrobiphenyls exhibit about the same relative reactivities. (auth)

2256 RADIATION-INDUCED POLYMERIZATION OF ISOBUTYLENE OXIDE. Bauer, R. S.; Spooncer, W. W. (Shell Development Co., Emeryville, Calif.). J. Polym. Sci., Part A-1; 8: 2971-7(Oct 1970).

In the absence of oxygen, liquid isobutylene oxide is polymerized by high energy radiation. The resultant polyethers may possess the same gross structures as those prepared by Lewis acid catalysis: $(CH_3)_2C(\diagup O\diagdown)CH_2 \rightsquigarrow (CH_3)_2C-CH_2-O\rangle_n$. The reaction is characterized by a small, apparent activation energy (2.7 kcal/mole), a polymerization rate proportional to the first power of the dose rate, inhibition by Lewis bases, and moderate inhibition by free-radical scavengers. The molecular weights of the polymers increase with decreasing temperatures of polymerizations. These results are discussed in terms of a cationic propagation mechanism. (auth)

Radiolysis

Refer also to abstracts 2588 and 3191.

2257 (CEA-R–4046) RADIOLYSIS OF CONCENTRATED NITRATE AND FORMATE SOLUTIONS. Hickel, Bernard (Commissariat a l'Energie Atomique, Saclay (France). Centre d'Etudes Nucleaires). Aug 1970. 64p. (In French). Dep. NTIS (U. S. Sales Only).

Thesis. Submitted to Paris Univ., France.

The influence of potassium nitrate and sodium formate on the decomposition of γ-irradiated water was studied. Radical and molecular yields were studied as a function of the concentration of the scavengers and their variation was compared with the theoretical prediction of the spur model. The influence of oxygen and the effects of γ rays on the scavengers were also investigated. The results obtained show that the yields of H_2, H_2O_2, and atomic hydrogen decrease as a function of the concentration of the scavengers, and the yield of solvated electrons and OH radicals increases. The total yield of decomposition of water increases to 4.6 ± 0.3. (France)

2258 (DP-Report-447) X-RAY IRRADIATION OF HELIUM CONTAINING GASEOUS IMPURITIES. Project DRAGON. Nencini, G. (Atomic Energy Establishment, Winfrith (England)). Jul 1966. 20p. Dep. NTIS.

Results of a study of the radiolysis of impurities in helium show that the effect of x radiation on helium–carbon dioxide mixtures is qualitatively the same as the effect of in-pile radiation, and a preliminary estimate indicates rough quantitative agreement also; the extent of the radiolysis is determined by energy transfer from the helium rather than by direct absorption of energy in the impurity; and yields in the ^{14}C exchange process between carbon monoxide and carbon dioxide are proportional to the integrated x-ray dose. (D.H.M.)

2259 (GA–10208) PULSE RADIOLYSIS STUDIES OF AQUEOUS SOLUTIONS OF AMINOTHIOLS AND COMPOUNDS RELATED TO NUCLEIC ACID. Three-Year Summary Report. Theard, L. M.; Peterson, F. C.; Voigt, R. L. (Gulf General Atomic, Inc., San Diego, Calif.). 15 Jun 1970. Contract AT(04-3)-167. 180p. Dep. NTIS.

Developments are reported for studies on: nanosecond pulse radiolysis of aqueous thymine solutions; and steady state and pulse radiolysis of aqueous chloride solutions of nucleic acid components. Copies of several articles previously published in journals are also included. Most of the experimental work reported was performed by the pulse radiolysis technique employing the 17-MeV Linac and associated experimental apparatus at Gulf General Atomic, San Diego, California. The major goal of this research is the elucidation of indirect mechanisms by which ionizing radiation induces chemical transformations in nucleic acid, its components, and related compounds, and in aminothiols and radiation sensitizing agents. (P.C.H.)

2260 (IRI–133-70-2) SLOW ELECTRONS AND NEGATIVE IONS IN ORGANIC LIQUIDS. Hummel, A. (Interuniversitair Reactor Instituut, Delft (Netherlands)). [1969]. 19p. (CONF-700610–10). Dep. NTIS (U. S. Sales Only).

From 4th International Congress of Radiation Research, Evian, France.

A simplified model of the behavior of charged entities in the

track of a fast electron slowing down in a liquid, based on a predominant contribution of pairs of charged species that can be treated with classical diffusion theory, is discussed. Comparison of the theory with results from measurements of the electric conductance of liquids under irradiation and from the observation of ions formed during a short burst of irradiation yields information about the spatial distribution and the behavior of the charged species in the track of a fast electron. (auth)

2261 (NP-18518) EFFECTS OF GAMMA RADIATION ON THE GAS YIELDS AND CRYSTALLINITY OF POLYTETRAFLUOROETHYLENE. Report 360. Pinkerton, D. M.; Sach, B. T. (Defence Standards Labs., Maribyrnong (Australia)). Apr 1970. 27p. Dep. NTIS (U. S. Sales Only).

Polytetrafluorethylene (PTFE) was γ irradiated in the presence of gaseous radical scavengers. Irradiations in vacuo resulted in small yields of low-molecular-weight fluorocarbons. The presence of CH_4 during irradiation led to $G(CH_3F) = 0.06$. Although H_2 is a major product from the radiolysis of C_2H_4, none could be detected when PTFE–C_2H_4 mixtures were irradiated. $G(H_2)$ from PTFE–CH_3SH was significantly reduced from that expected from CH_3SH alone. Both C_2H_4 and CH_3SH scavenged PTFE radicals and it is suggested that H atoms react rapidly with the polymer radicals, O_2 caused a marked increase in G(gaseous products); the additional gas being due almost entirely to the formation of CF_2O. The crystallinity of PTFE was found to increase with radiation dose in the order O_2 > vacuo > CH_3SH > C_2H_4. Initiation of a polymerization reaction of C_2H_4 by PTFE radicals is considered to explain the low rate of crystallinity increase observed in C_2H_4. The results were found to be consistent with the view that permanent scission is a predominant reaction in irradiated PTFE. However, the extent of the degradation appears to depend on recombination of fragments resulting from chain scission. By interfering with the recombination processes, O_2 and CH_3SH accelerate the rate of degradation in relation to PTFE irradiated in vacuo. (auth) (Australia)

2262 (RD/B/N-1279) γ-RADIOLYSIS OF CARBON MONOXIDE IN THE PRESENCE OF γ-ALUMINA. Russell, R. D. (Central Electricity Generating Board, Berkeley (England). Berkeley Nuclear Labs.). Jun 1970. 31p. Dep. NTIS (U. S. Sales Only).

Rapid chemisorption of carbon monoxide is observed when the gas is γ-irradiated in the presence of γ-alumina. This is explained by the formation of active surface sites by the energy absorbed by the alumina onto which the gas is adsorbed. Carbon dioxide, most probably formed by reaction of carbon monoxide with a surface oxygen atom, is recovered, as are also carbon monoxide and hydrogen, when the alumina is heated after the irradiation. (auth) (UK)

2263 (RD/B/N-1748) APPARATUS FOR THE STUDY OF RADIOLYTIC CARBON DEPOSITION FROM THE GAS PHASE. Sach, R. S.; Skinner, R. F. (Central Electricity Generating Board, Berkeley (England). Berkeley Nuclear Labs.). Jul 1970. 22p. Dep. NTIS (U. S. Sales Only).

A description is given of an apparatus designed to study the deposition of ^{14}C-labeled gas mixtures, containing CH_4, CO, or inactive gas, under γ radiation at temperatures up to 900°K and pressures up to 40 bars. The deposit is determined using simple oxidation techniques and counting the $^{14}CO_2$ produced. The analytical equipment is fully automatic. (UK)

2264 POSITIVE ION SCAVENGING IN THE RADIOLYSIS OF LIQUID CHLOROFORM. Baxter, J. N.; Bibler, N. E. (E. I. du Pont de Nemours and Co., Aiken, S. C.). J. Chem. Phys.; 53: 3444-9(1 Nov 1970).

The effects of the positive ion scavengers NH_3 and n-C_4H_9OH, on the organic product yields in the radiolysis of liquid $CHCl_3$ at 25°C were investigated. As the solute concentrations increased the values for $G(CH_2Cl_2)$, $G(C_2HCl_3)$, and $G(C_2Cl_6)$ increased, G sym-$C_2H_3Cl_3$) and $G(C_2Cl_4)$ remained unchanged, and $G(CCl_4)$ decreased. These results are consistent with a free radical mechanism for all the radiolysis products except CCl_4. The decrease in $G(CCl_4)$ indicates that CCl_4 is formed by a secondary positive ion reaction. The concentration dependence of this decrease can be described by the expression: $G(CCl_4)_o - G(CCl_4)_s = G(CCl_4)_o((\alpha[S])^{1/2}/\{1 + (\alpha[S])^{1/2}\})$, where $G(CCl_4)_o$ is the 100-eV yield in the absence of a scavenger, and α is an empirical parameter proportional to the reactivity of the solutes, and [S] is the concentration of the scavenger in moles per liter. Values of α were determined for each solute and compared to published values determined in cyclohexane. In chloroform, values for α were 4 to 19 times larger than in cyclohexane suggesting that the solutes are more efficient in the alkyl halide than in the hydrocarbon. One mechanism accounting for this efficiency increase is the formation of anions by the free electrons in the alkyl halide. This anion formation increases the average lifetimes of the ions in the alkyl halide and hence the efficiencies of the scavengers. The increase in the 100-eV yields of three of the products formed by the free radical mechanism indicates that the presence of a cation scavenger increases the radical yields. Thus, some of the charge neutralizations in pure $CHCl_3$ do not produce radicals. This observation is in accord with the existence of the collisionally stabilized $CHCl_3^-$ anion in the irradiated solutions. It is suggested that this anion may be an intermediate in the formation of CCl_4. (auth)

2265 RADIOLYSIS OF AQUEOUS SULPHURIC ACID SOLUTIONS. FORMATION OF PERSULPHATES IN GAMMA RADIATION FIELD. Sobkowski, Jerzy (Univ., Warsaw). Nukleonika; 15: 89-95(1970).

The radiolysis of 1 to 8 mole $\times$ 1^{-1} aqueous sulfuric acid solutions was studied. The persulfates formed were determined polarographically and hydrogen peroxide spectrophotometrically. The initial radiation yield of H_2O_2 formation decreased with the H_2SO_4 concentration increase. The respective yield of persulfate formed increased first with H_2SO_4 concentration, and reached a maximum at ~4 mole $\times$ 1^{-1}. The maximum resulted from the concurring processes of persulfate formation by irradiation of HSO_4^- ions and hydrolysis of the persulfates formed, the velocity of the latter reaction increasing with the growing concentration of hydrogen ions. A probable mechanism of the reaction of formation and decomposition of persulfates in the system studied is proposed. (auth)

2266 RELATION BETWEEN THE MASS SPECTRA AND THE REACTION PRODUCTS OF ELECTRON-IRRADIATED AROMATIC KETONES. Schaefer, L.; Ezell, R. D.; Green, G. L.; Jefferson, T. C.; Southern, J. F. (Univ. of Arkansas, Fayetteville). J. Chem. Soc., D; No. 17, 1127-8(9 Sep 1970).

Products from electron irradiation of aromatic ketones corresponded closely to the main patterns of the mass spectra of these ketones. In the irradiation of liquid acetophenone, propiophenone, n- and iso-butyrophenone, and valerophenone with 5- to 10-keV electrons the main reaction products were benzene (50%), toluene (50%), and traces of ethylbenzene in the case of acetophenone; benzene (71%), toluene (12%), and ethylbenzene (17%) in the case of propiophenone; mainly benzene, toluene, ethylbenzene, and traces of n- and iso-propylbenzene in the case of n- and iso-butyrophenone; and benzene, toluene, and ethylbenzene in the case of valerophenone. Tars were formed to the extent of 5 to 10%, more tar being formed with increasing voltage and the yields of long chain substituted benzenes being reduced. The irradiations were carried out by producing an electrical discharge in the liquids between W electrodes. Traces of solids could also be isolated from the reaction mixtures, including biphenyl, bibenzyl, diphenylmethane, and bibenzoyl. (UK)

2267 EVIDENCE FOR VERY EARLY EFFECTS IN THE RADIOLYSIS OF WATER. Sawai, Takeshi; Hamill, William H. (Univ. of Notre Dame, Ind.). J. Phys. Chem.; 74: 3914-24 (29 Oct 1970).

An investigation was made based on the hypothesis that very early electronic effects in aqueous systems (i.e., those that precede dipole relaxation) are susceptible to observation. As a possible example, high concentrations of neutral Cl^- produce large yields of Cl_2^- and an increase in $G(e_{aq}^-)$, which can be attributed to hole trapping. Extensive studies of charged species in the radiolysis of liquid and solid alkanes provide a partial guide to the physical and chemical effects to be expected in water prior to relaxation. Relative scavenging efficiencies of solutes for mobile electrons in CH_3OH-H_2O glasses at 77°K do not correlate consistently with the rate constants $k(e_{aq}^- + S)$ in water. The effects of phenol, acetone, Cd^{2+}, HCl, and NO_3^- on G_{H_2} in aqueous solutions correlate better with results for glassy CH_3OH-H_2O than with conventional rate constants. In aqueous solutions results for scavenging dry electrons and holes (by hypothesis) are described by a trial function algebraically equivalent to a conventional kinetic competition between first-order decay and second-order scavenging. Relative efficiencies of scavengers and primary yields of precursors appear as parameters, and internal consistency provides a test of the probably over-simplified model. Hole scavenging by anions appears to be a general phenomenon and OH^- does not occupy a unique position. Results in very acid solutions may be complicated by this anion effect. High yields of oxidized species, e.g., Cl_2^- and I_2^-, and an increase in $G(e_{aq}^-)$ at high concentrations of OH^-, Cl^-, and F^- support the dry electron model. (auth)

2268 EFFECT OF ION AND RADICAL SCAVENGERS ON THE CYCLOHEXYL RADICAL YIELD IN THE RADIOLYSIS OF CYCLOHEXANE. Bansal, Krishan M.; Schuler, Robert H. (Carnegie-Mellon Univ., Pittsburgh). J. Phys. Chem.; 74: 3924-32(29 Oct 1970).

XUM

Scavenging studies with iodine indicate that the yield of cyclohexyl radicals produced in the radiolysis of pure cyclohexane is ~5.7. Iodine concentrations in the range of 10^{-2} M, however, reduce the observed yield to ~4.2. This decrease is interpreted as being produced both by hydrogen atom and by positive ion scavenging reactions of iodine. The effect of a number of other solutes on the production of cyclohexyl radicals was also examined. Cyclopropane reduces the yield by an amount approximately equal to the yield of the positive ion reactions. Ethylene has a similar effect with a superimposed reduction which results from hydrogen atom scavenging. The various electron scavengers examined (CH_3Br, CH_3I, CH_3Cl, SF_6, N_2O, and CO_2) have differing effects which depend on the relative importance of secondary abstraction reactions. The comparison of CH_3Br and CH_3Cl is particularly interesting because the first solute causes a reduction approximately equal to the yield of electron capture while the second has essentially no effect. Nitrous oxide is unique in that an increase is observed in $G(C_6H_{11}\cdot)$, which is equal to the yield of electrons captured by the N_2O. The quantitative aspects of the various effects can be correlated quite well by expressions derived from a description of the concentration dependence of ionic processes in these systems if it is assumed that on the average one cyclohexyl radical is produced for each neutralization that occurs between a positive ion–electron geminate pair. The interpretation of the data is, however, more complex than in the case of hydrogen production because certain processes produce several cyclohexyl radicals while others produce none. (auth)

2269 KINETICS OF γ-INDUCED DECOMPOSITION OF METHYL IODIDE IN AIR. Tang, I. N.; Castleman, A. W. Jr. (Brookhaven National Lab., Upton, N. Y.). J. Phys. Chem.; 74: 3933-9(29 Oct 1970).

The ^{60}Co γ-induced decomposition of methyl iodide in air was investigated at 15°C over an initial concentration range of 2.8×10^{-12} to 2.4×10^{-7} mole/cc. The decomposition reaction is pseudo-first order with respect to methyl iodide at concentrations below 2.4×10^{-10} mole/cc and is zero order at 2.4×10^{-7} mole/cc. At intermediate methyl iodide concentrations, however, the decomposition does not follow a simple reaction order. A mechanism is proposed which quantitatively accounts for the observed reaction kinetics. (auth)

2270 ENERGY TRANSFER IN THE RADIOLYSIS OF SATURATED AND UNSATURATED BINARY HYDROCARBON SYSTEMS. Foeldiak, G.; Wojnarovits, L. (Inst. of Isotopes, Budapest). Acta Chim. Acad. Sci. Hung.; 65: 59-66(1970).

The G_{H_2}, G_{CH_4}, and $G_{C_2H_6}$ values in mixtures of various amounts of n-octane with benzene, cyclooctatetraene, and 1,3-cyclooctadiene, respectively, were determined. A comparison of the yields shows that the specific effect of the conjugated double bonds of 1,3-cyclooctadiene and cyclooctatetraene in decreasing the G values are identical and stronger than that of the unsaturated bonds of benzene. This is explained by an identical, complex energy transfer and radical capturing effect of double bonds of the same type, which is, however, different from the effect of other bond types. On the basis of the phenomena recognized, it was also possible to find an analogy between intermolecular and intramolecular energy transfer. (auth)

2271 REVERSIBILITY BETWEEN THE ELECTRON-EXCESS CENTER, $e^-(CH_3CN)_2$, AND METHYL RADICALS IN γ-IRRADIATED ACETONITRILE-h_3. Takeda, Keiji; Williams, Ffrancon (Univ. of Tennessee, Knoxville). Contract AT(40-1)-2968 J. Phys. Chem.; 74: 4007-8(29 Oct 1970).

The electron-excess center formed by γ irradiation of the high-temperature phase of crystalline acetonitrile at 77°K is characterized by a broad optical absorption with λ_{max} at 510 nm. Essentially the same center is produced in CH_3CN and CD_3CN. Reversibility of the electron-excess center was demonstrated by photobleaching experiments and confirmed by an isothermal experiment at 113°K. (M.C.G.)

2272 PULSE RADIOLYTIC INVESTIGATION OF SHORT-LIVED HYDRATES OF AROMATIC NITROSO COMPOUNDS. Gruenbein, W.; Fojtik, A.; Henglein, A. (Hahn-Meitner-Institut fuer Kernforschung, Berlin). Monatsh. Chem.; 101: 1243-52 (Jul-Aug 1970). (In German).

Short-lived hydrates of aromatic nitroso compounds are formed in the reduction of the corresponding nitro compounds in aqueous solution. The overall first order rate constant k_b of the dehydration of a nitrosobenzene hydrate at first increased with decreasing pH and finally approached a limiting value k. The results are explained by a two step mechanism:

$$X-C_6H_4-N\begin{matrix}OH\\OH\end{matrix} + H^+ \overset{K}{\rightleftharpoons} X-C_6H_4-N\begin{matrix}OH\\(+)\\OH\\H\end{matrix}$$

$$X-C_6H_4-N\begin{matrix}OH\\(+)\\OH\\H\end{matrix} \xrightarrow{k} X-C_6H_4N \rightarrow O + H_2O + H^+$$

The equilibrium constant K and the first order decay constant k were determined. k depends very little on the nature of the substituent X. The following relationship between K and the Hammet constant σ of X was found: $\log (K/K_0) = 2.2 \cdot \sigma$ (K_0 = dissociation constant for X = H). (auth)

2273 RADIOLYSIS OF THE ORIGINAL AND REINFORCED ED-5 TYPE EPOXY RESIN. Voskan'yants, V. I.; Deev, Yu. C.; Serenkov, V. I.; Burlak, L. F.; Pshenitsyna, V. P.; Pridachina, N. N. Plast. Massy; No. 8, 50-4(1970). (In Russian).

The behavior of the ED-5-type epoxy resin exposed to ionizing radiation was investigated. The original epoxy resin had a molecular weight of 400 and contained 22% of epoxy groups. It was irradiated in a 5-MeV linear electron accelerator and in a ^{60}Co γ source in vacuo, at doses ranging from 10 to 2500 Mrad at temperatures between 20° and 150°C. The L-19 material used for reinforcing had a molecular weight of 870 and an amine number of 4.2%. Irradiation of the resin resulted in an increase of the molecular weight; exposure to about 900 Mrad doubled the original molecular weight; at the same time the epoxy group content decreased. The radiolysis also caused the release of small amounts of gaseous hydrogen. The L-19 and the polyethylene polyamine had less radiation resistance than the epoxy. The latter is suited for use in which it may be exposed to strong radiation. (TTT)

2274 EVIDENCE FOR VERY EARLY IONIC EFFECTS IN WATER RADIOLYSIS. Bevan, P. L. T.; Hamill, W. H. (Univ. of Notre Dame, Ind.). Trans. Faraday Soc.; 66: 2533-40(Oct 1970).

Yields of oxidized and reduced products from the radiolysis of aqueous solutions were measured. It was assumed that both H_3O^+ (or H_2O^+) and e^- can be trapped prior to hydration by using sufficiently high concentrations of appropriate solutes, e.g., anions for H_3O^+. By analogy with conventional kinetics, charge scavenging was assumed to compete with first-order hydration or recombination. Values $G^0(H_3O^+) = G^0(e^-) \cong 3.8$ were obtained. (auth) (UK)

2275 RADIATION CHEMISTRY OF OROTIC ACID AS STUDIED BY PULSE RADIOLYSIS. Greenstock, C. L. (Mount Vernon Hospital, Middlesex, Eng.). Trans. Faraday Soc.; 66: 2541-50(Oct 1970).

The optical absorption spectra of the adduct species formed by H, OH, or e^-_{aq} addition to orotic acid peak at 345, 340, and 330 nm. and their molar extinction coefficients are 1100, 1700, and 8500 $M^{-1}\,cm^{-1}$ respectively. The pK_a for protonation of the electron-adduct lies between 3.3 and 4. The protonated form absorbs at shorter wavelengths (~320 nm) and has an extinction of several 1000 $M^{-1}\,cm^{-1}$. These properties are quite different from those of the H-adduct formed by H atom attack at the 5,6-double bond. At neutral pH, the same electron-adduct species was formed, either by direct electron attachment to orotic acid, or by electron transfer from the ethanol radical formed in N_2O saturated solutions. No such transfer occurred from the corresponding t-butanol radical. The absolute rate constants for OH and e^-_{aq} reactions were measured by following the buildup of these adducts, and for OH attack, by the bleaching of the 5,6-double bond chromophore. The values so obtained (5.2×10^9 and 1.4×10^{10} $M^{-1}\,s^{-1}$ respectively) agreed well with those obtained by competition kinetics or by e^-_{aq} decay. The electron reactivity showed a 2-fold decrease at the pK_a for ionization of the carbonyl groups as expected from diffusion theory. No such effect was observed for OH reaction rates, but there was an increased reactivity at low pH, which was not understood. (auth) (UK)

2276 ENERGY TRANSFER IN THE Al/Al_2O_3 SYSTEM. PART II. THE INFLUENCE OF γ-IRRADIATION ON THE DECOMPOSITION G-VALUE OF 2,4-DIAMINOAZOBENZENE ADSORBED ON THE SURFACE OF THE Al/Al_2O_3 SYSTEM. Siejka, Juliusz; Owczarczyk, Andrzej; Minc, Stefan (Inst. of Nuclear Research, Warsaw. Univ., Warsaw). Nukleonika; 15: 69-78 (1970). (In Polish).

Energy transfer during γ irradiation of the Al/Al_2O_3 system with 2,4-diaminoazobenzene adsorbed on the oxide layer surface was investigated. Reflection spectrophotometry was used to estimate the amount of adsorbate. The G-value of 2,4-diaminoazobenzene decomposition in adsorbed state was found to increase by about two orders of magnitude. The average energy of formation of the active, energy rich species in the oxide layer capable of diffusing to the surface and causing decomposition of the adsorbed indicator was determined. The results obtained are discussed, and a mechanism for the energy transfer process is proposed. (auth)

2277 KINETIC EVIDENCE THAT G_{OH} IN THE RADIOLYSIS OF AQUEOUS SULFURIC AND NITRIC ACID SOLUTIONS IS PROPORTIONAL TO ELECTRON FRACTION WATER. Matthews, R. W.; Mahlman, H. A.; Sworski, T. J. (Oak Ridge National Lab., Tenn.). J. Phys. Chem.; 74: 3835-6(15 Oct 1970).

Kinetic evidence for primary yields of both OH and SO_4^- radicals in the radiolysis of aqueous 4.0M sulfuric acid was obtained using Ce(IV)–Ce(III)–HCOOH mixtures in sulfuric acid. Similar evidence was obtained for OH and NO_3 radicals in 4.0M nitric acid. G_{OH} based on energy absorbed by water was not markedly affected by either sulfuric or nitric acid. (M.C.G.)

2278 GAS-CHROMATOGRAPHIC ANALYSIS OF C_1–C_6 HYDROCARBONS, PRODUCTS OF RADIOLYSIS OF GASEOUS ETHYLENE. Gawlowski, Janusz; Niedzielski, Jan; Bierzynski, Andrzej (Univ., Warsaw). Chem. Anal. (Warsaw); 15: 721-7(1970).

The method of qualitative and quantitative gas chromatographic analysis of a mixture of hydrocarbons (products from radiolysis of gaseous ethylene) is described. Propylene glycol UCON LB 550 X on diatomaceous earth was used for the analysis of all unsaturated pentanes and hexanes. The use of a column containing $Hg(ClO_4)_2$ on a firebrick behind that with UCON made possible the determination of C_1–C_6 alkanes. Analysis of C_2–C_4 unsaturated hydrocarbons required the use of two column combinations: UCON + dinonyl phthalate, and UCON + 3,3′,3′′ -(1,2,3-propanetriyltrioxy)tripropionitrile, respectively. These four columns made possible the determination of 32 hydrocarbons in concentrations down to 0.1 ppM. Retention indexes are also given for the compounds. (auth)

2279 RADIATION CHEMISTRY OF CARBOHYDRATES. PART XVII. RADICAL PROCESSES FOLLOWING γ-IRRADIATION OF FROZEN CONCENTRATED SOLUTIONS OF SUCROSE AND D-GLUCOSE AT 77K. Baugh, P. J.; Kershaw, K.; Phillips, G. O. (Univ. of Salford, Eng.). J. Chem. Soc., B; No. 8, 1482-9(1970).

The radical species trapped in D-glucose and sucrose ices following γ irradiation at 77°K have been examined by electron spin resonance. In addition to the doublet assigned to the perpendicular features of randomly oriented OH radicals, trapped electrons (e_t^-) were produced which could be removed with visible light (540 to 580 nm) and addition of electron scavengers. The e_t^- had a singlet spectrum with g-value 2.0014 ± 0.0004 and linewidth 13.5 ± 0.5 G in H_2O ices and 6.3 ± 0.3 G in D_2O ices. The proton coupling constant, on the assumption of interaction of e_t^- with 8 equivalent nuclei from 4 surrounding water molecules, was 5.26 ± 0.3 G, which was in reasonable agreement with the proton constants in alkaline and neutral ices. Spectra due to D-glucose and sucrose radicals, after thermal annealing to 190°K, can be resolved into a 1:1 doublet (g = 2.0030 ± 0.0004) with hyperfine splitting of 20.5 G and a 1:2:1 (triplet g = 2.0025 ± 0.0004) with hyperfine splitting of 29.5 G. Possible structures of the radicals were considered. G(carbohydrate radicals) and $G(e_t^-)$ increased linearly with solute concentration. Radical yields extrapolated from the concentrated carbohydrate ices to the solid state were in good agreement with experimental values determined for the polycrystalline state at 77°K, which for D-glucose and sucrose were G = 3.2 and 2.7, respectively. The results indicated that direct radiation action yields the carbohydrate radicals and there was no evidence that electronic excitation transfer from associated water molecules contributes to radical formation. Maximum $G(e_t^-)$ values, obtained by extrapolation were 0.9 for D-glucose and 0.7 for sucrose ices. Consideration was given to the nature of the electron trapping site. (auth) (UK)

2280 EFFECTS OF L.E.T. AND TEMPERATURE IN THE RADIOLYSIS OF CYCLOHEXANE. PART 2. DIFFUSION KINETIC MODELS. Burns, W. G.; Hopper, M. J.; Reed, C. R. V. (Atomic Energy Research Establishment, Harwell, Eng.). Trans. Faraday Soc.; 66: 2182-91(Sep 1970).

Two radiation-chemical diffusion models are described. In the first, the radical model, the effect of LET is due to the competing reactions of H· atoms. A Gaussian spherical or cylindrical initial distribution of H· atoms and $C_6H_{11}^{\cdot}$ radicals is set up, and the radicals allowed to diffuse and react, the H· atoms being capable of abstracting from C_6H_{12} to produce more $C_6H_{11}^{\cdot}$ or of reaction with each other and with other radicals. The relevant differential equations were discretized over a number n of steps in space into two series of (n + 1) simultaneous equations, and progression in time achieved using the Taylor series expansion. A simplification was introduced into the iterative procedure for solving the resulting set of (2n + 2) nonlinear equations. The cross-reaction term of H· with $C_6H_{11}^{\cdot}$ was ignored only for the purpose of achieving the next closest approximation, giving two sets of (n + 1) equations, instead of one set of (2n + 2), reducing the total computation required for convergence, although the number of iterations was increased. In the second model, the excited molecule model, the relevant competition is between the interaction and decomposition of excited molecules, and H· atoms are considered to yield $C_6H_{11}^{\cdot}$ radicals in a very fast ("hot") reaction. Since the species for which diffusion is important are all C_6 radicals or molecules, a common diffusion constant was assumed, and the Ganguly–Magee "prescribed diffusion" method of solution of overlapping Gaussian spherical distributions was used. (UK)

2281 EFFECTS OF L.E.T. AND TEMPERATURE IN THE RADIOLYSIS OF CYCLOHEXANE. PART 1. EXPERIMENTAL RESULTS AND COMPARISON WITH PREDICTIONS OF DIFFUSION KINETIC MODELS. Burns, W. G.; Reed, C. R. V. (Atomic Energy Research Establishment, Harwell, Eng.). Trans. Faraday Soc.; 66: 2159-81(Sep 1970).

For low-dose (~3×10^{19} eV g^{-1}) irradiations of liquid cyclohexane at room temperature, G values of hydrogen, bicyclohexyl, and cyclohexene were measured, using a number of different kinds of radiation, viz. ^{60}Co γ rays, ^4He ions of energy 58, 23, 8, 7, 3.03, 2.13, and 1.53 MeV, 115-MeV ^{14}N ions, and 22-MeV ^{20}Ne ions. The effect of changing temperature was determined for ^{60}Co γ rays and for 3-MeV ^4He ions. A search for high-molecular-weight products, determined by weighing, was also made in high-dose (1 to 9×10^{21} eV g^{-1}) irradiations at high dose rate (10^{21} to 10^{22} eV g^{-1} s^{-1}), using 7-MeV ^4He ions and 115-MeV ^{14}N ions; initial G values of 0.65 and 0.80 respectively for conversion to polymer were found. In some experiments, G values of minor products, ethane, ethylene, acetylene, propane, propene, butane, butenes, n-hex-1-ene, and cyclohexyl-cyclohexenes were also measured. Attempts were made to correlate the results for changing LET and temperature, and the results of others using scavengers, with two diffusion models, in which the effect of LET is due to the competing reactions of thermal hydrogen atoms and excited molecules, respectively. The latter model, in which LET effects are due to events prior to radical formation, was the more successful. G values for 115-MeV ^{14}N ions were higher than expected on the basis of their overall mean LET; an analysis in terms of secondary electrons suggested that only a small part of the discrepancy was due to energetic secondary electrons, so that other radial track effects may occur with high-energy heavy ions. (auth) (UK)

2282 RADIATION-INDUCED CONFORMATION CHANGES OF THE PYRIMIDINE RING IN A SINGLE CRYSTAL OF DIHYDROTHYMINE. Herak, J. N. (Inst. Rudjer Boskovic, Zagreb). Z. Naturforsch.; 25a: 1299-1302(Aug-Sep 1970).

Radioinduced radicals in a single crystal of dihydrothymine were studied with EPR. It was found that the 5-thymyl radical is the dominant radical species at room temperature. The orientation dependence of the hyperfine couplings can only be explained if one assumes that $C_{(5)}$, $C_{(6)}$, and $C_{(7)}$ lie in the plane defined by the rest of the nonhydrogen atoms of the ring. The highly disordered structure of the ring in the undamaged crystal is ordered if a proton bound to $C_{(5)}$ is removed. (auth)

2283 PRIMARY YIELDS IN THE γ-RADIOLYSIS OF AMMONIA. Eyre, J. A.; Smithers, D. (Univ. of Leeds, Eng.). Trans. Faraday Soc.; 66: 2199-2209(Sep 1970).

The effects of varying pressure (100 to 700 mmHg), temperature (20 to 370°C), and dose (up to 7×10^{19} eV/g) on $G(H_2)$ and $G(N_2)$ in γ-irradiated ammonia gas were studied. From the effects of additives, propene, benzene, carbon tetrachloride, methanol, isopropanol, cyclohexane, propane, nitric oxide, hydrazine on these yields, and assuming plausible reaction mechanisms, values of primary yields were calculated. $G_{H_2} = 0.70 \pm 0.02$, $G_e = 3.4 \pm 0.6$, $G_H = 7.0 \pm 0.6$, $G_{NH_2} + 2G_{NH} = 11.9 \pm 0.1$. (auth) (UK)

2284 RADIOLYSIS OF NITRIC ACID SOLUTIONS: L.E.T. effects. Kazanjian, A. R.; Miner, F. J.; Brown, A. K.; Hagan, P. G.; Berry, J. W. (Dow Chemical Co., Golden, Colo.). Trans. Faraday Soc.; 66: 2192-8(Sep 1970).

The radiolysis of nitric acid solutions was investigated using gamma, beta, and alpha radiation. Solutions were gamma-irradiated under various conditions and analyzed for all stable products. Solutions that were alpha- or beta-irradiated were analyzed for nitrite ions only. Nitrite ion, the major radiolysis product, was determined as a function of nitric acid concentration. A nitrite scavenger, p-nitroaniline, was added to prevent the nitrite ion from reacting prior to analysis. The nitride yields from alpha irradiation were appreciably lower than the yields from gamma and beta irradiations at lower acid concentrations but continually increased with increasing acid concentration. The nitrite yields from gamma or beta irradiation increased with increasing acid concentration up to about 1 M but then decreased.

XUM

Similarity of the gamma and beta yields substantiated this unusual trend. Previous investigations of neutral nitrate solutions always showed an increase in yields at the higher nitrate concentrations. A mechanism, based on LET effects on three radiolytic reactions, was postulated to explain the differences in yields between alpha and gamma (or beta) irradiation. (auth) (UK)

2285 ULTRASONIC ABSORPTION: A NEW TECHNIQUE. Woodcock, J. P. (Guy's Hospital Medical School, London). Ultrasonics; 8: 213-15(Oct 1970).

Ultrasonic absorption spectroscopy is described for investigating the biological and chemical damage caused by gamma irradiation on three solutions, erythrocytes, sodium salt of DNA in distilled water, and glucose in distilled water. (auth) (UK)

2286 ELECTRON SPIN RESONANCE (ESR) STUDIES OF RADIATION-INDUCED RADICALS OF α-D-GLUCOSE, β-D-GLUCOSE, AND D-GLUCURONIC ACID. Neubacher, H. (Justus Liebig-Univ., Giessen, Ger.). Biophysik, 6: 161-72(1969). (In German).

Electron spin resonance was used to determine the damaging effect of x radiation on α-D-glucose, β-D-glucose, and D-glucuronic acid. By measurement of saturation dependent on doses and time after irradiation several radicals of these investigated substances in the polycrystalline state were identified. It would seem, from these results, that radiation damage occurs in the form of radicals at each of the carbon atoms in the ring of the gluco-pyranose molecule. The radicals of the α-D-glucose and the β-D-glucose then migrate to the carbon atom C-1, whereas those of D-glucuronic acid migrate to the carboxyl group. The decrease of the spin–lattice relaxation time T_1 with increasing dose shows that there will be a comparatively homogeneous distribution of the radioinduced radicals in the crystal. (auth)

2287 RADIATION CHEMISTRY OF CARBON MONOXIDE AT VERY HIGH DOSE RATES. Willis, C.; Miller, O. A. (Atomic Energy of Canada Ltd., Chalk River, Ont.). Can. J. Chem.; 48: 3029-33(1 Oct 1970). (AECL-3696).

Carbon monoxide was irradiated with single intense pulses from an electron accelerator at a dose rate of $\sim 2 \times 10^{27}$ eV g^{-1} s^{-1}. The yield of carbon dioxide obtained was $G(CO_2) = 0.7 \pm 0.1$ with a very small yield of carbon suboxide, $G(C_3O_2) \leq 0.02$. Addition of propene reduced the carbon dioxide yield to almost zero while addition of propane had no effect. This suggests that propene acts as an oxygen atom scavenger rather than as a quencher of an excited state of carbon monoxide. However, rate constant data do not support this suggestion and it is concluded that the residual yield of carbon dioxide observed at high dose rates arises from the reaction: $CO^+ + CO \rightarrow CO_2 + C^+$, where CO^+ is in an $A^2\Pi$ or $B^2\Sigma^+$ state. (auth) (Canada)

2288 STUDIES ON THERMAL DEGRADATION OF γ-IRRADIATED POLYCAPROAMIDE BY MEANS OF MASS SPECTROMETRY. Muinov, T. M.; Mavlyanov, A. M.; Marupov, R. (Inst. of Physics and Tech., Dushanbe, USSR). Vysokomol. Soedin., Ser. A; 12: 1724-8(Aug 1970). (In Russian).

The composition of volatile products from thermal degradation of γ-irradiated and unirradiated polycaproamide and kinetics of the process were studied by means of mass spectrometry. The main product of degradation is caprolactam. The activation energies of both processes do not differ and are equal to 45 kcal/mole. The results show good correlation of the activation energies of thermal (E) and mechanical (U_0) degradation of polycaproamide. (auth)

2289 ELECTRON SPIN RESONANCE SPECTROSCOPY OF FREE RADICALS PRODUCED IN DL-VALINE, D-VALINE, N-ACETYL-DL-VALINE, AND GLYCYL-DL-VALINE BY X-IRRADIATION. Schnepel, Gerd Henning (Justus Liebig-Univ., Giessen, Ger.). Biophysik, 6: 145-60(1969). (In German).

Free radicals produced in polycrystalline DL-valine, D-valine, N-acetyl-DL-valine, and glycyl-DL-valine by x radiation were studied by electron spin resonance spectroscopy. The structure of some of them was found to be $(CH_3)_2C-R$, formed by loss of the H. Additionally, the existence of several types of radicals was determined. For the unpaired spin of some radicals the values of isotropic hyperfine coupling constants are given. (auth)

2290 CARBONIUM IONS IN RADIATION CHEMISTRY. II. ISOMERIZATION PROCESS IN PROTONATED CYCLOPROPANE AND CYCLOBUTANE IONS. Lias, S. G.; Rebbert, R. E.; Ausloos, P. (National Bureau of Standards, Washington, D. C.). J. Amer. Chem. Soc.; 92: 6430-40(4 Nov 1970).

The structures of propyl and butyl ions formed in the gas-phase radiolysis of appropriate alkanes were deduced from the structures of the neutral products formed in proton transfer reactions with ammonia, or from the isotopic structures of hydride (or deuteride) transfer reaction products formed in labeling experiments. n-Propyl ions rearrange within 10^{-10} sec to the sec-propyl or the protonated cyclopropane structure. Rearrangement to the sec-propyl ion is favored under all conditions but increases in importance with increasing internal energy content of the ion. Both isomerization reactions are reversible, but the rate constants of the reverse reactions are very low owing to the energy requirements of these processes. The isomerization of the sec-butyl ion to the t-butyl structure is observed; this rearrangement also increases in importance with increasing internal energy content of the ion. The H (or D) atoms in the secondary and tertiary carbonium ions are seen to undergo energy-dependent hydrogen-scrambling processes. The protonated cyclobutane ion formed by proton transfer to cyclobutane isomerizes mainly to the sec-butyl structure. The results presented here demonstrate that most of the propyl and butyl ions formed in the dissociation of butane and hexane parent ions, respectively, originate as primary carbonium ions from simple C–C cleavage processes, rather than being formed initially with the secondary structure, as they are at the threshold energies. (auth)

2291 THERMOLUMINESCENCE IN N-HEPTANE. Boustead, I. (Royal Military Coll. of Science, Shrivenham, Eng.). Proc. Roy. Soc. (London), Ser. A; 319: 237-46 (20 Oct 1970).

n-Heptane freezes to a polycrystalline glass at 77°K and after γ radiolysis was found to emit four glow peaks. It was demonstrated that trapping is a property of the heptane matrix while emission intensity and temperatures of maximum glow depend on the nature and concentration of the luminescent additive. Dose-dependence measurements of glow peak intensities showed that the three lowest temperature peaks can be explained in terms of electron trapping in a fixed number of traps, while the highest temperature peak was produced by traps which are subject to a radioinduced blocking mechanism. A possible blocking mechanism is proposed and it is shown that the traps are probably different types of cavity within the solid. The results were compared with earlier results for squalane, an amorphous hydrocarbon. (auth) (UK)

2292 RADIATION OXIDATION OF LIQUID DODECANE. Sistek, I. (Czechoslovak Academy of Sciences, Prague). Collect. Czech. Chem. Commun.; 35: 2849-53(Sep 1970).

The yields of hydrogen from the radiolysis of dodecane in the absence and presence of oxygen were measured. Oxygen had almost no effect on the hydrogen yield. In the presence of oxygen the yield of gaseous hydrocarbons decreased. Oxygen interfered in the ionic reactions. (M.C.G.)

2293 HYDROGEN ABSTRACTION BY PRIMARY SPECIES IN THE RADIOLYSIS OF FROZEN AQUEOUS SYSTEM. Gopinathan, Chakrapani; Moorthy, P. N.; Rao, K. N. (Bhabha Atomic Research Centre, Bombay). Indian J. Chem.; 6: 749-50 (Dec 1968).

ESR spectra of γ-irradiated frozen aqueous solutions of ethyl and isopropyl alcohols were examined in the presence as well as absence of acids, such as sulfuric acid. Relatively low concentrations of these alcohols prevent the formation of SO_4^- as well as that of H atoms. Also, presence of acid causes an intensification of the alcohol radical spectra as compared with the acid-free solutions. These results were interpreted in terms of α-hydrogen abstraction by primary ionic species as well as by excited water molecules. (auth)

Radioisotope Production

2294 (ORNL–4572–, pp 109-34) TRANSURANIUM-ELEMENT PROCESSING. (Oak Ridge National Lab., Tenn.).

Equipment was put into operation for making americium oxide–curium oxide microspheres. About 7 mg ^{249}Bk, 54 mg of ^{252}Cf, 380 μg of ^{253}Es, and about 5×10^8 atoms of ^{257}Fm were recovered from irradiated HFIR targets. Seven ^{252}Cf neutron sources were fabricated; 19.4 μg of isotopically pure ^{253}Es was produced; and 155 μg of ^{250}Cf (87% isotope purity) was produced. An unused cell in the TURF facility was equipped to provide space for purification and encapsulation of californium. A systematic study of actinide element chemistry and of comparative lanthanide element chemistry is being made. (M.C.G.)

2295 (ORNL–4572–, pp 225-30) IRRADIATION EFFECTS ON HETEROGENEOUS SYSTEMS. (Oak Ridge National Lab., Tenn.).

The Campbell reaction, isotope enrichment by (n, γ) reactions in molecular sieves, is being studied. Typical results showed a

generally similar response from both light and heavy rare earths. Enrichment factors were in the vicinity of 50. The reaction was also studied by α bombardment of a molecular sieve. (M.C.G.)

2296 CHARACTERISTICS OF TWO ^{113m}In GENERATORS. Rousselin, R. J.; Gauthier, Cl. (Laboratoire Central des Ponts et Chausees, Paris). Int. J. Appl. Radiat. Isotop.; 599-606 (Oct 1970). (In French).

Some characteristics of tin-113 and indium-113m are examined. The outputs of the indium-113m elution are measured for two Sn–In generators and also the contaminations of the eluate. The ^{113m}In half-life was measured; the value is 99.8 ± 0.2 mn. (auth) (UK)

Recoil Production and Reactions

Refer also to abstract 2305.

2297 CHEMICAL BEHAVIOR OF ^{60}Co IN AQUEOUS SOLUTIONS OF NEUTRON-IRRADIATED SODIUM ETHYLENEDIAMINE-TETRAACETATOCOBALTATE/III/ TETRAHYDRATE. Omori, T.; Shiokawa, T. (Tohoku Univ., Sendai). Radiochem. Radioanal. Lett.; 5: 37-42(16 Oct 1970).

In sodium ethylenediaminetetraacetatocobaltate(III) tetrahydrate, the recombination reaction of the recoil ^{60}Co atoms was investigated in aqueous solutions, in which the neutron-irradiated target was dissolved. The retention values were not affected appreciably by the time after solution, while the yields of ^{60}CoEDTA^{2-} and ^{60}Co^{2+} varied with time owing to the substitution reaction. A comparison of the rate of this substitution reaction with that of the normal isotopic exchange reaction suggests the existence of ^{60}Co-labeled complexes other than EDTA complexes. (auth)

2298 CARRIER EFFECTS ON ANION-EXCHANGE AND GEL CHROMATOGRAPHIC BEHAVIOR OF ^{32}P RECOIL SPECIES PRODUCED IN IRRADIATED INORGANIC PHOSPHATES. Ujimoto, Kikujiro; Nakamura, Terumasa; Asada, Hiroyuki; (and others) (Kyushu Univ., Fukuoka). J. Inorg. Nucl. Chem.; 32: 3177-90(Oct 1970).

In the course of the separation of ^{32}P recoil species produced in neutron-irradiated inorganic phosphorus compounds by anion-exchange chromatography and gel chromatography (molecular-sieve chromatography), it was found that the chromatographic patterns obtained in the presence and the absence of some carriers for oxo anions of phosphorus differed considerably. Certain carriers for oxo anions of phosphorus must be present in a solution of a target material in order to obtain the true distribution of ^{32}P recoil species by means of anion-exchange or gel chromatography. The distribution of ^{32}P recoil species in some orthophosphates were investigated in conjunction with the carrier effects. The carrier effects on ^{32}P recoil species produced in irradiated monothiophosphates were also examined. (auth) (UK)

2299 REACTIONS OF RECOILING SILICON ATOMS WITH PHOSPHINE, SILANE, AND DISILANE. Gaspar, Peter P.; Markusch, Peter (Washington Univ., St. Louis). J. Chem. Soc., D; No. 20, 1331-2(21 Oct 1970).

A high ratio of radioactive trisilane to disilane obtained from the reactions of silicon atoms in phosphine–disilane mixtures is evidence for insertion by: $^{31}SiH_2$ as the product-determining step. (auth) (UK)

2300 CHEMICAL STATE OF RADIORHENIUM FORMED IN SOME INORGANIC IRIDIUM COMPOUNDS IRRADIATED WITH 660-MeV PROTONS. Ianovici, Eugenia; Zaitseva, Natalia (Joint Inst. for Nuclear Research, Dubna, USSR). J. Inorg. Nucl. Chem.; 32: 3165-75(Oct 1970).

The chemical behavior of radiorhenium formed by the Ir(p, 3 pxn)Re nuclear reaction with 660-MeV protons was investigated. The effects of water of crystallization and ammonium ion as well as of the radiation dose on the yield of Re(VII) are described. The thermal annealing of radiorhenium in anhydrous and hydrated sodium hexachloroiridate(IV) was studied. The role of radioinduced defects and inherent crystal defects in the annealing process was also examined. A comparison between the fate of the radiorhenium recoil formed by high-energy proton irradiation in lattices containing rhenium and the fate of atoms produced in non-isotopic lattices is reported. (auth)

2301 BROMINE ISOMERS UNDER (n,γ) PROCESS. Lal, A. (Banaras Hindu Univ., India). Indian J. Pure Appl. Phys.; 6: 481-3 (1968).

The uncertainty regarding higher collection of active bromine on the electrodes was studied with ethyl bromide and a possible explanation of the preferential collection attempted on the basis of Auger electron hypothesis suggested by P. R. Geissler and J. E. Willard [J. Phys. Chem., 67 (1963), 1675]. The relative yields of ^{80}Br and ^{80m}Br following thermal neutron irradiation of $C_2H_4Br_2$, C_2H_5Br, and C_6H_5Br for varying durations of time (3 to 22 hr) with and without electric field applied across the collecting electrodes were determined. The ratio ^{80}Br to ^{80m}Br first decreased and then increased with an increase in the neutron irradiation time in the absence of an electric field across the collecting electrodes. This ratio is markedly influenced by an electric potential applied across the electrodes. It is higher in case of aromatic compounds than in the aliphatic ones. (auth)

2302 HOT ATOM CHEMISTRY OF SOLID INORGANIC PHOSPHORUS COMPOUNDS: ALKALI AND AMMONIUM ORTHOPHOSPHATES. Nakamura, Terumasa; Ujimoto, Kikujiro; Yoza, Norimasa; Ohashi, Shigeru (Kyushu Univ., Fukuoka). J. Inorg. Nucl. Chem.; 32: 3191-7(Oct 1970).

Alkali and ammonium orthophosphates in the solid state were irradiated with thermal neutrons at dry ice temperature. Recoil species in the irradiated materials were analysed by ion-exchange chromatography in the presence of carriers for some oxo anions of phosphorus. It was established that a series of ^{32}P-labelled polyphosphates from tri- to hexaphosphate is formed in irradiated potassium or ammonium dihydrogen orthophosphate. This work suggests the occurrence of a comparatively large hot zone in irradiated solid inorganic phosphates. (auth) (UK)

2303 REACTIONS OF RECOIL ^{35}S ATOMS WITH ORGANIC COMPOUNDS. I. THE DISTRIBUTION OF ^{35}S ATOMS ON MERCAPTOBENZOTHIAZOLE. Taki, Ko (Inst. of Physical and Chemical Research, Saitama, Japan). Bull. Chem. Soc. Jap.; 43: 2626-8(Aug 1970).

The distribution of ^{35}S atoms in the molecules of mercaptobenzothiazole (I) and methylmercaptobenzothiazole (II) was studied; some differences in the reactions of the ^{35}S atoms formed by the ^{35}Cl(n,p)^{35}C and ^{34}S(n,γ)^{35}S processes were also investigated. It was found that the reactions of the ^{35}S atoms in the presence and in the absence of benzoquinone and oxygen as a radical scavenger gave almost the same ^{35}S distribution. This suggests that all the reactions may be considered to be hot reactions and not thermal reactions. The radiochemical yield of the activated parent molecule (retention value) was about 2 to 5% for the ^{35}Cl(n,p)^{35}S process and about 30% for the ^{34}S(n,γ)^{35}S process. The distribution of the ^{35}S atoms in the molecule was much greater in the S_8-position than in the S_1-position in both compounds. The results cannot be reasonably interpreted, but it may be considered that the collisional exchange (a knock on exchange in terms of a billiard-ball model) of the S atom is easier in the S_8-position than in the S_1-position in the molecule. Also, the distribution of the ^{35}S atoms may be dependent on the stability of the bond-cleaved intermediate. (P.C.H.)

Radiochemistry

Refer also to abstract 2300.

2304 DETERMINATION OF THE STATE OF ^{129}I IN β-$^{129m}TeO_3$ BY NUCLEAR GAMMA RESONANCE. Lebedev, R. A.; Babeshkin, A. M.; Nesmeyanov, A. N.; Fatieva, N. L. (Moscow State Univ.). Radiochem. Radioanal. Lett.; 5: 83-90(16 Oct 1970).

Nuclear gamma resonance spectral reveal that the daughter isotope ^{129}I is present in β-$^{129m}TeO_3$ in two states, one of which is unstable. The character of changes to which the iodine atom is subjected in its transition from one state to the other is discussed. The configuration of the valence electron shell for the stable state is calculated. (auth)

2305 CHARGE STATES OF Np RECOIL ATOMS FOLLOWING α DECAY. Gal, J.; Hadari, Z.; Yanir, E. (Nuclear Research Center, Negev, Israel). J. Inorg. Nucl. Chem.; 32: 2509-12(Aug 1970).

Utilizing the Moessbauer effect the charge states of the Np ions in various Am sources were determined. The charge states were found to be +3 in all sources containing the Am ions in frozen solutions and +4 and +5 in all oxide sources. In most other Am salts the Np attained the valence of the host lattice. (auth) (UK)

Separation Processes

Refer also to abstracts 2075, 2110, 2193, 2201, 2294, 2383, 2384, 2416, 2417, 2773, 2774, and 2791.

2306 (ANL–7735) FUEL CYCLE TECHNOLOGY QUARTERLY REPORT, APRIL, MAY, JUNE 1970. Webster, D. S.; Jonke, A. A.; Bernstein, G. J.; Levitz, N. M.; Pierce, R. D.; Steindler, M. J.; Vogel, R. C. (Argonne National Lab., Ill.). Jul 1970. Contract W-31-109-eng-38. 89p. Dep. NTIS.

Research and development efforts on Argonne National Laboratory's fuel cycle technology projects are reported for the period

April through June 1970. Work was done in the following areas: (1) development of two conceptual designs for plants to declad 5 metric tons/day of LMFBR fuel in molten zinc, (2) construction of a fluid-bed pilot plant to continuously convert uranium plutonium nitrate (in aqueous solution) to oxides, and laboratory experiments to identify the oxide products (i.e., phases) obtained by drop-denitration of uranium nitrate and U–20% Pu nitrate solutions at 300 to 600°C, (3) evaluation of x-ray fluorescence spectrometry as an in-line analytical method for determining the Pu/U ratio of oxide fuels, and consideration of X-ray diffraction measurement of the lattice parameter of single-phase (U,Pu) oxide as an in-line method of determining the oxygen content (O/M ratio) of oxide fuels; and (4) the development of a critically favorable centrifugal contactor for the efficient handling of plutonium from LMFBR fuels in the plutonium isolation steps of a solvent-extraction process. Highlights of ANL investigations of liquid metal decladding since early 1968 are also presented. (auth)

2307 (CEA-N-1316) SEPARATION OF TECHNETIUM FROM FISSION PRODUCTS. Herment, Jacques (Commissariat a l'Energie Atomique, Grenoble (France). Centre d'Etudes Nucleaires). Sep 1970. 9p. (In French). Dep. NTIS (U. S. Sales Only).

The separation of short-lived technetium isotopes from fission products by ion exchange and solvent extraction was investigated. The decontamination factors obtained were 10^3 for halogens and 10^6 for the other fission products. (France)

2308 (CEA-R-3845) COALESCENCE OF ORGANIC SOLUTIONS DURING THE EXTRACTION OF ACIDS AND METALS BY TRIALKYLAMINES. Blain, Jean-Francois (Commissariat a l'Energie Atomique, Fontenay-aux-Roses (France). Centre d'Etudes Nucleaires. Paris Univ. (France). Faculte des Sciences). Jun 1970. 60p. (In French). Dep. NTIS (U. S. Sales Only).

Thesis.

The formation of two layers in trialkylammonium salt solutions in a low-polarity solvent can be explained on the basis of the settling of micelles. The light scattering and viscosity measurements show that the micelle size increases rather sharply before coalescence. The existence of micelles in the solution was confirmed by ultracentrifuge experiments. The behavior of these solutions is similar to that of colloidal soap solutions. The various parameters favoring the third phase formation are: anion size ($Cl^- \sim Br^- < NO_3^- < ClO_4^-$); extraction of excess acid: metal cation size ($UO_2^{2+} < Pu^{4+} \sim Th^{4+}$); decrease in the length of the n-alkyl chain in alkylammonium salts; decrease in solvent polarity. These phenomena could be explained on the basis of the affinity between alkylammonium salts and organic solvent. The composition of the three phases is independent of the initial amine concentration for a determined acid and metal. (auth) (France)

2309 (DOCKET-50201-55) WEST VALLEY REPROCESSING PLANT. Conversion of Existing Emergency Generator to Diesel Drive. (Nuclear Fuel Services, Inc., West Valley, N. Y.). 9 Nov 1970. 12p. Dep. NTIS.

The existing steam turbine generator set in the emergency power system is being converted to a diesel-driven generator. There will be no change in the generator itself; only the drive unit will be changed. A tentative schedule is given. (M.C.G.)

2310 (IS-T-411) SEPARATION OF LANTHANUM FROM A RARE EARTH CHLORIDE MIXTURE USING A MULTISTAGE MIXER-SETTLER EXTRACTOR. Casto, Martin George (Ames Lab., Iowa). Oct 1970. Contract W-7405-eng-82. 82p. Dep. NTIS.

Thesis.

A pilot plant scale, multistage box-type mixer-settler extractor was operated to demonstrate the feasibility of separating lanthanum from a mixture of rare earth chlorides of monazite origin using bis(2-ethylhexyl)phosphoric acid (D2EHPA) in Amsco Odorless Mineral Spirits for the organic solvent and dilute HCl as the aqueous scrub solution. Using 0.5M D2EHPA as the organic solvent, 0.1M HCl as the aqueous scrub solution, and 2.6M $RECl_3$ as the feed, steady state with respect to the rare earth concentration was achieved in both 10- and 20-stage mixer settler extractors. Several runs were made to find the operating conditions necessary to achieve a 95% pure lanthanum raffinate product from a feed containing 45.6% lanthanum, 10.0% cerium, 30.5% neodymium, 3.6% samarium, 8.0% praseodymium, and 2.4% gadolinium. Using a 20-stage extractor, operating conditions were found which produced a 97% lanthanum raffinate product with a 60% lanthanum recovery. On a cerium-free basis this corresponds to a 99% lanthanum product. A study of the dynamics of the system was also made using the 10-stage extractor, 0.5M D2EHPA, 0.1M HCl, and 2.7M $RECl_3$. Base operating conditions were chosen which produced an approximately 88 mole % lanthanum raffinate product. Once steady state was reached, intentional upsets of varying degree were made in the individual flow rates and interface positions to test their effect on the raffinate product concentration and on the operation of the mixer-settler. Six runs were made in this manner, each one testing the effect of a single variable. The relative importance of the various variables on the steady state concentration of the raffinate product was to be determined. It was found that the $RECl_3$ flow rate is by far the most important variable to be controlled and, if steady state is to be maintained, even small fluctuations in the $RECl_3$ flow rate cannot be tolerated. The other most important variables to control are, in order of importance; the HCl flow rate, the D2EHPA flow rate, and the settler interface positions. (auth)

2311 (IS-T-412) PREDICTION OF EQUILIBRIUM DATA FOR THE SOLVENT EXTRACTION SYSTEM $SmCl_3$–$NdCl_3$–$CeCl_3$–HCl–H_2O WITH THE EXTRACTANT DI-(2-ETHYLHEXYL) PHOSPHORIC ACID IN AMSCO. Ioannou, Tom Kyriacou (Ames Lab., Iowa). Oct 1970. Contract W-7405-eng-82. 130p. Dep. NTIS.

Thesis.

Equilibrium data for the system $CeCl_3$–HCl–H_2O–1 M D2EHPA (in Amsco Odorless Mineral Spirits) were obtained for a wide range of acidities and aqueous lanthanide concentrations. The equilibrium curves for $CeCl_3$ are of the same shape as the other lower lanthanides. A mathematical model was developed to predict the organic concentration as a function of the aqueous phase variables for the system. Equilibrium data were also obtained for the systems $SmCl_3$–$NdCl_3$–HCl–H_2O–1 M D2EHPA–Amsco and $SmCl_3$–$NdCl_3$–$CeCl_3$–HCl–H_2O–1 M D2EHPA–Amsco. The data for the binary salt system were obtained at total aqueous lanthanide concentrations of ~0.64 M and ~0.11 M over a wide range of acidities and mole fraction of Sm in the aqueous phase. The ternary salt system was studied at a total aqueous metal concentration of ~0.64 M over a wide range of acidities, mole fraction of Ce and mole fraction of Sm on a cerium-free basis in the aqueous phase. The total organic concentration for the above systems may be predicted by the sum of a series of linear terms analogous to Raoult's Law for ideal solutions, and terms measuring the interaction effects (deviations from ideality). The interaction effects were correlated empirically as a function of the aqueous phase variables and can be predicted with an average error of less than 4%. The separation factor $\beta_{Sm,Nd}$ for the binary and ternary systems was essentially constant for all conditions studied. Also, it was found that in the ternary system, the separation factor of each combination pair of elements remains the same as in the case where each pair is extracted together. (auth)

2312 (ORNL-4572) CHEMICAL TECHNOLOGY DIVISION ANNUAL PROGRESS REPORT FOR PERIOD ENDING MAY 31, 1970. (Oak Ridge National Lab., Tenn.). Oct 1970. Contract W-7405-eng-26. 307p. Dep. NTIS.

Separate abstracts were prepared for 17 of the 18 sections. The remaining section, biochemical technology, covered macromolecular separations, body fluids analyses, and water pollution studies. (M.C.G.)

For abstracts of individual sections see: 2152, 2195, 2294, 2295, 2313–2319, 2380, 2773–2775, 2821, and 3797.

2313 (ORNL-4572-, pp 1-36) MOLTEN-SALT REACTOR PROCESSING. (Oak Ridge National Lab., Tenn.).

A flowsheet is given for processing a MSBR fuel, based on the use of a fluorination–reductive extraction process for rare earth removal. The distribution of thorium, rare earths, and other elements between molten lithium halide-containing salts and liquid bismuth solutions is being studied. Equipment for semicontinuous engineering experiments on reductive extraction was put into operation. The metal-transfer process for removing rare earths from the fuel salt of single-fluid MSBR's was studied. The hydrodynamics of packed columns was studied using mercury and water to simulate bismuth and molten salt. Development of electrolytic cells and a frozen-wall fluorinator is discussed. Eight specially designed capsules were filled with $^{239}PuF_3$ powder for refueling additions to the MSRE. The distillation of irradiated fuel carrier salt was studied. (M.C.G.)

2314 (ORNL-4572-, pp 37-84) DEVELOPMENT OF AQUEOUS PROCESSES FOR FAST REACTOR FUELS. (Oak Ridge National Lab., Tenn.).

For shipment of LMFBR spent fuel, recent findings confirmed the desirability of the features of the cask concept that employs steel for shielding as well as structural material and that uses liquid sodium to transport heat from multiple fuel subassemblies to the inner wall of the cask. Heat transfer between LMFBR fuel rods and head-end processing were studied. A method of removing I, Kr, Xe, and T from PuO_2–UO_2 fuel specimens was evaluated.

Dissolution and feed preparation, solvent extraction using TBP, removal of iodine from off-gas, engineering studies, and radiation, shielding, and criticality studies are discussed. (M.C.G.)

2315 (ORNL-4572-, pp 85-97) DEVELOPMENT OF METHODS FOR REPROCESSING HTGR FUELS. (Oak Ridge National Lab., Tenn.).

Head-end methods are being developed for HTGR fuels. Studies with unirradiated fuels and irradiated Dragon fuels are described. (M.C.G.)

2316 (ORNL-4572-, pp 98-108) WASTE TREATMENT AND DISPOSAL. (Oak Ridge National Lab., Tenn.).

An economic analysis of wastes expected from the aqueous processing of fuels from three types of reactors, light water, liquid-metal-cooled fast breeder, and high-temperature gas-cooled, was completed. An improved version of the pot calcination process was developed for solidifying the high-level radioactive waste generated by the aqueous processing of LWR and LMFBR fuels. The encapsulation of fission products in solid media was studied. The permeability and separation factors for krypton, xenon, and several other gases were measured using sheets of thin silicone-rubber membrane. A conceptual design of a demonstrational salt-mine repository for the permanent storage of high-level and alpha-contaminated solid wastes is underway. (M.C.G.)

2317 (ORNL-4572-, pp 170-3) CONVERSION STUDIES IN THE LMFBR FUEL CYCLE. (Oak Ridge National Lab., Tenn.).

From Chemical Technology Division annual progress report for period ending May 31, 1970.

In the conversion of depleted UF_6 and $Pu(UO_3)_4$ solution to LMFBR core fuel assemblies, the estimated costs for the Sol-Gel Sphere-Pac process were about $20/kg less than those for three competing pellet processes. It is shown that substantial savings may be realized by shipping plutonium in the form of oxide spheres. Preparation of UO_2 spheroids is discussed. (M.C.G.)

2318 (ORNL-4572-, pp 174-80) PREPARATION OF $^{233}UO_2$ FOR LIGHT WATER BREEDER REACTORS. (Oak Ridge National Lab., Tenn.).

A process is being developed for purification of ^{233}U and preparation of ceramic-grade UO_2 powder. Plant modifications, equipment design for UO_2 conversion line, storage system, and site preparation are discussed. (M.C.G.)

2319 (ORNL-4572-, pp 181-95) SEPARATIONS CHEMISTRY RESEARCH. (Oak Ridge National Lab., Tenn.).

From Chemical Technology Division annual progress report for period ending May 31, 1970.

Separation methods and reagents are being developed. Data were obtained on extraction of 19 metals from sulfate and nitrate solutions using amines. The solvent extraction process for purification of beryllium was evaluated. A process for recovering uranium from wet-process phosphoric acid by extraction with DEHPA + TOPO was demonstrated. The displacement elution of transplutonium elements from ion exchange resins is being studied. Distribution equilibria and mechanisms are discussed. Studies are being made of the relative potentials of Bk(IV)-Bk(III) and Ce(IV)-Ce(III) couples. The relative basicities of most of the lanthanides and of americium and curium were measured. Aggregation and activity coefficients in solvent phases are discussed. (M.C.G.)

2320 (ORNL-TM-3204) THORIUM FUEL CYCLE DEVELOPMENT PROGRESS REPORT, NO. 15, OCTOBER 1970. (Oak Ridge National Lab., Tenn.). Nov 1970. Contract W-7405-eng-26. 22p. Dep. NTIS.

Development work on HTGR fuel recycle is reported under the following headings: head-end reprocessing development, refabrication development, TURF equipment design and engineering, and materials irradiation. (M.C.G.)

2321 RECOVERY OF TELLURIUM FROM SULPHATE SOLUTIONS BY EXTRACTION. Kunev, Dinko; Vasilev, Khristo; Chimbulev, Mincho. Rudodobiv Met. (Sofia); 24: No. 7, 51-3 (Jul 1969). (In Bulgarian).

The relative merits of two proposed extraction agents (dialkyldithiophosphate and diethylhexylphosphoric acid) for the recovery of Te from sulfate solutions are discussed on the basis of practical tests. Dialkyldithiophosphates were found to be the better type of agent for extracting Te from sulfate solutions, although they were none too selective. The use of diethylhexylphosphoric acid was not particularly promising, since the Te distribution coefficient was rather low and the admissible pH range inconveniently narrow. (Metals Abstr.)

2322 IMPROVEMENTS IN OR RELATING TO THE SEPARATION OF MIXTURES CONTAINING TWO OR MORE OF RADIUM, ACTINIUM, AND THORIUM. (to Commissariat a l'Energie Atomique). British Patent 1,206,712. 30 Sep 1970. Priority date 30 Jan 1967, France.

Radium, actinium, and thorium may be separated from a mixture containing two or more of these elements and their radioactive decay products by halogenating the mixture and subjecting the resulting halides to fractional sublimation in a vacuum. (B.L.M.)

2323 EXTRACTING URANIUM FROM SEA WATER. Keen, N. J. (United Kingdom Atomic Energy Authority, London). Indian East. Eng.; 112: 337-9(Jun 1970).

Methods for the extraction of uranium from seawater have been examined. Trials have been carried out at Portland harbor with seawater flowing through packed beds of granules of hydrous titanium oxide, which absorb uranium from seawater by ion exchange. The uranium can be leached from the absorber bed by treatment with ammonium carbonate solution and isolated. Several arrangements for presenting the absorber to the sea have received attention. Use of tidal energy to provide a larger head of water is contemplated. Capital costs, engineering difficulties and proper site selection are still some of the unsolved problems. It is hoped that these problems will be overcome and by the turn of the century the extraction of uranium from seawater will prove to be an economic and feasible project. (INIS)

2324 TECHNOLOGICAL ASPECTS OF REPROCESSING NUCLEAR FUEL AT EUROCHEMIC. van Geel, J. N. C. (Eurochemic, Mol, Belg.). Ingenieur (Utrecht); 82: 27-38 (10 Jul 1970). (In Dutch).

The Eurochemic plant for reprocessing spent nuclear fuel from different nuclear reactors is basically a chemical separation plant using classical operations such as dissolution, extraction, precipitation, and calcination. The nuclear character of the material treated limits the choice of equipment and its dimensions. This report describes these aspects as well as the experience gained after 3 years of operation. (Netherlands)

2325 SEPARATION OF URANIUM FROM SEA WATER BY PRECIPITATION METHOD. Yamabe, Takeo; Takai, Nobuharu (Tokyo Univ.). Nippon Kaisui Gakkaishi; 24: No. 1, 16-19(May 1970). (In Japanese).

In the method described, artificial seawater was prepared so as to contain 1 mg/l of uranium, and uranium was determined by the colorimetric method using Arsenazo III. The separation of uranium was carried out by formation of insoluble substances with phosphate. By this procedure, about 90% of the uranium in the seawater was collected into precipitates of phosphate. This method proved useful for the separation of uranium from seawater. (auth) (Japan)

2326 ISOLATION OF CERIUM FROM A MIXTURE OF RARE EARTHS WITH THE PRODUCTION OF A NITRIC MOTHER LIQUOR. Facchini, A.; Teatini, A.; Verganti, G. Chim. Ind. (Milan); 51: 970-5(Sep 1969). (In Italian).

Three methods of separating Ce from a NO_3-containing solution of a rare earth mixture {(i) hydrolysis, (ii) crystallization of hexanitrato-ammonium cerate $(NH_4)_2[Ce(NO_3)_6]$, and (iii) oxidation to hydroxide and leaching} were compared. Method (ii) was the most efficient, yielding Ce of 99% purity and a mother liquor containing HNO_3 and 180 g/l rare earths, including 10% residual Ce. (Metals Abstr.)

2327 MICROBIAL DEGRADATION OF AROMATIC HYDROCARBONS USED AS REACTOR COOLANTS. Catelani, D.; Mosselmans, G.; Nienhaus, J.; Sorlini, C.; Treccani, V. (Univ., Milan. Centro Euratom Ispra Servizio Protezione, Ispra, Italy). Experientia; 26: 922-3(15 Aug 1970).

Since the use of pure organic solvents is not possible in decontamination of organic reactor coolants, solvent emulsions and two-phase systems were used. A bacteriological pretreatment of waste waters from this decontamination process was attempted. The organisms able to grow on biphenyl, m-terphenyl, and on the thermic mixture (naphthalene, methylnaphthalene, biphenyl, and alkyl derivative of naphthalene) are described, together with the biological decontamination procedure of the waste waters. (M.C.G.)

2328 EXTRACTION OF RHENIUM AND MOLYBDENUM BY DIALKYLMETHYLBENZYLAMMONIUM SALTS. Angelova, Veselka; Doicheva, Rakhila. Rudodobiv Met. (Sofia); 24: No. 7, 40-3(Jul 1969). (In Bulgarian).

The general principles underlying the extraction of Re(VII) and Mo(VI) by various salts of the dialkylmethylbenzylammonium type are presented and discussed in relation to the pH of the aqueous phase and the type of anion in the salt. The distribution coefficient of Re depends both on the pH of the aqueous phase and the type of anion in the salt; Re may be extracted from both acid and alkaline

XUM

media by means of an agent of the $R_4N \cdot Cl$ type, but for the other salts the coefficient falls sharply at pH 4. The distribution coefficient of Mo is determined mainly by the concentration in the aqueous phase and the pH value. (Metals Abstr.)

2329 DECONTAMINATION OF MILK FROM RADIOACTIVE CAESIUM AND STRONTIUM BY MEANS OF ION EXCHANGERS OF POLISH MANUFACTURE. Kornacki, Kazimierz; Poznanski, Stefan; Jedrychowski, Lucjan. Nukleonika; 15: 79-88(1970). (In Polish).

Several ion exchangers produced in Poland were tested for their suitability in the removal of radioactive Cesium and strontium from milk. The products tested included: SD—product of the Chemical Cooperative "Xenon" in Łódź, FPC—product of the "Gamrat" Laboratory in Jasło, and MK-3—product of the Nitrogen Plant in Kedzierzyn. For comparison, the standard Amberlite IR-120 (USA) cation exchanger was also used. It was found that for removal of $^{85,89}Sr$ and ^{134}Cs, the cation exchangers SD and MK-3, respectively, were the most suitable, the latter being superior to the standard Amberlite IR-120. When a 1:1 mixture of the SD and MK-3 exchangers was used for joint decontamination of milk from these radionuclides, only 72% of $^{85+89}Sr$ and ^{134}Cs was removed as compared with 99.3% of ^{134}Cs on MK-3, and 92.3% of $^{85+89}Sr$ on the SD exchanger. At a milk flow rate through the column of $1/8$ and $1/16$ rbv/min (milk per resin volume per minute), no significant differences were noted in the degree of decontamination from radioactive cesium and strontium between the SD and MK-3 resins, whereas for Amberlite IR-120 the difference reached 10%. The ion exchangers of domestic production removed most intensively the particular radionuclides at 5°C, and Amberlite IR-120 was most efficient in the case of $^{85+89}Sr$ and ^{134}Cs at 35 and 20°C, respectively. For decontamination of Amberlite IR-120 about 20 rbv of the regenerating solution was used, whereas about 10 rbv was sufficient for regeneration of the SD and MK-3 exchangers. This is essential from the commercial viewpoint, since the price of the chemicals is important for the total cost of the milk decontamination process. (auth)

2330 ION-EXCHANGE SEPARATION OF URANIUM AND THORIUM FROM ORE PULPS AND CLEAR SOLUTIONS. Korkisch, J. (Univ., Vienna). At. Energy Rev.; 8: 535-619(Sep 1970).

Information is presented on separations of uranium and thorium by means of ion-exchange resins. Special attention is paid to methods that permit the anion-exchange separation of uranium from pulps obtained by the leaching with sulfuric acid of ores and other uranium-bearing materials. Numerous techniques are also described based on anion exchange, which can be used to separate uranium and/or thorium from a variety of other elements in pure aqueous or mixed aqueous—organic solvent systems containing carbonate, chloride, nitrate, phosphate, fluoride, thiocyanate, and organic complexing agents. Similarly, methods for the separation of uranium and thorium on cation-exchange resins are presented. Outlines of many techniques involving both anion- and cation-exchange separations and also distribution data are presented in tabular form. The review contains more than 800 references. (auth)

2331 IONIC FLOTATION OF URANIUM FROM DILUTED SOLUTIONS. Rabrenovic, R. (Institut za Tehnologi ju Mineralnih Sirozina, Belgrade). Rudy (Prague); 18: 139-41(Apr 1970).

A summary is given of the results of an extensive investigation on ionic flotation of uranium from dilute solutions obtained by leaching low-grade uranium ores from the Yugoslav localities of Gorenja Ves and Zletovska Reka. It follows from the results that by this procedure it is possible to concentrate successfully the uranium ions from these solutions in a common flotation cell used for the flotation of minerals. Together with the cation collector a corresponding liquid ion exchanger is introduced into the process as activator. Thus a uranium yield of about 97 to 99% can be attained with a procedure lasting not more than 3 min. The uranium content of the flotation product ranges from 3.8 to 18.5%. (auth) (INIS)

2332 STUDY OF THE FIXATION OF FLUORINE ON ANTIMONY PENTOXIDE IN HYDROCHLORIC ACID MEDIUM. Vialatte, B.; Barrandon, J. N.; Alexandrov, S.; (and others) (CEN de Saclay, Gif-sur-Yvette, France). Radiochem. Radioanal. Lett.; 5: 59-62(16 Oct 1970). (In French).

The experimental results of an investigation on the retention of fluorine on hydrated antimony pentoxide in hydrochloric acid as a function of time and normality are presented. The study was made in order to facilitate the determination of fluorine by charged particle or photon activation. (P.C.H.)

2333 FIXATION OF ALKALI METALS ON ANTIMONY PENTOXIDE HYDRATE IN STRONGLY ACID MEDIA. Bourrelly, I. N.; Cleyrergue, C.; Deschamps, N.; (and others) (CEN de Saclay, Gif-sur-Yvette, France). Radiochem. Radioanal. Lett.; 5: 43-9(16 Oct 1970). (In French).

The retention of the alkali metals, Na, K, Rb and Cs, on hydrated antimony pentoxide has been studied in hydrochloric, perchloric, and nitric acids. Curves showing the influence of time and acid normality on the retention are presented. The studies were made in order to facilitate the determination of alkali metals in rocks by activation. (P.C.H.)

2334 EXTRACTION OF NIOBIUM FROM AQUEOUS ORGANIC ACID MEDIA BY STRUCTURALLY RELATED TERT-AMINES. Abdel-Gawad, A. S.; Abdel-Rassoul, A. A.; Maghrawi, H. B.; Sherif, Sh. A. (Atomic Energy Establishment, Inshas, Egypt). Indian J. Chem.; 8: 293-5(Mar 1970).

The extraction ^{95}Nb from citric, oxalic, and acetic acids by a number of structurally related tertiary amines and the quaternary ammonium salt Aliquat 336 was investigated. Pronounced extractability of the metal ion with amines of high molecular weight was observed. In all the cases an increase in pH of solution results in a decrease in the per cent Nb extracted. With TOA the dependence on oxalate ion and amine concentration in the organic phase was also studied. (auth)

2335 SALTING OUT IN SOLVENT EXTRACTION OF ACIDS AND SOME RADIOACTIVE ELEMENTS. IV. SALTING OUT IN EXTRACTION OF HNO_3, $UO_2(NO_3)_2$, AND $Th(NO_3)_4$ BY AMINES AND TBP. Frolov, Yu. G.; Nasonova, G. I.; Gavrilov, N. V. At. Energ. (USSR); 29: 99-102(Aug 1970). (In Russian).

The possibility of determination of activity coefficients of tracer amounts of $UO_2(NO_3)_2$ in the presence of macroquantities of different salting-out agents on the basis of Mikulin's equation was shown. The advantage of utilization of osmotic coefficients for evaluating salting-out properties of electrolytes was confirmed. The effect of all factors defining the salting-out in a heterogeneous system was shown for extraction of HNO_3, $UO_2(NO_3)_2$, and $Th(NO_3)_4$ by amines and TBP. (auth)

2336 TREATMENT OF RUM JUNGLE URANIUM ORE. Allman, M. B.; Harris, J. A.; Bayly, M. G. (Territory Enterprises Pty. Ltd., Melbourne). At. Energy Aust.; 13: 22-38(1970).

Operational practice at the Rum Jungle uranium oxide plant in the Northern Territory is discussed with reference to crushing, grinding, leaching, solvent extraction and precipitation. Flow charts illustrate these systems and their interrelationship. A comparison is made with some overseas practices. Research and development in uranium separation is outlined. Aspects covered include precipitation from high-grade strip and solvent extraction investigations via TBP and amine/sulfate. cf. NSA 23: 40827. (Australia)

2337 ANION EXCHANGE BETWEEN BENTONITES AND ^{131}I IONS. Furnica, G. (Inst. of Hygiene, Bucharest). pp 611-21 of Symposium International de Radioecologie. Vol. I. Fontenay-aux-Roses, France; Commissariat a l'Energie Atomique (1970). (In French).

From Conference on Radioecology, Cadarache, France. See CONF-690918-(Vol.1).

Radioactive isotopes were used to study the retention by montmorillonitic bentonites of the I^- anion and the ion exchange capacity of the bentonites used was determined. Their activity was found to increase in proportion with their time of contact with $Na^{131}I$ solution. The bentonite-radioactive solution system (1g : 5ml) reached equilibrium after 12 hours, the bentonite having fixed 11.13 n Ci (i.e., 0.9×10^{-13}g ^{131}I) of the original quantity (12.304 n Ci) in the aqueous solution. The study was carried out with a calibrated solution (Amersham) containing 2.5×10^{-9}g $I^-/1.0 \times 10^{-13}$g ^{131}I. The anion exchange capacity measured on the bentonite used is extremely small, corresponding to 12.9×10^{-12} equiv/g bentonite. (auth) (France)

2338 ABSORPTION OF ELEMENTS BY CLAYS. Argiero, L.; Barzon, G. (CAMEN, Pisa, Italy). pp 655-64 of Symposium International de Radioecologie. Vol. I. Fontenay-aux-Roses, France; Commissariat a l'Energie Atomique (1970). (In French).

From Conference on Radioecology, Cadarache, France. See CONF-690918-(Vol.1).

The ion exchange capacity and the distribution coefficient for the elements Ru, Cs, and Ce were studied on several clays. Four groups of samples of quaternary sediments and three groups of pliocene sediments were examined. The difference between the exchange capacities of these two types of samples seems to be due to the presence of a vermiculite-type material in the quaternary soil. Another peculiarity observed is the aspect of the distribu-

tion coefficients, which increase rapidly while the Ci value of the initial concentration of the radioisotopes studied decreases. (auth) (France)

2339 ANION EXCHANGE PURIFICATION OF NEPTUNIUM BY IN SITU CONVERSION FROM A NITRATE TO A CHLORIDE SYSTEM. Conner, William V.; Proctor, Stephen G. (Dow Chemical Co., Golden, Colo.). Contract AT(29-1)-1106. J. Inorg. Nucl. Chem.; 32: 3259-62(Oct 1970).

A 200-g batch of neptunium oxide was purified using a combined nitrate and chloride anion exchange procedure, which utilized an in situ conversion of the loaded neptunium nitrate complex to the chloride complex. The in situ conversion reduced the processing time and neptunium losses previously experienced with a two-step nitrate and chloride process. No adverse effect on the purity of the NpO_2 product was observed. The actinide content of the purified NpO_2 product was <0.1 ppM of plutonium and americium, <0.2 ppM thorium, and 7 ppM uranium. The total of all impurities was 407 ppM. (auth) (UK)

2340 PROCESS FOR DECONTAMINATING LIQUID RADIOACTIVE EFFLUENTS CONTAINING RADIUM. (to Ugine-Kuhlmann, SA). French Patent 1,569,793. 28 Apr 1969. Filed 28 Mar 1968. (In French).

A procedure is described for the removal of radium from radioactive effluents from the treatment of uranium minerals by ion exchange using zeolites containing alkali metal or alkaline earth metal ions. The zeolite has the general formula $nSiO_2$, mAl_2O_3, pM_2O, zH_2O where $5 \leq n \leq 9$, $0.8 \leq m \leq 1.5$, and $2 \leq z \leq 15$ for $p = 1$. (P.C.H.)

2341 SEPARATION OF ^{234}Th FROM INACTIVE THORIUM, URANIUM, AND IRON BY ADSORPTION ON $Bi(IO_3)_3$, $Bi(IO_4)_3$, OR $Pb(IO_3)_2$. Sethi, Suman; Rai, Rama Shanker (Univ. of Rajasthan, Jaipur, India). Z. Anal. Chem.; 252: 5-7(1970).

Conditions are described under which rapid and quantitative separation of ^{234}Th occurs by adsorption on $Bi(IO_3)_3$, $Bi(IO_4)_3$, $Pb(IO_3)_2$. The activity is retained even in presence of considerable amounts of inactive thorium, uranyl, and ferric ions. It appears that the activity is adsorbed by counter-ion exchange followed by inhomogeneous mixed crystal formation. (auth)

2342 SEPARATION OF FISSION PRODUCED IODINE BY SURFACE IONIZATION. Venezia, A.; Amiel, S. (Soreq Nuclear Research Centre, Yavne, Israel). Nucl. Instrum. Methods; 87: 307-9(1970).

Iodine isotopes were extracted from a graphite fission fragment catcher by diffusion, and separated in high purity from the other fission products by negative surface ionization and electromagnetic separation. (auth)

2343 REVIEW OF ISOTOPIC METHODS APPLIED IN DISTILLATION AND RECTIFICATION. Zablotny, Wladyslaw (Inst. of Nuclear Research, Warsaw). Nukleonika; 15: 107-15(1970). (In Polish).

A review is given of investigations into the distillation process by the tracer method. The works discussed were carried out both on a laboratory and industrial scale with the aim to determine the degree of purification. The tracer method was also applied to establish the optimal parameters of the distillation process. The results obtained in the particular investigations contributed to a number of technological improvements increasing the output of the plants. (auth)

2344 DE-WATERING OF RADIOACTIVE SLUDGE BY SUPER-DECANTER CENTRIFUGE. Shimoura, Kazukuni; Tsutsui, Tenson (Kyoto Univ.). Nippon Genshiryoku Gakkaishi; 12: 582-5(1970). (In Japanese).

Volume reduction of radioactive sludge by de-watering is important in the chemical treatment of radioactive liquid wastes. The de-watering characteristics of a super-decanter type centrifuge for ferric hydroxide sludge was investigated experimentally. The results obtained include the relation of sludge removing efficiency to feed rate, the correlation of centrifugal force with volume reduction factor and with radioactivity eluted from the sludge. Addition of polymer as coagulating agent is effective in improving the treating capacity and in shortening the settling time after separation. Experiments were performed to determine the conditions for adding the polymer to obtain optimum coagulation of the sludge. (auth)

2345 REGULARITIES IN THE DISTRIBUTION OF TTA AND ITS SCANDIUM CHELATE INTO A SERIES OF ETHER SOLVENTS. Suzuki, Nobuo; Akiba, Kenichi; Asano, Hiroko (Tohoku Univ., Sendai). Anal. Chim. Acta; 52: 115-22(Oct 1970).

The distribution of a powerful chelating agent, TTA, and its typical trivalent metal chelate, that of scandium(III), between aqueous perchlorate solution ($\mu = 0.1$) and 12 ether solvents was determined at 25°. A good correlation was found between the distribution coefficient of TTA and the "solubility parameter" of the ether solvents, except bis(2-chloroethyl) ether. The distribution coefficient of the scandium chelate (P_M) was compared with that of TTA (P_{HA}), and it was confirmed that the relationship expressed by $\log P_M = n \log P_{HA} + \text{const.}$, is valid for the present system. (auth)

2346 IMPROVEMENTS IN OR RELATING TO DECONTAMINATION OF MATERIALS. Kudo, Tsutomu. British Patent 1,208,521. 14 Oct 1970. Priority date 10 Jan 1968, Japan.

A method of removing radioactive contaminants from a material, such as milk, comprises contacting the material with a phytin compound to adsorb the contaminant. Suitable compounds are Na-phytin, $C_6H_6O_{24}P_6CaMg_4Na_2 \cdot 5H_2O$, Ca-phytin, $C_6H_6O_{24}P_6Ca_6 \cdot 5H_2O$, Ca_4Na_2-phytin, $C_6H_6O_{24}P_6Ca_4Na_2 \cdot 5H_2O$, and Ca_3Na_2-phytin, $C_6H_{10}O_{24}P_6Ca_3Na_2 \cdot 5H_2O$. The pH of the solution should be from 3 to 9, and the phytin compound should be present in an amount of 10 to 80 g/l. The method is particularly suitable for the separation of strontium-90 from milk. (B.L.M.)

XUM

EARTH SCIENCES

Geology and Hydrology

Refer also to abstracts 2338, 2498, 2542, 2543, 2545, and 2547.

2347 (CSIRO-Trans-10140) PROBLEMS OF GAMMA-GAMMA LOGGING IN ORE MINING IN THE MECSEK. Szabo, J.; Somlyay, Z.; Szekely, E.; Tirkala, F.; Virag, P. Translated by G. Losonci (Commonwealth Scientific and Industrial Research Organization, Melbourne, Australia), from Magy. Geofiz.; 9: 237-41(1968). 7p. Dep. NTIS (U. S. Sales Only).

Improvements in utilization of $\gamma-\gamma$ borehole logging are considered. A suitable intensity radiation source, optimal probe length, and limit level of the instrument were evaluated. Two profiles, determined on the basis of these evaluations are discussed. (Australia)

2348 (NYO-3961-1) UTILITY OF RADIOISOTOPE METHODOLOGY IN ESTUARY POLLUTION CONTROL STUDIES, PART I. EVALUATION OF THE USE OF RADIOISOTOPES AND FLUORESCENT DYES FOR DETERMINING LONGITUDINAL DISPERSION COEFFICIENT IN ESTUARIES. Abood, Karin A.; Lawler, John P.; Disco, Michael D. (Quirk, Lawler and Matusky Engineers, New York). Aug 1969. Contract AT(30-1)-3961. 197p. Dep. NTIS.

A generalized procedure for a tracer field survey was developed. This handbook procedure is suitable for selection of the best tracer for measurement of dispersion and flow characteristics in freshwater rivers as well as estuaries. Comprehensive analysis shows that there are advantages and limitations to both groups of tracers. Radiotracers appear to meet the technical requirements of an ideal tracer better than other materials. However, the non-technical aspects associated with their use are responsible, to some extent, for hindrance to the adoption of radioisotope techniques by many investigators. (auth)

2349 (USGS-474-72) HYDRAULIC TESTS IN HOLE UA-1 AND WATER INFLOW INTO AN UNDERGROUND CHAMBER, AMCHITKA ISLAND, ALASKA. Ballance, Wilbur C. (Geological Survey, Denver, Colo.). Oct 1970. 54p. Dep. NTIS.

Hole UA-1 was center punched (a small-diameter exploratory hole drilled ahead of the large-diameter emplacement hole) from 1,524.0 to 1,981.2 (5,000 to 6,500 ft) and hydraulically tested to determine an ideal location for mining a chamber. Fifteen zones were tested; minor amounts of water bypassed the packers during five of the tests. The tested intervals ranged in length from 37.5 m (123 ft) to 211.5 m (694 ft). For purposes of comparison relative specific capacities were calculated from comparable 60.4 m (198 ft) intervals of tested rock, and ranged from 0.1162 m^3 per day per m (0.0065 gpm/ft) of drawdown to 0.0039 m^3 per day per m (0.0002 gpm/ft) of drawdown. The interval 1,745.0 to 1,836.4 m (5,725 to 6,025 ft) appears to be the best location for mining a chamber so far as water inflow is concerned. This interval, 91.4 m (300 ft), consists of about 27.4 m (90 ft) of breccia and 64.0 m (210 ft) of basalt. The inflow to a spherical chamber 18.3 m (60 ft) dia and placed in the center of the proposed 91.4 m (300 ft) interval, was calculated to be about 175 m^3 per day (32 gpm) after the first day and would stabilize at about 57 m^3 per day (10.5 gpm) after about 200 days. (auth)

2350 TO THE QUESTION OF THE LOADING CAPACITY OF THE RHINE FOR RADIOACTIVE NUCLIDES. 6. SORPTION OF RADIONUCLIDES ON SELECTED MINERALS. Schneider, H. (Bundesanstalt fuer Gewaesserkunde, Coblenz, Ger.). Gas-Wasserfach, Wasser - Abwasser; 111: No. 1, 21-6(1970). (In German).

The sorptive properties of artificial mono-mineralic fine sands of uniform grain size is investigated. Montmorillonite, kaolinite, muscovite, and biotite have a high sorptive power. The sorptive power of quartz oxides and magnetite and of microcline and albite is low. Hornblende and augite occupy a medium position. The highest affinity for the minerals show the cations ^{137}Cs, ^{90}Sr, and ^{65}Zn. Phosphorus-32, as complex phosphate anion, is less highly absorbed. The sorption of ^{131}I is negligible. (INIS)

2351 FISSION TRACKS ON (001) CLEAVAGES OF TOPAZ. Patel, A. R.; Patel, M. M. (Sardar Patel Univ., Gujarat, India). Indian J. Pure Appl. Phys.; 7: 491-3(Jul 1969).

Etching on (001) cleavages of natural topaz single crystals from Ropp Tin Mines, Nigeria, has shown two types of pits: with trails and without trails. The pits with the trails have been found to be comparatively larger in size than those without the trails. It has been observed that on matched pairs these pits have one-to-one correspondence in position, size and structure. When the negatives of matched pairs have been superposed the trails have been found to run along the same straight line. Correspondence in the etch patterns on the two sides of an etched thin (260 μ thick) plate of the crystal has been established with respect to pits without the trails. The etch patterns have been found to be displaced with respect to each other. A cleavage face has been successively etched for different periods and the etch patterns produced have been studied at each stage of etching. The implications are discussed. (auth)

2352 MEASUREMENT OF ENVIRONMENTAL RADIATION AT ARCHAEOLOGICAL EXCAVATION SITES. Mejdahl, V. (Danish Atomic Energy Commission, Risoe). Archaeometry; 12: 147-59(Aug 1970).

As part of a thermoluminescence dating programme the environmental radiation was measured at approximately thirty excavation sites, including three in Germany and one in Sweden. The measurements were carried out by means of a thermoluminescent phosphor, $CaSO_4$:Dy, contained in steel tubes that were hammered into the ground and left in position for approximately one month. The intensity at a height of one m above the ground and at depths ranging from 0 to 130 cm below the ground was determined, and the perturbing effect of large stones was studied. The variation of response with energy was investigated for quartz and feldspar grains imbedded in one cm thick clay tablets, and for $CaSO_4$:Dy. The response of the mineral grains exceeded the true exposure from soil radiation by 5.3%, and $CaSO_4$:Dy exposed in steel cylinders with a wall thickness of 1.5 mm overestimated the exposure by 6.6%. The exposure measured with our dosimeters is therefore fairly close to that recorded by a sherd. However, when a more accurate evaluation of environmental radiation is desired, the soil contribution to the response must be corrected. (auth) (UK)

2353 MODEL LEAD AND RADIOMETRIC AGES FROM THE CHURCHILL PROVINCE, CANADIAN SHIELD. Sinha, A. K. (Univ. of California, Santa Barbara). Goechim. Cosmochim. Acta; 34: 1089-1106(Oct 1970).

The isotopic composition of primary lead has been determined in 11 galenas and 26 feldspars from the Churchill Province, Canada. Samples were collected from a triangular area bounded by La Ronge, Saskatchewan, Lake Wollaston, Saskatchewan and Flin Flon, Manitoba. The galena lead model ages are consistent around 2030 Myr assuming a closed system isotopic evolution for their lead and 4550 Myr as the age of the earth. The least radiogenic lead from feldspars gives model ages similar to the galena ages, while others are more radiogenic and give anomalously younger ages even after correction for in situ uranium decay. The $^{208}Pb/^{204}Pb$ ratios of the galenas and the least radiogenic feldspars are indistinguishable. Rb-Sr ages determined on whole rocks and potassium feldspars from pegmatites and whole rocks give an isochron age of 1846 ± 60 Myr. This is probably the time of the formation of the galena ore bodies also. Feldspars from a belt of metamorphic rocks of possible pre-Hudsonian age contain lead with aberrant model ages, which are mostly much younger than the ages of the galenas and other feldspars. The difference between the radiometric and model ages seen in this area is of the same sign, but lesser magnitude than the difference found in the 2720 Myr old rocks of the Superior Province in Canada. On the other hand, ores and rocks younger than 1400 Myr generally have model ages less than radiometric ages. These observations cast doubt on the validity of closed system evolution models for common lead. (auth) (UK)

2354 IMPACT OF THE NATURAL SCIENCES ON ARCHAEOLOGY. Tite, M. S. (Univ. of Essex, Eng.). Contemp. Phys.; 11: 523-39(Nov 1970).

Some of the applications of physics to the solution of archaeological problems are reviewed. The use of magnetic, resistivity and electromagnetic surveying techniques for the location of buried features is described. Various methods of age determination are outlined while the problems associated with radiocarbon dating of organic material and thermoluminescent dating of pottery are discussed in detail. The techniques, including petrological examination, chemical analysis and isotopic analysis, employed in the physical examination of archaeological artefacts are described. Examples of the application of these techniques in establishing the source of the raw materials used in pottery, metal and stone implements and in elucidating the techniques of manufacture of pottery and metal objects are also given. (auth) (UK)

2355 THERMOLUMINESCENT DATING: REFINEMENT OF THE QUARTZ INCLUSION METHOD. Fleming, S. J. (Oxford Univ.). Archaeometry; 12: 133-45(Aug 1970).

XUM

In the early development of thermoluminescent dating the method was considered as a relative one that required calibration with known-age samples. Absolute ages independent of other chronology were first obtained using the inclusion technique (Fleming 1966). Subsequent modifications to this technique together with the results of a comprehensive test programme are described. (auth) (UK)

2356 ISOTOPIC COMPOSITION OF URANIUM IN GROUND WATERS. Gottikh, R. P.; Tyminskii, V. G.; Spiridonov, A. I.; Sel'dyakov, Yu. I.; Salmenkova, M. A. Tr., Vses. Nauch.-Issled. Inst. Yader. Geofiz. Geokhim.; No. 4, 255-65(1968). (In Russian).

Geochemical analysis of the behavior of uranium isotopes must include also an examination of the ^{234}U precursors, UX_1(^{234}Th) and UX_2(^{234}Pa). Thorium is removed faster by adsorption on fragmental material than uranium; thus when ^{238}U decays, the thorium is removed before the ^{238}U is transformed into ^{234}U. Thus, the ^{234}U derived from ^{234}Th and ^{234}Pa in the liquid phase does not have to be taken into account in the isotopic analysis of water samples. Water samples from artesian basins were used for studying the variations of the $^{234}U/^{238}U$ ratio; it was found that the ratio varies from 1.2 to 6.1. Water specimens from metamorphic and igneous rocks exhibited the highest ratios; this is probably due to the preferential leaching of ^{234}U and the relative youth of the rocks. The wide variations of the ratio indicate that the ratio may be used for the solution of hydrogeological and geochemical problems. The study also indicated that the α-spectrometric method yields the most precise results. The instrument provided with a semiconductor detector, used for the study, had a resolution of <2% for 5-MeV α particles and made it possible to measure shifts in the $^{234}U/^{238}U$ ratio in specimens containing 2×10^{-6} g of uranium with a precision of ±10%. The same method was also used to determine the ^{235}U. The ratio may be of interest to solve problems relating to the origin of the waters, their path and hydrodynamic questions. (TTT)

2357 SUBMARINE RADIOACTIVITY LOGGING TECHNIQUE. Dewan, John T. (to Schlumberger Technology Corp.). U. S. Patent 3,532,881. 6 Oct 1970. Filed 5 Jan 1968.

A typical embodiment of the invention enables characteristics of the bottom of a body of water to be measured and located with accuracy. Radioactivity logging equipment is housed within a sled that is towed along the bottom to scoop up mineral nodules or bottom samples in a mesh or grid. The sled and samples are lifted by towing cable about ten feet off the bottom to provide a suitable environment for gamma radiation spectrum analysis. The elevation above the bottom is measured by a fathometer within the sled. Hydrophone equipment on board the towing vessel responds to the sound pulses emitted by the fathometer in order to fix the position of the sled relative to known geographical references and thereby establish the precise location of each sample measurement. Optionally, an integral drill bit is fixed to one end of the sled for the purpose of boring through sediment. (auth)

2358 PROGRESS OF HYDROLOGY. VOLUME I. NEW DEVELOPMENTS IN HYDROLOGY. Proceedings of the First International Seminar for Hydrology Professors Held at Urbana, Illinois, July 13–25, 1969. A United States Contribution to the International Hydrological Decade. Urbana, Ill.; University of Illinois (1969). 511p. (CONF-690726-(Vol.1)).

Twenty of the papers presented at the conference are included in volume 1. Separate abstracts were prepared for 2. Eighteen papers are not within the scope of NSA. (L.C.L.)

For abstracts of individual papers see: 2359 and 2360.

2359 NUCLEAR TECHNIQUES IN HYDROLOGY. Payne, Bryan R.; Dincer, Targut (International Atomic Energy Agency, Vienna). pp 126-48 of Progress of Hydrology. Vol. I. New Developments in Hydrology. Urbana, Ill.; Univ. of Illinois (1969).

From 1st International Seminar for Hydrology Professors, Urbana, Ill. See CONF-690726-(Vol.1).

A short review of nuclear techniques and examples of their applications in a variety of hydrological conditions and problems is presented. The subjects discussed include nucleonic instruments, uses of artificially-injected radioisotope tracers, and the use of environmental isotope variations in waters of the hydrological cycle. (L.C.L.)

2360 PRINCIPLES OF THE APPLICATION OF NUCLEAR TECHNIQUES TO HYDROLOGIC INVESTIGATIONS. Thatcher, L. L. (Geological Survey, Denver). pp 149-93 of Progress of Hydrology. Vol. I. New Developments in Hydrology. Urbana, Ill.; Univ. of Illinois (1969).

From 1st International Seminar for Hydrology Professors, Urbana, Ill. See CONF-690726-(Vol.1).

The principles of the application of nuclear techniques used in hydrologic investigations are selectively reviewed with emphasis on applications of more general interest. The subjects discussed include: a review of relevant nuclear physics; uses of environmental isotopes; principles of ground water dating; and applications in local and regional ground water investigations, in surface water studies, and in water pollution studies. (L.C.L.)

2361 CAPTURE OF ^{60}Co BY SUSPENDED PARTICLES IN THE DANUBE. Radosavljevic, R.; Tasovac, T. (Boris Kidric Inst. of Nuclear Sciences, Vinca, Yugoslavia). pp 83-92 of Symposium International de Radioecologie. Vol. I. Fontenay-aux-Roses, France; Commissariat a l'Energie Atomique (1970).

From Conference on Radioecology, Cadarache, France. See CONF-690918-(Vol.1).

As a part of the program for the control of the radioactivity of the Danube, the behavior of different radionuclides is studied and the fixation of cobalt-60 by suspensions is investigated. The influence of different parameters on fixation is determined. (auth) (France)

2362 INTRODUCTION TO A STUDY OF THE PHYSICO-CHEMICAL BEHAVIOR OF RADIORUTHENIUM CONTAINED IN RADIOACTIVE EFFLUENT. Amavis, R. (European Atomic Energy Community, Luxemburg). pp 93-125 of Symposium International de Radioecologie. Vol. I. Fontenay-aux-Roses, France; Commissariat a l'Energie Atomique (1970). (In French).

From Conference on Radioecology, Cadarache, France. See CONF-690918-(Vol.1).

Since no completely satisfactory method exists for the radioruthenium purification of radioactive effluent before discharge, this radioelement is largely responsible for the pollution of the environment. The difficulties of its elimination are mainly due to a lack of knowledge of its physicochemical behavior in radioactive wastes. Research was devoted to the identification of the physico-chemical form in which ruthenium is present in an actual effluent, either before or after purification treatments. Various microchemical methods were used for this study. Different forms of radioruthenium were found, cationic, anionic, neutral, polynuclear,or colloidal in nature. From the results of this work certain hypotheses may be put forward concerning the behavior of radioruthenium in a natural water-containing medium: dilution, deposition, and retention on suspensions and sediments. (auth) (France)

2363 RETENTION OF CERTAIN RADIOACTIVE IONS BY THE SUSPENSIONS OF SURFACE BASINS AND BY CERTAIN ACTIVE EARTHS IN RUMANIA. Furnica, G. (Inst. of Hygiene, Bucharest). pp 181-200 of Symposium International de Radioecologie. Vol. I. Fontenay-aux-Roses, France; Commissariat a l'Energie Atomique (1970). (In French).

From Conference on Radioecology, Cadarache, France. See CONF-690918-(Vol.1).

A study was made of the retention, by mud taken from the river of Dimbovitza–Bucharest, of the isotopes ^{22}Na, ^{85}Sr, ^{110}Ag, ^{134}Cs, ^{65}Zn, ^{59}Fe, and ^{131}I dissolved in the water. These isotopes are fixed by the mud in different proportions, i.e., 15% Na, 45% Sr, 37% I, 97% Zn, 95% Fe, or 98% Cs. By elution of the mud retaining ^{22}Na, ^{85}Sr, or ^{110}Ag, a phenomenon of ion exchange between the radioactive ions and the natural product was observed. The sand fixes separately: 3.6% Na, 22% Ag, 72% Zn, 8.8% I, 99% Cs, 93% Sr, or 94% Fe. Treatment of the sand with 5% HNO_3 or 10% HCl alters the radioactive ion retention capacity. Similar determinations were made with montmorillonitic bentonites, the retention observed being greater with respect to Cs and smaller with respect to Na. (auth) (France)

2364 POINTS OF VIEW ON THE STUDY OF THE PHYSICO-CHEMICAL PROCESSES OF TRANSFER OF RADIORUTHENIUM IN CONTINENTAL MEDIUM. Bittel, R. (CEN, Fontenay-aux-Roses, France); Blum, J. M.; Jaumier, J. J.; Verot, J. L. pp 213-30 of Symposium International de Radioecologie. Vol. I. Fontenay-aux-Roses, France; Commissariat a l'Energie Atomique (1970). (In French).

From Conference on Radioecology, Cadarache, France. See CONF-690918-(Vol.1).

The physical chemistry of ruthenium is complicated because of its multi-valent states and corresponding saline and complex compounds. Two Ru isotopes, ^{106}Ru and ^{103}Ru are present in many liquid radioactive effluents and contribute to contamination of continental medium. The behavior of Ru in dispersion medium may be explained by the chemical states of the element. Experiments are proposed in order to obtain suitable data. The principal difficulties for experimenters result from: varied nature of Ru solutions; multiplicity of equilibrium between the different forms of Ru in dilute solutions; non accuracy of analyses. The first difficulty can be avoided by using well-defined Ru compounds, and the third by carrying out many analyses which may allow to have sufficient informations on the second difficulty. In a first

XUM

experimental work, synthesis of the well-defined Ru compounds was carried out. The conditions for using these compounds as well as the informations obtained from the experiments performed on these compounds in order to study Ru transfer in continental medium are discussed. (auth) (France)

2365 INFLUENCE OF SOME ORGANIC COMPOUNDS ON THE MOVEMENT OF ^{90}Sr IN SOILS. Himes, F. L.; Shufeldt, R. (Ohio Agricultural Research and Development Center, Columbus). pp 493-507 of Symposium International de Radioecologie. Vol. I. Fontenay-aux-Roses, France; Commissariat a l'Energie Atomique (1970).

From Conference on Radioecology, Cadarache, France. See CONF-690918-(Vol.1).

The leachates of undisturbed Canfield soil in lysimeters contain some ^{90}Sr. The influences of organic compounds and of soil organic matter on the movement of ^{90}Sr have been studies. The decreasing order of effectiveness of organic compounds on the quantity of ^{90}Sr adsorbed by most soil samples is: phytic acid, glucuronic acid, citric acid, pectic acid, pyrocatechol, glycine, and dextrose. The adsorption of ^{90}Sr by soil samples after treatment with dilute HF could be altered by methylation. Methylation of soil organic matter with diazomethane decreased the quantities of exchangeable and chelate Sr fractions proportionally more than the non-displaceable fraction. Methylation with CH_3OH-BF_3 decreased only the non-displaceable fraction. In general, the quantity of water soluble Sr was greater for soil samples that had been oven-dried than for samples kept continuously moist. (auth) (France)

2366 CALCULATION BY DIGITAL COMPUTER OF THE MIGRATION RATE OF ^{90}Sr IN THE SOIL. Reiniger, P.; Frissel, M. J.; Poelstra, P. (ITAL-EURATOM, Wageningen, Netherlands). pp 589-609 of Symposium International de Radioecologie. Vol. I. Fontenay-aux-Roses, France; Commissariat a l'Energie Atomique (1970). (In French).

From Conference on Radioecology, Cadarache, France. See CONF-690918-(Vol.1).

A mathematical model of strontium-90 transport in the soil is presented. The total transport rate is calculated by addition of the component rates, these being the rates of chromatographic transport, biological transport, and displacement by ploughing. The climatological parameters used in these calculations may be time variables. The biological parameters and those of the soil may be variables of time, of position in the soil profile or of both. The mathematical model uses the CSMP (continuous system modeling program) for the IBM 360/50 digital computer. The results of calculations for an experimental field with three pH levels and for a muddy soil are compared to the strontium-90 values measured over a period of eight years. (auth)(France)

Meteorology

Refer also to abstracts 2059, 2103, 2110, 2113–2115, and 2504–2506.

2367 (STI/DOC-10/117) ENVIRONMENTAL ISOTOPE DATA NO. 2: WORLD SURVEY OF ISOTOPE CONCENTRATION IN PRECIPITATION (1964–1965). Technical Reports Series No. 117. (International Atomic Energy Agency, Vienna (Austria)). 1970. 420p. IAEA $8.00.

The second volume of "Environmental Isotope Data: World Survey of Isotope Concentration in Precipitation" includes tabulated data on: the concentration of environmental isotopes, deuterium, ^3H, and ^{18}O in monthly samples of precipitation taken by a global network of 221 stations in the period from 1964 to 1966; meteorological conditions such as the amount of precipitation, vapor pressure, and temperature; and information for the period 1957 to 1964 that was received too late for inclusion in the first volume of this series. (L.C.L.)

2368 METEOROLOGICAL EVALUATION ON THE ENVIRONMENTAL CONTAMINATIONS DUE TO THE CHINESE NUCLEAR EXPLOSION TESTS (OCT. 1964 TO JAN. 1969). Kim, Sung Sam (Seoul National Univ.); Rho, Chae-shik; Son, Hyeongjin. New Phys. (S. Korea); 10: 53-64(Jun 1970). (In Korean).

Relationships between the radioactive contamination at ground level and the winds aloft and pressure patterns were analyzed. The following results were obtained: Surface contamination due to total deposits tends to be distributed to the south of the jet stream axis locating from west to east at upper and middle troposphere, and to the north of the axis at the lower troposphere. A distance of 2 to 3 latitudinal degrees was observed between the center axis line of surface contaminated area and the zero vorticity line at 500 mb level. The highest contamination occurred within 24 hours after the passages of surface front and/or trough except for the fifth test. (auth)

2369 IMPORTANCE OF GRAVITATIONAL COAGULATION ON THE SETTLING OF HIGH-MASS DENSITY AEROSOLS. Lindauer, G. C.; Castleman, A. W. Jr. (Brookhaven National Lab., Upton, N. Y.). Nucl. Sci. Eng.; 42: 58-63(Oct 1970).

The relative importance of Brownian and gravitational coagulation on the transient behavior of an aerosol undergoing coagulation and gravitational settling is discussed. A comparison is given of the particle size distribution and settling rates calculated for a typical high-mass density aerosol using a gravitational coagulation capture efficiency, ϵ of unity, an ϵ calculated as a function of particle radius, and an ϵ of zero. It is concluded that the use of $\epsilon = 1.0$ predicts a non-log-normal size distribution and seriously overestimates the aerosol deposition rate, particularly at short times after the onset of settling. (auth)

2370 FISSION PRODUCTS OF NUCLEAR EXPLOSIONS DETECTED ON THE TERRITORY OF THE G.D.R. II. Zindler, H. (Staatliche Zentrale fuer Strahlenschutz, Berlin). Kernenergie; 13: 186-8(Jun 1970). (In German).

Fission products from the 7th and 8th Chinese nuclear explosions partially entered the stratosphere. They returned to the troposphere by virtue of the intense upflow beginning in late winter and produced significant maxima of man-made radioactivity in near-ground air, precipitations, and fallout in the G.D.R. in the spring months of 1968 and 1969. Yearly sum of total beta activity in the 1968 fallout was about twice that of the preceding year because of this permanent supply of fresh fission products continued over some months, but it was only 4 percent of the 1963 value. The yearly sum for ^{90}Sr and ^{137}Cs activity in the 1968 fallout varied but little as compared to 1967. (auth)

2371 GENERAL REGULARITIES OF NATURAL RADIOISOTOPE DISTRIBUTION IN SOILS OF THE USSR. Baranov, V. I.; Morozova, N. G. (Inst. of Geochemistry and Analytical Chemistry, Moscow). pp 469-91 of Symposium International de Radioecologie. Vol. I. Fontenay-aux-Roses, France; Commissariat a l'Energie Atomique (1970).

From Conference on Radioecology, Cadarache, France. See CONF-690918-(Vol.1).

The chief genetic soil types of different climatic zones of the European part of the USSR were studied and the distribution of natural radioisotopes was established. Six hundred and seventy-five samples of soils and soil-forming rocks were analyzed. The content of natural radioelements (in air-dry material) of the investigated soils varied within wide ranges: for Ra from $n.10^{-13}$ to $n.10^{-10}$%, for Th from $n.10^{-6}$ to $n.10^{-3}$%, and for K from $n.10^{-2}$ to n%. From the obtained data, an attempt was made to draw up radiogeological maps in order to study the migration, accumulation, and diffusion of natural radioelements in soils. (auth) (France)

Mineralogy and Exploration

Refer also to abstract 3098.

2372 (RME-153) PRELIMINARY RECONNAISSANCE FOR URANIUM IN TEXAS, 1951 TO 1957. (Grand Junction Office (AEC), Colo. Geological Survey, Washington, D. C.). Jun 1970. 228p. Dep. GPO $1.75.

A compilation of preliminary reconnaissance reports on sites in Texas, examined in 1951 to 1957 for uranium deposits, is presented. Information on the geology, location, mineralogy, mining history, ownership, and radioactivity at each site is included. (L.C.L.)

2373 (RME-154) PRELIMINARY RECONNAISSANCE FOR URANIUM IN APACHE AND COCHISE COUNTIES, ARIZONA, 1950 TO 1957. (Grand Junction Office (AEC), Colo. Geological Survey, Washington, D. C.). Jun 1970. 86p. Dep. GPO $0.75.

A compilation of preliminary reconnaissance reports on sites in Apache and Cochise Counties, Arizona, examined in 1950 to 1957 for uranium deposits, is presented. Information on the geology, location, mineralogy, mining history, ownership, and radioactivity at each site is included. (L.C.L.)

2374 (RME-155) PRELIMINARY RECONNAISSANCE FOR URANIUM IN COCONINO COUNTY, ARIZONA, 1951 TO 1955. (Grand Junction Office (AEC), Colo. Geological Survey, Washington, D. C.). Jun 1970. 119p. Dep. GPO $1.00.

A compilation of preliminary reconnaissance reports on sites in Coconino County, Arizona, examined in 1951 to 1955 for uranium deposits, is presented. Information on the geology, location,

XUM

mineralogy, mining history, ownership, and radioactivity at each site is included. (L.C.L.)

2375 (RME-156) PRELIMINARY RECONNAISSANCE FOR URANIUM IN GILA COUNTY, ARIZONA, 1951 TO 1956. (Grand Junction Office (AEC), Colo. Geological Survey, Washington, D. C.). Jun 1970. 186p. Dep. GPO $1.50.

A compilation of preliminary reconnaissance reports on sites in Gila County, Arizona, examined in 1951 to 1956 for uranium deposits, is presented. Information on the geology, location, mineralogy, mining history, ownership, and radioactivity at each site is included. (L.C.L.)

2376 (RME-158) PRELIMINARY RECONNAISSANCE FOR URANIUM IN MOHAVE COUNTY, ARIZONA, 1952 TO 1956. (Grand Junction Office (AEC), Colo. Geological Survey, Washington, D. C.). Jun 1970. 169p. Dep. GPO $1.75.

A compilation of preliminary reconnaissance reports on sites in Mohave County, Arizona, examined in 1952 to 1956 for uranium deposits, is presented. Information on the geology, location, mineralogy, mining history, ownership, and radioactivity at each site is included. (L.C.L.)

2377 (RME-159) PRELIMINARY RECONNAISSANCE FOR URANIUM IN PIMA AND PINAL COUNTIES, ARIZONA, 1950 TO 1957. (Grand Junction Office (AEC), Colo. Geological Survey, Washington, D. C.). Jun 1970. 100p. Dep. GPO $1.00.

A compilation of preliminary reconnaissance reports on sites in Pima and Pinal Counties, Arizona, examined in 1950 to 1957 for uranium deposits, is presented. Information on the geology, location, mineralogy, mining history, ownership, and radioactivity at each site is included. (L.C.L.)

2378 CLOSED CIRCUIT TECHNIQUE FOR THE MEASUREMENT OF RADON/THORON RATIO IN SOIL-GAS. Tewari, S. G.; Ghosh, P. C.; Bhatnagar, A. S. (Dept. of Atomic Energy, New Delhi). Indian J. Pure Appl. Phys.; 6: 33-6(Mar 1968).

A closed circuit technique for measuring the $^{220}Rn/^{222}Rn$ ratio in soil gas as an aid to the geophysical method of prospecting by radon survey is discussed. This method is suitable for field applications and gives good statistical results in spite of limited available volume of soil gas and short half-life of Th. Significance of some experimental results have been discussed. (auth)

2379 ACTIVITIES OF THE PECHINEY GROUP IN THE NUCLEAR FUEL CYCLE. Pache, B. (Compagnie de Produits Chimiques et Electrometallurgiques Pechiney, Paris). Energ. Nucl. (Paris); 12: 318-22(Jul-Aug 1970). (In French).

The activities of the Pechiney group in the field of the nuclear fuel cycle are reported: prospecting, mining, marketing of uranium and manufacturing of fuel elements. (auth) (France)

Oceanography

Refer also to abstract 2357.

ENGINEERING

Nuclear Explosions

Refer also to abstracts 2312, 2370, 2420, and 2504–2506.

2380 (ORNL–4572–, pp 196-8) CHEMICAL APPLICATIONS OF NUCLEAR EXPLOSIONS. (Oak Ridge National Lab., Tenn.).
From Chemical Technology Division annual progress report for period ending May 31, 1970.

Fracturing of copper ore deposits with nuclear explosives, followed by leaching in place, is being studied, along with recovery of oil from shale. (M.C.G.)

2381 (UCRL–50898) NUCLEAR CRATERING ON A DIGITAL COMPUTER. Terhune, R. W.; Stubbs, T. F.; Cherry, J. T. (California Univ., Livermore. Lawrence Radiation Lab.). 24 Jul 1970. 29p. Dep. NTIS.

Computer programs based on the artificial viscosity method are applied to developing an understanding of the physics of cratering, with emphasis on cratering by nuclear explosives. Two established codes, SOC (spherical symmetry) and TENSOR (cylindrical symmetry), are used to illustrate the effects of variations in the material properties of various media on the cratering processes, namely shock, spall, and gas acceleration. Water content is found to be the most important material property, followed by strength, porosity, and compressibility. Crater-profile calculations are presented for Pre-Gondola Charley (20-ton nitromethane detonation in shale) and Sedan (100-kt nuclear detonation in alluvium). Calculations also are presented for three 1-Mt yields in saturated Divide basalt and 1-Mt yield in dry Buckboard basalt to show crater geometry as a function of the burial depth for large explosive yields. The calculations show, for megaton-level yields, that gas acceleration is the dominant mechanism in determining crater size and depends in turn on the water content in the medium. (auth)

2382 PROBLEMS ARISING FROM NUCLEAR BLASTING FOR OIL AND GAS PRODUCTION. Caspari, A. (Niedersaechsisches Landesamt fuer Bodenforschung, Hanover); Langer, M.; Wuestenhagen, K. Erdoel Kohle, Erdgas, Petrochem.; 23: 275-81(1970). (In German).

After a brief introduction into the relevant problems arising from the use of nuclear explosions for oil and gas production, a description is given of some projects in the USA which are either carried out or envisaged within the framework of the Plowshare program. These projects are Bronco, Ketch, Gasbuggy, and Rulison and are centered on the endeavors for reaching a more economical oil and gas exploitation by increasing the permeability of the carrier bed by nuclear explosions. Subsequently, a number of special problems resulting from the application of nuclear explosions for civil purposes, especially those connected with the assessment of damages (radioactivity, shock-waves, stability of the loaded rock), are discussed. In the future all cost accounting should consider the application of nuclear explosions for the construction of storage caverns for gas, liquid petroleum, crude oil, etc. (auth) (INIS)

Facilities and Equipment

Refer also to abstracts 2427, 2523, 2600, and 3038.

2383 (AAEC/TM–547) ASSESSMENT OF AIR-PULSING TECHNIQUES FOR LIQUID EXTRACTION COLUMNS. Fane, A. G.; Alfredson, P. G. (Australian Atomic Energy Commission Research Establishment, Lucas Heights). Jul 1970. 20p. Dep. NTIS (U. S. Sales Only).

Air-pulsing techniques for enhancement of hydraulic pulsation of liquids in extraction columns are reviewed. Relative advantages are discussed with reference to the special needs of fuel reprocessing plants. The imposed frequency system is considered the most promising. (Australia)

2384 (CEA-CONF–1579) HYBRID SIMULATION OF THE DYNAMICS OF A BATTERY OF MIXER–SETTLERS. Chazal, Guy; Hoclet, Odette (Commissariat a l'Energie Atomique, Saclay (France). Centre d'Etudes Nucleaires); Rouyer, Hubert (Commissariat a l'Energie Atomique, Fontenay-aux-Roses (France). Centre d'Etudes Nucleaires). 1970. 6p. (In French). (CONF-700826–1). Dep. NTIS (U. S. Sales Only).
From Conference on Hybrid Computation, Munich, Germany.

The dynamic behavior of a battery of mixer–settlers was studied with an EAI 8900 computer in order to determine the final equilibria in uranium and acid obtained in the different stages following various perturbations (charge, flow, titer in T.B.P., and temperature). The sensitivity of the solutions to given variations was studied, as in reality the control of such a chemical process cannot be achieved with great precision. Results in good agreement with experiment were obtained. (France)

2385 (DP-Report–230) THE CHARGE/DISCHARGE MACHINE FOR THE DRAGON REACTOR EXPERIMENT. Project DRAGON. Ribaux, P.; Demaurex, P.; Steigman, M. (Atomic Energy Establishment, Winfrith (England). Ateliers des Charmilles S. A., Geneva (Switzerland). Societe Anonyme des Ateliers de Secheron, Geneva (Switzerland)). Oct 1963. 38p. (CONF-631012–11). Dep. NTIS.
From Dragon Project Engineering Symposium, Bournemouth, Eng.

Design of the charge-discharge machine for Dragon reactor is described. Information is included on mechanical components, electrical equipment, power supply, protection devices, and instrumentation. (J.R.D.)

2386 (ORNL–TM–2526(Add.)) ADDENDUM: EXPERIMENTAL AND ANALYTICAL INVESTIGATIONS OF THE STRUCTURAL BEHAVIOR OF NOZZLE-TO-SHELL ATTACHMENTS. Greenstreet, W. L.; Gwaltney, R. C. (Oak Ridge National Lab., Tenn.). Nov 1970. Contract W-7405-eng-26. 46p. Dep. NTIS.

Experimental and analytical investigations of nozzle-to-shell attachments are being made under the general sponsorship of the U. S. Atomic Energy Commission and the Pressure Vessel Research Committee of the Welding Research Council. The Oak Ridge National Laboratory is the coordinating organization for this program. Both elastic and plastic behavior of single nozzle-to-shell attachments are being studied, as well as elastic behavior of multiple nozzles in closely spaced clusters. Seven independent organizations are participating in the program. The purpose of this addendum is to update the report "Experimental and Analytical Investigations of the Structural Behavior of Nozzle-to-Shell Attachments," USAEC Report ORNL-TM-2526. Several changes have been made in the program, primarily as a result of completion of work and the addition of new studies. (auth)

2387 (ORNL–TM–2746) INVESTIGATION OF THE NEED FOR VARIABLE ORIFICES IN MULTISTAGE FLASH EVAPORATORS. Van Winkle, R. (Oak Ridge National Lab., Tenn.). Nov 1970. Contract W-7405-eng-26. 67p. Dep. NTIS.

The suitability of various devices to regulate flashing brine flow through flash evaporators was reviewed. Plain orifices have little regulating capability. Baffles provide an impedance that decreases as water depth increases and thus offers a degree of brine flow regulation. The relationships involved in regulating fluid flow by the use of baffles have not been described well enough, to date, for use in design. Novel devices, which may provide practical means for flow regulation, include pressurized rubber-fabric dams (Fabridams) and spring-loaded flappers. A computer program, ORFIG, was developed to study perturbations in MSF operation due to changes in parameters such as steam flow, recycle flow, ocean temperature and fouling. The only type of reasonable perturbation which seemed to require variable orifices was turndown, if it is desired to minimize steam consumption in the turned-down condition. Point Loma operating data were studied to see the behavior of the brine flowing through fixed orifices as operating parameters were changed. Some of the runs showed severe blow-through of the fixed orifices or brine pile-up behind the fixed orifices in some stages, and the expected reduction in evaporator efficiency was observed when blow-through and transient fouling occurred. The main advantages of variable orifices would be in ability to operate at optimum brine levels to maximize output; ability to adjust efficiently to reductions in demand for product or to reductions in steam and recycle flow; and the reduction in effort required to tune a plant initially. On this basis it is recommended that OSW continue development and testing of variable flow-regulating devices. More urgently needed are better data for determining the characteristics of flow through fixed orifices and for experimental verification that fixed orifices with appropriate baffles can provide adequate regulation for large MSF plants. (auth)

2388 (RD/B/M–1753) LIQUID-NITROGEN CRYOSTAT FOR keV HEAVY-ION IRRADIATION EXPERIMENTS. Channing, D. A. (Central Electricity Generating Board, Berkeley (England). Berkeley Nuclear Labs.). Jul 1970. 8p. Dep. NTIS (U. S. Sales Only).

A liquid-nitrogen cryostat is described for KeV heavy-ion irra-

diation and isochronal annealing of specimens between 77 and 300°K. Temperatures are readily stabilized to better than ±1°K and, in anneals, the rise and fall-times from and to the reference temperature, 77°K, range up to 10 min and 7 min respectively. Access to the specimen is specifically provided for Moessbauer spectroscopy. (auth) (UK)

2389 OPTIMUM PLANNING FOR RADIATION FACILITIES. IRRADIATION FACILITIES. Shigematsu, Tomomichi (Japan Atomic Energy Research Inst., Takasaki). Genshiryoku Kogyo; 16: No. 5, 30-4(May 1970). (In Japanese).

The design of an irradiation facility depends on whether radioisotopes or particle accelerators are used and whether it is for industry or research. Optimal design of irradiation facilities for industrial uses in particular are described. Irradiation facilities, are described emphasizing uniformity of radiation exposure and hot cell design. Industrial irradiation facilities using radioisotopes are also described emphasizing the mechanisms and configuration for irradiation of solid, powder, and gaseous substances. Industrial irradiation facilities, using electron beams from accelerators are discussed dealing with the mechanisms and exposure methods for cross-linking in film-type materials and curing of coatings on building materials. (Japan)

2390 OPTIMUM PLANNING FOR RADIATION FACILITIES. TRACER FACILITIES. Iso, Yasuhiko (Japan Atomic Energy Research Inst., Tokyo). Genshiryoku Kogyo; 16: No. 5, 24-9 (May 1970). (In Japanese).

Tracer facilities are associated with the studies in physics, chemistry, and biology. Optimal design of such radioactive facilities is described. Components are determined by the facility purpose; this is also true of design parameters and design criteria. Fundamentals in design of facilities associated with personnel include protection from radiations by containment and separation. Radiation protection measures are necessary in experimental and storage areas. Design of a facility is described including the layout of rooms and the systems of discharging air and water; an example is given using the JAERI Radioisotope Utilization Development Laboratory. (Japan)

2391 SINTERING FURNACE. Masselot, Yves; Poujol, Georges (to Commissariat a l'Energie Atomique). British Patent 1,210,778. 28 Oct 1970. Priority date 27 Sep 1968, France.

An industrial furnace is described in which sintering and impurity trapping are separated from each other. Under these conditions trap cleaning can be carried out independently of either positioning or withdrawal of items to be sintered. Use of two traps makes possible positioning of a clean trap for operations involving charging and discharging items such as fissile material pellets thereby avoiding lengthening the sintering cycle. (J.R.D.)

2392 HIGH-PRESSURE PUMPS: SOLVED SEALING PROBLEMS. Bach, M. Maschinenmarkt; 76: 573-5(1970). (In German).

Bearing ring seals are preferred in Germany for boiler feeders. Since nuclear power plants are being built, the demand for zero- and controlled-leakage has increased. The circulating pumps of BWR's can be designed sufficiently safe in operating using series-connected bearing ring seals. For PWR's the pumps must have hydrostatic shaft seals. Thermal shocks must be considered for stage casing seals. (INIS)

2393 ENERGY FORECASTS NEED NEW APPROACHES. Morrisson, W. E. Elec. World; 170: No. 19, 35-7(4 Nov 1968).

Projecting total US energy requirements to 2000 will require changes in source material and conversion technologies. The medium range of electric energy requirements is $5,036 \times 10^9$ kWh requiring 1.5×10^6 MW generating capacity. Nuclear would generate 60%, fossil fuels 32%, and hydro 8%. If the economy turns to on-site fuel use, the electricity would come from fuel cells and none from conventional utilities. (Fuel Abstr.)

2394 LEVEL INDICATOR MADE OF Zr–20 PERCENT Nb SUPERCONDUCTING ALLOY. Bychkov, Yu. F.; Zamolodchikov, O. G.; Rozanov, A. N. Met. Metalloved. Chist. Metal., Sb. Nauch. Rabot; No. 8, 53-7(1969). (In Russian).

Superconducting level indicators using Zr–20 Nb ribbons were found suitable for measuring He levels in cryogenic systems especially those subject to strong magnetic fields. Production of similar indicators using Zr also appears feasible. Operation Zr–20 Nb level indicators in He may be less efficient because its superconducting transition is closer to the boiling point of He. (J.R.D.)

2395 METHOD OF AND SYSTEM FOR CONVEYING PARTICULATE ELEMENTS. (to Brown Boveri/Krupp Reaktorbau GmbH). British Patent 1,208,877. 14 Oct 1970. Priority date 25 May 1968, Germany.

A method of conveying particulate elements through an inlet into a closable vessel by means of a fluid is described. The fluid may be recirculated. The particulate elements may be conveyed for charging reactors with spherical fuel elements or moderator elements. The fluid may be gas such as air. (J.R.D.)

2396 ADVANCES IN SPACE SCIENCE AND TECHNOLOGY. VOLUME 10. Ordway III, Frederick I. (ed.). New York; Academic Press Inc. (1970). 302p. $17.00.

Five chapters on advances in space science and technology are presented. A separate abstract was prepared for one. Four were not within the scope of NSA. (L.C.L.)

For abstract of an individual chapter see: 2397.

2397 ASTRONAUTICS: AN OUTLINE OF UTILITY. Ruppe, Harry O. (Technical Univ., Munich). Advan. Space Sci. Technol.; 10: 139-271(1970).

A review of the past accomplishments and future expectations of astronautics is presented in order to answer the questions — why should astronautics be developed, and is the utility worth all the effort. The subjects discussed include the obvious utility of space flight as related to specific fields such as astronomy, communications, military applications, navigation, and physics, and speculation as to the benefits of astronautics to art, education, race survival, religion, and science. (L.C.L.)

2398 EFFECTS OF ELECTRODE SIZE ON THE PERFORMANCE OF A COMBUSTION-DRIVEN MHD GENERATOR. Rubin, Edward Stephen. Stanford, Calif.; Stanford Univ. (1969). 148p. University Microfilms Order No. 70-10,517. Thesis.

Experiments were conducted to investigate the effects of electrode size on the performance of a combustion-driven MHD generator. Three molybdenum electrode pairs were located 45 cm downstream of the entrance to a rectangular MHD channel. The center electrode pair was taken to represent an arbitrary pair in a segmented generator, and was shielded from end effects by the two remaining pairs of guard electrodes. The electrode temperature could be varied between 500 and 1600°K by controlling the electrode coolant, while the electrical conductivity in the electrode boundary layer regions was independently conditioned by the type of wall upstream of the electrodes. The upstream wall could be either hot (2200°) MgO brick or a cold (750°K) water-cooled plate. Two types of experiments were performed. First, the effects of electrode size on performance were examined for fixed values of all other pertinent geometrical and thermodynamic parameters, and the second type of experiment investigated electrode size effects in the presence of dissimilar boundary layers such as might arise from the coupling between electrode and gas boundary layer temperatures in a cold-electrode generator with hot interelectrode insulators. In all experiments two electrode sizes were operated simultaneously to avoid effects of uncertainties in day-to-day operating conditions. The electrode voltage drop data demonstrated a marked influence of electrode size on generator performance. At a given load current, larger electrodes were found to yield lower voltage losses, for similar conditions of surface and gas boundary layer temperature. However, for dissimilar boundary layers reflecting the coupling between electrode and boundary layer temperatures in a cold-electrode generator, total voltage losses for a large electrode pair were equal to or greater than those of a small electrode pair at the same surface temperature. Boundary layer resistances determined from the experimental voltage drops were compared to analytical predictions obtained using an approximate, then a more exact two-dimensional gasdynamic model which incorporated a variable electrical conductivity in the electrode-wall boundary layers. For anodes above about 700°K, the agreement between theory and experiment was quite favorable. At lower temperatures, however, anodes were found to be influenced by condensation on the electrode surface, which caused a departure from theoretical performance based only on a gasdynamic loss mechanism. For cathodes, the boundary layer resistance was also found to be gasdynamic in the case of a hot upstream wall, for an electrode current density not exceeding that of saturated thermionic emission at the electrode temperature. In all other cases, the presence of surface-sheath effects, associated with the emission of electrons from the cathode, was indicated. Some quantitative estimates of these were obtained for the conditions of the present experiments. In general, however, surface-sheath phenomena are not well understood, and there is a need for more detailed investigations. (Diss. Abstr. Int., B)

Heat Transfer and Fluid Flow

Refer also to abstracts 2387, 2633, 2634, 3865, 3876, and 3893.

XUM

Isotope Technology

Refer also to abstracts 2141, 2294, 2348, 2497, 2566, and 2643.

2399 (AED-C-12-22) BIBLIOGRAPHIES IN NUCLEAR SCIENCE AND TECHNOLOGY. SECTION 12: NUCLEAR SCIENCE LITERATURE OF EASTERN COUNTRIES. Ensslen, Benno (comp.) (Zentralstelle fuer Atomkernenergie-Dokumentation, Frankfurt am Main (West Germany)). Jul 1970. 71p. Dep. NTIS (U. S. Sales Only).

1497 references from literature published in eastern countries during 1967 to 1969 on the industrial and research applications of radioisotopes are presented. These applications are grouped according to the specific industrial fields and scientific disciplines in which they are used. An author index is included. (L.C.L.)

2400 (CEA-CONF-1623) USE OF THIN FILM SOLAR CELLS IN RADIOVOLTAIC GENERATORS. Bomal, R.; Manin, A.; Steinschaden, K. (Commissariat a l'Energie Atomique, Saclay (France). Centre d'Etudes Nucleaires). 1970. 15p. (CONF-700707-1). Dep. NTIS (U. S. Sales Only).

From International Meeting on Solar Cells, Toulouse, France.

A radiovoltaic generator was developed, using tritium as a beta emitter and cadmium telluride as a radiovoltaic converter. CdTe is a semiconductor generally used in thin film solar cells and is very cheap. The characteristics of both components and the reason of their choice are given, the generator and its performances are described. (France)

2401 GENERATOR OF SHORT PULSES OF HARD X-RAYS OF HIGH INTENSITY. Abramyan, E. A.; Vasserman, S. B.; Dolgushin, V. M.; Morkin, L. A.; Pecherskii, O. P.; Tsukerman, V. A. Dokl. Akad. Nauk SSSR; 192: 76-7(1 May 1970). (In Russian).

A steel vessel 180 cm in diameter and 500 cm long holds a pulse x-ray tube, a forming line or conductor, and a resonance pulse transformer of the Tesla type. The steel vessel is filled with a 50% mixture of nitrogen and sulfur hexafluoride at a pressure of 14 kg/cm^2. During testing of the generator the condenser bank with a capacity of 20 microfarads was charged up to 28 kilovolts. Under these conditions a tension of 7×10^6 volts was obtained on the conductor. The current through the pulse x-ray tube was 10 to 20 kiloamps. A dose of 10 r was recorded at a distance of 100 cm from the anode for a pulse of less than 50 nanoseconds duration. At this distance it was possible to x-ray lead 160 mm thick. The dose near the tube exit window attained 2×10^{11} r/sec. This equipment could be used to x-ray rapid processes. (TTT)

2402 SEPARATION OF URANIUM ISOTOPES. Pecqueur, Michel (CEA, Fontenay-aux-Roses, France). Bull. Inform. A.T.E.N. (Ass. Tech. Energ. Nucl.); No. 84, 12-26(Jul-Aug 1970). (In French).

Uranium isotope separation is an important item of the fuel cycle. Two processes can be foreseen at present for the construction of a plant. The first is the ultracentrifugation method which offers interesting long term prospects but suffers so far from limited industrial experience. The second is the gaseous diffusion process which can form a sound technical and economic basis for the launching of a large separation unit corresponding to the needs of European countries at the end of the decennium. Following up the experience acquired in its plant at Pierrelatte, France has undertaken large scale studies on gaseous diffusion and by 1972 will possess an exhaustive technical and economic record. The ultracentrifugation process was investigated also although the possible date of industrial application is still uncertain. Moreover, it may prove in the long run that the two processes are more complementary than competitive, gaseous diffusion being used for the high output sections of the cascade and centrifugation for the low output sections, especially if fairly high concentrations (5 or 7 percent) are to be adopted. Many political and industrial problems are involved in the prospect of setting up a multinational unit. (France)

2403 OUTPUT CALCULATION FOR CYLINDRICAL IRRADIATOR WITH ADDITIONAL AXIAL SOURCE. Primak-Mirolyubov, V. N. This paper was summarized in At. Energ. (USSR); 24: 379(Apr 1968) as paper No. 200. (In Russian).

A method for calculating the dose rates of γ complex cylindrical irradiators, is described. The results obtained permitted an estimation of the dynamic and static modes of irradiation, a determination of the conditions under which the output could be calculated without taking absorption in the medium into account and the compilation of tables and graphs needed for output calculations. (L.C.L.)

2404 SPHERICALLY SHAPED CARTRIDGES FOR EXTENDED SOURCES IN PILOT AND FULL-SCALE RADIATION-CHEMICAL PROCESSORS. Osipov, V. B.; Solodikhina, L. D.; Bodrov, D. P.; Simonov, V. M.; Dzhagatspanyan, R. V. This paper was summarized in At. Energ. (USSR); 25: 315(Oct 1968) as paper No. 233. (In Russian).

A spherical ^{60}Co cartridge consisting of a capsule and a lid joined to the capsule by means of a locking spring is used in the design of extended linear sources of variable activity. The cartridge cannot be dismantled once assembled. The ^{60}Co is encapsulated in the cartridge in a hot cell, using a standard M-20 manipulator and relatively uncomplicated production equipment. These cartridges loaded with ^{60}Co are capable of withstanding static loads as high as 7 tons/cm^2 and overloads to 25.5 g at a frequency of 11.5 Hz and amplitude of 12 mm. Radiation losses in the cartridge amount to ≈4.9%. The spherical cartridges loaded with ^{60}Co performed reliably and efficiently in the RS-2.5 radiation sulfochlorinator. There was no radioactive contamination of the distributor mechanism. (auth)

2405 THERMAL SEPARATION OF THE ORTHO AND PARA FORMS OF H_2 AND D_2. Mason, E. A. (Brown Univ., Providence); Sander, Stanley I. Chem. Phys. Lett.; 6: 620-2(15 Sep 1970).

The kinetic theory of nonspherical molecules is shown to account for the experimental observations on thermal diffusion in pH_2-oH_2 and oD_2-pD_2 mixtures, in terms of measured rotational collision numbers. (auth)

2406 ION EXCHANGE BEADS AS CALIBRATED MICROSCOPIC RADIOACTIVITY SOURCES. Hahn, Paul B.; Shleien, Bernard (Department of Health, Education, and Welfare, Winchester, Mass.). Anal. Chem.; 42: 1608-12(Nov 1970).

Spherical microscopic radioactivity sources with diameters ranging from 10 to 500 μm and activities from 1 to 25,000 dpm were prepared by equilibrating milligram quantities of ion exchange resin beads with microcurie quantities of radioactivity in aqueous solution. The correlation between activity taken up by an individual bead and its measured diameter was shown to be excellent, the relative standard deviation of source specific activities (dpm/unit volume) for beads from the same equilibration being on the order of 2%. The demonstrated ability to prepare these sources ranging in activity over four orders of magnitude from a variety of radionuclides and ion exchangers and to precisely calibrate them in terms of a microscopic diameter measurement makes available to the nuclear industry a new approach for preparing point source radioactivity standards. (auth)

2407 Pu-Be NEUTRON SOURCE SPECTRUM MEASURED BY ^{6}Li SEMICONDUCTOR SPECTROMETER. Yen, Yu-liang; Yang, Teh Li; Vincent, Diectrich H. (National Tsing Hua Univ., Hsinchu, Taiwan). Nucl. Sci. J. (Taiwan); 7: 1-11(Oct 1969).

The neutron spectrum of the 1-Curie Pu-Be neutron source which is in general use at Tsing Hua University has been obtained by using a ^{6}LiF sandwich-type semiconductor neutron spectrometer. Only those neutrons beyond 2 MeV are shown. Intensity maxima exist at 3.6, 6.8, 7.8, and 9.9 MeV. Comparison of the Pu-Be neutron spectra obtained by different methods, such as by nuclear emulsion, ^{3}He semiconductor neutron spectrometer, and ^{6}Li semiconductor neutron spectrometer, is made. Within its limits of error, the result of this paper is in agreement with the previously obtained source spectra. (auth)

Materials Testing

Refer also to abstracts 2601, 2660, 2770, 3471, and 3483.

2408 (ORNL-4570, pp 96-7) NONDESTRUCTIVE TESTING TECHNIQUES FOR LMFBR. (Oak Ridge National Lab., Tenn.).

From Metals and Ceramics Division annual progress report for the period ending June 30, 1970.

New methods, techniques and equipment for nondestructively inspecting materials for the LMFBR are being developed with emphasis on measuring cold work in stainless steel tubing. Design and development have begun on a prototype eddy-current instrument to identify both the size of a flaw and its depth below the surface. Since phase shift of the signal is important portions of a new modular phase-sensitive eddy-current instrument are being used as a starting point. Ultrasonic schlieren techniques are being applied to specimens of welds containing intentional flaws in both aluminum and stainless steel and the results are correlated with those obtained using other more conventional ultrasonic techniques. Techniques for measuring changes in magnetic permeability in both flat sheet and tubular specimens of Type 316 stainless steel as a means of determining the degree of cold work in the materials are being developed. Because of the good results on the

XUM

flat specimens using a breadboard, low-frequency bridge system, a series of calculations were performed to aid the design of a high-sensitivity prototype instrument for tubing. (auth)

2409 (ORNL–4570, pp 149-51) NONDESTRUCTIVE TEST DEVELOPMENT. (Oak Ridge National Lab., Tenn.).

From Metals and Ceramics Division annual progress report for the period ending June 30, 1970.

Analytical studies of eddy-current phenomena were continued including deriving new equations, and both writing and applying computer programs to use the equations to study cases of interest. Phase-sensitive instrumentation was modified to improve stability and sensitivity. Improved capabilities were developed for fabricating reference standards for ultrasonic inspection. The optical portion of the schlieren system was improved. Preliminary techniques using frequency analysis were developed to allow determination of the size and orientation of flaws without dependence upon the relative intensity of reflected signal. Quantitative radiation attenuation measurements were sensitive to changes in density or thickness as small as 0.5% in graphite. Development began on techniques for measuring radiographs with closed-circuit television. Good sensitivity has been demonstrated on measuring thickness of aluminum on uranium, using the fluorescent radiation from uranium excited by a ^{147}Pm source. Results of studies showed the feasibility of real-time infrared holography using liquid crystals as a display medium. (auth)

2410 (ORNL-TM-3113) MEASUREMENT OF RESIDUAL STRESSES. Cepolina, A. G.; Canonico, D. A. (Oak Ridge National Lab., Tenn.). Oct 1970. Contract W-7405-eng-26. 32p. Dep. NTIS.

A modification of the Sachs "boring-out" method for determining residual stresses has been developed. This technique permits the determination of the distribution of the stresses and their levels over extremely short increments of distances. This technique was used for measuring the residual stresses present in gas tungsten-arc welds made in Hastelloy N. The specimen was ½-in.-thick plate, 12 in. in diameter. Circular welds 6 in. in diameter were simultaneously deposited on both flat faces. The equations applicable for the calculation of residual stresses in this specimen geometry are as follows: $(\sigma_R)_{\frac{-}{R}} = (E\epsilon_T/2)[(R_0^2/R^2) - 1]$, and $\sigma_T = \sigma_R + (Rd\sigma_R)/d_R$, where σ_R = radial stress and σ_T = tangential stress. The maximum value of tangential residual stress was found to be about 50,000 psi and was not particularly affected by either the shielding gas or heat input. Stress relieving at 1600°F for 4.5 hr proved to be the optimum heat treatment and reduced the tangential residual stress to about 5000 psi. Lowering of the maximum residual stress to about 10,000 psi was achieved at 1400°F after 6 hr; however, lower temperatures even for times as long as 100 hr only reduced the maximum residual stress by about 25%. (auth)

2411 (TID–25573) LUMPED-PARAMETER ANALYSIS FOR SHEAR FAILURE IN THE END SLAB OF CYLINDRICAL PRESTRESSED CONCRETE PRESSURE VESSELS. Structural Research Series No. 363. Higashionna, R.; Schnobrich, W. C. (Illinois Univ., Urbana). Aug 1970. Contract W-7405-eng-26; Subcontract 2906. 95p. Dep. NTIS.

Investigations of end slabs revealed that the development of shear failure of these members in cylindrical concrete pressure vessels can be described in terms of two stages. In the initial stage a series of 45° cracks are formed. These cracks lead to a formation of an inverted dome. The second stage is characterized by the ultimate failure of the dome that was created in the previous stage. In development of an analytical method which can be used to predict cracks similar to those associated with the formation of the inverted dome, a lumped-parameter method of analysis was used. A computer program was developed to permit a high-speed processing of the resulting equations. One of the small-scale cylindrical vessels tested was analyzed. The mathematical procedure as formulated in this study is applicable up to about 70 to 80% of the ultimate load obtained in the experiment. The analytical model predicts the crack patterns leading to an inverted dome, although the complete shape of the dome was not defined. The over-all structural behavior as predicted by the model, within the range of its applicability, agrees favorably with the experimental result. The absence of information on a general failure criterion for concrete presented a problem in trying to define a failure criterion to be used in the analytical method. For lack of anything better the maximum strain theory has been used as a failure criterion in this study. Many investigators have pointed out an urgent need for a general failure criterion in the multiaxial state of stress. In order to further refine the lumped-parameter analysis to predict the behavior of the vessel in the later stages of its failure sequence the stress-strain relations for the multiaxial case must also be established. As this information becomes available, it can be incorporated into the analysis of PCRV's. (auth)

2412 STATISTICAL ANALYSIS OF THE INFORMATION TRANSFER PROCESS IN RADIOMETRIC BETATRON DEFECTOSCOPY. Vorob'ev, A. A.; Vorob'ev, V. A.; Pokrovskii, A. V.; Flesher, G. I.; Gorbukov, V. I. (Polytechnic Inst., Tomsk, USSR). Isotopenpraxis; 6: 187-91(May-Jun 1970). (In Russian).

A theoretical discussion and analysis of the bremsstrahlung beam spreading process are presented. The results provide for calculation of minimum detectable volume of some defect through principal design features of the gauge, testing velocity, material thickness, and collimation of beam with modification after filtration. Also, it describes how to set up formulae for selecting and calculating main features of the gauge. (auth)

2413 CALCULATING THE OPTIMUM THICKNESS OF THE FRONT SCREEN IN THE TRANSFER METHOD OF NEUTRON RADIOGRAPHY. Pekarskii, G. Sh. Izv. Vyssh. Ucheb. Zaved., Fiz.; No. 3, 143-4(1970). (In Russian).

In neutron transfer radiography a converter screen is used on which a radioactive image is formed. After the irradiation is complete the latent radioactive image is removed and placed in contact with a film to develop a visible image. The optimum screen thickness is determined by the maximum number of emitted electrons and by the quality of the image (the degree of smearing). The energy losses of electrons from the back side of the screen were taken into account. Calculations were carried out for a gold screen at thicknesses of 0.005, 0.01, 0.02, 0.03, 0.04, 0.05, 0.07, 0.09, 0.12, 0.15, and 0.19 mm. A ten-group approximation of energy groups from 0.1 to 1.0 MeV was used. The results show a significant difference in the optimum screen thickness calculated according to electron energy rather than the number of electrons. These results show that the energy losses of secondary radiation in the screen should be taken into account in determining the optimum screen thickness for neutron radiography. (TTT)

Radioactive Material Handling

Refer also to abstracts 2316, 2362, 2601, 2633, 2792, 2821, and 3649.

2414 (AD–707709) FILTRATION OF PARTICLES OF ATOMIC DIMENSIONS. Final Report. Saunders, A. W. Jr.; Patterson, R. L. Jr.; Lockhart, L. B. Jr. (Naval Research Lab., Washington, D. C.). 12 May 1970. 25p. (NRL–7047). NTIS.

Particles of atomic dimensions, as typified by the primary decay products of radon, were readily removed from an air stream by passage through coarse fibrous filters or even through screens, while the radon parent was unaffected. The inverse relationship between the efficiency of removal and the air velocity indicated that diffusion is the mechanism primarily responsible for deposition of these small particles. However, if the particles become attached to aerosols, their collection is governed by aerosol behaviors where collection depends both on filter characteristics and air velocity. These particles are readily collected on aerosol particles and provide a radioactive tag by which aerosol or filter behavior may be studied. Such measurements can be extended to size ranges and concentration levels below those convenient for other techniques. (auth) (USGRDR)

2415 (ARH–1819) VIBRATION TESTING OF L-3 AND L-10 SHIPPING CONTAINERS. Curren, E. F. (Atlantic Richfield Hanford Co., Richland, Wash.). Sep 1970. Contract AT(45-1)-2130. 22p. Dep. NTIS.

The resonant frequency of the L–3 shipping system was found to be 15.5 Hz; the L–10 system 19.4 Hz. These frequencies approximate the 17 Hz and 1 g conditions observed in an instrumented truck transport of a heavily shielded cask from Philadelphia, Pa. to Los Alamos, New Mexico. It was demonstrated in the test program that the pumping action postulated could occur and could create the conditions observed in shipments received at Hanford. Maximum pumping action occurred at or near the resonant frequency of each system; approximately 15.5 Hz for the L–3 systems and 19.4 Hz for the L–10 systems at accelerations from 0.1 to 0.9 g. The polyethylene bottle in both systems was found to be moving independently of the 2-R container and cage assembly in the resonant frequency range. A 3-liter bottle containing 3 liters of water was secured to a smaller shake table to enable visual observation of wave formation. The test was run as a sweep of frequencies from 5 to 20 Hz. While agitation of the fluid was evident across the spectrum of frequencies, the most violent agitation occurred at 17 Hz. Installation of a restraint between the closing flange of the 2-R container and the top of the bottle cap forced the bottle to vibrate at the same frequency as the 2-R container. The restraint dampens the standing wave formation such that the waves then have insufficient energy to force solution through the vents. The restraints used in the test program con-

XUM

sisted of short sections of rubber hose, sized to fit closely between the shoulder of the 83 mm bottle closures and the underside of the closing flange. The hose was 2½ inch I.D., with two fabric plies, manufactured by the Boston Woven Hose and Rubber Company, and designated Type OED. The use of restraining devices to eliminate the differential movements of the 3-liter and 10-liter bottles within their respective 2-R containers was effective in preventing the formation of the standing waves which force the solution through the vents of the bottle closures. (auth)

2416 (ARH-SA-67) OPERATING EXPERIENCE USING SILVER REACTORS FOR RADIOIODINE REMOVAL IN THE HANFORD PUREX PLANT. Raab, G. J.; Van der Cook, R. E. (Atlantic Richfield Hanford Co., Richland, Wash.). 17 Jun 1970. Contract AT(45-1)-2130. 15p. (CONF-701103-3). Dep. NTIS.

For Presentation at 63rd National Meeting of the American Institute of Chemical Engineers, Chicago, Ill.

Silver reactors have been successfully employed to remove radioiodine from dissolver off-gas streams. Overall plant iodine release to the atmosphere is typically 0.1 percent with the reactors and 1 percent without the reactors of the iodine charged to the plant. Typical plant operating data are presented. Operation has been safe and reliable. (auth)

2417 (BNWL-SA-3287) PROPERTIES OF THE Pu ESTIMATE BASED ON WEIGHTED Pu/U VALUES. Stewart, K. B.; Schneider, R. A. (Battelle-Northwest, Richland, Wash. Pacific Northwest Lab.). 1 Apr 1970. 32p. (SM-133/55; CONF-700701-6). Dep. NTIS.

From IAEA Symposium on Progress in Safeguards Techniques, Karlsruhe, Germany.

The results of analytical and simulation studies of the properties of the weighted Pu/U estimate of the amount of plutonium which is inputted into a separations facility are presented. Formulas that give the relative variance of the weighted Pu/U estimate in terms of the relative process and measurement variances of the batch Pu/U and uranium estimates are developed. The situation in which there is batch-to-batch compositing and that in which there is no compositing were both studied. (auth)

2418 (CONF-700322-, pp 357-78) USE OF SMALL ACCELERATORS IN NUCLEAR SAFEGUARDS RESEARCH. Evans, A. E. (Los Alamos Scientific Lab., N. Mex.).

From Proceedings of the second Oak Ridge conference on the use of small accelerators for teaching and research, March 23-25, 1970.

The Nuclear Safeguards Program is concerned with assuring that fissile material is not diverted from lawful use as nuclear reactor fuel into unlawful use as nuclear explosives. Recent ratification of the Nuclear Nonproliferation Treaty makes it necessary to apply this program worldwide to the nuclear power industry. A system of nondestructive quantitative physical measurement of fissile materials is necessary to implement the program. Passive techniques such as the counting of decay gamma rays and spontaneous fission neutrons will serve some purposes in the nondestructive assay of fissionable material, such as plutonium assay in thin, well-defined geometries. Many assay problems, however, call for active interrogation of the sample with either neutrons or high-energy photons. The LASL Safeguards Research program is dedicated principally to the development of methods of assay involving fast-neutron interrogation followed by the counting of delayed neutrons from fission. The method is applicable to the assay of many diverse objects, including process-line samples, fuel pellets, assembled fuel elements, and fissile-bearing scrap. Use of a variable-energy interrogating neutron source permits discrimination among fissionable isotopes. LASL uses four accelerators in its Safeguards program: a 350-keV Cockcroft–Walton accelerator, an "Accelerator I" 150-keV neutron generator, a KAMAN Type 1254 190-keV neutron generator mounted in a mobile assay laboratory, and a 3-MeV Van de Graaff accelerator. Application of these machines to delayed-neutron research is discussed. (auth)

2419 (KFK-1192) CRITICAL AND SAFE DIMENSIONS OF CONTAINERS FOR STORAGE AND MIXING OF PLUTONIUM-CONTAINING NUCLEAR FUEL. Wiese, H.-W. (Kernforschungszentrum, Karlsruhe (West Germany). Institut fuer Neutronenphysik und Reaktortechnik). May 1970. 14p. (In German). Dep. NTIS (U. S. Sales Only).

Production of fuels for breeder reactors involves the problem of storage and mixing of plutonium-containing nuclear fuel in containers under criticality safe conditions. An assembly is considered safe against criticality when its fuel volume is at most 80 per cent of the fuel volume of the critical assembly with the same atomic densities, the same geometrical form, and an additional 1-in.-water-reflector. Critical and safe dimensions are calculated for one storage and two mixing containers. Neutron–hydrogen scattering is treated in Transport- and in P_1-Approximation. (auth)

2420 (NVO-410-2) CARLSBAD SITE ROLL-UP PROGRAM, ON-SITE RADIOLOGICAL SAFETY REPORT. Tappan, John T.; Lorenz, Jerry J. (Reynolds Electrical and Engineering Co., Inc., Mercury, Nev. Radiological Sciences Dept.). Jul 1969. 25p. Dep. NTIS.

The Carlsbad Site in New Mexico was used once in 1961 for the Project Gnome test, and was subsequently designated to be restored to the public domain. The Carlsbad Roll-Up Program was implemented to remove and dispose of all surface contamination to whatever depth it was in excess of 0.1 mR/hr as measured with an open shield GM tube instrument. The procedures used and results obtained in the restoration of contaminated areas on the 640 acre Carlsbad Site are described. At the end of the program, no contact surface contamination was detected in excess of the established limit of 0.1 mR/hr. (L.C.L.)

2421 (ORNL-TM-3110) SAVANNAH RIVER AMERICIUM-CURIUM SLUG CARRIER. Shappert, L. B.; Klima, B. B. (Oak Ridge National Lab., Tenn.). Nov 1970. Contract W-7405-eng-26. 41p. Dep. NTIS.

The Savannah River Americium-Curium Slug Carrier was designed to transport large quantities of transuranium elements, plus associated mixed fission products in the solid form. The cask, its operating characteristics and procedures, and an analytical evaluation made to demonstrate its compliance with the regulations governing packages in which radioactive material is shipped are described. Computational procedures were used to determine the structural integrity and thermal behavior of the cask with respect to the general standards for packaging, structural standards, standards for normal conditions of transport, and the standards for the hypothetical accident conditions. Results of this evaluation show that the cask complies with all the applicable regulations. (auth)

2422 HANDLING OF RADIOACTIVE WASTES IN POLAND. Gabriel, L. (Central Research Inst. for Physics, Budapest). Atomtech. Tajek.; 13: 237-45(Apr 1970). (In Hungarian).

In order to ensure the safe and uniform handling of radioactive waste products throughout Poland, a treatment station was established at the Swierk Nuclear Research Institute in 1962. The station has been assigned the responsibility for the collection of all radioactive waste materials from the whole country, their transportation, and conversion into a form suitable for extended and subsequent ultimate storage. The station also takes care of the decontamination of tools, protective clothing, etc. The solid wastes are divided into 3 categories on the basis of the dose rate at the surface of the container: <50mR/hr; 50mR to 2R/hr; and >2R/hr. Material in the first 2 groups is collected in polyethylene bags, enclosed in metals drums and buried. Biological waste is embedded in concrete. Intermediate-level materials are collected in shielded containers. The various treatment methods for liquid waste, such as chemical processes and sorption treatment are outlined. The station was designed and built within Poland but some of the more complex units have been purchased in Belgium. (TTT)

2423 INVESTIGATIONS OF DECONTAMINATION ABILITY OF PAINTS. Berger, W.; Hepp, H.; Sauermann, P. F. (Farbenfabriken Bayer AG, Leverkusen, Ger. Gesellschaft fuer Kernforschung mbH, Karlsruhe, Ger. Kernforschungsanlage, Juelich, Ger.). Farbe Lack; 76: No. 1, 44-9(1970). (In German).

The decontamination ability of 22 paints and coating fabricated under the same conditions from different adhesives was determined by two independent authorities. The best results were obtained for silicone lacquers, 2-component polyurethane lacquers and coatings and for chloro- and cyclocaoutchouc paints. The decontamination ability seems to be property specific to the adhesive which may be transferred to other pollutions if the paint is chemically stable against the reactive medium. An isotope mixture consisting of $^{90}Sr/Y$, $^{106}Ru/Rh$, ^{137}Cs, and ^{60}Co in hydrochloric solution at pH of 4 was used; the solution had an activity of 10 $\mu Ci/cm^3$. (INIS)

2424 HANDLING AND TRANSPORT OF IRRADIATED FUELS. Sousselier, Yves (CEA, Fontenay-aux-Roses, France). Bull. Inform. A.T.E.N. (Ass. Tech. Energ. Nucl.); No. 84, 63-78 (Jul-Aug 1970). (In French).

The handling of the Chinon 3, St. Laurent des Eaux 1 and Bugey fuel elements and their storage in a swimming pool are described. The technical aspects of the packaging and transport of fuels from gas graphite power reactors and from light water reactors are discussed. Mention is made of the administrative side (approval of packaging systems and means of dispatch, regulations) and the economy of irradiated fuel transport. (France)

2425 DISPOSING OF NUCLEAR PLANT SOLID WASTES. Tuite, P. T. Power; 114: No. 11, 78-9(Nov 1970).

The environmental impact of nuclear power plants is examined in terms of radioactive waste processing methods and related economic considerations. Treated gaseous and liquid wastes are considered to be nonhazardous. However, the disposal of solid radioactive wastes derived from the processing of gaseous and liquid wastes or from solid matter in the reactor system is of prime importance. Process diagrams for the treating, packaging, transporting, and underground burial of solid wastes from pressurized water reactors and boiling water reactors are presented, and the unit costs of these operations are discussed. (L.C.L.)

2426 DEVELOPMENT OF A WASTE DISPOSAL METHOD FOR N REACTOR'S DECONTAMINATION WASTES. Kratzer, W. K.; Bainard, W. D. (Douglas United Nuclear, Inc., Richland, Wash.). pp 449-52 of Proceedings of the 26th Conference of the National Association of Corrosion Engineers, Philadelphia, Pa., March 2-6, 1970. Houston, Tex.; National Association of Corrosion Engineers (1970).

See CONF-700324.

The evolution of methods for decontamination and disposal of wastes from the Hanford reactor are reviewed. It is noted that early concepts involving ground disposal were later modified to on-site concentration by evaporation, and then to the presently used concept of railroad shipment to a concentration facility. (J.R.D.)

2427 DETACHABLE TERMINAL HEAD FOR A PNEUMATIC SYSTEM FOR TRANSFERRING ARTICLES. Baudoin, Jean-Claude; Drieu, Fernand; Marlin, Henri; Oger, Robert; Pennincq, Alex (to Commissariat a l'Energie Atomique). British Patent 1,211,315. 4 Nov 1970. Priority date 20 Jun 1968, France.

The head incorporates a casing which can be connected sealtight to one end of the conduit by a locking mechanism. The head is also supported by the conduit when it is unlocked. A breech-block is slideably mounted on the casing between a top position in which the breech-block closes and seals the casing and a bottom position in which the breech-block allows access to the casing and supports the article to be transferred. A remote control of pressures at the end of the casing for conveying articles is provided. (J.R.D.)

Vacuum Engineering

2428 MEASUREMENT OF TOTAL PRESSURE IN THE RANGE 10^{-8} TO 10^{-12} TORR. Leck, J. H. (Univ. of Liverpool). Vacuum; 20: 369-72(Sep 1970).

Various techniques that have been introduced to extend the working range of ionization gauges below 10^{-9} or 10^{-10} torr are briefly described. The modifications made to the Bayard–Alpert gauges to suppress both surface ion and X ray induced currents are included. The magnetron and orbitron gauges in which sensitivity is greatly increased by forcing the electrons to execute very long oscillatory paths in the ionization chamber are discussed. The cold cathode Penning gauge is mentioned. (auth) (UK)

2429 EXPERIENCES WITH CRYOPUMPS IN CALIBRATION DEVICES. Grosse, Gottfried; Messer, Guenter (Physikalisch-Technische Bundesanstalt, Berlin). Vacuum; 20: 373-6(Sep 1970).

A room-temperature calibration system is described in which calibrating pressures between 10^{-9} and 10^{-5} torr are maintained by a helium evaporator cryopump with a liquid helium consumption of 2 to 3 l/hr. The major advantage of this system is that, due to the high pumping speed of the cryopump, an orifice of relatively large conductance (100 l/sec) may be used. Hydrogen background pressures of 10^{-10} torr may be maintained for a sufficient time to permit the use of all test gases except helium and hydrogen. (auth) (UK)

2430 UHV MEASUREMENTS BY COLD CATHODE GAUGES. de Chernatony, L.; Crawley, D. J. (AEI Scientific Apparatus Ltd., Harlow, Eng.). Vacuum; 20: 389-91(Sep 1970).

The characteristics of cold cathode gauges are briefly described with particular reference to the Penning-type discharge cell adapted to work down to very low pressures. Such gauges have the great advantage of not contributing contaminants to the system from hot filaments, and from this point of view are highly attractive as standards of reference at very low pressures. Experimental results are presented which contrast their behavior with that of hot cathode devices. Some drawbacks are recognized in practice, but it seems likely that developments will increase their attraction for making accurate and reproduceable measurements down to the lowest pressures likely to be encountered. (auth) (UK)

2431 EXTERNAL COLLECTOR GAUGE FOR ULTRAHIGH VACUUM MEASUREMENT. Fletcher, B. (Edwards High Vacuum International Ltd., Crawley, Eng.). Vacuum; 20: 381-4(Sep 1970).

Developments designed to reduce the low pressure measurement limit of hot cathode ionization gauges are reviewed. The two main considerations when reducing the low pressure limit are residual current and sensitivity. An external collector gauge has a low residual current due to the ion collector being placed outside the grid volume. The evaluation of a gauge of this type is described. An increase in sensitivity obtained without an increase in residual current also has the effect of reducing the low pressure limit. It is shown that an improvement in sensitivity can be obtained by ensuring that the ratio of radial to tangential energy of electrons entering the grid is as high as possible. (auth) (UK)

XUM

INSTRUMENTATION

Radiation Detection Instruments

Refer also to abstracts 2122 and 3183.

General Detectors and Monitors

Refer also to abstracts 2474 and 3497.

2432 (AD-706587) TEST MEASUREMENTS ON SCINTILLATION GEIGER-MUELLER COUNTERS. Daggs, V. M.; Parr, W. H.; Krebs, A. T. (Army Medical Research Lab., Fort Knox, Ky.). 18 Jul 1951. 11p. NTIS.

The object of the study was to explore the possible application of scintillation Geiger Mueller counters to radiobiological studies. (auth) (USGRDR)

2433 (CEA-R-4063) CONSTRUCTION OF A SEMI-AUTOMATIC DEVICE FOR MEASURING NUCLEAR TRACKS. APPLICATION TO NEUTRON SPECTROMETRY AROUND THE LOW- AND MEDIUM-ENERGY ACCELERATORS AT SACLAY. Delsaut, Romeo. (Commissariat a l'Energie Atomique, Saclay (France). Centre d'Etudes Nucleaires). Oct 1970. 91p. (In French). Dep. NTIS (U. S. Sales Only).

Amongst the various methods commonly used for neutron spectrometry around accelerators, the use of nuclear emulsions is particularly interesting. This technique presents two major difficulties due to the fact that the analysis of the emulsions is lengthy and tedious, and that the neutrons measured around accelerators do not have a preferred direction. In order to solve these difficulties, a semiautomatic device for analyzing the emulsions was developed, which gives results used directly by a computer. The fixed emulsion was replaced by a mobile system of two emulsions perpendicular to each other. The validity of these methods was verified by measuring the spectrum of neutrons emitted by reaction $D(d,n)^3He$; the practical application is the determination of the spectrum of neutrons emitted by a plutonium fluorine source, and that of neutrons emitted in the Van de Graaff tandem chamber at Saclay. The results obtained are very satisfactory and indicate that the two techniques proposed make it possible to widen the field of application of nuclear emulsions to the spectrometry of neutrons having an unknown incident direction, and also improve the conditions in which the emulsion is analyzed. (France)

2434 (CERN-70-27) METHOD OF MEASUREMENT OF THE BEAM PROFILE FOR HIGH-INTENSITY PARTICLES (10^{12}/cm^2). Annoni, H.; Cordaillat, A.; Herz, A. J.; Mendola, O.; Oppel, R. (European Organization for Nuclear Research, Geneva (Switzerland)). 13 Oct 1970. 12p. (In French). Dep. NTIS (U. S. Sales Only).

This method allows a rapid and precise determination of the beam profile, the position of the maximum of the intensity and the absolute intensity (with an error of about 10%). At present, it can be used for intensities between 10^{11} and 2×10^{12} particles/cm^2. Thin plastic detector foils (cellulose nitrate) are exposed normal to the beam under study and the measurements are carried out with a microdensitometer. Nuclear-research emulsions have been used as a comparison standard. The first measurements were carried out in a proton beam of energy 600 MeV; the method can, of course, be applied to any other kind of high-intensity, high-energy beam. (auth)

2435 (RPI-328-202) PRECISION OF TANK CAPTURE CROSS SECTION MEASUREMENTS. Block, Robert C.; Hockenbury, Robert W. (Rensselaer Polytechnic Inst., Troy, N. Y. Dept. of Nuclear Science). [1970]. Contract AT(30-1)-328. 13p. (CONF-701002-1). Dep. NTIS.

From EANDC Symposium on Neutron Standards and Flux Normalization, Argonne, Ill.

The precision of neutron capture cross section measurements with large liquid scintillators, or "tanks", is reviewed with regard to recently reported measurements. A precision of 3% is currently obtained for thermal measurements while a precision of 10% is reported for heavy nuclei in the keV region. Anticipated improvements in the determination of the neutron flux dependence with energy and capture spectra measurements in the keV region should enable future tank measurements to achieve an accuracy of 3 to 5% in absolute capture cross sections in the keV region. On the other hand, a relative measurement in the keV region of two capture cross sections could conceivably be made to an accuracy of 5%, and with great care a precision of 2 to 3% should be possible. (auth)

2436 LOW TEMPERATURE SCINTILLATION RESPONSE OF UNACTIVATED SODIUM IODIDE TO GAMMA-RAYS. West, J. B.; Collinson, A. J. L. (Borough Polytechnic, London). J. Phys., B (London); 3: 1363-73(Oct 1970).

The pulse height per unit energy was measured for two pure sodium iodide crystals for gamma-ray excitation in the energy region 30 keV to 1 MeV, at temperatures between 77 K and 200 K. By using a specially calibrated crystal, it was possible to find the light output per unit energy in terms of photons per MeV. The purity of the crystals used was investigated by recording their emission spectra, and the variation of scintillation efficiency with specific ionization of the incident radiation was deduced from the gamma-ray response data. (auth) (UK)

2437 MAKING OF Ge(Li) DETECTOR AND ITS APPLICATION. Morimitsu, Wataru (Industrial Research Inst., Yokohama, Japan); Ishizuka, Yasuhiro. Kanagawa-ken Kogyo Shikenjo Kenkyu Hokoku; No. 29, 37-42(Mar 1970). (In Japanese).

The Ge(Li) detector, with its high energy resolution for γ-rays, is being used in various fields. In order to utilize it in industry, the coaxial-type Ge(Li) detector of relatively large size has been constructed for trial. The size is 30 mm dia × 45 mm long, and the effective volume is 22 cc; the detection efficiency is high. The energy resolution for gamma rays (FWHM) is 5.2 keV for the ^{60}Co of 1.33 MeV, 4.4 keV for the ^{137}Cs of 0.662 MeV, and 2.5 keV for the ^{57}Co of 122 keV. The detector was used for activation analyses of brass and neutron-irradiated Ti and also for counting air-borne dust particles. The result showed that the Ge(Li) gamma detector has superior performance, and can be utilized for various measurements. (Japan)

2438 NUCLEAR TRACK METHODS IN SOLIDS AND ITS DEVELOPMENT. PART 2. DISCRIMINATION OF INCIDENT PARTICLES AND OF THEIR ENERGY, AND APPLICATION OF PLASTICS. Sakanoue, Masanobu (Kanazawa Univ., Japan). Kagaku No Ryoiki; 24: 207-21(Mar 1970). (In Japanese).

In Part 1, the fundamentals of the nuclear track method in dielectric solids and its applications were described concerning the quantitative aspect of the track, that is, track density. In this article the fundamentals are explained in detail with regard to the qualitative aspect of the track such as track size and track length. The discrimination of incident particles and their energy can be made by the use of these qualitative characteristics of the tracks. Cellulose film and its application are described, and the applications of polycarbonate and other plastics are discussed. (Japan)

2439 IMPROVED METHOD IN THRESHOLD NEUTRON SPECTROSCOPY. Daddi, L. (CAMEN, Pisa, Italy). Energy. Nucl. (Milan); 17: 448-9(Jul 1970).

An improvement is presented of a method of threshold neutron spectroscopy utilizing four detectors. In this new approach the differential flux φ (E) is always obtained through two functions only; moreover, a digital IBM 7090 computer is utilized in data treatment. (W.H.K.)

2440 CORONA COUNTERS FOR NUCLEAR RADIATION DETECTION. Gilar, Oldrich; Pavlíček, Zdenek (TESLA, Premysleni, Czech.). Jad. Energ.; 16: 239-41(1970). (In Czech).

The design, operation, and characteristics of a new type of gas discharge counter are described. (W.H.K.)

2441 NUCLEAR RADIATION DETECTOR AND METHOD FOR MANUFACTURING SAME. Kozlov, Stanislav Fedorovich; Konorova, Elena Alexandrovna (to Ordena Lenina Fizichesky Institut Imeni PN Lebedeva). British Patent 1,205,115. 16 Sep 1970. Priority date 29 Mar 1967, Russia.

A diamond crystal detector for operation at room temperature is described. The crystal is sandwiched between contact plates to apply the electric field. The surface layers may be doped to form essentially a p-z'-n semiconductor, or the contact surfaces may be coated to form carrier blocking and injecting layers. (W.H.K.)

2442 POLYNOMIAL APPROXIMATION OF THE FAST NEUTRON SPECTRUM MEASURED BY THRESHOLD DETECTORS. Starodubtsev, S. V.; Ashirov, E. G.; Zinov'ev, N. V. This paper was summarized in At. Energ. (USSR); 25: 139(Aug 1968) as paper No. 211. (In Russian).

The fast neutron spectrum was measured in an experimental channel of the VVR-S reactor by using the threshold reactions ^{115}In $(n,n')^{115m}$In, ^{58}Ni $(n,p)^{58}$Co, ^{64}Zn $(n,p)^{64}$Cu, ^{27}Al $(n,p)^{27}$Mg, ^{24}Mg $(n,p)^{24}$Na, and ^{27}Al $(n,\alpha)^{24}$Na. For the mathematical pro-

cessing of the activation data the spectrum was approximated by the polynomial $\varphi(E) = \Sigma_{i=-3}^{2} \alpha_i E^i$. Using the method of least squares to solve the equations for the α's allowed the spectrum function to be represented by any set of powers of E from 2 to 6 without loss of information. In addition, the polynomial expansion of the spectrum was taken in various combinations with the function $\varphi(E)$ describing the fission spectrum, and with the exponential function $\varphi_0(E) = \exp(-E + \sqrt{2E})$. Altogether 23 different combinations of functions for approximating the spectrum were tested, yielding errors in activity, both positive and negative, of 0.5 to 70%. (W.H.K.)

2443 DETERMINATION OF FAST NEUTRON FLUX BY A ZnS(Ag) + PLEXIGLAS DETECTOR AND BY A BASSON DETECTOR. Kozlovskii, S. A.; Kyz'yurov, V. S.; Smetanin, A. A. This paper was summarized in At. Energ. (USSR); 24: 564-5 (Jun 1968) as paper No. 207. (In Russian).

ZnS(Ag) + Plexiglas fast-neutron detectors (B-type detectors) and Basson medium-energy neutron detectors are often used in studying the distribution of fast and medium-energy neutrons in a shield. When the flux of fast or medium-energy neutrons is to be determined from the readings of such detectors one has to make a correction for medium-energy neutrons counted by the ZnS(Ag) + Plexiglas detector and one for fast neutrons counted by the Basson detector. This is easily done for measurements in a known neutron spectrum, where the flux of neutrons with energies higher than a certain given threshold can be determined from the detector reading. The correction procedure is described. Also, the detector sensitivity as a function of neutron energy was studied experimentally. The neutron spectrum of a Po–Be-source was used as a calibration spectrum for the ZnS(Ag) – Plexiglas detector, that for the Basson detector was the spectrum of neutron leakage from a 30 cm thick iron prism. The maximum error in finding the flux of fast neutrons with energies greater than 0.5 to 1.5 MeV and intermediate neutrons with energies less than 0.5 to 1.5 MeV is 900% for measurements by a ZnS(Ag) + Plexiglas detector in iron, and 500% for measurements by a Basson detector in a fission spectrum. (W.H.K.)

2444 RESPONSE OF SUPERCONDUCTING WEAK LINKS TO PHOTONS. Chiao, R. Y. (Univ. of California, Berkeley). Phys. Lett.; 33A: 177-8(19 Oct 1970).

A theoretical study of radiation detectors using superconducting weak links was undertaken, with the Mercereau ring interferometer as a specific example. A single photon should depress the critical current fractionally by $2\pi\alpha \approx 4.6\%$. These detectors should possess sizeable post-detection gains, so that individual photons should be countable. (auth)

2445 POCKET RADIOMETER WITH OPTIC AND ACOUSTIC SIGNAL. Weber, H. (Humboldt-Univ., Berlin). Isotopenpraxis; 6: 184-7(May-Jun 1970). (In German).

The described pocket ionization radiometer may be used both for relative activity measurement in radiation monitoring service (contamination monitoring), and for semi-quantitative dose rate metering in the orientation radiation detection field, so that it may be included into the category of combined radiometers. Its features are small dimensions and low weight as well as ample adaptibility to different operating voltage and radiation intensity values. Apart from signalization of discrete pulses, it provides visual and acoustic signalization on conjunction with an integrating measuring circuit and connection of some measuring gauge or counter. (auth)

2446 CALIBRATION OF TWO-STAGE AIR SAMPLERS. Ettinger, Harry J.; Partridge, Jennings E.; Royer, George W. (Los Alamos Scientific Lab., N. Mex.). Amer. Ind. Hyg. Ass. J.; 31: 537-45(Sep-Oct 1970).

Three different two-stage samplers were calibrated using monodisperse aerosols produced by a spinning-disk aerosol generator. One, using a horizontal elutriator as the size selector, agreed with the criteria defining "respirable dust" adopted by the British Medical Research Council. The other two, using small cyclones as size selectors, agree with criteria proposed by the Los Alamos Conference and the ACGIH when operated at approximately half their initially recommended flow rates. Operation of these cyclones at the initially recommended flow rates underestimates the inhalation hazard. (auth)

2447 MODULATION TRANSFER FUNCTION EVALUATION OF SCINTILLATION CAMERA AND RECTILINEAR SCANNER. Alvi, Zahoor M. (Univ. of Southern California, Los Angeles); Bennett, Leslie R. Nucl.-Med.: 9: 203-17(30 Sep 1970).

A simple film density approach was used to obtain modulation transfer functions for a scintillation camera. Counting rate was measured in the case of a rectilinear scanner. Point sources were prepared of ^{131}I and ^{99m}Tc and point source images were obtained on X-ray film. Density distribution along the diameter of the images was converted into corresponding exposure values. Line spread functions were obtained as areas under the distribution curves and then MTF was solved for each spatial frequency considered. Plots of MTF versus spatial frequency show in one glance the relative responses of either the two imaging systems or the responses of one imaging system for two different commonly used radionuclides. (auth)

2448 SOME PRACTICAL CONSIDERATIONS ON COUNTING EFFICIENCY FOR ENVIRONMENTAL SAMPLES AND THE GAMMAGRAPH CALIBRATION. Jun, Jae Shik (Atomic Energy Research Inst., Seoul). New Phys. (S. Korea); 9: 75-82(Dec 1969).

A simple and relatively accurate method for determining the gross beta counting efficiency for various environmental samples and a calibration procedure for the measurement of natural background radiation dose rate with a Gammagraph are presented. It has been reaffirmed that a thallium-204 liquid standard source is an appropriate source for determining gross beta activity of reasonably old fission products, and the relative counting efficiencies of an end-window G–M counter for plane circular sources of relative size $d/r = 0$ to 2 were examined in both empirical and and theoretical ways. The Gammagraph calibration equations were considered to be sufficiently reliable for practical analysis of the measured radiation dose rate within the statistically estimated standard deviations of the slope and intercept of the regression equation and the 95% confidence band of the calibration line as a whole. (auth)

2449 PROPORTIONAL CHAMBERS. CERN Cour.; 10: 151-3(May 1970).

The design and development of multiwire position-sensitive proportional chambers are reviewed. A circuit diagram for an amplifier processing unit is presented, and the associated electronics is discussed. Some position-sensitive proportional chambers in use at various laboratories are surveyed. (W.H.K.)

2450 ADDITION OF NAPHTHALENE TO LIQUID SCINTILLATORS. AN ATTEMPTED INTERPRETATION ON THE BASIS OF ENERGY TRANSFER KINETICS. Germai, G. (Univ., Liege). Int. J. Appl. Radiat. Isotop.; 21: 587-94(Oct 1970). (In French).

In the field of radiation measurements the energy transferring mechanism has not been described in the case of liquid scintillators containing naphthalene although it is a usual component of scintillating solutions. The experiments described in this paper show that naphthalene acts as an intermediate and a secondary solvent. The transfer processes chain varies with the speed of the energy transfer from the solvent to the primary solute. The quenching law is still linear with regard to quencher concentration when the scintillator contains naphthalene, although the quenching constant of many quenchers is smaller than the one measured when naphthalene is absent. (auth) (UK)

2451 NUCLEAR INTERACTIONS IN Si(Li) DETECTORS DUE TO H, D, ^3He, AND ^4He BEAMS. Cahill, T. A.; Brady, F. P.; Corbett, S.; (and others) (Univ. of California, Davis). Nucl. Instrum. Methods; 87: 151-3(1970).

Measurements are reported of pulse height distributions in Si(Li) detectors due to nuclear interactions of monoenergetic protons, deuterons, ^3He and ^4He beams in the range 15 to 80 MeV. (auth)

2452 OPERATION OF LARGE AREA SILICON SURFACE-BARRIER DETECTORS AT LOW TEMPERATURES. Beda, A. G. (Inst. of Theoretical and Experimental Physics, Moscow). Nucl. Instrum. Methods; 87: 135-6(1970).

The fabrication and operation of silicon surface-barrier detectors with active areas of 254 mm^2 are described. The resolution of the detectors yielded a fwhm of approximately 9 keV at 77 K and 8.4 keV at 4.2 K for 194 keV conversion electrons of ^{203}Tl. (auth)

2453 SIMPLE APPARATUS FOR DELIVERY OF GAS FOR A FLOWTHROUGH PROPORTIONAL COUNTER AT ANY OPERATING PRESSURE. Hink, W.; Scheit, A. N.; Ziegler, A. (Univ., Wuerzburg, Ger.). Nucl. Instrum. Methods; 87: 137-40(1970). (In German).

Stabilization of gas pressure in flow proportional counters is an important problem since for example a relative variation of gas pressure of only 2.2×10^{-3} induces a change of gas gain of 1% under optimal operating conditions (defined by the maximum possible gas gain within the range of proportionality). This paper describes the construction and operation of a simple apparatus which reduces the variation of gas gain to less than 1% and which functions as a pycnostat under changes of temperature. (auth)

2454 NOTE ON THE FINITE SOLID-ANGLE CORRECTIONS FOR Ge(Li) DETECTORS. Anicin, I. V.; Bikit, I. S. (Boris

XUM

Kidric Inst. of Nuclear Sciences, Belgrade). Nucl. Instrum. Methods; 87: 145(1970).

The finite solid-angle correction factor calculations for coaxial Ge(Li) detectors (Nucl. Instr. and Meth., Vol. 76(1969) p. 192) are commented. (auth)

2455 CORRECTIONS TO COAXIAL Ge(Li) DETECTOR SOLID ANGLE CORRECTION FACTORS. Camp, D. C.; Van Lehn, A. L. (Univ. of California, Livermore). Nucl. Instrum. Methods; 87: 147-8(1970).

This letter discusses additional corrections (Nucl. Instr. and Meth., Vol. 76(1969) p. 192) needed for solid angle correction factors for coaxial detectors. (auth)

2456 STUDY ON THE MULTIPLE DIFFUSION OF NEUTRONS IN ^{6}Li-LOADED SCINTILLATORS COUPLED TO A PHOTOCATHODE OF THE ASSOCIATE PM. Fort, E. (CEA, Cadarache, France). Nucl. Instrum. Methods; 87: 115-24(1970). (In French).

A Monte Carlo method is used to study the multiple scattering of neutrons in ^{6}Li scintillators. The back-scattering by the photocathode of the photomultiplier is taken into account. The nuclear processes considered are absorption by the (n,α) reaction and inelastic scattering. For heavy nuclei the scattering is assumed to be isotropic in the center of mass system while for light nuclei published values of the angular distributions are employed. Three cases are considered: (1) A collimated beam of monoenergetic neutrons incident normally on a lithium glass scintillator type NE 905. (2) The same scintillator irradiated by neutrons from the $p(T,n)^3$He reaction with energy selection by means of the associated particle technique. The angular distribution and energy spectrum of the neutrons incident on the scintillator are altered by the multiple scattering of the ^{3}He particles in the target. (3) A collimated beam of monoenergetic neutrons incident normally on a I^{6}Li Harshaw type crystal enclosed in a protective capsule. The multiple scattering correction curves make it apparent which portion of the effect is due to what may be properly said to be multiple scattering and which portion is actually due to the effects of geometry. (auth)

2457 EFFECT OF THE MUTUAL OVERLAP OF ADJACENT GRAINS OF THE GRAIN COUNTING IN NUCLEAR EMULSIONS. Filisetti, O.; Lovera, G.; Minetti Mezzetti, E.; Tedde, P. G. (Politecnico, Turin). Nucl. Instrum. Methods; 87: 93-9(1970).

The results of grain counting are here reported; they concern the grain density along tracks of α-particles and protons, at the end of the range, in Ilford K0 emulsions, with different track dip angles in the original emulsion. The results are interpreted accounting for the mutual overlap effect of next developed grains along the track. This allows to normalize the statistical grain density distribution along inclined tracks to the one along horizontal tracks, with the purpose to discriminate the tracks of different particles (α-particles and protons). (auth)

2458 CONSTRUCTION OF A FAST CONSTANT FRACTION TRIGGER WITH INTEGRATED CIRCUITS AND APPLICATION TO VARIOUS PHOTOMULTIPLIER TUBES. Maier, M. R.; Sperr, P. (Technische Hochschule, Munich). Nucl. Instrum. Methods; 87: 13-18(1970).

A simple realization of a constant fraction of pulse height trigger with integrated circuits is described. Some results for time walk and time resolution are given which were obtained with Valvo XP 1021, RCA 8575, RCA C 31000 D photomultiplier tubes and 1.5" × 1.0" Naton 136 scintillator. The best values were measured with the RCA C 31000 D tubes, namely a resolution of 200 psec fwhm for 1 MeV energy loss in both scintillators, and a time walk of less than 60 psec with an energy range of 50 keV to 1 MeV. (auth)

2459 SPARK COUNTERS AS HIGH-TEMPERATURE NEUTRON DETECTORS. Eichholz, G. G. (Georgia Inst. of Tech., Atlanta). Nucl. Instrum. Methods; 87: 181-7(1970).

Cylindrical spark counters have been designed that employ boron nitride disks as converters and are capable of functioning as high level neutron detectors with a sensitivity of the order of 10^{-7} counts per incident neutron. These detectors have shown linear response in neutron fluxes up to 10^{10} n/cm^2 sec with argon filling. At higher radiation fields, breakdown occurs in the detector, presumably due to the accompanying gamma ray field. The detectors have been operated at temperatures up to 550°C; above that temperature satisfactory performance appears to be inhibited by the low leakage resistance of available insulators. The detectors have a large signal amplitude and operate best with external voltage quenching. (auth)

2460 SELF-QUENCHING GM COUNTERS WITH HEATED ANODE. Peeva, A.; Rijhikov, St. (Univ. of Sofia). Nucl. Instrum. Methods; 87: 237-40(1970).

The purpose of the present paper is to report the results of our studies on the behaviour of counters with current-heated anodes. The results have shown that by heating the anode, the counter regime is changed and this change depends on the type and amount of the quenching component. There is an optimal value of the quencher pressure (p_q) at which the counter works most effectively. By heating the anode, the counter discharge can be regulated within a definite interval (range). The heating permits to enhance the working capabilities of counters with worsened characteristics. The worsening may be due to cooling, ageing, inadequate pressure of the quenching, pressure of the quencher, etc. It is attempted to show that the effect of heating can be explained by the presence of quenching molecules in the space around the anode, thus emphasis is laid on the role of that space for the counter discharge. (auth)

2461 INVESTIGATION OF SOURCE-DEPENDENT CONTRIBUTIONS TO PHOTOMULTIPLIER NOISE. Johnson, F. A. (Defence Research Establishment, Ottawa). Nucl. Instrum. Methods; 87: 215-20(1970).

Fast pulses produced at the output of a photomultiplier as a result of the interaction of low-energy γ rays in the glass faceplate are shown to have similar characteristics to those due to Cherenkov events generated there by high-energy γ rays. In both cases the pulses can be distinguished from those produced by γ-ray interactions in a scintillator which is viewed by the photomultiplier. On the basis of fast-crossover-timing and pulse-height-distribution measurements it is concluded that visible light, produced in the glass faceplate by the low-energy γ rays, is responsible for the pulses observed. Other mechanisms by which similar pulses could be produced by low-energy γ rays are also considered, but separate identification would appear to be difficult. (auth)

2462 PERFORMANCE OF A PULSED-LIGHT FEEDBACK PREAMPLIFIER FOR SEMICONDUCTOR DETECTOR X-RAY SPECTROMETERS. Landis, D. A.; Goulding, F. S.; Jaklevic, J. M. (Univ. of California, Berkeley). Nucl. Instrum. Methods; 87: 211-13(1970).

Experimental results are reported for the energy resolution and counting-rate performance of an x-ray spectrometer using pulsed-light feedback to restore the input of a charge-sensitive preamplifier when required. (auth)

2463 USE OF THIN SEMICONDUCTOR POSITION SENSITIVE DETECTORS IN MAGNETIC SPECTROGRAPHS. Jolly, R. K.; Trentelman, G. F.; Kashy, E. (Michigan State Univ., East Lansing). Nucl. Instrum. Methods; 87: 325-8(1970).

Thin position sensitive silicon surface-barrier detectors in a magnetic-spectrograph have been found to yield good position resolution and a high degree of discrimination between various particles. (auth)

2464 TECHNIQUE FOR MOUNTING AN ANODE WIRE IN A 4π PROPORTIONAL COUNTER. Roy, J. C. (Univ. Laval, Quebec). Nucl. Instrum. Methods; 87: 323(1970).

A simple technique is described for mounting an anode wire in a 4π proportional counter. It consists in tying the wire to the eye of a sewing needle which is passed through the hole of the insulators. (auth)

2465 UNIFORM TENSION IN A PLANE ARRAY OF THIN PARALLEL WIRES. Wynchank, S. (Columbia Univ., New York, Brooklyn Coll.). Nucl. Instrum. Methods; 87: 317-18(1970).

A construction method for multiwire proportional chambers is proposed which winds the wires in a helix under constant low tension. The wires are then stretched uniformly, as required for high voltage operation. (auth)

2466 SIMPLE HOLDING SCALER. Thonnard, N. (Univ. of Kentucky, Lexington). Nucl. Instrum. Methods; 87: 313-15 (1970).

A simple and inexpensive holding circuit is described in which a separate register is not used to store the counts. Instead, neon lamps are used both as indicators and memory units. (auth)

2467 TRANSIENT RESPONSE OF COBALT SELF-POWERED NEUTRON DETECTORS. Boeck, H. (Oesterreichische Hochschule, Vienna); Stimler, M.; Strindehag, O. Nucl. Instrum. Methods; 87: 299-300(1970).

In the TRIGA reactor in Vienna the transient response of a self-powered detector with cobalt emitter has been studied. (auth)

XUM

2468 MEASUREMENT OF BACKWARD SCATTERING OF 14 MeV NEUTRONS. Bonazzola, G. C.; Bressani, T.; Chiavassa, E.; Venturello, G. (Univ., Turin. Istituto Nazionale di Fisica Nucleare, Turin). Nucl. Instrum. Methods; 87: 291-5(1970).

In this paper we describe an experimental arrangement which can be used for the measurement of differential cross sections at backward angles (140° – 178°) for elastic and inelastic scattering of 14 MeV neutrons. The angular resolution is better than 2°, the divergence of the incident neutron beam being 12°. An application to the time-of-flight with associated particle technique is given, for a ^{12}C target. Improvements are possible with the pulsed-beam technique. (auth)

2469 MASS-IDENTIFICATION OF ALPHA-PARTICLES AND HEAVY IONS BY TIME-OF-FLIGHT METHODS. Schneider, W. F. W.; Kohlmeyer, B.; Bock, R. (Univ., Marburg, Ger.). Nucl. Instrum. Methods; 87: 253-9(1970).

A time-of-flight technique has been applied to the mass identification of heavy ions from nuclear reactions in the mass-range $4 \leq A \leq 16$. The system described consists of a zero-time detector of the secondary emission type in connection with a surface barrier semiconductor energy detector at the end of the flight path. The apparatus exhibits a time resolution of 1.15 ns for α-particles and 0.8 ns for fission-fragments, and an efficiency of 83% and 99.9%, respectively. (auth)

2470 PRESENTATION OF EVIDENCE OF THE INFLUENCE OF THE TEMPERATURE ON THE GAIN OF A TUBULAR ELECTRON MULTIPLIER WITHOUT A WINDOW. Barat, C. (Centre d'Etude Spatiale des Rayonnements, Toulouse). Nucl. Instrum. Methods; 87: 247-52(1970). (In French).

The gain of twenty units of different channel electron multipliers is studied as a function of temperature for variable applied voltages and incident fluxes. The devices show an exponential reduction of gain when the temperature decreases dating from 50°C, upper limit of utilization. This reduction depends on the contamination of the layer and it is necessary to obtain accurate and stable characteristics to find a rapid desorption device of the inner channel surface. The interpretation of this law shows that the output current is proportional to the conduction layer current. (auth)

2471 RADIATION SENSITIVE MATERIALS. Sherwood, Harold Frank (to Eastman Kodak Co.). British Patent 1,208,024. 7 Oct 1970. Priority date 9 Nov 1966, United States.

A thin color-change layer is coated with a thin polymer film. After exposure to charged particles, the polymer film is etched and then the color-change layer is selectively developed (only the portions exposed by the etched tracks in the polymer film). In the preferred embodiment, the color-change layer is a photographic film. (W.H.K.)

Nuclear Spectroscopic Instrumentation

Refer also to abstracts 2144, 2407, 3535, and 3541.

2472 (AEEW-M-905) PROTON RECOIL COUNTER TECHNIQUES IN ZEBRA. Broomfield, A. M.; Carter, M. D. (Atomic Energy Establishment, Winfrith (England)). Dec 1969. 24p. Dep. NTIS (U. S. Sales Only). UK 4s. 6d.

Spherical hydrogen-filled proton recoil proportional counters are used for measurements of neutron spectra between 5 keV and 1 MeV in fast reactor assemblies built in ZEBRA. The technique used for these measurements and their analysis is described. (auth) (UK)

2473 (AERE-R-6318) SOME EFFICIENCY CALCULATIONS FOR ^6Li SUSPENDED TARGET SEMICONDUCTOR SANDWICH SPECTROMETERS. Lord, E. A.; Cousins, J. A. R.; Silk, M. G.; Clements, P. J. (Atomic Energy Research Establishment, Harwell (England)). Aug 1970. 14p. Dep. NTIS (U. S. Sales Only). UK 2s. 6d.

The geometric efficiency of lithium-6 semiconductor spectrometers of the suspended target type has been calculated for isotropic neutron fluxes. A wide range of diode separations has been studied. It is shown that the geometric efficiency is not well predicted by earlier "loss angle" calculations nor by extrapolations from the data available for surface target spectrometers. (UK)

2474 (IAEA-122, pp 150-63) THEORETICAL PHOTOPEAK COUNT-RATES IN Ge(Li) AND NaI(Tl) DETECTORS FROM GAMMA-RAY EMITTERS FORMED BY THERMAL NEUTRON ACTIVATION. Parr, R. M. (International Atomic Energy Agency, Vienna (Austria)).

Tables of calculated photopeak count-rates from gamma ray emitters formed by thermal neutron activation are presented for a 20 cm^3 lithium-drifted germanium detector, a 3 × 3 inch right circular thallium-activated sodium iodide scintillation detector, and an assumed ideal gamma ray detector. (W.H.K.)

2475 (INP-707) VINCA NOVA: AN AUTOMATIC UNIT FOR NEUTRON SPECTROMETER CONTROL. Brankowski, J.; Olejarczyk, W.; Sarga, T.; Sciesinski, J.; Zaleski, T. (Institute of Nuclear Physics, Krakow (Poland)). Jun 1970. 21p. Dep. NTIS (U. S. Sales Only).

A boron trifluoride proportional neutron spectrometer control unit is described. Its operational program can be accomplished manually or automatically by means of punched tape. The unit is constructed with solid-state elements. The logical structure and co-ordination of blocks are described. To illustrate the electronic details one block is described. The technical parameters of the Vinča Nova unit are given. (auth)

2476 α SPECTROMETRY OF LOW-ACTIVITY SPECIMENS. Szabo, G. Levente Magy. Geofiz.; 11: No. 1-2, 35-40(1970). (In Hungarian).

Lack of suitable equipment and difficulties encountered in the preparation of thin specimens were responsible for not using α-spectrometric methods as a prospecting tool for radioactive ores. These difficulties may be overcome by designing an instrument for such a specialized use. The features of such a modified α spectrometer, consisting of a double-grid ionization chamber with plane-parallel electrodes are described. The new detector presents several advantages over semiconductor detectors: it allows to measure sources with a large surface and it generates several signals for each single α particle. By making use of the logical connection between the anode, grid, and cathode pulses, the usual shortcomings of ionization chambers may be overcome. The experiments indicate that the required 70-keV resolution is not compromised by the eventual contamination of the commercial argon + methane mixture used in the instrument. (TTT)

2477 COMPUTER FOR PROCESSING γ-SPECTRA. Tishechkin, A. S. This paper was summarized in At. Energ. (USSR); 24: 462-3(May 1968) as paper No. 202. (In Russian).

In processing scintillation γ-spectra, besides solving the Fredholm equation and taking account of Compton broadening, it is necessary to make corrections for such phenomena as background, counting losses related to the instrument dead time, the photoefficiency of the crystal, the linearity of the instrument scale, the difference in amplification factors in various series of experiments, etc. All these corrections lead to the multiplication of the spectrum by a constant (function) or to the subtraction of a spectrum from a spectrum. A special computer has been developed to perform the following operations: (a) normalization of the spectrum; (b) taking account of the efficiency of the crystal; (c) taking account of background (subtracting a spectrum from a spectrum); (d) numerical differentiation of the spectrum; (e) resolution of a complex discrete spectrum into components; (f) regrouping of data taken in any number of channels into any other number of channels; (g) multiplication of the spectrum by the inverse matrix; (h) multiplication of the spectrum by the forward matrix; and (i) finding the actual spectrum by iterating use of the forward matrix. The computer has been constructed so as to allow the work to be programmed by inserting plugs into sockets mounted on the front panel of the equipment. Input and output are through a ST-2M telegraphic apparatus. The time to perform a single addition or subtraction, including the access time to two memory addresses and the time to transfer the result from the accumulator to the memory is less than 1 msec, while the time to perform a multiplication under the same conditions is of the order of 2.4 msec. The device has a ferrite core memory with a capacity of 256 words of 16 binary digits each. The memory may be divided into two or four equal parts. A cathode-ray tube permits visual scanning of input data and results. (auth)

2478 PREVENTION OF ALPHA COUNTER CONTAMINATION BY ELECTRODELESS DISCHARGE DEPOSITION OF Si_3N_4 THIN FILMS. Blumstein, C.; Melgard, R.; Stafford, W. (Trapelo/West, Richmond, Calif.). Radiochem. Radioanal. Lett.; 5: 29-35(16 Oct 1970).

Platinum disks plated with α-emitting isotopes can be covered with a thin film of silicon nitride using a low temperature rf generated discharge reaction of silane and nitrogen to reduce the contamination of alpha detectors. The low thickness film inhibits the escape of gaseous radioactive daughters and of radioactive recoil nuclei from the plated sample but has a negligible effect on the α spectrum. (auth)

2479 SOURCES AND PREVENTION OF RECOIL CONTAMINATION OF SOLID-STATE ALPHA DETECTORS. Sill,

XUM

Claude W.; Olson, Dale G. (Atomic Energy Commission, Idaho Falls, Idaho). Anal. Chem.: 42: 1596-1607(Nov 1970).

Most recoil contamination of the solid-state detectors used in alpha spectrometry results from radioactive chains in which short-lived, alpha-emitting daughters are produced either directly from alpha-emitting parents or indirectly by decay of a short-lived beta-emitting daughter which in turn was produced from an alpha-emitting parent. Spectra are given showing the recoil products resulting from various combinations of exposure and decay time for each of the four main radioactive series. Recoil contamination of the detector can be reduced by a factor of at least 10^3 with a loss in resolution of only 1 or 2 keV by leaving enough air in the counting chamber to produce 12 $\mu g/cm^2$ of absorber between the source and detector, and applying a negative potential of 6 volts to the source plate. Polonium-210 gives a marked pseudo-recoil effect, probably due to its own inherent volatility, and is by far the most serious long-term contaminant encountered. Its spontaneous volatilization from a stainless steel support can be virtually eliminated by heating the plate for 5 minutes at about 300°C without significant loss of resolution. (auth)

2480 PROTON-RECOIL SPECTROMETER USING SOLID-STATE DETECTORS AND PARTICLE IDENTIFICATION. Roy, R.; Slobodrian, R. J. (Univ. Laval, Quebec). Nucl. Instrum. Methods; 87: 1-6(1970).

A proton recoil neutron spectrometer using a thin radiator, three solid-state detectors and particle identification has been tested at 20 MeV neutron energy. Particle identification, a triple coincidence requirement between the detectors and the detection of recoil protons at 10° with respect to the neutron beam result in a very low background (<0.5%). Detailed mechanical and electronic designs of the spectrometer are presented. The system is compared with a time-of-flight spectrometer for energies between 20 and 80 MeV under conditions yielding energy resolutions of 2%. (auth)

2481 FAST NEUTRON SPECTRUM MEASUREMENTS IN THE MTR SCANDIUM AND IRON FILTERED BEAMS. Powell, J. E. (Argonne National Lab., Idaho Falls, Idaho); Rogers, J. W. Nucl. Instrum. Methods; 87: 29-36(1970).

The energy response of proton-recoil proportional counters was studied by making fast neutron spectrum measurements in the MTR scandium and iron filtered beams over the energy range of 200 eV to 1 MeV. Results of the measurements were compared with time-of-flight data. It was found that the calibration technique suggested by Bennett is adequate for accurate measurements if the hydrogen counter data is corrected for calibration pulse height losses due to shaping time constants in the linear amplifier. Further evidence of the energy loss per ion pair for hydrogen (W) being constant with energy down to 2 keV was found. Cutoff models suggested for the hydrogen W, which account for an energy variation near 2 keV, can cause errors in the measured neutron spectrum. The results also showed that W for methane is energy dependent in the region around 100 keV. (auth)

2482 METHOD FOR THE SEPARATION OF OVERLAPPING DECAYING PEAKS. Adam, G.; Katriel, J. (Nuclear Research Centre, Beer-Sheva, Israel). Nucl. Instrum. Methods; 87: 305-6(1970).

A computational method for the separation of overlapping decaying gamma rays peaks is proposed. The method, which takes advantage of the decay, overcomes some of the drawbacks of the standard peeling method. (auth)

2483 RESOLVING POWER OF COINCIDENCE MOESSBAUER SPECTROSCOPY. Levinson, Lionel M.; Shtrikman, S. (Weizmann Inst. of Science, Rehovoth, Israel). Nucl. Instrum. Methods; 87: 205-10(1970).

The narrowing of Moessbauer absorption lines resulting from time filtering effects is analyzed with regard to the possible utility of this technique in improving experimental line resolution. We demonstrate that in the absence of statistical noise, and provided the line shape is Lorentzian of known width and experimentally undistorted, it is always possible to solve for a completely unknown energy level scheme of a thin absorber, independent of whether or not the individual lines comprising the Moessbauer spectrum can be resolved by eye. We solve analytically a simple model to test the utility of time filtering as an aid to the determination of the parameters of Moessbauer spectra, taking into account the effects of statistical noise. Our calculation indicates that only minor improvement in accuracy can be achieved when non-zero coincidence delay times are introduced, and in view of the experimental difficulties involved in coincidence Moessbauer spectroscopy, it appears to us that time filtering methods are unlikely to compete successfully with computer techniques as a useful experimental tool for spectrum analysis. Some comments as to the relevance of the Heisenberg uncertainty principle to line narrowing are appended. (auth)

High Energy Physics Instrumentation

Refer also to abstract 2841.

2484 (INS-TCA-26) DEVICE FOR OBSERVING THE ENTRY DIRECTION OF AIR SHOWERS. Akiyama, Hiromitsu (Tokyo Univ. (Japan). Inst. for Nuclear Study). Oct 1969. 22p. (In Japanese). Dep. NTIS (U. S. Sales Only).

In observation of extensive air showers, it is important to know the direction of their entry by stereo-arrangement of the counters. The conventional system of the chronotron type is laborious in the film development, reading, etc. Scintillation detector arrays, transistorization of an electronic system, and also transistorized automatic digital recorder were developed previously. Subsequently, the device (transistorized) for observing the entry direction of air showers was completed. The detectors are located at the five corner points of a regular pyramid. The measured values are punched in the same tapes for particles counters in digital quantities. The tapes are processed directly in a computer, and the entry direction of air showers is given for each individual shower. Compared to the chronotron-type system, the maintenance and the data analysis are both greatly simplified. (Japan)

2485 (JINR-P13-5277) ELECTRIC DISCHARGE OF GAS BUBBLES IN LIQUIDS. Pisarev, A. F.; Selivanov, G. I.; Balandin, M. P.; Lytkin, L. K. (Joint Inst. for Nuclear Research, Dubna (USSR). Lab. of Nuclear Problems). 1970. 14p. (In Russian). Dep. NTIS (U. S. Sales Only).

The values of the field intensities, capable of inducing the bubble discharge in liquids, are calculated using the criteria and experimental dependences of the electric gas discharge in small gaps. The bubble discharge in liquid bubble chambers filled with the monatomic liquids is found to appear at the constant field intensity of about 200 kV/cm, and for the case of molecular liquids at 500-600 kV/cm. In high frequency fields, the discharge takes place at 50 and 300 kV/cm, respectively. (auth)

2486 (RHEL/R-205) COMPUTER GRAPHICS PATCHING OF FAILED CYCLOPS EVENTS FOR A SPARK CHAMBER EXPERIMENT. Bell, S. B. M. (Rutherford High Energy Lab., Chilton (England)). Aug 1970. 38p. Dep. NTIS (U. S. Sales Only). UK 7s.

A system of programs is described for the rescue of spark chamber events in an experiment to test CP conservation. The events were measured on the CYCLOPS flying spot digitizer and subsequently fail in the automatic analysis system. Selected regions of the events are displayed on a computer-controlled CRT and faults in the pattern recognition processes of track-finding are repaired by an operator using a light pen. The results are subsequently replaced in the automatic system. (auth) (UK)

2487 DEVELOPMENT OF THE TECHNICAL MEANS FOR THE CORRESPONDENCE BETWEEN ECC γ-RAY AND SPARK CHAMBER SHOWER. Dake, Shyoji (Kobe Univ., Japan); Hazama, Michio; Jitsuno, Kunihisa; Nishikawa, Kiyoshi; Sakata, Michinori. Uchusen Kenkyu; 14: 227-38(Oct 1969). (In Japanese).

Test experiment was performed to establish the correspondence between AS events and ECC γ-ray. The simultaneity was confirmed, by the accurate measurement of the direction of incident AS, and by locating precisely the position of incident high-energy γ-ray. The AS event was detected with wire spark chambers placed both above and below ECC. The set-up of the apparatus is shown. γ-ray energy spectrum was obtained after two months exposure, and a γ-ray map was made. The incident direction can be determined with an accuracy within ±1°. The distribution of zenith angle was determined for ECC γ-ray and for spark chamber events. Each particle in the core of shower could not be resolved in the spark chamber, but the core was found as an illumination peak. An attempt was made to establish the correspondence between the ECC γ-ray and the electron shower in the spark chamber by measuring the direction and the position of AS events. Six examples for good conformity were found and their photos are shown. (Japan)

2488 CORRESPONDENCE BETWEEN ECC γ-RAY AND SPARK CHAMBER EVENTS. Jitsuno, Kunihisa (Konan Univ., Kobe, Japan). Uchusen Kenkyu; 14: 283-5(Oct 1969). (In Japanese).

In order to detect high energy γ-rays in the core of air showers, an attempt has been made to establish the correspondence between air shower events and ECC γ-ray. The result is briefly reported in this article. The spark chambers used in the experiment were

of wire-metal type, 50 × 50 × 2 cm in size. The arrangement of the spark chambers and an ECC is shown. The angular distribution of the incident particles of shower was measured with the photographs of the spark chambers within the error of ±0.5°. This was then compared with the corresponding ECC γ-ray records. The examples of the measured angular distribution are shown. Six spark chambers were used with an ECC. In some photographs of the chamber placed under the ECC, the core of shower was found and ascertained by the correspondence with the ECC γ-ray record. The structure of the core could not be resolved in the spark chambers. (Japan)

2489 LARGE APERTURE CHERENKOV COUNTER. Aubert, J. J. (CERN, Geneva); Niebergall, F.; Willitts, T. R.; (and others). Nucl. Instrum. Methods; 87: 79-85(1970).

The design and performance of a large, multi-cell threshold Cherenkov counter is described. Electrons from $K^0 \rightarrow e\pi\nu$ decays are detected with an efficiency of better than 0.99 over an angular range of ±50° in one plane and of ±15° in the other. (auth)

2490 SPACE–TIME DETECTOR FOR COSMIC RAY SHOWERS. Porter, L. G.; Earnshaw, J. C.; Tielsch-Cassel, E.; Ahlstrom, J. C.; Greisen, K. (Cornell Univ., Ithaca, N. Y.). Contract AT(30-1)-3038. Nucl. Instrum. Methods; 87: 87-92 (1970).

We describe a detector to observe cosmic ray showers by the fluorescent light they produce in the atmosphere. The night sky is surveyed stereoscopically by two stations, individually consisting of 212 photomultipliers each of which views a small section of the sky. Such a station will be able to resolve both the spatial coordinates and the temporal evolution of very large showers (>10^{18} eV). We have successfully tested the apparatus using light scattered out of a pulsed beam as a simulation of an inverse shower. (auth)

2491 WIRE-SPARK-CHAMBER SYSTEM WITH ON-LINE COMPUTERS. Ford, W. T.; Piroue, P. A.; Remmel, R. S.; Smith, A. J. S.; Souder, P. A. (Princeton Univ., N. J.). Nucl. Instrum. Methods; 87: 241-5(1970).

We describe the performance of a system of wire spark chambers and 2 on-line computers (one being time-shared) used in an experiment at the Brookhaven A.G.S. to study the decay of K± mesons via the τ mode ($K^{\pm} \rightarrow \pi^{\pm}\pi^{\pm}\pi^{\mp}$). (auth)

2492 DESIGN OF THE SUPERCONDUCTING MAGNET FOR THE OMEGA PROJECT. Morpurgo, M. (CERN, Geneva). Particle Accel.; 1: 255-63(Jul 1970).

The design of a large superconducting magnet for a large spark chamber (the "Omega" magnet) cooled by forced circulation of supercritical helium is discussed. Details are given on the coil construction, on the hollow conductor and on the helium flow diagram. Some design problems, typical of forced circulation cooling, are considered. (auth)

Radiation Dosimeters

Refer also to abstracts 2448 and 3476.

2493 DK-0.2 DOSIMETER FOR RECORDING FAST NEUTRONS. Piskunov, L. I.; Bezel, V. S.; Potashev, P. I. This paper was summarized in At. Energ. (USSR); 24: 258-9(Mar 1968) as paper No. 187. (In Russian).

DK-0.2 ionization chamber dosimeters are sometimes recommended for individual dosimetry of fast neutrons. It was found that the induced activity of the dosimeter body is the main cause of ionization in such cases. The ionization effect produced in the DK-0.2 and KID-1 dosimeters by mixed gamma and neutron radiation was studied experimentally in order to clarify the quantitative relations. The investigations were carried out in a neutron activator with a Po(α,n)Be source (maximum output $2.2 \cdot 10^7$ neutrons/sec). The DK-0.2 and KID-1 dosimeters were irradiated under completely identical conditions with lead, cadmium, and paraffin screens. The gamma spectra of the induced activity from the dosimeter bodies were analyzed with an Al-100-1 amplitude analyzer. This analysis of the gamma spectra and the decay of the induced gamma activity of the metal body and of the inner plastic material of the DK-0.2 dosimeter chamber showed that the activation is due mainly to the formation of the isotopes ^{28}Al (E_γ = 1.7 MeV) and ^{56}Mn(E_γ = 0.8 MeV). Similar but less intense gamma spectra were obtained with KID-1 dosimeters. This indicates that their body contains metal impurities. The ionization produced by external gamma radiation and recoil protons is in first approximation identical for both types of dosimeter, and the difference between the readings of the DK-0.2 and the KID-1 dosimeters may be attributed to the induced gamma activity. According to calculations and experimental data one may assume that the factor of proportionality between ionization in the chamber and real radiation dose of the KID-1 dosimeter is 1.5 times greater than that of the DK-0.2 dosimeter. The investigations show that it is possible to use a DK-0.2 dosimeter for individual neutron dosimetry when the flux is much greater than the permissible limit. However, the dosimeter readings cannot be taken for tissue equivalents. (auth)

2494 SPATIAL DISTRIBUTION OF ABSORBED NEUTRON DOSE IN POLYETHYLENE. Briskman, B. A.; Savina, V. P. This paper was summarized in At. Energ. (USSR); 24: 565-6 (Jun 1968) as paper No. 208. (In Russian).

The distribution of absorbed dose (DAD) of neutron radiation in polyethylene specimens placed in dry channels of a VVR-type reactor was investigated experimentally with cellulose diacetate films. It is known that the absorbed dose in polyethylene irradiated in a nuclear reactor is the sum of the γ-dose and the fast-neutron dose. Calculations for the corrections for the gamma contribution are described. Within the limits of experimental error no change in the DAD was observed with changes in height and width of the specimen. The distance between the vertical channel and the reactor core did not affect the form of the attenuation curve for neutron dose. The DAD in a polyethylene specimen (γ = 0.92 g/cm^3) was calculated also: (1) by using the transport equation in the P_2-approximation; and (2) by using the Monte Carlo method with a computer. The results of the calculations are shown and are in good agreement with the experimental data. Under the conditions described, the relaxation length for the absorbed dose in polyethylene is deduced to be approximately 5 cm. (W.H.K.)

2495 EXPERIMENTAL STUDY OF THE SPATIAL ABSORBED-DOSE FIELDS OF REACTOR γ-RADIATION IN A POLYETHYLENE SAMPLE. Briskman, B. A.; Savina, V. P. This paper was summarized in At. Energ. (USSR); 24: 566-7 (Jun 1968) as paper No. 209. (In Russian).

In this investigation we studied the spatial absorbed-dose fields a.d.f. in polyethylene samples (high-pressure polyethylene, γ = 0.92 g/cm^3) situated in the dry vertical channels (diameter 7 to 20 cm) of a water-moderated water-cooled reactor at distances of 14 to 62 cm from the edge of the active zone. The samples had the form of parallelepipeds of rectangular cross section 5 by 6 and 3.5 by 3.5 cm, 6 cm in height, made from plates of various thicknesses, and a cylinder 5 cm in diameter and 6 cm long. As radiation detector we used cellulose diacetate film of mean thickness 130 μ. It is clear that in order to measure the a.d.f. of the γ-radiation of the reactor spectrum in mixed n- and γ-radiation it is essential either to filter the neutrons or to know the a.d.f. for the neutron radiation and the ratio of the radiochemical yields of the dosimetric system employed for neutron and γ-radiation respectively. Since either possibility arose, the measurements were made with the reactor switched off, using the background radiation of fission fragments. Extrapolation of the resultant data to the γ-radiation spectrum of a working water-moderated water-cooled reactor for polyethylene is valid because of the fact that the spectrum of the working reactor differs from that of the ^{235}U fission mainly for γ-quanta with energies greater than 2 MeV; the contribution of these to the absorbed dose in polyethylene is extremely small. In the case in question Compton scattering predominates. The spectrum of background γ-radiation during the first hour after stopping the reactor is determined by short-lived fission products and is thus practically identical with the ^{235}U-fission spectrum. The results of measurements made for one of the channels are presented in the form of a plane dose field. The weakening of the dose of γ-radiation over the depth of the sample is approximately 30%. Over the height and width of the sample the nonuniformity in the a.d.f. is never greater than 4%. Preliminary experiments carried out with ^{60}Co revealed the existence of a maximum on the first part of the attenuation curve and a relatively sharp fall at the end of the latter. In the reactor channels these end effects tend to merge, their behavior depending on the channel diameter. Within the limits of experimental error the attenuation does not appear to be dependent on the distance of the sample from the active zone of the reactor. (auth)

2496 DOSIMETRY COMPOSITION FOR MEASURING IONIZING RADIATION. Boehm, George Gustave Anton (to Radiation Processing Inc.). British Patent 1,206,385. 23 Sep 1970. Priority date 2 Apr 1968, United States.

A vinyl film dosimeter is described. An organic compound containing a terminal vinyl group is dispersed in a thin inert carrier. Intensity measurements of the vinyl peak at 11 microns is suggested for readout. (W.H.K.)

XUM

Radiometric Instruments

2497 (INR–1180) ANNUAL REPORT, 1969. (Institute of Nuclear Research, Warsaw (Poland)). 204p. (In Polish). Dep. CFSTI (U. S. Sales Only).

Research in the areas of nuclear physics, nuclear chemistry, reactor technology, isotope technology and radiometric instruments, and plasma physics is briefly summarized. Publications issued during this period are listed. (C.E.S.)

2498 FURTHER NOTE ON MOVING-SOURCE SOIL DENSITY GAUGE. Giftcioglu, O.; Taylor, D. (Univ. of Strathclyde, Scotland). Nucl. Instrum. Methods; 87: 329–31(1970).

This letter discusses a number of matters which arise when using a moving-source soil density gauge. All concern the choice of the index n in the (Id^n vs d) characteristic to obtain a (Id^n) maximum, which occurs within the range of d-values possible with a specific design of the instrument. Also considered is the choice of n when two or more values are possible. (auth)

2499 ABSORPTION CURVE MATCHING CIRCUIT IN NUCLEONIC MEASURING SYSTEM. Troutman, Paul H. (to Industrial Nucleonics Corp.). U. S. Patent 3,529,162. 15 Sep 1970. Filed 2 May 1967.

A nucleonic measuring system, which normally operates over a limited portion of a non-linear absorption curve, is extended in this case in its operation along that curve with substantially uniform sensitivity to weight-per-unit area changes, by automatically adjusting the sensitivity as a function of amplifier output voltage. (auth)

Miscellaneous Instruments and Components

Refer also to abstracts 2069, 2094, 2394, 2967, 2968, 3018, 3882, and 3905.

2500 (AI-AEC–12981) LMFBR TASK 25, TRANSIT TIME FLOWMETER. Quarterly Technical Progress Report, July–September 1970. Pekrul, P. J. (Atomics International, Canoga Park, Calif.). 12 Nov 1970. Contract AT(04-3)-701. 11p. Dep. NTIS.

The development of a flowmeter using noise-analysis techniques which will be suitable for use as a flow-measurement standard in large liquid-metal systems at temperatures to 1200°F or higher is described. Operation of the Transit Time Flowmeter depends upon the detection of small temperature variations (thermal eddies) at two points a known distance apart in a flowstream. The two signals are cross-correlated with a variable delay time. The delay time which gives maximum correlation is the transit time of the fluid between the sensors, which time is inversely proportional to the fluid velocity. (W.H.K.)

2501 (CONF-700322–, pp 105-11) PROGRAMMING TECHNIQUES FOR THE PDP-8/I COMPUTER. McDowell, J. D. (Tennessee Univ., Oak Ridge. Resident Graduate Program).

From Proceedings of the second Oak Ridge conference on the use of small accelerators for teaching and research, March 23–25, 1970.

Suggestions for conserving memory and for creating more elegant program structures using the PDP-8 language FOCAL are discussed. A compact kinematics program and several brief numerical function subprograms are presented as examples. (auth)

2502 (GEAP–11094) 10-DECADE WIDE RANGE NEUTRON MONITORING SYSTEM. Final Test Report. Green, W. K. ([General Electric Co., San Jose, Calif. Atomic Power Equipment Dept.]). Oct 1970. 272p. Dep. NTIS.

The design, testing, and evaluation (under actual reactor operating conditions) of a prototype counting–Campbelling wide-range thermal neutron flux measurement channel are described. The wide range neutron monitoring system was designed to monitor 10 decades of neutron flux when used with a General Electric Type NA04 fission chamber. To obtain this wide range capability, counting techniques are used for the low range (10^{-8} to 10^{-3}% power), and Campbelling techniques are used for the intermediate (10^{-3} to 3×10^{-1}% power) and high ranges (3×10^{-1} to 100% power). A failure mode analysis and instruction manual are included as appendices. (W.H.K.)

2503 (NYO–3906-4) ULTRASONIC THERMOMETRY FOR LMFBR SYSTEMS. Phase I Report. Fam, S. S.; Lynnworth, L. C.; Carnevale, E. H. (Panametrics, Inc., Waltham, Mass.). Sep 1968. Contract AT(30-1)-3906. 73p. Dep. NTIS.

A pulse-echo ultrasonic thermometer system for the development and operation of advanced liquid metal fast breeder reactors (LMFBR) was designed, constructed and tested. The thermometer was designed to determine fuel temperature up to 5000°F and the coolant ard cladding temperatures up to ~1200°F by measuring the round trip transit time in wire or tubular sensors. A new instrument was used to measure transit time automatically. Compatibility of the ultrasonic transmission line portion of the system with liquid sodium was demonstrated by immersing bare and sheathed wires up to 20 ft long in sodium up to 700°F, the maximum temperature attainable in the facility available for this test. The feasibilities of using the spacer wire to measure coolant temperature, and the cladding to measure its own temperature, were also demonstrated. Low frequency mechanical vibrations were shown not to noticeably affect the transit time measurements. Finally, a complete system was simulated in parts, demonstrating that pulses generated in a 100 psi pressure tight magnetostrictive transducer housing could be transmitted down a 50 ft SS 304 lead-in, a 20 ft portion of which was sheathed and heated to 1200°F, with another portion curved into a 2″ radius S-shape simulating access restrictions expected in LMFBR's. With this simulation system echoes were obtained from a 2″ Re sensor at 5000°F. The ultrasonic instrument automatically measured the time between these echoes to 0.1 μsec, corresponding to temperature resolution better than 1% at 5000°F. (auth)

2504 (UCRL–50892(Vol.2)) WEAPONS EFFECTS DISPLAY SYSTEM (WEDS MOD II): OPERATOR'S MANUAL. Peschel, D. J. (California Univ., Livermore. Lawrence Radiation Lab.). Aug 1970. 53p. Dep. NTIS.

The Weapons Effects Display System (WEDS MOD II) is a digital computer-driven device that generates and displays both prompt effects and radioactive fallout patterns predicted for nuclear detonations. Both types of patterns are projected as overlays on selectable maps that are themselves projected onto a CRT display screen. Numerical data are digitally displayed off screen. The system is contained within a console on which are the 29-in.-square display screen, a data readout panel, and operator control panels. An operator at the console inputs data for the detonation and controls the type and development of the display pattern. Each input parameter and display control is described along with the operating sequence to run either a prompt effects or fallout pattern problem. Error conditions sensed and displayed on the console for the operator are explained. Sample problems with photographs of the patterns are presented. An appendix describes how to initially load the computer programs and prepare the system for operation. (auth)

2505 (UCRL–50892(Vol.4)(Pt.5)) WEAPONS EFFECTS DISPLAY SYSTEM (WEDS MOD II): MAINTENANCE MANUAL. PART 5. SYSTEM WIRING TABLES. Peschel, D. J.; Hollis, J. C. (California Univ., Livermore. Lawrence Radiation Lab.). Aug 1970. 196p. Dep. NTIS.

Wiring tables are presented for the fallout and prompt effects logic interfaces. These interfaces are located in the right- and left-hand cabinets of the WEDS MOD II console. (auth)

2506 (UCRL–50922) GENERAL DESCRIPTION OF THE WEAPONS EFFECTS DISPLAY SYSTEM (WEDS MOD II). Berndt, C. W. (California Univ., Livermore. Lawrence Radiation Lab.). Sep 1970. 28p. Dep. NTIS.

An apparatus has been developed that calculates and displays weapons effects patterns superimposed on chart or map backgrounds. Fallout and prompt effects patterns are calculated and generated by a small digital computer and memory disc that are incorporated in the machine. Variables to the computer program are readily entered by means of switches and thumbwheels. Fallout patterns can be observed at half-hour increments from detonation through 48 hr, or the pattern may be called up directly for anytime during the first 48 hr. Radiation dose rate and total integrated dose may be read for specific points in any pattern. Prompt effects patterns show the range extent from ground zero for values of interest of blast, thermal, or nuclear radiation. Weapon yield, height of burst, and range of interest may be varied over a large scale with correlated immediate change in all related parameters. The machine and its support equipment are housed in a self-supporting semitrailer and a separate utility van that contains an air-conditioning plant and a power generator. (auth)

2507 COMBINATION OF AN ELECTRON MICROSCOPE AND A HEAVY-ION ACCELERATOR. Wohlenberg, T.; Carlsen, F.; Henriksen, L.; (and others) (Univ. of Copenhagen). Radiat. Eff.; 5: 279–80(Oct 1970).

XUM

In order to study heavy-ion damage in known crystallographic directions, a simple ion accelerator was attached under an electron microscope so that the ion beam enters at the bottom of the microscope on the optical axis. A test run on Al single crystals with 12-keV Cs^+ ions showed that this idea is workable. (D.L.C.)

2508 DEBYE–SCHERRER CAMERA FILTER ATTACHMENT FOR USE WITH RADIOACTIVE SPECIMENS. Runyan, J. E.; Olsen, C. E.; Kempter, C. P. (Los Alamos Scientific Lab., N. Mex.). Norelco Rep.; 17: No. 1, 16-17(Apr 1970).

The use of a thin filter to eliminate alpha and beta background with only a small attenuation of the x radiation for Debye–Scherrer powder patterns of radioactive samples is discussed. A beryllium filter is described. (W.H.K.)

2509 NUMERICAL CORRECTION OF MULTICHANNEL ANALYZER DATA FOR SYSTEM NONLINEARITY. Turner, C. E. Jr. (Ames Lab., Iowa). Nucl. Instrum. Methods; 87: 45-57(1970).

A correction technique using a computer for elimination of differential and integral nonlinearity in a multichannel pulse-height-analyzer (MCPHA) system is presented. Nonlinear histogram data are redistributed into a new set of channels having equal width by use of an accurate differential nonlinearity measurement and a suitable approximation. Experimental considerations of importance for achieving a rapid, accurate differential nonlinearity measurement are treated carefully for a time-to-amplitude converter (TAC) system. Tests of the procedure with a system comprised of a TAC, biased amplifier, and MCPHA are described. (auth)

2510 SIMPLE BINARY-TO-DECIMAL OR DECIMAL-TO-BINARY CONVERTER AND ADDING DEVICE. Biancastelli, R.; Bosio, C. (Istituto Superiore di Sanita, Rome). Nucl. Instrum. Methods; 87: 101-3(1970).

A simple binary-to-decimal or decimal-to-binary converter is described. The speed of this converter is proportional to the number to be converted; the time of conversion of a number of 8 bits can be less than 250 μs. From this converter one can easily obtain the add or subtract function too. (auth)

2511 PRINTOUT SYSTEM FOR ANALOG-TO-DIGITAL CONVERTERS. Biancastelli, R.; Bosio, C. (Istituto Superiore di Sanita, Rome). Nucl. Instrum. Methods; 87: 105-8(1970).

A readout system is described which can record from an arbitrary number of 256-channel analog-to-digital converters or other digital equipment connected in the "slave read mode." This readout system normally controls a typewriter at 6 characters per second, but the output pulse train may be easily modified to driving other output units. (auth)

2512 MAGNETIC FIELD PROBE FOR PRECISE MAGNETIC FIELD MEASUREMENTS. Kaltenbach, V.; Kuhlmann, W. R. (Kernforschungsanlage, Juelich, Ger.). Nucl. Instrum. Methods; 87: 131(1970). (In German).

The basic relations of Ref. 1 (Nucl. Instr. and Meth., Vol. 82 (1970) p. 245) are extended for applications with higher frequencies, so that the inductive components of the current induced in the rotating probe must be taken into account. (auth)

2513 VERSATILE MERCURY FILM PULSER. Fullwood, R. R. (Los Alamos Scientific Lab., N. Mex.). Nucl. Instrum. Methods; 87: 149-50(1970).

A convenient pulser is described having a rise time of less than 1 ns and capable of single shot and variable operation up to 60 Hz. The switch element is a mercury film magnetic latching relay capable of operation in any position. (auth)

Radiation Effects on Instruments and Instrument Components

2514 (SC-R-70-4351) APPLICATION OF NEUTRON DAMAGE MODELS TO SEMICONDUCTOR DEVICE STUDIES. Gregory, B. L.; Gwyn, C. W. (Sandia Labs., Albuquerque, N. Mex.). Dec 1970. 10p. Dep. NTIS.

A hybrid recombination model has been formulated for neutron irradiated silicon which correctly predicts the minority carrier recombination in both the neutral and space charge regions of a device. Exact, one-dimensional, numerical calculations have been performed using this model and compared to reported V–I characteristics of irradiated p^+n diodes. The calculated curves agree with the reported data within 20% over the seven decade span of currents in the investigations, for diode base resistivities from 0.25 Ω-cm to 17 Ω-cm. At low injection levels the calculated recombination occurs predominantly in the junction space charge region, whereas at high injection both the space charge region and neutral region can be important. Calculations have also been performed for the recombination occurring throughout a typical NPN silicon transistor. The results indicate that space charge region recombination is probably dominant in modern, narrow base transistors even at high injection levels. (auth)

XUM

LIFE SCIENCES

Biochemistry, Physiology, and Molecular Biology

Refer also to abstract 2134.

Basic Processes

Refer also to abstracts 2109 and 3907.

2515 UPTAKE OF ISOLATED METAPHASE CHROMOSOMES BY MAMMALIAN CELLS IN VITRO. Burkholder, G. D.; Mukherjee, B. B. (City of Hope Medical Center, Duarte, Calif. McGill Univ., Montreal). Exp. Cell Res.; 61: 413-22(Aug 1970).

In an autoradiographic investigation, it was found that isolated ^{3}H-thymidine-labeled metaphase chromosomes can penetrate into mammalian cells in vitro. The progressive changes in the cellular labeling patterns with time indicate that, in most cases, the ingested chromosome is degraded in the cytoplasm of the recipient cell and the chromosomal DNA is integrated into the host nuclear DNA. This integration of extracellular chromosomal DNA into the recipient cell DNA may involve DNA macromolecules rather than free nucleotides, and in most cases, the chromosomal DNA becomes randomly integrated among the chromosomes of the recipient cell. Rarely, whole extracellular chromosomes may become incorporated into a cell without being degraded, although this has not been established with certainty. (auth)

2516 NATURAL CESIUM AND TRANSPORT OF STABLE CESIUM IN A FISH-BREEDING POND. Wlodek, S.; Bysiek, M.; Grzybowska, D. (Centralne Laboratorium Ochrony Radiologiezne], Warsaw). pp 319-33 of Symposium International de Radioecologie. Vol. I. Fontenay-aux-Roses, France; Commissariat a l'Energie Atomique (1970). (In French).

From Conference on Radioecology, Cadarache, France. See CONF-690918-(Vol.1).

Neutron activation analysis was used to determine the natural cesium (autochtonic cesium) content in eight elements of an ecosystem: water, sediments, and six groups of aquatic organisms in a fish-breeding pond near Warsaw. The ecosystem was then enriched by the addition of stable cesium (allochtonic cesium) used as inactive tracer. The results of this research showed that: (1) The distribution of allochtonic cesium amongst the elements of the ecosystem is similar to that of the natural autochtonic cesium, except for groups in which the organisms living at the time of contamination were not replaced by new generations during the period of research; (2) The way in which cesium is accumulated by Phragmites communis and Cyprinus carpio indicates that absorption of this nuclide plays a much more important part than adsorption; (3) Cesium elimination in Cyprinus carpio during the first 50 days following contamination is vigorous. After this period the process is very slow. (auth) (France)

2517 NATURAL CESIUM IN FRESHWATER AND FISHES. Bigliocca, C. (EURATOM, Ispra, Italy); De Bortoli, M.; Polvani, C. pp 335-60 of Symposium International de Radioecologie. Vol. I. Fontenay-aux-Roses, France; Commissariat a l'Energie Atomique (1970).

From Conference on Radioecology, Cadarache, France. See CONF-690918-(Vol.1).

Data obtained in four lakes (Maggiore, Varese, Comabbio, and Monate) and in three fish species (Perca fluviatilis L., Scardinius erythrophtalmus L., and Lepomis gibbosus L.) living therein are reported. The neutron activation method for the study of natural cesium in the environment is briefly discussed. Among the fish species considered, P. fluviatilis showed a higher cesium concentration than S. erythrophtalmus and L. gibbosus. The cesium concentration in fishes did not appear to be a conservative property. In fact cesium concentration in the fishes of one lake (Varese) is lower than that of the fishes of the other lakes studied. In three lakes (not in Lake Varese) there is a certain positive correlation between cesium and potassium concentration in fishes. A discrepancy between the apparent concentration factors for fallout ^{137}Cs and natural Cs is confirmed. The ratio between the concentration factors is higher in Lake Varese and in P. fluviatilis. (auth) (France)

2518 SIMULTANEOUS DETERMINATION OF THE APPARENT ^{3}HOH, ^{82}Br, ^{125}I-HUMAN ALBUMIN AND ^{51}Cr RED CELL VOLUMES IN HUMAN SUBJECTS. Dyrbye, M. O.; Kragelund, E. (Gentofte Hospital, Copenhagen. Kommunehospitalet, Copenhagen). Scand. J. Clin. Lab. Invest.; 26: No. 1, 61-6(Aug 1970).

A technique for performing true simultaneous determinations of body fluid compartments by means of four radioisotopes is described. The accuracy of the method based upon in vitro experiments showed a 2 s.d. from 4.0 to 7.2%. The daily biological variations were from 0 to 2.8% (2 s.d.). A so-called steady state was approximately obtained by ^{3}HOH, ^{82}Br, and ^{51}Cr. Daily variations of ^{125}I-albumin volume could only be determined by injections twice or three times daily. As this was not done in these experiments, the daily variations of ^{125}I-albumin volume could not be calculated. 27 patients without fluid disturbances were examined and the results are given in tabular form. (auth) (Norway)

2519 OXIDATIVE AND GLYCOLYTIC ACTIVITY OF EJACULATED RAM SPERMATOZOA IN THE PRESENCE OF STEROID HORMONES. Murdoch, R. N.; White, I. G.; Seamark, R. F. (Univ. of Sydney. Waite Agricultural Research Inst., Glen Osmond, Australia). Acta Endocrinol.; 64: 557-88(1970).

Progesterone, 20α-OHP, 20β-OHP, androstanedione and testosterone depressed the respiration of washed ram spermatozoa and enhanced aerobic glycolysis. 17β-oestradiol, oestriol, androstenedione, 5β-androstanedione, pregnanedione and pregnanolone reduced respiration without stimulating aerobic glycolysis. Of the steroids tried, none stimulated anaerobic glycolysis. The steroids appeared to act principally on the oxidative phase of spermatozoal metabolism since the oxidation of isotopically labeled glucose, acetate and citric acid cycle intermediates were all depressed when spermatozoa were incubated in the presence of these steroids. (auth) (Denmark)

2520 NEW METHODS OF ENZYMIC SYNTHESIS OF RADIOACTIVE NUCLEOSIDES. Nejedly, Z. (Inst. of Research, Production, and Uses of Radioisotopes, Prague). Jad. Energ.; 16: 233-8(1970). (In Czech).

The catalytic properties of an unpurified enzyme preparation from cells of Brevibacterium ammoniagenes toward phosphoribosylation of the nucleic acid bases are pronouncedly specific and display a high efficiency toward phosphoribosylation of uracil where the conversion to uridine-5-'phosphate is quantitative, phosphoribosylation of adenine takes place with lower efficiency and guanine and cytosine are not practically phosphoribosylated at all. Using orotic acid-^{14}C and a complete inhibition of orotidine-5'-phosphate decarboxylase by means of 6-azauridine-5'-phosphate a 60% production of orotidine-5'-phosphate-^{14}C was achieved. The catalytic efficiency of the enzyme preparation remains preserved even upon substitution of 5-phosphoribosyl-1-pyrophosphate by its direct metabolic precursors. The catalytic effect of an unpurified cell-free extract from mice leukemic cells is characterized by extremely low substrate specificity. This enables the enzyme phosphorylation of both purine and pyrimidine nucleosides. Nucleotides of different stage of phosphorylation according to reaction conditions are thus obtained. (auth)

2521 HIGH-RESOLUTION AUTORADIOGRAPHY WITH ^{33}P. Holmgren, Paul Robert. Denton, Tex.; North Texas State Univ. (1969). 54p. University Microfilms Order No. 70-9135.

Thesis.

The use of ^{33}P in high resolution autoradiographic experiments was investigated. Phosphorus-33 emits β particles that have a much lower energy level and a longer half-life than ^{32}P. These characteristics make ^{33}P a more suitable radioisotope for radiographic experiments. The experiments showed that a large amount of radiophosphorus is lost to the preparatory solutions and a large amount is moved by diffusion within excised tissue during normal electron microscope preparation. Using liquid scintillation count methods to determine the relative uptake of radiophosphorus by the skin, liver, muscle, and kidney at 2, 4, and 12 hr after ^{33}P injection, it was concluded that the largest uptake at 2 hr was in the liver. Then, in descending order, the next largest was in the kidney, muscle, and skin tissues. At 4 and 12 hr after injection, the level of radiophosphorus in the liver and kidney reduced considerably, while only slight reductions were observed in the muscle and skin. Finally, it was concluded that radiophosphorus is first incorporated into the aqueous fraction of the four tissues studied and from there, incorporated into the other subcellular fractions of the cell such as the mitochondria. (Diss. Abstr.) (TSS)

2522 MEASUREMENT OF PLASMA DIGOXIN CONCENTRATION BY RADIOIMMUNOASSAY. Evered, D. C.; Chapman, C.; Hayter, C. J. (General Infirmary, Leeds, Eng.). Brit. Med. J.; 3: 427-8(22 Aug 1970).

A rapid, sensitive, and precise method for measuring the plasma digoxin concentration has been developed with the radioimmunoassay technique. Seventy patients receiving digoxin were shown to

have plasma digoxin concentrations between 0.4 and 5 ng./ml. Preliminary studies show that though there is a positive correlation between total daily dose and the plasma digoxin concentration, the relationship is not close, and a relatively wide range of plasma digoxin concentrations appear to be consistent with effective digitalization. (auth) (UK)

2523 TRACER TECHNIQUE FOR THE BEHAVIOUR OF DUSTS IN EXPERIMENTAL ANIMAL LUNGS USING AN AUTOMATIC AIR POLLUTION REPRODUCER AND A FILM SCINTILLATION COUNTER. Shigematsu, A.; Toyohara, M.; Iwasaki, T. (Research Inst. of Tuberculosis, Tokyo). Nucl. Instrum. Methods; 86: 279-84(1970).

A tracer technique using an air pollution reproducer and a film scintillation counter is described for measuring radioactivities of homogeneous dusts (^{14}C-charcoal, ^{14}C-methylcholanthrene and ^{35}S-sulfur dioxide) and heterogeneous dusts (^{14}C-methylcholanthrenesilica and ^{35}S-sulfur dioxide alumina) in mice lungs. (auth)

2524 MORPHOLOGICAL AND CLINICO-CHEMICAL STUDIES OF THYROID FUNCTION IN LACTATING CATTLE. Nyberg, Jan Anders. Acta Vet. Scand., Suppl.: No. 31, 1-124(1970).

The radioiodine uptake in the thyroid and the thyroxine secretion rate were measured in SRB cows from two Swedish areas. From 180 of these animals milk samples were collected for determination of the total iodine concentration. The following blood chemistry tests of thyroid function were used; determination of the resin or the erythrocyte uptake in vitro of ^{131}I-labeled L-triiodothyronine (T_3-resin uptake index and EU) and the concentration of protein-bound iodine (PBI) in serum, as well as calculation of the free thyroxine index (FTI). A description of the methods is presented. (Sweden)

Metabolism, Physiology, and Toxicology

Refer also to abstracts 2122–2126, 2544, 2546, 2548, and 2563.

2525 INFLUENCE OF AGE, TEMPERATURE, AND LIGHT ON THE EXPERIMENTAL CONTAMINATION OF ANODONTA CYGNEA (L) BY ^{137}Cs. Foulquier, L.; Grauby, A. (CEA, Cadarache, France). pp 269-318 of Symposium International de Radioecologie. Vol. I. Fontenay-aux-Roses, France; Commissariat a l'Energie Atomique (1970). (In French).

From Conference on Radioecology, Cadarache, France. See CONF-690918-(Vol.1).

Anodonta cygnea (L) is a fresh water bivalve very common in the Rhone basin. The influence of age, light, and temperature on the extent of cesium-137 contamination was studied in 7 experimental tanks in which only one factor changes, all other conditions remaining identical. The aim of the experiment is to compare total contamination values obtained under known conditions when three factors are varied. The results are perforated on cards and used to make a series of computerized statistical treatments (histograms, averages and standard deviations, factorial matrix analysis of covariance or correlation). (auth) (France)

2526 UPTAKE, LOSS, AND DISTRIBUTION OF RADIOCOBALT IN A FRESHWATER FISH. LEPOMIS, GIBBOSUS, L. Merlini, Margaret; Bittel, R. (EURATOM, Ispra, Italy). pp 399-412 of Symposium International de Radioecologie. Vol. I. Fontenay-aux-Roses, France; Commissariat a l'Energie Atomique (1970).

From Conference on Radioecology, Cadarache, France. See CONF-690918-(Vol.1).

The uptake of radiocobalt from water, the loss in non-active water, and the distribution of the radionuclide in various tissues and organs of a freshwater fish, Lepomis gibbosus, common to many lakes are presented. The internal organs are by far the richest in radiocobalt and the muscle tissue is the least active on a unit weight basis. The muscle tissue has a relatively slow rate of uptake. Eventual hazards to man, the ultimate consumer of freshwater fish, are discussed. (auth) (France)

2527 SOURCES OF VARIABILITY IN THE OBSERVED CONCENTRATION FACTORS FOR FALLOUT ^{90}Sr AND ^{137}Cs IN FRESHWATER FISHES. Gaglione, P. (EURATOM, Ispra, Italy); Moeller, F.; Polvani, C. pp 439-66 of Symposium International de Radioecologie. Vol. I. Fontenay-aux-Roses, France; Commissariat a l'Energie Atomique (1970).

From Conference on Radioecology, Cadarache, France. See CONF-690918-(Vol.1).

The concentration factors for ^{90}Sr and ^{137}Cs in three fish species (Perca fluviatilis, Scardinius erythrophtalmus, and Lepomis gibbosus) of four lakes near Varese (Northern Italy) have already been reported. In the present paper an analysis of variance on the observed concentration factors is described: it shows highly significant differences between lakes, between species, between years, and also between the different seasons in the year. The interactions between the four variables are significant, too, but not as much as the variables themselves; the main sources of variability are therefore not influenced. As a consequence of the interactions, a certain degree of correlation must be expected; it is shown to be of exponential form. (auth) (France)

2528 EXPERIMENTAL STUDY OF THE LIBERATION OF RADIONUCLIDES AND INORGANIC ELEMENTS FROM TWO TYPES OF FOREST BED. Saas, A.; Grauby, A. (CEA, Cadarache, France). pp 509-70 of Symposium International de Radioecologie. Vol. I. Fontenay-aux-Roses, France; Commissariat a l'Energie Atomique (1970). (In French).

From Conference on Radioecology, Cadarache, France. See CONF-690918-(Vol.1).

The liberation of radionuclides (^{141}Ce, ^{103}Ru, ^{106}Ru, ^{65}Zn, and ^{54}Mn) as a function of time and manner of decomposition was studied in order to establish the relative lixiviation rate and the form in which these elements are liberated. The same parameters were also studied for certain inorganic elements (Na, K, Ca, Mg, Mn, Zr, and Al). This gives an idea of the supply of inorganic elements and radionuclides to the soil and their availability, as the case may be, for a rapid return to plants (assimilable forms), for biological or biochemical reconstruction (organic-inorganic complexes), or for migration in the soil layers (soluble and pseudosoluble compounds). (auth) (France)

2529 AVAILABILITY OF RADIOCESIUM IN RELATION TO AMMONIUM FERTILIZATION AND POTASSIUM STATUS OF TWO SOILS FROM ALLONVILLE. Marckwordt, U.; Mousny, J. M. (EURATOM, Ispra, Italy). pp 571-87 of Symposium International de Radioecologie. Vol. I. Fontenay-aux-Roses, France; Commissariat a l'Energie Atomique (1970).

From Conference on Radioecology, Cadarache, France. See CONF-690918-(Vol.1).

A comparative study was carried out on the availability of ^{137}Cs in mineral soils, as influenced by varied concentrations of K or NH_4 ions in equilibrium soil solutions. A loess derived parabrownearth and a rendsina both located in Allonville near Amiens were used in this study. The results show that NH_4 ions greatly increase the water solubility of Cs and reduce its fixation by the clay fraction of soil, thus increasing the availability of Cs. The Cs fraction in the soil solution is considerably higher and the fixed Cs lower when the radionuclide is added to soils well supplied with available K. Cs availability decreases with deteriorating K status. By addition of K to the Cs contaminated rendsina, the Cs availability increases only slightly. A K fertilization of the contaminated loess leads to a small increase of Cs in soil solution. The Cs fixation, however, is also higher. As a result, NH_4 and K fertilization both have practical significance as a means to influence indirect Cs contamination of plants on mineral soils. (auth) (France)

2530 ACCUMULATION OF RADIONUCLIDES BY BACTERIA AND YEASTS. Kokke, R.; Van Kleeff, B. H. A.; Nieuwdorp, P. J.; Van Zuilekom, Jeannine T. (Technische Hochschule, Delft, Netherlands). pp 637-53 of Symposium International de Radioecologie. Vol. I. Fontenay-aux-Roses, France; Commissariat a l'Energie Atomique (1970).

From Conference on Radioecology, Cadarache, France. See CONF-690918-(Vol.1).

Microorganisms were grown in Petri-dishes on nutrient agar and a radionuclide was added. An X-ray film was placed on the top of the agar. Colonies of radionuclide-accumulating strains were revealed by autoradiography. The amount of blackening produced within a given period by the radionuclide added in a known concentration, was used as a semiquantitative parameter for the uptake by the organisms. This technique was used for the detection of fresh water organisms accumulating radionuclides. (auth) (France)

2531 RETENTION OF ORAL ^{47}Ca IN PATIENTS WITH INTESTINAL MALABSORPTION: REGIONAL ENTERITIS AND PANCREATIC INSUFFICIENCY. Sjoeberg, H. E.; Nilsson, L. H. (Karolinska Hospital, Stockholm. St. Eriks Hospital, Stockholm). Scand. J. Gastroenterol.; 5: 265-72(1970).

The retention of a single oral dose of ^{47}Ca was measured in a whole body counter 2 weeks after being adminstered to 11 patients with regional enteritis and 12 with pancreatic insufficiency. Two μCi of ^{47}Ca were given to the fasting patients together with 135 mg of calcium as $CaCl_2$ in water. In all but one of the regional enteritis patients resections of parts of the small intestine had been

XUM

performed. Three patients with pancreatic insufficiency had undergone operation with exclusion or resection of the upper small intestine. The mean retention of ^{47}Ca was significantly lowered in the group of patients with regional enteritis; eight retained less than the $-2\ \sigma$ limit for the control group. No significant decrease was found of the retention of an oral dose of ^{47}Ca given fasting patients with severely impaired pancreatic function. (auth) (Norway)

2532 PENETRATION OF RADIOACTIVE ISOTOPES THROUGH ENAMEL AND DENTINE. II. TRANSFER OF ^{22}Na IN FRESH AND CHEMICALLY TREATED DENTAL TISSUES. Arwill, T.; Myrberg, N.; Soremark, R. (Univ. of Umea, Sweden). Odontol. Revy; 20: No. 1, 47-54(1969).

The effect of various chemicals on the rate of penetration of ^{22}Na through the enamel and dentine of intact, homologous premolars was studied. Compounds with a low molecular weight that affect organic material caused an increased penetration, while high molecular weight compounds of similar chemical action and the lipid solvent compound chloroform had no effect. The enamel interprismatic spaces are small enough to restrict penetration of high molecular weight compounds and these spaces may be filled with an organic material that is low in lipid and can to some degree control the passage of ions. (Excerpta Med.)

2533 WHOLE-BODY MEASUREMENTS ON THE DISTRIBUTION OF ^{203}Hg IN HUMANS AFTER ORAL INTAKE OF METHYLRADIOMERCURY NITRATE. Falk, R.; Snihs, J. O.; Ekman, L.; Greitz, U.; Aaberg, B. (Statens Stralskyddsinstitut, Stockholm. Kungliga Veterinarhogskolan, Stokholm. Forsvarets Forskningsanstalt, Stockholm). Acta Radiol., Ther., Phys., Biol.; 9: No. 1, 55-72(Feb 1970).

Distribution measurements were made using a whole body counter on three subjects who had taken 2.6 μCi CH_3-^{203}Hg NO_3 orally. Profile curves showed that the uptake was specifically concentrated in two regions in the body, that correspond to the brain and the liver. The biologic half-life was calculated. The various sources of error are discussed and conclusions drawn concerning their effect on the final results. The radiation doses were estimated and were found to be acceptable. The results reported concern specifically the three subjects involved in the present series of measurements, but it may be assumed that these results are also applicable to other clinically healthy men, 35 to 45 years of age. (auth) (Sweden)

2534 ABSORPTION OF ^{51}Cr-EDTA IN ULCERATIVE COLITIS FOLLOWING RECTAL INSTILLATION. Rask-Madsen, J.; Schwartz, M. (Glostrup Hospital, Copenhagen). Scand. J. Gastroenterol.; 5: 361-8(1970).

Ethylene-diamine-tetra-acetic acid labeled with ^{51}Cr (^{51}Cr-EDTA) is practically nonabsorbable from the colonic mucosa of normal individuals following rectal instillation. In ulcerative colitis, however, its net absorption is considerable. Its magnitude may be determined by measuring the urinary radioactivity through a 48-hour period after rectal instillation of ^{51}Cr-EDTA, since the substance is eliminated by the kidneys at the same rate as inulin. Determination of the absorption of ^{51}Cr-EDTA seems to be a suitable clinical-physiological method for investigating the permeability of the colonic mucosa. (auth)

Radiation Effects

Refer also to abstracts 2285, 2289, and 2596.

2535 REPAIR OF X-RAY DAMAGE IN DNA OF CULTIVATED CELLS FROM PATIENTS HAVING XERODERMA PIGMENTOSUM. Kleijer, W. J.; Lohman, P. H. M.; Mulder, M. P.; Bootsma, D. (National Defense Research Organization TNO, Rijswijk, Netherlands. Medical Faculty, Rotterdam). Mutat. Res.; 9: 517-23(May 1970).

Repair replication and rejoining of single-strand breaks after x irradiation in human skin fibroblasts from normal donors and several patients with xeroderma pigmentosum were compared. The xeroderma strains showed different levels of repair replication following uv exposure. Repair replication and rejoining of breaks, that are considered to be part of the repair mechanism after damage due to x irradiation and uv irradiation, appeared to be performed in all xeroderma pigmentosum strains tested to the same level as in control strains. These results, and the observation that in the same xeroderma pigmentosum strains repair replication after uv irradiation was considerably reduced, suggest that the xeroderma strains investigated were deficient in the enzyme(s) involved in the excision of pyrimidine dimers from the DNA. (auth)

2536 DEUTERIUM-ISOTOPE EFFECT ON THE FLUORESCENCE YIELDS AND LIFETIMES OF INDOLE DERIVATIVES: INCLUDING TRYPTOPHAN AND TRYPTAMINE. Ricci, Robert W. (California Inst. of Tech., Pasadena). Photochem. Photobiol.; 12: 67-75(Jul 1970).

The fluorescence yields and lifetimes of indole, five of its alkyl derivatives, tryptophan, and tryptamine were determined in degassed, heavy and light water at room temperature. All of the compounds have radiative lifetimes nearly identical to the parent compound indole, and a comparison of these results with recently reported data on tryptophyl derivatives disclosed a striking uniformity in radiative lifetimes between indole and many amino acids and peptides that contain the indole group as the fluorescence unit. The fluorescence rate k_f in H_2O, was found to be $4.5 \times 10^7\ sec^{-1}$. The nonradiative decay rates were found to vary between 5.1 and $46 \times 10^7\ sec^{-1}$ and from a study of the deuterium-solvent isotope effect and the deuterium-substituent effect a mechanism for nonradiative deactivation is proposed that includes an isotopically dependent proton transfer and a pathway involving energy loss via the ring carbon hydrogen vibrations. Tryptophan at pH 7 was found to have a unique nonradiative decay scheme not evidenced at pH 1 or pH 10. (auth) (UK)

Immunology

Refer also to abstract 2587.

2537 TRANSPLANTATION ANTIGENS AND VIRAL CARCINOGENESIS. Haughton, Geoffrey; Nash, Donald R. (Univ. of North Carolina, Chapel Hill). Contract AT(40-1)-3634. Progr. Med. Virol.; 11: 248-306(1969). (ORO-3634-3).

Immunization in leukemia systems following treatment with x-irradiated tumor cells is described. It is hoped that immunology may one day provide a key to tumor control in man. (F.M.M.)

2538 EFFECTS OF RES BLOCKADE ON ANTIBODY FORMATION. III. PROLIFERATIVE CAPACITY OF ANTIGEN-REACTIVE STEM CELLS IN CARBON-TREATED MICE AFTER TRANSFER TO IRRADIATED RECIPIENTS. Friedman, H.; Sabet, T. Y. (Albert Einstein Medical Center, Philadelphia. Univ. of Illinois Coll. of Dentistry, Chicago). Immunology; 18: 883-95(Jun 1970).

The number of antigen-sensitive stem cells in spleens of mice treated with carbon particles to suppress the reticuloendothelial system was studied by a cell transfer system. X-irradiated recipient mice were injected with varying quantities of spleen cells from control and carbon-treated donor mice, followed immediately by challenge immunization with sheep erythrocytes. The number of individual haemolysin forming cells and antibody foci in spleens of recipient animals was determined. There was usually a maximum of 10 to 20 percent fewer foci in the spleens of irradiated mice treated with spleen cells from carbon-injected as compared to normal donor mice. Furthermore, the number of individual antibody forming cells appearing in spleens of irradiated mice restored with spleen cells from carbon-treated mice was only moderately less than that occurring in spleens of mice receiving cells from normal donors. Similarly, serum antibody titres were only moderately suppressed in recipient mice when the donors were carbon-treated. The day of administration of carbon into the donor affected the number of antibody forming cells and foci, as well as serum titres, in the recipient mice. Maximum inhibition occurred when the donors were injected with the carbon 1 to 3 days before sacrifice and cell transfer. Since each focus of antibody activity in a recipient spleen is considered due to proliferation of an individual antigen-reactive stem cells in the donor cell population, the results obtained suggest that only a portion of the immunodepression occurring in carbon-blockaded mice is due to stem cell inhibition. (auth) (UK)

2539 RESISTANCE OF MICE AND RATS TO CHALLENGE BY BABESIA RODHAINI AFTER INOCULATION WITH IRRADIATED RED CELLS INFECTED WITH B. RODHAINI. Phillips, R. S. (National Inst. for Medical Research, London). Nature (London); 227: 1255(19 Sep 1970).

A preliminary account is given of the successful protective immunization of mice and rats against the piroplasm Babesia rodhaini using irradiated piroplasms. Blood was taken from uninfected or infected donors, using heparin as anticoagulant, and kept on ice until irradiated at 22°C with about 1,000 R/min. of $^{60}Co\ \gamma$ radiation. Immunizing and challenge inocula were given intraperitoneally. The mice were injected with infected mouse red cells that had been irradiated with doses of 5, 10, 20, 40 and 80 kR, and during the succeeding 20 days recipient mice were examined for piroplasms. It was found that only doses of 40 kR or higher rendered the piroplasms non-infective. On day 20 after immunization the mice in the >40 kR group, together with control mice that had been injected with irradiated normal red cells, were challenged

with parasitized red cells. It was found that mice inoculated with irradiated piroplasms developed patent parasitaemas 3 to 4 days after the controls and that more of them survived. The protective immunization of rats was much more effective than with mice. It is thought that this type of approach to the control of economically important piroplasms could be worthwhile even when taking into account the problems associated with intraspecific variation. (UK)

2540 EFFECT OF WHOLE BODY X IRRADIATION ON DELAYED HYPERSENSITIVITY IN THE RAT. Visakorpi, R. (Univ. of Helsinki). Ann. Med. Exp. Biol. Fenn. (Helsinki); 48: 125-30(1970).

In rats irradiation with 800 rads 24 hours before immunization with bovine serum albumin (BSA) greatly reduced delayed skin reactivity. The latent period was prolonged and skin reactions were weak. There was little inhibition after 400 to 600 rads, although 400 rads delayed the appearance of detectable anti BSA antibody by nearly two weeks. Irradiation 1 to 2 hours after immunization also strongly inhibited delayed reactions, but irradiation 24 hours after immunization had less effect. Rats immunized one week after irradiation showed varying degrees of immunological recovery. Thus there seems to be a radiosensitive phase in both antibody production and delayed hypersensitivity at the time of induction of the immune response. (auth) (Finland)

Ecology

Refer also to abstracts 2361, 2362, 2517, 2525–2527, and 2564.

2541 SYMPOSIUM INTERNATIONAL DE RADIOECOLOGIE, CADARACHE, 8 AU 12 SEPTEMBRE 1969. VOL. I. (Proceedings of International Symposium on Radioecology, Cadarache, France, September 8–12, 1969. Volume 1). Fontenay-aux-Roses, France; Commissariat a l'Energie Atomique (1970). 684p. (In French and English). (CONF-690918–Vol.1)).

Separate abstracts were prepared for 26 of the 27 papers appearing in Volume I of these proceedings. The other paper discusses the use of tracers to study the absorption of organic materials from soils by plant roots. (E.R.B.)

For abstracts of individual papers see: 2337, 2338, 2361–2366, 2371, 2516, 2517, 2525–2530, 2542–2549, and 2565.

2542 TRANSPORT OF RADIONUCLIDES IN A MODEL AQUATIC SYSTEM. Gloyna, E. F. (Univ. of Texas, Austin). pp 3-31 of Symposium International de Radioecologie. Vol. I. Fontenay-aux-Roses, France; Commissariat a l'Energie Atomique (1970).

From Conference on Radioecology, Cadarache, France. See CONF-690918–(Vol.1).

Some selected investigations on radionuclide transport are described. The overall objective of these studies is to develop a mathematical model that reasonably predicts the transport of various radionuclides under different environmental conditions. The ecological environment was partially controlled, but all aspects were monitored. River systems were simulated with the aid of a research flume or "model" river. Laboratory and aquaria studies simulated closed ecosystems. Basic hydrodynamic relations were used to establish flow regimes; and uptake and release data were used to provide values for the various coefficients. (auth) (France)

2543 DEVELOPMENT OF THE RADIOCONTAMINATION OF IRRIGATION CANALS FED BY THE RHONE. Picat, P.; Grauby, A. (CEA, Cadarache, France). pp 33-81 of Symposium International de Radioecologie. Vol. I. Fontenay-aux-Roses, France; Commissariat a l'Energie Atomique (1970). (In French).

From Conference on Radioecology, Cadarache, France. See CONF-690918–(Vol.1).

The lower-Rhone-Languedoc irrigation canals are situated downstream from all the nuclear centers built on the Rhone basin, and their waters are used for irrigation and as drinking water. The physical and chemical properties of the water and sediments of these canals were studied. The average composition of the radioactive effluent discharged into the Rhone, and the results obtained from radioactivity measurements carried out in situ and in the laboratory on the samples taken, enabled the behavior of cesium, strontium, and ruthenium to be determined. The detectable radioactivity is localized on the sediment and is equally divided between ^{137}Cs and the other β emitters ($^{90}Sr/^{90}Y$, $^{106}Ru/^{106}Rh$). Laboratory studies confirmed the marked affinity of ^{137}Cs for the sediments in view of their very small particle size. (France)

2544 RADIOMANGANESE AND RADIOCOBALT FIXATION BY SEDIMENTS, FAUNA, AND FLORA IN THE MEUSE, DOWNSTREAM FROM THE FRANCO–BELGIAN ARDENNES POWER-STATION. Cantillon, G. (Institut d'Hygiene et d'Epidemiologie, Brussels); Kirchmann, R.; Van der Borght, O. pp 127-63 of Symposium International de Radioecologie. Vol. I. Fontenay-aux-Roses, France; Commissariat a l'Energie Atomique (1970). (In French).

From Conference on Radioecology, Cadarache, France. See CONF-690918–(Vol.1).

The Meuse is used to supply a large section of the Belgian population with water. It is therefore necessary to be sure of the quality of this water and to analyze not only the water itself, untreated and filtered, but also samples of various sorts liable to act as indicators. This paper describes a programme of samplings from muds, plants, and aquatic animals and gives the results obtained between 1965 (date previous to the start-up of the power plant) and the end of 1968. Results of experiments aimed at determining the Mn and Co fixation capacity of sediments, and the fixation and desorption of ^{54}Mn and ^{60}Co in aquatic mosses, are presented and discussed. (auth) (France)

2545 STUDIES ON THE SELFCLEANING CAPACITY ON RADIONUCLIDES OF A SMALL RIVER. Wanderer, E. (Oesterreichisch Studiengesellschaft fuer Atomenergie GmbH, Seibersdorf, Austria). pp 165-80 of Symposium International de Radioecologie. Vol. I. Fontenay-aux-Roses, France; Commissariat a l'Energie Atomique (1970).

From Conference on Radioecology, Cadarache, France. See CONF-690918–(Vol.1).

Hydrology and sedimentology of the main drainage canal of the Austrian reactor center Seibersdorf near Vienna were studied. Samples of mineral sediment organic detritus, as well as water plants (Cladophora) and crabs (Gammarus pulex) were prepared and their radioactivity determined. At first, suspended load in relation to water level and flow rate was estimated and the grain size distribution and composition determined. Laboratory experiments on the sorption capacity of the different grain sizes showed a maximum in the fractions 100 to 75 μ of mineral sediment and 30 × 15 μ of aquatic detritus. These two fractions contribute up to 67% of the total suspended load. Samples of the bottom sediment are taken on profiles and with glass cores. The differences in contamination of the different samples along the testing range show that the radionuclides from the wastes of the reactor center are adsorbed fairly well by the clay particles contained in suspended load. Water is cleaned by sedimentation of the accumulated particles. The dependence of contamination in sediment from the distance of the inlet point is shown. In a weir approximately 3 km downstream from the inlet system, a higher cleaning rate is caused by longer reaction time as well as by settling of smaller grain sizes (15 to 30μ), which prove to have the highest sorption capacity. Samples of waterplants (Cladophora) and crabs (Gammarus pulex) show a similar course. (auth) (France)

2546 CONCENTRATION FACTORS OF ^{90}Sr AND URANIUM OF HYDROBIONTS LIVING IN LAKES OF DIFFERENT TYPES. Kalnina, Z. K. (Inst. of Biology, Riga); Polikarpov, G. G.; Risik, N. S. pp 233-49 of Symposium International de Radioecologie. Vol. I. Fontenay-aux-Roses, France; Commissariat a l'Energie Atomique (1970).

From Conference on Radioecology, Cadarache, France. See CONF-690918–(Vol.1).

The ^{90}Sr concentration factors are found to be higher in the hydrobionts and substrates of a dystrophic lake than in those of mesotrophic-eutrophic and eutrophic lakes. An interesting phenomenon is revealed, that is, the microaccumulation of uranium in hydrobionts and substrates. Uranium was measured by use of dielectric detectors of charged particles. This permits determination of the uranium content and its microdistribution in studied samples. (auth) (France)

2547 ROLE OF FRESH-WATER VEGETATION IN THE MIGRATION AND TRANSLOCATION OF NATURAL RADIOACTIVE ELEMENTS IN A BODY OF WATER. Iskra, A. A.; Bakhurov, V. C.; Kulikov, N. V. (Inst. of Plant and Animals Ecology, Sverdlovsk, USSR). pp 251-68 of Symposium International de Radioecologie. Vol. I. Fontenay-aux-Roses, France; Commissariat a l'Energie Atomique (1970).

From Conference on Radioecology, Cadarache, France. See CONF-690918–(Vol.1).

As a result of the exploitation of deposits of non-ferrous, rare, disseminate, and radioactive elements, an increasing amount of natural radioactive elements is transferred to freshwater basins. Radioactive elements are dispersed and distributed among the major components, biomass, detritus, and ground. In this report experimental data on the influence of freshwater plants on the migration and transport of elements in model systems are given and estimates of their accumulation and concentration in biomass, detritus, and ground are presented. The major components of

XUM

bodies of water may be arranged in the following order according to the capacity of accumulation of radioactive elements: detritus > plants > ground, thorium being absorbed to a greater degree than radium and uranium. (auth) (France)

2548 STUDY OF FISSION PRODUCT TRANSFER AND FIXATION IN SOME FRESH WATER SPECIES UNDER CONDITIONS OF NON-EQUILIBRIUM. Beninson, D.; Cancio, D.; Menossi, C. (Comision Nacional de Energia Atomica, Buenos Aires). pp 361-97 of Symposium International de Radioecologie. Vol. I. Fontenay-aux-Roses, France; Commissariat a l'Energie Atomique (1970). (In French).

From Conference on Radioecology, Cadarache, France. See CONF-690918-(Vol.1).

The results of experiments carried out independently in the laboratory and in the field are presented. The laboratory experiments concern the transfer of radiostrontium and radiocesium in freshwater plants and molluscs. A quantitative model of this transfer is proposed, showing that contamination of the organisms depends only on the existing radioactivity level of the water and the temporal integral of past concentrations, not on the way in which the radionuclide concentration of the water has varied in the past. The validity of the model was confirmed for strontium in molluscs of the types Ampullaria, Planorbis, and Limnea, which are thus excellent biological integration indicators. However, where cesium is concerned, the results show that the cumulative effect is shorter and the temporal integral of the past is only valid for about two weeks. On the other hand aquatic plants of the Elodea type respond rapidly to variations in the cesium and strontium level of the water. Contamination then depends largely on the existing radioactivity level and to a lesser extent on the temporal integral of the past, which is only four days. The field studies were based on systematic recent fallout measurements both on the water of the river chosen for testing and on plants and molluscs, adequately arranged in special cages. The level of contamination due to ^{103}Ru, ^{144}Ce, ^{131}I, $^{95}Zr(^{95}Nb)$, and ^{140}Ba was followed. Analysis of the results shows that in every case the activity levels in the organisms vary rapidly with those of the water. It is shown that the concentration factors can be evaluated from the relations between the temporal integrals of contamination of the water and the organisms. The concentration factors obtained in this way vary from 20 to 300 for molluscs of the Diplodon and Ampullaria type depending on the nuclide and the species, and from 100 to 600 for plants of the Elodea and Cabomba type. (auth) (France)

2549 TRANSPORT OF RADIOCOBALT IN A SIMPLE ARTIFICIAL ECOSYSTEM IRRIGATED BY SUBMERSION. Bittel, R. (CEA, Fontenay-aux-Roses, France); Merlini, M.; Myttenaere, C.; Bourdeau, P. pp 413-38 of Symposium International de Radioecologie. Vol. I. Fontenay-aux-Roses, France; Commissariat a l'Energie Atomique (1970). (In French).

From Conference on Radioecology, Cadarache, France. See CONF-690918-(Vol.1).

The behavior of radiocobalt in ecosystems irrigated by submersion is studied. For this purpose, artificial rice-plantations under glass are used and conditions necessary for irrigation are created. Fresh water bivalves, Unio mancus elongatulus, are employed. A double labeling (^{60}Co in irrigation water and ^{58}Co in soil) has allowed the behavior of Co in soil, water, and organisms to be studied as a function of the origin and of the physicochemical nature of Co. The important results are as follows: preponderant absorption of Co from water by microorganisms; preponderant absorption of Co introduced in the ionic state; and faster migration of complexed Co. The above results are discussed in terms of radioprotection of food and environment. (auth) (France)

2550 INVESTIGATION OF FISSION PRODUCT DEPOSITION IN THE MOSCOW REGION DURING 1962–1966. Fedorov, G. A.; Konstantinov, I. E. This paper was summarized in At. Energ. (USSR); 25: 139-40(Aug 1968) as paper No. 222. (In Russian).

The monthly levels of fallout of ^{141}Ce, ^{144}Ce, ^{103}Ru, $^{106}Ru + ^{106}Rh$, $^{95}Zr + ^{95}Nb$, ^{140}La, ^{54}Mn, and ^{137}Cs in the Moscow region during 1962 to 1966 were determined. The fallout levels of ^{137}Cs and ^{90}Sr in the northern hemisphere in 1964 were slightly less than in 1963, but at certain points they exceeded the 1963 levels. The change of concentration of ^{137}Cs in certain agricultural products in 1966 are also reported. The total expected dose in atmosphere from fission product fallout in the region amounted to 113 Mrad and the tissue dose to internal organs was about 23 Mrad. (E.E.H.)

Genetics and Cytogenetics

Refer also to abstracts 2535 and 2585.

2551 (COO–873-28) MUTATION STUDIES WITH TOBACCO MOSAIC VIRUS. Technical Progress Report, December 1, 1969–November 30, 1970. (Arizona Univ., Tucson). Contract AT-(11-1)-873. 8p. Dep. CFSTI.

Studies conducted on intermediates in the biosynthesis of RNA in tobacco mosaic virus showed that double-stranded forms appeared as intermediates in the biosynthesis of single-stranded viral RNA. Two such forms were identified and named replicative form and replicative intermediate. Studies on the TMV-RNA replicative system were continued. Studies on the nature and location of new protein components appearing in tissue as a result of virus infection were conducted by exposing healthy leaf tissue to ^{14}C-leucine and virus infected tissue to ^{3}H-leucine. Investigations on hybridization of TMV-RNA with host DNA were continued. The following classes of defective mutants were studied: strains which induce synthesis of non-functional coat proteins which have quaternary packing structures distinctively different from that of the parental strain; strains which produce non-functional proteins which have no recognizable packing structure and which are insoluble in the buffers used to extract the infected tissue; and temperature sensitive mutants. Studies were continued on the antigenic structure of tobacco mosaic virus protein. (H.L.W.)

2552 (ORO–2909-9) NORTHWARD MIGRATION OF CITRUS BY MEANS OF RADIATION-INDUCED MUTATION. Progress Report, October 1, 1969–June 30, 1970. (North Carolina State Univ., Raleigh). Contract AT(40-1)-2909. 20p. Dep. CFSTI.

X_1 scions of a single seedling sweet orange (Citrus sinensis) were selected through successive bud grafts by three winters at an outdoor site near Raleigh, North Carolina, and the survivors tested in replicated survival trials near the North Carolina Atlantic coast. Thirty-five, or slightly over 1% of 3473 vegetative bud descendents of 461 initially irradiated buds survived the Raleigh test site. Five, or 2.3% of 218 non-irradiated buds of the control seedling survived. Preliminary results from testing the first four of the irradiated survivors show that when the proportion of stem (in %) which survived the winters of 1968-69, 1969-70 was determined, the four irradiated measured 40.0, 51.8, 70.3, and 69.8 vs 41.7 for the non-selected non-irradiated original seedling buds in 1968-69, and 7.3, 38.5, 35.9, and 33.1 vs 23.4 for the non-irradiated in 1969-70. Statistical analysis of each year taken singly and both years jointly indicated very high significance for the differences shown. The biological implications of the above results are not clear. It is not known whether the differences shown result from greater resistance to cold weather diseases, vessel blockage caused by intense cold, or disruption of tissue structure through ice formation, or from lower freezing points of the cells themselves. It is reasonable to conclude however, that the differences among the different scions in the proportion of stem surviving the winters were associated with the radiation treatment and that these differences were recognized in the irradiated generation. (auth)

2553 STUDIES ON THE INDUCTION OF TRANSLOCATIONS IN MOUSE SPERMATOGONIA. III. EFFECTS OF X-IRRADIATION. Evans, E. P.; Ford, C. E.; Searle, A. G.; West, B. J. (Medical Research Council, Harwell, Eng.). Mutat. Res.; 9: 501-6(May 1970).

Translocation frequencies were studied in mouse spermatocytes derived from x-irradiated spermatogonia. Over the range from 50 to 800 R, the dose–response relationship did not differ significantly from linearity, in agreement with previous findings of Léonard and Deknudt. It seems probable that the initial dose–response curve has the expected square-law component but becomes distorted by secondary factors between irradiation and meiotic examination of cells. Observed translocation frequencies were little affected by increasing length of time from 11 to 30 weeks between irradiation and examination, except for a possible decline at the highest dose (800 R). No significant frequency differences were found between mated and solitary males, or between those given whole-body or part-body (gonadal) irradiation. (auth)

2554 PARTIAL AND TOTAL SEX-CHROMOSOME LOSS INDUCED BY X-RAYS IN MATURE SPERMATOZOA OF DROSOPHILA MELANOGASTER. Traut, H.; Scheid, W.; Wind, H. (Univ., Muenster, Ger.). Mutat. Res.; 9: 489-99(May 1970).

Using a cytological technique (analysis of metaphase chromosomes of larval ganglia) the proportion of partial sex-chromosome losses induced by X-rays (4 kR) in mature spermatozoa of Drosophila melanogaster was determined. For this purpose a scheme has been devised allowing the detection of aberrant F_1 individuals already at the larval stage. More than 90% of the losses analyzed cytologically were found to be partial ones. The partial losses have been classified into three types: rod fragments, ring fragments, and fragments of similar size and shape as chromosome IV (point fragments). It is assumed that more of the rods and rings originate from the Y than from the X chromosome. A considerable part of the partial losses of each type (possibly all partial losses)

seems to require two breaks. Using a genetical technique the dose dependence of the frequency of partial plus total losses induced by x rays (0 to 4 kR) in mature spermatozoa was investigated. A statistically highly significant rise above linearity was obtained. The reason for the discrepancy between this result and that obtained by Pontecorvo (who got no indication of a two-track component) is probably the fact that germ cells of differential radiosensitivity were utilized in those studies. Special experiments revealed no influence of selection operating between the larval and imaginal stage of loss individuals. The rise above linearity of our dose–effect curve is in line with our cytological findings, namely that two-break events represent a considerable fraction of the partial losses analyzed. However, there is evidence that a part of these two-break aberrations is produced by one track only. (auth)

2555 FURTHER OBSERVATIONS ON THE X-IRRADIATION RESPONSE OF G_1 CELLS IN DRY SEEDS. Brunori, A.; Georgieva, Jordanka; D'Amato, F. (National Committee for Nuclear Energy, Rome. Univ., Pisa, Italy). Mutat. Res.; 9: 481-7(May 1970).

A previous DNA cytophotometric analysis on dormant seeds has shown that the shoot and root apices and the cotyledons in Pinus pinea and the root apices in Helianthus annuus and Lactuca sativa are composed exclusively of 2C cells (G_1 phase of the nuclear cycle for meristematic cells). When dormant seeds of these three species were x-irradiated, the G_1 cells responded to irradiation predominantly with chromosome break (B'') aberrations: in the first mitotic cycle postirradiation, the percent ratio of B'' breaks to total breaks ranged from about 94 to about 82 in Pinus, from about 92 to about 80 in Helianthus and from about 85 to about 69 in Lactuca. The chromatid (B') breaks found in the experiment may be accounted for by one or both of these possibilities: the meristems contain a fraction of their G_1 cells in late G_1, the stage that is known to respond to radiation with B' breaks; the B' breaks are, at least in part, the result of an indirect effect of irradiation. In Pinus pinea, the shoot apical cells are clearly less radiosensitive than root apical and cotyledon cells (these last two groups of cells show an identical radiation sensitivity). It is suggested that the lower radiation sensitivity of shoot apices may be caused by their specific metabolic features. (auth)

2556 UV-SENSITIVE MUTANT OF NEUROSPORA DEFECTIVE FOR PHOTOREACTIVATION. Tuveson, R. W.; Mangan, J. (Univ. of Illinois, Urbana. Univ. of Chicago). Mutat. Res.; 9: 455-66(May 1970).

A mutant (uvs-1 upr-1) with enhanced uv sensitivity was isolated from the uvs-1 upr-1$^+$ mutant of Neurospora crassa. The negative slope of the exponential uv dose response curve of the uvs-1 upr-1 mutant is approximately 1.8 times that of the uvs-1 upr-1$^+$ mutant. Although the mutant was selected for enhanced sensitivity in the dark, the mutant is simultaneously defective for photoreactivation (PR). The results of experiments in which PR was carried out at ice bath temperatures are consistent with the hypothesis that PR in microconidial strains of Neurospora crassa, when carried out with a broad spectrum fluorescent light, is a composite of two types of PR: direct (enzymatic) PR and indirect (photochemical reversal of uv lesions). It is suggested that the uvs-1 upr-1 mutant is defective for direct (enzymatic) PR. Attempts to demonstrate in vitro repair of uv-irradiated Bacillus subtilis transforming DNA by extracts from the uvs-1 upr-1$^+$ mutant and the lack of such repair by extracts from the uvs-1 upr-1 double mutant, were unsuccessful due to the presence of nucleases in the extracts. As judged by the ability of the enzyme extracts to solubilize tritium counts from labeled Bacillus subtilis phage DNA, Neurospora crassa produces a nuclease(s) capable of attacking unirradiated DNA as well as a nuclease(s) that degrades irradiated DNA with great efficiency. The uvs-1 upr-1 double mutant resulted from the alteration of a single nuclear gene (upr-1) as revealed by linear tetrad analysis. Since it was not possible to separate the upr-1 gene from its associated mating type gene (thus suggesting possible linkage between these loci), it was not feasible to test the effects of the upr-1 gene on crossing over. (auth)

2557 ULTRAVIOLET ACTION SPECTRA FOR MUTATION IN ESCHERICHIA COLI. Setlow, Jane K.; Boling, Maxon E. (Oak Ridge National Lab., Tenn.). Mutat. Res.; 9: 437-42(May 1970).

Ultraviolet action spectra for mutation to prototrophy in Escherichia coli were obtained when repair of premutational damage was inhibited or mostly absent, either because of the presence of acriflavine in the plating medium or because of a genetic defect; and when such repair was allowed to proceed at a normal rate. These action spectra were different. The former was similar to the action spectra for cellular inactivation and was interpreted as the result of pyrimidine dimers, whereas the latter was postulated to result from damage to purines. (auth)

2558 TIME-SPECIFIC EFFECT OF UV-IRRADIATION ON CELLS PROGRESSING FROM G_2 INTO METAPHASE. Barranco, S. C.; Humphrey, R. M. (Univ. of Texas, Houston). Mutat. Res.; 9: 524-6(May 1970).

These experiments were designed to determine whether uv radiation of Chinese hamster ovary cells would cause a delay in their progression from G_2 into metaphase earlier in the G_2 phase than when treated with protein or RNA synthesis inhibitors. Actinomycin D treated cells were used for controls. Exposure to uv caused progression delay at a time earlier in G_2 than the delay induced by actinomycin D. Ultraviolet radiation appears to interfere with the synthesis of division-specific protein. This protein is presumably synthesized on shortened mRNA's that are produced when transcription is prematurely terminated at the site of uv lesions. (E.E.H.)

2559 TABLES FOR DETERMINING THE STATISTICAL SIGNIFICANCE OF MUTATION FREQUENCIES. Kastenbaum, Marvin A.; Bowman, K. O. (Oak Ridge National Lab., Tenn. Computing Tech. Center, Oak Ridge, Tenn.). Mutat. Res.; 9: 527-49(May 1970).

The standard tables of the cumulative binomial distribution are arranged to provide values of α for specified values of $1 \leq c \leq n$, and $o \leq p \leq 0.5$. However, errors may be made by researchers who are not skilled in the use of tables of mathematical functions. Therefore, tables were designed specifically to provide minimum values of c, for a given n, p, and α values of c are given for all combinations of n = 1(1)100, p = 0.01(0.01)0.99, and α = 0.01, 0.05. (E.E.H.)

2560 EFFECTS OF X-IRRADIATION AND GAMMA IRRADIATION ON PARAMUTATION IN R HETEROZYGOTES IN MAIZE. Shih, Katherine Lu; Brink, R. Alexander (Univ. of Wisconsin, Madison). Genetics; 65: 473-82(Jul 1970).

The amount of change in level of aleurone pigmenting potential of standard R^r was significantly reduced in R^rR^{st} heterozygotes after direct x-irradiation (8,000R and 10,000R) of R^rR^{st} dormant seeds, as compared with that in unirradiated controls. Similar, although smaller, changes were obtained by x-irradiation of R^r/R^{sc}_{132} and $R^s_8/r^r(D)_4$ seeds. Under the conditions of the tests made, x rays were found to be distinctly less efficient as an artificial paramutagen than diethyl sulfate, as used in earlier experiments with R^rR^{st} seeds in our laboratory. Data were obtained suggesting that the action of high energy radiations was due to either derepression of the freshly paramutated $R^{r'}$ allele in R^rR^{st} heterozygotes, or to impairment of the paramutation process itself, or to both factors. Indecisive results were obtained in experiments designed to determine whether sensitivity of R alleles to high energy radiations varies in a regular way with stage of plant development. The changes in R^r and R^s testcross scores induced in heterozygotes with overtly paramutagenic alleles by high energy radiations were in one direction, namely, to higher levels of pigmenting potential. (auth)

2561 SCREENING FOR X-RAY-INDUCED CROSSOVER SUPPRESSORS IN DROSOPHILA MELANOGASTER: PREVALENCE AND EFFECTIVENESS OF TRANSLOCATIONS. Roberts, Paul A. (Oak Ridge National Lab., Tenn.). Genetics; 65: 429-48(Jul 1970).

A stock that makes it possible to screen chromosomes 1, 2, and 3 simultaneously for x-ray-induced dominant crossover suppressors was constructed. Out of 360 x-irradiated (4000 R) genomes from sperm that were screened with this stock, 70 translocations, 29 inversions and 3 transpositions were recovered. Some heterozygous translocations with distal breakpoints are more effective crossover suppressors than are inversions, lowering crossing over within a chromosome arm from a control value of 40% to less than 1%. The behavior of these translocations was interpreted to mean that distal regions of chromosome arms are important in the initiation of synapsis in D. melanogaster females. (auth)

Health Physics and Safety

Refer also to abstracts 2059, 2423, and 2821.

Radioactive Contamination and Decontamination

Refer also to abstracts 2329, 2346, 2361, 2362, 2420, 2525, 2527, and 2542–2546.

2562 AIR POLLUTION ON THE CERN SITE. Prantl, F. A.; Baarli, J. (CERN, Geneva). Ann. Occup. Hyg.; 13: 191-5(Jul 1970).

XUM

Air pollution by dust, fume and smoke at CERN derives mainly from construction areas within the site, from heating plant and from vehicle exhausts. A neighbouring airport and local factories also make a contribution. Aerosols from within the CERN accelerators are prevented from escaping into the atmosphere by exhaust ventilation with efficient filters. Activation of particles in the outside air by radiation penetrating the accelerator shielding is possible, but it is likely to be small, partly because it is known that the intensity of stray radiation is low and decreases rapidly with distance and also because the cross sections for the possible nuclear reactions are small. An investigation was undertaken to determine the extent and nature of the radioactivity of the particulate air pollution on the site, and to assess any possible influence from the radioactivity generated by operation of the CERN accelerators. (auth) (UK)

2563 STUDY AND RESULTS OF EXAMINATIONS CARRIED OUT AFTER INHALATION OF SO-CALLED SOLUBLE COMPOUNDS OF NATURAL URANIUM. PART I. Chalabreysse, J. (Commissariat a l'Energie Atomique, Pierrelatte, France). Radioprotection; 5: 1-17(1970). (In French).

Following an accident which took place in May 1965 at the Pierrelatte pilot plant, numerous tests carried out on a relatively large number of employees provided interesting statistics on the elimination of uranium inhaled in small doses by certain subjects. Several individual cases taken from the personnel directly exposed and suffering internal contamination, from staff exposed indirectly, from the cleaning staff and from personnel in charge of decontamination of the equipment were subjected to a special study. The equation on which the interpretation of internal contamination and of the urinary excretion norm is based was verified from a study of the results of these examinations. (France)

2564 SURVEY OF ENVIRONMENTAL ASPECTS OF NUCLEAR ENERGY. Dinunno, Joseph J.; Levin, Saul; Wright, J. H.; Davis, Owen H. Nucl. Eng. Int.; 15: 607-22 (Jul-Aug 1970).

The survey includes three review papers which cover the following topics: The impact in the USA of electrical power generation on the environment. Recent legislation, including regulations for radiation protection, thermal energy effects, and the AEC's research programme is discussed. The attitude of the nuclear industry to public health and safety. Measures taken to fulfil the industry's promise to provide safe power without pollution are described. A brief account of radiation from PWR's; ecological implications of thermal discharges; use of waste heat; work of the Westinghouse Environmental Systems Department. The survey concludes with a review of the papers presented at the Second International Radiation Protection Association Congress, held in Brighton, 1970. (UK)

Dosimetry and Monitoring

Refer also to abstracts 2446, 2494, 2495, 2584, and 3476.

2565 APPLICATIONS OF THE LIQUID SCINTILLATION SPECTROMETER TO RADIOECOLOGY. EMPHASIS IS PLACED ON THE DETECTION OF CHERENKOV RADIATION OF BETA-EMITTING NUCLIDES. Palais, C. J. (Intertechnique, Plaisir, France). pp 201-12 of Symposium International de Radioecologie. Vol. I. Fontenay-aux-Roses, France; Commissariat a l'Energie Atomique (1970).

From Conference on Radioecology, Cadarache, France. See CONF-690918-(Vol.1).

The modern liquid scintillation spectrometer is a convenient and accurate tool for the measurement of very low specific activity material containing tritium or carbon-14, by using classical liquid scintillation techniques combined with high-efficiency catalytic conversion of sample material to benzene. The same instrumentation shows great promise for the measurement of large samples with low specific activities of hard beta emitters such as ^{32}P, $^{90}Sr-^{90}Y$, $^{144}Ce-^{144}Pr$, $^{103}Ru-^{106}Ru$, by Čerenkov counting. The general advantages of both methods and some details on sample preparation and counting efficiency, are discussed. (auth)(France)

2566 UNIVERSAL NOMOGRAMS FOR CALCULATING ABSORBED DOSES FROM PLANE RADIATORS. Drozdov, V. E.; Suroegin, L. M.; Orlenko, P. A.; Tikhonov, V. P. This paper was summarized in At. Energ. (USSR); 25: 224(Sep 1968) as paper No. 226. (In Russian).

Plane sources radiation γ rays with energies from 0.5 to 3 MeV are frequently used at radiation processing and research establishments. To calculate such fundamental characteristics of the arrangement as its efficiency as a γ-ray emitter, the degree of nonuniformity of the dose distribution etc., it is necessary to know the distribution of absorbed dose rate (ADR) over the volume of the apparatus or irradiated objects. The calculation of the ADR is simplified by using universal graphs showing how γ-radiation of various energies from plane sources is attenuated in different materials. These graphs are presented and discussed. (W.H.K.)

2567 DIFFERENT INHERITED LEVELS OF DNA REPAIR REPLICATION IN XERODERMA PIGMENTOSUM CELL STRAINS AFTER EXPOSURE TO ULTRAVIOLET IRRADIATION. Bootsma, D.; Mulder, M. P.; Pot, F.; Cohen, J. A. (National Defense Research Organization TNO, Rijswijk, Netherlands. Medical Faculty of Rotterdam. Univ., Leiden). Mutat. Res.; 9: 507-16(May 1970).

Primary fibroblast cultures were established from eight patients having different degrees of clinical symptoms of xeroderma pigmentosum. Repair replication after exposure of cells to different doses of uv irradiation (predominantly 254 nm) was studied by means of [^{3}H] thymidine labeling and autoradiography. A decreased repair DNA synthesis in cells in G_1 and G_2 phase was found in all xeroderma pigmentosum cell cultures relative to control cell cultures obtained from healthy people. Cell strains originating from two severe cases of xeroderma showed no repair synthesis after short autoradiographic exposure times, although, after one month exposure a slight labeling was observed (10 to 20% of the control). The repair activity in cells from the other patients ranged from 70% for a light case to 50 and 30% for moderate cases of the disease. Cells obtained from related patients showed identical levels of repair activity, suggesting a genetically determined constant level of reduced repair replication. An xeroderma cell strain transformed by SV40 virus showed no repair replication as did the original strain before transformation. (auth)

2568 CALCULATION OF SPECTRA OF ENERGY DEPOSITED BY RECOIL HEAVY PARTICLES. Saigusa, T. (Oak Ridge National Lab., Tenn.). Health Phys.; 18: 547-60(May 1970).

Spectra of energy deposited in a semiconductor detector by heavy charged particles, which recoil in soft tissue, were obtained for incident monoenergetic neutrons of 15.09 MeV by a Monte Carlo calculation. In the calculation, the lowest energy of charged particles to be registered was extended to 1 keV, and the spectra of them produced in tissue and the detector were obtained for nine positions. The results from 50,000 incident neutrons were compared with the corresponding experimental data. While deviations were found in most of the energy ranges, they were significant only in the interval from 2 to 6 MeV. The effect of the bias level energy of the detector was also estimated in order to check the applicability of the measurements to dosimetry. The establishment of the bias level at an energy of 640 keV was found to give most of the total energy delivered to the detector by 15.09 MeV neutrons. (auth) (UK)

2569 VALUES OF C_λ FOR POLYSTYRENE AND LUCITE. Schulz, R. J. (Albert Einstein Coll. of Medicine, New York). Phys. Med. Biol.; 15: 563-5(Jul 1970).

The advantages of plastic phantoms over water phantoms for the calibration of high energy X- and γ-ray beams in terms of absorbed dose are discussed. The relationship between the absorbed dose in plastic and in water is derived. An expression for C_λ (the dose conversion factor) is given and the sources used for the data in the calculations of C_λ indicated. Values of C_λ for water, polystyrene, and Lucite and the ratios of mass energy absorption coefficients for water to polystyrene and Lucite are tabulated for energy up to 35 MeV. (UK)

Radiation Protection

2570 (KFK-1158) RADIATION PROTECTION AND SAFETY DEPARTMENT. Annual Report, 1969. Kiefer, H.; Koelzer, W. (eds.) (Kernforschungszentrum, Karlsruhe (West Germany)). 31 Mar 1970. 138p. (In German). Dep. CFSTI (U. S. Sales Only).

Radiation protection and personnel safety in the conventional and nuclear fields at the Karlsruhe Nuclear Research Center are duties of the Radiation Protection and Safety Department. The different duties are described, results of routine radiation monitoring measurements during 1969 are listed and recent results of investigations and developments in the Working Groups of the Department are covered. (auth)

2571 INCREASING TASKS OF RADIATION PROTECTION. Kosmowski, A. Wasser, Luft Betr.; 14: 149-51(1970). (In German).

As a result of the increased number of nuclear power plants

and the rapidly increased application of radioisotopes and radiation sources in research, medicine, and industry, knowledge and application of radiation protection methods increased significantly. For a better understanding of the problematic nature of radiation protection with regard to genetic exposure of the individual and the whole population, the biological radiation effects and natural and artificial radiation sources are reviewed. (INIS)

2572 RESPONSE TO CRITERIA FOR THE DESIGNATION OF PERSONS WORKING WITH UNSEALED RADIOACTIVE SUBSTANCES. Bush, D. (Univ. of Birmingham, Eng.). Nature (London); 227: 1150(12 Sep 1970).

Reference is made to Hughes (Nature 224: 728(1969)) who outlined the derivation of criteria which he adopts to decide if a worker using unsealed radioactive sources should be designated. In the present communication although it is considered that Hughes' general approach to the problem is appropriate, it is suggested that some of the numerical values of the parameters used in the derivation could be improved. These parameters are concerned with the derivation of maximum activity to be handled at one time, which in Hughes' criteria is considered too restrictive; also the inhaled fraction of total activity handled, which is considered to be too low; also maximum turnover per quarter, which is also too low for the radioiodines. (UK)

2573 DEFENCE OF CRITERIA FOR THE DESIGNATION OF PERSONS WORKING WITH UNSEALED RADIOACTIVE SUBSTANCES. Hughes, D. (Univ. of Leeds, Eng.). Nature (London); 227: 1151(12 Sep 1970).

The author replies to the criticisms of Bush (Nature 227: 1150 (Sept. 12th 1970)). With regard to the maximum activity to be handled at one time, the author states that his figures have not proved restrictive to university uses. With regard to the inhaled fraction of total activity handled, Hughes considered that his figures for ^{85}Kr and ^{133}Xe should be adjusted. With regard to maximum turnover per quarter, comments are made in the light of ICRP recommendations on individual monitoring of personnel. Further guidance on the levels at which designation is necessary is requested. (UK)

Safety Procedures

Refer also to abstract 3475.

Legal Aspects

2574 DEVELOPMENTS ON ASPECTS OF NORMS FOR RADIATION PROTECTION. Letavet, A. A.; Dibobes, I. K.; Teverovskii, E. N.; Terman, A. V. At. Energ. (USSR); 28: 225-31(Mar 1970). (In Russian).

A brief review is given of the recommendations made by the International Radiological Congress on radioprotection and permissible doses. Considerations are given on the concepts of justifiable risk, equivalent doses, permissible doses for the total population, and somatic doses for people handling radioactive materials. (R.V.J.)

Medicine

2575 ANNUAL REVIEW OF MEDICINE. VOLUME 20. DeGraff, Arthur C. (ed.). Palo Alto, Calif.; Annual Reviews, Inc. (1969). 506p.

Separate abstracts were prepared on two papers included in this book. Other papers discuss various pathological conditions in man. (C.H.)

For abstracts of individual chapters see: 2579 and 2580.

Protective Substances

Refer also to abstracts 2588 and 2597.

2576 EFFECT OF PRE- AND POST-IRRADIATION ADMINISTRATION OF MAGNESIUM PEMOLINE ON RADIORESISTANCE. LeVan, Hoa (Univ. of Illinois, Chicago). Int. Z. Klin. Pharmakol., Ther. Toxikol.; 1: 514-16(Oct 1968).

An evaluation was made of the protective effect of Mg Pemoline when administered to mice before and after irradiation at two different drug doses (0.7 and 70 mg/Kg). The time between injection and irradiation or irradiation and injection was not more than 5 to 10 min. The mice were exposed to a single whole-body dose of 750 R of x rays at 80 R/min. In the two groups injected with 70 mg/Kg of Mg Pemoline before and after irradiation, 100% of the mice still survived on the 7th postirradiation day while 21% of the control group had died. All the control mice were dead 2 weeks after irradiation, but 47% of the pre-exposure injection group and 42% of the post-exposure injection group were still alive. Up to the 14th day, there was no significant difference in the mortality rate between these two groups. On the following day, however, this difference became quite pronounced (40% vs 25% on the 15th day, and 35% vs 16% on the 16th day after exposure). From the 16th day to the 30th day after irradiation no more mortality was observed in these two groups. The mortality patterns of the two groups given 0.7 mg/Kg were similar to the previous experiment. On the 8th day after irradiation 25% of the control group had died while 100% of the pre-exposure injection group and 94% of the post-exposure injection group were still alive. It was concluded that the effect of Mg Pemoline in enhancing radioresistance in mice is independent of the drug doses (up to 2 weeks after irradiation) whether the animals are exposed to radiation before or after the drug administration. For long-term protection, however, the pre-irradiation treatment is more effective than the post-irradiation treatment. (BBB)

Radiodiagnosis

Refer also to abstracts 2122, 2127, 2447, 2518, 2533, and 3471.

2577 DENSITOMETRIC AND SCINTIGRAPHIC INVESTIGATIONS OF BRAIN TISSUE DURING REDUCED BLOOD FLOW. Piepgras, U.; Heuck, F.; Maerz, K.-D (Katharinenhospitals, Stuttgart). Radiologe; 9: 448-51(Dec 1969). (In German).

Only in cases involving major vessels, information about cerebral blood flow can be obtained by serial angiography. When the disturbance occurs in the regions of arterioles and capillaries, significant clues may be obtained by densitometry and scintigraphy with ^{99m}Tc. The case history of one patient demonstrates that the highest degree of diagnostic correctness can be reached by a combination of the two methods. (H.B.G.)

2578 ISOTOPE DIAGNOSIS OF PROCESSES INVOLVING THE POSTERIOR CEREBRAL FOSSA. Hirschbiegel, H.; Boeckem, K. (Univ., Duesseldorf). Radiologe; 9: 481-4(Dec 1969). (In German).

Diagnostic difficulties for detecting tumors located in the posterior fossa are discussed for radioisotopes such as ^{197}Hg, ^{203}Hg, ^{131}I RISA, and ^{99m}Tc. Among 500 brain tumors, diagnosed by scintigraphic methods, 54 were located in the posterior fossa. Utilization of computers proved to be effective for evaluation of data. Use of ^{131}I macroaggregates proved most promising because it avoided the usual difficulties caused by blood content of neck muscles and the circulatory system at the base of the brain. (H.B.G.)

2579 PLATELET LIFESPAN. Najean, Y.; Ardaillou, N.; Dresch, C. (Hopital Saint-Louis, Paris). Annu. Rev. Med.; 20: 47-62(1969).

Radioisotopic methods have allowed the measurement of platelet lifespan in man and in animals under normal conditions and in most thrombocytopenic states. They are very useful not only as diagnostic tools but also in making the decision on splenectomy. Numerous problems are still under study and the three following seem to us to be among the most important: the identification of precise platelet groups so that donor and recipient of platelet transfusions can be correctly matched; the definition of the exact role of senescence and random destruction so as to allow the indirect calculation of marrow production from the percentage renewal per day; and the development of a quantitative technique to measure thrombocytopoiesis. (76 references) (auth)

2580 ^{99m}Tc IN CLINICAL NUCLEAR MEDICINE. Gottschalk, Alexander (Univ. of Chicago, Argonne Cancer Research Hospital, Chicago). Annu. Rev. Med.; 20: 131-40(1969).

The chemical and physical properties of ^{99m}Tc are reviewed. The use of ^{99m}Tc-labeled compounds for scanning the brain, thyroid gland, lungs, reticulo-endothelial system, and kidney, for dynamic studies of blood circulation, and as a γ source for transmission scanning of lung anatomy in human patients is discussed. (67 references) (C.H.)

2581 VISUALIZATION OF ORGANS BY MEANS OF RADIONUCLIDES. Persson, Jan (Institutt for Atomenergi, Kjeller, Norway). Norsk Farm. Tidsskr.; No. 19, 537-44(1 Oct 1970). (In Norwegian).

After a general description of the principles of γ scanning using a scintillation camera, the uses of this method of visualizing the distribution of radioactivity within an organ such as the thyroid, lung, kidney, spleen, liver and brain are briefly described and the radioisotopes normally used for these examinations, and their specific activities and resulting doses are mentioned. The increasing use of ^{99m}Tc is noted and some remarks are made on the preparation of ^{99m}Tc-labeled products and on the contribution

XUM

the hospital pharmacist can make to nuclear medicine by making these available in a pharmaceutically safe form. (Norway)

Radiotherapy

Refer also to abstracts 2531 and 3473.

2582 (CONF-700322–, pp 393-406) FAST NEUTRON RADIOBIOLOGY AND RADIOTHERAPY. Boone, M. L. M.; Hevezi, J. M. (Wisconsin Univ., Madison).

From Proceedings of the second Oak Ridge conference on the use of small accelerators for teaching and research, March 23–25, 1970.

Fast neutrons appear to offer a number of advantages in the treatment of malignant disease over conventional x-ray modalities. These advantages are based on physical and radiobiological considerations pertaining to the ionization density produced by the radiation and the consequent biological responses to fast neutrons. Anoxic tumor cells are protected from the ionizing effects of conventional x irradiation by a dose modifying factor of 2 to 3 compared to well-oxygenated normal cells. It was found experimentally that this protection diminished as the ionization density produced by the radiation increased. Fast neutrons give rise to directly ionizing protons and other densely ionizing nuclear species in tissue and these particles are much more effective in dealing with the anoxic tumor cells than lightly ionizing electrons liberated by x irradiation. With the advent of new data supporting fast neutron radiotherapy, the Hammersmith group in London began treating patients with fast neutrons produced by a cyclotron. In general, the early results from the program are encouraging. Many tumors have regressed completely without the complications which plagued the Stone therapy program. The recent availability of D – T neutron generators capable of producing quantities of 14 MeV neutrons having favorable characteristics for use in fast neutron therapy may open the field to those centers without cyclotrons. Neutron source strengths obtainable with these machines are somewhat lower than desirable but this problem is being attacked by several groups of investigators. (auth)

2583 RADIOLOGIC SIDE-EFFECTS. INTRODUCTION. Scheer, K. E. Langenbecks Arch. Chir.; 325: 991-3(1969). (In German).

From the start, a sensible combination of the surgical procedure with radiotherapy and with cytostatic therapy should be planned for the treatment of malignant tumors. All three measures have unavoidable side effects of which the physician who is carrying out the treatment must be aware in order to be able to recognize complications in due time and thus be able to treat them. An additional danger is late damage after the application of ionizing radiation. In conclusion, late damage after the use of the radioactive contrast medium Thorotrast is discussed. (auth)

2584 COMPUTER PROGRAMS FOR IRRADIATION PLANNING IN HIGH-ENERGY THERAPY. Dobry, H.; Benedetti, G. R. (Siemens AG, Erlangen, Ger.). Electromedica; 38: 219-26(1970). (In German).

Data processing occupies a position of increasing importance in numerous fields of medicine. In radiotherapy the calculation of dose distributions is an essential future field of activity. The series of articles to be published will present a survey of the present state of the art in dose calculations for radiotherapy using electronic data processing, and an extensive description of programs developed for betatron and cobalt facilities. After a short explanation of the methods in question and of the program deck, the method of calculation for homogenous body cross sections is shown. (INIS) (S)

Radiation Effects on Animals

2585 ISOENZYME STABILITY IN HUMAN HETEROPLOID CELL LINES. Auersperg, N. (Univ. of British Columbia, Vancouver); Gartler, S. M. Exp. Cell Res.; 61: 465-7(Aug 1970).

A heteroploid human carcinoma cell line that retained the glucose-6-phosphate dehydrogenase (G6PD) in prolonged culture after serial irradiation is described. Cells were x-irradiated in doses of 100 to 1500 rads over a period of 30 months. In the course of the serial irradiation the chromosome number decreased from 120–130 to 59–62. Types of G6PD and phosphoglucomutase were determined after 41 months in culture. Results indicated that the transformation from a diploid to a heteroploid karyotype, as well as the prolonged culture of heteroploid human cells, was not invariably associated with and the appearance of type A G6PD. The persistence of the original G6PD type in the course of serial irradiation, in spite of a 50% reduction in chromosome number, supports previous indications of the stability of this isoenzyme in vivo and in vitro. (H.L.W.)

2586 ELECTROPHORETIC MOBILITY OF TUMOUR CELLS EXPOSED TO ULTRASOUND AND IONISING RADIATION. Repacholi, M. H. (Guy's Hospital Medical School, London). Nature (London); 227: 166-7(11 Jul 1970).

It is stated that little is known concerning the mechanism of interaction of combined ultrasound and ionizing radiation on cell surfaces, but success has been reported using such treatment on tumors. Ultrasonic radiation may remove mucropolysaccharide by shearing and streaming forces set up between the cell and the intercellular fluid, thus reducing the size of the surface charge. Ionizing radiation would then neutralize exposed groups, probably by free radical combination. In vivo, pre-irradiation with ultrasound might allow a reduction in x-ray dose required for tumor regression and enhance the action of lymphocytes. Some studies are described using Ehrlich ascites tumor cells extracted from mice. Electrophoretic mobility was measured at 25°C in a cylindrical electrophoresis cell, and results are shown in tabular form; histograms of the electrophoretic mobilities of cells exposed to x rays (55 R/min) and ultrasound (1 MHz, 10 W cm^{-2}, pulsed for 10 ms with 90 ms intervals for 5 min) are also shown. Exposure of cells to ultrasound and x rays (1000R) reduced the mobility by almost 30%, whereas ultrasonic radiation alone caused only a 16% reduction. The results appeared to indicate an additive effect. At the levels of ultrasound used the maximum shearing force acting on the cell was calculated as $\sim 2.5 \times 10^{-2}$ dynes, which exceeds the strength of the weakest covalent bonds in a macromolecule, and the ultrasound may thus be capable of shearing the mucopolysaccharide coat from the cell surface. (UK)

2587 RADIOLOGICAL STUDIES ON THE CHRONOLOGICAL RELATION BETWEEN MURINE SARCOMA VIRUS INFECTION AND CELL CYCLE. Yoshikura, H. (Faculte des Sciences, Orsay, France). J. Gen. Virol.; 8: 113-20(Aug 1970).

Intracellular replication of murine sarcoma virus was followed by Luria–Latarjet experiments. In experiments with unsynchronized cultures uv sensitivity of the cells infected with murine sarcoma virus as focus centers increased with the lapse of time after infection, and 16 hr after infection uv-resistant cells appeared that were probably producing mature virus. The uv-resistant population continued to increase thereafter. Ultraviolet sensitivities as focus centers of synchronized cells infected with murine sarcoma virus at different periods of the cell cycle were compared 23 hr after infection. The cells infected with the virus in the G I phase remained more sensitive to uv light than those infected with the virus in the S phase, i.e., the latent period was longer after G I phase infection than after S phase infection. An antimitotic agent colchicine, prevented the increase of uv resistance of the cells as focus centers. These facts suggest that murine sarcoma virus infection requires the division of the host cells and that virus replication is synchronized at this stage of the cell cycle. (auth) (UK)

Invertebrates

Refer also to abstracts 2539 and 2554.

2588 EFFECT OF X-IRRADIATION ON HYDRA IN THE PRESENCE OF ARGININE AND CITRULLINE AND STUDY OF THE RADIOLYTIC PRODUCTS. Podder, N. G. (Saha Inst. of Nuclear Physics, Calcutta); Mookerjee, A.; Saha, N. N.; Palit, R. Indian J. Exp. Biol.; 8: 37-8(Jan 1970).

Effects of x irradiation (25 kR) on the behavior and morphology of hydra in presence of arginine and citrulline were studied; the breakdown products due to irradiation of these amino acids were detected. The average mortality of hydra was 15% in arginine and 58% in citrulline and the average latent periods of survival in arginine and citrulline were 20 and 10 days respectively. Ammonia and formaldehyde were detected in irradiated amino acids. The results indicate that arginine is more radiosensitive when compared to distilled water and hydra culture solution, but is less radiosensitive when compared to citrulline. The greater degree of radiosensitivity of citrulline may be attributed to its degree of deamination. (auth)

Vertebrates

Refer also to abstracts 2538, 2540, 2553, 2558, and 2576.

2589 ABSENCE OF THYMIC INVOLVEMENT IN THE INHIBITION OF URETHAN LUNG ADENOMAGENESIS BY X-RADIATION. Bartlett, Gerald L. (Inst. for Cancer Research, Philadelphia, Univ. of Pennsylvania, Philadelphia). Int. J. Cancer; 5: 384-8(1970).

Since regional thoracic irradiation involves the thymus, as well

as lung tissue, inhibition of urethan lung adenomagenesis by thoracic irradiation might be mediated by radiation damage to the thymus. Experiments which show that lung tumor induction is not inhibited by surgical removal of the thymus and that the inhibitory effect of radiation is not reversed by grafts of normal thymus tissue are reported. Hence, the thymus is not essential to pulmonary adenomagenesis, and does not mediate the inhibitory effect of radiation. (auth) (Denmark)

2590 KINETIC MODEL OF STEM-CELLS AND PROERYTHROBLASTS POPULATIONS IN THE POSTIRRADIATION BONE MARROW INJURY. **Hradil, J.; Smid, A.; Mraz, J. (Purkyne Medical Research and Postgraduate Inst., Hradec Kralove, Czech.). Atomkernenergie; 16: 155-8(1970).**

An analog computer model expressing some features of erythropoiesis, especially the relations between the stem-cells and proerythroblasts populations, was developed. Two proportional plus integral action controllers work inside this system. These controllers are governing and checking the sizes of both compartments, the rates of cell differentiation and division. During the first phase of the radiation injury development a secondary decrease of stem-cells can be seen. A predominance of R_2 controller ensuring the function of proerythroblasts population and-consequently-the erythroid cells production is obvious. Later a predominance of R_1 controller appears. R_1 controller demonstrates the function of a mitotic inhibitor-chalone-acting in the sphere of the stem-cell population. Curves expressing the behavior of investigated cell populations were similar in testing animal experiments. (Irradiated rats were given allogenic bone marrow cells.) The model system employing quantitative changes of proerythroblasts is yielding some information about the behavior of the stem-cell population, above all about the output of cells for differentiation in erythropoiesis, about the recovery of the stem population size. By means of this model the rates of processes and their interrelations can be investigated. (auth)

2591 NEW OCULAR HAZARD OF MODE LOCKING IN CW LASERS. **Smart, D. (International Research and Development Co. Ltd., Newcastle-upon-Tyne, Eng.); Manson, N.; Marshall, J.; Mellerio, J. Nature (London); 227: 1149-50(12 Sep 1970).**

In experiments with rabbits to investigate threshold retinal damage produced by CW He–Ne lasers (Wavelength 632.8 nm) it was found that lasers with identical beam divergence and output power, but different amplifier/cavity parameters, produced different amounts of retinal damage. The source of this was traced to mode locking. The retinal damage was observable as small white spots, and damage in the pigment epithelium and receptor cells was shown under the electron microscope. A laser with a long cavity and high gain can be made to mode lock by introducing an absorption cell of excited Ne into the cavity, and when mode locked the laser generates a train of very high frequency pulses instead of a continuous output. Loss mechanisms in a multi-mode laser cavity, other than an absorption cell, can also mode lock the system. The peak power in a mode locked pulse is greater than the mean power by the ratio of the pulse repetition period to the pulse half-width, that in the case described was about 8, but could be 35 to 40. Pulsed laser studies showed that the parameter that determines whether the retina is damaged is retinal peak power density, and with a mode locked laser, the output of which is monitored with a conventional power meter, the retinal power density may be an order of magnitude greater than expected. (UK)

2592 FURTHER STUDIES ON THE RADIOSENSITIVITY OF THE RAT INCISOR. **Koppang, Hanna Stromme; Stokke, Torvald (Univ. of Oslo). Odontol. Tidskr.; 77: 47-61(15 Feb 1969).**

At higher dose levels (≅600r) lesions occurred to approximately the same extent in superior and inferior incisors. At lower doses (≅500r) lesions prevailed in superior incisors. With the exception of one observation (in a superior incisor after 400r), lingual lesions were diagnosed after 700r only, and in superior and inferior incisors to the same extent. Left and right incisors presented lesions with approximately the same frequency. (auth)

2593 EFFECTS OF MATERNAL X-IRRADIATION OF MICE ON THE GERM CELLS OF THEIR PROGENY. **Palayoor, Thomas; Batra, B. K. (Tata Memorial Centre, Bombay). Indian J. Exp. Biol.; 7: 89-92(Apr 1969).**

The germ cells of the progeny of adult female mice, x-irradiated and mated with their untreated brothers, were studied quantitatively at specific pre- and post-natal ages. At 16 days post coitum a numerical reduction of pre-leptotene and leptotene oocytes with a corresponding increase in zygotene and pachytene oocytes was observed. Higher rate of degeneration of oocytes was observed among all the age groups studied. The total oocyte count registered a marked fall when the animals attained puberty. It is suggested that irradiation of female mice eventuates disturbances in the normal pattern of germ cell development and the control of their population in the progeny. (auth)

2594 FINE STRUCTURE OF OSTEOSARCOMATA PRODUCED EXPERIMENTALLY IN RATS. **Cameron, D. A. (Sydney Univ.). Pathology; 2: 223-30(Jul 1970).**

Osteosarcomata induced in rats by ^{32}P injections had histological appearances resembling those in other experimental animals and in man. The fine structure of most of the component cells was like that generally ascribed to malignant cells and their structural organization was much more simplified than that of preosteoblasts undergoing hyperplasia in repair. They had relatively inconspicuous Golgi zones, limited endoplasmic reticulum and few mitochondria and it seemed unlikely that they played much part in matrix synthesis. Other cells more closely resembled osteoblasts and they were probably derived from the more primitive tumour cells rather than directly from the original bone cells. Presumably they secreted the matric component of the hard tissue of the tumours. This matrix did not have any features labeling it neoplastic and its fine structure resembled that of fracture callus. Calcification patterns did not differ from the normal. Cells were included within the matrix and were analogous to osteocytes although some of the superficial ones had features of the undifferentiated cells. The few multinucleated cells present resembled osteoblasts although most of them seemed to be non-functioning and lacked a brush border. The thin-walled blood vessels traversing the tumours were lined by endothelial cells and not by tumour cells. (auth) (Australia)

2595 STUDY OF THE BEHAVIOR OF NORMAL AND IRRADIATED BONE MARROW BY AN INTRAOCULAR TRANSPLANT TECHNIQUE. **Le Go, Roland; Gholamreza, Djalali-Behzad (CEN, Fontenay-aux-Roses, France). Compt. Rend., Ser. D; 270: 3144-7(22 Jun 1970). (In French).**

The technique of grafting in the anterior chamber of the eye was used to study the behavior of irradiated bone marrow in normal rats. The irradiated marrow, isolated by transplant to a nonirradiated medium, from the influence of humoral factors resulting from irradiation of the donor, shows an excellent proliferation potential even at lethal doses. (auth) (France)

Man

Refer also to abstracts 2535 and 2567.

Radiation Effects on Plants

Refer also to abstracts 2552 and 2555.

2596 MODIFICATION OF ACTIVITY OF CERTAIN REDOXY ENZYMES IN THE SPROUTS OF BEANS AND CLOVER FOLLOWING gamma IRRADIATION OF SEEDS. **Kuzin, A. M.; Seisebaev, A. T.; Babaeva, M. K. (Inst. of Biophysics, Moscow. Inst. of Experimental Biology, Alma-Ata, USSR). Izv. Akad. Nauk Kaz. SSR, Ser. Biol.; No. 4, 69-74(1968). (In Russian).**

It was found that γ-irradiation of fodder bean (of violet color) and red clover by 0.1 and 10 kR induced certain shifts in the catalase and peroxidase activity. At the beginning of the experiment it was increased and toward the end it was inhibited. No correlation was found between the variations of the activity level of cytochromeoxidase and the radiosensitivity of the plants studied. It was assumed that the different levels of variations of catalase activity and peroxidase during seed irradiation was related to the variable radiosensitivity. (R.V.J.)

2597 ACTION OF PLANT HORMONES ON DYNAMICS OF NUCLEIC ACIDS IN GROWING SPIKES OF IRRADIATED BARLEY PLANTS. **Zabolotskii, N. N.; Voronova, G. D. (All-Union Scientific Research Inst. for Fertilizers and Agricultural Soils, Moscow). Dokl. Akad. Nauk SSSR; 192: 1371-3(21 Jun 1970). (In Russian).**

Exposure of plants to ionizing radiation results in the breakdown of the biosynthetic system of the plant hormones involving disturbances in the formation of RNA and DNA. The radioprotective action of gibberellic acid (GA) and indolyl acetic acid (IAA) is probably due to the activation of the synthesis suppressed by the radiation. This problem was further examined by determining the effect of GA and IAA on the growth of barley spike. Because of their highly radiosensitive tissue, the spikes are well suited for such a study. The Viner type growing barley plants were exposed to 1700 R from a ^{60}Co γ source. GA or IAA was introduced within two days at a rate of 20 μg or 0.5 μg, respectively. The results indicated that both GA and IAA regenerate the growth of the spikes that was slowed down by exposure to γ radiation. The regeneration is related to the activation of the biosynthesis

XUM

of the nucleic acid due to the interaction of the plant hormones. It was concluded that the breakdown of the nucleic acid biosynthesis is not due to the apparatus involved in the biosynthesis but to interference in the highly radiosensitive process involved in the transinduction of DNA that in turn depends on hormonal activity. (TTT)

Radiation Effects on Microorganisms

Refer also to abstracts 2556 and 2557.

2598 EVIDENCE FOR THE CONTROL OF RESPIRATION BY DNA IN ULTRAVIOLET-IRRADIATED ESCHERICHIA COLI B/r CELLS. Swenson, O. A.; Schenley, R. L. (Oak Ridge National Lab., Tenn.). Mutat. Res.; 9: 443-53(May 1970).

Ultraviolet irradiation of Escherichia coli B/r cells causes a temporary inhibition of respiration. This inhibition begins about 60 min after irradiation. The duration of the inhibition depends, in part, upon the carbon source on which the cells were grown and its presence or absence at the time of irradiation. In cells grown on a mineral salts and glycerol medium irradiation with 520 erg/mm^2 at 254 nm almost completely inhibits respiration for 4 hr. The addition of exogenous amino acids to the growth medium favors early recovery of respiration. Experiments with caffeine show that excision of pyrimidine dimers is not necessary for the delayed inhibition of respiration, but is necessary for the subsequent recovery of respiration. If chloramphenicol, 5-fluorouracil, or an amber mutant of phage T4 is added to cells immediately after uv, the turnoff of respiration is prevented, but none of these agents reverses the inhibition once it has set in. These results indicate that uv-damaged DNA is transcribed and a protein important for the turnoff of respiration is formed. (auth)

2599 RECOVERING SPORES DAMAGED BY HEAT, IONIZING RADIATIONS, OR ETHYLENE OXIDE. Roberts, T. A. (Meat Research Inst., Bristol, Eng.). J. Appl. Bacteriol.; 33: 74-94(Mar 1970).

Factors affecting the recovery of spores damaged by heat, ionizing radiation and ethylene oxide are reviewed and discussed. Further data are presented for spores of a range of Clostridium sp. The sensitization of spores of Clostridium botulinum type A to sodium chloride by heat γ radiation, and combinations of γ radiation and heat was used to illustrate the effect of damage on the inhibition of growth. Attempts to maximize recovery showed Most Probable Number (MPN) counts to be no higher than plate counts in the same medium solidified with agar and incubated anaerobically. Media giving the greatest recovery (i.e. highest viable count) of undamaged spores did not necessarily give the greatest recovery of damaged spores. The use of additives such as starch, bicarbonate and germinants in counting media is discussed. Recovery of undamaged spores was not increased by sodium bicarbonate, but counts of heated and irradiated spores were increased by the addition of sodium bicarbonate to the plating medium. No increase in count was noted with any of the germinants studied. The optimum temperature for recovery of undamaged spores differed from that for damaged spores. The optimum pH was about the same for undamaged and damaged spores but growth of the former occurred over a wider pH range. Attempts to demonstrate repair of damage in spores of Clostridium sp. stored at 5 to 35° were unsuccessful. (auth)

XUM

METALS, CERAMICS, AND OTHER MATERIALS

Metals and Alloys

Refer also to abstracts 2379 and 3025.

2600 (BNL–50258) HIGH-TEMPERATURE LIQUID-METAL TECHNOLOGY REVIEW. A Bimonthly Technical Progress Review. Volume 8, Number 3. (Brookhaven National Lab., Upton, N. Y.). Jun 1970. 35p. Dep. NTIS.

Brief reviews are presented on information associated with liquid metal thermodynamics, fluid dynamics, heat transfer, corrosion, instrumentation, chemistry, component design, fabrication methods, safety, and metal purification. (J.R.D.)

2601 (ORNL–4570) METALS AND CERAMICS DIVISION ANNUAL PROGRESS REPORT FOR PERIOD ENDING JUNE 30, 1970. Peterson, Sigfred (comp. and ed.) (Oak Ridge National Lab., Tenn.). Oct 1970. Contract W-7405-eng-26. 257p. Dep. NTIS.

Research progress is reported in 47 sections. A separate abstract was prepared for each section. (J.R.D.)

For abstracts of individual sections see: 2408, 2409, 2602, 2605–2610, 2641–2645, 2668–2677, 2727–2731, 2758, 2759, 2768–2772, 2786–2792, 2805, 2816, 2817, and 2820.

2602 (ORNL–4570, pp 191-4) REACTOR EVALUATION. (Oak Ridge National Lab., Tenn.).

From Metals and Ceramics Division annual progress report for the period ending June 30, 1970.

Efforts devoted to evaluating and optimizing the reactor designs by analyzing the cost of fuel fabrication and evaluating the performance of nuclear fuels are reported. The basic computer code for fabrication cost analysis was modified to extend and refine its capabilities in examining various cladding and structural materials and to analyze more thoroughly cost of fuel preparation by pelletization. Also, a number of cost analyses for reactor fuel elements and on various fabrication processes for fuel elements were performed. The release of fission gases from mixed oxide fuels was investigated. The physical and tensile properties of Type 316 stainless steel were tabulated. The nuclear performance feasibility of molybdenum fuel cladding in an LMFBR was assessed. (auth)

Corrosion and Erosion

Refer also to abstract 2765.

2603 (AEC-tr–7096) RADIATION CORROSION. Byalobzheskii, A. V. Translation of Radiatsionnaya Korroziya, Izdatel'stvo Nauka, Moscow, 1967. 188p. (TT–70-50005; IPST-Cat.–5655). Dep. NTIS.

This book was abstracted from the original language and appeared in NSA as 22: 45750. (J.R.D.)

2604 (CONF-700322–, pp 155-71) APPLICATION OF HIGH-VELOCITY IONS TO METALLURGY RESEARCH. Needham, Paul B. Jr. (Bureau of Mines, College Park, Md. College Park Metallurgy Research Center).

From Proceedings of the second Oak Ridge conference on the use of small accelerators for teaching and research, March 23–25, 1970.

The equipment and methods used in conjunction with a 300 kV accelerator facility for fundamental research at the College Park Metallurgy Research Center (Maryland) are described. Problems such as oxidation, corrosion, and alloy techniques are being approached on an atomistic basis using several of the well-known interactions of charged particles with solids. Elastic and inelastic particle interactions with amorphous, polycrystalline and single crystal materials are being studied to explain the fundamental knowledge of oxidation kinetics, how corrosive environments initiate corrosion, the interaction of "real" metal surfaces with their environments, and how alloying elements alter the structure of metal surfaces. Experimental results on x-ray production cross-section and x-ray spectra studies of the oxidation kinetics of high-purity iron at moderate temperatures are presented. (L.C.L.)

2605 (ORNL–4570, pp 37-9) SURFACE REACTIONS OF METALS. (Oak Ridge National Lab., Tenn.).

From Metals and Ceramics Division annual progress report for the period ending June 30, 1970.

A model was developed for the oxidation of the ternary alloy U–7.5 wt % Nb–2.5 wt % Zr and the binary U–9.4 wt % Nb. Transient stresses on the order of 10^6 psi exist at the oxide-metal interface of these alloys, and these stresses can trigger phase transformations in the alloy and control oxide morphology. Flexure studies with tantalum at 550 to 850°C provided data for computing strain, strain energy, and stress levels that develop in the oxide and metal as tantalum oxidizes. Average stresses in excess of 10^6 psi exist in the oxide. Results of a flexure technique use also showed how specimen geometry and mechanical inhomogeneities may cause uniaxial bending to result from the uniform biaxial stress produced during oxidation. A study of the oxidation characteristics of the tantalum–tungsten alloys was initiated, in which a submicron, anodic-film sectioning technique was used in investigating possible small differences in the activation energy for diffusion of various tracer elements in tungsten. (auth)

2606 (ORNL–4570, pp 92-5) SODIUM CORROSION IN LMFBR SYSTEMS. (Oak Ridge National Lab., Tenn.).

From Metals and Ceramics Division annual progress report for the period ending June 30, 1970.

Various vanadium alloys were tested in capsules at 600°C to determine the effect of alloying elements on the reactivity of vanadium with impurities in sodium. Additions of both chromium and molybdenum to vanadium lower the affinity of vanadium for oxygen in sodium. The creep properties of vanadium were measured in vacuum and in low-pressure oxygen. The absorption of oxygen by vanadium during the creep test increased the creep rate at 600°C. However, the addition of 470 ppM O to the vanadium before creep testing had little effect on the creep rate at 600°C in vacuum. The simultaneous exposure of vanadium and Type 304 L stainless steel to sodium resulted in the mass transport of carbon and nitrogen to the vanadium, embrittling it within 3000 hr at 800°C. However, similar exposures to Type 321 stainless steel did not affect the mechanical properties of the vanadium. The oxidation behavior of Types 304 and 316 stainless steel was studied at 760°C in moist air and in a mixture of N_2–1% O_2–100 ppM H_2O. Type 316 stainless steel showed poorer resistance to scaling in moist air than did Type 304. However, both steels underwent negligible oxidation in the nitrogen mixture. Contacting the steels with Al_2O_3–SiO_2 thermal insulation did not affect their oxidation behavior in either test environment. Sodium accelerated the oxidation of Type 304 stainless steel in the nitrogen mixture when the sodium was introduced through a small crack in the stainless steel. However, increasing the sodium leak rate caused the sodium to move into surrounding thermal insulation, and the stainless steel specimen oxidized much less. (auth)

2607 (ORNL–4570, pp 103-5) ALKALI-METAL CORROSION OF REFRACTORY METALS. (Oak Ridge National Lab., Tenn.).

From Metals and Ceramics Division annual progress report for the period ending June 30, 1970.

A model was developed for the penetration of alkali metals into oxygen-contaminated tantalum and niobium. It was established that temperature-gradient mass transfer of zirconium and hafnium in refractory-alloy systems containing lithium is controlled by solid-state diffusion. To investigate the compatibility of materials with lithium under engineering conditions, a large T-111 forced convection loop was operated under conditions anticipated for the primary system of an advanced high-temperature space reactor. The loop was operated for 3000 hr at a 1370°C heater exit temperature. One field repair was required after 1750 hr to remove a leaking vent line. (auth)

2608 (ORNL–4570, pp 124-6) CORROSION OF ADVANCED STEAM GENERATOR ALLOYS. (Oak Ridge National Lab., Tenn.).

From Metals and Ceramics Division annual progress report for the period ending June 30, 1970.

Field corrosion tests of welds in advanced steam generator alloys are being conducted using steam. General corrosion is assessed by determining attack rates, characterizing scales, and calculating long-term corrosion from weight-gain data. Susceptibility to preferential corrosion is determined by examining for knife-line attack at weld fusion lines and by conducting U-bend tests. Inconel 625, Hastelloy X, and IN 102 as both base and filler metals, Incoloy 800 as base metal, and Inconel 82 as filler metal exhibited very good corrosion resistance at both 595 and 650°C. Welds containing Inconel 600 and austenitic stainless steel exhibited somewhat inferior behavior. No preferential or unusual attack was noted. (auth)

2609 (ORNL–4570, pp 175-90) MOLTEN-SALT REACTOR PROGRAM. (Oak Ridge National Lab., Tenn.).

From Metals and Ceramics Division annual progress report for the period ending June 30, 1970.

XUM

Samples of Hastelloy N and graphite were removed from the MSRE after 22,533 hr at 650°C. They were compatible with the fluoride salt environment; however, the Hastelloy N was embrittled by the thermal neutron irradiation. Development of a Hastelloy N of modified composition that has improved postirradiation ductility is reported. Additions of Ti, Hf, and Nb produced the finely dispersed MC-type carbide believed to be responsible for the improved properties. Some 50- to 100-lb commercial heats of this material have been procured; their fabricability and weldability are excellent. Continuing corrosion tests on standard Hastelloy N show that it has excellent compatibility with salts containing LiF, BeF_2, UF_4, and ThF_4. A higher corrosion rate was observed in the proposed new coolant salt, $NaBF_4$–8 mole % NaF. This higher rate is at least partially attributable to the ease with which this salt picks up moisture. Hastelloy N showed good compatibility with steam in tests to 6000 hr. Graphite test bodies from various cokes were fabricated for testing. The most isotropic bodies were produced from Robinson coke. In irradiation studies on numerous graphites, the crystallite growth rates decreased with increasing isotropy and with increasing crystallite size. Metallographic studies revealed the deterioration of the particle–particle boundaries and have emphasized the need for better binder materials. Several techniques were developed for reducing the surface permeability of graphite to gaseous fission products. The first irradiation of samples so treated showed an increase in the permeability after a fluence of about 1×10^{22} neutrons/cm^2 (>50 keV). The chemical compatibility of several materials with bismuth has been studied. Molybdenum, TZM, and Mo–0.5% Ti exhibited excellent compatibility, but Nb and Nb–1% Zr mass transferred very badly. Methods of putting adherent coatings of W and Mo on Ni- and Fe-base alloys have been partially developed. A molybdenum test stand for Chemical Technology Division experiments involving bismuth is being fabricated. This has involved the development of back-extrusion techniques for making 4-in.-dia. vessels and welding and brazing methods. (auth)

2610 (ORNL–4570, pp 205-12) WATER REACTOR SAFETY. (Oak Ridge National Lab., Tenn.).

From Metals and Ceramics Division annual progress report for the period ending June 30, 1970.

The deformation and rupture of Zircaloy-clad fuel rods during the thermal transient associated with a loss-of-coolant accident in a light-water reactor may play an important role in determining whether the outcome of such an accident is acceptable. Therefore, the failure of these rods in terms of their environmental history is being examined. Postulated accident conditions are also considered in assessing the effect of failure on the termination of the accident transient. The high-temperature deformation of Zircaloy is also being studied. (auth)

2611 (PEL–201) OXIDATION OF ZIRCONIUM ALLOY IN LIQUID SODIUM AT DIFFERENT OXYGEN LEVELS. Slatter, D. De L. (Atomic Energy Board, Pelindaba, Pretoria (South Africa)). Jun 1970. 19p Dep. NTIS (U. S. Sales Only).

Previous work on the corrosion of the zirconium alloy 3Z1 in sodium is reviewed. The reported anomalous corrosion behavior of this alloy between 400 and 500°C, where it shows a transition from a parabolic to a linear corrosion rate law, is based on work carried out at one specific oxygen concentration in the sodium. Results of an investigation of corrosion at different sodium oxide levels are presented. The experimental work was carried out in a sodium tank from which a small stream of sodium could be circulated through a cold trap to adjust the oxide level. The latter was established by periodically withdrawing samples and analyzing them by a vacuum distillation technique. Specimens of zirconium and 3Z1 were exposed to the sodium in the tank for 4 to 400 hours at oxygen levels of 30 and 100 ppM. The results were evaluated by weight change measurements, macroscopic and microscopic examination, x-ray diffraction and electron microprobe analysis. A special polishing technique had to be developed for the metallographic specimens. The 3Z1 specimens were found to form thick, dark oxide layers which progressively became less adherent with increase in corrosion time. This effect was less severe for sodium containing 30 ppM oxygen. The corrosion process followed an approximately linear oxidation law until break-away occurred. The oxidation commenced with a thin, adherent layer, growing in preferred localities which eventually coalesced to form very uneven surfaces prior to break-away. Break-away seems to occur within the oxide itself only when the layer reaches a certain thickness, and not at the metal/oxide interface. Attempts to correlate oxide growth localities with the phase structure of the parent metal were unsuccessful. Microprobe examination to determine compositional differences between the phase was inconclusive, as were efforts to determine, by x-ray diffraction, whether break-away was the result of structural changes within the oxide. In contrast, the zirconium in all cases formed a perfectly adherent thin oxide film and followed a parabolic corrosion law. The type 304 constructional material of the corrosion apparatus showed negligible corrosion. (auth)

2612 MECHANICAL PROPERTIES AND CORROSION RESISTANCE OF STEEL COATED WITH TITANIUM AND ZIRCONIUM CARBONITRIDES. Sintsova, I. T.; Kozlovskii, L. V. (Technological Inst., Leningrad). Zashch. Metal.; 6: 616-21 (Sep-Oct 1970). (In Russian).

Repeated diffusive saturation of steel with titanium and zirconium, applied in the form of powder, resulted upon heating of the system at 900 to 1150°C in a vacuum furnace, in the formation of a saturated system which was then carbonitrided to form a protective surface coating. In order to prevent the formation of a low-melting eutectic mixture between the diffusing metals and the steel base, Al_2O_3 was mixed with the refractory metal powder, and the mixture calcined to remove adsorbed hydrogen, water, and organic residues. Acetylene carbon black was used for carburizing and carbonitriding of the metallized specimens. The titanium-coated specimens exhibited a higher tensile strength than those coated with zirconium, because saturation with zirconium takes place more slowly. The higher atomic diameter of zirconium makes it more difficult to form substitution solid solutions. Carburization increased especially markedly the strength of forged steel specimens. The carbonitriding process also increased the wear resistance of the surface layer and the corrosion resistance without affecting the mechanical strength of the steel. (TTT)

2613 CORROSIVE BEHAVIOR OF ALLOYS OF THE TITANIUM–MOLYBDENUM–CHROMIUM SYSTEM. Tomashov, N. D.; Ruskol, Yu. S.; Filippov, A. F.; (and others) (Inst. of Physical Chemistry, Moscow). Zashch. Metal.; 6: 499-504 (Sep-Oct 1970). (In Russian).

The effect of chromium on the corrosion resistance of Ti–5% Mo and Ti–10% Mo alloys was investigated by a potentiometric method; the corrosion rate was determined on the basis of the current and weight loss measurements. The series tested included alloys containing 1, 3, 5, and 10% Cr in addition to the 5 or 10% Mo; a Ti–10% Cr alloy was also included. It was found that the β phase of Ti alloys, containing a stabilizing component, such as Mo, possesses an increased corrosion resistance, even when the two-phase $\alpha + \beta$ alloys are accumulated at the surface. In nonoxidizing media, the corrosion of the Ti–Mo–Cr alloys is decreased after introduction of sufficient amount of Cr, forming the single-phase β alloys. The alloys with an $\alpha + \beta$ structure exhibit the same corrosion rate as the Ti–Mo alloy. At potentials more positive than 1.2 V, the corrosion rate of the Ti–Mo–Cr alloys starts to increase. (TTT)

2614 STRESS CORROSION CRACKING OF PROCESS EQUIPMENT. Ashbaugh, W. G. (Union Carbide Corp., Texas City, Tex.). Chem. Eng. Progr.; 66: No. 10, 44-7 (Oct 1970).

Principles and parameters of stress cracking failures in materials are reviewed. Examples of chloride and caustic stress cracking in Inconel, stainless steel, and carbon steel are discussed. (J.R.D.)

2615 CORROSION BY LIQUID METALS. Proceedings of the Sessions on Corrrosion by Liquid Metals of the 1969 Fall Meeting of The Metallurgical Society of AIME, October 13–16, 1969, Philadelphia, Pennsylvania. Draley, Joseph E.; Weeks, John R. (eds.). Metallurgical Society of AIME Proceedings. New York; Plenum Publishing Corporation (1970). 625p. $29.00. (CONF-691007).

A total of 34 papers was presented at the meeting. A separate abstract was prepared for each of 27 papers. The remaining 7 papers were not within the scope of NSA. (G.M.C.)

For abstracts of individual papers see: 2205, 2616–2631, and 2705–2714.

2616 EVALUATION OF PARTICULATES DEPOSITED IN FLOWING NON-ISOTHERMAL SODIUM SYSTEMS. Roy, Prodyot; Dutina, Dragomir; Comprelli, Frank (General Electric Co., San Jose, Calif.). pp 1-20 of Corrosion By Liquid Metals. /Draley, Joseph E. (ed.). New York; Plenum Publishing Corp. (1970).

From Corrosion by Liquid Metals Conference, Philadelphia, Pa. See CONF-691007.

Recent experimental evidence suggests that the corrosion and deposition processes in a flowing non-isothermal sodium system are interdependent, and each exerts considerable influence over the extent and characteristics of the other. Therefore, a performance analysis of non-isothermal sodium systems must consider these processes as complementary and equal in significance to the overall system behavior. This report will focus on the factors which influence the composition and structure of particulates (deposits) and the location and rate at which they are de-

XUM

posited. In order to explore these factors, deposits from several areas were removed from experimental facilities for study. An analysis was completed on particulates collected from corrosion specimens positioned in the initial regions of cooled sections (1200 to 1070°F); the piping of an economizer (300 to 700°F); and a nickel filter (600°F). The particulates examined from each temperature region had distinct compositional characteristics and morphology. Based on these observations, relationships are proposed between the mechanisms of deposition of corrosion products and the structure and composition of the deposit at each temperature range examined. (auth)

2617 INTERACTION EFFECTS BETWEEN DISSIMILAR METALS IN HIGH VELOCITY SODIUM AT TEMPERATURES UP TO 760°C. I. MASS TRANSFER OF VANADIUM ONTO TYPE 321 STAINLESS STEEL. Romano, A. J.; Wachtel, S. J.; Klamut, C. J. (Brookhaven National Lab., Upton, N. Y.). pp 21-31 of Corrosion By Liquid Metals. /Draley, Joseph E. (ed.). New York; Plenum Publishing Corp. (1970).

From Corrosion by Liquid Metals Conference, Philadelphia, Pa. See CONF-691007.

Comparative corrosion studies are being carried out with potential fuel cladding materials for advanced Liquid Metal Fast Breeder Reactors. The materials under test at temperatures as high as 760°C include refractory metal-base, cobalt-base, and iron-base alloys. Two pumped loops, made entirely of stabilized stainless steels, are used to carry out the investigations. The corrosion specimens are exposed to high velocity sodium (22 ft/sec) in a 24''-long rising temperature region (between 710° and 760°C). In the tests, the oxygen content of the sodium was controlled over the range from <1 to 15 ppM. Post-test examination showed dissimilar metal mass transfer. In tests containing V-base alloys, significant amounts of V were detected on the surfaces of type 321 stainless steel specimens. X-ray fluorescence analysis showed that about 25 times more V was present on the surface of an exposed sample than on an unexposed standard. Microprobe analysis of two type 321 SS specimens that were exposed simultaneously throughout the entire run but at opposite ends of the test section, i.e., 710° vs 760°C, showed that the difference in their corrosion behavior was the depth to which the V penetrates each sample, not the surface concentration of V. In general, increased temperature, exposure time and oxygen concentration in the sodium appeared to increase the extent of dissimilar metal reactions. (auth)

2618 CORROSION OF TYPE 316 STAINLESS STEEL WITH SURFACE HEAT FLUX IN 1200°F FLOWING SODIUM. Hopenfeld, J. (Atomics International, Canoga Park, Calif.). pp 33-9 of Corrosion By Liquid Metals. /Draley, Joseph E. (ed.). New York; Plenum Publishing Corp. (1970).

From Corrosion by Liquid Metals Conference, Philadelphia, Pa. See CONF-691007.

The corrosion behavior of Type 316 stainless steel in flowing sodium was studied. The main features of the experimental loop were that the sodium at the inlet to the test section was saturated with corrosion products and the surface temperature of the test sample varied along its length and was always higher than the local bulk sodium temperature. The corrosion rate for Type 316 stainless steel in 1266°F sodium, flowing at 20.5 ft/sec, was determined to be 0.72 mils/yr. (G.M.C.)

2619 SODIUM CORROSION OF WESTINGHOUSE LIQUID METAL FAST BREEDER REACTOR (LMFBR) MATERIALS. Schrock, S. L.; Baysden, J. N.; Miller, R. L.; Lohr, D. E. (Westinghouse Electric Corp., Madison, Pa.). pp 41-62 of Corrosion By Liquid Metals. /Draley, Joseph E. (ed.). New York; Plenum Publishing Corp. (1970).

From Corrosion by Liquid Metals Conference, Philadelphia, Pa. See CONF-691007.

The sodium corrosion program on LMFBR materials concentrated primarily on the combination of Type 316 stainless steel (cladding) and Type 304 stainless steel (I.H.X. tubing) for the primary system, and the combination of Type 304 stainless steel (I.H.X. tubing) and Incoloy 800 (steam generator tubing) for the secondary system. To date, eight loop runs were completed on both types of systems which represented approximately 20,000 hours of operation at maximum temperatures ranging from 900 to 1325°F. The loops used in this program were designed as system mock-ups of the LMFBR. Parameters and ranges investigated during this program include temperature (900 to 1325°F), temperature difference, ΔT, (200 to 300°F), sodium oxide levels (<10 to ~25 ppM), velocity (3 to 20 fps), time (up to 10,000 hours), and material combinations. When the maximum temperature of the primary system (316 stainless steel–304 stainless steel) was 1100°F, the oxide level was less than 10 ppM, the ΔT was 300°F, and the velocity was 7 fps, the corrosion rate at 2500 hours was approximately 0.09 mils per year; if the velocity is increased to 20 fps, the corrosion rate was approximately 0.11 mils per year, indicating that the velocity had only a slight effect on corrosion. However, if the velocity was held at 20 fps, and the maximum temperature was increased to 1325°F, the corrosion rate was increased roughly by one order of magnitude to approximately 1.2 mils per year. For a mock-up of the secondary system (304 stainless steel–Incoloy 800) with a maximum temperature of 1100°F, a ΔT of 300°F, an oxide level of less than 10 ppM, and velocity of 15 fps, the corrosion rate at 2500 hours was approximately 0.08 mils per year. (auth)

2620 CORROSION OF STAINLESS STEEL IN OXYGEN-CONTAMINATED SODIUM AT 1200 F AND 1400 F. Hiltz, R. H. (MSA Research Corp., Evans City, Pa.). pp 63-80 of Corrosion By Liquid Metals. /Draley, Joseph E. (ed.). New York; Plenum Publishing Corp. (1970).

From Corrosion by Liquid Metals Conference, Philadelphia, Pa. See CONF-691007.

The corrosion of Types 304 and 316 stainless steel in oxygen-contaminated sodium (>20 ppM oxygen) was studied at 1200 and 1400°F. A gray surface scale, identified as sodium chromite, formed at 1200°F as a function of time and oxygen concentration. It began as a surface layer but penetrated along grain boundaries into the base metal. At 1400°F a green thin surface layer formed which was thought to be made up of two components. Less internal penetration occurred than would occur at an equivalent time and oxygen level at 1200°F. (G.M.C.)

2621 EFFECTS OF EXPOSURE TO FLOWING SODIUM ON VANADIUM ALLOYS IN STAINLESS STEEL CONTAINMENT SYSTEMS. Whitlow, G. A.; Hornak, R. J.; Schrock, S. L.; Bishop, E. C. (Westinghouse Electric Corp., Madison, Pa.). pp 115-35 of Corrosion By Liquid Metals. /Draley, Joseph E. (ed.). New York; Plenum Publishing Corp. (1970).

From Corrosion by Liquid Metals Conference, Philadelphia, Pa. See CONF-691007.

The effects of sodium exposure on the following vanadium alloys were studied. V–9Cr–3Fe–1.3Zr–0.05C (VANSTAR 7); V–8Cr–10Ta–1.3Zr–0.05C (VANSTAR 8); V–6Fe–5Nb–1.3Zr–0.05C (VANSTAR 9); and V–20Ti (for comparison). All alloys exhibited weight gains after exposure to flowing sodium containing less than 10 ppM oxygen in a Type 316 stainless steel loop system over the temperature range of 675 to 800°C. Removal of the interstitials, nitrogen, carbon, and oxygen from the stainless steel, and their absorption by the vanadium alloys was shown to account for the observed increase in weight after exposure. The kinetics of the corrosion process, the weight change data, and the mechanical property changes related to interstitial pick-up from the stainless steel were examined, using a layer chemical analysis technique. Interstitial concentration gradients in both the vanadium alloys and the stainless steel loop tubing were used to obtain activation energies for corrosion and interstitial diffusion coefficients in these materials. In addition to weight change and metallographic results, data are presented on the effects of this interstitial absorption on the mechanical properties of the vanadium alloys. After 1500 and 2650 hours of exposure to sodium, 800°C tensile elongation values greater than 20 percent were obtained for the VANSTAR alloys, but the room temperature ductility was very much reduced. Ways of reducing the interstitial absorption and mechanical property deterioration are discussed. Among these are the use of stabilized stainless steel loop construction at more realistic reactor operating temperatures, or modification of stainless to vanadium alloy surface area ratios. (auth)

2622 APPLICATION OF THERMODYNAMIC AND KINETIC PARAMETERS OF THE V–O–Na SYSTEM TO THE SODIUM CORROSION OF VANADIUM-BASE ALLOYS. Smith, D. L.; Kassner, T. F. (Argonne National Lab., Ill.). pp 137-49 of Corrosion By Liquid Metals. /Draley, Joseph E. (ed.). New York; Plenum Publishing Corp. (1970).

From Corrosion by Liquid Metals Conference, Philadelphia, Pa. See CONF-691007.

The conditions of temperature and oxygen concentration in sodium that result in a transition from oxygen solution and diffusion in vanadium (parabolic weight-gain kinetics) to non-adherent oxide film formation (linear weight-loss kinetics) were determined. In the oxygen-solution region, the distribution coefficient was used to determine the surface or equilibrium oxygen concentration in vanadium from a known oxygen concentration in sodium. In the oxide-formation region, the effect of velocity and oxygen concentration in sodium on the linear corrosion rate of vanadium was determined at 600°C. The corrosion process was controlled by oxygen diffusion in the liquid, over a wide range of experimental conditions, and was shown to be excessive for practical applications in a sodium environ-

XUM

ment. The beneficial effect of chromium as an alloying element to vanadium was demonstrated by the decrease in the distribution coefficient. This result, and the effect of chromium additions on the solubility of oxygen in vanadium are required to determine the position of the alloy–O_{Na}–oxide phase boundary. Problems encountered in the measurement and control of the oxygen concentration in sodium during early stages of this work resulted in a confirmation of the Rutkauskas Na_2O solubility curve over a limited temperature range. An analytical method, based upon equilibrium distribution coefficients in the V–O–Na system, was developed to accurately measure oxygen concentrations in sodium as low as 0.01 ppM. (auth)

2623 CORROSION OF OXYGEN CONTAMINATED TANTALUM IN NaK. Harrison, Robert W. (General Electric Co., Cincinnati). pp 151-75 of Corrosion By Liquid Metals. /Draley, Joseph E. (ed.). New York; Plenum Publishing Corp. (1970).

From Corrosion by Liquid Metals Conference, Philadelphia, Pa. See CONF-691007.

Refractory metals and alloys have excellent corrosion resistance to pure alkali metals; however, this inherent corrosion resistance is adversely affected by small amounts of oxygen. SNAP-8 boilers under evaluation employ NaK in a thermal bond annulus. This NaK contacts both tantalum tubing and weldments and it is therefore important to determine the effect of the oxygen concentration of tantalum on its corrosion resistance to NaK. Tantalum specimens with homogeneous oxygen concentrations ranging from 50 to 500 ppM were prepared by contamination at low pressure and subsequently exposed to NaK at 1350°F for 1000 hours to determine the threshold oxygen concentration for corrosion. Additional contaminated and uncontaminated specimens were welded in pure helium and helium contaminated with air to evaluate the combined effects of welding, welding gas purity, and pre-weld oxygen concentration of the tantalum on the corrosion resistance of the tantalum to NaK. Some specimens were also exposed at 1200°F for 100 hours to determine the effects of temperature and time on corrosion. The effects of the exposure to NaK were evaluated by weight change measurements, bend tests, metallographic examinations, microhardness measurements, and chemical analysis. (auth)

2624 SOME ALKALI METAL CORROSION EFFECTS IN A RANKINE CYCLE TEST LOOP. Phillips, Wayne M. (Jet Propulsion Lab., Pasadena, Calif.). pp 197-215 of Corrosion By Liquid Metals. /Draley, Joseph E. (ed.). New York; Plenum Publishing Corp. (1970).

From Corrosion by Liquid Metals Conference, Philadelphia, Pa. See CONF-691007.

A two-loop lithium-boiling potassium facility was constructed and tested at the Jet Propulsion Laboratory to simulate the major elements and working fluids of a two-loop, nuclear, turbo-plant concept of interest for spacecraft propulsion. During initial testing the niobium-1% zirconium loop was operated for approximately 1000 hr at potassium temperatures up to 1900°F with a yttrium hot trap in the lithium loop and a zirconium hot trap in the potassium loop. This operation produced no observable corrosion in the potassium loop and nominal corrosion in the lithium loop despite high impurity levels in the lithium. No dissimilar metal mass transfer was observed as a result of the hot traps. The hot traps were removed for the final phase of operation which was at potassium temperatures of up to 1900°F for approximately 1000 hr. This resulted in large increases in nitrogen and oxygen content of the containment alloy of the lithium system accompanied by extensive corrosion. Slight erosion of niobium components of the vapor portion of the potassium system was produced, but no erosion of the molybdenum alloy turbine wheel was observed. Impingement or cavitation damage was produced in the lithium centrifugal pump impeller. (auth)

2625 EFFECTS OF WELDING ATMOSPHERE PURITY ON THE LITHIUM CORROSION RESISTANCE OF REFRACTORY ALLOYS. Harrison, Robert W. (General Electric Co., Cincinnati). pp 217-50 of Corrosion By Liquid Metals. /Draley, Joseph E. (ed.). New York; Plenum Publishing Corp. (1970).

From Corrosion by Liquid Metals Conference, Philadelphia, Pa. See CONF-691007.

The effects of oxygen contamination, introduced during welding, on the lithium corrosion resistance of refractory alloys of interest in space power systems were investigated. Specimens of Nb–1Zr, FS–85 alloy (Nb–28Ta–10.5W–0.9Zr), and T-111 alloy (Ta–8W–2Hf) welded in atmospheres of pure helium, helium + 200 ppM air, and helium + 2.5 percent air were exposed in the as-welded and postweld annealed conditions to lithium at 1000°F for one and eight hours and at 1400°F for one hour. The effects of the lithium exposure were determined by weight change measurements, bend tests, chemical analysis, microhardness measurements, and metallographic examination. The effects of postweld heat treatment, lithium temperature, and exposure time on the corrosion behavior of these alloys were also determined. (auth)

2626 CORROSION OF METALS BY MOLTEN LITHIUM. DeVries, Gerrit (Naval Undersea Research and Development Center, San Diego, Calif.). pp 251-69 of Corrosion By Liquid Metals. /Draley, Joseph E. (ed.). New York; Plenum Publishing Corp. (1970).

From Corrosion by Liquid Metals Conference, Philadelphia, Pa. See CONF-691007.

A number of metals were tested to find their corrosion resistance to contaminated molten lithium at 600°F and 900°F. The effect of lithium on microstructure, tensile strength, and stress corrosion was found. The austenitic stainless steels, Types 302, 303, 304, 316, 347 and the ferritic stainless steels, Types 446, 430, 405 apparently were not impaired. Hardenable stainless steels were corroded when hardened but not when annealed. Alloy steels showed increased resistance when tempered at 1100°F for 24 hours. Titanium, molybdenum, tungsten, and chromium showed no evidence of attack. (auth)

2627 5000-HR TEST OF A EUTECTIC LEAD–BISMUTH CIRCUIT CONSTRUCTED IN STEEL AND NIOBIUM. Hodge, R. I.; Turner, R. B.; Platten, J. L. (Chalk River Nuclear Labs., Ont.). pp 283-303 of Corrosion By Liquid Metals. /Draley, Joseph E. (ed.). New York; Plenum Publishing Corp. (1970).

From Corrosion by Liquid Metals Conference, Philadelphia, Pa. See CONF-691007.

Solution-erosion and deposition processes were studied for a lead-bismuth eutectic circuit passing through steel tubing. The use of wrought niobium as a protective coating for the steel was assessed. Before filling the loop the lead-bismuth was treated with magnesium and zirconium in the charge pot. The loop was operated for 5000 hr with hot and cold leg temperatures of 500 and 375°C. (G.M.C.)

2628 CORROSION STUDIES OF LIQUID METAL HEAT PIPE SYSTEMS AT 1000° TO 1800°C. Johnson, G. D. (McDonnell Douglas Corp., Richland, Wash.). pp 321-37 of Corrosion By Liquid Metals. /Draley, Joseph E. (ed.). New York; Plenum Publishing Corp. (1970).

From Corrosion by Liquid Metals Conference, Philadelphia, Pa. See CONF-691007.

The compatibility of heat pipe structural alloys with different working fluids can be conveniently evaluated with reflux capsules. Capsule tests with refractory metal seamless tubing were conducted in vacuum at temperatures of 1000 to 1800°C and at times to 1000 hours. Systems evaluated to date are: TZM with indium; Nb–1Zr with lead, calcium, and barium; and Ta–10W with indium, calcium, lead, thallium, and barium. The observed corrosion behavior of the various systems was associated with the nature of oxygen in the particular system. Severe attack was observed in the lead and thallium systems, while calcium produced very little attack, especially in contact with Ta–10W. Corrosion occurring with calcium was mainly confined to very shallow intergranular penetration. (auth)

2629 CORROSIVE ACTION OF SELENIUM TOWARDS VARIOUS MATERIALS IN THE TEMPERATURE RANGE 300 TO 700°C. Janjua, M. B. I. (Noranda Research Centre, Pointe Claire, Quebec); Yannopoulos, J. C.; Cooper, W. Charles. pp 339-59 of Corrosion By Liquid Metals. /Draley, Joseph E. (ed.). New York; Plenum Publishing Corp. (1970).

From Corrosion by Liquid Metals Conference, Philadelphia, Pa. See CONF-691007.

Data are given on the corrosive effects of selenium at 300 to 700°C on metals and alloys (chromium, gold, zirconium, Hastelloys B, C, and F, stainless steels 304, 316, 316L, 410, 430, and 446), Inconel coated with ceramic (Nucerite), graphite, ceramics (Magnorite, silicon carbide, zirconia), and glasses (Pyrex, Vycor). (G.M.C.)

2630 ANODIC TREATMENT TO IMPROVE THE LIQUID ZINC CORROSION RESISTANCE OF TANTALUM. Sandor, L. V.; Kundig, K. J. A. (Republic Steel Research Center, Independence, Ohio). pp 393-403 of Corrosion By Liquid Metals. /Draley, Joseph E. (ed.). New York; Plenum Publishing Corp. (1970).

Tantalum as a container material for liquid zinc at elevated temperatures was evaluated. Metallographic examination revealed some dissolution of the base metal accompanied by embrittlement resulting from the formation of an acicular phase. An anodizing treatment in H_3PO_4 retarded liquid zinc attack

XUM

through the formation of an adherent protective film. Protection was complete under fully submerged conditions but was somewhat reduced where the coating was exposed to air. (auth)

2631 CORROSION AND MASS TRANSFER OF PURE IRON, NICKEL, CHROMIUM, AND COBALT IN 660° TO 760°C SODIUM. Fleitman, A. H.; Isaacs, H. S. (Brookhaven National Lab., Upton, N. Y.). pp 589-99 of Corrosion By Liquid Metals. /Draley, Joseph E. (ed.). New York; Plenum Publishing Corp. (1970).

From Corrosion by Liquid Metals Conference, Philadelphia, Pa. See CONF-691007.

Data are given on the corrosion and mass transfer of pure chromium, cobalt, iron, and nickel in sodium at 660 and 760°C. The effects of about 4 and 110 ppM oxygen in the sodium on the corrosion and mass transfer of the metals were studied. (G.M.C.)

2632 OXIDATION OF TANTALUM IN THE OXYGEN PLASMA OF A HIGH-FREQUENCY DISCHARGE. Mikhalkin, V. S.; Odynets, L. L. Elektrokhimiya; 6: 359-61(Mar 1970). (In Russian).

The kinetics of the oxidation of Ta in the O plasma of a high frequency electrodeless gas discharge were studied together with the electrical properties and protective characteristics of the resultant oxide films. The kinetic laws governing the oxidation of the metal surface in the gas discharge were closely analogous to those governing anodic oxidation in electrolytes; apparently very much the same mechanisms of oxide formation persisted in both cases. The quality of the oxide films depended to some extent on the electrical conditions. (Metal Abstr.)

2633 PROCEEDINGS OF THE 26th CONFERENCE OF THE NATIONAL ASSOCIATION OF CORROSION ENGINEERS, PHILADELPHIA, PA., MARCH 2–6, 1970. Houston, Tex.; National Association of Corrosion Engineers (1970). 651p. $30.00. (CONF-700324).

Ninety-one papers were presented at the conference. A separate abstract was presented for five papers. Papers for which no abstracts were prepared are concerned with deep ground anodes, construction material protection, automotive corrosion, underground cable corrosion, corrosion by pure water, coatings for pipes, refinery corrosion, military equipment corrosion, corrosion control by chemical alteration, and protective coatings. (J.R.D.)

For abstracts of individual papers see: 2426, 2634, and 2635–2637.

2634 INTERNAL CATHODIC PROTECTION OF WATER COOLED PLANT. Lowe, R. A.; Brand, J. W. L. F. (Corrosion and Welding Engineering, Ltd., Redhill, Eng.). pp 175-8 of Proceedings of the 26th Conference of the National Association of Corrosion Engineers, Philadelphia, Pa., March 2–6, 1970. Houston, Tex.; National Association of Corrosion Engineers (1970).

See CONF-700324.

Progress in the application of cathodic protection of seawater-cooled plants such as generating stations, refineries, and seawater evaporators, is reviewed. Discussions are included on strip anodes, automatic control of potential, special requirements, and repair. (J.R.D.)

2635 STRESS CORROSION CRACKING OF Ti AND Ti-6Al-4V ALLOY IN DINITROGEN TETROXIDE. Moreland, P. J.; Boyd, W. K. (Battelle Memorial Inst., Columbus, Ohio). pp 213-19 of Proceedings of the 26th Conference of the National Association of Corrosion Engineers, Philadelphia, Pa., March 2–6, 1970. Houston, Tex.; National Association of Corrosion Engineers (1970).

See CONF-700324.

The stress corrosion cracking behavior of titanium and Ti-6Al-4V alloy in liquid N_2O_4 has been investigated from thermodynamic considerations and autoradiographic, chemical, and potential studies. Studies were concerned with the N_2O_4-H_2O-O_2 system which is believed to produce HNO_3 and the N_2O_4-O_2 system to cause stress corrosion cracking. A hydrogen embrittlement mechanism involving HNO_3 in the commercial N_2O_4 appeared improbable. An electrochemical mechanism in which O_2 plays a major role has been proposed. (auth)

2636 CORROSION OF ADVANCED STEAM GENERATOR ALLOY WELDMENTS IN 1100 AND 1200 F (595 AND 650 C) STEAM. Hammond, Joseph P.; Patriarca, P.; Slaughter, G. M.; Maxwell, W. A. (Southern Nuclear Engineering, Inc., Dunedin, Fla.). pp 277-91 of Proceedings of the 26th Conference of the National Association of Corrosion Engineers, Philadelphia, Pa., March 2–6, 1970. Houston, Tex.; National Association of Corrosion Engineers (1970).

See CONF-700324.

Results of tests involving dissimilar heat-resisting alloy weldment corrosion by steam are presented. Fourteen combinations were exposed to steam at 1100 to 1200°F. Results are tabulated and discussed. (J.R.D.)

2637 CORROSION AND COOLANT CHEMISTRY INTERACTIONS IN PRESSURIZED WATER REACTORS. Miller, D. A.; Bryant, P. E. C. (Combustion Engineering, Inc., Windsor, Conn.). pp 292-300 of Proceedings of the 26th Conference of the National Association of Corrosion Engineers, Philadelphia, Pa., March 2–6, 1970. Houston, Tex.; National Association of Corrosion Engineers (1970).

See CONF-700324.

The corrosion behavior of Inconel 600 Zircaloy, and 300-series stainless steel in ammoniated and lithiated aqueous reactor solutions is reviewed. A model is proposed which relates changes in PWR reactivity, core pressure drop, and primary system radiation fields to the influence of coolant pH on corrosion product transport and deposition. Ammonium hydroxide is recommended as the pH control additive and means for alkali production and control are described. Methods for control of activated corrosion products are also discussed. (J.R.D.)

Preparation and Fabrication

Refer also to abstracts 2237 and 3219.

2638 (CEA-CONF-1625) SOLUTION OF TWO IMPORTANT PROBLEMS IN THE NUCLEAR INDUSTRY BY FLAME METAL SPRAYING. Faussat, Armand (Commissariat a l'Energie Atomique, Saclay (France). Centre d'Etudes Nucleaires). 1970. 12p. (In French). (CONF-700922–1). Dep. NTIS (U. S. Sales Only).

From 6th International Conference on Metal Spraying, Paris, France.

Two applications of flame metal spraying were developed to solve specific problems of uranium fuel elements clad with magnesium at Bugey nuclear power station. The spray deposits can be used to decrease the thermal transfer coefficient between uranium and magnesium alloys using an alumina layer and to form metallurgical bonding between uranium and magnesium alloys using an aluminum layer followed by a diffusion heat treatment. The latter application is now used in the fuel element industry. (auth) (France)

2639 (LIB/Trans–309) HIGH PURITY GAS PROTECTIVE SYSTEM FOR THE USE OF HIGH MELTING REACTIVE METALS AT HIGH TEMPERATURES. Bukau, F. (Kernforschungszentrum, Karlsruhe (West Germany). Institut fuer Reaktorentwicklung). Translated by I. Mumme (Australian Atomic Energy Commission Research Establishment, Lucas Heights), from report KFK–927. 93p. Dep. NTIS (U. S. Sales Only).

An abstract of this report, prepared from the original, appeared as NSA 23: 36071 (1969). (Australia)

2640 (NLCO–1058) PRESSURIZED LOW TEMPERATURE REDUCTION OF GREEN SALT. Trapp, J. H. (National Lead Co. of Ohio, Cincinnati). Sep 1970. Contract AT(30-1)-1156. 48p. Dep. NTIS.

The semicontinuous reduction of green salt by magnesium at 2400°F and 75 psig was studied on a laboratory scale. The use of pressure resulted in reduction of the uranium oxide constituents of the green salt as well as the UF_4, thereby producing a MgF_2 slag containing less than 200 ppM uranium. Based on these promising results, a pilot plant pressurized reduction facility was designed and built. The operation of this facility demonstrated that high-purity uranium could be produced from green salt containing up to 4.01% uranium oxides and that the by-product slag was low enough in uranium content (less than 0.1%) to be directly discardable. A number of operational problems remained when the experimental work was terminated: the necessity of sparging the reaction mixture with argon to achieve complete reduction; plugging of the feed tube; frequent failure of pour tube power connectors and graphite parts; and formation of a UC skin within the crucible which occasionally plugged the pour tubes. (auth)

2641 (ORNL–4570, pp 85-7) FABRICATION OF FAST BREEDER REACTOR CLADDING. (Oak Ridge National Lab., Tenn.).

From Metals and Ceramics Division annual progress report for the period ending June 30, 1970.

Activities in a program to develop methods of fabricating tubing free of defects and to relate mechanical properties at elevated temperatures to processing variables and defects are summarized. Ultrafine-grain size Type 304 stainless steel tubing was produced by controlling the degree of cold working and the temperatures at which the tubing was annealed between the cold working steps. This tubing is weaker than conventional tubing at elevated temperatures

XUM

but also is considerably more ductile. Using planetary swaging equipment now available, this process is not attractive as the primary tubing fabrication process because of surface defect generation. Defects in tubing can be generated during many stages of manufacturing. Machine marks on tube shells can produce defects in the final tubing. A method was developed to produce artificial defects and allow a more precise relationship to be developed between mechanical properties and fabrication defects. (auth)

2642 (ORNL–4570, pp 88-91) STAINLESS STEEL WELDING DEVELOPMENT. (Oak Ridge National Lab., Tenn.).

From Metals and Ceramics Division annual progress report for the period ending June 30, 1970.

The behavior of weldments in austenitic stainless steel are being studied at elevated temperatures as a function of both welding process and variables within a process for application to LMFBR vessels and components. Efforts are being made to determine reasons for the high degree of scatter reported for creep ductility and to develop optimized welding procedures for obtaining satisfactory mechanical properties. Minor changes in weld metal composition (within the allowable range for Type 308 filler metal) can produce significant variations in mechanical properties. The rupture life can be increased tenfold, for example, by increasing the carbon content of shielded metal-arc weld metal from 0.044 to 0.074 wt %. Coating differences are also important; lime-coated electrodes produced weaker but more ductile deposits than electrodes coated with titania or lime and titania. Submerged-arc welds exhibited lower creep strengths than did shielded metal-arc welds. Results of these studies are being correlated with metallographic interpretations, with special emphasis on scanning electron fractographs of the specimen surfaces. (auth)

2643 (ORNL–4570, pp 106-11) MATERIALS DEVELOPMENT FOR ISOTOPIC POWER PROGRAMS. (Oak Ridge National Lab., Tenn.).

From Metals and Ceramics Division annual progress report for the period ending June 30, 1970.

Research and development on materials for encapsulation of isotopic power fuels is being carried out in support of a variety of space and terrestrial (including undersea) programs. Capsules were machined from arc-cast tungsten extruded at 1775°C. Throughout fabrication and inspection, an electropolishing technique minimized propagation of cracks and revealed defects covered by metal smeared during machining. A CVD tungsten vent tube was welded to the capsule with W–25% Re filler metal and to a Type 304 stainless steel extension tube with Type 308 filler metal. The 1000-W (thermal) $^{244}Cm_2O_3$-fueled capsule was successfully seal welded in the hot cell with specially developed equipment and procedures. In a study of the compatibility of $^{244}Cm_2O_3$ with refractory metals, specimens exposed for up to 10,000 hr and 1850°C were examined. Tantalum alloys were penetrated at 1650°C and formed low-melting fuel mixtures at 1850°C; W–26% Re, TZM, and Mo showed the best compatibility. The creep testing of CVD tungsten test capsules at 1650°C by programmed pressurization with helium verified rupture times predicted from uniaxial creep data and showed good rupture ductility (11 and 18% circumferential strain). The evaporation of Hastelloy N and Haynes alloy No. 188 at 800 to 1050°C and 10^{-9} torr resulted in void formation, solutioning of some precipitates, and formation of others due to the selective evaporation of chromium and manganese. Platinum-base solid solution (Pt–5% Mo) and ordered (Pt_3Cr) alloys are being developed. The ordered alloy exhibits superior creep strength and slower evaporation than unordered alloys, and both have excellent oxidation resistance at 1000°C. The structure of a pseudobinary alloy $(Ni,Co)_3$ V can be controlled, although Ni_3 V and Co_3 V order on quenching. Aging at 700 and 800°C produces the ductile cubic $AuCu_3$-type ordered structure. However, longer aging forms a brittle hexagonal structure with a nine-layer stacking sequence. The activation energy for creep and the stress exponent are greater for the ordered alloy than for a similar disordered alloy. Capsules of Nb–1% Zr, Mo, and Mo–0.5% Ti with hemispherical ends were extruded at 1200°C. The tantalum alloys T-111 and Ta–10% W are being back extruded at 1300 and 1350°C with a plasma-sprayed molybdenum coating to protect from contamination and provide lubrication by MoO_3. Nonradioactive $SrTiO_3$ and Sr_2TiO_4 shows little interaction with Haynes alloy No. 25, Hastelloy C, or Type 316 stainless steel in 10,000 hr at 900 and 1100°C. However, SrO reacts significantly because of the silicon content of the alloys. Potassium in SrO from one process increases the interaction. Ultrasonic inspection was used to weld penetration in pressure-tested SNAP-23 capsules; results agreed within ±10 mils of metallographic measurements. For the Isotope Kilowatt Program, high-temperature thermal conductivity data on iron alloys were reviewed for radiation shield applications, and consumable-electrode vacuum remelting was recommended to obtain high-purity iron castings. (auth)

2644 (ORNL–4570, pp 157-60) DESALINATION. (Oak Ridge National Lab., Tenn.).

From Metals and Ceramics Division annual progress report for the period ending June 30, 1970.

Exploratory experiments were completed on fuel fabrication methods for the Unclad Metal Breeder Reactor (UMBR). This reactor, which would use Th–20 wt % U fuel elements, is a proposed low-cost source of heat for seawater distillation and power generation. The basic feasibility of casting to shape, casting a billet, and forming from a billet component shapes from which the fuel element can be assembled was demonstrated. The most attractive and economical production method for making fuel elements now appears to consist of some combination of rolling and forming component pieces from an ingot. The ingot may be produced by consumable electrode arc-melting or possibly from alloyed or elemental powders by compaction and extrusion. Specimens of Th and Th–20 wt % U were taken from a loop operated to determine the compatibility of these materials with sodium in Type 304 stainless steel at 800°F. No physical evidence of corrosion was found; even after 2000 hr the reaction product film was less than 0.1 mil. No intergranular attack was observed. (auth)

2645 (ORNL–4570, pp 214) ALLOY DEVELOPMENT FOR ARMY PULSED RADIATION FACILITY REACTOR. (Oak Ridge National Lab., Tenn.).

From Metals and Ceramics Division annual progress report for the period ending June 30, 1970.

In seeking an improved core alloy for pulsed reactor service, the toughness properties of several U–10% Mo alloys containing small additions (to 1.0%) of Al, Cr, Nb, Ta, and Ti were determined. After aging at the maximum embrittlement temperature of 475°C, the alloy U–10% Mo–0.3% Ti showed a clear superiority in notch toughness at all aging times to 64 hr. While inferior to the alloy containing 0.3% Ti, the alloy U–10% Mo–1% Ta exhibited impact properties that were independent of aging time. (auth)

2646 (RFP–1550) GAS COVERAGE FOR PIGMA WELDING. Brandon, Eldon D.; Bush, Walter L. (Dow Chemical Co., Golden, Colo. Rocky Flats Div.). 10 Nov 1970. Contract AT(29-1)-1106. 5p. Dep. NTIS.

A study was conducted to check differences in results when using argon and air to pressurize a welding chamber, and to determine the rate of torch gas flow required to give satisfactory arc shielding in pressurized inert gas metal-arc (PIGMA) welding. A series of gas metal arc welds was made on Type 1100 aluminum using 0.030-in.-diameter 718 aluminum electrode wire. The welds were made at 30 and 100 psia ambient pressure with 45, 60, 90, and 120 cfhr of helium/argon shielding gas through the torch. The chamber atmospheres were air and argon. Although the welds made in compressed air exhibited a somewhat rougher surface and were oxidized, the welds were sound. The use of argon prevented the oxidation. At 30 psia pressure, 45 cfhr torch gas coverage was adequate; at 100 psia pressure, at least 60 cfhr was required. (auth)

2647 RHENIUM AND ITS ALLOYS AS CONSTRUCTION MATERIAL. Mecklenburg, E. Z. Wirt. Fertigung; 65: 289-92(1970). (In German).

A survey of the fabrication, mechanical properties, and uses of Re, Re–Mo, and Re–W alloys is presented. Because of their high-temperature properties, high density, and relatively large neutron capture cross-section, the alloys are suitable for radiation shields and other reactor components. (INIS)

2648 MORPHOLOGICAL EFFECTS OF RELATIVE MOVEMENT BETWEEN SOLID AND LIQUID IN ELECTROCHEMICAL PROCESSES. Piontelli, R.; Rivolta, B.; Razzini, G. C. Electrochim. Metal.; 4: 218-32; 254(Jul-Sep 1969). (In Italian).

Metal deposition on rotating disc and cylindrical cathodes has been studied and the conditions which produce spiral or helical ridges noted. Cd, Cu, and Zn were deposited on Cu, Cd, Ni, Pb, and stainless steel, and the relative overvoltage of the two components was found to influence the deposition phenomena. Conditions producing spongy Zn deposits and the effect of gas flow were also investigated. (Metals Abstr.)

2649 ELECTRODEPOSITION OF COBALT–TUNGSTEN MAGNETIC ALLOYS. Rachinskas, V. S.; Syaurukaite, L. M.; Radzhyunene, B. S. (Inst. of Chemistry and Chemical Tech., Vilnyus, USSR). Zashch. Metal.; 6: 609-12(Sep-Oct 1970). (In Russian).

The effect of the anion of cobalt salts on the cathode processes, chemical composition and corrosion resistance of Co–W alloys, electrodeposited from various acid solutions, was investigated. The electrolyte contained Co^{2+} ions, 0.5 g/l, K_2WO_4, 10 g/l, and H_3BO_3, 30 g/l; containing Co as sulfate, chloride, bromide, aluminosulfate, acetate, or nitrate. The magnetic properties were determined from

XUM

the hysteresis loop. Increase of the current density resulted in a decrease of the W content of the alloy and an increase of the corrosion rate. Using higher deposition temperatures and chloride in the electrolyte helped to reduce the corrosion rate. The conditions of electrolysis which favored the reduction of the tungsten content increased the magnetic induction, improving the hysteresis curve of the deposited coating. The results agreed with those obtained in similar tests carried out with a sulfate electrolyte. (TTT)

2650 SHEAR SPINNING REWARDS DESIGNER WITH AUTOMATICALLY PRECISE PARTS. Stewart, Jack D. SAE (Soc. Automot. Eng.) J.; 78: No. 2, 43-5(Feb 1970).

Shear spinning reduces the thickness of a metal blank or preforms in a way that is exactly predicted by a sine law, thus producing precision parts on automatic tracer machines. Careful machine setup is required because tool radius, surface speed, feed and other factors affect the finish, precision, and fit of the part on the spinning mandrel. The necessary preform shape is easily calculated from the sine law. A table lists max. reductions for commonly shear spun materials such as stainless steel, maraging steel, Waspaloy, René 41, Al alloys, Cu, Ti alloys, and refractory alloys. (Metals Abstr.)

2651 THERMOMECHANICAL PROCESSING OF A MOLYBDENUM ALLOY USING HYDROSTATIC EXTRUSION. Raffo, Peter L. (Lewis Research Center, Cleveland, Illinois Inst. of Tech., Chicago). Met. Trans.; 1: 2967-70(Oct 1970).

Room-temperature hydrostatic extrusion was used to prepare Mo-TZC with superior high-temperature strength. This was accomplished by combining severe room-temperature strain hardening with the capacity for dynamic strain aging in a molybdenum alloy. (G.M.C.)

2652 COMPOSITE FILM METALLIZING FOR CERAMICS. Hollar, E. L.; Rebarchik, F. N.; Mattox, D. M. (Sandia Labs., Albuquerque, N. Mex.). J. Electrochem. Soc.; 117: 1461-2(Nov 1970).

A method for obtaining an adherent coating on ceramics that cannot be handled by traditional means is proposed. A transitional interface region, conducive to good bonding, is formed by deposition of an oxygen-active metal in a controlled gaseous environment. The deposition of the active metal is begun in a partial pressure of oxygen to allow partial oxidation of the deposited material and thus form a transition oxide and suboxide interfacial region. By decreasing the partial pressure of oxygen during the deposition, the composition of the interfacial region may be graded from the substrate material through a metal oxide–metal composite region to the pure metal. Metallizing fused silica was investigated. A refractory material was used in contact with silica in order to prevent scavenging. Of the four refractory metals, Nb, Ta, W, and Mo, investigated, niobium seemed to be the most stable under brazing conditions. The system niobium–silver with a copper–silver eutectic braze was used. (J.G.B.)

2653 KROLL PROCESS BERYLLIUM. Campbell, Thomas T.; Mussler, R. E.; Block, F. E. (Bureau of Mines, Albany, Oreg.). Met. Trans.; 1: 2881-7(Oct 1970).

High-purity beryllium metal was prepared on a laboratory scale by Kroll process procedures in which sodium was used as a reductant. Crude beryllium chloride, purchased from commercial sources, was purified by vacuum sublimation and fused-salt scrubbing. Purified beryllium chloride was vaporized and reacted at a controlled rate with molten sodium at temperatures ranging from 650 to 750°C to form beryllium sponge. Excess metal reductant and byproduct salt were removed from the sponge metal by vacuum distillation. Beryllium sponge metal was wet ball milled to –200 or –400 mesh powders. Beryllium powder metal, subsequently consolidated by isostatic pressing, was hot extruded and machined into tensile specimens for evaluation of mechanical properties. Evaluation indicates that the beryllium described in this study is of higher purity than comparable commercial grades of metal; also it is more ductile but has somewhat lower strength. The overall process appears to have an excellent potential from an economic standpoint. (auth)

2654 BERYLLIUM AND ITS ALLOYS. (ENGINEERING OUTLINE 246). Dyer, C. K. (Nottingham Univ., Eng.). Engineering; 210: 359-62(Oct 1970).

Data, in summary form, are presented on the extraction, metallurgy, and applications, including nuclear uses, of Be. A few basic properties are quoted. Uses of Be–Cu and Be–Ni are briefly outlined. (UK)

2655 NEW TECHNIQUE OF TARGET PREPARATION. Suzuki, T.; Baba, S.; Umezawa, H.; Amano, H. (Japan Atomic Energy Research Inst., Tokai). Nucl. Instrum. Methods; 87: 311-12(1970).

A technique for preparing targets (particularly rare earth elements and uranium) of various thicknesses ranging from 0.1 mg/cm^2 to 60 mg/cm^2 was developed by centrifuging powder suspended in liquid paraffin. The uniformity was investigated by measuring the penetrability of a collimated β-ray beam. The local fluctuation in thickness from the average value was found to be less than ±3% except at the very edge of each target. (auth)

2656 PREPARATION AND ETCHING OF MICROSECTIONS OF ZIRCONIUM AND ZIRCONIUM–NIOBIUM ALLOYS. Vollbrecht, W.; Rudorf, G. Freiberg. Forschungsh.; B141: 83-90 (1969). (In German).

Zr and Zr–Nb alloys are very prone to cold-working effects during conventional metallographic preparation; electrolytic polishing is normally used for these materials. Recommended solutions and procedure are given, and several micrographs of Zr and Zr–Nb alloys shown. (Metals Abstr.)

Properties Evaluations

Refer also to abstracts 2074, 2394, 2408, 2410, 2788, and 3217.

2657 (AD-464715) RECENT INFORMATION ON LONG-TIME CREEP DATA FOR COLUMBIUM ALLOYS. English, Jerome J.; Bartlett, Edwin S. (Battelle Memorial Inst., Columbus, Ohio. Defense Metals Information Center). 26 Apr 1965. Contract AF33(615)-1121. 6p. (DMIC-Memo-203). NTIS.

Recent information relating to long time creep parameters for niobium alloys is summarized. The available creep data for niobium alloys through mid-1963 were previously reported in DMIC memorandum 170. Long-time-creep test programs are being conducted by NASA Lewis Research Center, Thompson Ramo Wooldridge, and Oak Ridge National Laboratory. Data from these and other selected sources for time greater than 10 hours are compiled in this memorandum. (auth) (USGRDR)

2658 (AEC-tr-7095) METALLURGY OF PLUTONIUM. Vol'skii, A. N.; Sterlin, Ya. M. Translation of Metallurgiya Plutoniya, Izdatel'stvo Nauka, Moscow, 1967. 277p. (TT-70-50004; IPST-Cat.-5653). Dep. NTIS.

This book was abstracted from the original language and appeared in NSA as 23: 41609. (J.R.D.)

2659 (BMI-1889, Sect.A) DEVELOPMENT OF MECHANICAL-PROPERTY DESIGN DATA FOR REACTOR MATERIALS. (Battelle Memorial Inst., Columbus, Ohio). 14p.

In a program to evaluate the low-cycle-fatigue resistance of Incoloy 800, measurements were completed at 800°C on solution-annealed specimens. The curve fell somewhat above that developed earlier in tests at 1000°C. Attention was also given to the effect of incorporating hold times in compression or tension in the test stress cycle. For total strain ranges between 1.56 and 2.73 percent, cyclic fatigue life was greatly reduced at 1400 and 1200°F and slightly reduced at 1000°F when only tension 10-min hold times were applied. When only compression or both tension and compression 10-min hold times were used, the cyclic fatigue life at 1400, 1200, and 1000°F was but slightly reduced. (auth)

2660 (JAERI-Memo-4097) CREEP AND CREEP-RUPTURE TESTS OF DOMESTIC SUS 32 (AISI TYPE 316) STAINLESS STEEL AS A STRUCTURAL MATERIAL OF FAST BREEDING REACTOR. Collaboration Report, 1967–1969. Yokoi, S.; Monma, Y.; Fujimura, T.; Namatame, H.; Kodaira, T. (Japan Atomic Energy Research Inst., Tokyo). 10 Jun 1970. 49p. (In Japanese). Dep. NTIS (U. S. Sales Only).

Results of creep and creep-rupture tests of domestic SUS 32 (AISI Type 316) stainless steel are presented. The creep test was made at 500, 550, and 600°C on the specimens taken from heavy thickness plates (t = 30mm) and the creep-rupture test was made on the specimens of 316 stainless steel and their weld metals at 500 and 600°C. It was found that in creep tests on two different lots, one material showed a faster minimum creep rate at 500 and 550°C than the other. However, this tendency was reversed at 600°C. Adding nitrogen and niobium to 316 stainless steel as alloying elements is highly effective in increasing the creep-rupture strength. The rupture time of weld-metal specimens was about one order lower than the base metals at the same stress level at 600°C. All materials tested had good ductility at rupture. Creep properties of all materials tested satisfied the criteria of ASME Boiler and Pressure Vessel Code, Section VIII. (auth)

2661 (JAERI-Memo-4125) THE EFFECT OF COLD WORKING ON CREEP PROPERTIES OF AISI 316 TYPE STAINLESS STEEL. Furuta, Teruo; Ogawa, Yutaka; Nagasaki, Rukichi (Japan Atomic Energy Research Inst., Tokyo). Aug 1970. 29p. (In Japanese). Dep. NTIS (U. S. Sales Only).

Austenitic stainless steel is to be used as fuel cladding mate-

XUM

rials in the fast breeder reactor. It is noted that creep properties of stainless steel are well known, but little information is available on fuel cladding applications where stress is low and tubes are thin-walled. The investigation revealed that at the temperature of 650°C, secondary creep rate reached the minimum at about 10% prior to cold working at 4 ~ 8 kg/mm² stress range. At the temperature of 750°C, where recovery controls creep behavior of steel, secondary creep rate increased with prior cold working at the same stress range. (auth)

2662 (KFK-1193) CREEP AND CREEP STRENGTH OF VANADIUM-TITANIUM AND VANADIUM-TITANIUM-NIOBIUM ALLOYS WITH ADDITIONS OF SILICON AND GERMANIUM. Scholz, H.; Schirra, M. (Kernforschungszentrum, Karlsruhe (West Germany). Institut fuer Material und Festkoerperforschung). May 1970. 41p. (In German). Dep. NTIS (U. S. Sales Only).

The creep behavior of alloys composed of V-3Ti, V-3Ti-1Si, V-3Ti-1Ge, -2Ge, -4Ge, and V-3Ti-5Nb-1Si was investigated, at a temperature of 850°C and under a vacuum of 10^{-4} torr; the creep behavior of the alloy composed of V-3Ti-15Nb-1Si was investigated at the temperatures of 650, 750, 800, and 850°C. The creep rupture strength of the V-3Ti alloy is about 6 kg/mm² after 1000 hours. Germanium alloying did not result in a considerable increase in strength. A major increase in strength seems to be attained by adding 1% of Si to the V-3Ti alloy; however, the high strength of the V-3Ti-1Si alloy must be attributed to the high oxygen content of 2900 ppM. The strength may be enhanced also by the solid solution hardening element niobium. Cracks are not observed in the vanadium alloys under consideration, unless the samples have been embrittled on the surface by chemical reactions with the surrounding medium. Ductility behaves also in a favorable way, which excludes limitations to use from this point of view. The creep mechanism which occurred under the different experimental conditions were determined very roughly only. However, a change in the creep mechanism was observed for the alloy V-3Ti-15Nb-1Si in the temperature range between 650 and 750°C. Up to 650°C, dislocation movements are rate-determinant, while diffusion processes dominate above a temperature of 750°C. (auth)

2663 (MLM-1684) COMPATIBILITY OF ^{238}Pu DIOXIDE WITH PLATINUM AND PLATINUM-RHODIUM ALLOYS: INTERIM REPORT. Selle, J. E.; McDougal, J. R.; Schaeffer, D. R. (Mound Lab., Miamisburg, Ohio). 20 Jan 1970. Contract AT-33-1-GEN-53. 124p. Dep. NTIS.

Results of compatibility tests between production grade $^{238}PuO_2$ and platinum and platinum-rhodium alloys are presented. Test periods were as long as 360 days, and most of the work was done at 800, 1000, and 1200°C. Samples were analyzed by means of metallography, microhardness measurements, x-ray diffraction, and electron microprobe analysis. A chronology of the program to date is presented along with a discussion of the various results. The effects of impurities in the fuel, the presence of molybdenum or tantalum in the system, as well as the effects of a reducing atmosphere are presented and discussed. Attempts are made to interpret the results in terms of possible mechanisms. (auth)

2664 (N-70-32146) APPARENT SOLUBILITIES OF COMMERCIALLY PURE AND OXYGEN-DOPED TANTALUM AND NIOBIUM IN LIQUID POTASSIUM. Stecura, Stephen (National Aeronautics and Space Administration, Cleveland, Ohio. Lewis Research Center). Jul 1970. 34p. (NASA-TN-D-5875; E-5615). NTIS.

The apparent solubility of tantalum in potassium at 1055 and 1287°K is about 72 and 240 ppM by weight and that of niobium at 1055 and 1287°K is about 48 and 210 ppM by weight, respectively. The calculated heats of solution for tantalum and niobium solubilities in pure liquid potassium are 13.9 ± 1.3 and 17.1 ± 1.6 kcal/mole (58.2 and 71.5 kJ/mole), respectively. These apparent solubility data are believed to provide the upper limit for the true solubilities of tantalum and niobium between 1055 and 1287°K. Intentional doping of tantalum and niobium metals with oxygen increased the apparent solubilities of these two metals in liquid potassium. This effect of oxygen was related to K_3TaO_4 and K_3NbO_4 ternary oxides, respectively. These ternary oxides were recovered and identified. A hypothesis is proposed to explain these observations and those previously observed by others. (auth) (STAR)

2665 (NBS-SPEC. PUBL.-315-5) BIBLIOGRAPHY ON THE HIGH TEMPERATURE CHEMISTRY AND PHYSICS OF MATERIALS, JANUARY-MARCH 1970. Diamond, J. J. (ed.) (National Bureau of Standards, Washington, D. C.). Apr 1970. 82p. GPO $0.75.

A bibliography of references to research involving temperatures above 1000°C, which were noted by the contributors during the period is given. This is intended primarily as a current-awareness bibliography and there is no cross-referencing or indexing. About 750 references roughly grouped under fifteen subject headings are included. (auth)

2666 (NP-18468) THERMOMIGRATION IN METAL-INTERSTITIAL SOLID SOLUTIONS. Shaw, John Graham (Newcastle Univ. (Australia). Dept. of Metallurgy). Oct 1969. 178p. Dep. NTIS (U. S. Sales Only).

Thesis.

Thermomigration, the transport of matter induced by an applied temperature gradient, was investigated in a number of metal-interstitial solid solutions. In such systems only the interstitial solute moves, the solvent lattice serving as a fixed frame of reference. The solvent metals studied were iron, cobalt, nickel, titanium, vanadium, and palladium; both carbon and hydrogen were used as solutes. Carbon thermomigration was investigated in all six of these metals using a radioactive tracer technique and hydrogen thermomigration was investigated in palladium using the technique of thermo-osmosis. For the carbon studies, a substantial solute redistribution occurred towards the hotter regions in alpha iron and vanadium and towards the colder regions in palladium while for cobalt, nickel, and beta titanium very little segregation was observed. The heats of transport determined were: alpha iron, -14.1 ± 1.5 kcal/g atom; vanadium, -4.9 ± 1.0 kcal/g atom; palladium, +8.4 ± 1.5 kcal/g atom; cobalt, +1.5 ± 1.5 kcal/g atom; nickel, -1.6 ± 1.4 kcal/g atom; beta titanium, -1.0 ± 1.0 kcal/g atom. An order of magnitude variation in carbon concentration and the magnetic transformation appeared to have little or no effect on carbon thermomigration in alpha iron. For hydrogen in palladium, redistribution was also small, the heat of transport measured being +1.5 ± 0.5 kcal/g atom. An examination of the results obtained together with all of the published data for interstitial solute thermomigration has indicated two apparent trends which suggest that electronic effects could be of major importance in determining the redistributions observed. These trends relate to the sign and magnitude of the heat of transport for different interstitial solutes in the one solvent metal. This contention is further supported by a striking correlation between the sign of the heat of transport and the effective charge, the experimental quantity of interest in the essentially electronic phenomenon of electromigration. (auth)

2667 (NP-18491) INTERNAL FRICTION IN INDIUM SINGLE CRYSTALS. Technical Note 152. de Morton, M. E. (Defence Standards Labs., Maribyrnong (Australia)). May 1970. 7p. Dep. NTIS (U. S. Sales Only).

Low-frequency, internal-friction measurements made as a function of temperature on pure In in single-crystal form have shown three effects which could be resolved into the following mechanisms: a frequency-insensitive peak in internal friction observed at ~170°K and believed to be associated with the motion of twin boundaries; a relaxation measured at ~273°K and interpreted as originating from the motion of dislocations interacting with vacancies; and a background relaxation between 320°K and the melting point attributed to dislocation climb. (auth) (Australia)

2668 (ORNL-4570, pp 10-12) DEFORMATION OF CRYSTALLINE SOLIDS. (Oak Ridge National Lab., Tenn.).

From Metals and Ceramics Division annual progress report for the period ending June 30, 1970.

Progress has been made in understanding the nature of precipitation in Nb-Hf and Ta-Hf alloys. Work on dislocation theory has included extensive investigation of dislocations in anisotropic media. Computer programs have been written for simulation of solid solutions based on x-ray measurements and for predicting the changes in such solutions on deformation. (auth)

2669 (ORNL-4570, pp 23) MOESSBAUER STUDIES OF ALLOYS. (Oak Ridge National Lab., Tenn.).

From Metals and Ceramics Division annual progress report for the period ending June 30, 1970.

Mössbauer measurements provided information on the field about ^{61}Ni nuclei in nickel-palladium alloys. (auth)

2670 (ORNL-4570, pp 35-6) SUPERCONDUCTING MATERIALS. (Oak Ridge National Lab., Tenn.).

From Metals and Ceramics Division annual progress report for the period ending June 30, 1970.

A study of niobium with gadolinium or yttrium dispersions was extended to high ac frequencies. Initial results indicate that these materials may exhibit lower ac losses than pure niobium. The Debye temperature of pure technetium has been found to be 454°K by ultrasonic measurements at 4.2°K. A phenomenological model of flux pinning in hysteretic superconductors was derived, based on the assumption of thermally activated flux motion. Two material parameters available from this model should facilitate intercomparison of superconducting properties and metallurgical structure. This model was extended to the case of moving fluxoids flux flow and ac magnetization experiments. (auth)

XUM

2671 (ORNL–4570, pp 40-3) THEORETICAL RESEARCH. (Oak Ridge National Lab., Tenn.).

From Metals and Ceramics Division annual progress report for the period ending June 30, 1970.

A number of phenomena in solids are being investigated with particular emphasis on those that are related to the electronic states. New techniques are being developed for treating the electronic states of ordered and disordered solids theoretically. For the most part, the Korringa–Kohn–Rostoker method is used to study the energy bands of ordered metals and alloys, the LCAO method for ionic and covalent compounds, and the coherent potential approximation for disordered systems. (auth)

2672 (ORNL–4570, pp 112-15) METALLURGY OF REFRACTORY ALLOYS. (Oak Ridge National Lab., Tenn.).

From Metals and Ceramics Division annual progress report for the period ending June 30, 1970.

The aging characteristics of tantalum alloys containing 30, 50, and 60 wt % Hf were studied by x-ray diffraction, metallography, and hardness tests. Hardness increases to about 350 dph resulting from clustering and the precipitation of coherent α-hafnium. Thermodynamic and kinetic features of spinodal decomposition in a hypothetical binary system were studied with various quasichemical models. A model that incorporates atomic nonrandomness and concentration-dependent potential energies agrees qualitatively with experimental observations. The creep strength of TZM was related to the subgrain size. Transverse welds in T-111 creep specimens failed in the weld at high stresses and outside the weld at lower stresses, as predicted from a study of the effect of heat treatment on creep properties. The creep strength of annealed C-129Y was improved by annealing; however, the rupture ductility was reduced. A transition piece of tungsten between platinum and Ta–10 wt % W tubing extended the leak-tight life from 100 hr to between 500 and 1000 hr at 1200°C. The thermal conductivity of tantalum estimated from experimentally derived low-temperature phonon conductivity and Lorenz function values are within 3% of the recommended values to 3000°K. (auth)

2673 (ORNL–4570, pp 118-23) TUNGSTEN METALLURGY. (Oak Ridge National Lab., Tenn.).

From Metals and Ceramics Division annual progress report for the period ending June 30, 1970.

The program for the development of technology on the fabrication and properties of tungsten alloys for application in advanced reactor and isotope systems for space power is described. Variables are being optimized to extrude high-quality tungsten tubing and extruding tubing of advanced high-strength tungsten alloys. Over 800 in.^{2} of high-purity chemically vapor-deposited tungsten sheet was produced for mechanical property and welding studies. The fluorine content was varied between 5 and 30 ppM by controlling the temperature of the deposition chamber. Nodule formation was overcome in depositing alloys containing 1 to 5% Re by using metal-rich gas mixtures. A feasibility study showed that fully dense vanadium can be deposited by the hydrogen reduction of VCl_4 or VF_5 feed gas; however, elimination of interstitial impurities will require additional development. Improved methods are being developed for joining tungsten alloys with lower melting ductile filler metals. The variables for gas tungsten-arc welding of powder-metallurgy tungsten and arc-melted W–25% Re were determined both with and without molybdenum-rhenium alloy filler metal. Cracking in some of the welds of CVD tungsten was caused by high fluorine impurity contents. Additional long-time creep-rupture data at creep rates as low as 10^{-5}/hr were collected for arc-melted tungsten–rhenium alloys and high-purity CVD tungsten. At 1650°C the CVD material was the strongest on the basis of time to 1% creep in 1000 hr; however, W–5% Re is stronger if larger strains or 50% of the rupture stress is used as the criterion. Utilizing the correlation of creep strength developed by Sherby, excellent agreement of data for arc-melted tungsten with data from three other sources was realized. The creep rate varied with the hyperbolic sine of the stress. At very low stresses powder-metallurgy W–25% Re had a lower creep rate at 2200°C than at 1650°C. This anomalous behavior was attributed to the larger grain boundary area available for growth of creep cavities in the material tested at 1650°C. An electron microscopic study of the nucleation and growth of creep cavities in powder-metallurgy tungsten showed that gas bubbles apparently nucleate the cracks, which grow by merging with small cavities expanded by the crack front. It was determined that the creep strength of tungsten in 10^{-5} torr O_2 is substantially lower than in a vacuum of 10^{-8} torr. The W–25% Re alloy is stronger in a partial pressure of oxygen because a surface layer of the rhenium-rich sigma phase forms; however, in this environment the alloy ruptures at strains of 2 to 8%. (auth)

2674 (ORNL–4570, pp 136-42) HASTELLOY N IMPROVEMENT. (Oak Ridge National Lab., Tenn.).

From Metals and Ceramics Division annual progress report for the period ending June 30, 1970.

Carbide precipitates can be correlated strongly with the postirradiation creep properties of Hastelloy N. Alloys with more than 0.2% Si form coarse M_6C that is very stable, but the fracture strains are very low. Alloys with low silicon contents form M_2C, which is finely dispersed up to 650°C but coarsens rapidly at higher irradiation temperatures. The fracture strains are quite low for both forms of M_2C but much lower for the coarse, high-temperature form. Adding Nb, Ti, or Hf produces very finely dispersed MC and results in high postirradiation fracture strains. Several compositions have been found to have good properties, but the optimum concentrations of Nb, Ti, and Hf have not been determined yet. (auth)

2675 (ORNL–4570, pp 143-8) JOINING RESEARCH ON NUCLEAR MATERIALS. (Oak Ridge National Lab., Tenn.).

From Metals and Ceramics Division annual progress report for the period ending June 30, 1970.

The effects of minor quantities of the elements C, S, P, Ti, Al, Mn, and Si on the weldability of nickel-containing alloys such as Inconel 600 and Incoloy 800 are being determined. In heat-affected-zone studies on Incoloy 800, aluminum and titanium improved hot ductility, sulfur was deleterious, but phosphorus had little effect. An alloy with 0.08% C performed better than alloys with less carbon. Additional studies were concerned with alloys containing manganese and sulfur plus phosphorus. Heat-affected zone studies on Inconel 600 were focused on the effect of various elemental additions on microstructures. Significant grain-size differences were observed, and gross liquation in laminations was noted in high-sulfur alloys. Manganese did not affect the microstructure of sulfur-containing alloys unless phosphorus was added also. Filler metals were tested for use with Incoloy 800. Inconel 82T appeared to be best, but electroslag remelted Incoloy 800 also appeared satisfactory. Also an experimental phosphorus-containing composition exhibited a high yield strength and is promising. A study of austenitic stainless steels has centered on the effect of composition on the amount and morphology of the ferritic phases usually found in weld deposits. These phases are body-centered cubic δ-ferrite and body-centered tetragonal martensite. Measurements are made with the Magne–Gage and the quantitative television microscope. Even though the nickel and chromium equivalents remain the same, the compositions of the filler metals were very important in controlling the amount, size, and distribution of ferrite. One alloy predicted to have 100% austenite based on the Schaeffler diagram actually contained about 3% ferrite. (auth)

2676 (ORNL–4570, pp 170-3) HEAVY SECTION STEEL TECHNOLOGY. (Oak Ridge National Lab., Tenn.).

From Metals and Ceramics Division annual progress report for the period ending June 30, 1970.

Activities directed toward characterization of 12-in.-thick quenched-and-tempered steel plates and weldments and toward determination of the effect of irradiation on their mechanical properties are summarized. It was found that the mechanical properties of three plates were similar and satisfied the requirements of the ASTM A533, grade B, class 1, specification. Plate material from the surface locations is superior to material from the interior locations in tensile and impact properties. The characterization studies have increased understanding of flaw-initiated failures. The effects of the acuity of the notch in Charpy V-notch (C_V) specimens on dynamic and static fracture toughness are being analyzed. The weld metal and heat-affected zone (HAZ) of electroslag welds was characterized. The quarter-thickness tensile and impact properties of the weld metal and base metal are similar. The weld metal is somewhat poorer than the base metal in that it does not vary in properties through the thickness (even though the weldment has been double austenitized, double quenched, and tempered). Further, the ductile shelf energy of the weld metal is 80 ft-lb compared with 140 ft-lb for the base metal. The HAZ properties approximate those of the base metal. Changes in tensile and C_V properties from radiation were shown to depend on irradiation temperature; self-annealing occurred at 550°F and up. (auth)

2677 (ORNL–4570, pp 224-7) NERVA PROGRAM METALLURGICAL SUPPORT. (Oak Ridge National Lab., Tenn.).

From Metals and Ceramics Division annual progress report for the period ending June 30, 1970.

A Hall device magnetic probe has been designed, built, and tested for the nondestructive inspection of coolant channels in beryllium reactor components. This probe has demonstrated the feasibility and usefulness of the inspection technique. Outgassing of NERVA fuel elements is being measured under conditions similar to those expected in space operations; the rates for 11 different gases are determined semicontinuously during each test run, and the results are analyzed and plotted as a function of time and

XUM

temperature with the aid of a computer. Adhesion studies are concentrated on the effects of shear motion in controlled vacuum environments. Tensile data on Type 347 stainless steel were obtained to aid in the analysis of thermal fatigue problems in the NERVA nozzle. Study of irradiation effects in beryllium and selected carbonaceous materials requires a knowledge of their properties unirradiated. To provide this base-line data the thermal conductivity, electrical resistivity, and thermopower of several materials in the range 80 to 400°K were measured. (auth)

2678 TUBE MATERIALS IN NUCLEAR REACTOR CONSTRUCTION. **Richter, Herbert; Kleibeler, Hans-Juergen (Vereinigte Deutsche Metallwerke AG, Duisburg, Ger.). Schweiz. Arch. Angew. Wiss. Tech.: 35: 375-80(Nov 1969). (In German).**

Alloys used for reactor fuel cans, heat exchanger tubes, and pressure tubes in various types of nuclear reactors are discussed. (Metals Abstr.)

2679 EFFECT OF Nb AND Ag ON THE RECRYSTALLIZATION PROCESS IN Nb-Ag PERMALLOY. **Nagai, Takeshi; Henmi, Zenzo (Fujitsu Labs., Ltd., Kawasaki, Japan). J. Jap. Inst. Metals; 34: 943-8(Sep 1970). (In Japanese).**

A new Permalloy was developed by adding Nb and Ag to Permalloy (Fe-78.5% Ni alloy). After heat treatment the material had a low coercive force (Hc) and a high residual induction/peak induction (Br/Bm). Although magnetic domain wall migration was impeded by deformation strain in a cold worked Nb-Ag Permalloy, after recovery or recrystallization the material is saturated by low induction and then Hc decrease. The rolling texture in Nb-Ag Permalloy upon annealing is retained by Nb and Ag and consequently Br/Bm becomes high in Nb-Ag Permalloy. (auth) (Japan)

2680 IMPURITY DIFFUSION OF RARE EARTH METALS IN COPPER. **Badrinarayanan, S.; Mathur, H. B. (National Chemical Lab., Poona). Indian J. Pure Appl. Phys.; 8: 324-30 (Jun 1970).**

The impurity diffusion of the rare earth metal isotopes ^{141}Ce, ^{147}Pm, $^{152+154}Eu$, ^{160}Tb, ^{170}Tm and ^{177}Lu in copper metal was studied in the temperature interval 700 to 1010°C by the residual activity method of P. L. Gruzin [Dokl. Akad. Nauk USSR, 86 (1952), 289] and by the serial sectioning technique. Plots of the log specific activity versus the square of diffusion distance show, instead of the expected straight line, a curve which can be resolved into two straight line portions of very different slopes. The initial straight line portion of a greater slope has been attributed to the volume diffusion and the second straight line of a lower slope, which extends to depths beyond 20 μm, has been attributed to the diffusion through dislocations. The experimental results on the activation energy for impurity diffusion of the rare earth metal isotopes in copper are compared with those calculated from the elastic model of R. A. Swalin [Acta metall., 5 (1957), 443]. (auth)

2681 EFFECT OF TEMPERATURE AND DEFORMATION ON MECHANICAL CHARACTERISTICS OF MOLYBDENUM AND NIOBIUM. **Aleksyuk, M. M.; Rudenko, V. N. Tekhnol. Organ. Proizvod.; No. 3, 106-7(1969). (In Russian).**

The effects of temperature and rate of deformation on the mechanical properties of Nb and Mo were studied at 290 to 1870°K and a deformation rate of 10^{-4} to 10^{-1} sec^{-1}. It is shown that the specimen reactions follow a regular law. At 300 to 700°K the maximum strength of the tested materials increased insignificantly with increased rate of deformation; at 0.35 to 0.5 T_{melt} the increased rate of deformation resulted in considerably increased strength but the difference between the maximum strength and yield was reduced. The compression strength in alloys was less affected by the rate of deformation than in pure metals. (R.V.J.)

2682 STRENGTH OF NIOBIUM-MOLYBDENUM ALLOYS IN VACUUM AT HIGH TEMPERATURES. **Rudenko, V. N. Probl. Prochnosti; 1: No. 4, 72-4(Oct 1969). (In Russian).**

The mechanical properties (ultimate tensile strength (UTS), yield strength (YS), relative elongation, and relative transverse contraction) of Nb-10% Mo alloy, and a modified form of the alloy containing traces of Zr and C, were studied in vacuum (10^{-5} torr) at 20 to 1600°C. The ductility of the first alloy fell sharply with increasing temperature up to 800°C, after which it sharply increased, while the UTS and YS fell. These effects were attributed to the influence of gaseous impurities. The corresponding effects in the second alloy were rather less marked but more complicated. The addition of C and Zr increased the UTS, but reduced the YS: UTS ratio of the original material at 1300°C. (Metals Abstr.)

2683 LEAD SHIELD IN THE FIRST NUCLEAR-POWERED SHIP MUTSU. **Nara, Shigeru (Ishikawajima-Harima Heavy Industries Co. Ltd., Tokyo). Sempaku; 43: No. 3, 47-51; 72 (Mar 1970). (In Japanese).**

The radiation sources in the nuclear-powered ship Mutsu, for which shielding should be provided, are the reactor proper and main cooling system. The requirements for the shield in a nuclear-powered ship are stringent, compared to land-based reactor plants, especially concerning its weight and volume; the center of gravity must also be as low as possible. The total weight of the lead shield used for the secondary shielding is 420 t. The secondary shield of lead for the reactor containment vessel is described. The requirements are: the part of shield on the cover flange of the containment vessel must be removable; gap must be provided between lead blocks so as to absorb expansion of the pressure vessel, and also of the blocks themselves; the joint face of the blocks must be in a direction making as large angle as possible with radiation sources; and so on. The lead blocks are cast in steel-plate casings. (auth) (Japan)

2684 IMPACT OF HEAT ON A STRAIGHT TUBE. **Novak, J. (National Research Inst. for Machine Design, Bechovice, Czech.). Jad. Energ.; 16: 293-6(Sep 1970). (In Czech).**

The results of measurements of external and internal steel tube surfaces in the case of thermal shock generated by air flowing through the tubes are reported. The measurement results are compared with calculations. These problems were solved in connection with the first Czechoslovak nuclear power station. (auth)

2685 THERMODYNAMIC PROPERTIES OF ZINC-INDIUM DILUTE LIQUID SOLUTIONS. **Moser, Z. (Inst. of Bases of Metallurgy, Krakow). Bull. Acad. Pol. Sci., Ser. Sci. Tech.: 18: 481-6(1970).**

Results of measurements of electromotive force in cells containing electrolyte and Zn-In alloys are presented. The measurements were made at 714, 757, and 805°C and Zn concentrations of X_m = 0.0101 to 0.9000 mole fraction. Data and information are included on emf dependence on temperature and Zn activity as function of mole fraction. (J.R.D.)

2686 ADSORPTION OF OXYGEN AND NITROGEN ON TANTALUM FILMS. PART I. EXPERIMENTAL METHODS. **Fischer, Konrad; Fromm, Eckehard (Max-Planck-Institut fuer Metallforschung, Stuttgart). Z. Metallk.; 61: 710-17(Oct 1970). (In German).**

A volumetric method for experiments on the adsorption of gases on thin films is discussed. The pressure in the receiver, the electrical resistivity, and the temperature of the film were measured. Using these data, the amount of adsorbed gas and the sticking probability can be determined. The details of the apparatus, the experimental procedure and the production of pure tantalum films are described. (auth)

2687 EFFECTS OF IMPURITIES AND HEAT TREATMENT ON THE INTERNAL FRICTION OF TUNGSTEN AT HIGH TEMPERATURES. **Berlec, I. (General Electric Co., Cleveland). Met. Trans.; 1: 2677-83(Oct 1970).**

An improved internal friction technique was used to study the relaxation processes in pure tungsten and the following alloys: commercially doped tungsten (218W), W-1% ThO_2, 218W-3% Re, and 218W-20% Re. Internal friction experiments were performed on worked and recrystallized specimens in the temperature range of 300 to 3000°K. The effects of impurities and alloying additions on the damping and recrystallization behavior of tungsten are demonstrated. It is further shown that the internal friction curves can conveniently be used to determine the temperature of primary and secondary recrystallization. The important effect of impurities on the microstructure and high temperature strength is also revealed by the temperature dependence of shear modulus. (auth)

2688 INVESTIGATION OF THE CONVECTIVE-DIFFUSION LIMITED OXIDATION OF MOLYBDENUM BY THE ROTATING DISK METHOD. **Olander, D. R. (Univ. of California, Berkeley); Schofill, J. L. Jr. Met. Trans.; 1: 2775-84(Oct 1970).**

A rotating disk system was developed to study heterogeneous chemical reactions subject to gas phase diffusion limitations. The system was operated at temperatures up to 2000°K and disk speeds up to 15,000 rpm to investigate the reaction of oxygen and molybdenum. The independence of reaction or diffusion on radial position in the rotating disk system permitted kinetic data to be obtained from simple weight loss measurements as a function of disk temperature, oxygen partial pressure, and disk speed. Because of the availability of an exact solution of the diffusion-convection equation for the rotating disk, the diffusional contribution to the overall rate can be accurately assessed when both gas phase diffusion and surface reaction offer resistances of comparable magnitude. The results of this work demonstrated the importance of studying atmospheric pressure, high temperature

XUM

heterogeneous reactions in a flow system for which accurate prediction of diffusional limitations is possible. The rotating disk is an eminently satisfactory tool for such theoretical and experimental studies. (auth)

2689 PRECIPITATION OF Ni_3Nb PHASES IN A Ni–Fe–Cr–Nb ALLOY. Kirman, I.; Warrington, D. H. (Univ. of Sheffield, Eng.). Met. Trans.; 1: 2667-75(Oct 1970).

The age hardening of a Ni-Fe-Cr-Nb alloy containing 4.85 wt % Nb was studied using transmission electron microscopy. The major hardening phase in this alloy was γ^*, DO_{22}-ordered Ni_3Nb, which precipitated as a fine dispersion of square plates. It is shown that nucleation of γ^* plates may be dependent upon matrix excess vacancy concentration, but nucleation of γ^* plates was also observed at dislocations and extrinsic stacking faults. The γ^* phase was metastable with respect to the orthorhombic Ni_3Nb phase, β, which precipitated by either a cellular or an intragranular reaction, depending upon the aging temperature. It is proposed that the intragranular nucleation of β laths proceeds by the growth of stacking faults from within γ^* plates; the γ^* plates subsequently dissolve in favor of the β laths. Room temperature deformation of the γ^* dispersion is shown to produce faults within the γ^* plates; possible dislocation reactions occurring during this deformation are discussed. (auth)

2690 DEFORMATION BEHAVIOR OF POLYCRYSTALLINE METALS. Voehringer, O. Wiss. Z. Tech. Hochsch. Otto von Guericke Magdeburg; 13: 343-53(1969). (In German).

Problems related to polycrystalline plasticity are discussed in the light of recent investigations and data reported in the literature. Factors influencing polycrystalline plasticity, changes in grain structure caused by plastic deformation, and the deformation characteristics of pure and alloyed metals (with particular reference to Nb, Fe, Cu, and Cu–Sn alloys) are considered. (Metals Abstr)

2691 DIFFUSION IN BCC IRON BASE ALLOYS. Bowen, A. W.; Leak, G. M. (Univ. of Manchester, Eng.). Met. Trans.; 1: 2767-73(Oct 1970).

Using radiotracer techniques, volume diffusion measurements were carried out in the bcc phases of the following systems: iron containing 0 to 20 wt % Cr, iron containing 0 to 20 wt % V, and iron containing 0 to 6 wt % Ti. The activation energies and frequency factors were found to decrease with increasing solute content. A comparison is made between the experimental results and theoretical calculations in terms of the various relationships between activation energy, entropy, and frequency factor. (auth)

2692 DENSITIES OF LIQUID In–Bi, Sn–In, Bi–Sb, AND Bi–Cd–Tl ALLOYS. Berthou, P.-E.; Tougas, R. (Univ. of Montreal). Met. Trans.; 1: 2978-9(Oct 1970).

A method based on Archimedes' principle was used to measure the density of the following liquid alloys: Bi–Cd–Tl and In–Sn alloys at 122 to 440°C; Bi–In alloys at 73 to 660°C; and Bi–Sb alloys at 403 to 742°C. The density of pure liquid Bi, In, Sb, and Sn were also measured. (G.M.C.)

2693 EFFECT OF TEMPERATURE ON THE LOGARITHMIC CREEP OF ZIRCALOY-2. Snowden, K. U. (Australian Atomic Energy Commission Research Establishment, Sutherland). J. Nucl. Mater.; 36: 347-9(Sep 1970).

Results of creep tests for Zircaloy-2 at 25 to 428°C are presented. Zircaloy-2 exhibited a continuously decreasing creep rate with time. Below 400°C, the creep curves were found to have a logarithmic form. The creep strain could be represented by $\epsilon = \alpha \log_{10} t + \beta$, where t is the time under stress and α and β are constants independent of time. (G.M.C.)

2694 DETERMINATION OF OXYGEN CONCENTRATION AND MASS TRANSFER COEFFICIENTS IN SODIUM USING URANIUM. Isaacs, H. S. (Brookhaven National Lab., Upton, N. Y.). J. Nucl. Mater.; 36: 322-30(Sep 1970).

Uranium in sodium at 500 to 650°C was found to react with oxygen at a rate proportional to the oxygen concentration in the sodium. The rate of this reaction was controlled by the mass transfer of oxygen in the sodium and not by that in the uranium oxide formed as an adherent reaction product. Methods are discussed whereby uranium can be used to determine oxygen concentrations and mass transfer coefficients in sodium. (auth)

2695 PRODUCTION AND PROPERTIES: ZIRCALOY TUBES FOR NUCLEAR CLADDING. Kondo, Yutaka; Kodama, Tatsuro; Konishi, Takao. Sumitomo Search; No. 1, 49-58(May 1969).

Research, development, manufacture, and properties of Zircaloy, with particular ref. to improved inspection and quality, is described. A production flowsheet is included. Standard compositions for Zircaloy –2 and –4 are given. Physical properties and test data are reported, including flare ratio, hydraulic and bursting results, grain size, corrosion weight-gain, hydride orientations etc. (Metals Abstr.)

2696 INTERACTION BETWEEN SLIP DISLOCATIONS AND TWINS IN α-URANIUM. II. INTERACTION FORCES. Saxl, I. (Nuclear Research Inst., Rez, Czech.). Czech. J. Phys.; 20: 1157-65(1970).

The forces on dislocations propagating through twins are calculated using the anisotropic elasticity. The anisotropic boundary force is calculated assuming that the twin boundary is of the welded type. The stresses necessary for the passage of dislocations through twins are compared with the estimated stresses for a homogeneous thermally activated nucleation of twins. (auth)

2697 ELASTIC PROPERTIES AND INTERNAL FRICTION OF HYDROEXTRUDED Mo. Mochalov, G. A.; Evstyukhin, A. I.; Sidorenko, O. N.; Sevryugin, V. V. Met. Metalloved. Chist. Metal., Sb. Nauch. Rabot; No. 8, 88-98(1969). (In Russian).

The effects of cold plastic deformation by hydraulic extrusion on the modulus of elasticity of (Young's model), the modulus of slip, the coefficient of Poisson ratio and internal friction of various compositions of polycrystalline Mo were studied. The deformed material is characterized by smaller modulus of elasticity (Young's model), smaller modulus of slip, smaller coefficient of Poisson ratio, and by relatively high internal friction value dependent on dislocation density. The maximum value of modulus of defect (Young's model) of 8.03% was found for metalloceramic Mo alloy. The change in elastic properties of metalloceramic Mo upon hydroextrusion is associated with porosity disappearance. (J.R.D.)

2698 RECOVERY OF ELASTIC PROPERTIES AND INTERNAL FRICTION IN HYDROEXTRUDED Mo. Mochalov, G. A.; Evstyukhin, A. I.; Sidorenko, O. N. Met. Metalloved. Chist. Metal., Sb. Nauch. Rabot; No. 8, 99-115(1969). (In Russian).

Modulus (Young's model) recovery, slip modulus recovery, Poisson coefficient recovery, and internal friction recovery in hydroextruded Mo was studied. The specimens were subjected to various degrees of deformation and to the action of staircase-like annealing. Recovery of internal friction in deformed Mo as a result of annealing is complete at temperatures of 800 to 900°C. Elastic properties are recovered in two stages, the first stage at annealing in the range 800 to 900°C. The recovery of elastic and inelastic properties in Mo occurs in vacuum annealing at 200 to 2000°C under 10^{-5} mm Hg. (J.R.D.)

2699 INVESTIGATION OF STRESS RELAXATION IN TEMPERED AND DEFORMED U DURING BENDING. Tsvetaev, A. A.; Bovenko, V. N.; Golovanov, Yu. N. Met. Metalloved. Chist. Metal., Sb. Nauch. Rabot; No. 8, 58-63(1969). (In Russian).

Uranium metal containing 0.002% Fe, 0.001% Al, 0.003 Si, and 0.05 C was rolled in plates to a thickness of 0.4 to 0.5 mm thickness after salt bath annealing at 650°C. The effects of cold hardening on relaxation processes in elastically strained metals is independent of the process used. Cold-hardening can be related by exertion and recording of external forces if the thermal activation is sufficient for movement of the defects in the tension field and if heterogeneous defect concentrations can be equalized. A more detailed investigation is required to define the mechanism of defect redistribution in cold-hardened metals under strain by studying effects of temperature, cold-hardening, texture, and microstructure. (J.R.D.)

2700 TEMPERATURE EFFECTS ON MICROHARDNESS OF Zr–O ALLOYS. Korobkov, I. I. Met. Metalloved. Chist. Metal., Sb. Nauch. Rabot; No. 8, 48-52(1969). (In Russian).

Relations of temperature with hardness of Zr–O solid solutions were investigated. The effects of O mobility in these alloys were also investigated. It was found that the hardness in relation to temperature increases with O content to about 8 at.%. The peak hardness displacement was established as toward lower temperatures in proportion to the increased O content. (J.R.D.)

2701 BOND PARAMETERS OF SELF-DIFFUSION COMPONENT BINARY SYSTEM WITH PARTIAL THERMODYNAMIC FUNCTIONS. Smirnov, E. A.; Fedorov, G. B. Met. Metalloved. Chist. Metal., Sb. Nauch. Rabot; No. 8, 154-7(1969). (In Russian).

Processes of diffusion involving bond parameters were studied by investigating heterointerstitial relation coefficients and measurement of coefficients of self-diffusion in binary alloys. The relations of the exponential multiplier and the mole fraction to the thermodynamic multiplier component in binary Ni–Cr and Zr–U alloys were calculated for temperatures of 900 and 1100°C. A proportional relation was also found by comparing experimental and thermodynamic data for the systems under study. (J.R.D.)

XUM

2702 REDISTRIBUTION OF C IN CAST THERMALLY TREATED Mo. Nikishanov, V. V.; Ginzburg, S. S.; Evstyukhin, A. I.; Shulepov, V. I.; Yudkovskii, S. I. Met. Metalloved. Chist. Metal., Sb. Nauch. Rabot; No. 8, 199-205(1969). (In Russian).

The distribution of C in cast Mo and cast thermally treated Mo was studied by electron microscopy autoradiography. The structure of the material and radioisotope distribution were studied simultaneously using this method. Mechanical test results are the basis for the conclusion that the relatively low plasticity of Mo in cast and cast thermally treated specimens at 1600°C and the relatively high plasticity of Mo specimens after annealing at 1300°C are associated with heterogeneity of structure and distribution of assimilated impurities such as C. (J.R.D.)

2703 SELF-DIFFUSION IN W AND Nb AND DIFFUSION OF W IN Nb. Fedorov, G. B.; Zhomov, F. I.; Smirnov, E. A. Met. Metalloved. Chist. Metal., Sb. Nauch. Rabot; No. 8, 145-53(1969). (In Russian).

Layer recording and tracer techniques using ^{185}W and ^{95}Nb were used to investigate self-diffusion in Nb and W and diffusion of W in Nb. Specimens were prepared from zone refined W and Nb which were also cathode-ray remelted. Diffusion experiments were carried out at 1800 to 2200°C. Results show a close relationship between activation energy for self-diffusion and melting temperature. Similar relations were found between heats of melting and sublimation. (J.R.D.)

2704 EFFECTS OF ALLOYING Zr WITH Nb OR Mo ON DIFFUSION MOBILITY OF Nb AND Mo. Fedorov, G. B.; Smirnov, E. A.; Novikov, S. M. Met. Metalloved. Chist. Metal., Sb. Nauch. Rabot; No. 8, 41-7(1969). (In Russian).

The plot for activation energy of Zr diffusion shows that in alloys having identical alloying components the energy for Zr with Nb is lowest and increases in Zr–Mo alloys and reaches the highest values in Mo–Nb–Zr alloys. (J.R.D.)

2705 EVALUATION OF MATERIALS-COMPATIBILITY PROBLEMS IN THE EBR-II REACTOR. Ruther, W. E.; Claar, T. D.; Strain, R. V. (Argonne National Lab., Ill.). pp 81-96 of Corrosion By Liquid Metals. /Draley, Joseph E. (ed.). New York; Plenum Publishing Corp. (1970).

From Corrosion by Liquid Metals Conference, Philadelphia, Pa. See CONF-691007.

Three cases of slow, direct interaction of a material of construction with the high-temperature sodium coolant are discussed. Copper was dissolved from an exposed bus bar and transferred to other reactor parts. An ex-reactor investigation indicated that neither the deposited copper nor the copper in solution in the sodium reacted further with stainless steel surfaces. Beryllium copper (Berylco 25) wear bushings eroded and corroded in the high-temperature sodium. An aluminum bronze (Ampco 18-13) bushing proved to be a satisfactory replacement. Tantalum was slightly attacked by the sodium. The resultant fine, highly radioactive corrosion product increased handling difficulties during disposal. In addition, three instances of failure of thin sections of materials that are usually resistant to sodium are analyzed. In two instances the investigation indicated contamination of the component by a carbonaceous material prior to insertion in the reactor. In the third instance (valve bellows) exposure of the component to sodium containing oxygen prior to insertion in the reactor system is postulated as the cause of failure. (auth)

2706 RADIOACTIVE MATERIAL TRANSPORT IN FLOWING SODIUM SYSTEMS. Brehm, W. F.; Koehmstedt, P. L.; Kovacevich, E. A.; Shannon, D. W. (Battelle-Northwest Labs., Richland, Wash.). pp 97-113 of Corrosion By Liquid Metals. /Draley, Joseph E. (ed.). New York; Plenum Publishing Corp. (1970).

From Corrosion by Liquid Metals Conference, Philadelphia, Pa. See CONF-691007.

A summary is given on work that was done on the transport and deposition of activated corrosion products, including ^{60}Co, ^{51}Cr, and ^{54}Mn, in flowing sodium. Fluid boundary-layer resistance to deposition of species exists for many isotopes under a broad range of conditions. Deposited activity can either release from the deposition site and migrate through the loop, or diffuse into the base metal. Deposited corrosion product activity can create reactor maintenance problems. (G.M.C.)

2707 PENETRATION OF REFRACTORY METALS BY ALKALI METALS. Klueh, R. L. (Oak Ridge National Lab., Tenn.). pp 177-96 of Corrosion By Liquid Metals. /Draley, Joseph E. (ed.). New York; Plenum Publishing Corp. (1970).

From Corrosion by Liquid Metals Conference, Philadelphia, Pa. See CONF-691007.

Under certain conditions tantalum and niobium undergo rapid penetration by liquid alkali metals along grain boundaries and certain crystallographic planes. Penetration is observed only when oxygen dissolved in the refractory metal exceeds some threshold concentration. This concentration depends upon the refractory metal, the alkali metal, and the temperature. Penetration was first encountered in niobium and tantalum exposed to lithium, but has now also been found to occur when these metals are exposed to sodium, potassium, and the sodium-potassium eutectic. Oxygen levels required to effect penetration in niobium and tantalum by lithium, sodium, and potassium at 600°C are compared, and the rate of penetration is discussed in terms of a corrosion model. (auth)

2708 GRAIN BOUNDARY GROOVING OF IRON IN LIQUID SODIUM. Eberhart, J. G.; Cafasso, F. A.; Feder, H. M.; Kremsner, W. (Argonne National Lab., Ill.). pp 461-7 of Corrosion By Liquid Metals. /Draley, Joseph E. (ed.). New York; Plenum Publishing Corp. (1970).

From Corrosion by Liquid Metals Conference, Philadelphia, Pa. See CONF-691007.

Grain boundary grooving studies on α-iron in a liquid sodium environment indicated a mass transport mechanism of surface diffusion with an activation enthalpy of 1.7 ± 0.1 eV/atom. The surface diffusion coefficient was larger and the activation enthalpy was smaller than those reported for α-iron in vacuum. A grain boundary to interfacial tension ratio of 0.39 ± 0.08 was deduced from the groove angle. (auth)

2709 SOLUBILITIES OF SEVERAL TRANSITION METALS IN LIQUID LEAD–BISMUTH EUTECTIC. Rosenblatt, G.; Wilson, J. R. (Queen's Univ., Kingston, Ont.). pp 469-77 of Corrosion By Liquid Metals. /Draley, Joseph E. (ed.). New York; Plenum Publishing Corp. (1970).

From Corrosion by Liquid Metals Conference, Philadelphia, Pa. See CONF-691007.

Solubilities of cobalt, nickel, and chromium in liquid lead-bismuth eutectic were obtained over the low temperature range 400 to 500°C. Solubility equations and experimental heats of mixing were calculated for these metals over the temperature range. (auth)

2710 OXIDATION-REDUCTION REACTIONS FOR CHROMIUM AND 304 STAINLESS STEEL IN LIQUID SODIUM. Jansson, Sven A.; Berkey, Edgar (Westinghouse Research Labs., Pittsburgh). pp 479-513 of Corrosion By Liquid Metals. /Draley, Joseph E. (ed.). New York; Plenum Publishing Corp. (1970).

From Corrosion by Liquid Metals Conference, Philadelphia, Pa. See CONF-691007.

Solid electrolyte electrochemical cells were used to follow the oxygen activity in reactor grade liquid sodium [Na(l)] containing initially 10 to 20 ppM oxygen during reactions with chromium powder or 304 stainless steel over the temperature range of ~300 to 500°C. The measured emf values were used to calculate chemical potentials for oxygen (expressed as the logarithm of the oxygen pressure), to deduce effective oxygen concentrations, and to postulate the appropriate chemical reactions involved. Of particular importance was a run with an excess of chromium powder in sodium in which the system was equilibrated at a constant oxygen potential at 520°C that was tentatively identified as representative of the $Na(l)-Cr(s)-NaCrO_2(s)$ equilibrium. Emf values obtained upon cooling were taken to occur at equilibrium, and thus the results could be used to estimate thermochemical data for $NaCrO_2$. Sodium–stainless steel interactions yield complex emf behavior, indicating a number of competing mechanisms. To complement these runs, differently pretreated specimens of 304 stainless steel were exposed to different purity sodium and subsequently characterized by means of scanning electron microscopy, microprobe analysis, and x-ray diffraction. The results illustrate the role in alloy corrosion of enhanced diffusion along grain boundaries and in cold-worked surface layers and also the effect of sensitization. High oxygen content was observed to increase the amount of iron-rich precipitates on the specimens, indicating the importance of $Na_xFe_yO_z$ solution compounds. CrN(s) was found on cold worked surfaces exposed to air-contaminated sodium. (auth)

2711 SOLUBILITY AND REACTIONS OF OXYGEN IN SODIUM. Minushkin, B.; Kissel, G. (Brookhaven National Lab., Upton, N. Y.). pp 515-22 of Corrosion By Liquid Metals. /Draley, Joseph E. (ed.). New York; Plenum Publishing Corp. (1970).

From Corrosion by Liquid Metals Conference, Philadelphia, Pa. See CONF-691007.

Measurements of emf were made using solid electrolyte cells of the type: $Na_l, Na_2O_{(sat'd)} || ThO_2 - 15$ w/o $Y_2O_3 || Na_l, O_{(d)}$; $Au, O_{2(g)}$ 1 atm$|| ThO_2 - 15$ w/o $Y_2O_3 || Na_l, Na_2O_{(sat'd)}$; and $Au, O_{2(g)}$ 1 atm||

ThO_2–15 w/o Y_2O_3|Na_l,$Fe_{(s)}$,$O_{(d)}$. The first two cells were used to determine the solubility of oxygen in sodium and the standard molar free energy of formation of Na_2O, respectively, and to construct a free energy-temperature-composition diagram for the sodium-oxygen system, based on emf measurements. The last cell was used in a preliminary study of reactions between iron and oxygen dissolved in sodium. (auth)

2712 MEASUREMENTS OF THE SOLUBILITY OF IRON AND CHROMIUM IN SODIUM. Singer, R. M.; Fleitman, A. H.; Weeks, J. R.; Isaacs, H. S. (Brookhaven National Lab., Upton, N. Y.). pp 561-76 of Corrosion By Liquid Metals. /Draley, Joseph E. (ed.). New York; Plenum Publishing Corp. (1970).

From Corrosion by Liquid Metals Conference, Philadelphia, Pa. See CONF-691007.

The solubilities of Fe, Cr, and Ni were measured in liquid Na. Iron is more soluble than Ni and Cr in Na at T > 600°, yet Ni and Cr are selectively leached from stainless steels during corrosion. Concentrations of Fe and Cr in circuit Na (low oxygen) generally approximate their solubilities at T_{max}, whereas concentrations of Ni are generally less than its solubility at T_{max}. The location of Ni and Cr deposits as described by Roy et al. and by Bogers was shown to be consistent with the temperature dependence of the Ni and Cr solubilities. (auth)

2713 SEGREGATION OF IMPURITIES AND THE FORMATION OF PARTICLES IN SODIUM SYSTEMS. Isaacs, H. S.; Singer, R. M.; Becker, W. W. (Brookhaven National Lab., Upton, N. Y.). pp 577-87 of Corrosion By Liquid Metals. /Draley, Joseph E. (ed.). New York; Plenum Publishing Corp. (1970).

From Corrosion by Liquid Metals Conference, Philadelphia, Pa. See CONF-691007.

From experimental studies it appears that the formation of particles at the sodium/cover-gas interface does occur. Solubility experiments that presently are in progress now use sampling containers fitted with removable covers in an attempt to overcome the high surface concentrations of iron and chromium now known to exist on the surface. The latest solubility results for iron in sodium appear much lower using this new sampling technique. Particulates may be formed as a result of the cooler cover-gas as was observed in experiments involving copper and carbon deposits. The results obtained with copper deposition on molybdenum suggest that if this mechanism is the one for the formation of particulates, then, at low solubilities, the rate of formation of particles increases more rapidly with temperature than the rate of increase in solubility. These results may also be relevant in design of reactors using sodium as a coolant. Metal deposits would be expected to form on all surfaces in contact with the sodium-cover-gas interface. For example, any probe left in the sodium would form deposits which could lead to serious removal problems if the probe remained in the sodium for extended periods of time. In a similar manner the sodium surface in surge tanks could be expected to give rise to deposits on the container walls which may eventually lead to plugging of the tank. (auth)

2714 SOLUBILITIES OF MOLYBDENUM, TUNGSTEN, VANADIUM, TITANIUM, AND ZIRCONIUM IN LIQUID POTASSIUM. Stecura, Stephan (Lewis Research Center, Cleveland). pp 601-11 of Corrosion By Liquid Metals. /Draley, Joseph E. (ed.). New York; Plenum Publishing Corp. (1970).

From Corrosion by Liquid Metals Conference, Philadelphia, Pa. See CONF-691007.

The solubilities of five transition metals were studied in liquid potassium containing less than 20 ppM by weight of oxygen. The solubilities of molybdenum at 1040 and 1316°K, tungsten at 1055 and 1328°K, and vanadium at 1012 and 1341°K are 6 and 13, 20 and 130, and 6 and 70 ppM by weight, respectively. The solubilities of titanium and zirconium between 1020 and 1340°K are less than 4 and 10 ppM by weight, respectively. The heats of solutions for molybdenum, tungsten, and vanadium in liquid potassium are 6.7 ± 0.8, 17.6 ± 1.2, and 20.7 ± 1.4 kilocalories per mole, respectively. (auth)

2715 THERMAL CONDUCTIVITY, SPECIFIC ELECTRICAL RESISTIVITY, AND TOTAL EMISSIVITY OF REFRACTORY METALS AT HIGH TEMPERATURES. Neimark, B. E.; Voronin, L. K. High Temp. (USSR) (Engl. Transl.); 6: 999-1010(Nov-Dec 1968).

Translated from Teplofiz. Vys. Temp.; 6: 1044-56(Nov-Dec 1968).

An experimental setup for measuring λ, ρ, L, and ϵ_t by Bode's method is described. The results of these measurements are given for niobium, tantalum, and tungsten in the temperature range 1000–1700°C. Values are also given for λ, ρ, and L obtained by the Eger–Disselhorst method for the same metals in the range 100 to 1000°C. It is shown that the results obtained by the two methods agree well among themselves and also with the data of other authors. (auth)

2716 REACTION OF CARBON WITH NICKEL-BASE SOLID SOLUTION ALLOY CONTAINING CARBIDE-FORMING ELEMENT. Niki, Eiji; Masato, Kazuo (Tokyo Univ.). J. Jap. Inst. Metals; 34: 879-83(Sep 1970). (In Japanese).

The systems Ni–Ti–C, Ni–V–C, Ni–Zr–C, Ni–Nb–C, Ni–Mo–C, Ni–Ta–C, and Ni–W–C were studied by means of gas carburization and electron probe microanalysis in the nickel-rich portion. The solubility of carbon and each carbide-forming element in nickel at 1100°C were determined as follows ([A] is the atomic percent of A.): $\log [C] + 0.222 [Ti] = 1.000$, $3.5 \lesssim [Ti] \lesssim 10$; $\log [C] + 0.182 [V] = 1.699$, $8 \lesssim [V] \lesssim 15$; $\log [C] + 2.060 [Zr] = -0.721$, $0.05 \lesssim [Zr] \lesssim 0.3$; $\log [C] + 0.164 [Nb] = -0.066$, $1 \lesssim [Nb] \lesssim 8$; $\log [C] + 0.276 [Mo] = 1.505$, $7 \lesssim [Mo] \lesssim 10$; $\log [C] + 1.696 [Ta] = 3.301$, $2 \lesssim [Ta] \lesssim 3$; and $\log [C] + 0.105 [W] = -0.097$, $6 \lesssim [W] \lesssim 11$. The hardness of the carburized alloy was measured by a micro-hardness tester. The result showed that the increase in hardness was negligibly small with the carburization. It was thought that the hardening of the matrix itself is necessary for the hardness of the carburized layer under such a condition of carbide-dispersion as in the present work. (auth)

2717 BETA PROCESSING [FORGING] OF TITANIUM ALLOYS. Coyne, James E. Precis. Metal; 27: No. 11, 48-52; 88(Nov 1969).

Beta forging expands the forging range and reduces the energy needed to deform all Ti alloys. Investigations showed that β forging improves the tensile strength, creep strength, and fracture toughness of Ti–6Al–4V, Ti–8Al–Mo–1V, and Ti–6Al–2Sn–4Zr–2Mo alloys with no decrease in fatigue resistance. Improved shapes resulted in Ti alloy parts such as fan blades and landing gear wheels which need only minimal machining before use. Several new alloys also are now available which are capable of 160,000 to 170,000 lb/in^2 yield strength in section size up to 3.5 in. thick. Examples are Ti–8Mo–8V–2Fe–3Al and Ti–6Al–6V–4Mo–4Zn. The new β alloys such as Ti–3Al–8V–6Cr–4Mo–4Zr offer the possibility of increased strength in even heavier sections with improved fracture toughness. (Metals Abstr.)

2718 DEFORMATION PROPERTIES OF VANADIUM SINGLE CRYSTALS. Bressers, J. (CCR Petten, Netherlands); Heerschap, M.; de Meester, P. J. Less-Common Metals; 22: 321-6 (Nov 1970).

The preliminary results reported in this communication form a part of a systematic study in which the influence of temperature, strain-rate, and orientation on yield stresses and work-hardening characteristics is investigated. It is shown that vanadium exhibits a clear, three-stage hardening behavior under some of the temperature and orientation conditions used. (auth)

2719 X-RAY LINE BROADENING OF A QUENCHED ZIRCONIUM–1.25 WT. PERCENT CHROMIUM ALLOY. Rumball, W. M. (Atomic Energy of Canada Ltd., Chalk River, Ont.). J. Less-Common Metals; 22: 287-92(Nov 1970).

X-ray line-broadening (B) measurements were made on samples of a Zr–1.25 wt % Cr alloy cooled from the β-region at between 0.1 and 4500°C/sec. Line broadening increased with increased cooling rate and with increased Bragg angle, θ. Lattice distortion of the supersaturated quench products was anisotropic, the c axis contracting more than the a axis. Plotting the corrected line-broadening data in the form $B \cos \theta$ vs $\sin \theta$ showed that the grain size of the transformation product contributed most to the observed line broadening in the cooling-rate range studied. However, any incremental broadening above 2000°C/sec is largely due to increases in lattice distortion. Estimates of the contribution of grain size and lattice distortion to the hardness of the alloy, quenched at about 2240°C/sec, agree well with experimental results and explain the observed variation of hardness with cooling rate. (auth)

2720 COMPATIBILITY OF COPPER WITH TANTALUM–10 WT. PERCENT TUNGSTEN ALLOY AT ELEVATED TEMPERATURES. Harrison, J. L.; Coffey, D. L.; Burgan, C. E. (Monsanto Research Corp., Miamisburg, Ohio). J. Less-Common Metals; 22: 275-9(Nov 1970).

The compatibility of copper with Ta–10 wt % W at ~1100°C was studied. It was determined that the copper wets the Ta–10 wt % W grain boundaries, and that a eutectic is formed at the interface between the copper and the refractory alloy matrix at 1100°C. Limited tests with T–111 (Ta–8 wt % W–2 wt % Hf) indicate similar reactions with other tantalum-base alloys. (auth)

2721 INFLUENCE OF ALLOYING AND TEMPERATURE ON THE ELASTIC CONSTANTS OF TANTALUM. Armstrong, D. A.;

XUM

Mordike, B. L. (Univ. of Liverpool). J. Less-Common Metals: 22: 265-74(Nov 1970).

The elastic compliance constants of TaRe, TaW, TaMo, and TaNb single crystals were determined over the temperature range 80 to 1400°K. These constants were then used to derive the bulk modulus, shear moduli C_{44}, and $C' = \frac{1}{2}(C_{11} - C_{12})$ and the anisotropy factor. The results were also used to interpret solid solution hardening in tantalum-base alloys. (auth)

2722 INTERACTION OF WATER VAPOR WITH THE SURFACE OF TUNGSTEN. Ageev, V. N.; Ionov, N. I.; Ustinov, Yu. K. (Ioffe Inst. of Physics and Tech., Leningrad). Zh. Tekh. Fiz., 39: 1337-9(July 1969). (In Russian).

A time-of-flight mass spectrometer was used for studying the direct stream of desorbed particles during thermal desorption and water molecules adsorbed on a tungsten film. Three states of water adsorption were found, two of which (B_1 and B_2) were accompanied by the dissociation of molecules on the surface. The desorption of water molecules occurred at film temperatures of T < 1000°K ($\alpha - \beta_1$ phase) and O atoms were expelled at T > 1900°K (β_2 phase). (tr-auth)

2723 WORK-HARDENING PARAMETERS OF POLYCRYSTALLINE MATERIALS. Ramani, S. V.; Rodriguez, P. (Bhabha Atomic Research Centre, Bombay). Scr. Met.; 4: 755-60(Oct 1970).

A new method for the determination of the work-hardening parameters, h and m, which does not involve the work-hardening rates, was developed. It was successfully applied to Ta, Nb, mild steel, and Fe. (G.M.C.)

2724 WORK SOFTENING IN POLYCRYSTALLINE METALS. Longo, W. P.; Reed-Hill, R. E. (Univ. of Florida, Gainesville). Scr. Met.; 4: 765-70(Oct 1970).

Results of studies on the polycrystalline work softening of Cu, Al, Ag, Pb, Ni, Mo, and Al 6061 alloy are presented. The work-softening load drops became significant when the reloading yield stress exceeded the ultimate stress in a simple upper temperature tensile test. Work-softening is apparently a general phenomenon in fcc polycrystalline metals of high to moderate stacking fault energy and can also occur in some bcc and hcp metals. (G.M.C.)

2725 INFLUENCE OF TITANIUM ON THE HIGH-TEMPERATURE DEFORMATION AND FRACTURE BEHAVIOR OF SOME NICKEL-BASED ALLOYS. Sessions, C. E. (Oak Ridge National Lab., Tenn.). Scr. Met.; 4: 795-8(Oct 1970).

The influence of titanium on the high-temperature deformation and fracture behavior of nickel and Hastelloy N was investigated. The creep-rupture properties were measured at 650°C as a function of titanium (from 0 to 1.2%) and carbon contents (0.003 to 0.3% at constant 0.5% Ti) for laboratory heats of Hastelloy N. The effect of titanium on the phase equilibria of four commercial heats of Hastelloy N was defined. The carbide types, morphologies, and distributions established in these four heats were correlated with creep and tensile properties after aging at 650 or 760°C. This influence of titanium in the Ni–Mo–Cr alloy was compared with that in pure nickel alloyed with 0 to 1.5% Ti. (auth)

2726 HEAT CAPACITY OF TUNGSTEN NEAR THE MELTING POINT. Dikhter, I. Ya.; Lebedev, S. V. (Inst. of High Temperatures, Moscow). High Temp. (USSR) (Engl. Transl.); 8: 51-4(Jan-Feb 1970).

Translated from Teplofiz. Vys. Temp.; 8: 55-8(Jan-Feb 1970).

Measurements of the heat capacity were made under pulsed conditions during the process of heating tungsten wires, using a high-density current. The energy introduced was measured from oscillograms of the heating current and of the voltage drop in the wire. The temperature was recorded photoelectrically from oscillograms of the luminescence. Values of the heat capacity of solid and liquid tungsten were obtained in the temperature range 2600 to 4500°K. The specific heat of melting of tungsten was measured. (auth)

Structure and Phase Studies

Refer also to abstract 2160.

2727 (ORNL-4570, pp 1-4) CRYSTAL PHYSICS. (Oak Ridge National Lab., Tenn.).

From Metals and Ceramics Division annual progress report for the period ending June 30, 1970.

Using etch-pit patterns, electron microscopy, and x-ray topography, the quality of UO_2 single crystals grown by arc melting was studied by a modified floatingzone technique, and by vapor deposition. Eutectic-composite structures resulted from the directional solidification of melts consisting of uranium dioxide with 5 to 15 wt % W and (U,Th)O_2 with 10 wt % W. Results of scanning electron microscopy, x-ray diffraction, electrical conductivity, thermal conductivity, and mechanical strength studies on UO_2–W composites are summarized. The eutectic in the UO_2–W pseudobinary system was determined to be approximately 2640°C and 9 wt % W. Progress is reported in efforts to grow ThO_2 by an internal centrifugal zone growth technique at 26 MHz by the addition of 7 mole % Y_2O_3 to reduce the resistivity. As a preliminary step in a program to produce a transuranic-based laser, the Czochralski (crystal pulling) method has been used to prepare single-crystal boules of $CaWO_4$ and $CaWO_4$: Nd approximately 1 cm in diameter × 7 cm long. Melt growth of pure and doped crystals [Mg_2SiO_4, $KMgF_3$, $XSiO_4$: Ln (X = Zr, Hf, Th; Ln = Gd, Er, Yb), ThO_2 : ^{239}Pu, ThO_2 : ^{244}Cm + Tm] is discussed. Phase studies (under dynamic conditions) are summarized for the hydrothermal system SiO_2–RbOH–H_2O–Fe. Growth conditions and alkali ion impurities of RbOH-grown quartz are correlated by analysis of infrared and mass spectroscopic data. (auth)

2728 (ORNL-4570, pp 5-9) DEFORMATION, ANNEALING, AND INTERFACES IN METALLURGICAL PHENOMENA. (Oak Ridge National Lab., Tenn.).

From Metals and Ceramics Division annual progress report for the period ending June 30, 1970.

Quantitative metallography showed isothermal recrystallization in moderately deformed aluminum to be quantitatively consistent with a proposed edge-nucleated, growth-controlled model. A power-law dependence of grain-boundary migration rate on driving force may be related to impurities in solid solution capturing and controlling the boundary motion. The rolling texture of Cu_3Au, whether ordered or disordered, was similar to that of copper for all reductions in thickness between 20 and 96%. Ordering before rolling affected the subsequent recrystallization texture of Cu_3Au and enhanced the formation of the {001} ⟨100⟩ component. Recovery of niobium occurred in three stages corresponding to point defect annealing, dislocation rearrangements within cell walls, and coalescence of subgrains. Migration of low-angle grain boundaries in Nb–40% V left behind a trail of hair-pin shaped dislocation loops. A contribution was made to the theory of jogged screw dislocation glide and to the measurement of high-temperature creep of LiF single crystals. (auth)

2729 (ORNL-4570, pp 20-2) FUNDAMENTAL CERAMICS RESEARCH. (Oak Ridge National Lab., Tenn.).

From Metals and Ceramics Division annual progress report for the period ending June 30, 1970.

Results of a multidisciplinary study of uranium mononitride, and related rock-salt-structured actinide compounds are described. A synergistic increase in understanding of the behavior of UN is shown to derive from the interpretation of a number of different measurements. The studies reported include band structure calculations, optical constant measurements, physical property determinations, and low-temperature specific heat measurements. (auth)

2730 (ORNL-4570, pp 44-6) X-RAY DIFFRACTION. (Oak Ridge National Lab., Tenn.).

From Metals and Ceramics Division annual progress report for the period ending June 30, 1970.

A mathematical method for use in analysis of temperature-diffuse x-ray scattering in terms of mean atom displacements rather than normal vibration modes was developed. An analytic technique for separating components of diffuse x-ray scattering due to short-range order, static atom displacements, and thermal motion of atoms was derived. Results of studies on x-ray scattering from neutron-irradiated highly oriented graphite specimens were the basis of a model for the damaged structure that involves condensation of interstitial carbon atoms to form new basal planes. Aging reactions of gamma-stabilized uranium alloys have been followed by x-ray diffraction experiments at a series of aging conditions. Effects of sample deformation on the reactions are also being examined. Phase transitions in metallic samarium have been delineated by a high-temperature x-ray diffraction study. Progress in small-angle x-ray scattering includes modifications to experimental apparatus to improve signal-to-noise ratios, a further analysis of proportional counter characteristics, and the development of techniques for the measurement of absolute intensities. (auth)

2731 (ORNL-4570, pp 215-23) METALLOGRAPHY. (Oak Ridge National Lab., Tenn.).

From Metals and Ceramics Division annual progress report for the period ending June 30, 1970.

The electron microprobe continues to be an extremely useful

analytical tool. Its utility was extended to soft biological tissue with gratifying results. Multiple elemental cathode-ray tube x-ray displays can be shown in a single photograph by use of color film. Computer-plotted graphs can be made from x-ray intensities. The alpha metallography facility is operating very well. Low-moisture-containing abrasive vehicles helped reveal the microstructures of uranium-plutonium carbides, nitrides, and carbonitrides. A report on the metallography of radioactive materials at ORNL was presented. Some technique developments in alpha autoradiography improved microstructural evaluations. Reports on shatterproof coatings on glass and an improved illumination system for older research metallographs were published. The quantitative television microscope continues to be a useful quantitative tool. More accurate data are now obtained because of a better understanding of the instrument performance. (auth)

2732 (RFP-1582) HOMOGENIZATION OF URANIUM-BASE NIOBIUM ALLOYS. Jackson, Ross J.; Kangas, Clifford V. (Dow Chemical Co., Golden, Colo. Rocky Flats Div.). 13 Oct 1970. Contract AT(29-1)-1106. 9p. Dep. NTIS.

Three types of niobium segregation are considered in uranium-base niobium alloys: dendritic coring, macrobanding, and gross-ingot segregation. The origin and nature of these inhomogeneities are discussed, as are procedures for their identification and elimination. (auth)

2733 SUPERCOOLING IN THE SOLIDIFICATION OF Al–Cr, Al–Mn, AND Al–Zr BINARY ALLOYS. Ichikawa, Riei; Ohashi, Teruo; Ideda, Tetsuyuki (Nagoya Inst. of Tech., Japan). J. Jap. Inst. Metals; 34: 929-35(Sep 1970). (In Japanese).

An investigation was made on supercooling phenomena in Al-Cr, Al-Mn and Al-Zr binary alloys, which have a strong tendency to form metastable solid solutions by rapid cooling of these molten alloys, by means of an improved technique of thermal analysis and microscopic observation. It was found that, the square of the degree of supercooling was proportional to cooling rate in the solidification of the alloys of which the solute concentration was less than the maximum solid solubility (C_e) at the equilibrium state. In case of solute concentration more than C_e, this relation was satisfied under the conditions in which the primary crystals were metastable solid solutions. The minimum cooling rate to form the metastable solid solutions containing solute atoms above C_e increased a in the following sequence: 120°C/sec for Al-Mn, 180°C/sec for Al-Cr, and 190°C/sec for Al-Zr alloys, and when the cooling rate exceeded each minimum value the concentration of supersaturatedly dissolved solute and supercooling rose with cooling rate. A phase relation which gives the primary crystallization ranges of the metastable solid solutions ($C > C_e$), solid solutions ($C < C_e$), intermetallic compounds and pure solvent can be expressed by the three factors: composition (C), cooling rate (v) and supercooling (ΔT), that is, by $C-v-\Delta T$ nonequilibrium phase diagram. A relation between supercooling (ΔT) and dendrite spacing λ in μ) can be shown by $\log \lambda = 2n \log \Delta T + A$, where n = 0.32 and A is a constant. (auth) (Japan)

2734 STUDY OF THIN FILMS OF SAMARIUM BY X RAYS AND ELECTRON MICROSCOPY. Boulesteix, C. (Institut d'Optique, Orsay, France); Valiergue, L.; Gasgnier, M.; La Blanchetais, Ch. Henry. Thin Solid Films; 6: 51-71(Jul 1970). (In French).

X-ray diffraction studies on thin films of samarium metal revealed two phases: rhombohedric and dhcp. The film structure was found to be greatly influenced by the substrate temperature, the film thickness, and the metal purity. The intensity of the diffraction rings demonstrated preferential orientations of the crystallites. Subsequent annealing showed the formation of samarium sesquioxide and the transformation of phase C (bcc) into phase B (monoclinic). Electron microscopy showed, after annealing with electron beam, recrystallization of the film and formation of samarium sesquioxide phase B. (auth)

2735 ATHERMAL OMEGA TRANSFORMATION IN Zr–Nb ALLOYS. Perkins, A. J.; Yaffe, P. E.; Hehemann, R. F. (Case Western Reserve Univ., Cleveland). Met. Trans.; 1: 2785-90 (Oct 1970).

The athermal ω reaction in Zr-Nb alloys was investigated by transmission electron microscopy. In a 12 wt % Nb alloy, ω formed periodic arrays of plates on $\{112\}_\beta$ planes. These plates were 10 to 40Å thick and 150 to 200Å in dia. The ω electron diffraction reflections were relatively sharp in the 12% Nb alloy but became diffuse as the solute content was increased. The diffuse intensity existed as sheets parallel to $\{111\}_\beta$ reciprocal lattice planes. It is proposed that this diffuse intensity results from a large amplitude lattice vibration rather than from small particle size effects, i.e. ω forms when the bcc lattice becomes unstable to a transverse lattice vibration polarized in $\langle 111\rangle_\beta$ directions. Ti-V and Hf-Nb alloys exhibited diffuse diffraction effects identical to those in the Zr-Nb alloys. (auth)

2736 EFFECT OF GAS BUBBLES ON RECRYSTALLIZATION OF TUNGSTEN. Farrell, K.; Schaffhauser, A. C.; Houston, J. T. (Oak Ridge National Lab., Tenn.). Met. Trans.; 1: 2899-2905(Oct 1970).

Tungsten sheet deposited from WF_6 vapor was rolled at temperatures up to 1000°C and reductions in thickness up to 95%. Recovery and recrystallization were studied using hardness measurements and transmission electron microscopy. The temperatures for the onset of recrystallization during 1 hr anneals were 1600°C or more. Recrystallization was sluggish, requiring temperatures of 2100°C or more for completion. Transmission electron microscopy revealed that many small (<500 Å dia) gas bubbles were present on dislocations and recovered subgrain boundaries and caused scalloping of these boundaries and the advancing recrystallized grain boundaries. Coarsening of the bubbles to a relatively few larger bubbles permitted complete recrystallization. No solid inclusions were found. Annealing treatments that coarsened the gas bubbles prior to rolling caused accelerated recovery and complete recrystallization was observed at approximately 1200°C. It is concluded that small gas bubbles were the cause of the original high recrystallization temperatures and also influenced the size and shape of the recrystallized grains. (auth)

2737 STUDY OF THE SOLIDUS AND LIQUIDUS CURVES OF BINARY ALLOYS OF URANIUM WITH CARBON, MANGANESE, AND VANADIUM. Kuchar, Lumir; Wozniakova, Blanka (Inst. of Mining and Metallurgy, Ostrava, Czech.). Jad. Energ.; 16: 256-61(Aug 1970). (In Czech).

A method of computing solidus and liquidus curves is described. Initial points of the solidus and liquidus curves of constitutional diagrams U–C, U–Mn and U–V are studied. The equations of the curves and distribution coefficients of these alloys are computed by means of an ODRA 1003 computer and function dependencies are demonstrated graphically. (auth)

2738 CONTINUOUS AND DISCONTINUOUS PRECIPITATION REACTIONS IN U–1.5 PERCENT Mo ALLOYS. Giraud-Heraud, F.; Guillaumin, J.; Sifferlen, R. (Laboratories de la Societe Industrielle de Combustible Nucleaire, Veurey-Voroize, France). J. Nucl. Mater.; 36: 315-21(Sep 1970). (In French).

U/1.5% Mo alloys which have been cooled after a homogenization anneal undergo a series of transformations, with or without diffusion, leading to the formation of a complex population of structures. The description and study of these structures have been undertaken in many publications and some authors have attempted to interpret all the results with the help of a sole mode of precipitation of the α or β phases of Widmanstätten type. It seemed necessary to maintain a distinction between the structures with different morphologies. The crystallographic study of the structures formed in the neighborhood of the martensitic transformation point showed in effect the existence of two fundamentally different decomposition processes: one was continuous precipitation reaction, the other a discontinuous precipitation reaction leading to the formation of oriented or lamellar structures. The interference between these two mechanisms, which are initially independent, permits the explanation of the morphological changes in the alloy as they were affected by cooling rate. (auth)

2739 STABILIZATION OF THE PLUTONIUM β PHASE IN Pu–Ti ALLOYS. Spicer, B. R.; Hambling, P. G.; Ward, B. J. (United Kingdom Atomic Energy Authority, Aldermaston, Eng.). J. Nucl. Mater.; 36: 304-14(Sep 1970).

Four plutonium alloys with additions ranging from 1.8 to 3.6 at. % Ti were assessed with respect to retention of the β phase at room temperature when quenched from the homogenization temperature of 425°C in the δ phase. The ability of the retained β phase in the 3.6% Ti alloy, in two heat-treated conditions, to withstand room temperature storage, thermal cycling about room temperature, and low temperature treatments at –5, –25, and –79°C, was then investigated by monitoring changes in specimen density. Dilatometric and x-ray diffraction studies were used to assess the constitution of the Pu/3.6 at. % Ti samples; the data implied a mainly β phase structure at room temperature, with no α phase present, with about 3.5% retained δ phase and about 9.5% retained γ phase. Annealing the retained β phase at 175°C reduced the subsequent stability of the β phase at room and sub-zero temperatures due, it is inferred, to separation of Ti from solid solution at the annealing temperature. (auth)

2740 TETRAGONAL HYDRIDE IN LOW HYDROGEN CONTENT ZIRCALOY. Katz, O. M. (Westinghouse Bettis Power Lab., Pittsburgh). J. Nucl. Mater.; 36: 335-9(Sep 1970).

XUM

An extensive search by electron diffraction of many hydrides in low hydrogen content thin or thick samples of Zircaloy-4 showed only a tetragonal structure with a c/a very close to that of γ'. Volume fraction analyses confirmed that the hydride could not have exceeded 50 at. % hydrogen. (G.M.C.)

2741 KINETICS OF THE $\alpha-\beta$ PHASE CHANGE IN URANIUM ALLOYS. Aubert, Henri; Chamagne, Francoise; LeLong, Claude (CEN, Saclay, France). J. Nucl. Mater.; 36: 251-64(Sep 1970). (In French).

The kinetics of phase change were studied by isothermal dilatometry and microscopy for seven uranium alloys, principally uranium/chromium alloys. The eutectoidal and intermediate transformations were fairly well represented by an equation of the Johnson–Mehl type, but this was not the case for the martensitic transformation for which an applicable analytical model was not found. Heterogeneous nucleation in local sites in a network was observed at low temperatures for the intermediate transformation. A thermal cycle preceding the transformation modified the rate of transformation but did not affect the activation energy. The activation energy deduced from the transformed fraction or from the maximum slope of the curves y = f(t) was close to the activation energy of linear growth of the α grains. When the chromium content increased from 0.5 to 1.4 at. %, Q was constant for the martensitic transformation but increased from 30 to 43 kcal/mole for the bainitic. (auth)

2742 STUDY OF DISPERSED PRECIPITATES IN BETA AND OMEGA PHASES OF Zr–2.5 PERCENT Nb ALLOYS. Ambartsumyan, R. S.; Evstyukhin, A. I.; Bychkov, Yu. F.; (and others). Met. Metalloved. Chist. Metal., Sb. Nauch. Rabot; No. 8, 21-40 (1969). (In Russian).

The composition and quantities of these dispersed precipitates were studied by varied thermal treatments. The changes in Nb content in alpha solid solutions were also studied. X-ray diffraction, potential measurements during cooling, and microhardness measurements were made after quench hardening from 600 to 850°C, after tempering at 350 to 550°C, and after cooling at rates from 15 to 1500°C per minute. Alloy property changes were correlated with these treatments. To reach equilibrium in Zr–2.5% Nb alloys containing alpha and beta phases composed of 80 to 85% Nb it is necessary to anneal at 550°C after mechanical treatment. (J.R.D.)

2743 RADIOGRAPHY OF SUBSTRUCTURE OF POLYCRYSTALLINE Mo CONTAINING SMALL ADDITIONS OF ZrC. Rusakov, A. A.; Yudin, V. M.; Buzin, V. I.; Shulepov, V. I.; Nikishanov, V. V. Met. Metalloved. Chist. Metal., Sb. Nauch. Rabot; No. 8, 79-87(1969). (In Russian).

Diffractive microradiography of cast Mo showed a substructure of the first order, and in Mo with small additions of ZrC, subgrains of the first and second order are evident. Results showed that increases of ZrC in Mo result in grain size reduction for first and second order subgrains. Also an increased disorientation angle between first order subgrains occurs. The disorientation is specific between subgrains of the first and second order. There is an excess of dislocations inside and at the boundaries of first order subgrains. The merit of combined microradiography and autoradiography for correct interpretation of results is illustrated. (J.R.D.)

2744 INVESTIGATION OF SUBSTRUCTURE OF CAST Mo BY DIFFRACTIVE MICRORADIOGRAPHY. Rusakov, A. A.; Yudin, V. M.; Yal'tsev, V. N.; Buzin, V. I. Met. Metalloved. Chist. Metal., Sb. Nauch. Rabot; No. 8, 71-8(1969). (In Russian).

Methods of determining quantitative characteristics of Mo substructure by diffractive microradiography were studied. Formulas are presented for determining the Bragg angle from the radiographs obtained by varying the distance from the specimens to the film during exposure to unshielded reflections from the grains. Methods of removing separate grains in equatorial reflecting position were examined and the substructure of separate crystallites of coarse cast Mo were studied. (J.R.D.)

2745 AUTORADIOGRAPHIC INVESTIGATION OF CERTAIN PECULIARITIES OF DECOMPOSITION OF SOLID SOLUTION OF MOLYBDENUM. EFFECTS OF C ON THE STRUCTURE OF CAST UNALLOYED Mo AND ITS DILUTE ALLOYS. Nikishanov, V. V.; Evstyukhin, A. I.; Shulepov, V. I.; Lazorenko, V. M. Met. Metalloved. Chist. Metal., Sb. Nauch. Rabot; No. 8, 138-44(1969). (In Russian).

Results of investigation showed that the structure breakdown in cast Mo and its alloys with Zr and Cr upon addition of C is accompanied by decomposition of solid-solution phases at boundaries and in the cast grain. A 200°C temperature reduction increment during alloy deformation in the range from 1300 to 1600°C leads to particle dispersion in the second phase. Annealing Mo at 1200°C leads to development of dissolution processes and precipitation of particles in the second phase. Temperature increases in regions of intensive alloying leads to precipitation of secondary phase particles and an increase in coagulation rate. Autoradiographic investigations of welded Mo alloys showed that decomposition of solid-solution phases were slowed. Coagulation of second phase particles can occur in heat affected zones causing brittleness. (J.R.D.)

2746 RECOVERY OF DEFORMED Mo MONOCRYSTALS. Yastrebkov, A. A.; Oplesnin, B. A.; Lubenets, V. P.; Klement'eva, V. V. Met. Metalloved. Chist. Metal., Sb. Nauch. Rabot; No. 8, 128-37(1969). (In Russian).

Investigation revealed that (001) and (110) oriented Mo monocrystals can be deformed at room temperature by rolling up to 70% without disturbing the monocrystalline system. Anneal-induced recovery occurs in two stages. The first stage occurs at 500 to 1400°C involving a decrease in dislocation density strength loss, and decrease in width of x-ray interference lines. The second recovery stage at >1400°C involves formation of a polygonal structure. The rolled crystals will not recrystallize even if they are heated to melting. (J.R.D.)

2747 RECRYSTALLIZATION OF HYDROEXTRUDED Mo. Mochalov, G. A.; Evstyukhin, A. I. Met. Metalloved. Chist. Metal., Sb. Nauch. Rabot; No. 8, 116-27(1969). (In Russian).

Recrystallization information and diagrams are presented for Mo having various compositions which were subjected to plastic deformation by hydroextrusion. The annealing of specimens with various degrees of deformation was accomplished in vacuum at 10^{-5} mm Hg at 900 to 2000°C. (J.R.D.)

2748 APPLICATION OF TRANSMISSION ELECTRON MICROSCOPY AND ELECTRON DIFFRACTION TO ANALYSIS FOR MATERIALS SCIENCE. Tufts, Charles F. Norelco Rep.; 16: 25-47(Jul 1969).

Basic theory on image formation and diffraction effects is given for methods including replication electron microscopy, incident electron diffraction, transmission electron diffraction, transmission electron diffraction contrast microscopy, selected area electron diffraction and microscopy, and extraction replication electron microscopy. Tables list the mode of examination, basis for image formation, type of data obtained and location of samples by each method. Signals resulting from interaction of high-energy electrons with matter in a specimen are also tabulated for effects such as elastic or inelastic and coherent or incoherent scattering. Illustrations of the various methods show micrographs including Au deposits vacuum evaporated onto C substrates, longitudinal sections of W wires, an aggregate of ZnS crystals, the surface of an ZnS-type phosphor, the surface of a calcium fluoride phosphate crystal, crystallographic defects in Si semiconductors, deposits of SiC on single crystal Si and particles of thoria extracted from a Ni alloy containing 15% Mo and 4% thoria. (Metals Abstr.)

2749 PHASE DIAGRAM OF NIOBIUM–COBALT SYSTEM. Bataleva, S. K.; Kuprina, V. V.; Markiv, V. Ya.; (and others). Vestn. Mosk. Univ., Ser. II. Khim.; 11: 432-7(Jul-Aug 1970). (In Russian).

A phase diagram of the niobium–cobalt system is presented. Thermodynamic data and micrographs showing high-temperature structures are included. (J.R.D.)

2750 NOTE ON THE STRUCTURE OF $DyFe_3$ AND Dy_6Fe_{23}. Dariel, M. P.; Erez, G. (Nuclear Research Centre–Negev, Beer-Sheva, Israel). J. Less-Common Metals; 22: 360-2(Nov 1970).

The intermetallic compounds in the iron-dysprosium system present a special interest owing to the high magnetic moments of their individual components. Single phase samples were prepared for magnetic susceptibility and Mössbauer effect measurements. The crystallographic data of the two compounds $DyFe_3$ and Dy_6Fe_{23} are given. (auth)

2751 ANISOTROPIC THERMAL EXPANSION OF THE CRYSTAL LATTICE OF α HAFNIUM. Krug, Marion P.; Davis, B. E. (Bureau of Mines, Albany, Oreg.). J. Less-Common Metals; 22: 363-6(Nov 1970).

The two lattice parameters of hafnium with 2.1 wt % zirconium were determined from measurements on two single-crystal specimens at temperatures from 23 to 1600°C. These data are believed to be the most accurate thus far obtained for material of this composition, and, since hafnium of higher purity (with respect to zirconium) is difficult to obtain, they may be the best approximation to the thermal expansion data for pure hafnium. (auth)

2752 ABNORMAL MICROSTRUCTURE FORMED IN HOT ROLLED PLATES AND SHEETS OF $\alpha + \beta$ TITANIUM ALLOYS. Tokuda, Shoichi; Kawahara, Hiromichi; Taniguchi, Mitsuo;

Tsumori, Yoshikatsu (Kobe Steel, Ltd., Japan). J. Jap. Inst. Metals; 34: 949-57(Sep 1970). (In Japanese).

In order to make clear the formation process, the property and the effect on tensile properties of abnormal microstructure formed in hot rolled plates and sheets of $\alpha + \beta$ titanium alloys, experiments were carried out on Ti-5 Al-2 Cr-1 Fe, Ti-4 Al-3 Mo-1 V, Ti-6 Al-4 V, and Ti-8 Mn alloys. Hot rolling was carried out under various conditions so as to investigate the formation process of the abnormal microstructure observed by optical microscopy, and hardness of that microstructure formed was measured by the microhardness tester. Concentration of alloying elements at the abnormal microstructure was also measured by means of electron probe microanalyzer. Tensile tests were carried out on hot rolled plates and sheets with and without the abnormal microstructure to obtain the effect of the said microstructure. The abnormal microstructure in hot rolled plates and sheets was formed, with an elongated shape, by rolling from the abnormal microstructure already existing in slab. Formation of the abnormal microstructure depended on hot rolling temperature. The abnormal microstructure had increased hardness and contained more β stabilizing elements than its surroundings. On plates and sheets with the microstructure, the elongation decreased significantly and also severe anisotropy was detected. (auth)

2753 RARE-EARTH INTERMEDIATE PHASES WITH ZINC. Bruzzone, G.; Fornasini, M. L.; Merlo, F. (Univ., Genoa). J. Less-Common Metals; 22: 253-64(Nov 1970).

The existence and the structure of the rare earth-zinc intermediate phases in the range 75 to 88 at. % Zn was investigated: the compositions MZn_3, M_3Zn_{11}, MZn_4, $M_{13}Zn_{58}$, MZn_5, M_3Zn_{17}, and M_3Zn_{22} were examined. A part of the Er-Zn system was studied by differential thermal analysis. The different types of structure occurring in these intermetallic phases were correlated through the coordination number of the component atoms. The trend of the rare-earth coordination number appears to be related to the existence of ranges of the different phases. In the series of isomorphous compounds, the known, linear dependence of the lattice dimensions upon the rare-earth trivalent ionic radii is confirmed. (auth)

Radiation Effects

Refer also to abstract 3921.

2754 (BMI-1889) PROGRESS ON LMFBR CLADDING, STRUCTURAL, AND COMPONENT MATERIALS STUDIES DURING JULY 1969-JUNE 1970. Annual Report. Keller, Donald L. (Battelle Memorial Inst., Columbus, Ohio). Jul 1970. Contract W-7405-eng-92. 42p. Dep. NTIS.

Research progress is reported in two sections. A separate abstract was prepared for each section. (J.R.D.)

For abstracts of individual sections see: 2659 and 2755.

2755 (BMI-1889, Sect.B) STUDIES OF THE EFFECTS OF IRRADIATION ON CLADDING AND STRUCTURAL ALLOYS. (Battelle Memorial Inst., Columbus, Ohio). 40p.

An evaluation of two potential methods to inexpensively determine radiation-induced changes in mechanical properties of cladding materials was undertaken. Testing of ring specimens fabricated from tubing proved unsatisfactory in that friction effects associated with the loading method complicated interpretation of the data. Experiments with a microhardness technique involving the use of variable-angle cone indenters to determine stress-strain properties produced consistent results only with nonirradiated material. In studies of radiation effects on mechanical properties, a relationship was established between elevated-temperature (600°C) embrittlement and >50-A helium bubbles in the microstructure of Type 347 stainless steel. Such bubbles were observed in specimens annealed at 980°C but not in as-irradiated specimens, in which embrittlement effects were more severe. The effects of irradiation temperature on the mechanical properties of Types 347 and 348 stainless were studied also. In tensile tests below 450°C, specimens irradiated at 400°C exhibited the largest change in mechanical properties; those irradiated at 50°C showed an intermediate effect and those irradiated at 650°C the least change. Specimens tested at 750°C displayed an embrittlement effect that was independent of irradiation temperature. In efforts to explain the high helium contents of these irradiated alloys, calculations based upon Weitman's nickel transmutation hypothesis were carried out. Good correlations with analytical data were obtained. In a study of the response of materials of different microstructures to irradiation-induced embrittlement at elevated temperatures, a capsule containing Type 316 stainless steel tensile specimens with oriented grain structures was prepared for insertion in the EBR-II. In work concerned with the use of high-defect structures to control void formation during irradiation, explosive shock hardening of Type 316 stainless was found to produce large increases in yield strength, moderate increases in ultimate strength, and reductions in ductility. Steady-state creep rates at 650°C were reduced. In annealing studies, the shock-induced hardening was largely retained for 1500 hr at 700°C. Creep studies were initiated on alloys containing 0.012 and 0.046 wt % carbon in an investigation to evaluate low-carbon ferritic 2-1/4 Cr-1 Mo steel for LMFBR steam-generator tubing. (auth)

2756 (CEA-CONF-1638) STUDY OF ACICULAR PRECIPITATES IN IRRADIATED AUSTENITIC STEELS USING ELECTRON MICROSCOPY. Bisson, Andre; Vouillon, Michel (Commissariat a l'Energie Atomique, Saclay (France). Centre d'Etudes Nucleaires). 1970. 12p. (In French). (CONF-700920-1). Dep. NTIS (U. S. Sales Only).

From International Meeting on Fast Reactor Fuel and Fuel Elements, Karlsruhe, Germany.

Neutron irradiation of austenitic steel Type 316 at temperatures between 450 and 550°C gives rise to small precipitates in the (110) crystal planes. They are very thin long plates whose maximum dimension is in the (100) direction. They are about 50°A thick. The nature of these precipitates remains indeterminate but their instability indicates that they are not $M_{23}C_6$-type carbides. The precipitates constitute preferential cavity sites. (auth) (France)

2757 (NRL-7121) DEMONSTRATION OF IMPROVED RADIATION EMBRITTLEMENT RESISTANCE OF A533-B STEEL THROUGH CONTROL OF SELECTED RESIDUAL ELEMENTS. Hawthorne, J. Russell (Naval Research Lab., Washington, D. C.). 29 May 1970. 33p.

A successful demonstration test of metallurgically controlled radiation embrittlement sensitivity has been conducted with a large commercial melt of A533-B steel. The 30-ton melt represents a scaleup from the 300-lb laboratory melts which provided the first evidence of the potential for very low sensitivity to radiation embrittlement at power reactor pressure vessel service temperatures (≈550°F, 288°C). The primary objective of special melt specifications and melt planning was the reduction of copper and phosphorus contents to the lowest possible level. Restrictions were also imposed on the content of other residual impurity elements with known or suspected influences on radiation embrittlement resistance. For a broad experimental analysis, the melt was split to provide material representing the primary melt analysis (0.03% Cu) and a melt modification (0.13% Cu). Plates representing each analysis were also split and sections individually heat-treated to Class 1 or Class 2 strength conditions. All procedures used were standard mill practices. Radiation assessments showed the primary melt analysis to have very low sensitivity to radiation embrittlement at 550°F, thereby validating the composition specification approach for future melts. Transition temperature increases measured independently by Charpy-V (C_v) and dynamic tear (DT) test methods were 70°F or less for fluences up to 3.1×10^{19} n/cm^2 > 1 MeV. Based on DT results, the nil ductility transition (NDT) temperature of the Class 1 plate remained below 75°F after 550°F irradiation. Results for the 0.13% Cu melt modification provided direct confirmation of the primary, highly detrimental influence of copper content on radiation embrittlement resistance. The C_v 30-ft-lb transition temperature increases for the Class 1 and Class 2 plates were 140° and 125°F, respectively, for a fluence of 2.8×10^{19} n/cm^2 > 1 MeV. The enhancement of radiation sensitivity by copper content appeared independent of the strength class. Postirradiation DT characteristics of the primary melt analysis (Class 1 plate) were indicative of excellent fracture resistance at shelf level temperatures. The A533-B scaleup demonstration test fully supports the principles for control of radiation embrittlement sensitivity developed in laboratory research. A summary of 550°F radiation data for the ASTM A302-B reference plate and A533 standard production plate and weld metals places the results for the special melt in full perspective. The radiation embrittlement sensitivity of the primary melt analysis is shown to be only one third that of the reference plate and significantly less than that of A533 production materials. (auth)

2758 (ORNL-4570, pp 76-84) CLADDING AND STRUCTURAL MATERIALS. (Oak Ridge National Lab., Tenn.).

From Metals and Ceramics Division annual progress report for the period ending June 30, 1970.

The nature of the defects produced in Type 304 stainless steel during irradiation to fast fluences of the order of 10^{22} neutrons/cm^2 was characterized as a function of irradiation temperature. At about 300°C small defect clusters were formed, from 370 to 630°C voids were formed, and above 770°C only helium bubbles were visible. The voids caused a density decrease, which was a maximum at about 400°C, and the ductility was reduced. Type

XUM

304 stainless steel modified with 0.2% Ti had better ductility than the standard alloy. Part of the titanium-modified alloy stock has been fabricated into tubing and shown to have properties, if unirradiated, comparable with those of the standard alloy. Incoloy 800 was irradiated to thermal fluences of the order of 10^{21} neutrons/cm^2; most of the ^{10}B was converted to helium. Alloys containing 0.1% Ti had the best postirradiation ductilities. Some aging was noted and was most embrittling at 550°C. The defects produced in vanadium by irradiation to fast fluences of 10^{21} to 10^{22} neutrons/cm^2 over the range of 385 to 710°C were characterized. (auth)

2759 (ORNL–4570, pp 152-6) ALUMINUM IRRADIATION DAMAGE. (Oak Ridge National Lab., Tenn.).

From Metals and Ceramics Division annual progress report for the period ending June 30, 1970.

Irradiation-induced changes in the microstructure and mechanical properties of aluminum alloys are described. Loops and voids form from defects produced by displacement reactions. Transmutation-produced silicon precipitates as a new phase. Hydrogen and helium, injected by cyclotron or formed by an earlier irradiation, affect the distribution of voids and loops formed during later irradiations or quenching experiments, indicating that these transmutation-produced gases play an important role in the swelling of irradiated aluminum alloys. Void formation at about 60°C in various alloys was related to original composition and structure: voids form more rapidly in high-purity aluminum than in solid-solution alloys, while 6061 aluminum, which contains precipitated Mg_2Si, exhibits only a few tenths of a percent density change after irradiation to fluences as high as 5×10^{22} neutrons/cm^2 (>0.821 MeV). In high-purity aluminum irradiated to 1.0×10^{22} neutrons/cm^2 (>0.821 MeV), the presence of voids up to 1100 Å in diameter causes a 7% decrease in density. Irradiation of 6061 aluminum to high fast neutron fluences increases the tensile strength below 150°C while the ductility is moderately reduced. However, at 150°C and above, the ductility measured at low strain rates is severely reduced. (auth)

2760 STRESS-DEPENDENCE OF THE IN-REACTOR CREEP RATE OF HEAT-TREATED Zr–2.5 WT. PERCENT Nb AND COLD-WORKED ZIRCALOY-2. Fidleris, V. (Chalk River Nuclear Labs., Ont.). J. Nucl. Mater.; 36: 343-6(Sep 1970).

New in-reactor creep results on heat treated Zr – 2.5 wt % Nb pressure tube material are presented. A complex stress dependence composed of three distinct regions was observed. Published in-reactor results of the stress dependence of cold-worked Zircaloy-2 and heat treated Zr – 2.5 wt % Nb were discussed. (G.M.C.)

2761 EFFECT OF HELIUM ON VOID FORMATION IN IRRADIATED STAINLESS STEEL. Bloom, E. E.; Stiegler, J. O. (Oak Ridge National Lab., Tenn.). J. Nucl. Mater.; 36: 331-4 (Sep 1970).

The role of helium in void formation in irradiated stainless steel was investigated. A uniform concentration of 20×10^{-6} atom fraction helium was injected into Type 304 stainless steel prior to irradiation with a fast neutron fluence of 7.4×10^{21} neutrons/cm^2. It was found that helium was a very effective agent for nucleating voids during neutron irradiation. In steel which was not preinjected with helium the irradiation created about 70 helium atoms for every void. In practice, helium will be generated during neutron irradiation in quantities large enough to be significant. (G.M.C.)

2762 URANIUM SWELLING UNDER IRRADIATION. Lehmann, J.; Blanchard, P. (CEA, Saclay, France). Bull. Inform. Sci. Tech. (Paris); No. 148, 13-31(May 1970). (In French).

In neutron irradiated uranium, macroscopic dimensional variations due to radiation growth, accelerated creep, and swelling are observed. Uranium swelling mechanisms are described. The in-pile behavior of various fuel elements is reported and the results analyzed as a function of the fuel alloy composition and irradiation conditions. (auth) (France)

2763 PRELIMINARY STUDIES OF THE BEHAVIOR OF SURFACES UNDER BOMBARDMENT USING NUCLEAR REACTIONS. Quaglia, L.; Weber, G. (Univ., Liege). Radiochem. Radioanal. Lett.; 4: 89-98(3 Jun 1970). (In French).

The desorption of oxygen from the surface of high-purity metals during the bombarding by charged particles was investigated. In order to make possible the interpolation of the experimental points obtained at different times during desorption, the behavior of the metallic surface during the irradiation was studied. From this study, the valid experimental conditions were defined. (auth)

2764 STATE OF CARBON IN MARTENSITE AS INFLUENCED BY ELECTRON BOMBARDMENT. Kritskaya, V. K.; Il'ina, V. A.; Bystrov, L. N. (Central Scientific-Research Inst. of Ferrous Metallurgy, Moscow. Inst. of Metallurgy, Moscow). Dokl. Akad. Nauk SSSR; 186: 89-91(1 May 1969). (In Russian).

The influence of electron irradiation on carbon state in martensites was studied using specimens of U – 10 tempered steel irradiated in an accelerator at 68 and 41°C to 10^{18} to 10^{19} electrons/cm^2 doses using ~2 MeV electrons. The x rays obtained showed that the reduced tetragonality of the martensite lattice induced by electron bombardment was not an irreversible process as in the annealing of carbon steels. Data obtained confirmed that obtained for neutron irradiation. In both events the reduced tetragonality proved to be a reversible process. (R.V.J.)

Ceramics and Cermets

Refer also to abstracts 2601 and 2602.

Corrosion and Erosion

Refer also to abstracts 2629, 2633, and 3860.

2765 (KFK–1213) COMPATIBILITY TESTS WITH UC OF DIFFERING STOICHIOMETRIES AND Fe–Ni–Cr ALLOYS AND THE INFLUENCE OF STABILIZERS. Goetzmann, O.; Scherbl, D. (Kernforschungszentrum, Karlsruhe (West Germany). Institut fuer Material und Festkoerperforschung). Jun 1970. 28p. (In German). Dep. NTIS (U. S. Sales Only).

Compatibility tests were carried out at 900°C on Fe-Ni-Cr-alloys and UC of varying carbon contents and with stabilizers added. The carbon contents were 4.1; 4.8 and 5.22 wt %. Chromium and vanadium were used as stabilizers for fuels with the hyperstoichiometric composition and $Cr_{23}C_6$ and VC for the substoichiometric composition, respectively. The stabilizer was mixed with the fuel powder. The mixture was not annealed to reach an equilibrium. No great effect of the stabilizers on the reaction of the substoichiometric fuel with the cladding materials was detectable. There was always a strong reaction. The interactions between the stoichiometric and hyperstoichiometric UC and the cladding materials were less than those found with the substoichiometric UC. With the hyperstoichiometric UC there was a remarkable effect of the stabilizers on the reactions with the cladding materials. (auth)

Preparation and Fabrication

Refer also to abstracts 2151, 2195, 2312, 2317, 2318, and 2320.

2766 (CSIRO-Trans–9924) EFFECT OF ADDITIVES ON THE SINTERING OF ZIRCON. Motoi, S. Translated by M. Hintze (Commonwealth Scientific and Industrial Research Organization, Melbourne, Australia), from Kogyo Kagaku Zasshi; 70: 638-43(1967). 23p. Dep. NTIS (U. S. Sales Only).

The effect of various additives on physical aspects of the sintered zircon mass such as contraction during sintering, specific gravity, and strength was studied. Titania significantly accelerated the sintering process as did alumina, magnesia, $BaCO_3$, NaF, crystalline and noncrystalline silica, and silicate of soda. Thermal dissociation was retarded by addition of rare earth oxides and olivine sand. On the basis of these results sintered zircon was obtained with hardness = 91, sp gr = 4.3, bending strength 1450 kg/cm^2 and compressive strength 4120 kg/cm^2. (Australia)

2767 (DP-Report–378) MONITORING FLUIDISED BEDS BY PRESSURE MEASUREMENTS. Kingdon, J. (Atomic Energy Establishment, Winfrith (England)). Sep 1965. 20p. Dep. CFSTI (U. S. Sales Only).

A method of characterising fluidizing conditions by monitoring the gas pressures in the throat of a bed used to coat fuel particles is described. The steady-state and transitory conditions are demonstrated. (auth)

2768 (ORNL–4570, pp 47-61) FAST REACTOR OXIDE FUELS. (Oak Ridge National Lab., Tenn.).

From Metals and Ceramics Division annual progress report for the period ending June 30, 1970.

A program being conducted to advance the technology of $(U,Pu)O_2$ as a Liquid Metal Fast Breeder Reactor fuel is described. The determination of the properties and performance of sol-gel-derived oxide fuels fabricated by the Sphere-Pac and pelletizing techniques is emphasized. A variety of irradiation capsules were fabricated during the year. Sol-gel-derived pellets were fabricated with con-

trolled densities from 81 to 93% of theoretical. A Sphere-Pac method in which all of the plutonium is incorporated in the coarse fraction was developed. The Sphere-Pac process was used to load approximately 150 in. of $(U-20\%\ Pu)O_2$ 0.250 OD fuel pin material for irradiation tests in the Engineering Test Reactor, the ORR, and the EBR-II. Smear densities of these beds ranged from 80 to 85% of theoretical. Firing $(U,Pu)O_2$ pellets with less sorbed gas by sintering in $Ar-4\%\ H_2$ and cooling in pure argon to prevent resorption of hydrogen was demonstrated. Nineteen unencapsulated fuel pins were fabricated for an EBR-II Series II experiments along with 8 fuel pins for testing gas-cooled breeder reactor conditions in the EBR-II. One instrumented capsule was constructed for the ORR and two each containing four fuel pins for irradiation in the ETR. Characterization methods for $(U,Pu)O_2$ fuels, including determining the oxygen-to-metal ratio and determining the homogeneity of $(U,Pu)O_2$ were improved by alpha autoradiography, by electron microprobe analysis, by light microscopy, and by replica electron microscopy. Uninstrumented irradiations in the ETR to 9.7 at. % burnup and instrumented tests in the ORR have continued to confirm that Sphere-Pac fuels perform in reactors comparably to pelletized fuels of similar smear density. Two capsules were placed in the ETR to test sol-gel pellet and Sphere-Pac fuel swelling and fuel-cladding mechanical and chemical interaction under peak LMFBR design operating conditions of 590 W/cm with the cladding inside surface at 650°C. In an ORR instrumented test, Sphere-Pac and pellet fuels having a smear density 82% of theoretical exhibited identical thermal performance to low burnup. Five encapsulated Series I pins containing Sphere-Pac $(U,Pu)O_2$ continued irradiation in the EBR-II, reaching a peak burnup of 6.2% FIMA; three capsules will continue to 11.8% FIMA. Six fuel pins containing unirradiated sol-gel $(U,Pu)O_2$ survived power transients in the TREAT that melted 50 to 60% of the fuel in the peak power regions of two pins. Extensive design work was done on instrumented ORR tests of interaction between fuel and cladding during power cycling. In-reactor redistribution of uranium and plutonium was studied by postirradiation electron microprobe analysis and alpha autoradiography. (auth)

2769 (ORNL–4570, pp 62-7) ADVANCED LMFBR FUELS DEVELOPMENT. (Oak Ridge National Lab., Tenn.).

From Metals and Ceramics Division annual progress report for the period ending June 30, 1970.

Mixed (U,PU)N is being developed as an advanced fuel for the LMFBR. Since the principal aim is good performance under irradiation to burnups in excess of 100,000 MWd/metric ton, emphasis has to be placed on the manufacture of fuel for irradiation testing. Ten pins containing a total of 30 linear inches of (U,Pu)N sodium-bonded to type 316 stainless steel cladding were fabricated for testing in the ETR at heat ratings of 30 kW/ft. In fabrication development it was found that homogeneous (U,Pu)N pellets could be made by two independent routes. In one the (U,Pu)N is synthesized from uranium-plutonium alloy; in the other UN is blended with PuN, calcined, ground, and sintered into pellets. Reliable analytical techniques were developed for U, Pu, C, and O in (U,Pu)N. A consistent negative bias on nitrogen is observed with the micro-Kjeldahl method now being used. If excess nitrogen produced by fissioning of plutonium in (U,Pu)N causes a problem, it can be alleviated by the addition of vanadium or chromium as metals, V_2N, or Cr_2N. The buffering action of these additives is due to the formation of $(U,Pu)VN_2$ or $(U,Pu)CrN_2$. (auth)

2770 (ORNL–4570, pp 127-35) FUEL ELEMENT FABRICATION DEVELOPMENT. (Oak Ridge National Lab., Tenn.).

From Metals and Ceramics Division annual progress report for the period ending June 30, 1970.

Studies of research reactor fuels to obtain improved irradiation performance, lower fuel element costs, and higher fuel element reliability are being conducted. The preirradiation characteristics and irradiation performance of aluminum cermet fuels were correlated with excellent predictability of swelling at fission densities of $2.2 \times 10^{21}/cm^3$. Improvements in the bonding of nickel phosphide coatings to aluminum were insufficient for successful operation of coated fuel plates in the G-12 loop of ETR. Results of postirradiation examination of W-UO_2 cermets indicated that void volume and its deployment are important factors controlling the swelling of these high-temperature cermets. But mass transfer between the fueled cermet and its cladding may be the controlling factor for fuel element lifetime. Some fuel plates fabricated for the HFIR fuel assembly were modified to obtain production information. No fabrication problems were found in the manufacture of a small test lot of fueled plates containing the burned grade of oxide fuel. The use of an Al_2O_3 dispersoid on the filler side of the complex HFIR fuel plate core was investigated to reduce fuel plate rejection due to bond defects during manufacture. Fabrication studies on shaped cores revealed that the void left in the frame cavity by the shaping of the core is filled with aluminum from the frame and cover plate. It was found that the quantity of voids in aluminum-base dispersions is affected by the hot rolling temperature and the degree of cold work in addition to the type of materials used and concentration of ceramic fuel. But other fabrication variables such as compact density had no influence on the void volume of the final fuel plate. A study was completed of radiography and densitometry to determine the capabilities and limitations for measuring fuel inhomogeneity on aluminum fuel dispersion plates. To control many of the variables required for precision of fuel inhomogeneity measurements using radiography was extremely difficult. (auth)

2771 (ORNL–4570, pp 161-9) GAS-COOLED REACTOR PROGRAM. (Oak Ridge National Lab., Tenn.).

From Metals and Ceramics Division annual progress report for the period ending June 30, 1970.

All-ceramic fuels of $(Th,U)O_2$ or $(Th,U)C_2$ particles coated with pyrolytic carbon and SiC offer advantages as fission-product-retaining fuel for high-temperature gas-cooled reactors (HTGR's). In support of this program the preparation, characterization, and irradiation testing to high fast fluence of coating materials and simulated bonded-bed fuel elements were investigated. Bonded coated-particle beds prepared with high-density matrices containing high concentrations of stable filler materials survived irradiation to full HTGR fast fluences without loss of integrity or coating failures. Binder compositions that include large concentrations of alternate commercial filler materials were developed and are being tested. Excellent dimensional stability of high-density propylene-derived pyrolytic carbon coatings as compared with methane-derived coatings was also demonstrated to fast fluences twice the design maximum of HTGR's. A significant new activity is the development of coated particles derived from ion exchange resins. Certain types of resin particles retain their spherical shape when carbonized slowly in a fluidized bed, and stable two-layer coatings may be applied to them. Sufficient uranium may be absorbed in such particles before carbonizing to make them an attractive substitute for the small fissile particles in the HTGR fuel cycle. Efforts were also directed to the development of fuel elements for a gas-cooled fast breeder reactor (GCBR). Results of examination and evaluation of three sealed fuel pins that performed well during irradiation in the ORR are included. The $(U,Pu)O_2$ fuel and fuel pin for a test of a new manifolded-vented fuel element design was prepared. This instrumented, vented fuel pin began irradiation in the ORR and is operating satisfactorily. The $(U,Pu)O_2$ fuel for a set of eight GCBR fuel pins to be tested in EBR-II at temperatures ranging from 600 to 800°C was prepared. (auth)

2772 (ORNL–4570, pp 174) MILITARY REACTOR FUEL ELEMENT PROCUREMENT ASSISTANCE. (Oak Ridge National Lab., Tenn.).

From Metals and Ceramics Division annual progress report for the period ending June 30, 1970.

Technical surveillance and specification preparation in support of core procurement for the Antarctica reactor, the floating "Sturgis" nuclear power plant, and the Air Force Nuclear Engineering Test Reactor are summarized. (auth)

2773 (ORNL–4572–, pp 135-48) DEVELOPMENT OF THE THORIUM FUEL CYCLE. (Oak Ridge National Lab., Tenn.).

From Chemical Technology Division annual progress report for period ending May 31, 1970.

Recycle of the alcohol used in the microsphere-forming column was studied. Techniques were developed for drying and firing gel microspheres and preparation of microspheres in nonfluidized-bed columns. Preparation of test material for recycle test elements and ^{233}U storage, purification, and distribution are discussed. (M.C.G.)

2774 (ORNL–4572–, pp 149-69) SOL-GEL PROCESSES FOR THE URANIUM FUEL CYCLE. (Oak Ridge National Lab., Tenn.).

The CUSP process was used in engineering-scale equipment to prepare urania sols containing more than 230 kg of UO_2. In continued laboratory work to develop a solvent extraction process for the preparation of mixed UO_2-PuO_2 sol, a process is being studied in which CUSP-prepared urania sol is pretreated to remove excess formate and is then mixed with a high-nitrate plutonia sol produced by an alcohol extraction process. (M.C.G.)

2775 (ORNL–4572–, pp 242-50) PREPARATION AND PROPERTIES OF ACTINIDE OXIDES. (Oak Ridge National Lab., Tenn.).

Studies of a wide range of actinide and lanthanide sols were continued. Conditions were identified for production of dense microspheres and shards of U-Pu(80%-20%) monocarbide and carbonitride. The adsorption of CO_2 by three ThO_2 sols was measured. (M.C.G.)

XUM

2776 NUCLEAR FUEL MATERIAL HAVING A URANIUM CARBIDE BASE. Guinet, Philippe; Vaugoyeau, Henri (to Commissariat a l'Energie Atomique). British Patent 1,210,800. 28 Oct 1970. Priority date 20 Sep 1968, France.

A compact refractory fuel is described which is suitable for use in high temperature reactors. The material is made up of fine-grain UC containing UC_2 inclusions and coated with Be_2C. The composition range is U-33 to 39%, C-55 to 59%, and Be-1 to 12%. (J.R.D.)

2777 BORON AND BORON CARBIDE COATINGS BY VAPOR DEPOSITION. Cochran, Andrew A.; Stephenson, James B. (Bureau of Mines, Rolla, Mo.). Met. Trans.; 1: 2875-80(Oct 1970).

The formation of boron and boron carbide coatings by vapor-phase reactions was investigated. Optimum parameters were determined for hydrogen reduction of boron trichloride and for the formation of boron carbide coatings on graphite by reaction with the depositing boron. At 1300°C, about 85% of the boron was deposited. Tungsten substrates did not react with the boron deposit; other substrates reacted to various extents. The hydrogen reduction of boron tribromide was briefly investigated. Boron carbide was deposited at 1300°C by adding methane to the boron trichloride-hydrogen feed gas. The chemical composition of the vapor-deposited boron carbide approximated B_4C. A method of etching B_4C was developed to study its microstructure. When boron was deposited on graphite at 1500°C, very hard, uniform, strongly adherent coatings of B_4C were formed that might be useful in applications such as rocket nozzles and chemical reaction and processing vessels. (auth)

2778 ELECTRODYNAMIC VIBROCOMPACTION OF SINTERED NODULES OF URANIUM OXIDE. Papeleux, P.; Flipot, A. J. (CEN–Belgonucleaire, Mol-Donk, Belgium). J. Nucl. Mater.; 36: 275-87(Sep 1970). (In French).

Vibrocompaction of sintered UO_2 nodules and powders was studied on an installation equipped with an electrodynamic vibrator. The influence of the dimensions of the coarse fraction on the average fuel density was examined both theoretically and experimentally. This study showed that certain dimensions were advantageous and that the diameter of the nodules must therefore be chosen between 20 and 30% of the inner diameter of the cladding tube. The role of the other 2 fractions was mentioned. Experiments were carried out with different percentages of these fractions in order to establish a ternary diagram, which gave the compositions to be used as a function of the finally desired density. Fabrication parameters, such as time and vibration power are also discussed. Examinations of the vibrocompacted rods containing nodules proved the good quality of these pins. Densification of the rods was rather quick and easy: a judicious choice of the initial load made it possible to obtain a 87.9% theoretical density. The density fluctuations were ±1.3% as a maximum and very often below 1%. The different fabrication steps are also very reproducible and the technique is very versatile. (auth)

2779 FORMATION OF ALUMINUM PEARLS ON THE SURFACE OF SAP ALLOYS. Beghi, G.; Piatti, G.; Schleicher, H. W. (CCR–EURATOM, Ispra, Italy). J. Mater. Sci.; 5: 741-5(Sep 1970).

An abnormal phenomenon of aluminium "pearl"-formation at the surface of Al–Al_2O_3 alloys was observed occasionally in quite different experimental conditions. In order to obtain more information, a series of hot-hardness and hot-compression tests was performed on SAP specimens. Qualitative correlations between the experimental variables and the experimental results are described; tentative explanations are related to Sherby's hypothesis of a continuous alumina network and to the presence of a non-oxidizing atmosphere. (auth) (UK)

2780 PROCESS FOR PREPARING A SOL FOR MAKING PARTICLES OF AN ACTINIDE CARBIDE. Triggiani, Leonard Vincent (to W. R. Grace and Co.). British Patent 1,209,223. 21 Oct 1970. Filed 10 Apr 1968.

Reference is made to a method of preparing spherical actinide carbide particles (microspheres) of controlled size, including a method of making an aquasol of an actinide oxide and carbon from which the carbide particles can be made. Present methods for the preparation of these microspheres are laborious, costly, and give a low product yield; the particles furthermore tend to lack sphericity and uniform structure and often show surface irregularities. The process described comprises blending an aqueous solution of an actinide metal salt with an ammoniacal C dispersion, whereby an actinide oxide precipitate containing C is obtained, which is peptized into an aquasol composition. The carbide microspheres are prepared by passing droplets of the aquasol through a column containing an organic dispersion medium and ammonia, and the gel microspheres so obtained are sintered. Desirable features of this process are enumerated, and a number of examples of its application are described. The ammonia producing agent may be urea, hexamethylene-tetramine, actinide, ammonium carbonate, or ammonium cycanate, or ammonia solution itself may be used. An acid may be used for peptization. The sintering process may comprise a low temperature pretreatment step in H_2 and a high temperature treatment step in vacuum. The organic solvent may be butanol. Rare earths, Y, Zr, or Hf may also be incorporated as oxides. (UK)

2781 PRODUCTION OF URANIUM DIOXIDE. (to Westinghouse Electric Corp.). British Patent 1,210,057. 28 Oct 1970. Priority date 28 Mar 1968, United States.

A process for the production of ceramic-grade UO_2 powder comprises reacting UF_6, steam, and H_2 in a fluidized bed at a temperature ranging from 475 to 600°C. Intermediate reaction products are formed, including UO_2F_2 and U_3O_8, which are transmitted to a second fluidized bed where more steam and H_2 are added. The intermediates are heated to 575 to 650°C to form fine particles of UO_2. (B.L.M.)

2782 INVESTIGATION OF HYDROLYZABLE CARBIDES. III. YTTRIUM CARBIDE. Brozek, V.; Popl, M.; Hajek, B. (Technische Hochschule, Prague). Collect. Czech. Chem. Commun.; 35: 2724-37(Sep 1970). (In German).

Optimum conditions for production of YC_2 by reduction of Y_2O_3 with carbon were determined. The YC_2 samples produced at 2000 and 2100°C were decomposed by water, dilute sulfuric acid, and dilute potassium hydroxide solutions and the resulting products investigated with the help of ir, uv, and mass spectroscopy as well as gas chromatography. Products were analogous to those formed in the decomposition of LaC_2. (tr-auth)

2783 PURIFICATION AND SINGLE-CRYSTAL GROWTH OF V_2O_5. Haemers, J. (Univ., Ghent). Bull. Soc. Chim. Belg.; 79: 473-7(Jul-Aug 1970).

A means of obtaining single crystals of V_2O_5 of reasonable perfection is described. Starting from p.a. material preliminary purification as described is needed. (auth)

2784 IMPROVEMENTS IN AND RELATING TO THE PREPARATION OF NUCLEAR FUEL MATERIALS. Kosiancic, Eugene Joseph (to Babcock and Wilcox Co.). British Patent 1,211,211. 4 Nov 1970. Priority date 8 Nov 1966, United States.

A process for preparation of actinide oxide fuel materials is described. A compound of the actinide is precipitated from an aqueous solution of its salt forming an aqueous sol. The sol is gelled by addition of hydrogen peroxide to form an actinide peroxide. The gel is then calcined to produce the fuel material. (auth)

Properties Evaluations

Refer also to abstracts 2411, 2663, 2665, 3204, 3774, and 3875.

2785 (LA–4452) MECHANICAL PROPERTIES OF CARBIDE AND NITRIDE REACTOR FUELS. Tokar, M.; Nutt, A. W.; Leary, J. A. (Los Alamos Scientific Lab., N. Mex.). Jan 1970. Contract W-7405-eng-36. 9p. Dep. NTIS.

Mechanical-property evaluations of plutonium-bearing carbides and nitrides in study of fast reactor fuels are presented, along with a review of the literature on the mechanical properties of uranium and plutonium carbides and nitrides. (auth)

2786 (ORNL–4570, pp 13-15) DIFFUSION IN SOLIDS. (Oak Ridge National Lab., Tenn.).

From Metals and Ceramics Division annual progress report for the period ending June 30, 1970.

A mathematical analysis showed that diffusivities relative to two different frames of reference in multi-component systems are invariant. Uranium diffusion coefficients in UN_{1+x} were shown to be markedly dependent on nitrogen gas overpressure. The alpha-energy degradation method was confirmed directly by comparison with results obtained for uranium in tantalum by the anodizing-and stripping serial sectioning technique. Radio-frequency sputtering is being developed as a tool for determination of small diffusion coefficients. Cation self-diffusion coefficients are being determined and analyzed with regard to jump mechanism for both the monoxide and dioxide of titanium. Experiments on diffusion in refractories under high pressures and temperatures are planned. (auth)

2787 (ORNL–4570, pp 24-6) PHYSICAL CERAMICS STUDIES. (Oak Ridge National Lab., Tenn.).

From Metals and Ceramics Division annual progress report for the period ending June 30, 1970.

The effects of stoichiometry on the deformation mechanisms of UO_2 single crystals and on the creep of UN are being investigated. For UO_2 the principal slip system changes from {100} to {111} for sufficiently hyperstoichiometric crystals. A phenomenological model for sintering is being developed with topological ideas. In addition, new evidence for the role of dislocation movement in sintering was found. The phenomenon of desintering, the decrease of the bulk density of a sintered body on further heat treatment, was examined for sol-gel ThO_2. (auth)

2788 (ORNL–4570, pp 27-30) PHYSICAL PROPERTY RESEARCH. (Oak Ridge National Lab., Tenn.).

From Metals and Ceramics Division annual progress report for the period ending June 30, 1970.

Experimental investigations of heat transport in solids were continued. This effort included work on lattice or phonon conduction in UO_2 and LiF along with electronic and phonon transport in Ta, Cr, and $(Th_xU_{1-x})N$. In addition, the effect of configurational order on the transport properties and specific heat of Ni_3Fe was investigated. (auth)

2789 (ORNL–4570, pp 68-75) LMFBR FUEL ELEMENT DESIGN AND MODEL DEVELOPMENT. (Oak Ridge National Lab., Tenn.).

From Metals and Ceramics Division annual progress report for the period ending June 30, 1970.

Analytical methods are being developed to predict and evaluate the performance of LMFBR fuel pins and fuel elements. The program incorporates areas such as integrated fuel element performance modeling, modeling of fuel performance, and modeling of cladding performance. The work is coordinated with the related fuel and cladding development programs, providing methods for designing and interpreting irradiation tests, determining the influences of materials properties on fuel element performance, and identifying specific areas in which experimental research should be done. The integrated fuel performance model, FMØDEL, was completed and can perform calculations for fuel swelling, fission gas formation and release, and cladding mechanics. Fuel performance modeling is in an empirical stage, thus, much effort was directed toward further refinement of the models for the various aspects of fuel behavior. The work included light and electron microscopy and electron microprobe analysis of irradiated $(U,Pu)O_2$ to increase understanding of fuel swelling, fission gas release, actinide and fission product redistribution, and restructuring. Determinations of stresses in cladding exposed to service levels of temperature and pressure and the deformation of the cladding under these stresses were made. Exploratory tests were made on unirradiated type 316 stainless steel under cyclic stress and temperature. Creep of stainless steel tubing for LMFBR application was studied and methods for failure analysis were developed. Methods for treatment of the behavior of cladding under power cycling and reactor transients were also studied. (auth)

2790 (ORNL–4570, pp 98-102) FAST BREEDER NEUTRON ABSORBER MATERIALS. (Oak Ridge National Lab., Tenn.).

From Metals and Ceramics Division annual progress report for the period ending June 30, 1970.

Properties of boron carbide and factors that affect its irradiation performance are being studied to determine the mechanism of irradiation damage for this material, which is a prime candidate for use as a neutron absorber in fast reactors. Methods to control the size and numbers of intragranular voids that may affect the irradiation performance of boron carbide were found. These voids are believed to form as a consequence of a Kirkendall effect. Using an ion-bombardment milling technique, a transmission electron micrograph of boron carbide was obtained. The surfaces of intragranular voids were observed to be crystallographic faces. Boron carbide power irradiated at 350°C in a thermal reactor released approximately 5.3% of the gas generated. Results of scanning electron microscopy of irradiated and unirradiated boron carbide powder indicated no change in the appearance of the solid particle or fragmentation of the particles during irradiation. X-ray diffraction lines of these particles were more diffuse after irradiation. Irradiation led to the disappearance of a free graphite line that did not disappear in unirradiated material heat treated for equal times at the same temperature. (auth)

2791 (ORNL–4570, pp 195-200) THORIUM UTILIZATION. (Oak Ridge National Lab., Tenn.).

From Metals and Ceramics Division annual progress report for the period ending June 30, 1970.

The objective of the Thorium Utilization Program is to demonstrate economic techniques for conducting the Th-^{233}U fuel cycle for the High-Temperature Gas-Cooled Reactor. Fabrication processes and equipment must be developed to handle the highly radioactive recycle fuel, and the fuels produced must be demonstrated in an irradiation test program. The activities in the program this year included the maintenance of the Thorium-Uranium Recycle Facility and improvements of certain functional components in TURF, further development of various refabrication processing steps, with primary emphasis on a prototype remote fluidized-bed furnace for deposition of pyrolytic carbons from hydrocarbon gases. A principal activity was the fabrication of prototype Recycle Test Elements for irradiation in the Peach Bottom Reactor. A number of different types of fuel particles were fabricated, coated, and bonded into fuel sticks for incorporation in these elements. (auth)

2792 (ORNL–4570, pp 201-4) TRANSURANIUM PROGRAM. (Oak Ridge National Lab., Tenn.).

From Metals and Ceramics Division annual progress report for the period ending June 30, 1970.

The Transuranium Project is producing quantities of the heavier transuranium elements for research by successive neutron captures in plutonium, americium, and curium in the High Flux Isotope Reactor. Target elements are removed periodically and reprocessed to obtain the product actinides and to recycle target actinides to the HFIR. Special target elements of the higher isotopes are fabricated and irradiated in HFIR. In addition, product actinides are encapsulated. Activities included the fabrication of targets in TRU for HFIR, the fabrication of HFIR rabbits, the fabrication of special encapsulations for neutron and gamma sources, the evaluation of the performance of the target elements, and the improvement of the processing equipment in TRU. Fifteen target elements were fabricated during the year, 14 loaded with ^{244}Cu and one with ^{242}Pu. Nine hydraulic rabbits for use in the HFIR were fabricated containing ^{244}Pu, ^{253}Es, and ^{249}Bk. Seven neutron sources of ^{252}Cf and one gamma source were assembled. A failure model for the HFIR targets had predicted that increased porosity in the actinide-containing pellets would extend the target life. This model was confirmed by the operation of six targets with lower density pellets up to 82% FIMA and fast fluences up to 5.45×10^{22} neutrons/cm^2 (>0.81 MeV). These targets contain pellets ranging in density from 75 to 80%, compared with 90%-dense pellets in targets that had failed at about 60% FIMA. The causes of low-ductility failures in the HFIR targets and alloys more suitable for cladding use in the targets were studied. (auth)

2793 (ORNL-TM–3191) PROGRAM AND ABSTRACTS OF PAPERS FOR CONFERENCE ON CONTINUUM ASPECTS OF GRAPHITE DESIGN, NOVEMBER 9–12, 1970, GATLINBURG, TENNESSEE. (Oak Ridge National Lab., Tenn.). Nov 1970. 90p. (CONF-701105–(Absts.)). Dep. NTIS.

Abstracts of papers containing information on material characteristics and methods of predicting the mechanical properties of graphite under in-service conditions are presented. Information is included on material characterization, constitutive equations, structural analysis, fracture, thermal shock, and design criteria. (J.R.D.)

2794 (ORNL-tr–2388) MECHANICAL PROPERTIES OF CERAMICS BASED ON URANIUM AND PLUTONIUM. Padel, Andre (Commissariat a l'Energie Atomique, Fontenay-aux-Roses (France). Centre d'Etudes Nucleaires). Translated for Oak Ridge National Lab., Tenn., from report CEA-R–3953. 80p. Dep. NTIS.

This report was abstracted from the original language and appeared in NSA as 24: 36964. (J.R.D.)

2795 PROCESS FOR FORMING UNIFORM MICROSPHERES. (to W. R. Grace and Co.). British Patent 1,210,609. 28 Oct 1970. Priority date 26 Jul 1967, United States.

A method for preparing microspherical particles of carbides or oxides of the actinides; rare earths; transition metals in groups IVA, VA, and VIA; Be; Al; and Y, is described. An aqueous solution containing the desired metal is subjected to sonic vibrations breaking it into droplets. The droplets are gelled, dried and oxidized or reacted with carbon. (J.R.D.)

2796 INVESTIGATIONS ON CERMETS OF ThO_2–Ni AND ZrO_2–Mo WITH ADDITIONS OF CHROMIUM. Jangg, G.; Kieffer, R.; Gugel, E.; Jicinsky, G.; Kollwentz, W. (Technische Hochschule, Vienna. Forschungsinstitut der Cremer-Gruppe, Oeslau, Austria). Ber. Deut. Keram. Ges.; 47: 563-70(Sep 1970). (In German).

Two types of cermets were investigated: a system of two components with high but similar melting points (ZrO_2–Mo) and two binary systems with very different melting points (ThO_2–Ni and ThO_2–Cr). For ZrO_2–Mo both normal sintering and hot pressing are suitable as shaping methods, while with the other two cermets only hot pressing is successful, since ceramic components do not sinter at temperatures high enough to melt the metallic compo-

XUM

nents. ZrO_2–Mo cermets can be produced, over the whole range of their composition, with low residual porosities. Even with high proportions of ZrO_2 these cermets still have high cross-breaking strengths, high hardness values and are, owing to the similar expansion coefficients of their components, not very sensitive to thermal shock. Their relatively low resistance to oxidation increases with increasing proportion of the ceramic component and can be clearly improved by adding chromium to the bonding metal. On the basis of ThO_2, cermets could only be produced on the basis of an adequate metal matrix, i.e., with maximum 45% ThO_2. These cermets show low cross-breaking strengths but a good resistance to oxidation (which can again be improved, with ThO_2–Ni combinations, by adding chromium). (auth)

2797 BEHAVIOR OF SOLID FISSION PRODUCTS IN PYROLYTIC CARBON AND GRAPHITE. Walter, K. H.; Schifferstein, K.; Lange, G.; Meininghaus, H. R. (Brown Boveri/Krupp Reaktorbau GmbH, Juelich, Ger.). J. Nucl. Mater.; 36: 265-74(Sep 1970). (In German).

The behavior of fission products in pyrolytic carbon and graphite is particularly interesting in connection with the release of fission products from ceramic fuel elements for high-temperature reactors. The distribution of ^{95}Zr, ^{144}Ce, ^{134}Cs, and ^{137}Cs in the coating of irradiated fuel particles, and of ^{95}Zr, ^{89}Sr, ^{103}Ru, ^{106}Ru, ^{129}Te, ^{131}I, ^{137}Cs, ^{140}Ba, ^{141}Ce, and ^{144}Ce in the graphite which surrounds the fuel particles during irradiation, was investigated. The pyrolytic carbon coating formed an almost impenetrable barrier for iodine, tellurium and cesium. Strontium, barium, and cerium are released more readily. Measured concentrations of the fission products referred to in the graphite coatings are listed. (auth)

2798 ELASTIC CONSTANTS OF THE URANIUM AND PLUTONIUM CARBONITRIDES $UC_{1-x}N_x$ AND $(U_{0.85}Pu_{0.15})(C_{1-x}N_x)$. Padel, Andre; Groff, Alain; DeNovion, Charles-Henri (Centre d'Etudes Nucleaires, Fontenay-aux-Roses, France). J. Nucl. Mater.; 36: 297-303(Sep 1970). (In French).

The velocity of sound at room temperature in the carbonitrides $UC_{1-x}N_x$ and $U_{0.85}Pu_{0.15}C_{1-x}N_x$ were measured with the aim of determining their elastic constants. The Debye temperatures deduced from the elastic constants, extrapolated to zero porosity, were compared with those calculated on the basis of measurements of specific heat; agreement was good except for UN. Young's modulus and the Debye temperature are maxima for $x \simeq 0.80$, which corresponds to an optimum occupation of the bonding component of the 6d–2p band. (auth)

2799 EFFECT OF OXIDATION ON THE EMISSIVITY OF MOLYBDENUM DISILICIDE COATINGS. Zhorov, G. A.; Sivakova, E. V. High Temp. (USSR) (Engl. Transl.); 6: 995-8(Nov-Dec 1968).

Translated from Teplofiz. Vys. Temp.; 6: 1040-3(Nov-Dec 1968).

The total-radiation emissivity of molybdenum disilicide coatings deposited on molybdenum by vacuum siliconizing has been determined at temperatures above 1000°K. It is shown that the formation of an oxide film on the coating is accompanied by an increase in its emissivity. The maximum emissivity attained in this case persists over the temperature range in which the oxide film is stable. The temperature limits for this stability of the oxide film on the coatings have been determined in air and in a vacuum of 10^{-4} mm Hg. (auth)

2800 REACTIVITY OF CARBON: SOME CURRENT PROBLEMS AND TRENDS. Thomas, J. M. (University Coll. of Wales, Aberystwyth). Carbon; 8: 413-21(Oct 1970).

Facts and theories which are generally accepted are reviewed, particular attention being paid both to the phenomenological aspects of surface oxide formation and decomposition and to the occurrence of maxima in Arrhenius plots at elevated temperatures. Present theories, which are capable of offering a unified interpretation of the $C + CO_2$ and $C + H_2O$ reactions need to be extended to encompass the $C + O_2$ system. Problems, relating to reactivity, which were solved by, and the fresh challenges that emerged from, the techniques of optical and electron microscopy are summarized. Several unsolved problems are brought into focus, and future studies are discussed by reference to a variety of new techniques. (auth) (UK)

2801 SOLUTION HARDENING OF β-RHOMBOHEDRAL BORON. Carlsson, J.-O.; Lundstroem, T. (Univ. of Uppsala). J. Less-Common Metals; 22: 317-20(Nov 1970).

Solid solutions of transition metals in β-rhombohedral boron were investigated using x-ray techniques and microhardness measurements. The variation of microhardness with unit cell volume is discussed. (auth)

2802 DETERMINATION OF THE RATE OF VAPORIZATION OF CONGRUENTLY VAPORIZING COMPOSITIONS OF THE MONOCARBIDE PHASE OF NIOBIUM. Nikol'skaya, T. A.; Avarbe, R. G.; Vil'k, Yu. N. (State Inst. of Applied Chemistry, Leningrad). High Temp. (USSR) (Engl. Transl.); 8: 72-5(Jan-Feb 1970).

Translated from Teplofiz. Vys. Temp.; 8: 77-80(Jan-Feb 1970).

The rate of the congruent vaporization of six compositions of the monocarbide phase of niobium was experimentally determined in the interval 2480 to 3300°K. The method of least squares was used to obtain the dependence of the logarithmic rate of the congruent vaporization of niobium carbide on the reciprocal of the temperature. The congruent composition is determined by the temperature. (auth)

Structure and Phase Studies

Refer also to abstracts 2727, 2730, 2748, and 3210.

2803 (COO-716-66) AN INVESTIGATION OF SOME LANTHANIDE BORON, CARBON, NITROGEN, SILICON, CHALCOGEN AND HALOGEN SYSTEMS AT ELEVATED TEMPERATURES. Technical Progress Report, February 1, 1970–January 31, 1971. Eick, Harry A. (Michigan State Univ., East Lansing. Dept. of Chemistry). Contract AT(11-1)-716. 28p. Dep. NTIS.

Single crystals of thulium carbide were prepared and submitted to crystallographic examination. The kinetics of the vaporization of SmOBr were studied. The vaporization of $EuCl_2$ was studied at 1240 to 1705°K in order to establish accurate vapor pressure values and the derived thermodynamic quantities. Studies are underway on the vaporization of $EuF_{2.0}$ and EuOF. $YbBr_2$ was prepared and its crystal structure studied by x-ray diffraction. (J.G.B.)

2804 (IS-T-401) ERBIA–HAFNIA SYSTEM. Johnstone, James Keith (Ames Lab., Iowa). Oct 1970. Contract W-7405-eng-82. 137p. Dep. NTIS.

Thesis.

The phase relations in the erbia-hafnia system were studied after fixed-temperature anneals and at high temperatures by x-ray diffraction with emphasis placed on the cubic fluorite solid solution region. Solubility of erbia in hafnia is less than 1 mole %. Trace-quantity erbia dissolved in hafnia lowered the upper limit of the monoclinic to tetragonal transformation temperature from 1825 to 1725°C. The fluorite domain extends from 9 to 50 mole % Er_2O_3 at 1450°C and from 6 to 60 mole % erbia at 1900°C. A two-phase domain composed of fluorite and erbia solid solutions extends from 50 to 73 mole % erbia at 1450°C. The evidence suggests that the two-phase region is dome shaped and does not extend all the way to the liquidus curve. Above 73 mole % erbia, a single phase domain of erbia solid solution is present. The liquidus curve exhibits a maximum of 2845°C at 20 mole % erbia. A eutectic exists at 85 mole % erbia and 2340°C. The melting points of pure hafnia and erbia were found to be 2825 ± 20 and 2400 ± 20°C respectively. X-ray structure determinations detected ordering of the pyrochlore type at 33.3 mole % erbia in the fluorite domain. A previously unrecognized anomaly in the activation energy for total electrical conductivity was observed at ~33.3 mole % erbia. The anomalous activation energy was related to the pyrochlore structure and, in particular, to the migration of the oxygen ions occupying the (a) positions in the pyrochlore structure. An anomaly was also observed in the conductivity vs composition relation. This anomaly was also related to ordering of the pyrochlore type. (auth)

2805 (ORNL-4570, pp 31-4) SPECTROSCOPY OF IONIC MEDIA. (Oak Ridge National Lab., Tenn.).

From Metals and Ceramics Division annual progress report for the period ending June 30, 1970.

The physical chemistry of haloaluminate and chlorozincate systems was investigated, largely by absorption spectroscopy of molten mixtures. Information on structure and constitution of complex ions of Ni, Al, Zn, and Bi was derived. (auth)

2806 (ORNL-4611) FABRICATION VOIDS IN ALUMINUM-BASE FUEL DISPERSIONS. Martin, M. M.; Martin, W. R. (Oak Ridge National Lab., Tenn.). Oct 1970. Contract W-7405-eng-26. 34p. Dep. NTIS.

The introduction of fabrication voids explains variations in irradiation performance of many fuel dispersions for nuclear reactors. To obtain consistent and improved irradiation performance, the fabrication factors that control the amount of void volume must be understood. The void content of aluminum-base dispersion-type fuel plates was investigated at all stages of manufacture. Two grades of U_3O_8 and two grades of UAL_x were examined at various loadings up to 1.7 g U/cm^3 of core; this covered the range applicable to the High Flux Isotope Reactor

(HFIR) and the Advanced Test Reactor (ATR). The void content of the roll-clad aluminum-base dispersions depended on: the type and concentration of the fuel compound; the aluminum cladding alloy; and the amount of cold-rolling deformation at room temperature. For a particular material combination, the first roll-bonding reduction of as little as 15% in thickness established a constant void concentration for all subsequent hot-rolling passes. This equilibrium quantity of voids was insensitive to the initial density of fuel compact and the amount of −325-mesh fuel particles in the dispersions. The final void content of the completed fuel plate showed only a secondary dependency on hot deformation and heat treatment. (auth)

2807 (SC-T-70-4039) REPLY TO THE ARTICLE OF SPIRIDONOV. Beliaev, I. N.; Artamonova, S. M. Translated by Marcel I. Weinreich (Sandia Labs., Albuquerque, N. Mex.), from Izv. Akad. Nauk SSSR, Neorg. Mater.; 6: 1387(1970). 4p. Dep. NTIS.

The stability of the phase $Ho_2O_3 \cdot 2ZrO_2(HfO_2)$ and its affinity for pyrochlore structure are discussed. It is noted that the conclusions drawn concerning structure are unreliable because of the poor quality of the x ray picture used. (J.R.D.)

2808 PHASE EQUILIBRIA RELATIONS IN THE TERNARY SYSTEM BaO–SrO–Nb_2O_5. Carruthers, J. R.; Grasso, M. (Bell Telephone Labs., Inc., Murray Hill, N. J.). J. Electrochem. Soc.; 117: 1426-30(Nov 1970).

Phase equilibria in the binary system SrO–Nb_2O_5 and the Nb_2O_5-rich region of the ternary system BaO–SrO–Nb_2O_5 were investigated by differential thermal analysis, x-ray diffraction, strip heater, and Curie temperature measurement techniques. The ternary-phase fields of three tetragonal tungsten-bronze type structures were located. Only one of these structures is a ternary compound; it is located along the $SrNb_2O_6$–$BaNb_2O_6$ binary join, extending from 20 to 80 mole % $BaNb_2O_6$, and melts congruently near 50% $BaNb_2O_6$. The ternary solubility extends from about 4% excess (Ba + Sr) to about 1% excess Nb_2O_5. This phase possesses observable orthorhombic distortion in the $BaNb_2O_6$-rich region of the solid solution. The implications of the phase diagram for the crystal growth of these compounds are briefly discussed. (auth)

2809 COMPOSITION, THERMAL STABILITY, AND STRUCTURE OF URANIUM OXYCARBIDES. Emel'yanov, V. S.; Evstyukhin, A. I.; Solov'ev, G. I. Met. Metalloved. Chist. Metal., Sb. Nauch. Rabot; No. 8, 64-70(1969). (In Russian).

Solid solutions of U–O were prepared by sintering mixtures of UO_2 and UC at 1600°C and 50 to 100 kg/mm^2. These specimens were analyzed by chemical methods, metallography, and x ray. It was found that at 1600°C the solubility of O in UC is about 17 at. % which corresponds to the value of x in $UC_{x-1}O_x$ of 0.34 and to a lattice parameter value of 4983 Å. The solubility of O in UC at 1450°C is about 10 at. % corresponding to an x value of 0.20 and lattice parameter value of 4956 Å. At 1850° a change occurs in the oxycarbide which gives the appearance of metallic U. (J.R.D.)

2810 AN INVESTIGATION OF THE EARLY STAGE GRAPHITIZATION PROCESS BY NEUTRON INELASTIC SCATTERING. Leung, P. S.; Safford, G. J. (Sterling Forest Research Center, Tuxedo, N. Y.). Carbon; 8: 527-44(Oct 1970).

The spectra of the intramolecular and intermolecular vibrational frequencies for a series of heat-treat polynuclear aromatic hydrocarbons were measured in the frequency range 8 to 900 cm^{-1} by neutron inelastic scattering. The results show that the structural ordering of pyrolyzed carbon depends strongly on both the skeletal structures and the molecular dynamics of the original aromatic materials and of the early stage intermediate products. For materials that lead to well ordered graphites, temperature intervals are reached where a major and stable species with a defined skeletal structure is first formed and then persists, gradually becoming fused together to form the graphite layers. However, large amplitude skeletal or intramolecular vibrations or the formation of strained non-planar intermediates can both inhibit the formation of such unique planar species and the growth of a well ordered graphite. (auth) (UK)

2811 ORDERED ORTHORHOMBIC SUBNITRIDE OF VANADIUM. Potter, Donald; Altstetter, Carl (Univ. of Illinois, Urbana). Scr. Met.; 4: 849-52(Oct 1970).

The structures of quenched and aged vanadium–nitrogen alloys with up to 11 at. % N were examined in the electron microscope. (G.M.C.)

Radiation Effects

Refer also to abstracts 2769 and 3872.

2812 (DP-Report-320) X-RAY MICROPROBE STUDIES OF IRRADIATED FUEL PARTICLES. Project DRAGON. Quataert, D.; Schleicher, H. W. (Atomic Energy Establishment, Winfrith (England)). Feb 1965. 34p. (CONF-641031-9). Dep. NTIS.

From Symposium on Basic Research, Harwell, Eng.

Results of microprobe analyses of irradiated pyrocarbon-coated UC_2 particles are presented. The particles were irradiated at 1450 to 1650°C. Information is included on experimental procedures and findings related to the kernels and coatings. (J.R.D.)

2813 (JAERI-Memo-4128) THERMAL CONDUCTIVITY OF VIPAC UO_2 FUEL. II. IN-PILE MEASUREMENT IN TLG-1. Shirai, Eiji; Kitahara, Tanemichi; Fukushima, Masao; Kumagai, Katsuaki; Murata, Hideo; Kaieda, K.; Toyoshima, N.; Yamada, T. (Japan Atomic Energy Research Inst., Tokyo). Sep 1970. 37p. (In Japanese). Dep. NTIS (U. S. Sales Only).

Results of measurements of the thermal conductivity of vibratory compacted UO_2 fuel in the temperature range from 200 to 1500°C are presented. The fuel was irradiated in an in-pile gas loop, TLG-1, of the JRR-2 reactor with a special capsule. The design of the capsule and its preliminary examination are described. From the difference between the temperatures at the coolant gas and the surface of the outer capsule, the rod power of the fuel was calculated and the thermal conductivity was determined. The thermal conductivity in the range up to 1500°C is represented by the emperical equation $K = (1/27.8 + 0.021\ T)$ where T is the temperature of the fuel (°C). The thermal conductivity of the VIPAC UO_2 at temperatures near 1400°C was shown to be similar to that of the sintered UO_2 pellet. The post-irradiation examination of the capsule is also described. (auth)

2814 (N-70-27167) INVESTIGATION OF THE EFFECTS OF SUB-THRESHOLD HIGH-ENERGY ELECTRONS ON THE PROPERTIES OF SILICON PHOTOVOLTAIC CELLS. Final Report, February 3–November 3, 1969. Loferski, J. J.; Crisman, E. E. (Brown Univ., Providence, R. I. Div. of Engineering). Feb 1970. Contracts NAS7-100; JPL-952386. 13p. (NASA-CR-109851). NTIS.

For Jet Propulsion Lab., Pasadena, Calif.

Measurements of the photovoltaic characteristics of p-n lithium-doped cells, p-n conventional cells and n-p cells are described. An experimental comparison of damage rates in a lithium doped p-n cell with a conventional p-n cell at approximately 90°K has shown that no effects associated with displacement of lithium ions by electrons whose energy is too low to displace Si atoms has been detected. A difference in damage rates at 200 keV was observed with the lithium-doped cell exhibiting very little damage even though Li ions are not mobile at approximately 90° K. A deflection circuit to produce a scanned electron beam pattern is described. (auth) (STAR)

2815 (N-70-33138) MECHANISMS OF RECOVERY OF RADIATION DAMAGED SILICATE-TREATED ZINC OXIDE THERMAL CONTROL COATINGS. Colony, J. A.; Bass, J. A. (National Aeronautics and Space Administration, Greenbelt, Md. Goddard Space Flight Center). Jun 1970. 16p. (NASA-TM-X-63965; X-713-70-251). NTIS.

X-ray exposure of a silicate-treated zinc oxide coating results in a drastic reduction of near infrared reflectance. This damage is completely reversible upon exposure to an oxygen environment as is the case for ultraviolet-induced damage in coatings made from untreated zinc oxide. Thus, damage in both cases is due to loss of oxygen from the zinc oxide crystals. The rapid increase in bleaching rate with increase in temperature is due to an accelerated diffusion rate of molecular oxygen through the silicone binder as well as to possible increased kinetics of reaction of oxygen molecules with damaged pigment. Oxygen photolysis due to ultraviolet exposure during bleaching results in a suppression of bleaching rate. This is due to interaction of atomic oxygen with the methyl silicone binder which creates a barrier for diffusion of molecular oxygen. Comparisons between bleaching effects of the coating and of the treated pigment alone indicate consistent relative behavior as a function of environment. The mechanisms of damage and recovery, then, must be unaffected by the silicone binder. (auth) (STAR)

2816 (ORNL-4570, pp 16-19) ELECTRON MICROSCOPY. (Oak Ridge National Lab., Tenn.).

From Metals and Ceramics Division annual progress report for the period ending June 30, 1970.

XUM

Observations on voids produced in metals by irradiation and quenching are described, including the effects of cyclotron-injected gases, and preliminary experiments using electron irradiation to produce damage in aluminum are described briefly. Metallographic observations of silicon precipitates produced in aluminum as a result of neutron irradiation are summarized. Theoretical and experimental studies of the stability and growth of bubbles and cavities in metals are reported. Measurements of the energy stored in copper single crystals by room-temperature deformation are presented along with a brief discussion of the use of stored energy measurements in evaluating work-hardening theories. Observations on hydrogen absorption and embrittlement of steel are described. (auth)

2817 (ORNL–4570, pp 116-17) NITRIDE FUELS DEVELOPMENT. (Oak Ridge National Lab., Tenn.).

From Metals and Ceramics Division annual progress report for the period ending June 30, 1970.

A method of fabricating UN fuel pellets with only 150 ppM O contamination was developed. UN clad in T-111 was irradiated at a surface temperature of 1400°C to a burnup of about 1.75 at. % heavy metal. The test was terminated when cladding failure was detected. Failure is attributed to low cladding ductility under the conditions of the test. (auth)

Plastics and Other Materials

Refer also to abstracts 2249, 2629, 2730, and 3219.

2818 (BDX–613-170) EFFECTS OF AMINE CATALYSTS ON THE PHYSICAL PROPERTIES OF A RIGID URETHANE FOAM SYSTEM. Neet, T. E.; DeGisi, S. L. (Bendix Corp., Kansas City, Mo.). Sep 1970. Contract AT(29-1)-613. 22p. Dep. NTIS.

The effects of catalyst type and concentration upon the compressive properties of a rigid urethane foam system were investigated. Formulations containing six different catalysts and various concentrations of each were tested. Standard ASTM 1-inch-cube compressive specimens were prepared from both free-rise and molded billets. All data were normalized to nominal densities, 6.5 lb/ft^3 for the free-rise foam and 14.0 lb/ft^3 for the molded materials, thus enabling direct comparisons of strength values. The results of the investigation support the belief that the principal function of the catalyst in high-density molded urethane foams is to control the reaction of the foam constituents. (auth)

2819 (LCIE–342) EFFECT OF HIGH ENERGY RADIATIONS ON INSULATING MATERIALS. (Laboratoire Central des Industries Electriques, Fontenay-aux-Roses (France)). Jun 1970. 75p. (In French). Dep. NTIS (U. S. Sales Only).

Methods of estimating the permanent damage, in terms of the variations in the electrical and mechanical properties, suffered by insulations and cables subjected to irradiations are described. With the aid of the results obtained, the lifetimes of the materials were determined, and an attempt was made to define an acceptable dose limit. Six groups of different products were studied: (1) basic insulating materials, in the form of films or sheets, such as polyethylenes, polyamides, and heavy molecular plastics; (2) impregnating varnishes; (3) impregnated cloths; (4) enameled wire; (5) wire and cables; and (6) laminated copper for printed circuits. Two radiations were used: 1.3-MeV gamma and 6-MeV electrons. (France)

2820 (ORNL–4570, pp 213) ABSORBER MATERIALS FOR SULFUR DIOXIDE FROM FLUE GAS. (Oak Ridge National Lab., Tenn.).

From Metals and Ceramics Division annual progress report for the period ending June 30, 1970.

A comparison of the SO_2 absorption and H_2 regeneration characteristics of pure sodium aluminate and sodium aluminate modified with kaolinite and sodium silicate indicated that the pure sodium aluminate has serious limitations but is generally superior to the modified material as a possible flue-gas absorber. Extensive DTA, TGA, and x-ray experiments showed that formation of sodium aluminate from $NaAlCO_3(OH)$, the mineral dawsonite, is complex and involves at least one noncrystalline intermediate. (auth)

2821 (ORNL–4572–, pp 258–61) MISCELLANEOUS PROGRAMS. (Oak Ridge National Lab., Tenn.).

From Chemical Technology Division annual progress report for period ending May 31, 1970.

Tests to evaluate commercial protective coatings for potential use in various nuclear facilities were continued. Current exposure data on coatings γ irradiated in air and submerged in deionized water are presented. (M.C.G.)

2822 EFFECT OF NUCLEAR RADIATION ON THE PHYSICOMECHANICAL PROPERTIES OF LACQUER COATINGS. Knyazev, V. K.; Novikov, V. S.; Izotov, G. T.; Glushchenko, V. M.; Seregina, G. P. Lakokrasoch. Mater. Ikh. Primen.; No. 1, 42-4(Jan 1970). (In Russian).

It is shown that a series of coatings retain satisfactory properties under γ radiation at doses of 10 rad/hr. Physico-mechanical indices for evaluating the radiation stability of coatings relate mainly to the elasticity and resistance to shock. (INIS)

2823 CRYSTALLIZATION OF AMORPHOUS FILMS OF SILICON DIOXIDE DURING IONIC BOMBARDMENT AND SUBSEQUENT ANNEALING. Pavlov, P. V.; Shitova, E. V.; Zorin, E. I. (Gorky State Univ., USSR). Dokl. Akad. Nauk SSSR; 192: 559-61(1970). (In Russian).

A transition of glass from the amorphous to crystalline state is observed on irradiation with high-energy inert gas ions. Amorphous films of silicon dioxide on NaCl were irradiated with 50 keV ions of Ar^+, P^+, and B^+ at doses of 1×10^3 to 1×10^4 microcoulombs/cm^2, and were subsequently annealed at temperatures from 500 to 1000°C. Electrograms showed the growth of alpha-cristobalite in the amorphous silicon dioxide film. The heavier the bombarding ion and the greater the irradiation dose, the lower is the annealing temperature at which the crystallization begins to take place. (TTT)

PHYSICS (GENERAL)

Astrophysics and Cosmology

Cosmic Ray Exposure Ages

Refer also to abstract 2148.

2824 ORIGIN OF PALLASITES. Nordemann, Daniel; Tobailem, Jacques (CEA, Saclay, France). Compt. Rend., Ser. D; 271: 753-5(31 Aug 1970). (In French).

In the three pallasites Eagle Station, Springwater, and Krasnojarsk, ^{40}K and ^{26}Al were determined by gamma spectrometry. The results obtained showed that the origins of pallasites and chondrites are not identical, although their orbits during the million year preceding their fall are similar. (auth) (France)

Stars

Refer also to abstracts 2888, 2892, 3335, and 3562.

2825 MIXING BETWEEN STELLAR ENVELOPE AND CORE IN ADVANCED PHASES OF EVOLUTION. I. GENERAL TREATMENT AND BRIEF SUMMARY OF RESULTS. Sugimoto, Daiichiro (Nagoya Univ., Japan). Progr. Theor. Phys. (Kyoto); 44: 375-88 (Aug 1970).

Stellar structure in very advanced phases of evolution is discussed, taking into account the hydrogen-rich envelope. The star is divided into the envelope and the core. It is shown that the envelope with an extended surface-convection zone can be replaced, to a good approximation, by suitable boundary conditions at the outer edge of the core. Computing evolution of the core with these boundary conditions, one can discuss mixing between the stellar core and envelope through a deepening surface-convection zone; the condition for the mixing is formulated as an entropy condition at the edge of the core. A simplified model of the core is studied to understand how the mixing proceeds in the very advanced phases of evolution. Detailed numerical computation was made for the stars of masses about 30 and 12 $M_\odot$ through the oxygen-burning phase, and for the star of mass about 6 $M_\odot$ through the phase of carbon-shell burning. In the present paper, however, physical data used in this series of studies are given along with a brief summary of numerical results. (auth)

2826 NARROW-BAND INFRARED PHOTOMETRY OF α ORI. Low, F. J. (Univ. of Arizona, Tucson. Rice Univ., Houston, Tex.); Swamy, K. S. K. Nature (London); 227: 1333-4(26 Sep 1970).

Broad-band infrared photometry of cool giants and supergiants showed that many of these stars exhibit appreciable excess emission at 10 and 22 μ, and it was also shown that 10-μ excess in several stars, including α Ori, was confirmed to a band peaking at about 10 μ. It was also suggested that this peak corresponds to a peak in the emittance of silicate materials and that circumstellar dust composed of silicate produces the excess emission by thermal radiation of starlight. In order to provide an additional experimental test of this hypothesis a series of narrow-band photometric observations was made of α Ori, extending out to 24.5 μ, as the spectral emittance of of silicates is known to show a second peak near 20 μ, which should be even more diagnostic than the 10-μ peak. The curves obtained clearly showed the infrared excess, and comparisons were made with previous spectral emittance data for silicate materials, showing consistency with the new data. The total infrared excess was about 0.5% of the total flux emitted by the star, implying very low optical depth near 1 μ and suggesting a large diffuse cloud. The observations, however, placed moderately severe limits on the size of the circumstellar dust cloud. It is noted that a direct observational test of the thermal reradiation model is rendered possible. Assuming T = 250°K, a mean particle radius of 0.2 μ, and a distance of 180 psc, the number of grains producing the observed flux density at 22 μ is calculated as $\sim 1 \times 10^{26}$ g. (UK)

2827 NEW APPROACH TO THE EQUILIBRIUM CONFIGURATION OF STELLAR ENVELOPES. Singh, Bijai; Ram, Rishi (Banaras Hindu Univ., India). Bull. Cl. Sci., Acad. Roy. Belg.; 56: 357-66(1970).

Considering the physical structure of the stellar envelope, a new solution of the equation of equilibrium is obtained that is free of approximations. In a determination of the mass in the stellar envelope Chandrasekhar's solution requires further approximation in the process of integration, whereas the new solution obtained requires no approximation. In the particular case of vanishing radiation pressure, results are in full agreement with those of Chandrasekhar. The application of results in a stellar model is also discussed, and n_{eff} is calculated. The expression for n_{eff} assumes a simple form, and its typical values are the same as obtained by Chandrasekhar. (auth)

2828 INTERNAL SOLUTION FOR STATIONARY AXIALLY SYMMETRIC GRAVITATIONAL FIELDS. Sedrakyan, D. M.; Chubaryan, E. V. (Erevan State Univ.). Astrophysics (Engl. Transl.); 4: 227-33(1968).

Translated from Astrofizika; 4: 551-65(1968).

A method is developed for deriving the internal solutions of the Einstein equations for stationary axially symmetric gravitational fields in the Ω^2 approximation (Ω is the angular velocity). The problem is reduced to the integration of ordinary differential equations with given initial conditions. The method can be applied to any equations of state. (auth)

2829 APPLICATION OF THE METHOD OF CHARACTERISTICS TO THE SOLUTION OF THE TRANSFER EQUATION FOR A NONSTATIONARY RADIATION FIELD. Kaplan, S. A.; Morozov, S. F.; Piskunova, L. V. (Gorky Scientific Research Radiophysics Inst., USSR). Astrophysics (Engl. Transl.); 4: 205-8(1968).

Translated from Astrofizika; 4: 485-91(1968).

An account is given of the method of characteristics, which can be used to obtain a numerical solution of the transfer equations for a nonstationary radiation field with any scattering indicatrix and including the time shift. Relatively modest expenditure of computer time is necessary. An example illustrating the method is given. (auth)

2830 RADIATION FROM A GAS HEATED BY A SHOCK WAVE AND ITS ROLE IN THE EMISSION OF STELLAR ENVELOPES OF CLOSE BINARY SYSTEMS. Gorbatskii, V. G. (Leningrad State Univ.). Astrophysics (Engl. Transl.); 4: 209-14(1968).

Translated from Astrofizika; 4: 505-18(1968).

The intensity of radiation emitted by a gas layer heated by a shock wave is determined approximately as a function of frequency. In the range between visible radiation and soft x rays, this function is represented by the power law ν^{-s}, where $s < 2.5$. The U−B and B−V color indices are calculated for this radiation, and are then compared with the observed color indices in the region where the gas jet encounters the envelope ("hot spot") in the close binary systems UX UMa and U Gem. In the case of UX UMa the color indices are in agreement with the theoretical calculations for $s = \frac{1}{2}$, whereas for U Gem this occurs for $s \approx 2$. Estimates of the x-ray emission of the gas heated by the shock wave agree with observations for many known x-ray sources. (auth)

2831 DYNAMIC PARTICLE-SPIN ORIENTATION IN A COSMIC MEDIUM. Varshalovich, D. A. (Ioffe Inst. of Physics and Tech., Leningrad). Astrophysics (Engl. Transl.); 4: 215-21 (1968).

Translated from Astrofizika; 4: 519-36(1968).

The spins of atoms and molecules exposed to a directed flux of radiation assume a definite orientation after resonant scattering, and this results in a specific nonuniform population of magnetic sublevels. The conditions necessary and sufficient for this type of dynamic spin orientation are frequently satisfied in many astrophysical objects such as the upper atmospheres of stars and planets, the interplanetary and interstellar medium, and so on. Calculations of magnetic sublevel populations for all the possible resonant transitions that can occur in both polarized and unpolarized orienting radiation traveling in an arbitrary direction relative to the local magnetic field are reported. The properties of a medium containing paritcles with oriented spins and some astrophysical consequences of these properties are discussed. The extinction coefficient for the resonance radiation propagating through such a medium is given as a function of the magnetic sublevel population and the direction of observation. (auth)

2832 EFFECT OF NEUTRONIZATION OF THE CRITICAL PARAMETERS OF ISOTHERMAL WHITE DWARFS. Vartanyan, Yu. L.; Ovsepyan, A. V. (Erevan State Univ.). Astrophysics (Engl. Transl.); 4: 270-2(1968).

Translated from Astrofizika; 4: 643-6(1968).

Calculations are reported of the critical parameters of isothermal white dwarfs, including both general relativistic and neutronization corrections. The calculation was carried out by the energy method. (W.D.M.)

2833 POLYTROPIC MODELS IN THE NONRELATIVISTIC GENERALIZED THEORY OF GRAVITATION. Mnatsakanyan,

M. A.; Avakyan, R. M. (Erevan State Univ.). Astrophysics (Engl. Transl.); 4: 272-5(1968).
Translated from Astrofizika; 4: 646-50(1968).
It is shown that static polytropic models cannot have central densities exceeding a certain definite value. Physically, this means that the pressure at the center of the star due to the gravitational attraction of the masses ceases to increase with increasing mass of the star, and may even fall because the attraction characterized by the function k(y) becomes weaker. (W.D.M.)

2834 ANOMALOUS HYDROGEN LINE INTENSITIES IN THE SPECTRUM OF HD 152107. Kuznetsova, T. I. (Main Astronomical Observatory, Pulkovo, USSR). Astrophysics (Engl. Transl.); 4: 276-8(1968).
Translated from Astrofizika; 4: 651-5(1968).
The spectra of peculiar magnetic A stars were observed at the Crimean Observatory in 1962, 1963, and 1967. Analysis of the observational material established the existence of highly anomalous behavior of a number of absorption lines in the Balmer series of hydrogen. These properties were observed in three cases out of a long series of observations on the magnetic star HD 152107. (W.D.M.)

2835 LUMINOSITY FUNCTION AND STELLAR DENSITY IN THE NEIGHBORHOOD OF THE SUN. Arakelyan, M. A. (Byurakan Astrophysical Observatory, Erevan). Astrophysics (Engl. Transl.); 4: 256-65(1968).
Translated from Astrofizika; 4: 618-32(1968).
Data on stars in a sphere of radius 20 pc were used to construct the luminosity function and to determine the stellar density in the neighborhood of the Sun. The analysis was based on the author's method of determining densities from the distances of individual close stars. It is shown that the luminosity function has maxima at $M_V = 13$ and $M_V = 15$. The stellar density for $M_V \geq 15$ is almost entirely due to dwarfs with hydrogen emission lines. The existence of a local maximum in the stellar density at $M_V = 6$, which has been noted by a number of workers, was confirmed. This local maximum is connected with an excess of stars of the sixth magnitude in the immediate neighborhood of the Sun. Possible modifications of the method are considered while the distribution function for the distance of the k-th neighbor is determined. (auth)

2836 STRUCTURE AND EVOLUTION OF RAPIDLY ROTATING B-TYPE STARS. Sackmann, Inge-Juliana. Toronto; Univ. of Toronto (1968).
Thesis.
Sixty-four interior main-sequence models of slowly and rapidly rotating B-type stars were constructed. It was found that changes brought about by rotation were comparatively small. The total decrease of the luminosity is only 6 to 7% and that of the polar radius only 1 to 2% when the rotation is increased from zero to the maximum value. The percentage luminosity change produced by rotation is remarkably constant as the mass varies from 5 to 15 $M_\odot$; the corresponding change in the polar radius decreases as the mass increases. Equatorial velocities at maximum rotation vary from 484 to 597 km/sec in the mass range from 5 to 15 $M_\odot$; the critical angular velocity for the same increase of mass decreases from 1.70×10^{-4} radians/sec to $1/07 \times 10^{-4}$ radians/sec. (TSS) (Diss. Abstr. Int., B)

2837 INHOMOGENEITIES IN PLANETARY NEBULAE. Kirkpatrick, Ronald Crecelius. Austin, Tex.; Univ. of Texas (1969). 177p. University Microfilms Order No. 70-10,819.
Thesis.
The physical processes shown by Menzel and his contemporaries to be responsible for nebular emission are incorporated into axially symmetric theoretical emission models of planetary nebulae for comparison with observations. Also, several possible nebular circumstances that may coexist in planetary nebulae were analyzed: smooth density distributions in thermal equilibrium, crowded inhomogeneities in thermal equilibrium, sparsely distributed inhomogeneities in thermal equilibrium, and smooth density distributions not in thermal equilibrium. Detailed numerical models for smooth density distributions in thermal equilibrium were calculated on the basis of observational data for NGC 7009, NGC 7662, and IC 3568 and on the basis of typical observational characteristics for a homogeneous nebula and a "ring–lobe" nebula. For the line ratios of forbidden lines produced by the same ion, the agreement between theory and observation is fairly good; but the relative intensities for lines of different ions of the same element, notably [O II] and [O III], are in discord. Therefore, a grid of optically thin model condensations in thermal equilibrium was computed under the assumption that they are spherically symmetric with a Gaussian density profile. The agreement between observation and theory is more satisfactory for appropriate choices of condensation peak density, background density, and size relative to separation; but the agreement is still not perfect. It appears that the radiation field in the vicinity of the condensations must be much more dilute if the strengths of the lines of subordinate ions such as O II are to compare favorably with observation. (TSS) (Diss. Abstr. Int., B)

2838 HYDRODYNAMIC ATMOSPHERES OF A CEPHEID VARIABLE. Keller, Charles F. Jr. Bloomington, Ind.; Indiana Univ. (1969). 180p. University Microfilms Order No. 70-10,265.
Thesis.
Shallow-envelope, hydrodynamic calculations were carried out for a theoretical, Cepheid, variable star model corresponding to the deep-envelope model, BK7, studied by Cox, et. al. Improvements made in the present calculations include: (1) Finer zoning of the model—the stellar model is divided into concentric, spherical shells or zones. The shallow-envelope models were computed by rezoning the upper 9 zones of the deep-envelope model into 35 zones. (2) Treatment of the atmosphere by radiative transfer rather than by the diffusion approximation—in the deep-envelope model the flux is given by the diffusion approximation. This approximation is incorrect in the atmosphere because it assumes the medium to be optically thick. For the shallow-envelope models radiation flow in the atmosphere is computed from the equation of transfer. As time-dependent lower boundary conditions the velocity and flux at the 9th zone of BK7 were used. (TSS) (Diss. Abstr. Int., B)

2839 NEUTRAL HELIUM LINES IN NORMAL B-TYPE SPECTRA. Leckrone, David Stanley. Los Angeles; Univ. of California (1969). 316p. University Microfilms Order No. 70-14,300.
Thesis.
Spectroscopic observations of the profiles of a number of neutral helium lines were obtained for five main-sequence B stars. The helium abundances of three of these stars, υ Orionis, HR 2154, and π Ceti were estimated. Published profile and equivalent width data for the neutral helium lines of ι Herculis and γ Pegasi were utilized in estimating their helium content. The five stars analyzed range in spectral type from BO to B7. (TSS) (Diss. Abstr. Int., B)

2840 MODEL-ATMOSPHERE ANALYSIS OF THE PECULIAR A STAR KAPPA CANCRI. Aller, Margo Friedel. Ann Arbor, Mich.; Univ. of Michigan (1969). 129p. University Microfilms Order No. 70-14,460.
Thesis.
A detailed model atmosphere analysis was carried out for the manganese–mercury star Kappa Cancri using nine high-dispersion spectrograms for the spectral range $3100 < \lambda < 6500$Å and a published energy distribution. A grid of empirical model atmospheres was constructed, using scaled temperature distributions for Mihalas-type models in radiative equilibrium. The adopted model was selected from the grid by comparing the observed energy distribution and hydrogen-line profiles with the parameters predicted by the models. The model selected is characterized by $\theta = 0.36$ at $\log \tau_0 = 0.0$ and by $\log g = 3.6$. Equivalent widths were measured for more than 350 metal lines, line profiles were determined for the strong Si II lines at 3853 to 3862Å, and half widths and central line depths (corrected for instrumental broadening) were obtained for several lines of iron, chromium, and silicon. These data served to determine the stellar abundances and to further verify the model. A microturbulent velocity of 5 km/sec was determined from the shapes of the metal-line profiles from the abundance–equivalent width correlations and from the shape of the curve of growth. The abundances obtained are as follows: phosphorus overabundant by a factor of 300, manganese by a factor of 200, gallium by a factor of 2000, and mercury and xenon by factors of 10^3 or more; helium underabundant by a factor of 2, magnesium by a factor of 6 and calcium by a factor of 30. Among the iron-peak elements titanium and scandium are overabundant, iron is marginally overabundant and chromium and nickel are marginally underabundant. The types of abundance anomalies indicate that the composition of Kappa Cancri is similar to that of 3 Cen A and the other manganese stars. The extent of the manganese overabundance in each manganese star appears to be correlated with its effective temperature. (Diss. Abstr. Int., B)

Quasi-Stellar, Radio, and X-Ray Sources

2841 (CEA-CONF-1633) OPTICAL SPARK CHAMBER FOR THE SEARCH OF GAMMA-RAY SOURCES. Vasseur, J.; Paul, J.; Parlier, B.; Leray, J. P.; Forichon, M.; Agrinier, B.; Boella, G.; Maraschi, L.; Treves, A.; Buccheri, R.; Scarsi, L. (Commissariat a l'Energie Atomique, Saclay (France). Centre d'Etudes Nucleaires). 1970. 12p. (In French). (CONF-700825-1). Dep. NTIS (U. S. Sales Only).

From Symposium I.A.U. on New Techniques in Space Astronomy, Garching, Germany.

In order to observe the NP 0532 pulsar in the energy range above 50 MeV, six balloon flights took place in 1969. The system included a pointed telescope equipped with an 850 cm^2 optical spark chamber and a time-marker recording unit. A stereographic display allowed the reconstruction of the gamma-ray directions from the photographs of the sparks. The preliminary analysis indicated the probable existence of a pulsed emission of gamma rays coming from the Crab Nebula. (tr-auth) (France)

2842 RADIO EVOLUTION OF PULSARS. Aizu, Ko; Taketani, Mituo (Rikkyo Univ., Tokyo). Progr. Theor. Phys. (Kyoto); 44: 363-74(Aug 1970).

Phenomenological analysis of radio evolution of pulsars is made. Under an assumption that the periods of most pulsars have a similar time dependence, the age t of pulsars is determined statistically from the observed spindown time t_1: $t = 0.30t_1$. Period P, radio luminosity during the pulse L, called simply the luminosity, and size of the radio emitting region a, estimated as the pulse width times the light velocity, are shown to have time dependences of $P \propto t^{0.36\pm0.05}$, $L \propto t^{0.70\pm0.12}$, and $a \propto t^{0.23\pm0.06}$, respectively. This radio evolution is compared with that of supernova remnants, quasi-stellar objects, and radio galaxies directly or by means of the luminosity versus volume emissivity diagram. The evolutionary tracks are similar to each other in spite of different mechanisms involved. Finally, the observed luminosity function $N(L) \propto L^{-1.50\pm0.08}$ is compared with that calculated from the time dependence of the luminosity and it is shown that the slopes of both functions are consistent with each other if the selection effect in the present sample of pulsars is taken into account. Similarly, the birth rate of pulsars in the Galaxy is shown to be nearly equal to the explosion rate of Type II supernovae after the selection effect is taken into account. (auth)

2843 OPTICAL POLARISATION OF THE CRAB NEBULA PULSAR. Cocke, W. J.; Disney, M. J.; Muncaster, G. W.; Gehrels, T. (Univ. of Arizona, Tucson). Nature (London); 227: 1327-9(26 Sep 1970).

Among radio observations of pulsars, polarization measurements are among the most revealing and gave the first direct evidence for rotation. Various attempts have been made to measure the optical polarization properties of the Crab pulsar. The present authors reported variability of polarization on a time scale of minutes, but now believe that this finding was due to an instrumental effect. In the observations described it was found that the linear polarization in both pulses was high (~20%) in the wings, but fell to virtually zero near the pulse centers, and that the polarization vector swept rapidly through a large angle (~140%) in both pulses. There did not seem to be any variation in either pulse shape or polarization from night to night. When the interstellar polarization was subtracted, the linear polarization was well defined and varied smoothly through the pulses in a manner lending support to some sort of rotating model. The observations, however, did not take the simple form shown by the radio emissions of the Vela pulsar, in which the intensity and percentage polarization follow each other closely. In the Crab pulsar the radio and optical polarizations differed markedly from one another. No obvious relationship could be detected between the optical polarization of the pulsar and that of the Crab Nebula in its immediate environment. Details are given of the instrumentation used in the studies, the observational procedure, and the results. (UK)

2844 VERY-LONG-BASELINE INTERFEROMETRY OF GALACTIC OH SOURCES. Ronnang, B. O. (Chalmers Univ. of Tech., Goteborg); Rydbeck, O. E. H.; Moran, J. M. Radio Sci.; 5: 1227-31(Oct 1970).

Several hydroxyl radical microwave emission sources were studied in July 1969 with very-long-baseline interferometry (VLBI). The elements of the interferometer were the 84-foot telescope of the Onsala Space Observatory and the 120-foot telescope of the Haystack Facility; a baseline of 31.1×10^6 wavelengths, or a fringe spacing of 0.0066 sec of arc at a frequency of 1665 MHz, resulted. Earlier spectral-line interferometric observations have given detailed information on the angular sizes and spatial separations of the 1665-MHz OH sources in the W3 source. The measurements reported here confirm these results and give additional information on the complex structure of the various features. Four other galactic OH emission sources with unknown angular sizes were also investigated. Only one (the 5-km/sec component in the 1667-MHz spectrum of W49) gave reliable fringes. (auth)

2845 LOW-FREQUENCY SPECTRA OF EXTRAGALATIC RADIO SOURCES. Aslanyan, A. M.; Malumyan, V. G.; Sanamyan, V. A. (Byurakan Astrophysical Observatory, Erevan). Astrophysics (Engl. Transl.); 4: 252-5(1968).

Translated from Astrofizika; 4: 595-601(1968).

The low frequency spectra of 75 extragalactic radio sources are discussed. Most of these spectra can be divided into three types, namely: linear, "rising," and "descending." It is concluded that about 60% of all quasars have nonlinear spectra, about 65% of sources identified with radio galaxies have linear spectra, and about 90% of binary or multiple sources identified with radio galaxies have linear spectra. (auth)

2846 POLARIZATION AND TRANSFORMATION THEORY OF QUASI-MONOCHROMATIC RADIATION FIELDS. SUMMARY REPORT. Thiel, Manfred A. F. Beitr. Radioastron.; 1: 114-46 (Mar 1970). (In German).

A coherent derivation of several representations of the polarization state of quasi-monochromatic radiation fields, the relations between these representations, and the transformation of the polarization state when the radiation is transmitted through an instrument are given. (W.D.M.)

2847 INTERPRETING THE CURVATURE IN THE EXTRAGALACTIC RADIO SOURCE SPECTRUM BY MEANS OF A HIGH CUT-OFF ENERGY IN THE ELECTRON SPECTRUM. Ristow, D. Beitr. Radioastron.; 1: 149-60(May 1970).

An analysis of the 3C sources with convex spectra is given. An attempt is made to describe the spectrum by $I(f) \sim f^{\alpha} \exp(f/f_c)$ above 178 MHz and examine the distribution of the "critical" frequency f_c. The distribution function increases with f_c. There is no significant difference between quasars and radio galaxies. Therefore, the assumption that quasars develop into radio galaxies is not compatible with the assumption that the observed spectral curvature is a function of time only. Also brightness temperature, source diameter, and redshift do not show the correlation with the "critical" frequency as one would expect when f_c was due to a cut-off energy in the electron spectrum. (auth)

2848 MEASUREMENTS OF RADIO SOURCES AT 10.69 GHz. Zimmermann, P. Beitr. Radioastron.; 1: 161-8(May 1970). (In German).

The flux densities of 74 radio sources were measured at 10.69 GHz. The measurements were made with the 20-m telescope of the Institut für Weltraumforschung in Bochum. The telescope is protected by a radome. A cryogenically cooled parametric amplifier was used as receiver. Its noise temperature, including the Dicke switch, was 59°K. Due to the radome and the humidity of the atmosphere, the noise temperature of the whole system varied between 100 and 190°K. By applying the dual beam method, the influence of the varying noise contribution of the atmosphere could be largely reduced. By these variations, however, a lower limit was set to the still-measurable flux density. It was twice as high as that one resulting from the theoretical value gained from the noise temperature of the system. All the sources of the NRAO catalog with an expected flux density of ≥ 1 FU = 10^{-26} W·m^{-2}·Hz^{-1} were measured, each of them at least five times. The rms of the measured flux density was 8%. (auth)

2849 SPACED-RECEIVER OBSERVATIONS OF RADIO PULSES. Charman, W. N. (Atomic Energy Research Establishment, Harwell, Eng.); Jelley, J. V.; Fruin, J. H.; (and others). Nature (London); 228: 346-8(24 Oct 1970).

Preliminary observations were carried out to look for radio signals associated with gravitational waves. Although inconclusive, the observations from five receivers in the British Isles suggest the value of further experiments. (auth) (UK)

2850 CONTRIBUTION TO THE CO-ROTATING MAGNETIC FIELD MODEL OF THE PULSAR. Endean, V. G.; Allen, J. E. (Oxford Univ.). Nature (London); 228: 348-50(24 Oct 1970).

A new general solution of the electromagnetic field equations convenient for rotating field problems is used to analyze the case of low plasma number density. Two localized pulse-emitting regions rotating with the star and located at approximately twice the velocity of light radius away from the star, and on opposite sides of it, are predicted. (UK)

2851 PULSAR DISTRIBUTIONS WITHOUT MAGNETIC DECAY. Holt, S. S.; Romaby, R. (Goddard Space Flight Center, Greenbelt, Md.). Nature (London); 228: 351-2(24 Oct 1970).

Arguments have been put forward for the necessity of decay of the surface magnetic field of neutron stars with a characteristic time of a few million years in order to explain details of observed pulsar samples. In this connection the findings of Gunn and Ostriker (Astrophys. J., 160: 979(1970)) and Setti and Woltger (Astrophys. J. Lett., 159: L87(1970)) are briefly discussed. Among the evidence offered is the scarcity of long-period pulsars, and an

XUM

apparent decrease in surface magnetic field and pulsed radio luminosity with age. The present authors point out that the assumption of a period-dependent pulsed radio luminosity can explain the age dependence of both the surface field and the pulsed radio luminosity, although an additional assumption must be made to reconcile the proposal model with the two young pulsars NP 0531 and PSR 0833. If it is assumed that the radio luminosity is a fixed fraction of the total electromagnetic energy-loss rate of the rotating neutron star, such radio luminosity becomes explicitly period-dependent. The proposed model can also account for the other characteristics of the pulsar sample. (UK)

2852 FREQUENCIES FOR RADIO ASTRONOMY. Smith, F. G. (Nuffield Radio Astronomy Labs., Jodrell Bank, Eng.). Nature (London); 228: 419(31 Oct 1970).

At present the scope of research in radio astronomy is limited by the allocation of frequencies, some of which have to be shared with other radio services. When the International Telecommunications Union reconsiders all frequency allocations next year, astronomers are hoping for an improvement. (UK)

2853 ABSOLUTE TIME-OF-ARRIVAL MEASUREMENTS OF OPTICAL PULSES FROM THE CRAB PULSAR. Papaliolios, C.; Carleton, N. P.; Horowitz, P. (Harvard Univ., Cambridge, Mass.). Nature (London); 228: 445-50(31 Oct 1970).

An attempt is made to understand the characteristics of pulsar slowdown in terms of various possible emission mechanisms. Though magnetic-dipole radiation seems to be dominant, the deviations from a pure dipolar decay are large compared with errors in measurement and indicate the presence of more complicated braking mechanisms, small fluctuations, and major "jumps," or period discontinuities. Some rapid-relaxation effect is evident following the discontinuous jump in period in September 1969, but there is no evidence of the quasi-sinusoidal behavior reported before the jump by Arecibo. An alternative interpretation of the Arecibo data is given. (UK)

2854 PULSAR DISTANCES AND EMISSION. Prentice, A. J. R.; Buckee, J. W.; ter Haar, D. (Oxford Univ.). Nature (London); 228: 452-3(31 Oct 1970).

An extension is presented to the list of pulsar distances given in Nature, 222: 964(1969) and Mon. Not. Roy. Astron. Soc., 146: 423 (1969), comprising 18 additions. These additions are MP 0254, 0818, 1154, 1359, 1604 and 1706, 1857, 1911 and 1944, JP 1845, 1858, 1946, 1953, 2003, 2021, 2111 and 2319, and AP 2303. A suggestion that optical or infrared pulsed emission might be found at frequencies where the brightness temperature would become of the order of the effective temperature of the relativistic particles that produces the magneto-bremsstrahlung radiation is discussed. Values of these frequencies are given for seven pulsars, and from the data it appears that the most likely condidates to show pulsations in the infrared would be CP 0950 at ~1 μ and PSR 1642 and 1929 at ~2 μ. (UK)

2855 SURVEY BETWEEN 0 AND 20^0 NORTH DECLINATION USING THE OHIO STATE UNIVERSITY RADIO TELESCOPE AT 612, 1415, AND 2650 MHz. Fitch, Lewis Thomas. Columbus, Ohio; Ohio State Univ. (1969). 272p. University Microfilms Order No. 70-14,015.

Thesis.

A survey of the radio sky has been in progress at the Ohio State University for the past five years. Surveys previous to the one described in this dissertation have been conducted almost exclusively at 1415 MHz, and have been of more limited extent. This dissertation describes the instrumentation and procedures used to operate the radio telescope at three frequencies simultaneously, gives a listing and maps of the results of the survey, and shows comparisons to results obtained at other observatories for evaluating the accuracy of the results. The survey covers about 4,000 square degrees of sky between the declinations mentioned in the title, and lists 2,101 radio sources whose 1415-MHz flux densities were measured as being above 0.2 flux units. Peak flux densities at 612 MHz are also given for about 1200 of these sources and 2650-MHz peak flux densities are given for 115 sources whose flux densities were found to be above 0.6 f.u. Spectral indices are given for the sources measured at 612 MHz, and some three point spectra are shown for the previously uncataloged sources detected at 2650 MHz. (Diss. Abstr. Int., B)

2856 LABORATORY MODEL FOR RADIO STAR SCINTILLATION AND OTHER DIFFRACTION PHENOMENA. Morgan II, Millett Granger. San Diego, La Jolla, Calif.; Univ. of California (1969). 102p. University Microfilms Order No. 70-8844.

Thesis.

The diffraction of a radio star signal by a thin, weak, random-phase-changing screen, such as the Earth's ionosphere or the solar wind, was modeled in the laboratory using 40-khz airborne ultrasound and a diffracting screen of warm turbulent air. Initial measurements by Bartusek and Felgate had suggested that such modeling might prove a useful tool for exploring the techniques of signal processing necessary in the digital processing of such data and, in addition, might allow the empirical exploration of some diffraction geometries. Specifically, it was hoped that such a modeling experiment would assist in the interpretation of data gathered on a large solar wind–radio star scintillation system now nearing completion at UCSD. (TSS) (Diss. Abstr. Int., B)

Solar Phenomena

Refer also to abstract 2998.

2857 (AD-707256) PHOTOSPHERIC AND CHROMOSPHERIC MAGNETIC FIELDS AND THE BRIGHTNESS OF FACULAE AND FLOCCULI. Tsap, T. T. Translated for Air Force Cambridge Research Labs., L. G. Hanscom Field, Mass., from Izv. Krym. Astrofiz. Observ.; 39: 265-75(1969). 20p. (AFCRL-70-214; AFCRL-Trans-75). NTIS.

Photospheric and chromospheric longitudinal magnetic fields and the brightness of faculae and flocculi were compared. The relation between the brightness distributions at different depths in active regions on the Sun was investigated. The following results were obtained: (1) There is a close relation between the position of faculae observed in the light of the lines 5250 and 6102.7 Å and flocculi observed in K3Ca (+) lines and the Hα nucleus, as well as the position of the photospheric and chromospheric magnetic fields; (2) the correlation factors between the brightnesses of flocculi in the K3 line and the Hα nucleus are roughly identical with both photospheric and chromospheric fields; (3) the course of the brightness change in the case of a section through an active region in the lines 5250, 6102.7, K3, and the Hα nucleus is approximately equal, although there sometimes are small deviations. The results obtained agree well with the fact that the distributions of the magnetic field in the photosphere and chromosphere are close. (Severnyi, 1966 and 1960). (auth) (USGRDR)

2858 (N-70-32003) SOLAR INDICES FOR THE PERIOD JANUARY 1, 1955–DECEMBER 31, 1969. Euler, H. C. (National Aeronautics and Space Administration, Huntsville, Ala. George C. Marshall Space Flight Center). 8 Jun 1970. 548p. (NASA-TM-X-64526). NTIS.

The solar–geomagnetic indices listed may be used for model atmosphere studies. These tables contain daily sunspot number, solar 10.7-cm flux, and the daily geomagnetic A_p index. Also included are the three-hourly K_p and a_p indices and 27-, 54-, and 81-day running means of sunspot numbers and solar flux. (auth) (STAR)

2859 GEOPHYSICAL ACTIVITY OF SOLAR FLARES AS A FUNCTION OF THE BRIGHTNESS OF EMISSION OF METALS IN THEM. Odintsova, I. N.; Shilova, N. S. (Inst. of Terrestrial Magnetism, Ionosphere, and Radio Wave Propagation, Moscow). Geomagn. Aeron. (USSR) (Engl. Transl.); 10: 251-3(1970).

Translated from Geomagn. Aeron.; 10: 326-7(1970).

The geophysical activity of flares is investigated as a function of the emission intensity of the metal lines in them. The degree to which the emission of metals in a flare is enhanced, compared with emission in the undisturbed chromosphere, is known to differ in different flares. Some moderate- and low-intensity lines in the spectrum of the chromosphere that were examined are Mgb_1, Mgb_2; 5889.9, 5995.9, 4395.0, 4300.0 A Ti II; 4294.1, 4383.5, 4282.4 A Fe I; 4296.6, 4385.4, 4304.2, 3938.3 A Fe II. Flares occurring between 1956 and 1963 were analyzed, using only flares on the solar disc, because a flare on the limb may be part of another more intense flare next to it on the other side of the limb and the effects of these would be superposed. It is concluded that the spectrum of geophysically active ionizing radiation (affecting various layers of the ionosphere) from a flare of a given intensity becomes broader as the intensity of the emission of the metal lines in it increases. Thus, flares accompanied by strong metal emissions apparently originate in the lower layers of the solar atmosphere and are most active geophysically. (J.C.W.)

2860 DEPENDENCE OF GEOMAGNETIC ACTIVITY ON THE POLARITY OF THE INTERPLANETARY MAGNETIC FIELD. Hruska, A.; Hruskova, J.; Jacobs, J. A. (Univ. of Alberta, Edmonton). Can. J. Phys.; 48: 2447-50(15 Oct 1970).

Geomagnetic activity measured by the Kp index varies with the angle α between the Earth–Sun vector and the vector of the interplanetary magnetic field. The effect is due to the change in magnitude and in fluctuations of the magnetic field with α. (auth) (Canada)

2861 SOLAR NEUTRON FLUX IN THE ENERGY RANGE 20 TO 160 MeV. Kim, C. Y. (Univ. of Calgary, Alberta). Can. J. Phys.; 48: 2155-61(15 Sep 1970).

An attempt to measure the flux of high-energy solar neutrons was made by measuring the difference in flux from the direction of the Sun and from the symmetrical direction about the zenith, using oriented nuclear emulsions flown by balloon on July 30, 1966 from Fort Churchill, Manitoba. An excess of $(2.2 \pm 2.5) \times 10^{-2}$ neutrons cm^{-2} s^{-1} was observed from the direction of the Sun in the energy region of 20 to 160 MeV. On the day of the flight the sunspot number was 63, and no major solar flares were reported. (auth) (Canada)

2862 MASS MOTIONS IN SOLAR FLARES AND RELATED PHENOMENA. Proceedings of the Ninth Nobel Symposium Held June 10–12, 1968, in Anacapri, Italy. Oehman, Yngve (ed.). Nobel Symposium 9. New York; John Wiley and Sons, Inc. (1968). 245p. $22.00. (CONF-680671).

This volume contains all the papers presented at the symposium. It also contains the discussions following each paper, a list of the participants, a discussion on the topic of the symposium, and a summary of the symposium. The papers dealt with the following topics: mass motions in flares indicated by line profiles and filtergrams; mass motion in flares and moustaches indicated by special features; mass motion in loops, sprays, surges, etc.; theoretical aspects of flare related mass motions; and associated phenomena on stars. (Meteorological and Geophysical Abstracts)

2863 ASYMMETRY OF MOUSTACHES. Koval, A. N.; Severny, A. B. (Crimean Astrophysical Observatory, USSR). Solar Phys.; 11: 276-84(Feb 1970).

A careful photometry of moustaches is carried out to reveal asymmetry of their emission in the far wings ($\Delta\lambda \geq 1$ Å), if it exists. The presence of background continuous emission in spectra of moustaches demands special care with the photometry, and makes the current method of comparison of rest-intensities inadequate. The other sources of errors are also discussed. The blue asymmetry, as a systematic difference of intensities between the blue and the red wing shows itself in some cases, being 2 to 3 times larger than the probable errors. In most moustaches investigated, the accompanying background continuous emission shows a rapid increase to the violet. (auth)

Galaxies

2864 SIMULATION OF THE EVOLUTION OF STELLAR SYSTEMS. Hohl, Frank (Langley Research Center, Hampton, Va.). Simulation; 15: 131-40(Sep 1970).

Computer models for isolated disk galaxies and for infinite doubly periodic stellar systems are used to study the self-consistent motion of large numbers of interacting stars as they move in the plane of the galactic disk. The doubly periodic model is used to investigate the development of the gravitational instability for a plane stellar system. The results obtained show that the initial condensations that form are about two Jeans lengths in diameter. An isolated, initially cold, balanced disk is found to be violently unstable. Adding a sufficient amount of velocity dispersion will stabilize all small-scale disturbances. Most disks investigated are found to be unstable against slowly growing long-wavelength modes, and after about two rotations the disks tend to assume a bar-shaped structure. It is also found that the final mass distribution for most disks can be closely approximated by an exponential variation irrespective of the initial mass distribution. (auth)

2865 SPECTRAL OBSERVATIONS OF MARKARYAN GALAXIES WITH ULTRAVIOLET CONTINUUM. PART I. Weedman, D. W.; Khachikyan, E. E. (Univ. of Texas, Austin). Astrophysics (Engl. Transl.); 4: 243-51(1968).

Translated from Astrofizika; 4: 587-93(1968).

Preliminary results of spectral observations of 17 galaxies from the Markaryan list, which are characterized by strong ultraviolet continua, are reported. The observations were carried out on the 200, 84, 82, and 36" telescopes at the Mount Palomar, Kitt Peak, MacDonald, and Lick Observatories using high dispersions. The observations show that, with rare exceptions, the spectra of these galaxies contain emission lines but differ quite considerably from each other in the nature of these lines. Two of the galaxies were found to be of the Seyfert-type. The UBV data for some of the nuclei of Markaryan galaxies are also presented. (auth)

2866 MODEL OF THE MASS DISTRIBUTION IN M 31. PART I. Sizikov, V. S. (Leningrad State Univ.). Astrophysics (Engl. Transl.); 4: 266-9(1968).

Translated from Astrofizika; 4: 634-42(1968).

Solutions are reported for integral equations relating the angular velocity in the plane of symmetry and the surface brightness, on the one hand, and the mass distribution and luminosity on the other, in the nonmodel homogeneous nonsimilar spheroid in which the surfaces of constant mass density and constant luminosity are coinciding spheroids with variable sphericity. (auth)

2867 SOME PROPERTIES OF RADIO GALAXIES. Vardanyan, R. A.; Melik-Alaverdyan, Yu. K. (Byurakan Astrophysical Observatory, Erevan). Astrophysics (Engl. Transl.); 4: 278-9(1968).

Translated from Astrofizika; 4: 655-7(1968).

This note is concerned with the dependence of the properties of radio-emitting clouds on their distance from the nucleus of a radio galaxy that is genetically related to them. (W.D.M.)

2868 OBSERVATIONAL UPPER LIMITS TO THE ELECTROMAGNETIC ENERGY RADIATED BY NORMAL GALAXIES. Harwit, M. O. (Astronomical Inst., Prague); Houck, J. R.; Wagner, R. V. Nature (London); 228: 451-2(31 Oct 1970).

It has been suggested that typical galaxies emit energies of the order of their present rest-mass energies during their lifetime of $\sim 10^{10}$ yr, and the observations on which this theory is based indicate that the flux peaks sharply at $\sim 70\,\mu$. The constraints that can be placed on such models from observations of the isotropic background radiation at this and longer wavelengths are indicated. It is shown that the present upper limits on the flux still allow most of the energy emitted by galaxies to be in the infrared region. In order to interpret the meaning of the background radiation measurements, it is assumed that the galactic emission is confined to a narrow range of emitted wavelengths. Low's model is discussed, together with relevant observations, none of which is inconsistent with the expected large-scale isotropy. Maximum energies radiated by galaxies emitting at 70 to 2000 μ are tabulated. The results are consistent with Low's model in strongly evolutionary cosmologies, but this model is ruled out in steady-state cosmology. Although the upper limits indicated are not very restrictive, more sensitive broad-based background measurements, especially at $\sim 200\,\mu$, might be interesting. (UK)

Cosmology

Refer also to abstracts 3343 and 3423.

2869 (CSIRO-Trans-10207) BACKGROUND RADIATION OF THE UNIVERSE AND DIFFICULTIES WITH LEMAITRE's COSMOLOGICAL MODEL WITH A PLATEAU AT Z = 1.95. Syunyaev, R. S. Translated by M. A. Hintze (Commonwealth Scientific and Industrial Research Organization, Melbourne, Australia), from Astron, Tsirk.; No. 465, 1-5(Mar 1968). 7p. Dep. NTIS (U. S. Sales Only).

Evaluations of the density of intergalactic gas and of matter concentrated in galaxies are reviewed with respect to the Lemaitre model. Aggregated data on background radiation of the metagalaxy appears to contradict this model for plateau at Z = 1.95. (Australia)

2870 RELATIVISTIC GENERALIZED THEORY OF GRAVITATION. I. Saakyan, G. S.; Mnatsakanyan, M. A. (Erevan State Univ.). Astrophysics (Engl. Transl.); 4: 234-9(1968).

Translated from Astrofizika; 4: 567-79(1968).

The relativistic variant of the generalized theory of gravitation is discussed. The conservation laws are formulated, and a derivation is given of the field equations for the internal region of a spherically symmetric distribution of masses. The external solution, which is used as the condition on the surface of the configuration, is given. Models are developed for massive superdense static configurations with a very high mass defect and a gravitational red shift. (auth)

2871 CLASSICAL AND RELATIVISTIC FORCES OF INERTIA. Horak, Z. (Technical Univ., Prague). Czech. J. Phys.; B20: 1194-1208(1970).

It is shown that, in contrast to the classical physics and special relativity, the self-consistency of general relativity requires that the forces of inertia follow unambiguously from the field equations as inductive gravitational effects of the cosmic matter and that this requirement is perfectly satisfied, without supplementary hypotheses, for the Einstein universe, in full agreement with Mach's principle. (auth)

2872 STUDY OF THE GENERAL-RELATIVISTIC DYNAMICS OF THE KLEIN–ALFVEN COSMOLOGY. Moritz, Barry Kyler. College Park, Md.; Univ. of Maryland (1969). 162p. University Microfilms Order No. 70-10,291.

Thesis.

There has been, of late, considerable interest in a cosmology

involving matter–antimatter symmetry. One such cosmology known as the Klein–Alfven Cosmology, has previously been examined in the Euclidean approximation and in the general-relativistic static case. However, the Euclidean calculation has been shown invalid by the static one, and neither calculation accurately considers the effects of the relativistic decay products from proton–antiproton annihilation. In this thesis, the dynamic equations for this cosmology are derived, and the relevant cross sections and energy momentum transfer are determined in the general relativistic magnetohydrodynamic scheme. These equations were programmed for high-speed digital computers in certain simplified approximations. The results indicate that the Klein–Alfven Cosmology cannot explain the observed matter content of at least 10^{54} grams, as the contracting ambiplasma will not re-expand for masses of this order. The actual magnitude of the electron–positron annihilation cross section is re-examined and shown to be of critical importance in this cosmological model, as the radiative recombination process, which had previously been ignored, is much more efficient than the direct interaction. Although the nucleon annihilation rate is enhanced, the lepton rate goes up even faster, resulting in a decrease in the net radiation forces contributing to a turnaround. It is noted that, in these calculations, the separation mechanisms described by Alfven were ignored. However, the derived analytic equations contain all the information required for an almost arbitrarily complicated calculation, effectively limited by calculator size, speed, and the ingenuity of the programmer. (Diss. Abstr. Int., B)

2873 TRANSPORT COEFFICIENTS OF A RELATIVISTIC QUANTUM GAS. Israel, W.; Vardalas, J. N. (Univ. of Alberta, Edmonton). Lett. Nuovo Cim.; 4: 887-92(7 Nov 1970).

Transport phenomena in relativistic fluids are currently of great interest in connection with the study of conditions in neutron stars and the early history of the big bang. Integrations of the linearized Boltzmann collision equation for a classical relativistic gas have recently been carried out by several authors. Unfortunately, there seems to be little concensus about the correct expressions for the transport coefficients. A brief report is given on some results for a simple, self-gravitating quantum gas of neutral particles undergoing elastic binary collisions. (W.D.M.)

2874 PROPAGATION OF COSMIC RAYS IN THE NEUTRINO SEA. I. PROTONS IN COSMIC RADIATION. Rekalo, M. P. (Physical-Technical Inst., Kharkov). Ukr. Fiz. Zh.; 15: 923-31(Jun 1970). (In Russian).

It is shown that the energy spectrum of superhigh-energy protons in cosmic rays is very sensitive to the Fermi energy of the degenerate neutrino gas filling the Universe. The upper limit of the Fermi energy k_F of the neutrino in the Universe is equal to $k_F = 10^{-1}$ eV. This value is found in the assumption that energy dependence of the total cross section of the neutrino–proton interaction may be extrapolated in the high-energy region. This estimation is valid for neutrinos of all four kinds. Maximal energy of the protons for which the Universe is opaque is found for different cosmological models. (auth)

2875 PROPAGATION OF COSMIC RAYS IN THE NEUTRINO SEA. II. ELECTRONS AND NEUTRINOS IN COSMIC RADIATION. Rekalo, M. P. (Physical-Technical Inst., Kharkov). Ukr. Fiz. Zh.; 15: 932-40(Jun 1970). (In Russian).

An effect of the neutrino filling the Universe on the penetration of the high-energy cosmic electrons and neutrinos was investigated. The penetration of the electrons in the Universe is determined by the combined effects of the photons and neutrinos that are present in the Universe. The Universe is opaque for electrons of any high energy if $k_F \geq 6.3 \times 10^{-2}$ eV; the Universe is transparent for electrons in the energy interval 5×10^{20} eV $\leq E \leq 8 \times 10^{23}$ eV, if $k_F = 10^{-2}$ eV. Maximal energy of cosmic neutrinos is determined by the Fermi energy of the degenerate neutrino sea; for example, for $k_F = 10^{-3}$ eV, the Universe is transparent for neutrino energies less than 7×10^{27} eV. The influence was also studied of the highest-order weak interactions and six-fermion interaction on the penetration of the superhigh-energy cosmic rays. (auth)

2876 ANISOTROPY AND INHOMOGENEITY IN THE COSMIC BACKGROUND RADIATION. Conklin, Edward Kirkham. Stanford, Calif.; Stanford Univ. (1969). 138p. University Microfilms Order No. 70-10,443.

Thesis.

Homogeneity measurements were made at 10,690 MHz. The primary antenna beamwidth was 13 minutes of arc, and repeatedly scanned a strip of sky from 10 h to 22 h right ascension at declination +40.6°. After 36 scans, the rms fluctuation in antenna temperature in this region was 5.6 mK. By allowing for internal receiver noise and antenna efficiency, and considering the antenna as a spatial smoothing filter, upper limits to the rms intrinsic fluctuations in the background were derived. In most world models, these fluctuation limits require a density of point sources much greater than galaxies to explain the radiation, so that the alternate "primordial fireball" interpretation appears correct. Then the limits show that clusters of galaxies in the process of formation may be observable, that small-scale density fluctuations are lower than expected, and that intergalactic gravitational radiation has a very low mass density. Anisotropy measurements were made at 8000 MHz with an angular resolution of 15°. The input to a sensitive radiometer was switched between two antennas so that the system measured the temperature difference between points 5 h apart in right ascension over the entire small circle $\delta = +32°$. Observations were made at 3800 m altitude, as sea-level atmospheric fluctuations limited system sensitivity. After averaging about 25 complete runs, the rms deviation for a 30-minute period of right ascension was ~1.5 mK. Following removal of unwanted, mostly nonthermal radiation sources from the data, Fourier analysis of the remainder shows dipole and quadrupole anisotropies of 1.93 ± 0.58 and 1.14 ± 0.50 mK respectively. The strength of smaller scale anisotropies is ≤1.5 mK. The Earth's peculiar velocity, v, is related to the dipole anisotropy by $T' \cong T[1 + (v/c) \cos \theta]$, where T' is the temperature seen at look angle θ, and T is the isotropic temperature seen by a fixed observer. The anisotropy above implies $v = 255 \pm 76$ km/sec in the celestial equatorial plane, agreeing with estimates of peculiar motion in the local supercluster of galaxies. Mach's principle and Hubble's linear expansion law are thereby verified, and vorticity in the Universe, if present, is extremely small. The low value for the quadrupole anisotropy implies nearly isotropic expansion of a closed Universe, although viscosity may have reduced the anisotropy. If space is open, definite statements about expansion are not possible due to the restricted survey area. Smaller-scale anisotropy limits allow a maximum density fluctuation of ~10% over a linear scale of ~500 Mpc. An expected background temperature fluctuation of ~½% due to a quasar cluster was not seen, indicating either that the clustering is only apparent or that quasars are not as massive as supposed. (TSS)

2877 METHOD TO CALCULATE GRAVITATIONAL WAVES. Yadav, Basudeo P. Progr. Theor. Phys. (Kyoto); 44: 555-7(Aug 1970).

A method for calculating gravitational waves in the vicinity of wave fronts was investigated, giving a powerful formalism for successive calculations of gravitational wave fronts. Approximate calculations for thin sandwich waves are also obtained. (W.D.M.)

Planetary Phenomena

2878 SOLAR WIND FLOW PAST NONMAGNETIC PLANETS: VENUS AND MARS. Spreiter, John R. (Stanford Univ., Calif.); Summers, Audrey L.; Rizzi, Arthur W. Planet. Space Sci.; 18: 1281-99(Sep 1970).

The hydromagnetic theory of solar wind flow past the Earth is extended and modified so as to be applicable to nonmagnetic planets, such as Venus and Mars, that have a sufficient ionosphere to deflect the solar plasma around the planet and its atmosphere. The principal difference in the analysis stems from the fact that the current sheath that bounds the solar wind away from the planet is formed by interaction with the ionosphere rather than with the geomagnetic field as in the case of the Earth. After stating the principal assumptions and equations, the theory is applied to determine the shape of the ionosphere boundary, or ionopause, across which the Newtonian approximation for the pressure of the flowing plasma is balanced by the pressure of a stationary ionosphere. Specific numerical results are given for a wide range of ionospheric parameters representative of those proposed for Venus and Mars. The location of the bow wave and the properties of the flow field are then calculated using magnetohydrodynamic and gasdynamic considerations in a manner similar to that employed for the flow of the solar wind plasma past the Earth's magnetosphere. Examination of the results reveals a correspondence rule that enables results presently available for the location of the bow wave and the properties of the flow about the Earth's magnetosphere to be converted rapidly into those for a nonmagnetic planet by a simple relabeling of the scales. The results are shown to be in general accordance with observations made by Mariner 5 as it flew past Venus, although certain differences near the theoretical location of the ionopause suggest the presence of a thick boundary layer. A similar analysis of the data from Mariners 4, 6, and 7 indicates that Mars has a sufficient ionosphere for the theory to be applicable. Further comparison is relatively uninformative beyond revealing no inconsistencies with the theoretical results, however, because Mariner 4 did not approach close enough, and Mariners 6 and 7 were not equipped to make the necessary measurements. (auth) (UK)

XUM

2879 VERY-LONG-BASELINE INTERFEROMETRY OF DECAMETRIC RADIATION FROM JUPITER. Stannard, Kent M.; Dulk, George A.; Rayhrer, Benno (Univ. of Colorado, Boulder). Radio Sci.; 5: 1271-80(Oct 1970).

Very-long-baseline Michelson interferometry measurements were made on Io-related radio emissions from the planet Jupiter at 34 MHz. The data include a single baseline observation made on December 1, 1968, between the Arecibo Ionospheric Observatory and Boulder, Colorado (436,000 λ), and a three-station observation made on April 27, 1969, between the University of Maryland Radio Observatory in California, the University of Texas Radio Astronomy Observatory in Texas, and Boulder, Colorado (typically 100,000 λ). Frequency analysis of the cross-correlated signals shows that there is a tendency toward lower observed fringe rates than had been calculated. If the results are interpreted entirely in terms of source motion, the data imply a velocity near 200 km sec eastward. The phase fluctuations in the cross-correlated signals are attributed to interplanetary scintillation; however, source motion effects cannot be distinguished from scintillation. The implied rms phase variations at the scintillation screen are 0.7 radian at an elongation of 65° (December 1, 1967) and 0.3 radian at an elongation of 145° (April 27, 1969). (auth)

2880 VERY-LONG-BASELINE INTERFEROMETRY OF JUPITER AT 18 MHz. Carr, T. D. (Univ. of Florida, Gainesville); Lynch, M. A.; Paul, M. P.; (and others). Radio Sci.; 5: 1223-6(Oct 1970).

Very-long-baseline interferometry (VLBI) observations of the decametric bursts from Jupiter were initiated by the University of Florida in 1964, with a tape-recording intensity interferometry operating at 18 MHz over a baseline of 55 km. This was apparently the first VLBI. Since the source was unresolved, subsequent observations were made with progressively longer baselines. The longest baseline is 7900 km (between Kentucky and Chile). Preliminary results indicate that, if the S-burst sources are incoherent, at least some of them must be smaller than 0.1″ of arc. (auth)

2881 ISOTOPIC ANALYSIS OF MOON SOIL AND ROCKS. Subotowicz, Mieczyslaw. Postepy Fiz.; 21: 499-509(1970). (In Polish).

The main scientific problems of the investigation of the Moon in the Apollo program are discussed. The mineralogical and chemical composition of the Moon surface layer is presented. Rare gases are contained in the Moon breccia and fines and were transported in the solar wind. Using well-known methods of geological dating (K–Ar, Rb–Sr, U–Pb, and Th–Pb) the age of the Moon rocks was determined (3.8 to 4.7×10^9y). An analysis was made of the different isotope radioactivities induced by the interaction of primary cosmic rays with the Moon soil and rocks. The results of these radioactivity measurements are given. The data on the origin and history of cosmic rays and the history of the Moon surface layer were analyzed. There is a discussion of the influence of the possible Moon capture (Gerstenkorn theory) on the Pb-isotopic composition measured in some surface rocks on the Earth. The very destructive tidal effects during Moon capture and its approach up to the Roche limit were accompanied by local heating of the Earth crust, its possible melting and lava flow from the upper mantle of the Earth. This process is identified with the geological anorthosite event. For the time occurrence of these processes the age ($1.28 \pm 0.20 \times 10^9$y) was found from the Pb-isotopic composition analysis, a value identical with the geological dating of the anorthosite event: ($1.30 \pm 0.20 \times 10^9$y). (auth)

Atomic and Molecular Physics

Atomic, Electron, Ion, and Molecular Beams and Their Reactions

Refer also to abstracts 3111, 3188, 3465, and 3472.

2882 (CONF-700322–, pp 113-24) CHARGED PARTICLE EXCITED X RAYS. Spaulding, J. D. (Pacific Union Coll., Angwin, Calif.).

From Proceedings of the second Oak Ridge conference on the use of small accelerators for teaching and research, March 23–25, 1970.

Low-voltage accelerators are used to produce characteristic x rays by positive ion bombardment of metallic and nonmetallic samples. The x rays are measured with an ORTEC high-resolution Si (Li) x-ray system. Yields of photons per incident proton are tabulated for some of the samples. (auth)

2883 (N–70–25499) TRANSMISSION AND BACKSCATTER COEFFICIENTS OF 1.0 TO 3.0-MeV ELECTRONS INCIDENT ON SOME METALS AND ALLOYS. Miller, William E. (National Aeronautics and Space Administration, Langley Station, Va. Langley Research Center). Apr 1970. 31p. (NASA-TN-D–5724; L–6776). NTIS.

The transmission and backscatter coefficients of aluminum, titanium, vanadium, copper, gold, and the alloys Ti–6Al–4V and 50% copper–50% gold were determined experimentally for normally incident electrons of 1.0 to 3.0 MeV. From the transmission measurements, the extrapolated range of electrons as a function of energy was determined for each material. Analysis showed that the extrapolated range and maximum backscatter of electrons in an alloy can be calculated to within a few percent from the range and backscatter of electrons in the constituent elements. (auth)

2884 (NP–18490) SOME PHENOMENA PRODUCED BY POSITIVE ION BOMBARDMENT OF METAL SURFACES AT MEDIUM ENERGIES. Cawthron, E. R. (Australian National Univ., Canberra. Research School of Physical Sciences). Dec 1969. 163p. Dep. NTIS (U. S. Sales Only).

Thesis.

Secondary electron emission coefficients, apparent total ion scattering, and energy distributions of secondary electrons and scattered ions resulting from bombardment of polycrystalline and semicrystalline surfaces by ions of 5 to 50 keV were studied. Target materials were Ni, Mo, Ta, Pt, and reactor-grade graphite. Ions included H^+, H_2^+, H_3^+, D^+, D_2^+, D_3^+, He^+, C^+, N^+, N_2^+, O^+, O_2^+, Ne^+, Ar^+, and CO_2^+. The effects of incident-ion velocity, the atomic numbers of both incident ions and target materials, and angle of incidence of the ion on the emission and scattering processes were measured. A review of the theoretical basis of the work detailed descriptions of the apparatus used, and numerous tables and graphs of data are included. (A.G.W.)

2885 OBSERVED RADIATION FROM SURFACE PLASMONS IN ALUMINUM. Braundmeier, A. J. Jr.; Arakawa, E. T. (Oak Ridge National Lab., Tenn.). Z. Phys.; 239: 337–42 (1970).

Plasma radiation from thin films of aluminum bombarded by non-normally incident 80-keV electrons was investigated. Radiative decay of both volume plasmons and surface plasmons was observed with the surface plasmon radiation being very sensitive to contamination of the film surface by an oxide layer. The surface resonance occurs at 10.2 eV, whereas the volume resonance is at 15 eV. These values are in accord with electron energy-loss experiments. (auth)

2886 ELECTRON BACKSCATTER MEASUREMENTS FOR PERPENDICULAR AND NON-PERPENDICULAR INCIDENCE AT 1.0 MeV BOMBARDING ENERGY. Rester, D. H. (Ling-Temco Vought, Inc., Dallas); Derrickson, J. H. Nucl. Instrum. Methods; 86: 261-7(1970).

Total energy spectra of backscattered electrons for 1.0-MeV electrons with perpendicular incidence on targets of saturation thicknesses of Al, Fe, Sn, and Au are shown. The variation of the shape of the energy distributions with angle observed for Al and Fe is illustrated. Total backscatter coefficients of 0.08, 0.22, 0.37, and 0.51 were obtained for Al, Fe, Sn, and Au. Mapping of electrons backscattered from a saturation thickness of Al for an angle of incidence of 30° from the target plane was also carried out at 1.0 MeV. Angular distributions as a function of two angles and typical energy distributions are included. (auth)

2887 ALUMINIUM OXIDE FILMS PRODUCED BY A TWO STEP PROCESS AND ALPHA STOPPING POWER STUDIES. Mai, Trinh Thi Hoang; Drouin, R. (Univ. Laval, Quebec). Nucl. Instrum. Methods; 87: 297-8(1970).

A rapid method has been applied to fabricate self-supporting aluminium oxide films, and alpha stopping power studies have been made for films of different thicknesses and for alpha energies of 5.477, 6.617 and 8.786 MeV. The experimental results are in fair agreement with theoretical predictions and atomic additive rule on stopping powers. (auth)

Atomic and Molecular Properties

2888 (CONF-700322–, pp 281-8) MEASUREMENT OF ATOMIC LIFETIMES. Bashkin, S. (Arizona Univ., Tucson. Dept. of Physics).

From Proceedings of the second Oak Ridge conference on the use of small accelerators for teaching and research, March 23–25, 1970.

The application of beam–foil spectroscopy to the measurement of level lifetimes in monatomic systems is discussed. The use of these lifetimes in connection with the determination of element abundances in stars is treated in some detail. The proposed ex-

XUM

periment on the lifetimes of Stark levels is described. 25 references. (auth)

2889 (CONF-700322–, pp 289-95) ATOMIC PHYSICS OF FAST ION BEAMS: FINE STRUCTURE EXPERIMENTS. Sellin, I. A. (Oak Ridge National Lab., Tenn.).

From Proceedings of the second Oak Ridge conference on the use of small accelerators for teaching and research, March 23–25, 1970.

Methods for determination of fine structure level intervals, level metastability, and similar properties of ions not presently measurable by resonance techniques are discussed. One-, two-, and three-electron systems are treated as examples. (auth)

2890 EXCITATION OF IONIZED HELIUM STATES IN A COOLED HOLLOW-CATHODE DISCHARGE. Berry, H. G.; Roesler, F. L. (Univ. of Wisconsin, Madison). Phys. Rev., A; 1: 1504-17(May 1970).

A high-resolution study of the He II λ4686 Å (n = 3–4) line complex emitted from a cooled hollow cathode was made using a double-etalon spectrometer with photoelectric detection. Computer analysis of the digitally recorded spectra of this line yields fine-structure and isotope-shift measurements for the isotopes ^{3}He and ^{4}He, which agree with quantum electrodynamic theory to within ±0.0005 cm^{-1} for the best measured components. The excitation and de-excitation processes for this transition, which are active in the hollow-cathode, were analyzed. The results show that the anomalously large widths observed in ionized helium lines that have been electronically excited arise from large momentum transfers in the excitation process. Calculation of the momentum-transfer line profile in the process $He + e \rightarrow He^{+*} + e + e$ gives reasonable agreement with the observed profiles when the instrumental profile and neutral He Doppler profile are included. Measurements further confirm that the origin of the small anode-drift shift is a residual electric field within the discharge. (auth)

2891 HYPERFINE STRUCTURE AND STARK EFFECT INVESTIGATIONS OF THE STATES 4d5s5pz$^2F_{\frac{9}{2}}$ AND z$^2F_{\frac{9}{2}}$ IN THE YTTRIUM I SPECTRUM. Beer, H. (Technische Univ., Berlin). Z. Phys.; 239: 351-9(1970). (In German).

The hyperfine structure and the Stark effect shift of the 4d5s5pz$^2F_{\frac{9}{2},\frac{7}{2}}$ states in the Y I spectrum were investigated by level-crossing techniques. Between the Zeeman-effect region and the Paschen–Back region of hyperfine structure states some of the levels cross. The resonance radiation of these coherently excited levels shows an interference effect of the scattering amplitudes in the crossing region. The level-crossing signals give information about hfs splitting and lifetime of the excited states under investigation. The magnetic hfs splitting factors A of the 4d5s5pz$^2F_{\frac{9}{2},\frac{7}{2}}$ states and their lifetimes were determined. With an electric field parallel to the magnetic field a shift of the level-crossing signals of the 4d5s5pz$^2F_{\frac{9}{2},\frac{7}{2}}$ states was observed, and the Stark constants β were deduced. (auth)

2892 LAST RESOLVED LINE IN THE BALMER SERIES. Kurochka, L. N. (Univ., Kiev). Astrophysics (Engl. Transl.); 4: 240-2(1968).

Translated from Astrofizika; 4: 581-6(1968).

The number of the last resolved line in the Balmer series is given as a function of the electron concentration for the case where the line is broadened by the combined action of Stark and Doppler effects. (auth)

2893 HYPERFINE STRUCTURE ANOMALY OF ^{241}Pu AND ^{239}Pu AND THE NUCLEAR MOMENT OF ^{241}Pu. Edelstein, N. (Univ. of California, Berkeley). Phys. Lett.; 33A: 233-4 (2 Nov 1970).

The hfs anomaly of an s electron for the ^{241,239}Pu isotopes is shown to be $^{241}\Delta^{239} = -6.3 \pm 0.2\%$. The value for $\mu_N(^{241}Pu)$ is found to be -0.718 ± 0.017 nm. (auth)

2894 POSSIBILITY OF INDUCED AMPLIFICATION OF CHARACTERISTIC X RADIATION. Stankevich, Yu. L. Dokl. Akad. Nauk SSSR; 191: 805-6(1 Apr 1970). (In Russian).

The rapid growth in photoionization cross sections of internal electron shells of atoms with a decrease in the principal quantum number can be used to create an inverse population of internal shells. In principle it is possible to observe induced amplification of characteristic x radiation during pumping with x radiation. The life time of the inverse state should not exceed the life time of vacancies in the isolated atom. It is possible to obtain a quasi-stationary inverse population with multiple use of each atom. A condition of maintaining a quasi-stationary inverse population of two internal electron levels of an atom is that the total probability of the transition of a vacancy from a lower level A to an upper level B be less than the probability of filling a vacancy at level B from higher-lying levels. Available data indicate that this condition is fulfilled for vacancy transitions $1s_{\frac{1}{2}} \rightarrow 2p_{\frac{1}{2}}$($K_{\alpha 2}$ line) in elements with Z < 47 and $1s_{\frac{1}{2}} \rightarrow 2p$ ($K_{\alpha 1}$ line) at Z < 36. The favorable ratio of level widths in this region of Z values is due mainly to radiationless transitions of vacancies from the $2p_{\frac{1}{2}}$ and $2p_{\frac{3}{2}}$ levels. Maintenance of a stationary inverse state is possible in a range of temperatures at which the probability of radiationless recombination into valence levels is not less than the probability of vacancy transition between the levels being used. An estimate indicates that the inverse state can be maintained up to temperatures of 30 to 100 eV. The cross sections of induced radiation of the $K_{\alpha 1,2}$ lines are estimated. A comparison of the cross sections of induced radiation with the cross sections of resonance absorption of photons shows that amplification is possible if 2 to 3×10^{-3} of the total number of atoms are in an excited state at the same time. (TTT)

2895 APPROXIMATION IN SCATTERING THEORY. McCavert, P.; Rudge, M. R. H. (Queen's Univ., Belfast). J. Phys., B (London); 3: 1286-99(Oct 1970).

An approximation, based on what is termed regional trial functions, is used to calculate excitation cross sections between some optically connected states of hydrogen and of lithium, sodium, and potassium. The cross sections obtained in this approximation, which is simpler than the Born–Oppenheimer approximation, are compared with other theoretical and with experimental results. On the basis of this comparison it is suggested that the wave functions on which the calculation is based may form an acceptable first approximation in a more detailed variational treatment. (auth) (UK)

Positronium, Muonium, and Mesic Atoms and Molecules

2896 4f → 3d PIONIC TRANSITION IN ^{138}Ba, ^{140}Ce, AND ^{142}Ce. Jenkins, D. A. (Virginia Polytechnic Inst., Blacksburg, Va.); Powers, R. J.; Kunselman, A. R. Phys. Rev., C; 2: 429-34(Aug 1970).

The 4f → 3d pionic x rays in ^{138}Ba, ^{140}Ce, and ^{142}Ce were observed in order to measure the effect of the nuclear interaction on a pion in a 3d atomic level. The results are used to look for differences in the pion interaction with these nuclei. Within experimental error, no isotope shift in the ^{142}Ce-^{140}Ce results could be detected. The nuclear isotone shift in the x-ray energy and width for ^{140}Ce-^{138}Ba of 1.59 ± 0.30 and 1.3 ± 1.3 keV agrees with the values of 1.31 and 2.0 keV predicted from an optical-model calculation. (auth)

2897 PHENOMENOLOGICAL APPROACH FOR A π^- MESON NUCLEUS POTENTIAL. Blum, B. (Univ., Frankfurt am Main. Univ., Erlangen-Nuernberg, Ger.). Nucl. Phys.; B23: 155-67 (1970).

The observed level shifts and widths of π-mesic atoms are described in terms of an optical potential between the pion and the nucleus. A special form of this potential is proposed: herein the microscopic picture of the scattering and absorption of pions by bound nucleons served as a guideline; the parameters, however, are chosen freely to give a best fit to the experimental data. It turns out that only three parameters are necessary to describe satisfactorily the available data for all known 2p–1s and 3d–2p transitions. (auth)

2898 POSITRON ANNIHILATION IN QUENCHED CADMIUM METAL. Connors, D. C.; Crisp, V. H. C.; West, R. N. (Univ. of East Anglia, Eng.). Phys. Lett.; 33A: 180-1(19 Oct 1970).

Positron annihilation experiments in quenched samples of cadmium are described. The results give further support to a theory of trapping of positrons by defects. (auth)

2899 CHEMICAL SHIFTS OF THE μ^+. Breskman, D. (Lehigh Univ., Bethlehem, Pa.); Kanofsky, A. Phys. Lett.; 33B: 309-11(26 Oct 1970).

The differences in chemical shifts between a muon and a proton in simple diatomic halide molecules are calculated and shown to be about 2 ppM. A formula based on the shift of the μ^+ precession frequency is presented for determining reaction rates for μ molecule formation. (auth)

Collision Phenomena

Refer also to abstracts 3079 and 3110.

2900 (CONF-700322–, pp 305-19) ELECTRON SPECTROSCOPY WITH HEAVY IONS. Rudd, M. E. (Nebraska Univ., Lincoln. Behlen Lab. of Physics).

From Proceedings of the second Oak Ridge conference on the use of small accelerators for teaching and research, March 23–25, 1970.

XUM

Though of recent origin, the spectroscopy of electrons is becoming an important complement to the spectroscopy of the electromagnetic spectrum. In addition to avoiding the limitations of the optical selection rules, it allows easy access to the energy range of 25 to 250 eV, which is in the experimentally difficult far ultraviolet and soft-x-ray region. Auto-ionization and Auger processes yield discrete spectra, which can be analyzed by present techniques to yield information about multiple excitation states, inner shell vacancy states, and others. Such states may be excited by fast ions as well as by electrons or photons. Characteristics of such spectra are discussed, experimental methods described, and examples of spectra are shown. Also shown is an example of a process, analogous to the Doppler effect, in which the energy of the emitted electron is shifted because of the motion of the source atom. 19 references. (auth)

2901 (ORNL-AMPIC-13) BIBLIOGRAPHY OF ATOMIC AND MOLECULAR PROCESSES FOR JANUARY–DECEMBER 1969. (Oak Ridge National Lab., Tenn.). Nov 1970. 65p. Dep. NTIS.

Literature related to atomic and molecular collision research is presented in the annotated bibliography. Bibliographical sources consisted of eighty-two scientific journals and three abstracting journals. References are cataloged under ten major categories with appropriate subcategories. For each entry the following information is indicated: the reactants studied, the type research (experimental or theoretical), the energy range, the author(s), and journal or book reference. (auth)

2902 (SC-RR-70-695) EMISSION CROSS SECTIONS FOR H^+, Na^+, Ne^+, Rb^+, INCIDENT ON MOLECULAR NITROGEN. Hoffman, James M.; Miller, Glenn H.; Lockwood, Grant J. (Sandia Labs., Albuquerque, N. Mex.). Oct 1970. 62p. Dep. NTIS.

Selected radiations from a nitrogen target for incident ions of H, Ne, Na, and Rb were examined in the energy range 30 to 100 keV. In particular, the N_2^+ (3914 Å), N_2 (3371 Å), and N^+ (3995 Å, 4026 Å, 4043 Å, 4080 Å, 5003 Å, 5680 Å) absolute emission cross sections were measured. The H^+ data are compared to values previously reported. The use of Ne^+ and Na^+ permits a comparison for similar incident masses, but different chemical structure. On the other hand, the role of incident particle mass for similar chemical structure was studied by comparison of Na^+ and Rb^+. Included are recommendations for a more comprehensive program. (auth)

2903 COMPUTER PROGRAM FOR THE CALCULATION OF ELECTRON SCATTERING AND PHOTOIONIZATION CROSS SECTIONS OF ATOMIC SYSTEMS WITH CONFIGURATION $(np)^q$. Conneely, M. J. (Univ. of Nebraska, Lincoln); Lipsky, L.; Smith, K.; Burke, P. G.; Henry, R. J. W. Comput. Phys. Commum.; 1: 306-24(Sep 1970).

Program ATOMNP is intended for study of the scattering of an electron by an atom or ion with configuration $(np)^q$, where n = 2 or 3, and $0 \leq q \leq 6$, under the assumption that all the ground-state terms are closely coupled but no excited terms contribute. The method of solution is similar to the Hartree–Fock method for bound states in that the total wave function of the system is diagonal in total orbital angular momentum L, total spin S, and parity π and is represented by a sum of Slater determinants. Given L, S, and π the code sets up the system of coupled equations for the atom or ion being considered and solves them. The R matrix, and hence the S matrix, for the collision is obtained from the asymptotic form of these equations and multichannel photoionization cross sections are computed if required. The program is written in FORTRAN IV for the IBM 360/65. (A.G.W.)

2904 PHOTOELECTRIC CROSS SECTIONS OF 662-keV GAMMA RAYS IN Ta AND Pd. Raja Rao, M.; Parthasaradhi, K.; Jnanananda, Swami (Andhra Univ., Waltair, India). Indian J. Pure Appl. Phys.; 7: 271-3(Apr 1969).

Photoelectric cross sections of 662-keV gamma rays in Ta and Pd are determined utilizing the internal–external conversion technique and the internal conversion coefficient determined by absolute count. The results are found to be in agreement with the previous experimental values as well as with the compiled values of G. W. Grodstein [X-ray attenuation coefficients from 10 keV to 100 MeV, NBS Circular 583, 1957]. However, the recent theoretical values of R. D. Schmickley and R. H. Pratt [Phys. Rev., 164: 104(1967)] are found to be slightly overestimated in the case of Ta only. (auth)

2905 PHOTOELECTRIC CROSS-SECTIONS OF GAMMA RAYS IN Cu, Ag, AND Pt. Parthasaradhi, K. (Andhra Univ., Waltair, India). Indian J. Pure Appl. Phys.; 6: 385-6(1968).

Total photoelectric cross sections of gamma rays in Cu, Ag, and Pt are determined by subtracting the theoretical scattering cross sections (with coherence) from the experimental total gamma-ray cross sections in the energy region 50 to 412 keV. These values are compared with the theoretical photoelectric cross sections of R. D. Schmickley and R. H. Pratt [Tables of calculated photoelectric cross sections for energies 10 to 3000 keV. (Lockheed Missiles & Space Co., Lockheed, USA) 1967]. The observed discrepancies are attributed to the possibility of overestimation of the theoretical cross sections. A remeasurement of total gamma-ray cross sections in Pt at low energies is suggested. (auth)

2906 STUDIES ON THE EFFECTIVE ATOMIC NUMBERS IN ALLOYS FOR GAMMA-RAY INTERACTIONS IN THE ENERGY REGION 100 TO 662 keV. Parthasaradhi, K. (Andhra Univ., Waltair, India). Indian J. Pure Appl. Phys.; 6: 609-13(Nov 1968).

Experimental photoelectric, scattering, and total gamma-ray cross sections in five alloys, viz. tungsten steel, monel metal, sterling silver, solder, and bell metal, were determined at gamma energies 100, 130, 279, 411, and 662 keV, utilizing experimental total gamma-ray cross sections and accurate theoretical partial gamma-ray cross sections in individual elements. Employing these cross sections the effective atomic numbers in these alloys at all the energies were determined by interpolation from the respective plots of experimental cross sections versus atomic number of individual elements. It has been found that the effective atomic numbers for partial processes are different from one another, being higher for the photoelectric process, but remain more or less constant for individual processes at all energies. This is in conformity with the predictions of G. J. Hine [Phys. Rev., 84: 725(1952)] that the effective atomic number for gamma-ray interaction in materials composed of several elements cannot be represented by a single number and they have to be computed for each partial process differently giving different weights to each element present in the material. However, it has been found that the effective atomic number for total gamma-ray interaction varies with energy unlike that in individual elements. Maximum variation is found in tungsten steel. No significant variation is found in monel metal. The cases of other alloys lie between these two cases. It has been concluded that the significance of variation of the effective atomic number for total gamma-ray interaction in alloys depends on the relative domination of the partial cross sections since the numbers for these partial processes differ. This in turn depends on the respective proportions and the range of atomic numbers of the elements with which the alloy is composed. An approximate expression for the determination of the number for total gamma-ray interaction from the numbers of the partial processes is suggested. (auth)

2907 PHOTOELECTRIC CROSS SECTIONS OF GAMMA RAYS IN La, Gd, Hf, AND Th. Visweswara Rao, V.; Parthasaradhi, K. (Andhra Univ., Waltair, India). Indian J. Pure Appl. Phys.; 6: 642-3(1968).

Experimental photoelectric cross sections of gamma rays at 30, 40, 60, 80, and 100 keV in La, Gd, Hf, and Th are determined by subtracting the scattering cross sections from total experimental gamma-ray cross sections. These cross sections are found to be in satisfactory agreement with recent theoretical values reported in the literature within the range of errors except for a very little discrepancy (less than 1%) in Gd at 40 and 80 keV. (auth)

2908 NOTE ON TOTAL TO SUBSHELL PHOTOELECTRIC CROSS SECTION RATIOS. Parthasaradhi, K. (Andhra Univ., Waltair, India). Nucl. Instrum. Methods; 85: 147-50(1 Aug 1970).

An analysis of available estimated and deduced data on the total-to-subshell photoelectric cross-section ratios is made. Evidence for a little variation of total-to-K-shell ratio with energy is observed. Suitable values of the ratios are evolved from the analyzed data. Using these ratios, the subshell cross sections are estimated from the total experimental cross sections and good agreement is observed with the theoretical values of Schmickley and Pratt within the range of errors. It is concluded that the reported values of the ratios can be used to get the subshell photoelectric cross sections from the total photoelectric cross sections. (auth)

2909 INCOHERENT SCATTERING OF GAMMA RAYS BY K ELECTRONS. Singh, M. (Punjabi Univ., Patiala, India). Phys. Lett.; 33A: 70-1(5 Oct 1970).

The integrated K-electron–photon scattering cross sections obtained from the available differential cross sections for energies from 280 to 1002 keV with Z varying from 50 to 82 are found to be appreciably lower than the free-electron values. (auth)

2910 K-SHELL EXCITATION OF NITROGEN AND CARBON MONOXIDE BY ELECTRON IMPACT. van der Wiel, M. J.; El-Sherbini, Th. M.; Brion, C. E. (FOM-Instituut voor Atoom-en

Molecuulfysica, Amsterdam). Chem. Phys. Lett.; 7: 161-4 (15 Oct 1970).

The K-shell energy-loss spectra for N_2 and CO were measured using 10-keV electrons. In addition to the K-shell ionization continua, discrete transitions at 400.8 eV for N_2 and at 287.7 and 534.4 eV for CO are observed corresponding to excitation of the atomic K shells. Electron–ion coincidence studies provide information on the decay processes following K-shell excitation and ionization. (auth)

2911 ABSOLUTE MEASUREMENTS OF THE EXCITATION FUNCTIONS FOR THE KII LINE PRODUCED IN COLLISIONS BETWEEN K^+ IONS AND Ne ATOMS. Pop, S. S.; Krivskii, I. Yu.; Zapesochnyi, I. P.; Baletskaya, M. V. (Uzhgorod State Univ., USSR). Zh. Eksp. Teor. Fiz.; 59: 696-9(Sep 1970). (In Russian).

The emission spectrum arising in collisions between K^+ ions and Ne atoms is investigated. The absolute variation of the excitation functions for a number of K II and Ne I spectral lines is measured at energies ranging from threshold up to 30 keV. For most spectral lines of the potassium ion, the qualitative course of the excitation functions is the same. The highest values of the cross sections for the potassium ion lie between 0.3×10^{-18} and 1.7×10^{-18} cm^2, whereas the total excitation cross section for all K II lines in the visible part of the spectrum is $\sim 10^{-17}$ cm^2. A theoretical interpretation of the experimental data is presented on the basis of the Landau–Zener adiabatic model. (auth)

2912 RESONANCE CHARGE EXCHANGE BETWEEN A MOLECULAR ION AND DIATOMIC MOLECULE. Bylkin, V. I.; Palkina, A. A.; Smirnov, B. M. (Inst. of High Temperatures, Moscow). Zh. Eksp. Teor. Fiz.; 59: 992-9(Sep 1970). (In Russian).

The cross section for charge exchange between a molecular ion and its molecule is calculated. The potential for exchange interaction between the molecular ion and molecule for a given direction of their axes is calculated by the asymptotic method under the assumption that the distance between them is great compared with the size of the molecule. This quantity is found by taking into account anisotropy of the electron distribution in the molecule, exchange of valency electrons, and correlation between the spin and projections of the electron moment and atomic residue. The resonance charge-exchange cross section is calculated on the basis of the exchange interaction potential for not-very-small collision velocities such that, during a collision, the molecular ion and molecule axes do not have time to rotate. Limiting cases of collision rates for transitions between vibrational levels are considered. One case is that of small rates when transitions between vibrational states do not occur; another case is that of large rates when transitions between vibrational levels satisfy the Franck–Condon principle. The results of the calculations are compared with the experimental cross sections for resonance charge exchange between a molecular ion and its molecule. (auth)

2913 APPROXIMATE METHODS OF CALCULATION OF EXCITATION CROSS SECTIONS OF ATOMS AND IONS. Vainshtein, L. A. Tr. Fiz. Inst., Akad. Nauk SSSR; 51: 3-7(1970). (In Russian).

Approximate methods of calculation of excitation cross sections of atoms are surveyed. Emphasis is on methods of obtaining cross sections in a sufficiently wide range of energies for different applications. (tr-auth)

2914 EFFECTIVE EXCITATION AND IONIZATION CROSS SECTIONS OF IONS. Beigman, I. L.; Vainshtein, L. A. Tr. Fiz. Inst., Akad. Nauk SSSR; 51: 8-19(1970). (In Russian).

Methods and results of calculations of cross sections for excitation and ionization of ions by electron impact are presented. The rates of characteristic processes were calculated for a Maxwellian distribution of electron velocities. The results of the calculations were approximated by two-parameter analytical formulas. The parameters appearing in these formulas are given for a series of transitions in the isoelectronic sequence from He to Ne. (tr-auth)

2915 INSEPARABLE VARIABLES IN THE PROBLEM OF EXCITATION OF ATOMS BY ELECTRON IMPACT. Presnyakov, L. P. Tr. Fiz. Inst., Akad. Nauk SSSR; 51: 20-35(1970). (In Russian).

A method proposed in 1963 by the author and others for describing inelastic electron–atom collisions is considered in detail. A generalization of results for the case of excitation of hydrogen-like ions by electron impact is proposed. Cross sections calculated by the method discussed and by the Born approximation are given for a large number of transitions in hydrogen and alkali metal atoms. (tr-auth)

2916 ROLE OF INTERMEDIATE STATES IN EXCITATION OF ATOMS BY ELECTRON IMPACT. Vainshtein, L. A.; Presnyakov, L. P. Tr. Fiz. Inst., Akad. Nauk SSSR; 51: 36-43(1970). (In Russian).

In a series of cases the first Born approximation for the excitation of atoms by electron impact gives values less than experimental values. It is shown that such a situation arises when the probability of direct excitation is comparatively small and transition through intermediate states plays a significant role. Calculations for quadrupole transitions in He and Ne give results having an error typical of the Born method. Approximate methods of normalization of cross sections in second order are examined. (tr-auth)

2917 QUASI-CLASSICAL METHOD IN THEORY OF COLLISIONS OF ATOMS WITH HEAVY PARTICLES AND ELECTRONS. Vinogradov, A. V. Tr. Fiz. Inst., Akad. Nauk SSSR; 51: 44-54 (1970). (In Russian).

On the basis of analysis of the exact relation between the quantum-mechanical scattering amplitude and the quasi-classical range of probability, a simple modification of the quasi-classical approach to calculation of cross sections of inelastic collisions of atoms with electrons is proposed. The method is used for calculation of the cross section of excitation of the 4p–4d transition in the Ne atom and for calculation of the excitation of the dielectronic transition $4s^2-4p^2$ in the Ca atom. (tr-auth)

2918 CALCULATION OF EFFECTIVE SCATTERING CROSS SECTIONS WITH ATOMIC FUNCTIONS THAT TAKE INTO ACCOUNT CONFIGURATION INTERACTION. Beigman, I. L. Tr. Fiz. Inst., Akad. Nauk SSSR; 51: 55-62(1970). (In Russian).

A previously proposed semi-empirical method of calculation of wave functions using the two-configuration approach is presented. On the basis of this method, inelastic scattering of electrons by atoms and ions having two valence electrons is considered in the Born approximation. Calculations of cross sections of dielectronic transitions in the Ca atom and the O V ion are given. (tr-auth)

2919 CHARGE EXCHANGE AT MEDIUM COLLISION ENERGIES. Poluektov, I. A.; Presnyakov, L. P. Tr. Fiz. Inst., Akad. Nauk SSSR; 51: 63-73(1970). (In Russian).

The problem of charge exchange of neutral atoms with monovalent ions at energies from 1 to 100 keV is considered. In treating charge exchange into an excited state, the effect of an intermediate level, the ground state of the atom formed, is taken into account. Analytical approximations for the transition probabilities and cross sections are obtained. Calculated cross sections for the processes $p + He \rightarrow H(1s) + He^+$, $p + He \rightarrow H(2p) + He^+$, and $p + Ne$ H(2p) + Ne^+ agree well with experimental data. (tr-auth)

2920 INVESTIGATION OF TRANSITIONS BETWEEN EXCITED STATES OF NEON ATOMS IN COLLISIONS WITH ELECTRONS. Khaikin, A. S. Tr. Fiz. Inst., Akad. Nauk SSSR; 51: 90-123(1970). (In Russian).

The modulation method of measurement of rates of transitions between excited states of atoms is described in detail. The method is based on the perturbation of stationary populations of excited states by external irradiation, and it is applied in principle to random transitions, both spontaneous and collision-induced. The application of the method to measurement of rate coefficients for transitions between excited states induced by collisions with electrons was studied. Measurements made for the $s'-d'$, $p'-d'$, and $s'-p'$ transitions in Ne are described. The results obtained are compared with results of theoretical calculations using the first and second Born approximations. (tr-auth)

2921 STUDIES ON THE INCOHERENT SCATTERING CROSS-SECTIONS OF GAMMA RAYS BY ELECTRONS IN Al, Cu, Sn, Pb, AND U. Parthasaradhi, K. (Andhra Univ., Waltair, India). Indian J. Pure Appl. Phys.; 7: 511(Jul 1969).

Incoherent scattering cross sections were estimated by subtracting the other theoretical partial cross sections from the total gamma ray cross sections available in literature, for Al, Cu, Sn, Pb, and U, in the gamma energy region 30 to 2620 keV. A comparison with the theoretically deduced variation of free electron scattering cross sections with gamma energy shows a general agreement, although a few deviations are observed at lower gamma energies. These deviations are attributed to the effect of electron binding. (auth)

2922 ELASTIC SCATTERING OF ALKALI ATOMS FROM IODINE ATOMS AND MOLECULES AT THERMAL ENERGIES. Fluendy, M. A. D.; Horne, D. S.; Lawley, K. P.; Morris, A. W. (Univ. of Edinburgh). Mol. Phys.; 19: 659-71(1970).

High-resolution, small-angle measurements of the elastic differential cross sections were made for the systems K–I and K–I_2. In all cases the structure at small angles is found to arise predominantly from collisions occurring along the adiabatic potential. The off-diagonal matrix element of the electronic hamil-

tonian between the covalent and ionic states in the K–I system is found to be $\sim 6 \times 10^{-15}$ ergs. (auth) (UK)

Atomic Theory

2923 GENERAL PROGRAM FOR CALCULATING ANGULAR MOMENTUM INTEGRALS IN ATOMIC STRUCTURE. Hibbert, A. (Queen's Univ., Belfast). Comput. Phys. Commun.; 1: 359-77 (Sep 1970).

In configuration-interaction calculations, the matrix of the Hamiltonian operator must be evaluated with respect to a basis set of configuration wave functions. The two-electron interaction matrix elements involved may be written as a weighted sum of radial Slater integrals. The program described, WEIGHTS, calculates the coefficients of these integrals. The program is written in FORTRAN IV for the ICL 1907. (A.G.W.)

2924 DERIVATION OF SOMMERFELD–DIRAC FINE STRUCTURE FORMULA BY WKB METHOD. Lu, Pao (Arizona State Univ., Tempe). Phys. Rev., A; 1: 1283-5(May 1970).

By use of the WKB approximation in the spirit of Miller and Good, an expression was obtained, which connects the energy eigenvalues of two parts: One is supposedly known and the other is to be solved. The Balmer energy formula of the one-electron bound state is used as the known part and its relativistic counterpart, the Sommerfeld–Dirac fine-structure formula, is solved. An exact form of the relativistic energy-level formula can be obtained through this modified WKB expansion to order $\hbar^2$. (auth)

2925 APPRAISAL OF AN ITERATIVE METHOD FOR BOUND STATES. Robinson, Peter D.; Warnock, Tony T. (Univ. of Wisconsin, Madison). Phys. Rev., A; 1: 1314-20(May 1970).

An iterative method for determining bound-state eigenvalues and properties of the radial Schroedinger equation is appraised. The method stems from iterating the integral equation $\psi = \mu(T + \frac{1}{2}\gamma^2)^{-1}(-V\psi)$, where T and V are the kinetic- and potential-energy operators. The basic theory is briefly reviewed, and calculations are performed for the Coulomb and screened-Coulomb potentials. The lowest three μ eigenvalues, together with the expected values of $(\gamma r)^{-1}$, γr, and $(\gamma r)^2$, are obtained from a single iterated eigenfunction sequence. Convergence is rapid for eigenvalues but slow for expected values. There is some sensitivity to the choice of the numerical integration formula. Regarded as a numerical method, this approach may be most competitive for the determination of zero-energy potential-strength eigenvalues. Its disadvantages are listed. Analytical improvements to eigenfunctions can be easier to obtain by iteration than by perturbation, and some success has been achieved. A simple example suggests that the rate of convergence of an iterated eigenfunction sequence is less than that of a related perturbation sequence unless the choice of starting function is bad. (auth)

2926 METHOD OF OBTAINING BRUECKNER ORBITALS FOR ATOMS AND MOLECULES. Larsson, S. (Uppsala Univ.). Chem. Phys. Lett.; 7: 165-70(15 Oct 1970).

A method, resembling the Hartree–Fock method, is presented of obtaining Brueckner orbitals through a knowledge of pair correlation functions. The pair correlation functions may be obtained from approximate wave functions. They may also be Bethe–Goldstone type pairs or simpler types of pair function. (auth)

2927 METHODS OF MOLECULAR QUANTUM MECHANICS. McWenny, R.; Sutcliffe, B. T. A Series of Monographs. Theoretical Chemistry, Volume 2. London; Academic Press (1969). 316p. 168s.

The subject is considered under the following headings: introductory survey, mathematical methods, many-electron wave functions, the nature of the electron distribution, molecular orbitals and the self-consistent field, valence bond theory, some recent developments, electric and magnetic effects, the calculation of electronic wave functions. (UK)

2928 INTEGRAL-TRANSFORMATION TRIAL FUNCTIONS OF THE FRACTIONAL-INTEGRAL CLASS. Somorjai, R. L. (National Research Council of Canada, Ottawa); Bishop, David M. Phys. Rev., A; 1: 1013-18(Apr 1970).

Fractional integrals (Euler transforms) of conventional quantum-mechanical functions are proposed as special integral-transform trial functions. Calculations on the first four members of the He isoelectronic sequence with three different-order Euler transforms of both Slater and Gaussian 1s orbitals are reported. A pilot calculation for H_2 with an Euler transform of an LCGTO (linear combination of Gaussian-type orbitals) molecular orbital gives a total energy E = −1.10903 a.u. at R = 1.4 a.u. (exact value is −1.17444 a.u.). A generalization of the shape function used in this work is given and the general applicability of Euler transforms discussed. (auth)

Cosmic Radiation

Refer also to abstracts 2484, 2487, 2488, 2490, 2874, and 2875.

2929 THEORY OF THE ACCELERATION OF CHARGED PARTICLES IN A COSMIC PLASMA. Kats, M. E.; Yukhimuk, A. K. (Inst. of Geophysics, Kiev). Geomagn. Aeron. (USSR) (Engl. Transl.); 10: 253-5(1970).

Translated from Geomagn. Aeron.; 10: 328-30(1970).

Recent investigations of the acceleration mechanisms of charged particles permit use of experimental data in the determination of the spectrum of turbulent pulsations. The spectral energy density of turbulent pulsations and the integral intensity spectrum of charged particles are computed in the quasi-linear approximation. A magnetized plasma has various oscillations that can be unstable and the particles diffuse in the velocity space because of Cherenkov and cyclotron resonances with various waves. Particles are analyzed whose velocity is much greater than the phase velocity of a wave. In this case, ion–acoustic oscillations build up and the dynamics of the instability is investigated. (J.C.W.)

2930 COSMIC-RAY ENERGY SPECTRUM IN INTERSTELLAR SPACE. Charakhch'yan, A. N.; Charakhch'yan, T. N. (Lebedev Inst. of Physics, Moscow). Geomagn. Aeron. (USSR) (Engl. Transl.); 10: 187-9(1970).

Translated from Geomagn. Aeron.; 10: 240-3(1970).

The cosmic-ray energy spectrum in the absence of solar activity was obtained from a study of 11-year cosmic-ray variations. It practically coincides with the spectrum of galactic cosmic rays observed near the Earth in periods of minimum solar activity. Therefore, the cutoff of the galactic cosmic-ray spectrum in the low-energy range apparently reflects the property of the spectrum of particles arriving from interplanetary space. (auth)

2931 SATELLITE MEASUREMENT OF THE RELATIVE ABUNDANCE OF RELATIVISTIC COSMIC-RAY LH NUCLEI. Ely, John T. A. (Univ. of Washington, Seattle). Can. J. Phys.; 48: 2427-33(15 Oct 1970).

A Cherenkov-scintillator telescope was flown on the low-altitude polar orbiting OV1-10 satellite. Charge resolution was accomplished in the Z = 9 to 17 range for energies above ~0.6 BeV/nucleon. The data indicate an even–odd ratio for the integral energy spectra of these nuclei which decreases from 6 to 3 as the threshold increases from 0.6 to about 3 BeV/nucleon. This behavior is shown to be consistent with a positive energy dependence of path length. The measurements are presented and compared with the other published satellite results and one balloon experiment. (auth)

2932 INFLUENCE OF PRIMARY MASS ON STRUCTURE OF EXTENSIVE AIR SHOWERS. Thielheim, K. O. (Univ., Kiel). Z. Naturforsch.; 25a: 1254-8(Aug-Sep 1970). (In German).

Results of Monte Carlo simulations of extensive air shower development are discussed with respect to the influence of primary mass on shower characteristics (energy spectrum and lateral distribution of hadrons, frequency of nuclear active "multicores," mean total energy of hadrons, fluctuation of total hadron energy, mean total number of muons, fluctuation of total muon number, mean central electron density, frequency of electromagnetic "multicores"). Critical comments are presented concerning some empirical data. (auth)

Direct Energy Conversion

Refer also to abstracts 3129 and 3133.

2933 CONCERNING THE OPTIMUM DISTRIBUTION OF SPECIFIC RESISTANCE TENSORS OF WORKING SUBSTANCES IN MAGNETOHYDRODYNAMIC CHANNELS. Lur'e, K. A. Prikl. Mat. Mekh.; 34: 270-91(Mar-Apr 1970). (In Russian).

The problem considered was set up and partially studied previously. The conditions that must be satisfied by the distribution of specific resistance in the working material in a channel with terminal electrodes in order for the current in the external circuit to reach a maximum value are studied. The specific resistance is considered to be a tensor function of coordinates; the tensor is assumed to be symmetrical and its principal values are piecewise-continuously differentiable functions. (tr-auth)

2934 NONLINEAR TRANSPORT OF ELECTRONS AND IONS IN A PLASMA DIODE. Biron, Didier Francois. Stanford, Calif.; Stanford Univ. (1969). 106p. University Microfilms Order No. 70-10,427.

Thesis.

A set of Boltzmann Equations for the velocity-dependent angular fluxes, together with Poisson's equation, is used to describe the

XUM

charged particle distribution. In order to get analytical results, part of the acceleration term is neglected; the introduction of a transform allows the reduction of each Boltzmann equation to an equivalent one-speed neutron transport problem. A set of complete eigenfunctions is then derived, and it is shown that general boundary conditions can be satisfied. The solution of the problem is thus reduced to that of a Hammerstein integral equation. (TSS)

2935 THERMAL CYCLE FOR A DIRECT FLOW, SUPERSONIC, COMPRESSORLESS MHD GENERATOR. Poletavkin, P. G. (Inst. of High Temperatures, Moscow). High Temp. (USSR) (Engl. Transl.); 6: 1061-70(Nov-Dec 1968).

Translated from Teplofiz. Vys. Temp.; 6: 1108-17(Nov-Dec 1968).

A new MHD generator thermal cycle is proposed and evaluated. This cycle does not involve heat regeneration and a high-temperature heat exchanger. Cycle efficiency has values to 50%. The feasibility is proposed of a very simple MHD generator installation that has no moving parts, is capable of long-term operation, and is completely constructed from ordinary industrial materials. A direct flow, supersonic, compressorless MHD generator may operate in an open cycle on combustion products, as well as in a closed cycle with an inert working gas. In such operation the high temperature (up to 2100°K) of the working gas in open-cycle operation is obtained in a combustion chamber and in closed-cycle operation in a high-temperature nuclear reactor. The extreme expansion of the working gas in the new thermal cycle establishes conditions favorable to attainment of nonequilibrium electrical conductivity in the MHD channel (at the expense of power dissipated as Joule heat). This occurs in combustion products, as well as in an inert gas, when some form of easily ionized seed material is not used; this eliminates the difficult problem of introduction and removal of seed. By means of water (ice) mist injection into the working gas, compression of the mixture is accomplished with little change in temperature and with minimum work. (auth)

2936 ANALYSIS OF A SCHEME OF POWER PLANT WITH AN MHD GENERATOR AND THERMOCOMPRESSOR. Kovbasyuk, V. I.; Medin, S. A. (Inst. of High Temperatures, Moscow). High Temp. (USSR) (Engl. Transl.); 6: 1071-5(Nov-Dec 1968).

Translated from Teplofiz. Vys. Temp.; 6: 1118-23(Nov-Dec 1968).

A thermodynamic analysis is made of a scheme of an electric power plant with an MHD generator and thermocompressor—a device in which there occurs an increase of total pressure in a high-speed flow of hot gas with injection of a coolant. Along with having a high efficiency, this scheme provides a more complete static character of the plant and permits realization of a high-temperature heat exchanger without a pressure drop. The optimal operating conditions of the thermocompressor are determined and the examined cycle is compared with the usual Brayton cycle. Results of calculating the scheme of a prospective open-cycle power plant with an MHD generator and thermocompressor are presented. (auth)

2937 CHOICE OF A WORKING SUBSTANCE FOR SINGLE-COMPONENT LIQUID-METAL MAGNETOHYDRODYNAMIC UNITS OF THE CONDENSATION TYPE. Shpil'rain, E. E.; Boldyrev, V. M.; Postnikova, I. N. (Inst. of High Temperature, Moscow). High Temp. (USSR) (Engl. Transl.); 8: 162-5(Jan-Feb 1970).

Translated from Teplofiz. Vys. Temp.; 8: 174-6(Jan-Feb 1970).

A study was made of the effect of the choice of the working substance on the effective efficiency of a liquid-metal magnetohydrodynamic unit of the condensation type. It is shown that, under definite assumptions, the efficiency does not depend on the heat capacity of the liquid of the working body. (auth)

2938 ELECTROGASDYNAMIC GENERATOR WITH NEUTRALIZATION OF SPACE CHARGE. Borok, A. M. High Temp. (USSR) (Engl. Transl.); 8: 166-70(Jan-Feb 1970).

Translated from Teplofiz. Vys. Temp.; 8: 177-81(Jan-Feb 1970).

The possibility of building a high-power electrogasdynamic generator for direct conversion of heat energy into electrical energy is discussed. Operation of the generator at high gas pressures is studied. Calculating formulas and typical variants of the units are given. (auth)

2939 USE OF A TURBULENT WASHER FOR REMOVAL OF AN IONIZING ADDITIVE IN OPEN-CYCLE MAGNETOHYDRODYNAMIC POWER GENERATORS. Val'dberg, A. Yu.; Mostinskii, I. L.; Nekhoroshev, R. S. (Inst. of High Temperatures, Moscow). High Temp. (USSR) (Engl. Transl.); 8: 171-6(Jan-Feb 1970).

Translated from Teplofiz. Vys. Temp.; 8: 182-7(Jan-Feb 1970).

A liquid method is described for the removal of an ionizing additive, working in an experimental unit with a magnetohydrodynamic generator. Experimental data are given on the collection efficiency of a submicron potassium carbonate dust from the combustion products of natural gas using a turbulent washer. The dependence of the residual dust content of the gas on the hydraulic resistance of the tubular pulverizer is obtained, and the expenditures of power with a purely mechanical collection method are determined $\eta = 1 - \exp[-2.32 \times 10^{-3} K_T^{0.75}]$, where η is the turbulent washing efficiency; K_T is the energy in kJ, expended by a turbulent washer for the treatment of 1000 m^3 of gas. Methods for obtaining the required collection efficiency of the additive with the lowest expenditures of power are indicated. Data are given on the conversion of potassium carbonate to bicarbonate, with contact between an aqueous solution of K_2CO_3 and the combustion products. (auth)

2940 LAWS GOVERNING THE OPERATION OF THE METALLIC ELECTRODES OF A MAGNETOHYDRODYNAMIC GENERATOR.. Zelikson, Yu. M.; Kirillov, V. V.; Reshetov, E. P.; Flid, B. D. (Inst. of High Temperatures, Moscow). High Temp. (USSR) (Engl. Transl.); 8: 181-9(Jan-Feb 1970).

Translated from Teplofiz. Vys. Temp.; 8: 193-202(Jan-Feb 1970).

Results of the operation of metallic electrodes under conditions close to the operating conditions of a magnetohydrodynamic generator are presented. Copper and stainless steel electrodes, with water and air cooling were investigated. It is shown that the nonlinear nature of the volt–ampere characteristic is mainly determined by processes involving the passage of an electrical current through the region of metallic electrodes close to the electrodes. In current regions from 0.1 to 0.15 A, with threshold voltages of 70 to 120 V, a discharge of an arc type develops at the cathode. It is established that arc conditions of operation of the electrodes have a substantial effect on the character of the oscillations of the current passing through the electrodes. On the basis of the data obtained, there is plotted the time dependence of the mean current at one spot of the total current. In experiments on measurements of the heat balance there is established the presence of additional heat losses to the electrode, brought about by passage of the current. (auth)

Fluid Physics

Refer also to abstract 3127.

2941 MASS EXCHANGE OF A CIRCULAR CYLINDER IN PRESENCE OF TRANSVERSE MAGNETIC FIELD. Lisovskaya, S. I.; Blum, E. Ya.; Kulis, P. B.; Fedin, A. G. (Inst. of Physics, Riga). Latv. PSR Zinat. Akad. Vestis, Fiz. Teh. Zinat. Ser.; No. 3, 69-73(1970). (In Russian).

Results of an experimental investigation into the total and local convective mass exchange of a circular cylinder in a transverse MHD flow are presented. The variations of the mass exchange intensity are due mainly to the interaction between the diffusion current and the magnetic field. At small values of the interaction, the mass exchange variations can be explained by the effects met in ordinary hydrodynamics; however, these variations are very small. (auth)

2942 SOME TOPICS IN MAGNETOHYDRODYNAMICS. Buckmaster, John David. Ithaca, N. Y.; Cornell Univ. (1969). 102p. University Microfilms Order No. 70-11,219.

Thesis.

Three problems are investigated. The first section is an investigation of MHD boundary layers in a transverse magnetic field when the magnetic Reynolds number (Rm) is small. The main purpose is to understand something about the suppression of separation by a strong magnetic field, with particular emphasis on the behavior near a rear stagnation point. In the second section the equations of inviscid magnetohydrodynamics are studied for small Rm (magnetic Reynolds number) and large N (interaction parameter). The limit equations, in which the nonlinear inertia terms do not appear, can not fully describe general inviscid flow situations, suggesting the existence of inviscid boundary layers in which the missing terms must be reinstated. The third section is concerned with the impulsively started flow around an insulator in a perfectly conducting inviscid liquid. The velocity is much slower than the Alfven-wave speed so that a linear analysis is possible. The time development is followed for an arbitrarily shaped body and arbitrary free-stream electric field, with particular emphasis on the steady state. (TSS) (Diss. Abstr. Int., B)

2943 NONISOTHERMAL MHD DUCT FLOW. Thomson, William Joseph. Moscow, Idaho; Univ. of Idaho (1969). 166p. University Microfilms Order No. 70-10,711.

Thesis.

The partial differential equations describing the simultaneous transport of momentum, energy and magnetic field, are derived

for fully developed MHD flow in finite ducts. The fluid properties are allowed to vary to the extent that electrical conductivity and viscosity are assumed to be temperature-dependent. For heated or cooled electrically insulating walls, numerical solutions are obtained by utilizing a modified Gauss–Siedel algorithm. It is shown that consideration of variable fluid properties results in friction factors and bulk flow rates that differ from constant property solutions by as much as a factor or two, and by 50% even for small variations. For ducts operated as electromagnetic flow meters, variable fluid properties produce flowmeter sensitivities 30% above ideality for cooling at the walls, and up to 60% below ideality for heated walls. Analysis leads to the conclusion that it is the nature of the current distributions in the duct which is important in predicting the character of nonisothermal MHD-duct flow. Consequently, it is not possible to account for fluid-property variations in terms of "weighted" fluid parameters such as average Hartmann numbers. (Diss. Abstr. Int., B)

2944 HEAT TRANSFER IN THE TURBULENT FLOW OF AN ELECTRICALLY CONDUCTING LIQUID IN A CIRCULAR TUBE IN A LONGITUDINAL MAGNETIC FIELD. Zhilin, V. G.; Berman, M. I. (Inst. of High Temperature, Moscow). High Temp. (USSR) (Engl. Transl.); 6: 1016-19(Nov-Dec 1968).

Translated from Teplofiz. Vys. Temp.; 6: 1061-5(Nov-Dec 1968).

The heat transfer associated with the turbulent flow of an electrically conducting liquid in a circular tube in a longitudinal magnetic field is calculated for a constant density of the thermal flux at the walls of the tube. The calculation is based on the well-known integral relation of Lyon, experimental data relating to velocity profiles, and an assumption as to the equality of the coefficients of turbulent heat and momentum transfer. By using these results (extrapolated as necessary) and existing experimental data, an interpolation formula for heat transfer under the conditions $2300 \leq Re \leq 1.5 \times 10^5$, $0 < Pr \leq 3.0 < Ha \leq 614$ is obtained. (auth)

2945 TENTH SYMPOSIUM ON ENGINEERING ASPECTS OF MAGNETOHYDRODYNAMICS, CAMBRIDGE, MASSACHUSETTS, MARCH 26–28, 1969. Jackson, W. D.; Klepeis, J. E. (eds.). Cambridge, Mass.; Massachusetts Institute of Technology (1969). 209p. (CONF-690348).

Papers are included on the following topics: plasma instabilities; channel flows and boundary layers; liquid metal systems and generators; nonequilibrium conditions, diagnostics, and conductivity; nonequilibrium pre-ionizer, generator, and accelerator studies; combustion-plasma generators and electrode studies; power plant performance, and open- and closed-cycle generator experiments. (M.H.R.)

2946 PERTURBATION OF STOKES FLOW PAST A HOLLOW SPHERE IN MAGNETOHYDRODYNAMICS. Levy, Therese (Univ., Paris). J. Mec.; 9: 189-211(Jun 1970). (In French).

The steady flow of an incompressible, viscous, and electrically conducting fluid past a hollow sphere in a magnetic field was studied, the flow and the magnetic field upstream being uniform and parallel. The Hartmann number M, the magnetic Reynolds number R_m and the Reynolds number R were assumed small; furthermore R_m and R were small compared to M, when R_m and R were equal to zero, the solution required the matching of two asymptotic expansions for each quantity, one of them valid near the body and the other far from it. The influence of R_m and R on this solution was studied up to the $O(R_m)$ and O(R) orders respectively. To these orders, though the flow velocity and the magnetic field are influenced by R_m and R, the drag on the sphere is not. (tr-auth) (France)

2947 BREAKAWAY PARAMETER OF THE TURBULENT MAGNETOHYDRODYNAMIC BOUNDARY LAYER. Vatazhin, A. B.; Gotovtsev, A. V. High Temp. (USSR) (Engl. Transl.); 8: 113-19(Jan-Feb 1970).

Translated from Teplofiz. Vys. Temp.; 8: 123-9(Jan-Feb 1970).

Using the well-known gas-dynamic hypothesis with respect to the effect on the flow in a cross section of the breakaway of the boundary layer only in the immediate vicinity of this cross section, a determination was made of the breakaway parameter, ξ_{cr}, of the turbulent boundary layer in a conducting liquid in the presence of magnetic and electric fields. The principal dimensionless parameters that characterize the degree of action of the electromagnetic field on the breakaway of the flow in the boundary layer are found. Calculations were made of ξ_{cr}, for both incompressible and compressible gases, taking account of heat transfer through the wall. It is shown that, using an electromagnetic field, it is possible to increase considerably the breakaway parameter of the boundary layer, which makes it possible to delay and, in certain cases, even to prevent its breakaway. (auth)

Geophysics (Upper Atmosphere)

Refer also to abstract 2860.

2948 (AD–709200) MUTUALLY INTERACTING INSTABILITIES IN THE MAGNETOSPHERE. Report for July 1968–July 1969. Cornwall, John M. (Aerospace Corp., El Segundo, Calif.). 29 Jun 1970. Contract F04701-69-C-0066. 25p. (TR–66(5260-20)-18; SAMSO-TR–70-233). NTIS.

The mutual interaction of a drift-wave instability and a high-frequency instability is studied. When both instabilities are present in a plasma, the usual dispersion relation for the drift wave is modified by terms involving the wave intensity of the high-frequency instability; generally, damping results. An example is worked out: the Mikhailovskii–Rudakov drift Alfven mode, in the presence of an electron-cyclotron instability. For auroral magnetospheric parameters, high-frequency damping is comparable to the usual linear growth rate for the drift instability. (auth) (USGRDR)

2949 (AD–709359) ARCTIC IONOSPHERE AND AURORA: AIRBORNE INVESTIGATIONS. Environmental Research Papers. Buchau, J.; Pittenger, E. W.; Sizoo, A. H. (Air Force Cambridge Research Labs., L. G. Hanscom Field, Mass.). May 1970. 62p. (AFCRL–70-280; AFCRL-ERP–322). NTIS.

A highly instrumented NKC 135 jet aircraft was used in an extensive Arctic research program that started in 1967. To date, 69 flights have been made and ionospheric and optical data covering major parts of the auroral oval, mainly the midday and the night sectors, were collected. During the winter months of 1967, 1968, 1969, and 1970, special emphasis was put on the investigation of the day sector. These flights covered a rather unique and poorly investigated area of the auroral oval. A thorough analysis of the data collected in the day sector reveals the existence of a band of continuous-particle precipitation south of the location of the discrete aurora. This precipitation hardens towards the south and results in E and D region ionization. These observations compare very well with measurements of precipitating particles performed by satellite. The investigation of the evening and night sectors showed similar but less organized trends than on the day side. During several flights the continuity of the auroral oval was verified. The investigation indicates that with additional measurements, it may be possible to develop a model of the Arctic ionosphere. With control measurements from a few ideally located ground stations, the dynamics of the Arctic ionosphere might then be utilized for forecasting propagation conditions in the Arctic. (auth) (USGRDR)

2950 (AD–709363) QUIESCENT AND DISTURBED PROTON AND ELECTRON DISTRIBUTIONS. Environmental Research Papers. Webb, Virgil H.; Rothwell, Paul L.; Katz, Ludwig (Air Force Cambridge Research Labs., L. G. Hanscom Field, Mass.). Jun 1970. 21p. (AFCRL–70-334; AFCRL-ERP–324). NTIS.

Ionizing radiation within the Earth's magnetosphere presents a potential hazard to men as well as to sensitive equipment operating in this region. Thus, investigation of the detailed structure, as well as the variability of this radiation, is an important aspect of the continuing studies of the environment within Air Force operations. Air Force satellite OV1-13, instrumented to measure the differential energy spectra of protons and electrons, was launched on April 6, 1968 into a polar orbit with an apogee and perigee of 9300 and 570 km, respectively. Both proton and electron data for energies between 0.1 and 1.0 MeV, obtained during the June 9, 1968 magnetic storm, are presented in the form of flux distributions and E_0 vs L plots with emphasis being placed on the late-morning sector of the outer belt. (auth) (USGRDR)

2951 (AD–709723) PROTON ENERGY DISTRIBUTIONS FROM 0.060 TO 3.3 MeV AT 6.6 EARTH RADII. Stevens, John R.; Martina, E. Frank; White, R. Stephen (Aerospace Corp., El Segundo, Calif. California Univ., Riverside. Dept. of Physics). 15 Jul 1970. 38p. (TR–59(6260-20)-4; SAMSO-TR–70-262). NTIS.

Proton differential fluxes are reported for 12 energies from 0.060 to 3.3 MeV at 6.6 Earth radii for the time period of October 2 to 13, 1968. The proton energies were measured with a surface barrier semiconductor detector and a stacked discriminator pulse height analyzer on the Air Force Office of Aerospace Research Satellite OV2-5 (1968-81A). The typical quiet time fluxes decreased by 8 orders of magnitude over the measured energy interval. During this time the energy spectrum varied from $E^{-3.5}$ to $E^{-6.0}$. Below 200 keV the energy distributions flatten but never peak above the energy of the lowest channel, 68 keV. Energy spectra associated with the two magnetic storms on October 2 and October 12 are presented. After the storms the fluxes were higher than before. This is particularly true at the lower energies

XUM

measured. Quiet-time pitch-angle distributions near the local noon–midnight meridian clearly show the east–west effect caused by the radial gradient in the fluxes. The pitch-angle distributions at local midnight show the drift loss cone predicted by Roederer. (auth) (USGRDR)

2952 (N–70–33955) MEASUREMENT OF AVERAGE ELECTRON DENSITY BETWEEN 75 AND 80 KILOMETERS. Reynolds, D. A.; Sechrist, C. F. Jr. (Illinois Univ., Urbana. Aeronomy Lab.). 1 May 1970. 86p. (NASA-CR–109850). NTIS.

Instrumentation capable of recording variables necessary for the computation of average electron density between 75 and 80 km was developed. The instrumentation is used in conjunction with the existing partial-reflection facility. Data output of the instrumentation is recorded on paper tape in binary-coded decimal form. To handle the paper tape, a program was developed that produces, for each data acquisition interval, a mean electron density at 77.5 km and data necessary for a time plot of electron density at 77.5 km. (auth) (STAR)

2953 ATMOSPHERIC RESPONSE TO HEATING WITHIN A STABLE AURORAL RED ARC. Roble, R. G.; Dickinson, R. E. (National Center for Atmospheric Research, Boulder, Colo.). Planet. Space Sci.; 18: 1489-98(Oct 1970).

The electron conduction hypothesis for the stable auroral red arc is assumed; i.e., energy conducted in the electron gas from the magnetosphere along the geomagnetic field lines into the ionosphere heats the ambient F-region electrons. These, in turn, excite the (^{1}D) term of atomic oxygen by electron impact giving rise to the λ6300 emission characteristic of the arc. A two-dimensional model of a red arc is constructed using solutions of the one-dimensional electron heat-conduction equation so that the calculated two-dimensional λ6300 volume emission-rate contours model the contours determined from photometric observations. The resulting electron temperature, λ6300 volume emission-rate, and neutral heating-rate contours are obtained for the arc model. More than 99% of the energy conducted from the magnetosphere is transferred to the neutral gas in the ionosphere through elastic and inelastic collisions of the electrons and ions with the neutrals. A two-dimensional steady-state dynamic model of the neutral thermosphere incorporating thermal conduction, viscosity, and ion drag is used to calculate the temperature perturbation and circulation pattern within the arc region. The pressure forces originating from the red-arc heating drive a thermal cell with upward motion in the red-arc region and a slow subsidence over a much greater area outside the arc. The adiabatic warming and cooling by these motions significantly reduce the neutral temperature increase within the red arc compared to the increase obtained in the absence of motions, but the warming and cooling enlarge the horizontal scale of the region of temperature increase. (auth) (UK)

2954 NEUTRAL-AIR WINDS IN THE IONOSPHERIC F REGION FOR AN ASYMMETRIC GLOBAL PRESSURE SYSTEM. Challinor, R. A. (Radio and Space Research Station, Slough, Eng.). Planet. Space Sci.; 18: 1485-7(Oct 1970).

Corrections are made for data in a previous paper by the author (NSA 23:42083) in which F-region neutral-air winds driven by both pressure gradients and moving ions were calculated. Unfortunately, the directions of the ion velocities used in the previous calculations were in error by 180°. The effect of ion velocities on the winds is generally small, and negligible at medium and high latitudes, so that the major conclusions reached before were valid. (auth) (UK)

2955 VARIATIONS IN THE EARTH'S SURFACE MAGNETIC FIELD FROM THE MAGNETOPAUSE CURRENT SYSTEM. Olson, W. P. (McDonnell Douglas Astronautics Co., Santa Monica, Calif.). Planet. Space Sci.; 18: 1471-84(Oct 1970).

The magnetic field at the Earth's surface produced by the magnetopause current system was calculated with solar wind conditions (density, speed, and direction) taken as constant throughout the year. The strength and shape of this current system (and its associated field) depend upon the orientation of the geomagnetic dipole axis with respect to the direction of the solar wind. The magnetopause currents therefore produce seasonal as well as daily variations in the Earth's surface magnetic field. The daily variations display several of the major features of the observed S_q pattern, including seasonal changes and dependence on longitude. Also in agreement with the observations, the daily field has a maximum at about 11:30 a.m. (local time) owing to the direction of the solar wind (8° west of the optical Sun–Earth line). The magnetopause currents produce both annual and semiannual variations similar in form to the observed patterns. When the contribution from Earth-induced currents is taken into account, the magnetopause current system is found to be the source of about 20% of the daily and seasonal variations in the Earth's surface magnetic field. It is concluded that the ionospheric dynamo is not the only source of the S_q variations and that at least two other magnetospheric current systems, the neutral sheet and ring currents, may also make contributions to the quiet magnetic variations at the surface of the Earth. (auth) (UK)

2956 THERMAL COUPLING BETWEEN THE UPPER F2 REGION AND THE MAGNETOSPHERE: HEAT FLUXES AND ENERGY PRODUCTION. Bauer, P.; Lejeune, G.; Petit, M. (Centre National d'Etude des Telecommunications, Issy-les-Moulineaux, France). Planet. Space Sci.; 18: 1447-70(Oct 1970).

Measurements of electron and ion temperatures and electron density in the F region over Saint-Santin during the winter predawn period allow a determination of the energy given to the ambient electron gas by the photoelectron flux streaming into the magnetosphere. The energy input per thermal electron is 0.75 eV s^{-1} during the predawn period and 2.25 eV s^{-1} during daytime. The corresponding photoelectron flux is always larger than 10^9 cm^{-2} s^{-1} if angular scattering is ignored in the magnetosphere. The magnetospheric electron temperature ranges from 3000 to 5500°K, and the difference between the ion temperature and the electron temperature is of the order of 100°K. (auth) (UK)

2957 E_s LAYER CHARACTERISTICS DETERMINED FROM SPACED IONOSONDES. Goodwin, G. L.; Summers, R. N. (Univ. of Queensland, Australia). Planet. Space Sci.; 18: 1417-32(Oct 1970).

An analysis was made of ionograms recorded for approximately 1900 hr during 12 months with an average of six ionosonde receivers distributed over an area of some 700 km^2. The E_s-layer characteristics (measured by fE_s and f_bE_s) remained essentially constant for one-third of the time during which E_s was recorded. Changes in E_s characteristics for two-thirds of the time were practically all ascribed to the movements of small-scale E_s frontal irregularities during the daytime, but at night a large minority of the changes was attributed to the formation and dissipation of E_s layers having horizontal dimensions of the order of a few hundred km. Changes in fE_s could not be ascribed to the movement of E_s layer edges. The small-scale frontal irregularities, which produced range-spreading of E_s echoes, consisted apparently of ridges and troughs of enhanced and diminished E_s electron density respectively. Velocities of horizontal motion of the irregularities were estimated from the time delays between the occurrences of maxima or minima in fE_s or f_bE_s recorded on the various spaced ionograms. Irregularity wavelengths were generally 10 to 40 km. (auth) (UK)

2958 STATISTICAL PROPERTIES OF WORLD-WIDE FLUCTUATIONS IN THE MAGNETIC FIELD. Bhargava, B. N.; Rao, D. R. K. (Colaba Observatory, Bombay). Planet. Space Sci.; 18: 1381-5(Sep 1970).

The common periods with which world-wide geomagnetic fluctuations occur in the period range of 6 to 150 min during disturbed conditions were computed from spectrum analysis of horizontal force at several equatorial stations. The spectrums suggest a dominant period with peak power near 120 min and a half-power width of about 100 min. Shorter-period secondary oscillations with periods around 25 and 37 min were also noticed in the spectrums. The longer-period oscillations appear to be caused by changes in the solar wind structure. The periods associated with relatively faster oscillations agree fairly well with the eigenperiods computed by several workers from their studies of the natural resonances of the geomagnetic tail. (auth) (UK)

2959 EFFECT OF MAGNETICALLY CONJUGATE PHOTOELECTRONS ON O I(6300 A). Noxon, J. F.; Johanson, A. E. (Harvard Univ., Cambridge, Mass.). Planet. Space Sci.; 18: 1367-79(Sep 1970).

Predawn enhancement of the O I(6300 Å) line at Boston, U. S. A., (L = 3.1) appears to be primarily due to an increase in F-region ionic recombination. A residual component due to direct excitation of atomic oxygen by magnetically conjugate photoelectrons is probably present. The upper limit on this component is about 20 Rayleighs (R). (auth) (UK)

2960 SELF-CONSISTENT THEORY OF THE MAGNETOTAIL. Beard, David B.; Bird, Michael; Huang, Yao Hui (Univ. of Kansas, Lawrence). Planet. Space Sci.; 18: 1349-55(Sep 1970).

The magnetic fields were calculated everywhere in the magnetotail, assuming the magnetotail to be a cylinder of constant radius with a sheet of current bisecting its center; the current magnitude and spatial dependence are a best fit to present satellite observa-

XUM

tions. Particle motions were then computed in this calculated field. It was shown that these computed particle motions yield electrical currents that closely approximate the initial assumed current source of the magnetic field. These computed currents furnish an excellent basis for a second cycle of field, particle motion, and current computation for a rapidly convergent self-consistent calculation. The magnetic field at the center of the neutral sheet (including the planetary dipole field) is perpendicular to the current sheet, relatively small (~1 to 2 gamma), unidirectional, and monotonically decreasing with distance from the planet permitting no X-type field configuration as required for field annihilation or reconnection. (auth) (UK)

2961 PRE-DAWN ENHANCEMENT OF lambda6300 A AIRGLOW AT HIGHER MIDLATITUDES. Nichol, D. G. (Univ. of Tasmania, Hobart, Australia). Planet. Space Sci.; 18: 1335-47(Sep 1970).

All-sky records of λ6300 Å airglow intensity were obtained at Hobart (geomagnetic latitude, 54°S) for the years 1968 and 1969. These observations cover geomagnetic latitudes 44 to 64°S. A winter predawn enhancement (P.D.W.) of about 50 R is observed for this line down to about 60°S. The commencement time of the phenomenon is usually inconsistent with the increase in production of photoelectrons at the magnetically conjugate point (M.C.P.). In addition ionospheric evidence points to an increase in the dissociative recombination of O_2^+ as being a major cause of the enhancement. However, it is proposed that M.C.P. photoelectrons do play an important role in the P.D.E. but that the commencement of the P.D.E. is controlled by the morphology of the neutral atmosphere winds superposed on effects due to exospheric cooling. (auth) (UK)

2962 MINOR-ION DIFFUSION IN THE F2 REGION OF THE IONOSPHERE. Schunk, Robert W.; Walker, James C. G. (Yale Univ., New Haven). Planet. Space Sci.; 18: 1319-34(Sep 1970).

The ionospheric diffusion coefficients were evaluated to the second approximation of Chapman and Cowling in order to check the first approximation values which are currently in use. It was found that the first approximation to the ambipolar diffusion coefficient is quite accurate, but that similar diffusion coefficients for the minor ions are in error by as much as a factor of 2. Coulomb collisions couple minor ion drift velocities closely to the velocity of the O^+ ions. Consequently, minor ion densities in the F-region are very sensitive to fluxes of ionization into or out of the ionosphere. To illustrate this sensitivity solutions are presented of the continuity equations for O^+, H^+, He^+, and N^+ ions in the F-region for a range of topside boundary conditions. It is found that H^+ densities are significantly reduced if the upward O^+ flux approaches 9×10^8 cm^{-2} sec^{-1} or if the upward H^+ flux approaches 2.5×10^7 cm^{-2} sec^{-1}. For He^+ the corresponding limits are 4×10^8 cm^{-2} sec^{-1} of O^+ or 4.3×10^6 cm^{-2} sec^{-1} of He^+, and for N^+ the limits are 2×10^8 cm^{-2} sec^{-1} of O^+ or 9.5×10^5 cm^{-2} sec^{-1} of N^+. (auth) (UK)

2963 STUDY OF THE IRREGULARITIES IN THE NIGHT-TIME EQUATORIAL E REGION USING A LANGMUIR PROBE AND PLASMA NOISE PROBE. Prakash, Satya; Gupta, S. P.; Subbaraya, B. H. (Physical Research Lab., Ahmedabad, India). Planet. Space Sci.; 18: 1307-18(Sep 1970).

A rocket-borne Langmuir-probe and plasma-noise-probe experiment, conducted at 2300 hr IST on 29 August 1968 from Thumba near the magnetic equator, revealed the existence of electron densities varying between 10^3 and 10^4/cm^3 in the height range of 95 to 120 km and a deep valley in the 120 to 140 km region. The electron density in the valley was of the order of a few hundreds per cm^3. Large-scale structures in the electron density profile in the 95 to 120 km region were observed with vertical scale sizes of a few kms and a horizontal extent of the order of 50 km. In these structures the electron density was observed to vary by factors lying between 4 and 25. Small-scale irregularities with scale sizes lying in the ranges 30 to 300 m and 1 to 15 m that were present in the ambient medium were detected during the flight. While these irregularities were found to occur randomly and in the form of bursts, most of them were located only in regions where the background electron density exhibits large negative gradients. The positions of occurrence of the 30 to 300 m irregularities were found to confirm qualitatively that these irregularities are generated by a cross-field instability mechanism which needs a background electron density gradient with a specific sign. While the smaller scale size irregularities (1 to 15 m) also occur in regions where the cross-field instability mechanism can operate they cannot be directly explained on the basis of the present theories of the cross field instability. Hence either the present theories need modification, or there exists another mechanism which is responsible for these irregularities. However, even if a separate mechanism were to exist, the present data indicate that depending on the relative orientation of the ambient electric field and the electron density gradients, the cross-field instability mechanism can promote or inhibit the production of these irregularities. (auth) (UK)

2964 MID-LATITUDE MAGNETIC BAYS AND AURORAL ABSORPTION. Lichtenstein, Pearl R. (Rensselaer Polytechnic Inst., Troy, N. Y.). Planet. Space Sci.; 18: 1301-6(Sep 1970).

One hundred and thirty two simple isolated magnetic bay events at Fredericksburg, Virginia, were studied in terms of their H, Z, and D components and found to fall into several distinct groups. Nighttime bays are sharp, highly correlated with 18 MHz auroral absorption at midlatitude stations, and their H and Z components reverse sign near 2100 hr LT. Daytime bays are generally diffuse and only slightly correlated with midlatitude riometer absorption. The high degree of correspondence between sharp bays and riometer absorption suggests that the same precipitating particles may be responsible for both. (auth) (UK)

2965 PENETRATION OF SOLAR PARTICLES TO IONOSPHERIC HEIGHTS AT LOW LATITUDES. Lanzerotti, L. J.; Graedel, T. E. (Bell Telephone Labs., Murray Hill, N. J.). Nature (London); 228: 45(3 Oct 1970).

Recently presented evidence for the possiblity of the penetration of high-energy solar particles to ionospheric heights at the equator is discussed (Ganguly and Rao, Nature 225: 169 (1970)). This is interesting in the context of recent work on the penetration of solar particles to low magnetospheric L values at the equator. The evidence is examined and it is concluded that there is little basis for the contention that solar particles can penetrate directly to low altitudes and thus influence ionospheric absorption at the equator. Proton data obtained by the Bell Laboratories instrument on ATS-1 at synchronous altitude were examined for evidence of solar particle enhancement at the time reported by Ganguly and Rao; no evidence for such enhancement was found. The data from the solar-proton monitoring experiment on Explorer 34 were also examined for proton enhancement. Association with flares is also discussed. (UK)

2966 SEASONAL CHANGES IN THE IONOSPHERE. Munro, G. H. (Univ. of Sydney). Nature (London); 228: 147-8(10 Oct 1970).

In most studies of the changes that occur in the ionosphere during the year, statistical methods have been employed, but this type of examination tends to mask the fundamental changes. An important feature is that, in the southern hemisphere, the change is abrupt in the Sept.–Oct., equinox but more gradual in March–April. These changes appeared consistently during Australian investigations of travelling ionospheric disturbances as a reversal of the N–S component of TID travel in late Sept. or early Oct. This effect also showed in satellite observations. It was indicated that a magnetic storm could trigger the change. A closer examination of a comprehensive set of travelling disturbance data, covering a period of 12 years, is described (April 1948 to Oct. 1959), covering a complete sunspot cycle. The data clearly showed that the seasonal change in direction was not a smooth transition, but that there were fluctuations between summer and winter directions lasting for a few weeks, this pattern being particularly obvious in Sept.–Oct. The main changes all occurred within the first ten days of Oct., the actual day apparently depending on a magnetic increase. In order to confirm that the effect was essentially equinoctial, a check of magnetic indices and disturbances was made for the other months of the years. It appears that the Sept.–Oct. equinox is a period of instability in the ionosphere, and that the ionosphere is then particularly susceptible to fluctuations in the magnetic field, which result in changes in the distribution of ionisation and corresponding changes in the direction of travel of disturbances. (UK)

2967 IMPEDANCE MEASUREMENTS OF A LOOP ANTENNA IN THE TOPSIDE IONOSPHERE. Gregory, P. C. (Univ. of Manchester, Jodrell Bank, Eng.). Planet. Space Sci.; 18: 1357-65(Sep 1970).

Measurements at three frequencies of the resistive and reactive impedance of a small loop antenna flown on the satellite Ariel III are presented. The reactive impedance was observed to remain constant and equal to its free space value while the resistive component exhibited a large increase with increasing electron plasma frequency. The additional antenna resistance does not result from an increased electromagnetic radiation resistance and it appears very unlikely that electron plasma waves are responsible. (auth) (UK)

2968 SIMPLE SENSOR FOR THE MEASUREMENT OF ATOMIC OXYGEN HEIGHT PROFILES IN THE UPPER ATMOSPHERE. Henderson, W. R. (Aeronomy Lab., Boulder, Colo); Schiff, H. I. Planet. Space Sci.; 18: 1527-34(Oct 1970).

XUM

A sensor suitable for measuring the height profile of atomic oxygen in the atmosphere above 70 km is described. It consists of a thin film of silver deposited on a pyrex rod of dimensions sufficiently small to permit molecular flow transport to its surface at these altitudes. The instantaneous atom flux to the surface can be evaluated from the rate of change of the electrical resistance of the film. Laboratory calibrations on a series of such sensors indicate an accuracy of at least 25% by simultaneous measurements with four sensors and increased accuracy with the use of additional sensors. Its small size, simplicity, specificity for O atoms, and modest power and telemetry requirements make these sensors most attractive for use in rocket and satellite instrument packages. (auth) (UK)

2969 RELATIONSHIP BETWEEN OUTER-BELT ELECTRON INTENSITY AND GEOMAGNETIC ACTIVITY INDEXES. Vernov, S. N.; Kuznetsov, S. N.; Lopatina, G. B.; Stolpovskii, V. G. (Moscow State Univ.). Geomagn. Aeron. (USSR) (Engl. Transl.); 10: 167-71(1970).

Translated from Geomagn. Aeron.; 10: 214-20(1970).

The relationship between the intensity of electrons with $E_e \geq 150$ keV on $L \geq 5$ and the geomagnetic activity indexes is investigated. It is found that on $L \sim 6$ there is good anticorrelation between electron intensity and the AU index. In the unstable radiation zone there is good correlation between electron intensity and the K_p index. It is demonstrated that the AU, Al, and K_p indexes have independent values, and each characterizes a specific aspect of geomagnetic disturbance. (auth)

2970 SPECTRUM OF ALFVEN OSCILLATIONS OF THE MAGNETOSPHERE. Gul'el'mi, A. V. (Inst. of Terrestrial Physics, Moscow). Geomagn. Aeron. (USSR) (Engl. Transl.); 10: 182-6(1970).

Translated from Geomagn. Aeron.; 10: 234-9(1970).

The spectrum of one-dimensional (Alfvén) oscillations of the magnetosphere is found by numerical integration. Three modes are examined: toroidal and undulating, which approximate the oscillations of thin magnetic shells, and twisted. It is shown that if plasma concentration decreases along the lines of force more slowly than r^{-6}, the nonequidistance of the harmonics of all three modes is positive. The natural frequencies of the three modes are practically indistinguishable, starting from the third to fourth harmonics. (auth)

2971 MEASUREMENT OF IONOSPHERIC PARAMETERS FROM RECORDS AT SPACED POINTS OF THE DOPPLER AND FARADAY EFFECTS OF COHERENT SIGNALS FROM GEOPHYSICAL ROCKETS. Misyura, V. A.; Krakhmal'nikov, E. B.; Zinchenko, G. N.; Firsakov, A. S.; Slutsker, S. M. Geomagn. Aeron. (USSR) (Engl. Transl.); 10: 190-4(1970).

Translated from Geomagn. Aeron.; 10: 244-9(1970).

Results are reported of measurements of the vertical electron density profiles, the integral content of electrons in a vertical column of the ionosphere, and of horizontal gradients to a height of ~500 km. The Doppler and Faraday effects of coherent signals from geophysical rockets were recorded at several spaced points at middle latitudes in the Soviet Union. (auth)

2972 RELATIONSHIP BETWEEN F2-LAYER IONIZATION IN THE NORTHERN AND SOUTHERN HEMISPHERES DURING THE SOLSTICES. Besprozvannaya, A. S. (Arctic and Antarctic Scientific Research Inst., Leningrad). Geomagn. Aeron. (USSR) (Engl. Transl.); 10: 195-8(1970).

Translated from Geomagn. Aeron.; 10: 250-4(1970).

A comparison is made between the noon critical F2-layer frequencies in the northern and southern hemispheres for: 1) different zenith distances of the Sun at a given latitude and at corresponding latitude in the opposite hemisphere and 2) different zenith distances of the Sun at fixed latitudes in the northern and southern hemispheres. (auth)

2973 DEPENDENCE OF THE PLASMA SCALE HEIGHT IN THE UPPER F2 REGION ON MAGNETIC ACTIVITY. Fatkullin, M. N. (Inst. of Terrestrial Magnetism, Ionosphere, and Radio Wave Propagation, Moscow). Geomagn. Aeron. (USSR) (Engl. Transl.); 10: 199-203(1970).

Translated from Geomagn. Aeron.; 10: 255-61(1970).

The influence of magnetic activity on the scale height of the plasma in the outer part of the F2 region is investigated on the basis of Alouette-1 data. The distributions of H_0 (scale height for $a_p = 0$) and of $\Delta H/\Delta a_p$ are computed for the midnight hours in the summer of 1963. The effective temperature of the ionosphere is computed for a height of 300 km for quiet and disturbed conditions, as are the latitudinal and vertical distributions of the average ion mass. (auth)

2974 METHOD OF FINDING THE N(h) PROFILE BY ANALOG COMPUTER TECHNIQUES. Kadukhin, G. F.; Shlionskii, Sh. G. (Inst. of Terrestrial Magnetism, Ionosphere, and Radio Wave Propagation, Moscow). Geomagn. Aeron. (USSR) (Engl. Transl.); 10: 208-10(1970).

Translated from Geomagn. Aeron.; 10: 268-72(1970).

A method is described for computing the N(h) profile from ionograms by searching on a special-purpose analog-digital computer permitting computation of nonmonotonic N(h) profiles by using for the computation program the integral equation of the relationship between the N(h) profile and the ionogram without inversion or other transformations. (auth)

2975 COMPLETE FUNCTIONS IN THE ANALYSIS AND REPRESENTATION OF DISTANT ATMOSPHERICS ON THE BASIS OF THE COORDINATES OF THEIR ZEROS. Kostygov, K. I.; Zorin, V. A. (Leningrad State Univ.). Geomagn. Aeron. (USSR) (Engl. Transl.); 10: 211-14(1970).

Translated from Geomagn. Aeron.; 10: 273-7(1970).

In the analysis and representation of atmospherics, certain classes of complete functions and expansions of them as infinite or finite products involving the zeros of the function are used. Simple representations of distant atmospherics as complete functions of finite degree are constructed that are based on the results of experimental analysis of the forms observed and that arise as a solution of the problem of reconstructing a signal from the known coordinates of its zeros. (auth)

2976 STATISTICAL PATTERNS OF AURORAL HYDROGEN EMISSION. Sobolev, V. G. (Inst. of Terrestrial Physics, Moscow). Geomagn. Aeron. (USSR) (Engl. Transl.); 10: 225-7(1970).

Translated from Geomagn. Aeron.; 10: 291-4(1970).

The dependence of the intensity of hydrogen emission and of the relative position of hydrogen fields and visible auroras on magnetic activity is analyzed on the basis of observations at Loparskaya and Zvenigorod from 1957 to 1966. The influence of the relative position of hydrogen fields and of auroras on the H_α contour at the magnetic zenith is estimated. (auth)

2977 DEVELOPMENT OF A POLAR STORM. Khorosheva, O. V.; Darchieva, L. A. (Moscow State Univ.). Geomagn. Aeron. (USSR) (Engl. Transl.); 10: 228-30(1970).

Translated from Geomagn. Aeron.; 10: 295-9(1970).

The conclusion is reached on the basis of magnetic field and auroral data that disturbances (polar storms) appear and develop simultaneously over the entire auroral oval. The result is interpreted as the consequence of the simultaneous dumping of a soft plasma along the entire boundary of trapped radiation. The conclusions derived by some researchers that there is a time shift in the course of a storm at different meridians, which is usually interpreted as the longitudinal drift of the disturbance source, are believed to be erroneous. The time shift is thought to be the consequence of the incorrect determination of the instant of commencement of a storm. (auth)

2978 DEVELOPMENT OF AN ELEMENTARY MAGNETIC DISTURBANCE. Ivliev, D. Ya.; Pudovkin, M. I.; Zaitseva, S. A. (Leningrad State Univ.). Geomagn. Aeron. (USSR) (Engl. Transl.) 10: 231-4(1970).

Translated from Geomagn. Aeron.; 10: 300-4(1970).

The development of an elementary magnetic storm in the polar cap is examined. It is shown that the appearance of an auroral electrojet on the night side of the auroral zone is preceded by that of a specific magnetic disturbance on the day side of the polar cap. The current system of this disturbance is investigated. (auth)

2979 MERIDIONAL MOVEMENT OF AURORAL ABSORPTION BAYS. Driatskii, V. M.; Shumilov, O. I. (Arctic and Antarctic Scientific Research Inst., Leningrad). Geomagn. Aeron. (USSR) (Engl. Transl.); 10: 235-9(1970).

Translated from Geomagn. Aeron.; 10: 305-11(1970).

Galactic noise records show a systematic delay in the appearance of auroral absorption at stations located to the north and south of some average geomagnetic latitude, 65 and 66°. The rate of northward movement decreases gradually with distance from the region of initial injection. (auth)

2980 POSSIBLE REASON FOR THE DEPENDENCE OF THE DISTANCE TO THE MAGNETOSPHERE BOUNDARY ON GEOGRAPHIC LONGITUDE. Rudneva, N. M. (Inst. of Terrestrial Magnetism, Ionosphere, and Radio Wave Propagation, Moscow). Geomagn. Aeron. (USSR) (Engl. Transl.); 10: 240-2(1970).

Translated from Geomagn. Aeron.; 10: 312-15(1970).

The distance to the boundary of the magnetosphere can depend on the strength of electric currents flowing along geomagnetic lines of force in it. The main geomagnetic field differs at different longitudes. These differences may result in the direction of electric currents appearing in the magnetosphere along lines of force being different at different longitudes. The relatively low density

XUM

of these currents may create the dependence of the distance to the magnetosphere boundary on geographic longitude. (auth)

2981 INTERPLANETARY MAGNETIC FIELD FLUX AND THE K_p INDEX OF MAGNETIC ACTIVITY. Ivanov, K. G.; Mikerina, N. V. (Inst. of Terrestrial Magnetism, Ionosphere, and Radio Wave Propagation, Moscow). Geomagn. Aeron. (USSR) (Engl. Transl.); 10: 256-7(1970).

Translated from Geomagn. Aeron.; 10: 331-2(1970).

A formula is expressed for the K_p index of magnetic activity as a function of equivalent planetary amplitudes a_p, expressed in units of 2γ. After assuming an expression for a_p, a more specific expression is given for K_p. The variations of K_p during magnetospheric storms must correlate with the magnetic field and with the factor determining the large-scale variation of the interplanetary field. The best correlation must be with the flux of reconnecting lines of force that include the field and velocity. A confirmation of this analysis is made from the variations of S, reconnecting lines of force, and the corresponding variations of K_p with allowance for the lag of observations on Earth behind observations in space, according to Mariner-2 data, Sept. 9 to 13, 1962. (J.C.W.)

2982 MAGNETIC FIELD OF THE NEUTRAL SHEET IN THE TAIL OF THE MAGNETOSPHERE. Ivanov, K. G. (Inst. of Terrestrial Magnetism, Ionosphere, and Radio Wave Propagation, Moscow). Geomagn. Aeron. (USSR) (Engl. Transl.); 10: 257-8(1970).

Translated from Geomagn. Aeron.; 10: 333-4(1970).

The magnetic field of the neutral sheet in the tail of the magnetosphere may decrease with proximity to the Earth because the volume of magnetic tubes that move toward the Earth decreases and can lead to an increase in the gas pressure and a decrease in magnetic pressure in the tubes. A computation of this decrease of the field with proximity to the Earth is made for magnetically quiet conditions and for the morning sector of the magnetosphere. The distribution of the magnetic field in the tail of the magnetosphere was taken from Explorer-33 data. Assuming the computation approximate and the experimental data dependent on local time, the agreement is satisfactory. (J.C.W.)

2983 MEASUREMENT OF TOTAL ELECTRON CONTENT IN THE POLAR IONOSPHERE FROM THE RECORDED SIGNALS OF THE 3D SATELLITE. Solodovnikov, G. K.; Misyura, V. A.; Migunov, V. M.; Gorbachev, I. I. Geomagn. Aeron. (USSR) (Engl. Transl.); 10: 258-60(1970).

Translated from Geomagn. Aeron.; 10: 334-5(1970).

Results are given of the determinations of the total electron content in the polar ionosphere of both hemispheres during high solar activity from data on the Faraday effect of signals from the 3d satellite at a frequency of 20 MHz at Murmansk and at the Antarctic station Mirny in May to July, 1968. Data from 210 observations at Murmansk and 106 at Mirny were analyzed. Results show that an increase in electron density with solar activity is much smaller in the polar ionosphere than at middle latitudes, probably due to the difference in ionization processes and the movement of charges in these regions. (J.C.W.)

2984 CYCLIC VARIATIONS OF THE PARAMETERS A_0 AND n OF THE LATITUDE DEPENDENCE OF F2-LAYER IONIZATION AT NOON. Besprozvannaya, A. S.; Yudovich, L. A. (Artic and Antarctic Scientific Research Inst., Leningrad. Inst. of Terrestrial Magnetism, Ionosphere, and Radio Wave Propagation, Moscow). Geomagn. Aeron. (USSR) (Engl. Transl.); 10: 261-2(1970).

Translated from Geomagn. Aeron.; 10: 336-7(1970).

An analytical formula is given that was proposed on the basis of the hypothesis of the relationship between ionization at magnetically conjugate points for describing the geographic distribution of F2-layer ionization at noon. A_0 and n are geographic distribution parameters and are found empirically. From graphs that were constructed, it is shown that A_0 is a function of $\log \phi_{10.7}$ (solar radio noise flux ϕ at $\lambda = 10.7$ cm) for the four seasons. The second parameter of the geographic distribution described by the formula is the exponent n of the cosine of the zenith angle of the sun and varies differently in the cycle in different seasons. In years of maximum solar activity the n values are low in winter and increase sharply with increasing solar declination both in the northern and southern hemispheres. (J.C.W.)

2985 INFLUENCE OF THE MAGNETIC FIELD ON THE LONGITUDINAL DISTRIBUTION OF THE MEAN ANNUAL CHARACTERISTIC OF F2-LAYER IONIZATION. Likhachev, M. A. (Siberian Physical-Technical Inst., Tomsk, USSR. Tomsk State Univ., USSR). Geomagn. Aeron. (USSR) (Engl. Transl.); 10: 262-3(1970).

Translated from Geomagn. Aeron.; 10: 338-9(1970).

A statistical analysis of the latitudinal distribution of the mean annual characteristic showed that ionization parameter $\bar{y}$ has a small dispersion and can serve as a reliable zonal characteristic of the mean annual state of ionization for middle latitudes (NSA 23: 20786). A comparison of $\bar{y}$ deviations at individual stations at middle latitudes in the eastern and western hemispheres revealed also a pattern in the longitudinal distribution associated with the effect of the constant geomagnetic field on F2-layer ionization. Influence of the magnetic field was investigated using f_0F2_{max} data from 18 middle-latitude stations in the northern hemisphere at closely located geographic latitudes and different geomagnetic latitudes. The results obtained indicate that, in the course of a year, the ionization level at the F2-layer maximum at a single geographic latitude is lower at stations located in closer proximity to the north geomagnetic pole. The magnitude of this effect is controlled by the average annual solar activity level. (J.C.W.)

2986 INFLUENCE OF TRAVELING DISTURBANCES ON THE DRIFT OF SMALL-SCALE INHOMOGENEITIES IN THE IONOSPHERIC F2 LAYER. Zagulyaeva, V. A.; Kashin, A. A.; Sharadze, Z. S. (Inst. of Terrestrial Magnetism, Ionosphere, and Radio Wave Propagation, Moscow. Moscow State Univ. Tbilisi State Univ., USSR). Geomagn. Aeron. (USSR) (Engl. Transl.); 10: 264-5(1970).

Translated from Geomagn. Aeron.; 10: 340-1(1970).

An attempt is made to determine the influence of traveling disturbances on the drift of small-scale inhomogeneities in the F2 layer. Drifts were recorded continuously over 1 to 2 hours by spaced reception at two frequencies simultaneously. The investigations were made at Tbilisi in Dec. 1966 and Feb. 1967. It was found that traveling disturbances, accompanied by vertically traveling ones, formed near $N_{max}F2$ and gradually lowering, produced quasi-periodic drift variations. Computations of N(h) profiles in the same time interval also showed quasi-periodic variations in electron density at fixed levels in the ionosphere with a period of 30 min. It was found that drift begins to fluctuate 10 to 15 min before the appearance of vertically traveling disturbances near $N_{max}F2$. The changes in drift behavior observed in the presence of traveling disturbances can be explained by the slope mechanism. The quasi-periodic variations in drift velocity with a period of 10 to 40 min point to the wave-like nature of traveling ionospheric disturbances, which are interpreted as internal gravity waves. (J.C.W.)

2987 INFLUENCE OF ATMOSPHERIC VARIABILITY ON DIURNAL VARIATIONS OF IONIC STRUCTURE IN THE F1 REGION. Koshelev, V. V.; Shchepkin, L. A. (Siberian Inst. of Terrestrial Magnetism, Ionosphere, and Radio Wave Propagation, Irkutsk, USSR). Geomagn. Aeron. (USSR) (Engl. Transl.); 10: 265-7(1970).

Translated from Geomagn. Aeron.; 10: 342-3(1970).

Results are presented of modeling the ionic structure using the diurnally varying atmospheric model of Jacchia. Values of the coefficients of the basic ionospheric reactions were chosen that are not inconsistent with the experimental data, and which give internal consistency between the given model of the neutral atmosphere and the observed diurnal variations of electron density. It was found that within the framework of the stationary model, the relative concentration of the 0^+ ions ($[0^+]/n_e$) increases in the morning hours until noon and symmetrically decreases toward evening. The relative concentrations of the molecular O_2^+ and NO^+ ions vary in the opposite way. The modeling is based on data on diurnal variations in n_e at various heights obtained at Slough in June, 1953 from vertical ionospheric soundings. Diurnal variations are given of the relative concentrations $[O^+]/n_e$, $[NO^+]/n_e$, and $[O_2^+]/n_e$ at 150, 170, 190, and 210 km heights. An important result is the possibility of a theoretical explanation of the reduction in $[O^+]/n_e$ when solar zenith angles $\chi < 55°$. (J.C.W.)

2988 CONNECTION BETWEEN THE PARAMETERS OF THE F2 AND F1-LAYERS AND THE PREDICTION OF DIURNAL N(h)-PROFILES AND h'f CHARACTERISTICS. Shapiro, B. S. (Inst. of Terrestrial Magnetism, Ionosphere, and Radio Wave Propagation, Moscow). Geomagn. Aeron. (USSR) (Engl. Transl.); 10: 267-9(1970).

Translated from Geomagn. Aeron.; 10: 344-5(1970).

The form and parameters of the diurnal N(h) profiles and h'f characteristics of the F region are known to change sharply at the appearance or disappearance of the F1 layer. The dependence of the appearance of F1 layer on the critical frequencies of F2 can be explained by the fact that the quantity f_0F2 reflects a change in the loss coefficient in the F region, upon which the formation of F1 layer intrinsically depends. Forecasts of N(h) have been constructed from previous data and give the probability of the appearance and the effective size-shape factors of the F1 layer, independent of the prediction of f_0F1 and f_0F2. The author indicates a possibility of connecting the appearance and size-factors of F1 to f_0F1 (by the ratio of f_0F1/f_0F2). This prediction

XUM

allows for the values at which the bifurcation of the F region will occur, what its extent will be, and how the parameters N(h) and h'f will vary. From the theory of the formation of F1, it may be assumed that for given values of the sunspot number and the solar zenith angle, the bifurcation of the F trace is tied to a definite ratio of f_0F1/f_0F2. Equations are given to predict the bifurcation of the F region as a function for quiet conditions, and using the same data, the bifurcation of the F region may be predicted during a storm. An attempt is made to indicate in the forecasts for daytime magnetic disturbances, the index K that must precede a predicted bifurcation of the F region by 6 to 7 hours, provided the decrease in f_0F2 is ascribed to an increase in the loss coefficient under the influence of an increase in the temperature during a storm. (J.C.W.)

2989 INFLUENCE OF THE DEPTH OF THE INTERLAYER IONIZATION VALLEY OF F-REGION HEIGHTS. Vinnikova-Gulyaeva, T. L. (Inst. of Terrestrial Magnetism, Ionosphere, and Radio Wave Propagation, Moscow). Geomagn. Aeron. (USSR) (Engl. Transl.); 10: 269-71(1970).

Translated from Geomagn. Aeron.; 10: 346-7(1970).

The estimation of the interlayer ionization distribution may be made after obtaining the N(h) profile of the F region. In the inversion of the integral equation, connecting the true with the virtual heights of the ionosphere, it is assumed that ionization increases monotonically with height. This condition does not hold in the interlayer region if it has an ionization valley. In this case it is suggested that the heights of the E layer in this region be excluded from analysis as carrying one-sided information and be replaced by a single-valued equivalent ionization distribution. Examples are illustrated of computations of N(h) with a deep and shallow valley by the least squares method on the assumption that the first derivative is constant. Previous papers devoted to nonmonotonic computations of N(h) mention that the solution in the F region is obtained regardless of the depth of the valley, utilizing the "new start" and other methods for the computation of F-region heights without allowance for the solution in the E region. The author believes it more natural to use all the data of an ionogram and to select a suitable valley depth in computing the heights of the F region. The idea of replacing the nonmonotonic interlayer ionization by an equivalent linear distribution has been previously explored. (J.C.W.)

2990 INFLUENCE OF THE F2 LAYER ON IONOSPHERIC SCATTER LINKS (d < 2000 KM) IN THE SHORT-WAVE FREQUENCY RANGE. Ashkaliev, Ya. F. (Ionospheric Sector, Alma-Ata, USSR). Geomagn. Aeron. (USSR) (Engl. Transl.); 10: 272-3(1970).

Translated from Geomagn. Aeron.; 10: 350-1(1970).

Weak, but constant signal levels used on ionospheric scatter links are interpreted as scattering on electron density inhomogeneities in the ionospheric D–E region at 75 to 90 km. Using lower frequencies in the short-wave range, absorption in the D layer ceases to be negligibly small. There is reason now to expect that irregularities of electron density in the F2 region will have some influence on signal strength at the reception point. When short-wave radio waves are used on ionospheric scatter links, the MUF–F2 may be commensurate with the operating frequency during some periods of the day. Part of the incident power from those inhomogeneities whose MUF at a given moment is greater or equal to the operating frequency may be reflected. An experimental relationship between the drop in scattered power and excess of operating frequency over the MUF–F2 was obtained during a 3-year observation on radio-wave propagation at frequencies greater than the MUF–F2 in the range 9.9 to 19.8 MHz. On ionospheric scatter links (d < 2000 km) operating in the short-wave range, allowance must be made for the effect of scattering from the F2 region when the operating frequency is equal to or less than 1.4 MUF–F2. (J.C.W.)

2991 THEORY OF PERIODIC WIND CURRENTS IN THE LOWER IONOSPHERE. Khantadze, A. G. (Inst. of Geophysics, Tbilisi, USSR). Geomagn. Aeron. (USSR) (Engl. Transl.); 10: 274-6(1970).

Translated from Geomagn. Aeron.; 10: 351-3(1970).

Experimental and theoretical data are presented in describing the general patterns of periodic wind currents in the D and E regions. The velocity vector of the nonstationary wind rotates clockwise in the northern hemisphere in the course of a day and describes a closed circle or ellipse performing one (diurnal wave) or two (semi-diurnal) rotations per day. The shape of the curve and its orientation depend on height and latitude. The amplitude of the rotating vector increases as a spiral with height between 70 and 120 km and rotates clockwise. There is no significant relationship between wind velocity and height above this level. The data are analyzed. It is concluded that turbulence in the lower ionosphere produces the vertical pattern of periodic winds, specifically, the increase and right-handed rotation of the nonstationary wind with height. The wind current is affected by the deflecting force of the rotation of the Earth. Compared with the influence of the periodic inducing force, this influence will be the greater, the smaller the period of the latter. The hodograph of wind velocity with time is a circle or an ellipse, depending on the type of tidal forces. In the general case of periodic winds in the lower ionosphere, the temporal wind variation is actually determined by external inducing sources and its spatial distribution depends on the turbulent state of the medium. (J.C.W.)

2992 SOME RESULTS OF A STUDY OF INHOMOGENEITIES IN THE LOWER IONOSPHERE. Zhalkovskaya, L. V. (Inst. of Geology and Geophysics, Novosibirsk, USSR). Geomagn. Aeron. (USSR) (Engl. Transl.) 10: 276-7(1970).

Translated from Geomagn. Aeron.; 10: 354-5(1970).

Small-scale inhomogeneities and their motions in the lower ionosphere were studied by spaced reception of signals from a medium-wave radio broadcasting station in Aug. and Sept., 1967. The measurements were made only at night. The surface wave was tuned out by tuning the antenna to the minimum during the daytime. Results were analyzed for 20-minute intervals every 2.5 sec. The geometric dimensions of the inhomogeneities were determined. It was found that the dimensions of the inhomogeneities range from 600 to 2000 m for the major axis, and from 300 to 900 m for the minor axis. The inhomogeneities are elongated along the magnetic meridian. The recording sessions are separated into evening, night, and morning. Since tuning out of the surface wave was achieved by orienting the frame antenna to the minimum during the daytime, the antenna received only the horizontal component at night, produced by the rotation of the polarization plane in the ionosphere. The interpretation of the data is complicated since the angle of rotation is small and the antenna receives only an insignificant fraction of the signal, subject to polarization fadings. Results compare satisfactorily with other studies. (J.C.W.)

2993 SPACED SOUNDING OF THE E_s LAYER. Ovezgel'dev, O.; Bakaldina, V. D. (Inst. of Terrestrial and Atmospheric Physics, Ashkhabad, USSR). Geomagn. Aeron. (USSR) (Engl. Transl.); 10: 277-8(1970).

Translated from Geomagn. Aeron.; 10: 355-6(1970).

Spaced soundings of the ionospheric sporadic E layer were performed in the summer of 1966 at two points approximately 20 km apart to study the spatial structure of this layer. The same equipment was used with an identical antenna system at each observational point. The same measurement sounding program was used, both intermittently and simultaneously. Comparison of the temporal variations of the frequency characteristics of the E_s layer, f_oE_s and f_bE_s, at the two observation points showed a difference, and graphs showed a relative shifting to each other. The absolute value of the time-shift ranges from 0 to 4 min. To estimate the discrepancies between the frequency characteristics of the E_s layer quantitatively, a mathematical value is constructed with allowance for the corresponding time shifts, and then histograms were constructed of the frequency distribution. It is concluded that the E_s layer has a large horizontal ionization gradient and ionization inhomogeneities average approximately 10% over a distance of about 20 km. (J.C.W.)

2994 INFLUENCE OF THE LOWER IONOSPHERE ON THE APPEARANCE OF RADIO-WAVE REFLECTIONS FROM THE E_s LAYER. Chernysheva, S. P.; Ryss, I. K. (Rostov State Univ., Rostov-on-Don, USSR). Geomagn. Aeron. (USSR) (Engl. Transl.); 10: 279-80(1970).

Translated from Geomagn. Aeron.; 10: 356-7(1970).

The cutoff frequency, f_oE_s, and the probability of E_s appearance (pE_s) are used as sporadic E-layer characteristics. Whereas f_oE_s is associated with a change in ionization in the E_s itself, pE_s does not reflect the state of ionization of this layer. A change in absorption in the lower ionosphere must be reflected on pE_s because this parameter characterizes the appearance of radio-wave reflections from the E_s and not the appearance of this layer itself. Simultaneous data on total absorption measurements and vertical soundings were used to determine the diurnal pattern of the median absorption values in the D region in March 1966 for several frequencies and computed absorption in the region below the blanketing frequency from ionograms showed a sporadic-E layer at the same frequencies. Absorption data increases and decreases are discussed for various times of the day in the D region. As the height of the sun above the horizon increases, so does absorption in the D region and the electron density in the E_s. Consequently, the probability of reflections from the E_s increases until the absorption values reach their maximum. The maximum f_{min} value for March is 2 MHz and then pE_s for frequency below 2 MHz decreases to zero and is minimal for f_oE_s of higher frequencies. Absorption decreases after noon and reflections from

E_s appear. The probability of the appearance of E_s increases at first as absorption decreases and then it decreases because electron density in the E_s decreases with absorption. (J.C.W.)

2995 RELATIONSHIP BETWEEN THE GEOMAGNETIC FIELD AND THE SPORADIC E LAYER. Kolesnikova, T. V.; Starovatov, A. A.; Filonova, L. D. (Ionospheric Sector, Alma-Ata, USSR). Geomagn. Aeron. (USSR) (Engl. Transl.); 10: 280-1(1970).

Translated from Geomagn. Aeron.; 10: 358-9(1970).

Studies between the relationship of the geomagnetic field and the sporadic-E layer have shown contradictory results. On the basis of data for 1964, 1965, and 1966 at Alma-Ata, the deviations of the average hourly f_oE_s values from the monthly average and the seasonal variations of Δf_oE_s were found. The $\Delta H(\gamma)$ values for the H component of the geomagnetic field were found. The parameters are out of phase in summer and during the equinox, while the correlation is positive in winter. In summer and during the equinox, when E_s of the c- and h-types are most frequently observed, the relationship between f_oE_s and H is negative, while in winter when layers of the l- and f-type prevail, the relationship is positive. The E_s blanketing frequency is known to experience significant short-period variations in the course of a day. In 1966, approximately 220 f_bE_s bursts were recorded. It is interesting that geomagnetic field variations were synchronous with the f_bE_s variation in 39% of the cases for the H component, 43% for the Z component, and 27% for the D component. An E_s layer of the c-type can be accompanied by the formation of a local current system whose magnetic field either adds up with the current system in the normal E region, or is subtracted from it. H and Z components can either increase or decrease. The variations of the D vector can be understood if it is assumed that the magnetic field of a regional current system may not coincide with the direction of the vector of the magnetic field of currents flowing in the E region. (J.C.W.)

2996 INVESTIGATIONS OF THE LOWER IONOSPHERE DURING THE SOLAR ECLIPSE OF SEPTEMBER 22, 1968. Yampol'skii, V. S. (Omsk Pedagogical Inst., USSR). Geomagn. Aeron. (USSR) (Engl. Transl.); 10: 282-4(1970).

Translated from Geomagn. Aeron.; 10: 360-2(1970).

The field strength of medium-wave radio broadcasting stations was recorded on eclipse day Sept. 22, and on control days from Sept. 20 to 24, 1968. The geographic latitude of the reflection points was 53 to 57.5° and the longitude, 57 to 78°. The characteristics of the links and of the eclipse conditions at the reflection points are tabulated. The field strength E at the reception point changes because of the interference of the ground and ionospheric waves. Equivalent frequency $f_{eq} = f \cos \varphi$ where f is the transmitter frequency and ϕ is the angle of incidence of radio waves upon the ionosphere. The eclipse effect appeared on links with a small f_{eq} practically at the same time as the Moon began to obscure the solar disc, while on links with a large f_{eq}, it appeared approximately 10 min before the maximum phase of the eclipse. Records on control days show the effect of sunset on the strength of the total field. The reflection level changed during the eclipse and this resulted in a change in the phase difference between the ionospheric and ground waves and, consequently, quasi-periodic variations in field strength were observed at the reception points. The maximum rate of change of the reflection level V_{max} is traced as a function of f_{eq}, i.e., of the initial reflection height. The nature of this relationship indicates that cosmic rays produce stronger ionization in the lower part of the ionosphere than does solar radiation. An eclipse is a good time to verify that not only the rate of movement of the reflection level, but also its direction could be determined from the results of spectral analysis. This analysis of the field strength of radio broadcasting stations on links of different length and with different transmitter frequencies makes it possible to estimate the horizontal dimensions of the ionospheric region that moves simultaneously in the vertical direction. (J.C.W.)

2997 MEASUREMENT OF THE PHASE OF VLF SIGNALS DURING THE SOLAR ECLIPSE OF SEPTEMBER 22, 1968. Protopopov, L. A.; Khadzhi, B. A. (Inst. of Radio Engineering and Electronics, Moscow). Geomagn. Aeron. (USSR) (Engl. Transl.); 10: 284-5(1970).

Translated from Geomagn. Aeron.; 10: 363-4(1970).

The phases of signals from the vlf radio station GBR (16 kHz) and the lf station RES (100 kHz) were recorded for 6 hours, the visual duration of the solar eclipse, on Sept. 22, 1968. The phase drift due to the frequency instability of the reference generator was excluded from the phase records on the two channels. The resultant curve for the GBR signal for Sept. 22 shows only the end of the transition from night to day. The eclipse effect was manifest in the time interval from 13 to 16 hr and consisted in an increase in phase (transition from day to night and then to day). The curve for Sept. 26 is compared with the Sept. 22 observations. On the RES signal curves, irregular variations increased somewhat during the eclipse. There were no marked regular deviations from the normal RES phase pattern on Sept. 26. This can probably be explained by the much shorter propagation path of this signal, as compared with the GBR signal, and by the different orientation of this link with respect to the west–east line. (J.C.W.)

2998 SOME CHARACTERISTICS OF THE RELATIONSHIP BETWEEN GEOMAGNETIC AND SOLAR ACTIVITIES. Berishvili, G. P. (Inst. of Geophysics, Tbilisi, USSR). Geomagn. Aeron. (USSR) (Engl. Transl.); 10: 287-9(1970).

Translated from Geomagn. Aeron.; 10: 365-6(1970).

Information from the Tbilisi geomagnetic storm catalog (1900–1964) is used to tabulate data to determine the characteristics of the relationship between the tendency of storms to recur on their intensity. The tendency of storms to recur increases with their intensity (δN is the number of storms in the sequences in percent of the total number of storms). Then the data are separated into time periods for study from 1900–1939 and 1940–1964. The data are also available from the Pavlovsk geomagnetic storm catalog. Data show that in 1940–1964 and 1900–1964, the tendency toward storm recurrence increases with storm intensity. During 1900–1939, the change in tendency of storms to recur as a function of their intensity is almost the same according to the Tbilisi and Pavlovsk data (1878–1939). Results from the comparisons confirm the change in the last years of the studied periods for some patterns in solar–terrestrial relationships. It is also concluded that the frequency of occurrence and the relative proportion of storms in the sequences are much larger in 1940–1964 than in 1900–1939. The theoretical and empirical probabilities of the formation of storm sequences of different multiplicity were computed and compared to determine if the increase in storm frequency in the second part of the period affects the character of storm recurrence because of the increase in this period of the randomness of the formation of sequences. (J.C.W.)

2999 PULSATING AURORAS AT CONJUGATE POINTS. Gokhberg, M. B.; Kazak, B. N.; Raspopov, O. M.; (and others) (Inst. of Terrestrial Physics, Moscow. Polar Geophysical Inst., Moscow. Leningrad State Univ.). Geomagn. Aeron. (USSR) (Engl. Transl.); 10: 289-91(1970).

Translated from Geomagn. Aeron.; 10: 367-70(1970).

Simultaneous photometric observations on auroral intensity were carried out at the conjugate points Sogra and Kerguelen from Feb. to April, 1968. The data obtained confirm the results obtained earlier that auroras pass conjugate points simultaneously in the form of rayed arcs. It is concluded that auroral intensity variations are synchronous within 1 min at both stations. The periods when auroras were recorded simultaneously at Sogra and Kerguelen confirm the results obtained earlier on the parallel development of particle precipitation at conjugate points. It is known that the dumping of particles at these points is manifested not only in the appearance of auroras, but also in riometric absorption and x-ray bremsstrahling. Pulsating auroras are individual spots approximately 10 km long with a lifetime of several seconds. Pulsating auroras are accompanied by magnetic field pulsations. Auroral agitation is a term used to designate irregular geomagnetic micropulsations that last several hours and accompany pulsating auroras. The appearance of pulsating auroras is accompanied by auroral agitation of the magnetic field. The characteristics of appearance of pulsating auroras at conjugate points are studied. Along with Sogra and Kerguelen, auroral pulsations were recorded at a great speed at Loparskaya. Analyses are performed and compared for observations at the three stations. (J.C.W.)

3000 CLASSIFICATION OF SHORT-PERIOD PULSATIONS OF EARTH'S ELECTROMAGNETIC FIELD. Vinogradova, V. N. (Siberian Inst. of Terrestrial Magnetism, Ionosphere, and Radio Wave Propagation, Novosibirsk, USSR). Geomagn. Aeron. (USSR) (Engl. Transl.); 10: 292-4(1970).

Translated from Geomagn. Aeron.; 10: 371-3(1970).

A new classification was used to process the short-period pulsations records at Irkutsk during the IQSY. The processing consisted first of identifying pulsations with one of two main types of pulsations and second, in determining the period to relate the pulsations to some subgroup. Each subgroup of pulsations covers a sufficiently broad range of periods so that attention must be paid only to pulsations that enter the boundary intervals of the periods. The distribution of Pc by periods is shown. The dependence of the Pc periods on magnetic activity and the time of day must be taken into account and the variance of the Pc periods with respect to K_p is presented in a graph. The

XUM

diurnal distribution of the frequency of appearance of pulsations of various types is investigated. The relative frequency of occurrence of pulsations of various types and subgroup at minimum solar activity (1964) is categorized. The diurnal distribution of the frequency of pulsations with T > 45 sec is categorized according to hours and frequency of occurrence. Here pulsation records were made at high speed, and the periods were determined of all pulsations visible on the records except Pi. The frequency of pulsations with T > 45 sec has a main maximum at 18 to 21 hr. A similar diurnal pattern was obtained previously for pulsations with T > 60 sec. The patterns of occurrence of Pc3–Pc4, Pc4, and Pc5 contradict the conclusions of other authors. (J.C.W.)

3001 ALTITUDE PROFILE OF AIRGLOW HYDROXYL EMISSION. Harrison, A. W. (Univ. of Calgary, Alberta). Can. J. Phys.; 48: 2231-4(1 Oct 1970).

A rocket-borne cooled (S-1) filter photometer was flown from Resolute Bay, Northwest Territories 75°N during geomagnetically quiet conditions. The derived altitude profile of the (6 to 2) hydroxyl band emission shows a peak at 95 km. An airglow background of 2.7 R A^{-1} or less at 8380 A is reported for altitudes above 125 km. (auth) (Canada)

3002 RELATIVE INTENSITIES OF THE O_2^+ 1NG AND N_2 1PG BAND SYSTEMS IN NORMAL AND TYPE-B AURORAE. Harris, F. R.; Peterson, R. N.; Bradley, D. T. (Churchill Research Range, Fort Churchill, Manitoba). Can. J. Phys.; 48: 2283-95(1 Oct 1970).

A wavelength scanning spectrometer was used to study the intensities of selected O_2^+ 1NG and N_2 1PG bands in the visible spectra of normal and type-B aurorae. Peak differential brightnesses were considered. It was found that $I(O_2^+ 1NG)/I(N_2 1PG)$ is constant to within 70% in both normal and type-B aurorae of intensities IBC I through IBC III. The relevance of these observations, in view of previously published results on the subject of type-B aurorae is discussed. (auth) (Canada)

3003 MEASUREMENTS OF THE SHAPE OF IONOSPHERIC IRREGULARITIES USING SATELLITE TRANSMISSIONS. Dixon, A. F.; Forsyth, P. A. (Univ. of Western Ontario, London). Can. J. Phys.; 48: 2097-2100(15 Sep 1970).

Amplitude and phase scintillations were observed in the radio signals propagated at a frequency of 40 MHz from a satellite to two stations on the ground separated by a distance of about 10 km. By comparison of the signal fluctuations at the two stations the size and shape of F-region ionospheric irregularities were deduced. The lengths of irregularities oriented along the magnetic field ranged from 3 to 30 km with axial ratios of 11 to 60. (auth)

3004 NONLINEAR FREQUENCY SHIFT IN WHISTLER AND HYDRODYNAMIC PROPAGATION. Frey, Jean Pierre (Centre d'Etudes Nucleaires, France); Roux, Alain. Can. J. Phys.; 48: 2130-4(15 Sep 1970).

Nonlinear effects for the electron- and ion-cyclotron modes propagating in the magnetosphere were studied by using the Vlasov equation; the frequency shift was deduced to the third order. Going to the case of a cold plasma for the whistler mode, it was found that frequency shift vanishes, a result in agreement with Tidman and Stainer, based on the moments equations, but in contradiction with Watanabe's results derived from the Vlasov equation. For the hydromagnetic waves the effect does exist, but is not sufficient to explain the frequency–time displays (sonagrams) of the so-called "pearl" events. (auth) (Canada)

Low-Temperature Physics and Cryogenic Equipment

Refer also to abstract 3228.

3005 POINT TRANSFORMS AND THE HARD-CORE FERMI SYSTEM. Witriol, Norman M. (Brandeis Univ., Waltham, Mass. Physical Sciences Lab., Redstone Arsenal, Ala.). Phys. Rev., A; 1: 1775-82(Jun 1970).

The method of point transforms, assuming pairwise additivity, as developed by Eger and Gross, is applied to the many-body hard-core Fermi system. The ground-state energy and Landau parameters are found to second order in the hard-core radius. The dilute-gas-limit results are in agreement with those of Huang and Yang and of Abrikosov and Khalatnikov. Methods of extending the calculation to denser systems via the determination of the cutoff function of the transformation are discussed. (auth)

Superfluidity

3006 TEMPERATURE VARIATIONS PRODUCED BY HEAT CURRENTS IN LIQUID HE II. Loos, W. (Technische Univ., Munich). Z. Phys.; 239: 343-4(1970).

From linearized two-fluid hydrodynamics it is shown that there is a spatially constant temperature rise if a heat current is switched on in a channel of infinite length. This leads to a maximum possible heat current vanishing at T_λ. In a spherical geometry there is a similar temperature rise, but it decays exponentially with time. (auth)

3007 TRANSFORMATION OF FIRST (SECOND) SOUND INTO FOURTH SOUND IN SUPERFLUID HELIUM. Kaganov, M. I.; Sanikidze, D. G.; Tkeshelashvili, O. G.; Yampol'skii, V. A. (Physical-Technical Inst. of Low Temperature, Kharkov. Inst. of Cybernetics, Tbilisi, USSR. Donetsk Physical-Technical Inst., USSR). Zh. Eksp. Teor. Fiz.; 59: 812-19(Sep 1970). (In Russian).

Normal incidence of sound waves from superfluid helium onto the surface of a porous body saturated with helium is considered. The porous body is assumed to consist of plane-parallel capillaries that are normal to the surface. The coefficient of transformation of first (second) sound into fourth sound and also the reflection coefficient and the coefficient of transformation of the sounds at the surface are calculated for pure ^{4}He as well as for ^{3}He–^{4}He solutions. (auth)

3008 WIDTH OF THE SURFACE LAYER OF LIQUID ^{4}He. Cole, Milton W. (Univ. of Chicago). Phys. Rev., A; 1: 1838-40(Jun 1970).

It is noted that a divergence predicted for the contribution of capillary waves to the surface-layer thickness disappears if the effect of gravity is included. The resulting finite value for ^{4}He is computed as a function of temperature, and a comparison is made with the static contribution to the thickness. Application to other liquid systems is discussed. (auth)

3009 PHENOMENOLOGICAL ^{6}He–^{4}He POTENTIAL AND THE PROPERTIES OF LIQUID HELIUM (^{4}He). Khanna, K. M. (International Centre for Theoretical Physics, Trieste, Italy). Czech. J. Phys.; 20: 1166-74(1970).

The properties of liquid ^{4}He whose particles are interacting among themselves through an equivalent two-body Gaussian potential are studied by using the Bogolyubov method. It is shown that the value of the hard-core radius $\sigma \leq 2.2$ Å; the most probable values for m^*/m lie between 1.292 and 9 and that for Δ/k between 8 and 16°K. The results are compared with the experimental and theoretical values known so far. The energy gap Δ and the effective mass m^* increase as the value of k increases, keeping the density ρ fixed. The resultant two-body interaction between the helium atoms is repulsive in the temperature range $T \to 0$. (auth)

3010 SURFACE TENSION OF LIQUID ^{4}He. Dickson, D. P. E.; Caroline, D.; Mendoza, E. University Coll. of North Wales, Bangor). Phys. Lett.; 33A: 139-40(19 Oct 1970).

The surface tension of liquid ^{4}He was measured by means of electronically monitored capillary rise between 1.24 and 3.60°K. The results are in good agreement with those obtained by Allen and Misener from optical observation of capillary rise. (auth)

3011 LOW-TEMPERATURE DENSITIES AND THE SOLUBILITY OF ^{3}He IN LIQUID ^{4}He UNDER PRESSURE. Watson, Gary Ernest. Ithaca, N. Y.; Cornell Univ. (1969). 103p. University Microfilms Order No. 70-5785.

Thesis.

At its saturated vapor pressure, ^{3}He is soluble in liquid ^{4}He to only about 6.5% at absolute zero. A model calculation for a hard-sphere mixture of fermions and bosons by van Leeuwen, Mossel, and Cohen predicts that this limiting solubility will decrease to zero at an external pressure of 5 atm. A calculation based on the effective interaction theory of Bardeen, Baym, and Pines (BBP), however, indicates that the solubility should increase initially with increasing external pressure. Measurements of the molar volumes of dilute mixtures of ^{3}He in liquid ^{4}He at temperatures to 50 mK and pressures to 22 atm are reported here. The dielectric constant of the mixture was measured with a capacitor coil combination along with a tunnel diode oscillator. The dielectric constant of the mixture obtained from frequency measurements was then converted to molar volume by the use of the Clausius–Mossotti relation. The measurements were accurate to .003 cm^3/mole. The mixture was cooled with a ^{3}He–^{4}He dilution refrigerator. (TSS) (Diss. Abstr. Int., B)

3012 STABILITY OF SUPERFLOW AND ION MOBILITY IN ^{3}He–^{4}He MIXTURES. Kramer, Lorenz. Stanford, Calif.; Stanford Univ. (1969). 79p. University Microfilms Order No. 70-10,479.

XUM

Thesis.

The limit of metastable existence of parallel superflow through channels is found by examining the second variation of the free energy. The corresponding critical velocity V_{c1} is calculated with the two-fluid equations derived by a Boltzmann equation method from Landau's quasi-particle model and with the Ginzburg–Pitaevskii theory. V_{c1} reduces to the Landau velocity for $T \to 0$ and tends to zero for $T \to T_\lambda$. The behavior of the system above V_{c1} is discussed. The drag force F due to the creation of rotons by a heavy impurity moving with an average velocity near the Landau velocity is computed. At zero temperature F is zero up to the Landau velocity and then rises rapidly with a finite initial slope. At finite temperature the variation of F at the Landau velocity smooths out. Since the cross section for roton production is not known, absolute values cannot be established for the drag force. An attempt is made to explain some recent mobility measurements of ions in dilute ^{3}He–^{4}He mixtures and in pure ^{3}He at very low temperatures. First, the general formula for the drag force of a heavy impurity in a gas is derived by a new Boltzmann equation method. The simple theory of a heavy impurity moving through a very rarefied Fermi gas (Knudsen limit) gives only very rough agreement with the experimental results of ^{3}He–^{4}He mixtures. Two modifications are introduced. The structure of the negative ion (electron bubble) is assumed to depend on ^{3}He concentration, and a correction to the Knudsen limit is made. The theory is in fair agreement with the experiments on negative ions for temperatures above about 0.1°K. The application of the theory to pure highly degenerate ^{3}He shows that the mobility remains finite at T = 0 and rises for increasing temperature due to the correction to the Knudsen limit. Both results are in agreement with experiment. (Diss. Abstr. Int., B)

3013 GROUND STATE OF LIQUID HELIUM FOUR. Francis, William Porter. Ithaca, N. Y.; Cornell Univ. (1969). 135p. University Microfilms Order No. 70-5767.

Thesis.

A trial wave function describing the ground state of a quantum system of N interacting bosons is written in the Jastrow form, a product of pair functions. With the interaction potential chosen to represent liquid ^{4}He, and with the parameterized form of the pair function chosen to include a long-range term that has been found necessary for the representation of the phonon modes known to exist in liquid helium, a minimum-energy variational calculation was performed. The essential results are that including the phonon modes in the wave function definitely lowers the energy, corrects the behavior of the structure function and the momentum distribution of the particles in the low-wave-number region, and decreases the Bose–Einstein condensate fraction. The value of the lower limit on the wavelength of the phonon modes was determined variationally to be about three interparticle spacings. (Diss. Abstr. Int., B)

3014 NEW DERIVATION OF THE EQUATIONS OF MOTION FOR THE COMPLEX ORDER PARAMETER OF HELIUM II. Haug, H.; Weiss, K. (Philips Research Labs., Eindhoven, Netherlands). Phys. Lett.; 33A: 263–4(2 Nov 1970).

Anderson's canonical equations of motion for the phase of the order parameter and the particle number are generalized to inhomogeneous situations. With these equations, Froehlich's equations of motion for the density and the velocity of condensate of helium II are rederived. (auth)

3015 HIGH-TEMPERATURE SERIES EXPANSIONS FOR GRIFFITHS' MODEL OF ^{3}He–^{4}He MIXTURES. Oitmaa, J. (Monash Univ., Clayton, Australia). Phys. Lett.; 33A: 230-1 (2 Nov 1970).

The first nine terms of the high-temperature series expansion for the free energy are obtained for Griffiths' model of a system exhibiting a tricritical point. The series for the face-centered cubic lattice is analyzed to obtain a phase diagram. (auth)

3016 MEASUREMENT OF $\eta\rho_n$ VERSUS T NEAR T_λ OF DILUTE ^{3}He–^{4}He MIXTURES AND THEIR IMPLICATION FOR PURE ^{4}He. Webeler, R. W. H.; Allen, G. Lewis Research Center, Cleveland). Phys. Lett.; 33A: 213-14(2 Nov 1970).

Precision measurements of $\eta\rho_n$ in the vicinity of their respective lambda points were made for pure ^{4}He and for three mixtures of ^{3}He in ^{4}He. Consideration of the precise ½% mixture curve leads to the conclusion that neither the viscosity nor its first derivative is discontinuous at T_λ for this mixture, and to the inference that the same is true for pure ^{4}He. (auth)

3017 SUPERFLUIDITY OF ^{3}He. Bookbinder, James Henry. San Diego, La Jolla, Calif.; Univ. of California (1969). 236p. University Microfilms Order No. 70-8843.

Thesis.

The previous treatments of the question of superfluidity in ^{3}He, which have not shown conclusively whether this phase should or should not occur, are summarized. The most promising calculation was by Pitaevskii, whose determination of the screened quasiparticle transition amplitude $\tilde{T}_j$ was carried out in the limiting case of large angular momentum j. In estimating T_c this was extrapolated to j = 2 by Gor'kov and Pitaevskii (G.P.). The work of G. P. was found to contain an inadequate approximation (the D-wave Born approximation) plus also an algebraic error. When these corrections are made, their formula for T_c then yields the unattainably low value $T_c \sim 10^{-100}$ deg. $\tilde{T}_j$ $(0 \le j \le 10)$ was projected precisely in second-order perturbation theory. As the bare vertex function, the off-energy-shell K-matrix was used, the particular form of which was chosen so that K would satisfy two exact identities (Ward Identities). It was found that G.P.'s extrapolation underestimates the effective D-wave interaction. In fact, the polarization (bubble) diagram is an attractive correction to K_j, for j = 2 and $j \ge 6$, in contrast to Pitaevskii's result that the second-order diagram for $\tilde{T}_j$ is repulsive. The three approximations involved in Pitaevskii's large-j calculation were studied carefully. Theoretical arguments are given, and numerical evidence is furnished, which indicate that as j increases his limit is being approached asymptotically, but so slowly that Pitaevskii's analytical result does not hold for angular momenta of interest (i.e., for j < 20). The possibility of D-state superfluidity is discussed. The present work indicates that T_c may be as high as 10^{-4} deg, but the transition temperature is such a sensitive function of the calculated theoretical parameters that it is difficult to furnish a precise estimate for T_c. To make the dissertation self-contained, and to carefully define the notation and terminology, a summary of many-body techniques, K-matrix theory and the theory of superconductivity are presented. (Diss. Abstr. Int., B)

3018 STUDIES OF ^{4}He BY X-RAY SCATTERING. Hallock, Robert Bruce. Stanford, Calif.; Stanford Univ. (1969). 172p. University Microfilms Order No. 70-10,462.

Thesis.

The intensity of copper K_α x-rays scattered from helium-4 was measured as a function of scattering angle in both the gas phase at 5°K and the liquid phase at several lower temperatures. By measuring the intensity scattered from neon, these measurements were normalized and hence the structure factor for helium-4 was obtained in both phases. To carry out these measurements it was necessary to design and construct a low temperature x-ray spectrometer. The completed instrument is capable of maintaining temperatures as low as 0.32°K for several weeks at a time. Data collection was made completely automatic. The gas phase was shown to be distinctly non-ideal. At 0.32°K the liquid structure factor agrees with a prediction of Feynman and is linear in momentum transfer up to a value of 0.4 $Å^{-1}$. Above this value of the momentum transfer, the liquid structure factor exhibits a gentle but definite change of slope and falls below the prediction of Feynman. Hence it has been shown that the Bijl–Feynman dispersion relation appears to remain valid up to a momentum transfer of 0.4 $Å^{-1}$. This change of slope agrees with a qualitative prediction made by Miller, Pines and Nozieres. The measurements indicate that the strong shoulder predicted by Massey is not present. At higher temperatures (up to 2.0°K) the zero momentum transfer extrapolation of the structure factor agrees well with the expected behavior deduced from the isothermal compressibility. (Diss. Abstr. Int., B)

Superconductivity

Refer also to abstracts 2444, 2670, 3752.

3019 (NYO–3029-48) HARD SUPERCONDUCTING MATERIALS. Progress Report, December 1, 1969–November 30, 1970. Silcox, J.; Webb, W. W. (Cornell Univ., Ithaca, N. Y. Dept. of Applied Physics). Contract AT(30-1)-3029. 16p. Dep. NTIS.

Research is reported on: critical currents in hard superconductors, intrinsic fluctuations in superconductors, radiation effects and instabilities in weak superconductors, superconducting surface sheath, and superconducting thin films. (D.L.C.)

3020 (ORNL-TM-3206) COMPARISON OF CALCULATED AND MEASURED LOWER CRITICAL FIELD FOR SOME Nb–Ti ALLOYS. Lubell, M. S.; Kernohan, R. H. (Oak Ridge National Lab., Tenn.). Oct 1970. 24p. Dep. NTIS.

An expression is obtained from the Maki theory for H_{c1} (0) in terms of three measurable material constants T_c, ρ_n, and H_{c2}' (0). The calculations are compared to the measured H_{c1} vs T extrapolated to T = 0°K for three vacuum annealed Nb–Ti alloys. Values of H_{c1} (0) are also determined from the computation of Harden and Arp. Both sets of calculated values differ greatly from the measured values showing that the Maki theory is not applicable for $\kappa_{GL} < 30$, and the computation of Harden and Arp is not valid at

XUM

T = 0°K in disagreement with recent results of Echarri et al. Analysis of data available in the literature supports the conclusions. Comparison of the magnetization data near T_c with the theory of Neumann and Tewordt shows reasonable agreement. (auth)

3021 (UCRL-Trans-1409) THE SUPERCONDUCTIVITY OF TERNARY β-TITANIUM ALLOYS. Raub, Christoph Julius Translated for Univ. of California Lawrence Radiation Lab., Berkeley, from Z. Phys.; 178: 216-20(1964). 6p. Dep. NTIS.

An abstract of this paper, prepared from the original language, appeared as NSA 18: 21112.

3022 DEPRESSION IN ORDER PARAMETER OF A SUPERCONDUCTOR WITH KONDO EFFECT. Singh Nagi, A. D. (Univ., Frankfurt am Main. Univ. of Waterloo, Ont.). Phys. Lett.; 33A: 80-1(5 Oct 1970).

It is shown that the depression in order parameter, $[-\delta\Delta(\gamma, T_C/T_K)]$, at fixed distance γ, has a pronounced maximum when the ratio of Kondo temperature to critical temperature is about 12. $\gamma \gg \xi_0$ (coherence length) is assumed. (auth)

3023 TRANSITION TEMPERATURE OF SUPERCONDUCTORS. Klose, W.; Hertel, P. (Univ., Saarlandes, Saarbruecken, Ger.). Z. Phys.; 239: 331-6(1970). (In German).

An iteration procedure allows one to find an equation for the critical temperature T_c of superconductors starting from the linearized Eliashberg equations without using any cutoff parameters or a Coulomb pseudopotential. Explicit calculation of T_c for a simple model leads to the expression of Morel and Anderson and McMillan (Phys. Rev., 125: 1263(1962) and 167: 331(1968)) thereby allowing for a physical interpretation of the commonly used approximation for the Coulomb pseudopotential. (auth)

3024 DIRECT OBSERVATION OF SINGLE MAGNETIC FLUX QUANTA IN SUPERCONDUCTING TUBES. III. Lischke, B. (Technische Univ., Berlin). Z. Phys.; 239: 360-78(1970). (In German).

By use of electron interferometry the trapped magnetic flux was investigated in superconducting microcylinders (inner diameter <1 μm). Even in thin-walled cylinders (wall thickness < penetration depth) at temperatures near the superconducting transition, the flux was found to be quantized in integer multiples hc/2e. In the appendix an interpretation of the magnetic Aharonov-Bohm effect as a local interaction between the excluded field and the electromagnetic field of the electron is discussed. (auth)

3025 SUPERCONDUCTIVITY AND PHYSICAL METALLURGY. Seeger, Alfred (Max-Planck-Institut fuer Metallforschung, Stuttgart). Met. Trans.; 1: 2987-96 (Nov 1970).

After a brief summary of the historical development of the field of superconductivity and the background required for the topics treated in the present paper, some of the relationships between superconductivity and physical metallurgy are discussed. These are mainly in two areas: (1) The distribution of magnetic flux in superconductors may show fine structures (boundaries between normal and superconducting regions in the intermediate state of type-I superconductors; quantized flux-lines in the Shubnikov phase of type-II superconductors) on such a scale that they interact strongly with the metallurgical microstructure of the superconducting materials, such as grain boundaries, dislocations, precipitates, and so forth. (2) Ideally, the flux-lines in a type-II superconductor form a two-dimensional lattice (Abrikosov lattice). The decoration technique of Träuble and Essmann has permitted the direct observation of these flux-lines lattices and has revealed that they contain a rather high density of defects. Most of them are known from the studies of defects in crystals, such as grain boundaries, dislocations, stacking faults, and vacancy and interstitial lines, but also disclinations, which were predicted by theory but have not yet been observed in metals, were investigated. (auth)

3026 SUPERCONDUCTIVITY CRITICAL TRANSITION TEMPERATURE IN THIN TIN FILMS. Man'kovskii, K. K.; Pilipenko, V. V.; Komnik, Yu. F.; Dmitrenko, I. M. (Physical-Technical Inst., Kharkov). Zh. Eksp. Teor. Fiz.; 59: 740-52(Sep 1970). (In Russian).

The critical temperature for the superconducting transition in thin films depends on many factors such as the thickness and degree of equilibrium of the film, type of backing, development of surface, texture, etc. The effect of various factors on T_c of thin tin films is investigated by a "comparative" method, i.e., with a series of samples obtained in conditions when all but one parameter influencing the structural properties of the films and T_c are held constant, the variable parameter being, for example, the condensation temperature or film thickness. Structural characteristics of thin tin films are also studied. It is shown that tin films obtained on lowering the temperature even after heating possess less-perfect structures than do films obtained at room temperature. This is the cause of growth of T_c with decrease of the condensation temperature below 250°K. Increase of the condensation temperature above 250°K also results in an increase of T_c, despite the fact that such characteristics as the specific resistance of the films are improved by the ratio $\delta = R_{293}/R_{4.2}$ increases. A growth of T_c with decrease of thickness in the region of the critical thickness L_K is observed in tin films obtained at ~300°K. Various explanations offered by current theories of the variation of T_c of thin tin films are discussed. (auth)

3027 MAGNETIZATION OF THE SUPERCONDUCTING ALLOY Ti-22 AT. PERCENT Nb. Karasik, V. R.; Vasil'ev, N. G.; Ershov, V. G. (Lebedev Inst. of Physics, Moscow). Zh. Eksp. Teor. Fiz.; 59: 790-8(Sep 1970). (In Russian).

By means of the modified Bean model, it is shown that the critical-state concept can be applied to a superconducting alloy with a rigidly fixed vortex lattice. The effect of Pauli paramagnetism on the ratio H_{c2}/H_{c2} near T_c is investigated. The existence of a proximity effect in the alloy Ti-22 at. % Nb containing ω-phase particles is proved. (auth)

3028 RESONANT ABSORPTION OF ULTRASOUND BY NUCLEI IN AN INTERMEDIATE STATE SUPERCONDUCTOR. Khabibullin, B. M. (Physical-Technical Inst., Kazan). Zh. Eksp. Teor. Fiz.; 59: 805-11(Sep 1970). (In Russian).

The ultrasound absorption coefficient for nuclear quadrupole levels in the intracrystalline electric field in an intermediate-state metal is calculated. Absorption is due to the following factors: (a) modulation of the critical field in normal superconducting layers under the action of ultrasound deformations; (b) nuclear motion induced by ultrasound with respect to the interface between the superconducting and normal phases $R_z(t)$; this leads to the appearance in the N-S transition region of a varying field $H(t) = R_z(t)\,\lambda^{-1}H_{K0}\exp(-|z_i - z_n|\lambda^{-1})$ (λ is the transition layer thickness, z_n and z_i are the coordinates of the N-S boundary and i-th nucleus, respectively). An expression is derived that describes the dependence of absorption on temperature and direction of propagation of longitudinal ultrasound relative to the direction of the external field and the boundary plane. (auth)

3029 FLUCTUATION RESISTANCE OF A TUNNEL JUNCTION AT TEMPERATURES EXCEEDING THE CRITICAL. Kulik, I. O. (Physical-Technical Inst. of Low Temperatures, Kharkov). Zh. Eksp. Teor. Fiz.; 59: 937-44(Sep 1970). (In Russian).

Fluctuation conductivity effects in superconducting tunnel junctions at temperatures above T_c are analyzed. It is shown that, in a high-frequency field, the fluctuation component of the junction current exhibits quantum interference effects, viz. (1) generation of radiation at the Josephson frequency with a spectral width, which is defined by the inverse relaxation time of the Cooper pairs Γ; (2) appearance of singularities in the volt-ampere characteristic when the junction is irradiated by a high-frequency wave, the position of the singularities being defined by the formula $V_n = n\hbar\Omega/2e$ (Ω is the irradiation frequency and $\Omega \gg \Gamma$); and (3) an oscillating dependence of the slope of the volt-ampere characteristic at zero current as a function of amplitude of the high-frequency signal. (auth)

3030 ROLE OF BOUNDARY SINGULARITIES IN SUPERCONDUCTIVITY. Shekhtman, A. Z. Zh. Eksp. Teor. Fiz.; 59: 957-64(Sep 1970). (In Russian).

The boundary singularities of the electron proper energy at zero absolute temperature and their effect on the character of single-electron excitations in a metal at low temperatures are studied for a metal model involving electron-phonon interaction. It is not assumed that the metal is necessarily a superconductor at low temperatures. It is shown that already in the zero approximation (second order in perturbation theory), the real part of the electron proper energy $\Sigma^{(0)}$ at T = 0 may contain boundary singularities of the x ln x type which result in deviation of the analytical properties of the single-electron Green function from the properties following from the Lehman expansion. Allowance for the sum of the main sequence for Σ does not affect the result. The anomalies in the analytic properties of the single-electron Green function that are observed can be explained by violation of the adiabatic hypothesis. It is suggested that, in the given case, violation of the adiabatic hypothesis is a consequence of the tendency of a metal to undergo a phase transition into the superconducting state. (auth)

3031 SIMULATED SUPERCONDUCTIVITY IN THIN FILMS. Ivlev, B. I. (Inst. of Theoretical Physics, Moscow). Zh. Eksp. Teor. Fiz.; 59: 1036-42(Sep 1970). (In Russian).

XUM

The behavior of a thin superconducting film with paramagnetic impurities in an external uhf field is investigated by a method developed by Gorkov and Eliashberg for nonstationary effects in superconducting alloys. It is found that, in the gapless superconductivity region, there exists such a range of external field amplitudes and frequencies for which the transition temperature to the superconducting state and the critical current increase with respect to the values observed in the absence of an external varying field. The results are shown to be in qualitative agreement with the experimental data. (auth)

3032 HOW JOSEPHSON DISCOVERED HIS EFFECT. Anderson, Philip W. (Bell Telephone Labs., Murray Hill, N. J.). Phys. Today; 23: No. 11, 23-5; 27; 29(Nov 1970).

Incidents in the history of the discovery of the Josephson effect are reviewed. The publication, significance, and applications of this discovery are discussed. (M.H.R.)

3033 PRECIPITATES AND FLUX LINE PINNING IN A SUPERCONDUCTING Pb–Na ALLOY. Petermann, Juergen (Univ., Goettingen, Ger.). Z. Metallk.; 61: 724-33(Oct 1970). (In German).

In a type-II superconducting Pb–7 at. % Na alloy several states of precipitation were produced and investigated by electron microscopy. Measurements of differential magnetization permitted calculation of the "critical flux gradient" $\partial B/\partial r$ as a function of the magnetic flux B and, thus, computation of the pinning forces of the precipitates per unit volume of the flux line (FF) lattice. Homogeneous coherent precipitate particles were spherical and aligned along ⟨100⟩ if their radius was $\bar{r} > 210$ Å, and rod shaped if their radius $\bar{r} > 470$ Å. For crystals oriented approximately along ⟨100⟩ a maximum in the magnetization curves and in $\partial B/\partial r$ (B) was observed; it could be related to a geometric correlation between particle spacing and the flux-line lattice parameter. The maximum pinning force exerted by a particle on a flux line was computed for this case and compared to theoretical estimates. For specimens oriented close to ⟨111⟩ no corresponding maxima were observed. Measurements covering discontinuous precipitates in polycrystalline specimens were also performed. (auth)

3034 UPPER LIMIT ON ELECTRON–PHONON INTERACTION IN VANADIUM CARBIDE. Bloom, D. W. (Univ. of Colorado, Boulder); Finegold, L.; Lye, R. G.; Radebaugh, R.; Siegwarth, J. D. Phys. Lett.; 33A: 137-8(19 Oct 1970).

Single crystals of VC_x (x = 0.87, 0.84, 0.81, 0.76) were not superconducting above 30 mK, indicating that the electron–phonon enhancement of the densities of states determined from electronic specific heats is less than 30%. (auth)

3035 EVIDENCE OF A PHASE TRANSITION IN AN ASSEMBLY OF POINT CONTACTS. Rosenblatt, J.; Cortes, H.; Pellan, P. (Institut National des Sciences Appliquees, Rennes, France). Phys. Lett.; 33A: 143-4(19 Oct 1970).

A system of about 10^4 point contacts shows a transition to the resistanceless state at a temperature much smaller than the superconducting transition temperature. (auth)

3036 FLUCTUATIONS OF ORDER PARAMETER AND HALL EFFECT. Fukuyama, H. (Tohoku Univ., Sendai); Ebisawa, H.; Tsuzuki, T. Phys. Lett.; 33A: 187-8(19 Oct 1970).

The effects of fluctuations of the order parameter in superconductors on the Hall effect are investigated in a weak magnetic field in the region above T_c. (auth)

3037 GENERATION OF HARMONICS AND SUBHARMONICS OF THE JOSEPHSON OSCILLATION. Sullivan, D. B.; Peterson, Robert L.; Kose, V. E.; Zimmerman, J. E. (National Bureau of Standards, Boulder, Colo.). J. Appl. Phys.; 41: 4865-73(Nov (1970).

The observation of harmonics and subharmonics of the Josephson oscillation is shown to be in agreement with a rather simple model of the junction. The generation of harmonics provides an explanation of induced steps in the current–voltage characteristic which occur at submultiples of the usual induced step voltages. The subharmonic oscillation is seen to be a relaxation-like process which can be easily understood in terms of a mechanical analog. (auth)

3038 SUPERCONDUCTING MAGNET SUSPENSION SYSTEMS: PERSISTENT MODE OPERATION. Atherton, David L. (Ferranti–Packard Ltd., Toronto). Can. J. Phys.; 48: 2451-3 (15 Oct 1970).

The lift force generated by a rectangular superconducting magnet operating in the constant flux (persistent mode) and moving over an infinite conducting plane is derived from the lift equation for such a magnet operating in a constant-current mode. (auth)

3039 DEFECT STRUCTURE AND CRITICAL CURRENT DENSITY IN THE HIGH FIELD SUPERCONDUCTORS V_3Ga, $(VZr)_3Ga$, AND $(VHf)_3Ga$. Nembach, Eckhard (Univ., Goettingen, Ger.). Z. Metallk.; 61: 734-42(Oct 1970). (In German).

Using electron microscopy and x-ray diffraction, the reasons for the excellent current-carrying capacity of the hard superconductor V_3Ga were investigated. The result is: the compound is only partially ordered and very fine-grained. The smaller the grains, the higher is the critical current density. Only grain boundaries act as pinning centers for flux lines; three interaction mechanisms for this are discussed. A further increase of the critical current density is possible by adding Zr or Hf to the V substrate. These elements decrease the grain size of V_3Ga through heterogeneous nucleation; moreover, there are particles of a second phase that pin flux lines too. Unfortunately, it was not possible to prevent the fine-grained material from recrystallizing. The recrystallization decreases j_c, because it reduces the number of pinning centers. (auth)

3040 HAMILTONIANS OF QUANTUM STATISTICS AND MODEL HAMILTONIAN OF THE THEORY OF SUPERCONDUCTIVITY. Petrina, D. Ya. (Inst. of Theoretical Physics, Kiev). Teor. Mat. Fiz.; 4: 394-411(Sep 1970). (In Russian).

The general Hamiltonian of quantum statistics and model Hamiltonian of the theory of superconductivity in infinite volume are investigated. The Hamiltonians considered are rigorously defined as the operators on Hilbert space of the sequences of translation–invariant functions. The general Hamiltonian is not symmetric, but possesses a real spectrum. The model Hamiltonian is symmetric and its spectrum possesses a gap between the energies of the ground state and the excited state. (auth)

3041 SUPERCONDUCTING PENETRATION DEPTH IN LEAD. Gasparovic, Richard Francis. New Brunswick, N. J.; Rutgers–The State Univ. (1969). 114p. University Microfilms Order No. 70-10,067.

Thesis.

The temperature dependence of the change in the superconducting penetration depth λ from its value at T = 0 was measured for a high-quality bulk polycrystalline lead specimen. It was found that the temperature dependence of λ in lead, a strong coupling superconductor, is essentially identical to that of a weak coupling (BCS) superconductor. Near the transition temperature T_c, $d\lambda/dy = 418 \pm 9$ A°, where $y = (1 - t^4)^{-\frac{1}{2}}$, $t = T/T_c$. The energy gap Δ_0 deduced from a detailed comparison of the measurements with the weak-coupling theory as developed by Nam is $2\Delta_0 = 3.75\ kT_c$, in contrast to the value $2\Delta_0 = 4.3\ kT_c$ found by more direct measurements. This reduction in the apparent size of Δ_0 is shown to result from strong-coupling effects, which are neglected in the weak-coupling formalism. By studying several single-crystal specimens, a small anisotropy in $d\lambda/dy$ was found, the magnitude of which can be accounted for by an anisotropic energy gap. A slight anisotropy in the form of the temperature dependence of λ was also observed at low temperatures. From a critical analysis of various experimental investigations, consistent values for the coherence length and London penetration depth of Pb, viz., $\zeta_0 = 960$ A° and $\lambda_L(0) = 305$ A°, were derived. (Diss. Abstr. Int., B)

3042 FLUCTUATIONS IN SUPERCONDUCTIVE FILMS IN A MAGNETIC FIELD. Redi, Martha Harper. New Brunswick, N. J.; Rutgers–The State Univ. (1969). 95p. University Microfilms Order No. 70-10,095.

Thesis.

The effects of thermodynamic fluctuations of the superconductive order parameter were studied for certain dynamical properties of superconducting films in a perpendicular magnetic field just above the transition point. The microscopic Matsubara thermal Green's function technique was used to calculate the fluctation conductivity and the effect on the tunneling density of states of superconductive films. The theoretical predictions are shown to agree with experiment. (Diss. Abstr. Int., B)

3043 ELECTRICAL CONDUCTIVITY IN PURE TYPE-II SUPERCONDUCTORS NEAR H_{c2}. Hibler III, William David. Ithaca, N. Y.; Cornell Unit. (1969). 170p. University Microfilms Order No. 70=5770.

Thesis.

The electric conductivity for pure type-II superconductors for magnetic fields near H_{c2} is calculated. The calculation is carried out in the extreme pure limit for frequencies and relaxation times such that $\omega\tau > 1$. The conductivity in the absence of fluctuations, i.e., with a static vortex lattice, is calculated in a manner similar to the procedure used by Brandt, Pesch and Tewordt to obtain the density of states. In particular the off-diagonal elements in the Gorkov factorization are determined by using the Gorkov integral

XUM

equations, and the response function is shown to have the periodicity of the lattice of fluxoids in the center of mass coordinates. Using this periodicity, an expression for the response function may be obtained. This expression is reduced to a more tractable form by using the fact that the coherence length ξ is smaller than the penetration depth λ and the approximation, justified in the thesis, that the fourier transform of the Brandt Green's function $G^B(\underset{\sim}{k}, \underset{\sim}{K}, \xi_1)$ for $\underset{\sim}{K} \neq 0$ is small compared to $G^B(\underset{\sim}{k}, O, \xi_1)$ where $\underset{\sim}{K}$ is the reciprocal fluxoid lattice vector corresponding to the fourier transform with respect to the sum coordinates of the Green's function. From the resulting expression for the response function the real part of the conductivity is calculated numerically in the extreme anomalous, ql large, limit; and the imaginary part of the conductivity is calculated by expanding in powers of Δ. Next, it is verified (first shown by Maki) that the fluctuations of the order parameter couple to the external field and in the pure limit, for the orientation $\underset{\sim}{J}_{osc} \perp \underset{\sim}{H}_o$, the fluctuations cancel the imaginary part of the conductivity whereas in the orientation $\underset{\sim}{J}_{osc} \parallel \underset{\sim}{H}_o$ the fluctuations have no effect on the conductivity. The contribution of the fluctuations to the real part of the conductivity is also estimated and found to be small. The values of the conductivity are used to calculate values of the surface impedance and are compared to experimental measurements made previously by the author and Bruce Maxfield. The theory predicts a decrease in the surface impedance at H_{c2} which is highly frequency dependent. For frequencies in the megahertz region where the experimental measurements were taken, the theory predicts a sharper decrease in R_s/R_n as a function of magnetic field near H_{c2} than observed experimentally. It is pointed out, however, that for these frequencies the limit $\omega\tau >$ 1 is probably not valid and higher frequency measurements are necessary. (Diss. Abstr. Int., B)

3044 EXCITATIONS IN A BOSE GAS AT FINITE TEMPERATURES. I. SHIELDED POTENTIAL IN THE HARTREE APPROXIMATION. Cheung, T. H.; Griffin, Allan (Univ. of Toronto). Can. J. Phys.; 48: 2135-54(15 Sep 1970).

Making use of the finite-temperature version of Belyaev's field-theoretical description description of an interacting Bose gas, the self-energy diagrams which correspond to the collisionless shielded potential approximation (SPA) are summed. This generalizes Bogolyubov's first-order results by replacing the bare repulsive interaction by a dynamically shielded interaction and includes the effect of the excited atoms. This theory is completely equivalent to that of Tserkovnikov if the ideal Bose gas approximation is used for the polarization function which screens the two-particle interaction. The excitation spectrum is found to have a single resonance. No convincing evidence for the additional high-frequency second-sound mode obtained by Tserkovnikov was found. (auth) (Canada)

3045 SUPERRADIANCE IN ARRAYS OF SUPERCONDUCTING WEAK LINKS. Tilley, D. R. (Philips Research Labs., Eindhoven, Netherlands). Phys. Lett.; 33A: 205-6 (2 Nov 1970).

M superconducting weak links in series can interact with a cavity mode so that the dc voltage is the same across each link, and the photon number is proportional to M^2. (auth)

3046 CONDENSATION ENERGY OF A SUPERCONDUCTOR. Carbotte, J. P.; Vashishta, P. (McMaster Univ., Hamilton, Ont.). Phys. Lett.; 33A: 227-8(2 Nov 1970).

The condensation energy was calculated for a number of superconductors for which the Eliashberg kernels are known from tunneling data. (auth)

3047 APPLICATION OF THE CORRELATION FUNCTION METHOD TO CALCULATION OF THE ANISOTROPY OF H_{c2} IN CUBIC SINGLE CRYSTALS. Harms, Klaus-Dieter (Univ., Goettingen, Ger.). Z. Naturforsch.; 25a: 1161-8(Aug-Sept 1970). (In German).

The upper critical magnetic field for a monocrystalline superconductor with cubic symmetry is calculated, using the correlation function method. The symmetry of the system leads to an eigenvalue equation which is solved with perturbation-theoretical methods. The upper critical field is calculated for dirty superconductors in the lowest order for which anisotropy is present. For clean superconductors, a higher order is calculated. Some results are critically compared with those in a paper by Hohenberg and Werthamer. (auth)

Equipment and Devices

Refer also to abstracts 2492, 3038, 3499, and 3504–3514.

3048 (AERE-R-6532) LOW TEMPERATURE CRYOSTAT FOR SINGLE CRYSTAL AND POWDER X-RAY DIFFRACTION. Sampson, C. F. (Atomic Energy Research Establishment, Harwell (England)). Sep 1970. 10p. Dep. NTIS (U. S. Sales Only). UK 2s. 6d.

A low-temperature cryostat for single-crystal and powder x-ray diffraction was designed and manufactured. The main body of the cryostat is conventional, having an outer vacuum container enclosing nitrogen and helium bins with their associated radiation shields extending throughout the lower volume of the cryostat. A small reservoir is extended from the He bin into the lower volume of the cryostat. The reservoir has a heater wound onto it, and a needle-valve control allows liquid He from the main He bin to pass into the reservoir. There are also facilities for allowing the entry of an exchange gas (i.e., He) into the reservoir. The extended radiation shields from the vacuum, nitrogen, and helium bins and from the reservoir in the region of the specimen are 0.005 Be and are machined from hot-pressed material. Temperature measurements are made using a carbon resistor and thermocouples. Temperatures down to 1.3°K were achieved by filling the reservoir with liquid He, isolating, and pumping on the exhaust line. (auth) (UK)

3049 HIGH-ENERGY NEUTRON SCATTERING FROM LIQUID ^{4}He. II. INTERFERENCE AND TEMPERATURE EFFECTS. Sears, V. F. (Chalk River Nuclear Labs., Ont.). Phys. Rev., A; 1: 1699-1704(Jun 1970).

The scattering of high energy neutrons from liquid ^{4}He was discussed in an earlier article on the basis of the Gram–Charlier series expansion of the incoherent scattering function. In the present paper, interference effects ignored previously are taken into account approximately and are shown to give rise to an oscillation in the half-width of the scattering function as a function of the momentum transfer. The temperature dependence of the scattering is investigated by deriving approximate expressions for the parameters in the Gram–Charlier expansion in terms of their values at T = 0, together with the observed thermodynamic properties of liquid ^{4}He. Reasonable agreement with the neutron-scattering data of Cowley and Woods is obtained. (auth)

3050 ENERGY TRANSPORT BY CRYOGENIC CABLES. Bogner, G.; Schmidt, F. (Siemens AG, Erlangen, Ger.). Naturwissenschaften; 57: 414-22(Sep 1970). (In German).

The properties of the basic components of cryogenic cables, such as conducting materials, thermal and electrical insulation, and cooling requirements, are described. Some of the most important concepts of superconducting and hydrogen- or nitrogen-cooled normal metal cables are introduced. A rough technical and economic comparison of cable types so far proposed shows that cryogenic cables become attractive only at power rates above 1000 MVA; this is especially true of superconducting ac cables. (auth)

3051 SPIN–LATTICE RELAXATION OF LIQUID ^{3}He AND ^{3}He–^{4}He MIXTURES. Horvitz, E. Philip (Rice Univ., Houston, Tex.). Phys. Rev., A; 1: 1708-12(Jun 1970).

The relaxation times T_1 and T_2 of ^{3}He nuclei in pure liquid ^{3}He and in liquid ^{3}He–^{4}He mixtures were measured in the temperature range 0.9°K < T < 2.6°K. Reproducible relaxation times longer than those previously reported have been obtained by employing an extensive cleaning procedure. The Pyrex sample chamber and filling capillary were repeatedly cleaned in the presence of several mm of pure ^{4}He by heating the glass to almost melting and, at the same time, touching the glass surface with a Tesla coil. This coil creates a high-frequency discharge that drives absorbed gases off the wall. T_1 for pure ^{3}He was found to have the value and the temperature dependence predicted by the modified Bloembergen–Purcell–Pound theory to within ±3%. T_1 is proportional to the diffusion coefficient, and increases from 350 sec at 1.0°K to 450 sec at 1.8°K. T_2 was found to be approximately equal to T_1. These long relaxation times were significantly shortened by contamination of the clean chamber with air or by inadequate purification of the ^{3}He sample. Since the work on pure ^{3}He showed that wall effects could be minimized by cleaning, it was considered of interest to measure T_1 in ^{3}He–^{4}He mixtures. The relaxation times of a 33% ^{3}He solution were determined in an extensively cleaned system. Above the λ point, T_1 is about 50% greater than for pure ^{3}He, while just below this temperature it increases sharply by about 15%. Measurements of T_1 of other mixtures were made in partially cleaned systems. The results were affected by wall relaxation and bulk impurities. Some conclusions about T_1 are drawn from these data. (auth)

Plasma and Thermonuclear Physics

Refer also to abstract 2497.

Confinement and Heating

Refer also to abstract 3142.

3052 (CEA-CONF-1595) SPACE-TIME EVOLUTION OF A TOKAMAK-TYPE PLASMA. Mercier, C.; Soubbaramayer (European Atomic Energy Community. Commissariat a l'Energie Atomique, Fontenay-aux-Roses (France). Centre d'Etudes Nucleaires). 1970. 4p. (CONF-700817-20). Dep. NTIS (U. S. Sales Only).

A mathematical model was set up to compute the space-time evolution of a Tokamak type plasma. Two examples of applications show that the model can be used to do extrapolation calculations of Tokamak machines or to carry out numerical experiments to test possible interpretations of measurements. (tr-auth) (France)

3053 (CEA-CONF-1597) PLASMA CONTAINMENT IN A CIRCULARIZED QUADRUPOLAR MAGNETIC WELL: DECA II B. Launois, D.; Lecoustey, P.; Nicolas, M.; Tachon, J. (European Atomic Energy Community. Commissariat a l'Energie Atomique, Fontenay-aux-Roses (France). Centre d'Etudes Nucleaires). 1970. 4p. (CONF-700817-18). Dep. NTIS (U. S. Sales Only).

From 4th European Conference on Controlled Fusion and Plasma Physics, Rome, Italy.

The focalization of magnetic lines out of a quadrupolar well reduces the wall-plasma interaction. Such a trap confines a 500-eV hydrogen plasma with an initial density of 10^{12} cm^{-3}. The decay time is 400 μsec. (tr-auth) (France)

3054 (CEA-CONF-1611) ION HEATING BY BEAM PLASMA INTERACTION. Bottiglioni, F. (European Atomic Energy Community. Commissariat a l'Energie Atomique, Fontenay-aux-Roses (France). Centre d'Etudes Nucleaires). 1970. 4p. (CONF-700817-5). Dep. NTIS (U. S. Sales Only).

From 4th European Conference on Controlled Fusion and Plasma Physics, Rome, Italy.

A powerful electron beam was injected longitudinally in a magnetic mirror configuration. By ionization of the H_2 gas, a plasma was produced that was heated by interacting with the beam itself. The hot plasma density and the ion temperature were, respectively, a few 10^{11} cm^{-3} and a few hundred eV. (tr-auth) (France)

3055 (IPPJ-100) STOCHASTIC MODEL OF ELECTRON CYCLOTRON HEATING IN A MAGNETIC MIRROR. Kawamura, Takaichi; Momota, Hiromu; Namba, Chusei; Terashima, Yoshinosuke (Nagoya Univ. (Japan). Inst. of Plasma Physics). Aug 1970. 24p. Dep. NTIS (U. S. Sales Only).

The mechanism of heating of electron plasmas by high-power microwaves in a magnetic mirror is investigated theoretically, in reference to the experiments in a device named TP-M. A microwave mode propagating perpendicular to the magnetic field is assumed to be responsible for heating, as there exist higher harmonic resonances, the main features of the experiments. The heating mechanism can be interpreted in terms of a stochastic process, a random walk in velocity space. It is numerically confirmed that the localized resonance zones of finite width exist and electrons are effectively heated only in the resonance zones, and that the presence of a randomization process of the relative phase relation between the wave and the electron gyration is essential to heating. On the basis of the numerical analysis the heating process is analytically treated. Electrons are supposed to pass the resonance zones repeatedly in the course of oscillatory motions between turning points, and the relative phase relation is assumed to be random at each passage through the resonance zone. The heating rate is calculated and is found to be in agreement with the experimental value. The causes of phase randomization and the observed saturation of electron temperature are also discussed. (auth) (Japan)

3056 (ORO-1171-1, pp 78-97) TURBULENT HEATING IN MIRROR MACHINES AT OAK RIDGE NATIONAL LABORATORY. Alexeff, I.; Estabrook, K.; Hirose, A.; (and others) (Oak Ridge National Lab., Tenn.).

From Proceedings of the symposium on thermonuclear fusion reactor design, June 2-5, 1970.

A survey is given of past experiments in turbulent heating in mirror machines at ORNL. The two classes of instabilities present in the experiments are discussed, i.e., plasma electron oscillations and plasma ion oscillations. (M.O.W.)

3057 CONTROL-THEORETIC APPROACH TO THE PLASMA CONFINEMENT PROBLEM. Wang, P. K. C. (Univ. of California, Los Angeles); Janos, W. A. J. Optimization Theory Appl.; 5: 313-29(Apr 1970).

The problem of confining a collisionless plasma by means of external electromagnetic fields is formulated as an optimal control or variational problem. The paper begins with a formal development of the equations governing the plasma motion. Then, various mathematical formulations of the confinement problem are discussed. Specific results are obtained for the simplified case where confinement is achieved by means of a spatially uniform, time-varying magnetic field. Physical interpretations of these results are also given. (auth)

3058 SOME COMMENTS ON THE STOCHASTIC HEATING OF PARTICLES IN MAGNETIC MIRROR SYSTEMS. Krlin, L. (Inst. of Plasma Physics, Prague). Czech. J. Phys.; 20: 1175-85(1970).

The heating of particles in a magnetic mirror system by means of the stochastic hf field is discussed. The diffusion in perpendicular energies and in the amplitudes of axial motion of particles is solved as well as the influence of the escape of particles through mirrors on the absorbed energy. The solution is in a one-particle approximation. (auth)

3059 EFFECTS OF TIME-VARYING FIELDS ON PLASMA CONTAINED IN A TOROIDAL OCTUPOLE MAGNETIC FIELD. Lencioni, Donald Eugene. Madison, Wis.; Univ. of Wisconsin (1969). 199p. University Microfilms Order No. 69-22,421. Thesis.

A gun-injected hydrogen plasma contained in a toroidal octupole magnetic field was studied to determine the effects caused by the time variation of the field. The plasma properties were measured primarily with Langmuir probes. A high-impedance floating double probe was developed for measurements made in the presence of fluctuating floating potentials. The experimentally observed evolution of the plasma distribution was compared to a mathematical model based on the flux invariance of the plasma motion. The model also included a finite gyroradius approximation and a decay term to simulate plasma losses. An analysis was made of the MHD stability of an adiabatic flux preserving plasma motion and compared to experimental observations. A calculation was made of the component of the inductive electric field parallel to the lines of force, and it was found to be much larger than the Dreicer critical field. Measurements of the parallel current flow were used to study the plasma conductivity, which was found to have the form $\sigma = 4 \times 10^{-8}\, n(cm^{-3})/\sqrt{T_e(eV)}$ mho m^{-1}. This was analyzed in terms of known theoretical results and the expected effects due to magnetic mirrors. (TSS) (Diss. Abstr. Int., B)

3060 EFFECT OF INERTIA ON LOSSES FROM A PLASMA IN TOROIDAL EQUILIBRIUM. Zehrfeld, H.-P.; Green, B. J. (Institut fuer Plasmaphysik, Garching, Ger.). Nucl. Fusion; 10: 251-8(Sep 1970).

The MHD equilibrium of a resistive, low-density plasma in a model stellarator field is investigated. The effect of inertia on plasma motion is treated exactly and its influence on plasma loss determined. The results are valid for arbitrary aspect ratio. For the existence of a stationary equilibrium it is shown that there are two unconnected regions of solution, described in terms of the mass fluxes the long and the short way within a magnetic surface. For the region containing the case of the well-known classical resistive diffusion it is argued that the increase in plasma loss due to inertia is strongly limited and does not appreciably exceed the classical diffusion rate. (auth)

Diagnostics

Refer also to abstract 3206.

3061 (CEA-CONF-1628) SPECTROSCOPIC DIAGNOSTICS OF NONEQUILIBRIUM PLASMAS. Drawin, H. W. (European Atomic Energy Community. Commissariat a l'Energie Atomique, Fontenay-aux-Roses (France). Centre d'Etudes Nucleaires). 1970. 55p. (CONF-700706-2). Dep. NTIS (U. S. Sales Only).

From 5th Plasma Physics Symposium, Herceg-Novi, Yugoslavia.

The spectroscopic diagnostics of plasmas not locally in thermodynamic equilibrium are based upon certain fundamental equations that give a spectroscopic description of the plasma. The relevant equations are those of Boltzmann collisions. In general, the analysis commences with an equation of this type and its higher-order moments, taking into account the initial and the boundary conditions. A collision equation was established that could be applied to any type of particle in a continuous or a discrete energy state. In order to effect a plasma diagnostic, the measurable quantities must be associated with the fundamental quantities appearing in the collision equations, such as line-emission coefficients, temperatures, particle densities, and distribution functions. These associations were made for elastic and inelastic processes with the radiative collision model. Relations describing changes in population density, momentum, and energy were established for each type of particle. The results obtained on the intensities of the spectral lines arising from plasmas that were stationary or transient, homogeneous or inhomogeneous, the continuum, and Thomson and Rayleigh scattering are briefly reviewed. (France)

XUM

3062 USE OF THE HIGH-FREQUENCY STARK EFFECT IN PLASMA DIAGNOSTICS. Cooper, W. S.; Hicks, W. W. (Univ. of California, Berkeley). Phys. Lett.; 33A: 188-9(19 Oct 1970).

New numerical calculations of the high-frequency Stark effect in He are used to estimate the range of validity of similar calculations based on perturbation theory, and pitfalls in using this effect in plasma diagnostics are pointed out. (auth)

3063 ENERGY-MASS ANALYSIS FOR HIGHLY IONIZED STEADY-STATE PLASMA. Ishimaru, Hajime (Nagoya Univ., Japan). Jap. J. Appl. Phys.: 9: 1154-62(Sep 1970).

The design and the construction of an electrostatic analyzer for low-energy charged particles and time-of-flight mass spectrometer with mass resolving power of less than 30 for 50-eV ions are described. With application of gated counting methods, accurate energy distributions for each ion species were obtained. Ion temperature and density ratio of each ion species for highly ionized steady-state plasma were also determined. (auth)

3064 MULTIWAVE STUDIES OF RELAXATION PHENOMENA IN ARGON PLASMA. Lobastov, Yu. S.; Testov, V. G. (Inst. of High Temperatures, Moscow. Inst. of Radiotechniques and Electronics, Moscow). Teplofiz. Vys. Temp.; 7: 358-9 (Mar-Apr 1969). (In Russian).

Relaxation phenomena in argon plasma were studied in a shock tube with a rectangular 7×7 cm^2 cross section channel with a two-dimensional flow, using radio waves smaller than the plasma cluster. An oscillogram of radiophysical parameter($\lambda = 8$ mm) variations behind the incident wave in argon at $p_0 = 2$ mm Hg, $M = 10$ is shown; in this case $T_{e\ max} = 8500°K$. The time to reach the maximum absorption and reflection was less than the time of natural emission. The short trailing-edge emission pulse was specified by a sharp increase of reflection coefficient. (R.V.J.)

3065 PLASMA DIAGNOSTICS OF A WEAK-CURRENT ARC DISCHARGE BY MEANS OF A LIGHT PROBE. Batenin, V. M.; Chinnov, V. F. (Inst. of High Temperatures, Moscow). High Temp. (USSR) (Engl. Transl.); 6: 940-6(Nov-Dec 1968).

Translated from Teplofiz. Vys. Temp.; 6: 981-8(Nov-Dec 1968).

Optical probing of a cylindrical, symmetric electrical arc burning in an argon atmosphere with the addition of potassium was carried out. The character of deviation of the population of the resonance level of potassium from the equilibrium value was established in various regions of the plasma volume. It was shown experimentally that violation of the Boltzmann distribution for excited atoms does not lead to a noticeable deviation from ionization equilibrium with electron temperature as described by the Saha equation. (auth)

3066 LASER METHODS OF MEASUREMENT OF PLASMA DENSITY. Petrov, G. D. Izmer. Tekh.; No. 12, 5-9(Dec 1968). (In Russian).

Laser holography, methods of coupled resonators and pulsations, and also methods that use the scattering of higher-energy radiation by the electrons of the plasma as suitable for the measurement of charged-particle density are examined. Results of the appraisal of sensitivity and accuracies are given, and the limits of applicability of each method are determined. (tr-auth)

3067 SCHLIEREN METHOD AND ITS APPLICATION FOR PLASMA DIAGNOSTICS. Hermoch, V. (Inst. of Physics, Prague). Czech. J. Phys.; 20: 939-49(1970).

The schlieren method for measuring electronic and atomic density gradients in plasma has been used in recent years. This paper points out the advantages of this rarely used optical method describing the principle, characteristics, and application. (auth)

3068 DETERMINATION OF ION DENSITY FROM STARK BROADENING OF THE H_β LINE NEAR ELECTRIC DISCHARGE IN H_2 BEAM CLUSTERS. Klingelhoefer, R.; Moser, H.; Roehl, H. (Univ., Karlsruhe, Ger. Kernforschungszentrum, Karlsruhe, Ger.). Z. Naturforsch.; 25a: 1360-2(Aug-Sep 1970). (In German).

A transient plasma column is produced by discharging a 0.1-μF capacitor at 20 kV along a beam of hydrogen clusters. The time dependence of the ion density is obtained from Stark-broadening measurements of H_β (4861 Å). A maximum density of 6.6×10^{16} ions/cm^3 is achieved, the initial density of the neutrals in the beam being 8.5×10^{17} H_2 molecules/cm^3. The background number density in the surrounding vacuum amounts to about 7×10^{10} molecules/cm^3. (auth)

3069 PLASMA DIAGNOSTICS. Brand, G. F.; Millar, D. D. (Univ. of Sydney). At. Energy Aust.; 13: 9-20(Jul 1970).

Diagnostic techniques used in plasma physics are discussed. Spectroscopic measurements of electron temperature and density are covered, as well as diagnostic methods based on plasma–electromagnetic wave interactions. Measurements by Alfvén waves, microwaves (by transmission or interferometry) and laser light (by interferometry and Thomson scattering) are reviewed. (Australia)

3070 PROPERTIES OF FREE JETS OF IONIZED NITROGEN. Myronuk, Donald Joseph. Urbana, Ill.; Univ. of Illinois (1969). 125p. University Microfilms Order No. 70-13,427.

Thesis.

The results of an experimental study to measure temperatures and electron densities of a free jet of ionized nitrogen gas at atmospheric pressure are presented. A spectroscopic method that utilized the 4955-Å continuum radiation of nitrogen to investigate the exhaust plume of a plasma jet of a simple design, yielded gas temperatures in the range of 9000°K to 15,800°K and electron densities in the range of 5×10^{15}/cm^3 to 10^{17}/cm^3. Nitrogen-mass flow rates were 0.05 and 0.1 grams per second with arc currents of 200 and 300 A. The study made possible an estimation of Prandtl numbers, which included radiation effects and ranged in value from 0.06 to 0.75 in the free jet. There is general agreement between these values and other available data in the temperature range of 2000 to 12,000°K. A value of the order of 12 was determined for the jet spread parameter associated with free jets. Other items of interest are plasma jet noise levels, the application of a fluidic velocity probe to determine average velocity profiles in the hot jet and the deflection of the jet by an applied electric field. (Diss. Abstr. Int., B)

3071 VARIABLE SENSITIVITY OPTICAL MACH-ZEHNDER AND HOLOGRAPHIC INTERFEROMETRY FOR PLASMA DIAGNOSTICS. Weigl, Frederic. Austin, Tex.; Univ. of Texas (1969). 119p. University Microfilms Order No. 70-10,883.

Thesis.

Techniques both to increase and decrease the sensitivity of nondiffuse optical holographic interferometry for use with transparent experimental media are developed. Applications to plasma diagnostics are emphasized. The simultaneous recording of double-exposure holographic interferograms at two or more optical wavelengths is discussed. Two experimental techniques to accomplish this are investigated experimentally using a pulsed argon laser and Polaroid 55 P/N film. One technique uses a single multiple-wavelength reference beam, while the other uses multiple single-wavelength reference beams. (Diss. Abstr.) (TSS)

3072 EXPANSION OF THE MEASUREMENT LIMITS OF ELECTRON DENSITY IN A PLASMA USING A LASER INTERFEROMETER WITH PHASE MODULATION OF THE OPTICAL SIGNAL. Dushin, L. A.; Privezentsev, V. I. (Physical-Technical Inst., Kharkov). High Temp. (USSR) (Engl. Transl.); 8: 148-50(Jan-Feb 1970).

Translated from Teplofiz. Vys. Temp.; 8: 159-62(Jan-Feb 1970).

The scheme of an optical laser interferometer permitting measurement of $n_e L$ of a plasma within the limits from 10^{14} to 10^{17} cm^{-2} is discussed. (auth)

3073 X-RAY SPECTROSCOPIC MEASUREMENT OF THE TEMPERATURE OF ATOMIC AND IONIC TRANSFER IN A PLASMA. Lacaze, Rose-Marie (Univ., Paris); Bonnelle, Christiane; Terrier, Marc; Vervisch, Pierre; Valentin, Pierre. Compt. Rend.; Ser. B; 271: 614-17(28 Sep 1970). (In French).

A new method is described for the temperature measurement of the heavy particles of a plasma within a pressure and temperature range where conventional methods do not exist. (tr-auth) (France)

3074 EVALUATION OF THE ACCURACY OF PROBE MEASUREMENTS OF THE VELOCITY OF FREE-MOLECULAR PLASMA FLOWS. Petrov, G. D. Izmer. Tekh., No. 5, 38-9 (May 1969). (In Russian).

The theory of the operation of a probe in rarefied plasma was given by Bernstein and Rabinowitz (Phys. Fluids, No. 2 (1959)), and experimental results in determining the velocity field are provided by Sonin (Rocket Technology and Austronautics, No. 9 (1966)). The anisotropy of the velocities was not then measured, and the values obtained for the velocity field were only tentative. In this note, the author provides a theoretical evaluation of the precision in measuring the velocity of plasma flow with a plane probe. (L.M.T.)

Kinetics (General)

3075 (CEA-CONF-1627) BASIC COLLISION PROCESSES IN PLASMAS; COLLISION CROSS SECTIONS. Drawin, H. W.

(European Atomic Energy Community. Commissariat a l'Energie Atomique, Fontenay-aux-Roses (France). Centre d'Etudes Nucleaires). 1970. 39p. (CONF-700706-1). Dep. NTIS (U. S. Sales Only).

From 5th Plasma Physics Symposium, Herceg-Novi, Yugoslavia.

In plasmas, molecules and molecular ions have translational, rotational, vibrational, electronic, and chemical energy; atoms and atomic ions have translational, electronic, and chemical energy, and electrons have only translational energy. Collisions between these particles lead to energy transfers between these different types of energies, and a table, which has the form of a matrix, gives a simple classification of these interaction processes. The rules and regularities in collision processes are recalled: energy and momentum conservation, spin conservation, adiabaticity, nonadiabaticity and level crossing, and Franck–Condon principle. The general behavior of some selected cross sections is reviewed. (France)

3076 FIZIKA GAZORAZRYADNOI PLAZMY. VYPUSK 1. (Physics of Gas-Discharge Plasma. Number 1). Trekhov, E. S. (ed.). Moscow; Atomizdat (1968). 100p.

Ten articles are included on the theory of high-frequency discharges for the cases of vortex electrodeless discharges and jets. Tabulated data are given on the vortex discharge (skin effect) in argon and air at atmospheric and low pressures. The influence of parameters of an electrodeless plasmatron on the performance of hf generators, applicability of electrodynamic models to a hf arc discharge stabilized by axial gas purging, and problems on generation of plasma jets in circulating hf arc discharges are discussed. (R.V.J.)

3077 STUDY OF THE VELOCITY RELATIONS IN THE RAIL ACCELERATOR WITHOUT AN EXTERNAL MAGNETIC FIELD. Maloch, J.; Sestak, B.; Sobra, K.; Stanek, Z. (Technical Univ., Prague). Czech. J. Phys.; 20: 1186-93(1970).

The experimental results of the measurement of the plasma cluster velocity in the rail accelerator and their theoretical analysis are presented. The experimental setup with simple pulse electromagnetic valves enabling a discharge to be struck is described. The dependences of the plasma cluster velocity on the voltage between electrodes and on different capacitances of the condenser battery are studied. (auth)

3078 PLASMA DEFLAGRATION AND THE PROPERTIES OF A COAXIAL PLASMA DEFLAGRATION GUN. Cheng, Dah Yu (Univ. of Santa Clara, Calif.). Nucl. Fusion; 10: 305-17 (Sep 1970).

The concept of plasma deflagration is investigated theoretically and experimentally. Deflagration is a heating process that adds energy to a flowing stream under expansion. The equations governing the process are the same as the detonation "snowplough" process; therefore, deflagration is nothing more than the second solution of the set of conservation equations. The deflagration process is thoroughly studied in the field of chemical combustion. An analogy between combustion and magnetized plasma is made, and the second law of thermodynamics is invoked in the discussion on the limits of the existence of deflagration solutions. The deflagration process that occurs in a gaseous discharge can accelerate particles to very high velocities at relatively low thermal energy. The deflagration discharge wave always propagates towards the high gas pressure and the high magnetic field region. The wave can be made stationary by injecting neutral gas into the wave. The discharge zone is thick, which reduces the local current density with a given total current and the erosion of electrodes can thus be reduced. A coaxial plasma gun was designed, based on the deflagration principle, which demonstrates the features predicted by the deflagration hypothesis. The energy of the plasma stream thus produced exceeds 10 keV ($>10^8$ cm/sec with D_2). The discharge wave is found to be thick, and the wave is quasi-stationary inside the gun barrel. Besides the high-velocity capabilities, the gun can focus the plasma to a very small area. This provides a unique opportunity to perform plasma injection experiments with strong magnetic fields (>100 kG). (auth)

Kinetics (Experimental)

3079 INVESTIGATION OF CHARGE EXCHANGE OF A DENSE PLASMA CURRENT IN A MAGNESIUM TARGET. Kartashev, K. B.; Pistunovich, V. I.; Platonov, V. V.; Filimonova, E. A. Zh. Eksp. Teor. Fiz.; 59: 779-84(Sep 1970). (In Russian).

Charge exchange of a plasma cluster with an ion density $n_i \approx 10^{12}$ cm^{-3} in an ultrasonic magnesium jet is investigated experimentally. It is shown that charge exchange takes place in accordance with the classical model of pair collisions; in this case no appreciable scattering of the particles with increase of the target thickness up to $n_M l \approx 2 \times 10^{16}$ cm^{-2} is observed. Scattering occurring at $n_M l \gtrsim 3 \times 10^{16}$ cm^{-2} cannot be ascribed exclusively to Coulomb scattering since the accuracy of measurement of the target thickness is not sufficient for this. It is found that an ultrasonic magnesium jet may serve as a "shutter" for a plasma moving with a velocity $<5 \times 10^7$ cm/sec. (auth)

3080 TRANSFORMATION OF THE DISTRIBUTION FUNCTION OF AN ELECTRON BEAM DURING CYCLOTRON INTERACTION WITH A PLASMA. Shustin, E. G.; Popovich, V. P.; Kharchenko, I. F. (Inst. of Radio Physics and Electronics, Erevan). Zh. Eksp. Teor. Fiz.; 59: 657-60(Sep 1970). (In Russian).

The longitudinal and transverse energy distribution of electrons in a beam interacting with a magnetoactive plasma waveguide is investigated experimentally. It is shown that upon excitation by the beam of waves with frequencies $\omega_c < \omega < \sqrt{\omega_p^2 + \omega_c^2}$, an appreciable increase of the electron transverse motion energy occurs. It is thus confirmed experimentally that transformation of electron longitudinal energy into transverse energy occurs in the interaction between the beam and plasma due to the anomalous Doppler effect. (auth)

3081 METHOD OF MEASURING ELECTRICAL CONDUCTIVITY OF PLASMA WITH A HIGH TIME RESOLUTION. Poberezhskii, L. P. High Temp. (USSR) (Engl. Transl.); 6: 933-9(Nov-Dec 1968).

Translated from Teplofiz. Vys. Temp.; 6: 973-80(Nov-Dec 1968).

Factors influencing resolving power in time and the accuracy of systems measuring the electrical conductivity of an ionized gas flow based on the change of the circuit Q are analyzed. The technique of measuring electrical activity with a time resolution of less than 1 μsec and range of measurable values of conductivity from hundredths to thousands of mho/cm is described. (auth)

3082 INVERSE FARADAY EFFECT IN A PLASMA. Deschamps, J.; Fitaire, M.; Lagoutte, M. (Faculte des Sciences, Orsay, France). Phys. Rev. Lett.; 25: 1330-2(9 Nov 1970).

It was shown experimentally that a magnetic field is created by the electrons of a plasma subjected to high-power pulses of circularly polarized microwaves. The experimental results confirm the predictions concerning this phenomenon, known as the inverse Faraday effect. (auth)

3083 MEASUREMENT OF THE RADIAL DISTRIBUTION OF ELECTRIC FIELD STRENGTH IN HYDROGEN ARCS WITH AXIAL MAGNETIC FIELD. Schwenn, R. (Institut fuer Plasmaphysik, Garching, Ger.). Z. Naturforsch.; 25a: 1310-16(Aug-Sep 1970). (In German).

In a stationary hydrogen arc with axial magnetic field, the radial distribution of the axial electric field E_z was measured by shooting a double-potential probe across the arc. It was found that E_z strongly decreases outside the magnetic flux tube defined by the cathode radius and tends to zero. The measured distribution of E_z agrees qualitatively with computations allowing for the observed rotation profile. In a very-fast-rotating arc with a hollow anode, E_z was found to vanish not only outwards, but also towards the axis, as predicted by the theory. (auth)

3084 MEASUREMENT OF RADIATIVE LOSSES IN A PULSED PLASMA ACCELERATOR USING THE BOLOMETRIC METHOD. Derevshchikov, V. A.; Rusakov, N. V. (All-Union Scientific-Research Inst. for Electromechanics, Moscow). High Temp. (USSR) (Engl. Transl.); 8: 15-18(Jan-Feb 1970).

Translated from Teplofiz. Vys. Temp.; 8: 17-21(Jan-Feb 1970).

A method is proposed for measuring radiative losses in an erosional pulsed plasma accelerator, using quick-response radiation pickups, located at a considerable distance from the radiating volume of the plasma, to separate the effects of bombardment by particles of the plasma and the action of radiation. Measurements were made of energy losses due to radiation in end-type and coaxial accelerator models. In an end-type model the losses are 16 to 24% for an aluminum central electrode and 7 to 10% for a lithium electrode; in a coaxial model, they are 3 to 5%. The fact that the greatest fraction of the radiative losses occurs in the vacuum-ultraviolet region of the spectrum indicates that the use of optical filters is undesirable in such measurements. (auth)

Kinetics (Theoretical)

3085 (LYCEN-7061) DISTRIBUTION OF ION DENSITIES IN AN ARC DISCHARGE. Bajard, M.; Hadinger, G.; Hadinger, G.; Tauth, Th. (Lyon Univ. (France). Institut de Physique Nucleaire). 8 Jul 1970. 12p. (In French). Dep. NTIS (U. S. Sales Only).

XUM

The general equations of the elementary processes involved in the plasma are considered, and the characteristics of an arc discharge introduced. Quantitative relations between the concentrations of the ionic carriers and the different positive charges as a function of the j_Z, Z_m, $\langle Z \rangle$ and Z parameters, and the recombination and charge exchange cross sections, are obtained. The case of xenon is discussed, and cross sections calculated from the measured ion currents given. (tr-auth) (France)

3086 PHASE TRANSITION AND NEGATIVE CLUSTERS IN AN IMPERFECT PLASMA OF METAL VAPOR. Khrapak, A. G.; Yakubov, I. T. (Inst. of High Temperatures, Moscow). Zh. Eksp. Teor. Fiz.; 59: 945-50(Sep 1970). (In Russian).

An equilibrium, highly imperfect, and partially ionized plasma is considered. Under certain conditions, interaction between charged and neutral particles may result in the formation of very heavy negative charged clusters. Estimates indicate that this may induce phenomena of the phase-transition type under conditions that are encountered in some experiments. (auth)

3087 EFFECTIVE DIELECTRIC CONSTANT OF CYLINDRICAL PLASMA AT MICROWAVE REGIONS. Lau, Bong Whan (Korea Univ., Seoul); Chung, Jae Sun; Kim, Sung Wun; Min, Suk Ki. New Phys. (S. Korea); 10: 65-70(Jun 1970). (In Korean).

To clarify the dielectric behavior of cylindrical plasmas at microwave regions, the Tonks–Dattner resonance was studied. From the condition of minimum points in the resonance curves, the relative dielectric constant that incorporated the collisions, thermal motions, and finiteness of boundary was derived. Then with the insertion of this expression into the condition of maximum points one gets the equation of corresponding relative dielectric constant. To verify experimentally these theoretical results, TE_{10} modes at 9 and 16 GHz were used in the generation of perturbed electric fields. With these practical conditions, the real and imaginary parts of dielectric constants changing with the discharge currents were determined, and the tendency of greater dielectric loss with decreasing discharge currents was confirmed. (auth)

3088 NUMERICAL CALCULATIONS AND DESCRIPTION OF TOROIDAL ARCS BY MODEL THEORIES. Wynands, A.; Druxes, H.; Schmitz, G. (Technische Hochschule, Aachen). Z. Phys.; 239: 306-21(1970). (In German).

Contrary to cylindrical arcs, there appear asymmetric thermal, electric, and magnetic values. The displacement of the maximum of temperature out of the center of cross section to the center of curvature may be a criterion for this asymmetry. The effects of curvature are realized analytically by a model theory. Furthermore, a theory of conform mapping of the numerical results of a cylindrically symmetric arc to a torus geometry yields to values that are in good agreement with numerical solutions of the energy balance of the toroidal geometry. In addition convection caused by the asymmetry of the Lorentz forces, is pointed out. (auth)

3089 NONLINEAR PROBLEM ON COLLISION OF ANTIPARALLEL FLOWS OF A RAREFIED PLASMA. Sigov, Yu. S. (Inst. of Applied Mathematics, Moscow). Dokl. Akad. Nauk SSSR; 192: 534-7(21 May 1970). (In Russian).

The nonstationary problem on nonlinear electrostatic oscillations in mutually penetrating fluxes of rarified plasma is solved by numerical methods within the framework of a single-dimensional model. Solutions of the type of collision-free shock waves can be expected in problems of this kind under definite conditions. An electron–proton plasma moves at an average velocity along the x axis, and at time $t = 0$ collides with the same plasma at plane $x = 0$. The plasma is strongly nonisothermal. The behavior of the system is described by the Vlasov equations. In order to solve the nonlinear set of equations a discrete model of the plasma is used in which the phase space is broken up into NQ cells by dividing the configurational and momentum spaces into N and Q cuts, respectively. A self-consistent solution is obtained by a simultaneous numerical integration over each interval with respect to time. The time dependence of the potential energy is about 10% of the total energy at saturation. The space distribution of ions, and the distribution of particles in phase space have the form of a collision-free shock wave. Small-scale oscillations caused by ion bunching are modulated by the main harmonic of the ion–ion oscillations. Behind the shock-wave front there takes place strong scattering and thermalization of ions on electrostatic oscillations. (TTT)

3090 TRANSVERSE CONTRIBUTIONS TO THE NONLINEAR CONDUCTIVITY–TERNARY CORRELATION RELATIONS IN NONRELATIVISTIC PLASMAS. Golden, K. I.; Silevitch, M. B. (Northeastern Univ., Boston). Phys. Lett.; 33A: 162-3(19 Oct 1970).

The statistical-mechanical perturbation theoretic method of Kubo is used to calculate the nonlinear response of an equilibrium collection of classical plasma particles and radiation field oscillators; the equilibrium system is in a constant external magnetic field. (auth)

3091 HIGH-SPEED PLASMA FLOW IN A CUSPED MAGNETIC FIELD. Tanaka, Masatoshi (Japan Atomic Energy Research Inst., Tokai). Jap. J. Appl. Phys.; 9: 1163-6(Sep 1970).

High-speed plasma flow, the flow velocity of which is much larger than the thermal velocity of the ions, in a cusped geometry is investigated. The density distribution of the plasma in a plane perpendicular to the axis is assumed to be known and the ions there to have a Maxwellian distribution of velocities. The ion distribution in the downstream is calculated in the free-particle approximation. (auth)

3092 WAVE RADIATION BY A CHARGE IN NONEQUILIBRIUM PLASMA. Radzievskii, V. N. (Inst. of Physics, Kiev). Ukr. Fiz. Zh.; 15: 989-99(Jun 1970). (In Russian).

Interaction of a charged particle with fluctuation fields in a nonequilibrium magnetoactive plasma was considered. Spectral densities of correlation functions of the electric field fluctuations were determined in such a plasma. The energy losses of a particle were calculated as a result of its resonance and Doppler interactions with low-frequency fluctuation fields. (auth)

3093 CALCULATION OF THE ELECTRICAL CONDUCTIVITY OF PARTIALLY IONIZED PLASMA. Asinovskii, E. I.; Batenin, V. M. (Inst. of High Temperatures, Moscow). High Temp. (USSR) (Engl. Transl.); 6: 927-32(Nov-Dec 1968).

Translated from Teplofiz. Vys. Temp.; 6: 966-72(Nov-Dec 1968).

Known methods of calculating electrical conductivity of partially ionized plasma are analyzed. The inapplicability of the lower approximations of the Enskog–Chapman theory and formulas based on the additivity of specific resistances of plasma components in the case when the electron–atom cross section is an increasing function of electron velocity is shown. The limits of applicability of the Lorentz model to partially ionized plasma are found. (auth)

3094 COMPUTER STUDIES OF PLANAR PLASMA CONFIGURATIONS. Burn, Robert Daniel Jr. Stanford, Calif.; Stanford Univ. (1969). 75p. University Microfilms Order No. 70-10,435.

Thesis.

Three computer models simulating the motion of a plasma in both one and two dimensions were applied to the sheet or planar pinch. Both the relativistic regime, including field-retardation effects, and the nonrelativistic regime were investigated. In all cases both electric and magnetic interactions were allowed. The sheet pinch was completely stable both to spreading and fast-wave instabilities, but exhibited tearing-mode instabilities in the slow wave regime. Typically, the tearing consisted of an initial breakup into multiple strands, which subsequently underwent coalescence. (Diss. Abstr. Int., B)

3095 SYNCHROTRON RADIATION IN TOKAMAKS. Rosenbluth, M. N. (Inst. for Advanced Study, Princeton, N. J.). Nucl. Fusion; 10: 340-3(Sep 1970).

The radiation and self-absorption in the low-temperature limit, where $v/c \ll 1$ and the field inhomogeneity provides all the broadening, are calculated for Tokamak devices. (M.O.W.)

3096 SPECTRA OF MAGNETOHYDRODYNAMIC TURBULENCE IN COLLISIONLESS PLASMA. Livshits, M. A.; Tsytovich, V. N. (Inst. of Physics, Moscow). Nucl. Fusion; 10: 241-50(Sep 1970).

Steady-state frequency spectra are considered for Alfvén and magnetohydrodynamic waves created when the waves interact nonlinearly. The principal form of nonlinear interaction is scattering by plasma particles. A study is made of the stability conditions for the power-type spectra $W_{\omega\Omega} = (1/\omega^{\nu})W_{\Omega}$. It is demonstrated that power-type spectra with $\nu \geq 1$ are stable; at $\nu = 1$ to 2 the power-type nature of the spectrum is not disturbed during establishment of the steady state, as distinct from other values of ν. (auth)

3097 PLASMA MOTION AND EQUILIBRIUM IN UNSYMMETRIC MAGNETIC FIELDS. Lehnert, B. (Royal Inst. of Tech., Stockholm). Nucl. Fusion; 10: 283-92(Sep 1970).

The motion and equilibrium of a plasma confined by an arbitrary magnetic field are investigated, where the lines of force are either closed inside the confinement volume or form a bottle between two magnetic mirrors. (a) Stationary states are treated for which macroscopic fluid motions are allowed to take place in the plasma. Such states represent a larger class of equilibria than the static ones where the plasma is assumed to be at rest all over space. (b) For a hot plasma confined in a closed magnetic bottle the fluid motions decay at essentially the same rate as the pressure gra-

dients and the electric currents. (c) A modified deduction is presented of the average guiding-center drifts from field line to field line in the $\alpha\beta$ space defined by the magnetic field. The drifts include contributions from the electric field and the magnetic gradient. (d) The contribution to the macroscopic particle flux from the gyro motion is averaged along the field lines to form a corresponding flux in $\alpha\beta$ space. An average macroscopic fluid velocity is further obtained by superimposing the contributions from the guiding-center drifts and the gyro motion. (e) The mechanisms producing density changes and charge-separation phenomena are treated in terms of the average macroscopic fluid velocity. They are found to be due to the average guiding-center drifts only. (f) An analysis is performed in terms of the velocities in $\alpha\beta$ space of equilibria for which local fluid velocities are allowed to exist in the plasma. For a particular class of such states an electric field can be set up which, on the average, keeps the plasma at rest on each field line. (g) The results indicate that plasma confinement should become possible in ring-current configurations with magnetically screened supports, provided that the plasma remains stable and that there are no excessive losses in the small weak field regions close to the leads where this analysis is inapplicable. (auth)

3098 APPLICATION OF THE MONTE-CARLO METHOD TO THE SOLUTION OF KINETIC PROBLEMS OF LOW-TEMPERATURE PLASMA. Malama, Yu. G.; Lebedev, S. N. Tr., Vses. Nauch.-Issled. Inst. Yader. Geofiz. Geokhim.; No. 3, 74-80(1968). (In Russian).

Earlier proposals concerning the use of an argon or helium plasma jet for the detection of hydrocarbon deposits were followed up. The required theoretical treatment involves the Maxwellization of the high-temperature plasma jet and of the gases obtained by the evaporation of the ores exposed to the jet. The Monte-Carlo technique was used to solve the Maxwellization process for a spatially homogeneous mixture of two gases; specific geophysical questions that arise under actual field conditions were also taken into account. The method was used to solve kinetics problems, calculating the dependence of the distribution function on time and deriving other parameters, such as the number of collisions per unit time, etc. Although the strict theoretical foundations must still be developed, the new "periodic boundary conditions method" appears to be useful for solving problems in chemical and physical kinetics. (TTT)

3099 KINETIC EQUATIONS FOR AUTOCORRELATION FUNCTIONS IN DILUTE GASES. Chappell, W. R. (Univ. of Colorado, Boulder). Contract DA-31-124-ARO-D-139. J. Statist. Phys.; 2: 267-77(1970).

It is shown that, in the case of a dilute gas of neutral particles, kinetic equations for autocorrelation functions such as $\langle \hat{f}(r,v,t)\hat{f}(r',v',t')\rangle$, where $\hat{f}(r,v,t) = \Sigma_{i=1}^{N}\delta(r - r_i(t))\delta(v - v_i(tt))$, can be obtained in a very simple manner by the use of the truncated BBGKY hierarchy. The resulting equations correspond to the low-density limit of the results of van Leeuwen and Yip. Moreover, the derivation does not make use of the Bogolyubov adiabatic approximation, and therefore includes non-Markovian effects that can be important in describing light scattering from gases and the collisional narrowing of atomic dipole radiation. The resulting equations in the long-wavelength limit correspond to the non-Markovian Boltzmann equation for the self-correlation part and the non-Markovian, linearized Boltzmann equation for the total autocorrelation function. (auth)

3100 IMPEDANCE OF A PARALLEL-PLATE CAPACITOR IN A COMPRESSIBLE, INHOMOGENEOUS, COLLISIONAL MAGNETOPLASMA. Chai, Hi Dong Boston; Northeastern Univ. (1968). 194p. University Microfilms Order No. 69-18,547.

Thesis.

A qualitative study of impedance of a section of an infinitely large parallel-plate capacitor in plasma is presented, using one-dimensional macroscopic hydrodynamic equations and Maxwell's equations. First, starting from the definition of impedance (ratio of voltage to current), an impedance formula is derived as an integral of the first-order velocity function. This reduces the problem into one of finding the velocity, which is a solution to an ordinary, inhomogenous second-order differential equation. Secondly, the impedance of a capacitor in a homogenous, compressible, collisional magnetoplasma is obtained. Totally reflecting and totally absorptive boundary conditions are used, and their results compared. For the inhomogenous plasma, a parabolic zero-order density profile is assumed. Impedance is obtained using a difference method. Effects of collision, uniform magnetic field, capacitor plate separation, and sheath on impedance are analyzed. Also, a possibility of using impedance variation over a range of frequencies in diagnosing plasma parameters for low-density plasmas such as the ionosphere is discussed. (Diss. Abstr. Int., B)

3101 SCATTERING OF LASER LIGHT BY HIGH-DENSITY PLASMAS. Schaefer, Robert Anthony. Ann Arbor, Mich.; Univ. of Michigan (1969). 122p. University Microfilms Order No. 70-14,633.

Thesis.

The predominant scattering process is the Thomson scattering of photons by the free electrons in the plasma. A differential scattering cross section is related to the autocorrelation of the space–time dependent electron density fluctuations in the plasma. In the analysis, particular care is taken to include the effects of all internal electromagnetic field fluctuations. The transverse electric and magnetic fields are included in the kinetic equations. It is found that, if the plasma is in thermal equilibrium and there is no applied electromagnetic field, the scattering cross section for photons is completely independent of the transverse internal-field fluctuations. However, if an electric current is flowing through the plasma and the current may be represented by an electron drift in the plasma, a correction to the previously calculated scattering cross section is found due to the internal transverse field fluctuations. This correction may be of sizeable magnitude under certain experimental conditions, e.g., very high electron density. The scattering of photons by a plasma in a strong applied magnetic field is also considered and the effect of the internal transverse field fluctuations is found to be negligible. It is concluded that, for the diagnosis of a dense plasma by the laser light scattering technique, the internal transverse field fluctuations must be considered or their neglect must be justified. (Diss. Abstr. Int., B)

3102 OPTICALLY THIN HYDROGEN PLASMA WITH SELF-CONSISTENT ELECTRON VELOCITY DISTRIBUTION. Oxenius, J. (EURATOM–CEA, Fontenay-aux-Roses, France). Z. Naturforsch.; 25a: 1302-10(Aug-Sep 1970).

Occupation numbers of the atomic levels and degree of ionization of a stationary optically thin hydrogen plasma are calculated for temperatures in the range $8{,}000°K \lesssim T \lesssim 16{,}000°K$ and for electron densities in the range $10^9\ cm^{-3} \lesssim n_e \lesssim 10^{17}\ cm^{-3}$. The electron velocity distribution is not supposed to be Maxwellian, rather, it is obtained in a self-consistent way from the corresponding kinetic equation, which is solved simultaneously with the equations that describe the statistical steady state of the atomic levels. Besides spontaneous radiative bound–bound transitions and radiative recombinations, inelastic electron–atom collisions as well as elastic electron–electron and electron–atom collisions are taken into account. Hydrogen atoms are approximated by model atoms having four bound levels and a continuum. The numerical results show that, for temperatures $T \lesssim 10{,}000°K$, the tail of the electron distribution function differs markedly from that of a Maxwell distribution, except in the case of high electron densities. Likewise, the self-consistently calculated values of the atomic occupation numbers and of the degree of ionization there deviate strongly, up to several orders of magnitude, from those obtained by assuming a Maxwellian velocity distribution of the electrons. (auth)

3103 FLOW OF COMPRESSIBLE PLASMAS IN INHERENT FIELDS OF ARC DISCHARGES. Huegel, Helmut (DFVLR, Stuttgart). Z. Naturforsch.; 25a: 1317-32(Aug-Sep 1970). (In German).

The flow of compressible plasmas in axisymmetric channels of constant or variable cross sections under the influence of electromagnetic bodyforces and of Joule heating is described in terms of magnetogasdynamics. The existing electric and magnetic fields are not independently applied, but originate as the electric field and self-induced magnetic field from a dc arc discharge. Under the condition of low magnetic Reynolds numbers, a quasi-one-dimensional description of the flow is given, using the flow parameters velocity, Mach number, pressure, density, and temperature. For these quantities, five coupled first-order differential equations are obtained. A qualitative discussion outlines typical solutions and points out some features that are the same for flows in arc discharges and for flows in so-called crossed fields. The conditions for a continuous passage through the sonic point are discussed. For flows in diverging nozzles, results of numerical integration are presented. Experimental investigations are reported that verify the self-magnetic effect in nozzle flows. At arc currents of 500 to 3000 A, measured values of thrust and Mach number show satisfactory agreement with theoretical results. (auth)

3104 RADIAL PRESSURE PROFILE IN AN MPD HYDROGEN ARC. I. 5-MOMENTS APPROXIMATION. Bohn, W. L.; McCann, T. E. (DFVLR, Stuttgart). Z. Naturforsch.; 25a: 1332-43(Aug-Sep 1970). (In German).

Within the framework of the five-moments approximation, the radial pressure profile of an MPD arc is calculated as a function

XUM

of the ambient pressure and the superimposed magnetic field. In addition to the well known pressure increase due to ambipolar diffusion, the typical axisymmetric MPD geometry provides further pressure increase or decrease by the interaction of current density (Hall effect) or mass flow with the magnetic field. Characteristic pressure profiles for assumed current and flow fields and for various superimposed magnetic field strengths are shown in numerous diagrams and are discussed by use of the generalized Ohm's law. A significant pressure decrease due to mass entrainment becomes evident. Deviations from LTE are considered in the frozen-flow approximation. The theoretically predicted pressure decrease in the axial region of the plasma flow of an MPD arc subjected to mass entrainment agrees qualitatively with experimental results. (auth)

3105 RADIAL PRESSURE PROFILE IN AN MPD HYDROGEN ARC. II. 13-MOMENTS APPROXIMATION. McCann, T. E.; Bohn, W. L. (DFVLR, Stuttgart). Z. Naturforsch.; 25a: 1344-53(Aug-Sep 1970). (In German).

The calculation of the radial pressure profile of an MPD arc as a function of the ambient pressure and the superimposed magnetic field, developed in the preceding paper, is extended to the 13-moments approximation. The higher-moments approximation introduces additional thermomagnetic forces and changes significantly the structure of the velocity-dependent part of the external viscous forces. While the Hall effect and the mass flow are practically unaffected by the higher approximation, as far as their influence on the radial pressure profile is concerned, the ambipolar diffusion leads to an appreciably smaller pressure increase than the 5-moments theory. Qualitative differences of the two approximations are discussed beyond the scope of pressure profiles via the generalized Ohm's law. Quantitative results for a partially as well as for a fully ionized plasma are shown in diagrams. The importance of thermomagnetic forces (especially the Nernst effect) for MPD arcs is clearly pointed out. (auth)

3106 DEVIATIONS FROM THE THERMODYNAMIC EQUILIBRIUM IN AN ATOMIC HYDROGEN PLASMA. Peyraud, Nelly. J. Phys. (Paris); 31: 565-80(Jul 1970). (In French).

The quasi-static theory of a partially ionized plasma with partial trapping of the radiation is applied to an atomic hydrogen plasma. An analytic expression is given for the non-Maxwellian discrepancies in the tail of the distribution function in terms of the partial opacity of the plasma to the resonant radiation. The local influence of these discrepancies on the Boltzmann (for the ratio of populations in the resonance and the ground levels) and Saha's laws in a slab of plasma is studied. (tr-auth) (France)

3107 THEORY OF A PLASMA CATHODE. Ul'yanov, K. N. (All-Union Order of Lenin Electrotechnical Inst., Moscow). High Temp. (USSR) (Engl. Transl.); 8: 10-14(Jan-Feb 1970).

Translated from Teplofiz. Vys. Temp.; 8: 12-16(Jan-Feb 1970).

The operation of a plasma cathode is considered when the nonemitting negative electrode is located in the plasma, while the positive electrode is located in a vacuum. The ionization in the plasma equalizes itself by volumetric recombination. Expressions are obtained for the currents and the form of the volt–ampere characteristics for the plane, cylindrical, and spherical cases. (auth)

3108 EFFECT OF NONHOMOGENEOUS INTERATOMIC ELECTRICAL FIELDS ON A RADIATING ATOM IN A LOW-TEMPERATURE PLASMA. Grechikhin, L. I. (Inst. of Physics, Minsk). High Temp. (USSR) (Engl. Transl.); 8: 19-24(Jan-Feb 1970).

Translated from Teplofiz. Vys. Temp.; 8: 22-8(Jan-Feb 1970).

In many cases the concentration of charged particles in a plasma can be found from the broadening of the spectral lines due to the action of a nonhomogeneous field. For diagnostic purposes use can be made of the "polar effect," as well as of the forbidden transitions of the S–nF series and of the phenomenon of the supplementing of the spectral lines in a multiplet. (auth)

Production

Refer also to abstract 3052.

3109 (CEA-CONF-1610) PLASMA FORMATION BY DISSOCIATION OF AN ACCELERATED HYDROGEN CLUSTER BEAM. Bottiglioni, F.; Coutant, J.; Fois, M. (European Atomic Energy Community. Commissariat a l'Energie Atomique, Fontenay-aux-Roses (France). Centre d'Etudes Nucleaires). 1970. 4p. (CONF-700817-6). Dep. NTIS (U. S. Sales Only).

The dissociation rate of a hydrogen cluster beam crossing an electron target was calculated with a model involving spontaneous breaking of multicharged clusters. (tr-auth) (France)

3110 (IN-1425) BIBLIOGRAPHY OF LASER PUBLICATIONS OF INTEREST TO EMISSION SPECTROSCOPISTS. V. Baldwin, Jon M. (Idaho Nuclear Corp., Idaho Falls). Aug 1970. Contract AT(10-1)-1230. 15p. Dep. NTIS.

Thirty references are listed in connection with laser beam interactions with gases, seventy-seven for laser beam interactions with condensed phases, and thirty for applications of lasers to analysis. Many of the references in the second group concern plasma production by laser beams. (J.G.B.)

3111 (LYCEN-7065) PRODUCTION OF MULTICHARGED IONS IN A REFLEX SOURCE WITH AXIAL EXTRACTION. Bajard, M.; Chabert, A.; Droc, M.; Hadinger, G.; Jacquet, G.; Tauth, Th. (Lyon Univ. (France). Institut de Physique Nucleaire). 23 Jul 1970. 16p. (In French). Dep. NTIS (U. S. Sales Only).

A test bench for reflex sources is described, and the first experimental results with an axial extraction source are given. Various extraction geometries were tested and a diaphragmed expansion cup was selected. The measurements were made with this cup. The internal and external characteristics of the nitrogen, neon, and argon ion sources are discussed. Currents composed of quadruply ionized particles were easily detected. (tr-auth) (France)

3112 APPARATUS FOR THE PRODUCTION AND INVESTIGATION OF HIGH-PRESSURE HEAVY-CURRENT LONG ARCS. Borovik, E. S.; Petrenko, V. I.; Knyazev, Yu. R.; Mitin, R. V.; Kantsedal, V. P. (Physical-Technical Inst., Kharkov). High Temp. (USSR) (Engl. Transl.); 6: 1076-80(Nov-Dec 1968).

Translated from Teplofiz. Vys. Temp.; 6: 1124-9(Nov-Dec 1968).

An apparatus was designed for the production and investigation of an arc discharge at pressures of up to 1000 atm, arc lengths up to 10 cm, and currents up to 100 A in continuous operation and 100 kA in pulsed operation. The method of producing high pressures by means of a thermocompressor is described. A brief account is given of the main results obtained in the investigation of continuous and pulsed high-pressure discharges. (auth)

3113 INVESTIGATION OF DENSE PLASMA FORMATION USING ELECTRON BEAM INJECTION INTO MAGNETIC TRAP. Bredikhin, M. Yu.; Il'chenko, A. M.; Maslov, A. I.; (and others). At. Energ. (USSR); 29: 276-82(Oct 1970). In Russian).

The possibility of a dense plasma formation using fast electron beam–neutral gas interaction in a magnetic mirror configuration was investigated. In contrast to recent works, a neutral supersonic stream was used to inject neutrals into a region of interaction. Thereby, a necessary pressure gradient was created without any differential pumping. As a result of the experiments the conditions of exponential plasma density growth were found as a function of the beam–plasma discharge parameters. It turns out that the time of plasma density increase to values $\geq 7 \times 10^{13}$ cm^{-3} is less that 10 μsec. The lifetime of the dense plasma is several times more than the time of electron beam injection. On the basis of these experiments it is concluded that a plasma with density 5 to 7×10^{14} cm^{-3} can be produced by using an interaction of an electron beam with a neutral supersonic stream. (auth)

3114 VERY-HIGH-DENSITY PLASMAS FOR THERMONUCLEAR FUSION. Linhart, J. G. (EURATOM–CNEN, Frascati, Italy). Nucl. Fusion; 10: 211-34(Sep 1970).

It is shown that, for plasma-confinement times below the Bohm diffusion time, fusion reactors are conceivable only when densities above 10^{19} ions/cm^3 are considered. Two classes of such reactors are examined: the nonself-destructive and the self-destructive devices. A review is given of experiments and of theories concerning both classes of the plasma focus, the axial flow-pinch, the inertial confinement, the laser and electron-beam produced plasmas and the plasmas produced by projectile impact. Nonfusion applications are also discussed. Reactor and trigger criteria are derived in the appendices. (auth)

3115 CROSSED-FIELD EXPERIMENT TO STUDY PLASMA FORMATION PROCESSES AND RESULTING GUIDE-FIELD SPATIAL AND ENERGY DISTRIBUTIONS. Harder, Carroll Ross. Madison, Wis.; Univ. of Wisconsin (1969). 150p. University Microfilms Order No. 70-3549.

Thesis.

A crossed-field plasma experiment was constructed to investigate the utility of the device as a source of plasma for thermonuclear research. The physics of plasma formation was investigated and the resulting plasma examined. The source was designed and constructed with special emphasis on the contouring of electrodes to constant flux surfaces in an attempt to reduce parallel electric and magnetic field components and plasma interaction with electrode surfaces. The source evolution is discussed with respect to efforts expended to eliminate or control shorting, which still persists. The plasma formation pro-

cess was investigated in some detail. Source internal-shorting mechanisms were studied with the conclusion that two shorting paths exist. The plasma exiting the source was studied with respect to axial acceleration mechanisms and the ion energy spectrum. (TSS) (Disser. Abstr.)

3116 POSSIBILITIES OF A SHOCK TUBE IN OBTAINING AND INVESTIGATING A DENSE LOW-TEMPERATURE PLASMA. Lomakin, B. N.; Fortov, V. E.; Shchekotov, O. E. High Temp. (USSR) (Engl. Transl.); 8: 143-7(Jan-Feb 1970).

Translated from Teplofiz. Vys. Temp.; 8: 154-8(Jan-Feb 1970).

The possibilities of a shock tube with preheating for obtaining a dense low-temperature plasma are considered. The propagation of forward and reverse shock waves in Cs vapors is calculated. The ideality of the plasma in a large canonical ensemble was calculated using the Debye theory. The system of conservation equations was integrated step-wise in a digital computer together with the thermodynamic equations. Optimum experimental conditions were determined. (auth)

Stability

3117 (CEA-CONF-1598) BOUNCE EFFECTS IN THE NEGATIVE MASS INSTABILITY. Launois, D.; Laval, G.; Pellat, R.; Tachon, J. (European Atomic Energy Community. Commissariat a l'Energie Atomique, Fontenay-aux-Roses (France). Centre d'Etudes Nucleaires). 1970. 4p. (CONF-700817-19). Dep. NTIS (U. S. Sales Only).

Unstable modes at bounce harmonic satellites of the ion cyclotron frequency exist for any density. The thermal spreading reduces slightly the unstable domain. The decreasing of ion bounce frequency does not stabilize dilute plasma. (tr-auth) (France)

3118 PARAMETRIC INSTABILITY OF NONHOMOGENEOUS PLASMA. Domrin, V. I.; Ramazashvili, R. R. Krat. Soobshch. Fiz.; No. 7, 62-7(Jul 1970). (In Russian).

It was found that inhomogeneous plasma instability at $\omega = \omega_e(\omega$ frequency of electromagnetic wave) develops as a parametric instability; however, it begins at higher field intensities. It was also shown that, in high-energy fields, instability induced by heterogeneity may develop more rapidly than the instability developed due to the relative motion of charges in the wave field. (R.V.J.)

3119 ON THE COLLISIONAL DRIFT INSTABILITY IN A Q-MACHINE. Nocentini, A. (Univ., Trieste, Italy). Lett. Nuovo Cim.; 4: 859-61(7 Nov 1970).

The influence of the cathodes of a double-ended Q machine on the collisionless drift instability has been studied (B. Bertotti and A. Nocentini: Plasma Phys., 12, 39(1970)) using Vlasov's equation. This treatment is extended here to the collisional regime, taking into account electron collisions by a Krook term, which conserves the number of particles. (M.O.W.)

3120 INFLUENCE OF A STATIONARY ELECTRIC FIELD ON THE CYCLOTRON INSTABILITY OF DENSE PLASMA. Davydova, T. A. (Inst. of Physics, Kiev). Ukr. Fiz. Zh.; 15: 959-70(Jun 1970). (In Russian).

The stability is considered of cyclotron oscillations in a cylinder of a relatively high-density plasma ($\omega_{0i}^2 \gtrsim \omega_i^2$, where ω_{0i} and ω_i are the ion plasma and cyclotron frequencies) in the presence of the nonuniform electric field $E_0(r)$. It is shown that the negative electric field ($E_0 < 0$) gives rise to stabilization of the plasma oscillations. Instability remains if $E_0 > 0$; but the resonance magnetic field increases with a rise in the electric field. (auth)

3121 LOW-FREQUENCY INSTABILITIES OF THE HIGH-FREQUENCY SKIN LAYER IN A PLASMA WITH NON-UNIFORM PARAMETERS. Sidorov, V. P.; Tsypin, V. S.; Utkina, L. A. (Physico-Technical Inst., Sukhumi, USSR). Nucl. Fusion; 10: 293-304(Sep 1970).

Low-frequency instabilities caused by nonuniformity of the macroscopic parameters of a plasma located in a constant magnetic and a high-frequency (hf) electric field are discussed. The instabilities of a completely ionized plasma are studied, with allowance for Coulomb collisions. It is shown that the effect of "induced" longitudinal friction significantly changes the spectrum of natural oscillations of the drift-dissipative type. The influence of the hf field on hydrodynamic drift-temperature, drift-cyclotron, and centrifugal instabilities is considered. The hf field is found to have both a stabilizing and a destabilizing influence. (auth)

3122 STABILITY OF A PLASMA CONTAINED BY A STRONGLY NON-UNIFORM MAGNETIC FIELD. Gordeev, A. V. (Inst. of Atomic Energy, Moscow). Nucl. Fusion; 10: 319-24 (Sep 1970).

The hydrodynamic instability of a plasma contained by a strongly nonuniform magnetic field H_0 was investigated in the frequency region $eH_0/m_ic < \omega < eH_0/m_ec$. It is shown that, in a plasma with a sufficiently high collision frequency ν, a high-frequency tearing mode (encountered earlier in single-fluid hydrodynamics for frequencies $\omega < eH_0/m_ic$) can develop. In particular, a plasma cylinder with a strong longitudinal magnetic field along which a current is flowing may prove unstable with respect to the perturbation under consideration. It is also shown that there is no Suydam instability in the high-frequency region. (auth)

3123 DYNAMIC STABILIZATION OF A CONFINED PLASMA. Samain, A. (EURATOM-CEA, Fontenay-aux-Roses, France). Nucl. Fusion; 10: 325-35(Sep 1970).

A formalism is presented that is suitable for the analysis of a collisionless plasma sheet confined by a static magnetic field in the presence of a small-amplitude alternating electromagnetic field. Each particle is described by angular and action variables that allow the calculation of the stationary state of the plasma, in the presence of the alternating field, by a variational method. A dispersion relation for the actual eigenmodes of the plasma is also derived. This formalism is used to study a stabilizing effect of the alternating field that takes place when the field has a standing-wave structure along the direction of the confinement. This effect is associated with the mean particle velocities induced along the direction of the diamagnetic current. It is shown that the drift modes and the interchange modes in the plasma may be stabilized, when discarding the parametric amplification effects and the nonlinear Landau effects, if the values assumed by these mean velocities are spread over an interval of the order of the diamagnetic velocity. (auth)

3124 CYCLOTRON INSTABILITY IN A PLASMA CYLINDER. Klopovskii, K. S. (Inst. of Atomic Energy, Moscow). Nucl. Fusion; 10: 235-9(Sep 1970).

Ion-cyclotron instability of oscillations was studied in a plasma cylinder in which cold magnetized electrons perform Langmuir oscillations in the magnetic field direction while the ions (with an anisotropic velocity distribution) oscillate across the magnetic field. Dispersion equations are obtained for waves rotating in the direction of ion rotation and in the opposite direction. It is shown that the wave buildup is most intense in waves propagated in the direction of ion rotation. (auth)

3125 EFFECT OF A HIGH-FREQUENCY ELECTRIC FIELD ON THE DEVELOPMENT OF ION-ACOUSTIC INSTABILITY IN A CURRENT-CARRYING PLASMA. Kostyukova, Yu. S.; Nekrasov, F. M. (Physical-Technical Inst., Sukhumi, USSR). Nucl. Fusion; 10: 277-81(Sep 1970).

The effect of a high-frequency (hf) electric field on ion-acoustic oscillations in a magnetized nonisothermal ($T_e \gg T_i$) current-carrying plasma is examined, in which the direct current velocity w_0 and the amplitude of the electron oscillatory velocity $u_0 = eE_0/m\Omega_0$ satisfy the condition $w_0, u_0 \ll v_{Te}$. Only those plasma perturbations are considered for which the inequality $\Omega_0 \ll k_z v_{Te}$ is fulfilled, k_z being the wave vector component parallel to the constant magnetic field. Expressions are derived for growth rates in the regions $\Omega_0 \ll \omega_s$ and $\Omega_0 \gg \omega_s$, and for the case where the parametric resonance condition $\Omega_0 = \omega_s$ is fulfilled (Ω_0 is the hf field frequency, ω_s is the ion-acoustic oscillation frequency). (auth)

3126 NONLINEAR STABILIZATION OF BEAM INSTABILITY. Leont'ev, N. I.; Timoshenko, A. P.; Udovichenko, Yu. K. Zh. Eksp. Teor. Fiz.; 59: 649-53(Sep 1970). (In Russian).

Partial stabilization of beam instability in the interaction between an electron beam and a preformed decay plasma is demonstrated experimentally. (auth)

3127 DEVELOPMENT OF THE MHD ELECTROTHERMAL INSTABILITY WITH BOUNDARY EFFECTS. Nelson, A. H. (Imperial Coll. of Science and Tech., London). (AIAA (Amer. Inst. Aeronaut. Astronaut.) J.; 8: 1753-9(Oct 1970).

An analytic treatment of the linear development of the electrothermal instability with boundary effects is presented. The plasma is assumed to be bounded in one direction only, namely between two parallel walls of finite separation lying parallel to the applied magnetic field. The procedure of the calculation is to Laplace transform the linear electrothermal equations in time, solve the resulting spatial differential equations under the appropriate boundary conditions, and then transform back into real time to obtain the development of a given initial perturbation. Two cases are considered, viz., continuous insulator walls, and infinitely finely segmented electrode walls. In general, an initially plane wave perturbation in the electron density is split into an infinite number of modes, of which usually only a finite number are unstable. As the Hall parameter increases, more and more modes

XUM

are successively destabilized. However, the critical Hall parameter for destabilization of a given mode usually increases as the wavelength parallel to the walls increases, so that, at least for some geometries, long-wavelength perturbations are more stable. In the case of segmented electrodes, it may be possible to achieve enhanced stability for a given wavelength by adjusting the external circuitry. (auth)

Thermonuclear Processes

3128 (IPPJ–95) MAGNETIC AND DRIFT SURFACES, CURRENT CONFIGURATION OF STELLARATOR FIELD. Miyamoto, Kenro (Nagoya Univ. (Japan). Inst. of Plasma Physics). Aug 1970. 23p. Dep. NTIS (U. S. Sales Only).

Magnetic surfaces and drift surfaces of a single charged particle of a stellarator field are analyzed by using an average method. The dependences of the rotational transform angle and the magnetic well depth on the parameters of current configuration of the stellarator field are studied in case of long and short pitch of helical windings to find the optimum parameters. The relation of magnetic and drift surfaces are examined and a condition for their small deviation is deduced. The properties of isobar surfaces are examined. (auth) (Japan)

3129 (JUL–667-PP) STEADY-STATE GENERATION OF ROTATING MULTIPOLES FOR PLASMA EXPERIMENTS IN THE Mcs RANGE. Bastian, C. (Kernforschungsanlage, Juelich (West Germany). Institut fuer Plasmaphysik). Jun 1970. 61p. Dep. NTIS (U. S. Sales Only).

The cyclic delay-line connection of three interlaced multipole coils and of three capacitors has two ringing modes producing multipolar magnetic field patterns that rotate in opposite directions around the axis of permutation of the coil assembly. Sustainment of a prescribed mode is made possible by a three-phase (Mc) cw transmitter system driven through feedbacks. Rotating multipolar patterns with shear or axial gradient of the amplitude can be realized in the same way. This leads to the concept of inductive plasma turbines, with possible applications to plasma beam acceleration and direct energy conversion. (auth)

3130 (ORO–1171-1) PROCEEDINGS OF THE SYMPOSIUM ON THERMONUCLEAR FUSION REACTOR DESIGN, JUNE 2–5, 1970. Kristiansen, M.; Hagler, M. O. (eds.) (Texas Tech Univ., Lubbock. Plasma Lab.). 1 Aug 1970. 442p. (CONF-700614). Dep. NTIS.

Individual abstracts were prepared for eleven articles. Two articles were previously abstracted as NSA 24: 37492 and 24: 47060. Only abstracts appear in the proceedings for the remaining papers. (M.O.W.)

For abstracts of individual papers see: 3056, 3131–3139, and 3891.

3131 (ORO–1171-1, pp 3-37) INJECTOR REQUIREMENTS FOR OPEN ENDED FUSION REACTORS. Forsen, Harold K. (Wisconsin Univ., Madison. Dept. of Nuclear Engineering).

From Proceedings of the symposium on thermonuclear fusion reactor design, June 2–5, 1970.

The filling problem of the present- and next- generation plasma physics experiments of the mirror type is discussed. These projections should also be relevant for the startup requirements of possible reactors, although no attempt was made to take the time history of buildup into account. (M.O.W.)

3132 (ORO–1171-1, pp 38-77) LECTURE NOTES [ON TOROIDAL FUSION REACTORS]. Mills, R. G. (Princeton Univ., N. J.).

From Proceedings of the symposium on thermonuclear fusion reactor design, June 2–5, 1970.

Fundamental considerations for toroidal fusion reactors are discussed in terms of the following: (1) nuclear physics, (2) plasma physics, (3) reactor considerations, (4) hypothetical machines, and (5) sizes and costs. The control and ignition of toroidal fusion reactors are discussed. An extensive bibliography is given. (M.O.W.)

3133 (ORO–1171-1, pp 141-66) THERMAL ENERGY CONVERSION SYSTEM FOR A FUSION REACTOR. Carlson, G. A. (California Univ., Livermore. Lawrence Radiation Lab.). (UCRL–72479).

From Proceedings of the symposium on thermonuclear fusion reactor design, June 2–5, 1970.

An analysis is presented that describes a self-consistent, workable blanket for a D–T fusion reactor. The very high neutron energy flux at the first wall is effectively distributed throughout a blanket constructed of niobium, using lithium as a moderator–coolant and sodium heat pipes to transfer heat radially. The lithium also provides adequate tritium breeding. The blanket is made up of modules containing small-diameter tubes that must be designed to withstand only small internal pressures. The heavily loaded vacuum wall is external to the blanket, in a low-temperature, neutron-free environment. The analysis includes heat-transfer calculations for the first wall, the heat pipes, and the lithium coolant. Fluid-flow calculations include consideration of magnetically induced pressure gradients. (auth)

3134 (ORO–1171-1, pp 256-331) WHY FUSION. (Gough, William C. (Division of Research (AEC), Washington, D. C.).

From Proceedings of the symposium on thermonuclear fusion reactor design, June 2–5, 1970.

The use of controlled fusion power is discussed in relation to population expansion, living standards, raw materials, pollution, and energy resources. (M.O.W.)

3135 (ORO–1171-1, pp 334-42) WALL EROSION BY SPUTTERING IN CONTROLLED THERMONUCLEAR FUSION DEVICES. Daniel, James M.; Finfgeld, C. R. (Roanoke Coll., Salen, Va. Dept. of Physics). (ORO–3557-11).

From Proceedings of the symposium on thermonuclear fusion reactor design, June 2–5, 1970.

Existing data relevant to the sputtering problem in thermonuclear devices are reviewed. Using this data, an estimate was made of the wall lifetime as a function of burnup fraction. Those yields that will be the primary determinants of erosion rates are also identified, and recommendations as to which quantities ought to be determined more accurately are made. (M.O.W.)

3136 (ORO–1171-1, pp 344-75) ACCOMMODATING FOR UNCERTAINTIES AND INTERPLANT VARIATIONS IN THE ENGINEERING OF A FUSION PLANT-TORCH COMPLEX. Sabri, Zeinab A. (Wisconsin Univ., Madison. Dept. of Nuclear Engineering).

From Proceedings of the symposium on thermonuclear fusion reactor design, June 2–5, 1970.

Uncertainties in the design parameters of a fusion plant are investigated. The plant is assumed to consist of a power reactor supplying a part of a city with electrical energy. The waste energy from the reactor is to be utilized by a fusion torch. The torch processes scrap material to reduce it to its basic elements. Sensitivity of the power output of the reactor and the cost per unit energy to uncertainties in confinement time and plasma density is evaluated. A proper plasma density is obtained in case of uncertainty in plasma temperature. The design criterion for a feasible self-heated fusion reactor is obtained, taking into account uncertainties in the parameters involved. The expected value of the density–confinement time product is found to differ in some extent from that evaluated using average values for the parameters where uncertainty resides. The torch is considered next. The variation in the waste energy throughput to the torch is taken into account. A utilization factor for the energy supplied to the torch is derived. Also obtained is the optimal capacity of the torch that gives maximum venture profit. The case of pulsed supply of scrap material in the presence of a variable processing rate is finally considered. Utilization factors on daily basis are obtained for the supply and the process. The optimal capacity of the storage and the effect of overflow are discussed. (auth)

3137 (ORO–1171-1, pp 376-86) EXPERIENCE TEACHING A FUSION DESIGN SEMINAR. Miley, George H. (Cornell Univ., Ithaca, N. Y. Dept. of Applied Physics).

From Proceedings of the symposium on thermonuclear fusion reactor design, June 2–5, 1970.

Experience in conducting a seminar for the purpose of designing a 5000-MWe CTR for siting in or near New York City is discussed. The class was divided into two groups: one worked on a closed, steady-state device similar to a stellarator or Tokamak, while the second was assigned a pulsed mirror-type device. Some parameters of the two concepts are described. (M.O.W.)

3138 (ORO–1171-1, pp 387-411) SOME THOUGHTS ON THE DESIGN OF A THERMONUCLEAR SPACE POWER SYSTEM. Samaras, Demetrios George (Air Force Office of Scientific Research, Washington, D. C.).

From Proceedings of the symposium on thermonuclear fusion reactor design, June 2–5, 1970.

Basic considerations for designing a thermonuclear power plant for use in space are discussed. Energy conversion, starting systems, control systems, and auxiliaries are described. (M.O.W.)

3139 (ORO–1171-1, pp 425-39) SELECTED BIBLIOGRAPHY FOR FUSION REACTOR DESIGN STUDIES. Gough, W. C. (Atomic Energy Commission, Washington, D. C.).

From Proceedings of the symposium on thermonuclear fusion reactor design, June 2–5, 1970.

This listing includes approximately 225 articles dealing with design aspects of thermonuclear reactors. (M.O.W.)

3140 SYNTHESIS OF DIFFERENTLY CHARGED NUCLEI IN PLASMA WITH STRONG ELECTRIC CURRENT. Vil'koviskii, E. Ya. Dokl. Akad. Nauk SSSR; 192: 307-8(11 May 1970). (In Russian).

Gurevich (Zh. Eksp. Teoret. Fiz., 40: 1825(1961)) found two steady states of motion of multicharged ion admixtures in plasma with main ions of $Z_{io} < Z$ charge. An attempt is reported here of synthesizing nuclei of admixture ions found in the second state in reactions $^6Li + {}^2D \rightarrow {}^7Li + p + 5$ MeV, $^6Li + {}^2D \rightarrow 2\ {}^4He + 22.4$ MeV, $^3He + {}^2D \rightarrow {}^4He + p + 18.3$ MeV. Graphs of the energy of various processes in plasma as functions of the temperature showed that, in ^6Li, D, and ^3He reactions, the energy yield exceeded plasma radiation at $T \sim 10^6$ to $10^{7\circ}K$. It was found that synthesis of various-charge nuclei in plasma with high electric current was possible under conditions of Coulomb conductivity. Additional heating of plasma at the expense of ^3He, D reactions may help to achieve thermonuclear synthesis in the D,D reaction. The influence of the two steady states in the motion of admixture ions on the collective processes in plasma was not yet resolved. However, the synthesis reactions offer another possibility of detecting the second steady state, using the products of the synthesis with the ordinary spectral methods. (R.V.J.)

3141 HIGH-CURRENT HALL ACCELERATOR. Cole, H. C. (Culham Lab., Abingdon, Eng.). Nucl. Fusion; 10: 271-5 (Sep 1970).

A high-current two-stage dc Hall accelerator is investigated to determine its possible application in controlled thermonuclear fusion work. Detailed measurements are made on the electrical characteristics of the device for currents of up to ~3 kA and potential differences of up to ~1 kV. It is shown that the impedance of the device, and consequently the energy of the accelerated plasma, increases directly with B_r over the range investigated. The output of accelerated plasma also increases with B_r and maximum values of ~500 A equivalent are obtained. The presence of a rotating cathode spot is shown by means of high-speed framing photographs. An important characteristic of the device is its flexibility, the total number of particles produced depending on the duration and magnitude of the gas feed and current pulse. The output of the device is compared with fusion reactor requirements, and the way in which it could be scaled up to meet these requirements is considered. (auth)

3142 POLOIDAL FIELDS AND THE MINIMUM MEAN MAGNETIC FIELDS IN A TWO-PATH STELLARATOR. Karpenko, I. K. This paper was summarized in At. Energ. (USSR); 25: 518-19(Dec 1968) as paper No. 251. (In Russian).

An approximate analytical solution of the problem identified by Furth et al., (2nd Conference on Plasma Physics, Culham, 1965 (Paper CN 21/106)) of combination of the two fields of a two-path stellarator with toroidal geometry and a "poloidal" field is discussed, using the familiar method described by Mercier (Nucl. Fusion, 3: 89(1963) and 4: 213(1964) and Solov'ev and Shafranov (Problems in Plasma Theory, No. 5, Atomizdat, Moscow, 1967). In the vicinity of the magnetic axis of such a system there are closed toroidal magnetic surfaces. It is shown that by proper selection of the current in the bars lying in the principal plane of the torus, it is possible to get greater stability of the magnetic surfaces and depth of magnetic well. (L.M.T.)

3143 POSSIBILITY OF THE EXISTENCE OF MAGNETIC WELLS IN THE COMBINED FIELD OF ONE- AND TWO-PATH STELLARATORS. Karpenko, N. K. This paper was summarized in At. Energ. (USSR); 25: 519-20(Dec 1968) as paper No. 252. (In Russian).

Solov'ev and Shafranov (Problems in Plasma Theory, No. 5, Atomizdat, Moscow, 1967) showed that, in vacuum magnetic configurations of one- and two-path stellarators of straight geometry, mimimum B does not exist. In order to obtain magnetic wells, it is necessary to study the topological structure of the combined fields of one- and two-path stellarators. Moreover, in these systems one can hope for increased values of rotational transform at the magnetic axes and their vicinity, because each stellarator has different angles of turning of the lines of force. Starting with the expressions of Solov'ev and Shafranov for the scalar magnetic potential of the combined fields, the author develops expressions concerning V' and V'' (first and second derivatives of the specific volume) for which magnetic wells may or may not exist. (L.M.T.)

Wave Phenomena

3144 (CEA-CONF-1601) AMPLITUDE AND DAMPING OF PLASMA WAVE ECHOES. Guillemot, M.; Matthieussent, G.; Olivain, J.; Perceval, F.; Quemeneur, A. (European Atomic Energy Community. Commissariat a l'Energie Atomique, Fontenay-aux-Roses (France). Centre d'Etudes Nucleaires). 1970. 4p. (CONF-700817-16). Dep. NTIS (U. S. Sales Only).

From 4th European Conference on Controlled Fusion and Plasma Physics, Rome, Italy.

A theory taking into account diffusion in velocity space shows that a spatial plasma echo exhibits new features when either the second wave amplitude or the distance between the transmitters is increased. Good agreement is found between this theory and experiment. (tr-auth) (France)

3145 (CEA-CONF-1607) HARMONIC ABSORPTION OF MICROWAVES IN MAGNETIZED LOW-DENSITY PLASMA. Cano, R.; Fidone, I.; Schwartz, M.; Zanfagna, B. (European Atomic Energy Community. Commissariat a l'Energie Atomique, Fontenay-aux-Roses (France). Centre d'Etudes Nucleaires). 1970. 4p. (CONF-700817-10). Dep. NTIS (U. S. Sales Only).

Increased ionization and temperature due to harmonic cyclotron absorption were observed in a low-density, warm, magnetized plasma subjected to high-power microwaves. (tr-auth) (France)

3146 (CEA-CONF-1608) CHANGE IN THE POLARIZATION OF AN ELECTROMAGNETIC WAVE IN A SHEARED MAGNETIC FIELD. Cano, R.; Etievant, C.; Fidone, I.; Zanfagna, B. (European Atomic Energy Community. Commissariat a l'Energie Atomique, Fontenay-aux-Roses (France). Centre d'Etudes Nucleaires). 1970. 4p. (CONF-700817-11). Dep. CFSTI (U. S. Sales Only).

From 4th European Conference on Controlled Fusion and Plasma Physics, Rome, Italy.

The experiment described showed that an extraordinary electromagnetic wave propagating across a plasma column, confined by a slightly sheared magnetic field, is partially converted into an ordinary mode at the upper hybrid resonance. (tr-auth) (France)

3147 (CEA-CONF-1612) DRIFT WAVES IN A COLLISIONLESS PLASMA. Blanc, P.; Brossier, P.; Deschamps, P.; Gravier, R. (European Atomic Energy Community. Commissariat a l'Energie Atomique, Fontenay-aux-Roses (France). Centre d'Etudes Nucleaires). 1970. 4p. (CONF-700817-4). Dep. NTIS (U. S. Sales Only).

From 4th European Conference on Controlled Fusion and Plasma Physics, Rome, Italy.

Pressure-gradient-driven drift waves were observed in a collisionless, low-density, 5.40-m-long plasma. Comparisons with the theoretical predictions show a reasonable agreement. (tr-auth) (France)

3148 (CEA-CONF-1614) TWO ION COLLISIONAL ABSORPTION OF LOW FREQUENCY ELECTROMAGNETIC WAVES IN A TOROIDAL HARD-CORE CONFIGURATION. Adam, J.; Alvarez de Toledo, F.; Feltin, D. (European Atomic Energy Community. Commissariat a l'Energie Atomique, Fontenay-aux-Roses (France). Centre d'Etudes Nucleaires). 1970. 4p. (CONF-700817-2). Dep. NTIS (U. S. Sales Only).

From 4th European Conference on Controlled Fusion and Plasma Physics, Rome, Italy.

The absorption of the fast hydromagnetic wave propagating in a two-species plasma (H + D) was investigated in a Levitron-type device. In agreement with the calculations, the wave could be excited for experimental parameters appropriate to the collisional absorption, and the damping length outside the emission coil was found to be minimum for $\omega_{cH} > \omega > \omega_{cD}$. (tr-auth) (France)

3149 (CEA-CONF-1616) INFLUENCE OF TRAPPED PARTICLES ON THE DRIFT WAVES. Samain, A. (European Atomic Energy Community. Commissariat a l'Energie Atomique, Fontenay-aux-Roses (France). Centre d'Etudes Nucleaires). 1970. 4p. (CONF-700817-22). Dep. NTIS (U. S. Sales Only).

From 4th European Conference on Controlled Fusion on Plasma Physics, Rome, Italy.

The stability of the drift modes of a collisionless magnetically confined plasma slab is considered when shear is present and the field intensity is modulated. In the absence of such a modulation, the drift modes are generally convective and strongly localized in the direction of the plasma confinement. The field modulation introduces a coupling between these localized convective modes. Under proper conditions, unstable eigenmodes consisting of a sequence of convective localized modes may exist throughout the plasma. (France)

3150 (IPPJ-93) EFFECTS OF R.F. ELECTRIC FIELD ON DISPERSION OF ION WAVES. Aihara, Shuko; Takamura, Shuichi; Takayama, Kazuo (Nagoya Univ. (Japan). Inst. of Plasma Physics). Jul 1970. 28p. Dep. NTIS (U. S. Sales Only).

The wavelength of an ion wave decreases in rf electric field.

XUM

The slowing down of an ion wave becomes small as the frequency of the ion wave increases. These phenomena can be explained by the additional pressure produced by the spatial modulation of the rf field on account of the ion wave. A new branch of the dispersion relations of ion waves in a high-frequency electric field is described. (auth) (Japan)

3151 (IPPJ-94) NONLINEAR EFFECT OF LARGE-AMPLITUDE ION ACOUSTIC WAVES. Kawai, Y.; Ikegami, H. (Nagoya Univ. (Japan). Inst. of Plasma Physics). Jul 1970. 17p. Dep. NTIS (U. S. Sales Only).

Large-amplitude ion–acoustic waves are propagated in a streaming-ion plasma and amplitude oscillations are observed. In the course of the amplitude oscillation, multiple exchange of energy between resonant ions and the wave is detected by an ion energy analyzer. The use of the energy analyzer eliminates a possibility of the amplitude oscillation caused by interference between a wave mode and a ballistic mode. (auth) (Japan)

3152 IONIZATION-DIFFUSION OSCILLATIONS IN A PLASMA. Alanakyan, Yu. R.; Aivazyan, Yu. M. (All-Union Scientific-Research Inst. for Physical-Technical and Radiotechnical Measurements, Stantsiya Kryukovo, USSR). Zh. Eksp. Teor. Fiz.; 59: 1032-5(Sep 1970). (In Russian).

A new type of low-frequency proper oscillation in a partially ionized bounded plasma is found. The oscillations are due to ionization processes, ambipolar diffusion, and recombination of charged particles at the walls. (auth)

3153 REFLECTION AND ABSORPTION OF ELECTROSTATIC WAVES IN AN INHOMOGENEOUS PLASMA. Landt, D. L.; Lonngren, K. E. (Univ. of Iowa, Iowa City). Phys. Lett.; 33A: 170-1(19 Oct 1970).

The experimental observation of the reflection and absorption of an electrostatic wave at frequencies of the order of an electron plasma frequency in an inhomogeneous plasma is reported. (auth)

3154 INFLUENCE OF PULSE LENGTH ON THE SPATIAL ECHO IN A COLLISIONLESS PLASMA. David, Georges (Paris Univ.). Compt. Rend., Ser. B; 271: 363-6(10Aug 1970). (In French).

It was shown that, when the external pulses are Gauss functions of width α, the electric field of the spatial echo is finite and proportional to an exp $(-a/\lambda_D)$ where λ_D is the plasma Debye length. (tr-auth) (France)

3155 VARIATION OF ATTENUATION OF ACOUSTIC WAVES THROUGH PLASMA WITH ION–PLASMA FREQUENCY. Gaur, S. C.; Saxena, A. P. (Government Coll. of Engineering and Tech., Raipur, India). Indian J. Pure Appl. Phys.; 8: 86-9(Feb 1970).

From an analysis of the equation of motion in an elastic medium, the dispersion relation for the propagation of a plane acoustic wave in a plasma was obtained. A study of the relation shows that attenuation of the sound waves due to reflections from the plasma boundaries should start when the acoustic frequency $\omega = \omega_{pi}$ (plasma-ion frequency). An experimental study of the variation of the attenuation of acoustic signal through a plasma with the applied potential also shows a minimum at the state of the plasma when $\omega = \omega_{pi}$. Beyond this frequency, the attenuation increases asymptotically, indicating the transition of the plasma from the state of transparency to opacity. The variation of the percentage of attenuation with the acoustic frequency is found to be an oscillatory function and the amplitudes of this function show a regular decrease with the increase in the applied voltage of the plasma. (auth)

3156 EXISTENCE OF NEWTONIAN-VELOCITY SOUND IN PLASMA. Sinkevich, O. A. (Inst. of High Temperatures, Moscow). Teplofiz. Vys. Temp.; 7: 354-5(Mar-Apr 1969). (In Russian).

Propagation of small perturbations in plasma penetrated by electrical currents from external sources is calculated, considering that the condition $Re_m \ll 1$ (Re_m is the Reynolds magnetic number) is fulfilled. (R.V.J.)

3157 ELECTRON PLASMA WAVE GROWTH. Nunez, Paul L. San Diego, La Jolla, Calif.; Univ. of California (1969). 100p. University Microfilms Order No. 70-8845.

Thesis.

Transfer of energy from the particles of an electron beam to longitudinal plasma waves is studied by means of plasma kinetic theory. The fundamental equations of plasma physics that have been used successfully in the study of wave propagation are first discussed. Next, Landau's linear theory of collisionless damping of plasma waves is reviewed. The quasi-linear theory of collisionless damping of plasma waves is then presented and applied to the beam–plasma problem. The quasi-linear equations for the evolution of the wave-field energy and distribution function are analyzed. It is shown that the fundamental condition of validity of the quasi-linear theory is that the wave spectrum must be sufficiently broad so that a particle trapped in one portion of the wave spectrum receives a large number of random "bumps," due to random components of the wave, during the time it takes the particle to be accelerated over a wavelength. The contributions to the evolution of the wave field and distribution function due to the spontaneous emission of waves by plasma particles are then included in the quasi-linear theory. It is shown that spontaneous emission may cause the field energy to grow on a shorter time scale than in conventional quasi-linear theory. The effect of two-body collisions of resonance particles with the bulk plasma particles is also included in the quasi-linear theory. A comparison of the effects of collisions and quasi-linear random wave-particle interactions on the evolution of the resonance distribution function is made. It is shown that, in an equilibrium plasma, quasi-linear velocity space diffusion is small compared to the diffusion due to two-body collisions. If, however, the plasma contains a large random wave field, as may be the case in the beam–plasma problem, quasi-linear diffusion may be dominant. The limitation of the field energy growth due to collision drag on the beam particles is also discussed. Numerical solutions of the quasi-linear equations modified by spontaneous emission and two-body collision effects are obtained. It is shown that except for logarithmic dependences the solutions depend on two parameters, the constant part of the diffusion coefficient and the spontaneous emission coefficient. The evolution of the resonant field energy density and distribution function are presented for various combinations of these parameters. Finally, a summary of the various phenomena that may limit the growth of the resonant field energy in a plasma containing an electron beam is presented. (Diss. Abstr. Int., B)

3158 PROBLEM OF MAGNETO-ACOUSTIC WAVE PROPAGATION IN LAMELLAR MEDIA. Ponomarenko, V. G. (Donetsk State Univ., USSR). Ukr. Fiz. Zh.; 15: 1014-20(Jun 1970). (In Russian).

The problem is solved on reflection of magneto-acoustic waves from an arbitrary number of electroconducting liquid (or gaseous) layers in a constant uniform magnetic field. General expressions are obtained for coefficients of reflection and transparency in case of an arbitrary magnetic field. A particular case of one layer is considered at greater length. (auth)

3159 KINETICS OF MAGNETOHYDROMAGNETIC WAVES. I. Aleksin, V. F.; Khodusov, V. D. (Physical-Technical Inst., Kharkov. Physical-Technical Inst., Donetsk, USSR). Ukr. Fiz. Zh.; 15: 1021-8(Jun 1970). (In Russian).

The Hamiltonian of interaction of magnetohydromagnetic waves (Alfven and slow and fast magneto-acoustic) is obtained. A kinetic equation for the function of wave distribution and mean relaxation time are written. For waves with constant phase, increases in small-intensity waves are obtained when they interact with a large-intensity wave. (auth)

3160 ELECTRON PLASMA INDUCED OSCILLATIONS IN A MAGNETIC FIELD. Zhdanov, A. I.; Repalov, N. S.; Khizhnyak, N. A.; (and others) (Physical-Technical Inst., Kharkov). Ukr. Fiz. Zh.; 15: 914-22(Jun 1970). (In Russian).

Cold plasma nonlinear oscillations were investigated in a magnetic field. The resonance conditions between the beat frequencies of electron oscillations and ion plasma frequency were found. By means of an analog computing complex, the efficiency of energy transfer of rf oscillations to low-frequency ones, as well as the efficiency of frequency multiplication at the plasma internal resonance, was studied. (auth)

3161 ION–ACOUSTIC WAVES IN STREAMING-ION PLASMA. Kawai, Yoshinobu (Nagoya Univ., Japan). J. Phys. Soc. Jap.; 29: 1354-65(Nov 1970).

Ion–acoustic waves are excited in a streaming-ion plasma. The comparison between the experimental results and the theory about the effects on the higher-order modes is made. Discussions on the wave mode and the ballistic mode are described in detail. The wave mode among wave-like fluctuations was detected by an ion-energy analyzer. Waves are excited by a grid immersed in a plasma. When the voltage applied to the grid is increased, oscillations of the amplitude are observed. In the course of the amplitude oscillations, multiple exchange of energy between resonant ions and the wave is detected by the ion-energy analyzer. (auth)

3162 DECAY INSTABILITY OF CYCLOTRON HARMONIC PLASMA WAVES. Amano, Tsuneo (Osaka Univ.); Okamoto, Masao. J. Phys. Soc. Jap.; 29: 1366-76(Nov 1970).

The decay instability of cyclotron harmonic plasma waves is

investigated by solving the nonlinear Vlasov equation to the second order in powers of the wave amplitude. For a Maxwellian plasma, it is shown that a single cyclotron harmonic wave with frequency $\omega_0(k_0)$ can decay into two other modes with $\omega_1(k_1)$ and $\omega_2(k_2)$, when the three waves satisfy the decay condition: $\omega_0 = \omega_1 + \omega_2$, $k_0 = k_1 + k_2$. For a ring-velocity distribution, it is shown that a mode with ω_0 decays into a negative energy wave ω_1 and a positive one ω_2 under the matching condition: $\omega_0 = \omega_1 \sim \omega_2$, $k_0 = k_1 \sim k_2$, where $\sim$ denotes the difference. The growth rates of the decay instability are solved numerically and the results are illustrated. (auth)

3163 ELECTROSTATIC LOW-FREQUENCY OSCILLATIONS IN AN INHOMOGENEOUS MAGNETOPLASMA. Nishida, Yasushi; Hatta, Yoshisuke (Tohoku Univ., Sendai). J. Phys. Soc. Jap.; 29: 1341-54(Nov 1970).

Starting from macroscopic equations with electrostatic approximation, the wave modes and the instability conditions are discussed on both anti-drift and pseudo-ion cyclotron waves. When the magnetic field is not so strong as to affect the ion motion, the anti-drift wave is shown to become unstable by taking the electron transverse motion into account. The pseudo-ion cyclotron mode is introduced as a part of the branch of drift or drift-dissipative wave by taking the effects of finite ion inertia into account, and the instability conditions are also discussed. Both positive-column and diffusion-type plasma in a longitudinal uniform magnetic field are used to check the theory. In a mercury positive column anti-drift waves are observed, and in a helium positive column or a diffusion-type plasma, pseudo-ion cyclotron waves. The discrepancy between the theoretical and the experimental results, especially in a diffusion-type plasma, is discussed from the standpoint of the effects of a radial electric field. (auth)

3164 CONTRIBUTION TO THE THEORY OF ECHO PHENOMENA IN A PLASMA. Sitenko, A. G.; Nguyen-Van-Chong; Pavlenko, V. N. (Inst. of Theoretical Physics, Kiev). Nucl. Fusion; 10: 259-67(Sep 1970).

Echo effects that are due to the nondamping nature of the distribution function oscillations that occur under the influence of time-displaced perturbations are considered. The case of two external perturbations is studied. The high-frequency and low-frequency echo oscillations occurring in a plasma under the influence of external charges are investigated; in particular, echo effects associated with oscillation conversion are considered. It is shown that one can have, in a plasma, echo phenomena associated with oscillations whose dispersion is determined by the nature of external perturbations of the distribution function. Echo oscillations in a nonequilibrium plasma in which there is directed particle motion are considered. It is shown that re-excitation of strongly damping short-wave oscillations in a plasma may be accompanied by long-wave echo oscillations leading to plasma instability. (auth)

3165 LOW-FREQUENCY RESONANCES AND AVERAGED POTENTIAL IN A NON-ISOTHERMAL PLASMA, TAKING ACCOUNT OF ION COLLISIONS. Nikolov, N.; Shivarova, A. (Univ., Sofia). Nucl. Fusion; 10: 269-70(Sep 1970).

The interaction of a low-frequency electromagnetic field with a plane nonisothermal plasma layer ($T_e \gg T_i$) in the one-dimensional case, where the frequency of the field is much less than the ion Lagnmuir frequency, is investigated. Using the effective ion collision frequency, the perturbed plasma parameters are determined in a single-fluid hydrodynamic approximation. By averaging the equations of motion, an expression is derived for the averaged potential and averaged force under conditions of strong spatial dispersion, taking into account ion collisions. (auth)

3166 HEURISTIC APPROACH TO LANDAU DAMPING. Gratton, F.; Gratton, J. (Univ. of Buenos Aires). Nucl. Fusion; 10: 339-40(Sep 1970).

A longitudinal plasma oscillation with electric field $E \sim \exp(-i\omega t)$ and wave number k is considered. The plasma is separated into two parts, the resonant beam particles with velocity $v = \omega/k$, and the main plasma (i.e., the plasma without the resonant particles). A brief derivation of the Landau damping factor is given. (M.O.W.)

3167 DRIFT WAVES DUE TO A PRESSURE GRADIENT IN A COLLISIONLESS PLASMA. Blanc, Pierre; Brossier, Philippe; Deschamps, Pierre; (and others) (EURATOM-CEA, Fontenay-aux-Roses, France). Compt. Rend., Ser. B; 271: 618-21(28 Sep 1970). (In French).

Drift waves due to the pressure gradient were identified in a collisionless hydrogen plasma of 10^{10} cm^{-3} density and confined by a homogeneous magnetic field. The theoretical predictions are in good agreement with the experimental results. (tr-auth) (France)

Shielding

Refer also to abstracts 3476, 3480, and 3538.

3168 RECONSTRUCTION OF THE SPECTRAL AND ANGULAR-DISTRIBUTION FUNCTION OF SOURCES OF γ RADIATION. Churin, S. A. This paper was summarized in At. Energ. (USSR); 28: 50(Jan 1970) as paper No. 361/5351. (In Russian).

A flow of radiation specified by the spectral and angular-distribution N_0 on a plane barrier of specified thickness is considered. The possibility of finding N_0 for an isotropic point source of gamma radiation from ^{137}Cs (E = 0.660 MeV) inside homogeneous or stratified media, and also behind plane homogeneous barriers is investigated. Reflection and transmission matrices obtained by the Monte Carlo method are used to solve the problem. Results for two energy regions of scattered γ quanta were analyzed. These results were obtained in three experiments with sources located as follows: behind a layer of aluminum 2 cm thick; behind two sheets of iron each 1 cm thick; and between a layer of iron 1 cm thick and a layer of aluminum 2 cm thick. (TSS)

3169 GAMMA-RAY ENERGY-ABSORPTION RATES IN IRON AND LEAD. Chitnis, V. D. (Iowa State Univ., Ames). Indian J. Pure Appl. Phys.; 6: 361-3(1968).

A laminated shield is designed for a source of gamma radiation. The shield consists of alternate layers of iron and lead. The Monte Carlo technique is used for the determination of the energy absorption rates in the laminated shield. The total thickness of the composite shield is kept constant and the ratio of the thickness of the iron slab is varied. The dose rate at the outer boundary of shield is found to be dependent on this ratio. (auth)

3170 SHIELDING CALCULATIONS BY MEANS OF THE MONTE CARLO METHOD. Kschwendt, H. (Europaeische Gemeinschaften (CID), Luxemburg); Diettrich, O. Atomwirt., Atomtech.; 15: 540-1(Nov 1970). (In German).

For computation of shielding requirements, routine Monte Carlo methods possess only limited applicability. A new type of Monte Carlo method, especially designed for shielding, is under development. Practical usefulness and limitations of the new technique at the present stage are demonstrated with two examples. Since insufficient statistics prevent direct calculation of heat production in the containment vessel, the neutron flux at the core surface was analytically smoothed out as to distribution of both energy and angle. The values obtained were then utilized for the next computation. (H.B.G.)

3171 EXPONENTIAL ANGULAR COEFFICIENTS OF NEUTRONS FOR HYDROGEN-FREE MEDIA. Degtyarev, S. F.; Staroverov, V. B.; Tarasov, V. V.; Tikhonov, V. K.; Tsypin, S. G. This paper was summarized in At. Energ. (USSR); 24: 374(Apr 1968) as paper No. 194. (In Russian).

The results obtained from measurements of the angular distributions of a flux of scattered fast neutrons with energies >1 MeV and of the total neutron flux leaving the hydrogen-free plane shields (BeO, B_4C, Al, W, Pb, Li) are analyzed for the case of a plane infinite monodirectional neutron source (reactor spectrum). The angular distributions of the flux of scattered fast neutrons with energies >1 MeV depend weakly upon the shield material and its thickness (beginning with some minimum value) and for the range of angles $15° \lesssim \theta \lesssim 80°$ are approximated by the relationship $(-\theta/\theta_0)$, where θ is the angle between the normal to the shield surface and the direction to the detector and θ_0 is the exponential angular coefficient ($\sim 40°$). Values of the exponential angular coefficients θ_0 for hydrogen-free media are tabulated. The angular distribution of the flux of fast neutrons leaving the hydrogen-free shields is shown. It was noted that as the energy threshold of neutron registration drops to the thermal region the angular distributions become more isotropic and θ_0 reaches $\sim 100°$. (auth)

3172 GAMMA-RAY SHIELDING BY HIGH-DENSITY CONCRETES WITH DENSITIES FROM 3.2 UP TO 3.8 g/cm^3. Krueger, F. W. (VEB Kombinat Kraftwerksanlagenbau, Berlin). Kernenergie; 13: 172-8(Jun 1970). (In German).

Iron ores, scrap, or baryte were used for the production of high-density concretes with densities from 3.2 up to 3.8 g/cm^3. The influence of different chemical composition on the shielding effect was studied for energies ranging from 0.3 up to 10.0 MeV. For concretes with iron-bearing aggregates and baryte concretes respectively, this influence turns out to be so small that, in practice, averaged shielding parameters may be used for shield calculations. They are given for the two types of concrete considered. On the basis of these parameters, concretes with iron-bearing aggregates and baryte concretes were compared. It is shown that

XUM

both types of concrete practically possess the same shielding properties within the range of medium energies (from 0.8 up to 3.5 MeV). For energies below 0.8 MeV and above 3.5 MeV, a considerable reduction of shield mass per unit area is possible when baryte concretes are being used. Plots are given from which quantitative data on the benefit made by using baryte concrete may be taken. (tr-auth)

3173 ATTENUATION OF MONOENERGETIC SOURCE NEUTRONS IN DIFFERENT SHIELDING MATERIALS. Perlini, G. (EURATOM–CCR, Ispra, Italy); Nicks, R.; Penkuhn, H.; (and others Nucl. Eng. Design; 13: 377-89(Aug 1970).

Energy-dependent attenuation parameters for several important shielding materials were measured by means of a Van de Graaff accelerator. These parameters serve for the determination of energy-dependent removal cross sections, which are to be fed into the removal diffusion codes. In particular, the procedure by which removal cross sections for the SABINE program are being computed is explained. The variation of the removal cross section as a function of atomic mass was examined. A detailed description is given of the experimental device, the method, and the results of the measurements. (auth)

3174 OPTIMUM ARRANGEMENT OF LAMINATED IRON–WATER SHIELDS. Fuse, T.; Yamaji, A.; Miura, T. (Ship Research Inst., Ibaraki, Japan). Nucl. Eng. Design; 13: 390-4(Aug 1970).

The radiations from a reactor were measured after passage through a laminated iron/water shield with the iron slab movable in the shield. Calculations by the MAC-RAD code were also made for comparison. The calculated values of neutron fluxes agreed with those by experiments. But the calculated gamma-ray dose rates did not agree with the experimental results. The difference in shielding effects was significant between the optimum and the least effective arrangement of iron and water layers. The optimum arrangement was the thick iron/water/thin iron configuration, rather than a homogeneous mixture of iron and water layers. (auth)

3175 USE OF THE DISCRETE ORDINATES S_n METHOD IN RADIATION SHIELDING CALCULATIONS. Stevens, P. N. (Oak Ridge National Lab., Tenn.). Nucl. Eng. Design; 13: 395-408 (Aug 1970).

Recent developments have led to the widespread use of the "discrete ordinates" method in the deep-penetration shielding calculation. Events leading to this breakthrough in technology are described. A detailed derivation of the discrete ordinates difference equations is presented, along with a review of the calculational procedures that are peculiar to the shielding problem. Advantages and disadvantages of the method are discussed and a list of current computer codes is included. (auth)

3176 PRACTICAL ASPECTS OF MULTI-DIMENSIONAL MONTE CARLO SHIELDING CALCULATIONS. Mittelman, Phillip S.; Kalos, Malvin H. (Mathematical Applications Group, Inc., White Plains, N. Y.). Nucl. Eng. Design; 13: 409-14(Aug 1970).

Multidimensional Monte Carlo programs exist that are capable of solving most radiation-shielding problems. There are, however, practical problems that must be faced in applying these programs to specific situations. These problems concern geometrical description (input and computer algorithms), source description, importance sampling, scoring techniques, and cross-section treatment. New techniques under development promise to reduce the present difficulties and make Monte Carlo a practical engineering tool for radiation-transport calculation. (auth)

3177 ADVANCED MONTE CARLO CONCEPTS IN RADIATION SHIELDING CALCULATIONS: METHODS AND APPLICATIONS. Jordan, Thomas M. (ART Research Corp., Los Angeles). Nucl. Eng. Design; 13: 415-22(Aug 1970).

Flux evaluated at a point represents the most useful solution to the transport equation in complex geometries. Several Monte Carlo concepts that arise in obtaining accurate point fluxes are described. These concepts include random sampling of source distributions biased by point-to-point kernel approximations of importance. The use of analytic techniques, whenever possible, is also discussed with emphasis on the use of energy-dependent samples. (auth)

3178 KERNEL METHODS FOR RADIATION SHIELDING CALCULATIONS. Trubey, D. K. (Oak Ridge National Lab., Tenn.). Nucl. Eng. Design; 13: 423-47(Aug 1970).

The development and use of kernel methods in solving problems of radiation shield design and radiation transport are reviewed. Two classes of kernels are identified: empirical and computational. Various techniques are analyzed, and examples are given. The relevant computer codes in the collection of the Radiation Shielding Information Center are listed and briefly described. It is concluded that kernel methods are valuable for quick estimates, hand calculations, checks of transport computer code results, and engineering parameter studies. However, the method can give underestimates for situations that the applied kernel cannot treat properly. (auth)

3179 COMPUTER CODES FOR SHIELDING CALCULATIONS: 1970. Maskewitz, Betty F.; Trubey, D. K. (Oak Ridge National Lab., Tenn.). Nucl. Eng. Design; 13: 448-9(Aug 1970).

Materials available from the Radiation Shielding Information Center are mentioned briefly. Fifteen current computer codes and essential information for each are tabulated. (M.H.R.)

3180 TIME OPTIMISATION FOR THE GAMMA TRANSPORT CODES BIGGI ¾. Penkuhn, H. (EURATOM–CCR, Ispra, Italy). Nucl. Eng. Design; 13: 450-4(Aug 1970).

It is discussed how, by a change in the storing technique of variables, the computer time needed by the BIGGI gamma codes can be reduced by a considerable factor. Such an accelerated version of BIGGI (called PIPE) is in test, its neutron analog being prepared. (auth)

3181 GAMMA-RAY SPECTRA ARISING FROM THERMAL-NEUTRON CAPTURE IN ELEMENTS FOUND IN SOILS, CONCRETES, AND STRUCTURAL MATERIALS. Maerker, R. E.; Muckenthaler, F. J. (Oak Ridge National Lab., Tenn.). Nucl. Eng. Design; 13: 455-6(Aug 1970).

Gamma-ray spectra arising from the capture of thermal neutrons were measured for several naturally occurring elements of interest to the shielding community. The spectral intensities in units of photons per 100 captures are tabulated as sums over 0.5 MeV intervals. These results have an estimated accuracy of ±15% and include the contributions from both discrete and continuum gamma rays. The present results do not go below 1 MeV. The measurements were made at the Tower Shielding Facility with a carefully calibrated 5 × 5 in. NaI(Tl) detector. Results are presented for: Si, Ca, K, Na, Ba, Fe, Al, Cu, Ti, Zn, Cl, Ni, S, and Type 321 stainless steel. (M.H.R.)

3182 INVESTIGATION OF THE ENERGY DISTRIBUTION OF SINGLY SCATTERED AND MULTIPLY SCATTERED GAMMA RADIATION. II. DOUBLY BACK SCATTERED AND TRIPLY BACK SCATTERED RADIATION. Wechselberger, E. (Univ., Tuebingen, Ger.). Atomkernenergie; 16: 146-52 (1970). (In German).

Spectral measurements of the tertiary and quaternary radiation are dealt with and the effects of slab material, geometrical arrangement, primary energy, and beam geometry on the energy distribution are examined. It is seen that: The mean quantum energy decreases with each additional backscattering; but the degradation decreases considerably with increasing order of backscattering. The diminution of the intensity in backscattering is dependent on the slab material, on the angle, and on the order of scattering; it amounts to one to two powers of ten. The effective atomic number of the last backscattering wall controls decisively the number and energy distribution of the photons, whereas the preceding walls only alter substantially the number of photons. The portion of Eigen radiation in the total radiation increases with the order of backscattering. At the same time the influence of primary energy and beam geometry diminishes, so as to equal in practice the spectra of quaternary radiation of ^{60}Co and ^{137}Cs. (auth)

3183 DETERMINATION OF THE ENERGY SPECTRUM OF A GAMMA-RAY FLASH. Fabian, H. U.; Nemsmann, U. (Univ., Kiel). Atomkernenergie; 16: 143-5(1970).

A method is presented for the determination of the energy spectrum of a gamma-ray flash by evaluating the filtration curve using the maximum-likelihood approximation. Instead of measuring the filtration curve simultaneously with many absorber layers and detectors only one detector and absorber was used, and the measurement was performed successively. The method was programmed in ALGOL-code and tested by reproducing some known spectra. A measured filtration curve for the radiation field of a gamma-flash generator and the corresponding computed energy spectrum are given in diagrams. (auth)

3184 GREEN'S FUNCTIONS FOR MULTIDIMENSIONAL NEUTRON TRANSPORT IN A SLAB. Garrettson, Garrett Aquila, Stanford, Calif.; Stanford Univ. (1969). 162p. University Microfilms Order No. 70-10,455.

Thesis.

The problem of determining the neutron density throughout a bare, homogeneous slab with an arbitrary neutron source is considered. Under the assumptions of one speed, steady state, and isotropic scattering, the integral form of the Boltzmann neutron transport equation for the neutron density is given. To obtain the

neutron density from an arbitrary uncollided source, the point (uncollided) source Green's function is found by transforming the Boltzmann equation into an integral equation that can be solved exactly and then two alternate expressions for the transform inversions are given. Some numerical results are obtained by this theory, including the neutron density in a slab from a normal pencil beam and from an isotropic point source, as well as tables to determine the poles of the transform in a plane. The results indicate that the theory can be economically applied to certain engineering problems, such as performing benchmark calculations to check shielding design codes. (TSS)

Solid-State Physics

3185 (CONF-700801) PROCEEDINGS OF THE TENTH INTERNATIONAL CONFERENCE ON THE PHYSICS OF SEMICONDUCTORS, CAMBRIDGE, MASSACHUSETTS, AUGUST 17–21, 1970. Keller, Seymour P.; Stern, Frank (IBM Watson Research Center, Yorktown Heights, N. Y.); Hensel, John C. (eds.) (Bell Telephone Labs., Murray Hill, N. J.). 880p. Dep. NTIS.

A total of 155 papers are presented in 23 technical sessions dealing with: hot electrons, multiphonon processes, phonons, polarons and magneto-optics, excitons and for uv, surfaces and magnetic semiconductors, optical properties and impurities, metal–semiconductor transition, tellurium band structure, fundamental optical properties, surface quantization and tunneling, excitons at high concentrations, energy band effects, amorphous semiconductors, acoustoelectric effects, light scattering, low mobility and disordered semiconductors, spin-dependent and other transport, and recent advances. (D.L.C.)

3186 ABSTRACTS OF REPORTS PRESENTED AT THE 22nd CONGRESS OF THE BRAZILIAN SOCIETY FOR SCIENCE PROGRESS HELD IN THE CITY OF SALVADOR, BRAZIL, JULY 1970. Notas Fis., Cent. Brasil, Pesqui. Fis.; 16: 1-73(May 1970). (In Portuguese and English). (CONF-700703).

Abstracts are included for 37 of the 1000 papers presented. The topics of most of the abstracts are in the field of physics. (W.H.K.)

Radiation Effects

Refer also to abstracts 2227, 2507, 2514, 2814, 3469, and 3477.

3187 (CONF-700322–, pp 63-77) RADIATION DAMAGE STUDIES WITH LOW-ENERGY HYDROGEN ISOTOPES: AN UNDERGRADUATE SOLID STATE PROGRAM. Goldsmith, George J.; Downey, Daniel; Gorman, Michael; Martin, Edward (Boston Coll., Chestnut Hill, Mass. Dept. of Physics).

From Proceedings of the second Oak Ridge conference on the use of small accelerators for teaching and research, March 23–25, 1970.

The education program for senior physics majors at Boston College on radiation damage studies in semiconductors is described. Crystal preparation and experimental procedures for deuteron damage studies in cadmium sulfide crystals using a 400-keV Van de Graaff accelerator are discussed. Electrical and optical properties of cadmium sulfide were studied, and some results are presented. (W.H.K.)

3188 (CONF-700322–, pp 141-53) ION CHANNELING AND BLOCKING PHENOMENA: TOOLS FOR RESEARCH AND TEACHING. Appleton, B. R. (Oak Ridge National Lab., Tenn.).

From Proceedings of the second Oak Ridge conference on the use of small accelerators for teaching and research, March 23–25, 1970.

This paper is presented for the consideration of the low-energy-accelerator user who may be interested in beginning a research and/or teaching program in solid state and atomic physics that makes use of the channeling and blocking phenomena as tools. It is by no means a comprehensive treatment of these phenomena and their applications. Instead, it includes only the basic model considerations and the consequences these phenomena impose on the Rutherford scattering process that make the combined technique a useful investigative tool. Essential features required for interpreting the energy spectra of the scattered ions are noted and sufficient references are included to guide the interested researcher to more detailed applications. 12 references. (auth)

3189 (COO–1053-14) [RELATIONSHIP BETWEEN ION IMPACTS AND CLUSTERS IN GOLD CRYSTAL FOILS.] Final Progress Report, June 15, 1969–August 31, 1970. Hines, R. L. (Northwestern Univ., Evanston, Ill.). 9 Oct 1970. Contract AT(11-1)-1053. 3p. Dep. NTIS.

Imperfection clusters produced by ^{131}Xe ion impacts in Au crystals were studied using weak-beam images in electron microscopy. No structure is observed at low energies, but above 15 keV, pairs or triplets of closely spaced subclusters appear. From the cluster size distribution, the cluster diameter was found to be mainly 10 to 60 Å. The ratio of clusters to ion impacts increases with energy above 2 keV, reaching a limiting value of unity near 20 keV. Theoretical calculations of the weak beam contrast for a prismatic dislocation loop on a 111 plane agree with experiment. (D.L.C.)

3190 (COO–1053-15) RADIATION EFFECTS OF ION BOMBARDMENT. Final Report, June 15, 1958–August 31, 1970. Hines, R. L. (Northwestern Univ., Evanston, Ill.). 9 Oct 1970. Contract AT(11-1)-1053. 7p. Dep. NTIS.

Research was conducted on the use of positive-ion bombardment to simulate fast-neutron bombardment. Some papers resulting from the research are listed. (D.L.C.)

3191 INFRARED ABSORPTION IN GAMMA-RAY IRRADIATED SINGLE CRYSTAL OF SODIUM NITRITE. Lee, Moon Nam; Kwun, Sook-Il (Seoul National Univ.). J. Korean Phys. Soc.; 3: 9-14(Mar 1970).

An extra peak in the infrared absorption spectrum of γ-irradiated $NaNO_2$ crystals was found. The normal peak at 825 cm^{-1} in the infrared spectrum is usually attributed to the bending vibration mode of the NO_2^- ion in $NaNO_2$ virgin single crystals. But γ-irradiated (by ^{60}Co 750-Ci) $NaNO_2$ shows another peak at 835 cm^{-1} with the peak height dependent on the dose. The dependency of the ratio of intensity at 825 to 835 cm^{-1} on dose is shown. The temperature range covered is from 15 to 185°C. The extra peak at 835 cm^{-1} is thought to be due to the bending vibration mode of the NO_2 free radical in the γ-irradiated $NaNO_2$. To support the model, a Faraday rotation experiment was performed, resulting in a Faraday rotation angle of 2.5° in the [100] direction, 0.9° in the [0$\bar{1}$0] direction, and 0.8° in the [100] direction at 115°C with a crystal irradiated with 10^7 R. Evidence is presented that, in the γ-irradiated $NaNO_2$, the NO_2 free radical behaves as a paramagnetic species. (auth)

3192 EFFECT OF γ RADIATION ON THE VOLT-AMPERE CHARACTERISTICS OF DIODES. Mirsagatov, Sh. A.; Isamukhamedova, D. K.; Yunusov, M. S. (Physical-Technical Inst., Tashkent). Izv. Akad. Nauk Uzb. SSR, Ser. Fiz.-Mat. Nauk; No. 2, 57-9(1970). (In Russian).

The volt–ampere characteristics of silicon carbide diodes were investigated after exposure to 10^4 to 10^9R of γ radiation, at currents ranging from 10^{-9} to 10^{-1}A, in both directions. Study of the dependence of the current on the radiation dose at constant voltage at room temperature indicated that the linear portions of the curve represent the more radiation-sensitive range. In the forward direction, the $I \sim V$ relationship changes into $I \sim V^4$ or V^5 after exposure to 1.5×10^8R. The rectification coefficient of $K = I_{direct}/I_{inverse} = 28$ before the exposure became 7000 after exposure to 3×10^9R. Study of the temperature coefficients revealed that defects with an activation energy of 0.03, 0.08, and 0.3 eV are created by exposing the system to 10^9R of γ radiation. The defects in the SiC may be of donor or acceptor types. (TTT)

3193 QUICK-RESPONSE ENERGY TRANSFER IN KBr:Tl CRYSTALS. I. OPTICAL FLASH. Nagli, L. E.; Rot, M. L. (Inst. of Physics, Riga). Latv. PSR Zinat. Akad. Vestis, Fiz. Teh. Zinat. Ser.: No. 3, 52-9(1970). (In Russian).

A quick-response flash of activator luminescence in a KBr : Tl phosphor, x-irradiated at room temperature and stationary stimulation in the $F(M_2)$ range of the absorption band were studied. Data on spectral composition kinetics of flash extinction, as well as on the influence of the direct current on the flash, in a temperature range 80 to 290°K were obtained. It is supposed that complex centers $Tl^{3+}(F)$ and $Tl^{2+}(M)$ are responsible for the quick-response flash. After the photoextinction in the $F(M_2)$ absorption band, the thermal emission of the electrons in the conductivity zone in the given case, apparently, could not be realized. (auth)

3194 QUICK-RESPONSE ENERGY TRANSFER IN KBr:Tl CRYSTALS. II. PHOTOSCINTILLATIONS. Nagli, L. E.; Rot, M. L. Latv. PSR Zinat. Akad. Vestis, Fiz. Teh. Zinat. Ser.: No. 3, 60-4(1970). (In Russian).

KBr : Tl phosphor luminescence, x-irradiated at 290°K and excited by short light pulses ($\tau = 2 \times 10^{-7}$ sec) in a $F(M_2)$-region absorption band, was investigated. Data on spectral composition, attenuation kinetics, and the external electric field influence on M_2 scintillations were obtained. A hypothesis on the tunnel transition of the energy in the Tl^{2+} M centers is suggested. (auth)

3195 EPR STUDY OF ISOTHERMAL ANNEALING KINETICS OF CHROMIUM IONS IN X-IRRADIATED RUBY. Liu, D. C. (Lewis Research Center, Cleveland). Phys. Lett.; 33A: 140-1(19 Oct 1970).

By using the EPR technique, dynamic measurements showed that

the thermal recovery of the chromium ions to the +3 state in x-irradiated ruby was a first-order process. The activation energy of this process was found to be 1.37 ± 0.07 eV. (auth)

3196 EFFECT OF X IRRADIATION ON FERROELECTRIC PROPERTIES OF BARIUM TITANATE SINGLE CRYSTAL. Sinha, S. K. (Patna Univ., India). Indian J. Pure Appl. Phys.; 7: 798-800(Dec 1969).

The effects of x irradiation on the coercive force, dielectric loss, and dielectric constant of barium titanate single crystal were studied. The coercive force and dielectric loss increase initially with increasing amount of irradiation up to a certain limit (44 R) beyond which they decrease. On the other hand, the dielectric constant of the crystal initially decreases with increasing amount of irradiation up to nearly the same limit and begins to increase beyond this limit. All the ferroelectric parameters of the crystal regain their original values before irradiation if the crystal is heated to 400°C and then cooled. But the position of the hysteresis loop on the screen changes, indicating the production of an intrinsic bias in the crystal. An attempt was made to explain these observations on the basis of the assumption that trapped electrons produce polarizable centers in the crystal lattice. (auth)

3197 STORED ENERGY MEASUREMENTS IN ELECTRON-IRRADIATED Pt BELOW 40°K. Feese, K.; Hoffmann, D.; Wollenberger, H. (Kernforschungsanlage, Juelich, Ger. Institut fuer Allgemeine Metalkunde und Metalphysik, Aachen). Cryst. Lattice Defects; 1: 245-53(Oct 1970).

The stored-energy release of electron-irradiated Pt foils was measured between 10 and 40°K during heating up with a constant heating rate. The calorimeter is described in detail. The reproducibility and the absolute accuracy of the measurements were carefully determined. The annealing curves of the stored energy differed from those of the electrical resistivity by a temperature-dependent background. This background could be separately determined by irradiating with electrons whose energy was too low to produce Frenkel defects. After correcting the annealing curves for this background, the stored-energy release in stage I_C to I_E $\Delta E_{I_C\text{-}I_E}$ divided by the irradiated sample mass m and the electron dose ϕ was obtained to be $(1.0 \pm 0.25) \times 10^{-19}$ $(W_s/g\ cm^{-2})$. By comparing this value to the resistivity annealing in equivalent irradiation experiments, one obtains the ratio of the formation energy of a Frenkel defect and the resistivity contribution per unit concentration of Frenkel defects $E_F / \rho_F = 3.0 \times 10^3$ (eV/Ω cm). Using an estimated value of $E_F = 6$ eV, one obtains $\rho_F = 20 \times 10^{-4}$ Ω cm. With this value one obtains quite reasonable results for the total cross section of defect production and the spontaneous recombination volume. (auth)

3198 INFLUENCE OF AGGREGATION PROCESSES ON THE V-BAND ABSORPTION IN Ca-DOPED KCl CRYSTALS. Berg, K. J.; Froehlich, F.; Gehrke, E. (Univ. of Halle, Ger.). Cryst. Lattice Defects; 1: 255-9(Oct 1970).

Shape and intensity of V center absorption in Ca-doped KCl crystals after x-ray irradiation at room temperature are shown to vary systematically with thermal pretreatment. One finds that this fact is correlated with aggregation processes of the divalent impurities and can be interpreted by the existence of three different, closely neighboring V absorption bands, whose proportion, with respect to the total V absorption, is a function of the thermal treatment. The three absorption bands are assumed to arise from V centers in the structure, of which dipoles, trimers, or larger dipole agglomerates of the impurities are involved. (auth)

3199 SEMICONDUCTOR LAYERS AND STRUCTURAL CHANGES PRODUCED BY ION IMPLANTATION. Konorova, E. A. (Lebedev Inst. of Physics, Moscow); Sergienko, V. F.; Vavilov, V. S.; (and others). Cryst. Lattice Defects; 1: 269-74(Oct 1970).

Ion implantation of impurities into natural diamond crystals leads to the formation of conductive thin layers near the surface. These layers were used as injecting electrodes in charged-particle counters and might be used for other types of devices working at high temperature. The data on the properties of semiconducting layers are presented. The ion implantation leads also to the formation of strained regions due to radiation damage that extend into the crystal volume. This phenomenon was investigated by x-ray topography and by other methods. (auth)

3200 POSSIBLE UNIFIED UNDERSTANDING OF DEFECTS INDUCED IN n-TYPE GERMANIUM BY ELECTRON BOMBARDMENT. Hiraki, Akio (Osaka Univ.). Cryst. Lattice Defects; 1: 277-9(Oct 1970).

The differences between the annealing behavior of 30°K and 77°K bombardments of Sb-doped Ge are discussed with respect to the "permanent" defects (stable at 77°K). A consistent model is proposed for the permanent defects introduced at 30 and 77°K. The 150°K-defects are likely in the form of divacancy–interstitial complex whose annihilation results in the releases of vacancies. (D.L.C.)

3201 EFFECTS OF THE RADIATION DAMAGE ON THE CHANNELING OF MeV PROTONS IN KBr CRYSTALS. Morita, K; Tachibana, K.; Itoh, N. (Nagoya Univ., Japan). Phys. Lett.; 33A: 257-8(2 Nov 1970).

The effects of the radiation damage on the backscattering of channeled protons from KBr crystals are studied. The radiation-induced dechanneling along ⟨100⟩ and ⟨110⟩ is analyzed and the structure of the interstitial center formed by radiation is discussed. (auth)

3202 THERMALLY STIMULATED CONDUCTIVITY OF IRRADIATED ALKALI HALIDES. Hanley, Peter Ronald. Ithaca, N. Y.; Cornell Univ. (1969). 170p. University Microfilms Order No. 70-5987.

Thesis.

Thermally stimulated conductivity (TSC) that is attributed to the release of charge from electronic and ionic defects during thermal annealing of single crystals of KBr and NaCl was examined. A ^{60}Co gamma source, or a monoenergetic neutron source employing the $^7Li(p,n)^7Be$ reaction, was used to create and/or excite these defects. Irradiations were performed at either 10 and 77°K followed by linear rise annealing to room temperature, at rates ranging from 2×10^{-3} to 2×10^{-2} K° per second. A field of 1000 V/cm was applied to the crystal just before annealing. The current resolution of the electrometer–crystal system was $\geq 1 \times 10^{-15}$ A. Typical TSC peaks ranged from about 10^1 to 10^5 times this amplitude for neutron or gamma dose of the order of 10^{13} neutrons or 10^{14} photons, respectively. The prominent low-temperature TSC peak occurs at 34°K after gamma irradiation at 10°K. This effect is characterized by an activation energy of 0.093 ± 0.005 eV and is correlated with optical absorption measurements at the H center. Two small peaks on the leading edge of the H center correlate with an optical absorption effect that has been attributed to interstitial–vacancy recombination of anion defects. Since the H center peak is not present after the 10°K neutron exposure and the two small peaks predominate, it is concluded that gamma rays at low temperatures predominately form the H center, and that low-temperature neutron exposure results in the Br^- interstitial. The amplitude of the Br^- peaks are sensitive to the energy of the bombarding neutrons. In contrast, the prominent TSC peak after 77°K gamma irradiation occurs from 110 to 120°K, and is characterized by an activation energy of 0.27 ± 0.02 eV. This effect correlates with annealing of the V_1 center. Although this peak is prominent after 10°K neutron exposure, it is not present after the 10°K gamma irradiation. Hence, when the H center can be formed, the V_1 TSC peak is not observed. The observed reaction kinetics of the H and Br^- peaks can be explained by these assignments, and the appearance of the V_1 peak is also consistent with expectations based on these assignments. (Diss. Abstr. Int., B)

3203 INFRARED ABSORPTION STUDY OF SILICON IMPLANTED WITH HIGH-ENERGY NITROGEN IONS. Dexter, Richard John. Blacksburg, Va.; Virginia Polytechnic Inst. (1970). 71p. University Microfilms Order No. 70-9911.

Thesis.

Nitrogen, the only group V impurity that has never been diffused into silicon by thermal methods, has been implanted into the silicon lattice by several authors. Most of this effort has been to study the properties of the p–n junctions produced and the distribution profiles of the implanted ions. Kleinfelder has given a value of .142 eV for the ionization energy of the nitrogen donor. Schwuttke, et al., have found that a buried layer of silicon nitride formed when high-energy nitrogen ions are implanted in silicon. This work reports the first intensified effort to establish the donor ionization energy of high-energy implanted nitrogen in silicon by infrared spectroscopy and further establishes that the buried layer consists of silicon nitride and silicon oxynitride molecules. Infrared spectra of unannealed samples showed absorption peaks at 1.9, 2.7, 3.25, and 5.6 μ. These peaks can be annealed out at 760°C in a few minutes and are attributed to radiation damage effects in the silicon lattice. When fluences of less than 2×10^{16} nitrogen ions per cm^2 were used, peaks were observed that indicate that the ionization energy of the nitrogen donor in silicon might be as shallow as 45.8 MeV. Long, high-temperature anneals on heavily bombarded samples formed an absorption peak at 11.7 μ that was assigned to silicon nitride and peaks at 10.2, 10.7, 11.0, 11.2, and 11.5 μ that were assigned to silicon oxynitride molecules. (Diss. Abstr. Int., B)

Physical Properties

Refer also to abstracts 2669, 2671, 2729, 2805, 2885, 2898, 3034, and 3048.

3204 (AD-708547) SPECTRAL EMITTANCE OF NEODYMIUM, SAMARIUM, ERBIUM, AND YTTERBIUM OXIDES AT HIGH TEMPERATURES. Guazzoni, Guido E.; Shapiro, Stuart J. (Army Electronics Command, Fort Monmouth, N. J.). May 1970. 45p. (ECOM-3281). NTIS.

Spectral emittance of solid specimens of Er_2O_3, Yb_2O_3, Sm_2O_3, and Nd_2O_3 was obtained by comparison of sample emission with the emission of a standard black-body cavity maintained at the same sample true temperature. The spectral emittance has been characterized in a wavelength range of 0.4- to 5.0-μ and at sample temperatures from 1520 up to 1870°K corresponding to surface radiation flux densities of 10 to 50 W/cm^2. This flux density range is of practical interest for thermophotovoltaic energy conversion applications. Preliminary observations of spectral transmittance and reflectance are also reported. (auth) (USGRDR)

3205 (UCRL-19681) DENSITY OF ELECTRONIC STATES IN α-PHASE IN ALLOYS CONTAINING Cd AND Sn. Phillips, Norman E.; Brock, J. C. F.; Lambert, Marcel H.; Merriam, M. F. (California Univ., Berkeley. Lawrence Radiation Lab.). Sep 1970. Contract W-7405-eng-48. 6p. (CONF-700921-1). Dep. NTIS.

From 12th International Conference on Law Temperature Physics, Kyoto, Japan.

Low-temperature heat capacity measurements on α-phase indium alloys were used to obtain the Debye characteristic temperature, the density of electron–phonon coupling constant. The results show further evidence for Brillouin zone boundary–Fermi surface interactions, and are discussed from this point of view. (auth)

3206 PINCHING PROCESSES IN SEMICONDUCTOR PLASMAS. Tacano, Munecazu; Kataoka, Shoei (Electrotechnical Lab., Tokyo). J. Phys. Soc. Jap.; 29: 1241-7(Nov 1970).

Adiabatic compression model for the linear pinch in avalanching n-InSb is studied experimentally. The pinching radial velocity and the final pinched radius are determined from the cross sectional dependence of the pinch time and compared with the theory. Semiconductor plasma is heated up to a temperature just below the melting point according to the adiabatic compression in the low and intermediate sample axial current. (auth)

3207 LOCAL ATOMIC ARRANGEMENT IN In–Pb ALLOYS. Koike, Yoshiyasu (Material Research Lab., Kawasaki, Japan); Sivertsen, John M. J. Phys. Soc. Jap.; 29: 1235-41(Nov 1970).

Local-order and size-effect coefficients were measured from diffuse x-ray scattering of In–Pb solid solutions. The sign of the observed local-order coefficient α_1 is positive, indicating that clustering is preferred in this system. This is expected from heats of formation in the liquid phase measured by other investigators and also from the electron screening model of an alloy. From measured size-effect coefficients β_1 and local-order coefficients α_1 it is found that relatively large atom size accommodations, compared with other systems, take place in this system. (auth)

3208 MAGNETIC ANISOTROPY IN RARE-EARTH METALS. Nielsen, M. (Atomenergikommissionen Research Establishment, Risoe, Denmark); Moeller, H. Bjerrum; Lindgard, P. A.; Mackintosh, A. R. Phys. Rev. Lett.; 25: 1451-4(16 Nov 1970).

The magnetic field dependence of the energy of long-wavelength magnons in Tb–10% Ho was studied by inelastic neutron scattering. The results agree with the "frozen-lattice" model, provided that the second-order magnetoelastic effect is taken into account. The planar anisotropy is almost entirely the result of magnetoelastic effects. The temperature dependences of the anisotropy parameters were deduced from the results. (auth)

3209 APPLICATION OF THE FLUCTUATION MODEL FOR ELECTRON SCATTERING IN LIQUID ALLOYS TO HALL COEFFICIENTS FOR Hg–Tl AND Hg–In SYSTEMS. Menon, M. N. (Univ. of Washington, Seattle); Lichter, B. D. Met. Trans.; 1: 2699-2703(Oct 1970).

The Hall coefficients of liquid Hg–Tl alloys were measured at 20°C using a double ac method. Samples were subjected to an ac current of 77 Hz and an ac magnetic field of 60 Hz, and the resulting Hall voltages were measured at the difference frequency of 17 Hz using a phase-sensitive detection system. The results for alloys of compositions up to 38.9 at. % Tl are accurate to ±4%. The measured Hall coefficients are significantly lower than the free electron values and agree with earlier measurements of Andreev and Regel. Using data for Hg–Tl and Hg–In alloys, the validity of a fluctuation scattering model was investigated. Calculated Hall coefficients agree well with measured values obtained for the Hg–Tl system, but are lower than reported experimental values for the Hg–In system. Both systems are anomalous with respect to a previously observed correlation between electron concentration and excess free energy of formation of the alloys. (auth)

3210 ELECTRICAL CONDUCTIVITY AND DEFECT STRUCTURES IN NON-STOICHIOMETRIC UO_{2+x}. Ishii, Tamotsu; Naito, Keiji; Oshima, Keichi (Tokyo Univ.). J. Nucl. Mater.; 36: 288-96(Sep 1970).

Electrical conductivity (σ) of UO_{2+x} was measured as a function of oxygen partial pressure (Po_2) from 500 to 1400°C in the O/U composition between 2.013 and 2.113. These data were used for the discussion of imperfection models for nonstoichiometric UO_{2+x} with reference to the analysis obtained from the relation between excess oxygen (x) and oxygen partial pressure. The slope of log–log plots of σ against Po_2 decreased with increasing temperature from 1 at 500°C to $\frac{1}{4}$ at 1400°C in the O/U range $0.02 < x < 0.11$. With increasing temperature, interstitial oxygens began to react with lattice oxygens and a complex was produced. At high temperatures the complex decomposed to individual oxygen ion with a localized hole. The charge carrier of the conduction was a hole localized to an excess oxygen or a complex, and the electrical conduction was explained by the hopping mechanism. (auth)

3211 SPECTROSCOPIC PROPERTIES OF SOLID SOLUTIONS OF ERBIUM AND YTTERBIUM OXIDES. Gruss, Leonard (Frankford Arsenal, Philadelphia); Salomon, Robert E. J. Phys. Chem.; 74: 3969-72(29 Oct 1970).

Solid solutions of Er_2O_3 and Yb_2O_3 were prepared over the entire composition range. The visible and ultraviolet diffuse reflectance spectra, the magnetic susceptibility, and the lattice parameters of these solutions were determined. An unusual competition in the intensity stealing of an ultraviolet charge-transfer band was observed and analyzed. (auth)

3212 EFFECT OF PRESSURE ON THE FERMI SURFACE OF Zr. Schirber, J. E. (Sandia Labs., Albuquerque, N. Mex.). Phys. Lett.; 33A: 172-3(19 Oct 1970).

Pressure derivatives of Fermi surface cross sections of Zr along major symmetry directions were obtained, using the fluid He phase-shift technique. The values range from -8×10^{-4} to 3×10^{-3} kbar^{-1}, as compared to the free-electron-scaling prediction of $\sim 7 \times 10^{-4}$ kbar^{-1}. (auth)

3213 CHEMICALLY STIMULATED LUMINESCENCE IN RARE EARTH OXIDES. Sweet, J. R.; White, W. B.; Henisch, H. K.; Roy, R. (Pennsylvania State Univ., University Park). Phys. Lett.; 33A: 195-7(19 Oct 1970).

Strong luminescence from Tb^{3+}-(~0.1%) doped Y_2O_3 and Lu_2O_3 is activated by a hydrogen diffusion flame. Forty-five spectral lines are resolved, the strongest of which exhibits maximum intensity at 160°C. Activation appears to be by neutral OH* species in the flame. (auth)

3214 OPTICAL DENSITY AND THICKNESS OF $NbSe_2$ AND $Nb_{1.04}Se_2$ LAMELLAE. Myers, G. E.; Montet, G. L. (Argonne National Lab., Ill.). Thin Solid Films; 6: R7-8(Jul 1970).

A rapid, nondestructive method was devised for determining the thickness of thin $NbSe_2$ samples cleaved from layered single crystals. A plot of optical density vs thickness shows a reasonably straight line, and an absorption coefficient of 3.45×10^5 cm^{-1} at 545 nm is found for both $NbSe_2$ and $Nb_{1.04}Se_2$. (D.L.C.)

3215 ELECTRICAL RESISTIVITY OF UPt. Lawson, A. C. (Univ. of California, San Diego, La Jolla). Phys. Lett.; 33A: 231-2(2 Nov 1970).

The electrical resistivity of the ferromagnet UPt shows T^2 behavior at low temperatures and a large spin-disorder resistivity above the ordering temperature. (auth)

3216 INTERNATIONAL MEETING ON ACCURATE DETERMINATION OF X-RAY INTENSITIES AND STRUCTURE FACTORS, CAMBRIDGE, ENGLAND, 24 TO 28 JUNE 1968. Arndt, U. W.; Mathieson, A. McL. (eds.). Acta Crystallogr., Sect. A; 25: 1-276(1 Jan 1969). (CONF-680619).

Forty papers are included that treat various topics related to the x-ray intensity and structure factors of single crystals: errors and corrections, attenuation coefficients, multiple diffraction and diffuse scattering, Debye–Waller factor, Pendellösung figures, electron diffraction, atom form factors, x-ray photography, comparison with neutron diffraction, elements, alloys, and compounds, charge and momentum density. (D.L.C.)

3217 OBSERVATION OF MAGNETIC DOMAIN STRUCTURES OF THE INTERMETALLIC COMPOUNDS $SmCo_5$, $LaCo_5$, AND $CeCo_5$. McCurie, R. A.; Carswell, G. P. (Bradford Univ., Eng.). J. Mater. Sci.; 5: 825-8(Sep 1970).

The alloys used were prepared by melting very pure oxygen-free samarium, lanthanum, and cerium with cobalt in an induction furnace. The $SmCo_5$ and $CeCo_5$ were shown by x-ray diffraction analysis to be single-phase in the as-cast state with the hexagonal $CaCu_5$ structure. The $LaCo_5$ required homogenisation for 4 days at 1000°C before the $LaCo_5$ single phase was obtained. The specimens were polished down to 1 μ diamond paste and domain structures obtained by the Bitter technique. All the structures were typical of those for strongly uniaxial materials, the specimens were all polycrystalline, and only one domain structure was seen on each grain. The domain structures obtained are shown and discussed. $SmCo_5$ and $CeCo_5$ were found to be appreciably harder than $LaCo_5$ and less anisotropic. Since the grains on all the specimens were too small for their orientations to be conveniently determined by x-ray diffraction, the domain patterns provided a useful technique for the measurement of hardness as a function of orientation. More detailed measurements of Vickers and Knoop hardness are currently in progress. (UK)

3218 CORRECTIONS TO MAGNON DISPERSION RELATIONS AS DETERMINED BY THE NEUTRON DIFFRACTION TECHNIQUE. Antonini, B.; Medina, R.; Menzinger, F. (CNEN, Rome). Nucl. Instrum. Methods; 87: 125-30(1970).

Spin-wave dispersion relations in ferromagnets can be determined by the neutron-diffraction technique. A new procedure of analyzing the experimental data is described. It is shown that the use of the complete magnon cross section gives a magnon intensity profile appreciably different from the conventional rectangular profile used in the analysis of scattering data. This result is shown to affect the values of the magnon stiffness constant and the shape of the dispersion relations. (auth)

3219 PURE CHEMICAL ELEMENTS FOR SEMICONDUCTORS, 1969. Sittig, Marshall. Electronics Materials Review No. 1. Park Ridge, N. J.; Noyes Development Corporation (1969). 351p. $35.00.

This review presents techniques for producing pure chemical elements for semiconductors and is based on the U. S. patent literature since 1960. The elements are: Sb, As, Bi, B, Ga, Ge, In, P, Se, Si, Te, Tl, and Zn. Company, inventor, and patent number indexes are included. (D.L.C.)

Moessbauer Effects and NMR

Refer also to abstract 2483.

3220 (COO-1700-12) NUCLEAR MAGNETIC RESONANCE STUDY OF THE CRYSTALLINE COMPOUNDS OF THE $NbBe_x$ SYSTEM. Bennett, Robert A.; Hooper, H. O. (Wayne State Univ., Detroit, Mich. Dept. of Physics). [nd] 25p. Dep. NTIS.

Nuclear magnetic resonance techniques were employed to study powder samples of the compounds $NbBe_2$, $NbBe_3$, Nb_2Be_{17} and $NbBe_{12}$. The nuclear quadrupole coupling constants and Knight shifts were determined for the Nb sites in these compounds. The ^{93}Nb NMR from $NbBe_2$ is a single unsplit line with no quadrupole coupling constant and with a Knight shift of 0.70 ± .03%. The ^{93}Nb NMR from $NbBe_3$ indicates the presence of three Nb sites identified by the values of eqQ/h = 0 MHz, 24.2 ± 0.2 MHz, 30.1 ± 0.3 MHz and corresponding Knight shifts of 0.693 ± 0.03%, 0.724 ± 0.03%, 0.532 ± 0.03%. The first of these lines is identified as less than 2% impurity of $NbBe_2$. The ^{93}Nb NMR of $NbBe_{17}$ exhibits a quadrupole coupling, eqQ/h = 5.93 ± 0.15 MHz, and an anisotropic Knight shift, K_{axial} = 0.014% and $K_{isotropic}$ = 0.34 ± 0.02%. The ^{93}Nb resonance from $NbBe_{12}$ was split by a very large quadrupole interaction yielding eqQ/h = 21.73 ± 0.3 MHz with a Knight shift of 0.552 ± 0.02%. The beryllium NMR was examined, yielding little information, since no measurable quadrupole interaction or Knight shift were present. This study illustrates the variety of environments of the niobium nuclei among these beryllides and within a single beryllide. The NMR results are discussed in relation to the results of x-ray studies of these compounds. (auth)

3221 NMR STUDIES OF SPONTANEOUS POLARIZATION IN ROCHELLE SALT. Fitzgerald, Maurice Edward. Troy, N. Y.; Rensselaer Polytechnic Inst. (1969). 135p. University Microfilms Order No. 70-11,318.

Thesis.

Several related problems concerning single-crystal ferroelectric Rochelle salt were investigated experimentally using the quadrupole NMR spectrum of ^{23}Na. Using the symmetry properties of the crystal structure to improve accuracy, the quadrupole coupling constant in the lower, nonferroelectric phase of undeuterated Rochelle salt was measured: e^2Qq/h = 1363 ± 4 kHz; asymmetry parameter η = 0.737 ± 0.004. The quadrupole coupling constant is different from that in the lower phase of deuterated Rochelle salt measured by Blinc, Petkovsek, and Zupancic. Careful measurements were made near the phase transitions of the microscopic spontaneous polarization by the method of Oja and Casabella, that is, by measurements of quadrupole satellite separation in the ferroelectric phase. No discontinuity or thermal hysteresis was observed, confirming the second-order nature of the phase transitions. The effects of γ irradiation on the nonferroelectric phases on the microscopic polarization were also investigated. Irradiation at +30°C in the upper nonferroelectric phase produced stable effects: the spontaneous polarization and the ferroelectric temperature range were reduced; no internal-bias fields were produced, as is the case with irradiation in the ferroelectric phase. By contrast, irradiation at 77°K produced unstable effects. No internal-bias field was initially produced. As the temperature was slowly raised above the lower transition, an internal-bias field began to build up. Further annealing effects occurred when the temperature was raised above the upper transition to about +30°C, but thereafter, the sample properties remained stable and no further annealing was observed. These observations may be tentatively explained by the transformation of the initially formed radiation-damage centers into different types of damage centers as the temperature is increased. These transformations cause effects similar to irradiation at the temperature at which the transformation takes place. (Diss. Abstr. Int., B)

3222 RECOILLESS ABSORPTION MEASUREMENTS OF THE 25.6-keV GAMMA RAYS OF ^{161}Dy EMITTED FROM FOUR-VALENT DYSPROSIUM IONS. Khurgin, B.; Ofer, S.; Rakavy, M. (Hebrew Univ., Jerusalem). Phys. Lett.; 33A: 219-20 (2 Nov 1970).

A narrow emission line for the 25.6-keV gamma rays of ^{161}Dy emitted from a ^{161}Tb(^{161}Dy) in CeO_2 source is reported. The isomer shift between a Dy^{4+} source to a Dy^{3+} source was found to be (3.71 ± 0.04) mm/sec. A value of −1.241 ± 0.004 was found for g(25.6 keV)/g(0) of ^{161}Dy. (auth)

3223 RADIATIVE DETECTION OF SINGLE-PASSAGE NUCLEAR MAGNETIC RESONANCE. Barclay, J. A.; Chaplin, D. H.; Don, C. G.; Wilson, G. V. H. (Monash Univ., Clayton, Australia). Phys. Lett.; 33A: 215-16(2 Nov 1970).

Single-passage NMR and spin−lattice relaxation of oriented ^{60}Co nuclei in iron was detected by observing the γ-radiation anisotropy. (auth)

3224 MOESSBAUER SPECTROMETER CALIBRATION USING ^{57}Fe ENRICHED METALLIC IRON. Abou-Elnasr, T. Z. A.; Moon, P. B.; Reid, C. N. (Univ. of Birmingham, Eng.). Nucl. Instrum. Methods; 87: 303(1970).

The line shift in the Moessbauer spectrum of metallic iron caused by martensite may be removed by annealing. (W.H.K.)

3225 INVESTIGATION OF SUPPRESSED NUCLEAR ABSORPTION OF RESONANT γ RAYS UNDER LAUE DIFFRACTION CONDITIONS. EFFECT OF OSCILLATIONS OF THE REFLECTION INTENSITY. Smirnov, G. V.; Sklyarevskii, V. V.; Artem'ev, A. N. JETP Lett. (USSR) (Engl. Transl.); 11: 400-2(20 Jun 1970).

Translated from Zh. Eksp. Teor. Fiz., Pis'ma Red.; 11: 579-82 (20 Jun 1970).

The suppression of nuclear resonant absorption was reported earlier by the authors under conditions when diffraction is primarily by electrons (JETP Lett., 8: 181(1968) and 11: 363(1970)). The suppression effect is reported here for the case of diffraction predominantly by resonant nuclei, i.e., when the ratio of the amplitudes $f_{nuc}^{res}/f_{el} \gg 1$. A beam of 14.4-keV γ quanta with divergence 0.5° and 6° in the vertical plane was incident directly from the source (20 mCi of ^{57}Co in Pd) on a single crystal of hematite (α-Fe_2O_3) 95 μ thick, enriched to 85% ^{57}Fe. The (111) plane emerged on the surface of the crystal. The crystal was mounted in a position of symmetrical Bragg reflection ($10\bar{1}$) in the Laue geometry (θ = 9°54′). The conditions were chosen such that only one component of the γ radiation with polarization 1 took part in the effect of suppression of the nuclear absorption. Results clearly demonstrate the suppression effect for resonant nuclei. Reference is made to an analogous experiment by Voitoveskii et al. (JETP Lett., 11: 91(1970)) using ^{119}Sn γ rays and a tin crystal. (L.M.T.)

Theory

3226 (IN-1420) ELECTRON GROUND STATES IN MOLECULAR AND VALENCE-BONDED CRYSTALS. McMurry, H. L.

(Idaho Nuclear Corp., Idaho Falls). Oct 1970. Contract AT(10-1)-1230. 21p. Dep. NTIS.

This work is a first step toward calculating the potential functions which govern crystal vibrations from a fundamental understanding of how the ground state electronic energy changes when internuclear distances depart from their equilibrium values. The motivation arises from the need to calculate the slow neutron scattering of crystalline moderators (graphite, Be, BeO, etc.). To do this, the crystal vibrational frequencies and normal modes must be known. To calculate the frequencies and normal modes, the changes in potential energy with departures of internuclear distances from equilibrium must be known. These potential functions are usually obtained by empirical or semi-empirical processes in which parameters in assumed models are adjusted so calculated frequencies agree with available experimental data. However, experimental data on crystal vibrations have increased to the point where potential functions with sound physical bases are becoming necessary in order to get good agreement between theory and experiment. The work reported here aims at providing this basis. It also leads toward using experimental data for better evaluation of ideas about the electron structure of crystals. The method draws on ideas which have been developed for calculating electronic ground state energies in large molecules. For the crystal, the atoms within any primitive cell play the role of molecules and the theory essentially expresses how the molecular wave functions interact from one primitive cell to another. However, the crystalline wave functions are written so they possess the symmetry properties associated with the translation operations of the crystal and this simplifies the equations. The final result is a method for calculating the ground state electronic wave function for the equilibrium configuration. These wave functions should be useful for making perturbation calculations of the change in ground state energy with changes in internuclear distances. They may be useful, also, in guiding the search for models with a minimum number of potential constants which are needed to give calculations in agreement with experiment. (auth)

3227 PSEUDOPOTENTIALS AND MODEL POTENTIALS IN SOLID STATE PHYSICS. Pindor, Andrzej (Univ. of Warsaw). Postepy Fiz.; 21: 437-45(1970). (In Polish).

The ideas of pseudopotential and model potential of an atom in a solid are presented. Their physical interpretation and some of the applications are discussed. (auth)

Theoretical Physics

Refer also to abstracts 2927, 3040, and 3237.

3228 HARTREE–FOCK THEORY AND THE LAMBDA TRANSFORMATION IN QUANTUM STATISTICAL MECHANICS. II. DEGENERATE BOSE SYSTEM. Tuttle, E. R. (Univ. of Denver). Phys. Rev., A; 1: 1758-71(Jun 1970).

A Hartree–Fock theory of the quantum Ursell expansion for Fermi fluids was developed previously. The same techniques are used here to derive a theory of degenerate Bose fluids from the x-ensemble theory of Lee and Yang. It is shown that this theory is equivalent to the Λ-transformed theory recently derived by Mohling, RamaRao, and Shea. The present approach considerably simplifies the formalism and eliminates the need for the Λ transformation. By working entirely in a quasi-particle framework, the problems with unphysical line factors that have appeared in earlier theories are avoided. Finally, a greatly simplified Λ transformation is obtained for use in problems in which the potential contains an infinitely repulsive core. (auth)

3229 COMPARISON OF TWO PERTURBATION METHODS. Singh, S. R.; Smith, V. H. Jr. (Queen's Univ., Kingston, Ont.). Int. J. Quant. Chem.; 4: 519-27(Sep 1970).

Polikanov's perturbation method for the solution of the radial Schroedinger equation is shown to be equivalent to the usual Rayleigh–Schroedinger method but with full normalization instead of intermediate normalization. The energy corrections are shown to be the same to all orders. The computational advantages of Polikanov's method are discussed. The method is illustrated by considering the two-electron ions in the Hartree–Fock approximation. (auth)

3230 SOLUTION OF THE DIRAC EQUATION IN A MAGNETIC FIELD. Sen Gupta, N. D. (Tata Inst. of Fundamental Research, Bombay). Indian J. Pure Appl. Phys.; 6: 459-60 (1968).

It is shown that, in a steady magnetic field, the Dirac equation can be reduced to the problem of simultaneous linear homogeneous partial differential equations of two unknown scalar functions. The solutions are further simplified for application in two special cases, when the magnetic field is (i) symmetric about an axis, and (ii) invariant with respect to translation along a direction. The problem in these cases reduces to the solution of a second-order partial differential equation. (auth)

3231 FOLDY–WOUTHUYSEN TRANSFORMATIONS AND RELATED PROBLEMS. de Vries, E. (Univ., Groeningen, Netherlands). Fortschr. Phys.; 18: 149-82(1970).

A number of problems that remained or originated with the appearance of the Foldy–Wouthuysen transformation are reviewed: (1) The interpretation of the Fouldy–Wouthuysen (FW) transformation for a free particle. (2) The stepwise transformation method of Fouldy and Wouthuysen is compared with the method of Eriksen. (3) Pauli's elimination method is analyzed. (M.O.W.)

3232 BOUNDS FOR SOME EQUILIBRIUM PROPERTIES OF AN ELECTRON GAS. Kugler, Alfred A. (Institut Max von Laue, Grenoble, France). Phys. Rev., A; 1: 1688-96(Jun 1970).

Upper and lower bounds are derived for the average potential energy and Helmholtz free energy of an electron gas with uniform positive background. In the ground-state limit, upper and lower bounds are given for the average kinetic energy, average potential energy, and total ground-state energy. Inequalities are derived for the static form factor S(k) and wave-number-dependent dielectric function $\epsilon(k,0)$, making use of exact sum rules for the Fourier-transformed density–density commutator and of the assumption that $S(k) \leq 1$. Comparison is made with the exact behavior of these quantities for small k. The sum rules are used to construct an approximate nonlinear integral equation for the ground-state static form factor of the electron gas. (auth)

3233 ELECTRON IN A QUANTIZED FIELD OF A PLANE ELECTROMAGNETIC WAVE. Berson, I. Ya. (Inst. of Physics, Riga). Latv. PSR Zinat. Akad. Vestis, Fiz. Teh. Zinat. Ser.; No. 3, 3-8(1970). (In Russian).

The solution of the problem on electron movement in a quantized field of a monochromatic electromagnetic wave obtained by the author previously (Zh. Eksp. Teoret. Fiz., 56: 1627(1969)) is generalized for a case with a plane random electromagnetic wave. The p-electron quasi impulse is found to satisfy the equation $\bar{p}^2 + m^2 + a(\bar{p}) = 0$, where: m is the effective electron mass, having the same expression as in the classical case of the wave, whereas the term $a(\bar{p})$ is found to appear due to electromagnetic wave quantization and to approach zero with increasing quantization volume. (auth)

3234 IDENTITY CONCERNING THE PROJECTION OPERATORS IN NONEQUILIBRIUM STATISTICAL MECHANICS. George, Cl. (Univ. Libre, Brussels). Bull. Cl. Sci., Acad. Roy. Belg.; 56: 386-93(1970).

The possibility of projecting out of the complete dynamical behavior of a many-body system the coherent behavior associated with a thermodynamical description rests on a relation between asymptotic operators. A direct proof of this relation is presented. (auth)

3235 COMMENTS ON THE CYCLOTRON RESONANCE EXPERIMENTS OF THE LOS ALAMOS GROUP. Robinson, L. C. (Sydney Univ.). Nucl. Fusion; 10: 337-9(Sep 1970).

Time dependence of the absorbed cyclotron energy for a small perturbation experienced by an electron in transit through two identical helices of constant pitch was analyzed. Diagrams are given of the energy of cyclotron motion absorbed by the electron as functions of helix pitch and electron velocity. (M.O.W.)

3236 APPLICATIONS OF LIE SERIES IN ATOMIC PHYSICS. Cap, F. F.; Weil, J. W. (Univ., Innsbruck). At. Energy Rev.; 8: 621-92(Sep 1970).

A survey was made of the most important properties of Lie series, particular emphasis being laid on second-order ordinary differential equations where several detailed calculations are presented, on some special types of equations derived therefrom, and on partial first-order differential equations. The applications discussed are eigenvalue problems of reactor physics for which numerical results obtained both with customary methods and Lie series are given, neutron diffusion (with a discussion of the advantages of Lie-series method), reactor dynamics (basic differential equations, space-independent xenon dynamics), transport theory (transport equation, spherical-harmonic equations, solutions, transfer matrices), accelerator problems, plasma flows (MHD equations, channel flows and computing programs, (LIE-PN program, diffusion and neutron shielding, critical mass and eigenvalue problems, ARLEKIN, Mathieu- and Weber-function program, satellite-orbit program, LIESE). (auth)

3237 NEW APPROACH FOR THE JUSTIFICATION OF ENSEMBLES IN QUANTUM STATISTICAL MECHANICS. II.

XUM

Keizer, Joel E. (Univ. of California, Santa Cruz). J. Statist. Phys.; 2: 233-49(1970).

The results of the first paper in this series are generalized to include spin, permutation symmetry, and time dependence. In particular, the question of time invariance of localness in the Heisenberg picture is discussed and it is conjectured that an operator that is initially local will remain local over time. In order to treat macroscopic systems, it is shown that the ensemble decomposition of the previous paper can be used to "coarse-grain" configuration space. Finally, a physical interpretation of the ensemble decomposition in terms of "redundant macroscopic information" is used to give a derivation of the generalized microcanonical average. (auth)

3238 NEW APPROACH FOR THE JUSTIFICATION OF ENSEMBLES IN QUANTUM STATISTICAL MECHANICS. I. Keizer, Joel E. (Univ. of California, Santa Cruz). J. Statist. Phys.; 2: 213-32(1970).

In this and the following paper, a new approach for the justification of ensembles in statistical mechanics is given. The essential physical idea is that a measurement is an average of values arising from disjoint regions in three-space. This idea is given a mathematical basis in terms of a class of operators called "local operators," and the first paper is devoted primarily to the development of the properties of local operators. In particular, a complete characterization of the bounded local operators on L_2 spaces of finite measure is given. Two results of importance for statistical mechanics are also derived. First, it is shown that the observables of quantum mechanics are local operators. Second, it is shown that the expectation value of an observable for a pure state can be written formally as an ensemble average. In the following paper, these results are used to develop a new approach for the justification of statistical ensembles. (auth)

3239 STATISTICS OF A RANDOM PLUS CONSTANT VECTOR WITH APPLICATION TO ACOUSTIC AND ELECTROMAGNETIC-WAVE SCATTERING. Seifer, Arnold D. (General Dynamics Corp., Groton, Conn.); Jacobson, Melvin J. J. Statist. Phys.; 2: 279-89(1970).

A two-dimensional random-walk problem is investigated, where a vector fixed in amplitude (magnitude) is added to one that is random in phase (direction angle). This problem can arise from a study of the effect of multipath interference from an acoustic or electromagnetic-wave source, where an arrival of constant amplitude is combined with an incoherent background of randomly scattered components of the incident field. The source is considered to have harmonic time dependence. This study follows from an earlier paper, in which the required properties of the incoherent background were derived. In the present study, the joint distribution of the resultant amplitude and of the phase angle between the resultant and the fixed arrival is determined. Further, expressions are developed for the first and second moments of the resultant phase, amplitude, decibel-amplitude, and intensity. Many properties of these moments are described. (auth)

3240 APPLICATION OF DISTRIBUTION THEORY TO MARTIN'S METHOD IN POTENTIAL SCATTERING. Whipp, A. T. (Univ. of Liverpool). Proc. Cambridge Phil. Soc.; 68: 709(18 Nov 1970).

In order to study the convergence of a series arising from the use of Martin's method in potential scattering a framework consisting of a modification to Schwartz's formulation of distribution theory is set up. This modification makes essential use of norms on the spaces of test functions and linear functionals. By making the norm on the space of test functions satisfy extra axioms a bound is obtained on the norm of a generalized convolution of two linear functionals, and this bound is used to prove the convergence of the series. The proof of convergence is generalized to cover the multichannel problem. The method used may also be applied to many other physical problems. (auth) (UK)

3241 THE VARIATIONAL SOLUTION OF THE SCHROEDINGER EQUATION OF FINITE FERMION SYSTEMS. I. HARTREE–FOCK APPROXIMATION AND INDEPENDENT PAIR MODEL. Szasz, Levente; Schroeder, John (Fordham Univ., New York). Z. Naturforsch.; 24a: 1855-6(Nov 1969).

A method is outlined here and in Part II for obtaining the variational solution of the Schroedinger equation for finite fermion systems. The new method is based on a trial function (called correlated wave function) of the form $\Psi = \Psi_F + \Psi_C$, where Ψ is the Hartree–Fock wave function built from the orbitals $\Phi_1 \ldots \Phi_A$ and $\Psi_C = \sum_{i<j} f^{(2)}(ij) + \Sigma f^{(3)}(ijl) + \ldots f^{(A)}(1,2, \ldots, A)$. (M.O.W.)

3242 THE VARIATIONAL SOLUTION OF THE SCHROEDINGER EQUATION OF FINITE FERMION SYSTEMS. II. THREE-PARTICLE CORRELATIONS AND HIGHER ORDER EFFECTS. Szasz, Levente; Schroeder, John (Fordham Univ., New York). Z. Naturforsch.; 24a: 1856-7(Nov 1969).

Solutions of the Schroedinger equation are obtained in steps, and at each step, the 2-, 3-, ..., n-th order correlation functions are calculated ($n \leq n \leq A$) from independent equations, but nothing in the energy expression is neglected. The calculation of the n-th order function requires the knowledge only of the lower-order functions. (M.O.W.)

3243 ENERGY-MOMENTUM CONSERVATION FOR COLLISION, CREATION, AND ANNIHILATION PROCESSES: GEOMETRICAL DERIVATION FROM A VERY SIMPLE CLASSICAL ACTION PRINCIPLE. Dorling, J. (King's Coll., London. Univ. of Sussex, Brighton, Eng.). Amer. J. Phys.; 38: 1023-8(Aug 1970).

It is shown by a geometrical argument that the action principle $\delta \Sigma_i m_{0i} \int d\tau_i = 0$ (m_{0i} is the rest mass of the ith particle taking part in the process; $d\tau_i$ is an infinitesimal element of proper-time along the ith particle's trajectory; the integrals are over all trajectories between any two space-like hypersurfaces) leads directly to energy–momentum conservation for collisions and creation and annihilation processes. This action principle could be interpreted as a principle of maximum total "particle time" if the rest masses were thought of as the frequencies of certain periodic processes defined along the particle trajectories. (auth)

XUM

PHYSICS (HIGH ENERGY)

Particle Interactions and Properties (Experimental)

Electromagnetic

3244 ELECTROPRODUCTION OF PIONS ON A PROTON AT THRESHOLD AND STRUCTURE OF THE NUCLEON. Titov, Yu. I.; Severin, N. F.; Afanas'ev, N. G.; (and others). JETP Lett. (USSR) (Engl. Transl.); 12: 129-31(20 Aug 1970).
Translated from Zh. Eksp. Teor. Fiz., Pis'ma Red.; 12: 186-9(20 Aug 1970).

A number of spectra of the inelastic scattering of electrons in the region at the electroproduction threshold were measured. The cross sections for inelastic scattering as functions of the pion 3-momentum in the cms of the pion and recoil nucleon are shown. Also shown are the results of the determination of the neutron charge form factor by the chi-squared method. (J.F.P.)

3245 THEORETICAL DESIGN OF THE EXPERIMENT TO STUDY SCATTERING OF ELECTRONS AND POSITRONS BY ELECTRONS. Bhiday, M. R.; Bhise, V. M.; Shastri, A. G. (GS Inst. of Tech. and Science, Indore, India). Indian J. Phys.; 43: 499-506(Sep 1969).

Experiments to measure the electron-electron and positron-electron scattering cross sections using a transverse magnetic field are in progress. The theoretical design study of these experiments is discussed. Monoenergetic beams of electrons or positrons are incident nearly normally to the scattering foil placed in the plane of the magnetic field. It is shown that the scattered and recoil particles due to electron-electron or positron-electron collisions with energy transfer q are focussed on two lines along the magnetic field. Relations between the x and z coordinates of the scattered particles, when focussed on the lines and the angles of scattering, are derived enabling the design and exact positioning of the scintillators in order to achieve a high collection efficiency and good resolution. (auth)

3246 PHOTOPRODUCTION OF ρ^0 MESONS ON DEUTERONS BETWEEN 1 AND 5 GeV. Hilpert, H. G. (Technische Hochschule, Aachen); Lauscher, P.; Matziolis, M.; (and others). Nucl. Phys.; B23: 45-74 (1970).

The reactions $\gamma d \rightarrow d\pi^+\pi^-$ and $\gamma d \rightarrow pn\pi^+\pi^-$ were investigated in a deuterium bubble chamber. Invariant mass spectra are presented; ρ^0 production is dominant in both reactions. Differential and total cross sections for ρ^0 production have been determined. The results are compared with the reaction $\gamma p \rightarrow p\rho^0$ within the framework of the impulse approximation, assuming equal ρ^0 photoproduction amplitudes on the proton and the neutron. (auth)

3247 PHOTOPRODUCTION OF ω-MESONS FROM NUCLEI. Braccini, P. L. (Univ., Pisa, Italy. Istituto Nazionale di Fisica Nucleare, Pisa, Italy); Bradaschia, C.; Castaldi, R.; (and others). Nucl. Phys.; B24: 173-81(1970).

An experiment of ω-photoproduction from nuclei (C, Al, Zn, Ag, Ta, Pb; 5.7 GeV mean photon energy) performed at DESY is reported. The experimental apparatus detects the $\pi^0\gamma$ decay of the produced ω-mesons. Results about the ω-photon coupling $\gamma_\omega^2/4\pi$ and about the ω-nucleon total cross section σ_ω are derived. The dependence of these results on the different possible models of analysis is discussed. (auth)

3248 PHOTOPRODUCTION OF K^0 MESONS FROM PROTONS AND FROM COMPLEX NUCLEI. Albrow, M. G. (Univ. of Manchester, Eng.); Aston, D.; Barber, D. P.; (and others). Nucl. Phys.; B23: 509-24(1970).

The momenta spectra of neutral K-mesons photoproduced from protons and other nuclei by bremsstrahlung were measured for photon energies up to 5 GeV. The cross sections for production of K_L^0 from protons integrated over momenta from 1.5 GeV/c to the maximum were 11.8 ± 3.5, 14.0 ± 3.7, 33.4 ± 6.9 and 35.3 ± 7.5 μb/sr/equivalent quantum at 3½° to bremsstrahlung beams with maximum energies of 3.5, 4.0, 4.5 and 5.0 GeV, respectively. At 9° the cross sections, similarly defined, were 3.6 ± 3.0 and 6.0 ± 3.5 μb/sr/equivalent quantum at 3.5 and 4.0 GeV, respectively. The cross sections for production from nuclei, at 3½° and with bremsstrahlung of maximum energy 4.5 GeV, were 32.0 ± 8.0, 49.1 ± 6.0 and 45.9 ± 15.7 μb/sr/equivalent quantum per nucleon for Be, Al and Cu, respectively. The observed spectra cannot be explained in terms of simple processes; the K-mesons are probably produced in association with several other particles. A description is given of the ferrite core wire spark chambers used in this experiment, including the readout logic and on-line computer system. (auth)

3249 PRODUCTION OF EXTERNAL BREMSSTRAHLUNG IN DIFFERENT MATERIALS. Gopal, S.; Gopal, K.; Sanjeevaiah, H.; Sanjeevaiah, B. (Univ. of Mysore, India). Indian J. Pure Appl. Phys.; 7: 512-3(Jul 1969).

Variation in the intensity of external bremsstrahlung, emitted in the forward direction, with thickness of different materials was studied using P-32 source. Exponential character in the ratio of the intensity to the number of atoms per cm^2 is noticed over a limited thickness. (auth)

3250 EXPERIMENTAL INVESTIGATION OF DIRECT ELECTRON–POSITRON PAIR PRODUCTION IN COPPER BY ELECTRONS OF 5.8 MeV KINETIC ENERGY. Feist, H.; Reich, H. (Physikalisch-Technische Bundesanstalt, Brunswick). Z. Phys.; 239: 437-46(1970). (In German).

The direct production of positrons by electrons in copper was investigated using the 5.8-MeV electron beam from the 6-MeV microtron of the Physikalisch-Technische Bundesanstalt. Cross sections were derived from the measurements under the assumption that the positrons produced directly and those produced indirectly by bremsstrahlung photons have the same angular distribution. The values obtained are greater than those calculated numerically by Lõns by a factor of 1.3 to 1.45. It is shown that there is an essential contribution of direct positron production to the electron positron conversion factor in thin foils consisting of elements with low atomic number. The experimental set-up is described in detail. Its main feature is the use of a special positron transmission line with bending magnet in order to overcome background difficulties. (auth)

3251 PHOTOPRODUCTION OF Y* RESONANCES ABOVE 1800 MeV. Lu, D. C.; Greenberg, J. S.; Hughes, V. W.; (and others) (Yale Univ., New Haven). Phys. Rev., D; 2: 1846-51 (1 Nov 1970).

The photoproduction of K^+ mesons and hyperons with strangeness S = −1, in reactions of the type $\gamma + p \rightarrow Y^* + K^+$, was studied in the Y* mass range 1800 to 2600 MeV with a missing-mass spectrometer by analyzing the structures in the K^+ yield as a function of the end point bremsstrahlung energy. The K^+ yield was observed at the laboratory angle of $\theta_K = 10°$ and at the K^+ momenta of 2.5 and 2.0 BeV/c. A fit to the K^+ yield curve suggests, in addition to a smooth background, resonancelike structure at 1820 ± 20, 2025 ± 20, 2250 ± 20, and 2530 ± 25 MeV. Widths and photoproduction cross sections for these states were measured. (auth)

3252 BOUND ON VIRTUAL COMPTON SCATTERING AT 185 AND 460 MeV/c^2. Randolph, J. K.; Eisner, A. M.; Feldman, G. J.; (and others) (Harvard Univ., Cambridge, Mass.). Contract AT(30-1)-2751. Phys. Rev., D; 2: 1852-9(1 Nov 1970).

The photoproduction of asymmetric electron-positron pairs from carbon was measured to study the production of virtual photons of energies (masses) 1.8 GeV (185 MeV/c^2) and 4.5 GeV (460 MeV/c^2). The interference between such a Compton production mechanism and the dominant Bethe–Heitler production was determined by observing the change in the yield for electron-positron pairs when the electron and positron were interchanged. The measured interference cross section is consistent with zero and with most models treating Compton production as due to the decay of the ρ meson into electron-positron pairs. (auth)

3253 SCATTERING OF HIGH-ENERGY PIONS ON ELECTRONS. Waterman, F. M.; McNulty, P. J. (Clarkson Coll. of Tech., Potsdam, N. Y.). Phys. Rev., D; 2: 1820-3 (1 Nov 1970).

A total of 50 knock-on electrons with emission angles less than or equal to 10° were located by along-the-track scanning of 105.4 m of 16.2-GeV/c negative-pion track in nuclear emulsion. The measured electron energies were found to be in agreement with kinematics. The spectrum of these high-energy δ rays is in agreement with both theory and previous bubble chamber results. A serious scanning deficiency at small angles in along-the-track scanning was found, and its implications for experiments searching for anomalous scattering on electrons are discussed. (auth)

3254 ASYMMETRY AND BACKGROUND IN $\eta \rightarrow 3\pi$. Taggart, Keith. (Case Western Reserve Univ., Cleveland). Phys. Rev., D; 2: 1960-3(1 Nov 1970).

XUM

The problem of the asymmetry observed in the decay $\eta \rightarrow \pi^+\pi^-\pi^0$ is considered. Bernstein, Feinberg, and Lee suggested that an asymmetry in the average energies of the charged pions in this decay would be proof of C violation in the electromagnetic interaction among hadrons. Recall, however, that the η is identified as a peak in the invariant-mass distribution of three pions from a reaction like $\pi^-p \rightarrow \pi^+\pi^-\pi^0n$. Yuta and Okubo proposed that the observed effect is due to interference between the η channel for this reaction and direct 3π production background processes. The background size and its possible contributions to the asymmetry are calculated using a simple model which takes into account only tree diagrams (no closed loops) with constant vertices and ignores the effects of spin. Forty percent of the background observed in the experiment of Gormley et al. is accounted for but it is found that the largest asymmetry which can be produced through interference is 10^{-5}, as compared to the experimentally observed 1.5×10^{-2}. It is concluded that if the observed asymmetry persists, then charge-conjugation invariance is violated by the decay. These results agree with the analysis of Stein of the experimental background. He concluded that the background could account for an asymmetry of at most 2.7×10^{-3}. (auth)

3255 RECOIL PROTON POLARIZATION IN ETA PHOTOPRODUCTION. Heusch, C. A.; Prescott, C. Y.; Rochester, L. S.; Winstein, B. D. (California Inst. of Tech., Pasadena). Phys. Rev. Lett.; 25: 1381-5(9 Nov 1970).

The polarization of the recoil proton in the process $\gamma p \rightarrow p\eta^0$, at 90° in the center-of-mass system was measured at incoming photon energies from 0.8 to 1.1 GeV. Detection of all three particles in the final state $p\gamma\gamma$ permitted observation of this process with little background. Subsequent rescattering off carbon nuclei yielded sizable polarization values for the protons, indicating considerable S-P-wave interference in the production process. (auth)

3256 DETERMINATION OF THE PHOTOPRODUCTION PHASE OF ρ^0 MESONS. Alvensleben, H.; Becker, U.; Chen, M.; (and others) (Deutsches Elektronen-Synchrotron, Hamburg. Massachusetts Inst. of Tech., Cambridge). Phys. Rev. Lett.; 25: 1377-80(9 Nov 1970).

Large-angle electron–positron pairs from the reaction $\gamma + Be \rightarrow Be + e^+ + e^-$ in the e^+e^- invariant-mass region $610 < m < 850$ MeV/c^2 were measured. The phase of the photoproduction amplitude of the ρ meson at 4.1 to 6.1 GeV was found to deviate from pure imaginary by $11.8 \pm 4.4°$ which corresponds to a ratio of the real to imaginary ρ-nucleon amplitude of $\beta = 0.2 \pm 0.1$. (auth)

3257 POLARIZATION OF HIGH-ENERGY PHOTONS USING HIGHLY ORIENTED GRAPHITE. Berger, C. (Cornell Univ., Ithaca, N. Y.); McClellan, G.; Mistry, N.; (and others). Phys. Rev. Lett.; 25: 1366-70(9 Nov 1970).

The feasibility of a new method of polarizing high-energy photons, by preferential attenuation of photons polarized in one plane as a result of coherent pair production on passage through a single crystal of specific orientation is discussed. Highly oriented graphite is a particularly favorable material. The method, feasible at presently available energies, is predicted to be especially useful at higher energies. (auth)

3258 PRECISE MEASUREMENT OF THE NEUTRAL BRANCHING RATIOS OF THE η MESON. Buttram, Malcolm T.; Kreisler, Michael N.; Mischke, Richard E. (Princeton Univ., N. J.). Contract AT(30-1)-4159. Phys. Rev. Lett.; 25: 1358-61(9 Nov 1970).

The neutral branching ratios of the η meson were determined from the energy spectrum of single γ rays in the η center of mass. The sample of 7200 events after background subtraction yields $(\eta \rightarrow \gamma\gamma)/(\eta \rightarrow \text{neutrals}) = (53.5 \pm 1.8)\%$, $(\eta \rightarrow \pi^0\gamma\gamma)/(\eta \rightarrow \text{neutrals}) = (2.6 \pm 1.9)\%$, and $(\eta \rightarrow 3\pi^0)/(\eta \rightarrow \text{neutrals}) = (43.9 \pm 2.4)\%$ under the assumption that no other neutral decay modes contribute. The quoted errors include an estimate of possible systematic effects. (auth)

Weak

Refer also to abstracts 2489 and 2491.

3259 MEASUREMENT OF THE LIFETIME OF THE Λ-He^5 HYPERNUCLEUS. Bohm, G. (Institut fuer Hochenergiephysik, Berlin); Klabuhn, J.; Krecker, U.; (and others). Nucl. Phys.; B23: 93-8(1970).

The mean lifetime of the $_\Lambda He^5$ hypernucleus was estimated in nuclear emulsion using the $\pi^- + p + {}^4He$ decays both at rest and in flight. The result obtained is $\tau(_\Lambda He^5) = (2.74^{+0.68}_{-0.39}) \cdot 10^{-10}$ sec. This result together with the experimental value of Γ^-, the ratio of the non-mesonic to π^- mesonic decay rates for $_\Lambda He^5$, was used to determine the ratio $R = \Gamma(_\Lambda He^5 \rightarrow \pi^- + p + {}^4He)/\Gamma(\Lambda^0 \rightarrow \pi^- + p)$. (auth)

3260 NUCLEAR INTERACTIONS BY ACCELERATOR AND COSMIC-RAY MUONS. Wada, T. (Osaka City Univ.). Lett. Nuovo Cim.; 4: 833-7(31 Oct 1970).

A preliminary report is given on the results of the analysis of nuclear interactions induced by cosmic-ray and accelerator muons studied using a cloud chamber and nuclear emulsions respectively. The differential cross section of these interactions is written using structure functions. The structure functions are listed for the cloud-chamber and the cosmic-ray data respectively. The structure function is also plotted against the energy transfer. These three results agree approximately with the exception of a single point. (J.F.P.)

Strong (Baryon-Induced)

3261 (UCI-34-P-149-1) STUDY OF NEW HEAVY BOSONS IN PROTON–ANTIPROTON INTERACTIONS. Progress Report, October 1, 1969–September 30, 1970. Schultz, J.; Condon, P. (California Univ., Irvine. Dept. of Physics). Contract AT(04-3)-34. 26p. Dep. NTIS.

Experimental research on new heavy bosons in antiproton–proton interactions during the period from October 1, 1969 to September 30, 1970 is reported. The discussion covers resonance formation experiments, elastic processes, resonance production experiments, and other results. (J.F.P.)

3262 POLARIZATION IN ELASTIC PROTON–PROTON SCATTERING BETWEEN 0.86 AND 2.74 GeV/c. Albrow, M. G.; Andersson/Almehed, S.; Bosnjakovic, B.; (and others) (CERN, Geneva). Nucl. Phys.; B23: 445-65(1970).

Polarization and differential cross section data for elastic proton-proton scattering between 0.86 and 2.74 GeV/c are presented. A comparison is made with existing phase-shift analyses. (auth)

3263 GENERAL FEATURES OF $\bar{p}p$ ANNIHILATION INTO SIX CHARGED PIONS AT 6.94 GeV/c INCIDENT MOMENTUM. Alexander, G.; Bar-Nir, I.; Dagan, S.; (and others). (Tel-Aviv Univ., Israel). Nucl. Phys.; B23: 557-73(1970).

The reactions $\bar{p}p \rightarrow 3\pi^+3\pi^-m\pi^0$ ($m \geq 0$) were studied at an incident momentum of 6.94 GeV/c. The following cross sections were obtained: $\sigma(\bar{p}p \rightarrow 3\pi^+3\pi^-) = 0.25 \pm 0.03$ mb, $\sigma(\bar{p}p \rightarrow 3\pi^+3\pi^-\pi^0) = 1.57 \pm 0.11$ mb, and $\sigma(\bar{p}p \rightarrow 3\pi^+3\pi^-m\pi^0) = 3.65 \pm 0.24$ mb, ($m \geq 2$). The angular distributions and the transverse and longitudinal momentum distributions for the outgoing pions are presented and compared with the Lorentz-invariant phase space. The collimation, asymmetry and two-particle correlation parameters are given. The role of boson resonance production was investigated. (auth)

3264 MEASUREMENT OF THE EFFECTIVE DEUTERON–PROTON ELASTIC SCATTERING CROSS SECTION AT 180° WITH INCIDENT DEUTERONS OF 3.76 GeV/c. Banaigs, J. (Departement Saturne, Saclay, France); Berger, J.; Duflo, J.; (and others). Nucl. Phys.; B23: 596-604(1970). (In French).

The deuteron-proton differential elastic cross section was measured at exactly 180°, using 3.76 GeV/c incident deuterons. The value found is 12 ± 2.4 μb/sr. The variation of the cross section was studied for cm angles between 180 and 174.5°. A drop of the cross section was observed at 180° after a maximum near 180°. These results were compared with recent theoretical predictions. (auth)

3265 $\Delta^{++}(1236)$ $\Delta^-(1236)$ PRODUCTION IN pn COLLISIONS AT 6.98 GeV/c. Shapira, A.; Yekutieli, G.; Yaffe, D.; (and others) (Weizmann Inst. of Science, Rehovot, Israel). Nucl. Phys.; B23: 583-95(1970).

The reaction $pn \rightarrow \Delta^{++}\Delta^-$ with $\sigma = 1.1 \pm 0.2$ mb is studied at 6.98 GeV/c. Comparison with the reactions $\bar{p}p \rightarrow \bar{\Delta}\Delta$ and $pp \rightarrow \Delta\Delta$ at different incident momenta shows that their cross section behaves like $P_{lab}^{-2.5 \pm 0.3}$, consistent with one-pion exchange. The production and decay of $\Delta^{++}\Delta^-$ at small momentum transfer agrees with the OPE model with sharp cutoff at $R = 1.3$ fm. The decay correlations are also compared with some quark-model predictions. (auth)

3266 PROTON–NEUTRON ELASTIC SCATTERING ON A DEUTERIUM TARGET. Marshak, M. L. (Univ. of Michigan, Ann Arbor); Schmueser, P.; Day, J. L.; (and others). Phys. Rev., D; 2: 1808-19(1 Nov 1970).

The feasibility of measuring the ratio of proton–neutron to proton–proton elastic scattering using the second extracted proton beam of the Argonne ZGS and a liquid-deuterium target is dis-

cussed. The forward proton was detected by a 35-m-long spectrometer consisting of magnets and scintillation and Čerenkov counters. The recoil nucleon was detected by a steel-scintillator sandwich counter. The efficiency of this counter was measured using tagged neutrons in coincidence with the spectrometer and calculated using a Monte Carlo simulation of the nuclear cascade. A scintillation counter determined whether the recoil nucleon was charged or neutral. At a test point of $p_0 = 12.4$ GeV/c, $\theta^* = 37°$, and $t = -2.2$ (GeV/c)^2, a pn-to-pp cross-section ratio of 1.05 ± 0.14 was found. The pp cross section was $(d\sigma/d\Omega)_{c.m.} = 5.8 \pm 0.6$ μb/sr, and the pn cross section was $(d\sigma/d\Omega)_{c.m.} = 6.1 \pm 1$ μb/sr. The ratio of pp scattering from deuterium to pp scattering from hydrogen, corrected for geometrical effects, was 0.75 ± 0.09. The future of this technique for measuring pn cross sections is discussed and the results of the test are compared with the predictions of the Glauber multiple-scattering formalism. Available pn data is also plotted as a function of $\beta_{c.m.}{}^2 p_\perp^2$. (auth)

3267 ANTIPROTON–NEUTRON ELASTIC SCATTERING AT 3.5 GeV/c. Reynolds, B. G.; Weaver, K. E.; Bishop, J. M.; Huwe, D. O.; Malko, J. A. (Ohio Univ., Athens). Phys. Rev., D; 2: 1767-76(1 Nov 1970).

The $\bar{p}n$ differential elastic cross section for $-t \geq 0.15$ (GeV/c)^2 was measured. The data are compared with existing data from $\bar{p}p$ and np elastic scattering experiments in this energy region. The data show a dip in the cross section at $-t \simeq 0.45$ (GeV/c)^2 and a secondary maximum at $-t \simeq 0.7$ (GeV/c)^2. No evidence is seen for backward peaking in $\bar{p}n$ elastic scattering at this energy. Evidence is presented for I = 1, t-channel exchange in $\bar{N}N$ scattering. (auth)

3268 TOTAL CROSS-SECTION MEASUREMENTS. Giacomelli, G. Progress in Nuclear Physics. Volume 12, Part 2. Oxford; Pergamon Press Ltd. (1970). 151p. $6.00.

The review of total cross sections for particle interactions covers mainly elementary hadron collisions. Experimental methods, the computation of the pure isospin cross sections for the deuteron problem, analysis of experimental errors, and analysis of the total cross section data are discussed. (J.F.P.)

3269 UPPER LIMIT ON THE $\omega \to 2\pi$ DECAY RATE FROM $\bar{p}n$ ANNIHILATIONS AT REST. Bizzarri, R. (Univ Rome. Istituto Nazionale di Fisica Nucleare, Rome); Ciapetti, G.; Dore, U.; (and others). Phys. Rev. Lett.; 25: 1385-8(9 Nov 1970).

Antiproton-neutron annihilations at rest (L = 0) into G-parity states of opposite sign are incoherent. This permits a measurement of the ratio $R = (\omega \to \pi^+\pi^-)/(\omega \to \pi^+\pi^-\pi^0)$ in the absence of of ω-ρ interference. In this way the upper limit $R < 4.3\%$ at the 97.5% confidence level ($\Delta\chi^2 = 4$) is found. (auth)

Strong (Meson-Induced)

Refer also to abstract 3381.

3270 (INFN-PD–70/2) THE ANNIHILATION $\bar{p}n \to \pi^+\pi^-\pi^-$ BETWEEN 1.0 AND 1.6 GeV/c AND ITS COMPARISON WITH THE VENEZIANO MODEL. Bettini, A.; Cresti, M.; Mazzucato, M.; (and others) (Padua Univ. (Italy). Istituto di Fisica. Istituto Nazionale di Fisica Nucleare, Padua (Italy)). Sep 1970. 18p. Dep. NTIS (U.S. Sales Only).

The reaction $\bar{p}n \to \pi^-\pi^+\pi^-$ between 2.08 and 2.29 GeV c.m. energy was analyzed. The population of the 3π Dalitz plot (a total of 2328 events at all energies) is strongly nonuniform and shows a structure that can be qualitatively interpreted with simple Veneziano type formulae. The moments of the angular distributions of the three-pions plane are also examined. (auth)

3271 (UCRL–19809) RESONANCE PRODUCTIONS IN K^+p INTERACTIONS AT 4.6 GeV/c AND 9 GeV/c. Fu, Chumin (California Univ., Berkeley. Lawrence Radiation Lab.). 10 Aug 1970. Contract W-7405-eng-48. 135p. Dep. NTIS.

Thesis.

A study is made of the reaction $K^+p \to K^+\pi^-\pi^+p$ at 9 GeV/c and GeV/c. The Brookhaven National Laboratory 80-inch hydrogen bubble chamber was employed for both experiments. It is found that one-pion exchange (OPE) plays a very important role in both the $K^0_{890}\Delta^{++}_{1236}$ and the $K^0_{1420}\Delta^{++}_{1236}$ double resonance productions and the low $\Delta^{++}_{1236}\pi^-$ mass enhancement in the $K^+\pi^-\Delta^{++}_{1236}$ channel. The decay properties of the double resonance channels indicate that OPE dominates over a larger t range in the lower energy (4.6 GeV/c) data than in the higher energy (9 GeV/c) data. In the small $K^+\pi^-$ mass region [$M(K^+\pi^-) < 1.54$ GeV], the contribution from the nonpion exchange is not negligible for $|t'| \gtrsim 0.05$ (GeV/c)^2 at 9 GeV/c and $|t'| \gtrsim 0.3$ (GeV/c)^2 at 4.6 GeV/c. It becomes more important as $|t'|$ increases. Thus a Kπ scattering analysis can be performed only in a region where the $|t'|$ values lie below these limits. A mass peak at ~1.1 GeV in the $K^+\pi^-$ mass spectrum is observed in the large $|t'|$ region [$|t'| \geq 0.05$ (GeV/c)^2] in the $K^+\pi^-\Delta^{++}_{1236}$ channel at 9 GeV/c. Presumably it is produced mainly via non-pion exchange. The low $\Delta^{++}_{1236}\pi^-$ mass enhancement can be described by a double peripheral model. The dominant mechanism is a Pomeron and a pion (P, π) double Regge-pole exchange. The model gives good agreement with the data provided that both $-t_{K^+\to K^+}$ and $-t_{p\to\Delta^{++}}$ are less than 0.5 (GeV/c)^2 and $M(K^+\pi^-) \geq 1.54$ GeV. Problems involved with the extrapolation into the small $K^+\pi^-$ mass region are discussed. The importance of the contribution from the extrapolation and its implication to the Kπ scattering analysis are also investigated. (auth)

3272 (UCRL–20050) REACTION $\pi^+p \to \Delta^{++}A_2^0$ AT 3.7 GeV/c. Barnham, K. W. J.; Abrams, G. S.; Butler, W. R.; Coyne, D. G.; Goldhaber, G.; Hall, B. H.; MacNaughton, J.; Trilling, G. H. (California Univ., Berkeley. Lawrence Radiation Lab.). Jul 1970. Contract W-7405-eng-48. 10p. (CONF-700806–43; CONF-700627–1). Dep. NTIS.

From 15th International Conference on High Energy Physics, Kiev, USSR.

From 4th International Conference on Resonant Particles, Athens, Ohio.

Preliminary results are presented for associated production of A_2^0 and Δ^{++} in the reaction $\pi^+ + p \to p + 2\pi^+ + \pi^- + \pi^0$ at 3.7 GeV/c. A fairly narrow A_2^0 signal is observed, and some evidence is seen for a dip in the differential cross section for production of this state at $t \sim 0.6$ GeV^2 or $t' = 0.15$ to 0.35 GeV^2. (J.F.P.)

3273 DOUBLE-REGGE POLE ANALYSIS OF $\pi^+p \to \pi^+\pi^-\Delta^{++}$ AT 13.1 GeV/c. Gaidos, J. A.; Ezell, C. R.; Lamsa, J. W.; Willmann, R. B. (Purdue Univ., Lafayette, Ind.). Nucl. Phys.; B23: 84-92(1970).

A double-Regge model is applied to the reaction $\pi^+p \to \pi^+\pi^-\Delta^{++}$ at 13.1 GeV/c. A good description of the data is given in terms of two amplitudes involving Pomeranchuk/π and Pomeranchuk/Δ exchanges. (auth)

3274 PRODUCTION OF THE $\bar{K}^{*0}$ (890) Δ^- (1236) FINAL STATE IN K^-d INTERACTIONS AT 5.5 GeV/c. Werner, B. (Northwestern Univ., Evanston, Ill.); Davis, R.; Ammar, R.; (and others). Nucl. Phys.; B23: 37-44(1970).

A cross section of 286 ± 45 μb was measured for the reaction $K^-n \to \bar{K}^{*0}(890)\Delta^-(1236)$ at a beam momentum of 5.5 GeV/c. The data show a forward diffraction peak with a slope of 5.7 ± 0.7 (GeV/c)$^{-2}$ and the decay correlations indicate that although pion exchange contributes to the production mechanism, it is apparently less dominant than in the related reaction $K^+p \to K^{*0}(890)\Delta^{++}(1236)$. Significant differences are observed between these two reactions in both the cross section and the decay correlations. These differences cannot be explained in terms of a one-pion exchange model with absorption. (auth)

3275 ANALYSIS OF $p\pi^+\pi^-$ ENHANCEMENT PRODUCED IN THE REACTION $\pi^+p \to \pi^+p\pi^+\pi^-$ AT 5 GeV/c. Cirba, E. (Ecole Polytechnique, Paris); Vanderhaghen, R.; Drevermann, H.; (and others). Nucl. Phys.; B23: 533-40(1970).

The $p\pi^+\pi^-$ effective mass spectrum is studied in the mass range from 1.2 to 2.3 GeV in the reaction $\pi^+p \to \pi^+p\pi^+\pi^-$ at 5 GeV/c. A resonant-type enhancement is observed at 1.71 ± 0.01 GeV whose position is consistent with that of the S_{11} pion-nucleon resonance rather than the D_{15} or F_{15} states, but whose width 66 ± 26 MeV is considerably narrower than that of the S_{11}. No evidence for an intermediate two-body decay is found. From the small value of the four-momentum transfer distribution slope 3.2 ± 0.4 GeV^{-2} a diffractive mechanism can be excluded. The $p\pi^+\pi^-$ spectrum also shows a rapid increase near threshold, which, after elimination of peripheral $\Delta\rho$ events appears as a broad diffractive-like enhancement (average slope 11.0 ± 1.0 GeV^{-2}); the shape of this threshold effect has been obtained from a study of the variation of the four-momentum transfer distribution along the mass spectrum. (auth)

3276 SPIN-PARITY ANALYSIS OF THE 3π SYSTEM IN THE REACTION $\pi^-p \to p\pi^-\pi^+\pi^-$ AT 3.9 GeV/c. Abramovich, M.; Blumenfeld, H.; Bruyant, F.; (and others) (CERN, Geneva). Nucl. Phys.; B23: 466-80(1970).

A spin-parity (J^P) analysis of the 3π system is presented for a sample of events of the type $\pi^-p \to p\pi^-\pi^+\pi^-$. Using the maximum-likelihood fitting procedure, the behavior of different J^P states for the intermediate $\rho\pi$ system was investigated as a function of the 3π effective mass. The analysis gives a clear indication for a $J^P = 2^+\rho\pi$ resonance at the mass of the A_2. (auth)

3277 ASSOCIATED PRODUCTION IN K^+p INTERACTIONS AT 3.5 GeV/c. Bishop, J. M.; Goshaw, A. T.; Erwin, A. R.; Walker, W. D.; Weinberg, A. (Univ. of Wisconsin, Madison). Contract AT(11-1)-881. Nucl. Phys.; B23: 547-56(1970).

XUM

In a recently completed experiment using 3.54 GeV/c K^+ mesons in the BNL 80-inch chamber, the two-prong plus one or two V^0 topology was investigated for events with associated production. No evidence was found for any production of any hypercharge 2 states. (auth)

3278 DETERMINATION OF THE I = 3/2 Kπ ELASTIC-SCATTERING CROSS SECTION FROM THE REACTION $K^-n \rightarrow pK^-\pi^-$ AT 3 GeV/c. Bakker, A. M. (Zeeman-Laboratorium, Amsterdam); Hoogland, W.; Kluyver, J. C.; (and others). Nucl. Phys.; B24: 211-20(1970).

The low energy I = 3/2 Kπ elastic-scattering cross section was obtained from an analysis of the reaction $K^-n \rightarrow pK^-\pi^-$ using the Chew–Low extrapolation method. For cm energies of the Kπ system between threshold and 1.2 GeV the cross section amounts on the average to ≈2 mb. (auth)

3279 PRODUCTION OF STRANGE PARTICLES IN π^+p INTERACTIONS AT 5.5 GeV/c. Cooper, W. A.; Manner, W.; Musgrave, B.; Pollard, D.; Voyvodic, L. (Argonne National Lab., Ill.). Nucl. Phys.; B23: 605-29(1970).

Results are presented on some final states involving strange particles produced in 5.5 GeV/c π^+p collisions. Production of Δ(1238), $Y_1^*(1385)$ and K*(890) resonances is pronounced in both quasi two-body and three-body reactions. Total and partial cross sections are given for several channels. The reactions $\pi^+p \rightarrow Y_1^*(1385)K^+$ and $\pi^+p \rightarrow Y_1^*(1385)K^*(890)$ are compared with the predictions of an absorptive peripheral model. (auth)

3280 MEASUREMENTS OF π^-p ELASTIC SCATTERING FROM 1.71 TO 5.53 GeV/c. Fellinger, M. (Iowa State Univ., Ames); Gutman, E.; Lamb, R. C.; (and others). Phys. Rev., D; 2: 1777-82(1 Nov 1970).

The π^-p elastic scattering differential cross section was obtained at 18 incident momenta from 1.71 to 5.53 GeV/c. The measurements were taken over a limited range of squared four-momentum transfer t near the forward direction. The statistical accuracy and resolution of these data are comparable to, or better than, existing data. The parameter b in the expression $d\sigma/dt = Ae^{bt}$ was determined at each of our incident momenta, and a large (~25%) enhancement in b as a function of momentum is observed at a c.m. energy of ~2290 MeV. The relation of this bump in b with the well-established bump in the total π^-p cross section at ~2200 MeV is discussed. (auth)

3281 INTERPRETATION OF SMALL-ANGLE π^-p ELASTIC SCATTERING FROM 1.71 TO 3.01 GeV/c. Hull, J. R.; Leacock, R. A. (Iowa State Univ., Ames). Phys. Rev., D; 2: 1783-9(1 Nov 1970).

Elastic scattering at small angles in the reaction $\pi^-p \rightarrow \pi^-p$ was investigated for Regge recurrences in the region 1.17 to 3.01 GeV/c. From examination of differential-cross-section data at low t values additional evidence is found for the existence of both the established $N_\gamma(2210)$ and the predicted $N_\alpha(2220)$. The resonance parameters obtained for the $N_\alpha(2220)$ are mass 2245 MeV, width 330 MeV, elasticity 0.15. (auth)

3282 π^-p REACTIONS AT 456, 505, AND 552 MeV/c. Sason, D. H. (Oxford Univ.); Mulvey, J. H.; Chinowsky, W. Phys. Rev., D; 2: 1790-1803(1 Nov 1970).

The results of an experiment to study the reactions $\pi^-p \rightarrow \pi\pi N$ at incident momenta of 456, 505, and 552 MeV/c in a hydrogen bubble chamber are presented. The most prominent features of the data in the $\pi^+\pi^-n$ final state are a high-mass peak in the $M^2(\pi^+\pi^-)$ spectrum (which moves upward in mass and becomes less significant as the incident momentum increases), and Δ^- production. It is shown that the $\pi^+\pi^-$ enhancement can be explained by the introduction of an I = J = 0 ππ interaction, and two forms for this interaction are investigated. Within the framework of an isobar model, values of the πN partial-wave inelasticities are derived and these are compared with the predictions of πN elastic phase-shift analyses. It is shown that the branching ratio $\pi N : \pi\Delta : \sigma N$ of the P_{11} partial wave depends strongly on the assumed form of ππ final-state interaction. (auth)

3283 STUDY OF THE REACTION $\pi^+p \rightarrow \Sigma^+K^+$ BETWEEN 1850- AND 2090-MeV c.m. ENERGY. Kalmus, G. E.; Borreani, G.; Louie, J. (Univ. of California, Berkeley). Phys. Rev., D; 2: 1824-37(1 Nov 1970).

Angular distributions and polarization measurements (obtained from bubble-chamber data) are presented at seven incident π^+ momenta in the reaction $\pi^+p \rightarrow \Sigma^+K^+$. Results of a partial-wave analysis as well as an s-, t-, and u-channel analysis are presented. The branching fraction of the Δ(1950) → Σ^+K^+ was found to be (2.0 ± 0.4)%. (auth)

3284 ENERGY ESTIMATION FROM THE ANGULAR DISTRIBUTION OF 20-GeV/c PION INTERACTIONS IN PHOTOGRAPHIC EMULSION. Goza, E. R. (Louisiana State Univ., Baton Rouge); Krzywdzinski, S.; Kim, C. O.; Park, J. N. Phys. Rev., D; 2: 1838-45(1 Nov 1970).

Interactions of 20-GeV/c negative pions in photographic emulsion were analyzed in order to compare and test the methods of energy estimation commonly used in high-energy cosmic-ray investigations. The energy of each pion interaction was determined from the angular distribution of the secondary particles using the median-angle, Castagnoli, E_{ch}, and $E(\theta)$ methods. The interactions were divided into various groups according to the number N_h of evaporation prongs and the number n_s of secondary particles. The median-angle, Castagnoli, and $E(\theta)$ methods all overestimate the energy of the group with $N_h \leq 5$ ($n_s \geq 4$) by factors of 1.5, 1.2, and 1.1, respectively. These same methods underestimate the energy of the group with $N_h > 5$ ($n_s \geq 4$) by factors of 1.3, 2.0, and 2.3, respectively. The E_{ch} method underestimates the energies of the groups with $N_h \leq 5$ ($n_s \geq 4$) and $N_h > 5$ ($n_s \geq 4$) by factors of 1.3 and 1.5, respectively. These underestimates by the E_{ch} method become 0.9 and 1.0 if the general practice of including the effect of neutral secondaries to the E_{ch} method is adopted. For all the various groupings of N_h and n_s considered, the E_{ch} method yields the most consistent and uniform results with the smallest standard deviations than any of the other three methods. (auth)

3285 EXPERIMENTAL COMPARISON BETWEEN ON- AND OFF-MASS-SHELL INELASTICITIES IN π^-p SCATTERING. II. Colton, Eugene (Univ. of California, Berkeley); Schlein, Peter E.; Ma, Z. Ming; Smith, Gerald A. (Phys. Rev., D; 2: 2108-9(1 Nov 1970).

It is shown that the experimental cross-section ratio of the reactions pp → Δ^{++} (neutrals) and pp → Δ^{++} (π^-p) (at 6.6 GeV/c) for low momentum transfer to the Δ^{++} ($|t| < 0.2$ GeV^2) is approximately the same as the cross-section ratio $\sigma(\pi^-p \rightarrow \text{neutrals})/\sigma(\pi^-p \rightarrow \pi^-p)$ for π^-p effective mass less than 1.56 GeV. The disagreement observed between the ratios for masses greater than 1.56 GeV can be explained by increased values of t_{min} and non-Δ^{++} background in the pp reactions. These results imply that pion exchange dominates pp → Δ^{++} (neutrals) for low momentum transfer to the Δ^{++}. (auth)

3286 COMMENT ON EVIDENCE FOR THE H MESON. Chaudhary, Banvir; Marquit, Erwin (Univ. of Minnesota, Minneapolis). Contract AT(11-1)-1764. Phys. Rev., D; 2: 2110-11 (1 Nov 1970).

It is shown that the contamination due to η′ decaying into $\rho^0\gamma$ cannot explain the H enhancement in the 3π system reported earlier in the reaction $\pi^+d \rightarrow pp\pi^+\pi^-\pi^0$ for an incident pion momentum of 3.65 GeV/c. A more likely explanation is provided by the suggestion that the enhancement is primarily due to the distortion of the phase space by a ρ-band cut. (auth)

3287 BRANCHING RATIOS OF THE K(1420) MESON. Aguilar-Benitez, M. (Brookhaven National Lab., Upton, N. Y.); Bassano, D.; Eisner, R. L.; (and others). Phys. Rev. Lett.; 25: 1362-6(9 Nov 1970).

A new measurement of the decay rates of the K(1420) produced in K^-p interactions is presented. In addition to improved statistics, the K(1420) is observed in final states where the absence of the Q enhancement allows an unambiguous determination of the branching ratios. The values obtained agree with SU(3) predictions. (auth)

3288 OBSERVATION OF COHERENT INTERFERENCE PATTERN BETWEEN ρ AND ω DECAYS. Alvensleben, H.; Becker, U.; Bertram, William K.; (and others) (Deutsches Elektronen-Synchrotron, Hamburg. Massachusetts Inst. of Tech., Cambridge). Phys. Rev. Lett.; 25: 1373-7(9 Nov 1970).

A high-statistics experiment measuring the structure of e^+e^- mass spectrum from photoproduction of ρ and ω mesons is reported. At 5.1 GeV, based on 4000 events, analysis of the spectra yields a ratio of vector-meson–photon coupling constants $\gamma_\omega^2/\gamma_\rho^2 = 9.4^{+2.1}_{-1.8}$ and a $\rho-\omega$ phase difference $\varphi_{\omega\rho} = 41° \pm 20°$. (auth)

3289 DIFFERENCE IN ENERGY DEPENDENCE FOR A_2^- AND A_2^0 PRODUCTION. Carroll, J. T. (Univ. of Wisconsin, Madison); Firebaugh, M. W.; Garfinkel, A.; (and others). Contract AT(11-1)-881. Phys. Rev. Lett.; 25: 1393-5(9 Nov 1970).

A comparison of A_2^- and A_2^0 production is presented. The cross section for the production of A_2^0 falls much more rapidly with increasing energy than the A_2^- cross section. The characteristics of the production processes seem to be very similar in other respects. These facts are hard to understand in terms of a Regge picture of the production process. (auth)

3290 EVIDENCE FOR A STRUCTURE IN THE NEUTRAL A_2 MASS REGION. Basile, M.; Dalpiaz, P.; Frabetti, P. L.; (and others) (CERN, Geneva. Istituto Nazionale di Fisica

Nucleare, Bologna. Univ., Bologna. CNRS, Strasbourg). Lett. Nuovo Cim.; 4: 838-47(31 Oct 1970).

The regularity of the neutral A_2 mass spectrum was investigated in the reaction $\pi^- + p \rightarrow A_2^0 + n$ at 3.16 GeV. A missing-mass spectrometer coupled with a system of large electromagnetic shower detectors was used. Strong evidence was found for the existence of structure in the A_2^0 mass spectrum. (J.F.P.)

Particle Interactions and Properties (Theoretical)

3291 HEURISTIC DERIVATION OF THE PERIHELIC PRECESSION. Arjun, Tan Tung (Visva Bharati Univ., Santiniketan, India). Chin. J. Phys. (Taiwan); 8: 24-5(Apr 1970).

The perihelic precession of mercury constitutes an exclusive test of general relativity. However, this effect can be obtained without recourse to general relativity using special relativity, that is, the equivalence principle and Newtonian results. Another method, a heuristic one, of derivation which is different from that of previous work is proposed. (auth)

General

3292 (ITF-70-32) ON THE ADDITIONAL INVARIANCE OF THE RELATIVISTIC EQUATIONS OF MOTION. Fushchich, V. I. (Akademiya Nauk Ukrainskoi SSR, Kiev. Institut Teoreticheskoi Fiziki). 1970. 17p. Dep. NTIS (U. S. Sales Only).

An additional (implicit) symmetry of equations of motion is studied which is invariant with respect to the Poincare group. It is shown that any relativistic equation of motion is invariant with respect to the Lie algebra of the inhomogeneous de Sitter group. The relativistic two-component equation describing a free motion of the spinless particle with zero mass is found. (auth)

3293 (JINR-P2-5343) QUASIELASTIC SCATTERING OF PARTICLES ON DEUTERONS. Tarasov, A. V.; Tseren, Ch. (Joint Inst. for Nuclear Research, Dubna (USSR). Lab. of Nuclear Problems). 1970. 13p. (In Russian). Dep. NTIS (U. S. Sales Only).

In the energy region, where the Glauber approximation cannot be applied, a number of simple expressions was obtained for the cross section of a particle scattered by a deuteron at a certain angle. These expressions include the effects of the double interaction of the particle with the deuteron nucleons. (auth)

3294 (NYO-4204-5) BJORKEN LIMIT AND THE JIN-MARTIN LOWER BOUND. Bitar, Khalil M. (European Organization for Nuclear Research, Geneva (Switzerland). (American Univ., Beirut (Lebanon). Dept. of Physics); Khuri, N. N. (Rockefeller Univ., New York). [1970]. Contract AT(30-1)-4204. 61p. Dep. NTIS.

The restrictions that analyticity, unitarity (positivity), and current conservation place on the asymptotic behavior in q_0 at fixed $\vec{q}$ of the connected, covariant amplitude $\widetilde{M}^c_{\mu\nu}(q,\vec{q})$ are investigated; where $\widetilde{M}^c_{\mu\nu}$ is the connected part of the forward amplitude for the scattering of a charged conserved current on a proton target. The main tool is a theorem of Jin and Martin which was used to give lower bounds for forward amplitudes. The main result is to establish a rigorous lower bound on the contribution of the class-I intermediate states to M^c_{00}. The bound gives $|M^I_{00} + p_0/mq_0|>C|q_0|^{-2}$, $C > 0$, for large complex q_0. This is larger by a factor (q_0^{+4}) than the asymptotic behavior of M^c_{00} needed in order to have the Bjorken limit definition of the space-space equal time commutator agree with the naive quark commutator. This bound has the following consequences: The existence of operator Schwinger terms is shown to be equivalent to the existence of a frame of reference for which the contribution of class-II intermediate states does not exactly cancel the $O(q_0^{-2})$ contribution of the class I states. The existence of the Bjorken limit definition of the space-space commutator depends on yet another cancellation between the $O(q_0^{-3})$ contributions to $\widetilde{M}^c_{00}$ of the class-I and -II states, and the cancellation also of all terms between $O(q_0^{-2})$ and $O(q_0^{-3})$. The sum rule whose validity is needed to guarantee this cancellation is known to diverge in perturbation theory. It is also shown to be divergent when the $P \rightarrow \infty$ limit is allowed. The convergence of the Cottingham formula can only be guaranteed if in all frames of reference all the contributions between $O(q_0^{-2})$ and $O(q_0^{-4})$ of the class-I states are exactly cancelled by the class-II contributions and if in addition the remaining contribution at $O(q_0^{-4})$ of the class-I states is also exactly cancelled out. The separation of the absorptive part of the amplitude into class-I and -II contributions is carried out explicitly through a fully reduced LSZ formula. The class-I states are the usual s-channel states and the so-called Z-graph states. The class-II states are those that couple directly to the current, contribute only for timelike q, and are physically quite distinct from the class-I states. (auth)

3295 (TPJU-12/70) PHYSICAL BOUNDS FOR THE COMPONENTS OF STATISTICAL TENSORS. Kotanski, A.; Sredniawa, B.; Zalewski, K. (Jagellonian Univ., Krakow (Poland). Dept. of Theoretical Physics). May 1970. 13p. Dep. NTIS (U. S. Sales Only).

Numerical values of the physical bounds for the components of single and double statistical tensors for spins ≤ 2 are calculated. The symmetry properties of these bounds are derived. Correlations between the values of different tensor components are not considered. (auth)

3296 PHYSICAL BOUNDS FOR THE COMPONENTS OF STATISTICAL TENSORS. Kotanski, A. (Jagellonian Univ., Krakow); Sredniawa, B.; Zalewski, K. Nucl. Phys.; B23: 541-6 (1970).

Numerical values of the physical bounds for the components of single and double statistical tensors for spins ≤ 2 are calculated. The symmetry properties of these bounds are derived. Correlations between the values of different tensor components are not considered. (auth)

3297 GEOMETRIC REPRESENTATION OF THE UNCERTAINTY RELATION. Arjun, Tan Tung (Visva-Bharati Univ., Santiniketan, India). Chin. J. Phys. (Taiwan); 8: 26-7(Apr 1970).

A geometric representation of the uncertainty relation $\Delta p \cdot \Delta q \geq h$ was given by Freeman. However, some more interpretations of the same are given for a transition of particles which have their antiparticles. (auth)

3298 COMMUTATORS AND LORENTZ COVARIANCE. Jacob, Gerhard (International Centre for Theoretical Physics, Trieste, Italy); Stech, Berthold. Z. Phys.; 239: 379-86 (1970).

The Lorentz transformation property of the right hand side of equal time commutators give conditions on Schwinger terms of commutators involving time derivatives. In particular, it is seen that current algebra relations imply special locality properties for the current divergence. Thus, an important element of the hypothesis of partially conserved currents is already contained in the current commutation rules. (auth)

3299 LOCAL CURRENT COMMUTATORS. Stech, Berthold (Univ., Heidelberg. Kernforschungszentrum, Karlsruhe, Ger.). Z. Phys.; 239: 387-94(1970).

The predictive power of current algebra relations is discussed using models for the spectral functions of current commutator matrix elements. The functions constructed fulfill the requirements of covariance, locality and spectrum conditions. Thus, the current algebra constraints can easily be imposed. In these models the form factors are described by superpositions of poles. For simplicity only spin-zero states are taken into account. (auth)

3300 ESTIMATES OF THE UNITARITY INTEGRAL. Krupsch, J. (CERN, Geneva). Commun. Math. Phys.; 19: 65-82(1970).

The elastic unitarity integral is studied for amplitudes which satisfy a Mandelstam representation without subtraction. The double spectral functions are taken to belong to function spaces which allow local, even nonintegrable, singularities. The existence of fixed point solutions is derived and the additional restrictions due to inelastic unitarity are discussed. (auth)

3301 IMPLICATIONS OF FULL CAUSALITY FOR NEUTRINO AND OTHER PARTICLE PRODUCTION RATES. Csonka, Paul L. (Univ. of Oregon, Eugene). Phys. Rev., D; 2: 1923-5(1 Nov 1970).

If the correct physical theory satisfies full causality, then, in our neighborhood of the universe, the total production rate for certain particles (e.g., neutrinos) may be different from what one would normally expect. (auth)

3302 WEAKLY COUPLED NEUTRAL CURRENTS. Albright, C. H. (Northern Illinois Univ., DeKalb. Ames Lab., Iowa); Oakes, R. J. Phys. Rev., D; 2: 1883-1901(1 Nov 1970).

A general analysis of interactions of the current-current form involving neutral vector and axial-vector hadron and lepton currents is given and compared with present experimental information. While the restrictions placed upon such neutral current interactions by existing data are found to be rather severe, a number of theoretically attractive possibilities remain. Still consistent with experiment are models obeying the $\Delta I < 3/2$, $\Delta Y < 2$ rule, a

universal model based on the SU(2) algebra of charges, a model with a strangeness-conserving isovector neutral hadron current and symmetrically coupled lepton currents, and models in which the neutral currents couple only in a superweak fashion. In contrast, a model which incorporates the octet rule as a built-in symmetry appears to be ruled out on the basis of present information. (auth)

3303 COVARIANT PHASE-SPACE CALCULATIONS OF n-BODY DECAY AND PRODUCTION PROCESSES. II. Kumar, Rajendra (Univ. of Delhi). Phys. Rev., D; 2: 1902-14(1 Nov 1970).

Lorentz-invariant phase-space integrals in the multicluster form are transformed into definite integrals over a set of "symmetric" Mandelstam variables. The momentum configuration of the particle clusters (in the center-of-mass system and in the lab system) as well as of the individual particles (in the cm. system, in the lab system, and in the rest frame of the decaying cluster) is explicitly given in terms of a complete set of kinematical variables, i.e., $3N-10$ independent Mandelstam variables and signs of $N-4$ quadrilinear invariants. This enables all possible scalar products formed from the 4-momenta of particles to be expressed in terms of the independent variables. Expressions for the angular correlation between two of the final-state particles or clusters and the simultaneous distribution in energies of two of the final-state particles are given explicitly, and distributions in invariant momentum transfers are discussed. (auth)

3304 GREEN'S PARAPARTICLES AND THE UNIFIED THEORY OF IDENTICAL PARTICLES. Carpenter, K. M. (Cambridge Univ., Eng.). Ann. Phys. (N. Y.); 60: 1-26(Sep 1970).

Green's paraparticles are discussed within a previous unified theory of identical particles. A general theorem concerning scattering of identical particles is proved and discussed. A previous result that the existence of a many-particle state with any permutation symmetry implies the existence of states of fewer particles with all permutation symmetries contained in the former is deduced very easily within the unified theory. (auth)

3305 ISOSCALAR FACTORS OF CLEBSCH-GORDAN COEFFICIENTS OF UNITARY GROUPS. Jucys, A. A. (Inst. of Physics and Mathematics, Vilnyus, USSR). Liet. Fiz. Rinkinys, Liet. TSR Mokslu Akad., Liet. TSR Aukst. Mokyklos; 10: No. 1, 5-12 (1970). (In Russian).

The expression for the isoscalar factors of the Clebsch–Gordan coefficients of the group U_k in the reduction of the Kronecker product of two irreducible representations, one being arbitrary the other symmetrical, was obtained. The analogy between this expression and the expression for the transformation matrix elements obtained in preceeding work is noted. The symmetry property in a particular case giving the Regge symmetry of SU_2 group Wigner coefficients is indicated. (auth)

3306 UNIVERSAL LIGHT CONE COMMUTATOR. Brandt, R. A. (New York Univ., N. Y. CERN, Geneva). Phys. Lett.; 33B: 312-16(26 Oct 1970).

An operator generalization of a previously considered universal light cone current commutator is proposed. It involves the vector $J_\mu^a(x)$ and scalar $S^a(x)$ elements of the U(12) algebra as well as the vector P_μ and scalar M^2 elements of the Poincaré enveloping algebra. The requirements imposed by the proposal on the light cone behavior of the current commutator are deduced and discussed. (auth)

3307 POLARIZED POSITIVELY CHARGED HYDROGEN ION BEAMS FROM CHARGE EXCHANGE COLLISIONS BETWEEN METASTABLE H(2S) ATOMS AND HALOGENS. Brueckmann, H.; Finken, D.; Friedrich, L. (Kernforschungszentrum, Karlsruhe, Ger. Univ., Karlsruhe, Ger.). Nucl. Instrum. Methods; 87: 155-6(1970).

Charge exchange collisions with halogens can be favorably used to produce polarized positively charged hydrogen ion beams in a Lamb shift type ion source. Tensor polarizations up to $P_{33} = -0.75$ were achieved. Iodine exhibits a yield of two times the yield known for the production of polarized negatively charged hydrogen ions from argon. (auth)

Electromagnetic

Refer also to abstract 3254.

3308 (DESY–70/45) ON INELASTIC DIFFRACTIVE RHO-PHOTOPRODUCTION AND COMPTON SCATTERING. Wolf, Guenter (Deutsches Elektronen-Synchrotron, Hamburg (West Germany)). Sep 1970. 16p. Dep. NTIS (U. S. Sales Only).

Inelastic diffractive ρ^0 photoproduction via diffractive rho-isobar production and via double peripheral scattering was studied. The integrated cross section is found to rise slowly with energy reaching ~3 μb at 20 GeV and ~4 μb at 100 GeV. The differential cross section $d\sigma/dt$ equals, in $\mu b/GeV^2$, ~7 exp(4t) at 5 GeV and ~15 exp (5.5t) at 10 GeV. The rho mass is predicted to be shifted in the same way as in $\gamma p \to \rho^0 p$. In addition a shift of the isobar mass should be observed. The same procedure was used to estimate the differential cross section for inelastic diffractive Compton scattering on protons; $d\sigma/dt$ comes out to be approximately energy independent for $E_\gamma > 5$ GeV and of the order of 0.2 exp(6t) ($\mu b/GeV^2$). (auth)

3309 (DESY–70/46) MEASUREMENT OF PROTON COMPTON SCATTERING AT 6 GeV AND SMALL MOMENTUM TRANSFERS. Buschhorn, G.; Criegee, L.; Dubal, L.; (and others) (Deutsches Elektronen-Synchrotron, Hamburg (West Germany)). Sep 1970. 12p. Dep. NTIS (U. S. Sales Only).

Compton scattering on protons was measured at a mean photon energy of 6 GeV and four-momentum transfers $-t$ between 0.06 and 0.60 $(GeV/c)^2$. The differential cross section shows a diffraction-like behavior. The cross section extrapolated to $t = 0$ is in fair agreement with the optical point. Discrepancies with the vector meson dominance model are pointed out. (auth)

3310 (DESY–70/50) SIMPLE INTERPRETATION OF INELASTIC ELECTRON-NUCLEON SCATTERING. Weisskopf, Victor F. (Deutsches Elektronen-Synchrotron, Hamburg (West Germany)). Oct 1970. 8p. Dep. NTIS (U. S. Sales Only).

The main features of the deep inelastic scattering of electrons by neutrons and protons can be explained by a simple model of the nucleon consisting of partons. It turns out that the best results are obtained if the nucleon is assumed to be a linear combination of states with three quarks and a varying number of quark-antiquark pairs with the usual fractional charges. (auth)

3311 (NYO–4204–4) DEEP INELASTIC e-p STRUCTURE FUNCTIONS IN A LADDER MODEL WITH SPIN ½ NUCLEONS. Blaha, Stephen (Rockefeller Univ., New York). [1969]. Contract AT(30-1)-4204. 46p. Dep. NTIS.

The asymptotic behavior of the inelastic electron-proton structure functions, W_1 and W_2, is found in the limit $|q^2| \to \infty$ with $\omega = 2\,q \cdot p/|q^2|$ fixed (q is the electron 4-momentum transfer and p the target nucleon 4-momentum) using a ladder model for the virtual Compton amplitude. Neutral vector mesons are exchanged between the (spin ½) proton legs. In addition, this model (with slight modifications) gives the asymptotic behavior for a ladder model in which pseudoscalar mesons are exchanged, and the asymptotic behavior for a truss bridge graph model in a mixed $\phi^3 - \phi^4$ field theory. In all of these models both W_1 and νW_2 do not scale by factors of $\ln |q^2|$ (with the exception of νW_2 in the truss bridge model). In addition, it is found that the structure functions are essentially Bessel functions with the argument $\ln |q^2| \ln \omega$ in the $|q^2| \to \infty$ limit for fixed $\omega \gg 1$. (auth)

3312 (NYO–4204–6) REGGE ANALYSIS OF ELECTROPRODUCTION AND PHOTOPRODUCTION. Pagels, Heinz (Rockefeller Univ., New York). [1970]. Contract AT(30-1)-4204. 11p. Dep. NTIS.

By combining the Froissart–Gribov definition of the partial wave amplitude with the DGS representation the analytic properties of the Regge residue functions $\beta(q^2,\alpha_1)$ in q^2 = virtual photon mass are established. The analysis suggests a simple extrapolation from the photoproduction data on nucleons at high energy to electroproduction in the deep inelastic region. For the structure functions we find $F_2^p(\rho) = 0.275 + 0.13\rho^{-\frac{1}{2}}$ and $F_2^p(\rho) - F_2^n(\rho) = 0.15\rho^{-\frac{1}{2}}$ as $\rho \to \infty$ consistent with recently reported data. (auth)

3313 AN ANALYSIS OF SINGLE PION PHOTOPRODUCTION IN THE SECOND RESONANCE REGION. Moorhouse, R. G.; Rankin, W. A. (Univ. of Glasgow). Nucl. Phys.; B23: 181-217(1970).

Single pion photoproduction data off protons in the second resonance region was analyzed, using an isobar model, in an attempt to determine how well the electromagnetic couplings of the $S_{11}(1520)$, $D_{13}(1520)$ and $P_{11}(1470)$ resonances are determined by the existing data. It is found that both D_{13} couplings can be classed as well determined and the S_{11} coupling as fairly well determined. Within significant limits the photonic coupling of the Roper or $P_{11}(1470)$ resonance is undetermined by the existing data and possible experiments to resolve the ambiguities are discussed. (auth)

3314 PRODUCTION CROSS SECTION OF $\gamma\gamma \to e^+e^-\mu^+\mu^-$. Masujima, Michio (Massachusetts Inst. of Tech., Cambridge). Nucl. Phys.; B24: 182-6(1970).

Production cross section for the process $\gamma\gamma \to e^+e^-\mu^+\mu^-$ is calculated in the impact factor representation. Up to the eighth order in e, the cross section approaches the constant 2.82×10^{-3} μb at infinite energy. (auth)

XUM

3315 PHOTOPRODUCTION AT HIGH ENERGIES. Maor, Uri (Univ. of California, Berkeley). Nucl. Phys.; B24: 1-15 (1970).

A review of photoproduction is presented, covering only new preprints from the SLAC List in Particle and Fields, which were circulated during the period January 1 to April 30, 1970. Some new experimental results and theoretical analyses of vector meson photoproduction are first given. Photoproduction of pseudoscalars and recent contributions on the vector dominance model are summarized. (L.B.S.)

3316 ELECTROMAGNETIC MESON DECAYS. TWO MODELS IN AN EFFECTIVE LAGRANGIAN APPROACH. Honerkamp, J. (Univ., Bonn). Nucl. Phys.; B24: 140-56 (1970).

Electromagnetic meson decays are discussed in an effective-Lagrangian approach. The relevant couplings are introduced by a breaking Lagrangian which transforms as a member of the $(3,3^*) + (3^*,3)$ representation of SU(3) × SU(3). Two models are discussed which lead to different sum-rules for the decay width. The non-linear model allows only values for $\Gamma(X \to 2\gamma)$ greater than 506 keV, once $\Gamma(\eta \to 2\gamma)$ and $\Gamma(\pi^0 \to 2\gamma)$ are given. The linear model leads to very small values for $\Gamma(X \to 2\gamma)$ but is preferred by the experimental facts. (auth)

3317 AN INVESTIGATION OF SOME APPROXIMATIONS INVOLVED IN THE THEORY OF THE INTERACTIONS OF PARTICLES AND NUCLEI AT HIGH ENERGIES. Newmeyer, Jeff; Trefil, J. S. (Univ. of Illinois, Urbana). Nucl. Phys.; B23: 315-32(1970).

The optical limit of the Glauber multiple-scattering theory is investigated by comparing this limit with results of explicit calculations in the theory, and it is shown that to very small A, the optical-limit results are virtually indistinguishable from the exact ones. The sensitivity of the theory to different choices of nuclear densities is also investigated, and it is found that for small-angle coherent scattering, the theory is relatively insensitive to this choice, but that for incoherent scattering the dependence is somewhat greater. The sensitivity of the value of the rho-nucleon total cross section to different choices of wave functions and different approximations is also investigated in the theory and it is shown that the changes in $\sigma_{\rho N}$ introduced by such considerations are ≈15%, and hence too small to explain the discrepancies in the $\sigma_{\rho N}$ reported by different experimental groups. (auth)

3318 CONSPIRACY, DUALITY, AND $\pi^{\pm}$, DELTA PHOTOPRODUCTION. Minami, S. (Osaka City Univ.). Lett. Nuovo Cim.; 4: 877-82(7 Nov 1970).

The properties of meson trajectories are studied considering conspiracy and duality. A possible model is suggested in which the characteristic properties of forward $d\sigma/dt$ for photoproduction of $\pi^{\pm}$ and Δ are described, respectively, in terms of the destructive and constructive interference effects between the amplitudes due to the π and A_1 trajectories. (J.F.P.)

3319 PHASES AND FORWARD CROSS SECTIONS IN VECTOR-MESON PHOTOPRODUCTION. Greenhut, Gary K. (Northeastern Univ., Boston). Phys. Rev., D; 2: 1915-23 (1 Nov 1970).

Using a quark model for forward scattering and Regge-pole parametrization of meson–nucleon scattering amplitudes, $d\sigma/dt|_{t=0}$ and the phases of the forward scattering amplitudes are calculated for ρ^0, ω, and φ photoproduction and compared with the experimental data. (auth)

3320 DIFFRACTION DISSOCIATION AND THE REACTION $\gamma \to \pi^+\pi^-p$. Pumplin, Jon (Stanford Univ., Calif.). Phys. Rev., D; 2: 1859-68(1 Nov 1970).

The diffraction dissociation process for the reaction $\gamma p \to \pi^+\pi^-p$ is analyzed in detail. Much of the analysis is relevant to reactions initiated by hadrons. A procedure is suggested for adding nonresonant background (the "Söding term") to ρ^0 production without double counting, and numerical calculations are presented. (auth)

3321 HIGH-ENERGY PHOTOPRODUCTION OF PSEUDOSCALAR MESONS IN A QUARK MODEL. Chand, Ramesh; Sundaram, A. (Inst. of Mathematical Sciences, Madras). Phys. Rev., D; 2: 1952-5(1 Nov 1970).

In the crossed t channel the high-energy photoproduction of pseudoscalar mesons in photon–nucleon collisions is investigated in our SU(3) quark model. Taking the physical baryon octet as 8 (physical) = $8' \cos\theta + 8 \sin\theta$, where 8 and 8′ arise from $3 \otimes \bar{3}$ and $3 \otimes 6$, respectively, it is found that the value $\theta = 20°$, which explains the high-energy data on meson–baryon scattering, also explains the recent high-energy data on the photoproduction of pseudoscalar mesons. In particular, it is found that for $\theta = 20°$, (i) $R(K^+\Lambda)/R(K^+\Sigma^0) = 1.5$, and (ii) the value of the strange-quark-to-nonstrange-quark coupling parameter is $b = 0.4 \pm 0.04$. (auth)

3322 POSSIBLE BINDING OF A MAGNETIC MONOPOLE TO A PARTICLE WITH ELECTRIC CHARGE AND A MAGNETIC DIPOLE MOMENT. Sivers, Dennis (Univ. of California, Berkeley). Phys. Rev., D; 2: 2048-54(1 Nov 1970).

It is argued that Dirac monopoles, if they exist, could be strongly bound to those naturally occurring free nuclei with magnetic dipole moments, and the effect this binding would have on the interpretation of experimental monopole searches is discussed. (auth)

3323 EFFECT OF A TRANSVERSE MOMENTUM DISTRIBUTION IN THE PARTON MODEL. Gardiner, C. W.; Majumdar, D. P. (Syracuse Univ., N. Y.). Phys. Rev., D; 2: 2040-7(1 Nov 1970).

The parton model for the inelastic lepton–nucleon scattering is generalized to include a realistic momentum distribution of the partons. In this formalism each parton is given a component of momentum which is orthogonal in a four-vector sense to the nucleon momentum. An approximation scheme is developed to take into account the effect of this orthogonal (transverse) momentum distribution of the partons. It is found to generate an additional scale-invariant contribution to the structure function $\nu W_2(\nu, Q^2)$ as well as a non-scale-invariant contribution, as is expected. The scale-invariance-breaking term is found to be a power series in Q^2/ν^2 and vanishes as ν or Q^2 goes to infinity for a fixed $\omega = 2M\nu/Q^2$. The effect of the transverse momentum distribution is explicitly displayed and discussed for a few momentum distribution functions. The data on inelastic e–p scattering are then analyzed for any significant deviations from scale invariance, and it is concluded that there is evidence for such deviations. On the assumption that the systematic errors in the data are small, some fits are made which display the dependence on Q^2. Finally, an attempt is made to fit the data with the formalism developed in the initial part of the paper. For this purpose use is made of a model for the partons, proposed previously to explain the data in the approximation that scale invariance is satisfied. Some comments are made on the properties of partons which are necessary to fit the data and on the present status of scale-invariance breaking. (auth)

3324 MUON–PROTON SCATTERING AND POSSIBLE ANOMALOUS INTERACTION OF THE MUON. Kiang, D.; Ng, S. H. (Dalhousie Univ., Halifax, Can.). Phys. Rev., D; 2: 1964-5(1 Nov 1970).

It is argued that a possible anomalous interaction of the muon of the form $i\bar{\psi}\gamma_\lambda\psi\chi_\lambda$ can be large enough to account for the μ–p/e–p cross-section ratio and yet it is not inconsistent with the present comparison for the theoretical and experimental values of the anomalous magnetic moment of the muon. (auth)

3325 CROSS SECTIONS FOR TWO-PAIR PRODUCTION AT INFINITE ENERGY. Cheng, Hung (Massachusetts Inst. of Tech., Cambridge); Wu, Tai Tsun. Phys. Rev., D; 2: 2103-5(1 Nov 1970).

The total cross sections are given for the following three high-energy processes: (i) $\gamma + \gamma \to e^+ + e^+ + e^- + e^-$, (ii) $\gamma + \gamma \to \pi^+ + \pi^+ + \pi^- + \pi^-$ are given, and (iii) $\gamma + \gamma \to \pi^+ + \pi^- + e^+ + e^-$. Up to the eighth order, all of them approach constants in the high-energy limit. These constants are 6.5, 0.23×10^{-5}, and 0.26×10^{-3} μb, respectively, for (i), (ii), and (iii). The corresponding photon–photon elastic scattering amplitudes in the forward direction are also given. The creation of μ pairs is also briefly discussed. (auth)

3326 ρ-MESON MASS SHIFT IN PHOTOPRODUCTION PROCESSES. Mannheim, P. D. (Tel-Aviv Univ., Israel); Maor, U. Phys. Rev., D; 2: 2105-7(1 Nov 1970).

It is argued that the ρ-meson mass shift, the mass dependence of the forward peak, and the structure of the spin-density matrix observed in photoproduction experiments are correlated and can be well parametrized utilizing crossing symmetry and t-channel kinematics. (auth)

3327 CONTINUOUS-MOMENT SUM RULES AND PION PHOTOPRODUCTION DATA. Vasavada, Kashyap V. (Indiana–Purdue Univ., Indianapolis). Phys. Rev., D; 2: 2098-2100 (1 Nov 1970).

Continuous-moment sum rules with different weight functions are studied for the single-pion photo-production process. Even granting the usual ambiguities on the high-energy side, it seems that presently available very low-energy data may be in considerable error. (auth)

3328 ELECTROMAGNETIC MANY-BODY FORCES. Chanmugam, G.; Schweber, S. S. (Brandeis Univ., Waltham, Mass.). Phys. Rev., A; 1: 1369-75(May 1970).

A method for obtaining electromagnetic many-body forces using canonical transformations is described. The Hamiltonian thus derived is more general than that of Primakoff and Holstein. (auth)

XUM

3329 DESER-GILBERT-SUDARSHAN REPRESENTATION AND ELECTROPRODUCTION STRUCTURE FUNCTIONS. Acharya, R.; Saxena, R. P. (Chalmers University of Tech., Gotenborg). Lett. Nuovo Cim.; 4: 828-32(31 Oct 1970).

A clear derivation of the scaling laws from the Deser-Gilbert-Sudarshan representation is given. Also it is shown that the asymptotic behavior of a given spectral function (required of scaling) is a direct reflection of the dominant singularity of the corresponding causal function of the light cone. (J.F.P.)

3330 PION ELECTROMAGNETIC FORM FACTOR WITH DIPION UNITARITY. Kanazawa, Akira; Haruyama, Masahiro (Hokkaido Univ., Sapporo). Progr. Theor. Phys. (Kyoto); 44: 437-43(Aug 1970).

The pion electromagnetic form factor which is consistent with the dipion unitarity and the analyticity is constructed, and it is compatible with the Veneziano-Lovelace-type pion-pion scattering amplitude. Several assumptions are made which restrict the validity of the result in the low and intermediate energy regions. The form factor thus obtained can be fixed uniquely by giving the ρ-meson trajectory α, the P-wave scattering length a_s and the zero point x_0 of the numerator function of the partial wave amplitude. Assuming $\alpha = 0.5 + t/2m_\rho^2$, an excellent fit can be obtained to the Novosibirsk data with $m_{\bar{\rho}} = 730$ MeV and $x_0 = \infty$ for $a_s = 17m_\pi^2$, the soft-pion prediction of current algebra, or with $m_{\bar{\rho}} = 720$ MeV and $x_0 = x_{04}$ for the hard-pion value $a_s = 14.5m_\pi^2$, where x_{04} is the 4th zero of the Veneziano-Lovelace-type scattering amplitude. The P-wave scattering phase shift is calculated also. In the spacelike region the form factor decreases slower than that of the ρ-dominance prediction with increasing the absolute value of four-momentum transfer squared. (auth)

3331 SOME ATTRIBUTES OF REAL AND VIRTUAL PHOTONS. awson, J. D. (Rutherford High Energy Lab., Chilton, Eng.). Contemp. Phys.; 11: 575-80(Nov 1970).

The interaction of charges by exchange of photons can be clearly and accurately described in the mathematical language of quantum electrodynamics; nevertheless attempts to describe such phenomena in verbal terms can be very confusing. This arises because it is not possible to form a consistent detailed mental picture of the process, as can normally be done in classical physics. Despite these difficulties, an attempt is made to discuss some basic properties of photons from a physical point of view, with special reference to two distinct descriptions of the wave aspects of virtual photons. These are in terms of, firstly, plane waves for which $\omega^2/c^2 \neq k^2$, and secondly, evanescent waves for which $\omega^2/c^2 = k^2$, but the component of k along one of the axes is imaginary. (auth) (UK)

Weak

3332 (ITF-70-59) OBTAINING THE LIMITING RELATIONS FOR CORRELATION AVERAGES. Bogolyubov, N. N. Jr. (Akademiya Nauk Ukrainskoi SSR, Kiev. Institut Teoreticheskoi Fiziki). 1970. 13p. (In Russian). Dep. NTIS (U. S. Sales Only).

The theorems necessary for obtaining many-time correlation averages are formulated under some rather general auxiliary conditions. The technique proposed is valid for a wide class of model systems with four-fermion interaction. (auth)

3333 (NYO-2171-323) DETECTION OF THE WEAK INTERMEDIATE BOSON THROUGH ITS HADRONIC DECAY MODES. Cline, D. (Wisconsin Univ., Madison. Dept. of Physics); Mann, A. K. (Pennsylvania Univ., Philadelphia. Dept. of Physics); Rubbia, C. (Harvard Univ., Cambridge, Mass. Dept. of Physics). 6 Jul 1970. 11p. Dep. NTIS.

It is shown that the hadronic decay modes of the weak intermediate boson W produced by high energy neutrinos provide a unique and unambiguous experimental signal of the production and decay of the W, even in the absence of any information about the number, the configuration or the momenta of the decay products. This method of detecting the hadronic decay modes of the W, in conjunction with previously utilized methods for detecting the leptonic decay modes, should allow a search for the W to be made which is independent of any assumptions about the hadronic to leptonic branching ratio of the W. (auth)

3334 (NYO-4204-3) WEAK INTERACTIONS AT HIGH ENERGIES. Pais, A. (Rockefeller Univ., New York). [1970]. Contract AT(30-1)-4204. 56p. Dep. CFSTI.

A review of high-energy neutrino beam semi-leptonic interactions is presented. Elastic form factor determinations from differential cross sections and polarization effects, total cross sections including sum rules and scaling, and problems beyond the quasi-two-body approximation are considered. (J.F.P.)

3335 WEAK INTERACTION OF PHOTONS AND NEUTRINO BREMSSTRAHLUNG. Chaudhuri, P. R. (Indian Statistical Inst., Calcutta). Can. J. Phys.; 48: 2357-61(15 Oct 1970).

Assuming that photons can interact weakly with neutrinos, the cross section for the neutrino bremsstrahlung $e^- + Z \rightarrow e^- + \nu + \bar{\nu} + Z$ was calculated. From this, the rate of stellar energy loss due to neutrino pair emission was derived and is compared with the result obtained on the basis of the current-current coupling theory. Also, for a comparative study, the neutrino luminosity was calculated according to both the theories. (auth) (Canada)

3336 INELASTIC NEUTRINO-NUCLEON SCATTERING AND THE q^2 DEPENDENCE OF REGGE RESIDUE FUNCTIONS. Palmer, David R. (Univ. of Colorado, Boulder). Nucl. Phys.; B24: 47-60(1970).

Inelastic neutrino-nucleon scattering is considered within the context of Harari's duality model. It is argued that the Regge residue function associated with the vector-axial-vector interference term should be rapidly damped at large $|q^2|$. A causal representation is used to show a rapidly damped residue function is consistent with scale invariance and Regge asymptotic behavior. The scaling function $F_3(\omega)$ is then shown to approach a nonzero constant as $\omega = |q^2|/\nu \rightarrow 0$ in contrast to previously suggested behavior. (auth)

3337 POSSIBLE EFFECTS OF LEPTON NON-LOCALITY IN THE DECAYS $K \rightarrow \pi e^+ e^-$ AND $K \rightarrow \pi\nu\bar{\nu}$. Singh, S. K.; Wolfenstein, L. (Carnegie-Mellon Univ., Pittsburgh). Nucl. Phys.; B24: 77-92(1970).

Decays of the form $K \rightarrow \pi l\bar{l}$ may occur even if there are no primitive weak neutral lepton currents; in this case the effective lepton coupling is non-local. A general discussion of the consequences of this non-locality is given and applied to the following models for these decays: (i) second order in the usual weak interaction theory, (ii) Kummer-Segrè-Christ model, (iii) Okubo model of CP violation, and (iv) models involving heavy leptons. (auth)

3338 SOME COMMENTS ON PARITY-VIOLATING WEAK NNrho-VERTEX. Danilov, G. S. (Ioffe Inst. of Physics and Tech., Leningrad). Nucl. Phys.; B24: 165-72(1970).

The hypothesis of Olesen and Rao about the cancellations between the Schwinger and the sea-gull terms in expressions for the divergence of the weak NNρ vertex is discussed. It is shown that under some very general assumptions this cancellation should not take place. An explicit expression is derived for the sea-gull term in the parity violating part of the NNρ vertex in terms of the Heisenberg operator of the fields. (auth)

3339 LEPTONIC DECAYS OF POLARIZED BARYONS. II. Linke, Volkard (Univ., Heidelberg). Nucl. Phys.; B23: 376-86 (1970).

For the weak electronic decay of a polarized hyperon formulas are given, which express explicitly the various energy-dependent asymmetry coefficients in the angular distribution of the decay products in terms of the weak form factors. (auth)

3340 COHERENT, INCOHERENT, AND INELASTIC CROSS SECTIONS FOR W-MESON PRODUCTION BY MUONS AND NEUTRINOS. Reiff, J. (Univ. of Utrecht). Nucl. Phys.; B23: 387-96(1970).

Cross sections for W-meson production by muons and neutrinos are calculated for vector-boson masses of 3 and 6 GeV and incident lepton energies of 50, 75 and 100 GeV. It is found that muon cross sections are up to a factor 1000 smaller than the corresponding neutrino cross sections, that W-mesons produced by muons are not polarized, while W-mesons produced by neutrinos are left-handed polarized, that in both processes the total inelastic cross sections are of the same order as the incoherent cross sections, and the $\sigma(N^*)$ (i.e.; the parts of the inelastic cross sections referring to N^*) form a very small part in the total inelastic cross sections. The inelastic cross sections are calculated with the form factors W_1 and W_2, where the SLAC data are used. W_1 is modified so that it is consistent with positive definiteness and use scaling. (auth)

3341 S-WAVE NON-LEPTONIC DECAYS AND GAUGE FIELDS. Kimel, I. (Univ. of Michigan, Ann Arbor). Nucl. Phys.; B23: 574-82(1970).

S-wave non-leptonic decay amplitudes are obtained from a gauge-field model and the results are also interpreted from the point of view of mixing of particle fields. The model gives different effective enhancements for K- and hyperon decays as required by experiment. (auth)

3342 SOME PROPERTIES OF NONSTRONG AMPLITUDES IN A VENEZIANO-TYPE MODEL. Humpert, B. (Cavendish

Lab., Cambridge, Eng.). Lett. Nuovo Cim.; 4: 897-907(7 Nov 1970).

A previous scheme for constructing current amplitudes is investigated. The construction of hadronic currents for lepton–hadron scattering in the Veneziano approach, the one-current amplitude, the two-current amplitude with adjacent currents, and the two-current amplitude with nonadjacent currents, and a comparison of the two-current amplitudes of this model and its determined parameters with previous asymptotic sum rules are treated. (J.F.P.)

3343 MODEL OF THE NEUTRINO IN THE GENERAL THEORY OF RELATIVITY WITH VELOCITY GROUPS G_3 ON V_2. Golubyatnikov, A. N. (Moscow State Univ.). Dokl. Akad. Nauk SSSR; 192: 55-8(1 May 1970). (In Russian).

The model of the neutrino is considered in the general theory of relativity which is described by the Dirac-Einstein equations, where the energy tensor is the momentum. All the general solutions of these equations are found that are invariant with respect to 3-dimensional groups G_3 acting on 2-dimensional nonisotropic transitive surfaces V_2. The type of measuring units allowed in this case are well known. Expressions are given for constants that characterize the gravitational field created by the particle in vacuum. The effect of a homogeneous free neutrino flux on the geometry of space is considered within the framework of the general solution that was obtained. Periodic compression of space takes place at the velocity of light. From these results it is possible to account strictly for the effect of completely polarized neutrino fluxes on the geometry of space during expansion of the universe. For a neutrino density of 5×10^{-14} g/sec^2 · cm, the distance between points of space compression is found to be 4.5×10^{30} cm. (TTT)

3344 QUANTUM MECHANICS OF CHARGED RELATIVISTIC VECTOR BOSONS WITH ANOMALOUS MAGNETIC MOMENT IN EXTERNAL ELECTROMAGNETIC FIELDS. I. Borgardt, A. A.; Karpenko, D. Ya. (Donetsk State Univ., USSR). Ukr. Fiz. Zh.; 15: 1091-4(Jul 1970). (In Russian).

Energy levels and wave functions of the W boson are found in constant electric and magnetic fields. These problems have an exact solution for the present type of the potential. (auth)

3345 AXIAL-VECTOR K_{l4}-DECAY FORM FACTORS BASED ON CURRENT ALGEBRA. Chhajlany, S. C.; Pandit, L. K.; Rajasekaran, G. (Tata Inst. of Fundamental Research, Bombay). Phys. Rev., D; 2: 1934-9(1 Nov 1970).

The axial-vector K_{l4}-decay form factors given by current algebra were reevaluated using the vector K_{l3}-decay form factors and the ratio f_K/f_π, obtained on the basis of broken chiral $SU_3 \otimes SU_3$ and SU_3 symmetries. It is shown that the assumption of near constancy of these form factors leads to good agreement with the experimental data, using consistently the single Cabibbo angle $\sin\theta_V = \sin\theta_A = 0.22$. (auth)

3346 BARYON POLE MODEL FOR S-WAVE HYPERON DECAY. Ram Mohan, L. R. (Purdue Univ., Lafayette, Ind.). Contract AT(11-1)-1428. Phys. Rev., D; 2: 2101-2(1 Nov 1970).

The role of the decuplet particle poles in a baryon pole model for the parity-violating amplitude is investigated from the algebraic point of view. The conditions under which the baryon pole model, with decuplet poles, reproduces the results of the K^* pole model and of current algebra are analyzed. (auth)

3347 CHIRAL-SYMMETRY-BREAKING CORRECTIONS TO THE $K \to 3\pi$ SOFT-PION THEOREM. Ali, Ahmad (Univ. of Islamabad, Rawalpindi, Pakistan); Riazuddin; Fayyazuddin. Phys. Rev., D; 2: 2093-5(1 Nov 1970).

First-order corrections, due to chiral symmetry breaking, to the $K \to 3\pi$ soft-pion theorem are calculated. The corrections turn out to be independent of any assumption of specific properties of the chiral-symmetry-breaking Hamiltonian. (auth)

3348 UNIVERSALITY OF WEAK BILINEAR TRANSITIONS AND ITS RELATION TO THE FUNDAMENTAL WEAK INTERACTIONS. Katuya, Mituaki; Fujii, Kanji (Hokkaido Univ., Sapporo). Progr. Theor. Phys. (Kyoto); 44: 486-99(Aug 1970).

According to the pole model, the strengths of weak bilinear transitions in various processes are investigated in the present stage of knowledge. In order to clarify whether or not the phenomenological strengths of weak bilinear transitions are obtained from the fundamental four-fermion interaction, the bilinear transitions based on factorization approximation are studied. It is shown that the parity-conserving transition $(K-\pi)$ consistent with the fundamental four-fermion interaction with Cabibbo factor cannot be definitely said to contradict the experimental data and that for parity-violating bilinear transitions two standpoints are possible: (1) the four-fermion interaction with Cabibbo factor leads to consistent results, although this interaction is inconsistent with experiment when the K^*-pole dominance and the factorization approximation are assumed to be valid and (2) this interaction is unfavorable. The second standpoint suggests the existence of some kind of new primary interaction which may be of bilinear type on the urbaryon line. Along this line of thought, a speculation on topological property of urbaryon diagrams and other discussions will be given. (auth)

3349 NONLEPTONIC HYPERON DECAYS AND BREAKING OF CHIRAL $SU(3) \otimes SU(3)$. Ohya, Katsuhiko (Nihon Univ., Tokyo). Progr. Theor. Phys. (Kyoto); 44: 473-85(Aug 1970).

Nonleptonic decays are discussed in connection with the breaking of chiral $SU(3) \otimes SU(3)$. An effective $\partial_\mu J^\gamma_\mu(x)$ interaction of nonleptonic decays, which is reduced to $Hw(x) = -iG[Q^\gamma(x_0) + Q^\gamma_5(x_0), m_0(S^c(x) + \lambda S^8(x))]$ is given. The amplitudes of the decays calculated in hard-pion limit give a good agreement with experiment both for S-waves and P-waves. In addition, it is shown that the f/d ratio of scalar spurion is −3.06, which is very close to that of mass-splitting −3.05, and $\lambda = 2.01$. Therefore $m_0(S^0(x) + \lambda S^8(x))$ can be identified as a mass operator, and then the strength of weak $\partial_\mu J^\gamma_\mu(x)$ interaction is estimated to be $G = 0.232 \times 10^{-5}$. (auth)

3350 EXISTENCE OF μ^* AND DUALITY IN WEAK PROCESSES. Hosoda, Masataka; Saito, Takesi (Osaka Univ.). Progr. Theor. Phys. (Kyoto); 44: 546-7(Aug 1970).

The existence of a resonant state μ^* in a final (μ^-, π^+) state is assumed, and its contribution to the K_{l3} decay form factors is examined. (L.B.S.)

3351 LEPTON CONSERVATION, μ-e SYMMETRY, NEUTRAL CURRENTS, AND THE PRINCIPLE OF UNIVERSALITY. Tsai, S. Y. (Ninon Univ., Tokyo). Progr. Theor. Phys. (Kyoto); 44: 558-60(Aug 1970).

It is demonstrated that, in the framework of the two-distinct two-component neutrino theory, the charged weak lepton current L_λ, consistent with the conservation law of the total lepton number, is always consistent also with the separate conservation of the electron number and the muon number provided that L_λ obeys the principle of universality. (L.B.S.)

Strong (General)

Refer also to abstract 3454.

3352 (IRB-TP-2-70) INELASTIC PROCESSES AND BACKWARD SCATTERING IN A MODEL OF MULTIPLE SCATTERING. Dadic, I.; Martinis, M.; Pisk, K. (Institut Rudjer Boskovic, Zagreb (Yugoslavia)). [1970]. 37p. Dep. NTIS (U. S. Sales Only).

The relativistic model of multiple scattering is discussed on the basis of similarity which may be established between the model and the nonrelativistic potential scattering. The problem of nonrelativistic high energy forward and backward scattering as obtained from the Klein-Gordon type equation as well as the many channel situation and the treatment of exchange forces are considered in detail. It is found that all the usual high energy approximations require a smooth and nonsingular-at-origin behavior of the potential. Many of the results are found to be analogous to the results obtained by other means in the relativistic case. In particular, by assuming that the relativistic "effective potential" defined in the model multiple scattering by means of single scattering is smooth and nonsingular at origin, the eikonal type approximations for forward and backward scattering are obtained. Restrictions due to unitarity on the high energy behavior of the derived scattering amplitude are discussed in terms of Martin's unitarity bound. A generalization of the procedure to an arbitrary inelastic process is given. Some interesting relations between forward and backward amplitudes at high energies are obtained. It is also shown that the model contains the absorption model as a special case, and corrections due to backward scattering and to the "random phase assumption" are obtained. Unitarity places restrictions on the freedom of choice of the single scattering amplitude; in fact, the limit of the high energy behavior of the exchange interactions is found. (auth)

3353 BASIC OPERATORS OF THE DUAL-RESONANCE MODEL. Gross, David J.; Schwarz, John H. (Princeton Univ., N. J.). Contract AF49(638)-1545. Nucl. Phys.; B23: 333-57(1970).

Rules for constructing arbitrary Feynman diagrams of the dual-resonance model are presented. Specifically, the twisted propagator, with all spurious states projected out, is explicitly constructed in terms of a one-dimensional integral. The propagator can be used together with the symmetric vertex operator to construct any

XUM

dual diagram. With the aid of the projected propagator an operator proof of duality is presented and a formula for N-point functions with arbitrary external states is constructed. These operators are also used to obtain simple forms for the three primitive one-loop operators of the model, as well as the counter-terms necessary for their renormalization. (auth)

3354 EMPIRICAL MERGER OF GEOMETRICAL AND REGGE PICTURES FOR ELASTIC HADRON SCATTERING. Barger, V.; Cline, D. (Univ. of Wisconsin, Madison). Contract AT(11-1)-881. Nucl. Phys.; B23: 227-35(1970).

From a survey of data on forward elastic scattering the following are found: (i) consistency with shrinkage from a Pomeranchuk trajectory slope $\alpha'_P = 1/2$; (ii) evidence for a scaling relation between the t-dependence of the Pomeranchuk residue and its total cross section; (iii) a geometrical interpretation of the non-shrinking part of forward elastic peaks. Predictions are made for hyperon-nucleon scattering based on (ii) and (iii). (auth)

3355 REMARKS ON THE THERMODYNAMICAL MODEL OF STRONG INTERACTIONS. Hagedorn, R. (CERN, Geneva). Nucl. Phys.; B24: 93-139(1970).

The thermodynamical model of strong interactions is described with the emphasis on aspects neglected in previous papers and on its relation to other recent developments and proposals in high-energy physics. The following topics are covered: Kinematical aspects: "limiting fragmentation"; The pure thermodynamical part; A glance of Feynman's ideas; Main results of the thermodynamical model; and Philosophy: the case for bootstrap and non-existence of "truly elementary" material building blocks. (auth)

3356 PHENOMENOLOGICAL MODEL FOR A POSSIBLE FAILURE OF THE POMERANCHUK THEOREM. Terazawa, Hidezumi (Cornell Univ., Ithaca, N. Y.). Phys. Rev., D; 2: 1983-4(1 Nov 1970).

A phenomenological model for a possible failure of the Pomeranchuk theorem is proposed. This predicts the following relations among asymptotic total cross sections: $\sigma_T(\pi^-p) - \sigma_T(\pi^+p) = \sigma_T(K^-n) - \sigma_T(K^+n)$, $\sigma_T(K^+p) = \sigma_T(K^+n)$, $\frac{2}{3}[\sigma_T(K^-n) - \sigma_T(K^+n)] \leq \sigma_T(K^-p) - \sigma_T(K^+p) \leq 2[\sigma_T(K^-n) - \sigma_T(K^+n)]$, $\sigma_T(pp) = \sigma_T(pn)$, and $\frac{2}{3}[\sigma_T(\bar{p}n) - \sigma_T(pn)] \leq \sigma_T(\bar{p}p) - \sigma_T(pp) \leq 2[\sigma_T(\bar{p}n) - \sigma_T(pn)]$. All of these are consistent with the recent Serpukhov data. (auth)

3357 NEW REGGE MODELS OF ASYMPTOTIC BEHAVIOR. Barger, V. (Univ. of Wisconsin, Madison); Phillips, R. J. N. Phys. Rev., D; 2: 1871-8(1 Nov 1970).

The properties and predictions of several new Regge models, suggested by the Serpukhov total-cross-section data, are analyzed and compared. Forward elastic πN, KN, $\bar{K}$N, NN, and $\bar{N}$N scattering are considered, for Regge models incorporating strong multi-Pomeranchukon cuts, or Regge dipoles, or complex secondary trajectories. Total cross sections are fitted. Forward real parts, charge-exchange scattering, and regeneration are predicted, within subtraction constants. High-energy extrapolations are shown. (auth)

Strong (Baryon No. = 0)

Refer also to abstracts 3278 and 3460.

3358 (DESY-70/49) CALCULATION OF N$\bar{N}$ BOUND STATES FROM A RELATIVISTIC OBE MODEL AND THE MESON SPECTRUM. Schierholz, G.; Wagner, S. (Deutsches Elektronen-Synchrotron, Hamburg (West Germany)). Sep 1970. 28p. Dep. NTIS (U. S. Sales Only).

Nucleon-antinucleon (N$\bar{N}$) bound states are calculated in the framework of relativistic quantum mechanics. The potential is taken from a previous treatment of nucleon-nucleon (NN) interaction with parameters adjusted to elastic NN phase shifts and the deuteron. The OBE potential is given by the field theoretic Born terms of π, η, σ, ϵ, ρ and ω exchange contributions which are supplied with form factors. The NN and N$\bar{N}$ channels are related by crossing. In the case of N$\bar{N}$ the π and ω exchange contribution to the potential change sign is compared to the NN case. This way the ω exchange gives rise to a repulsive core for NN and to short-range attractive forces for N$\bar{N}$. In contrast to similar calculations by other authors the input mesons are obtained as bound states below 1000 MeV in the N$\bar{N}$ channels. In addition there are bound states, mostly between 1 GeV and N$\bar{N}$ threshold, corresponding to ϕ, ρ', δ, A_1, A_2, f, f' and a B for both T = 1 and T = 0. The uncoupled partial waves with L = J contain at most one bound state for each isospin. The coupled L = J ± 1 partial waves $^3S_1 - {}^3D_1$ and $^3P_2 - {}^3F_2$ contain two T = 0 bound states which reflect the mixed singlet-octet mesons ω, ϕ and f, f'. Most of the calculated bound states are close to experimentally observed mesons, but the bound states corresponding to the ω and the fictitious σ mesons appear at negative energies. The bound state energies are particularly sensitive to the choice of the ω and scalar meson coupling constants and to the form factor parameters. (auth)

3359 CONSISTENCY CONDITION FOR THE $A_1\rho\pi$ SYSTEM FROM UNITARIZED CURRENT ALGEBRA. Ecker, G. (Univ., Vienna). Nucl. Phys.; B23: 173-80(1970).

Using recent attempts to incorporate unitarity into the current-algebra approach additional information on the $A_1\rho\pi$ system is obtained. When the resulting consistency condition is applied to the original hard-pion model of Schnitzer and Weinberg, the parameter δ, which is related to the magnetic moment of the A_1 meson, can be determined. The result turns out to depend crucially on the exact value of g_ρ, the coupling constant of the isovector current to the ρ-meson. (auth)

3360 LOWER BOUND FOR THE $\pi^0\pi^0$ SCATTERING LENGTH. Wit, R. (CERN, Geneva). Nucl. Phys.; B23: 168-72(1970).

Under some additional assumptions it is shown that the threshold value of the forward scattering amplitude F(4,0,0) is greater than −2.2 pion Compton wavelengths. (auth)

3361 HARD-PION CALCULATION WITHOUT CURRENT ALGEBRA. De Azcarraga, J. A.; Renner, B. (Cambridge Univ., Eng.). Nucl. Phys.; B23: 236-46(1970).

Following the suggestions of earlier authors the hypothesis that apart from fixing the scale of the weak axial-vector current, the main results of current algebra are largely implied in the concept of meson-pole dominance, which includes the famous PCAC principle. For definiteness the hard-pion analysis of the $A_1\pi\rho$ vertex by Schnitzer and Weinberg is re-examined, not assuming anything about the commutator of two axial-vector currents but retaining all their other assumptions, specifically those about meson-pole dominance. It is found, as expected, that these latter assumptions are powerful enough to determine the system up to the scale of the axial-vector current. As a by-product of our analysis, a highly interesting corollary on Weinberg sum rules is found which allows an otherwise permissible non-compact alternative to the usual SU(2) × SU(2) current algebra to be excluded on mere covariance and positivity requirements. (auth)

3362 METHOD TO STUDY EVENTS WITH TWO MISSING NEUTRAL PARTICLES. SEARCH FOR THE REACTIONS $p\bar{p} \to 2\omega^0 \to 2\pi^+ + 2\pi^- + 2\pi^0$ IN ANNIHILATIONS AT REST. Bloch, M.; Fontaine, G.; Lillestoel, E. (College de France, Paris). Nucl. Phys.; B23: 221-6(1970).

A method for the study of events with two missing neutral particles is described. For certain dynamical configurations, measurements on events of the type $Z \to X + Y \to (A + a^0) + (B + b^0)$, where X and Y are narrow-width resonances or unstable particles, can be plotted in a way which gives a specific signal for the reaction. Application of the method in annihilations at rest shows that the reaction $p\bar{p} \to \omega^0\omega^0$ may account for 1.4 ± 0.6% of the total number of annihilations. (auth)

3363 SIMPLE DERIVATION OF THE KSRF RELATION. Johnson, Robert C. (Durham Univ., Eng.). Nucl. Phys.; B23: 247-52(1970).

A simple derivation of the KSRF relation is given, and its underlying assumptions are examined in detail. (auth)

3364 MANY PI-MESON SYSTEMS. Jasselette, P. (Univ., Liege). Nucl. Phys.; B23: 481-508(1970).

An analysis of many π-meson systems previously made by Pais is reconsidered for greater values of N. A new difficulty is resolved by a recurrence procedure. Results are given for N up to 20. (auth)

3365 CROSSING-SYMMETRIC AMPLITUDE FOR THE POMERANCHUK TRAJECTORY. Chow, G. Y.; Chen, H. (Saginaw Valley Coll., University Center, Mich.). Nucl. Phys.; B23: 358-64(1970).

A simple crossing-symmetric amplitude for the Pomeranchuk trajectory is constructed for $\pi\pi$ elastic scattering. The amplitude exhibits the forward diffraction peak and various desirable properties of the Pomeranchuk trajectory. The expected high-energy behavior is achieved by locating the proper cut structure in the s- and t-planes. Comments are made on the unitarization of the amplitude. (auth)

3366 ANGULAR-MOMENTUM DISTRIBUTION IN DUAL-RESONANCE MODELS. Fritzsch, H. (Max-Planck-Institut fuer Physik und Astrophysik, Munich). Lett. Nuovo Cim.; 4: 893-6 (7 Nov 1970).

In this investigation of the angular-momentum structure of resonances in dual-resonance models the high-energy asymptotic

behavior is emphasized. Since the level-counting procedure for resonances is equivalent to the level-counting in the case of a Bose gas consisting of an infinite number of harmonic oscillators, this thermodynamical description is used. Also the Bose-gas description is analogous to the Bethe Fermi gas model of atomic nuclei, thus methods similar to those used in nuclear physics can be used to compute the angular momentum distribution of resonances at high energies. (J.F.P.)

3367 INTERFERENCE PHENOMENA IN DECAYS $\rho \rightarrow e^+ + e^-$ AND $\omega \rightarrow e^+ + e^-$. Zima, V. G. (Donetsk Inst. of Physics and Tech., USSR). Ukr. Fiz. Zh.; 15: 1132-4(Jul 1970). (In Russian).

With some simple assumptions, it is shown that full constructive or destructive $\rho-\omega$ interference would change the cross section for the reaction $\pi + p \rightarrow n + e^+ + e^-$ by +50% or −50%, respectively. (auth)

3368 ON-SHELL SUBTRACTED DISPERSION RELATIONS AND LOW-ENERGY THEOREMS FROM CURRENT ALGEBRA. Dahmen, Hans D. (Univ., Heidelberg. Kernforschungszentrum, Karlsruhe, Ger.); Rothe, Klaus D. Z. Phys.; 239: 409-22 (1970).

A method discussed earlier is applied to the case of $\pi\pi$ and πN scattering and to electroproduction. As an example for the $\pi\pi$ scattering amplitude a subtracted, covariant on-shell dispersion relation is derived in which the subtraction polynomial is determined by the corresponding low energy theorem plus possibly small corrections. It is also shown how this same method may be applied to the derivation of low energy theorems. (auth)

3369 UNITARY AND CROSSING-SYMMETRIC S-, P-, AND D-WAVE LOW-ENERGY PION–PION SCATTERING. Carrotte, John B.; Johnson, Robert C. (Univ. of Durham, Eng.). Phys. Rev., D; 2: 1945-51(1 Nov 1970).

Crossing-symmetric solutions to the pion–pion partial-wave dispersion relations are obtained, using the inverse-amplitude method. The presence of the ρ meson with its physical mass and width is assumed, the amplitudes are constrained to contain Adler zeros, and general sum rules and inequalities are satisfied. Favored solutions contain a very broad isoscalar S-wave resonance, and have a small decreasing isospin-2 S-wave phase shift. The D waves are very small. The over-all agreement with phenomenology and with other S-matrix calculations is very good. (auth)

3370 DISTRIBUTIONS OF CHARGED PIONS. Horn, D.; Silver, R. (California Inst. of Tech., Pasadena). Contract AT(11-1)-68. Phys. Rev., D; 2: 2082-4(1 Nov 1970).

Statistical considerations are used to derive a new distribution for charged pions in multiparticle production reactions. The distribution is in good agreement with experiment. (auth)

3371 EVALUATION OF THE $\pi\pi$ SCATTERING LENGTHS USING ON-MASS-SHELL PIONS. Golestaneh, A. A. (Mount Union Coll., Alliance, Ohio); Carlson, C. E. Phys. Rev., D; 2: 2084-9(1 Nov 1970).

The $\pi\pi$ scattering lengths were evaluated using current algebra but without the use of a power-series expansion or extrapolation of the scattering amplitude. The usual Lehmann–Symanzik–Zimmermann reduction was used in terms of an axial-vector current $J = A + c\partial\phi$, where A is the usual axial-vector current, c is the Goldberger–Treiman constant, and ϕ is the pion field. The scattering amplitude is decomposed into four terms, three of which are due to the equal-time commutators; two of these three are evaluated using the σ model in order to show that the usual current algebra of the current A holds for the current J. The other terms are evaluated in terms of single-particle intermediate states; it is shown that among these states, only s waves contribute at threshold. Assuming that the ϵ resonance is the only s wave dominating the low-energy ($\pi\pi$) scattering, a relation is found connecting the form factors arising from the equal-time commutators of the current J to the ϵ-pion coupling constant. Finally, the scattering lengths are obtained corresponding to isospins 0 and 2, and ϵ resonance width 200 MeV, as $a_0 = 0.278m^{-1}$ and $a_2 = -0.044m^{-1}$, where m is the pion mass. (auth)

3372 BROKEN SCALE INVARIANCE AND THE WIDTH OF A SINGLE DILATON. Crewther, R. J. (California Inst. of Tech., Pasadena). Contract AT(11-1)-68. Phys. Lett.; 33B: 305-8 (26 Oct 1970).

It is found that, in the scale-invariant limit, the pion-dilaton axial coupling constant $F_{\sigma\pi}$, the vacuum-dilation stress-energy tensor constant F_σ, and the pion decay constant f_π satisfy $F_\sigma F_{\sigma\pi} f_\pi = \frac{1}{2}$. This relation, assumed to be approximate in the real world, leads to a large dilaton width. (auth)

3373 OFF-SHELL $\pi\pi$ VENEZIANO AMPLITUDE. Ahmed, M. A.; Taha, M. O. (International Centre for Theoretical Physics, Trieste, Italy. Univ. of Khartoum, Sudan). Progr. Theor. Phys. (Kyoto); 44: 444-7(Aug 1970).

An off-shell extension of the Veneziano $\pi\pi$ amplitude is proposed. It is discussed in relation to the off-shell ρ-exchange Feynman graph, the Lovelace on-shell amplitude and the Adler consistency condition. (auth)

3374 VENEZIANO AMPLITUDES FOR πA_1 SCATTERING. Ahmed, M. A.; Taha, M. O. (Univ. of Khartoum, Sudan). Progr. Theor. Phys. (Kyoto); 44: 448-55(Aug 1970).

Veneziano representations for the processes $\pi A_1 \rightarrow \pi A_1$ and $\pi A_1 \rightarrow \pi\pi$ are constructed for the I = 2 eigenamplitudes of the t-channel. The representations given for the physical I = 2 amplitudes involve the ρ-coupling constants and a single arbitrary parameter. Some previous constructions for $\pi A_1 \rightarrow \pi\pi$ in the literature are seen to be special cases of these representations. (auth)

3375 NON-DUALITY OF POMERANCHON TERM AND QUARK LINE PICTURE. Yoshida, Toshihiro (Kyoto Univ.). Progr. Theor. Phys. (Kyoto); 44: 551-3(Aug 1970).

It is shown that the duality concept seems not to hold for the Pomeranchuk term in the quark-line picture for $\pi\pi$, πN, and NN processes. (L.B.S.)

3376 PHENOMENOLOGICAL CURRENT ALGEBRA VERTEX. Wise, Michael Louis. Waltham, Mass.; Brandeis Univ. (1969). 170p. University Microfilms Order No. 70-12,033. Thesis.

The most general vertex function determined by current algebra is constructed. Though the vertex function of three vector currents is emphasized, the methods employed are readily generalized to other currents, higher point functions, and matrix elements of currents, where the Ward identity techniques of Schnitzer and Weinberg are used to impose the current algebra constraints. It is found that the vertex function naturally separates into two parts, a "canonical" part and a "noncanonical" part. The "canonical" part depends only on the propagator, while the "noncanonical" part depends on two partially symmetric scalar functions. Any choice of these scalar functions will yield a theory which satisfies all of the current algebra constraints. Thus a convenient framework is provided for constructing dynamical models consistent with the current algebra. The Johnson–Low Bjorken (JLB) theorem is found to be consistent with the matrix elements of the algebra of fields. More generally it places conditions on the noncanonical part, and hence various models for the space-space equal-time commutators correspond to different choices for the scalar functions. The origin of the possible breakdown of the JLB theorem is investigated and a generalized Bjorken theorem is presented. The methods developed are applied to the $\pi\rho A_1$ system. The decays $A_1 \rightarrow \rho\pi$ and $\rho \rightarrow \pi\pi$ are parameterized in a convenient manner. Since a realistic model may require an underlying fermion field, subtracted representations for the propagators are derived and the regularized Ward identities for the currents are investigated. It is concluded that whereas current algebra will greatly restrict the class of strong interaction models additional dynamical information must be found to enable one to calculate the remaining undetermined scalar functions. (Diss. Abstr. Int., B)

Strong (Baryon No. = 1)

3377 (ITF–70-65) DISPERSION–THEORETIC MODEL OF πN-SCATTERING BACKWARD PEAKS. Lendel, A. I.; Lend'el, V. I. (Akademiya Nauk Ukrainskoi SSR, Kiev. Institut Teoreticheskoi Fiziki). 1970. 15p. Dep. NTIS (U.S. Sales Only).

The structure of backward differential cross section of πN scattering is explained by using the backward dispersion relations for the real part of $\pi \pm$ N-scattering amplitude. Excellent agreement of the proposed model with the experiment is obtained. (auth)

3378 (ITF–70-77) SOME INELASTIC MESON–BARYON REACTIONS IN GENERALIZED VENEZIANO MODEL. Enkovski, L. L.; Kukhtin, V. V.; Timokhin, V. V. (Akademiya Nauk Ukrainskoi SSR, Kiev. Institut Teoreticheskoi Fiziki). 1970. 22p. Dep. NTIS (U. S. Sales Only).

Inelastic MB scattering processes $\pi^-p \rightarrow pK^0K^-$, $\pi^-p \rightarrow \Lambda K^+\pi^-$, $\pi^-p \rightarrow nK^0\bar{K}^0$, $\pi^-p \rightarrow \Sigma^0K^0\pi^0$, $\pi^-p \rightarrow \Lambda K^0\pi^0$, $\pi^-p \rightarrow \Sigma^0K^+\pi^-$ are investigated in the framework of the 5-point Veneziano amplitude. Cross sections and effective mass distributions are calculated. (auth)

3379 (JINR–E1-5259) COMPILATION OF DATA ON THE REAL PARTS OF THE K^+p FORWARD SCATTERING AMPLITUDES. Dumbrais, O. V.; Dumbrais, T. Yu.; Queen, N. M.

(Joint Inst. for Nuclear Research, Dubna (USSR)). 1970. 15p. Dep. NTIS (U. S. Sales Only).

A compilation of experimentally determined values of the real parts of the K^+p forward scattering amplitudes is given in a form in which these data may be used directly in analyses of forward dispersion relations. (auth)

3380 (JINR-P2-5263) STATIC MODEL OF THE S WAVES IN πN SCATTERING AND THE t-CHANNEL PECULIARITIES. Meshcheryakov, V. A.; Rerikh, K. V. (Joint Inst. for Nuclear Research, Dubna (USSR). Lab. of Theoretical Physics). 1970. 18p. Dep. NTIS (U. S. Sales Only).

The main t-channel peculiarities corresponding to ρ and σ-mesons are taken into account on the basis of the precise Wander's solution in the static model of the s-wave πN-scattering. A good description of the experimental data on s-waves up to 260 MeV in 1.c.s. is obtained. (auth)

3381 (JINR-P2-5320) DESCRIPTION OF EXPERIMENTAL DATA ON πN AND KN SCATTERING IN THE HIGH-ENERGY REGION ON THE BASIS OF THE COMPLEX ANGULAR MOMENTA THEORY. I. Dzhgarkava, M. I.; Kazarinov, Yu. M.; Potashnikova, I. K.; Silin, I. N. (Joint Inst. for Nuclear Research, Dubna (USSR). Lab. of Nuclear Problems). 1970. 18p. (In Russian). Dep. NTIS (U. S. Sales Only).

The published experimental data on πN- and KN-scattering in the energy range from 6 to 55 GeV and in the range of transferred momenta up to 1 GeV/c were treated for the purpose of checking the Regge pole hypothesis. The results of experiments on measurements of the total interaction cross sections, of differential cross sections of elastic scattering and the scattering with the charge exchange, of the Wolfenstein parameters R and A and the data of the known resonance belonging to p, p', ρ, ω, and A_2 trajectories were used. The results show that at more than 40 free parameters only qualitative description of the experimental data can be obtained. (auth)

3382 (TPJU-1/70) AMBIGUITIES IN THE EXPERIMENTAL DETERMINATION OF RESONANCE PRODUCTION AMPLITUDES. Gizbert-Studnicki, P.; Golemo, A.; Zalewski, K. (Jagellonian Univ., Krakow (Poland). Dept. of Theoretical Physics). Feb 1970. 14p. Dep. NTIS (U. S. Sales Only).

Experiments with unpolarized particles determine only partially the scattering amplitudes. For reactions $0^- + 1/2^+ \to 0^- + 1/2^+$ the most general transformation of the amplitudes, which leaves the experimental results unchanged, is given. Implications for the quark model are also discussed. (auth)

3383 (TPJU-2/70) POLARIZATION OF Λ AND Σ HYPERONS IN TWO-BODY Y* PRODUCTION PROCESSES AND THE QUARK MODEL. Bialas, Andrzej; Kotanski, Andrzej (Jagellonian Univ., Krakow (Poland). Dept. of Theoretical Physics). Feb 1970. 12p. Dep. NTIS (U. S. Sales Only).

The two-body Y* production processes with $0^- 3/2^+$, $1^- 3/2^+$ and $3/2^+ 3/2^+$ final states are considered. The measurements of the polarization of Λ and Σ hyperons are discussed in the framework of the additive quark model. Several constraints are derived. The results provide strong and qualitatively new tests of the additivity assumption. In addition, a short summary of the experimental methods of determining the polarization moments of hyperons is given. (auth)

3384 (TPJU-3/70) REGGE POLE MODEL WITH VENEZIANO RESIDUES FOR REACTIONS $0^- 1/2^+ \to 0^- 3/2^+$. Gizbert-Studnicki, P.; Golemo, A.; Zalewski, K. (Jagellonian Univ., Krakow (Poland). Dept. of Theoretical Physics). Feb 1970. 21p. Dep. NTIS (U. S. Sales Only).

A Regge pole model for the reactions $\pi N \to \pi\Delta$, $\pi N \to \eta\Delta$ and $KN \to K\Delta$ is proposed. The description of the decay distributions and differential cross sections is good. The model contains six free parameters: the intercepts of the ρ and A_2 trajectories, a universal slope, the η, η' mixing angle, and two coupling constants. The number of free parameters is kept low by the use of the quark model and of the Veneziano formula for the residues. The predictions for the differential cross-sections of the π^+p processes at 16 GeV/c are also given. (auth)

3385 ANALYSIS OF THE SERPUKHOV TOTAL CROSS SECTION DATA WITH THE ALGEBRA OF VERTEX STRENGTHS. Horwitz, L. P. (Univ. of Denver); Ne'eman, Y. Nucl. Phys.; B23: 75-83(1970).

The energy dependence required of the CHN amplitudes by the Serpukhov data is studied. The behavior of the singlet-even amplitude is found to have a break. There may be systematic errors in the new data, but it appears that the universal couplings provided by CHN, with essentially the same D/F found at lower energies for the baryon-even amplitude couplings, still provide a consistent interpretation. (auth)

3386 APPLICATION OF THE VENEZIANO MODEL WITH PION AND POMERON EXCHANGE TO THE REACTION $K^-p \to nK^-\pi^+$ AT 10 GeV/c. Bartsch, J. (Technische Hochschule, Aachen); Deutschmann, M.; Honecker, R.; (and others). Nucl. Phys.; B23: 1-18(1970).

The generalized Veneziano model is applied to the reaction $K^-p \to nK^-\pi^+$ at 10 GeV/c. This reaction requires facing two of the major difficulties of the model, namely (i) pomeron exchange, (ii) dominant contribution of pion exchange, with possibility of some vector-meson contribution. The analysis is made first without pomeron exchange on a subset of the events, then on all events, with pomeron exchange included. It is found that though pion exchange is the dominant process, satisfactory descriptions of differential cross sections and longitudinal momentum distributions are obtained only when a contribution of about 15% from vector-meson exchange is included. Pomeron exchange, when considered, contributes about 25% of the cross sections. Most of the experimental distributions at 10 GeV/c are satisfactorily described, but the predicted variation of the cross section with incident momentum is different from experiment, indicating that the model, as employed, still has some difficulties. (auth)

3387 SUM RULES AND SYMMETRIES. Gunson, J. Russell (Carleton Univ., Ottawa). Can. J. Phys.; 48: 2376-82(15 Oct 1970).

The results of saturating sum rules are shown to be the same as those obtained previously in a bootstrap model. It is also shown how these models tie in with intermediate coupling theory of Kuriyan and Sudarshan, which explains why higher symmetry results are obtained from these models. It is then demonstrated how certain amplitudes correspond to specific t-channel spin, in the p-wave limit. Because of this, spin-symmetric results are obtained. Finally a soluble model is presented, in which the mass of the isobars is linear in isospin. (auth) (Canada)

3388 FURTHER EVIDENCE FOR EXCHANGE DEGENERACY WITH SU(3) SYMMETRY AND ABSORPTIVE CORRECTIONS IN HYPERCHARGE-EXCHANGE REACTIONS. Meyers, C.; Noirot, Y.; Rimpault, M.; Salin, Ph. (Faculte des Sciences, Bordeaux). Nucl. Phys.; B23: 99-115(1970).

All hypercharge- and charge-exchange reactions for meson-baryon scattering ($0^- 1/2^+ \to 0^- 1/2^+$) are analyzed with exchange degeneracy, SU(3) symmetry and absorptive corrections. Good agreement for polarization and differential cross sections, including the line-reversed reactions $K^-p \to \pi^-\Sigma^+$ and $\pi^+p \to K^+\Sigma^+$, is obtained in terms of essentially a single parameter. (auth)

3389 APPLICATION OF MULTI-REGGE THEORY TO PRODUCTION PROCESSES. Lipes, Richard G. (California Inst. of Tech., Pasadena). Nucl. Phys.; B24: 16-46(1970).

Both kinematic (phase space) and dynamical aspects of production processes are described and reviewed within the framework of multi-Regge theory. Those techniques that rely on additional theoretical assumptions are not treated. As an illustrative example, the case of three-body final states is developed in considerable detail. A simplified multi-Regge amplitude is assumed and formulas for the resulting differential cross sections are given. The emphasis of this work is the analysis of experimental data containing potential multi-Regge events. (auth)

3390 REGGE-CUT EFFECTS IN PION-NUCLEON SCATTERING. Carreras, B.; White, J. N. J. (Daresbury Nuclear Physics Lab., Eng.). Nucl. Phys.; B24: 61-76(1970).

A detailed calculation of absorptive-model Regge-cut corrections in πN elastic and charge-exchange scattering is presented, for energies above 5 GeV and momentum transfers <1 $(GeV/c)^2$, with particular regard to the dependence on the elastic spin-flip amplitudes. (auth)

3391 FITTING $K^-p \to \bar{K}^0\pi^-p$ WITH A GENERALIZED VENEZIANO MODEL. Schreiner, Philip A. (Univ. of California, Los Angeles); Stork, Donald H.; Clark, Allan G.; Saxon, D.; Lyons, L. Nucl. Phys.; B24: 157-64(1970).

Fits are made to new $K^-p \to \bar{K}^0\pi^-p$ data at 3.3 GeV/c with a generalized Veneziano model that includes both vector and pseudoscalar exchanges. Tests of the exchange degeneracy properties of the Regge trajectories show that the model prefers exchange degeneracy of the K*(890) and non-exchange degeneracy of the $\Delta(1238)$. Several defects in the model are noted. (auth)

3392 REACTION $\pi^-p \to \pi^0\pi^0n$ AT T_π = 378 MeV AND THE S-WAVE $\pi\pi$ PHASE SHIFT. Botke, J. C. (Univ. of California, San Diego, La Jolla). Nucl. Phys.; B23: 253-68(1970).

A phenomenological study of the reaction $\pi^-p \to \pi^0\pi^0n$ at an incident pion kinetic energy of 378 MeV is conducted within the framework of the isobar model. Through a study of both the total

XUM

and differential cross-section data, constraints on both the elastic partial-wave absorption parameters and the J = I = 0 $\pi\pi$ phase shift are obtained. In particular, $\alpha_0 = 0.2^{+0.8}_{-1}\ \mu^{-1}$ is found. (auth)

3393 K^+p PHASE SHIFT ANALYSIS. Carreras, B. (Daresbury Nuclear Physics Lab., Eng.); Donnachie, A. Nucl. Phys.; B23: 525-32(1970).

Two phase-shift-analysis solutions in K^+p scattering are presented, both with an attractive S-wave. The consistency of the solutions with dispersion-relation calculations is discussed. (auth)

3394 COMPARISON OF NUCLEON FORM FACTORS OBTAINED FROM THE VENEZIANO MODEL WITH EXPERIMENT. Konetschny, W. (Technische Hochshule, Vienna); Majerotto, W. Lett. Nuovo Cim.; 4: 883-6(7 Nov 1970).

In previous work a simple Veneziano model was assumed for the baryonic matrix elements of the vector and axial currents. Under certain assumptions formulas for the isovector form factor of the nucleon and for the weak axial form factor could be derived and are given. The nucleon form factor is also expressed in terms of the Sachs form factors, which are more appropriate for analysis of experimental data. In this way the isovector and isoscalar nucleon form factors are found, listed, and compared with experiment. (J.F.P.)

3395 FACTORIZATION TEST FOR THE POMERANCHUKON IN THREE-PARTICLE FINAL STATES. Bari, M. B. (Univ. of Durham, Eng. Univ. of Islamabad, Rawalpindi, Pakistan); Razmi, M. S. K. Phys. Rev., D; 2: 2054-6(1 Nov 1970).

A factorization test for the Pomeranchukon is suggested for reactions with three particles in the final state. It is applied to the available experimental data on $\pi N \to \pi\pi N$ and $NN \to \pi NN$ and is found to be satisfied reasonably well. (auth)

3396 FIXED-u FINITE-ENERGY-SUM-RULE CALCULATIONS AND THE CERN πN AMPLITUDES. Sowash, Laurence J.; Signell, Peter (Michigan State Univ., East Lansing). Phys. Rev., D; 2: 2096-8(1 Nov 1970).

It is shown that Regge asymptotic πN scattering amplitudes constructed from the CERN model-independent experimental (EXP) phase shifts possess better convergence properties than the same amplitudes constructed from the CERN resonance-model dispersion-relation (TH) phases used previously in fixed-u finite-energy sum rules. The EXP phases provide a better description of the πN data since they are fitted to them directly, while the TH phases are only an attempt to approximate the EXP phases by a resonance model satisfying dispersion-relation constraints. However, substituting the EXP phases for the TH ones does not greatly alter the sum-rule results. The calculations are also extended to higher moments and suggestions are made for improving the calculation. (auth)

3397 MESON–BARYON INTERACTIONS WITH BROKEN SU(3) AND THE BARYON SPECTRUM IN RELATIVISTIC QUANTUM MECHANICS. Katz, J. (Purdue Univ., Lafayette, Ind.); Wagner, S. Phys. Rev., D; 2: 2070-81(1 Nov 1970).

The multichannel relativistic Schrödinger equation is solved for the $\frac{1}{2}^+$ and $\frac{3}{2}^+$ partial-wave amplitudes and their Regge recurrences with an energy-dependent potential obtained by computing the baryon-exchange contribution to the pseudoscalar-meson–baryon interaction. As discussed previously, the model yields the usual $\frac{3}{2}^+$ decuplet and predicts in addition a 27-dimensional representation and a radially excited decuplet in this partial wave. It is shown that in the range of parameters which fit the usual decuplet, there are also decuplet orbital excitations in the $\frac{7}{2}^+$ and $\frac{11}{2}^+$ partial-wave amplitudes which correspond to the known experimental resonances. The $\frac{1}{2}^+$ octet is obtained as deeply bound states, and a second $\frac{1}{2}^+$ octet or a $\overline{10}$ representation is predicted, depending on whether the F/D ratio is less than or greater than 0.34. In addition, an orbital excitation of the octet occurs in the $\frac{5}{2}^+$ partial-wave amplitude at very high energies. The P-wave phase shifts are in qualitative agreement with experiments, but there are deviations for the P_{33} effective range near threshold and for the P_{13} phase shifts at higher energies. (auth)

3398 MESON–NUCLEON SCATTERING AND ASYMPTOTIC CONSERVATION OF HELICITY. Pfeffer, Robert (Stevens Inst. of Tech., Hoboken, N. J.); Cheng, Wen-kwei; Dutta-Roy, Binayak; Renninger, George. Phys. Rev., D; 2: 1965-9(1 Nov 1970).

The validity and consistency of the hypothesis of asymptotic conservation of s-channel helicity, and the dynamical hypothesis that the P′ Regge trajectory decouples from the A amplitude in πN and KN diffraction scattering are described. Sum rules which follow from these hypotheses are shown to be quite consistent with the experimental data. (auth)

3399 KINEMATICS OF PRODUCTION PROCESSES AT HIGH ENERGY AND THE REGGE-POLE HYPOTHESIS. Luxton, G. (California Inst. of Tech., Pasadena). Contract AT(11-1)-68. Phys. Rev., D; 2: 1926-34(1 Nov 1970).

Production processes are examined in the limit of infinite energy at points at which the kinematics simplifies. In the limit of zero momentum transfer to one of the outgoing particles, and subject to a condition on the transverse momentum of this particle, it is found that the momenta in a crossed channel tend to a collinear limit. This result is shown to yield nontrivial information concerning the direct-channel reaction, and predictions are made for the reactions $\pi N \to \pi\pi N$ and $\pi N \to \pi\rho N$. The latter prediction is compared with data that suggest that in a certain sense the Pomeranchon behaves like an ordinary Regge pole. Also, the Regge-pole contribution for a $2 \to 3$ process is examined at a momentum-transfer point of wrong signature, and a minimum is predicted for the reaction $\pi p \to \pi\eta n$ at $t_{pn} \simeq -0.5\ \mathrm{GeV}^2$, in the context of the Regge-pole model. (auth)

3400 VECTOR-MESON PRODUCTION IN MESON–NUCLEON COLLISIONS IN A QUARK MODEL. Chand, Ramesh (Inst. of Mathematical Sciences, Madras). Phys. Rev., D; 2: 1955-9(1 Nov 1970).

In an SU(3)-symmetric quark model, the production of vector mesons in high-energy $PN \to VB$ collisions is investigated in the crossed t channel. It is assumed that the physical baryon octet is given by $8(\text{physical}) \equiv 8' \cos\theta + 8 \sin\theta$, where 8 and 8′ octets arise from $3 \otimes \bar{3}$ and $3 \otimes 6$, respectively. It is found that the value $\theta = 20^\circ$, which leads to predictions in reasonable agreement with the available data on high-energy meson–baryon scattering and the photoproduction of pseudoscalar mesons, is also consistent with the available data on the vector-meson production. Also, independently of the mixing angle θ, a number of sum rules are obtained. (auth)

3401 APPLICATION OF THE HARD-PION METHOD TO THE BARYON–MESON FOUR-POINT FUNCTIONS. Matolcsi, Tamas (Computer Center, Budapest); Nagy, Tibor. Magy. Fiz. Foly.; 18: 151-61(1970). (In Hungarian).

A new summation method was developed for evaluating the σ terms on the basis of correlations involving the 3-point function. The 3-point and 4-point functions containing 2 baryon spaces were treated by the hard-pion method; this method may be used to describe the interactions between baryons and mesons. The results were applied to the study of the $B \to B'\pi\, l\nu$ decays. Comparison of the results with those obtained by soft-pion calculations revealed that the coefficients are either identical or quite similar. Nonleptonic decays are also examined. (TTT)

3402 COMPLEX REGGE POLES IN THE CUT j PLANE: PION–NUCLEON CHARGE-EXCHANGE SCATTERING. Desai, Bipin R. (Univ. of California, Riverside); Kaus, Peter; Park, Robert T.; Zachariasen, F. Contract AT(11-1)-134 P107A. Phys. Rev. Lett.; 25: 2389-92(9 Nov 1970).

The structure of the pole-cut combination in πN charge-exchange scattering for $t \le 0$ is represented by a pair of complex poles. Excellent fits to the πN charge-exchange differential cross section, polarization, and total cross-section difference $\sigma_t(\pi^-p) - \sigma_t(\pi^+p)$ are obtained for the two examples considered, $\mathrm{Im}\alpha = g\sqrt{-t}$ and $\mathrm{Im}\alpha = g$. The phases of the residues are allowed to vary and a zero in $\mathrm{Im}A'^{(-)}$ (the "crossover" zero) is obtained. (auth)

3403 ON THE γ_5-GAUGE INVARIANCE AND HELICITY CONSERVATION IN HIGH-ENERGY MESON–BARYON SCATTERING. Sewerynski, M. (International Centre for Theoretical Physics, Trieste, Italy). Lett. Nuovo Cim.; 4: 819-24(31 Oct 1970).

The consequences of the γ_5-gauge invariance hypothesis are examined for meson–baryon scattering. The examples chosen are $0^- + \frac{1}{2}^+ \to 0^\pm + \frac{1}{2}^+$ and $0^- + \frac{1}{2}^+ \to 0^\pm + 3/2^+$ interactions. In the case of $0 + \frac{1}{2} \to 0 + \frac{1}{2}$ scattering the hypothesis of γ_5 gauge invariance automatically leads to the dominance of the helicity-nonflip amplitudes, that is to helicity conservation. For the case $0 + \frac{1}{2} \to 0 + \frac{3}{2}$, helicity is conserved if suitable high-energy behavior for B_1 (appearing in the T-matrix) is assumed. (J.F.P.)

3404 EXOTIC EXCHANGE STATE AND NEW SUM RULES. Seth, V. P. (Allahabad Univ., India). Progr. Theor. Phys. (Kyoto); 44: 432-6(Aug 1970).

Series of sum rules were obtained for the amplitudes of the scattering processes which has exotic state in its crossed channel and they are well satisfied when saturated with all the known intermediate states. (auth)

3405 DECAY WIDTHS OF RESONANCES AND COMPOSITE MODEL. THE LINEARITY OF g–J PLOT AND UNIVERSAL

QUARK COUPLING. Hirano, Masanobu; Ito, Akihiro; Iwata, Kenzo (Hokkaido Univ., Sapporo). Progr. Theor. Phys. (Kyoto); 44: 561-2(Aug 1970).

It is shown that the composite model, in which the baryon consists of quarks linked by harmonic oscillator potentials, predicts a regularity among decay widths for resonances with non-zero strangeness as well as zero-strangeness resonances such as N^- and Δ. It is found that the g-J plot of strange baryon resonances is almost parallel to that of N^-,Δ resonances, from which it is concluded that the interaction strength of all quarks is almost universal. (L.B.S.)

Strong (Baryon No. ≥ 2)

Refer also to abstracts 3721 and 3766.

3406 (IFVE-STF-69-71) $\bar{p}$-MESON PRODUCTION IN HIGH ENERGY PION-COLLISIONS WITH NUCLEI. Babaev, Z. R.; Balashov, V. V.; Korenman, G. Ya.; Korotkich, V. L.; Tecku, B. [Gosudarstvennyi Komitet po Ispol'zovaniyu Atomnoi Energii SSSR, Serpukhov. Institut Fiziki Vysokikh Energii]. 1969. 11p. (In Russian). Dep. NTIS (U. S. Sales Only).

On the basis of Glauber multiple scattering theory theoretical calculations of coherent and incoherent processes such as $\pi^-A \rightarrow \rho^-A^1$ and $\pi^-A \rightarrow \rho^0A^1$ are carried out. The calculations were made at the energy of 30 GeV of incident π-mesons on nuclei from A = 20 up to A = 208. Besides an estimation is made to compare analogous processes in selecting rules $\gamma A \rightarrow \pi^0 A$ at different energies. (auth)

3407 (JINR-E2-5329) POISSON DISTRIBUTION OF SECONDARY PARTICLES IN STRAIGHT-LINE PATHS APPROXIMATION. Barbashov, B. M.; Kuleshov, S. P.; Matveev, V. A.; Pervushin, V. N.; Sisakyan, A. N. (Joint Inst. for Nuclear Research, Dubna (USSR). Lab. of Theoretical Physics). 1970. 19p. Dep. NTIS (U. S. Sales Only).

The problem of multiple production of "soft" mesons in high-energy two-nucleon collisions is considered in the framework of standard quantum field theory models. The straight-line paths approximation is used to obtain the Poisson distribution of the secondary particle number and to investigate the average particles as a function of the choice of the integral cutoff parameters in various asymptotic regions. (auth)

3408 THE dpn AND tdn COUPLING CONSTANTS FROM FORWARD NEUTRON-DEUTERON DISPERSION RELATIONS. Locher, M. P. (Massachusetts Inst. of Tech., Cambridge). Contract AT(30-1)-2098. Nucl. Phys.; B23: 116-24(1970).

Forward dispersion relations for nd scattering using unpolarized total cross sections are evaluated at low energies (E_{lab} < 20 MeV). Comparison with real parts deduced from near forward differential cross sections allows the coupling strengths of the nearlying p- and t-pole to be determined in an attractively direct way, free from theoretical information on nd amplitudes, in principle. The present best fit gives a very consistent picture. The dnp strength is right on the value deduced from triplet np scattering, indicating a quite accurate determination of the (less well known) tnd coupling constant. (auth)

3409 RELATIVISTIC DISPERSION THEORY OF THE DEUTERON STRUCTURE. Bebel, D.; Biebl, K. J. (Humboldt-Univ., Berlin). Nucl. Phys.; B24: 187-205(1970).

Integral equations for the imaginary parts of the πdNN scattering amplitudes are obtained which allow the calculation of the imaginary parts of the dNN vertex-function invariants including one-, two- and three-pion exchange effects in the anomalous region and in the nearby part of the normal spectrum. In the anomalous region the equations can be exactly solved by a finite number of iterations yielding recursive formulas for the vertex-function discontinuities across the three iterative anomalous branch cuts t_n connected with n-pion exchange. The formalism is especially appropriate for the calculation of corrections to the ladder approximation (e.g., contributions from vertex diagrams with crossed pion lines) and for the calculation of the deuteron Regge-vertex function. (auth)

3410 ROPER RESONANCE AND THE SHORT-RANGE STRUCTURE OF THE DEUTERON. Weber, H. J. (Univ. of Virginia, Charlottesville). Nucl. Phys.; B24: 206-10(1970).

The structure of the nucleon is used to describe the high-momentum region of the deuteron. In particular, the reaction $pp \rightarrow d\pi^+$ at threshold is analyzed in terms of a nucleon and a Roper-resonance pole. (auth)

3411 ANALYSIS OF DIFFERENTIAL AND TOTAL CROSS-SECTION DATA FOR HIGH-ENERGY pp AND p anti p INTERACTIONS. Drechsler, Wolfgang; Suaya, Roberto (Stanford Univ., Calif.). Phys. Rev., D; 2: 1879-83 (1 Nov 1970).

An analysis of pp and $p\bar{p}$ data in terms of a K-matrix model for the Pomeranchuk exchange and the absorptive corrected P′ and ω Regge-pole contributions is presented. The model provides a quantitative understanding of high-energy pp and $p\bar{p}$ total cross-section measurements and the measured ratio of the real to the imaginary part of the pp elastic forward scattering amplitude. The structure observed in $(d\sigma/dt)_{p\bar{p}}$ around $t = -0.8$ GeV^2 and in $(d\sigma/dt)_{pp}$ at $t = -1.2$ GeV^2, the shrinkage patterns in both differential cross sections, and the crossover phenomenon are explained in the framework of this model. (auth)

3412 SHADOW CORRECTION IN DEUTERIUM. Rudin, Robert A. (Cooper Union, New York). Phys. Rev., D; 2: 1869-70(1 Nov 1970).

The cross-section defect for high-energy hadron–deuteron scattering is calculated by two methods. The widely employed "shadow" correction is shown to give a larger value than the "eikonal" calculation. A new black-sphere derivation is presented which supports the "eikonal" result. The calculation chosen may significantly affect the analysis of experimental data. (auth)

3413 OPTICAL MODEL OF ELASTIC PROTON–PROTON SCATTERING. Weingarten, Donald (National Accelerator Lab., Batavia, Ill.). Phys. Rev., D; 2: 1939-44(1 Nov 1970).

The energy and momentum-transfer dependence of the differential cross section ($k_\perp \gtrsim 0.8$ GeV/c, $k_{lab} \gtrsim 8$ GeV/c), the position of "breaks;" and the parameter $b = [\partial \ln (d\sigma/d\Omega)/\partial t]_{t=0}$ are reproduced by a smooth absorber determined by two energy-independent parameters. It is assumed that the absorber representing a proton flattens in a manner suggested by the Lorentz transformation. (auth)

3414 FIELD-THEORETICAL NUCLEON–NUCLEON POTENTIAL. Partovi, M. Hossein; Lomon, Earle L. (Massachusetts Inst. of Tech., Cambridge). Contract AT(30-1)-2098. Phys. Rev., D; 2: 1999-2032(1 Nov 1970).

A formulation is presented for the derivation of a Schrödinger-equation potential from a field-theoretical model. The relativistic two-body equation of Bethe and Salpeter is reduced using a generalization of the Blankenbecler–Sugar method. The resulting equation is shown to be identical with the nonrelativistic Lippmann–Schwinger equation upon a unitarity-preserving identification of the amplitudes. An equivalent potential is thereby defined and expressed as a solution of an integral equation. The second- and fourth-order potentials are calculated, and their energy dependence and nonlocality are studied. An approximation scheme is developed for expanding the configuration-space potentials in the powers of the momentum operator. Terms up to and including the first power are retained, giving rise to a potential composed of central, spin-orbit, tensor, and spin–spin parts. The contributions of the meson resonances η, ρ, and ω are included to second order. The complete potential is numerically calculated using masses and coupling parameters taken from meson experiments; no parameter of the potential is searched upon. The resulting potential is remarkably similar to that of Hamada and Johnston (outside half a pion Compton wavelength), particularly for the parts that are relatively well determined by nucleon–nucleon scattering data. Further extensions of the program, including the treatment of the nucleon resonances and pair suppression, are discussed, and an outline of such extensions is given. (auth)

3415 DEUTERON–DEUTERON SCATTERING AT 2.2 AND 7.9 GeV/c: THEORETICAL INTERPRETATION. Goshaw, A. T. (Princeton Univ., N. J.); Oddone, P. J.; Bazin, M. J.; Sun, C. R. Contract AT(30-1)-2137. Phys. Rev., D; 2: 2057-60(1 Nov 1970).

Franco's treatment of dd elastic scattering is extended by including the quadrupole deformation of the deuteron. The results of numerical computations of the cross sections at 2.2 and 7.9 GeV/c are presented where comparison with experimental results is possible. (auth)

3416 ONE-BOSON-EXCHANGE POTENTIAL MODEL FOR THE AN INTERACTION. Brown, J. T. (Colorado School of Mines, Golden); Downs, B. W.; Iddings, C. K. Contract AF-AFOSR-30-67. Ann. Phys. (N. Y.); 60: 148-87(Sep 1970).

A one-boson-exchange potential model for the AN interaction is described. The effect of the ΣN channel is included explicitly. The potential includes contributions from the following bosons: pseudoscalar and vector octets, and scalar and vector unitary singlets. The approximations needed to obtain a potential for a general baryon–baryon interaction are discussed, and certain ambiguities are pointed out. In particular, it is considered to what extent the addition of momentum-dependent corrections would be an improve-

XUM

ment over the extreme nonrelativistic limit. By numerical calculations, the parameters of the model are then adjusted to reproduce experimental low-energy Λp data. SU(3) is used to relate the meson–baryon couplings. The principal search parameters are the mass and coupling of the scalar unitary singlet boson, the vector coupling of the vector unitary singlet boson, and the radius of a phenomenological spin-independent hard core. Λp cross sections are then calculated from zero energy up through the Σ-production threshold. Some of the ambiguities present in a local potential are investigated numerically. For this model it is found that the values of the search parameters are not especially sensitive to these ambiguities. (auth)

3417 ENERGY DEPENDENCE OF THE SLOPE OF THE FORWARD PEAK IN ELASTIC PROTON–PROTON SCATTERING. Kawasaki, Mamoru; Kobayashi, Masanori; Yonezawa, Minoru (Hiroshima Univ.). Progr. Theor. Phys. (Kyoto); 44: 557-8 (Aug 1970).

A simple diffraction model is discussed that explains the shrinkage of the forward peaks observed in recent Serpukhov data for elastic p + p interactions above 20 GeV/c. (L.B.S.)

3418 HIGH-ENERGY PROTON–PROTON SCATTERING. ABSORPTION EFFECT AND ONE-BOSON-EXCHANGE CONTRIBUTION. Sato, Sukeyo; Ueda, Tamotsu (Osaka Univ.). Progr. Theor. Phys. (Kyoto); 44: 419-31(Aug 1970).

Proton–proton scattering at high energy (E_{lab} = 5 to 31 GeV) is studied in terms of the one-boson-exchange model with form factors and absorption effects. The polarizations and the real-imaginary ratios of the forward amplitude are well reproduced with parameters which are adjusted so as to fit the differential cross sections. It is pointed out that these two observables embody a property of vector-meson-exchange contribution. An energy-dependent vector-meson coupling constants is chosen. Related problems are discussed. (auth)

3419 SIMPLE MODEL FOR WIDE-ANGLE, HIGH-ENERGY, ELASTIC, PROTON–DEUTERON SCATTERING. Pazdzerskii, V. I. (Tashkent State Univ.). Izv. Akad. Nauk Uzb. SSR, Ser. Fiz.-Mat. Nauk; No. 2, 85-6(1970). (In Russian).

Wide-angle pd scattering at energies above 1 GeV is characterized by a large back-scattering peak which decreases rapidly as the energy increases. Scattering of the high-energy particles on deuterons is expressed by the impulse approximation which corresponds to single scattering, yielding a forward-scattering peak, while Glauber's correction takes the double scattering into account. However, this does not explain the back-scattering effects, which require the presence of a similar particle. A potential mechanism able to explain the appearance of a back-scattering peak is described; it involves a double, high-energy forward scattering and substitution of the protons in the deuteron. The model proposed by K. Foley et al. was used to obtain the 2-particle amplitude. The calculations were carried out for Gaussian, Hulten and exponential functions. The model was found to describe satisfactorily the value of the observed angular distribution in the range of the back-scattering range, to cos $\theta = -0.7$. (TTT)

Particle Invariance Principles and Symmetries

Refer also to abstracts 3349 and 3432.

3420 (IFVE-STF-69-102) ON ONE REALIZATION OF REPRESENTATIONS OF THE QUATERNION GROUP. Leznov, A. N.; Fedoseev, I. A. (Gosudarstvennyi Komitet po Ispol'zovaniyu Atomnoi Energii SSSR, Serpukhov. Institut Fiziki Vysokikh Energii). 1969. 7p. (In Russian). Dep. NTIS (U. S. Sales Only).

The representations of the quaternion group are realized in the space of functions on its maximal compact subgroup. The character of the representations is found, and the equations for the invariant Hermitian form are given. (auth)

3421 (KFKI-70-19-HEP) SL(2,C) REPRESENTATIONS IN EXPLICITLY ENERGY DEPENDENT BASIS. II. Szego, K.; Toth, K. (Magyar Tudomanyos Akademia Kozponti Fizikai Kutato Intezete, Budapest). [1969]. 15p. Dep. NTIS (U. S. Sales Only).

A systematic treatment is presented for the transformation matrix elements between different types of basis sets in the SL(2,C) representation space and for the boost matrix elements. The treatment is based on the theory of invariant bilinear functionals and makes use of the knowledge of explicit basis functions. New expressions are given for the SU(2) ⇌ E(2) and SU(1,1) ⇌ E(2) overlap functions, and it is shown, that they can be considered as Fourier-transform of a function, which is also known. Some relations are proved between boost functions and transformation matrix elements. A new and relatively simple expression is derived for the boost matrix elements $d^{j\sigma\sigma}_{jmj'}(\xi)$ in SU(2) basis. (auth)

3422 SOME RESULTS ON THE ALGEBRAIC REALIZATION OF CHIRAL SU(2) x SU(2) SYMMETRY. Collins, P. V.; Renner, B. (Cambridge Univ., Eng.). Nucl. Phys.; B23: 436-44 (1970).

The saturation of generalized Adler–Weisberger relations is considered, and certain results of Gilman and Harari are derived; among these the approximate relation $m_A^2 \approx 2m_\rho^2$, from weaker assumptions than have been reported before. (auth)

3423 TIME-REVERSAL VIOLATION AND THE ARROWS OF TIME. Aharony, A. (Tel-Aviv Univ., Israel); Ne'eman, Y. Lett. Nuovo Cim.; 4: 862-6(7 Nov 1970).

The relation of a microscopic arrow of time to the behavior of the neutral-kaon beam is discussed. Also the relations of this microscopic arrow of time with the cosmological and thermodynamical arrows are considered. (J.F.P.)

3424 ELECTROMAGNETIC FINAL-STATE INTERACTIONS AND TESTS OF TIME-REVERSAL INVARIANCE IN NUCLEAR BETA DECAY. II. Brodine, John C. (Carnegie-Mellon Univ., Pittsburgh). Phys. Rev., D; 2: 2090-3(1 Nov 1970).

Expressions are given for the electromagnetic final-state interaction contribution to D, the triple-product correlation coefficient, in the nuclear β-decay transitions $\frac{1}{2}^+ \to \frac{3}{2}^+$, $\frac{3}{2}^+ \to \frac{5}{2}^+$, and $\frac{1}{2}^+ \to \frac{1}{2}^+$ to all orders of $Z\alpha/v_e$ in the Coulomb interaction. The contribution to D from the final-state magnetic scattering is investigated to order α. (auth)

3425 POSSIBLE NONELECTROMAGNETIC VIOLATION OF ISOSPIN, CHARGE-CONJUGATION, AND TIME-REVERSAL INVARIANCE BY AN INTERACTION AT THE LEVEL OF ELECTROMAGNETISM. Pati, Jogesh C. (Univ. of Maryland, College Park). Phys. Rev., D; 2: 2061-70(1 Nov 1970).

It is proposed that there exists a basic interaction L_V, not involving the photon, whose strength is similar to that of electromagnetism and which violates isospin, C, CP, and T invariance "maximally," while conserving P and CT. Simultaneously, it is assumed that electromagnetism conserves C, CP, and T. It is proposed that such an interaction arises through the coupling of a vector-meson field V^0_μ to a hadronic current $J_{V\mu}$ with strength g_V comparable to the electric charge e (if V^0 is not too heavy). It is also assumed that V^0 is not involved in other basic interactions (apart from gravity). Some arguments are provided to show that V^0 should be heavier than at least $3m_\pi$. Possible ways of producing and detecting the V^0 meson, which acts as an I-spin schizon like the photon, are discussed. It is suggested that the problem of the sign of the n–p mass difference and that of the forbiddenness of the $\eta \to 3\pi$ decay based on partial conservation of axial-vector current, current algebra, softness of any one pion, and the conventional electromagnetic interaction, may be resolved owing to the existence of the V^0 interaction. A specific model for L_V, based on Lévy's generalization of the σ model to SU(3), is presented to demonstrate that $\eta \to 3\pi$ forbiddenness is avoided in this model via the contribution of the V^0 interaction. One expects to see (under the proposed hypothesis) noticeable $\pi^+ - \pi^-$ energy asymmetry in the $\eta \to \pi^+ + \pi^- + \pi^0$ decay, no such asymmetry in the $\eta \to \pi^+ + \pi^- + \gamma$ decay, no noticeable T-violating effects in the $\gamma + d \rightleftharpoons n + p$ reactions, and an electric dipole moment of the neutron in the region $10^{-22} - 10^{-23}$ e cm. It is suggested that these measurements should enable a choice to be made between L_V and other existing theories of CP violation. (auth)

3426 27-PLET UNITARY SYMMETRY OPERATOR. Castilho Alcaras, J. A. (Duke Univ., Durham, N. C.); Biedenharn, L. C.; Hecht, K. T.; Neely, G. Contract Nonr-1224(59). Ann. Phys. (N. Y.); 60: 85-147(Sep 1970).

The unitary spin-tensor operator transforming as the representation [4 2 0] in SU(3) (the 27-plet) is discussed in detail. Using a recent result for the unique (nonarbitrary) splitting of the multiplicity, complete algebraic formulas are determined for the complete 27-plet operator. Symmetry properties of the 27-plet operator are given. Applications to both particle and nuclear physics are discussed. (auth)

3427 SEARCH FOR VIOLATION OF CP INVARIANCE IN τ^4 DECAY. Ford, W. T.; Piroue, P. A.; Remmel, R. S.; Smith, A. J. S.; Souder, P. A. (Princeton Univ., N. J.). Contracts NOO14-67-A-0151; AT(30-1)-2137; AT(30-1)-4159. Phys. Rev. Lett.; 25: 1370-3(9 Nov 1970).

A comparison of the Dalitz-plot distributions of 1.6 million τ^+ decays ($K^+ \to \pi^+\pi^+\pi^-$) and an equal number of τ^- decays is given. No significant asymmetry was found in any region of the plot. In

XUM

terms of the difference in the slope parameters a^+ and a^- for the odd-pion c.m.-energy spectra, the asymmetry is $\Delta = (a^+ - a^-)/(a^+ + a^-) = -0.0070 \pm 0.0053$. Also a preliminary result is presented for the slope parameter itself: $a = 0.283 \pm 0.005$. New measurements of the τ^+ decay rates and their difference confirm previous results. (auth)

3428 CHIRAL SYMMETRY IN THE UNIFIED FERMION THEORY. II. LINEARIZATION. Arafune, Jiro; Hiida, Kichiro; Ohta, Tadayuki (Tokyo Univ.). Progr. Theor. Phys. (Kyoto); 44: 512-32(Aug 1970).

Chiral U(n) × U(n) transformations are investigated in the unified theory of the fundamental Dirac field q. The transformation laws are nonlinear with respect to q. It is shown in the unquantized theory that the laws can be linearized by the redefinition of the field, Q = Uq, where U is a unitary matrix depending on q and q*. Discussions are given on the conditions that U is non-singular as a function of q and q* at the origin, q = q* = 0. It is shown that the transformation from q to Q is in general neither canonical in the unquantized theory nor unitary in the quantized theory. (auth)

3429 POSSIBLE CPT NONCONSERVATION IN K^0 DECAY. Kitani, Kohei (Tokyo Inst. of Tech.). Progr. Theor. Phys. (Kyoto); 44: 500-11(Aug 1970).

A consistent model example of field theory is presented in which CPT nonconservation is allowed. This is the generalization of the model proposed previously on $K_L \to 2\pi$ with CPT nonconservation which is based on the fact that there exist two sets of field operators for a pair-conjugate isomultiplet and that in the case of half-integer isospin these two sets of field operators are connected nonlocally with each other and transformed differently under the CPT transformation. It is found from the causality condition that only the decay process of a pair-conjugate multiplet with half-integer isospin into "neutral state" allows CPT nonconservation. Some discussions on CP- and possible CPT-nonconserving K^0 decay $K_L \to 2\pi$, $\pi l\nu$ are given and possible CPT nonconserving processes are enumerated. (auth)

Field Theories

General

3430 (JINR-P2-5373) ON THE INVARIANCE OF THE NONRELATIVISTIC HAMILTONIAN-JACOBI EQUATION IN THE PRESENCE OF THE ELECTROMAGNETIC FIELD. Strel'tsov, V. N. (Joint Inst. for Nuclear Research, Dubna (USSR). Lab. of High Energy). 1970. 5p. (In Russian). Dep. NTIS (U. S. Sales Only).

It is shown that the nonrelativistic Hamiltonian-Jacobi equation for a particle in the electromagnetic field is invariant relative to nonrelativistic "phase" transformations. (auth)

3431 GEODESICS AND THE LYTTLETON-BONDI ELECTRODYNAMICS. Burman, R. R. (Univ. of Western Australia, Perth). Phys. Lett.; 32A: 448(7 Sep 1970).

Paths of charged particles in the Lyttleton-Bondi electrodynamics are expressed as geodesics of an affine connection. (auth)

3432 RELATIVISTIC SYMMETRY GROUPS OF UNIFORM ELECTROMAGNETIC FIELDS. Janner, A. (Katholieke Univ., Nijmegen, Netherlands); Ascher, E. Physica; 48: 425-46 (31 Aug 1970).

The relativistic symmetry group of a uniform electromagnetic field (space- and time-independent) is defined as the largest subgroup of the Poincaré group leaving the corresponding electromagnetic field tensor invariant. It is shown that all such relativistic symmetry groups are semi-direct products of the group of all translations in space and time by the relativistic point group (the homogeneous symmetry group) of the field. They are larger than the corresponding Shubnikov groups usually indicated as symmetry groups of electromagnetic fields in space-time. The determination of the point groups gives insight into methods useful for deriving relativistic symmetry groups. The isomorphism and homeomorphism classes as well as the geometric classes of relativistic point groups are established. (auth)

Quantum Field Theory

Refer also to abstract 3428.

3433 (ITF-70-33) ON THE REPRESENTATION OF THE JOST-LEHMANN-DYSON TYPE. Vladimirov, V. S.; Zharinov, V. V. (Akademiya Nauk Ukrainskoi SSR, Kiev. Institut Teoreticheskoi Fiziki). 1970. 25p. Dep. NTIS (U. S. Sales Only).

The integral representation is obtained for functions holomorphic in tube domains over arbitrary proper cones C and -C and in a neighborhood of a real n-divided open set φ, and belonging to the algebras H(C) and H(-C). As an application the corresponding Jost-Lehmann-Dyson type representation is derived. Reported at the Seminar of the Department of Mathematical Methods in Theoretical Physics. (auth)

3434 (JINR-P2-5363) INVARIANTS IN THE NONRELATIVISTIC APPROXIMATION. Strel'tsov, V. N. (Joint Inst. for Nuclear Research, Dubna (USSR). Lab. of High Energy). 1970. 6p. (In Russian). Dep. NTIS (U. S. Sales Only).

The procedure of proving the invariability of the known invariants of special theory of relativity in nonrelativistic and Galilean approximation is discussed. (auth)

3435 (TPJU-13/70) EXAMPLES OF QUANTUM FIELD THEORIES WITHOUT DIVERGENCES. Rayski, Jerzy (Jagellonian Univ., Krakow (Poland). Dept. of Theoretical Physics). May 1970. 12p. Dep. NTIS (U. S. Sales Only).

The field concept is considered. Then the examples of a bounded interaction and of a temperate action are treated. (J.F.P.)

3436 BETHE-SALPETER EQUATION. THE WARD-TAKAHASHI IDENTITY AND THE LADDER APPROXIMATION. Golden, J. M. (Univ. of Edinburgh). Nucl. Phys.; B23: 19-36 (1970).

The Ward-Takahashi identity for composite particles is derived and the triangle approximation to the vertex function of a composite particle is discussed. The method of stereographic transformation applied to the scalar-scalar equation in the ladder approximation is generalized. The generators of the O(4) symmetry exposed by this method are shown to be hermitean in a physical scalar product. A perturbation calculation is carried out from a known exact solution. An ansatz for the spinor-antispinor bound state amplitude is made and the resulting equations are simplified with the help of certain identities, involving the O(4) spherical harmonics, which are derived. (auth)

3437 GAUGE INVARIANCE AND THE CHARGE OPERATOR IN THE HEISENBERG PICTURE. Pugh, R. E. (Univ. of Toronto). Can. J. Phys.; 48: 2101-6(15 Sep 1970).

The transformations of the renormalized interpolating fields generated by the gauge transformation of the free asymptotic fields restrict the interpolating fields to satisfying certain commutation rules. These commutation rules, in turn, give a non-phenomenological charge operator for the interpolating Heisenberg fields. Redundant states and the eigenvalue problem with the indefinite metric are discussed. (auth) (Canada)

3438 VALIDITY OF QUANTUM ELECTRODYNAMICS. Niederle, Jiri; Tolar, Jiri (CSAV, Prague). Cesk. Cas. Fys.; 20: 274-88(1970). (In Czech).

The present status of the validity of quantum electrodynamics is dealt with and, in particular, low- and high-energy test experiments. (auth)

3439 BHABHA'S EQUATION AND THE ELECTROMAGNETIC FIELD. Baisya, H. L. (Trinity Coll., Dublin). Nucl. Phys.; B23: 633-40(1970).

The electromagnetic interaction of the Bhabha field with spin $^3/_2$ and two-mass states is discussed and the quantization is performed. It is shown using the Bhabha theory that $\psi(x) = \psi(x|\sigma)$ holds even for spin $^3/_2$ field. (auth)

3440 QUANTIZATION OF INTERACTING FIELDS. Henneberger, Walter C. (Southern Illinois Univ., Carbondale. Univ., Wuerzburg, Ger.). Nucl. Phys.; B23: 365-75(1970).

It is shown that the canonical quantization scheme does not lead to a unique formulation of quantum field theory because of the freedom to make time dependent unitary transformations involving a (classical) Boson field, before quantization. As examples, alternative formulations of both non-relativistic and relativistic quantum electrodynamics, in agreement with the correspondence principle, are given. These yield an S-matrix which is free of all divergences, at least to the second order. (auth)

3441 FOLDY-WOUTHUYSEN, LORENTZ, AND LORENTZ-TACHYON TRANSFORMATIONS. Saavedra, I. (Univ., Chile, Santiago). Lett. Nuovo Cim.; 4: 873-6(7 Nov 1970).

A compact algebra is applied to the free Dirac equation for the various wave equations which can be generated and the corresponding transformations, which are shown to be the tilting operators for each case. The tilting operators appearing in the formalism are, on the one hand, the Foldy-Wouthysen and the Cini-Touschek operators respectively and, on the other, the Lorentz transformation which takes the Dirac spinors to their

rest system form and a new transformation corresponding to a Lorentz–tachyon transformation, taking a Dirac tachyon to its transcendent state. (J.F.P.)

3442 EXPONENTIAL REPRESENTATIONS OF THE CANONICAL COMMUTATION RELATIONS. Fabrey, James D. (Massachusetts Inst. of Tech., Cambridge. Univ. of North Carolina, Chapel Hill). Commun. Math. Phys.; 19: 1-30(1970).

A class of representation of the canonical commutation relations is investigated. These representations, which are called exponential representations, are given by explicit formulas. Exponential representations are thus comparable to tensor product representations in that one may compute useful criteria concerning various properties. In particular, they are all locally, and nontrivial exponential representations are globally disjoint from the Fock representation. Also, a sufficient condition is obtained for two exponential representations not to be disjoint. An example is furnished by Climm's model for the $:\phi^4:$ interaction for boson fields in three space–time dimensions. (auth)

3443 FACTORIZATION AND DUALITY OF MULTILOOP DIAGRAMS. Ida, Masakuni; Matsumoto, Hideki; Yazaki, Shigeo (Tokyo Univ.). Progr. Theor. Phys. (Kyoto); 44: 456-72(Aug 1970).

Simple rules for expressing an arbitrary Feynman-like diagram in the harmonic oscillator formalism are given. They assure the full factorization and the duality relation in an obvious way. This is achieved by investigation of gauge properties of the three-resonance vertex. The correspondence of the present model with that of Kikkawa, Sakita and Virasoro is clarified by giving conventions which allow all dots attached to the resonance lines to be omitted. The problem of divergences is not discussed in this work. (auth)

3444 GAUGE, RENORMALIZATION, AND THE GOTO–IMAMURA–SCHWINGER TERM IN QUANTUM ELECTRODYNAMICS. Hayakawa, Mizuaki; Yokoyama, Kan-ichi (Hiroshima Univ.). Progr. Theor. Phys. (Kyoto); 44: 533-45(Aug 1970).

According to the conventional rules of calculation, the significance of the Gotō-Imamura-Schwinger term in quantum electrodynamics is investigated in connection with gauge and renormalization. The results are as follows: (1) If the G-I-S- term is present, the unrenormalized photon self-energy part defined in the Feynman gauge can be neither covariant nor gauge invariant. (2) The G-I-S term plays the role of changing the gauge of the photon propagation function pathologically. (3) Consequently, unless it is eliminated by some manipulation, covariant gauge formulation is generally impossible in the renormalization process. (auth)

3445 COMMENTS ON NISHIJIMA AND SATO'S PAPER ON THE HNZ CONSTRUCTION. Yoshimura, Tetz (Univ. of Adelaide). Progr. Theor. Phys. (Kyoto); 44: 548-9(Aug 1970).

Modifications of the arguments of Nishijima and Sato (Prog. Theor. Phys. 42: 692(1969)) on the HNZ construction of field operators for composite particles are considered without relying upon the perturbation theoretical estimation of divergences. (L.B.S.)

3446 QUANTUM THEORY OF WHEELER–FEYNMAN ELECTRODYNAMICS. Davies, P. C. W. (University Coll., London). Proc. Cambridge Phil. Soc.; 68: 751-64(Nov 1970).

A quantum mechanical theory of the action-at-a-distance electrodynamics of Wheeler and Feynman is given using an S-matrix approach. The response of the universe is introduced, and a perturbation expansion leads to the usual expression for the spontaneous transition rate between atomic energy levels, an effect normally attributed to quantized field oscillators. The Feynman propagator is then recovered, leading to the familiar self-energy formulas. Finally, a comparison of the formal structure of the new theory with the conventional is shown to establish a complete mathematical equivalence to all orders in the expansion. (auth) (UK)

Gravitation and General Relativity

Refer also to abstracts 2828, 2870, and 3343.

3447 (IFVE-SEF-69-59) GENERALIZATION OF THE TOLMAN EQUALITY. Folomeshkin, V. N. [Gosudarstvennyi Komitet po Ispol'zovaniyu Atomnoi Energii SSSR, Serpukhov. Institut Fiziki Vysokikh Energii]. 1969. 5p. (In Russian). Dep. NTIS (U. S. Sales Only).

The generalization of the Tolman equality $\int_0^R T_0^0 r^2 dr = \int_0^R (T_0^0 - T_\alpha^\alpha)\sqrt{-g}r^2 dr$, where R is the radius of a spherically-symmetric body in the case of an arbitary upper limit of the integration, is proposed. The obtained equality is given in a form: $T_1^1 r^3 = \int_0^r T_0^0 r^2 dr - (1/\sqrt{g})\int_0^r (T_0^0 - T_\alpha^\alpha)\sqrt{-g}r^2 dr$ and transfers into the usual Tolman equality at $r \gg R$. (auth)

3448 EQUATION FOR NONSTATIC MATTER DISTRIBUTIONS OF SPHERICAL SYMMETRY IN GENERAL RELATIVITY. Kuchowicz, Br. (Univ. of Warsaw). Phys. Lett.; 33A: 73-4 (5 Oct 1970).

A procedure for deriving exact solutions of the gravitational field equations is presented under the following assumptions: perfect fluid and isotropic pressure, a general metric of spherical symmetry, dependence of the metric tensor components on both r and t. This is an extension to the nonstatic case of a previously reported approach. Two examples of solutions are given, too. (auth)

3449 GRAVITATIONAL PRESSURE IN FRIEDMAN–LOBACHEVSKII SPACE. Fikhtengol'ts, I. G. (Leningrad Inst. of Precise Mechanics and Optics). Dokl. Akad. Nauk SSSR; 191: 1028-30(11 Apr 1970). (In Russian).

Space is described in terms of a fundamental tensor, and the Riemann tensor is derived. After suitable development of the space, time and gravity relations, a term is obtained that can be interpreted as a gravitational pressure (the pressure of gravitational radiation). An expression is obtained for the curvature of the space with the gravitational pressure being taken into account. (TTT)

3450 IMPOSSIBILITY OF A DEFOCUSING QUADRUPOLE-LENS SYSTEM. Moses, R. W. Jr.; Symon, K. R. (Univ. of Wisconsin, Madison). Phys. Rev. Lett.; 25: 1356-7(9 Nov 1970).

It is proven that in an orthogonal quadrupole system a beam entering parallel to the optic axis is necessarily brought to at least one point or line focus. (auth)

Scattering Theory

Refer also to abstract 3240.

3451 (ITF-70-49) SOLUTION OF UNITARITY CONDITION FOR THE ELASTIC SCATTERING AMPLITUDE FOR HIGH ENERGIES. Savrin, V. I.; Tyurin, N. E.; Khrustalev, O. A. (Akademiya Nauk Ukrainskoi SSR, Kiev. Institut Teoreticheskoi Fiziki). 1970. 17p. (In Russian). Dep. NTIS (U. S. Sales Only).

The method of obtaining the elastic scattering amplitude for high energies is suggested based on using the unitarity condition for the partial amplitudes. To calculate imaginary and real parts of the elastic scattering amplitude, and also Legendre coefficients of inelastic channel contribution of the reaction, one should give some real functions as well (the phases of purely elastic scattering corresponding to two-particle unitarity condition). The comparison of the given method with quasi-potential consideration is carried out. (auth)

3452 BOGOLYUBOV CAUSALITY IN S-MATRIX THEORY. Peres, Asher (Israel Inst. of Tech., Haifa). Nucl. Phys.; B23: 125-54(1970).

The restrictions imposed on the S-matrix by the Bogoliubov causality condition are investigated. It is shown that when the latter is expressed in terms of S-matrix elements, it yields a set of integrodifferential equations, which may serve as the basis of a complete non-perturbative dynamical theory. For that purpose, the S-matrix must be generalized to virtual processes which do not conserve energy and momentum (but where all particles are on their mass shells). This generalization differs from the more familiar off-mass-shell extrapolation of field theory, but both methods lead to identical results, at least in perturbation theory. (auth)

3453 SIGN OF REGGE-POLE RESIDUES IN THE VENEZIANO MODEL. Neveu, A.; Scherk, J. (Laboratoire de Physique Theorique et Hautes Energies, Orsay, France). Nucl. Phys.; B23: 630-2(1970).

The problem of the location of the negative residues appearing in a Veneziano term is studied. It is found that if the parameters satisfy certain relations, there is only a finite number of ghost states in the region of the resonances. (auth)

3454 STRUCTURE OF HIGH-ENERGY TWO-BODY NONDIFFRACTIVE REACTIONS. Ross, M.; Henyey, F. S.; Kane, G. L. (Univ. of Michigan, Ann Arbor). Nucl. Phys.; B23: 269-314(1970).

The structure of two-body scattering amplitudes is considered, concentrating on those reactions in which the "internal" quantum numbers exchanged correspond to the quantum numbers of a single particle, different from those of the vacuum. Conventional Regge-

XUM

pole models (in which dips as a function of t are caused by "nonsense" factors) are compared with the strong-cut model (in which dips are caused by a diffractive mechanism). In the conventional models, the systematics of the angular structure are determined by the nature of the exchange, as well as by the helicity structure and factorization. In the strong-cut model, the systematics of the angular structure are determined exclusively by the helicity structure of the amplitude (except for slight modification in the case of pion exchange, due to the proximity of the pion pole to the physical region); most important is the net helicity flip of the amplitude. Experimental data are examined, particularly with regard to dips near $-t$ (or $-u$) ≈ 0.2 or 0.6, and near $t = 0$. It is found that whenever a distinction can be made, the strong-cut model is favored over the conventional models (even including cuts determined by conventional absorption models). Further experimental tests are proposed. Double-particle exchange processes, energy dependence, effects of t-channel unitarity and duality are discussed. (auth)

3455 PROOF OF THE EXISTENCE OF FUNCTIONS THAT SATISFY EXACTLY BOTH CROSSING AND UNITARITY. IV. NEARLY CONSTANT ASYMPTOTIC CROSS SECTIONS. Atkinson, D. (CERN, Geneva). Nucl. Phys.; B23: 397-412 (1970).

A proof of the existence of functions that satisfy a Mandelstam representation with the crossing symmetry appropriate to pion-pion scattering, elastic unitarity below the inelastic threshold, and the inelastic inequalities above it, is generalized to a restricted class of amplitudes that need an arbitrary, finite number of subtractions. Although the leading angular momentum singularity is constrained not to rise above unity in the elastic region, it is possible for the total cross section to display an almost constant asymptotic behavior. (auth)

3456 NEW APPROACH TO THE REGGEON CALCULUS. II. Short, R. D. (Cambridge Univ., Eng.). Nucl. Phys.; B23: 413-35(1970).

The method of Polkinghorne for evaluating the asymptotic behavior of amplitudes involving Feynman propagators and reggeons is extended to diagrams containing three-reggeon vertices, and a general procedure for this class of diagrams is constructed. (auth)

3457 CONSISTENCY OF A MODEL FOR PION–PION SCATTERING. Johnson, Robert C. (Durham Univ., Eng.). Phys. Rev., D; 2: 2112-14(1 Nov 1970).

The consistency with phenomenological $\pi-\pi$ scattering phase shifts of a model of the subthreshold dipion interaction is tested, using convergent dispersion sum rules. The model is found to be satisfactory, provided the isoscalar S-wave interaction just above threshold is not very large. The value of a hitherto undetermined parameter is estimated. (auth)

3458 SOLUBLE TWO-CHANNEL PROBLEMS IN POTENTIAL SCATTERING. Kamal, A. N.; Kreuzer, H. J. (Univ. of Alberta, Edmonton). Phys. Rev., D; 2: 2033-9(1 Nov 1970).

Three soluble two-channel models with square-well, δ-function, and separable potentials, respectively, are presented. The structure of the cross sections, the presence of resonances and bound states, and one-channel approximations with generalized optical potentials are discussed in some numerical detail. The qualitative relevance of our results in particle physics is indicated. (auth)

3459 RESCATTERING, OMNES EQUATION, AND ZEROS IN RESONANCE PEAKS. Resnick, L. (Carleton Univ., Ottawa). Phys. Rev., D; 2: 1975-83(1 Nov 1970).

The production of a resonance in a collision is studied from a semiphenomenological point of view as a rescattering effect. The framework is an integral equation of the Muskhelishvili–Omnès type, with the rescattering parameters (e.g., phase shift) assumed known. In particular, the possibility of structure (e.g., zeros) in the line shape is investigated. Coupled singular equations are also examined, and an explicit solution is obtained in a particular case. (auth)

3460 IMPROVED UPPER BOUND ON THE IMAGINARY PART OF ELASTIC SCATTERING AMPLITUDES. Jacobs, Matthew A.; Joseph, Anthony; Nussinov, Shmuel; Rangwala, Abbas A. (Tel-Aviv Univ., Ramat Aviv, Israel). Phys. Rev., D; 2: 1970-4(1 Nov 1970).

The method of Singh and Roy, which obtains a bound on the imaginary part of the elastic scattering amplitude, given σ_{tot} and σ_{el}, is generalized to allow inclusion of other given data such as $d\sigma/dt$ at fixed points. A calculation is described in which one additional experimental point is given. The upper bound is compared with the experimental data for $\pi^{\pm}p$, $K^{\pm}p$, pp, and $p\bar{p}$ elastic scattering at various energies in the near-forward direction. It is found that this single extra piece of given data extends by a factor of about 3 the range for which the original bound remained close to the data and at the largest t value considered ($t \approx -0.5$ BeV^2) improves this bound by a factor of about 4. (auth)

3461 GILBERT-LIKE DISPERSION RELATIONS FOR THE FORM-FACTORS. Kamal, A. N. (Univ. of Alberta, Edmonton). Can. J. Phys.; 48: 2420-2(15 Oct 1970).

New dispersion relations are obtained for the form-factors. A sum rule for the r.m.s. radius is derived and tested. (auth) (Canada)

3462 COMPLEX ANGULAR MOMENTUM AND IMPACT PARAMETER AMPLITUDE. Adachi, Toshimi (Tokyo Metropolitan Tech. Coll.). Progr. Theor. Phys. (Kyoto); 44: 562-4 (Aug 1970).

It is shown that the impact parameter representation leads to an expression for the Froissart–Gribov type continuation of the partial wave amplitude without introducing signature and assuming the Mandelstam form for the scattering amplitude explicitly. It is also shown that the singularities in the complex l-plane lead to a cut on the negative real axis of the impact parameter plane in the impact parameter amplitude. (L.B.S.)

Particle Accelerators

Refer also to abstracts 2120, 2434, 2655, and 3542.

3463 (CONF-700322) PROCEEDINGS OF THE SECOND OAK RIDGE CONFERENCE ON THE USE OF SMALL ACCELERATORS FOR TEACHING AND RESEARCH, MARCH 23–25, 1970. Duggan, Jerome L. (Oak Ridge Associated Universities, Inc., Tenn.). 466p. Dep. CFSTI.

Separate abstracts were prepared for the 33 papers presented. (W.H.K.)

For abstracts of individual papers see: 2118–2121, 2218, 2418, 2501, 2582, 2604, 2882, 2888, 2889, 2900, 3187, 3188, 3464–3475, 3526, 3527, 3543, and 3560–3562.

3464 (CONF-700322–, pp 1-19) CHARGED PARTICLE NUCLEAR PHYSICS EXPERIMENTS FOR A TEACHING LABORATORY. Treado, Paul A.; Lambert, James M. (Georgetown Univ., Washington, D. C. Dept. of Physics).

From Proceedings of the second Oak Ridge conference on the use of small accelerators for teaching and research, March 23–25, 1970.

A modest accelerator facility can provide the basis for a charged particle nuclear physics laboratory course that is stimulating for both students and faculty. Experiments that can be presented are discussed that range from historically significant elastic scattering measurements to contemporary investigations of reaction mechanisms. (auth)

3465 (CONF-700322–, pp 21-31) BEAM-FOIL EXCITATION USING LOW-ENERGY ACCELERATORS: APPLICATIONS TO RESEARCH AND TEACHING IN ATOMIC PHYSICS. Dotchin, L. W.; Chupp, E. L.; Pegg, D. J. (New Hampshire Univ., Durham. Dept. of Physics).

From Proceedings of the second Oak Ridge conference on the use of small accelerators for teaching and research, March 23–25, 1970.

The University of New Hampshire 400 keV Van de Graaff accelerator has been used for research and teaching in beam-foil spectroscopy. The experimental method is discussed in detail, and the advantage of using low energy accelerators in beam-foil research is illustrated. The need for accurate experimental determination of atomic transition probabilities is pointed out, and some recent UNH measurements on beam-foil excited carbon are presented. An experiment on beam-foil hydrogen is shown to be an excellent teaching tool. The experiment introduces the student to some of the basic techniques involved in nuclear and atomic beam measurements performed on accelerators. (auth)

3466 (CONF-700322–, pp 49-61) STUDIES OF THE (p,α) REACTION WITH A 400-keV VAN DE GRAAFF ACCELERATOR. Quinton, A. R. (Massachusetts Univ., Amherst).

From Proceedings of the second Oak Ridge conference on the use of small accelerators for teaching and research, March 23–25, 1970.

A new instructional program is described wherein students gain experience with a small accelerator. Coulomb scattering is used to gain familiarity with procedures and techniques common in nuclear physics research. The ^{6}Li(p,γ)^{4}He and the ^{7}Li(p,α)^{4}He reactions are used for spectrometer calibration purposes followed by an intensive study of resonant yields from ^{19}F(p,α)^{16}O. Resonance shapes, straggling, energy loss, angular distributions and kinematic

shifts are the principal topics of the course. The implications of the results for nuclear structure are discussed. (auth)

3467 (CONF-700322–, pp 79–88) EDUCATIONAL APPLICATIONS OF NUCLEAR ELECTRONICS. French, Walter R. Jr. (Nebraska Wesleyan Univ., Lincoln. Dept. of Physics).

From Proceedings of the second Oak Ridge conference on the use of small accelerators for teaching and research, March 23–25, 1970.

A versatile nuclear laboratory has been developed which is used for both undergraduate instruction and faculty or student research. This paper deals with some of the design features of this laboratory, the nuclear instrumentation used, and some types of experiments that can be performed. A 200 kilovolt Cockcroft–Walton accelerator capable of 2.5×10^{11} n/sec is used for fast and thermal activation analysis. Three multichannel analyzers, including one with 4096 channels, the necessary support electronics, and lithium-drifted germanium, sodium iodide, anthracene, plastic phosphor, silicon surface barrier, and other detectors are available. These permit experiments involving high resolution gamma spectroscopy, precision gamma energy measurements, NaI gamma spectroscopy, beta scintillation spectroscopy, high resolution alpha spectroscopy, fission fragment energy measurements, as well as short half lives or lifetimes of excited states. Undergraduate students have shown a genuine interest in working in the laboratory, and they have been able to do a wide variety of experiments of a substantial nature with the facilities described. (auth)

3468 (CONF-700322–, pp 125–32) TIME-OF-FLIGHT EXPERIMENTS FOR LOW-ENERGY ACCELERATORS. Carter, H. K. (Furman Univ., Greenville, S. C.).

From Proceedings of the second Oak Ridge conference on the use of small accelerators for teaching and research, March 23–25, 1970.

Modern day electronics makes it quite easy to resolve time events that are only a few nanoseconds apart in time. The associated particle time-of-flight technique has been used successfully in neutron time-of-flight spectroscopy for the last 14 years. Several time-of-flight experiments suitable as an undergraduate laboratory are discussed. The first experiment is an alpha-alpha time-of-flight experiment for the $^{7}Li(p,\alpha)\alpha$ reaction. The flight time of the alpha particle is measured as a function of flight path. The experimental reciprocal velocities (nanosec/meter) are compared to the calculated values. Other experiments that yield charged particles of favorable energies are discussed. Finally, neutron time-of-flight experiments for the $T(d,n)^{4}He$ and $D(d,n)^{3}He$ reactions are outlined. (auth)

3469 (CONF-700322–, pp 173–84) UNIQUE 150-keV ION ACCELERATOR FOR ION IMPLANTATION. Kleinfelder, W. J.; Johnson, W. S. (International Business Machines Corp., Hopewell Junction, N. Y. East Fishkill Lab.).

From Proceedings of the second Oak Ridge conference on the use of small accelerators for teaching and research, March 23–25, 1970.

A comparison is made between heavy ion accelerators with 1) high potential target chambers and low potential sources and 2) ones of the more conventional arrangement utilizing grounded targets. Advantages of the former arrangement include low radiation level, economy, and construction simplicity. In addition, the ion velocity in the mass analysis magnet is low thus allowing adequate separation with smaller magnets, and is independent of final acceleration potential thereby eliminating readjustment of the magnet when a different energy is desired. The principal difficulties with high potential targets involve beam current measurement, peripheral equipment at the target, and working near the target when the accelerator is operating. Two systems in the 100 keV to 150 keV range which utilize these concepts have been built. One of these systems has been operating for 3-½ years, the other for more than a year. Systems similar to these can be constructed in-house from readily available parts. (auth)

3470 (CONF-700322–, pp 259–79) ATOMIC PHYSICS WITH A LOW-VOLTAGE TANDEM. Ryding, G. (High Voltage Engineering Corp., Burlington, Mass.).

From Proceedings of the second Oak Ridge conference on the use of small accelerators for teaching and research, March 23–25, 1970.

The suitability of a low voltage tandem accelerator for atomic physics experiments is discussed. Recent advances in negative ion source techniques are presented together with some recent heavy ion stripping data, which indicate the energy and intensities of ion beams accelerated by a tandem. Experiments concerning heavy ion charge changing collisions and large angle coincidence measurements which have been performed with a small tandem are also described. (auth)

3471 (CONF-700322–, pp 321–44) ROLE OF ACCELERATORS IN NEUTRON RADIOGRAPHY. Barton, John P. (Argonne National Lab., Ill.).

From Proceedings of the second Oak Ridge conference on the use of small accelerators for teaching and research, March 23–25, 1970.

The state of the art of neutron radiography using accelerators is reviewed. Evidence is provided that within the past two years the field has taken firm roots. Several initial application facilities are reporting successful operation, and the scope for future development is considerable. Accelerator source facilities should be complementary to reactor source facilities, allowing on-site inspection of items that demand only moderate quality neutron radiographs. Limitations of the technique are, at present, set by neutron shortage and interference effects; research and development studies of new moderation, collimation, and detection systems should be very valuable. (68 references) (auth)

3472 (CONF-700322–, pp 379–92) INELASTIC ELECTRON–ATOM INTERACTIONS IN THE 50 TO 150 keV ENERGY RANGE. Baggerly, L. L.; Davis, D. V.; Heroy, D.; Faulk, J.; Mistry, V.; Quarles, C. A. (Texas Christian Univ., Fort Worth).

From Proceedings of the second Oak Ridge conference on the use of small accelerators for teaching and research, March 23–25, 1970.

Using a modified Cockcroft–Walton 150 kV accelerator we are studying various inelastic electron-atom interactions in the range of incident electron energy from 50 to 150 keV. The experimental techniques used are generally similar to those of low energy nuclear physics, although the study of electrons in this energy range has presented some rather special experimental problems. Some of the experiments currently in progress are the measurement of the total cross section for K shell ionization of copper, silver, tin and gold and for L shell ionization of gold; the measurement of the differential cross section for bremsstrahlung production from various thin foil targets; and the measurement of inelastic electron spectra. We are also setting up a coincidence experiment to try to measure the differential cross section for K shell ionization and to study the cross section for bremsstrahlung differential in photon energy, electron angle and photon angle. In this paper we would like to briefly review the subject of inelastic electron interactions at these intermediate energies, to describe some of our experimental problems and techniques, and to discuss some of the experiments that we have in progress. (auth)

3473 (CONF-700322–, pp 407–29) NEUTRON SOURCES FOR RADIOTHERAPY. Herring, D. F. (Enviro-Med, Inc., La Jolla, Calif.).

From Proceedings of the second Oak Ridge conference on the use of small accelerators for teaching and research, March 23–25, 1970.

A review of the state-of-the-art of accelerator designs which may be useful in neutron therapy is presented. The accelerator system requirements are analyzed by examining the demands placed on the accelerator by the nature of its use in treating patients. Next, a review of the experimental data pertaining to neutron beams suitable for therapy is given. Then, the practical aspects of the accelerator concepts which appear to offer the best means of providing a useful therapeutic beam of fast neutrons are analyzed and the limitations of each are discussed. Finally, some conclusions are drawn concerning specifications for a neutron source. These specifications are intended to assist the therapist and the accelerator manufacturer in establishing design concepts for neutron therapy accelerators. (28 references) (W.H.K.)

3474 (CONF-700322–, pp 431–9) TARGET TECHNOLOGY FOR MEDIUM AND HIGH-POWER APPLICATIONS. Cossutta, D. D. (Multivolt Ltd., Crawley (England)).

From Proceedings of the second Oak Ridge conference on the use of small accelerators for teaching and research, March 23–25, 1970.

Several designs of stationary and rotating target systems intended for medium and high power accelerators are described. Different methods of heat removal are discussed with particular reference to the power handling capability of various target systems. A number of high power rotating targets reported in the literature over the last few years are described in more detail and their features and performance characteristics compared. Results are reported of measurements carried out recently with a high power rotating target assembly at the UKAEA AWRE Aldermaston. (auth)

3475 (CONF-700322–, pp 441–8) RADIATION SAFETY IN THE OPERATION OF A LOW-ENERGY ACCELERATOR. Dickson, Howard; Cloutier, Roger J.; Smithwick, Grover; Watson, Evelyn E.; Berger, James D. (Oak Ridge Associated Universities, Inc., Tenn.); Roberts, Edmond Jr. (Union Carbide Corp., Oak

XUM

Ridge, Tenn. Y-12 Plant); Butler, Hal M.; Haywood, Fred F. (Oak Ridge National Lab., Tenn.).

From Proceedings of the second Oak Ridge conference on the use of small accelerators for teaching and research, March 23–25, 1970.

The health physics aspects of operating a low-energy accelerator (less than 1 MeV) are reviewed to help accelerator users formulate guidelines for maintaining a safe facility. Radiation protection standards, licensing and registration, radiation dose limits, accelerator hazards, administrative control, shielding, warning and safety devices, radiation monitoring, personnel monitoring, and tritium and other targets are discussed. (W.H.K.)

3476 (JINR–16–4888) PROCEEDINGS OF CONFERENCE ON RADIATION DOSIMETRY AND PHYSICS OF ACCELERATOR SHIELDING, DUBNA, OCTOBER 7–10, 1969. (Joint Inst. for Nuclear Research, Dubna (USSR)). 1970. 257p. (In Russian). (CONF-691049).

Twenty-three papers are presented on shielding calculations, radiation dose calculations, and various dosimeter systems. (W.H.K.)

3477 (LYCEN–7063) USE OF A VAN DE GRAAFF GENERATOR TO SIMULATE THE TRANSIENT EFFECTS DUE TO RADIATION IN SEMICONDUCTORS. Gaillard, R.; Genre, R.; Guyon, J.; Samuell, J. J. (Lyon Univ. (France). Institut de Physique Nucleaire). Jul 1970. 14p. (In French). Dep. NTIS (U. S. Sales Only).

An original simulation method was developed, which uses a Van de Graaff type proton accelerator. This method was aimed at distinguishing the transient effects induced in semiconductor devices by short intense pulses of ionizing radiation. The phenomena studied was the production of hole electron pairs. In order to achieve a valid simulation, it was necessary to use a beam focusing device capable of delivering a dose of at least 10^9 rads/s, and an appropriate pulsing device. The electronic circuit and the mechanical organization of the equipment are described. Problems involved in the observation and measurement of the pulsed proton current and the induced photocurrent in a bipolar transistor are examined in detail. (France)

3478 WATER-DIELECTRIC GENERATOR FOR PRODUCING INTENSIVE FAST-ELECTRON AND HARD DECELERATED X-RAY PULSES. Pecherskii, O. P.; Sidoruk, A. M.; Tarasov, V. D.; Tsukerman, V. A. Dokl. Akad. Nauk SSSR; 192: 1266-7 (21 Jun 1970). (In Russian).

Production of bursts of high-intensity, hard x-rays for periods of several tens of nanoseconds requires high voltages and electron currents. This was achieved by using a coaxial conductor in a compressed gas up to a voltage of 3 to 7 MV, created by an electrostatic generator on a resonance-type Tesla transformer. The dimensions of high-voltage pulse generators and their internal resistance may be greatly reduced by using a material with a high dielectric constant as insulator. Pure water was chosen for this purpose. If the resistivity of the water dielectric lies between 1 and 3 kohm, the voltage is reduced only by a few percent. Replacement of the gaseous dielectric with water reduces ninefold the rate of propagation of electric waves, reducing its wave resistance by a similar amount. If the total internal resistivity is 10 kohm, the amplitude of the electron current through the accelerating tube will lie between 70 and 120 kA and the x-ray dose at 100 cm from the target amounts from 5 to 10 R, assuming that the pulse lasts for 60 nanoseconds. Thus, use of water increases the dose rate by an order of magnitude by reducing the duration of the burst and increasing the electron current. (TTT)

3479 ROLE OF INSTABILITIES IN THE PRODUCTION OF MONOENERGETIC ELECTRON BEAMS IN LINEAR ACCELERATORS. Zhileiko, G. I.; Snedkov, B. A. This paper was summarized in At. Energ. (USSR); 24: 256(Mar 1968) as paper No. 183. (In Russian).

The problems associated with the production of monoenergetic (zero energy spread) electron beams in linear accelerators are discussed. Frequency instabilities and power instabilities of the accelerating field are discussed. Temperature effects on the waveguide sections and resonators are considered, and the mechanical tolerances for iris waveguides are discussed. (W.H.K.)

3480 ATTENUATION OF SCATTERED SYNCHROCYCLOTRON RADIATION IN A SHIELD. Zaitsev, L. N.; Kimel, L. R.; Komochkov, M. M.; Sidorin, V. P.; Sichev, B. S.; Ulitin, O. A.; Cherevatenko, E. P. This paper was summarized in At. Energ. (USSR); 24: 182(Feb 1968) as paper No. 180. (In Russian).

An experimental investigation of the attenuation of scattered synchrocyclotron radiation in ordinary and hematite concretes is presented. The arrangement with ordinary concrete consisted of a block 2150 × 1780 × 1230 mm in a beam of scattered radiation having a hard spectrum. The experimental data on the attenuation of fluxes of scattered neutrons of various energies and of gamma dose rates as a function of shield thickness are given. High energy neutron fluxes (E > 20 MeV) and fast neutrons are attenuated in nearly the same exponential fashion for shield thicknesses d > 20 cm. The experimental points were obtained by taking into account the calculated neutron background arising from penetration through the lateral surfaces of the set up. The attenuation curve for resonance neutrons (E ≈ 1.44 eV) calculated by age theory and the calculated attenuation curve for the capture gamma dose rate are given. The attenuation distance for the high-energy scattered neutron flux in ordinary concrete found experimentally equalled 18.8 ± 1.5 cm. The experimentally determined attenuation length for high energy neutrons from a beryllium target bombarded with 170 to 660 MeV protons is 42–61 cm, which is about 2.2 to 3.2 times as large as the value for the same group of neutrons of scattered radiation. The experimental and calculated data on the distribution of fluxes of scattered neutrons of various energy groups and the dose rates for capture gamma radiation are in satisfactory agreement. (auth)

3481 CALCULATION OF THE PHASE FOCUSING OF INTENSIVE ION BUNCHES. Avramenko, M. I.; Kuznetsov, V. S. This paper was summarized in At. Energ. (USSR); 25: 520-1 (Dec 1968) as paper No. 253. (In Russian).

Direct action accelerators which operate under nanosecond conditions are now used to an ever-increasing extent. If beam chopping and the initial velocity modulation are effected before acceleration, the initial bunches can be approximated by charged ellipsoids of revolution. In the case of linear modulation and a homocentric beam, the axial and radial ion velocities are proportional to the corresponding coordinates, which are measured from the bunch center point. In this case, the bunch will retain its ellipsoidal form not only in the equipotential space, but also in a uniform external electric field whose strength satisfies the condition $E \ll V_0/\alpha_0$, where V_0 is the potential at the entrance to the accelerating tube, and α_0 is the length of the axial semi-axis of the bunch in front of the tube. Then, in order to determine the ion bunch parameters, it is sufficient to solve the equations of motion for the two end particles. These equations and solutions to the equations are presented. (W.H.K.)

3482 INVESTIGATION OF BEAM TRANSVERSAL CHARACTERISTICS AT INPUT OF THE IHEP PROTON SYNCHROTRON. Demikhovskii, D. A.; Myae, E. A.; Troyanov, E. F. At. Energ. (USSR); 29: 272-5(Oct 1970). (In Russian).

The results of measurements of the beam emittance, injected into the IHEP proton synchrotron from the linac at beam currents from 10 to 90 mA, are presented. The instantaneous current distribution in the phase space was measured. It was found, that during the injection momentum the emittance becomes changed and displaced along the angular coordinate. As the result, the effective emittance is considerably larger than the instantaneous one. The values of deformation and of angular displacement grow as the beam current increases. The most probable cause of it is the accelerating voltage drop due to the beam loading of the linac resonators. The current distribution curves with respect to emittance are presented. The dependence of the emittance, that corresponds to the initial injection momentum, upon the beam current has been found. It is indicative of considerable influence of the beam space charge upon the particle focussing in the linac. The causes of particle losses inside the injection channel are discussed. (auth)

3483 DESIGN OF AN ELECTRON LINEAR ACCELERATOR FOR INDUSTRIAL USE. Maekawa, Akiji (Hitachi Ltd., Tokyo); Takeda, Yasutsugu; Matsui, Isao; Suzuki, Isamu; Saito, Ryusei. Hihakai Kensa; 19: 405-10(Aug 1970). (In Japanese).

Requirements for an industrial linear electron accelerator include good movability, light weight, and short accelerator tubes. In order to meet the requirements, the following parts or items were newly designed or examined: high frequency power source, electron output voltage, electron source, and accelerator dimensions. The present apparatus has five degrees of movability freedom, a magnetron with isolator, a pulse modulator common to an electron source and a magnetron, accelerator tube length of 0.8 m, electron output voltage 4 to 5 MV, and x-ray output 500 roentgen/min at 1 m from a target. Using this apparatus, a radiogram according to JIS is taken with a film as wide as 400 mm without an equalizer at the position of 1 m from the target. It has been applied to the inspection of big steel and iron blocks up to a thickness of 470 mm. (auth) (Japan)

3484 TRUDY VSESOYUZNOGO SOVESHCHANIYA PO USKORITELYAM ZARYAZHENNYKH CHASTITS, MOSKVA, 9–16 OKTYABRYA 1968 GODA. TOM I. (Proceedings of the All-Union Conference on Particle Accelerators, Moscow, 9–16 October 1968. Volume I). Vasil'ev, A. A. (ed.). Moscow; Vsesoyuznyi Institut Nauchnoi i Tekhnicheskoi Informatsii (1970). 684p. (CONF-681029-(Vol.1)).

One hundred and nine papers are presented. Topics include the development of different types of accelerators; magnets and power supplies; ion and electron sources and direct-voltage accelerators; targets, beam separation and transport systems, injection, and extraction; and air-core and superconducting electromagnets and assemblies and equipment for magnetic measurements. (W.H.K.)

3485 TRUDY VSESOYUZNOGO SOVESHCHANIYA PO USKORITELYAM ZARYAZHENNYKH CHASTITS, MOSKVA, 9–16 OKTYABRYA 1968 GODA. TOM II. (Proceedings of the All-Union Conference on Particle Accelerators, Moscow, 9–16 October 1968. Volume II). Vasil'ev, A. A. (ed.). Moscow; Vsesoyuznyi Institut Nauchnoi i Tekhnicheskoi Informatsii (1970). 596p. (CONF-681029-(Vol.2)).

Ninety-eight papers are presented. Topics include radio electronic systems for accelerators; high-power radiotechnical facilities and accelerating systems; particle dynamics and new acceleration methods; and auxiliary systems and accelerator equipment of different types. (W.H.K.)

3486 MAGNETIC TRACKING OF COMPENSATED ELECTRON BEAMS IN THE ACCELERATION REGION. Bosamykin, V. S. Zh. Tekh. Fiz.; 40: 1173-6(Jun 1970). (In Russian).

Studies were made of the motion of compensated electron beams accelerated by a homogeneous electric field up to relativistic energy in a longitudinal magnetic field. The profile of the cylindrical beam was determined by an equation obtained by partial approximation. A short review is given of various cases. Equations were obtained for intrinsic electron beam path in longitudinal electric and magnetic fields compensated by a relativistic flow in a magnetic field and also for the boundary electron of relativistic compensated flow moving in the absence of external fields. (tr-auth)

3487 CALCULATIONS OF ELECTROSTATIC ENERGY ANALYZER FOR SOLID AND HOLLOW CYLINDRICAL BEAMS OF CHARGED PARTICLES. Kozlov, I. G.; Strizhenko, V. S. (Saratov State Univ., USSR). Zh. Tekh. Fiz.; 40: 1236-44(Jun 1970). (In Russian).

Calculations for electrostatic energy analyzers for solid and hollow cylindrical charged particle fluxes were made with a higher degree of accuracy and higher order of focusing than previously. Dispersion and specific dispersion, according to the energy, were calculated in the focusing point, and expressions were found for the resolving power of a charged particle energy analyzer using the field of cylindrical condenser as analyzing element. Data obtained can be used for construction of ion beam energy analyzers. (R.V.J.)

3488 STUDIES OF RESONANCES OF NONLINEAR SYNCHROTRON OSCILLATIONS. Kononenko, S. G.; Reprintsev, L. V.; Shenderovich, A. M. Zh. Tekh. Fiz.; 40: 1282-9(Jun 1970). (In Russian).

Theoretical and experimental studies of external and parametric resonances of large amplitude synchrotron oscillations showed that resonance perturbations may produce stationary induced synchrotron oscillations on the subharmonics of the perturbation. The stability of such oscillations was studied and the influence of radiative attenuation and quantum fluctuations of radiation was estimated. The maximum amplitudes of induced oscillations as functions of the perturbation force were determined. (R.V.J.)

3489 CURRENT CONFINEMENT BY SPACE CHARGE IN SECTIONED ELECTRON ACCELERATOR TUBES. Kaz'min, G. S. (Tomsk Inst. of Radioelectronics and Electron Techniques, USSR). Zh. Tekh. Fiz.; 40: 1290-6(Jun 1970). (In Russian).

Acceleration of parallel electron beams of annular cross section in a sectioned system with the Pierce optics was studied. It is shown that for the given cross section of open channel, the spatial charge, the current, and energy of the beam have the tendency to diminish with the rise of the calculated intensity in the tube. The applied injection into a uniformly accelerating field of the converging beam with intensity one order of magnitude smaller than the total working intensity in the tube, results in significantly larger maximum current in the tube at an identical open channel cross section. Numerical integrated equations for the boundary electron motion were used for calculating the beam parameters at the moment of injection which is the moment of the maximum current. (tr-auth)

3490 TWO-POTENTIAL LENS WITH DISTORTED FOCUSING LAYER. Brodskii, G. N.; Yavor, S. Ya. (Ioffe Inst. of Physics and Tech., Leningrad). Zh. Tekh. Fiz.; 40: 1304-7 (Jun 1970). (In Russian).

The motion of charged particles in the vicinity of the mean plane (the symmetry plane) of axial-symmetric electric and magnetic fields was studied previously. An attempt was made of studying their focusing effect using electric fields confined at both sides by equipotential regions with various potential magnitudes. Such a lens was considered to be a two-potential (immersion) lens which differed from the corresponding two-dimensional lens by the distortions of the equipotential. (R.V.J.)

3491 ELECTRON-OPTICAL PROPERTIES OF TWO-POTENTIAL TWO-DIMENSIONAL LENS. Brodskii, G. N.; Yavor, S. Ya. (Ioffe Inst. of Physics and Tech., Leningrad). Zh. Tekh. Fiz.; 40: 1310-13(Jun 1970). (In Russian).

Analytical expressions were obtained for focusing distances, positions of the main planes, and the aperture errors in the focus. (tr-auth)

3492 EXPERIMENTAL PROGRAMME AT THE CERN PROTON SYNCHROTRON. CERN Cour.; 10: 139-45(May 1970).

The 18 available beams are described; electronics experiments using counter and spark chamber techniques are outlined; nuclear structure experiments are discussed; and experiments at the three bubble chambers (2 meter and 81 centimeter hydrogen chambers and 1.2 meter heavy liquid chamber) are surveyed. (W.H.K.)

3493 REALIZATION OF THE MAGNETIC GUIDE FIELD IN THE ISOCHRON-CYCLOTRON AT JUELICH. Thimmel, Hermann Michael. Wiss. Ber. AEG-Telefunken; 43: No. 1, 67-72(1970). (In German).

The design and development of the magnet system for the guide field for the Juelich isochronous cyclotron are described. Construction of the pole shoes and compensating coil system is discussed, and results of field correcting measurements are presented. (W.H.K.)

3494 DIELECTRIC LOADED WAVEGUIDES AS PARTICLE SEPARATORS. Kustom, R. L.; Chang, C. T. M.; Dawson, J. W. (Argonne National Lab., Ill.). Nucl. Instrum. Methods; 87: 19-27(1970).

Rectangular and circular dielectric loaded waveguides support propagating modes which have transverse deflecting fields which enable them to be used as rf particle separators for elementary particle beams. Electric fields in excess of 4.0 MV/m have been achieved in sample structures. The spark limit of these structures is as yet undetermined. Possible applications include traveling wave separators for beams of 1.0 to 5.0 GeV/c and "quasi"-point deflectors for beams in excess of 20 GeV/c. (auth)

3495 ANALYSIS OF THE FIRST-ORDER EFFECTS OF MISALIGNMENTS IN A BEAM TRANSPORT SYSTEM. Lobb, D. E. (Univ. of Victoria, B. C.). Nucl. Instrum. Methods; 87: 59-72(1970).

The usual first-order matrix treatment for charged particle trajectories through beam transport system elements is applied to the case where the element axis is displaced from the system axis. The method used is to transform the trajectory coordinates at the input to the element to new coordinates expressed with respect to the element axis, to trace this trajectory through the element using the usual first-order theory and to transform the output coordinates to coordinates with respect to the system axis. It is shown that if the element is rotated about the direction of the incoming beam the distribution of trajectories about the central trajectory is changed; for all other misalignments the only first-order effect is the displacement of the central trajectory. The results are examined to determine the misalignments that have the greatest effect on the displacement of the central trajectory. It is shown that satisfying the position tolerances at input and output of the element easily satisfies the required angular tolerance for rotations about axes normal to the incoming central trajectory. (auth)

3496 STATUS AND DEVELOPMENT OF SUPERCONDUCTING 2^{+} GeV ACCELERATOR AT HEPL. Chambers, E. E. (Stanford Univ., Calif.). Nucl. Instrum. Methods; 87: 73-6 (1970).

The design of the accelerator which is substantially complete is discussed. In particular, the design of the niobium accelerating structure, the refrigerator, dewar, and low temperature transport system, and the injector and control system are explained. Projections of further developments are considered. (auth)

XUM

3497 SENSITIVE PROFILE AND POSITION MONITOR FOR ELECTRON AND POSITRON BEAMS. Kneissl, U.; Kuhl, G. (Justus-Liebig-Univ., Giessen, Ger.). Nucl. Instrum. Methods; 87: 77-8(1970). (In German).

A sensitive profile and position monitor for low intensity electron and positron beams is described. It consists of a thin rotating plastic scintillator which is viewed by a photomultiplier. Peak currents down to 10^{-9} A can well be monitored. (auth)

3498 RAPID EMITTANCE SCANNER. Kolata, J. J.; Surratt, R. E. (Naval Research Lab., Washington, D. C.). Nucl. Instrum. Methods; 87: 141-4(1970).

An emittance-measuring device which can operate at the rate of two measurements per second has been developed. It consists of a rotating wire scanner interfaced to a small on-line computer. (auth)

3499 RESISTANCE IN SMALL, TWISTED, MULTICORE SUPERCONDUCTING WIRES. Voelker, Ferd (Univ. of California, Berkeley). Particle Accel.: 1: 205-7(Jul 1970).

We have been testing twisted, multicore, superconducting wires with a nominal 0.008 in. diameter, and we find that there is no clear-cut value for critical current. Instead, the resistance of a given wire increases continuously as the current-density or field is increased, until a range is reached where the wire becomes unstable and resistivity increases with time. If the current or field is not reduced quickly the wire will go normal. Four samples of wire are reported on. One was a single core whose characteristics were compared with the multicore wires. One sample was mechanically defective and had approximately 25 percent broken strands in a one-inch length. (auth)

3500 PROTON POLARIZATION MEASUREMENTS AT HIGH MAGNETIC FIELDS AND LOW TEMPERATURES. Nicholas, D. J.; Williams, W. G.; Banks, P. H. T.; Cragg, D. A. (Rutherford High Energy Lab., Chilton, Eng.). Nucl. Instrum. Methods; 87: 301-2(1970).

Proton polarizations and relaxation times have been measured in a glycerol/water mixture doped with porphyrexide at a magnetic field of 47.8 kG and over the temperature range $0.5 \leq T \leq 1.2$°K. The results are compared with those obtained at 25 kG. (auth)

3501 DESIGN STUDIES FOR A LARGE PROTON SYNCHROTRON AND ITS LABORATORY. Adams, J. B.; Wilson, E. J. N. (CERN, Geneva). Nucl. Instrum. Methods; 87: 157-79(1970).

Analysis of the growth pattern of CERN-Meyrin leads to a model for the development of the proposed European 300 GeV Laboratory. The model must allow for flexibility in the development of the machine so that one may exploit future technological advances, e.g. pulsed superconducting magnets. The maximum use must be made of existing capital investment and infrastructure yet provision must also be made for a steady expansion in experimental utilization for 30 years to come. Various types of synchrotron with separated and combined-function lattices and missing-magnet, missing-power and fixed-energy configurations have been designed and costed. Their relative merits are discussed in the context of the model for the new Laboratory. (auth)

3502 DESIGN OF DIELECTRIC-LOADED RECTANGULAR DEFLECTORS. Hahn, H. (Brookhaven National Lab., Upton, N. Y.). Particle Accel.: 1: 275-9(Jul 1970).

The deflecting properties of dielectric-loaded rectangular deflectors excited in the dominant LSM_{10} mode are theoretically investigated and the essential results for S-band deflectors are summarized graphically. It is concluded that due to its long attenuation length a rectangular waveguide loaded symmetrically with beryllium oxide slabs is ideally suited to Blewett-type rf beam separators. This approach represents a realistic method of producing usable beams of elementary particles for counter experiments at the Brookhaven Alternating-Gradient Synchrotron. (auth)

3503 SMOOTHING AND DIFFERENTIAL ANALYSIS OF MAGNETIC FIELD AND GRADIENT MEASUREMENT. Young, Jonathan D. (Univ. of California, Berkeley). Particle Accel.: 1: 269-70(Jul 1970).

We discuss mini-max fifth-degree smoothing and modified quintic spline fitting of a set of median plane magnetic field measurements consisting of (1) the vertical component as a function of one variable, and (2) the first derivative thereof. We assume that the measurements have been made for at least five uniformly spaced values of the argument. In particular the application of this process to measurements made for the field in the Bevatron (Berkeley) is discussed. (auth)

3504 SUPERCONDUCTING TWO TESLA BENDING MAGNET. Fast, R. W.; Strauss, B. P.; Cohn, C. M.; Heim, J. R.; Scholefield, E. H. (National Accelerator Lab., Batavia, Ill.). Particle Accel.: 1: 265-8(Jul 1970).

A superconducting 2 tesla dipole model magnet has been designed, fabricated, and tested at the National Accelerator Laboratory. The magnet is of a type called "superferric" since it consists of an iron yoke and superconducting coil. The magnet provided a 4 cm × 10 cm free aperture and generated a magnetic field uniform to ±0.1 percent or less within a full horizontal aperture of 5.3 cm. The current density in the conductor at 2 T was 36 kA/cm^2, the stored energy was 8000 J and the magnet could be charged to 2 T in about 5 minutes. The iron was refrigerated to 4.2°K, and about 75 liters of LHe were required for cooldown from 80°K. The cryostat heat leak was 3 liters/h. A 3 m long prototype 2 T superferric magnet is under construction. (auth)

3505 SUPERCONDUCTING BEAM LINE. Desportes, H.; Morgan, M.; Purcell, J. (Argonne National Lab., Ill.). Particle Accel.: 1: 247-53(Jul 1970).

A complete superconducting beam line, including two bending magnets and eight quadrupoles, has been designed for use in a new experimental area at the ZGS. This beam line was expected to replace one of the conventional lines, provided it was competitive on a capital cost basis, and to provide a considerable practical experience with the many problems involved in the operation of a system of this type. It was intended to have the complete magnets constructed by industry and bids were received from eight vendors, showing their wide interest in the project, their high level of competence and the competitive range of their prices. (auth)

3506 DESIGN OF A 600-MeV MICROTRON USING A SUPERCONDUCTING LINAC. Allen, J. S.; Axel, P.; Hanson, A. O.; (and others) (Univ. of Illinois, Urbana). Particle Accel.: 1: 239-45(Jul 1970).

A proposed 600 MeV racetrack microtron is described which uses a superconducting linac as the accelerating section. This linac, which is being constructed, will use niobium cavities cooled to 1.8°K and will provide a continuous electron beam, except for the 1.3 GHz microstructure. The electron beam will be recirculated through the linac 20 times by two 180° bending magnets having uniform fields of about 14 kG. Focusing of the recirculating electrons is provided on each return path by a quadrupole pair close to each magnet. Calculations show that the requirements for space and phase stability are easily satisfied and that the microtron arrangement offers an electron beam with exceptional energy resolution. (auth)

3507 SUPERCONDUCTING ACCELERATOR RESEARCH AND DEVELOPMENT AT SLAC. Wilson, P. B.; Neal, R. B.; Loew, G. A.; (and others) (Stanford Univ., Calif.). Particle Accel.: 1: 223-38(Jul 1970).

This paper surveys current and planned research and development of SLAC on superconducting linear accelerators. Ultimately, the goal is to convert the present machine to a two-mile 100-GeV superconducting linac. The technological problems which stand in the way of this achievement are being attacked on two fronts: on the one hand, a better understanding of the properties of superconducting materials, such as residual loss, electric field breakdown and magnetic field quenching is being sought through experiments with individual samples and cavities; on the other hand, many of the design, fabrication and control problems which are the concern of the accelerator builder are being met head-on by the immediate construction of a short superconducting accelerator. The latter project, appropriately named "Leapfrog," utilizes a 15-cavity niobium traveling-wave resonant ring structure operating in the $2\pi/3$ mode. Many of the parameters for this test accelerator, such as the frequency (2856 MHz) and the accelerating field (33 MV/m), are the same as those envisaged for the two-mile machine. Detailed computer studies have been made to optimize the accelerator structure geometry. The paper concludes with a description of a feasibility study for the proposed two-mile accelerator. Design parameters are discussed and construction schedules and costs are estimated. (auth)

3508 REFRIGERATION OF SUPERCONDUCTING MAGNETS. Green, Michael A. (Univ. of California, Berkeley). Particle Accel.: 1: 213-21(Jul 1970).

This paper describes the Lawrence Radiation Laboratory helium refrigeration system and its use on superconducting magnets. A discussion of our operational techniques includes reliability and maintenance of components, cold transfer line techniques, and large magnet cooldown and operation. The validity of assumptions used in previous studies of large refrigeration systems for accelerator experimental areas is discussed. As a result of operational experience a revised set of recommendations for large experimental area refrigeration systems is made. The inter-

relationship of cryostat design on the refrigeration is briefly discussed. (auth)

3509 EXPERIMENTAL SUPERCONDUCTING TRANSFORMER FOR CURRENT STEP-UP. Voelker, Ferd; Acker, Robert C. (Univ. of California, Berkeley). Particle Accel.; 1: 209-11(Jul 1970).

For certain applications one would like to use relatively few turns of a high current conductor to make superconducting magnets. High current conductors introduce the problem of large heat leaks, and also the problem of a high current power supply. These problems would be simplified if one could make a suitable current step-up transformer. A design equation for such a transformer is presented. An experimental test was performed on a transformer made of superconducting solenoids which we had on hand. It had a primary current of 79.2 A, and supplied 670 A to a small load solenoid. The transformer was operated in two modes. In the first, the primary current was held constant for 24 hours. The magnetic field in the load solenoid was monitored and the rate of decay in field could be measured. In the second mode, the primary current was regulated to maintain constant field in the load solenoid. The time constant of the secondary circuit was 1.4×10^6 seconds. Such a system could be operated for a number of weeks without recycling. (auth)

3510 SUPERCONDUCTIVITY FOR HIGH ENERGY PHYSICS AT LRL-BERKELEY. Gilbert, W. S.; Meuser, R. (Univ. of California, Berkeley). Particle Accel.; 1: 199-203(Jul 1970).

The LRL-Berkeley superconducting program related to high energy physics is described in functional terms. DC magnets for use in accelerator experimental areas are discussed as are pulsed magnets as would be appropriate to a proton synchrotron. Fundamental studies and areas of cryogenic engineering and system investigations are outlined. (auth)

3511 APPLICATION OF PULSED SUPERCONDUCTING MAGNETS TO SYNCHROTRONS. Bronca, G.; Levy-Mandel, R.; Neyret, G.; Parain, J. (CEN, Saclay, France). Particle Accel.; 1: 187-98(Jul 1970).

The behavior of superconductors in variable fields is summarized. Some experimental results are given, concerning the behavior of the coils and their losses; emphasis is put on electrical methods. Comments on the design of superconducting dipoles and quardupoles are developed, and the main parameters of an experimental dipole are listed. A step towards bigger machines could be the conversion of an existing machine; as an example, it is proposed to turn Saturne into a 15-GeV synchrotron. Finally, some possible schemes using superconducting magnets in future plans for the European accelerator are sketched, taking into account the expected improvements in available amounts of power supply. (auth)

3512 SUPERCONDUCTING SYNCHROTRON MAGNETS. Sampson, W. B.; Britton, R. B.; Dahl, P. F.; (and others) (Brookhaven National Lab., Upton, N. Y.). Particle Accel.; 1: 173-85(Jul 1970).

The design of superconducting synchrotron magnets is discussed and experimental measurements of magnetic field distributions are presented for a number of model magnets. The use of iron in such magnets is evaluated and measured values of the external and internal fields are given. Conductor requirements are examined and compared with measured critical currents. The theory of ac losses is reviewed and experimental results presented in support of calculations. (auth)

3513 SUPERCONDUCTING ENERGY TRANSFER SYSTEMS. Smith, P. F.; Lewin, J. D. (Rutherford High Energy Lab., Chilton, Eng.). Particle Accel.; 1: 155-72(Jul 1970).

A synchrotron magnet power supply concept has been devised which consists solely of a system of coupled superconducting coils. By relative rotation of the coils, energy can be transferred from the system to the superconducting synchrotron magnet. The total energy remains constant during transfer so that no external work is required; the absence of resistive losses ensures that the process is quasi-stationary and completely reversible (apart from residual mechanical and electrical damping effects of order 0.01 percent). Energy transfers in the range 10^6–10^9 J could be achieved with systems typically 3 to 6 m diameter. Several possible schemes of this type have been studied theoretically. This paper describes the most promising of these, and crystallizes the significant theoretical results and practical conclusions. The original presentation of the idea has been improved in several ways: (1) a modified circuit, allowing the geometry to be simplified to three concentric coils; (2) inclusion of small variable control inductors to automatically produce forward or reverse rotation; and (3) addition of a transformer which facilitates matching and increases the proportion of energy transferred. In addition to the basic circuit theory, preliminary theoretical assessments of a number of practical aspects of the device are now in progress; items discussed include field and current distributions, choice of coil topology, mechanical stresses, ac losses, cost optimization, dynamic response, and replenishment of losses. (auth)

3514 RUTHERFORD LABORATORY SUPERCONDUCTING SYNCHROTRON PROGRAMME: NOTES ON WORK IN PROGRESS. Smith, P. F. (Rutherford High Energy Lab., Chilton, Eng.). Particle Accel.; 1: 151-4(Jul 1970).

Studies are in progress covering all aspects of superconducting synchrotrons. This brief review summarizes recent results and current thoughts on conductor development, magnet prototype development, and machine design problems. (auth)

3515 RECENT WORK ON THE DUBNA COLLECTIVE ION ACCELERATOR. Sarantsev, V. P. (Joint Inst. for Nuclear Research, Dubna, USSR). Particle Accel.; 1: 145-50(Jul 1970).

The main steps on the collective method of acceleration development in Dubna and the present situation of this work are described. (22 references) (auth)

3516 METHOD FOR LOCATING THE MEDIAN SURFACE OF AN AVF CYCLOTRON MAGNET. MacKenzie, G. H.; Richardson, J. Reginald (Univ. of British Columbia, Vancouver). Nucl. Instrum. Methods; 87: 319-22(1970).

A Hall probe device is described which locates the median surface of inhomogeneous magnetic fields: its precision is 0.010″ for the particular field studied. (auth)

3517 ACCURATE NON-INTERCEPTING BEAM CURRENT INTEGRATOR FOR PULSED ACCELERATOR BEAMS. Gardiner, S. N.; Matthews, J. L.; Owens, R. O. (Univ. of Glasgow). Nucl. Instrum. Methods; 87: 285-90(1970).

A non-intercepting integrator has been developed for the pulsed beam from the Glasgow 140 MeV electron linear accelerator. The system uses the signal from windings on a toroidal mu-metal core placed around the electron beam path to drive a gated integrator. The response of the integrator has been compared with that of a Faraday cup. The linearity and long term stability are found to be better than ±0.1%. (auth)

3518 RADIAL MOTION OF THE ELECTRONS AND THE EMITTANCE OF THE BUNCH FROM A LOW-ENERGY SUPERCONDUCTING LINEAR ACCELERATOR. Septier, A.; Bousoukaya, M. (Faculte des Sciences, Orsay, France). Nucl. Instrum. Methods; 87: 273-84(1970). (In French).

Trajectories of electrons in low energy, low current T.W. and S.W. superconducting linacs, with no external magnetic focusing are studied. An analytical solution is given to the equation of radial motion, in a T.W. linac, for electrons moving in synchronism with the accelerating wave; trajectories of electrons injected in a narrow phase domain around the synchronous particles are easily found by numerical integration of a simplified equation. In S.W. linacs, numerical integration of the complete set of motion equations shows an important focusing effect, even in the phase stability domain, due to the reflected wave, in the case of electrons injected in short bunches, when the mean injection phase angle ϕ_0 is chosen not too far from the wave crest. In these conditions, the accelerating structure is equivalent to a hf converging lens, and approximate expressions are given for the focal distance of short cavities. Emittance diagrams at the output of the linac are given in both cases for different values of the injection phase, and an average brightness of the beam has been calculated. (auth)

3519 POLARIZED ION SOURCE FOR THE U-120 CYCLOTRON. 2. ACCELERATION AND EXTRACTION OF POLARIZED DEUTERONS. Bejsovec, V.; Bem, P.; Mares, J.; Trejbal, Z. (Inst. of Nuclear Research, Rez, Czech.). Nucl. Instrum. Methods; 87: 233-6(1970).

A polarized ion source was built at the U-120 cyclotron using the method of radial injection. The intensity of the beam of oriented deuterons having the vector polarization $\langle it_{11} \rangle = -0.25 \pm 0.05$ in the target chamber attains 75 pA. (auth)

3520 POLARIZED ION SOURCE FOR THE U-120 CYCLOTRON. 1. REALIZATION OF A NEW METHOD OF RADIAL INJECTION OF IONS INTO CYCLIC ACCELERATORS. Bejsovec, V.; Bem, P.; Mares, J.; Trejbal, Z. (Inst. of Nuclear Research, Rez, Czech.). Nucl. Instrum. Methods; 87: 229-32(1970).

There has been developed a new method of radial injection of ions from an external ion source for the U-120 cyclotron which exploits the effects of double charge exchange. The reached injection efficiency for protons and deuterons is $\xi_i = 0.14$, the efficiency of acceleration and extraction of deuterons is $\xi_a = 0.01$. (auth)

XUM

3521 BEAM ELLIPSE MATCHING: WAIST-TO-WAIST TRANSPORT. Silbar, R. R. (Los Alamos Scientific Lab., N. Mex.). Nucl. Instrum. Methods; 87: 221-7(1970).

We derive the most general form of the beam transport transformation matrix that takes a given initial beam ellipse into a given final beam ellipse. The result is specialized to waist-to-waist transport and applied to the problem of drift-thin lens-drift. A large number of interpretative comments are made concerning the results of this analysis. (auth)

3522 INJECTION, EXTRACTION, OR SPLITTING OF A BEAM WITH HIGH CURRENT SEPTUM MAGNETS. Paulin, A. (SIN–ETH, Zurich). Nucl. Instrum. Methods; 87: 189-96(1970).

The technological possibility to build a high current septum magnet with a septum thickness of only 1 mm is shown. Through cooling with water, 14 W/mm^3 and more could be handled. The calculations show that with a proper septum form a broad region of magnetic fields needed for either beam splitter or inflector could be created. A proton beam of 0.3 μA/mm^2 can easily be split in any ratio between 0 and 100%. (auth)

3523 IMPROVEMENTS IN OR RELATING TO ELECTRON EMITTING CATHODES FOR IRRADIATION MACHINES. McCann, John David; Whittaker, Brian; Fuller, Robin Walter Ellecker (to United Kingdom Atomic Energy Authority). British Patent 1,204,316. 3 Sep 1970. Filed 26 Sep 1966.

The electron-emitting cathode described comprises a flexible plaited or woven graphite or carbon filament having an electron emitting coating. The filament is preferably of low mass per unit length, and may be tubular and mountable on a wire, thus comprising a central refractory metal core having a loose fitting graphite or carbon sleeve. The coating may be applied to the filament in the form of an aqueous slurry comprising La_2O_3, boron, carbon and water, with subsequent air drying, outgassing, and heating at 1700°C for a few seconds in vacuum. (UK)

3524 EFFECT OF LOCAL HETEROGENEITIES OF MAGNETIC FIELDS ON PULSATION OF EDGES OF ELECTRON BEAMS. Bakhrakh, L. E.; Benin, S. D.; Murzin, V. V. Radiotekh. Elektron.; 15: 883-5(Apr 1970). (In Russian).

Several authors have theoretically investigated the effect of local inhomogeneities of a focusing magnetic field on the pulsations at the edges of electron beams. An experimental investigation of the problem is briefly reported here, whereby transverse dimensions and current density distributions in the beam cross section were measured by a movable-slit method. An electron beam with current up to 10 mA, and accelerated by a potential of 300 to 1000 V, was focused by a homogeneous magnetic field of a solenoid and passed through a local inhomogeneity present in the field; the inhomogeneities were produced with the help of Armco washers or by using constant circular magnets mounted coaxially with the solenoid. The pulsations were examined for different entrance phases of the beam into the region of the inhomogeneity; the entrance phase was varied by axial displacements of the electron gun relative to the inhomogeneity. Results showed good agreement with the theoretical studies, and the possibility of correcting the beam-edge pulsations by proper selection of the beam entrance phase into the inhomogeneous region is indicated. (L.M.T.)

PHYSICS (NUCLEAR)

Neutron Interactions with Matter

Refer also to abstracts 2130, 3049, 3181, 3184, 3208, 3226, 3471, 3473, 3474, and 3927.

3525 (CEA-N-1312) THE PROGRAM IGOR. STRAIGHT LINE ATTENUATION. ADJUSTMENT OF THE ATTENUATION NUCLEI IN SPHERICAL GEOMETRY. Simon, Michel (Commissariat a l'Energie Atomique, Fontenay-aux-Roses (France). Centre d'Etudes Nucleaires). Jun 1970. 13p. (In French). Dep. CFSTI (U. S. Sales Only).

The use of calculation codes dealing with neutron propagation according to a straight line attenuation model requires a knowledge of the displacement cross sections Σ (I) of each medium traversed. The program IGOR determines values of the Σ (I) in spherical geometry from the flux which should be obtained at the media interfaces. An alternative makes it possible to provide a set of displacement cross sections and the program then calculates the flux at points chosen by the user. IGOR is written in FORTRAN IV for the IBM 360. (auth) (France)

3526 (CONF-700322-, pp 33-47) STUDENT EXPERIMENTS UTILIZING A NEUTRON GENERATOR. Veit, J. J.; Lindsay, R. H. (Western Washington State Coll., Bellingham).

From Proceedings of the second Oak Ridge conference on the use of small accelerators for teaching and research, March 23-25, 1970.

Several laboratory courses at Western Washington State College have been improved by the use of a small accelerator as a high-flux neutron generator. After five years we are convinced of its value to stimulate students and to bridge the gap between the teaching laboratory and research. Five student experiments which utilize the neutron generator are discussed, and six others which are used in several courses in nuclear physics and in engineering physics are briefly mentioned. All experiments can be completed in less than three hours, with time for faculty-student discussion. (auth)

3527 (CONF-700322-, pp 185-204) APPLICATION OF NEUTRON GENERATORS TO ACTIVATION ANALYSIS. Nargolwalla, S. S. (National Bureau of Standards, Washington, D. C.).

From Proceedings of the second Oak Ridge conference on the use of small accelerators for teaching and research, March 23-25, 1970.

This review summarizes some of the key developments in neutron generator technology which have had a significant bearing in the acceptance of neutron generators for the precise and accurate determination of a large number of elements at the semi-micro and macro levels of concentration by neutron activation analysis. Recent advances in the design and utilization of experimental hardware such as sample-placement devices, experimental designs and special long-lived neutron producing targets are discussed. Descriptions of some investigations pertaining to the evaluation of systematic errors in activation analysis with neutron generators are presented, and various aspects of analytical significance related to the use of this type of radiation source are emphasized. In this regard, advantages offered by the neutron generator for the analysis of light elements are given. Research in the area of cross section measurements and their implications in light of the practical sample due to degradation of the nominal 14.7 MeV neutrons is described. Typical sensitivities obtainable with present-day neutron outputs from neutron generators are critically examined and anomalies between expected theoretical sensitivities and experimental sample response in high energy neutrons are discussed. Pertinent applications of neutron generator activation analysis techniques in the areas of metallurgy, biochemistry, mineralogy and standard materials are described. Special attention is drawn to the introduction of this technique to the solution of industrial quality control problems. A brief treatment of the on-line analytical capabilities of neutron generators, particularly of the sealed-tube type, is given. In this connection, efforts made toward the computerization of analytical procedures and data reduction are emphasized. In conclusion, the contribution of this analytical technique in terms of sensitivity, specificity, accuracy and precision, and possible future developments of the fast neutron facility is discussed. 31 references. (auth)

3528 (KFKI-70-12-RPT) CALCULATION OF RESONANCE INTEGRALS: CODES RIFFRAFF AND RAO4. Szatmary, Z.; Bagyinszki, A. (Magyar Tudomanyos Akademia Kozponti Fizikai Kutato Intezete, Budapest). 24 Jun 1970. 11p. Dep. NTIS (U. S. Sales Only).

Codes RIFFRAFF and RAO4 calculate resonance integrals and homogenized cross sections for the multigroup slowing down code GRACE. RIFFRAFF calculates the space-energy variation of the flux in a cylindrical two-region cell. RAO4 calculates average cross sections in homogeneous mixtures of nuclei on the basis of a very simple physical model. Both codes are written in Fortran for the ICT-1905 computer. (auth)

3529 (KFKI-70-14-RPT) GRACE: A MULTIGROUP FAST NEUTRON SPECTRUM CODE. Szatmary, Z.; Valko, J. (Magyar Tudomanyos Akademia Kozponti Fizikai Kutato Intezete, Budapest). [1970]. 40p. Dep. NTIS (U. S. Sales Only).

GRACE is a multigroup fast neutron spectrum code which solves the asymptotic neutron transport equation in slab geometry using the Greuling-Goertzel approximation for the slowing down neutron source. The code permits the use of both B_1 and P_1 approximations. In the multigroup structure of GRACE a thermal group has been included making an iteration to criticality of the slab possible. (auth)

3530 (LA-4484) TWENTY-FIVE GROUP CROSS SECTIONS USED IN THE LOS ALAMOS ROVER PROGRAM. Sapir, Joseph (Los Alamos Scientific Lab., N. Mex.). Jul 1970. Contract W-7405-eng-36. 93p. Dep. CFSTI.

The most recent 25 energy-group cross sections used in the neutronic analyses of Rover reactors are presented. (auth)

3531 (LA-4506) PHOXE: A FORTRAN-IV CODE TO CHECK FORMAT SYNTAX, CONSISTENCY, AND PHYSICAL REALISM OF ENDF/B PHOTON PRODUCTION DATA. Dudziak, Donald J. (Los Alamos Scientific Lab., N. Mex.). Apr 1970. Contract W-7405-eng-36. 68p. Dep. NTIS.

The PHOXE code reads the photon production data files in ENDF/B format, checking them for format syntax, consistency, and "physics" errors. Suspected errors are flagged on an output listing immediately after the record in which they are detected. Some preprocessing of the data is performed, both for error checking and for listing convenient quantities (e.g., average photon energy of a continuum) useful to a reviewer. The intent of this code is to provide an aid to cross-section evaluators and reviewers in their attempts to produce an ENDF/B data set free of typographical, syntax, and simple "physics" errors. An attempt was made to include any reasonable check capable of being automated and which does not require an interactive capability with any system external to ENDF/B (e.g., a reviewer or data bank). The code is presently operational on CDC 6600 and IBM 360 computers and is available from the Radiation Shielding Information Center as PSR-21. (auth)

3532 VARIABLE PHASE-SPACE NEUTRON TRANSPORT ANALYSIS. Harms, Archie Arkadius. Seattle; Univ. of Washington (1969). 156p. University Microfilms Order No. 70-8457.

Thesis.

Methods of analysis associated with nodal phase-space representations relevant to neutron transport processes are discussed. The mathematical methods chosen include the classical modal formalism and the more recent mathematical programming formalism. The one-speed neutron transport model and the multigroup neutron diffusion model are selected for the basic description of neutron-nuclei processes. A unified modal-nodal angular density representation, designated by the acronym NP_L, is formulated within the context of one-speed neutron transport theory. This NP_L formalism is mathematically examined by deriving appropriate orthogonality and recurrence relations. It is subsequently shown that several widely used solution methods of one-speed neutron transport theory are but special cases of this more inclusive representation. As a second approach to the analysis of phase-space structures of neutron transport processes, a mathematical programming approach is developed and applied within the framework of multigroup neutron diffusion theory. This formalism is motivated by the practical need of specifying reduced spatial-energy structures which are optimal with respect to a specific computational objective. In keeping with the conceptual basis of mathematical programming, a response function is established such that the attainment of its extremum identifies the spatial-energy structure of interest. The distinguishing feature of the problem considered herein is the piece-wise continuity of the neutronic description embodied in the multigroup diffusion method. To incorporate this feature, an original extremal algorithm is developed with combines a random sampling technique with a steepest descent approach in piece-wise constant, non-convex, multidimensional phase-space. The analytical-computational features of this extremal algorithm are illustrated by performing model calculations. It is shown that the problem of

XUM

identifying a global minimum on a representative response surface can be treated with satisfaction. In addition, it is algebraically and computationally demonstrated that a particular class of constraint conditions can be incorporated by repeated application of the extremal algorithm. Applying the extremal algorithm to the multigroup neutron diffusion model in nuclear reactor calculations, it is found that information extracted from an initial detailed reference calculation can be used to specify reduced spatial-interval and/or reduced energy-group structures while minimizing the error in the effective multiplication constant. This suggests that the extremal algorithm represents a potentially useful tool in preliminary nuclear reactor design and survey calculations. (Diss. Abstr. Int., B)

3533 CALCULATION OF THE COHERENT NEUTRON SCATTERING FROM POLYCRYSTALLINE BERYLLIUM. **Borgonovi, G. M. (Gulf General Atomic Inc., San Diego, Calif.); Sprevak, D. Nucl. Sci. Eng.: 42: 137-42(Nov 1970).**

A calculation of the one-phonon neutron-scattering law for polycrystalline beryllium has been performed. This scattering law is an improvement over the results of the incoherent approximation and allows a more accurate computation of the total cross section below the Bragg cutoff. (auth)

3534 QUASI-ELASTIC INCOHERENT COLD NEUTRON SCATTERING IN LIQUID CYCLOHEXANOL. **de Mul, F. F.; Bregman, J. D. (Interuniversitair Reactor Instituut, Delft, Netherlands). Phys. Lett.: 33A: 87-8(5 Oct 1970).**

Using fast Fourier methods, the time-of-flight spectra of liquid cyclohexanol are transformed into intermediate scattering functions from which the resolution is removed. It is shown that rotational jump diffusion is an important mechanism for the molecular motions. (auth)

3535 SPECTRAL FUNCTION REPRESENTATION OF TIME AND ENERGY DEPENDENT NEUTRON DENSITY IN FAST MEDIA. PART 1. MEDIA WITHOUT MULTIPLICATION. SLOWING-DOWN SPECTROMETER. **Collatz, S. (Zentralinstitut fuer Kernforschung, Rossendorf, Ger.). Kernenergie: 13: 243-5(Aug 1970).**

The time-dependent neutron density in fast media is represented with spectral functions of the time-independent part of the transport operator in the buckling approximation. In this first part of the paper the problem is solved for the non-multiplying case. With this the special problem of slowing-down spectrometer is studied. (auth)

3536 ONE PHONON EXCITATION IN TITANIUM HYDRIDE BY LOW ENERGY NEUTRONS. **Lee, Y. J.; Suh, I. H.; Kang, H. D. (Atomic Energy Research Inst., Seoul). J. Nucl. Sci. (Seoul): 10: No. 1, Pt. 1, 1-5(Jun 1970).**

A preliminary experiment was conducted on the inelastic scattering of low-energy neutrons from H atoms in the optical mode in TiH_2. Monoenergetic neutrons from a double-crystal monochromator on a TRIGA-MARK-II reactor was used, and total cross sections were measured at 0.05 to 0.2 eV. A plot of total cross section of H in TiH_2 vs energy shows a minimum at ~0.12 eV. (D.L.C.)

3537 ATTENUATION OF 14 MeV NEUTRONS IN WATER. **Marshall, T. O. (Radiological Protection Service, Sutton, Eng.). Health Phys.: 19: 571-4(Oct 1970).**

The attenuation of 14-MeV neutrons in water was measured under approximately broad beam conditions, the transmitted neutrons being measured in terms of dose-equivalent rate. The relaxation length was found to be 16.3 cm with a random error of ±4% with a less than 5% chance that the error is greater than this value. Systematic errors are considered to be small in comparison with the random error. The transmitted neutrons irrespective of water thickness and the γ-ray dose rate emerging from the shield were found to be an important consideration for water thicknesses greater than about 100 cm. (auth) (UK)

3538 SPATIAL, ENERGY, AND ANGULAR DISTRIBUTIONS OF NEUTRONS IN LITHIUM. **Daruga, V. K.; Degtyarev, S. F.; Kukhtevich, V. I.; Nikolaev, A. N.; Polivanskii, V. P.; Sinitsyn, B. I.; Suvorov, A. P.; Tarasov, V. V.; Tikhonov, V. K.; Tsypin, S. G. This paper was summarized in At. Energ. (USSR); 24: 374(Apr 1968) as paper No. 193. (In Russian).**

Experimental and theoretical investigations of the spatial, energy, and angular distribution of neutrons in metallic lithium are reported. The source was the zero power RIZ reactor against which were placed three containers of lithium each 600 × 1350 × 1400 mm. The detectors were a ZnS(Ag) fast neutron counter, a fast neutron scintillation spectrometer with a stilbene crystal discriminating against γ rays, and also thermal- and intermediate-neutron detectors. In measurements of the spatial and energy distributions, all of the detectors were located in channels; in studying the angular distributions of fast neutrons, the ZnS(Ag) counter was placed in a special collimator that could be shifted to various angles with the outer normal to the lithium container. Data are presented on: the energy distribution of fast neutron fluxes obtained experimentally and calculated by the ROZ program; the spatial distributions of neutron fluxes of various energy groups for various lithium thicknesses; data on the angular distributions of fluxes of neutrons with energies greater than 1 MeV; and the total flux. It is shown that the calculated and experimental results are in satisfactory agreement. (auth)

3539 RECENT THEORETICAL DEVELOPMENTS IN THE INTERPRETATION OF THE NEUTRON DIFFUSION LENGTH EXPERIMENT. **Williams, M. M. R. (Queen Mary Coll., London). Nucl. Energy; 11: 100-7(Jul-Aug 1970).**

The development of the theory associated with the neutron diffusion length experiment is discussed. Some of the earlier treatments based on various approximations to the energy-dependent Boltzmann equation are considered. These are one-speed diffusion theory in the infinite medium, one-speed diffusion theory with transverse leakage, one-speed transport theory in the infinite medium, energy-dependent diffusion theory in the infinite medium, energy-dependent transport theory with transverse leakage, energy-dependent transport theory in the infinite medium, one-speed transport theory with transverse leakage, and energy-dependent transport theory with transverse leakage. The general solutions of the equations appropriate to these situations are given; and the consequences of the results obtained, discussed in an experimental context. Although an exact solution to the Boltzmann equation was obtained for the slab system using a one-term degenerate-kernel approximation, the inclusion of isotropic elastic-scattering phenomena prevents an exact solution. The applications and future advances of the theories are indicated. (UK)

3540 NUMERICAL CALCULATION OF THE MILNE PROBLEM EXTRAPOLATION LENGTH. **Cohen, E. Richard (North American Rockwell Corp., Thousand Oaks, Calif.). Nucl. Sci. Eng.: 42: 231-2(Nov 1970).**

For the solution of the Milne problem in the context of neutron transport, an expression for the extrapolation length Z_0 is given in terms of a definite integral and evaluated numerically to eight digits. An attempt is made here to provide a numerical value of Z_0 to increased accuracy to serve as a benchmark against which approximate solutions of the transport equation can be compared. It is found that twenty digit accuracy can be achieved with the integrand evaluated at only 8 points. (M.H.R.)

3541 CALCULATIONS OF NEUTRON TIME-ENERGY DISTRIBUTIONS IN HEAVY MODERATORS. **Williamson, T. J. (Naval Postgraduate School, Monterey, Calif.); Albrecht, R. W. Nucl. Sci. Eng.; 42: 97-100(Oct 1970).**

Short-comings of Monte Carlo and analytical techniques for making detailed neutronics calculations for heavy moderating isotopes have been partially overcome by use of the discrete stochastic model. The new model differs from the usual time-dependent multigroup theory in the method of calculating transition probabilities and in handling the stepping interval. Restrictions due to computer size have been eased in the following way. As the neutron population moves downward in energy following a short burst from the source, the matrix is allowed to move with it to generate new rows of transition probabilities at the bottom of the matrix and to increase time steps. In this way a 700 × 700 matrix can effectively be handled as a 200 × 200 matrix. Various assumptions are made concerning normal mode space dependence and the treatment of elastic scattering. The model is applied to the lead slowing down spectrometer, and the neutron density and time-dependent capture and leakage rates are calculated. (R.W.R.)

3542 DEGASSING AT LOW TEMPERATURE OF TITANIUM TARGETS IMPREGNATED WITH HYDROGEN ISOTOPES. **Germai, G.; Guillaume, M.; Peters, J. M. (Univ., Liege). Int. J. Appl. Radiat. Isotop.; 21: 595-8(Oct 1970). (In French).**

The measurement of the tritium loss rates of titanium targets for accelerator neutron sources obtained by different procedures is described. The results are compared. At normal temperature and pressure, the tritium loss rate of a given target decreases with time. By means of experiments under vacuum and at low temperature, it is shown that, in degassing, tritium is occluded. The health hazards are considered. (auth) (UK)

Nuclear Properties and Reactions, A≤ 5

Refer also to abstracts 3750 and 3768.

3543 (CONF-700322–, pp 95-104) EXPERIMENTS UTILIZING THE $D(^3He,p)^4He$ REACTION. **Carlton, Robert F. (Middle Tennessee State Univ., Murfreesboro).**

From Proceedings of the second Oak Ridge conference on the

use of small accelerators for teaching and research, March 23–25, 1970.

Several experiments utilizing the $D(^3He,p)^4He$ reaction and which would be suitable for use in a modern physics laboratory with a low energy accelerator are discussed. Angular distributions at four incident energies are presented, as well as the yield curve for the reaction. Two coincidence experiments, one using a basic coincidence circuit and one employing the time of flight (TOF) method, are discussed and the results are presented for the protons and alphas resulting from a ^3He bombarding energy of 350 keV. The energy loss and energy straggling of the high energy protons are studied for two absorber materials and various absorber thicknesses, and the results are compared with theory. Other instructive experiments utilizing the reaction are suggested. (auth)

3544 (LYCEN–7041) A STUDY OF ELASTIC α SCATTERING BY ^4He WITH THE AID OF SEPARABLE NONLOCAL POTENTIALS. Pigeon, Jacques (Lyon Univ. (France). Institut de Physique Nucleaire). May 1970. 89p. (In French). Dep. NTIS (U. S. Sales Only). Thesis.

The (α,α) interaction is described in terms of nonlocal separable potentials. A formalism for the scattering of particles without spin and without internal structure was presented by considering nonlocal separable potentials in the presence of Coulombian potentials. For incident energies inferior to the threshold for the inelastic channels the experimental situation was obtained with simple potentials and a minimum number of parameters. This formalism was applied to the α elastic scattering by ^4He at energies between 0 and about 40 MeV. At higher energies absorption phenomena were no longer negligible and manifest themselves by the appearance of complex phase shifts. The introduction of internal structure effects satisfactorily explained experimental phase shifts remote from the 40 MeV region. In this region, a compound nucleus type resonance was introduced in order to maintain compatibility with the experimental situation. (auth) (France)

3545 (LYCEN–7047) STUDY OF SOME NUCLEI OF THE 1p AND 2s-1d SHELLS USING THE HARTREE–FOCK METHOD. Delalex, Anne-Marie (Lyon Univ. (France). Institut de Physique Nucleaire). Jun 1970. 82p. (In French). Dep. NTIS (U. S. Sales Only). Thesis.

With the view of making comparisons with experimental results, the Hartree–Fock method for calculating the configurational energies of light nuclei is described. In particular, 4n nuclei with 1p and 2s-1d shells were studied. The phenomenological potentials of Volkov, Manning, Brink, Boeker and Monsonego were used to study the spherical nuclei ^4He, ^{16}O and ^{40}Ca and the deformed nuclei ^8Be and ^{12}C. The results obtained were in good agreement with those obtained by other workers. The conditions appropriate to the application of this method are described. The representation consisted of harmonic oscillator states considered on a cylindrical base and corresponding to three complete shells. The possibility of the deformation of the average field when an anisotropic harmonic oscillator was taken as the Hamiltonian of a particle was considered. Such a representation initially has two degrees of freedom, but it can be adapted to the cases of harmonic wells of different depths and degrees of deformation. The results indicate the advantages of the base used. In fact, the results obtained by the Hartree–Fock method may be improved upon by increasing the dimensions of the base, however this involves more computer time and consequently greater expense. It was more advantageous to use a cylindrical base, which after deformation, could allow for energies very near to those obtainable with an extended isotropic base. The program has many possibilities; other phenomenological potentials may be introduced. A restriction that must be made is their radial dependence must remain Gaussian. Spin-orbit coupling reactions may also be studied. (France)

3546 (ORNL–TM–3168) RADIATIVE CAPTURE OF DEUTERONS BY PROTONS AT 20 AND 30 MeV. Belt, Bobby Dean (Oak Ridge National Lab., Tenn.). Nov 1970. Contract W-7405-eng-26. 130p. Dep. NTIS. Thesis.

The energy spectrum of the ^3He particles from the radiative capture of deuterons by protons has been measured using 19.8- and 29.6-MeV deuteron beams from the Oak Ridge Isochronous Cyclotron. Precise γ-ray angular distributions, which cover the entire angular range (0°–180°), were constructed from the data for both energies and were fitted by the least-squares method to functions of the γ-ray angle obtained from a multipole expansion of the electromagnetic field. It was found that terms usually retained in this expansion, i.e., M1, E1, E2 and E1/E2 interference, could not account for all the observed features. The addition of terms higher than quadrupole removed some of the discrepancy. In addition, the total cross sections were determined to ±4% accuracy. They were found to be about 10% below recent calculations. (auth)

3547 (RLO–1388-126) ENERGY DEPENDENCE OF QUASI-FREE SCATTERING IN THE D(p,pn)p REACTION. Braithwaite, W. J.; Calarco, J. R.; Cameron, J. M.; Storm, Derek W. (Washington Univ., Seattle). [1970]. 20p. Dep. NTIS.

The cross section was measured for the reaction $^2H(p,pn)^1H$ at 14, 17, 20, and 23 MeV incident energies. The proton and neutron counter angles were chosen to emphasize the quasifree p-n scattering process. The neutron counter efficiency was measured in order to obtain the absolute differential cross sections. The experimental results agree well with a modified simple impulse approximation, which is discussed. (auth)

3548 BRUECKNER REACTION MATRIX AND SEPARABLE POTENTIALS. Gmitro, M. (International Centre for Theoretical Physics, Trieste, Italy); Sotona, M. Phys. Rev., C; 2: 356-65 (Aug 1970).

The binding energy of ^4He and ^{16}O was calculated using reaction matrix elements of Tabakin's potential. A separable form of the potential was used to reduce the basic equation to a simple linear algebraic system. The Pauli operator Q defined in terms of harmonic-oscillator intermediate states permits an easy and accurate calculation. The numerical results for the binding energies include the first- and second-order contributions. A very resonable agreement between the experimental and theoretical values was obtained, since the occupied-state energies are made nearly self-consistent and a cancellation of other important higher-order contributions was achieved by a shift of the entire harmonic-oscillator spectra. (auth)

3549 NEUTRON–NEUTRON FINAL STATE INTERACTIONS IN THE REACTION $^2H(d,pp)2n$. von Witsch, W.; Niiler, A.; Sandler, J.; Spiger, R. J.; Phillips, G. C. (Rice Univ., Houston, Tex.). Nucl. Phys.; A150: 461-6(1970).

The reaction $^2H(d,pp)2n$ was studied at a bombarding energy of 12 MeV, detecting the two protons in coincidence at angles of ±20° as well as +20° and −15°. In both cases, a narrow band was observed in a three-dimensional plot of the yield versus the energies of the two detected protons, E1 and E2, with most of the yield concentrated in the area where E1 ≈ E2. This suggests a two-step sequential process of the type $d + d \rightarrow (2p) + (2n) \rightarrow p + p + n + n$. In a missing mass plot for the third, undetected "particle" a pronounced, narrow peak appears at low relative energies in the (nn) system. (auth)

3550 RADIATIVE PION CAPTURE IN ^{12}C. Bistirlich, James A.; Crowe, Kenneth M.; Parsons, Anthony S. L.; Skarek, P.; Truoel, P. (Univ. of California, Berkeley). Phys. Rev. Lett.; 25: 689-93(7 Sep 1970).

The spectrum of high-energy gamma rays following the capture of negative pions in ^{12}C was measured with high resolution. The observed structure in the giant resonance region is the first direct experimental proof of the influence of collective excitations in radiative pion capture. This supports recent theories concerning the analogy between this process and muon capture. (auth)

3551 VARIATION OF CHARGE RADII OF THE NUCLEI OF $^{124,126,128,130}Te$ FROM THE DATA ON ISOTOPE SHIFTS OF X-RAY $K\alpha_1$ LINES. Mezentsev, A. F.; Sumbaev, O. I.: Marushenko, V. I.; Ryl'nikov, A. S.; Ivanov, G. A.; Egorov, A. I.; Popova, G. M. (Ioffe Inst. of Physics and Tech., Leningrad). Yadern. Fiz.; 11: 1141-5(Jun 1970). (In Russian).

Variation of the charge radii $\Delta\langle r^2\rangle$ of nuclei in Te isotopes in the region of neutron numbers N = 74 to 78 is measured using the isotope shift method for the x-ray K_{α_1} lines. It is established that the experimental values $\gamma \equiv \Delta\langle r^2\rangle/\Delta\langle r^2\rangle_{R\sim A}{}^{1/3}$ are somewhat lower than theoretical ones which take account of deformation of the nuclei, i.e., in this region of the N values the same anomaly takes place as that previously studied by the authors on the Ba isotopes (N = 78 to 82). (auth)

3552 p-p AND p-t FINAL STATE INTERACTIONS IN THE REACTION $^3He(d,tp)p$. Warner, R. E. (Oberlin Coll., Ohio); Corey, B. E.; Petersen, E. L.; Bercaw, R. W.; Poth, J. E. Nucl. Phys.; A148: 503-15(1970).

Absolute coincidence cross sections were measured for the reaction $^3He(d,tp)p$ at E_d = 20.7 MeV. Deep minima were observed in the cross sections when the relative energy of either p + p or t + p was below ≈20 keV. Predictions of the Watson–Migdal theory and of the PWBA and DWBA theories of Henley, Richards and Yu gave good agreement with the shapes of the spectra near these minima, but the required normalization factors varied widely from one geometry to another. Decay of the 21.2 MeV ^4He state, but not the 20.0 MeV state, was observed. (auth)

3553 THE D(p,d*)p CROSS SECTION FROM THE D(p,2p)n REACTION. Niiler, A. (Los Alamos Scientific Lab., N. Mex.);

XUM

von Witsch, W.; Phillips, G. C.; Joseph, C.; Valkovic, V. Phys. Rev., C; 1: 1342-52(Apr 1970).

Three-body breakup spectra from a kinematically complete measurement of the D(p,2p)n reaction are analyzed to yield the cross section for the production of d*, a quasiparticle consisting of a neutron and proton in a $^1S_0$ configuration. An excitation function of the D(p,d*)p reaction is obtained for the proton bombarding energy range 9 to 13 MeV. In agreement with measurements and predictions of the (p,d*) cross section on several nuclei, the D (p,d*)p cross section is about an order of magnitude less than the elastic D(p,d)p cross section. The D(p,d*)p excitation function shows a peak at the bombarding energy E_p = 1025 MeV which coincides with a ^{3}He excitation energy of 12.4 MeV. This peak might be interpreted as either a state in ^{3}He or a threshold effect. (auth)

3554 EXPERIMENTAL TEST OF THE IMPULSE APPROXIMATION IN THE ^{2}H(p,2p)n REACTION. Takeutchi, F.; Yuasa, T.; Kuroda, K.; Sakamoto, Y. (Faculte des Sciences de Paris, Orsay, France). Nucl. Phys.; A152: 434-48(1970).

The deuteron break-up reaction has been studied by bombarding liquid deuterium with 156-MeV protons. The kinematic conditions were completely determined by measuring the angles θ_1, θ_2 of the two outgoing protons and the energy E_1 of one of them. The partial differential cross section $d^3\sigma/d\Omega_1 d\Omega_2 dE_1$ was measured for a range of kinematic conditions including large momentum transfers. The results are compared to calculations based on the simple impulse approximation (spectator model) and those including the effects of multiple scattering terms and final-state interactions. (auth)

3555 ANALYSIS OF THE ANGULAR DISTRIBUTIONS OF THE REACTIONS ^{4}He(p,d)^{3}He, ^{4}He(p,t)2p, ^{4}He(p,^{3}He)pn, AND ^{3}He(p,d)2p. Harbison, S. A. (King's Coll., London); Griffiths, R. J.; Stewart, N. M.; Johnston, A. R.; Squier, G. T. A. Nucl. Phys.; A152: 503-15(1970).

The angular distribution of the reaction ^{4}He(p,d)^{3}He at 49.5 MeV has been measured over the cm angular range of 11 to 165°. This angular distribution, together with the angular distributions of the reactions ^{4}He(p,t)2p, ^{4}He(p,^{3}He)pn, ^{3}He(p,d)2p at 49.5 MeV and ^{3}He(p,d)2p at 30.5 MeV reported previously, have been analyzed in terms of the plane-wave Born approximation, DWBA, and diffraction theories. (auth)

3556 ANALYSIS OF POLARIZATION AND CROSS-SECTION DATA FOR THE p-^{3}He SYSTEM AT 30 AND 50 MeV. Harbison, S. A. (King's Coll., London); Griffiths, R. J.; Stewart, N. M.; Johnston, A. R.; Squier, G. T. A. Nucl. Phys.; A150: 570-86(1970).

Differential cross-section and polarization measurements on the p-^{3}He system at 30 and 50 MeV have been analyzed in terms of real phase shifts. It is shown that there is not sufficient data at either energy to define a unique solution. (auth)

3557 SCATTERING OF 7.8-MeV POLARIZED NEUTRONS FROM ^{4}He AND THE PHASE SHIFTS BELOW 8 MeV. Stammbach, Th.; Taylor, J.; Spalek, G.; Walter, R. L. (Duke Univ., Durham, N. C. Triangle Universities Nuclear Lab., Durham, N. C.). Phys. Rev., C; 2: 434-40(Aug 1970).

The polarization analyzing power for the elastic scattering of 7.80- and 3.38-MeV neutrons from ^{4}He has been measured at laboratory angles ranging from 40 to 140°. Polarized neutrons were produced in the ^{9}Be(α,n)^{12}C reaction at 45° (lab) with a mean α energy of 2.55 MeV. Results of a phase-shift analysis are given and are found to agree with optical-model calculations reported by Satchler et al. (auth)

Nuclear Properties and Reactions, 6 ≤ A ≤ 19

Refer also to abstracts 2468, 3247, 3545, 3548, 3693, 3694, 3748, and 3928.

3558 (AD-704484) MEASUREMENT OF THE CHARGE FORM FACTORS FOR ^{6}Li AND ^{7}Li BY ELECTRON SCATTERING. Monson, William Albert (Naval Postgraduate School, Monterey, Calif.). Jun 1969. 33p. CFSTI. Thesis.

The charge form factors of the stable lithium isotopes, lithium-six and lithium-seven, were measured. The root-mean-square radius of ^{6}Li was determined to be 2.43 F. The root-mean-square of ^{7}Li was determined to be 2.33 F. (auth) (USGRDR)

3559 (AWRE-O-45/70) ELASTIC AND INELASTIC SCATTERING OF NEUTRONS IN THE ENERGY RANGE 2 TO 5 MeV BY ^{10}B AND ^{11}B. Porter, D.; Coles, R. E.; Wyld, K. (Atomic Weapons Research Establishment, Aldermaston (England)). Aug 1970. 46p. Dep. NTIS (U. S. Sales Only). UK 7s.

The time-of-flight method was used to study fast neutron elastic and inelastic scattering on ^{10}B and ^{11}B in the energy region between 2 and 5 MeV. The elastic angular distributions were compared with the predictions of a non-local optical model. Calculations show qualitative agreement with experiment. The results obtained for neutron excitation of the 0.717 MeV state in ^{10}B substantiate previous findings and in addition excitation functions were determined for the 1.740, 2.154 and 3.590 MeV states in ^{10}B. Comparisons of the differential and integrated inelastic cross sections were made with compound nucleus calculations derived from Hauser-Feshbach theory with fluctuations (HFW) using neutron optical potentials obtained from fits to the elastic angular distributions with estimates of optical potentials for (n,p), (n,t) and (n,α) reaction modes included. Apart from resonance effects, agreement is fair. For ^{11}B, the excitation of the 2.140 MeV state was determined and compared with existing data. Finally comparisons are given of the differential and integrated cross section for inelastic scattering to this state with the HFW theory utilizing the neutron optical model parameters deduced from fits to the elastic angular distributions. The rise of the cross section above threshold is shown to be much slower than that theoretically predicted. (auth)

3560 (CONF-700322–, pp 89-94) STUDY OF THE CHARGED PARTICLE SPECTRA FROM THE ^{9}Be + D REACTION. Lin, Jung (Tennessee Technological Univ., Cookeville. Dept. of Physics).

From Proceedings of the second Oak Ridge conference on the use of small accelerators for teaching and research, March 23–25, 1970.

Deuterons were accelerated to an energy of 350 keV with a 400 kV Van de Graaff accelerator. These deuterons were then allowed to bombard a self supported ^{9}Be target. Charged particles from the following reactions are observed: ^{9}Be (d,t) ^{8}Be (Q_m = 4.952 MeV), ^{8}Be → α + α; ^{9}Be (d,p) ^{10}Be (Q_m = 4.589 MeV); ^{9}Be (d,^{7}Li) α (Q_m = 7.152 MeV). The angular distribution of the triton group from the ^{9}Be (d,t_0) ^{8}Be was measured. This distribution shows a broad peak at $\theta_t \sim 100°$, it is described quite well by a series of Legendre polynomials of which the highest term is A_3P_3. Angular distributions were also measured for the ground state and first excited state (3.683 MeV) proton groups for ^{9}Be (d,p) ^{10}Be. The ground state proton angular distribution is compared to the theoretical predication from an exchange stripping mechanism. (auth)

3561 (CONF-700322–, pp 133-40) STUDY OF THE LEVELS IN ^{11}B BY THE ^{10}B(d,p)^{11}B REACTION. Humphrey, D. L.; Helms, T. E.; McGimsey, L. S. (Western Kentucky Univ., Bowling Green).

From Proceedings of the second Oak Ridge conference on the use of small accelerators for teaching and research, March 23–25, 1970.

The ^{10}B(d,p)^{11}B reaction has been studied at an incident energy of 350 keV. The purpose of the experiment was to study the level structure of ^{11}B by observing the proton spectra for the reaction and the de-excitation gamma rays from ^{11}B. In addition the ground state alpha particle for the ^{10}B(d,α)^{8}Be reaction along with the continuum for the breakup of ^{8}Be into α_1 and α_2 were observed. The measured energies of the charged particles as a function of the angle in the center of mass system were compared with the calculated results. The angular distribution of seven proton groups and one alpha group was also determined. (auth)

3562 (CONF-700322–, pp 297-304) CAPTURE OF ALPHA PARTICLES BY ^{12}C. Tombrello, T. A. (California Inst. of Tech., Pasadena).

From Proceedings of the second Oak Ridge conference on the use of small accelerators for teaching and research, March 23–25, 1970.

The capture of alpha particles by ^{12}C probably represents the crucial reaction in the route through which ^{16}O and the heavier nuclei are formed in stars; knowledge of this cross section in the relevant energy range (up to 400 keV) is therefore important for any complete study of nucleosynthesis. Since a direct measurement seems precluded by the low cross section [σ(400 keV) < 10^{-17} barns], indirect techniques must be used to infer the necessary information. Because this type of difficulty is common in many reactions of astrophysical importance, the ^{12}C(α,γ)^{16}O reaction is an excellent example of the experimental and theoretical difficulties that arise. It is worth noting that both in this example and in many similar cases, the resolution of the difficulties has not been entirely satisfactory, indicating that many challenging opportunities still remain for work in this area. (auth)

3563 (JINR-P15-5156) INVESTIGATION OF THE PROTON POLARIZATION IN THE REACTION ^{12}C(^{3}He,p$_0$)^{14}N. Eler, G.; Krivopustov, M. I.; Wiebicke, H.-J.; Asfur, F.; Sizov, I. V.; Shirmer, G. (Joint Inst. for Nuclear Research, Dubna (USSR). Lab. of Neutron Physics). 1970. 28p. (In Russian). Dep. NTIS (U. S. Sales Only).

Experimental data on polarization of protons in the reaction ^{12}C(^{3}He,p)^{14}N(ground state) are presented. The measurements were performed with the aid of an electrostatic generator using

a ring geometry polarimeter. The proton polarization values are obtained for six energies of ^{3}He ions in the range from 2.4 to 3.6 MeV for the angles of 20-70° (the energy and angle in the lab. system). The analysis of experimental data is performed according to the resonance theory of nuclear reactions. (auth)

3564 (KFK-1190) EXCITATION FUNCTIONS AND DIFFERENTIAL CROSS SECTIONS FOR THE ^{9}Be(n,α) REACTION WITH 8 TO 30 MeV NEUTRONS. Kropp, L.; Forti, P. (Kernforschungszentrum, Karlsruhe (West Germany). Institut fuer Angewandte Kernphysik). Jul 1970. 21p. Dep. NTIS (U. S. Sales Only).

A new four parameter time-of-flight experiment (particle type and energy, neutron energy and emission angle) yielding differential cross section data of neutron-induced reactions was performed. Energy distributions of α-particles from the ^{9}Be(n,α) reaction were measured at several angles for neutron energies ranging from 8 to 30 MeV. Angular distributions and excitation functions for the three lowest states of ^{6}He (ground state, 1.7 and 3.4 MeV) are evaluated. (auth)

3565 (NP-18476) STUDY OF DISTORTION IN THE REACTIONS (COPLANAR AND NONCOPLANAR) ^{12}C(p,2p)^{11}B$_{1P}$ AND ^{40}Ca(p,2p)^{39}K$_{2S}$ AT 156 MeV. Hourany, Eid (Paris Univ., Orsay (France). Faculte des Sciences). 13 Feb 1970. 73p. (In French). Dep. NTIS (U. S. Sales Only).

Thesis.

The correlation of the angular distributions (coplanar and noncoplanar) for the reactions ^{12}C(p,2p)^{11}B in the 1P3/2 state and ^{40}Ca(p,2p)^{39}K in the 2S1/2 state was measured, in view of studying over a large kinematic region the mechanism of the reaction (p,2p) and the distortion affecting the three protons of the reaction in the nuclear material. At 156 MeV and for targets of ^{12}C and ^{40}Ca the distortion affecting the (p,2p) reaction was not sufficiently important to produce a strong localization of the reaction in the nucleus. The shape of the experimental angular distributions was the same as those of the distributions calculated using the momentum approximation and plane waves. Several optical potentials explained the results, but an optical potential explaining the coplanar distribution of the (p,2p) reaction did not necessarily explain the noncoplanar distribution. The use of optical potentials, derived from the elastic scattering of protons, in the (p,2p) reactions, was a reasonable approach. (France)

3566 (SAL-14) ELECTRODISINTEGRATION OF CARBON. Wong, Cho Fai (Saskatchewan Univ., Saskatoon. Saskatchewan Accelerator Lab.). Jan 1970. 126p.

Thesis.

Energy spectra and angular distributions of protons from ^{12}C and ^{13}C produced by electron beams of energies E_0 = 45.9 and 43 MeV respectively have been measured by using a magnetic spectrometer and solid state detectors. The (e,pe') cross sections were converted to the corresponding (γ,p) cross sections using the EI virtual photon spectrum. The equivalent photodisintegration cross sections of ^{12}C agree with the proton spectra obtained with real photons in other laboratories. Both the energy spectrum and angular distribution of protons from ^{12}C indicate that the center of the giant resonance is at 22.5 MeV excitation and is predominantly of the $p_{\frac{3}{2}}^{-1}d_{\frac{5}{2}}$ configuration. The angular distribution of ^{12}C was found to be forward peaked at large energies, a phenomenon observed in previous measurements. The measurement on ^{13}C shows a broadening of the giant resonance peak which is centered at around 24 MeV excitation energy and assigned predominantly T = 3/2. Compared to the real photon measurements, the measurements show a larger cross section in the low energy region ($E_P \leq 5$ MeV) which cannot be explained by the nonground state transitions alone. The center of the giant resonance in ^{13}C is higher than that of ^{12}C by approximately 1.5 MeV which is the difference of the thresholds of (γ,p) from the two carbon isotopes. Shifting the energy scales by this amount, the energy spectra of ^{12}C and ^{13}C resemble each other except for possible J-splitting and T-splitting. In particular, the four finer peaks in the 24 MeV region of ^{13}C may correspond to the J-splitting of the levels at 22.5 and 25.5 MeV in ^{12}C by the coupling of a $p_{\frac{1}{2}}$ neutron to the core. The angular distribution of ^{13}C indicates that protons are primary due to d-wave emission with slight evidence of having a larger magnitude in the directions forward of 90° at higher energies. Thus, the angular distributions of both ^{12}C and ^{13}C indicate a predominant d-wave emission. The result of the present measurements suggest that, for the most part, the valence neutron acts as a spectator during the photo-excitation of the giant resonance in carbon. (auth)

3567 (SAL-15) STUDY OF HIGH-ENERGY PHOTONEUTRONS EMITTED FROM THE 1P-SHELL IN ^{12}C. Miller, H. G. (Saskatchewan Univ., Saskatoon. Saskatchewan Accelerator Lab.). Mar 1970. 91p.

Photoneutron spectra from ^{12}C were measured at bremsstrahlung end tip energies from 64 to 128 MeV in 2-MeV steps. The spectra were obtained simultaneously at five angles using time-of-flight techniques. The measured cross sections exhibit "kinematic resonances" corresponding to the emission of a single neutron from the 1P-shell in ^{12}C. The angular distributions of these P-shell neutrons are forward asymmetric, the asymmetry increasing with neutron energy. The results are compared with the single-particle and cluster theories. It was found that the angular distributions and the differential cross section at 90° can be explained best by the quasi-alpha model and therefore it is concluded that dynamic correlations between nucleons in the same shell are more important than those between nucleons in different shells. (auth)

3568 PROTON TOTAL REACTION CROSS SECTIONS FOR LIGHT NUCLEI BETWEEN 24 AND 46 MeV. McGill, William Fleming. Los Angeles; Univ. of California (1969). 104p. University Microfilms Order No. 70-8247.

Thesis.

Total reaction cross sections for protons incident on beryllium, carbon, oxygen, fluorine, aluminum, and silicon were measured at energies of 45.9, 42.9, 39.5, 36.6, 34.0, 30.3, 27.2, and 24.5 MeV. A beam attenuation technique was used, and the uncertainties in the measurements averaged between 2 and 3%. A gradual decrease with increasing energy was observed for all nuclei studied. A comparison of the results with existing optical model analyses indicated excellent agreement for aluminum and silicon. Agreement was fair for oxygen and carbon, and poor for beryllium. This indicates a decrease in the effectiveness of the optical model in the description of light nuclei. Differential cross sections for aluminum were measured at energies of 25.2, 30.8, 34.7, 40.7, and 47.3 MeV, and differential cross sections for silicon were measured at energies of 25.2, 34.7, 40.7, and 47.3 MeV. These data include angles between 20 and 125° and were measured in order to obtain correction terms for the reaction cross section measurements. Optical model analyses of these data were made, and agreement with experimental values was excellent. (Diss. Abstr. Int., B)

3569 MEASUREMENT OF THE LIFETIMES IN ^{12}B, ^{14}N, AND ^{16}O. Gallmann, A. (Univ. Laval, Quebec); Haas, F.; Balaux, N.; Heusch, B.; Toulemonde, M. Can. J. Phys.; 48: 1595-1606(1 Jul 1970). (In French).

Lifetimes of nuclear states were measured by the Doppler-shift attenuation method. Gamma radiations from the ^{11}B(d,pγ) ^{12}B, ^{19}F(p,$\alpha\gamma$)^{16}O, and ^{12}C(^{3}He,pγ)^{14}N reactions were observed with a Ge(Li) detector at θ_γ = 7, 90 and 173°. The following lifetimes were obtained: ^{12}B, 0.953 MeV, $\tau = (2.0 \pm 0.4) \times 10^{-13}$ s, ^{16}O, 8.88 MeV, $\tau = (1.5 \pm 0.3) \times 10^{-13}$ s, ^{14}N, 6.44 MeV, $\tau = (6.3 \pm 0.4) \times 10^{-13}$ s. Upper limits were set for very fast lifetimes, and transition energies were also determined. The partial widths of the radiative transitions from the 6.44 MeV state of ^{14}N were compared with theoretical predictions. The amplitude of a $(p_{\frac{1}{2}})^{-2}$ configuration in the wave function of this level was evaluated using the partial width of the 6.44 → 3.95 MeV transition determined in the present work. (auth) (Canada)

3570 EXCITED STATES (4p-3h) IN REACTION ^{13}C(^{6}Li,d)^{17}O AND ^{13}C(^{7}Li,t)^{17}O. Gol'dberg, V. Z.; Davydov, V. V.; Ogloblin, A. A.; Sakuta, S. B.; Chuev, V. I. Yadern. Fiz.; 12: 30-4(Jul 1970). (In Russian).

The reactions (^{6}Li, d) and (^{7}Li, t) on ^{13}C at the Li energies E = 25.6 MeV and 30.1 MeV, respectively, were investigated. Experimental support is provided for the hypothesis on weak binding of four particles in the (sd) shell and of three holes in the ($p_{\frac{1}{2}}$) shell. The results are in good agreement with the calculations. The measurements enable one to establish the spin and parity of 7.56-MeV level in ^{17}O to be $\frac{5}{2}^-$. (auth)

3571 WIDTHS OF THE 6.92 MeV AND 7.12 MeV LEVELS OF ^{16}O. Swann, C. P. (Franklin Inst., Swarthmore, Pa.). Nucl. Phys.; A150: 300-4(1970).

The radiative widths of the 6.92 MeV 2^+ and 7.12 MeV 1^- levels of ^{16}O have been measured by the resonance fluorescence technique using a 30 cm^3 Ge(Li) diode. The source of exciting radiation was the Doppler-broadened gamma rays from the ^{19}F(p,$\alpha\gamma$)^{16}O reaction. Widths of 110 ± 5 meV and 62 ± 5 meV were obtained for the 6.92 MeV and 7.12 MeV levels, respectively. By comparison with the accurately known energy of the upper line the energy of the lower line was measured to be 6.9172 ± 0.0008 MeV. (auth)

3572 COMPOUND-NUCLEUS DIRECT INTERACTION INTERFERENCE IN THE ^{12}C(d,p$_0$)^{13}C REACTION AT 3.4 MeV. Leonard, J. W. (Univ. of Oregon, Eugene); Wells, D. O. Nucl. Phys.; A153: 657-64(1970).

A complete analysis of the interference between linearly combined direct interaction and compound nucleus amplitudes has been made for the ^{12}C(d,p$_0$)^{13}C reaction near the 3.4-MeV resonance. In contrast to previous work, all partial waves have been included in the calculations at this resonance, which can reasonably be assumed to be isolated. The results agree fairly well with the ex-

XUM

perimental excitation functions at forward angles, and they indicate that the discrepancy between previous measurements of the total width from ^{12}C + d and ^{10}B + α experiments may be due to interference effects in the former reaction. (auth)

3573 ISOBARIC SPIN DOUBLETS IN ^{9}Be EXCITED WITH THE $^{10}B(d,\alpha)^{8}Be$ REACTION. Callender, W. D.; Browne, C. P. (Univ. of Notre Dame, Ind.). Phys. Rev., C; 2: 1-12(Jul 1970).

The 2^+ levels in ^{8}Be at 16.6 and 16.9 MeV were investigated using the $^{10}B(d,\alpha)^{8}Be$ reaction at several angles and bombarding energies from 4.0 to 12.0 MeV. A pattern of interference between these two levels was observed at all angles and energies except at a deuteron energy of 4.0 MeV. Fits were made to the α-particle spectra using two different formulas for the differential cross section. The results are interpreted in terms of the isobaric spin purity of the levels and isobaric spin mixing in the reaction. The latter is found to vary from 4 to 99%. The effects of other 2^+ levels on the 16.6- and 16.9-MeV levels are also discussed. Differential-cross-section ratios of the 1^+ doublet at 17.6 and 18.1 MeV were simultaneously measured. This ratio depends upon deuteron bombarding energy in a way consistent with the change in isobaric spin mixing in the reaction. The 3^+ doublet at 19.05 and 19.22 MeV was investigated. Only one particle group is observed. Various explanations in terms of interference in this region are discussed. The excitation energy and width of the higher 1^+ level were found to be 18.146 ± 0.005 MeV and 138 ± 6 keV, respectively, based on an adopted value of 17.638 MeV for the excitation energy of the lower 1^+ level. (auth)

3574 POLARIZATION OF NEUTRONS FROM (d,n) REACTIONS ON ^{11}B, ^{14}N, AND ^{15}N. Busse, W.; Efken, B.; Hilscher, D.; Scheer, J. A.; Wenning, W. (Hahn–Meitner Institut fuer Kernforschung, Berlin). Nucl. Phys.; A152: 354-68(1970).

The angular dependence of the differential cross section and polarization for the reactions $^{11}B(d,n)^{12}C$ to the ground state and first-excited state of ^{12}C, and $^{14}N(d,n_0)^{15}O_{g.s.}$ have been measured at E_d = 5.5 MeV from 10° to 160°; for $^{14}N(d,n_0)^{15}O$, the energy dependence of the polarization at a lab angle of 25° has been measured between 4.2 and 6.0 MeV. For angles where the differential cross section is small but the polarization is large, a possibility to estimate the compound nucleus contribution is presented. The polarization and differential cross section of the reactions ^{11}B, ^{14}N, $^{15}N(d,n)$ are analyzed with DWBA theory. For the nitrogen isotopes a fair agreement is achieved. No such agreement was possible for the reaction $^{11}B(d,n)$; the transition to the first-excited state seems to be a mixture of a $1p_{\frac{1}{2}}$ and $1p_{\frac{3}{2}}$ proton transfer. (auth)

3575 ELECTROMAGNETIC TRANSITIONS IN ^{19}Ne. Gill, R. D.; Bharuth-Ram, K.; Jackson, K. P.; Bell, R. A. I.; Robertson, B. C.; L'Ecuyer, J.; Chapman, N. G.; Rose, H. J. (Nuclear Physics Lab., Oxford). Nucl. Phys.; A152: 369-86(1970).

The Doppler shift attenuation observed with a Ge(Li) γ-ray detector was used to gain information on the decay rates of some of the bound states of ^{19}Ne. The values $\tau = 4.1^{+3.1}_{-1.4}$ ps, τ = 28 ± 15 fs, τ = 180 ± 60 fs and τ = 330 ± 130 fs have been determined for the 1508, 1536, 1615 and 2795 keV levels respectively. Level energies and decay schemes are reported and angular correlation studies taken together with the lifetime results and mirror level arguments show that the spin-parity sequence for the levels studied is $5/2^-$, $3/2^+$, $3/2^-$ and $5/2^+$ respectively. The results are compared with model calculations. (auth)

3576 DETERMINATION OF $^{14}N(n,2n)^{13}N$ REACTION CROSS SECTION FOR 14.7 MeV NEUTRONS. Ishikawa, Hiroaki (Japan Atomic Energy Research Inst., Tokyo). J. Nucl. Sci. Technol. (Tokyo); 7: 534-8(Oct 1970).

The cross section for the $^{14}N(n,2n)^{13}N$ reaction with 14.7-MeV neutrons was determined. In this experiment, the $^{27}Al(n,p)^{27}Mg$ reaction was selected as reference standard for its generation of the nuclide ^{27}Mg which has a half-life very close to that of ^{13}N. The full-energy peaks of the γ-ray spectrum obtained by a multichannel pulse-height spectrometer was analyzed with γ-ray energy resolution determined by means of normal probability plots. The resulting value for the cross section is 8.2 ± 1.1 mb, which is in remarkably good agreement with the value reported in the literature. (auth)

3577 QUASIELASTIC ELECTRON SCATTERING IN A SQUARE-WELL SHELL MODEL. Donnelly, T. W. (Stanford Univ., Calif. Univ. of Toronto). Nucl. Phys.; A150: 393-416 (1970).

The process of quasielastic electron scattering from ^{12}C and ^{40}Ca is studied within the framework of a square-well shell model. The nuclear potential well parameters are assigned prior to the electron scattering calculation by fitting separation energies, elastic electron scattering form factors and results obtained from nucleon scattering experiments. The general behavior of the calculated cross section is investigated over a wide range of excitation energies and three-momentum transfers and detailed comparisons with recent experimental data are presented. (auth)

3578 STUDY OF ^{6}Li + ^{12}C REACTIONS. Johnson, D. J.; Waggoner, M. A. (Univ. of Iowa, Iowa City). Phys. Rev., C; 2: 41-59(Jul 1970).

A comprehensive investigation of the ^{6}Li + ^{12}C reaction was carried out for particle groups corresponding to the following states of the residual nuclei involved: 0.0-, 0.871-, 3.058-, 3.846-, and 4.551-MeV for ^{17}O; 0.0-, (6.05 + 6.13)- (unresolved), (6.92 + 7.12)-, and 8.88-MeV for ^{16}O; 0.0-MeV for ^{15}O; and 0.0-, 3.945-, and (4.91 + 5.10)-MeV for ^{14}N. Yield curves were measured for protons, deuterons, and α particles at laboratory angles of 0° and 40° at ^{6}Li bombarding energies from 5.6 to 14.0 MeV. Angular distributions were measured at 9.0, 10.0, 11.2, 12.0, 13.0, and 14.0 MeV for all of the above groups and from 5.6 to 6.6 MeV at 0.200-MeV intervals for most of the groups. A comparison is made of the accumulated α-particle data and two-mode plane-wave and single-mode distorted-wave direct-reaction models. The proton, deuteron, and α-particle data are also compared with the statistical compound-nucleus model. (auth)

3579 THREE-BODY BOUND-STATE CALCULATIONS FOR SOME LIGHT NUCLEI. Leung, Charles Chi-hei. Waco, Tex.; Baylor Univ. (1969). 133p. University Microfilms Order No. 70-7667.

Thesis.

The approximate method of solving the three-body bound-state Schroedinger equation advocated by Eyges and Mitra is generalized to a wave function method which preserves the hermiticity of the Fredholm kernel and permits an angular-momentum analysis. This method is applied to the groundstate calculation of three nuclei in chosen three-body models — namely, ^{12}C as (α,α,α), ^{6}Li ad (α,N,N) and ^{9}Be as (N,α,α) — in which the particles are taken to be elementary and the Coulomb effects are removed. The interactions are two-body nonlocal but separable potentials determined by fitting the two-body scattering data and binding energies. The energies in MeV below the three-body thresholds of the ground and the first excited states of the same J^π obtained for ^{12}C are −12.2 and −6.6, for ^{6}Li −3.32 and −0.92, and for ^{9}Be −5.11 and −2.55, respectively. When the Coulomb energies are taken to be 5.44, 1.0, and 3.5 MeV for ^{12}C, ^{6}Li, and ^{9}Be, respectively, the deviation of the calculated ground-state energy is 4% for ^{12}C, 29% for ^{6}Li, and 2% for ^{9}Be. The equivalence between this method and the Faddeev–Lovelace formalism is established by comparing the three-body equation obtained for ^{12}C and the corresponding equation obtained by Harrington. The wave functions obtained for the three-alpha system are applied to calculate the root-mean-square radius of the nucleus. The values found from the use of different model potentials are compatible with the experimental matter radius of ^{12}C. (auth) (Diss. Abstr. Int., B)

3580 REALISTIC FORCES AND DEFORMED STATE ADMIXTURES IN ^{18}O. Trlifaj, L.; Sotona, M. (Nuclear Research Inst., Rez, Czech.). Czech. J. Phys.; 20: 865-78(1970).

The structure of states in ^{18}O is investigated by assuming two-neutron configurations in the (2s − 1d) shell, with an admixture of deformed (SU_3) configurations of the same shell composed of two neutrons and two protons transferred from the $1p_{\frac{1}{2}}$ shell. The residual realistic Elliott potential matrix and Tabakin potential with some corrections of the second order of nuclear matter theory are assumed. Splitting of levels between the $1d_{\frac{5}{2}}$ and $1p_{\frac{1}{2}}$ shells is used as a free parameter. The calculated level positions and E2 transition probabilities with the effective charge 0.5e for nucleons are in good agreement with experiment for some of the cases. (auth)

3581 QUASI-ELASTIC SCATTERING OF 160-MeV PROTONS BY ALPHA CLUSTERS IN LIGHT NUCLEI. I. CARBON. Gottschalk, B. (Northeastern Univ., Boston); Kannenberg, S. L. Phys. Rev., C; 2: 24-40(Jul 1970).

Alpha-cluster knockout from ^{9}Be, ^{12}C, and ^{16}O by 160-MeV protons was investigated. The outgoing proton and α particle were detected in coincidence and their momenta measured with good resolution. Knockout, sequential decay, and spallation reactions were observed. Proton and α detection angles were varied so as to test the plane-wave impulse-approximation (PWIA) model of the knockout reaction over a wide range of the effective p–cluster interaction. The method, apparatus, and carbon results are discussed in this paper. Measured values of the fully differential cross section $d^3\sigma/d\Omega_\alpha d\Omega_p dT_p$) are given, and they are shown to vary nearly as predicted by the PWIA. The errors due to finite detector sizes (finite momentum resolution) are discussed in some detail. The recoil correction to the usual PWIA expression for the cross section is derived. The branching ratio to the first excited state of the residual ^{8}Be nucleus, as

well as the effective number of α clusters in ^{12}C, are discussed and compared with theoretical predictions. (auth)

3582 CALCULATION OF SPECTRUM OF EVEN-PARITY LOW-LYING LEVELS FOR ^{17}O NUCLEUS. Rybachenko, V. F.; Sadovoi, A. A. Yadern. Fiz.; 11: 1192-9(Jun 1970). (In Russian).

Matrix elements from the nucleon–nucleon potential over the angular harmonics are presented in a form convenient for calculations. The distances between the levels $5/2^+$, $1/2^+$, $3/2^+$, of the ^{17}O nucleus are calculated in the approximation of the minimal global momentum K. Reasonable agreement with experiment is obtained, even for nucleon–nucleon potentials which do not satisfy the conditions of saturation of nuclear matter. (auth)

3583 STRONG ABSORPTION MODEL ANALYSIS OF THE REACTIONS (^{3}He,^{7}Be) AND (^{3}He,^{6}Li) ON ^{16}O AND ^{12}C AT 24.5 AND 28.0 MeV. Ohta, Masahisa; Saeki, Bunzo; buro (Konan Univ., Kobe, Japan). Mem. Konan Univ., Sci. Ser.; No. 12, 1-14(Nov 1969).

The angular distributions for $^{16}O(^3He, ^6Li)^{13}N$, $^{16}O(^3He, ^7Be)^{12}C$, and $^{12}C(^3He, ^7Be)^8Be$ reactions are analyzed by means of the strong-absorption model with the smooth cut-off and the Coulomb effect. The large value of β (the interaction parameter in Yukawa-type form factor) and very small value of σ(the diffuseness parameter) as compared with the case of DWBA yield good agreement with the experimental data. The theoretical pattern of the oscillation represents a reasonable feature in all cases. (auth)

3584 STUDY OF γ TRANSITIONS IN ^{19}O. Fintz, P.; Hibou, F.; Rastegar, B.; Gallmann, A. (Laboratoire de Physique Nucleaire et d'Instrumentation Nucleaire, Strasbourg). Nucl. Phys.; A150: 49-55(1970). (In French).

The $^{18}O(d, p\gamma)^{19}O$ reaction has been investigated at E_d = 5 MeV. A Ge(Li) detector and a NaI(Tl) crystal were used to detect γ-rays in coincidence with reaction particles detected near 180°. Excitation energies have been obtained for the ^{19}O levels at 1470 ± 3, 2369 ± 4, 2777 ± 3, 3157 ± 3 and 3944 ± 3 keV and gamma-ray branching ratios have been determined for these levels. (auth)

3585 ASSYMMETRIES PRODUCED BY 28-MeV VECTOR POLARIZED DEUTERONS IN THE ELASTIC SCATTERING $^{12}C(d,d)^{12}C$, $^{28}Si(d,d)^{28}Si$, AND $^{40}Ca(d,d)^{40}Ca$. Burq, J.-F.; Hadinger, G.; Kouloumdjian, J.; Meyer, J. (Univ., Lyon). Nucl. Phys.; A149: 488-500(1970). (In French).

The asymmetries which appear in the elastic scattering of vector polarized deuterons of 28 MeV were studied. An interpretation with the optical model explains the experimental asymmetries very satisfyingly. (auth)

3586 THICK-TARGET $^{16}O(d,n)^{17}F$ YIELD CURVES. Bahnsen, R. M.; Wylie, W. R.; Lefevre, H. W. (Univ. of Oregon, Eugene). Phys. Rev., C; 2: 859-65(Sep 1970).

A thick-target method has been used to measure absolute differential cross sections for the reactions $^{16}O(d,n)^{17}F$ and $^{16}O(d,n)^{17*}F$ (0.500 MeV) from 2.0 to 4.2 MeV. Excitation functions were taken at 20° intervals from 0–160° in the lab system. Satisfactory fits to the angular distributions required Legendre polynomials of order 6 or higher. The cm Legendre coefficients A_0 and A_1 are presented as a function of lab deuteron energy for the ground-state data. The total cross sections for production of ground-state and first-excited-state neutrons are also given as a function of energy. (auth)

3587 ELASTIC ELECTRON SCATTERING FROM ^{12}C AND ^{16}O. Sick, I.; McCarthy, J. S. (Stanford Univ., Calif.). Contract Nonr 225 (67). Nucl. Phys.; A150: 631-54(1970).

Electron scattering cross sections for carbon and oxygen between q = 1 fm^{-1} and 4 fm^{-1} are given. The data are analyzed in terms of a phenomenological charge distribution and new information concerning the tail and the center of the charge distribution are obtained. The presence of dispersion effects appears to be necessary to explain the cross sections in the first diffraction minimum. The effect of a finite potential and short range-correlations on the form factor are discussed. (auth)

3588 INVESTIGATION OF THE 5.96-MeV DOUBLET IN ^{10}Be. Grant III, Walter Henry. New Orleans; Tulane Univ. (1969). 52p. Thesis.

The $^9Be(d,p)^{10}Be$ reaction was performed at an incident deuteron energy of 2.90 MeV. Particle-gamma correlations between the proton group populating the doublet at 5.96 MeV in ^{10}Be and the associated gamma decays were measured using a collinear geometry. Spin assignments of J = 1 and J = 2 were confirmed, and the multipole mixture of the transition from the J = 2 member of the doublet to the $J^\pi = 2^+$ first excited state was deduced to be δ (E2/M1) = .11 ± .05, and a positive parity was assigned to that member of the doublet. Shell model structure and the application of isospin to A = 10 nuclei are discussed. (Diss. Abstr. Int., B)

3589 REACTION $^{11}B(p,^4He)$ FOR PROTON-BEAM ENERGIES OF 0.675, 1.00, AND 1.388 MeV. Alessi, Victor Elliot. Washington, D. C.; Georgetown Univ. (1970). 135p. Thesis.

The reaction $^{11}B(p,3\alpha)$ was studied at proton-beam energies of 0.675, 1.00, and 1.388 MeV. The mode of decay of the reaction was found to be sequential at those energies. The width of the 2.9 MeV first-excited state of ^8Be was studied and found to be 1.0 MeV. At kinematically allowed angles an analysis of the shapes of the coincidence spectra, using Breit–Wigner line shapes, revealed the coherent interference of the first- and second-emitted ^4He particles from this reaction. A phenomenological model was proposed to explain the interference. (Diss. Abstr. Int., B)

3590 THE $^{14}N(^3He,\alpha)^{13}N$ REACTION. Knudson, A. R. (Naval Research Lab., Washington, D. C.); Young, F. C. Nucl. Phys.; A149: 323-36(1970).

Differential cross sections for the $^{14}N(^3He,\alpha)^{13}N$ reaction leading to the ground, 2.37 and (3.51 + 3.56) MeV states of ^{13}N have been measured for incident energies from 2.5 to 8.5 MeV. Large fluctuations are observed in excitation functions at 50°, 90° and 165°. Angular distributions over the range from 5° to 165° exhibit pronounced forward and backward peaking at 4.5 and 5.5 MeV, but relatively less backward peaking at 7.0 MeV. Differential cross sections for the elastic scattering of ^3He from ^{14}N at 4.5 and 7.0 MeV have been measured and used to determine optical potentials. Distorted wave analyses of reaction angular distributions at 7.0 MeV to the ground and 2.37 MeV states have been made. Spectroscopic factors were extracted assuming a direct pickup reaction mechanism. Calculations of the angular distribution to the 2.37 MeV state, assuming a direct knockout reaction mechanism, were made and are compared with the pickup calculations. (auth)

Nuclear Properties and Reactions, 20 ≤ A ≤ 89

Refer also to abstracts 2435, 3247, 3545, 3565, 3568, 3577, 3585, 3694, 3695, 3704, and 3722.

3591 (AAEC/TM-542) THE CALCULATION OF (n,2n) CROSS SECTIONS USING THE HAUSER–FESHBACH THEORY. Bertram, W. K. (Australian Atomic Energy Commission Research Establishment, Lucas Heights). May 1970. 14p. Dep. NTIS (U. S. Sales Only).

The statistical theory of Hauser and Feshbach was used to calculate the (n,2n) cross sections of ^{63}Cu, ^{197}Au, ^{203}Tl, ^{232}Th, and ^{238}U, for incident neutron energies below the (n,3n) threshold. Results were compared with experiment and with the results from the evaporation model. (auth) (Australia)

3592 (COO–1120-106) INTERMEDIATE COUPLING IN THE N = 29 AND Z = 29 NUCLEI. Larner, D. (Kansas Univ., Lawrence. Nuclear Structure Lab.). [1970]. Contract AT(11-1)-1120. 54p. Dep. NTIS.

Levels are calculated for the N = 29 and Z = 29 nuclei, ^{51}Ti, ^{53}Cr, ^{55}Fe, $^{61,63,65}Cu$. The model used is the intermediate coupling model, with quasi-vibrational core, as developed by True and Thankappan. A pattern search routine is used to fit the five parameters to the levels and stripping strengths. Except for the case of ^{53}Cr, levels and strengths are fit fairly well. In particular in ^{55}Fe we identify the states at 1.917 MeV and 2.051 MeV as $3/2^-$ and $1/2^-$ states, respectively. B(E2) values for transitions to the ground state are calculated, and the comparison with data for ^{63}Cu and ^{65}Cu shows good agreement. However, there is no experimental B(E2) data available for the other nuclei. (auth)

3593 (COO–1530-21) STRUCTURE OF ^{51}Cr VIA $^{48}Ti(^4He,n\gamma)$ AND $^{51}V(p,n\gamma)$ PROMPT γ-RAY SPECTROMETRY. Sarantites, Demetrios G.; Winn, Willard G. (Washington Univ., St. Louis, Mo. Dept. of Chemistry). [1970]. Contract AT(11-1)-1530. 74p. Dep. NTIS.

The level structure of ^{51}Cr has been studied in some detail via prompt γ-ray energy and intensity measurements utilizing a NaI(Tl)-Ge(Li) anti-compton spectrometer and a 511-γ-511 escape peak spectrometer via the $^{51}V(p,n\gamma)$ reaction with proton energies in the range 2.6-6.0 MeV and via the $^{48}Ti(^4He,n\gamma)$ reaction with $^4He^{++}$ energies in the range 12.0-15.0 MeV. Many of the γ-rays associated with levels in ^{51}Cr were identified with the $(^4He,n\gamma)$ or the $(p,n\gamma)$ reaction by means of n-γ coincidence measurements employing an organic phosphor as the fast neutron detector and a Ge(Li) γ-ray detector. Characterization of many levels populated in the $(p,n\gamma)$ reaction was achieved by means of thresholds for individual γ-rays obtained from measurement of excitation functions of individual γ-rays and from the γ-γ coincidence relationships established in on-beam γ-γ coincidence measurements in the $^{51}V(p,n\gamma)$ reaction at E_p =

XUM

5.0 MeV employing a NaI(Tl) and a Ge(Li) detector. It was thus established that 39 levels in ^{51}Cr are populated in these reactions. The levels at 2255.7, 2385.6, 2767.1 and 3001.6 or 3004.1 keV which were observed in these experiments have not been reported previously. The rest of the levels studied in this work have been studied previously by means of (d,p), (p,d) and (n_{th},γ) reactions. With the exception of the first six levels, the levels reported here have not been reported previously in the (p,nγ) or the (^{4}He,nγ) reactions. For the levels below 2704 keV in ^{51}Cr branching ratios for deexcitation of these levels by γ-decay were obtained by averaging the measured angular correlation of each γ-ray about the beam direction. The new γ-ray information from the present study was used in conjunction with the results of previously reported (d,p) reaction studies to make definite J^π assignments to many stripping levels in ^{51}Cr and to place limits to the J^π values for many levels which were reported earlier to exhibit proton angular distribution patterns from the (d,p) reaction non-characteristic of a stripping reaction. In this work a number of γ-rays were assigned to levels in ^{51}V that are populated via the ^{51}V(p,p'γ) and ^{48}Ti(^{4}He,pγ) reactions and which were found to compete to a small extent with the (p,nγ) and (^{4}He,nγ) reactions. A tentative decay scheme for the deexcitation of levels in ^{51}V is offered. The level structure of ^{51}Cr and of ^{51}V is compared with previously reported results of the Coriolis coupling model for the $f_{\frac{7}{2}}$ shell and good qualitative agreement in the level ordering is found. (auth)

3594 (NP-18464) STUDY OF THE MECHANISM OF THE (^{3}He,α) REACTION AT LOW ENERGY. APPLICATIONS TO THE STUDY OF ^{27}Si AND ^{31}S LEVELS. Rotbard, Georges (Paris Univ., Orsay (France). Faculte des Sciences). 1970. 41p. (In French). Dep. NTIS (U. S. Sales Only). Thesis.

The method of calculating the pick-up cross sections using the DWBA was recalled. The experimental apparatus used for measuring these cross sections for the (^{3}He,α) reactions on ^{28}Si and ^{32}S was then described. The aim of the research was to discover whether the spectroscopic factors could be measured by the (^{3}He,α) reaction at energies in the region of the coulomb barrier, and to determine the values of these factors for the levels of ^{27}Si and ^{31}S. The excitation energy for 11 levels of ^{27}Si, 15 levels of ^{31}S, the angular distributions at 7.6 MeV for the reactions populating the fundamental levels and several excited levels of ^{27}Si and ^{31}S were obtained; the excitation functions for the reactions ^{28}Si (^{3}He,α)^{27}Si at 20° and ^{32}S(^{3}He,α)^{31}S at 55° (the angles chosen were the maxima of the angular distribution) and the angular distributions for several incident alpha energies of the reactions populating the fundamental and the two first excited states of ^{27}Si and the fundamental level of ^{31}S were investigated. The analysis of the results in conjunction with those obtained at higher energy, led to the conclusion that for the (^{3}He,α) reaction at an incident energy of about 8 MeV there is competition between direct pick-up and other reaction mechanisms. The experimental values of the spectroscopic factors were in satisfactory agreement with those calculated using the shell model with residual interaction. There was, however, a contradiction with the values obtained using the weak coupling model or a single particle model in a deformed potential. (auth) (France)

3595 (ORNL-4551) V NEUTRON ELASTIC- AND INELASTIC-SCATTERING CROSS SECTIONS FROM 4.19 TO 8.56 MeV. Perey, F. G.; Kinney, W. E. (Oak Ridge National Lab., Tenn.). Oct 1970. Contract 7405-eng-26. 80p. Dep. NTIS.

Numerical values for neutron elastic-scattering cross sections for natural V(99.76%^{51}V, 0.24%^{50}V) and cross sections per atom of natural V for inelastic scattering to levels in ^{51}V for incident neutron energies from 4.19 to 8.56 MeV are presented. The data are in good agreement with the results of others. The ENDF/B V elastic angular distributions are in good agreement with experimental data at forward angles but are displaced about 10° toward 0° beyond the first minimum. The ENDF/B excitation functions are in good agreement with experiment although the inelastic functions stop at 2.6 MeV. The data partially fill priority III requests to NCSAC. (auth)

3596 (TID-25503) STUDY OF THE NUCLEI ^{61}Cu, ^{64}Cu, ^{67}Ga, AND ^{68}Ga USING THE (p,n) REACTION. Bass, William Thomas (Tennessee Univ., Knoxville). Aug 1970. 85p. Dep. CFSTI. Thesis.

Neutron time-of-flight techniques were used to study the (p,n) reaction on the nuclei ^{61}Ni, ^{64}Ni, ^{67}Zn, and ^{68}Zn. The locations of excited states in the residual nuclei up to 3 MeV excitation energy were measured with about 10 keV energy resolution. Some 20 to 70 excited states were identified in the residual nuclei. Level energies were assigned with certainties of 2 keV for low-lying states and 5 to 7 keV for higher (2 to 3 MeV) states. In general the (p,n) cross sections do not exhibit a strong dependence on the properties of the residual state (spin, parity, shell-model configuration, collectivity). However, a certain quantization of the observed peak areas was found. This feature led to a study of the predicted cross sections for final states of different spins and parities using an evaporation mechanism in a form referred to as the Hauser-Feshbach process. An optical model was used to predict barrier transmission functions for incident and exit channels of the compound nucleus. Transmission functions were only required for partial waves of low l-value at the energies used in the present experiment. The method was more sensitive to the spin of the residual nucleus than to final parity. Therefore, in general, only spin predictions were attempted. Spins were assigned to 10 to 20 levels in ^{64}Cu, ^{67}Ga, and ^{68}Ga. The results were in good agreement with known data. (auth)

3597 STRUCTURE OF THE LOW LYING LEVELS OF THE ^{33}S NUCLEUS INVESTIGATED BY THE ^{32}S(d,p)^{33}S REACTION. Bobrowska, A.; Chyla, K.; Strzalkowski, A.; Tomza, U.; Wiktor, S. (Inst. of Nuclear Physics, Krakow). Acta Phys. Pol.; B1: 201-10(Jul-Sep 1970).

An investigation of the ^{32}S(d,p)^{33}S reaction was made at a deuteron bombarding energy of 12.3 MeV. The energy spectra were measured by magnetic analysis and the obtained angular distributions were compared with the predictions of DWBA, using the deuteron optical model parameters obtained from an analysis of the elastic scattering of deuterons on ^{32}S nuclei. The absolute values of spectroscopic factors, extracted on this basis, indicate a significant contribution of higher configurations in the ground state wave function of the ^{32}S nucleus. There are no arguments which permit the identification of the observed states of the ^{33}S nucleus as rotational states. (auth)

3598 ELASTIC SCATTERING OF 39.6-MeV PROTONS BY THE NICKEL ISOTOPES. Liers, Henry Soehlke. Minneapolis; Univ. of Minnesota (1969). 116p. Thesis.

Proton elastic differential cross-section and polarization measurements were made on the isotopes of 58, 60, 62, 64 Ni at 39.6 MeV. Generally, both the cross-section and polarization measurements cover an angular range between 20 and 120°, except in the case of the cross-section data taken on ^{58}Ni and ^{60}Ni which were measured to 160°. Apart from absolute normalizations, errors range from 2.0 percent at small angles to 6.0 percent at large angles for the cross-section data and from 0.01 at small angles to 0.08 at large angles for the polarization data. Similar data were also taken on the isotopes of 64, 66, 68 Zn and are included for the sake of completeness and comparison. These data were analyzed using a standard optical model and two versions of a model recently proposed by Greenlees, Pyle, and Tang. From this analysis, information concerning variations of root-mean-square radii of the matter, neutron, and real central potential form factors in an isotopic sequence is extracted along with similar information concerning the integral over the volume of the potentials obtained. The cross sections and polarizations predicted by the models are compared with the data to determine if one model is preferred over the other. Also, by using different models the model dependency of the aforementioned root-mean-square radii and integrals is investigated. (Diss. Abstr. Int., B)

3599 ELASTIC AND INELASTIC SCATTERING OF 28-MeV PROTONS FROM IRON, COBALT, NICKEL, AND ZINC. Lewis, Paul Spurgeon Jr. Los Angeles; Univ. of Southern California (1969). 140p. University Microfilms Order No. 70-8532. Thesis.

Differential cross sections for elastic scattering of 28.0 MeV protons from natural isotopic mixtures of Fe, Co, Ni and Zn were measured at thirty-six scattering angles between 10.0 and 150.0 degrees. Cross sections for scattering from the first excited states of Fe, Ni and Zn and the integrated cross sections for scattering from all excited states with Q-values down to −8.0 MeV were also measured. Good fits to the scattering data were obtained with the optical model. The parameters found were in general agreement with those found by Satchler at 30.3 MeV. However, the real potential depth required to fit the Ni data was approximately 1.3 MeV greater than predicted by Satchler's linear function of the nuclear asymmetry, and the variation of potential depths between elements was not well represented by a linear function. The best fits were obtained with parameter sets in which the imaginary potential had a larger radius and smaller peak width for Ni than for its neighbors. The dip in σ_R at Ni was not reproduced in the optical model predictions. (Diss. Abstr. Int., B)

3600 HIGH EXCITED LEVELS OF ^{27}Al. Wakatsuki, Tetsuo; Takahashi, Noriaki; Suzuki, Katsumichi; Itahashi, Takahisa (Osaka Univ.). J. Phys. Soc. Jap.; 29: 815-26(Oct 1970).

The spectrum and angular distribution of alpha particles scattered by ^{27}Al at 22.2 MeV bombarding energy were measured. Among the prominent peaks in the spectrum, those corresponding to excited states at 5.434, 6.547, 7.28 and 7.50 MeV were studied

by measuring the gamma ray spectrum in coincidence with scattered alpha particle. From the measured gamma ray branching ratios, ($5/2$, $7/2$, $9/2$)$^+$ was assigned to the former two levels and $7/2^-$ was assigned to the latter two levels. In addition, from gamma ray transition rate considerations, $3/2^-$, $9/2^+$ and ($3/2$, $5/2$)$^+$ were found appropriate for 4.055, 4.508 and 5.491 MeV levels, respectively. (auth)

3601 STUDY OF ^{57}Co BY THE ^{56}Fe(p,γ)^{57}Co REACTION. O'Brien, B. J.; Coote, G. E. (Inst. of Nuclear Sciences, Lower Hutt, N. Z.). Nucl. Phys.; A153: 593-609(1970).

The yield curve for the ^{56}Fe(p,γ)^{57}Co reaction was measured for proton energies from 1210 to 2575 keV. Gamma-ray spectra were measured with a Ge(Li) detector at 14 resonances and angular distribution measurements made at 5 resonances. A Q-value for this reaction of 6026.7 ± 0.7 keV was obtained. The angular distributions were analyzed to give the following J$^\pi$(keV) assignments of ^{57}Co bound states and resonance levels: J(1224) = $3/2$, J$^\pi$(1757) = $3/2^-$, J$^\pi$(1897) = $1/2^-$, J(1919) = $5/2$, J(2132) = $5/2$, J(3850) = $3/2$, J(3989) = $5/2$, J$^\pi$(7252) = $3/2^-$, J$^\pi$(7266) = $1/2^-$, J(7523) = $5/2^+$, J$^\pi$(7632) = $3/2^-$ and J$^\pi$(8192) = $5/2^+$. From spin assignments, the resonance E_p = 1262.1 keV was identified as the isobaric analog of the ^{57}Fe ground state. A Coulomb displacement energy for ^{57}Co–^{57}Fe of 8881.5 ± 6.0 keV is deduced. The low-lying energy levels are examined with respect to the center-of-gravity theorem. (auth)

3602 STUDY OF THE ^{28}Si(^{3}He,p)^{30}P REACTION. Groeneveld, K. O.; Hubert, B.; Bass, R.; Nann, H. (Univ., Frankfurt am Main). Nucl. Phys.; A151: 198-210(1970).

The ^{28}Si(^{3}He,p)^{30}P reaction was investigated at incident energies between 4.3 and 11 MeV. Angular distributions to the ground state and the four lowest excited states were measured. Contributions to the measured cross sections from the compound and direct reaction mechanism are estimated. The data are analyzed using PWBA and DWBA in order to extract L-values and spectroscopic information. The results are compared with shell-model calculations. (auth)

3603 PROTON SCATTERING CALCULATIONS FROM ^{23}Na AND ^{25}Mg. Ottaviani, P. L.; Zuffi, L. (Comitato Nazionale Energia Nucleare, Bologna). Nucl. Phys.; A152: 570-8(1970).

The scattering cross sections of 17.5-MeV protons from five low-lying states in ^{23}Na and five low-lying states in ^{25}Mg were analyzed with the coupled-channel method. Excitations of rotational bands built on different single-particle states have been taken into account. The interaction potential used contains a macroscopic non-spherical optical part, which gives rise to the collective effects, and a microscopic effective part, which allows the single-particle excitations. (auth)

3604 LEVELS IN ^{55}Fe FROM THE DECAY OF ^{55}Co. Luukko, A.; Paukku, P.; Penttinen, S. (Univ. of Helsinki). Z. Phys.; 239: 429-36(1970).

The decay of 18 h ^{55}Co has been investigated. Twenty-one gamma rays were observed. The following levels in the daughter nucleus ^{55}Fe were populated in the decay: g.s. ($3/2^-$), 411.0 keV ($1/2^-$), 931.5 keV ($5/2^-$), 1316.7 keV ($1/2^-$), 1408.7 keV ($1/2^-$), 2144.1 keV ($5/2^-$), 2212.5 keV ($5/2^-$), 2301.4 keV ($3/2^-$), 2578.2 keV ($5/2^+$), 2871.9 keV ($5/2^-$, $1/2^-$), 2939.0 keV ($5/2^-$, $1/2^-$), and 3108.6 keV ($3/2^-$, $1/2^-$). (auth)

3605 ^{28}Si NUCLEUS IN THE PROJECTED HARTREE–FOCK MODEL. Castel, B. (Queen's Univ., Kingston, Ont.); Parikh, J. C. Phys. Rev., C; 1: 990-4(Mar 1970).

The structure of the ^{28}Si nucleus is studied using a variational procedure. The method of angular-momentum projection from a deformed intrinsic state is applied, and each J$^\pi$ state is projected from a determinant which is variationally "best" for that state. This more general variational procedure includes important vibrational correlations, which in ^{28}Si have hexadecapole character. The level spacings in the energy spectrum improve considerably compared to those in the Hartree–Fock method followed by angular momentum projection, and this leads to a much better agreement with the experimental spectrum. The E2 transition probabilities, except for the $6^+ \rightarrow 4^+$ transition, are also in good agreement with the experiments. (auth)

3606 STUDY OF THE ^{28}Si(d,p)^{29}Si REACTION MECHANISM IN THE RANGE OF E_d = 2 TO 6 MeV. Strohbusch, U.; Bakowsky, W.; Lacek, H. (Univ., Freiburg i. B.). Nucl. Phys.; A149: 605-24(1970).

Angular distributions of the ^{28}Si(d,p$_i$)^{29}Si reaction have been measured for transitions to the three lowest states of ^{29}Si in the energy interval of 2.00-6.12 MeV and for the transition to the fourth state in the range from 2.00 to 4.60 MeV. The excitation functions of the differential cross sections are analyzed on the basis of Ericson's fluctuation theory. The mean compound level width and the magnitude of the direct interaction are deduced from this analysis. Average angular distributions and average excitation functions are compared with DWBA and Hauser–Feshbach calculations. The magnitude of compound interaction is determined. Spectroscopic factors are deduced. Spin dependence of the averaged l = 2 angular distributions is seen at all energies down to 2.5 MeV. It could not be reproduced by the DWBA plus Hauser–Feshbach calculations. Evidence of gross structure not due to the statistical compound mechanism is found. Excitation functions of Legendre polynomial coefficients are discussed. There is some indication that the maximum order of the deuteron partial waves effective in the direct interaction is larger than that of the partial waves contributing to the compound process. (auth)

3607 DECAY OF ^{55}Cr. Hill, John C. (Texas A and M Univ., College Station). Nucl. Phys.; A150: 89-96(1970).

The decay of ^{55}Cr to levels in ^{55}Mn was investigated using Ge(Li) gamma detectors. On the basis of energy, intensity, and coincidence measurements a new decay scheme is proposed. In addition to levels at 1528 and 2252 keV seen in earlier decay studies, levels at 126, 2268, and 2368 keV were observed. Spin assignments are postulated for all levels. (auth)

3608 REACTION Q VALUES FROM NEAR-THRESHOLD NEUTRON SPECTRA. Kneff, D. W. (Univ. of Oregon, Eugene); Lefevre, H. W.; Din, G. U. Phys. Rev. Lett.; 25: 1210-13(26 Oct 1970).

A thick-target time-of-flight technique has been employed to measure neutron energies for (p,n) resonance levels near threshold in medium-weight nuclei. Combining the results with proton energy measurements of these resonances, the following ground state (p,n) Q values have been deduced: ^{41}K, −1203.8 ± 0.5 keV; ^{45}Sc, −2843.6 ± 4.0 keV; ^{51}V, −1533.7 ± 1.5 keV; and ^{57}Fe, −1618.2 ± 2.0 keV. (auth)

3609 DECAY OF ^{63}Ga. Dulfer, G. H.; Beertema, H. E.; Verheul, H. (Vrije Univ., Amsterdam). Nucl. Phys.; A149: 518-22(1970).

The decay of ^{63}Ga was investigated with Ge(Li) detectors. Energies and relative intensities of the γ-rays were determined. The half-life of ^{63}Ga was found to be 31.4 ± 0.8 sec. A decay scheme is presented in which the log ft values for the level feedings are given. (auth)

3610 HEAVY-ION REACTIONS AS A TECHNIQUE FOR DIRECT MASS MEASUREMENTS OF UNKNOWN Z > N NUCLEI. Cerny, Joseph; Cardinal, C. U.; Jackson, K. P.; Scott, D. K.; Shotter, A. C. (Oxford Univ.) Phys. Rev. Lett.; 25: 676-8 (7 Sep 1970).

The reactions ^{40}Ca(^{12}C,t)^{49}Mn and ^{40}Ca(^{12}C,^{3}He)^{49}Cr have been observed with ground-state cross sections of the order of 1 μb/sr. The results for ^{49}Mn are consistent with its predicted mass excess of −37.72 ± 0.08 MeV. (auth)

3611 MEASUREMENTS OF THE CROSS SECTIONS FOR FORMATION OF COMPOUND NUCLEI IN HEAVY-ION REACTIONS. Kowalski, L.; Miller, J. M.; D'Auria, J.; Jodogne, J.-C. (Columbia Univ., New York). Radiat. Eff.; 5: 277-8(Oct 1970).

Mica detectors were used to measure the compound-nucleus part of the reaction cross section in ^{27}Al foils bombarded by ^{16}O and ^{20}Ne beams of various energies. The measured cross sections are compared with total reaction cross sections and calculated complete fusion cross sections. The results show that up to ~100 MeV, nearly all the inelastic collisions lead to the formation of compound nuclei; at higher energies, other processes begin to occur. It is suggested that there is some critical value of angular momentum (~30) above which compound nuclei are not formed. (D.L.C.)

3612 EXCITATION OF STATES BETWEEN 3 AND 6 MeV IN ^{31}P AND ^{32}S BY INELASTIC SCATTERING OF 14-MeV NEUTRONS. Bonazzola, G. C. (Univ., Turin. Istituto Nazionale di Fisica Nucleare, Turin); Bressani, T.; Chiavassa, E.; Maringelli, M. Atti Accad. Sci. Torino. I. Cl. Sci. Fis., Mat. Natur.; 104: 381-9(May-Jun 1970).

The inelastic scattering of 14-MeV neutrons from levels between 3 and 6 MeV in ^{31}P and ^{32}S with a resolution of about 500 keV is described. The time-of-flight technique with associated particle detection was used, the flight path being 2.5 meters. Angular distributions were measured from 30 to 90° in steps of 10°. The shape of an isolated peak was determined by scattering from ^{12}C. The results are analogous to those from proton inelastic scattering at 17.5 MeV. (R.W.R.)

3613 DIFFERENTIAL CROSS SECTIONS, POLARISATIONS, AND PROTON-GAMMA ANGULAR CORRELATIONS FOR ^{54}Fe, ^{60}Ni(p,p) AND (p,p'γ) AT 10 MeV. Ahmed, M.; Lowe, J.; Rolph, P. M.; Karban, O. (Univ. of Birmingham, Eng.). Nucl. Phys.; A147: 273-82(1970).

Data are presented for the differential cross sections and polarizations for ^{54}Fe(p,p) and ^{60}Ni(p,p) and for the cross sections, proton asymmetries, and the spin-flip angular correlation for

XUM

$^{54}Fe(p,p'\gamma)$ and $^{60}Ni(p,p'\gamma)$ (first excited states). The incident energy is 10 MeV in each case. The cross section and angular correlation results are compared with the predictions of a simple model involving direct and compound nucleus contributions, permitting an estimate of the magnitude of the direct component to be made. The inelastic asymmetry data are not well described by this model. (auth)

3614 SCATTERING OF FAST DEUTERONS AT LARGE ANGLES. Berezhnoi, Yu. A.; Evlanov, M. V. (Kharkov Inst. of Physics and Tech.). Ukr. Fiz. Zh.; 14: 1919-22(Nov 1969). (In Russian).

The scattering and spallation of deuterons on black nuclei were studied using adiabatic approximations. At small angles the results coincide with the diffraction model. Calculations were made of differential cross sections of the elastic and inelastic scattering and spallation of 50-MeV deuterons by nickel nuclei at large angles of deuteron center-of-mass emission or the neutron–proton system formed during deuteron spallation. The differential cross sections at large angles exhibited diffractional characteristics and conform to the phase rules. (R.V.J.)

3615 QUASI-ELASTIC SCATTERING OF 1115-MeV ELECTRONS BY NUCLEONS OF ^{32}S NUCLEI. Dementii, S. V.; Afanas'ev, N. G.; Arkatov, I. M.; Vlasenko, V. G.; Gol'dshtein, V. A.; Kuplennikov, E. L.; Startsev, V. I. (Kharkov Inst. of Physics and Tech.). Ukr. Fiz. Zh.; 14: 1911-12(Nov 1969). (In Russian).

Previously, it was shown that inelastic scattering of electrons on ^{12}C and ^{28}Si nuclei at large excitation energies of the first continuum in the electron spectrum can be described by the mechanism of quasi-elastic scattering on intra-nuclear nucleons. Data obtained for scattering of 1115-MeV electrons on ^{32}S nuclei in the region of the quasi-elastic continuum at 17.5, 21, 27.5, 31, and 34° were analyzed. It was observed that the mean square radius of the distribution of the charge in ^{32}S nucleus $(Z_p^2)^{1/2} = 2.5 \pm 0.2f$, obtained on the basis of the quasi-elastic method, differed 20% from the $(Z_p^2)^{1/2} = 3.12f$ magnitude obtained by the method of elastic electron scattering. A similar discrepancy (13%) was observed earlier in the case of ^{12}C and ^{28}S radii calculated according to the quasi-elastic electron scattering and elastic electron scattering. (R.V.J.)

3616 STUDY OF PROTON HOLE STATES IN $1f_{7/2}$ NUCLEI BY THE (p,2p) REACTION AT 46 MeV. Bertrand, F. (Univ. of Southern California, Los Angeles); Waddell, C.; Eisberg, R.; Ingham, D.; Makino, M. Contracts AT(04-3)-136; AT(11-1)-34. Nucl. Phys.; A152: 337-343(1970).

Proton hole states in the $1f_{7/2}$ nuclei ^{46}Ti, ^{54}Fe, ^{56}Fe, ^{58}Ni and ^{60}Ni were studied using the (p,2p) reaction with 46-MeV protons. The measured binding energies and angular correlations are consistent with the binding energies and orbital angular momentum assignments ($1f_{7/2}$, $2s_{1/2}$ and $1d_{3/2}$) obtained from proton pick-up reactions. (auth)

3617 PROPERTIES OF LOW-LYING ^{53}Mn LEVELS FROM THE $^{52}Cr(p,\gamma)^{53}Mn$ REACTION; DECAY OF THE $2p_{3/2}$ ANALOGUE STATE. Maripuu, S. (Rijksuniversiteit, Utrecht). Nucl. Phys.; A149: 593-604(1970).

The $^{52}Cr(p,\gamma)^{53}Mn$ reaction has been used to obtain excitation energies, γ-ray branching ratios, amplitude mixing ratios, spins, parities and mean lives of ^{53}Mn levels up to 3.5 MeV. The $E_p = 1006$ keV resonance is probably the analogue of the $E_x = 0.56$ MeV, $J^\pi = 1/2^-$ level in ^{53}Cr. Its strength, spin and γ-ray branching have been determined. (auth)

3618 MAGNETIC MOMENT OF THE 10 μsec LEVEL IN ^{58}Co. Bertschat, H.; Christiansen, J.; Mahnke, H.-E.; Recknagel, E.; Schatz, G.; Sielemann, R.; Spellmeyer, B.; Witthuhn, W. (Hahn-Meitner-Institut fuer Kernforschung, Berlin). Nucl. Phys.; A151: 193-7(1970).

The methods of the stroboscopic observation of the nuclear Larmor precession as well as the conventional time-differential spin precession were applied to the 10.2 μsec state of ^{58}Co populated by the nuclear reaction $^{57}Fe(d,n)$. The g-factor has been determined to be $g = +1.046 \pm 0.002$. By means of the g-factor and the measured anisotropy of the observed γ-rays, the nuclear properties of the low-lying states in ^{58}Co are discussed. (auth)

3619 SPINS AND MEAN LIVES OF ^{34}Cl LEVELS. Brandolini, F.; Filosofo, I.; Signorini, C.; Morando, M. (Univ., Padua. INFN Padua). Nucl. Phys.; A149: 401-10(1970).

The spins of the 0.46, 0.66, 1.23 and 1.89 MeV states in ^{34}Cl have been established as J = 1, 1, 2 and 2, respectively, from angular correlation measurements in the $^{32}S(He\text{-}3,p\gamma)^{34}Cl$ reaction. The branching ratios of these states and some mixing ratios were also obtained. The mean lives of the ^{34}Cl levels at 0.46, 0.66 and 1.23 MeV, $\tau_m = 9 \pm 4$, 14^{+11}_{-6} and >14 ps, respectively, were found from DSA measurements in the reaction $^{31}P(\alpha,n\gamma)^{34}Cl$. The $1^+ \rightarrow 0^+$, $\Delta T = 1$, M1 transitions are quite slow as compared to similar transitions in other self-conjugated nuclei; this can be understood from shell-model arguments. (auth)

3620 MUONIC ATOMS. II. ISOTOPE SHIFTS. Macagno, E. R. (Columbia Univ., New York); Bernow, S.; Cheng, S. C.; (and others). Phys. Rev., C; 1: 1202-21(Apr 1970).

Isotope shifts in the muonic spectra of $^{40}_{20}Ca$, ^{44}Ca; $^{50}_{24}Cr$, ^{52}Cr, ^{53}Cr, ^{54}Cr; $^{63}_{29}Cu$, ^{65}Cu; $^{92}_{42}Mo$, ^{95}Mo, ^{96}Mo, ^{97}Mo; $^{116}_{50}Sn$, ^{117}Sn, ^{118}Sn, ^{119}Sn, ^{120}Sn, ^{122}Sn, ^{124}Sn; $^{142}_{60}Nd$, ^{143}Nd, ^{144}Nd, ^{145}Nd, ^{146}Nd, ^{148}Nd, and ^{150}Nd are measured using a stable high-resolution Ge(Li) spectrometer system. The results are compared with values calculated for assumed nuclear charge distributions. In the case of the Nd isotopes, the half-density radius and the skin thickness are determined from the measured K and L x-ray energies. An interesting shell-closing effect is observed among the Cr isotopes. The muonic isotope shifts are used to extract specific-mass shifts from optical measurements. Even in Nd, these specific-mass shifts are very large, and not at all negligible in the analysis of optical results. The isotope shifts in Sn follow favorably the theoretically predicted general trend. The great reduction of the isotope shift between $^{122-124}Sn$ as reported in an optical investigation is not found in the muonic case. Lastly, a comparison is made between the muonic results and recent electronic x-ray measurements. These are found to be in reasonable agreement. (auth)

3621 LEVEL STRUCTURE OF ^{88}Sr FROM THE DECAY OF 17.8 min ^{88}Rb. Kawase, Y. (Kyoto Univ., Osaka). Nucl. Phys.; A154: 127-40(1970).

Gamma transitions in the decay of 17.8 min ^{88}Rb have been investigated by using a Ge(Li) detector and angular correlations of four cascades have been measured with the multicounter goniometer. Five gamma transitions of 338, 485, 1027, 1366 and 2112 keV were newly found in singles and coincidence spectra measured with Ge(Li) and NaI(Tl) detectors. The spins and parities of levels at 3489, 4514, 4846 and 4855 keV were assigned to be 1^+, 2^-, 3^- and 2^-, respectively, from the results of angular correlation measurements and log ft values. The angular correlation measurements have also shown that the multipolarities of the gamma transitions of 1366, 2676 and 3009 keV are of purely dipole character and the E2/M1 mixing ratio of the 1382 keV $2_2^+ - 2_1^+$ transition agrees well with the single-particle limit. Some qualitative discussions are given concerning the level structure of the ^{88}Sr nucleus. (auth)

3622 ANGULAR CORRELATION STUDIES OF THE LOW-LYING LEVELS OF ^{57}Co. Coop, K. L.; Graham, I. G.; Titterton, E. W. (Australian National Univ., Canberra). Nucl. Phys.; A149: 463-87(1970).

Proton–gamma angular correlations and gamma-ray branching ratios were measured for the first nine excited states of ^{57}Co using the $^{54}Fe(\alpha,p\gamma)$ reaction. In contradiction to earlier reports, the 1.754 and 2.127 MeV states were found to be single, well isolated states, and the 1.687 MeV state was observed to have a large gamma-ray branch (44%) to the ground state. From the data obtained here and in previous experiments, J^π values were deduced for the following levels whose energies are shown in MeV: 1.222, $5/2^-$ ($5/2^-$); 1.375, $3/2^-$; 1.502, $1/2^-$; 1.687, $11/2^-$ ($1/2^-$, $5/2^-$); 1.754, $3/2^-$; 1.894, $1/2^-$; 1.917, $3/2^-$; 2.127, $5/2^-$ and 2.307, $1/2^-$ ($5/2^-$). Possible, but less probable, assignments have been enclosed in parentheses. (auth)

3623 ISOSPIN SPLITTING OF THE GIANT DIPOLE RESONANCE IN ^{64}Zn. Cook, B. C.; Morrison, R. C.; Schamber, F. H. (Ames Lab., Iowa). Phys. Rev. Lett.; 25: 685-8 (7 Sep 1970).

The (γ,n_0) reaction is discussed as a probable channel for observation of the $T = T_0 + 1$ component of the giant dipole resonance, and experimental evidence is presented in support of this conjecture in the case of ^{64}Zn. (auth)

3624 INVESTIGATION OF HIGH SPIN STATES IN ^{55}Fe FROM THE $^{55}Mn(p,n\gamma)$ REACTION. Pilt, A. A.; Sheppard, D. M.; Olsen, W. C.; Carola, T. P. G.; Twin, P. J. (Univ. of Alberta, Edmonton). Nucl. Phys.; A150: 439-48(1970).

Electromagnetic decay properties of the low-lying states in ^{55}Fe were studied using the $^{55}Mn(p,n\gamma)^{55}Fe$ reaction. The measurement of γ-ray angular distributions together with predictions based on the compound nuclear statistical model has permitted unique spin assignments to be made to the following excited states in ^{55}Fe: 1.316 MeV ($^7/_2$), 1.408 MeV ($^5/_2$), 2.144 MeV ($^5/_2$), 2.211 MeV ($^3/_2$), 2.301 MeV ($^9/_2$) and 2.470 MeV ($^3/_2$). Some multipole mixing ratios were also determined. Comparison is made with the shell-model calculations of Ohnuma and Vervier. (auth)

3625 SPECTROSCOPY OF $^{65\ 67\ 69}Ga$ BY (d,n) REACTION. Couch, R. G. (Oak Ridge National Lab., Tenn.); Biggerstaff, J. A.; Perey, F. G.; Raman, S.; Seth, Kamal K. Phys. Rev., C; 2: 149-60(Jul 1970).

The $^{64,66,68}Zn(d,n)$ $^{65,67,69}Ga$ reactions were studied by neutron

time-of-flight method. Absolute differential cross sections were measured and analyzed in terms of the distorted-wave Born approximation. Spin and parity assignments for several levels are proposed on the basis of l values and transition strengths. The experimental results for ^{67,68}Ga are compared with existing theoretical calculations. Only limited agreement is found. (auth)

3626 EVIDENCE FOR ROTATIONAL STRUCTURE IN ^{43}Sc. Forster, J. S. (Chalk River Nuclear Labs., Ont.); Ball, G. C.; Ingebretsen, F.; Monahan, C. F. Phys. Lett.; 32B: 451-3 (17 Aug 1970).

The Doppler-shift attenuation method has been used to obtain mean lives (ps) for the following levels in 43Sc: 880-keV, $^{5}/_{2}^{+}$, $5.8^{+2.2}_{-1.6}$; 1336-keV, $^{7}/_{2}^{+}$, 2.0 ± 0.4; 1931-keV, $^{9}/_{2}^{+}$, 3.4 ± 0.8 and 2552-keV, $(^{11}/_{2}^{+})$, 0.74 ± 0.06. This new information supports the existence of a $K^{\pi} = {}^{3}/_{2}^{+}$ rotational band in ^{43}Sc based on the 151-keV, $^{3}/_{2}^{+}$ level. (auth)

3627 PROTON STRIPPING TO PARTICLE-HOLE STATES IN ^{40}Ca AND ^{42}Ca. Forster, J. S.; Bearpark, K.; Hutton, J. L.; Sharpey-Schafer, J. F. (Univ. of Liverpool). Nucl. Phys.; A150: 30-48(1970).

Angular distributions have been measured for the ground state and eight excited states in ^{40}Ca and for the ground and fourteen excited states in ^{42}Ca in the ^{39,41}K(^{3}He, d)^{40,42}Ca reactions at a ^{3}He energy of 11.0 MeV. The elastic scattering of ^{3}He from ^{39}K has also been measured at a ^{3}He energy of 11.0 MeV. Zero-range DWBA calculations have been made and l_p values assigned to the states observed. Good agreement is found between the spectroscopic factors from th ^{39}K(^{3}He,d)^{40}Ca analysis and the predictions of Gerace and Green. The quartet of states arising from the $(1d_{\frac{3}{2}}^{-1}, 1f_{\frac{7}{2}})$ proton configuration is identified in ^{42}Ca. (auth)

3628 FINE STRUCTURE OF ANALOGUE STATES IN ^{59}Cu, ^{61}Cu, ^{63}Cu, and ^{65}Cu. Browne, J. C. (Duke Univ., Durham, N. C. Triangle Universities Nuclear Lab., Durham, N. C.); Newson, H. W.; Bilpuch, E. G.; Mitchell, G. E. Nucl. Phys.; A153: 481-501(1970).

Differential cross sections were measured at lab angles of 160°, 135°, 120° and 90° for proton elastic scattering on ^{58}Ni, ^{60}Ni, ^{62}Ni and ^{64}Ni at energies ranging between 1.8 and 3.3 MeV. The ^{64}Ni(p, n)^{64}Cu total yield was measured from threshold (≈2.50 MeV) to 3.3 MeV. All data were taken using the TUNL 3 MV Van de Graaff accelerator and high-resolution electrostatic analyzer-homogenizer system. A total resolution of 300 to 450 eV was realized using thin solid targets of the enriched nickel isotopes. There were nine l = 1 analog states identified in the elastic scattering data. In almost all cases, the analog state was fragmented into individual fine structure resonances. Spins, parities, total and partial widths were extracted from the data. Spectroscopic factors were obtained using the resonances parameters from the data and calculated single-particle widths. Coulomb energy differences were also extracted for the nine l = 1 analog states. (auth)

3629 INVESTIGATION OF THE (^{3}He,p) REACTION ON THE Ca ISOTOPES A = 42, 43, 44, AND 48. Schlegel, W. (Max-Planck-Institut fuer Kernphysik, Heidelberg); Schmitt, D.; Santo, R.; Puehlhofer, F. Nucl. Phys.; A153: 502-23(1970).

The (^{3}He, p) reaction on the Ca isotopes A = 42, 43, 44 and 48 was investigated at 15 and 18 MeV incident energy using a magnetic spectrograph. Angular distributions were measured and analyzed by means of the DWBA. Spins and L-values for the final levels in the Sc nuclei were deduced. The spectra are compared with the results of shell-model calculations. For the reaction ^{48}Ca(^{3}He, p)^{50}Sc a quantitative analysis of the cross sections was performed using the wave functions of Hughes and Soga. The systematics of the (^{3}He, p) cross sections for transitions to analog states were studied by measurements on a target consisting of a mixture of several Ca isotopes. A consistent DWBA analysis for these as well as for the corresponding (t, p) transitions was performed. (auth)

3630 INELASTIC SCATTERING OF 31-MeV ALPHA PARTICLES FROM ^{64}Zn AND ^{66}Zn. Alpert, N.; Alster, Jonas; Martens, E. J. (Northeastern Univ., Boston). Phys. Rev., C; 2: 974-80(Sep 1970).

The (α, α') reaction on ^{64}Zn and ^{66}Zn has been studied using the 31-MeV α-particle beam from the Massachusetts Institute of Tech nology cyclotron, with an over-all energy resolution of 80 to 120 keV. Angular distributions are presented, both for levels with known spin, and for levels whose spin and parity have not been previously determined. New 3^{-}, 4^{+}, and 5^{-} assignments are made both by comparison with levels of known spin and with the distorted-wave Born approximation. Good angular distributions are presented for the weak states at 1.81 MeV (2^{+}) and 2.32 MeV (4^{+}) in ^{64}Zn. They are both out of phase with the 2^{+} and 4^{+} single-excitation states. The slope of the angular distribution for the 2.32-MeV (4^{+}) level is shallower than for the single-excitation 4^{+} state, while the slopes are the same for the 2^{+} states. Transition strengths in ^{64}Zn and ^{66}Zn are compared. Fractionation of 3^{-} strength in ^{64}Zn has been observed, but it is smaller than that found in the calcium isotopes. (auth)

3631 INVESTIGATION OF ^{65}Zn BY (p,n) AND (p,nγ) EXPERIMENTS. Weidinger, A.; Finckh, E.; Jahnke, U.; Schreiber, B. (Hahn-Meitner-Institut fuer Kernforschung, Berlin). Nucl. Phys.; A149: 241-52(1970).

The compound nuclear reaction ^{65}Cu(p,n)^{65}Zn has been investigated by the neutron time-of-flight method at E_p = 3.62, 4.06 and 4.50 MeV. In addition, γ-ray spectra have been measured at four different proton energies with a Ge(Li) detector. A new level at E^{*} = 864 keV in ^{65}Zn is found. The measured (p,n) angular distributions and integrated cross sections agree well with predictions of the Hauser-Feshbach model. From a comparison of the measured and calculated cross sections the J^{π} values of the states at 207, 909 and 1468 keV have been determined as $^{3}/_{2}^{-}$; for six other states, possible spin values are given. The level scheme is compared with predictions from the weak-coupling model and the shell model. (auth)

3632 ANALYSIS OF THE ^{41}K LEVEL STRUCTURE FROM THE ^{40}Ar(^{3}He,d)^{41}K STRIPPING REACTION. Lankford, W. F.; Edge, R. D. (Univ. of South Carolina, Columbia). Nucl. Phys.; A148: 497-502(1970).

An argon gas target was bombarded by a 10 MeV ^{3}He beam, and the deuteron spectra measured at angles from 13 to 90°. The energy levels were investigated to an excitation of 6.57 MeV and the angular distributions were compared to DWBA predictions. Angular momentum assignments were made for the principal peaks and the corresponding spectroscopic factors were determined. The strength of the 1.31 MeV level is attributed to the T < configuration state in ^{41}K. (auth)

3633 STUDIES ON THE ^{21}Ne(p,d)^{20}Ne AND ^{21}Ne(d,p)^{22}Ne REACTIONS. Howard, A. J.; Pronko, J. G.; Hirko, R. G. (Yale Univ., New Haven). Contract AT(30-1)-3223. Nucl. Phys.; A150: 609-24(1970).

Angular distribution measurements have been performed on the ^{21}Ne(p,d)^{20}Ne and ^{21}Ne(d,p)^{22}Ne reactions at E_p = 20 MeV and E_d = 10.2 MeV, respectively. In the ^{21}Ne(p,d)^{20}Ne reaction, the prolific formation of the $J^{\pi} = 2^{+}$, 1.63 MeV state was characterized by l_n = 2 pickup, and the distribution associated with the 4^{+}, 4.25 MeV state was suggestive of a weak l_n = 2 pickup. All of the observed l_n = 1 pickup strength is associated with formation of the 2^{-}, 4.97 MeV ^{20}Ne level. The ^{21}Ne(d,p)^{22}Ne results indicate that l_n = 2 transfer is involved in the formation of the 1.28, 3.36, 5.52, 5.63 and 6.65 MeV ^{22}Ne states. The angular distribution observed for the 2^{+}, 4.46 MeV state and also the unresolved 5.33, 5.36 MeV composite of states required both l_n = 0 and l_n = 2 components in the associated distorted-wave Born approximation fits. The spectroscopic factors extracted from the present results are compared with those predicted by the Nilsson model without mixing: Applications of the angular momentum projection rule to the ^{21}Nd(d,n)^{22}Ne reaction are considered. (auth)

3634 CROSS SECTIONS FOR THE PHOTOPRODUCTION OF ^{28}Al AND ^{29}Al FROM PHOSPHORUS. Anderson, D. W.; Swift, S. C. (Univ. of Oklahoma, Norman). Nucl. Phys.; A150: 625-30(1970).

Bremsstrahlung activation curves were measured for the reactions ^{31}P(γ,2p)^{29}Al and ^{31}P(γ,2pn)^{28}Al in 0.5 MeV steps from 23.0 to 62.0 MeV. The cross sections obtained from these curves show peaks at 32.6 ± 0.7 MeV, 41.2 ± 0.8 MeV and 51.0 ± 1.5 MeV for both reactions. The cross section integrated to 62 MeV for the (γ,2p) reaction is 5.6 ± 0.6 MeV · mb and for the (γ,2pn) reaction is 7.6 ± 0.8 MeV · mb. (auth)

3635 EFFECTS OF THE DIRECT INELASTIC SCATTERING ANISOTROPY FOR FAST NEUTRONS IN SODIUM. Benzi, V.; Bignami, A.; Cenacchi, G.; Simonini, R. (CNEN, Bologna). Energ. Nucl. (Milan); 17: 597-600(Oct 1970).

By means of the generalized optical model the anisotropic angular distribution of the neutrons inelastically scattered via direct interaction by ^{23}Na is estimated below 2 MeV. The effects of such an anisotropy on the energetic distribution of neutrons slowed down in bulk sodium are analyzed by using the Monte Carlo method. (auth)

3636 ELASTIC SCATTERING OF 30.3-MeV POLARIZED PROTONS FROM ^{58}Ni, ^{120}Sn, AND ^{208}Pb. Greenlees, G. W. (Rutherford High Energy Lab., Chilton, Eng. Univ. of Minnesota, Minneapolis); Hnizdo, V.; Karban, O.; Lowe, J.; Makofske, W. Phys. Rev., C; 2: 1063-70(Sep 1970). (COO-1265-88).

Results are presented for the elastic scattering of 30.3-MeV polarized protons from targets of ^{58}Ni, ^{120}Sn, and ^{208}Pb. The angular region from 10 to 165° is covered with an absolute accuracy

in the polarization measurements of about 0.01. The data, together with corresponding differential cross-section data previously reported, are analyzed using the optical model. Two forms of the model are used: (1) the standard version with independent geometries and ten parameters; and (2) the folding version of Greenlees, Pyle, and Tang with eight parameters. Good fits to the data are obtained, particularly for ^{208}Pb. Evidence is presented to support the suggestion that such models are most satisfactory for large nuclei (^{208}Pb), and that for smaller nuclei (^{120}Sn and ^{58}Ni) second-order corrections ignored in the model are playing a non-negligible role. (auth)

3637 J-DEPENDENCE IN l = 2(^{3}He,α) REACTIONS ON ^{24}Mg, ^{28}Si, AND ^{30}Si. Kattenborn, H. (Max-Planck-Institut fuer Kernphysik, Heidelberg); Mayer-Boericke, C.; Mertens, B. Nucl. Phys.; A138: 657-70(1969).

In order to investigate a possible j-dependence in the l = 2 angular distributions of ^{3}He induced direct reactions in the region of the 1d-shell nuclei, (^{3}He,α) reactions on the target nuclei ^{24}Mg, ^{28}Si and ^{30}Si were measured at incident energies E_{inc} of 18 and 20 MeV. The stability of the shape of the angular distributions against variations of E_{inc} demonstrates that the direct reaction contribution prevails even at backward angles in the region of small cross sections. There is a difference between the shape of the $\Delta j = 3/2^+$ and $\Delta j = 5/2^+$ angular distributions at $\theta_{cm} = 45°$ which is common to all nuclei studied; at this angle the $\Delta j = 3/2^+$ curves show a deep minimum which is absent in the case of the $\Delta j = 5/2^+$ angular distributions. This systematic experimental j-dependence can be reproduced by DWBA calculations; the theoretical results agree well with the experimental ones in the region of large cross sections up to about 60°. (auth)

3638 DECAY OF 2.4 MIN ^{71g}Zn AND 3.9-h ^{71m}Zn TO LEVELS OF ^{71}Ga. Zoller, W. H.; Walters, W. B.; Gordon, G. E. (Massachusetts Inst. of Tech., Cambridge). Contract AT(30-1)-905. Nucl. Phys.; A142: 177-203(1970).

The decay schemes of 2.4-min ^{71g}Zn and 3.9 h ^{71m}Zn have been studied with the use of Ge(Li) and NaI(Tl) detectors and a multiparameter analyzer system. In the case of ^{71m}Zn decay, it was possible to observe coincidences in a Ge(Li)-Ge(Li) configuration. The short half-life of ^{71g}Zn limited coincidence studies of that isomer to NaI(Tl)-Ge(Li). A total of 24 γ-rays are assigned to decay of ^{71g}Zn and 60 to that of ^{71m}Zn. Excited states of ^{71}Ga are observed at 390, 487, 512, 910, 965, 1107, 1109, 1395, 1476, 1494, 1499, 1632, 1702, 1720, 2065, 2247, 2294, 2451, 2488, 2601, 2720, 2805 and 2816 keV. Several $1/2^+$ and $7/2^+$ or $9/2^+$ levels are populated above 2200 keV by allowed β^- decay of $9/2^+$ ^{71m}Zn. It is not clear if those levels can best be described as 2^+, 4^+, and 3^- vibrations coupled with the $g_{9/2}$, $p_{3/2}$, $p_{1/2}$ and $f_{5/2}$ particle states or as members of rotational bands built on the Nilsson components of the $g_{9/2}$ orbital. (auth)

3639 ENERGY LEVELS IN ^{72}Ge FROM RADIOACTIVE DECAY STUDIES OF ^{72}Ga AND ^{72}As. Rester, Alfred Carl Jr. Nashville; Vanderbilt Univ. (1969). 141p. Thesis.

The following experiments were performed on the ^{72}Ga decay: (1) gamma ray singles spectrum measurements with a Ge(Li) x-ray spectrometer and 30 cm^3 Ge(Li); (2) internal conversion measurements with a Si(Li) detector; (3) gamma–gamma coincidence measurements with Ge(Li) detectors and a two-parameter analysis system; (4) electron–gamma, delayed coincidence measurements with an anthracene detector and a 30 cm^3 Ge(Li) detector. Of the 71 definitely observed gamma ray transitions, 68 were placed in a decay scheme with 22 excited states, including energy levels at 691.2, 834.02, 1463.88, 1728.24, 2064.80, 2402.0, 2463.74, 2514.65, 2583.5, 2754.1, 2943.45, 3035.41, 3094.7, 3324.92, 3341.68, 3439.3, 3455.2, 3566.0, 3678.1, 3707.1, 3758.6, and 3815.4 keV. All of the measurements except for the delayed coincidence were also made on the decay of ^{72}As. A total of 60 gamma ray transitions was observed. Of these, 55 were placed in a decay scheme consisting of 27 excited states at the following energies: 691.2, 834.00, 1463.96, 1728.27, 2064.82, 2402.2, 2463.80, 2514.71, 2755, 2939.89, 2943.5, 3035.74, 3094.2, 3325.0, 3337.7, 3341.8, 3419.5, 3455.28, 3550.7, 3678.2, 3708.6, 3803.7, 3816.1, 3872.0, 3983.8, 3986.0, and 3995.0 keV. Accurate and rapid analysis of gamma-ray spectra taken with Ge(Li) detectors and large multichannel analyzers requires computerization. FORTRAN programs were developed for this purpose which are tailor-made for restricted computing budgets. These programs determine the peak parameters (channel number, F.W.H.M., area and height), energies, and intensities of the majority of photopeaks in a spectrum, place transitions in a known decay scheme, and search for new energy levels. Multiplets are not stripped, but this is no great problem when using Ge(Li) detectors. The programs have been successfully employed in precision energy and intensity measurements, the analysis of complex gamma spectra and the construction of decay schemes. Comparison of results with those of other groups indicate that, within their capabilities, the programs give results which are as accurate as those from more elaborate programs. (Diss. Abstr. Int., B)

3640 BETA DECAY OF ^{42}Ti. Aldridge, Ann Marshall. Tallahassee; Florida State Univ. (1969). 86p. Thesis.

The reaction ^{40}Ca(^{3}He,n)^{42}Ti was used to investigate the positron decay of ^{42}Ti to ^{42}Sc. Decays to both the 0^+ ground state of ^{4}Sc and to the 1^+ level at 615 keV were observed. The half-life of ^{42}Ti was measured by three methods; by observing its positron activity as a function of time, by observing the 615 keV gamma ray activity following the positron decay to the 1^+ level in ^{42}Sc as a function of time, and by observing the decrease in intensity of the 615 keV gamma peak at eight successive time intervals. A weighted average value of 0.173 ± 0.014 sec for the ^{42}Ti half-life was obtained from these three measurements. The branching ratio for the ^{42}Ti decay to the 1^+ level in ^{42}Sc was obtained by measuring the total gamma ray and positron yields. From the ratio of these two yields a branch of 56 ± 14% to the 1^+ level in ^{42}Sc was obtained. From these measurements of the half-life and the branching ratio and from the end-point energies of the positrons calculated from the masses involved, ft-values of 2720 ± 800 sec and 1282 ± 500 sec for the decays to the 0^+ and 1^+ levels in ^{42}Sc were calculated. These experimentally determined ft-values were compared with ft-values calculated from postulated wave functions for the levels in ^{42}Sc and ^{42}Ti. (Diss. Abstr. Int., B)

3641 ENERGY LEVELS OF ^{37}K FROM ^{36}Ar(p,p)^{36}Ar AND ^{36}Ar(p,p'γ)^{36}Ar. Thwaites, T. T. (Pennsylvania State Univ., University Park). Nucl. Phys.; A150: 531-44(1970).

The elastic and inelastic scattering of protons from ^{36}Ar has been investigated from 2.1 to 5.3 MeV using a gas target. Experimental energy resolution varied from 11 keV to 5 keV over this range. The results are interpreted in terms of 56 states in ^{37}K between the energies of 4.0 and 7.0 MeV excitation with the aid of single-level dispersion theory. The width and spin and parity or proton l-value are determined for the 38 states seen in the elastic scattering. Upper limits are placed on the total widths of levels seen only in the inelastic scattering. (auth)

3642 STATIC QUADRUPOLE MOMENTS OF THE FIRST EXCITED STATES OF ^{58,60,62}Ni. Lesser, P. M. S.; Cline, D.; Purvis, J. D. (Univ. of Rochester, N. Y.). Nucl. Phys.; A151: 257-72(1970).

Measurements of the relative thick-target yields of γ-rays deexciting the 2^+ first excited states in ^{58,60,62}Ni, following Coulomb excitation by carbon, oxygen and sulfur ions, have been used to determine the relative static quadrupole moments of these states as well as the relative reduced transition probabilities, B(E2; $0_1^+ \rightarrow 2_1^+$). The measured yields were compared with calculations using a Coulomb excitation coupled channels computer code in order to extract the quadrupole moments and B(E2) values. The following results are obtained if the effects of higher excited states are ignored: $Q(^{58}Ni) - 0.94Q(^{60}Ni) = -(0.122 \pm 0.039)e \cdot b$, $B(E2; 0_1^+ \rightarrow 2_1^+)_{^{58}Ni}/B(E2; 0_1^+ \rightarrow 2_1^+)_{^{60}Ni} = 0.783 \pm 0.014$, $Q(^{62}Ni) - 1.11Q(^{60}Ni) = -(0.075 \pm 0.092)e \cdot b$, $B(E2; 0_1^+ \rightarrow 2_1^+)_{^{62}Ni}/B(E2; 0_1^+ \rightarrow 2_1^+)_{^{60}Ni} = 0.964 \pm 0.026$. A previous experiment provided measurements of the absolute static quadrupole moment and B(E2) for ^{60}Ni and these are used to obtain absolute values for ^{58}Ni and ^{62}Ni. The experimental results are compared with various shell-model calculations as well as macroscopic model predictions. Qualitative agreement between theory and experiment is obtained. (auth)

3643 SYSTEMATICS OF (n,α), (n,p), AND (n,2n) REACTION CROSS SECTIONS OF MEDIUM WEIGHT NUCLEI FOR 14.5-MeV NEUTRONS. Hille, Peter. Oesterr. Akad. Wiss., Math.-Naturwiss. Kl.; 177: 463-79(1968). (In German).

Experimental values for (n,α), (n,p), and (n,2n) reaction cross sections of medium-weight nuclei for 14.5-MeV neutrons were compiled from the available literature. After establishment of certain criteria, unreliable data were eliminated. The remaining values showed a measuring error of less than 30%. These cross sections indicated a clear systematic relationship. The symmetry parameter (N-Z)/A apparently played a significant role. No shell effect was detected. Cross sections of nuclei with even mass numbers did not differ significantly from those of their neighboring nuclei with uneven mass numbers. (tr-auth) (83 references)

3644 DECAY OF THE ^{62}Co ISOMERS. Jongsma, H. W.; de Lange, J. C.; Boddendijk, J. C.; Kamermans, R.; Verheul, H. (Vrije Univ., Amsterdam). Nucl. Phys.; A150: 520-30(1970).

The single and coincident γ-ray spectra following the decay of the ^{62}Co isomers were measured. New γ-transitions in the decay of the 13.5 min respectively 1.4 min isomer with energies: 0.7778, 0.8749, 1.1291, 1.7535, 2.3020 and 2.8826 MeV respectively 1.8863, 2.3458, 3.271 and 3.370 MeV have been observed. The intensity of the direct feeding from the 1.4 min isomer to the ground state of ^{62}Ni was determined to be <0.5%. (auth)

Nuclear Properties and Reactions, A ≥ 90

Refer also to abstracts 2893, 2896, 3222, 3247, 3591, 3620, 3636, 3749, and 3751.

3645 (AERE-R-6529) CONCERNING THE HALF-LIFE OF ^{144}Ce. Cabell, M. J.; Wilkins, M. (Atomic Energy Research Establishment, Harwell (England)). Sep 1970. 3p. (EANDC(UK)-130AL). Dep. NTIS (U. S. Sales Only). UK 1s. 2d.

An evaluation of published data leads to the conclusion that the half-life of ^{144}Ce is 284.4 ± 0.4 days. (auth)

3646 (CNEA-275) GAMMA-GAMMA COINCIDENCES IN ^{140}Ce. de Aisenberg, E. Y.; Proto-Otero, A. N. (Comision Nacional de Energia Atomica, Buenos Aires (Argentina)). 1970. 17p. (In Spanish). Dep. NTIS (U. S. Sales Only).

Coincidence spectra from ^{140}Ce were measured with NaI(Tl) 3 in. × 3 in. crystals. The (398-2348) and (868-920) keV γ-γ coincidences were established. Two new levels at 2746 and 3348 keV are then proposed. (auth)

3647 (COO-1746-46) DIRECTIONAL CORRELATION AND INTENSITY STUDIES OF ELECTROMAGNETIC TRANSITIONS IN ^{181}Ta. Avignone III, F. T.; Trueblood, J. H. (South Carolina Univ., Columbia. Dept. of Physics); Grabowski, Z. W. (Purdue Univ., Lafayette, Ind. Dept. of Physics). [1970]. 28p. Dep. CFSTI.

Gamma-gamma directional correlations have been measured in ^{181}Ta using a 25 cc Ge(Li) detector and a 3″ × 3″ NaI(Tl) detector. Extra-nuclear perturbations were avoided by dissolving the ^{181}Hf source in a solution of HF. The following correlation coefficients were measured: $A_2 = -0.295 \pm 0.005$, $A_4 = -0.069 \pm 0.008$ for the 133γ − 482γ cascade, $A_2 = +0.197 \pm 0.012$, $A_4 = -0.008 \pm 0.020$ for the 133γ−(346γ)−136γ cascade, and $A_2 = +0.110 \pm 0.010$, $A_4 = 0.022 \pm 0.014$ for the 133γ − 346γ cascade. The E2 internal conversion particle parameters for the 133 keV transition were determined by measuring the 133K − 482γ, the 133 LM − 482γ and the 133γ − 482γ correlations in the same solid source. The results are b_2(133K) = 1.79 ± 0.11 and b_2(133 LM) = 1.18 ± 0.10 which are in good agreement with theory. The following internal conversion coefficients were also measured: $\alpha_K(136) = 1.46 \pm 0.15$, $\alpha_K(137) = 2.2 \pm 0.6$, $\alpha_K(482) = 0.0234 \pm 0.0015$, and $\alpha_K(615) = 1.32 \pm 0.20$. The directional correlation data imply E2/M1 multipole mixing ratios of $\delta(136) = 0.45 \pm 0.02$ and $\delta(482) = 5.8^{+0.9}_{-0.7}$ where δ is defined in terms of emission matrix elements. This value for δ(482) and a weighted average of the present and four previous values of $\alpha_K(482)$ were used to re-evaluate the internal conversion penetration parameter as $\lambda(482) = 175^{+7}_{-4}$. (auth)

3648 (JINR-E7-5319) NEUTRON-RICH ISOTOPES OF LIGHT ELEMENTS PRODUCED IN TRANSFER REACTIONS WITH HEAVY IONS. Artyukh, A. G.; Avdeichikov, V. V.; Gridnev, G. F.; Eroe, J.; Mikheev, V. L.; Volkov, V. V.; Wilczynski, J. (Joint Inst. for Nuclear Research, Dubna (USSR). Lab. of Nuclear Reactions). 1970. 24p. (CONF-700815-5). Dep. NTIS (U. S. Sales Only).

From Conference on the Properties of Nuclei Far from the Region of Beta Stability, Leysin, Switzerland.

For the first time transfer reactions with heavy ions were used for production of neutron-rich isotopes of light elements. 11 new isotopes of carbon, nitrogen, oxygen, fluorine and neon and all the known heaviest isotopes of helium, lithium, beryllium and boron were obtained. Evidence for particle instability of ^{13}Be and ^{14}Be was obtained. For identification, a new method was used which combines a magnetic analysis and dE/dx, E technique. (auth)

3649 (KFK-1214) STUDIES OF RADIATIVE NEUTRON CAPTURE AND DELAYED FISSION GAMMA-RAY SPECTRA FROM URANIUM AND PLUTONIUM AS A BASIS FOR NEW NONDESTRUCTIVE SAFEGUARDS TECHNIQUES. Matussek, P.; Michaelis, W.; Weitkamp, C.; Woda, H. (Kernforschungszentrum, Karlsruhe (West Germany). Institut fuer Angewandte Kernphysik). Jul 1970. 19p. (CONF-700701-5; SM-133/33). Dep. NTIS (U. S. Sales Only).

From IAEA Symposium on Progress in Safeguards Techniques, Karlsruhe, Germany.

The thermal-neutron induced gamma-ray spectra from ^{235}U and ^{239}Pu samples were studied with a Ge(Li) detector. The integral spectrum is a superposition of gamma rays from the neutron capture reaction, prompt gamma rays from fission, and delayed gamma rays emitted from fission products. In order to separate the different parts, two experimental setups were used. The prompt fission and capture gamma-ray spectra were obtained by means of a 4π plastic scintillator for the detection of prompt fission neutrons, the detector being operated in coincidence and anticoincidence with the Ge(Li) detector, respectively. A combination of three mechanical choppers covering a decay time range from μs to 1 s served for the measurement of the different components of the delayed spectra. The separation of the radiative capture, prompt fission, and delayed fission, and delayed fission components of the total thermal neutron gamma-ray spectrum greatly facilitates the interpretation of the different gamma-ray lines observed. In particular, the structure of the capture spectra can, in many cases, be unambigously related to hitherto known excited states and interpreted in terms of the nuclear structure of the compound nucleus. On the basis of the data measured new approaches for detection, identification, and quantitative analysis of nuclear fuel are proposed that are nondestructive, prompt, accurate, and isotope specific. The results of the measurements are discussed in view of this application. For obtaining optimum penetrability for the primary radiation the application of a filtered beam of keV neutrons in the case of the radiative capture reaction and of nonthermal neutrons or high-energy photons in the case of the delayed fission spectra is suggested. (auth)

3650 (LYCEN-7030) DECAY SCHEME OF 7 MIN ^{168}Lu. Charvet, A.; Duffait, R.; Emsallem, A.; Chery, R. (Lyon Univ. (France). Institut de Physique Nucleaire). May 1970. 22p. Dep. NTIS (U. S. Sales Only).

The electron-capture decay ^{168}Lu (7 min) → ^{168}Yb was investigated using Ge(Li) and Si(Li) detectors. Single, coincidence and sum gamma-ray spectra, conversion lines, and β-γ coincidence relations were studied. The results obtained for the ground-state band and the gamma and beta vibrational bands are in good agreement with those of earlier investigations. Above the gamma vibrational band, 16 levels are established having the following energies (in keV), spin values and parities: 1479.8 (3,4); 1551.2, 3 or 4$^+$; 1597.8, 4$^-$; 1650.4, 3 or 4$^-$; 1674.1, 5 or 6$^+$; 1770.1, 5$^-$; 1819.4, 3 or 4$^-$; 1842.1, 5 or 6$^-$; 1972.8, 5 or 6$^-$; 1998.7, 5$^-$; 2110.5, (5) 6$^-$; 2135.4, (4); 2203.8, (3) 4$^+$; 2242.9, 4$^+$; 2404.6, (3) 4$^+$; 2427.8, 4$^+$. The decay scheme accounts for 76 of the 110 transitions presently observed. The Q value of the electron-capture decay of ^{168}Lu (7 min) and the half-life of the 1998.7 keV level determined were 4360 ± 80 keV and (12.4 ± 1.1) × 10^{-9}s, respectively. The structure of ^{168}Lu (7 min) and of the levels of ^{168}Yb are discussed in terms of the conventional nuclear models. (France)

3651 (NP-18485) STUDY OF NEUTRON-CAPTURE GAMMA-RAY SPECTRA FROM ALIGNED NEODYMIUM AND SAMARIUM NUCLEI. Reddingius, Ewout Roelof (Leiden Rijksuniversiteit (Netherlands)). 1969. 95p. Dep. NTIS (U. S. Sales Only).

Thesis.

Neutron capture in the thermal energy range was used to study neodymium and samarium. The linear polarization and anisotropy of the gamma rays from aligned ^{143}Nd and ^{149}Sm were measured by cooling these nuclei to 0.01 K by using adiabatic demagnetization. These anisotropy measurements were done with natural Nd and Sm. Since the samples contained several stable isotopes, all of which could contribute to the results, separate measurements were made on targets enriched in ^{145}Nd, ^{147}Sm, and ^{152}Sm to allow subtraction of their contributions. Decay schemes are presented for the nuclides ^{144}Nd, ^{146}Nd, ^{148}Sm, ^{150}Sm, and ^{153}Sm. (R.W.R.)

3652 (UCRL-19957) SEARCH FOR SUPERHEAVY ELEMENTS IN NATURE BY DETECTION OF EVENTS WITH LARGE NUMBERS OF NEUTRONS. Cheifetz, E.; Giusti, E. R.; Bowman, H. R.; Jared, R. C.; Hunter, J. B.; Thompson, S. G. (California Univ., Berkeley. Lawrence Radiation Lab.). Aug 1970. Contract W-7405-eng-48. 14p. (CONF-700815-3). Dep. NTIS.

From Conference on the Properties of Nuclei Far from the Region of Beta Stability, Leysin, Switzerland.

Some preliminary results are reported on a search for the presence of "superheavy elements" in nature. Large samples (10-50 kg) of various substances including W and Pb ores as well as manganese nodules were examined for the presence of spontaneous fission events in which large numbers of neutrons are emitted. The method utilized a large Gd loaded liquid scintillator with 60-70% efficiency for detecting neutrons. The system was located in a tunnel of depth ~275 meters in order to reduce interference from cosmic rays. In the materials tested no events above background were detected. This limit corresponds to half lives in the region 10^{23} years relative to the principal component of the samples. (auth)

3653 INELASTIC DEUTERON SCATTERING FROM ^{151}Eu. Boss, Gerald Ralph. Kalamazoo, Mich.; Western Michigan Univ. (1969). 57p.

Thesis.

The low-lying states of ^{151}Eu were studied by scattering 12-MeV deuterons from a thin target enriched to 97% in ^{151}Eu. Deuterons

inelastically scattered at 60, 90, 125, and 155° were analyzed with a split-pole magnetic spectograph. Nineteen energy levels of ^{151}Eu were identified. The data from the present work were compared to existing samarium data in order to assign the multipolarity of each transition on the basis of the angular distribution of the inelastically scattered deuterons. The angular distributions and the cross section to reduced transition probability ratios for the known electric quadrupole transitions to levels at 196, 307, and 503 keV in ^{151}Eu were consistent with those for quadrupole transitions in ^{150}Sm. A consideration of the magnitudes of the cross sections indicated that a majority of these eight states must be excited by electric octopole transitions. (Masters Abstr.)

3654 GAMMA-RAY SPECTRUM OF ^{192}Au. Plajner, Z.; Frana, J.; Spalek, A.; Vobecky, M.; Fiser, M. (Nuclear Research Inst., Rez, Czech.). Czech. J. Phys.; 20: 840-56(1970).

The gamma-ray spectrum of 5 h ^{192}Au was measured by means of a germanium detector. About 200 new transitions were found in addition to the transitions known from the conversion electron measurement of Nyman et al. (Arkiv f. fysik 29 (1965), 321) and 82 internal conversion coefficients were determined from the relations between conversion line- and gamma-ray intensities. From energies, intensities and multipolarities of transitions the existence of 20 new levels is very probable, in many cases with spin-parity assignments too. (auth)

3655 ELASTIC SCATTERING OF 1.33 MeV GAMMA RAYS FROM TIN. Terdal, J. Edward. Kalamazoo, Mich.; Western Michigan Univ. (1969). 30p.

Thesis.

A theoretical summary of the inelastic and elastic scattering processes of gamma radiation is given, as well as a discussion of the experimental approach used to observe elastic scattering. Previous experimental methods are compared and the advantage of using a lithium drifted germanium detector is presented. This thesis also gives a value for the elastic cross section of 1.33-MeV gamma rays scattered from tin at 30°, using such a detector. (Masters Abstr.)

3656 STUDY ON THE REACTOR NEUTRON-INDUCED FISSION OF ^{231}Pa. Kemmer, J.; Kim, J. I.; Born, H.-J. (Technische Hochschule, Munich). Radiochim. Acta; 13: 181-7(Jun 1970).

Using a recoil technique in combination with a direct gamma spectrometry it is possible to determine the fission yields of 17 mass chains in the reactor neutron-induced fission of ^{231}Pa without any chemical elaborations. The position of the maximum of the light and the heavy mass peak is found around mass number 91 and 138, respectively, with yields of 7.2%. The peak widths at half height and at $^1/_{10}$ of the height are 13.0 and 22.0 amu, respectively. The average number of neutron emitted per fission is found to be 2.4. (auth)

3657 DECAY OF ^{124}Sb. Sud, S. P.; Trehan, P. N. (Panjab Univ., Chandigarh, India). J. Phys. Soc. Jap.; 29: 827-36(Oct 1970).

Gamma rays in the decay of ^{124}Sb were investigated with scintillation spectrometers using $\gamma-\gamma$ coincidence, sum-peak coincidence and $\gamma-\gamma$ angular correlation techniques. The 4π-sum coincidence spectrometer study indicates a crossover transition from the 2693 keV level. The $\gamma-\gamma$ coincidence studies confirm the existence of levels at 2040 and 2773 keV and several weak gamma rays observed from these levels. The directional correlation for nine gamma ray cascades was measured. From the results of these directional correlation measurements it was possible to assign spin and parity 4+ to the 1248- and 1962-keV levels. It was possible to limit the spin assignment to 2040-keV level to 1, 2 and 3 from angular correlation measurements on 715-(722)-603 keV cascade. This assignment was further limited to 2+ or 3+ on the basis of comparison of experimental level structure to that of theoretical level structure. The mixing ratio for several gamma rays was determined. (auth)

3658 SEARCH FOR DOUBLE-PHOTON DECAY IN ^{90}Zr. Vanderleeden, J. C.; Jastram, P. S. (Ohio State Univ., Columbus). Phys. Rev., C; 1: 1025-35(Mar 1970).

A search was made for double-photon decay occurring in the $0^+ \rightarrow 0^+$ transition in ^{90}Zr, with the aid of a "fast–slow" coincidence spectrometer which permits two-dimensional pulse-height analysis, and which is modified to suppress higher-order accidental coincidences and to accumulate prompt and delayed coincidences simultaneously. Coincident γ rays are observed; however, neither the energy spectra nor the angular correlation corresponds to two-photon decay. Analysis of the observed spectrum yields an upper limit to the probability of double-photon decay of $W_{\gamma\gamma}/(W_{pair} + W_e) \leq 1.2 \times 10^{-4}$. The significance of the negative result is discussed in this paper, while the process that accounts for the observed twofold coincidence spectrum is the subject of the following two articles. (auth)

3659 LOW-ENERGY GAMMA TRANSITIONS IN ^{171}Tm. El-Nesr, M. S. (Atomic Energy Establishment, Cairo). Z. Naturforsch.; 25a: 1043-5(Jul 1970).

The low-energy gamma-ray spectrum of ^{171}Er was studied with the use of both Ge(Li) gamma-ray and a high resolution iron-free double-focusing beta-ray spectrometer. The data provide K-conversion coefficients and multipolarities of eight gamma-rays. Spin and parity assignments $^7/_2{}^+$, $^3/_2{}^+$, $^5/_2{}^+$, and $^5/_2{}^+$ are given to the 636, 676, 738, and 913 keV levels, respectively. (auth)

3660 EXCITATION ENERGY DEPENDENCE OF NEUTRON YIELDS AND FRAGMENT KINETIC ENERGY RELEASE IN THE PROTON INDUCED FISSION OF ^{233}U AND ^{238}U. Bishop, C. J.; Vandenbosch, R.; Aley, R.; Shaw, R. W. Jr.; Halpern, I. (Univ. of Washington, Seattle). Nucl. Phys.; A150: 129-42(1970).

The yields and energies of neutrons emitted from fission fragments of known mass were measured as a function of proton bombarding energy for ^{233}U and ^{238}U. The familiar sawtooth dependence of ν, the number of neutrons emitted per fragment, on the fragment mass was found to be considerably washed out with increasing bombarding energy, with the depth of the minimum at $A \approx 132$ decreasing more rapidly than that at $A \approx 80$. As the bombarding energy is increased the yield of neutrons from the heavy fragment increases more rapidly than does that of the light fragment. The results are interpreted in terms of qualitative considerations on energy-apportionment between fragments at the time of scission. Structure in the variation of the total fragment kinetic energy with mass ratio was observed to decrease at higher bombarding energies. The nuclear level density parameter a of the final fragments has been obtained as a function of fragment mass from the neutron kinetic energy and yield data. The a-values are observed to increase for fragments near closed shells and to decrease for mid-shell fragments as the excitation energy is increased. (auth)

3661 MUONIC ATOMS. I. DYNAMIC HYPERFINE STRUCTURE IN THE SPECTRA OF DEFORMED NUCLEI. Hitlin, D. (Columbia Univ., New York); Bernow, S.; Devons, S.; Duerdoth, I.; Kast, J. W.; Macagno, E. R.; Rainwater, J.; Wu, C. S.; Barrett, R. C. Phys. Rev., C; 1: 1184-1201(Apr 1970).

Precise measurements, using a stable high-resolution Ge(Li) spectrometer, are made of the K(2p-1s) and L(3d-2p) muonic x-ray spectra for nine deformed even-even nuclei: ^{150}Nd, ^{152}Sm, ^{162}Dy, ^{164}Dy, ^{168}Er, ^{170}Er, ^{182}W, ^{184}W, and ^{186}W. From these measurements, parameters describing the nuclear charge distribution are determined. Nuclear-polarization corrections are included in the analysis. The accuracy of the determination of the parameters of the nuclear charge distribution is limited by theoretical rather than experimental uncertainties. Isotope shifts are determined and compared with optical and electronic x-ray results. (auth)

3662 MULTIPLE COULOMB EXCITATION OF ^{152}Sm, ^{166}Er, AND $^{172\ 174\ 176}$Yb. Sayer, R. O.; Stelson, P. H.; McGowan, F. K.; Milner, W. T.; Robinson, R. L. (Oak Ridge National Lab., Tenn.). Phys. Rev., C; 1: 1525-38(Apr 1970).

Multiple Coulomb excitation of the ground-state rotational band of ^{152}Sm, ^{166}Er, and ^{172,174,176}Yb is measured in order to test the predicted ratios of the B(E2) values for a rotational sequence of states. The deexcitation γ rays from the rotational levels are observed in ^{16}O–γ and α-γ coincidence spectra with a Ge(Li) detector. Experimental excitation probabilities are compared to the probabilities calculated with the de Boer–Winther Coulomb-excitation computer program. The B(E2, $2 \rightarrow 4$) and B(E2, $4 \rightarrow 6$) values are determined to accuracies of 6-10%. The B(E2, $6 \rightarrow 8$) values were determined to accuracies of 15–25%. For the poor-rotor ^{152}Sm, the results indicate some increase in the B(E2) values over the rigid-rotor predictions for the higher transitions. The observed increase is less than that predicted by "centrifugal stretching" based on the level positions. However, the results for the four good-rotor nuclei show smaller B(E2) values between higher rotational states than those given by the rigid-rotor values, rather than the larger values predicted by centrifugal stretching. (auth)

3663 FISSION YIELDS OF SEVERAL IODINE ISOTOPES AND HALF-LIFE AND FISSION YIELD OF ^{135}Te. Delucchi, A. A.; Greendale, A. E. (Naval Radiological Defense Lab., San Francisco). Phys. Rev., C; 1: 1491-7(Apr 1970).

Measurements are made of the independent fission yields of several iodine isotopes in thermal-neutron-induced fission of ^{235}U. These yields are obtained by isolation of iodine-fission products at early times after fission by a new, fast radiochemical procedure. The fractional cumulative fission yield and half-life of ^{135}Te are also determined from the experimental results. Fission yields measured are: ^{131}I, $(4.2 \pm 0.4) \times 10^{-2}$% independent; ^{132}I, $(1.74 \pm 0.11) \times 10^{-2}$% independent; ^{133}I, 0.176 ± 0.009% independent; ^{134}I, 0.90 ± 0.08% independent; ^{135}I, 0.44 ± 0.07 fractional independent; ^{135}Te, 0.52 ± 0.07 fractional cumulative. The half-life of ^{135}Te is determined to be 11.2 ± 2.6 sec. (auth)

3664 g-FACTOR OF 1127.8 keV, $2'^{+}$ SECOND EXCITED STATE IN ^{106}Pd. Singh, Vikram (Panjab Univ., Chandigarh, India). J. Phys. Soc. Jap.; 29: 1111-15(Nov 1970).

The g-factor of the $2'^{+}$, second excited state in ^{106}Pd has been measured by using the integral reversed field method of the perturbed angular correlations. For this purpose the internal hyperfine fields at palladium in iron host were used. The value of the g-factor obtained is g = 0.385 ± 0.115. The present measured value analyzed in the light of hydrodynamical model confirmed that $2'^{+}$, second excited state of ^{106}Pd is a member of triplet of the two phonon vibrational state. (auth)

3665 ANGULAR DISTRIBUTIONS OF FISSION FRAGMENTS AND THE CROSS SECTION FOR NEUTRON-INDUCED ^{249}Bk FISSION. Vorotnikov, P. E.; Dubrovina, S. M.; Kosyakov, V. N.; Chistyakov, L. V.; Shigin, V. A.; Shubko, V. M. (Kurchatov Atomic Energy Inst., Moscow). Nucl. Phys.; A150: 56-60(1970).

The cross section and angular distributions of fission fragments in neutron-induced ^{249}Bk fission were measured in the energy range from 0.6 MeV to 1.8 MeV as well as 4.6 MeV. The fission cross section increases monotonically from ≈10 mb at 0.65 MeV to 1.4 b at 1.8 MeV with increasing neutron energy. The fission threshold, determined as the energy at which the cross section reaches one half of its "plateau" value, is equal to 1.07 MeV. In accordance with the smooth behavior of the cross section, the angular distributions of fragments reveal small anisotropy ≈1.1, and do not vary appreciably over the whole energy range investigated. (auth)

3666 INHIBITED (^{3}He,d) TRANSITIONS TO $3s_{\frac{1}{2}}$ ISOBARIC ANALOG STATES. McGrath, R. L.; Cue, N.; Hering, W. R.; Lee, L. L. Jr.; Liebler, B. L.; Vager, Z. (State Univ. of New York, Stony Brook). Phys. Rev. Lett.; 25: 682-5(7 Sep 1970).

The (^{3}He,d) reaction cross sections on ^{90,92,94}Zr and ^{92,94,96,98}Mo targets have been measured to unbound isobaric analog states. All expected transitions are observed except those of $3s_{\frac{1}{2}}$ analog states which are inhibited. Distorted-wave Born approximation calculations do not explain the anomaly. Other possible explanations are suggested. (auth)

3667 EFFECTIVE NEUTRON CAPTURE CROSS SECTION AND HALF-LIFE OF ^{155}Eu. Mowatt, R. S. (Atomic Energy of Canada Ltd., Chalk River, Ont.). Can. J. Phys.; 48: 1933-5 (15 Aug 1970). (AECL-3633).

The half-life of ^{155}Eu was measured to be 4.65 ± 0.20 yrs and the absorption cross section was found to be 4040 ± 125 b by a depletion method using a Ge(Li) detector. The sample of ^{155}Eu was irradiated in the NRU pneumatic carrier where the flux has a small epithermal component. These values are very different from values of $T_{\frac{1}{2}} \sim 1.8$ yrs and $\sigma \sim 13{,}000$ b reported previously. (auth) (Canada)

3668 SPECTROSCOPY OF EVEN TIN ISOTOPES BY INELASTIC SCATTERING OF 24.5 MeV PROTONS. Beer, O.; El Behay, A.; Lopato, P.; Terrien, Y.; Vallois, G.; Seth, Kamal K. (CEN, Saclay, France). Nucl. Phys.; A147: 326-68(1970).

Elastic and inelastic scattering of 24.5-MeV protons by even isotopes of tin, ^{116,118,120}Sn and ^{122,124}Sn, has been studied with an energy resolution better than 20 keV. Approximately 30 levels in each isotope have been resolved up to an excitation energy of 4 MeV. Elastic scattering angular distributions have been analyzed to yield optical-model parameters and the inelastic scattering angular distributions have been analyzed in the distorted wave Born approximation (DWBA) using collective form factors to determine l and β_l corresponding to a large number of the transitions observed. The systematics of the states of each J^{π} are discussed and the results are compared to recent theoretical calculations. (auth)

3669 ENERGY LEVELS OF ^{243}Am EXCITED BY THE ^{242}Pu(^{3}He,d) AND ^{242}Pu(α,t) REACTIONS. Elze, Th. W.; Huizenga, J. R. (Univ. of Rochester, N. Y.). Nucl. Phys.; A149: 585-92 (1970).

The ^{242}Pu(^{3}He,d)^{243}Am and ^{242}Pu(α,t)^{243}Am reactions were studied with 30 MeV ^{3}He and ^{4}He beams. Rotational bands built upon the following Nilsson proton configurations in ^{243}Am were identified (bandhead energies in parentheses): $5/2^{-}[523\downarrow]$(0 keV), $5/2^{+}[642\uparrow]$ (84 keV), $3/2^{-}[521\uparrow]$(267 keV), $7/2^{+}[633\uparrow]$(466 keV). Experimental spectroscopic factors observed in both reactions were found to be in reasonable agreement with each other, as well as with theoretical spectroscopic factors calculated with Nilsson wave functions. Nilsson state assignments made previously are confirmed. (auth)

3670 LEVEL STRUCTURE OF ^{105}Pd STUDIED FROM THE DECAY OF ^{105}Ag. Kawakami, H.; Hisatake, K. (Tokyo Inst. of Tech.). Nucl. Phys.; A149: 523-44(1970).

The level structure of ^{105}Pd was investigated by measuring internal conversion electrons following the decay of ^{105}Ag with a $\sqrt{2}\,\pi$ air core β-ray spectrometer. Seventy-three conversion lines including five new transitions and three new conversion lines were observed. The 443 and 644 keV transitions were revealed to be doublets. The L-subshell ratios of the 64, 90, 155, 183, 280, 319, 344, 392, and 443 keV transitions were measured with the resolution between 0.024 and 0.082%, and the multipolarities and the mixing ratios of these transitions were determined. The level energies and the spin-parities of ^{105}Pd are as follows: 0[$5/2^{+}$], 280.51[$3/2^{+}$], 306.25[$7/2^{+}$], 319.18[$5/2^{+}$], 344.52[$1/2^{+}$], 442.23[$7/2^{+}$($5/2^{+}$)], 489.11[$11/2^{-}$], 560.75[$1/2^{+}$,$3/2^{+}$,$5/2^{+}$], 644.50($7/2^{-}$), 650.69[$3/2^{+}$], 673.18 [$1/2^{+}$,($3/2^{+}$,$5/2^{+}$)], 727.17[$5/2^{+}$], 782.1[$5/2^{+}$,$7/2^{+}$], 962.37[$1/2^{+}$,$3/2^{+}$,$5/2^{+}$] and 1087.93 keV [$3/2^{-}$]. The level structure of ^{105}Pd is discussed in terms of the core excitation and quasi-particle excitation. (auth)

3671 THE DECAY OF THE ISOMERS OF ^{102}Rh. Konijn, J.; Lingeman, E. W. A.; Diederix, F.; Meijer, B. J.; Koldewijn, P.; Klaasse, A. A. C. (Instituut voor Kernphysisch Onderzoek, Amsterdam). Nucl. Phys.; A138: 514-28(1969).

Energies and relative intensities of the gamma rays following the decays of 1057 d and 206 d ^{102}Rh have been measured with Ge(Li) counters of the coaxial type. Improved decay schemes are presented based on $\gamma-\gamma$ coincidence and $\gamma-\gamma$ angular correlation measurements using Ge(Li) counters. A level at 943.6 keV is definitely established as the missing 0^{+} level of the two-phonon triplet. The following energies in keV, spins and parities of levels are assigned: ground state (0^{+}), 475.0 ± 0.2 (2^{+}), 943.6 ± 0.3 (0^{+}), 1103.2 ± 0.2 (2^{+}), 1106.1 ± 0.4 (4^{+}), 1521.5 ± 0.2 (3^{+}), 1580.6 ± 0.2 ($1,2^{+}$), 1797.8 ± 0.6 (4^{+}), 1837.3 ± 0.2 (0^{+}), 1872.9 ± 0.4 (6^{+}), 2036.9 ± 0.2 (2^{+}), 2218.8 ± 0.2 (5^{+}) and 2261.2 ± 0.2 ($1^{+},2^{+}$) in ^{102}Ru and ground state (0^{+}) and 556.5 ± 0.2 (2^{+}) in ^{102}Pd. The spins and parities of the ^{102}Rh isomers most likely are 1^{-} and 5 for the 206 d and 1057 d activities, respectively. Evidence for an isomeric transition has been found. Gamma-ray energies and relative intensities of radiation following the decay of ^{101}Rh are also reported. (auth)

3672 HINDRANCE FACTORS FOR UNIQUE FIRST-FORBIDDEN BETA TRANSITIONS IN DEFORMED NUCLEI. Sharma, R. P.; Nielsen, H. L.; Hansen, P. G. (Univ. of Aarhus, Denmark). Nucl. Phys.; A152: 225-31(1970).

The absolute transition probabilities for first-forbidden unique beta transitions in ^{159}Dy, ^{169}Er and ^{185}W have been measured. These values along with the earlier reported values for ^{166}Ho and ^{172}Tm have been compared with the theoretical transition probabilities calculated from the Nilsson model with pairing corrections included. On this scale the observed transitions are hindered by the following factors: ^{159}Dy 3.2, ^{166}Ho 1.4, ^{169}Er 0.9, ^{172}Tm 10.9, and ^{185}W 2.5. (auth)

3673 A STUDY OF THE LOW-ENERGY TRANSITIONS ARISING FROM THE PROMPT DE-EXCITATION OF FISSION FRAGMENTS. Watson, R. L.; Wilhelmy, J. B.; Jared, R. C.; Rugge, C.; Bowman, H. R.; Thompson, S. G.; Rasmussen, J. O. (Univ. of California, Berkeley). Nucl. Phys.; A141: 449-80 (1970).

A four-dimensional experiment has been performed in which the energies of coincident complementary fragment pairs, internal conversion electrons, and K X-rays emitted as a result of the spontaneous fission of ^{252}Cf were recorded event by event using a multiparameter analyser. The fission fragment energies were used for mass identification and the x-ray energies supplied precise atomic number identification. The analysis of the conversion electron spectra has resulted in the assignment of numerous transitions to new isotopes, the determination of many transition half-lives, and the procurement of limited information concerning multi-polarities. It was concluded, based on the x-ray and conversion electron data, that most of the large number of observed low-energy transitions associated with heavy fragments are attributable to odd-mass or doubly odd nuclei and that surprisingly little contribution to the low-energy spectra is associated with doubly even nuclei in the rare earth-region. Low-energy transitions in doubly even nuclei were found to be more prevalent among the light fragments. Data are presented supporting the assignment of a high intensity 241 keV transition as the 2^{+} to 0^{+} transition in ^{110}Ru. An examination of this transition in terms of the energy predicted on the basis of rotational behavior and with regard to the systematics of neighboring doubly even Ru isotopes reveals evidence which strongly suggests that ^{110}Ru belongs to a new region of stable deformation. (auth)

3674 COULOMB EXCITATION OF ^{209}Bi AND THE WEAK-COUPLING MODEL. Broglia, R. A.; Lilley, J. S.; Perazzo, R.; Phillips, W. R. (Univ. of Minnesota, Minneapolis). Phys. Rev., C; 1: 1508-24(Apr 1970).

Some relative and absolute γ-ray transition probabilities are measured for the low-lying levels in ^{209}Bi by observing the Coulomb excitation and subsequent decay of the states. Thick bismuth targets are bombarded with 19-MeV α particles, and γ-ray yields at 0°, 30°, 45°, 60°, and 90° are observed with a 25-cm^{3} LiGe de-

XUM

tector. Determinations are made of the transition strengths to the $f_{\frac{5}{2}}$ (0.897-MeV), the $i_{\frac{13}{2}}$ (1.608-MeV), the $f_{\frac{7}{2}}$ (2.822-MeV), and the septuplet of levels near 2.6 MeV, formed by coupling an $h_{\frac{9}{2}}$ particle to the 3^- octuple state in ^{208}Pb, excited by E2, E3, E2, and E3 Coulomb excitation, respectively. Approximate E1 transition strengths for ground-state decays of the 2.563-, 2.581-, and 2.598-MeV levels are determined from the Doppler broadening of the γ peaks. Branches are observed corresponding to decays from the 2.741- and 2.600-MeV states to the 1.608 ($I^{13}/_2^+$) level, and from the 2.822-, 2.615-, and 2.581-MeV levels to the 0.897 ($I^{7}/_2^-$) state. The γ-ray strengths and relative transition rates are compared with the predictions of a particle-vibration coupling model. (auth)

3675 ANGULAR CORRELATION OF THE 460 keV-27.7 keV GAMMA-GAMMA CASCADE IN ^{129}I. Sanders, R. (Univ. Groningen, Netherlands). Nucl. Phys.; A138: 583-7(1969).

Normalized expansion coefficients $A_{22} = -0.0148 \pm 0.0029$ and $A_{44} = -0.0068 \pm 0.0043$ have been found for the angular correlation of the 460 keV–27.7 keV cascade in ^{129}I, in contradiction with some earlier measurements. These results are consistent with a spin $^3/_2$ or $^5/_2$ assignment of the 487-keV level. For both spins the E2/M1 mixing ratio of the 460 keV transition is given. Unfortunately, no conclusion can be drawn about the sign of the mixing ratio of the 27.7-keV transition. (auth)

3676 DECAY OF ^{169}Hf. Aten, A. H. W. Jr.; Kapteyn, Johanna C. (Instituut voor Kernphysisch Onderzoek, Amsterdam). Radiochim. Acta; 13: 219(Jun 1970).

A nuclide decaying with a half-life of 3.3 ± 0.3 min in the hafnium fraction isolated from activated ^{170}Yb is attributed to ^{169}Hf. This nuclide is seen to grow into ^{169}Lu. The 3.3-minute ^{169}Hf decays in part by β^+ emission; the decay is accompanied by the emission of gamma rays of 123.3, 369.3, and 492.3 keV. These data suggest the existence of a level at 492.3 keV in ^{169}Lu. (R.W.R.)

3677 BAND-MIXING EFFECTS IN THE EVEN–EVEN DEFORMED NUCLEI ^{154}Gd, ^{160}Dy, AND ^{168}Er. Keller, George Earl. Baton Rouge, La.; Louisiana State Univ. (1969). 211p. University Microfilms Order No. 70-9066. Thesis.

The gamma rays emitted in the decay of ^{154}Eu, ^{160}Tb, and ^{168}Tm to excited states of ^{154}Gd, ^{160}Dy, and ^{168}Er, respectively, were detected with Ge(Li) detectors and analyzed on a 4096-channel analyzer. For the prominent gamma rays emitted by each nucleus, the energies were determined to within 10 to 40 keV and the relative intensities were determined to within 2 to 4%. The energies were measured relative to a set of energy standards. The estimated uncertainty in the relative efficiency calibration used to obtain gamma intensities was 5%. The analysis of the gamma-ray spectra was accomplished by using a computer technique to fit a Gaussian function to each photopeak in the spectra. The gamma energies and intensities were used to calculate ratios of reduced E2 transition probabilities for levels in the β- and γ-vibrational bands of the even–even deformed nuclei ^{154}Gd, ^{160}Dy, and ^{168}Er. The B(E2) ratios, which are sensitive to the mixing of the ground-state rotational band and the vibrational bands, are compared to the predictions of the collective model. The models formulated from a purely macroscopic approach do not make realistic predictions of the ratios. Only for the nucleus ^{154}Gd is there even limited agreement between these theories and experiment. For the more deformed nuclei ^{160}Dy and ^{168}Er, the nonadiabatic models overestimate the effect of band mixing. The B(E2) ratios are compared to the theoretical predictions of the adiabatic symmetric-rotor model, which is valid for the case of no band mixing, to obtain band-mixing parameters, for each ratio in each nucleus, within the framework of the phenomenological band-mixing model. The band mixing in the nucleus is accurately described by this model, as a consistent set of z_2 parameters is obtained for B(E2) ratios for transitions from levels in the band. For ^{154}Gd, which was the only nucleus for which a β band was observed, a two-parameter analysis (including mixing of the β and γ bands) of the B(E2) ratios of the γ band does not result in a consistent set of mixing parameters, z_2 and $z_{2\gamma}$. The B(E2) ratios from the β band of ^{154}Gd and the γ band of ^{160}Dy are not described by the band-mixing model. The results indicate, however, that the model is promising—especially if additional second-order effects such as variation of the quadrupole moments from band to band are included. The mixing parameters are compared with the various microscopic models formulated from the pairing-plus-quadrupole-fields approach. These models are seen to be nearly adequate in the predictions of the mixing parameters. The energy shifts of the ground-state rotational band are analyzed within the framework of band mixing. It is concluded that band mixing can not account for the observed shifts and that the microscopic models underestimate the effect of band mixing. (TSS) (Diss. Abstr. Int., B)

3678 NON-LOCAL BARRIER AND ANISOTROPY OF ALPHA EMISSIONS FROM ORIENTED ^{237}Np NUCLEI. Chaudhury, M. L. (Indian School of Mines, Dhanbad). J. Phys., A (London): 3: 378-89(Jul 1970).

A formula for the angular distributions of alpha particles from oriented nuclei is presented by assuming the barrier to be the usual anisotropic electrostatic potential superimposed by a non-local alpha–nucleus interaction potential. A spherically symmetric form of this latter potential was used successfully in a previously published work and is taken to be axially symmetric, described by a deformation parameter ϵ_1. For simplicity the author restricts his considerations to spheroidal deformations of the nuclear surface. Calculations show that the anisotropy coefficient is positive for either sign of a given value of the quadrupole moment Q of the parent nucleus, depending on the values of ϵ_1. The significance of this finding in the light of the results of experiments on ^{237}Np nuclei is discussed. The main contribution of this work is to show that the observed anisotropy of alpha emissions from oriented ^{237}Np nuclei can now be interpreted without difficulty, regardless of the sign of Q of this nuclide. (auth) (UK)

3679 NEUTRON FISSION CROSS SECTIONS FOR ^{231}Th, ^{233}Th, ^{235}U, ^{237}U, ^{239}U, ^{241}Pu, AND ^{243}Pu FROM 0.5 TO 2.25 MeV USING (t,pf) REACTIONS. Cramer, J. D.; Britt, H. C. (Los Alamos Scientific Lab., N. Mex.). Nucl. Sci. Eng.; 41: 177-87(Aug 1970).

Experiments were performed using the (t,p) stripping reaction followed by fission to provide experimental measurements of fission probabilities. The neutron-induced fission cross sections of the corresponding even–odd neutron targets can be deduced from these experimental (t,pf) data with the aid of an optical-model calculation of the cross section for the formation of the compound nucleus by neutron absorption. Experimental measurements of the (n,f) cross section of the longer-lived targets such as ^{235}U and ^{241}Pu are used to test the validity of this technique by directly comparing experimental results and computed results from (t,pf) experiments. Ratios of Γ_n/Γ_f are determined from these experimental data and are compared to previously published values. (auth)

3680 FRAGMENT ANGULAR DISTRIBUTIONS AND CHANNEL ANALYSIS OF FISSION OF ^{232}Th BY NEUTRONS. Ermagambetov, S. B.; Smirenkin, G. N. Yadern. Fiz.; 11: 1164-77 (Jun 1970). (In Russian).

Angular distributions of fragments from fission of ^{232}Th by neutrons were measured at 18 neutron energy values from 0.95 to 2.3 MeV. Channel analysis of experimental data on the fission cross section and the angular anisotropy is carried out. Results of the experiment and the analysis are interpreted in the framework of the double-bump fission barrier. Sources of considerable uncertainty in the channel analysis of the (n, f) reaction are suggested. (auth)

3681 DEEXCITATION OF THE 931.1-keV 2_2^+ STATE OF ^{152}Gd. Gono, Yasuyuki (Tokyo Univ.); Fujioka, Manabu; Toriyama, Tamotsu. J. Phys. Soc. Jap.; 29: 255-8(Aug 1970).

The gamma-ray spectrum and the conversion-electron spectrum were measured in the decay of the ^{152}Tb activity. The L-subshell electron lines of the 586.7-keV $2_2^+ \rightarrow 2_1^+$ transition were separated by the iron-free beta-ray spectrometer. The M1–E2 mixing ratio δ^2 and the dimensionless ratio X of E0–E2 mixing of the 586.7-keV transition are found to be $\delta^2 \leqq 0.16$ and $0.034 \leqq X \leqq 0.038$, respectively. The E2 branching ratio B(E2; $2_2^+ \rightarrow 0_2^+$): B(E2; $2_2^+ \rightarrow 2_1^+$): B(E2; $2_2^+ \rightarrow 0_1^+$) is determined to be 0.023 : 1.0 : 5.6. (auth)

3682 TRANSITION MULTIPOLARITIES IN THE DECAY OF ^{197m}Hg. Plajner, Z.; Rezanka, I.; Spalek, A.; Frana, J.; Josovic, M.; Fiser, M. (Nuclear Research Inst., Rez, Czech.). Czech. J. Phys.; 20: 917-25(1970).

Multipolarities of 130-, 279-, and 409-keV transitions in the decay of ^{197m}Hg were determined by magnetic electron and gamma-ray spectroscopy. The multipolarities of other transitions were verified. The results are compared with core excitation, Alaga and Ialongo, and pairing-plus-quadrupole calculations. (auth)

3683 M1 GAMMA-RAY STRENGTH FUNCTIONS FOR DEFORMED NUCLEI. Shapiro, Charles Stephen. Stony Brook, N. Y.; State Univ. of New York (1969). 82p. University Microfilms Order No. 69-17,303. Thesis.

A shell-model calculation which can give a qualitative explanation for these strong M1 transition rates in deformed nuclei is presented. The experimental and theoretical results are discussed in terms of the M1 gamma-ray strength functions. The strength functions peak at an energy near 7.5 MeV, and in this way they resemble an M1 giant resonance at an energy near 7.5 MeV. The M1 transition strengths in the strength functions are derived from the M1 matrix elements between the particle-hole states and the ground state of the nucleus. The particle-hole states are assumed to be eigenfunctions of a very general nuclear Hamiltonian. The Hamiltonian is the sum of three terms: H = H(Nilsson) + H(short-range) + H(long-range). The short-

range part of the Hamiltonian is approximated by the pairing interaction, and the long-range part is approximated by a schematic spin–spin interaction. Two sets of theoretical results are presented. The first set consists of the Tamm–Dancoff (TD) and random-phase-approximation (RPA) calculations with values for the parameters that are obtained from the comparison between other nuclear structure calculations and other types of experimental data. In the first set of results the TD calculated strength functions for several deformed nuclei in the rare earth region have about three times the strength of the experimental strength functions for energies near the energies of the M1 primary transitions. The RPA calculated strength functions have about twice the strength of the experimental strength functions. Also, in the energy region of the primary transitions the experimental strength function for ^{168}Er appears to be increasing with increasing energy, but the theoretical strength functions decrease with increasing energy. However, for ^{239}U, the only heavy nucleus for which there is available data, the RPA and TD strength functions have values which are about 30% below the experimental values. In the second set of results the rare-earth theoretical strength functions are shifted upward one MeV. Such a shift in energy is within the uncertainty of the calculation due to the uncertainty of the parameters. In this case good qualitative agreement is obtained between the theoretical and experimental strength functions. Branching rules are also derived and compared with the experimental data. The theoretical predictions, however, are not in good agreement with the experimental branching rules. The explanation for this is discussed. (auth) (Diss. Abstr. Int., B)

3684 DIRECTIONAL CORRELATION STUDIES IN THE DECAY OF ^{177g}Lu. Hrastnik, B.; Basar, I.; Diksic, M.; Ilakovac, K.; Kos, V.; Ljubicic, A. (Rudjer Boskovic Inst., Zagreb). Z. Phys.; 239: 25-9(1970).

Directional gamma–gamma correlations of the strong 208.4–112.9-keV and of the weak 71.6–249.7-keV cascade transitions in the decay of ^{177g}Lu were measured. The correlation coefficients $A_{22} = -0.203 \pm 0.012$ of the strong and $A_{22} = -0.105 \pm 0.005$ of the weak cascade are determined. The mixing ratio E2/M1 of -3.7 ± 0.3 for the 112.9-keV transition and the M2/E1 of -0.0173 ± 0.0065 for the 71.6-keV transition are obtained. The deduced M2 admixture in the 71.6-keV transition is in good agreement with the theoretical estimates of Weisskopf and of Nilsson. (auth)

3685 2^+_1 MIXING AT ISOBARIC ANALOG RESONANCES IN $N \approx 82$ NUCLEI. Hiddleston, H. R.; Riley, P. J. (Univ. of Texas, Austin). Phys. Lett.; 32B: 425-7(17 Aug 1970).

Evidence is discussed for the mixing of single particle configurations built on the 2^+_1 core into the isobaric analog resonances formed by proton scattering on nuclei in the $N \approx 82$ region. Analysis of on-resonance angular distribution data for decay to the 2^+_1 state has provided inelastic proton partial widths and spectroscopic factors. It is shown that the parent analog wave functions are well described by including the above mixing. (auth)

3686 STATIC AND TRANSIENT HYPERFINE MAGNETIC FIELDS AT Ba ISOTOPES RECOILED IN IRON. Kugel, H. W.; Polga, T.; Kalish, R.; Borchers, R. R. (Univ. of Wisconsin, Madison). Phys. Lett.; 32B: 463-4(17 Aug 1970).

The hyperfine magnetic field at Ba nuclei recoiled into Fe is negative, and the transient magnetic field acting on the recoiling nuclei is found to be consistent with systematics. (auth)

3687 ELASTIC ELECTRON–NICKEL SCATTERING. Ficenec, J. R. (Virginia Polytechnic Inst., Blacksburg); Trower, W. P.; Heisenberg, J.; Sick, I. Phys. Lett.; 32B: 460-2(17 Aug 1970).

Electron-nickel elastic differential cross sections were measured at 300 MeV for the five stable isotopes. The isotopic dependence of the charge distribution is found from a phase shift analysis employing a parabolic Fermi shape modified by a damped oscillatory function. (auth)

3688 STUDY OF THE ^{207}Pb(d,p)^{208}Pb REACTION. Earle, E. D. (Chalk River Nuclear Labs., Ont.); Ferguson, A. J.; Van Middelkoop, G.; Bartholomew, G. A.; Bergqvist, I. Phys. Lett.; 32B: 471-2(17 Aug 1970).

Excitation energies and γ-ray branching ratios are obtained for ^{208}Pb levels below 7.5 MeV. These data combined with known spectroscopic factors and radiation widths give information on level assignments and correlations of E1 radiation and neutron strengths. (auth)

3689 ALPHA-PARTICLE SCATTERING FROM ^{204,206,208}Pb AND ^{209}Bi AT INCIDENT ENERGIES NEAR THE COULOMB BARRIER. Goldring, G. (Weizmann Inst. of Science, Rehovoth, Israel); Samuel, M.; Watson, B. A.; Bertin, M. C.; Tabor, S. L. Phys. Lett.; 32B: 465-7(17 Aug 1970).

Alpha particles elastically scattered from ^{204,206,208}Pb and ^{209}Bi were observed over the energy range 14 to 23 MeV at several angles. An optical-model analysis indicates that the surface of the nuclear potential is determined quite well. (auth)

3690 HYPERFINE INTERACTIONS ON ^{237}Np AND ^{239}Np IMPLANTED INTO COPPER AND NICKEL. Ansaldo, E. J.; Grodzins, L. (Massachusetts Inst. of Tech., Cambridge). Contract AT(30-1)-2098. Phys. Lett.; 32B: 479-81(17 Aug 1970).

Alpha–gamma perturbed angular correlations after recoil implantation have been used to study the hyperfine interactions acting on neptunium isotopes in metals. The interaction in copper is shown to be nonstatic and is probably of quadrupole character. The effective magnetic hyperfine field on ^{239}Np in nickel has been determined to be -0.170 ± 0.040 MOe. (auth)

3691 ROTATIONAL BANDS OF ^{166}Ho. Bollinger, L. M.; Thomas, G. E. (Argonne National Lab., Ill.). Phys. Lett.; 32B: 457-9(17 Aug 1970).

Nuclear states of ^{166}Ho were studied by means of the average-resonance-capture method of neutron-capture γ-ray spectroscopy. An exceptionally large number of states were observed and their spins and parities determined. These states form 16 rotational bands that are in generally good agreement with what is expected from the collective model. (auth)

3692 EFFECT OF SPIN-ORBIT AND SPIN–SPIN FORCES ON MAGNETIC MOMENTS OF DEFORMED NUCLEI. Chernyshev, A. S. (Voronezh State Univ., USSR). Yadern. Fiz.; 11: 1182-91(Jun 1970). (In Russian).

The effect of deformation on renormalization of the magnetic moment by spin forces is considered by using the Fermi-liquid theory method. It is shown that for deformed nuclei the effect of spin forces only is insufficient to explain the experiment. Including the effect of spin-orbit forces makes it possible to obtain good agreement with experiment, with the constant of spin interaction being very close to the spherical value of this parameter. (auth)

3693 DOUBLE-BETA DECAY. van Klinken, J. (Univ., Groningen, Netherlands). Ned. Tijdschr. Natuurk.; 35: 358-70 (Dec 1969). (In Dutch).

The double-beta ($\beta\beta$) decay represents the spontaneous decay of an (A,Z) nucleus to an (A,Z + 2) one. Its existence has been predicted but was proved only in 1968. Several isotopes which are currently considered stable may actually decay slowly. The $\beta\beta$ decay of ^{130}Te to ^{130}Xe is reviewed, alternate ways of the decay process are outlined, and the analytical problems are examined. The study requires a high-purity pre-Cambrian ore with a noble gas daughter and a highly specific spectrometer. This instrument obtained from the Max Planck Institute indicated that the Te ore from the Colorado Plateau contained 70% excess Xe. Its age was calculated by the K–Ar decay method as 1.27×10^9 years, indicating a $T_{\frac{1}{2}}(^{130}\text{Te})$ of $10^{21.3 \pm 0.1}$ years. A previous experiment, involving the use of Ca enriched with 97% of ^{48}Ca as a source in a 610 m deep salt mine in Ohio to measure the $^{48}\text{Ca} \xrightarrow{\beta\beta} {}^{48}\text{Ti}$ decay, is also discussed. The source acts as an electrode in a streamer ionization chamber. The calculations indicate that the $\beta\beta$ decays may be observed, but the margin of error is nearly prohibitive. (TTT)

3694 ACCURATE DETERMINATION OF THE ENERGY OF GAMMA RAYS FROM ^{7}Be, ^{40}K, AND ^{113}Sn, AND THE DECAY OF ^{113}Sn. Jansen, J. F. W.; Meijer, B. J.; Koldewijn, P. (Instituut voor Kernphysisch Onderzoek, Amsterdam). Radiochim. Acta; 13: 171-6(Jun 1970).

The energy of the gamma rays emitted by ^{7}Be, ^{40}K, and ^{113}Sn has been determined with a germanium detector system calibrated with gamma rays from other nuclides. The measured spectra were analyzed with different computer programs. The results, 477.61 ± 0.02 keV (^{7}Be), 1460.95 ± 0.07 keV (^{40}K), 255.04 ± 0.04 keV (^{113}Sn), and 391.71 ± 0.02 keV (^{113}Sn) are compared with other determinations. In the decay of ^{113}Sn two weak gamma rays were found with energies of 638.9 ± 0.5 keV and 646.4 ± 0.5 keV. The latter is interpreted as the cross-over gamma ray from the 646-keV level to the ground state. (auth)

3695 ANGULAR DISTRIBUTIONS OF 1 TO 40 keV NEUTRON SCATTERING. Samosvat, G. S. (Joint Inst. for Nuclear Research, Dubna, USSR). Yadern. Fiz.; 11: 1152-63(Jun 1970). (In Russian).

Energy-averaged angular distributions of neutrons scattered by nuclei of Sr, Mo, Rh, Cd, Sn, Sb, Te, I, La, and Th in the energy region 1 to 40 keV were measured. For each element except La all the information obtained can be described by a single parameter ω_1/E, where ω_1 is the coefficient of the first polynomial in the expansion of the differential scattering cross section in Legendre polynomials and E is the neutron energy. The systematic behavior of this parameter is compared with calculations from the optical model, and a good qualitative agreement with potentials describing other data on the interaction of neutrons with nuclei is obtained. In connection with the anomalous nega-

XUM

tive values of ω_1, the problem of the signs of the s- and p-scattering amplitudes is considered for La. Two possible explanations of the anomaly are proposed: optical potential with a suppressed imaginary part or the production of the doorway state. (auth)

3696 INVESTIGATION OF THE STATISTICAL PERTURBATION OF A GAMMA–GAMMA ANGULAR CORRELATION IN ^{166}Er IN DIFFERENT LIQUID SOURCES. Forker, M.; Wagner, H. F.; Bodenstedt, E. (Univ., Bonn). Nucl. Phys.; A138: 644-56(1969).

Time differential measurements of the 1379–81 keV angular correlation of ^{166}Er have been performed for two liquid sources of different chemical composition, Er^{3+} in 1 N HCl and Er^{3+} in 1 N $HClO_4$ at room temperature (T = 22°C). Within the accuracy of these experiments the attenuations can be described by single exponential functions as predicted by the theory of Abragam and Pound. The results are: (i) hydrochloric acid: $\lambda_2 = (0.1110 \pm 0.0075) \cdot 10^9\ s^{-1}$, $\lambda_4 = (0.3146 \pm 0.0078) \cdot 10^9\ s^{-1}$, $\lambda_4/\lambda_2 = 2.84 \pm 0.20$. (ii) perchloric acid: $\lambda_2 = (0.0921 \pm 0.0087) \cdot 10^9\ s^{-1}$, $\lambda_4 = (0.3079 \pm 0.0084)\ 10^9\ s^{-1}$, $\lambda_4/\lambda_2 = 3.34 \pm 0.33$. No indication of a Dillenburg–Maris effect was found. Possible influences of complex formations are studied. (auth)

3697 CIRCULAR POLARIZATION OF GAMMA RAYS FROM ^{124}Sb, ^{134}Cs, AND ^{110m}Ag. Pingot, O. (Centre de la Faculte Polytechnique, Mons, Belgium). Nucl. Phys.; A150: 587-92(1970). (In French).

The $\beta\gamma$ circular polarization correlation of the $3^-(\beta^-\ 621\ keV)\ 3^-(\gamma\ 1692)2^+$ cascade in ^{124}Sb, the $4^+(\beta^-\ 662)4^+\ (\gamma\ 796)2^+\ (\gamma\ 605)0^+$ in ^{134}Cs and the $6^+(\beta^-\ 529)6^+\ (\gamma\ 937)4^+\ (\gamma\ 885)2^+\ (\gamma\ 658)0^+$ in ^{110m}Ag have been studied by using a Compton effect polarimeter. The measured asymmetry parameters are 0.172 ± 0.004, −0.0702 ± 0.0024 and 0.0549 ± 0.0013, respectively. (auth)

3698 STUDIES OF THE LEVEL SCHEME OF ^{152}Eu WITH CONVERSION ELECTRONS FROM NEUTRON CAPTURE. Kaiser, Walther (Technische Hochschule, Munich). Z. Naturforsch.; 25a: 602-7(May 1970). (In German).

With the beta spectrometer at the research reactor near Munich the conversion electron spectrum of ^{152}Eu from slow neutron capture has been measured. In the range between 0 and 350 keV approximately 500 lines were found. For the low-energy states a level scheme is proposed and compared with earlier level schemes of ^{152}Eu. New transitions for the 9.3 h-isomer were found. (auth)

3699 TRANSITION PROBABILITIES OF EXCITED NUCLEAR STATES IN ^{125}Te. Marelius, A.; Lindskog, J.; Awwad, Z.; Vaelivaara, K. G.; Haegglund, S. E.; Pihl, J. (Uppsala Univ.). Nucl. Phys.; A148: 433-43(1970).

The lifetimes of eight excited states in ^{125}Te have been measured by the delayed coincidence technique. A comparison is made between experimental and theoretical M1 and E2 transition probabilities. (auth)

3700 LOCATION AND DESCRIPTION OF SOME LOW-LYING HIGH-SPIN STATES IN ^{155}Gd. Loevhoeiden, G. (Univ. of Copenhagen); Waddington, J. C.; Hagemann, K. A.; Hjorth, S. A.; Ryde, H. Nucl. Phys.; A148: 657-72(1970).

The reaction ^{154}Sm(α,3n)^{155}Gd has been used to populate states in ^{155}Gd. Cascade and crossover transitions are observed within a strongly perturbed rotational band which is populated up to spin $25/2$. A calculation in which the Nilsson-model Hamiltonian is extended to include Coriolis and $\Delta N = 2$ couplings can successfully account for the experimental energies, intensities and angular distributions in the positive-parity band. This calculation suggests that the band is a rather complete mixture of the $1/2^+[660]$, $3/2^+[651]$, $5/2^+[642]$, $7/2^+[633]$, $1/2^+[400]$ and $3/2^+[402]$ Nilsson orbitals. Rotational bands built on the intrinsic states $3/2^-[521]$ and $11/2^-[505]$ are also observed. The moment of inertia for the $11/2^-[505]$ band is discussed. (auth)

3701 DIRECT REACTION STUDIES OF VIBRATIONAL NUCLEI IN THE MASS-105 REGION. Dittmer, David Louis. Pittsburgh; Univ. of Pittsburgh (1969). 106p. University Microfilms Order No. 70-7875.

Thesis.

The isotopes ^{104}Pd, ^{106}Pd, and ^{105}Rh were studied with high resolution by the single nucleon transfer reactions ^{105}Pd(d,t)^{104}Pd, ^{105}Pd(d,p)^{106}Pd, and ^{104}Ru(^{3}He,d)^{105}Rh, and by the triton pickup reactions ^{107}Ag(p,α)^{104}Pd, ^{109}Ag(p,α)^{106}Pd, and ^{108}Pd(p,α)^{105}Rh. Van de Graaff bombarding energies of 17 MeV for deuterons, 18 MeV for ^{3}He, and 12 and 15 MeV for protons were employed and particle analysis was accomplished with an Enge split-pole spectrograph. Experimental angular distributions were compared with distorted wave Born approximation (DWBA) calculations, which included finite-range and non-locality corrections for the (d,p) and (^{3}He,d) stripping, and yielded l-value assignments, J^π limits and spectroscopic factors for the levels populated in the residual nuclei. Previous energy level schemes for these nuclei had been derived primarily from radioactive decay and were incomplete. The present studies resolve some earlier discrepancies and extend the spectroscopy of ^{104}Pd and ^{106}Pd up to 3.2 MeV excitation and of ^{105}Rh to 2 MeV. Results of these investigations are consistent with a description of the low-lying levels of the Pd isotopes by classic vibrational theory and suggest that the low excitation of ^{105}Rh arise from a coupling of the collective modes of the core to the odd proton configuration. Of particular interest is the result that the previously postulated doublet at 1.33 MeV in ^{104}Pd is in fact a nearly degenerate (18 keV) triplet, in accordance with a two-phonon quadrupole vibration model. Sums of spectroscopic factors for ^{105}Pd(d,t) and ^{105}Pd(d,p) measurements led to U_{lj}^2 values for the 2d and $3s_{1/2}$ neutron single particle orbitals for ^{105}Pd that are in good agreement ($.38 \le U_{2d}^2 \le .42$, $.73 \le U_{3s_{1/2}}^2 \le .80$). The low yield (p,$\alpha$) transitions leading to ^{104}Pd, ^{106}Pd and ^{105}Rh furnished additional spectroscopic information, but were of principal interest as a reaction mechanism study. Zero-range DWBA calculations were performed assuming a triton cluster transfer model and produced a particularly good duplication of the experimentally observed $p_{1/2}$, p_3 j-dependence. Comparisons of the experimental angular distributions and energy dependence with distorted wave theory gave convincing evidence that direct triton pickup is the dominant mechanism. (Diss. Abstr. Int., B)

3702 RECOIL STUDIES OF FISSION PRODUCTS FORMED IN THE FISSION OF ^{238}U BY PROTONS OF ENERGIES 25 TO 85 MeV. Ramamoorthy, A. N.; Saha, G. B.; Yaffe, L. (McGill Univ., Montreal). Nucl. Phys.; A150: 545-69(1970).

The recoil properties of ten fission products with masses ranging from 72 to 136 formed in the fission of ^{238}U with protons of energies 25 to 85 MeV have been determined radiochemically by the integral-range method. From the recoil properties of the products and the Monte Carlo cascade calculations the average kinetic energy, cascade deposition energy, and anisotropy parameter for each fission product has been calculated. The kinetic energy and the excitation energy of the primary fragments leading to the observed fission product, and the total kinetic energy and the total excitation energy of the primary fragment pair have also been calculated. The results indicate that up to a bombarding energy of 40 MeV fission takes place predominantly by the compound nucleus mechanism, with an increasing contribution of the direct interaction mechanism as the bombarding energy increases. The kinetic energy deficit was found to decrease with increasing bombarding energy. The fission products formed from the symmetric mode of fission have a larger separation distance between the charge centers of their respective primary fragments than those for the asymmetric mode of fission. (auth)

3703 COULOMB EXCITATION OF ^{151}Eu AND ^{153}Eu. Lewis, Trevor James. University Park, Pa.; Pennsylvania State Univ. (1969). 98p. University Microfilms Order No. 70-7225.

Thesis.

De-excitation gamma rays following Coulomb excitation of ^{151}Eu and ^{153}Eu were studied with a 2 cm^3 Ge(Li) spectrometer. Thick targets of natural europium metal were used to obtain excitation curves with 5 to 12 MeV alpha particles. Reduced transition probabilities were measured with 7 to 11 MeV alpha particles and 4.5 to 6 MeV protons. Pressed powder targets of Eu_2O_3 enriched to 97% in ^{151}Eu and ^{153}Eu were used to determine the isotopic origins of the observed transitions. A 2 × 2 in. NaI(Tl) spectrometer was used to study gamma rays of 800 to 2200 keV. In ^{151}Eu, gamma rays of 111, 196.1, 244.0, 258.9, 286.1, 307.1, 476, 481.6, 502.9, 522.9, and 600.1 keV were found. These transitions were attributed to previously known levels of 196.1, 307.1, and 502.9 keV. Additional levels of 244.0, 600.1, and possibly 721 keV are proposed. A 383 keV transition in ^{151}Eu remains unassigned. In ^{153}Eu, gamma rays of 83.3, 110.0, 151.5, 192.6, 486, 534.8, 568.9, and 617.1 keV were found. These were attributed to previously known levels of 83.3, 151.5, and 192.6 keV, and to previously proposed levels of 568.9 and 617.1 keV. The 568.9 and 617.1 keV levels are tentatively interpreted as a $9/2^+$ gamma vibration and a $5/2^+$ beta vibration, respectively. Gamma rays of 76, 97.5, 175, and possibly 427 keV may originate in either ^{151}Eu or ^{153}Eu. No transitions above 617.1 keV could be attributed to Coulomb excitation. (Diss. Abstr. Int., B)

3704 DECAY OF ^{185}Os, ^{74}As, AND ^{51}Cr. Kane, John William Jr. University, Ala.; Univ. of Alabama (1969). 101p. University Microfilms Order No. 70-9362.

Thesis.

The decay of ^{185}Os, ^{74}As and ^{51}Cr was investigated with high-resolution solid-state detectors and with standard scintillation counters. Gamma-ray energies and intensities were determined using Ge(Li) detectors and multichannel analyzers. Gamma–

gamma coincidence studies were conducted with a Ge(Li)-NaI system. A Si(Li) detector was used for measuring the internal conversion electron spectra. By standardizing a Ge(Li) gamma-ray spectrometer and a Si(Li) electron spectrometer, the internal conversion coefficients of various transitions were determined. ^{185}Os decays by electron capture to ^{185}Re. Gamma-rays of the following energies (in keV) and relative intensities (in parentheses) were assigned to the decay of ^{185}Os: 71 ± 1, 124.8 ± 0.2 (0.14), 163.1 ± 0.1 (0.55), 234.1 ± 0.1 (0.48), 592.2 ± 0.1 (1.92), 646.0 ± 0.1 (100), 717.2 ±0.1 (3.8), 874.7 ± 0.1 (5.4), 880.1 ± 0.1 (4.5), and 934 ± 1 (0.037). The internal conversion coefficients for the 592, 646 and 717 keV transitions were found to be $(2.8 \pm 0.4) \times 10^{-2}$ (α_K), $(1.2 \pm 0.1) \times 10^{-2}$ (α_K) and $(3.0 \pm 0.4) \times 10^{-3}$ (α_L), respectively. The nucleus ^{74}As decays by negatron emission to ^{74}Se and by positron emission and electron capture to ^{74}Ge. The following gamma-ray energies (in keV) and relative intensities (in parentheses) were assigned to the decay of ^{74}As: 595.9 ± 0.5 (100), 608.3 ± 0.5 (0.93), 635.0 ± 0.5 (24.8), 887.0 ± 0.5 (0.070), 1205.0 ± 0.5 (0.49), 1600 ± 3 (0.012), and 2199 ± 3 (0.015). Only the 635.0 ± 0.5 keV transition is assigned to the negatron decay mode. ^{51}Cr decays by electron capture to ^{51}V with a half-life of 28 days. Based on the present measurements, it is concluded that in addition to the ground state only a single level in ^{51}V at 320.1 ± 0.5 keV is populated by the decay of ^{51}Cr. This level de-excites only by a transition to the ground state. The K-shell internal conversion coefficient of the 320.1 keV transition was measured as $(1.57 \pm 0.08) \times 10^{-3}$ and the K/L ratio as 11.0 ± 0.5. A proposed decay scheme consistent with the experimental results is given for the three radioactive nuclei. Assignment of spin and parity is made on the basis of the experimental results and interpretation of the data in terms of various nuclear models. (Diss. Abstr. Int., B)

3705 THE g FACTOR OF THE 114 keV STATE IN ^{149}Pm. Tandon, P. N.; Devare, H. G. (Tata Inst. of Fundamental Research, Bombay). Indian J. Pure Appl. Phys.; 7: 1-3(Jan 1969).

The g factor of the 114-keV first excited state in ^{149}Pm was measured using the integral reversed-field method of perturbed angular correlation. Both the 542-114 and the 424-114 keV cascades through this level were used. Measurements were made at two different magnetic fields of 12.8 and 8.5 kgauss. The possible attenuation due to time-dependent perturbations was also measured using the 424-114 keV cascade by studying the anisotropy as a function of time. The results obtained are $G_2 = 0.8 \pm 0.03$ and g = 1.02 ± 0.13. This value of g corresponds to a value of $\mu = 2.55 \pm 0.33$ nm, the spin of the level being $\frac{5}{2}$. (auth)

3706 HALF-LIVES OF EXCITED LEVELS IN ^{125}Te AND ^{132}I. Hosangdi, R. R.; Tandon, P. N.; Devare, S. H. (Tata Inst. of Fundamental Research, Bombay). Indian J. Pure Appl. Phys.; 7: 604-6(Sep 1969).

The half-life of the 321-keV level in ^{125}Te has been measured to be $T_{\frac{1}{2}} = (0.68 \pm 0.03)$ nsec using conventional delayed coincidence measurements. In ^{132}I, the half-lives of the levels at 49.7 and 277.9 keV have been measured to be (0.93 ± 0.04) and (1.41 ± 0.07) nsec, respectively. The nature of these levels is discussed on the basis of these measurements. (auth)

3707 LIFETIMES OF 321- AND 113-keV LEVELS OF ^{177}Hf. Rao, B. V. Narasimha; Jnanananda, Swami (Andhra Univ., Waltair, India). Indian J. Pure Appl. Phys.; 6: 555-7(1968).

The lifetimes of 321 and 113 keV levels of ^{177}Hf have been measured with a delayed coincidence spectrometer, the values being 647 ± 32 and 523 ± 25 psec, respectively. The experimental transition probabilities of the three E1 transitions decaying from the 321 keV level are compared with the single particle as well as Nilsson estimates and a good agreement is found with the latter. (auth)

3708 HALF-LIFE OF THE 181-keV LEVEL OF ^{99}Tc Rama Rao, M. T.; Ramamurty, V. V.; Lakshminarayana, V. (Andhra Univ., Waltair, India). Indian J. Pure Appl. Phys.; 6: 553-4(1968).

The half-life of the 181-keV level in ^{99}Tc is measured by the delayed coincidence method using a time-to-amplitude converter of the Green and Bell type. NaI(Tl) crystals in conjunction with RCA 6810A photomultipliers are used as detectors. Observing the 740-181 keV gamma–gamma coincidences and adopting the slope method, the half-life of the 181-keV level is obtained as (3.42 ± 0.10) nsec. The 181-keV gamma ray E2 transition probability is estimated and is found to show an enhancement of (8.2 ± 1.3) over the single particle estimate. On the basis of the observed enhancement, a pure configuration $(p_{\frac{1}{2}})^2(g_{\frac{9}{2}})^3$ for the 181-keV level is rejected. Assuming the ground and the 181-keV states in ^{99}Tc to be described by pure De Shalit wave functions, it is observed that the expected value of B(E2) from these wave functions is in good agreement with the experimental value. Alternatively, the value of B(E2) is estimated assuming the ground state wave function furnished by L. S. Kisslinger and R. A. Sorensen [Rev. mod. Phys., 35(1963), 853] and a pure De Shalit wave function for the 181-keV level. It is noticed that a slight modification of the amplitudes of the particle and particle + phonon parameters in the ground state wave function is necessary to obtain an exact agreement of B(E2) with the experimental value. The core plus several particle model does not seem to apply to the 181-keV level in ^{99}Tc. (auth)

3709 EVIDENCE FOR A DIRECT REACTION MECHANISM IN THE PRODUCTION OF FISSION ISOMERS. Repnow, R.; Metag, V.; Fox, J. D.; Von Brentano, P. (Max-Planck-Institut fuer Kernphysik, Heidelberg). Nucl. Phys.; A147: 183-92(1970).

Targets of ^{233,235,236,238}U were bombarded with deuterons and protons in the energy range from 11 to 20 MeV. Excitation functions for the production of fission isomers were obtained and are interpreted in terms of direct reaction processes. The most probable reactions are (d,pxγ) and (d,pnxγ) leading to isomers assigned to ^{236}U and ^{238}U with half-lives of 70 nsec and 110 nsec, respectively. (auth)

3710 FRAGMENT ANGULAR DISTRIBUTIONS IN THE FISSION OF HEAVY NUCLEI BY 103 MeV HELIUM IONS AND 51.5 MeV DEUTERONS. Gindler, J.; Muenzel, H.; Buschmann, J.; Christaller, G.; Michel, F.; Rohde, G. (Nuclear Research Center, Karlsruhe, Ger.). Nucl. Phys.; A145: 337-50(1970).

Fragment angular distributions in the fission of ^{209}Bi, ^{233}U, ^{234}U, ^{235}U and ^{238}U by 51.5-MeV deuterons and 103-MeV helium ions, including the fission of ^{197}Au by the latter projectiles, have been measured using solid state detectors. The c.m. angular distributions have been calculated and fitted by a series of Legendre polynomials. The $W(\theta)/W(90°)$ anisotropies of the fragments have been calculated from the polynomial series and compared with anisotropies measured with similar projectiles, but of different energy. Variational trends observed in the anisotropy with projectile, projectile energy and the fission parameter Z^2/A are qualitatively explained in terms of changes in the total angular momentum I and its projection K on the nuclear symmetry axis. Fission cross sections measured for the various reactions are compared with total reaction cross sections calculated for an optical-model potential. (auth)

3711 TWO-QUASIPARTICLE STATES IN ^{164}Ho. Jones, H. D.; Sheline, R. K. (Florida State Univ., Tallahassee). Nucl. Phys.; A150: 497-519(1970).

Thirty-one levels in ^{164}Ho have been observed up to an excitation energy of 994 keV utilizing 12 MeV deuterons and the reaction ^{165}Ho(d,t)^{164}Ho. The ground state Q-value was determined to be −1730 ± 15 keV. The spectrum has been interpreted in terms of the coupling of the [523↑] Nilsson proton orbital with the neutron orbitals prominent in the (d,t) spectrum of ^{163}Dy. Based on this interpretation, the singlet–triplet splitting energies for the [523↓], [642↑], [521↑], [402↓] and [400↑] neutron orbitals coupled to the [523↑] proton orbital were determined to be −144, +67, +171, −85 and +102 keV, respectively. Theoretical calculations of these energies made for a zero-range spin-dependent central potential gave values of −248, +74, +160, −82 and +73 keV, respectively. (auth)

Nuclear Theory

Refer also to abstracts 2497, 3317, 3322, 3340, 3414, 3424, 3426, 3577, 3579, 3580, 3655, and 3692.

3712 (AAEC/TM-545) USE OF HAUSER–FESHBACH THEORY FOR PREDICTING INELASTIC SCATTERING OF NEUTRONS BY NUCLEI. Bertram, W. K. (Australian Atomic Energy Commission Research Establishment, Lucas Heights). Jul 1970. 24p. Dep. NTIS (U. S. Sales Only).

Cross sections for inelastic scattering of neutrons by nuclei are investigated using the Hauser–Feshbach theory. With transmission coefficients calculated from the optical model using a potential equivalent to the nonlocal potential of Perey and Buck, it is shown that it is possible to predict inelastic scattering cross sections with satisfactory results, provided corrections due to level width fluctuations are taken into account. (auth) (Australia)

3713 (CEA-N-1333) DELAYED NEUTRON EMISSION. EMISSION PROBABILITIES AND ENERGY SPECTRA. de Tourreil, Roland (Commissariat a l'Energie Atomique, Fontenay-aux-Roses (France). Centre d'Etudes Nucleaires). Aug 1970. 33p. (In French). Dep. CFSTI (U. S. Sales Only).

The model used to describe the process starts from the β^- decay of the precursor nuclide; then the excited nucleus obtained loses its energy by emission of γ-rays or neutrons. The results

obtained show, in particular, that the structure of the neutron energy spectra can be well reproduced together with the correct emission probabilities Pm. (auth) (France)

3714 (ITF-70-35) ELECTRODISINTEGRATION OF LIGHT NUCLEI. Sitenko, A. G.; Pasichnyi, A. A.; Tartakovskii, V. K. (Akademiya Nauk Ukrainskoi SSR, Kiev. Institut Teoreticheskoi Fiziki). 1970. 19p. (In Russian). Dep. NTIS (U. S. Sales Only).

The electrodisintegration of nuclei, i.e., the inelastic electron scattering process accompanied by knocking-out of nucleons is discussed. The case of ultrarelativistic electrons and light nuclei is considered. The Coulomb and magnetic interaction between the electron and nucleons is taken into account. As the wave functions for the primary and finite states of nucleons, the exact solutions of Shroedinger's equation with the Woods–Sakson real self-consistent potential are used. The numerical calculations of the electrodisintegration differential cross section for nu ^{12}C are performed. An investigation is made of the role of the nucleon wave deformation effects in the finite state. It is shown that by the calculations on the basis of the shell model with the real potential it is possible to obtain an agreement with experimental data both with respect to the maxima positions and the momentum distributions shapes under the electrodisintegration of light nuclei. The electron energy spectra inelastically scattering by light nuclei are calculated. The calculated spectra well agree with experimental data. (auth)

3715 (NBS-MON-118) PHOTONUCLEAR REACTIONS. Hayward, Evans (National Bureau of Standards, Washington, D. C.). Aug 1970. 46p. GPO $0.50.

Photonuclear reactions are reviewed in the approximate energy range 10 to 30 MeV. Various sum rules are discussed and applied to experimental data. Several different theories are described and their predictions compared with experiment, and as often as possible open questions and discrepancies are pointed out. 146 references. (auth)

3716 (ORNL-TM-3153) APPROXIMATE HIGH-ENERGY ALPHA-PARTICLE-NUCLEUS-COLLISION MODEL. Gabriel, T. A.; Santoro, R. T.; Alsmiller, R. G. Jr. (Oak Ridge National Lab., Tenn.). 1 Oct 1970. 29p. Dep. NTIS.

An alpha-particle-nucleus-collision model, which assumes that the nucleons within the alpha particle can be treated separately and independently except for their relative spatial locations when they enter the nucleus, is described. Because of the assumptions that are made, calculations based on the model can be carried out using the intranuclear-cascade code of Bertini. Calculated data on the energy and angular distribution of emergent nucleons and on the cross sections for the production of various residual nuclei from alpha-particle-nucleus collisions are found to be in very approximate agreement with existing experimental data. (auth)

3717 COMMENT ON THE NUMBER OF DEGREES OF FREEDOM IN FLUCTUATION ANALYSIS. Harney, H. L. (Max-Planck-Institut fuer Kernphysik, Heidelberg); Richter, A. Phys. Rev., C; 2: 421-5(Aug 1970).

Different methods of calculating the number of degrees of freedom N_{eff} in statistical cross-section fluctuations are compared. The underlying physical assumptions of the methods are discussed critically, and numerical examples for N_{eff} are given. (auth)

3718 SINGLE-PARTICLE RESONANCES IN THE RENORMALIZED RANDOM-PHASE-APPROXIMATION TREATMENT OF NUCLEON–NUCLEUS SCATTERING. Garside, L.; Weigel, M. (Univ. of California, Berkeley). Phys. Rev., C; 2: 374-9(Aug 1970).

The method of Garside and MacDonald is used to treat the single-particle resonances in the renormalized random-phase-approximation treatment of scattering. The resonances are shifted by an additional potential to single-particle bound states, which can be handled in the usual manner. The coupling to the continuum is done analytically using separable matrix elements. (auth)

3719 MESON DYNAMICS AND THE NUCLEAR MANY-BODY PROBLEM. I. THE FREE-NUCLEON PROBLEM. Brown, W. D.; Puff, R. D.; Wilets, L. (Univ. of Washington, Seattle). Phys. Rev., C; 2: 331-49(Aug 1970).

Relativistic nucleon-meson field theory is cast in a form appropriate to the nuclear many-body problem. Martin–Schwinger thermodynamic Green's functions are employed. The n-nucleon Green's functions satisfy a set of coupled equations which is formally identical to those of the usual potential many-body problem. Here, however, the two-body potential is replaced by a time-dependent interaction in which the mesons are formally eliminated in favor of higher-order nucleon correlations. A general program of increasing complexity for obtaining approximate solutions to the equations is discussed. It is necessary to solve the "vacuum" (one-, two-, etc., nucleon propagator) first. This has been done in the "Hartree–Fock" approximation which sums all diagrams containing a single continuous nucleon line with all possible uncrossed π and ω meson lines. Peaks in the spectral function are identified with masses of known N* resonances. The appearance of the ghost states, which arise in the process of mass and wave-function renormalization, is discussed. The resultant Green's function is used to calculate the magnetic moment of the nucleon, yielding a significantly better isovector component of the magnetic moment than the usual perturbation theory, although the isoscalar component is poor in both cases. (auth)

3720 COULOMB DISTORTION IN HEAVY-ION REACTIONS. Jensen, A. S.; Wong, C. Y. (Univ. of Copenhagen, Oak Ridge National Lab., Tenn.). Phys. Rev., C; 1: 1321-5 (Apr 1970).

The dynamics of nuclear distortion is studied for two spherical nuclei under the influence of their mutual Coulomb interactions. Both the quadrupole and the octupole degrees of freedom are considered. Realistic stiffness and effective-mass parameters are employed. It is found that the energy needed to bring the two nuclei into contact increases as a result of the distortions. However, in the most favorable case, the increase is only a few percent. This is much smaller than previous estimates using either the liquid-drop model or the adiabatic model. (auth)

3721 SHELL-MODEL STRUCTURE OF THE p-SHELL HYPERNUCLEI. Lee, T. Y.; Hsieh, S. T.; Chen-Tsai, C. T. (Tsing Hua Univ., Hsinchu, Taiwan). Phys. Rev., C; 2: 366-74 (Aug 1970).

A systematic study of the effective two-body $\Lambda-N$ interaction is made in an exact manner from the binding-energy data of the p-shell hypernuclei within the framework of the intermediate-coupling shell model. The binding energy is expressed in terms of the five independent potential integrals of the two-body $\Lambda-N$ interaction, and the latter are determined by a least-squares fit to the experimental data. The energy levels and the γ transitions are calculated, and the structures of the p-shell hypernuclei are discussed. The potential integrals are then analyzed in terms of phenomenological potentials. A large contribution to the binding energy by noncentral forces, especially the tensor forces, is found. The effect of the existence of a three-body ΛNN force is also discussed. (auth)

3722 GENERALIZED PAIRING IN LIGHT NUCLEI. II. SOLUTION OF THE HARTREE–FOCK–BOGOLYUBOV EQUATIONS WITH REALISTIC FORCES AND COMPARISON OF DIFFERENT APPROXIMATIONS. Goodman, A. L. (Univ. of California, Berkeley); Struble, G. L.; Bar-Touv, J.; Goswami, A. Phys. Rev., C; 2: 380-95(Aug 1970).

The Hartree–Fock–Bogoliubov (HFB) equations with generalized isospin pairing are numerically solved without any approximations, except imposing certain self-consistent symmetries. Realistic forces are used to make definite conclusions concerning the shapes of nuclei and the existence of isospin pairing. Comparison with previous approximations shows that in the s-d shell the HFB equations may not be quantitatively approximated by HF + BCS, HB–BCS, or by iterating between HF and BCS. Isospin pairing offers an explanation for axial symmetry in ^{24}Mg and ^{32}S and for the existence of low-lying vibrational states in ^{36}Ar. (auth)

3723 REGGE TRAJECTORIES AND NUCLEAR STRUCTURE. Shapiro, I. S. (Inst. of Theoretical and Experimental Physics, Moscow). Yadern. Fiz.; 12: 53-60(Jul 1970). (In Russian).

Regge trajectories are compared in many-particle (collective) and shell models. It is shown that the existence of analog resonances is difficult to reconcile with the behavior of the shell trajectories. On the basis of the formulas obtained for nuclear trajectories, the question of rotation-like spectra is discussed. (auth)

3724 GILBERT–SCHMIDT EXPANSION FOR POTENTIALS WITH HARD CORE. Narodetskii, I. M. (Inst. of Theoretical and Experimental Physics, Moscow). Yadern. Fiz.; 12: 61-9 (Jul 1970). (In Russian).

The expansion of the Gilbert–Schmidt type for the t matrix is considered for the case when the potential contains a hard core. It is shown that the t matrix is a sum of two terms, the first of which is due to the repulsing core and the second is due to the attracting part of the potential. The following examples are considered: the repulsing part as a rectangular well and as $V_1(r) = -V_1[\exp(r/b) + c]^{-1}$. Solutions of some transcendent equations appearing from determination of the Gilbert–Schmidt eigen values for these potentials are tabulated. (auth) .

XUM

3725 α DECAY AND NUCLEAR INTERACTIONS. Kadmenskii, S. G.; Kalechits, V. E. (Voronezh State Univ., USSR). Yadern. Fiz.; 12: 70-8(Jul 1970). (In Russian).

A new approach to the theory of the α decay is developed, which accounts consistently for the nuclear interactions between the α particle and the daughter nucleus. It contains no fitting parameter, like the nuclear force cut off, R_0. The partial α-decay width is expressed in the diagonal case via the sum of the one-nucleon optical potentials. The possibilities, connected with the nondiagonal components of the nuclear interaction, are discussed. The one-particle partial width and the spectroscopic factor for the α decay of ^{210}Po are calculated. (auth)

3726 DESCRIPTION OF M1 TRANSITIONS BETWEEN ROTATIONAL STATES OF DEFORMED NUCLEI. Zakrevskii, N. V. (Leningrad State Univ.). Yadern. Fiz.; 12: 79-81(Jul 1970). (In Russian).

M1 transitions between lower rotational states of even-even deformed nuclei are considered based on the rotation model, taking into account the difference in parameters of mass and charge distributions in the nucleus. The values of log $(\delta/E)^2$ are calculated for transitions between states with $I^\pi K$ 2 + 2 → 2 + 0 and 3 + 2 → 2 + 0 for even-even nuclei with A ≥ 150. The calculations are compared with experiment and with predictions of other collective models. (auth)

3727 STATES $I^\pi = 1^+$ IN EVEN-EVEN DEFORMED NUCLEI. Gabrakov, S. I.; Kuliev, A. A.; Pyatov, N. I. (Joint Inst. for Nuclear Research, Dubna, USSR). Yadern. Fiz.; 12: 82-90(Jul 1970). (In Russian).

Properties of excitations $I^\pi = 1^+$ (K = 0 or 1) in even-even deformed nuclei are studied. Calculations with residual pair and spin-spin interactions show that the spectroscopic 1^+ states (up to the energies of about 4 MeV) are weakly collectivized and have low values of B(M1, 0 → 1). Collective 1^+ states with maximal values of B(M1) may be expected in the energy regions 10–11 MeV (K = 0) and 12–13 MeV (K = 1), though separate excitations with B(M1) ~ $B(M1)_{sp}$ may appear also in the energy region of neutron resonance capture. The excitation structure and the dipole sum rule for M1 transitions are investigated. (auth)

3728 EFFECTIVE MASS OF ALPHA PARTICLES IN SUPERFLUID NUCLEAR MATTER. Khanna, K. M. (Dibrugarh Univ., India); Sikand, M. S. Indian J. Pure Appl. Phys.; 6: 390-2(Jul 1968).

By assuming that the nucleons in the surface region of nuclear matter have clustered into α-particles which interact with each other and that the α-particles are bosons, the effective mass of α-particles has been calculated and it is shown that the resultant interaction between α-particles, for the assembly in the stable superfluid state, is repulsive. The transition temperature from the superfluid to the normal state increases as the density of α-particles increases. (auth)

3729 TRANSFORMATION COEFFICIENTS IN THE HYPERSPHERICAL APPROACH TO THE THREE-BODY PROBLEM. Raynal, J.; Revai, J. (CEN de Saclay, Gif-sur-Yvette, France). Nuovo Cim.; 68A: 612-22(21 Aug 1970).

The transformation from one set of Jacobi coordinates to another for hyperspherical functions is closely related to the Talmi–Moshinsky transformation for two particles in an oscillator well. The corresponding coefficients are calculated analytically. (auth)

3730 HYPERSPHERICAL-EXPANSION APPROACH TO NUCLEAR BOUND STATES. I. Badalyan, A. M. (Inst. of Theoretical and Experimental Physics, Moscow); Calogero, F.; Simonov, Yu. A. Nuovo Cim.; 68A: 572-90(21 Aug 1970).

A simple lower bound for the magnitude of the binding energies of (suitably defined) doubly magic nuclei is presented. It states that these quantities are minorized by the corresponding quantities evaluated for a two-body problem with an effective potential that is an appropriate (and explicitly defined) integral transform of the original two-body nucleon-nucleon central potentials. (auth)

3731 SHORT-RANGE CORRELATIONS IN THE THREE-BODY PROBLEM AND THE FADDEEV EQUATIONS. Osman, A. (Cairo Univ.). Nucl. Phys.; A153: 524-8(1970).

For potentials containing repulsive cores, a separable expansion for the t-matrix is developed. The resulting Faddeev equations form a set of coupled equations in one continuous variable. The three-body binding energy is calculated using a Gaussian form for the repulsive and attractive parts of the potential. (auth)

3732 MULTI-STEP STRIPPING ON DEFORMED NUCLEI WITH NON-ROTATIONAL STATES INVOLVED. Dumitrescu, C.; Lukyanov, V. K.; Petkov, I. Z.; Schulz, H.; Wiebicke, H. J. (Joint Inst. for Nuclear Research, Dubna, USSR). Nucl. Phys.; A149: 253-60(1970).

An expression for the deuteron stripping cross section is obtained, taking into account the intermediate excitations of the rotational and non-rotational types. All the rotational states are included using the adiabatic approximation, while the other types of nuclear excitations are treated by the coupled equations. The result is illustrated using perturbation theory. The spectroscopic amplitudes of the intermediate transitions are calculated in the framework of the microscopic nuclear model. The theory is applied to the ^{154}Gd(d,p)^{155}Gd stripping reaction. A detailed analysis is made. (auth)

3733 TWO-NUCLEON DENSITY FUNCTIONS AND CORRELATION FUNCTIONS WITH REALISTIC SINGLE-PARTICLE WAVE FUNCTIONS. Jackson, Daphne F.; Murugesu, S. (Univ. of Surrey, Guildford, Eng.). Nucl. Phys.; A149: 261-72(1970).

Two-nucleon density functions and Pauli correlation functions are calculated for ^{6}Li, ^{12}C, ^{16}O and ^{40}Ca using realistic single-particle wave functions. The results are compared with those obtained using oscillator functions. The extent to which uncertainties introduced by the use of different wave functions may obscure investigation of the dynamical correlations is discussed. (auth)

3734 STRUCTURE OF THE POTENTIAL ENERGY SURFACE AT LARGE DEFORMATIONS. Mosel, Ulrich (Univ. of Tennessee, Knoxville. Oak Ridge National Lab., Tenn.); Scharnweber, Dieter. Phys. Rev. Lett.; 25: 678-81(7 Sep 1970).

The two-center shell model has been generalized to the shape of two overlapping spheroids with equal mass. In this model shell corrections have been calculated and the potential energy surface of two heavy nuclei has been investigated. The influence of fragment shells in the model gives rise to structure in this surface which supports assumptions of earlier models for the scission point. (auth)

3735 CORRECTION TO THE NUCLEAR-MATTER CALCULATIONS OF SECOND ORDER IN v/c. Bhakar, B. S. (Univ. of Manitoba, Winnipeg). Phys. Rev., C; 2: 905-11(Sep 1970).

A calculation of the correction, second order in v/c, to the binding energy of nuclear matter in the first-order Hartree–Fock approximation yields a result of +0.5 MeV per particle at k_F = 1.36. The correction becomes large very quickly as the Fermi momentum increases. These results are based on the nonlocal separable potential of Tabakin. (auth)

3736 CHARGE ASYMMETRY OF THE INTERNUCLEON POTENTIAL. Yap, C. T. (Univ. of Singapore). Nucl. Phys.; A142: 161-6(1970).

Experimental measurement of the β circularly polarized γ-correlation for the β^- decay from the J = 2^+, T = 1 ground state of ^{20}F to the J = 2^+, T = 0 state of ^{20}Ne yields a non-vanishing value for the Fermi nuclear matrix element M_F. Assuming the validity of the conserved vector current theory, this M_F should be zero identically if there are no charge-dependent effects. The non-vanishing value of M_F is attributed to charge-dependent effects and the calculation yields a value in fair agreement with that obtained experimentally. It is also found that any charge asymmetry of the internucleon potential is of the order of a tenth of a percent or so. (auth)

3737 POSITIVITY CONDITIONS FOR VELOCITY-DEPENDENT AND QUADRATIC SPIN–ORBIT POTENTIALS. Calogero, F.; Simonov, Yu. A. (Inst. of Theoretical and Experimental Physics, Moscow). Phys. Rev. Lett.; 25: 881-4 (28 Sep 1970).

It is proved that if velocity-dependent and/or quadratic spin-orbit potentials are present, they must satisfy very restrictive positivity conditions; otherwise the many-body Hamiltonian has a spectrum that is not bounded below. These conditions are not fulfilled by several currently available nuclear potentials. (auth)

3738 ALPHA-PARTICLE MODEL FOR NUCLEAR MATTER. Bhattacharya, P.; Khanna, K. M. (Indian Inst. of Tech., Kharagpur). Indian J. Pure Appl. Phys.; 7: 224-6(Apr 1969).

By assuming an interacting alpha-particle structure of nuclear matter, the variation of normal-superfluid phase transition temperature (T_c) with the density (ρ_α) of alpha-particle has been studied. It has been found that for T_c > 3 MeV, as the density ρ_α increases, T_c also increases and the transition temperature of an interacting system is less than that of a non-interacting system. The transition from normal to superfluid state is a first order phase transition. (auth)

3739 THEORY OF A SELF-CONSISTENT STATIC FIELD IN THE PRESENCE OF TWO-PARTICLE–TWO-HOLE ADMIXTURES. Padjen, R.; Ripka, G. (Centre d'Etudes Nucleaires de Saclay, Gif-sur-Yvette, France). Nucl. Phys.; A149: 273-301(1970).

The problem of two-particle–two-hole (2p-2h) admixtures is studied and applied to doubly even N = Z 2s-1d shell nuclei. A proper diagonalization corresponding to a resummation of Gold-

stone diagrams is derived. The problem of spurious effects, such as the non-conservation of angular momentum, is studied and a method is devised to check the validity of approximate eliminations of spurious effects. The effect of 2p-2h admixtures on the equilibrium deformation is first studied in a simplified calculation using Nilsson orbits. Then a fully self-consistent theory is formulated of the static average field in the presence of 2p-2h admixtures. A topological analysis of Goldstone diagrams, due to Bloch, yields a simple stationary expression for the ground state energy. The theory is illustrated by a complete numerical application in the 2s-1d shell. (auth)

3740 DEFINITION OF THE SINGLE-NUCLEON POTENTIAL. Baranger, Michel (Oak Ridge National Lab., Tenn.). Nucl. Phys.; A149: 225-40(1970).

The definition is the familiar one which regards a single-particle energy as an average of actual energy levels weighted with spectroscopic factors. It is shown to be related to the short-time behavior of the single-nucleon propagator. This leads to a Feynman expansion which is then compared with the expansion of the exact energies, related to the long-time behavior. The first expansion contains only a small fraction of the diagrams occurring in the second, namely those diagrams in which the two external lines issue from a common two-body vertex. This particular definition of the single-nucleon potential is capable of playing a central role in comparisons between BHF calculations and experiment. Short-range correlations can be eliminated and present no difficulty. Finally, a similar time-development leads to the Feynman expansion of the width of the single-nucleon strength distribution. (auth)

3741 LEAST-SQUARES ADJUSTMENT OF THE COUPLING CONSTANTS IN β-DECAY. Paul, H. (Reaktorzentrum, Seibersdorf, Austria). Nucl. Phys.; A154: 160-76(1970).

An attempt is made to determine the best values of the coupling constant ratios C_A/C_V, C_S/C_V, C_T/C_V, C'_V/C_V, C'_A/C_A, C'_S/C_V, C'_T/C_A from all relevant measurements on allowed decays (75 data), by a least-squares adjustment program. With two exceptions, no assumptions on matrix elements are made, i.e., only neutron decay and pure Fermi or Gamow–Teller transitions are used. Lepton conservation and $C_P = 0$ are assumed. Induced terms and the influence of finite nuclear size and screening are neglected. $C_S/C_V = -0.001 \pm 0.006$, $C_T/C_A = -0.0004 \pm 0.0003$ if $C_S = C'_S$, $C_T = C'_T$, but without assumptions on the remaining ratios. Further, $C'_V/C_V = 0.82^{+0.40}_{-0.13}$, $C'_A/C_A = 1.10 \pm 0.06$, independent of C_S, C_T. If $C'_V = C_V$, $C'_A = C_A$ is assumed, one finds $C_A/C_V = -1.262 \pm 0.008$, independent of C_S, C_T. Inclusion of ft(n) and ft(^{14}O) yields $C_A/C_V = -1.240 \pm 0.007$. For the time reversal parameter, $\varphi = 178.6 \pm 0.9°$ for a pure V–A interaction with $C_i = C'_i$. (auth)

3742 ON THE CALCULATION OF THE REACTION MATRIX IN FINITE NUCLEI. Sauer, P. U. (Massachusetts Inst. of Tech., Cambridge). Contract AT(30-1)-2098. Nucl. Phys.; A150: 467-77(1970).

A method is suggested for calculating the reaction matrix in finite nuclei from any local or non-local potential. It employs a harmonic oscillator Pauli operator and purely kinetic particle states. Particle and hole states are properly orthogonalized. Bare reaction matrix elements to be used in shell-model calculations for A = 18 nuclei are given as sample results. They are based on the soft-core Reid potential. (auth)

3743 EVALUATION OF THE SCREENING CORRECTION TO ALLOWED β-DECAY FOR LIGHT ELEMENTS. Wilkinson, D. H. (Nuclear Physics Lab., Oxford). Nucl. Phys.; A150: 478-80 (1970).

The screening correction to allowed β-decay is given to order α^3 and is compared with the "exact" value for light elements. (auth)

3744 ON THE SENSITIVITY OF β-TRANSITIONS TO THE SHAPE OF THE NUCLEAR CHARGE DISTRIBUTION. Behrens, H. (Univ., Karlsruhe, Ger. Kernforschungszentrum, Karlsruhe, Ger.); Buehring, W. Nucl. Phys.; A150: 481-96(1970).

Fermi and other β-decay functions have been calculated using refined nuclear charge distributions like Gaussian and Fermi-type distributions. The sensitivity of the functions to the shape of the distribution is discussed in detail. The necessary changes in the beta-decay formulae are also explained. While these modifications are simple and straightforward, the usefulness of the β-decay formulae turns out to be questionable because of convergence difficulties introduced by the refined charge distributions. (auth)

3745 OFF-MASS-SHELL FORM FACTORS OF THE NUCLEON. Nyman, Ebbe M. (Univ. of Helsinki). Nucl. Phys.; A154: 97-104(1970).

The electromagnetic vertex of the nucleon is studied in the case where a virtual nucleon becomes real by emitting or absorbing a γ-ray. This process is described by two form factors, in addition to the charge of the particle. Using dispersion relations in the mass of the nucleon, and assuming threshold dominance, a scaling law is obtained for the two form factors. Their numerical values are determined by the same method, in analogy with previous work by Drell and Pagels. (auth)

3746 NEUTRON MATTER: BINDING ENERGY AND MAGNETIC SUSCEPTIBILITY. Oestgaard, E. (Univ. of California, San Diego, La Jolla). Nucl. Phys.; A154: 202-24(1970).

The binding energy and the magnetic susceptibility of neutron matter is calculated by means of Brueckner theory. A modified Brueckner–Gammel method is used to solve the Bethe–Goldstone equation, calculate the reaction matrix or G-matrix, and obtain the interaction energy contribution from two-body correlations. For simplicity, the approximation of a reference energy spectrum with an effective mass and quadratic momentum dependence is used for the input energy spectrum, which in principle should be fitted to self-consistent single-particle energies. The intermediate-state potential energies are, however, chosen to be equal to zero. Hence, the three-body and possibly higher-order energy contributions should be estimated by separate calculations. The Bethe–Goldstone equation is solved numerically by iteration to give the perturbed two-body wave functions. Afterwards, the G-matrix elements are calculated by numerical integration. The binding energy is calculated as a function of the Fermi momentum and the pure neutron-matter system seems to be unbound at any density, even at very low densities. In addition to the binding energy, also the magnetic susceptibility is estimated. To this end, the spin symmetry energy is calculated in terms of the derivatives of the G-matrix with respect to the Fermi momentum. A ferromagnetic transition is found to occur at a density much higher than the typical nuclear-matter density. Our method is, however, probably too simple to be reliable at such a high density. (auth)

3747 STUDY OF A GENERALIZED OPTICAL POTENTIAL. Cirelli, R. (Univ., Milan. Istituto Nazionale di Fisica Nucleare, Milan); Dalla Fina, G. F.; Pizzigoni, M. Nuovo Cim.; 69B: 83-94(11 Sep 1970).

Some questions about the scattering amplitude for a complex nonlocal potential superposition of Yukawa potentials with a complex weight function $\sigma(t; q'^2, q^2)$ are studied. Under reasonable conditions on $\sigma(t; q'^2, q^2)$ it is shown that the kernel of the Lippmann–Schwinger equation for T(z) is of the Hilbert–Schmidt class and that the von Neumann series converges for $|z|$ large enough. The analyticity properties and asymptotic behaviors of the Born terms $T^{(\omega)}(q', q)$ are studied. The properties thus established for $T^{(\omega)}(q', q)$ are used for the study of the analyticity properties of the total amplitude T(s, t) ending with a dispersion relation in s. (auth)

3748 MUON CAPTURE RATE IN ^{6}Li AND THE PCAC HYPOTHESIS. Delorme, J.; Ericson, M. (Institut de Physique Nucleaire de Lyon, Villeurbanne, France). Phys. Lett.; 32B: 443-4(17 Aug 1970).

The recent claim by Kim and Mintz that there is evidence for large renormalization effects in the pseudo-scalar form factor from the transition ^{6}Li → ^{6}He in muon capture is critically discussed. (auth)

3749 ON THE BREAK-UP OF ^{6}Li IN THE COULOMB-FIELD. Wittern, H. W. (Univ., Tuebingen, Ger.). Phys. Lett.; 32B: 441-2(17 Aug 1970).

Inclusion of the nuclear forces may account for the anomalies occurring in the angular distributions of the sub-Coulomb disintegration process. (auth)

3750 MODIFIED IMPULSE APPROXIMATION CALCULATION OF THE N–N QUASI-FREE SCATTERING AND THE CHEW–LOW EXTRAPOLATION IN THE D(p,NN)N REACTION. Paic, G. (Univ. of California, Los Angeles); Young, J. C.; Margaziotis, D. J. Phys. Lett.; 32B: 437-40(17 Aug 1970).

The results of a calculation from a simple impulse approximation modified by the introduction of a cut-off radius in the deuteron ground-state wave function are compared with recent measurements of the D(p, 2p)n and D(p, pn)p reactions. (auth)

3751 BRANCHING RATIOS FOR E1 TRANSITIONS DE-EXCITING THE OCTUPOLE STATES IN EVEN–EVEN DEFORMED NUCLEI. Kocbach, L.; Vogel, P. (Univ. of Bergen). Phys. Lett.; 32B: 434-6(17 Aug 1970).

The relative B(E1) values are calculated using the Coriolis-coupled wave functions for the octupole states. The few entering ratios of intrinsic E1 matrix elements are determined by a least-squares fit. The agreement between the calculated results and the experimental data for transitions to the ground state rotational band and to the γ-vibrational band is satisfactory. (auth)

3752 NUCLEAR JOSEPHSON EFFECT IN HEAVY ION SCATTERING. Dietrich, K. (Niels Bohr Inst., Copenhagen). Phys. Lett.; 32B: 428-30(17 Aug 1970).

The transfer of a pair of nucleons in sub-Coulomb scattering of two heavy ions is treated in a semiclassical theory. If both reaction partners are superconducting, a large enhancement factor is found. (auth)

3753 EFFECT OF SHORT-RANGE CORRELATIONS AND CHARGE-DEPENDENT NUCLEAR FORCES ON THE ENERGY OF THE ANALOG STATE. Di Toro, M. (Massachusetts Inst. of Tech., Cambridge. Univ., Catania, Italy); Nunberg, P.; Riihimaeki, E. J. Contract AT(30-1)-2098. Phys. Rev., C; 2: 13-23(Jul 1970).

The effect of short-range correlations on the displacement energy (energy difference between the analog and the parent state) is computed to first order in perturbation theory. The plane-wave approximation is used for intermediate states. Both the contributions of the Coulomb interaction and of a charge-dependent component of the nuclear two-body interaction are taken into account. (auth)

3754 ANALYSIS OF NUCLEAR SEPARATION ENERGIES. Banerjee, D. (University Coll. of Science, Calcutta). Phys. Rev., C; 2: 110-15(Jul 1970).

It is observed that the proton separation energies S_p for even–even nuclei do not vary linearly with proton number in a strict sense. S_p values for even–even isotones with the same j, the angular momentum of the last proton orbit, lie on a straight line. The systematics of nucleon separation energies are explained on the basis of the shell model for nuclei. It is assumed that the central potential well in which nucleons are supposed to move remains constant for a group of neighboring isotones with the last proton orbit characterized by the same j. This is also taken to be valid for isotopes with the last neutron orbit characterized by the same j. Furthermore, the interaction between the extracore neutrons, extracore protons, and their mutual interactions are simulated by average effective two-body interaction matrix elements. (auth)

3755 REAL PART OF THE ALPHA–NUCLEUS POTENTIAL OBTAINED BY THE DOUBLE FOLDING PROCEDURE. Budzanowski, A.; Dudek, A.; Grotowski, K.; Strzalkowski, A. (Jagellonian Univ., Krakow. Inst. of Nuclear Physics, Krakow). Phys. Lett.; 32B: 431-3(17 Aug 1970).

The real part of the optical potential for alpha particle–nucleus interaction was calculated by the double-folding procedure from the nucleon–nucleon potential and matter distributions in both interacting nuclei. Angular distributions calculated with Yukawa, Gaussian, and effective nucleon–nucleon interactions are compared with experimental data for $^{58}Co(\alpha,\alpha)$ scattering. (auth)

3756 LOW-ENERGY THEOREM FOR NUCLEON–NUCLEON BREMSSTRAHLUNG. Liou, M. K. (Univ. of Manitoba, Winnipeg). Phys. Rev., C; 2: 131-8(Jul 1970).

The low-energy theorem is derived for nucleon–nucleon bremsstrahlung. It is assumed that the two nucleons interact through a potential which can be any model, nonlocal as well as local. For those potentials which depend explicitly upon momentum and/or angular momentum operators, the gauge terms arising from these operators are included in the derivation. These gauge terms are always important in the study of the off-energy-shell effects of the two-nucleon interaction, and for the npγ process they are essential in the derivation of the low-energy theorem. It is found that the gauge terms are canceled precisely by parts of the terms which represent the photons emitted by the internal nucleon lines. (auth)

3757 ACCURACY OF THE IONPIN–ERICSON THEORY OF NUCLEAR DIFFRACTION SCATTERING. Abul-Magd, A. Y. (International Centre for Theoretical Physics, Trieste, Italy); Simbel, M. H. Nucl. Phys.; A148: 449-56(1970).

The prediction of the approximate formula for the differential cross section of the elastic scattering of strongly absorbed particles obtained in the Inopin–Ericson theory of diffraction scattering is compared with the results of calculations using the corresponding exact formula. It is found that the approximate formula is in good agreement with the exact one for scattering angles larger than the Coulomb deflection angle. (auth)

3758 T = 1 PAIRING HAMILTONIAN IN A TWO-LEVEL MODEL. Dussel, G. G.; Maqueda, E.; Perazzo, R. P. J. (CNEA, Buenos Aires). Nucl. Phys.; A153: 469-80(1970).

The T = 1 pairing Hamiltonian is exactly solved in a two-level model and both energy eigenvalues and transition matrix elements are obtained. The system undergoes a phase transition for a value G_c of the coupling constant. In both limits, $G \ll G_c$ and $G \gg G_c$ vibrational and rotational patterns are observed. The exact results are compared to the RPA and to a Nilsson-like treatment. (auth)

3759 HIGHER-ORDER BUBBLE CORRECTIONS TO TWO-BODY MATRIX ELEMENTS IN THE 1s 0d SHELL. Ellis, P. J.; Siegel, S. (Rutgers–The State Univ., New Brunswick, N. J.). Nucl. Phys.; A152: 547-60(1970).

The renormalization of two-body matrix elements in the 1s 0d shell has been considered by explicitly summing to second and all orders the perturbation theory diagrams of the Tamm–Dancoff and random phase approximations. The equivalence to the phonon coupling approach is demonstrated. Large enhancements are found compared to the first order result, and it is shown that difficulties arise due to the instability of the $J'' = T'' = 0$ phonon. The spectra and γ-transitions in mass 18 are discussed. (auth)

3760 DENSITY OF PARTICLE-HOLE STATES IN THE EQUIDISTANT-SPACING MODEL. Boehning, M. (Technische Hochschule, Munich). Nucl. Phys.; A152: 529-46(1970).

For the most simple model of the nucleus, a system of independent fermions with equally spaced single-particle levels, the density of particle-hole states is calculated. The exact result, obtained by combinatorial methods, is compared with a level-density formula which is derived by means of the statistical approximation in the conventional way. Even simplifying approximations of this formula are in good agreement with the exact result. (auth)

3761 IMPACT-PARAMETER AMPLITUDES FOR LARGE-ANGLE POTENTIAL SCATTERING. II. Hahn, Yukap (Univ. of Connecticut, Storrs). Phys. Rev., C; 2: 775-81(Sep 1970).

In continuation of previous study of the impact-parameter representations of potential scattering amplitudes at large angles, various approximate forms of the impact phases along the trajectories parallel to the initial, final, and average momenta are numerically evaluated and compared. The necessity of phase averaging in the symmetric forms of the amplitudes is pointed out. None of the presently available approximations seems to be sufficiently accurate to reliably replace the phase-shift analysis at large angles. (auth)

3762 RELATION BETWEEN THE 2I + 1 RULE AND CHANNEL CORRELATION. Hsu, Chu Chung (Univ. of Maryland, College Park). Phys. Rev., C; 2: 767-9(Aug 1970).

The fluctuation cross section is derived as a function of the reduced-width correlation coefficient and also as a function of the channel cross correlation, with the resulting indication that the fluctuation cross section depends strongly on the channel cross correlation. The total average cross section is shown to be proportional to the quantity 2I + 1 only when the total level width is sufficiently large. Finally, the author suggests that only for experiments in the region of very large Γ_μ should the total cross sections be compared with the 2I + 1 rule. In order to get the above condition, low energy with a high Q value is highly desirable. (auth)

3763 ROLE OF MESONS IN NUCLEAR SATURATION. Haftel, Michael I. (Naval Research Lab., Washington, D. C.); Tabakin, Frank; Richards, Keith C. Nucl. Phys.; A154: 1-11 (1970).

The binding energy of nuclear matter is calculated with the Bryan–Scott one-boson exchange potential. Saturation occurs at higher density and binding than is found for the Yukawa-core Reid potential. The increase in binding and density arises because the Bryan–Scott interaction has somewhat weaker tensor and core-repulsion terms. The role of each meson in producing saturation is analyzed. It is found that the ω-meson produces the dominant repulsion and the σ_0 meson produces the dominant attraction. The π-meson's strong tensor force plays an important role in producing an energy minimum. All of the mesons make contributions to nuclear saturation, but it is found that the η-meson plays a relatively minor role. (auth)

3764 NEW METHOD FOR DISTORTED-WAVE ANALYSIS OF STRIPPING TO UNBOUND STATES. Vincent, C. M.; Fortune, H. T. (Argonne National Lab., Ill.). Phys. Rev., C; 2: 782-92 (Sep 1970).

The distorted-wave Born approximation (DWBA) cross section is discussed for a reaction of the form A(d,pn)A in which n is not observed. The slowly convergent oscillating radial integrals are evaluated by contour integration in the complex radius plane. This avoids the computation of wave functions out to the large distances that the Huby–Mines technique requires. The present technique is also useful for stripping to very weakly bound states. We find that the DWBA angular distribution for stripping to a resonant n state is closely reproduced by using a form factor for the resonant energy of n. The width of the resonance, rather than the spectroscopic factor, is found to be measured by the absolute magnitude of the cross section. The results of calculations with the present method are compared with the results of the Huby–Mines method

XUM

for the $^{16}O(d,p)^{17}O$ reaction leading to the resonant 5.08-MeV state of ^{17}O. (auth)

3765 SPIN DEPENDENCE OF DENSITY OF EXCITED NUCLEAR STATES. Ignatyuk, A. V.; Stavinskii, V. S. Yadern. Fiz.; 11: 1213-20(Jun 1970). (In Russian).

The effect of the discrete structure of the nucleon one-particle spectrum on the behavior of the spin dependence parameter σ^2, moment of inertia $F_{||}$, and r.m.s. of one-particle momentum projection $\overline{m^2}$ is studied. The nuclear excitation energy dependence effect on the variation of these parameters is considered. (auth)

3766 EFFECT OF TENSOR FORCES IN RESIDUAL PAIR NUCLEON INTERACTION. Dokutovich, V. A.; Rudak, E. A. (Inst. of Physics, Minsk). Yadern. Fiz.; 11: 1221-4(Jun 1970). (In Russian).

The dependence of matrix elements of the tensor forces on the resulting spin of a pair of interacting nucleons is investigated. A possible account of a contribution from the tensor forces by means of a variation of the central interaction parameters is considered. (auth)

3767 DISTRIBUTION OF RADIATION WIDTHS FROM (p,γ) REACTIONS. Nemashkalo, B. A.; Kresnin, A. A.; Storizhko, V. E. (Physical-Technical Inst., Kharkov). Yadern. Fiz.; 11: 1231-6 (Jun 1970). (In Russian).

Distributions of the total radiation widths from (p,γ) reactions for light and intermediate nuclei are analyzed. It is shown that the distribution of the total radiation widths obeys the Thomas–Porter distribution with the number of the degree of freedom ≈ 2. Near the magic numbers there is an increase of dispersion, while for the odd–odd nuclei the dispersion of distributions decreases that may be due to different densities of low-lying levels of these nuclei. (auth)

3768 THEORY OF THE DIPOLE SUM RULE FOR THREE-PARTICLE NUCLEI WITH REALISTIC NUCLEAR FORCES. Kozlov, M. I.; Fetisov, V. N. (Lebedev Inst. of Physics, Moscow). Yadern. Fiz.; 11: 1225-30(Jun 1970). (In Russian).

The applicability of the theory of three-nucleon systems with realistic two-particle nuclear forces to the photoeffect problem is studied. Close correspondence of theoretical and experimental integral cross sections of photosplitting of nuclei with $A = 3$ for the Yale potential and for the Hamada–Johnston and Gammel–Brueckner potentials is obtained. The integral cross section σ_0 and its isospin components $\sigma_0(T)$ weakly depend on the concrete forms of nuclear forces. The integral contribution of transitions to the final states with the isospin $T = 1/2$ in the three-particle channel of the photo-splitting is discussed. (auth)

3769 OPTICAL POTENTIALS AND ELASTIC SCATTERING OF t AND ^{3}He. Kadmenskii, S. G.; Kalechits, V. E.; Furman, V. I. (Voronezh State Univ., USSR). Yadern. Fiz.; 11: 1237-41(Jun 1970). (In Russian).

Theoretical optical potentials for t and ^{3}He are calculated based on one-nucleon optical potentials. Parameters of these potentials differ from the phenomenological values in the depth of the real part, in the radius and in variable diffusion. The elastic scattering of t for a number of nuclei from ^{24}Mg up to ^{118}Sn at 12 to 20 MeV and elastic scattering of ^{3}He for nuclei from ^{12}O up to ^{207}Pb at 20 to 65 MeV are studied on the basis of these potentials. The agreement of the theory with the experiment is obtained both in position of the maxima and in their absolute values for angles up to 90°, especially for ^{3}He. (auth)

3770 CALCULATION OF COULOMB ENERGY DIFFERENCES. Damgaard, Joergen (Univ. of Copenhagen); Scott, C. K.; Osnes, E. Nucl. Phys.; A154: 12-22(1970).

The correction to Coulomb displacement energies from monopole polarization is calculated with a model and discussed. Corrections from polarizations of higher multipolarity are found to be small. (auth)

3771 SCATTERING BY MODIFIED GAUSSIAN POTENTIAL. Krori, K. D.; Borgohain, P. (Cotton Coll., Gauhati, India). Indian J. Pure Appl. Phys.; 6: 674-7(1968).

The Gaussian potential has been modified taking into account the possible physical conditions obtaining inside and outside a spherical nucleus and certain aspects of scattering have been discussed in the light of this modified potential. Small nuclei have also been treated as a special case. (auth)

3772 NUCLEAR MATTER CALCULATIONS WITH HARD-CORE AND LONG-RANGE POTENTIALS. Khanna, K. M. (Dibrugarh Univ., India); Das, G. B. L. Indian J. Pure Appl. Phys.; 7: 474-7(Jul 1969).

Properties of an extended system of alpha-particles interacting through a hard sphere and long-range interaction and having densities less than that corresponding to nuclear saturation have been studied. The calculated transition temperature, in the case of hard-core potential, varies from 1.006 to 2.683 MeV as the density of the alpha-particles is varied, and in the case of long-range potential it varies from 0.258 to 2.095 MeV as the density and the strength of the potential change. It is concluded that an assembly of interacting alpha-particles, interacting via a purely repulsive interaction, is a stable assembly. (auth)

3773 CRITICAL TEMPERATURE OF TRANSITION OF NUCLEAR MATTER. Khanna, K. M. (Dibrugarh Univ., India). Indian J. Pure Appl. Phys.; 6: 1-6(Mar 1968).

The magnitude of the critical temperature of transition of a nuclear system consisting of an equal even number of protons and neutrons has been calculated by assuming that nuclear matter is composed of an assembly of interacting alpha-particles. The critical temperature is found to be a function of the density of nuclear matter and of the effective mass of alpha-particles. By assuming that the ratio m^*/m for alpha-particles is the same as that for the nucleons, it is found that the critical temperature for transition to the superfluid state for an interacting nuclear matter is more than that for a non-interacting nuclear matter. The result is opposite to the one obtained for liquid He-4 for which the transition temperature is less than that for an ideal gas of bosons. (auth)

REACTOR TECHNOLOGY

Commercial Power Reactors

Refer also to abstracts 2393 and 2619.

3774 (DP-Report-439) RECORD OF PROGRAMME AND DISCUSSIONS AT SYMPOSIUM OF PAPERS FROM DRAGON CONTRACTORS HELD AT A.E.R.E., HARWELL, 14th–16th MARCH 1966. Project DRAGON. Clough, D. J.; Gibson, J. A.; Logsdail, D. H.; Pattison, J.; Rose, K. S. B.; Wiblin, E. R. (Atomic Energy Research Establishment, Harwell (England)). Jun 1966. 40p. (AERE-R-5219). Dep. NTIS.

Information on the development of the Dragon Reactor is presented under the following topics: graphite physics; plutonium fuel studies; fuel particles and coatings; fission product technology; and coolant chemistry. (D.C.C.)

3775 (DP-Report-539) ON THE QUALIFICATION OF FISSION PRODUCT RELEASE. Project DRAGON. Preinreich, G. (Atomic Energy Establishment, Winfrith (England)). Apr 1967. 22p. Dep. NTIS.

A comparison of experimental methods for determining the fission product release from ThC_2–UC_2 coated particle fuel is presented. The methods described include: annealing method, closed capsule irradiation experiments, and fission product determination on fuel rods. Advantages and disadvantages of each method are analyzed. Concepts of release qualification are compared. (D.C.C.)

3776 STEAM PLANT FOR THE 1970S. Proceedings of the Institution of Mechanical Engineers, London, 23rd–25th April 1969. Proc. Inst. Mech. Eng. (London); 183: 1-162(1968–69). (CONF-690445).

The design, manufacture and erection, commissioning and servicing of steam power facilities are examined and discussed. The direction of development in the 1970s is explored by twelve papers presented to the Convention. They cover factors such as availability and reliability, increased unit size, advancing steam conditions, standardization and cost effectiveness. A separate abstract was prepared for two of the papers. (UK)

For abstracts of individual papers see: 3899 and 3900.

3777 EXPERIENCE WITH SIMPLE METHODS FOR EVALUATING ZERO-POWER EXPERIMENTS AT THE RHEINSBERG NUCLEAR POWER STATION REACTOR. Mueller, A. (VEB Kombinat Kraftwerksanlagenbau, Berlin). Kernenergie; 13: 169-72(Jun 1970). (In German).

On the occasion of commissioning the Rheinsberg nuclear power station, comparatively simple methods were derived for evaluating zero-power experiments. Direct evaluation of the neutron flux time dependence proved to be advantageous for determining the temperature coefficient of reactivity. Rod drop experiments also give appropriate results for power reactors with high-efficiency absorbers if in the evaluation the spatial variation of the neutron flux is taken into account. The use of a simple flux synthesis model for the description of a partially inserted absorber element efficiency curve in evaluating the different efficiencies measured may lead to larger errors. An improvement of this evaluation method by taking three-dimensional effects into account is regarded to be necessary. The importance of the calculational determination of power reactor operation regime increases because of the restricted possibilities and complexity of power reactor experiments as well as conditional validity of simple evaluation methods. (5 references) (auth)

3778 NUCLEAR POWER PIPING, USAB B31.7–1969. USA Standard Code for Pressure Piping. New York; American Society of Mechanical Engineers (1969). 226p. $10.00.

The piping code provides requirements for the design, materials, fabrication, assembly, erection, installation, and examination of three classes of nuclear piping systems for nuclear power plant service. The three classes of piping systems denote three levels of quality which are required for varying service limits. (D.C.C.)

3779 STATE OF CONSTRUCTIONS ON THE MIHAMA ATOMIC POWER STATION. Okano, Shigeo (Kansai Electric Power Co. Inc., Osaka). Karyoku Hatsuden; 20: 1251-6(Dec 1969). (In Japanese).

The Mihama Power Reactor, under construction on the coast of Japan Sea in Fukui Prefecture is described with emphasis on the difference from conventional thermal power stations. At the power station are two PWRs: Unit 1 with 340 MW(e) and Unit 2 with 500 MW(e). Various facilities are located on the site, which is within a national park. Unit 1 will go into operation in October 1970, and Unit 2, in June 1972. The course of construction to the present is described. Aspects are reviewed concerning the power station construction, including geological survey, anti-earthquake design of the shields, and quality of construction-process. (Japan)

3780 STATE OF CONSTRUCTIONS ON THE FUKUSHIMA ATOMIC POWER STATION. Nomura, Akio (Tokyo Electric Power Co. Inc.). Karyoku Hatsuden; 20: 1248-50(Dec 1969). (In Japanese).

Construction of the Fukishima Power Reactors, Units 1, 2, and 3, is proceeding. Unit 1, a 460 MW(e) BWR, is 80% complete. The foundations are now complete for Unit 2, a 784 MW(e) BWR. Plans for Unit 3, a 784 MW(e) BWR plant, are being considered for approval by the Government. (Japan)

3781 SWISS NUCLEAR INDUSTRY: TRADITIONAL QUALITY AND WORLD-WIDE DISTRIBUTION. Feuz, P. (Schweizerische Vereinigung fuer Atomenergia, Bern). Neue Tech., B; 11: 219-22 (1969). (In German).

Contributions by Switzerland to the nuclear industry are discussed. Because of its small size and limited internal market, Switzerland abandoned the development of its own nuclear reactors in 1967. In spite of this fact, the Swiss industry is able to manufacture almost any component of nuclear power stations of highest quality, especially gas turbines and electrical equipment. Nuclear engineering capability is advanced enough to design entire power stations and to monitor the construction. A commercial breakthrough in high-temperature reactors would open a promising future for Swiss turbines and generators. (H.B.G.)

Operation and Economics

3782 (DOCKET-1151-3) ELK RIVER REACTOR. Monthly Operating Report No. 82. (Rural Cooperative Power Association, Elk River, Minn.). Aug. 1969. 17p. (COO-651-78). Dep. CFSTI.

3783 (DOCKET-50029-140) YANKEE NUCLEAR POWER STATION. Operation Report No. 118, October 1970. (Yankee Atomic Electric Co., Westboro, Mass.). 20 Nov 1970. 8p. Dep. NTIS.

3784 (DOCKET-50171-58) PEACH BOTTOM ATOMIC POWER STATION, UNIT 1. Monthly Operations Report No. 55, September 1970. (Philadelphia Electric Co., Pa.). 19 Nov 1970. 12p. Dep. NTIS.

3785 (DOCKET-50206-94) SAN ONOFRE NUCLEAR GENERATING STATION, UNIT 1. Operation Report, October 1970. (Southern California Edison Co., Los Angeles). Nov 1970. Contract AT(30-1)-3270. 7p. (NYO-3270-43). Dep. NTIS.

3786 (DOCKET-50206-97) SAN ONOFRE NUCLEAR GENERATING STATION, UNIT 1. Malfunction of Safety Injection System Valves. (Southern California Edison Co., Los Angeles). 16 Nov 1970. 6p. Dep. NTIS.

3787 (DOCKET-50213-82) CONNECTICUT YANKEE ATOMIC POWER PLANT. Automatic Plant Trip and Reactor Coolant System Cooldown to 502°F. (Connecticut Yankee Atomic Power Co., Westboro, Mass.). 4 Nov 1970. 3p. Dep. NTIS.

3788 (DOCKET-50213-84) CONNECTICUT YANKEE ATOMIC POWER PLANT. Operation Report No. 70-10, October 1970. (Connecticut Yankee Atomic Power Co., Haddam). 24 Nov 1970. Contract AT(30-1)-3250. 14p. (NYO-3250-53). Dep. NTIS.

3789 (DOCKET-50245-42) MILLSTONE NUCLEAR POWER STATION, UNIT 1. Failure of Gas Turbine Generator on Test. (Millstone Point Co., Wethersfield, Conn.). 17 Nov 1970. 3p. Dep. NTIS.

3790 (DP-Report-438) DRAGON OPERATIONS THIRD QUARTERLY PROGRESS REPORT, DECEMBER 1965–FEBRUARY 1966. Project DRAGON. Chapman, B. G. (Atomic Energy Establishment, Winfrith (England)). Jun 1966. 17p. Dep. NTIS.

Operations and maintenance requirements during December 1965 to February 1966 are described. Unscheduled shutdowns and unusual occurrences are reviewed. (D.C.C.)

XUM

3791 (DP-Report-474) THE FIRST YEAR AT FULL POWER. Project DRAGON. Chapman, B. G.; Danby, F. D. (Atomic Energy Establishment, Winfrith (England)). Aug 1967. 15p. Dep. NTIS.

A review of operations and maintenance requirements during the first year at full power capability is presented. (D.C.C.)

3792 (DP-Report-483) DRAGON OPERATIONS GROUP FOURTH QUARTERLY PROGRESS REPORT, MARCH-MAY 1966. Project DRAGON. Chapman, B. G. (Atomic Energy Establishment, Winfrith (England)). Oct 1966. 14p. Dep. NTIS.

Operations and maintenance requirements during March to May 1966 are described. Unscheduled shutdowns and unusual occurrences are reviewed. (D.C.C.)

3793 (DP-Report-488) DRAGON OPERATIONS GROUP FIFTH QUARTERLY PROGRESS REPORT, JUNE-AUGUST 1966. Project DRAGON. Chapman, B. G. (Atomic Energy Establishment, Winfrith (England)). Nov 1966. 17p. Dep. NTIS.

Operations and maintenance requirements during June to August 1966 are described. Unscheduled shutdowns and unusual occurrences are reviewed. (D.C.C.)

3794 (DP-Report-531) DRAGON OPERATIONS GROUP SIXTH QUARTERLY PROGRESS REPORT, SEPTEMBER-NOVEMBER 1966. Project DRAGON. Chapman, B. G. (Atomic Energy Establishment, Winfrith (England)). Mar 1967. 22p. Dep. NTIS.

Operations and maintenance requirements during September to November 1966 are described. (D.C.C.)

3795 (DP-Report-561) OPERATIONAL DATA FOR CHARGE I. Project DRAGON. Hunt, C.; Joyce, M. D. (Atomic Energy Establishment, Winfrith (England)). Aug 1967. 93p. Dep. NTIS.

The data handling system devised for the Dragon Reactor is described. The access procedures to the magnetic tape storage are outlined so that assessment teams can produce computer subroutines to obtain, analyze, and present data to suit specific needs. Operations data for Charge 1 are listed. 6 references. (D.C.C.)

3796 (DP-Report-579) EVALUATION OF THE DATA FROM THE FIRST DRAGON CHARGE. Project DRAGON. Ashworth, F. P. O.; Preinreich, G. F. F. J.; Reed, D. L. (Atomic Energy Establishment, Winfrith (England)). Nov 1967. 79p. Dep. NTIS.

The data derived from the Dragon Reactor during the 20 MW operation concerning fission product release and deposition in the circuit, the fuel burnup, and the activity of the coolant are presented. 12 references. (auth)

3797 (ORNL-4572-, pp 236-41) REACTOR EVALUATION STUDIES. (Oak Ridge National Lab., Tenn.).

From Chemical Technology Division annual progress report for period ending May 31, 1970.

The development of computational models for use in the planning of optimal electrical power systems in the U. S. is described. The completion of the Oak Ridge Systems Analysis Code, the development of a dynamic programming algorithm for the dispatching of power generating plants, and the completion of a study of the feasibility of applying advanced dynamic programming procedures to the expansion planning of nuclear power plants and fuel reprocessing plants are reviewed. (D.C.C.)

3798 (ORNL-TM-3142) CONSIDERATION OF NUCLEAR POWER EXPANSION FOR PUERTO RICO, INCLUDING SURPLUS CAPACITY PENALTIES. Holmes, J. M. (Oak Ridge National Lab., Tenn.). Dec 1970. Contract W-7405-eng-26. 23p. Dep. NTIS.

An analysis is made to estimate the optimum time interval for installation of nuclear power plants in Puerto Rico. Data on projected demands for the Puerto Rican system between 1970 and 2000 are used as the basis. The model includes effects such as the net penalties for excess capacity, cost-size scaling factors for capital and operating costs, maximum reactor capacity (size) constraints, and salvage values. The optimum capacity expansion interval for an interest rate of 6% and no excess capacity penalty is about 2.5 years. When the price of the excess power sold as nonfirm power is reduced by 0.4 mill/kwhr, the optimum interval does not change. If the penalty for excess capacity is greater than 20% of the capital cost for one year's expansion in capacity, the expansion interval should not be more than one year. The effects of negative penalty costs (net benefits) are also evaluated. If the operating cost savings for nuclear fuel compared with fossil fuel amounts to 0.9 mill/kwhr, the optimum capacity expansion interval will be about 3.9 years. At the current system growth rate this corresponds to a reactor size of about 800 MW(e). (7 references) (auth)

3799 (WAPD-MRP-132) PRESSURIZED WATER REACTOR (PWR) PROJECT. Technical Progress Report, January 24-April 25, 1970. (Bettis Atomic Power Lab., Pittsburgh, Pa.). Contract AT(11-1)-Gen-14. 22p. Dep. NTIS.

Operations and maintenance requirements for the Shippingport Pressurized-Water Reactor during January 24, 1970 to April 25, 1970 are described. Physics measurements for Core 2 are listed. (D.C.C.)

3800 NUCLEAR ENERGY IN THE GERMAN ELECTRICAL INDUSTRY IN 1969. Atomwirt., Atomtech.; 15: 535-6(Nov 1970). (In German).

In comparison to 1968, the total production of electricity within the German Federal Republic increased by 10.2% in 1969. Of the total electricity generation, 3.3% was generated by nuclear power stations, which represents approximately 180% increase over 1968. Sources of energy are listed as to fuel, utilization, and contribution to the overall energy amount. (H.B.G.)

3801 TEN YEARS OF THE KAHL NUCLEAR POWER PLANT. Facius, H. (Kraftwerk Union AG., Frankfurt am Main). Atomwirt., Atomtech.; 15: 518-21(Nov 1970). (In German).

The Kahl nuclear power plant, a boiling water reactor, became critical in November 1960 as the first power reactor in West Germany. Because of advancement in reactor technology, the installation is now outdated; however, it played a decisive role in the introduction of nuclear energy into the Federal Republic and still possesses a certain degree of usefulness. Most important are experiences about its excellent operational performance, its safety, its low emission of radioactivity into the environment, and its assistance in developing legal aspects of atomic energy for West Germany. (tr-auth)

3802 CANADIANS FORSEE ½ MILL NUCLEAR FUEL COST. McConnell, L. G. Elec. World; 170: No. 22, 29-31 (25 Nov 1968).

Total fuel cost for Ontario Hydro's 508 MW(e) heavy water moderated, natural U fueled Pickering reactors, based on actual prices and expected burn-up of 223 MWh/kg is estimated at 0.63 mill/kWh. The plant should cost $226.40 per net kW and attain a total energy cost of 3.52 mill per net kWh at 80% capacity factor and 7.66% capital charge. With future reductions in fuel cost and spent fuel use, net fuel cost during station life is expected to average 0.5 mill/kWh for a total energy cost <3.39 mills. (Fuel Abstr.)

3803 ANALYSIS OF NUCLEAR FUEL MANAGEMENT TECHNIQUES FOR UTILITIES. Fulford, Phillip James. Lafayette, Ind.; Purdue Univ. (1968). 242p. University Microfilms Order No. 70-10,663.

Thesis.

Nuclear fuel management techniques are analyzed from the utility or reactor owner point of view. The information and decision flows required for sound management are presented as a formalized system. The major areas of the fuel cycle open to managerial discretion are shown and their relative importance estimated. Particular methods of financial calculations are reviewed and a new technique for preparing results in a manner suitable for utility use is presented. This is presented as the code CINCAS-II. Nucleonics calculational techniques are studied by examining particular potentially useful computer programs. In some cases it is found that simple modifications are all that are needed. In other cases more extensive changes or additions are needed. The very useful nodal power density code FLARE was completely rewritten to allow full core representations. This is presented as the code FLARE-P. Recommendations for further improvements in nuclear fuel management techniques are made. (Diss. Abstr.)

3804 OPTIMIZATION OF NUCLEAR POWER SYSTEM. THE METHOD AND CONCEPTS. Takei, Mitsuo (Japan Energy Economic Research Inst., Tokyo). Genshiryoku Kogyo; 16: No. 6, 41-5(Jun 1970). (In Japanese).

The question of optimization of a nuclear power generation system concerns the economic aspect for the long-range future, the mode of analysis of the power generation system, and the associated factors. In the case of Japan, immediate problems on the analysis of a future system are the determination of Pu price in the dual-economy stage, and the fuel cycle in an FBR and its economy. (Japan)

Safety and Siting

3805 (DOCKET-1155-84) LA CROSSE BOILING WATER REACTOR. Proposed Change to Technical Specifications. Installation of Automatic Gain Control System. (Dairyland Power Cooperative, La Crosse, Wis.). 25 Nov 1970. 4p. Dep. NTIS.

3806 (DOCKET-50003-59) INDIAN POINT STATION, UNIT NO. 1. Survey of Environmental Radioactivity, August 1, 1969–March 31, 1970. (Consolidated Edison Co. of New York, Inc., New York). 10 Sep 1970. 24p. Dep. NTIS.

3807 (DOCKET-50010-70) DRESDEN NUCLEAR POWER STATION, UNIT 1. Comments on Uniform Monitoring, Recording, and Reporting Guide. (Commonwealth Edison Co., Chicago, Ill.). 23 Nov 1970. 6p. Dep. NTIS.

3808 (DOCKET-50133-42) HUMBOLDT BAY POWER PLANT, UNIT NO. 3. Facility License No. DPR-7, Amendment 1. (Division of Reactor Licensing (AEC), Washington, D. C.). 23 Nov 1970. 4p. Dep. NTIS.

Authorized limits for the possession and use of radioisotopes at the reactor are presented. (D.C.C.)

3809 (DOCKET-50206-95) SAN ONOFRE NUCLEAR GENERATING STATION, UNIT 1. Preliminary Safety Analysis Report, Amendment 20. (Southern California Edison Co., Los Angeles). 13 Nov 1970. 4p. Dep. NTIS.

Additional data requested by the Division of Reactor Licensing are presented on the reactor design and operations. Included are data on excess reactivity, expected fuel burnup, moderator temperature, fissile Pu inventory, and anticipated Pu bone dose from the most serious accident analyzed. (D.C.C.)

3810 (DOCKET-50206-96) SAN ONOFRE NUCLEAR GENERATING STATION, UNIT 1. Provisional Operating License No. DPR-13, Amendment 3. (Division of Reactor Licensing (AEC), Washington, D. C.). 13 Nov 1970. 8p. Dep. NTIS.

Authorization for the use of 4 mixed-oxide fuel assemblies in the reactor and the "checkerboard" loading configuration of the core for Cycle 2 is presented. Additional information concerning burnup limits is included. (D.C.C.)

3811 (DOCKET-50213-83) CONNECTICUT YANKEE ATOMIC POWER PLANT. License No. DPR-14. Technical Specifications Proposed Change No. 16, Rev. No. 1. (Connecticut Yankee Atomic Power Co., Hartford). 10 Nov 1970. 32p. Dep. NTIS.

Revised and additional information concerning administrative controls of reactor operations is presented. Personnel qualifications and responsibilities are listed. (D.C.C.)

3812 (DOCKET-50213-85) CONNECTICUT YANKEE NUCLEAR POWER PLANT. 1970 Inservice Inspection. (Southwest Research Inst., San Antonio, Tex.). 17 Sep 1970. 66p. Dep. NTIS.

For Connecticut Yankee Atomic Power Co., Westboro, Mass.

3813 (DOCKET-50219-115) OYSTER CREEK NUCLEAR POWER PLANT, UNIT NO. 1. Preliminary Safety Analysis Report, Amendment 64. (Jersey Central Power and Light Co., Morristown, N. J.). 18 Nov 1970. 6p. Dep. NTIS.

Requested information on scram circuit modifications in the protection system is presented. (D.C.C.)

3814 (DOCKET-50220-52) NINE MILE POINT NUCLEAR STATION. Revisions to Second Addendum to Technical Supplement to Petition to Increase Power Level. (Niagara Mohawk Power Corp., Syracuse, N. Y.). 23 Nov 1970. 3p. Dep. NTIS.

3815 (DOCKET-50237-85) DRESDEN NUCLEAR POWER STATION, UNIT 2. Plant Design and Analysis Report. Volume I. (Commonwealth Edison Co., Chicago, Ill.). 17 May 1965. 500p. Dep. NTIS.

Revised design parameters of the Dresden Power Reactor Unit 2 are presented. Included also are additional data on the reactor requested by the Division of Reactor Licensing. (D.C.C.)

3816 (DOCKET-50237-86) DRESDEN NUCLEAR POWER STATION, UNIT 2. Plant Design and Analysis Report. Volume III. Plant Site and Environs. (Commonwealth Edison Co., Chicago, Ill.). 15 Apr 1965. 325p. Dep. NTIS.

3817 (DOCKET-50237-87) DRESDEN NUCLEAR POWER STATION, UNIT 2. Safety Evaluation. (Division of Reactor Licensing (AEC), Washington, D. C.). 24 Nov 1965. 97p. Dep. NTIS.

For Commonwealth Edison Co., Chicago, Ill.

3818 (DOCKET-50247-42) INDIAN POINT NUCLEAR GENERATING UNIT NO. 2. Inspections Performed on the Pressurizer. (Consolidated Edison Co. of New York, Inc., New York). 9 Nov 1970. 5p. Dep. NTIS.

3819 (DOCKET-50247-43) INDIAN POINT NUCLEAR GENERATING UNIT NO. 2. Preliminary Safety Analysis Report, Amendment 25 (Includes Final Facility Description and Safety Analysis Report, Suppl. 15). (Consolidated Edison Co. of New York, Inc., New York). 12 Nov 1970. 407p. Dep. NTIS.

Revised design parameters of the Indian Point Power Reactors Unit 2 are presented. Included also are additional data on the reactor requested by the Division of Reactor Licensing. (D.C.C.)

3820 (DOCKET-50247-44) INDIAN POINT NUCLEAR GENERATING UNIT NO. 2. Safety Evaluation. (Division of Reactor Licensing (AEC), Washington, D. C.). 16 Nov 1970. 116p. Dep. NTIS.

For Consolidated Edison Co. of New York, Inc., New York.

3821 (DOCKET-50249-43) DRESDEN NUCLEAR POWER STATION, UNIT 3. Proposed Operating License and Safety Evaluation. (Commonwealth Edison Co., Chicago, Ill.). 18 Nov 1970. 98p. Dep. NTIS.

3822 (DOCKET-50250-35) TURKEY POINT PLANT, UNITS NO. 3 AND NO. 4. Preliminary Safety Analysis Report, [Amendment 30], Suppl. 30. (Florida Power and Light Co.). 24 Nov 1970. 24p. (DOCKET-50251-33). Dep. NTIS.

Revised design parameters and operations aspects of the Turkey Point Power Reactor Units 3 and 4 are presented. (D.C.C.)

3823 (DOCKET-50254-22) QUAD-CITIES STATION, UNITS 1 AND 2. Preliminary Safety Analysis Report, Amendment 13, Answers to Questions. (Commonwealth Edison Co., Chicago, Ill. Iowa-Illinois Gas and Electric Co., Davenport, Iowa). 6 Nov 1970. 312p. (DOCKET-50265-18). Dep. NTIS.

Additional data requested by the Division of Reactor Licensing on the reactor and reactor operations are presented. (D.C.C.)

3824 (DOCKET-50254-23) QUAD-CITIES STATION, UNITS 1 AND 2. Preliminary Safety Analysis Report, Amendment 14. (Commonwealth Edison Co., Chicago, Ill. Iowa-Illinois Gas and Electric Co., Davenport, Iowa). 16 Nov 1970. 88p. (DOCKET-50265-19). Dep. NTIS.

Design specifications and seismic stress analysis for the pressure vessel are presented. Additional data on the reactor requested by the Division of Reactor Licensing are included. (D.C.C.)

3825 (DOCKET-50254-24) QUAD-CITIES STATION, UNITS 1 AND 2. Preliminary Safety Analysis Report, Amendment 15. Supplementary Information to Foundation Grouting (Amendment 8). (Commonwealth Edison Co., Chicago, Ill. Iowa-Illinois Gas and Electric Co., Davenport, Iowa). 16 Nov 1970. 30p. (DOCKET-50265-20). Dep. NTIS.

3826 (DOCKET-50254-25) QUAD-CITIES STATION, UNITS 1 AND 2. Environmental Report. (Commonwealth Edison Co., Chicago, Ill. Iowa-Illinois Gas and Electric Co., Davenport, Iowa). 16 Nov 1970. 105p. (DOCKET-50265-21). Dep. NTIS.

Information concerning radioactive and thermal discharges from the reactor is presented. The effects of reactor operations on the environment are analyzed. (D.C.C.)

3827 (DOCKET-50259-20) BROWNS FERRY NUCLEAR PLANT, UNITS 1, 2, AND 3. Preliminary Safety Analysis Report, Amendment 10. (Tennessee Valley Authority, Chattanooga. Office of Power). 18 Nov 1970. 156p. (DOCKET-50260-20; DOCKET-50296-19). Dep. NTIS.

Revised design parameters of the Browns Ferry Power Reactor Units 1, 2, and 3 are presented. Included also are additional data on the reactor requested by the Division of Reactor Licensing. Proposed technical specifications are listed. (D.C.C.)

3828 (DOCKET-50261-46) H. B. ROBINSON UNIT NO. 2. Request for Allowance for Use of Respiratory Protective Equipment. (Carolina Power and Light Co., Raleigh, N. C.). 12 Nov 1970. 4p. Dep. NTIS.

3829 (DOCKET-50266-32) POINT BEACH NUCLEAR PLANT, UNIT 1. Initial Integrated Leak Rate Test of the Reactor Containment Building. Final Report. (Bechtel Corp., San Francisco, Calif.). 20 Jul 1970. 315p. Dep. NTIS.

For Westinghouse Electric Corp., Atomic Power Div., Pittsburgh, Pa.

XUM

3830 (DOCKET-50266-33) POINT BEACH NUCLEAR PLANT, UNIT 1. Containment Structural Test. (Bechtel Corp., San Francisco, Calif.). Revised 29 Oct 1970. 71p. Dep. NTIS.

3831 (DOCKET-50266-34) POINT BEACH NUCLEAR PLANT, UNIT 1. Review of the Statistical Significance of Tendon Surveillance. (Bechtel Corp., San Francisco, Calif.). Rev. 1, 20 Oct 1970. 47p. Dep. NTIS.

3832 (DOCKET-50266-35) POINT BEACH NUCLEAR PLANT, UNIT 1. Facility Operating License DPR-24; Technical Specifications Change No. 1. (Division of Reactor Licensing (AEC), Washington, D. C.). 17 Nov 1970. 6p. Dep. NTIS.

Revised activity limits for the reactor coolant are presented. Revised procedures for handling liquid radioactive waste are listed. (D.C.C.)

3833 (DOCKET-50267-23) FORT ST. VRAIN NUCLEAR GENERATING STATION, UNIT 1. Preliminary Safety Analysis Report, Amendment 16. (Public Service Co. of Colorado, Denver). 5 Nov 1970. 316p. Dep. NTIS.

Additional data requested by the Division of Reactor Licensing on the reactor and reactor operations are presented. Environmental surveillance data during April to June 1970 are included. (D.C.C.)

3834 (DOCKET-50269-28) OCONEE NUCLEAR STATION, UNITS 1, 2, AND 3. Preliminary Safety Analysis Report, Amendment 23. (Duke Power Co., Charlotte, N. C.). 19 Nov 1970. 5p. (DOCKET-50270-28; DOCKET-50287-25). Dep. NTIS.

Additional information on the emergency and protection systems is presented. (D.C.C.)

3835 (DOCKET-50271-34) VERMONT YANKEE NUCLEAR POWER STATION. Preliminary Safety Analysis Report, Amendment 16 (Includes Additions and Revisions to Final Safety Analysis Report, Vol. 4, App. I). (Vermont Yankee Nuclear Power Corp., Rutland). 21 Oct 1970. 212p. Dep. NTIS.

Revised design parameters of the Vermont Yankee Power Reactor are presented. Included also are additional data on the reactor requested by the Division of Reactor Licensing. (D.C.C.)

3836 (DOCKET-50309-24) MAINE YANKEE ATOMIC POWER STATION. Preliminary Safety Analysis Report, Amendment 16. (Maine Yankee Atomic Power Co., Wiscasset). 9 Nov 1970. 66p. Dep. NTIS.

Administrative controls for reactor operations are described. Personnel qualifications and responsibilities are listed. (D.C.C.)

3837 (DOCKET-50309-25) MAINE YANKEE ATOMIC POWER STATION. Environmental Report. (Maine Yankee Atomic Power Co., Wiscasset). Oct 1970. 46p. Dep. NTIS.

Information concerning chemical, radioactive, and thermal discharges from the reactor is presented. The effects of reactor operations on the environment are analyzed. (D.C.C.)

3838 (DOCKET-50317-20) CALVERT CLIFFS NUCLEAR POWER PLANT, UNITS 1 AND 2. Environmental Report. (Baltimore Gas and Electric Co., Md.). 16 Nov 1970. 214p. (DOCKET-50318-20). Dep. NTIS.

Information concerning chemical, radioactive, and thermal discharge from the reactor is presented. The effects of reactor operations on the environment are analyzed. (D.C.C.)

3839 (DOCKET-50324-17) BRUNSWICK STEAM ELECTRIC PLANT, UNITS 1 AND 2. Design Report Nos. 4, 5, and 6. (Carolina Power and Light Co., Raleigh, N. C.). 15 Nov 1970. 261p. (DOCKET-50325-17). Dep. NTIS.

Seismic stress analysis of the primary and secondary containment structures is presented. Preparation and testing programs for Class 1 and Class 2 backfill are described. (D.C.C.)

3840 (DOCKET-50329-24) MIDLAND PLANT, UNITS 1 AND 2. Safety Evaluation. (Division of Reactor Licensing (AEC), Washington, D. C.). 24 Nov 1970. 130p. (DOCKET-50330-23). Dep. NTIS.

For Consumers Power Co., Jackson, Mich.

3841 (DOCKET-50338-26) NORTH ANNA POWER STATION, UNITS 1 AND 2. Detailed Statement on the Environmental Considerations. (Division of Reactor Licensing (AEC), Washington, D. C.). 9 Nov 1970. 43p. (DOCKET-50339-25). Dep. NTIS.

Information concerning chemical, radioactive, and thermal discharges from the reactor is presented. The effects of reactor operations on the environment are analyzed. (D.C.C.)

3842 (DOCKET-50341-21) ENRICO FERMI ATOMIC POWER PLANT, UNIT 2. Preliminary Safety Analysis Report, Amendment 12. (Detroit Edison Co., Mich.). 18 Nov 1970. 118p. Dep. NTIS.

Revised and additional information on the radioactive waste systems and the electrical power systems is presented. Additional data on the reactor requested by the Division of Reactor Licensing are also included. (D.C.C.)

3843 (DOCKET-50344-18) TROJAN NUCLEAR PLANT. Detailed Statement on the Environmental Considerations. (Division of Reactor Licensing (AEC), Washington, D. C.). 13 Nov 1970. 106p. Dep. NTIS.

Information concerning chemical, radioactive, and thermal discharges from the reactor is presented. The effects of reactor operations on the environment are analyzed. (D.C.C.)

3844 (DOCKET-50346-18) DAVIS-BESSE NUCLEAR POWER STATION. Safety Evaluation. (Division of Reactor Licensing (AEC), Washington, D. C.). 2 Nov 1970. 137p. Dep. NTIS.

For Toledo Edison Co., Ohio and Cleveland Electric Illuminating Co., Ohio.

3845 (DOCKET-50348-14) JOSEPH M. FARLEY NUCLEAR PLANT, UNITS 1 AND 2. Preliminary Safety Analysis Report, Amendment 8. (Alabama Power Co., Birmingham). 9 Nov 1970. 365p. (DOCKET-50364-8). Dep. NTIS.

Revised design parameters of the Joseph M. Farley Power Reactor Units 1 and 2 are presented. Included also are additional data on the reactor requested by the Division of Reactor Licensing. (D.C.C.)

3846 (DOCKET-50352-9) LIMERICK GENERATING STATION, UNITS 1 AND 2. Preliminary Safety Analysis Report, Amendment 2, Suppl. 2. (Philadelphia Electric Co., Pa.). 24 Nov 1970. 104p. (DOCKET-50353-9). Dep. NTIS.

Revised design parameters of the Limerick Power Reactor Units 1 and 2 are presented. Included also are additional data on the reactor requested by the Division of Reactor Licensing. (D.C.C.)

3847 (DOCKET-50354-9) NEWBOLD ISLAND NUCLEAR GENERATING STATION, UNITS 1 AND 2. Preliminary Safety Analysis Report, Amendment 3. (Public Service Electric and Gas Co., Newark, N. J.). 25 Nov 1970. 366p. (DOCKET-50355-9). Dep. NTIS.

Revised design parameters of the Newbold Island Power Reactor Units 1 and 2 are presented. Included also are additional data on the reactor requested by the Division of Reactor Licensing. (D.C.C.)

3848 (DOCKET-50358-8) WM. H. ZIMMER NUCLEAR POWER STATION, UNITS 1 AND 2. Preliminary Safety Analysis Report, Amendment 2. (Cincinnati Gas and Electric Co., Ohio. Columbus and Southern Ohio Electric Co., Columbus, Ohio. Dayton Power and Light Co., Ohio). 20 Nov 1970. 80p. (DOCKET-50359-7). Dep. NTIS.

Revised and additional data concerning the hydrology of the reactor site are presented. (D.C.C.)

3849 (DOCKET-50361-11) SAN ONOFRE NUCLEAR GENERATING STATION, UNITS 2 AND 3. Preliminary Safety Analysis Report, Amendment 3. (Southern California Edison Co., Los Angeles. San Diego Gas and Electric Co., Calif.). 24 Nov 1970. 343p. (DOCKET-50362-10). Dep. NTIS.

Revised design parameters of the San Onofre Power Reactor Units 2 and 3 are presented. Included also are additional data on the reactor requested by the Division of Reactor Licensing. (D.C.C.)

3850 (DOCKET-50373-6) LA SALLE COUNTY STATION, UNITS 1 AND 2. Preliminary Safety Analysis Report, Vol. 5. (Commonwealth Edison Co., Chicago, Ill.). 3 Nov 1970. 439p. (DOCKET-50374-6). Dep. NTIS.

Information on LaSalle County Power Reactor Units 1 and 2 is presented under the following headings: pressure boundary integrity criteria; proposed technical specifications; supplemental design criteria; quality assurance program; station atmospheric release limit calculations; conformance to AEC general design criteria; and operational nuclear safety analysis. (D.C.C.)

3851 STANDARDS AGREEMENT FOR IAEO REACTOR SAFETY CONTROL. Boulanger, W. Atomwirt., Atomtech., 15: 521-2(Nov 1970). (In German).

The board of governors of the IAEO accepted a standard agreement proposed by a special Control Committee. The

Safety and Siting

3805 (DOCKET-1155-84) LA CROSSE BOILING WATER REACTOR. Proposed Change to Technical Specifications. Installation of Automatic Gain Control System. (Dairyland Power Cooperative, La Crosse, Wis.). 25 Nov 1970. 4p. Dep. NTIS.

3806 (DOCKET-50003-59) INDIAN POINT STATION, UNIT NO. 1. Survey of Environmental Radioactivity, August 1, 1969-March 31, 1970. (Consolidated Edison Co. of New York, Inc., New York). 10 Sep 1970. 24p. Dep. NTIS.

3807 (DOCKET-50010-70) DRESDEN NUCLEAR POWER STATION, UNIT 1. Comments on Uniform Monitoring, Recording, and Reporting Guide. (Commonwealth Edison Co., Chicago, Ill.). 23 Nov 1970. 6p. Dep. NTIS.

3808 (DOCKET-50133-42) HUMBOLDT BAY POWER PLANT, UNIT NO. 3. Facility License No. DPR-7, Amendment 1. (Division of Reactor Licensing (AEC), Washington, D. C.). 23 Nov 1970. 4p. Dep. NTIS.

Authorized limits for the possession and use of radioisotopes at the reactor are presented. (D.C.C.)

3809 (DOCKET-50206-95) SAN ONOFRE NUCLEAR GENERATING STATION, UNIT 1. Preliminary Safety Analysis Report, Amendment 20. (Southern California Edison Co., Los Angeles). 13 Nov 1970. 4p. Dep. NTIS.

Additional data requested by the Division of Reactor Licensing are presented on the reactor design and operations. Included are data on excess reactivity, expected fuel burnup, moderator temperature, fissile Pu inventory, and anticipated Pu bone dose from the most serious accident analyzed. (D.C.C.)

3810 (DOCKET-50206-96) SAN ONOFRE NUCLEAR GENERATING STATION, UNIT 1. Provisional Operating License No. DPR-13, Amendment 3. (Division of Reactor Licensing (AEC), Washington, D. C.). 13 Nov 1970. 8p. Dep. NTIS.

Authorization for the use of 4 mixed-oxide fuel assemblies in the reactor and the "checkerboard" loading configuration of the core for Cycle 2 is presented. Additional information concerning burnup limits is included. (D.C.C.)

3811 (DOCKET-50213-83) CONNECTICUT YANKEE ATOMIC POWER PLANT. License No. DPR-14. Technical Specifications Proposed Change No. 16, Rev. No. 1. (Connecticut Yankee Atomic Power Co., Hartford). 10 Nov 1970. 32p. Dep. NTIS.

Revised and additional information concerning administrative controls of reactor operations is presented. Personnel qualifications and responsibilities are listed. (D.C.C.)

3812 (DOCKET-50213-85) CONNECTICUT YANKEE NUCLEAR POWER PLANT. 1970 Inservice Inspection. (Southwest Research Inst., San Antonio, Tex.). 17 Sep 1970. 66p. Dep. NTIS.

For Connecticut Yankee Atomic Power Co., Westboro, Mass.

3813 (DOCKET-50219-115) OYSTER CREEK NUCLEAR POWER PLANT, UNIT NO. 1. Preliminary Safety Analysis Report, Amendment 64. (Jersey Central Power and Light Co., Morristown, N. J.). 18 Nov 1970. 6p. Dep. NTIS.

Requested information on scram circuit modifications in the protection system is presented. (D.C.C.)

3814 (DOCKET-50220-52) NINE MILE POINT NUCLEAR STATION. Revisions to Second Addendum to Technical Supplement to Petition to Increase Power Level. (Niagara Mohawk Power Corp., Syracuse, N. Y.). 23 Nov 1970. 3p. Dep. NTIS.

3815 (DOCKET-50237-85) DRESDEN NUCLEAR POWER STATION, UNIT 2. Plant Design and Analysis Report. Volume I. (Commonwealth Edison Co., Chicago, Ill.). 17 May 1965. 500p. Dep. NTIS.

Revised design parameters of the Dresden Power Reactor Unit 2 are presented. Included also are additional data on the reactor requested by the Division of Reactor Licensing. (D.C.C.)

3816 (DOCKET-50237-86) DRESDEN NUCLEAR POWER STATION, UNIT 2. Plant Design and Analysis Report. Volume III. Plant Site and Environs. (Commonwealth Edison Co., Chicago, Ill.). 15 Apr 1965. 325p. Dep. NTIS.

3817 (DOCKET-50237-87) DRESDEN NUCLEAR POWER STATION, UNIT 2. Safety Evaluation. (Division of Reactor Licensing (AEC), Washington, D. C.). 24 Nov 1965. 97p. Dep. NTIS.

For Commonwealth Edison Co., Chicago, Ill.

3818 (DOCKET-50247-42) INDIAN POINT NUCLEAR GENERATING UNIT NO. 2. Inspections Performed on the Pressurizer. (Consolidated Edison Co. of New York, Inc., New York). 9 Nov 1970. 5p. Dep. NTIS.

3819 (DOCKET-50247-43) INDIAN POINT NUCLEAR GENERATING UNIT NO. 2. Preliminary Safety Analysis Report, Amendment 25 (Includes Final Facility Description and Safety Analysis Report, Suppl. 15). (Consolidated Edison Co. of New York, Inc., New York). 12 Nov 1970. 407p. Dep. NTIS.

Revised design parameters of the Indian Point Power Reactors Unit 2 are presented. Included also are additional data on the reactor requested by the Division of Reactor Licensing. (D.C.C.)

3820 (DOCKET-50247-44) INDIAN POINT NUCLEAR GENERATING UNIT NO. 2. Safety Evaluation. (Division of Reactor Licensing (AEC), Washington, D. C.). 16 Nov 1970. 116p. Dep. NTIS.

For Consolidated Edison Co. of New York, Inc., New York.

3821 (DOCKET-50249-43) DRESDEN NUCLEAR POWER STATION, UNIT 3. Proposed Operating License and Safety Evaluation. (Commonwealth Edison Co., Chicago, Ill.). 18 Nov 1970. 98p. Dep. NTIS.

3822 (DOCKET-50250-35) TURKEY POINT PLANT, UNITS NO. 3 AND NO. 4. Preliminary Safety Analysis Report, [Amendment 30], Suppl. 30. (Florida Power and Light Co.). 24 Nov 1970. 24p. (DOCKET-50251-33). Dep. NTIS.

Revised design parameters and operations aspects of the Turkey Point Power Reactor Units 3 and 4 are presented. (D.C.C.)

3823 (DOCKET-50254-22) QUAD-CITIES STATION, UNITS 1 AND 2. Preliminary Safety Analysis Report, Amendment 13, Answers to Questions. (Commonwealth Edison Co., Chicago, Ill. Iowa-Illinois Gas and Electric Co., Davenport, Iowa). 6 Nov 1970. 312p. (DOCKET-50265-18). Dep. NTIS.

Additional data requested by the Division of Reactor Licensing on the reactor and reactor operations are presented. (D.C.C.)

3824 (DOCKET-50254-23) QUAD-CITIES STATION, UNITS 1 AND 2. Preliminary Safety Analysis Report, Amendment 14. (Commonwealth Edison Co., Chicago, Ill. Iowa-Illinois Gas and Electric Co., Davenport, Iowa). 16 Nov 1970. 88p. (DOCKET-50265-19). Dep. NTIS.

Design specifications and seismic stress analysis for the pressure vessel are presented. Additional data on the reactor requested by the Division of Reactor Licensing are included. (D.C.C.)

3825 (DOCKET-50254-24) QUAD-CITIES STATION, UNITS 1 AND 2. Preliminary Safety Analysis Report, Amendment 15. Supplementary Information to Foundation Grouting (Amendment 8). (Commonwealth Edison Co., Chicago, Ill. Iowa-Illinois Gas and Electric Co., Davenport, Iowa). 16 Nov 1970. 30p. (DOCKET-50265-20). Dep. NTIS.

3826 (DOCKET-50254-25) QUAD-CITIES STATION, UNITS 1 AND 2. Environmental Report. (Commonwealth Edison Co., Chicago, Ill. Iowa-Illinois Gas and Electric Co., Davenport, Iowa). 16 Nov 1970. 105p. (DOCKET-50265-21). Dep. NTIS.

Information concerning radioactive and thermal discharges from the reactor is presented. The effects of reactor operations on the environment are analyzed. (D.C.C.)

3827 (DOCKET-50259-20) BROWNS FERRY NUCLEAR PLANT, UNITS 1, 2, AND 3. Preliminary Safety Analysis Report, Amendment 10. (Tennessee Valley Authority, Chattanooga. Office of Power). 18 Nov 1970. 156p. (DOCKET-50260-20; DOCKET-50296-19). Dep. NTIS.

Revised design parameters of the Browns Ferry Power Reactor Units 1, 2, and 3 are presented. Included also are additional data on the reactor requested by the Division of Reactor Licensing. Proposed technical specifications are listed. (D.C.C.)

3828 (DOCKET-50261-46) H. B. ROBINSON UNIT NO. 2. Request for Allowance for Use of Respiratory Protective Equipment. (Carolina Power and Light Co., Raleigh, N. C.). 12 Nov 1970. 4p. Dep. NTIS.

3829 (DOCKET-50266-32) POINT BEACH NUCLEAR PLANT, UNIT 1. Initial Integrated Leak Rate Test of the Reactor Containment Building. Final Report. (Bechtel Corp., San Francisco, Calif.). 20 Jul 1970. 315p. Dep. NTIS.

For Westinghouse Electric Corp., Atomic Power Div., Pittsburgh, Pa.

XUM

3830 (DOCKET-50266-33) POINT BEACH NUCLEAR PLANT, UNIT 1. Containment Structural Test. (Bechtel Corp., San Francisco, Calif.). Revised 29 Oct 1970. 71p. Dep. NTIS.

3831 (DOCKET-50266-34) POINT BEACH NUCLEAR PLANT, UNIT 1. Review of the Statistical Significance of Tendon Surveillance. (Bechtel Corp., San Francisco, Calif.). Rev. 1, 20 Oct 1970. 47p. Dep. NTIS.

3832 (DOCKET-50266-35) POINT BEACH NUCLEAR PLANT, UNIT 1. Facility Operating License DPR-24; Technical Specifications Change No. 1. (Division of Reactor Licensing (AEC), Washington, D. C.). 17 Nov 1970. 6p. Dep. NTIS.

Revised activity limits for the reactor coolant are presented. Revised procedures for handling liquid radioactive waste are listed. (D.C.C.)

3833 (DOCKET-50267-23) FORT ST. VRAIN NUCLEAR GENERATING STATION, UNIT 1. Preliminary Safety Analysis Report, Amendment 16. (Public Service Co. of Colorado, Denver). 5 Nov 1970. 316p. Dep. NTIS.

Additional data requested by the Division of Reactor Licensing on the reactor and reactor operations are presented. Environmental surveillance data during April to June 1970 are included. (D.C.C.)

3834 (DOCKET-50269-28) OCONEE NUCLEAR STATION, UNITS 1, 2, AND 3. Preliminary Safety Analysis Report, Amendment 23. (Duke Power Co., Charlotte, N. C.). 19 Nov 1970. 5p. (DOCKET-50270-28; DOCKET-50287-25). Dep. NTIS.

Additional information on the emergency and protection systems is presented. (D.C.C.)

3835 (DOCKET-50271-34) VERMONT YANKEE NUCLEAR POWER STATION. Preliminary Safety Analysis Report, Amendment 16 (Includes Additions and Revisions to Final Safety Analysis Report, Vol. 4, App. I). (Vermont Yankee Nuclear Power Corp., Rutland). 21 Oct 1970. 212p. Dep. NTIS.

Revised design parameters of the Vermont Yankee Power Reactor are presented. Included also are additional data on the reactor requested by the Division of Reactor Licensing. (D.C.C.)

3836 (DOCKET-50309-24) MAINE YANKEE ATOMIC POWER STATION. Preliminary Safety Analysis Report, Amendment 16. (Maine Yankee Atomic Power Co., Wiscasset). 9 Nov 1970. 66p. Dep. NTIS.

Administrative controls for reactor operations are described. Personnel qualifications and responsibilities are listed. (D.C.C.)

3837 (DOCKET-50309-25) MAINE YANKEE ATOMIC POWER STATION. Environmental Report. (Maine Yankee Atomic Power Co., Wiscasset). Oct 1970. 46p. Dep. NTIS.

Information concerning chemical, radioactive, and thermal discharges from the reactor is presented. The effects of reactor operations on the environment are analyzed. (D.C.C.)

3838 (DOCKET-50317-20) CALVERT CLIFFS NUCLEAR POWER PLANT, UNITS 1 AND 2. Environmental Report. (Baltimore Gas and Electric Co., Md.). 16 Nov 1970. 214p. (DOCKET-50318-20). Dep. NTIS.

Information concerning chemical, radioactive, and thermal discharge from the reactor is presented. The effects of reactor operations on the environment are analyzed. (D.C.C.)

3839 (DOCKET-50324-17) BRUNSWICK STEAM ELECTRIC PLANT, UNITS 1 AND 2. Design Report Nos. 4, 5, and 6. (Carolina Power and Light Co., Raleigh, N. C.). 15 Nov 1970. 261p. (DOCKET-50325-17). Dep. NTIS.

Seismic stress analysis of the primary and secondary containment structures is presented. Preparation and testing programs for Class 1 and Class 2 backfill are described. (D.C.C.)

3840 (DOCKET-50329-24) MIDLAND PLANT, UNITS 1 AND 2. Safety Evaluation. (Division of Reactor Licensing (AEC), Washington, D. C.). 24 Nov 1970. 130p. (DOCKET-50330-23). Dep. NTIS.

For Consumers Power Co., Jackson, Mich.

3841 (DOCKET-50338-26) NORTH ANNA POWER STATION, UNITS 1 AND 2. Detailed Statement on the Environmental Considerations. (Division of Reactor Licensing (AEC), Washington, D. C.). 9 Nov 1970. 43p. (DOCKET-50339-25). Dep. NTIS.

Information concerning chemical, radioactive, and thermal discharges from the reactor is presented. The effects of reactor operations on the environment are analyzed. (D.C.C.)

3842 (DOCKET-50341-21) ENRICO FERMI ATOMIC POWER PLANT, UNIT 2. Preliminary Safety Analysis Report, Amendment 12. (Detroit Edison Co., Mich.). 18 Nov 1970. 118p. Dep. NTIS.

Revised and additional information on the radioactive waste systems and the electrical power systems is presented. Additional data on the reactor requested by the Division of Reactor Licensing are also included. (D.C.C.)

3843 (DOCKET-50344-18) TROJAN NUCLEAR PLANT. Detailed Statement on the Environmental Considerations. (Division of Reactor Licensing (AEC), Washington, D. C.). 13 Nov 1970. 106p. Dep. NTIS.

Information concerning chemical, radioactive, and thermal discharges from the reactor is presented. The effects of reactor operations on the environment are analyzed. (D.C.C.)

3844 (DOCKET-50346-18) DAVIS-BESSE NUCLEAR POWER STATION. Safety Evaluation. (Division of Reactor Licensing (AEC), Washington, D. C.). 2 Nov 1970. 137p. Dep. NTIS.

For Toledo Edison Co., Ohio and Cleveland Electric Illuminating Co., Ohio.

3845 (DOCKET-50348-14) JOSEPH M. FARLEY NUCLEAR PLANT, UNITS 1 AND 2. Preliminary Safety Analysis Report, Amendment 8. (Alabama Power Co., Birmingham). 9 Nov 1970. 365p. (DOCKET-50364-8). Dep. NTIS.

Revised design parameters of the Joseph M. Farley Power Reactor Units 1 and 2 are presented. Included also are additional data on the reactor requested by the Division of Reactor Licensing. (D.C.C.)

3846 (DOCKET-50352-9) LIMERICK GENERATING STATION, UNITS 1 AND 2. Preliminary Safety Analysis Report, Amendment 2, Suppl. 2. (Philadelphia Electric Co., Pa.). 24 Nov 1970. 104p. (DOCKET-50353-9). Dep. NTIS.

Revised design parameters of the Limerick Power Reactor Units 1 and 2 are presented. Included also are additional data on the reactor requested by the Division of Reactor Licensing. (D.C.C.)

3847 (DOCKET-50354-9) NEWBOLD ISLAND NUCLEAR GENERATING STATION, UNITS 1 AND 2. Preliminary Safety Analysis Report, Amendment 3. (Public Service Electric and Gas Co., Newark, N. J.). 25 Nov 1970. 366p. (DOCKET-50355-9). Dep. NTIS.

Revised design parameters of the Newbold Island Power Reactor Units 1 and 2 are presented. Included also are additional data on the reactor requested by the Division of Reactor Licensing. (D.C.C.)

3848 (DOCKET-50358-8) WM. H. ZIMMER NUCLEAR POWER STATION, UNITS 1 AND 2. Preliminary Safety Analysis Report, Amendment 2. (Cincinnati Gas and Electric Co., Ohio. Columbus and Southern Ohio Electric Co., Columbus, Ohio. Dayton Power and Light Co., Ohio). 20 Nov 1970. 80p. (DOCKET-50359-7). Dep. NTIS.

Revised and additional data concerning the hydrology of the reactor site are presented. (D.C.C.)

3849 (DOCKET-50361-11) SAN ONOFRE NUCLEAR GENERATING STATION, UNITS 2 AND 3. Preliminary Safety Analysis Report, Amendment 3. (Southern California Edison Co., Los Angeles. San Diego Gas and Electric Co., Calif.). 24 Nov 1970. 343p. (DOCKET-50362-10). Dep. NTIS.

Revised design parameters of the San Onofre Power Reactor Units 2 and 3 are presented. Included also are additional data on the reactor requested by the Division of Reactor Licensing. (D.C.C.)

3850 (DOCKET-50373-6) LA SALLE COUNTY STATION, UNITS 1 AND 2. Preliminary Safety Analysis Report, Vol. 5. (Commonwealth Edison Co., Chicago, Ill.). 3 Nov 1970. 439p. (DOCKET-50374-6). Dep. NTIS.

Information on LaSalle County Power Reactor Units 1 and 2 is presented under the following headings: pressure boundary integrity criteria; proposed technical specifications; supplemental design criteria; quality assurance program; station atmospheric release limit calculations; conformance to AEC general design criteria; and operational nuclear safety analysis. (D.C.C.)

3851 STANDARDS AGREEMENT FOR IAEO REACTOR SAFETY CONTROL. Boulanger, W. Atomwirt., Atomtech., 15: 521-2(Nov 1970). (In German).

The board of governors of the IAEO accepted a standard agreement proposed by a special Control Committee. The

agreement was proposed as preliminary guidelines for negotiations about safety measures of the IAEO with those countries that ratified the nuclear non-proliferation treaty. In the first section of the agreement, principles for application of IAEO control standards are outlined as well as verification procedures with respect to responsibilities of the countries concerned. (tr-auth)

3852 POWER, POLLUTION, AND THE IMPERILED ENVIRONMENT. I. Friedlander, Gordon D. IEEE (Inst. Elec. Electron. Eng.), Spectrum; 7: No. 11, 40-50(Nov 1970).

Predicted electric power requirements for the U. S. are presented. Problems related to chemical and thermal effluents from steam power plants and nuclear power plants are described. (D.C.C.)

Power Reactor Development

Refer also to abstracts 2369, 2385, 2601, 2609, 2641, 2660, 2754, and 2755.

3853 FEDERAL EXPENDITURES FOR ATOMIC ENERGY FOR FISCAL YEAR 1971. Atomwirt., Atomtech.; 15: 534-5 (Nov 1970). (In German).

The budget proposal of the German Federal Republic for fiscal 1971 contains 1.181 billion DM for support of peaceful application of nuclear energy. Of this amount, approximately 335 million DM are projected for operation, 215 million DM for investment in nuclear installations, 125 million DM for uranium supply, and 158 million DM for research and development of experimental reactors. Increased amounts are allocated for direct transformation of nuclear energy, reprocessing of burned up nuclear fuel, reactor safety, development of monitoring equipment and diagnostic equipment for medicine and biology. Details of the budget proposal comparing the years 1969, 1970, and 1971 are tabulated. (H.B.G.)

3854 STUDY CONCERNING THE ANALYSIS AND EVALUATION OF A GAS COOLED FAST BREEDER. Mochizuki, Hiroji (Kawasaki Heavy Industries, Ltd., Kobe, Japan). FAPIG (Tokyo); No 54, 94-104(Sep 1969). (In Japanese).

The technical problems of a gas cooled fast reactor are analyzed. Analysis is performed for a CO_2 cooled, metal-clad UO_2-PuO_2 fueled reactor. Thermal, nuclear and structural characteristics, safety analysis, core nuclear and thermal survey, and general evaluation are included. The effect of channel parameters on core concerning thermal characteristics is a main problem of the analysis of thermal characteristics. The secondary steam cycle efficiency is considered. The ratio of structural material to coolant and fuel in the core is considered. Configurations with variations of the ratio of core height and diameter are analyzed. The heat transfer of the gas cooled reactor is poorer than that of a Na cooled reactor. The results of the analyses, however, show that a reactor with same performance as a Na cooled reactor can be constructed if a proper fuel rod diameter and a coolant flow cross-section are adopted. A large breeding ratio is easily obtained because the absorption and moderation effects by the gas coolant are negligible. (Japan)

3855 PRELIMINARY DESIGN ON THE PROTOTYPE FAST REACTOR. Nakano, Hideo (Fuji Electric Co. Ltd., Tokyo). FAPIG (Tokyo); No. 54, 106-13(Sep 1969). (In Japanese).

A preliminary design has been completed on the prototype fast reactor. The specifications given by PNC are: electric output of 300 MW; mixed oxides fuel, cooled by sodium, with a burn-up of 100,000 MWd/t; breeding ratio above 1.2; load factor 80%, and with the plant life of 30 years. The preliminary design is outlined. Main features of the design are as follows: reactor construction is of the three-loop type; the fuel exchange utilizes a system of single rotation plug and rotary arm; the steam generators are of the divided type, with 4 evaporators, 4 superheaters and 2 reheaters per loop; and primary sodium-circulation main pumps are installed on the high-temperature side of piping. (Japan)

Kinetics and Dynamics

Refer also to abstracts 3922, 3930, and 3932.

3856 (KFK-851) INHERENT STABILITY OF STEAM-COOLED BREEDER REACTORS. Frisch, W.; Huebschmann, W. (Kernforschungszentrum, Karlsruhe (West Germany)). Mar 1969. 29p. (In German). (EUR-4153). Dep. NTIS (U. S. Sales Only).

The stability of the uncontrolled steam-cooled fast breeder reactor is investigated theoretically. This reactor permits oscillations of the power and the steam pressure. The possibility of such oscillations depends on the core stability, the delay time for the energy transport from the fuel to the evaporator, and the energy storage capacity of the cycle. The core stability proper depends on the reactivity coefficients and the pin power, among other factors. If the power decreases, the reactor approaches instability. For a given reactor, the distance from the stability limit is shown as a function of reactor power and reactivity coefficient ratio. The influence of other parameters on the stability limit is shown. The load dependent stability diagram chosen is compared with the usual stability presentation for full power. 6 references. (auth)

3857 ASYMPTOTIC STABILITY BY LIAPUNOV'S DIRECT METHOD IN THE CASE OF CIRCULATING FUEL REACTOR. Adamski, J. (Technical Univ., Warsaw). Bull. Acad. Pol. Sci., Ser. Sci. Tech.; 18: 503-8(1970).

The investigation of the asymptotic stability of the shutdown equilibrium state of the reactor with circulating fuel is performed by means of Krasovskii's functional method. In this case Liapunov's direct method cannot be applied directly for the reactor is described by means of space independent differential-difference non-linear kinetic equations. The main drawback of the applied method is that the analysis can be done only for the numerical values of parameters. (auth)

Control Systems

Refer also to abstract 2790.

3858 (DP-Report-486) SEIZURE TESTS ON A DRAGON ARTICULATED CONTROL ROD. Project DRAGON. Woodley, H. J. (Atomic Energy Establishment, Winfrith (England)). Nov 1966. 9p. Dep. NTIS.

A prototpye articulated control rod of the type now installed in the Dragon Reactor has been subjected to simulated working conditions in order to determine whether or not seizure of the universal joints is liable to occur during service. Tests were carried out over a period of 163 days. 84 days being taken by a static test and 79 days by a dynamic test. During this period there was no actual seizure but there was a slight change in the indication of the joint closing characteristics. (auth)

Shielding

3859 WEIGHT OPTIMIZATION OF REACTOR SHIELDING USING TRANSMISSION-MATRIX METHODS. Leech, William Dale. Ames, Iowa; Iowa State Univ. (1969). 68p. University Microfilms Order No. 70-13,605.

Thesis.

A quick and accurate method of calculating dose rates outside the primary shield of a nuclear reactor is developed. This method is then used to investigate minimum weight reactor shield configurations. The fast neutron dose at the outside of the shield is obtained by using the removal cross section concept in diffusion theory. The thermal neutron distribution in the shield is obtained from the two group diffusion equations using Fermi age theory for the slowing down of the fast neutrons. The primary and secondary gamma rays are treated by transmission matrix techniques. The optimization is carried out by determining the weight of various primary shield configurations and then searching for a minimum weight. Studies are conducted on iron-water slab shields, lead-water slab shields, iron-water cylindrical shields, and lead-water cylindrical shields. Fast reactor lead-water slab shields are also investigated. For a thermal reactor the input quantities of thermal neutron flux and primary gamma dose are varied and changes in the dose at the outside of the shield are shown. (Diss. Abstr.)

Cooling Systems

Refer also to abstracts 2263, 2500, 2503, and 2637.

3860 (DP-Report-491) CARBON TRANSPORT STUDIES FOR HELIUM COOLED HIGH TEMPERATURE REACTORS. Project DRAGON. Everett, M. R.; Kinsey, D. V.; Roemberg, E. (Atomic Energy Establishment, Winfrith (England)). Nov 1966. 174p. Dep. NTIS.

The chemical, in-pore and mass transfer controlled regimes, applicable to the thermal corrosion of H.T.R. graphites when exposed to volume parts per million impurity levels in a helium carrier, are analyzed. Deviations from the thermal graphite corrosion rates caused by catalytic effects arising from metal-

XUM

lic impurities in the graphite and also the effects of radiation producing active species which might accelerate these reactions are investigated. Factors controlling the rates of possible back-reactions of CO on catalytically active metal surfaces around 500°C in the primary circuit are studied. The effect of these rates on the possible carbon transport mechanism in a reactor coolant is discussed. 78 references. (auth)

3861 (DP-Report-552) HELIUM UTILISATION ON DRAGON DURING THE APPROACH TO POWER AND FIRST CHARGE IRRADIATION. Project DRAGON. Gow, H. B. F.; Gray, P. S.; Hamilton, J. D. (Atomic Energy Establishment, Winfrith (England)). Jun 1967. 13p. Dep. NTIS.

Figures for the He utilization in Dragon during the approach to power and first core irradiation are given. During power operation 8.5 kg/week of helium were required to maintain the coolant inventory of 240 kg. Of this amount 5.4 kg/week were accounted for by plant operations, the remaining 3.1 kg being required to compensate for general losses. The levels of leakage achieved during construction were adequately maintained during operation. (auth)

3862 (DP-Report-553) IMPURITY REMOVAL FROM THE DRAGON REACTOR DURING INITIAL COMMISSIONING. Project DRAGON. Gray, P. S.; Neset, K. M.; Stonier, D. R. (Atomic Energy Establishment, Winfrith (England)). May 1967. 23p. Dep. NTIS.

The processes used for removal of water and organic distillate from the reactor primary circuit before and during the hot tests are described. Results are given and compared with experimental predictions. (auth)

3863 (DP-Report-554) THE REMOVAL AND REPLACEMENT OF A PRIMARY HEAT EXCHANGER TUBE BUNDLE AND CIRCULATOR ON THE DRAGON REACTOR. Project DRAGON. Capp, P. D.; Watts, C.; Gray, P. S. (Atomic Energy Establishment, Winfrith (England)). Jun 1967. 29p. Dep. NTIS.

The removal and subsequent replacement of a primary heat exchanger tube bundle and gas bearing circulator from the Dragon Reactor is described. Details of mechanical, health physics and chemical aspects of the problem are given. Finally the replacement of a number of heat exchangers and/or circulators is considered. (auth)

3864 DETECTION OF SODIUM BOILING IN FAST SODIUM-COOLED REACTORS BY NEUTRON MEASUREMENTS. Asmussen, Keith Eugene. Ames, Iowa; Iowa State Univ. (1969). 141p. University Microfilms Order No. 70-13,566.

Thesis.

Methods of void measurement are reviewed in general, and three techniques currently receiving attention for possible use in sodium-cooled fast breeder reactors are discussed in particular. A method based on neutron flux noise measurements is then studied qualitatively. The Natural Mode Approximation method is used to solve the space and time dependent multi-group diffusion equations. A two-energy group, one delayed-neutron group model is used for a bare parallelepiped reactor. The time-dependent coefficients of the Natural Mode approximation are utilized in a space-dependent neutron flux noise formulation. The space-dependent noise formulation permits the calculation of the cross spectral density between space points or energy groups, or both. The input driving function required in this analysis is the spectral density of the perturbation. Results are presented corresponding to white fission noise and several postulated boiling perturbation spectral densities. The role of temperature feedback is demonstrated by a simple point-kinetics model. (Diss. Abstr.)

Fuels

Refer also to abstracts 2638, 2768, 2769, 2771, 2772, 2789, and 2812.

3865 (AECL-3414) HEAT TRANSFER MEASUREMENTS ON TREFOIL FUEL BUNDLES IN THE POST-DRYOUT REGIME WITH DATA TABULATION. Groeneveld, D. C.; Thibodeau, M.; McPherson, G. D. (Atomic Energy of Canada Ltd., Chalk River (Ontario)). Aug 1970. 23p. Dep. NTIS (U. S. Sales Only). AECL $1.00.

Heat transfer tests in the post-dryout regime were done on a string of three fuel bundles irradiated in the NRX reactor. The bundles consisted of a cluster of three elements (15.24 mm OD, 500 mm long) in a 37.44 mm ID test section. Measurements were taken at a pressure of 63 bars, at mass velocities ranging from 110 to 220 g/cm^{2}s, at heat fluxes of 33 to 116 W/cm^2 and at steam qualities of 30 to 60% with both clean and crudded fuel sheath surfaces. Dimensional changes in the fuel during post-dryout operation may explain anomalous temperature patterns. The data are correlated with a revised Miropol'skiy equation. 18 references. (auth)

3866 (CEA-N-1379) EL 600: FUEL MANAGEMENT STUDIES. Chabrillac, Marcel; Goldstein, Stephen; Naudet, Roger; Sulc, Petr (Commissariat a l'Energie Atomique, Saclay (France). Centre d'Etudes Nucleaires). Oct 1970. 39p. (In French). Dep. NTIS (U. S. Sales Only).

EL 600 is a Canadian type, heavy water moderated and cooled reactor design. The fuel flow in the horizontal channels is of the bidirectional push-through type. The initial loading and the fuel management strategy are defined. It is possible to achieve good economy conditions for the first loading utilization and to retain during the transient period a good flattening of the power distribution. The arrangement of depleted fuel elements in the first loading, the number and nature of the recycles, and the dates of the first loadings are studied. Solutions corresponding to the loading of 13 elements by channel are compared to those with 12 elements by channel, as well as simultaneous unloading of a number of elements greater than 2. The strategy being chosen, the management is simulated with the tricycle code, in order to define the actual dates of the successive loadings and the fluctuations of the power map. 3 references. (auth) (France)

3867 (DP-Report-476) UTILISATION OF FUEL RESOURCES IN DIFFERENT REACTOR TYPES. Project DRAGON. Marien, P. (Atomic Energy Establishment, Winfrith (England)). Aug 1966. 12p. Dep. NTIS.

The net amount of nuclear fuel consumed in existing reactors is inversely proportional to the average net burnup, and the amount required for the fuel cycle inventory of new plant is inversely proportional to the initial fuel cycle rating. The total annual fuel requirements are determined by the net burnup, the initial rating, the nuclear generating capacity, the average load factor and the rate of construction of new plant. The net burnup is defined as the ratio of the electrical energy produced to the net amount of fuel to be supplied for consumption. In the case of reprocessing fuel cycles the make-up fuel requirements only are considered in these studies. Different reactor types use different definitions for the rating and the burnup and this makes the comparison of the fuel requirements of a nuclear power programme, using different reactor types, difficult. In addition to the values quoted for rating and burnup, information is normally required concerning fuel enrichment, fuel composition, thermal efficiency, in-pile and out-of-pile fuel life. In order to eliminate these difficulties, more general definitions of burnup and rating are adopted and a fuel utilization factor is introduced which combines the consumption and investment fuel requirements. 13 references. (auth)

3868 (DP-Report-477) FUEL CYCLES IN HIGH TEMPERATURE REACTORS. THE INFLUENCE OF FUEL ELEMENT HETEROGENEITY ON A PARTLY ENRICHED URANIUM CYCLE. Project DRAGON. Blomstrand, J. H.; Bruneder, H. (Atomic Energy Establishment, Winfrith (England)). Aug 1966. 48p. Dep. NTIS.

The influence of fuel lumping in low enriched cycle on the fuel cycle performance is investigated for a high temperature reactor. 4 references. (auth)

3869 (DP-Report-478) FUEL CYCLES IN HIGH TEMPERATURE REACTORS. COMPLETE CORE REPLACEMENT AND PART RELOADED SYSTEMS IN THE $^{235}U/Th$ AND $^{235}U/^{238}U$ CYCLES. Project DRAGON. Bruneder, H. (Atomic Energy Establishment, Winfrith (England)). Aug 1966. 114p. Dep. NTIS.

Fuel cycles for high temperature are discussed and compared with each other. The data and a fairly detailed amount of results for homogeneous fuel cycles of a Complete Core Replacement or 4-zones management scheme are presented. Reprocessing with fuel segregation and no reprocessing is contemplated. 93% enriched ^{235}U is used as make-up fuel and Th as fertile material. In addition, homogeneous low enriched U cycles are studied without reprocessing. 19 references. (auth)

3870 (DP-Report-497) POST-IRRADIATION GAS RELEASE MEASUREMENTS ON FUEL ELEMENTS FROM THE FIRST 20 MW RUN OF THE DRAGON REACTOR. Project DRAGON. Aumueller, L.; Barr, P.; Pollitt, N.; Stow, G.; Vivante, C. (Atomic Energy Establishment, Winfrith (England)). Jan 1967. 22p. Dep. NTIS.

Measurements are presented of fission gas release from individual fuel compacts from 4 fuel elements irradiated for 100 days in the first 20 MW run of the Dragon Reactor. 9 references. (auth)

3871 (DP-Report-538) MEASUREMENT OF THE BURN-UP OF THE DRAGON FIRST CHARGE FUEL ELEMENTS USING GAMMA SPECTROMETRY. Project DRAGON. Bartlett, A. C.; Reed, D. L. (Atomic Energy Establishment, Winfrith (England)). May 1967. 51p. Dep. NTIS.

A sufficiently accurate, nondestructive method is described for estimating the burnup of the Dragon First Charge fuel elements based on the determination of the $^{95}Zr/^{95}Nb$ shutdown activity in the fuel by γ spectrometry. The measured burnup for each fuel element is compared to the predicted burnup and an average axial burnup profile is shown to be representative of the whole reactor core. 10 references. (auth)

3872 (DP-Report-559) THE COMPARISON OF CARBON-ATOM DISPLACEMENT RATE IN GRAPHITE IN THE DRAGON REACTOR, THE PETTEN HTR AND LOW ENRICHMENT HTR. Project DRAGON. Reed, D. L. (Atomic Energy Establishment, Winfrith (England)). May 1967. 42p. Dep. NTIS.

The way in which the physical behaviour of graphite irradiated in different reactors can be related to one another by using a common fast neutron dose scale is described. The dose scale used is achieved by converting the measured nickel or iron fast neutron dose to an equivalent fission dose (or fluence). A relationship is established between the carbon atom displacement rate and the equivalent fission flux. Using high energy neutron spectra calculated by a Monte Carlo method the carbon atom displacement rate per unit equivalent fission flux in DRAGON and the Petten HFR were respectively 1.51 and 1.75 times that in PLUTO (or DIDO). With the same methods of fast neutron spectrum calculation in a typical low enrichment HTR with a power density of 8 MW/m^3 it was found that the time required to reach a DIDO nickel dose of 2×10^{22} n cm^{-2} in the graphite moderator immediately adjacent to the fuel was 15.4 years. In addition the carbon atom displacement rate per unit equivalent fission flux in the moderator was found to vary between 1.46 and 2.26 times that in PLUTO (or DIDO). 11 references. (auth)

3873 (DP-Report-573) FUEL CYCLES IN HIGH TEMPERATURE REACTORS: THE THORIUM CYCLE IN ON-LOAD REFUELLED SYSTEMS. Project DRAGON. Blomstrand, J. H. (Atomic Energy Establishment, Winfrith (England)). Jun 1967. 155p. Dep. NTIS.

The thorium fuel cycle in on-load refuelled High Temperature Gas Cooled Reactors is described. Ways in which the fuel cycle performance is influenced by nuclear parameters, design parameters and fuel management are analyzed. The particular fuel cycles that can be expected to yield optimum performance are then established. A comprehensive analysis of these cycles with regard to both nuclear performance and economics is presented. This analysis covers cycles based on reprocessing as well as once-through cycles, the use of U-235 as well as plutonium as fissile make-up fuel and the use of a feed-breed fuel management as well as cycles based on a single type of fuel element. The results are intercompared and discussed. 15 references. (auth)

3874 (DP-Report-595) CALCULATION OF THE RELEASE OF FISSION PRODUCTS FROM COATED PARTICLES. Project DRAGON. Walther, H. (Atomic Energy Establishment, Winfrith (England)). Oct 1967. 30p. Dep. NTIS.

The steady state fractional release of fission products from coated particles has been calculated as a contribution both from mechanically intact particles and from broken particles, treated as bare kernels. This model is discussed for solid fission products because of the introduction of an evaporation term for the particle surface. Calculations for triplex coated fuel particles are presented. 24 references. (auth)

3875 (EURFNR-834) SOME CONSIDERATIONS ON COATED PARTICLES, WITH OXIDE FUEL, AND GRAPHITE AND SILICON CARBIDE COATING, FOR GAS-COOLED FAST REACTOR APPLICATION. Donne, M. Dalle; Schumacher, G. (Kernforschungszentrum, Karlsruhe (West Germany). Institut fuer Neutronenphysik und Reaktortechnik). Jul 1970. 35p. (EUR-4318; KFK-1254). Dep. NTIS (U. S. Sales Only).

Work Performed under United States-Euratom Fast Reactor Exchange Program.

Recently, coated particles with a SiC outer coating layer have been proposed for Gas Cooled Fast Reactor applications. SiC is a very fragile material. Although under fast irradiation it can creep at relatively low temperatures, a very low strain (>0.3%) can produce hairline cracks. A SiC coating layer can therefore withstand only moderate overpressures when subjected to large fast neutron exposures. The pressure inside the particle due to gas fission products and Co-CO_2 is calculated. The operation temperature of the particle due to the condition strain ≤0.3% is given as a function of SiC layer thickness in conditions typical for GCFR's application. 29 references. (auth)

3876 (RCN-123) CACES: AN ALGOL PROGRAM FOR SOLVING DIFFUSION TYPE ELLIPTIC DIFFERENTIAL EQUATIONS IN A PLANE INVOLVING ARBITRARY BOUNDARY CONDITIONS AND SHAPE. Vonka, V. (Reactor Centrum Nederland, Petten). Aug 1970. 68p. Dep. NTIS (U. S. Sales Only).

An ALGOL program is described which solves elliptic differential equations. These equations have to be of the diffusion type, i.e., no terms with mixed derivatives are allowed. They also can be non-linear. The coordinates consist of any pair of cartesian or cylindrical coordinates defining a plane. The method uses a two-level iteration procedure with overrelaxation factors, calculated either with Chebyshev or Legendre polynomials, and incorporates also an extrapolation facility. The program is very flexible through the use of additional problem oriented procedures. These can be read in on tape together with the main program. The complete text of the ALGOL 60 program is given with a description of the format of the input tape. (10 references) (auth)

3877 PROGRESS IN FUEL ELEMENTS FOR GAS-GRAPHITE REACTORS. Boudouresques, B. (CEA, Saclay, France). Bull. Inform. Sci. Tech. (Paris); No. 148, 3-11(May 1970). (In French).

The main changes which occurred in the design of fuel elements for gas-graphite reactors include: the adoption of Mg-Zr alloys as canning material for the G.2 and G.3 fuel elements, the choice of a tubular element for the Chinon 1 reactor, that of a jacket supporting the element in Chinon 2, and the development of annular and graphite core elements. The use of the latter type of element should make it possible to achieve very good performances as far as the level, the operational temperature and the reliability are concerned. (auth) (France)

3878 LIMITS IN THE USE OF TUBULAR GRAPHITE CORE AND ANNULAR FUEL ELEMENTS. Faussat, A. (CEA, Saclay, France). Bull. Inform. Sci. Tech. (Paris); No. 148, 55-65(May 1970). (In French).

The limits in the use of a fuel element are an important factor in the calculation of the price of the nuclear kWh. The best conditions to obtain maximum energy from fuel elements, compatible with the resistance of components and materials, and with the safety of the installation are reported. (auth) (France)

3879 RELIABILITY AND SAFETY OF FUEL ELEMENTS FOR GAS-GRAPHITE REACTORS. Ollier, H. (CEA, Cadarache, France). Bull. Inform. Sci. Tech. (Paris); No. 148, 67-79(May 1970). (In French).

Various types of fuel cladding failures are described. The results of observations made on failed elements in power reactors or on Pegase fuel rods are given. The failures due to fuel oxidation or to unsticking are described. The use of a graphite core made of low porosity graphite increases the reliability of the elements. (auth) (France)

3880 PREDICTION OF THE BURNOUT HEAT FLUX FOR ROD CLUSTERS. Nagai, Masayuki (Hitachi Ltd., Ibaraki, Japan). Hitachi Hyoron; 52: 439-43(May 1970). (In Japanese).

The purpose of this study is to investigate the burnout heat flux for rod clusters, and to find a new method of prediction. Many parameters relate to the burnout heat flux, and the effect of the parameters is investigated. The important parameters considered for the prediction are flow rate, boiling length, the minimum gap between fuel rods and the dimension of sub-channel under severe thermal conditions. An empirical formula for burnout heat flux is derived as a quadratic formula of the parameters by using least square fitting. The experimental data used to determine the formula are 1000 psia (70 atm) of pressure, more than 0.5×10^6 lb/ft^2 · h (2.4×10^6 kg/m^2 · h) of flow rate and 0 to 0.5 of outlet vapor weight rate. Formulas are obtained for outside fuel rods and for inside fuel rods separately. Experimental values are compared with the calculations from empirical formulas and are in agreement within ±10% of error. (Japan)

3881 EXTREMELY LONG PERIOD FUEL CYCLE. 2. MERIT OF POWER REACTOR DEVELOPMENT. Iinuma, Takamasa (Science and Technology Agency, Tokyo). Atomu; 15: No. 3, 40-66(Mar 1970). (In Japanese).

A study of fuel cycles for each power reactor type is presented. The amount of U required, the amount of U enrichment and separation, the amount of nuclear fuel fabrication and the amount of spent fuel reprocessing are analyzed. These amounts are calculated on an annual basis. In the calculations, the period is 60 years. (Japan)

XU

Auxiliary and Emergency Systems

3882 (DP-Report-487) THE MEASUREMENT OF SUB VPM LEVELS OF WATER AND HYDROGEN UNDER PLANT CONDITIONS USING A PRESSURISED GOLDSMITH ELECTROLYTIC HYGROMETER. Project DRAGON. Gray, P. S.; Gordon, I. (Atomic Energy Establishment, Winfrith (England)). Nov 1966. 15p. Dep. NTIS.

A pressurizable version of the Goldsmith and Cox hygrometer was developed and the variation of efficiency with working pressure and flow investigated. An improvement in efficiency was noted at higher working pressures and at pressures above 75 psia levels as low as 0.01 vpm can be measured. The use of the instrument was extended to the measurement of hydrogen by preoxidizing the hydrogen to water over hot copper oxide. Successful operating experience under plant conditions is described and some useful further developments, in the construction of the instrument, noted. (auth)

Operation and Economics

Refer also to abstract 3914.

3883 (DP-Report-466) PARAMETRIC SURVEY OF THE LOW ENRICHED URANIUM CYCLE IN A HIGH TEMPERATURE REACTOR. Project DRAGON. Mancini, G.; Schloesser, J.; Weicht, U. (Atomic Energy Establishment, Winfrith (England)). Apr 1967. 38p. Dep. NTIS.

The low enriched $^{235}U/^{238}U$ fuel cycle for high temperature gas cooled reactors was investigated using a modified version of the BASS program. The modifications were made to include the effects of thermal flux depression in large fuel cells and the effects of a heterogeneous fuel arrangement. Burnup and fuel cycle cost data are presented in which various core parameters were varied independently, and more detailed calculations are included for a reference core. (H.D.R.)

3884 (DP-Report-469) FUEL CYCLES AND REACTOR PHYSICS FEED/BREED AND OTHER THORIUM CYCLES. Project DRAGON. Schroeder, E. (ed.) (Atomic Energy Establishment, Winfrith (England)). Apr 1967. 65p. Dep. NTIS.

Fuel cycle and reactor physics analyses for thorium fuel cycles in HTGRs are summarized. Both once-through fuel cycles and fuel cycles with reprocessing are examined. Factors affecting the fuel cycle include: the effects of xenon override of fuel costs; temperature coefficient; control rod effectiveness; reactivity swing during loading; spatial xenon oscillation; and reactivity worth of the radial reflector. The relative merits and disadvantages of the various fuel cycle alternatives are discussed. 15 references. (H.D.R.)

3885 (DP-Report-546) THERMAL PERFORMANCE OF THE DRAGON REACTOR. Project DRAGON. Black, W. S. A.; Brown, C. L.; Green, I. S. (Atomic Energy Establishment, Winfrith (England)). Oct 1967. 68p. Dep. NTIS.

The results of performance measurements made during operation with the first charge of fuels are described. Both steady state and transient conditions are considered. (auth)

3886 (DP-Report-571) AN INTERIM REPORT ON FISSION PRODUCT DISTRIBUTION IN DRAGON AFTER THE FIRST 20 MW RUN. Project DRAGON. de Nordwall, H. J.; Brown, P. E.; Davis, I.; Heap, C. R. (Atomic Energy Research Establishment, Harwell (England)). Mar 1967. 54p. (AERE-M-1862). Dep. NTIS.

An overwhelming majority of fission products remained in their fuel particles. Of the few released, mainly from accidental contamination on the surface of the coated particles, only a small fraction left the fuel element. The utility of graphite as a canning material for surface temperatures up to 1050°C has been demonstrated on a satisfactory scale with fuel temperatures above those to be expected in a high temperature reactor operated on a Th fuel cycle. Neutron activation of impurities and steel constituents was responsible for more than 90% of the coolant circuit activities measured in a heat exchanger and a circulator. Neither operational safety, fission product release during a loss of coolant nor component maintenance are likely to be seriously influenced by releases at these levels. (auth)

3887 (DP-Report-575) A FUEL CYCLE THEORY WITH TWO COMPUTER PROGRAMMES FOR ON-LOAD REFUELLED THERMAL CONVERTER REACTORS. PART 1. A FUEL CYCLE THEORY. PART 2. TWO COMPUTER PROGRAMMES. Project DRAGON. Blomstrand, J. H.; Haubert, P. (Atomic Energy Establishment, Winfrith (England)). Jun 1967. 118p. Dep. NTIS.

A general fuel cycle theory for on-load refuelled reactors with special emphasis to thermal converters is derived from the neutron balance and the material balance conditions at fuel cycle equilibrium. The theory is applied to fuel cycles based either on a once-through fuel management or reprocessing and recycling of the recovered fissile material. Various modes of recycle are treated. The theory is generalized to fuel managements involving the use of more than one type of fuel element. The application of the theory to numerical analysis on digital computers is discussed. (auth)

3888 (DP-Report-581) SELF-SUSTAINING MIXED FAST AND THERMAL REACTOR SYSTEMS. Project DRAGON. Rennie, C. A. (Atomic Energy Establishment, Winfrith (England)). Jul 1967. 15p. Dep. NTIS.

A scheme is discussed for producing nuclear power, with a mixture of fast and thermal reactors, which is self-sustaining in fissile material once the initial fuel inventory has been supplied. One advantage of such a scheme is that it is flexible in its application to any required growth curve and that for a long time it needs less fissile material feed than either a purely fast or a purely thermal system. In addition, in this scheme, fast reactors which produce excess fissile material are always operated at as high a load factor as possible, in fact above the average load factor of the system as a whole, while the low load factor contribution is supplied by thermal reactors which always consume fissile material and, hence, are not as adversely affected by operating at lower load factors. Another advantage is that the cost of electricity generated by such a mixed system should be lower than that in an all fast or all thermal reactor system, and this is the most significant reason of all for considering such a scheme. (auth)

3889 (DP-Report-582) DRAGON OPERATIONS GROUP SEVENTH QUARTERLY PROGRESS REPORT, DECEMBER 1966–FEBRUARY 1967. Project DRAGON. Chapman, B. G. (Atomic Energy Establishment, Winfrith (England)). Jul 1967. 26p. Dep. NTIS.

Following the completion of the shutdown inspection and maintenance program, the reactor was started. Faults in the generator control system for the main circulators caused reactor shutdown on December 22, 1966. After a number of modifications to the circulator electrical supply system, the reactor was restarted on January 4, 1967. The reactor operated intermittently until February 22 when leaks in the primary heat exchanger tubes forced a shutdown to develop a method for plugging the tubes. The unscheduled shutdowns and unusual occurrences are tabulated. (H.D.R.)

3890 (DP-Report-592) DRAGON OPERATIONS GROUP EIGHTH QUARTERLY PROGRESS REPORT, MARCH 1967–MAY 1967. Project DRAGON. Chapman, B. G. (Atomic Energy Establishment, Winfrith (England)). Dec 1967. 15p. Dep. NTIS.

Various methods were investigated for plugging both ends of leaking tubes in the primary heat exchangers. The plugging was accomplished by the use of an expandable mechanical sealing plug, and a system for venting the helium leakage into the secondary circuits was designed and installed. Following reactor startup, a number of physics measurements and chemical impurity injection experiments were carried out. The unscheduled shutdowns and unusual occurences are summarized. (H.D.R.)

3891 (ORO-1171-1, pp 206-55) STATUS REPORT ON FAST BREEDER REACTORS (WHY BREEDERS). Melese-d'Hospital, Gilbert (Gulf General Atomic, Inc., San Diego, Calif.). (GA-10171).

From Proceedings of the symposium on thermonuclear fusion reactor design, June 2–5, 1970.

World reserves of low-cost uranium and growth of nuclear power require commercial fast-breeder reactors some time between 1980 and 1990. High-grain breeders consume small amounts of uranium and therefore will extend existing resources of economic fission fuels by orders of magnitude. While development work on fast breeders has been going on for approximately two decades, large electric-power-producing breeders are still some years in the future. Technical feasibility of fast breeders has been proven, but competitiveness of large breeders with more conventional fossil-fired or thermal-reactor plants is still to be demonstrated. Advanced breeders, such as gas-cooled fast reactors with carbide fuels and direct-cycle gas turbines, promise to have power costs comparable to the most optimistic estimates made for fusion reactors by the end of this century. (auth)

Safety and Siting

Refer also to abstract 2610.

3892 (BNWL-SA-3360) SOME OBSERVATIONS ON NOBLE GAS PARTITIONING IN DYNAMIC AIR-WATER SYSTEMS. Mishima, J.; Schwendiman, L. C. (Battelle-Northwest, Richland, Wash. Pacific Northwest Lab.). 25 Aug 1970. Contract AT(45-1)-1830. 17p. (CONF-700816-5). Dep. NTIS.

From 11th AEC Air Cleaning Conference, Richland, Wash.

Radioactive noble gases produced in fission would be released from reactor fuel elements which might fail from thermal stresses in the serious overheating incidents considered as design-basis accidents. Although in most design-basis accidents considered for reactor safety analysis iodine isotopes released prove to be the limiting isotopes; noble gas isotopes released in particular reactors and circumstances could contribute importantly to the dose to people at the site boundary. Suppression of steam following a serious meltdown in some water reactor designs is through quenching in a water system and the degree to which the noble gases remain in the water must be known to evaluate the significance of the noble gases released to the environment either in the water or in the air. Experiments were conducted to help determine to what degree and how rapidly krypton-85 dissolved in water will disengage in a few dynamic water–air systems and from stagnant pools. Krypton-85 carried in inert krypton was dissolved in hot water contained in an aluminum vessel with a very small air space. After equilibration, the vessel was discharged in various ways and the disengagement rate noted. Rate of release from stagnant water in small vessels was also measured. The "immediate" release upon gravity draining ranged from small amounts to over 40%. In quiescent shallow pools release to air varied with the surface/volume ratio and temperature regime. During a 2-hour cooling period the krypton loss ranged from 14 to 43% of that initially present. Liquid scintillation counting techniques were used to measure krypton-85 concentrations in the water phase. Methods and techniques are described. (9 references) (auth)

3893 (IITRI-578-P-21-39) WATER DECOMPRESSION EXPERIMENTS AND ANALYSIS FOR BLOWDOWN OF NUCLEAR REACTORS. Final Report. Gallagher, Edward V. (IIT Research Inst., Chicago, Ill.). Jul 1970. Contract AT(11-1)-578. 233p. Dep. NTIS.

Small-scale experiments that simulated blowdown of nuclear reactors were conducted, and analytical models were formulated to describe the idealized experiments. The experimental and calculated pressure-time variations compared well for the range of temperatures, pressures and geometries treated. The range of these parameters was representative of prototype commercial water-cooled reactors. The conclusions reached were generally consistent with those being developed from larger scale experiments in the LOFT program allowing for differences in emphasis on specific parts of the blowdown problem. The hydrodynamic forces during blowdown are found to be governed largely by nonsteady, sonic choking. One-dimensional, nonsteady, frictionless flow gives a good approximation to the blowdown process. An isentropic-equilibrium-expansion path represents a very good approximation to the equation-of-state for blowdown and metastable pressures temporarily below equilibrium values either are not present, or are unimportant. For ruptures having flow area much larger than that at the rod bundle (simulated core) ends, the time-dependent net load on the core corresponds roughly to the decaying saturation pressure level of the fluid upstream. For rupture sizes smaller than the flow area at the core constriction, net loads on the core are the order of only a few hundred psi or less. The effects of heat addition from the rod bundles upon net load on the core were not significant for the low-magnitude energy input rates treated in these experiments (approximately decay heat levels). However, at higher input rates (say full prototype rate) heat addition from rods might produce higher net load, particularly for small rupture sizes. (16 references) (auth)

3894 INDUSTRIAL EXPERIENCE WITH FUEL ELEMENTS AND ACTIVATION IN THE BOILING WATER REACTORS. Engel, H. (Allgemeine Elektricitaets-Gesellschaft, Frankfurt am Main). Atomwirt., Atomtech.; 15: 523-7(Nov 1970). (In German).

In a nuclear power plant, the reactor core represents the main source of radioactivity. Especially important are fission products in fuel elements that escape into the primary cooling circuit because of cladding defects. Experiences about the treatment of radioactivity emission from a nuclear power station are closely associated with the operational behavior of fuel elements. Only of minor significance is the problem, typical for boiling water reactors, of direct radiation-induced activation caused by the primary circuit within the turbine circuit that may lead to contamination of components. (tr-auth)

3895 DETERMINISM AND STATISTICS IN REACTOR SAFETY. Knecht, O. (INTERATOM Internationale Reaktorbau GmbH., Bensberg, Ger.). Atomwirt., Atomtech.; 15: 528-30 (Nov 1970). (In German).

Problems of reactor safety are discussed from the standpoint of determinism and probability. In the case of serious reactor accidents, radiation detectors should indicate doses prevailing within the containment vessel. Instruments for such high dose rates, however, are not available commercially. They should be designed for pressure and temperature conditions existing in serious reactor accidents. 10 references. (H.B.G.)

3896 COMMENTS ON DETERMINISM AND STATISTICS IN REACTOR SAFETY. Merz, L. Atomwirt., Atomtech.; 15: 530-1(Nov 1970). (In German).

Reactor safety is discussed from the standpoint of determinism and probability. In deterministic considerations, single events form the focal point and require analysis for causative determining factors. In probability considerations, the single event is considered as part of a collective system. Thus, reactor accidents can be considered either from the standpoint of determinism as single events or from the standpoint of probability as constituent of a large entity. (H.B.G.)

Power Conversion Systems

3897 (DP-Report-591) PRESSURE DROP MEASUREMENTS MADE ON A DRAGON HEAT EXCHANGER FITTED WITH VARIOUS DESIGNS OF WATER CATCH-POT. Project DRAGON. Woodley, H. J. (Atomic Energy Establishment, Winfrith (England)). Dec 1967. 26p. Dep. NTIS.

Experimental work carried out in order to optimize the design of a device which can be fitted into Dragon heat exchangers in order to contain the water contents of the section of the secondary circuit concerned, in the event of failure of one or more of the heat exchanger tubes, is described. The final design of catch-pot consisted of a length of 5¼ in. OD by 5 in. ID tubing with a conical section welded to the lower end, the overall length being 36 in. If used this device would be welded in position at the lower end of the heat exchanger. Water would be contained in the annulus formed by the tube and the heat exchanger casing. This design of catch-pot, at room temperature and with a standard helium flow of 3.5 lb/s, caused a maximum increase in pressure drop of 0.85 psi across the heat exchanger. It is estimated that this value would increase to 1.385 psi when the temperature of the helium flowing into the heat exchanger is 730°C. (auth)

3898 EXAMPLES OF DIFFERENCES BETWEEN STEAM GENERATORS FOR CONVENTIONAL AND NUCLEAR POWER PLANTS. Mutke, R. (Vereinigte Kesselwerke AG, Duesseldorf, Ger.). Mitt. Ver. Grosskesselbetr.; 49: 145-53(Jun 1969). (In German).

Construction of steam generators is discussed for conventional fossil fuel plants and nuclear power stations. In the former, heat transfer occurs from gases at high temperatures and close to atmospheric pressure. In the latter, heat exchange depends on the reactor type and occurs at various pressures and temperatures. Steam generators are discussed for gas-cooled, water-cooled, and sodium-cooled reactors. Design and manufacturing of heat exchangers for the three reactor types are outlined as well as operating experience obtained in West Germany. (5 references) (H.B.G.)

3899 NUCLEAR WET-STEAM TURBINES. Harris, F. R. (AEI Turbine Generators Ltd., Manchester, Eng.). Proc. Inst. Mech. Eng. (London); 183: 14-24(1968-69).

From Convention Arranged by the Steam Plant Group, London, England. See CONF-690445.

Turbines which operate on steam initially slightly wet are required by several varieties of nuclear reactor at present in service. Such turbines differ substantially from conventional fossil-fuel turbines and special measures are necessary to avoid erosive damage and to achieve reasonable efficiency. Water separation by various methods during the expansion is universal, and steam-to-steam reheat is common. Some reactors produce radioactive steam with a high oxygen content, requiring further precautions. Examples are given of wet-steam turbines already in service, and under construction, and estimates are made of the limiting ratings that can at present be contemplated. (auth) (UK)

3900 BOILERS FOR NUCLEAR PLANT. Holmes, R. L. (Clarke, Chapman and Co. Ltd., Durham, Eng.); Southwood,

XU

J. R. M.; Whitehouse, P. R. Proc. Inst. Mech. Eng. (London); 183: 64-70(1968-69).

The development of heat exchangers for gas-cooled reactors is reviewed, indicating the influence that the reactor design has had on the Magnox system and, more recently, on the reactors of the advanced gas-cooled type. The possible line of development of boilers for the proposed High-Temperature Reactor is discussed which is the logical development of the present A.G.R. system. Particular problems such as the choice of tube surface and the preferred method of fabricating individual units are described. Other items discussed are the choice of tube material for the developing gas conditions, the problem of control in once-through systems, and the problem of operation with varying load conditions which will arise when the installed nuclear capacity exceeds the base load. Reference is also made to the degree to which boiler units of the above type can be fabricated in other countries. (auth) (UK)

Research and Test Reactors

Refer also to abstracts 2497, 2645, 2705, and 3851.

3901 (ANL-7442) FINAL SAFETY ANALYSIS REPORT ON THE USE OF PLUTONIUM IN ZPR-6 AND -9. Kato, W. Y.; Rusch, G. K.; Dates, L. R.; Till, C. E.; Ancarani, A.; van Doorninck, J.; Cheever, C. L.; Bohn, E. M. (Argonne National Lab., Ill.). Feb 1970. Contract W-31-109-eng-38. 270p. Dep. NTIS.

The split-table type critical facilities, ZPR-6 and -9 are described. The modifications which were made to the reactor cells and facilities are discussed. The hazards associated with the use of up to 1400 kg of plutonium fuel in each of the facilities are analyzed. Reactor operating procedures and the principles of reactor management are discussed in detail. A discussion of a maximum credible accident and a design basis accident is presented. (auth)

3902 (BNWL-1514) ANALYSIS OF THE PHOENIX FUEL EXPERIMENTS. Heeb, C. M. (Battelle-Northwest, Richland, Wash. Pacific Northwest Lab.). Oct 1970. Contract AT(45-1)-1830. 87p. Dep. NTIS.

A depletion experiment on a Pu-Al-alloy fueled core in the Materials Testing Reactor (MTR) is described. The supporting integral experiments and the installed neutronic behavior of this "Phoenix core" are described briefly. The analysis of these experiments is described in detail. It was found that increasing the absorption of the 1 eV ^{240}Pu resonance to agree with measured k_∞ values results in eigenvalues which are within 1% of the experimental values over a range in ^{240}Pu concentrations from 8% to 23%. The observed reactivity time behavior of the core shows a more abrupt loss of reactivity with time than had been calculated. A method of partitioning the computed reactivity time slope is presented which defines the contribution each burnable isotope makes to the total slope. A comparative analysis of two methods plus nuclear data is carried out using this technique to illustrate the complexities involved in burnup analysis. (30 references) (auth)

3903 (CEA-N-1348) THE NATURAL-CONVECTION IRRADIATION DEVICE "ESTHER." Leclere, Jacques; Lhermenier, Andre; Fages, Denis; Lauthier, Jean-Claude (Commissariat a l'Energie Atomique, Fontenay-aux-Roses (France). Centre d'Etudes Nucleaires). Oct 1970. 47p. (In French). Dep. NTIS (U. S. Sales Only).

In order to perform radiation experiments on fast reactor fuels, a device which was to be used in the Siloe and Osiris swimming pool reactors was designed and constructed. The Ester device is characterized by natural convection cooling. The temperature distribution is analogous to that in a reactor channel. The temperature is adjusted by a variable thermal barrier. The flux level is increased by moving towards the core. This device can dissipate between 800 and 900 W/cm. Its main interest lies in the circulation of Na or NaK along the fuel element. (auth) (France)

3904 (IJS-571) COLD NEUTRON SOURCE EFFICIENCY IN A TANGENTIAL BEAM HOLE. Dimic, V.; Petkovsek, J. (Institut Jozef Stefan, Ljubljana (Yugoslavia)). Nov 1969. 11p. Dep. NTIS (U. S. Sales Only).

Cold neutron beam intensity has been measured for differently shaped moderator chambers at different positions in a 15 cm diameter tangential beam hole of the reactor Triga Mark II. Measurements have been performed at ambient temperatures. It has been found that the most favourable configuration for moderator is a "black body" scatterer with a gain factor 19 relative to the empty beam hole and 1.7 relative to 15 cm long graphite slab. The cold neutron source inserted into the tangential beam hole is described. Measurements of the gain factor for a graphite slab, methyl alcohol and methane are discussed. 14 references. (auth)

3905 (IN-1441) ULTRASONIC VOID FRACTION DETECTOR USING COMPRESSIONAL STRESS WAVES IN A WIRE HELIX. Arave, A. E. (Idaho Nuclear Corp., Idaho Falls). Oct 1970. Contract AT(10-1)-1230. 18p. Dep. NTIS.

An ultrasonic void fraction detector to measure steam voids in water is being developed for the Loss of Fluid Test (LOFT). The detector is a 3/16 inch wire wound into a 6 turn, ¼ inch diameter, 4 inch long helix. The attenuation of a 200 Hz compressional stress wave as it propagates in the helix is a function of the void fraction at the helix surface. A magnetostrictive transducer is used on one end of the helix as a transmitter and another on the other end as a receiver. (auth)

3906 (JAERI-Memo-4130) ANALYSIS OF JMTR FLUX VARIATION DURING OPERATION. Tanaka, Toshiyuki; Omura, Tatsuro; Fukuda, Toru (Japan Atomic Energy Research Inst., Tokyo). Aug 1970. 53p. (In Japanese). Dep. NTIS (U. S. Sales Only).

Neutron flux variation during reactor operation with small size cores is influenced by reactor control rod position change, fuel burnup, etc. In order to solve this problem in JMTR, attention is paid to shim rod arrangement and the withdrawal sequence. The analysis of neutron flux change and the variational effects in irradiation holes are calculated. These results are compared with those of in-core irradiation experiments and JMTR physics experiments for their evaluation. The calculational model is accurate and JMTR neutron flux variation is at most from 10 to 20% in ordinary irradiation holes. If attention is paid to Xe buildup processes, the variational factor is about 10%. (auth) (Japan)

3907 (NP-18462) USE OF THE GRENOBLE HIGH FLUX REACTOR IN BIOLOGY. Duee, Emile D. (Grenoble Univ. (France). Faculte des Sciences). 1970. 24p. (In French). Dep. NTIS (U. S. Sales Only).

Thesis.

After some remarks on the subject of neutron diffraction, with special reference to biological uses, the possibilities of applying this method to the determination of protein structure are examined on the basis of already published experimental results. Because of the nondestructive nature of neutrons for proteins, neutron diffraction is an ideal method for the study of proteins of high molecular weight which are difficult to crystallize and very sensitive to x rays. The advantages of the equipment foreseen for the Grenoble high flux reactor are discussed. 30 references. (auth) (France)

3908 (WHAN-FR-18) CCTL MARK I AND MARK II PROTOTYPIC FFTF SUBASSEMLY COMPRESSION TEST DEVELOPMENT WORK. Baker, R. B.; Blahnik, D. E. (Battelle-Northwest, Richland, Wash. Pacific Northwest Lab.). Aug 1970. Contract AT(45-1)-1830. 74p. Dep. NTIS.

For WADCO Corp., Richland, Wash.

The subassembly compression test work performed by the FFTF Fuels Department on fuel subassemblies with 217 wire-wrapped fuel pins is discribed. These ductless subassemblies were compressed over a 4-foot length span by flat plates on six sides, and the side wall load was measured as a function of across-the-flats dimensions. The subassemblies were compression tested to determine the springiness that exists within the subassembly when it is compressed symmetrically from a nominal duct internal size down to a region where there are no gaps between wires and fuel cladding and where the fuel pins are temporarily deformed due to bending and torsion loads. (auth)

3909 HYDRODYNAMIC STIMULATION OF VIBRATIONS AND THEIR STABILIZATION IN THE CORE OF THE GRENOBLE HIGH FLUX REACTOR. Hein, D. (Maschinenfabrik, Augsburg, Ger.); Kloepper, H.; Mayinger, F. Atomwirt., Atomtech.; 15: 541-2(Nov 1970). (In German).

To study the behavior of fuel elements in the Grenoble high flux reactor, a full-scale model of the core was constructed. The experimental arrangement permitted water flow rates up to 2,000 m^3/hr. By means of sensitive detectors, lateral movement of the fuel elements were recorded as was the pressure on the supporting surface. Experimental results showed that hydraulic centralization of the fuel elements satisfied all requirements and that the fuel element support was not excessively strained even through highly variable forces. (H.B.G.)

3910 THERMOHYDRAULIC DESIGN OF THE REFLECTOR SPACE IN THE GRENOBLE HIGH FLUX REACTOR. Hein, D. (Maschinenfabrik, Augsburg, Ger.); Kloepper, H.; Mayinger, F. Atomwirt., Atomtech.; 15: 538-9(Nov 1970). (In German).

The Grenoble high flux reactor involves such a high neutron flux that the core must be compact. Sufficient and safe removal of heat demands a high velocity of the cooling medium in the core. In the reflector space into which the radiation channels penetrate, however, the fluid velocity must be low and free of turbulence. Problems arising in this connection are studied theoretically and examined experimentally. (H.B.G.)

3911 BRITISH HIGH FLUX BEAM REACTOR. Engelstaff, P. A. (Atomic Energy Research Establishment, Harwell, Eng.). Nature (London); 228: 324-8(24 Oct 1970).

A review is given of the reasons for proposals for such a reactor, together with the history leading to these proposals. The main reason is to provide a reactor better suited to the application of neutron scattering techniques in the study of condensed matter. The present proposal relates to a reactor having 12 horizontal beam holes fed by different neutron sources, together with several inclined holes. A limited number of irradiation facilities is also provided. It is proposed to operate the reactor at 100 MW, with a maximum available flux of 1.5×10^{15} $n/cm^2/sec$. The fuel is an Al–U alloy and the coolant is heavy water at 28.2×10^4 kg/m^2. The instrumentation and neutron beam programme are briefly described. The proposed studies include atomic distributions in crystals, magnetization distributions and liquid structure, crystal lattice vibrations, liquid dynamics, molecular dynamics, and defect and domain scattering. (UK)

3912 EXPERIMENTAL STUDIES ON 20 PER CENT ENRICHED URANIUM-LIGHT WATER ASSEMBLY. 3. CRITICAL BUCKLING MEASUREMENTS. Mitake, S.; Watarumi, C.; Miyawaki, Y.; Takeda, E. (Tokyo Inst. of Tech.). Bull. Tokyo Inst. Technol. (Engl. Ed.); No. 96, 1-21(Mar 1970).

The experiment performed on 20% enriched U light water subcritical assembly is reported. The experimental procedures used are the exponential pile method and the substitution method. Experimental results were analyzed by the fitting with hyperbolic function besides the usual exponential function. In the analysis for the exponential experiment the neutron flux distribution inside a homogeneous sub-critical assembly having a plane source at the bottom was considered, and the buckling of the system was obtained. Axial flux distribution and Cd ratio were measured, and the measured flux distribution was in good agreement with theoretical calculation. Transversal flux distribution curve was also obtained. Reflector saving value was determined by the U density in the core. Critical buckling B_c^2 and critical mass were calculated. In the substitution method, the central part of a nuclear assembly having known characteristics is replaced by another system having the same constitution with the reactor core to be investigated. Theoretical and experimental analyses were performed. This method was consistent with the exponential method. (Japan)

Rocket and Space Reactors

Refer also to abstracts 2601 and 2677.

Process Heat and Desalination Reactors

Refer also to abstract 2644.

3913 (ORNL-NDIC-8) TITLE-AUTHOR-COMPANY INDEX TO REPORTS PUBLISHED BY THE U. S. DEPARTMENT OF THE INTERIOR, OFFICE OF SALINE WATER. Johnsson, K. O. (Oak Ridge National Lab., Tenn.). Nov 1970. Contract W-7405-eng-26. 84p. Dep. NTIS.

A permuted index of the titles, authors, companies, and numbers of the approximately 575 research and development progress reports issued by the Office of Saline Water, U. S. Department of the Interior, through July 1970 is presented. The index was prepared with the aid of a computer and is presented in the form of computer printout. (auth)

3914 POWER BOUNDARY LIMIT BETWEEN REACTOR HEAT OUTPUT AND PROCESS HEAT AND ELECTRICITY. Bortlik, Jiri (Power Research Inst., Prague). Jad. Energ.; 16: 253-5(Aug 1970). (In Czech).

With the step-wise development of nuclear power the heat delivery from nuclear sources comes to the fore. The fundamental principle is the power boundary limit between a nuclear heating station and a nuclear heat and power plant that influences substantially the whole concept of central heat supply. The results of calculations of capacity limits of nuclear heat and power plants are discussed. The effects of individual basic input data of the evaluated heating system are indicated, together with technical and economic evaluation. (auth)

3915 MULTI-PURPOSE UTILIZATION OF NUCLEAR REACTORS IN CHEMICAL INDUSTRY. Tsujii, Junro (Ube Industries, Ltd., Yamaguchi, Japan). FAPIG (Tokyo); No. 54, 114-23(Sep 1969). (In Japanese).

The following are described: introduction of nuclear energy into chemical plants; high-temperature gas cooled reactors; molten salt reactors (the features in the respects of fuel-utilization efficiency, economy and safety); an agro-chemical complex by nuclear energy, utilizing desalination of water, and fertilizer manufacture; and problems with multi-purpose utilization of nuclear reactors (and also an industrial-complex project in Japan). (Japan)

3916 INTRODUCTION OF NUCLEAR REACTORS IN IRON MANUFACTURE INDUSTRY. Ando, Masao (Kobe Steel, Ltd., Japan). FAPIG (Tokyo); No. 55, 166-71(Dec 1969). (In Japanese).

The utilization of nuclear energy (HTGR) for iron manufacture is described. If a UHP (high-power electric furnace), with low-cost power from a nuclear reactor is utilized, the economic prospects are promising. The alternative is a combination of blast furnace and nuclear reactor. Advantages are a reduction in coal consumption and the use of an existing facility. But, there is the drawback of having to develop suitable heat-exchanger materials because of the high temperature of a reducing gas. (Japan)

Marine and Portable Power Reactors

Refer also to abstract 2683.

3917 (DOCKET-50238-74) N. S. SAVANNAH. Furnace Sensitized Stainless Steel, Additional Information. (First Atomic Ship Transport, Inc., New York). 13 Nov 1970. 10p. Dep. NTIS.

3918 PROIZVODSTVO SUDOVYKH REAKTOROV I PAROGENERATOROV. (Production of Marine Reactors and Steam Generators). Man'ko, P. A.; Soloimskii, B. E. Leningrad; Izdatel'stvo Sudostroenie (1969). 220p.

The technological developments in the production of the main structures and operating systems of ship reactors and steam generators, their design, construction, biological protection, and certain questions of reliability are examined. The main parameters of nuclear power plants and the contemporary construction of reactors and steam generators are described. Special attention is devoted to the consideration of construction materials used in heat exchangers, to methods of arrangements of tubes in tube sheets, and to quality control methods. 43 references. (tr-auth)

3919 NESTATSIONARNYE REZHIMY SUDOVYKH YADERNYKH NARO-PROIZVODYASHCHIKH USTANOVOK. (Non-Stationary Operation of Marine Nuclear Steam-Producing Installations). Mitenkov, F. M.; Motorov, B. I. Leningrad; Izdatel'stvo Sudostroenie (1970). 200p.

The mathematical modeling of transient and emergency operation of ship power plants using water cooled reactors is described. The selection and basis of models for engineering studies of non-stationary operation by using digital computers are discussed. Recommendations are given for the practical application of proven models. The basis for simplification of calculations of characteristics of various ship reactor systems are analyzed. 92 references. (tr-auth)

Production Reactors

3920 (BNWL-B-8) N-REACTOR HYBRID SIMULATION. Lodge, J. D. (Battelle-Northwest, Richland, Wash. Pacific Northwest Lab.). Oct 1970. Contract AT(45-1)-1830. 82p. Dep. NTIS.

The overall simulation model of N-reactor has been converted from an all-analog model to a hybrid model. The entire secondary system is simulated on the PDP-7 digital computer, while the primary system, which includes the reactor core, primary flow and pressurizer, is modeled on the 2133 analog. All control is done with the analog controller simulator. Programming and operating procedures for the hybrid model are included. (auth)

3921 (DUN-SA-144) TESTING AND SURVEILLANCE OF HANFORD PRODUCTION REACTOR ZIRCALOY TUBES. Al-

XUM

exander, W. K. (Douglas United Nuclear, Inc., Richland, Wash.). 13 Oct 1970. Contract AT(45-1)-1857. 14p. Dep. NTIS.

A description of nondestructive tests performed on Zircaloy tubes in the K Reactors is presented. Results of the tests are analyzed. Surveillance and destructive testing programs for Zircaloy tubes in the N Reactor are described. Tests results are presented. (D.C.C.)

Reactor Theory

Refer also to abstract 3528.

Kinetics

Refer also to abstracts 3857, 3859, and 3880.

3922 (ANL–7696) SOME IMPROVEMENTS IN VARIATIONAL FLUX SYNTHESIS METHODS. Woodruff, William L. (Argonne National Lab., Ill.). May 1970. Contract W-31-109-eng-38. 132p. Dep. NTIS.

Three synthesis models are proposed which reflect a consistent application of the semidirect method of the calculus of variations and the various suggested improvements. Although the emphasis is on flux synthesis in space-time neutron-diffusion theory, the concepts and methods can be applied to any diffusion or transport problem. The methods can also be applied to static flux synthesis problems. A brief introduction to the calculus of variations in areas relevant to the flux-synthesis problem is provided. The neutron-diffusion theory problem is presented, and the basic continuous variational formulation is discussed. Some of the early work with discontinuous models for space synthesis is reviewed. The time and space-time models are discussed. Consideration of external boundary conditions and the inclusion of delayed neutrons are analyzed. (51 references) (auth)

3923 (BNWL–1412) USER'S MANUAL FOR THE 1DX–2DB–3DB–PERT-V CODE PACKAGE. Hardie, R. W.; Little, W. W. Jr. (Battelle-Northwest, Richland, Wash. Pacific Northwest Lab.). Jul 1970. Contract AT(45-1)-1830. 83p. Dep. CFSTI.

The 1DX, 2DB, 3DB, and PERT-V codes have been programmed to read and write standard interface files containing groups of similar data. These data files and their use by the above codes are presented. Briefly, 1DX is a one-dimensional diffusion theory program designed to compute resonance shielded multigroup cross sections using data in the "Russian" format and collapsed-group cross sections using flux-weighting over any specified reactor zone. 2DB and 3DB are two- and three-dimensional diffusion theory burnup codes containing a material shuffling scheme. The above codes also perform criticality searches on time absorption, reactor composition, reactor dimensions, and buckling using either a flux or adjoint model. PERT-V is a one- and two-dimensional perturbation code designed to calculate reactivity coefficient traverses, the effective delayed neutron fraction, the neutron generation time, and the inhour/δk conversion factor. All codes are programmed in FORTRAN-4 for a 65K core and utilize variable dimensioning. 6 references. (auth)

3924 (CNAEM–73) NORDHEIM EQUATION ACCORDING TO P_1-APPROXIMATION. Ertek, Cetin; Gencay, Sarman; Guersu, Yurtcan (Cekmece Nuclear Research Center, Istanbul (Turkey)). Dec 1969. 10p. Dep. NTIS (U. S. Sales Only).

A Nordheim type equation relating the reactivity to the stable and transient periods of the reactor is established in the frame of P_1-approximation. Its characteristics are investigated and compared to the same kind of equation given by elementary diffusion theory. (auth)

3925 (DP–1238) CALCULATION OF RELATIVE REACTION RATES IN INTERACTING CYLINDRICAL CELLS. Clark, Hugh K. (Du Pont de Nemours (E. I.) and Co., Aiken, S. C. Savannah River Lab.). Sep 1970. Contract AT(07-2)-1. 43p. Dep. NTIS.

A computer program, written in FORTRAN 4, is described for calculating relative reaction rates in reactors composed of interacting cylindrical cells of different types, and the input requirements are listed. The program, INCYCE, permits intracell transport of neutrons to be calculated either from collision probabilities or from the assumption of a cosine distribution for the currents at all interfaces. Intercell transfer of neutrons is calculated on the basis of the assumption that the current entering or leaving a cell has a cosine distribution and that the current leaving a cell is uniform. Comparison is made with some critical experiments. The agreement in terms of buckling and ratios of thermal neutron densities is fairly good. (9 references) (auth)

3926 (EIR–166) CORONA: A PROGRAM FOR TWO-GROUP CONTROL ROD CALCULATIONS IN A REFLECTED REACTOR. Juillerat, T.; Koehler, P.; Lerch, C. (Eidgenoessisches Institut fuer Reaktorforschung, Wuerenlingen (Switzerland)). May 1970. 27p. Dep. NTIS (U. S. Sales Only).

CORONA (Control Rod Analysis) calculates the effective multiplication constant and two-group fluxes in a cylindrical reactor with fully or partially inserted control rods. The fuel lattice, which must be homogenized, may be surrounded by a radial reflector. Material properties in the axial direction are assumed constant. No control rods are allowed in the reflector. The method of solution is based on the heterogeneous theory with diffusion theory being used in core and reflector. Boundary conditions at control rod surfaces make use of effective extrapolation lengths which must be supplied to the program as input parameters. The theory on which the program is based is outlined and ALGOL and FORTRAN input schemes are described. A sample output is presented. (auth)

3927 (JAERI-Memo–4109) PULSED NEUTRON RESEARCH IN JAPAN (FROM 1965 TO 1970). Kaneko, Yoshihiko; Sumita, Kenji (Japan Atomic Energy Research Inst., Tokyo). Aug 1970. 27p. Dep. NTIS (U. S. Sales Only).

The activities in the field of pulsed neutron research in Japan since 1965 are reviewed. The activities are reviewed in the following five chapters: (1) neutron slowing-down and thermalization in reactor materials; (2) application to multiplying media; (3) neutron wave and pulse propagation; (4) time of flight experiment by use of electron linear accelerator; and (5) pulsed reactors. (40 references) (auth) (Japan)

3928 (JAERI-Memo–4110) GROUP STRUCTURE AND ACCURACY OF GROUP CONSTANTS IN THE VICINITY OF 2.85-keV RESONANCE SCATTERING OF SODIUM. Tone, Tatsuzo; Hasegawa, Akira (Japan Atomic Energy Research Inst., Tokyo). Aug 1970. 38p. (In Japanese). Dep. NTIS (U. S. Sales Only).

Interrelations between group structure and the accuracy of group constants in the vicinity of the 2.85 keV resonance scattering of sodium were examined, mainly based on the JAERI group-constant set. Large differences of elastic removal cross section were observed between 70- and 25-group structures. The differences bring larger variations in k_{eff} than in sodium void effect, and the results obtained from fine-spectrum calculations show that σ_{er} from 70-group structure is better than from 25-group structure. (25 references) (auth) (Japan)

3929 ANALYTICAL STABILITY CRITERIA FOR SPACE-DEPENDENT SYSTEMS. Crawford, Raymond Maxwell Jr. Los Angeles; Univ. of California (1969). 216p. University Microfilms Order No. 70-8125.

Thesis.

The space-time behavior of nuclear reactor systems governed by a set of coupled, nonlinear, partial differential equations is considered. A stability theorem and several corollaries are presented and proved using the methods of functional analysis and the theory of semi-groups. The three reactor models specifically developed and considered are the Simple Temperature Feedback Model, the Adiabatic Model, and the Prompt Feedback Model. Although the stability theorem can be applied to more general cases, these three models were specifically considered as illustrative examples. In each case, a sufficient condition for stability, and an upper bound for the solution norm was obtained. The Prompt Feedback Model was considered in particular detail. This model was used to compare various methods of stability analysis. The Point Kinetics reduction, the Lyapunov method, the Comparison function method, and the Semi-Group method were used in this comparison. It is shown that the Semi-Group method can be applied directly to the system equations to obtain both a criterion of stability and a realistic solution estimate. The solution estimate was subsequently compared to the actual numerical solution obtained using a modified version of WIGLE. In all cases considered this comparison verified that the Semi-Group method does indeed yield an upper bound for the solution transient following an initial system perturbation. (Diss. Abstr.)

3930 MINIMAL-ERROR FEW-GROUP CRITICAL MASS DETERMINATION. Harms, A. A. (McMaster Univ., Hamilton, Ont.); Johnson, R. D. J. Nucl. Sci. Technol. (Tokyo); 7: 539-41(Oct 1970).

A programming methodology to aid in the specification of an optimal few-group energy segmentation in reactor calculations is discussed. An application of the programming formalism for maximum numerical accuracy and minimum computation time is presented for a few-group criticality calculation. Results are compared to those obtained by an alternative procedure of specifying energy groups. 7 references. (D.C.C.)

3931 INSTRUMENT FOR ANALYSIS OF NEUTRON CORRELATION WITH SHIFT REGISTERS. Murata, Y. (Musashi Inst. of Tech., Tokyo); Izumi, A. Nucl. Instrum. Methods; 87: 261-72(1970).

A new method and an instrument for measuring neutron fluctuation in a thermal neutron multiplying system are reported in the present paper. In former experimental techniques, such as Feynmann-α and Rossi-α, only a part of the information on neutron fluctuation was analyzed. On the other hand, the new method is based on recognition of the pattern of neutron pulses in the time domain. The recorded data in the magnetic core are analyzed in various forms of neutron correlation with a computer; moreover, information of a higher order than that which has been measured up to the present, can be obtained. The instrument is basically composed of shift-registers and a core-memory of 4K words. It can recognize 4096 kinds of correlated patterns. Wide application of the instrument is expected in experiments of neutron fluctuation. (auth)

Experimental Applications

3932 REACTOR NEUTRON FLUCTUATION SIMULATOR USING PULSED NEUTRON SOURCE. Yasuda, Hideshi; Sumita, Kenji (Osaka Univ). J. Nucl. Sci. Technol. (Tokyo); 7: 527-33(Oct 1970).

The fission phenomena in a multiplying medium are simulated by neutron bursts in a non-multiplying medium produced by a pulsed neutron source. To simulate the chain reaction, the pulsed neutron source is triggered by neutronic signals from a detector installed in that medium. The kinetic parameters can be changed at will by regulating the detector sensitivity, the system medium and the burst yield of the pulsed neutron source. This simulator has been tested on experiments with Rossi-α, Feynmann-α and pulse die away methods and is also applied to the experiments with waiting time method and observation of neutron families to verify the recently developed theory in this domain. The results prove that, in principle, the number of neutrons in this simulator can represent the probabilistic nature of the neutrons in a multiplying medium described by one point model. Furthermore, the newly developed theory for reactor parameter measurement has been substantiated with use of the simulator. The simulator in its present form is restricted in applicable range to $k_{eff} = 0 \sim 0.66$ by limitations in the performance of the pulsed neutron source used. 5 references. (auth)

Reactor Components, Fuels, and Accessories

Refer also to abstracts 2379, 2386, 2392, 2395, 2411, 2502, 2601, 2602, 2758, 2762, 2770, 2780, 2795, 2813, 2817, and 3226.

3933 SIMULATOR FOR BWR TYPE TSURUGA NUCLEAR POWER STATION. Tachibana, Akira (Japan Atomic Power Co., Tokyo); Matsuda, Hiroyoshi; Kai, Takaaki; Kubota, Narinobu; Sugiyama, Sakae. Hitachi Hyoron; 52: 412-18(May 1970). (In Japanese).

A training simulator is installed at Tokai Training Institute to provide realistic training for the men operating BWR type Tsuruga nuclear power station. The simulator is the combination of a control board and an analog computer, and utilizes a part of the simulator already installed for Tokai Nuclear Power Plant. The control board contains the controls for a reactor and primary systems, the operation of control rods, the controls for feed water and recirculation flow, and the operation of auxiliary equipment. The graphic panel is adopted so that trainees may operate and watch the simulated system simultaneously. This simulator has three operational modes: start up range mode, intermediate range mode, and power range mode. (Japan)

GENERAL

3934 (ANL-Trans-862) CONSTANT ELECTRICAL FIELD SURFACES. Felici, Noel. Translated for Argonne National Lab., Ill., from Rev. Gen. Elec.; 59: 479-501(1950). 63p. Dep. NTIS.

3935 (BNL-tr-354) LIMITING TRANSITION FROM NON-RELATIVISTIC QUANTUM MECHANICS TO CLASSICAL MECHANICS. Strel'tsov, V. N. (Joint Inst. for Nuclear Research, Dubna (USSR)). Translated by S. J. Amoretty (Brookhaven National Lab., Upton, N. Y.), from report JINR-P2-4944. 13p. Dep. CFSTI.

3936 (CALT-822-16) SIMPLE MODEL FOR AMORPHOUS ANTIFERROMAGNETS. Hasegawa, Ryusuke (California Inst. of Tech., Pasadena. W. M. Keck Lab. of Engineering Materials). Dec 1970. Contract AT(04-3)-822. 10p. Dep. NTIS.

3937 (COO-958-19) ELECTROCHEMISTRY AND SPECTRA OF METAL-AMMONIA AND METAL-AMINE SOLUTIONS AND KINETICS OF ELECTRON-ATTACHMENT REACTIONS. Technical Progress Report, September 16, 1969-September 25, 1970. (Michigan State Univ., East Lansing). Contract AT(11-1)-958. 13p. Dep. NTIS.

3938 (COO-1198-753) MARTENSITIC TRANSFORMATIONS IN FERROUS AND NON-FERROUS SYSTEMS: SOME HEURISTIC COMPARISONS. Lieberman, David S. (Illinois Univ., Urbana. Dept. of Metallurgy and Mining Engineering). [1970]. Contract AT(11-1)-1198. 24p. (CONF-700923-1). Dep. NTIS.
From 6th International Conference on Metal Spraying, Paris, France.

3939 (COO-1247-21) TRANSPORT AND DEFECT PROPERTIES OF THIN METALLIC WIRES. Progress Report No. 8. Bass, Jack (Michigan State Univ., East Lansing). 30 Sep 1970. Contract AT(11-1)-1247. 29p. Dep. NTIS.

3940 (COO-1248-22) MOBILITY AND COEFFICIENTS OF SLIP OF POLYSTYRENE LATEX PARTICLES. Wahi, Bhupinder N. (Minnesota Univ., Minneapolis. Particle Technology Lab.). Jun 1970. 92p. Dep. NTIS.
Thesis.

3941 (COO-1431-10) SIZE DISTRIBUTIONS OF ANTIPHASE DOMAINS IN Cu_3Au. Mikkola, D. E.; Sakai, M.; Poquette, G. E. (Michigan Technological Univ., Houghton. Dept. of Metallurgical Engineering). [1969]. 5p. (CONF-690966-1). Dep. NTIS.
From 3rd Bolton Landing Conference on Ordered Alloys, Bolton Landing, N. Y.

3942 (COO-1569-67) NUCLEAR ORIENTATION STUDIES OF LOCAL MOMENTS IN NOBLE METAL HOSTS. Holliday, R. J.; Weyhmann, W. (Minnesota Univ., Minneapolis. School of Physics and Astronomy). Sep 1970. Contract AT(11-1)-1569. 62p. Dep. NTIS.

3943 (COO-1680-10) EXCHANGE OF INTERLAYER CATIONS IN MICACEOUS MINERALS. Progress Report, September 30, 1969-September 30, 1970. Scott, A. D.; Ismail, F. T. (Iowa State Univ. of Science and Technology, Ames. Dept. of Agronomy). Contract AT(11-1)-1680. 17p. Dep. NTIS.

3944 (COO-1758-26) FACTORS AFFECTING THYROID HORMONE SECRETION RATES AND UTILIZATION RATES IN MAMMALS USING ^{131}I AS A TRACER. Technical Progress Report, 1970. Anderson, Ralph R. (Missouri Univ., Columbia. Dept. of Dairy Husbandry). Contract AT(11-1)-1758. 8p. Dep. NTIS.

3945 (COO-1758-27) FACTORS AFFECTING THYROID HORMONE SECRETION RATES AND UTILIZATION RATES IN MAMMALS USING ^{131}I AS A TRACER. Comprehensive Report, 1968-1970. Anderson, Ralph R. (Missouri Univ., Columbia). Contract AT(11-1)-1758. 7p. Dep. NTIS.

3946 (COO-1761-13) THEORETICAL AND EXPERIMENTAL ASPECTS OF SELECTION AS APPLIED TO BIOLOGICAL GROUPS. Progress Report, February 1-October 31, 1970. (Ohio State Univ., Columbus). Contract AT(11-1)-1761. 9p. Dep. NTIS.

3947 (COO-1761-14) THEORETICAL AND EXPERIMENTAL ASPECTS OF SELECTION AS APPLIED TO BIOLOGICAL GROUPS. Progress Report, 1968-1970. (Ohio State Univ., Columbus). 26p. Dep. NTIS.

3948 (DESY-70/48) OPTICAL ABSORPTION OF METALS IN THE X-UV RANGE. Kunz, C. (Deutsches Elektronen-Synchrotron, Hamburg (West Germany)). Sep 1970. 18p. Dep. NTIS (U. S. Sales Only).

3949 (GA-9203) FASEII: A COMPUTER PROGRAM FOR THE STRESS ANALYSIS OF THIN CYLINDRICAL SHELLS AND FLAT PLATES. A User's Manual. Prince, N. (Gulf General Atomic, Inc., San Diego, Calif.). 29 Jan 1969. Contract W-7405-eng-26; Subcontract 2848. 49p. Dep. NTIS.
For Oak Ridge National Lab., Tenn.

3950 (GA-9952) SHELL5: SHELL-3D VERSION 5, A COMPUTER PROGRAM FOR THE STRUCTURAL ANALYSIS OF ARBITRARY THREE-DIMENSIONAL THIN SHELLS. A User's Manual. Prince, N. (Gulf General Atomic, Inc., San Diego, Calif.). 30 Jan 1970. Contract W-7405-eng-26; Subcontract 2848. 94p. Dep. NTIS.
For Oak Ridge National Lab., Tenn.

3951 (HUX-3780-29) COMPARISON OF 3D CLASSICAL TRAJECTORY AND TRANSITION-STATE THEORY REACTION CROSS SECTIONS. Koeppl, G. W.; Karplus, M. (Harvard Univ., Cambridge, Mass. Dept. of Chemistry). [1970]. 6p. Dep. NTIS.

3952 (HUX-3780-33) THEORETICAL STUDIES IN CHEMICAL KINETICS. Annual Report, 1970. Karplus, Martin (Harvard Univ., Cambridge, Mass.). Contract AT(30-1)-3780. 5p. Dep. NTIS.

3953 (IN-1410) APPLICATION OF SOLBRIG'S CELL-DIPOLE METHOD TO MOLECULAR CRYSTALS. McMurry, H. L. (Idaho Nuclear Corp., Idaho Falls). Oct 1970. Contract AT(10-1)-1230. 13p. Dep. NTIS.

3954 (IS-2389) LOCK-IN DETECTOR. Mourlam, Louis Jr.; Rhinehart, Wayne A. (Ames Lab., Iowa). Sep 1970. Contract W-7405-eng-82. 34p. Dep. NTIS.

3955 (IS-2416) USE OF MAN-COMPUTER INTERACTION IN ROOT-FINDING AND NUMERICAL PROBLEM-SOLVING. Ripley, Gerald David; Lambert, R. J. (Ames Lab., Iowa). Oct 1970. Contract W-7405-eng-82. 172p. Dep. NTIS.
Thesis. Submitted by Gerald David Ripley.

3956 (IS-T-383) ELECTRONIC HEAT CAPACITY OF ReO_3. Keller, David Anthony (Ames Lab., Iowa). Nov 1970. Contract W-7405-eng-82. 102p. Dep. NTIS.
Thesis.

3957 (IS-T-384) PREPARATION AND SOME HIGH TEMPERATURE PROPERTIES OF THE RARE EARTH TRIFLUORIDES. Henderson, David Courtland (Ames Lab., Iowa). Nov 1970. Contract W-7405-eng-82. 137p. Dep. NTIS.
Thesis.

3958 (IS-T-388) INFRARED SPECTRA OF SUBSTITUTIONAL H^- AND D^- IMPURITIES (U-CENTERS) IN CsBr AND CsI. Olson, Clifford Gerald (Ames Lab., Iowa). Oct 1970. Contract W-7405-eng-82. 84p. Dep. NTIS.
Thesis.

3959 (IS-T-390) CRYSTAL AND MOLECULAR STRUCTURES OF SELECTED ORGANOMETALLIC COMPOUNDS AND SOME DIRECT METHODS. Martin, Leslie Leon (Ames Lab., Iowa). Nov 1970. Contract W-7405-eng-82. 140p. Dep. NTIS.
Thesis.

3960 (IS-T-399) MAGNETIC THERMOMETRY FROM 1 TO 30 K. Cetas, Thomas Charles (Ames Lab., Iowa). Nov 1970. Contract W-7405-eng-82. 177p. Dep. NTIS.
Thesis.

3961 (IS-T-406) SURFACE STUDIES OF SIMPLE HYDROCARBONS ON IRIDIUM BY FLASH DESORPTION. Burns, Robert Arthur (Ames Lab., Iowa). Nov 1970. Contract W-7405-eng-82. 89p. Dep. NTIS.
Thesis.

3962 (IS-T-410) NUCLEAR MAGNETIC RESONANCE DETERMINATION OF THE ACTIVATION VOLUME FOR SELF-DIFFUSION IN ALUMINUM. Engardt, Ralph Duane (Ames Lab., Iowa). Nov 1970. Contract W-7405-eng-82. 100p. Dep. NTIS.
Thesis.

3963 (IS-T-423) TECHNIQUE FOR COOLING SINGLE CRYSTALS BELOW 90°K FOR X-RAY DIFFRACTION, AND THE CRYSTAL STRUCTURES OF $H_2Ta_6Cl_{18}\cdot 6H_2O$, AND THE PHOTODIMER OF 1,1-DIMETHYL-2,5-DIPHENYL-1-SILACYCLOPENTADIENE. Thaxton, Charles Burton (Ames Lab., Iowa). Nov 1970. Contract W-7405-eng-82. 71p. Dep. NTIS.
Thesis.

3964 (LA-4360-TR) DETERMINATION OF THE DECOMPOSITION TIME OF HEXOGEN UNDER THE EFFECT OF SHOCK WAVES. Voskoboinikov, I. M.; Bogomolov, V. M.; Margolin, A. D.; Apin, A. Ya. Translated by Helen J. Dahlby (Los Alamos Scientific Lab., N. Mex.), from Vzryvnoe Delo, Nauch.-Tekh. Gorn. Obshchest., Sb.; No. 63/20, 51-6(1967). 4p. Dep. NTIS.

3965 (LA-4507) DIRECT DIGITAL READOUT AND COMPUTER CALCULATION OF AMINO ACID ANALYSIS DATA. Shepherd, G. R.; Roberts, C. N.; Dean, P. N.; Hiebert, R. D.; Glascock, R. B. (Los Alamos Scientific Lab., N. Mex.). Mar 1970. Contract W-7405-eng-36. 34p. Dep. NTIS.

3966 (MHSMP-15) NON-CONTACT GAGING. Black, L. W. (Mason and Hanger-Silas Mason Co., Inc., Amarillo, Tex.). Oct 1970. Contract DA-11-173-AMC-487(A). 3p. Dep. NTIS.

3967 (NYO-2150-63) ELECTROMAGNETIC GENERATION OF ULTRASOUND IN METALS. Wallace, W. D. (Cornell Univ., Ithaca, N. Y. Lab. of Atomic and Solid State Physics). Aug 1970. Contract AT(30-1)-2150. 47p. Dep. NTIS.

3968 (NYO-2171-325) SELF-ADJOINT ALGEBRAS OF UNBOUNDED OPERATORS. Powers, Robert T. (Pennsylvania Univ., Philadelphia). [1969]. Contract AT(30-1)-2171. 63p. Dep. NTIS.

3969 (NYO-2391-121) LOW LYING EVEN PARITY RESONANCES IN $KI:Ag^+$. Kirby, R. D. (Cornell Univ., Ithaca, N. Y. Illinois Univ., Urbana). [1969]. Contract AT(30-1)-2391. 12p. Dep. NTIS.

3970 (NYO-3794-11) DETERMINATIONS OF ELEMENTARY REACTION RATE CONSTANTS FOR THE REACTION OF HYDROGEN ATOMS WITH VARIOUS SUBSTRATE MOLECULES IN THE GAS PHASE. Annual Progress Report, 1969-70. (Carnegie-Mellon Univ., Pittsburgh, Pa. Dept. of Chemistry). 1 Oct 1970. Contract AT(30-1)-3794. 125p. Dep. NTIS.

3971 (NYO-3798-9) MOESSBAUER SPECTROSCOPY OF BIOCHEMICALS CONTAINING IRON. Progress Report No. 5, October 1, 1969-September 30, 1970. (Catholic Univ. of America, Washington, D. C. Dept. of Chemistry). 1 Oct 1970. Contract AT(30-1)-3798. 14p. Dep. NTIS.

3972 (ORNL-tr-2398) MAGNETIC MEASUREMENTS IN THE COPPER-MANGANESE SYSTEM. Scheil, Erich; Wachtel, Ernst. Translated by R. Gregg Mansfield (Oak Ridge National Lab., Tenn.), from Z. Metallik.; 48: 571-82(1957). 27p. Dep NTIS.

3973 (RFP-1515) PARAMETERS FOR PRESSURIZED INERT GAS METAL ARC WELDING OF ALUMINUM. Brandon, Eldon D. (Dow Chemical Co., Golden, Colo. Rocky Flats Div.). 15 Oct 1970. Contract AT(29-1)-1106. 38p. Dep. NTIS.

3974 (SC-R-68-1784) BASIC RESPONSE PHENOMENOLOGY ANALYTICAL TECHNIQUES. Herrmann, Walter (Sandia Labs., Albuquerque, N. Mex.). Aug 1968. 46p. (CONF-670723-2). Dep. NTIS.
From Defense Atomic Support Agency Effects Conference, Columbus, Ohio.

3975 (SC-RR-70-561) STOCHASTIC APPROACH TO BIOBURDEN ESTIMATION AND PREDICTION. Preliminary Report. Roark, A. L. (Sandia Labs., Albuquerque, N. Mex.). Aug 1970. Contract W-12-853. 63p. Dep. NTIS.

3976 (SC-RR-70-645) SMOPAS: SANDIA MATRIX-ORIENTED PRODUCTION ASSEMBLY SYSTEM. Houghton, Arthur V. (Sandia Labs., Albuquerque, N. Mex.). Oct 1970. 22p. Dep. NTIS.

3977 (SC-T-70-4041) NOTES ON I. N. BELIAEV AND S. M. ARTAMONOVA'S PAPER "SOME PHYSICO-CHEMICAL PROPERTIES OF COPRECIPITATED HOLMIUM AND ZIRCONIUM, HYDROXIDES AND HOLMIUM, AND HAFNIUM HYDROXIDES." Spiridonov, F. M. Translated by Marcel I. Weinreich (Sandia Labs., Albuquerque, N. Mex.), from Izv. Akad. Nauk SSSR, Neorg. Mater.; 5: 93(1969). 5p. Dep. NTIS.

3978 (SC-T-70-4043) SYSTEM HfO_2-Er_2O_3. Spiridonov, F. M.; Komissarova, L. N. Translated by Fredric D. Killebrew (Sandia Labs., Albuquerque, N. Mex.), from Zh. Neorg. Khim.; 15: 875-8(1970). 7p. Dep. NTIS.

3979 (TID-25562) STRUCTURAL STUDIES OF METAL COORDINATION COMPOUNDS. Terminal Report, 1959-1969. Quagliano, James V. (Florida State Univ., Tallahassee). Contract AT(40-1)-2503. 20p. Dep. NTIS.

3980 (UCLA-10-P-14-90) MEASUREMENT OF RECURSIVE PROGRAMS. Report No. 70-43. Cerf, V. G. (California Univ., Los Angeles. School of Engineering and Applied Science). May 1970. Contract AT(11-1)-Gen-10. 114p. Dep. NTIS.

3981 (UCLA-10-P-14-94) INSTRUMENTING COMPUTER SYSTEMS AND THEIR PROGRAMS. Bussell, Bertram; Koster, Robert (California Univ., Los Angeles). [1969]. Contract AT(11-1)-Gen-10. 32p. Dep. NTIS.

3982 (UCLA-10-P-14-X-56) PROJECT SUMMARY. (California Univ., Los Angeles). [nd]. Contract AT(11-1)-Gen-10. 13p. Dep. NTIS.

3983 (UCLA-12-793) SUBCELLULAR FRACTIONATION OF CULTURED GLIAL CELLS. Cotman, C.; Herschman, H.; Taylor, D. (California Univ., Los Angeles. Lab. of Nuclear Medicine). [1970]. Contract AT(04-1)-Gen-12. 19p. Dep. NTIS.

3984 (UCLA-12-794) REGULATION OF THE PYRUVATE KINASE OF AN ESTABLISHED RAT LIVER CELL LINE (RLC) IN CULTURE BY INSULIN, GLUCOSE, AND SERUM. Gerschenson, L. E.; Andersson, Myrna (California Univ., Los Angeles. Lab. of Nuclear Medicine and Radiation Biology). [1970]. Contract AT(04-1)-Gen-12. 9p. Dep. NTIS.

3985 (UCLA-12-795) TEMPERATURE-MEDIATED HYPER-INDUCTION OF FATTY ACID DESATURATING ENZYME. Fulco, Armand J. (California Univ., Los Angeles. Lab. of Nuclear Medicine and Radiation Biology). [1969]. Contract AT(04-1)-Gen-12. 9p. Dep. NTIS.

3986 (UCLA-12-796) DISTRIBUTION OF POLYSOMES IN MOUSE BRAIN TISSUE. Lerner, Michael P.; Wettstein, Felix O.; Herschman, Harvey R.; Stevens, Jack G.; Fridlender, Bertold R. (California Univ., Los Angeles). [1970]. Contract AT(04-1)-Gen-12. 34p. Dep. NTIS.

3987 (UCRL-14248(Rev.1)) ISOP: A THREE-DIMENSIONAL ISOMETRIC PLOTTING SUBROUTINE. Hunt, Carolyn R. (California Univ., Livermore. Lawrence Radiation Lab.). 8 Sep 1970. 23p. Dep. NTIS.

3988 (UCRL-19601) HIGH-VOLTAGE ELECTRON MICROSCOPY STUDY OF SLIP BAND GROWTH IN COPPER. Kosel, T.; Washburn, J. (California Univ., Berkeley. Lawrence Radiation Lab.). Aug 1970. Contract W-7405-eng-48. 5p. (CONF-700819-6). Dep. NTIS.
From 2nd International Conference on the Strength of Metals and Alloys, Pacific Grove, Calif.

3989 (UCRL-19665) CALIBRATION OF AN INFRARED PYROMETER. McCoy, G. A.; Olstad, R. A.; Olander, D. R. (California Univ., Berkeley. Lawrence Radiation Lab.). Sep 1970. Contract W-7405-eng-48. 56p. Dep. NTIS.

3990 (UCRL-19686) LOW-TEMPERATURE HEAT CAPACITIES OF DILUTE SOLUTIONS OF Fe AND Cr IN Cu. Triplett, B. B.; Phillips, Norman E. (California Univ., Berkeley. Lawrence Radiation Lab.). Aug 1970. Contract W-7405-eng-48. 7p. (CONF-700921-2). Dep. NTIS.
From 12th International Conference on Low Temperature Physics, Kyoto, Japan.

3991 (UCRL-20303) ATOM PROBE FIELD ION MICROSCOPE. Stolt, Kaj Gunnar (California Univ., Berkeley. Lawrence Radiation Lab.). [Aug 1970]. Contract W-7405-eng-48. 50p. Dep. NTIS.
Thesis.

3992 (UCRL-20309) SINTERING AND FERROELECTRIC PROPERTIES OF LEAD ZIRCONATE TITANATE CERAMICS. Atkin, Robert B. (California Univ., Berkeley. Lawrence Radiation Lab.). Sep 1970. Contract W-7405-eng-48. 49p. Dep. NTIS.
Thesis.

3993 (UCRL-50874) SYSTEMATIC DEVELOPMENT OF DIFFERENCE FORMULAE, TO ARBITRARY ORDER, FOR THE

NUMERICAL DIFFERENTIATION AND INTEGRATION OF A TAYLOR-EXPANSIBLE FUNCTION. Sherman, Nevin W. (California Univ., Livermore. Lawrence Radiation Lab.). 14 May 1970. 101p. Dep. NTIS.

3994 (UCRL-50909) MULTIAXIAL STRESS STUDIES ON RIGID POLYURETHANE FOAM. Zaslawsky, Maurice (California Univ., Livermore. Lawrence Radiation Lab.). 21 Jul 1970. 93p. Dep. NTIS.

3995 (UCRL-50921) QUANTITATIVE PHASE ANALYSIS OF ROCKS BY X-RAY DIFFRACTOMETRY. Braun, Robert L.; Ramspott, Lawrence D. (California Univ., Livermore. Lawrence Radiation Lab.). 10 Sep 1970. 21p. Dep. NTIS.

3996 (UCRL-50926) EQUIPMENT AND TECHNIQUE FOR FORMING SENSITIZED PHOTOGRAPHIC FILM TO A SPHERICAL SHAPE. Pierce, Edward L. (California Univ., Livermore. Lawrence Radiation Lab.). 3 Sep 1970. 22p. Dep. NTIS.

3997 (UCRL-50927) CRITICAL FLUENCE NEEDED TO DESTROY THIN METAL FILMS BY LASER DEPOSITION. Boltwood, C. M. Jr.; Richards, L. M. (California Univ., Livermore. Lawrence Radiation Lab.). 2 Feb 1970. 19p. Dep. NTIS.

3998 (UCRL-50930) OPERATION OF A 12-INCH FAST GATE VALVE WITH A PRESSURE CARTRIDGE. Betten, P. R.; Holl, P. M. (California Univ., Livermore. Lawrence Radiation Lab.). 26 Aug 1970. 8p. Dep. NTIS.

3999 (UCRL-50931(Pt.1)) COMPUTERIZED FULLY AUTOMATIC ANALYTICAL MASS SPECTROMETER. PART 1. MECHANICAL DESIGN. Crawford, Richard W.; Stump, Ronald K.; Frazer, Jack W. (California Univ., Livermore. Lawrence Radiation Lab.). 11 Sep 1970. 16p. Dep. NTIS.

4000 (UCRL-72587(Rev.1)) CLUSTERING AND GIANT MOMENTS IN Cu-Ni ALLOYS. Jach, J.; Borg, R. J.; Lai, D. Y. F. (California Univ., Livermore. Lawrence Radiation Lab.). 13 Nov 1970. 11p. (CONF-701104-2). Dep. NTIS.

From 16th Annual Conference on Magnetism and Magnetic Materials, Miami Beach, Fla.

4001 (UCRL-Trans-1417) DIECKMANN REACTION. Vul'fson, N. D.; Zaretskii, V. I. Translated for Univ. of California, Lawrence Radiation Lab., Berkeley, from Reakts. Metody Issled. Org. Soedin.; 12: 9-48(1963). 39p. Dep. NTIS.

4002 (UCRL-Trans-10487) REGULATING FACTOR IN METHIONINE BIOSYNTHESIS. Rudiger, H.; Jaenicke, L. Translated for Univ. of California, Lawrence Radiation Lab., Livermore, from Naturwissenschaften; 57: 132(1970). 3p. Dep. NTIS.

4003 (UCRL-Trans-10496) DENSITIES OF PURE IRON, COBALT, AND NICKEL IN THE MOLTEN STATE. Saito, T.; Sakuma, Y. Translated by Y. Isozaki for Univ. of California, Lawrence Radiation Lab., Livermore, from J. Jap. Inst. Metals; 31: 1140-4(1967). 17p. Dep. NTIS.

4004 (UCSD-34-P-127-5) A CONTINUED STUDY OF THE DEEP CIRCULATION AND DEEP FISH POPULATIONS IN THE PACIFIC OCEAN. Annual Report. (California Univ., La Jolla, San Diego). 24 Feb 1969. Contract AT(11-1)-34. 34p. Dep. NTIS.

4005 (UCSD-34-P-143-23) APPLICATION OF COMPRESSIONAL COOLING TO THE STUDY OF NUCLEAR ORDERING IN SOLID ^{3}He. Johnson, R. T. (California Univ., San Diego. Dept. of Physics). 1969. Contract AT(11-1)-34. 165p. Dep. NTIS.

4006 (WAPD-TM-944) EFFECT OF HNO_3-HF PICKLING ON STRESS CORROSION CRACKING OF Ni-Cr-Fe ALLOY 600 IN HIGH-PURITY WATER AT 660F. Rentler, R. M.; Welinsky, I. H. (Bettis Atomic Power Lab., Pittsburgh, Pa.). Oct 1970. Contracts AT(11-1)-Gen-14; N5015. 17p. Dep. NTIS.

4007 (WHAN-FR-25) CREEP RATE CORRELATION IN SOLUTION-TREATED TYPE 304 AND 316 STAINLESS STEELS. Bates, J. F.; Gilbert, E. R.; Lovell, A. J. (WADCO Corp., Richland, Wash.). Oct 1970. Contract AT(45-1)-2170. 12p. Dep. NTIS.

CORPORATE AUTHOR INDEX

In the Corporate Author Index, technical report literature is indexed by the organization or institution responsible for issuing the report. Entries are given for all report literature and for published literature for which a corporate author approach is especially desirable, e.g., symposium and conference proceedings.

Each entry under a corporate author gives the publication title and the *NSA* volume and abstract numbers. Report numbers, where applicable, are given in parentheses at the end of the entry.

A

AEROSPACE CORP., EL SEGUNDO, CALIF.
Mutually interacting instabilities in the magnetosphere, 25:2948 (AD-709200)
Proton energy distributions from 0.060 to 3.3 MeV at 6.6 earth radii, 25:2951 (AD-709723)
AIR FORCE CAMBRIDGE RESEARCH LABS., L. G. HANSCOM FIELD, MASS.
Arctic ionosphere and aurora: airborne investigations, 25:2949 (AD-709359)
Quiescent and disturbed proton and electron distributions, 25:2950 (AD-709363)
AIR FORCE OFFICE OF SCIENTIFIC RESEARCH, WASHINGTON, D. C.
Some thoughts on the design of a thermonuclear space power system, 25:3138 (ORO-1171-1, pp 387-411)
AKADEMIYA NAUK UKRAINSKOI SSR, KIEV. INSTITUT TEORETICHESKOI FIZIKI.
Additional invariance of relativistic equations of motion, 25:3292 (ITF-70-32)
Dispersion--theoretic model of πN-scattering backward peaks, 25:3377 (ITF-70-65)
Electrodisintegration of light nuclei, 25:3714 (ITF-70-35)
Inelastic meson--baryon reactions in generalized Veneziano model, 25:3378 (ITF-70-77)
Obtaining the limiting relations for correlation averages, 25:3332 (ITF-70-59)
Representation of the Jost--Lehmann--Dyson type, 25:3433 (ITF-70-33)
Solution of unitarity condition for the elastic scattering amplitude for high energies, 25:3451 (ITF-70-49)
AKTIEBOLAGET ATOMENERGI, STUDSVIK (SWEDEN).
Relative signs of principal elements of the α-proton hyperfine coupling tensor in NH_2CONHO, 25:2219 (NP-18449)
ALABAMA POWER CO., BIRMINGHAM.
Joseph M. Farley Nuclear Plant, Units 1 and 2. Preliminary safety analysis report, Amendment 8, 25:3845 (DOCKET-50348-14)
AMERICAN UNIV., BEIRUT (LEBANON). DEPT. OF BIOCHEMISTRY.
Bjorken limit and Jin--Martin lower bound, 25:3294 (NYO-4204-5)
AMES LAB., IOWA.
Crystal and molecular structures of selected organometallic compounds, 25:3959 (IS-T-390)
Electronic heat capacity of ReO_3, 25:3956 (IS-T-383)
Erbia--hafnia system, 25:2804 (IS-T-401)
Infrared spectra of substitutional H^- and D^- impurities in CsBr and CsI, 25:3958 (IS-T-388)
Lock-in detector, 25:3954 (IS-2389)
Magnetic thermometry from 1 to 30 K, 25:3960 (IS-T-399)
Nuclear magnetic resonance determination of the activation volume for self-diffusion in aluminum, 25:3962 (IS-T-410)
Prediction of equilibrium data for solvent extraction system $SmCl_3$--$NdCl_3$--$CeCl_3$--HCl--H_2O with extractant D2EHPA-Amsco, 25:2311 (IS-T-412)
Preparation and some high temperature properties of rare earth trifluorides, 25:3957 (IS-T-384)
Separation of lanthanum from a rare earth chloride mixture using a multistage mixer-settler extractor, 25:2310 (IS-T-411)
Surface studies of simple hydrocarbons on iridium by flash desorption, 25:3961 (IS-T-406)
Technique for cooling single crystals below 90°K for X-ray diffraction, and crystal structures of $H_2Ta_6Cl_{18}.6H_2O$, and photodimer of 1,1-dimethyl-2,5-diphenyl-1-silacyclopentadiene, 25:3963 (IS-T-423)
Use of man-computer interaction in root-finding and numerical problem-solving, 25:3955 (IS-2416)
ARGONNE NATIONAL LAB., ILL.
Final safety analysis report on the use of plutonium in ZPR-6 and -9, 25:3901 (ANL-7442)
Fuel cycle technology quarterly report, April, May, June 1970, 25:2306 (ANL-7735)
Role of accelerators in neutron radiography, 25:3471 (CONF-700322-, pp 321-44)
Some improvements in variational flux synthesis methods, 25:3922 (ANL-7696)
ARIZONA UNIV., TUCSON.
Prog. rpt. on mutation studies with tobacco mosaic virus, annual, 12/69--11/70, 25:2551 (COO-873-28)
ARIZONA UNIV., TUCSON. DEPT. OF PHYSICS.
Measurement of atomic lifetimes, 25:2888 (CONF-700322-, pp 281-8)
ARMY ELECTRONICS COMMAND, FORT MONMOUTH, N. J.
Spectral emittance of Nd, Sm, Er, and Yb oxides at high temperatures, 25:3204 (AD-708547)
ARMY MEDICAL RESEARCH LAB., FORT KNOX, KY.
Test measurements on scintillation Geiger--Mueller counters, 25:2432 (AD-706587)
ATELIERS DES CHARMILLES S.A., GENEVA (SWITZERLAND).
Charge/discharge machine for Dragon reactor, 25:2385 (DP-Report-230)
ATLANTIC RICHFIELD HANFORD CO., RICHLAND, WASH.
Operating experience using silver reactors for radioiodine removal in the Hanford Purex Plant, 25:2416 (ARH-SA-67)
Vibration testing of L-3 and L-10 shipping containers, 25:2415 (ARH-1819)
ATOMIC ENERGY BOARD, PELINDABA, PRETORIA (SOUTH AFRICA).
Oxidation of zirconium alloy in liquid sodium at different oxygen levels, 25:2611 (PEL-201)
ATOMIC ENERGY CENTRE, LAHORE (PAKISTAN).
Investigations of thermal and 14-MeV neutron activation analysis in Pakistan, 25:2125 (IAEA-122, pp 27-36)
ATOMIC ENERGY COMMISSION, WASHINGTON, D. C.
Selected bibliography for fusion reactor design studies, 25:3139 (ORO-1171-1, pp 425-39)
ATOMIC ENERGY ESTABLISHMENT, WINFRITH (ENGLAND).
Calculation of the release of fission products from coated particles, 25:3874 (DP-Report-595)
Carbon transport studies for helium cooled high temperature reactors. project dragon, 25:3860 (DP-Report-491)
Charge/discharge machine for Dragon reactor, 25:2385 (DP-Report-230)
Comparison of carbon-atom displacement rate in graphite in Dragon reactor, Petten HTR and low enrichment HTR, 25:3872 (DP-Report-559)
Complete core replacement and part reloaded systems in $^{235}U/Th$ and $^{235}U/^{238}U$ cycles, 25:3869 (DP-Report-478)
Determination of total C in SiC coated Dragon fuel particles, 25:2064 (DP-Report-494)
Dragon operations third quarterly progress report, December 1965--February 1966, 25:3790 (DP-Report-438)
Evaluation of data from first Dragon charge, 25:3796 (DP-Report-579)
First year at full power, 25:3791 (DP-Report-474)
Fuel cycles and reactor physics feed/breed and other Th cycles, 25:3884 (DP-Report-469)
Fuel-cycle theory for on-load refuelled thermal converter reactors. I and II, 25:3887 (DP-Report-575)
Helium utilization on Dragon during approach to power and first charge irradiation, 25:3861 (DP-Report-552)
Impurity removal from Dragon reactor during initial commissioning, 25:3862 (DP-Report-553)
Influence of fuel element heterogeneity on partly enriched U cycle, 25:3868 (DP-Report-477)
Measurement of burn-up of Dragon first charge fuel elements, 25:3871 (DP-Report-538)
Measurement of sub vpm levels of water and hydrogen under

plant conditions, 25:3882 (DP-Report-487)
Monitoring fluidised beds by pressure measurements, 25:2767 (DP-Report-378)
Operational data for charge I, 25:3795 (DP-Report-561)
Parametric survey of the low enriched uranium cycle in a high temperature reactor. project dragon, 25:3883 (DP-Report-466)
Post-irradiation gas release measurements on fuel elements from Dragon reactor, 25:3870 (DP-Report-497)
Pressure drop measurements made on a dragon heat exchanger fitted with various designs of water catchpot. project dragon, 25:3897 (DP-Report-591)
Prog. rpt. on Dragon operations, 12/66--2/67, 25:3889 (DP-Report-582)
Prog. rpt. on Dragon operations, 3/67--5/67, 25:3890 (DP-Report-592)
Prog. rpt. on Dragon operations, 3--5/66, 25:3792 (DP-Report-483)
Prog. rpt. on Dragon operations, 6--8/66, 25:3793 (DP-Report-488)
Prog. rpt. on Dragon operations, 9-11/66, 25:3794 (DP-Report-531)
Proton recoil counter techniques in ZEBRA, 25:2472 (AEEW-M-905)
Pyrolysis of methane in bed of particles, 25:2151 (DP-Report-569)
Qualification of fission product release, 25:3775 (DP-Report-539)
Removal and replacement of primary heat exchanger tube bundle and circulator on Dragon Reactor, 25:3863 (DP-Report-554)
Seizure tests on Dragon articulated control rod, 25:3858 (DP-Report-486)
Self-sustaining mixed fast and thermal reactor systems, 25:3888 (DP-Report-581)
Thermal performance of the Dragon reactor, 25:3885 (DP-Report-546)
Thorium cycle in on-load refueled systems, 25:3873 (DP-Report-573)
Utilisation of fuel resources in different reactor types. project dragon, 25:3867 (DP-Report-476)
X-ray irradiation of helium containing gaseous impurities. project dragon, 25:2258 (DP-Report-447)
X-ray microprobe studies of irradiated fuel particles, 25:2812 (DP-Report-320)

ATOMIC ENERGY OF CANADA LTD., CHALK RIVER (ONTARIO).
Heat transfer measurements on trefoil fuel bundles in the post-dryout regime-with data tabulation, 25:3865 (AECL-3414)

ATOMIC ENERGY RESEARCH ESTABLISHMENT, HARWELL (ENGLAND).
Concerning the half-life of ^{144}Ce, 25:3645 (AERE-R-6529)
Fission product distribution in Dragon after first 20 MW run, 25:3886 (DP-Report-571)
Low temperature cryostat for single crystal and powder x-ray diffraction, 25:3048 (AERE-R-6532)
Record of programme and discussions at symposium of papers from Dragon contractors held at A.E.R.E., Harwell, 14--16 March 1966, 25:3774 (DP-Report-439)
Some efficiency calculations for ^{6}Li suspended target semiconductor sandwich spectrometers, 25:2473 (AERE-R-6318)

ATOMIC WEAPONS RESEARCH ESTABLISHMENT, ALDERMASTON (ENGLAND).
Elastic and inelastic scattering of neutrons in energy range 2 to 5 MeV by ^{10}B and ^{11}B, 25:3559 (AWRE-O-45/70)

ATOMICS INTERNATIONAL, CANOGA PARK, CALIF.
Prog. rpt. on Transit Time Flowmeter, 7--9/70, 25:2500 (AI-AEC-12981)

AUSTRALIAN ATOMIC ENERGY COMMISSION RESEARCH ESTABLISHMENT, LUCAS HEIGHTS.
Assessment of air-pulsing techniques for liquid extraction columns, 25:2383 (AAEC/TM-547)
Calculation of (n,2n) cross sections using Hauser--Feshbach theory, 25:3591 (AAEC/TM-542)
Use of Hauser--Feshbach theory for predicting inelastic scattering of neutrons by nuclei, 25:3712 (AAEC/TM-545)

AUSTRALIAN NATIONAL UNIV., CANBERRA. RESEARCH SCHOOL OF PHYSICAL SCIENCES.
Some phenomena produced by positive ion bombardment of metal surfaces at medium energies, 25:2884 (NP-18490)

B

BALTIMORE GAS AND ELECTRIC CO., MD.
Calvert Cliffs Nuclear Power Plant, Units 1 and 2. Environmental report, 25:3838 (DOCKET-50317-20)

BATTELLE MEMORIAL INST., COLUMBUS, OHIO.
Development of mechanical-property design data for reactor materials, 25:2659 (BMI-1889, Sect.A)
Progress on LMFBR cladding, structural, and component materials studies during July 1969--June 1970. Annual report, 25:2754 (BMI-1889)
Studies of the effects of irradiation on cladding and structural alloys, 25:2755 (BMI-1889, Sect.B)

BATTELLE MEMORIAL INST., COLUMBUS, OHIO. DEFENSE METALS INFORMATION CENTER.
Recent information on long-time creep data for columbium alloys, 25:2657 (AD-464715)

BATTELLE-NORTHWEST, RICHLAND, WASH. PACIFIC NORTHWEST LAB.
Analysis of the Phoenix fuel experiments, 25:3902 (BNWL-1514)
CCTL Mark I and Mark II prototype FFTF subassembly compression test development work, 25:3908 (WHAN-FR-18)
N-reactor hybrid simulation, 25:3920 (BNWL-B-8)
Properties of the Pu estimate based on weighted Pu/U values, 25:2417 (BNWL-SA-3287)
Some observations on noble gas partitioning in dynamic air-water systems, 25:3892 (BNWL-SA-3360)
User's manual for the 1DX--2DB--3DB--PERT-V code package, 25:3923 (BNWL-1412)

BECHTEL CORP., SAN FRANCISCO, CALIF.
Point Beach Nuclear Plant, Unit 1. Containment structural test, 25:3830 (DOCKET-50266-33)
Point Beach Nuclear Plant, Unit 1. Initial integrated leak rate test of the reactor containment building. Final report, 25:3829 (DOCKET-50266-32)
Point Beach Nuclear Plant, Unit 1. Review of the statistical significance of tendon surveillance, 25:3831 (DOCKET-50266-34)

BELL TELEPHONE LABS., MURRAY HILL, N. J.
Proceedings of the Tenth International Conference on the Physics of Semiconductors, Cambridge, Mass., 8/17--21/70, 25:3185 (CONF-700801)

BENDIX CORP., KANSAS CITY, MO.
Effects of amine catalysts on the physical properties of a rigid urethane foam system, 25:2818 (BDX-613-170)

BETTIS ATOMIC POWER LAB., PITTSBURGH, PA.
Effect of HNO_3--HF pickling on stress corrosion cracking of Ni--Cr--Fe Alloy 600 in high-purity water at 660F, 25:4006 (WAPD-TM-944)
Prog. rpt. on PWR project, 1/24--4/25/70, 25:3799 (WAPD-MRP-132)

BOSTON COLL., CHESTNUT HILL, MASS. DEPT. OF PHYSICS.
Radiation damage studies with low-energy hydrogen isotopes, 25:3187 (CONF-700322-, pp 63-77)

BROOKHAVEN NATIONAL LAB., UPTON, N. Y.
High-Temperature Liquid-Metal Technology Review, Vol. 8, No. 3, 6/70, 25:2600 (BNL-50258)

BROWN UNIV., PROVIDENCE, R. I. DIV. OF ENGINEERING.
Effects of sub-threshold high-energy electrons on properties of Si photovoltaic cells, 25:2814 (N-70-27167)

BUREAU OF MINES, COLLEGE PARK, MD. COLLEGE PARK METALLURGY RESEARCH CENTER.
Application of high-velocity ions to metallurgy research, 25:2604 (CONF-700322-, pp 155-71)

C

CALIFORNIA INST. OF TECH., PASADENA.
Capture of alpha particles by ^{12}C, 25:3562 (CONF-700322-, pp 297-304)

CALIFORNIA INST. OF TECH., PASADENA. W. M. KECK LAB. OF ENGINEERING MATERIALS.
Simple model for amorphous antiferromagnets, 25:3936 (CALT-822-16)

CALIFORNIA UNIV., BERKELEY. LAWRENCE RADIATION LAB.
Atom probe field ion microscope, 25:3991 (UCRL-20303)
Calibration of an infrared pyrometer, 25:3989 (UCRL-19665)
Density of electronic states in α-phase In alloys containing Cd and Sn, 25:3205 (UCRL-19681)
High-voltage electron microscopy study of slip band growth in copper, 25:3988 (UCRL-19601)
Low-temperature heat capacities of dilute solutions of Fe and Cr in Cu, 25:3990 (UCRL-19686)
Reaction $\pi^+p \rightarrow \Delta^{++}A_2^0$ at 3.7 GeV/c, 25:3272 (UCRL-20050)
Resonance productions in K^+p interactions at 4.6 GeV/c and 9 GeV/c, 25:3271 (UCRL-19809)
Search for superheavy elements in nature by detection of events with large numbers of neutrons, 25:3652 (UCRL-19957)
Sintering and ferroelectric properties of lead zirconate titanate ceramics, 25:3992 (UCRL-20309)

CALIFORNIA UNIV., IRVINE. DEPT. OF PHYSICS.
Prog. rpt. on new heavy bosons in proton--antiproton interactions, 10/1/69--9/30/70, 25:3261 (UCI-34-P-149-1)

CALIFORNIA UNIV., LA JOLLA, SAN DIEGO.
Deep circulation and deep fish populations in the Pacific Ocean, annual 2/24/69, 25:4004 (UCSD-34-P-127-5)

CALIFORNIA UNIV., LIVERMORE. LAWRENCE RADIATION LAB.
Clustering and giant moments in Cu--Ni alloys, 25:4000 (UCRL-72587(Rev.1))
Computerized fully automatic analytical mass spectrometer. I, 25:3999 (UCRL-50931(Pt.1))
Critical fluence needed to destroy thin metal films by laser deposition, 25:3997 (UCRL-50927)
Equipment and technique for forming sensitized photographic film to a spherical shape, 25:3996 (UCRL-50926)
General description of Weapons Effects Display System, 25:2506 (UCRL-50922)
ISOP: a three-dimensional isometric plotting subroutine, 25:3987 (UCRL-14248(Rev.1))
Multiaxial stress studies on rigid polyurethane foam, 25:3994 (UCRL-50909)
Nuclear cratering on a digital computer, 25:2381 (UCRL-

XUM

50898)
Operation of a 12-inch fast gate valve with a pressure cartridge, 25:3998 (UCRL-50930)
Quantitative phase analysis of rocks by x-ray diffractometry, 25:3995 (UCRL-50921)
Systematic development of difference formulae, to arbitrary order, for the numerical differentiation and integration of a Taylor-expansible function, 25:3993 (UCRL-50874)
Thermal energy conversion system for a fusion reactor, 25:3133 (ORO-1171-1, pp 141-66)
Weapons Effects Display System: Maintenance Manual. Pt. 5, 25:2505 (UCRL-50892(Vol.4)(Pt.5))
Weapons Effects Display System: Operator's Manual, 25:2504 (UCRL-50892(Vol.2))

CALIFORNIA UNIV., LOS ANGELES.
Distribution of polysomes in mouse brain tissue, 25:3986 (UCLA-12-796)
Instrumenting computer systems and their programs, 25:3981 (UCLA-10-P-14-94)
Project summary, 25:3982 (UCLA-10-P-14-X-56)

CALIFORNIA UNIV., LOS ANGELES. LAB. OF NUCLEAR MEDICINE AND RADIATION BIOLOGY.
Regulation of pyruvate kinase of an established rat liver cell line (RLC) in culture by insulin, glucose, and serum, 25:3984 (UCLA-12-794)
Subcellular fractionation of cultured glial cells, 25:3983 (UCLA-12-793)
Temperature-mediated hyper-induction of fatty acid desaturating enzyme, 25:3985 (UCLA-12-795)

CALIFORNIA UNIV., LOS ANGELES. SCHOOL OF ENGINEERING AND APPLIED SCIENCE.
Measurement of recursive programs, 25:3980 (UCLA-10-P-14-90)

CALIFORNIA UNIV., RIVERSIDE. DEPT. OF PHYSICS.
Proton energy distributions from 0.060 to 3.3 MeV at 6.6 earth radii, 25:2951 (AD-709723)

CALIFORNIA UNIV., SAN DIEGO. DEPT. OF PHYSICS.
Application of compressional cooling to study of nuclear ordering in solid ^{3}He, 25:4005 (UCSD-34-P-143-23)

CARNEGIE-MELLON UNIV., PITTSBURGH, PA. DEPT. OF CHEMISTRY.
Prog. rpt. on reaction rate of hydrogen in gas phase, annual, 1969--70, 25:3970 (NYO-3794-11)

CAROLINA POWER AND LIGHT CO., RALEIGH, N.C.
Brunswick Steam Electric Plant, Units 1 and 2. Design report Nos. 4, 5, and 6, 25:3839 (DOCKET-50324-17)
H. B. Robinson Unit No. 2. Request for allowance for use of respiratory protective equipment, 25:3828 (DOCKET-50261-46)

CATHOLIC UNIV. OF AMERICA, WASHINGTON, D. C. DEPT. OF CHEMISTRY.
Prog. rpt. on Moessbauer spectroscopy of biochemicals containing iron, annual, 10/69--9/70, 25:3971 (NYO-3798-9)

CEKMECE NUCLEAR RESEARCH CENTER, ISTANBUL (TURKEY).
Nordheim equation according to P_1-approximation, 25:3924 (CNAEM-73)

CENTRAL ELECTRICITY GENERATING BOARD, BERKELEY (ENGLAND). BERKELEY NUCLEAR LABS.
Apparatus for the study of radiolytic carbon deposition from the gas phase, 25:2263 (RD/B/N-1748)
γ-radiolysis of carbon monoxide in presence of γ-alumina, 25:2262 (RD/B/N-1279)
Liquid-nitrogen cryostat for keV heavy-ion irradiation experiments, 25:2388 (RD/B/M-1753)

CINCINNATI GAS AND ELECTRIC CO., OHIO.
Wm. H. Zimmer Nuclear Power Station, Units 1 and 2. Preliminary safety analysis report, Amendment 2, 25:3848 (DOCKET-50358-8)

CLEVELAND ELECTRIC ILLUMINATING CO., OHIO.
Davis--Besse Nuclear Power Station. Safety evaluation, 25:3844 (DOCKET-50346-18)

COLUMBUS AND SOUTHERN OHIO ELECTRIC CO., COLUMBUS, OHIO.
Wm. H. Zimmer Nuclear Power Station, Units 1 and 2. Preliminary safety analysis report, Amendment 2, 25:3848 (DOCKET-50358-8)

COMISION NACIONAL DE ENERGIA ATOMICA, BUENOS AIRES (ARGENTINA).
Determination of traces of hafnium in aluminum--uranium alloys, 25:2063 (CNEA-276)
Gamma--gamma coincidences in ^{140}Ce, 25:3646 (CNEA-275)
Use of electrophoresis in thin films for control of the radiochemical purity of tracer compounds, 25:2062 (CNEA-271)

COMITATO NAZIONALE PER L'ENERGIA NUCLEARE, ROME (ITALY).
Establishment of laboratory for determination of Pu in biological samples, 25:2108 (RT/PROT-(70)14)

COMMISSARIAT A L'ENERGIE ATOMIQUE, FONTENAY-AUX-ROSES (FRANCE). CENTRE D'ETUDES NUCLEAIRES.
Amplitude and damping of plasma wave echoes, 25:3144 (CEA-CONF-1601)
Basic collision processes in plasmas; collision cross sections, 25:3075 (CEA-CONF-1627)
Bounce effects in the negative mass instability, 25:3117 (CEA-CONF-1598)
Change in the polarization of an electromagnetic wave in a sheared magnetic field, 25:3146 (CEA-CONF-1608)
Coalescence of organic solutions during the extraction of acids and metals by trialkylamines, 25:2308 (CEA-R-3845)
Delayed neutron emission, 25:3713 (CEA-N-1333)
Drift waves in a collisionless plasma, 25:3147 (CEA-CONF-1612)
Harmonic absorption of microwaves in magnetized low-density plasma, 25:3145 (CEA-CONF-1607)
Hybrid simulation of the dynamics of a battery of mixer--settlers, 25:2384 (CEA-CONF-1579)
Influence of trapped particles on the drift waves, 25:3149 (CEA-CONF-1616)
Ion heating by beam plasma interaction, 25:3054 (CEA-CONF-1611)
Mechanical properties of ceramics based on uranium and plutonium, 25:2794 (ORNL-tr-2388)
Natural-convection irradiation device ''Esther'', 25:3903 (CEA-N-1348)
Plasma containment in a circularized quadrupolar magnetic well: DECA II B, 25:3053 (CEA-CONF-1597)
Plasma formation by dissociation of an accelerated hydrogen cluster beam, 25:3109 (CEA-CONF-1610)
Program IGOR, 25:3525 (CEA-N-1312)
Space--time evolution of Tokamak-type plasma, 25:3052 (CEA-CONF-1595)
Spectroscopic diagnostics of nonequilibrium plasmas, 25:3061 (CEA-CONF-1628)
Two ion collisional absorption of low frequency electromagnetic waves in a toroidal hard-core configuration, 25:3148 (CEA-CONF-1614)

COMMISSARIAT A L'ENERGIE ATOMIQUE, GRENOBLE (FRANCE). CENTRE D'ETUDES NUCLEAIRES.
Separation of technetium from fission products, 25:2307 (CEA-N-1316)

COMMISSARIAT A L'ENERGIE ATOMIQUE, SACLAY (FRANCE). CENTRE D'ETUDES NUCLEAIRES.
Acicular precipitates in irradiated austenitic steels using electron microscopy, 25:2756 (CEA-CONF-1638)
Construction of semi-automatic device for measuring nuclear tracks, 25:2433 (CEA-R-4063)
EL 600: fuel management studies, 25:3866 (CEA-N-1379)
Hybrid simulation of the dynamics of a battery of mixer--settlers, 25:2384 (CEA-CONF-1579)
Optical spark chamber for the search of gamma-ray sources, 25:2841 (CEA-CONF-1633)
Radiolysis of concentrated nitrate and formate solutions, 25:2257 (CEA-R-4046)
Solution of two important problems in the nuclear industry by flame metal spraying, 25:2638 (CEA-CONF-1625)
Use of thin film solar cells in radiovoltaic generators, 25:2400 (CEA-CONF-1623)

COMMONWEALTH EDISON CO., CHICAGO, ILL.
Dresden Nuclear Power Station, Unit 1. Comments on uniform monitoring, recording, and reporting guide, 25:3807 (DOCKET-50010-70)
Dresden Nuclear Power Station, Unit 2. Plant design and analysis report. Volume III. Plant site and environs, 25:3816 (DOCKET-50237-86)
Dresden Nuclear Power Station, Unit 2. Plant design and analysis report. Volume I, 25:3815 (DOCKET-50237-85)
Dresden Nuclear Power Station, Unit 2. Safety evaluation, 25:3817 (DOCKET-50237-87)
Dresden Nuclear Power Station, Unit 3. Proposed operating license and safety evaluation, 25:3821 (DOCKET-50249-43)
La Salle County Station, Units 1 and 2. Preliminary safety analysis report, Vol. 5, 25:3850 (DOCKET-50373-6)
Quad-Cities Station, Units 1 and 2. Environmental report, 25:3826 (DOCKET-50254-25)
Quad-Cities Station, Units 1 and 2. Preliminary safety analysis report, Amendment 13, answers to questions, 25:3823 (DOCKET-50254-22)
Quad-Cities Station, Units 1 and 2. Preliminary safety analysis report, Amendment 14, 25:3824 (DOCKET-50254-23)
Quad-Cities Station, Units 1 and 2. Preliminary safety analysis report, Amendment 15. Supplementary information to foundation grouting (Amendment 8), 25:3825 (DOCKET-50254-24)

CONNECTICUT YANKEE ATOMIC POWER CO., HADDAM.
Connecticut Yankee Atomic Power Plant. Operation report No. 70-10, October 1970, 25:3788 (DOCKET-50213-84)

CONNECTICUT YANKEE ATOMIC POWER CO., HARTFORD.
Connecticut Yankee Atomic Power Plant. License No. DPR-14. Technical specifications Proposed Change No. 16, Rev. No. 1, 25:3811 (DOCKET-50213-83)

CONNECTICUT YANKEE ATOMIC POWER CO., WESTBORO, MASS.
Connecticut Yankee Atomic Power Plant. Automatic plant trip and reactor coolant system cooldown to 502°F, 25:3787 (DOCKET-50213-82)
Connecticut Yankee Nuclear Power Plant. 1970 inservice inspection, 25:3812 (DOCKET-50213-85)

CONSOLIDATED EDISON CO. OF NEW YORK, INC., NEW YORK.
Indian Point Nuclear Generating Unit No. 2. Inspections performed on the pressurizer, 25:3818 (DOCKET-50247-42)
Indian Point Nuclear Generating Unit No. 2. Preliminary safety analysis report, Amendment 25 (includes final facility description and safety analysis report, Suppl. 15), 25:3819 (DOCKET-50247-43)
Indian Point Nuclear Generating Unit No. 2. Safety evaluation, 25:3820 (DOCKET-50247-44)
Indian Point Station, Unit No. 1. Survey of environmental radioactivity, August 1, 1969--March 31,

1970, 25:3806 (DOCKET-50003-59)
CONSUMERS POWER CO., JACKSON, MICH.
Midland Plant, Units 1 and 2. Safety evaluation, 25:3840 (DOCKET-50329-24)
CORNELL UNIV., ITHACA, N. Y.
Low lying even parity resonances in KI:Ag+, 25:3969 (NYO-2391-121)
CORNELL UNIV., ITHACA, N.Y. DEPT. OF APPLIED PHYSICS.
Experience teaching a fusion design seminar, 25:3137 (ORO-1171-1, pp 376-86)
Prog. rpt. on hard superconducting materials, annual, 12/69--11/70, 25:3019 (NYO-3029-48)
CORNELL UNIV., ITHACA, N. Y. LAB. OF ATOMIC AND SOLID STATE PHYSICS.
Electromagnetic generation of ultrasound in metals, 25:3967 (NYO-2150-63)

D

DAIRYLAND POWER COOPERATIVE, LA CROSSE, WIS.
La Crosse Boiling Water Reactor. Proposed change to technical specifications. Installation of automatic gain control system, 25:3805 (DOCKET-1155-84)
DAYTON POWER AND LIGHT CO., OHIO.
Wm. H. Zimmer Nuclear Power Station, Units 1 and 2. Preliminary safety analysis report, Amendment 2, 25:3848 (DOCKET-50358-8)
DEFENCE STANDARDS LABS., MARIBYRNONG (AUSTRALIA).
Effects of gamma radiation on gas yields and crystallinity of PTFE, 25:2261 (NP-18518)
Internal friction in In single crystals, 25:2667 (NP-18491)
DETROIT EDISON CO., MICH.
Enrico Fermi Atomic Power Plant, Unit 2. Preliminary safety analysis report, Amendment 12, 25:3842 (DOCKET-50341-21)
DEUTSCHES ELEKTRONEN-SYNCHROTRON, HAMBURG (WEST GERMANY).
Calculation of N anti N bound states from relativistic OBE model and meson spectrum, 25:3358 (DESY-70/49)
Inelastic diffractive rho-photoproduction and Compton scattering, 25:3308 (DESY-70/45)
Measurement of proton Compton scattering at 6 GeV and small momentum transfers, 25:3309 (DESY-70/46)
Optical absorption of metals in the X--UV range, 25:3948 (DESY-70/48)
Simple interpretation of inelastic electron-nucleon scattering, 25:3310 (DESY-70/50)
DIVISION OF REACTOR LICENSING (AEC), WASHINGTON, D. C.
Davis--Besse Nuclear Power Station. Safety evaluation, 25:3844 (DOCKET-50346-18)
Dresden Nuclear Power Station, Unit 2. Safety evaluation, 25:3817 (DOCKET-50237-87)
Humboldt Bay Power Plant, Unit No. 3. Facility License No. DPR-7, Amendment 1, 25:3808 (DOCKET-50133-42)
Indian Point Nuclear Generating Unit No. 2. Safety evaluation, 25:3820 (DOCKET-50247-44)
Midland Plant, Units 1 and 2. Safety evaluation, 25:3840 (DOCKET-50329-24)
North Anna Power Station, Units 1 and 2. Detailed statement on the environmental considerations, 25:3841 (DOCKET-50338-26)
Point Beach Nuclear Plant, Unit 1. Facility Operating License DPR-24; technical specifications Change No. 1, 25:3832 (DOCKET-50266-35)
San Onofre Nuclear Generating Station, Unit 1. Provisional Operating License No. DPR-13, Amendment 3, 25:3810 (DOCKET-50206-96)
Trojan Nuclear Plant. Detailed statement on the environmental considerations, 25:3843 (DOCKET-50344-18)
DIVISION OF RESEARCH (AEC), WASHINGTON, D. C.
Why fusion, 25:3134 (ORO-1171-1, pp 256-331)
DOUGLAS UNITED NUCLEAR, INC., RICHLAND, WASH.
Testing and surveillance of Hanford production reactor Zircaloy tubes, 25:3921 (DUN-SA-144)
DOW CHEMICAL CO., GOLDEN, COLO. ROCKY FLATS DIV.
Gas coverage for PIGMA welding, 25:2646 (RFP-1550)
Homogenization of uranium-base niobium alloys, 25:2732 (RFP-1582)
Parameters for pressurized inert gas metal arc welding of aluminum, 25:3973 (RFP-1515)
DU PONT DE NEMOURS (E.I.) AND CO., AIKEN, S. C. SAVANNAH RIVER LAB.
Calculation of relative reaction rates in interacting cylindrical cells, 25:3925 (DP-1238)
DUKE POWER CO., CHARLOTTE, N.C.
Oconee Nuclear Station, Units 1, 2, and 3. Preliminary safety analysis report, Amendment 23, 25:3834 (DOCKET-50269-28)

E

EIDGENOESSISCHES INSTITUT FUER REAKTORFORSCHUNG, WUERENLINGEN (SWITZERLAND).
CORONA: program for two-group control rod calculations in reflected reactor, 25:3926 (EIR-166)
ENVIRO-MED, INC., LA JOLLA, CALIF.
Neutron sources for radiotherapy, 25:3473 (CONF-700322-, pp 407-29)
EUROPEAN ATOMIC ENERGY COMMUNITY.
Amplitude and damping of plasma wave echoes, 25:3144 (CEA-CONF-1601)
Basic collision processes in plasmas; collision cross sections, 25:3075 (CEA-CONF-1627)
Bounce effects in the negative mass instability, 25:3117 (CEA-CONF-1598)
Change in the polarization of an electromagnetic wave in a sheared magnetic field, 25:3146 (CEA-CONF-1608)
Considerations on coated particles, with oxide fuel, and graphite and Si carbide coating, for GCFR application, 25:3875 (EURFNR-834)
Drift waves in a collisionless plasma, 25:3147 (CEA-CONF-1612)
Harmonic absorption of microwaves in magnetized low-density plasma, 25:3145 (CEA-CONF-1607)
Influence of trapped particles on the drift waves, 25:3149 (CEA-CONF-1616)
Ion heating by beam plasma interaction, 25:3054 (CEA-CONF-1611)
Plasma containment in a circularized quadrupolar magnetic well: DECA II B, 25:3053 (CEA-CONF-1597)
Plasma formation by dissociation of an accelerated hydrogen cluster beam, 25:3109 (CEA-CONF-1610)
Space--time evolution of Tokamak-type plasma, 25:3052 (CEA-CONF-1595)
Spectroscopic diagnostics of nonequilibrium plasmas, 25:3061 (CEA-CONF-1628)
Two ion collisional absorption of low frequency electromagnetic waves in a toroidal hard-core configuration, 25:3148 (CEA-CONF-1614)
EUROPEAN ORGANIZATION FOR NUCLEAR RESEARCH, GENEVA (SWITZERLAND).
Bjorken limit and Jin--Martin lower bound, 25:3294 (NYO-4204-5)
Measurement of beam profile for high-intensity particles, 25:2434 (CERN-70-27)

F

FIRST ATOMIC SHIP TRANSPORT, INC., NEW YORK.
N. S. Savannah. Furnace sensitized stainless steel, additional information, 25:3917 (DOCKET-50238-74)
FLORIDA POWER AND LIGHT CO.
Turkey Point Plant, Units No. 3 and No. 4. Preliminary safety analysis report, Amendment 30, Suppl. 30, 25:3822 (DOCKET-50250-35)
FLORIDA STATE UNIV., TALLAHASSEE.
Structural studies of metal coordination compounds, 25:3979 (TID-25562)
FURMAN UNIV., GREENVILLE, S.C.
Time-of-flight experiments for low-energy accelerators, 25:3468 (CONF-700322-, pp 125-32)

G

GENERAL ELECTRIC CO., SAN JOSE, CALIF. ATOMIC POWER EQUIPMENT DEPT.
10-decade wide range neutron monitoring system. Final test report, 25:2502 (GEAP-11094)
GEOLOGICAL SURVEY, DENVER, COLO.
Hydraulic tests in hole UA-1 and water inflow into an underground chamber, Amchitka Island, Alaska, 25:2349 (USGS-474-72)
GEOLOGICAL SURVEY, WASHINGTON, D. C.
Preliminary reconnaissance for uranium in Apache and Cochise Counties, Arizona, 1950 to 1957, 25:2373 (RME-154)
Preliminary reconnaissance for uranium in Coconino County, Arizona, 1951 to 1955, 25:2374 (RME-155)
Preliminary reconnaissance for uranium in Gila County, Arizona, 1951 to 1956, 25:2375 (RME-156)
Preliminary reconnaissance for uranium in Mohave County, Arizona, 1952 to 1956, 25:2376 (RME-158)
Preliminary reconnaissance for uranium in Pima and Pinal Counties, Arizona, 1950 to 1957, 25:2377 (RME-159)
Preliminary reconnaissance for uranium in Texas, 1951 to 1957, 25:2372 (RME-153)
GEORGETOWN UNIV., WASHINGTON, D.C. DEPT. OF PHYSICS.
Charged particle nuclear physics experiments for a teaching laboratory, 25:3464 (CONF-700322-, pp 1-19)
GOSUDARSTVENNYI KOMITET PO ISPOL'ZOVANIYU ATOMNOI ENERGII SSSR, SERPUKHOV. INSTITUT FIZIKI VYSOKIKH ENERGII.
anti rho-Meson production in high energy pion-collisions with nuclei, 25:3406 (IFVE-STF-69-71)
Generalization of Tolman equality, 25:3447 (IFVE-SEF-69-59)
Realization of representations of the quaternion group, 25:3420 (IFVE-STF-69-102)
GRAND JUNCTION OFFICE (AEC), COLO.
Preliminary reconnaissance for uranium in Apache and Cochise Counties, Arizona, 1950 to 1957, 25:2373 (RME-154)
Preliminary reconnaissance for uranium in Coconino County, Arizona, 1951 to 1955, 25:2374 (RME-155)
Preliminary reconnaissance for uranium in Gila County, Arizona, 1951 to 1956, 25:2375 (RME-156)
Preliminary reconnaissance for uranium in Mohave County, Arizona, 1952 to 1956, 25:2376 (RME-158)
Preliminary reconnaissance for uranium in Pima and Pinal

XUM

Counties, Arizona, 1950 to 1957, 25:2377 (RME-159)
Preliminary reconnaissance for uranium in Texas, 1951 to 1957, 25:2372 (RME-153)

GRENOBLE UNIV. (FRANCE). FACULTE DES SCIENCES.
Use of the Grenoble high flux reactor in biology, 25:3907 (NP-18462)

GULF GENERAL ATOMIC, INC., SAN DIEGO, CALIF.
FASEII: a computer program for the stress analysis of thin cylindrical shells and flat plates, 25:3949 (GA-9203)
Pulse radiolysis studies of aqueous solutions of aminothiols and compounds related to nucleic acid, 25:2259 (GA-10208)
SHELL5: SHELL-3D Version 5, a computer program for the structural analysis of arbitrary three-dimensional thin shells, 25:3950 (GA-9952)
Status report on fast breeder reactors, 25:3891 (ORO-1171-1, pp 206-55)

H

HARVARD UNIV., CAMBRIDGE, MASS.
Prog. rpt. on theoretical studies in chemical kinetics, annual, 1970, 25:3952 (HUX-3780-33)

HARVARD UNIV., CAMBRIDGE, MASS. DEPT. OF CHEMISTRY.
Comparison of 3D classical trajectory and transition-state theory reaction cross sections, 25:3951 (HUX-3780-29)

HARVARD UNIV., CAMBRIDGE, MASS. DEPT. OF PHYSICS.
Detection of the weak intermediate boson through its hadronic decay modes, 25:3333 (NYO-2171-323)

HIGH VOLTAGE ENGINEERING CORP., BURLINGTON, MASS.
Atomic physics with a low-voltage tandem, 25:3470 (CONF-700322-, pp 259-79)

I

IBM WATSON RESEARCH CENTER, YORKTOWN HEIGHTS, N.Y.
Proceedings of the Tenth International Conference on the Physics of Semiconductors, Cambridge, Mass., 8/17--21/70, 25:3185 (CONF-700801)

IDAHO NUCLEAR CORP., IDAHO FALLS.
Application of Solbrig's cell-dipole method to molecular crystals, 25:3953 (IN-1410)
Bibliography of laser publications of interest to emission spectroscopists. V, 25:3110 (IN-1425)
Electron ground states in molecular and valence-bonded crystals, 25:3226 (IN-1420)
Ultrasonic void fraction detector using compressional stress waves in a wire helix, 25:3905 (IN-1441)

IIT RESEARCH INST., CHICAGO, ILL.
Water decompression experiments and analysis for blowdown of nuclear reactors. final report, 25:3893 (IITRI-578-P-21-39)

ILLINOIS UNIV., URBANA.
Conference on progress of hydrology, Urbana, Ill., 7/69. I, 25:2358
Low lying even parity resonances in KI:Ag+, 25:3969 (NYO-2391-121)
Lumped-parameter analysis for shear failure in the end slab of cylindrical PCRV, 25:2411 (TID-25573)

ILLINOIS UNIV., URBANA. AERONOMY LAB.
Measurement of average electron density between 75 and 80 kilometers, 25:2952 (N-70-33955)

ILLINOIS UNIV., URBANA. DEPT. OF METALLURGY AND MINING ENGINEERING.
Martensitic transformations in ferrous and non-ferrous systems: some heuristic comparisons, 25:3938 (COO-1198-753)

INSTITUT JOZEF STEFAN, LJUBLJANA (YUGOSLAVIA).
Cold neutron source efficiency in a tangential beam hole, 25:3904 (IJS-571)

INSTITUT RUDJER BOSKOVIC, ZAGREB (YUGOSLAVIA).
Inelastic processes and backward scattering in a model of multiple scattering, 25:3352 (IRB-TP-2-70)

INSTITUTE OF NUCLEAR PHYSICS, KRAKOW (POLAND).
Vinca Nova: automatic unit for neutron spectrometer control, 25:2475 (INP-707)

INSTITUTE OF NUCLEAR RESEARCH, WARSAW (POLAND).
Prog. rpt. on nuclear research, annual, 1969, 25:2497 (INR-1180)

INTERNATIONAL ATOMIC ENERGY AGENCY, VIENNA (AUSTRIA).
Environmental isotope data, 25:2367 (STI/DOC-10/117)
Medical activation analysis research program of IAEA Laboratory, 25:2124 (IAEA-122, pp 15-26)
Meeting on uses of activation analysis in studies of mineral element metabolism in man, Teheran, Iran, 6/68, 25:2122 (IAEA-122)
Photopeak count-rates in Ge(Li) and NaI(Tl) detectors, 25:2474 (IAEA-122, pp 150-63)

INTERNATIONAL BUSINESS MACHINES CORP., HOPEWELL JUNCTION, N.Y. EAST FISHKILL LAB.
Unique 150-keV ion accelerator, 25:3469 (CONF-700322-, pp 173-84)

INTERUNIVERSITAIR REACTOR INSTITUUT, DELFT (NETHERLANDS).
Slow electrons and negative ions in organic liquids, 25:2260 (IRI-133-70-2)

IOWA-ILLINOIS GAS AND ELECTRIC CO., DAVENPORT, IOWA.
Quad-Cities Station, Units 1 and 2. Environmental report, 25:3826 (DOCKET-50254-25)
Quad-Cities Station, Units 1 and 2. Preliminary safety analysis report, Amendment 13, answers to questions, 25:3823 (DOCKET-50254-22)
Quad-Cities Station, Units 1 and 2. Preliminary safety analysis report, Amendment 14, 25:3824 (DOCKET-50254-23)
Quad-Cities Station, Units 1 and 2. Preliminary safety analysis report, Amendment 15. Supplementary information to foundation grouting (Amendment 8), 25:3825 (DOCKET-50254-24)

IOWA STATE UNIV. OF SCIENCE AND TECHNOLOGY, AMES. DEPT. OF AGRONOMY.
Prog. rpt. on exchange of interlayer cations in micaceous minerals, annual, 9/30/69--9/30/70, 25:3943 (COO-1680-10)

ISTITUTO NAZIONALE DI FISICA NUCLEARE, PADUA (ITALY).
Annihilation anti pn + $\pi^+\pi^-\pi^-$ between 1.0 and 1.6 GeV/c and its comparison with Veneziano model, 25:3270 (INFN-PD-70/2)

J

JAGELLONIAN UNIV., KRAKOW (POLAND). DEPT. OF THEORETICAL PHYSICS.
Ambiguities in the experimental determination of resonance production amplitudes, 25:3382 (TPJU-1/70)
Examples of quantum field theories without divergences, 25:3435 (TPJU-13/70)
Physical bounds for the components of statistical tensors, 25:3295 (TPJU-12/70)
Polarization of Λ and Σ hyperons in two-body Y* production processes and quark model, 25:3383 (TPJU-2/70)
Regge pole model with Veneziano residues for reactions $0^- \frac{1}{2}^+ \to 0^- \frac{3}{2}^+$, 25:3384 (TPJU-3/70)

JAPAN ATOMIC ENERGY RESEARCH INST., TOKYO.
Analysis of JMTR flux variation during operation, 25:3906 (JAERI-Memo-4130)
Creep and creep-rupture tests of stainless steel as structural material of fast breeding reactor, 25:2660 (JAERI-Memo-4097)
Effect of cold working on creep properties of stainless steel, 25:2661 (JAERI-Memo-4125)
Group structure and accuracy of group constants in vicinity of 2.85-keV resonance scattering of Na, 25:3928 (JAERI-Memo-4110)
Pulsed neutron research in Japan, 1965--70, 25:3927 (JAERI-Memo-4109)
Thermal conductivity of VIPAC UO_2 fuel. II, 25:2813 (JAERI-Memo-4126)

JERSEY CENTRAL POWER AND LIGHT CO., MORRISTOWN, N. J.
Oyster Creek Nuclear Power Plant, Unit No. 1. Preliminary safety analysis report, Amendment 64, 25:3813 (DOCKET-50219-115)

JET PROPULSION LAB., PASADENA, CALIF.
Effects of sub-threshold high-energy electrons on properties of Si photovoltaic cells, 25:2814 (N-70-27167)

JOINT INST. FOR NUCLEAR RESEARCH, DUBNA (USSR).
Conference on radiation dosimetry and physics of accelerator shielding, Dubna, 10/69, 25:3476 (JINR-16-4888)
Data on real parts of K^{+-} forward scattering amplitudes, 25:3379 (JINR-E1-5259)
Limiting transition from nonrelativistic quantum mechanics to classical mechanics, 25:3935 (BNL-tr-354)

JOINT INST. FOR NUCLEAR RESEARCH, DUBNA (USSR). LAB. OF HIGH ENERGY.
Invariance of nonrelativistic Hamiltonian--Jacobi equation in presence of electromagnetic field, 25:3430 (JINR-P2-5373)
Invariants in the nonrelativistic approximation, 25:3434 (JINR-P2-5363)

JOINT INST. FOR NUCLEAR RESEARCH, DUBNA (USSR). LAB. OF NEUTRON PHYSICS.
Investigation of proton polarization in reaction $^{12}C(^3He,p_0)^{14}N$, 25:3563 (JINR-P15-5156)

JOINT INST. FOR NUCLEAR RESEARCH, DUBNA (USSR). LAB. OF NUCLEAR PROBLEMS.
Description of experimental data on πN and KN scattering in high-energy region on basis of complex angular momenta theory. I, 25:3381 (JINR-P2-5320)
Electric discharge of gas bubbles in liquids, 25:2485 (JINR-P13-5277)
Quasielastic scattering of particles on deuterons, 25:3293 (JINR-P2-5343)

JOINT INST. FOR NUCLEAR RESEARCH, DUBNA (USSR). LAB. OF NUCLEAR REACTIONS.
Neutron-rich isotopes of light elements produced in transfer reactions with heavy ions, 25:3648 (JINR-E7-5319)

JOINT INST. FOR NUCLEAR RESEARCH, DUBNA (USSR). LAB. OF THEORETICAL PHYSICS.
Poisson distribution of secondary particles in straight-line paths approximation, 25:3407 (JINR-E2-5329)
Static model of s waves in πN scattering and t-channel peculiarities, 25:3380 (JINR-P2-5263)

K

KANSAS UNIV., LAWRENCE. NUCLEAR STRUCTURE LAB.
Intermediate coupling in the N = 29 and Z = 29 nuclei, 25:3592 (COO-1120-106)
KENTUCKY UNIV., LEXINGTON. DEPT. OF CHEMISTRY.
Determination of elements in lunar material by 14-MeV neutron activation, 25:2118 (CONF-700322-, pp 205-20)
KERNFORSCHUNGSANLAGE, JUELICH (WEST GERMANY). INSTITUT FUER PLASMAPHYSIK.
Steady-state generation of rotating multipoles for plasma experiments in Mcs range, 25:3129 (JUL-667-PP)
KERNFORSCHUNGSZENTRUM, KARLSRUHE (WEST GERMANY).
Inherent stability of steam-cooled breeder reactors, 25:3856 (KFK-851)
Prog. rpt. of the Radiation Protection and Safety Department, annual, 1969, 25:2570 (KFK-1158)
KERNFORSCHUNGSZENTRUM, KARLSRUHE (WEST GERMANY). INSTITUT FUER ANGEWANDTE KERNPHYSIK.
Excitation functions and differential cross sections for $^{9}Be(n,\alpha)$ reaction with 8 to 30 MeV neutrons, 25:3564 (KFK-1190)
Studies of radiative neutron capture and delayed fission gamma-ray spectra from uranium and plutonium as a basis for new nondestructive safeguards techniques, 25:3649 (KFK-1214)
KERNFORSCHUNGSZENTRUM, KARLSRUHE (WEST GERMANY). INSTITUT FUER MATERIAL UND FESTKOERPERFORSCHUNG.
Compatibility tests with UC of differing stoichiometries and Fe--Ni--Cr alloys and the influence of stabilizers, 25:2765 (KFK-1213)
Creep and creep strength of V--Ti and V--Ti--Nb alloys with additions of Si and Ge, 25:2662 (KFK-1193)
KERNFORSCHUNGSZENTRUM, KARLSRUHE (WEST GERMANY). INSTITUT FUER NEUTRONENPHYSIK UND REAKTORTECHNIK.
Considerations on coated particles, with oxide fuel, and graphite and Si carbide coating, for GCFR application, 25:3875 (EURFNR-834)
Critical and safe dimensions of containers for storage and mixing of plutonium-containing nuclear fuel, 25:2419 (KFK-1192)
KERNFORSCHUNGSZENTRUM, KARLSRUHE (WEST GERMANY). INSTITUT FUER RADIOCHEMIE.
Complex compounds of hexavalent actinides with pyridine carboxylic acids, 25:2194 (KFK-1070)
KERNFORSCHUNGSZENTRUM, KARLSRUHE (WEST GERMANY). INSTITUT FUER REAKTORENTWICKLUNG.
High purity gas protective system for the use of high melting reactive metals at high temperatures, 25:2639 (LIB/Trans-309)

L

LABORATOIRE CENTRAL DES INDUSTRIES ELECTRIQUES, FONTENAY-AUX-ROSES (FRANCE).
Effect of high energy radiations on insulating materials, 25:2819 (LCIE-342)
LEIDEN RIJKSUNIVERSITEIT (NETHERLANDS).
Neutron-capture gamma-ray spectra from aligned Nd and Sm nuclei, 25:3651 (NP-18485)
LOS ALAMOS SCIENTIFIC LAB., N. MEX.
Determination of Ti, Zr, Hf, Nb, Ta, Mo, and W in uranium alloys, 25:2065 (LA-4529)
Direct digital readout and computer calculation of amino acid analysis data, 25:3965 (LA-4507)
Mechanical properties of carbide and nitride reactor fuels, 25:2785 (LA-4452)
PHOXE: a FORTRAN-IV code to check format syntax, consistency, and physical realism of ENDF/B photon production data, 25:3531 (LA-4506)
Twenty-five group cross sections used in Los Alamos Rover program, 25:3530 (LA-4484)
Use of small accelerators in nuclear safeguards research, 25:2418 (CONF-700322-, pp 357-78)
LYON UNIV. (FRANCE). INSTITUT DE PHYSIQUE NUCLEAIRE.
Decay scheme of 7 min ^{166}Lu, 25:3650 (LYCEN-7030)
Distribution of ion densities in an arc discharge, 25:3085 (LYCEN-7061)
Elastic α scattering by ^{4}He, 25:3544 (LYCEN-7041)
Oxygen determination in silicon by means of alpha particles, 25:2128 (LYCEN-7060)
Production of multicharged ions in a reflex source with axial extraction, 25:3111 (LYCEN-7065)
Study of some nuclei of the 1p and 2s-1d shells using the Hartree--Fock method, 25:3545 (LYCEN-7047)
Use of a Van de Graaff generator to simulate the transient effects due to radiation in semiconductors, 25:3477 (LYCEN-7063)

M

MAGYAR TUDOMANYOS AKADEMIA KOZPONTI FIZIKAI KUTATO INTEZETE, BUDAPEST.
Calculation of resonance integrals: codes RIFFRAFF and RA04, 25:3528 (KFKI-70-12-RPT)
GRACE: multigroup fast neutron spectrum code, 25:3529 (KFKI-70-14-RPT)
SL(2,C) representations in explicitly energy dependent basis. II, 25:3421 (KFKI-70-19-HEP)
MAINE YANKEE ATOMIC POWER CO., WISCASSET.
Maine Yankee Atomic Power Station. Preliminary safety analysis report, Amendment 16, 25:3836 (DOCKET-50309-24)
Maine Yankee Atomic Power Station. Environmental report, 25:3837 (DOCKET-50309-25)
MASON AND HANGER-SILAS MASON CO., INC., AMARILLO, TEX.
Non-contact gaging, 25:3966 (MHSMP-15)
MASSACHUSETTS INST. OF TECH., CAMBRIDGE.
Tenth symposium on engineering aspects of magnetohydrodynamics, Cambridge, Massachusetts, March 26--28, 1969, 25:2945
MASSACHUSETTS UNIV., AMHERST.
Reaction (p,α) with a 400-keV Van de Graaff accelerator, 25:3466 (CONF-700322-, pp 49-61)
MICHIGAN STATE UNIV., EAST LANSING.
Prog. rpt. on electrochemistry and spectra of metal--ammonia and metal--amine solutions and kinetics of electron-attachment reactions, 9/16/69--9/25/70, 25:3937 (COO-958-19)
Prog. rpt. on transport and defect properties of thin metallic wires, annual, 9/69--9/70, 25:3939 (COO-1247-21)
MICHIGAN STATE UNIV., EAST LANSING. DEPT. OF CHEMISTRY.
Prog. rpt. on investigation of some lanthanide boron, carbon, nitrogen, silicon, chalcogen and halogen systems at elevated temperatures, annual, 2/70--1/71, 25:2803 (COO-716-66)
MICHIGAN TECHNOLOGICAL UNIV., HOUGHTON. DEPT. OF METALLURGICAL ENGINEERING.
Size distributions of antiphase domains in Cu_3Au, 25:3941 (COO-1431-10)
MIDDLE TENNESSEE STATE UNIV., MURFREESBORO.
Experiments utilizing $D(^{3}He,p)^{4}He$ reaction, 25:3543 (CONF-700322-, pp 95-104)
MILLSTONE POINT CO., WETHERSFIELD, CONN.
Millstone Nuclear Power Station, Unit 1. Failure of gas turbine generator on test, 25:3789 (DOCKET-50245-42)
MINNESOTA UNIV., MINNEAPOLIS. PARTICLE TECHNOLOGY LAB.
Mobility and coefficients of slip of polystyrene latex particles, 25:3940 (COO-1248-22)
MINNESOTA UNIV., MINNEAPOLIS. SCHOOL OF PHYSICS AND ASTRONOMY.
Nuclear orientation studies of local moments in noble metal hosts, 25:3942 (COO-1569-67)
MISSISSIPPI UNIV., UNIVERSITY. DEPT. OF CHEMICAL ENGINEERING.
Infrared and Raman spectra of trivalent lanthanide--Di-(2-ethylexyl) phosphoric acid solvent extraction organic equilibrium phases, 25:2193 (CONF-700403-8)
MISSOURI UNIV., COLUMBIA.
Prog. rpt. on factors affecting thyroid hormone secretion rates and utilization rates in mammals using ^{131}I as a tracer, 1968--70, 25:3945 (COO-1758-27)
MISSOURI UNIV., COLUMBIA. DEPT. OF DAIRY HUSBANDRY.
Prog. rpt. on factors affecting thyroid hormone secretion rates and utilization rates in mammals using ^{131}I as a tracer, annual, 1970, 25:3944 (COO-1758-26)
MOUND LAB., MIAMISBURG, OHIO.
Compatibility of ^{238}Pu dioxide with platinum and platinum--rhodium alloys, 25:2663 (MLM-1684)
MULTIVOLT LTD., CRAWLEY (ENGLAND).
Target technology for medium and high-power applications, 25:3474 (CONF-700322-, pp 431-9)

N

NAGOYA UNIV. (JAPAN). INST. OF PLASMA PHYSICS.
Effects of r.f. electric field on dispersion of ion waves, 25:3150 (IPPJ-93)
Magnetic and drift surfaces, current configuration of stellarator field, 25:3128 (IPPJ-95)
Nonlinear effect of large-amplitude ion acoustic waves, 25:3151 (IPPJ-94)
Stochastic model of electron cyclotron heating in a magnetic mirror, 25:3055 (IPPJ-100)
NATIONAL AERONAUTICS AND SPACE ADMINISTRATION, CLEVELAND, OHIO. LEWIS RESEARCH CENTER.
Apparent solubilities of commercially pure and oxygen-doped tantalum and niobium in liquid potassium, 25:2664 (N-70-32146)
Radiation-induced preparation of metals from their aqueous salt solutions, 25:2237 (N-70-32826)
NATIONAL AERONAUTICS AND SPACE ADMINISTRATION, GREENBELT, MD. GODDARD SPACE FLIGHT CENTER.
Mechanisms of recovery of radiation damaged silicate-treated zinc oxide thermal control coatings, 25:2815 (N-70-33138)
NATIONAL AERONAUTICS AND SPACE ADMINISTRATION, HUNTSVILLE, ALA. GEORGE C. MARSHALL SPACE FLIGHT CENTER.
Solar indices, 1/55--12/69, 25:2858 (N-70-32003)
NATIONAL AERONAUTICS AND SPACE ADMINISTRATION, LANGLEY STATION, VA. LANGLEY RESEARCH CENTER.
Transmission and backscatter coefficients of 1.0 to 3.0 MeV electrons incident on some metals and alloys, 25:2883 (N-70-25499)
NATIONAL BUREAU OF STANDARDS, WASHINGTON, D. C.
Application of neutron generators to activation analysis, 25:3527 (CONF-700322-, pp 185-204)

Bibliography on neutron generators in activation analysis, 25:2130 (NBS-TN-533)
Bibliography on the high temperature chemistry and physics of materials, January--March 1970, 25:2665 (NBS-SPEC. PUBL-315-5)
Photonuclear reactions, 25:3715 (NBS-MON-118)
Pollution analysis: bibliography of the literature of activation analysis, 25:2129 (NBS-TN-532)

NATIONAL INST. FOR METALLURGY, JOHANNESBURG (SOUTH AFRICA).
Determination of niobium and tantalum by chromatographic method, 25:2066 (NIM-834)
Determination of uranium in ore samples by liquid--liquid extraction and spectrophotometric determination, 25:2067 (NIM-906)

NATIONAL LEAD CO. OF OHIO, CINCINNATI.
Direct reading spectrometric method using AgCl--LiF carrier to determine impurities in nuclear-grade U_3O_8 samples, 25:2068 (NLCO-1071)
Pressurized low temperature reduction of green salt, 25:2640 (NLCO-1058)

NAVAL POSTGRADUATE SCHOOL, MONTEREY, CALIF.
Measurement of charge form factors for ^6Li and ^7Li by electron scattering, 25:3558 (AD-704484)

NAVAL RESEARCH LAB., WASHINGTON, D. C.
Filtration of particles of atomic dimensions, 25:2414 (AD-707709)
Improved radiation embrittlement resistance of steel, 25:2757 (NRL-7121)

NEBRASKA UNIV., LINCOLN. BEHLEN LAB. OF PHYSICS.
Electron spectroscopy with heavy ions, 25:2900 (CONF-700322-, pp 305-19)

NEBRASKA WESLEYAN UNIV., LINCOLN. DEPT. OF PHYSICS.
Educational applications of nuclear electronics, 25:3467 (CONF-700322-, pp 79-88)

NEW HAMPSHIRE UNIV., DURHAM. DEPT. OF PHYSICS.
Beam-foil excitation using low-energy accelerators, 25:3465 (CONF-700322-, pp 21-31)

NEW MEXICO UNIV., ALBUQUERQUE. DEPT. OF CHEMISTRY.
Studies in fast neutron activation analysis, 25:2120 (CONF-700322-, pp 231-48)

NEW YORK OPERATIONS OFFICE (AEC), N. Y. HEALTH AND SAFETY LAB.
Manual of standard procedures, third issuance, 1970, 25:2059 (NYO-4700(3rd Ed.))

NEWCASTLE UNIV. (AUSTRALIA). DEPT. OF METALLURGY.
Thermomigration in metal-interstitial solid solutions, 25:2666 (NP-18468)

NIAGARA MOHAWK POWER CORP., SYRACUSE, N. Y.
Nine Mile Point Nuclear Station. Revisions to Second Addendum to technical supplement to petition to increase power level, 25:3814 (DOCKET-50220-52)

NORTH CAROLINA STATE UNIV., RALEIGH.
Prog. rpt. on Northward migration of Citrus by means of radiation-induced mutation, annual, 10/69--6/70, 25:2552 (ORO-2909-9)

NORTH CAROLINA STATE UNIV., RALEIGH. DEPT. OF CHEMICAL ENGINEERING.
Applications of accelerators in the radiation chemistry of polymers, 25:2218 (CONF-700322-, pp 345-56)

NORTHWESTERN UNIV., EVANSTON, ILL.
Prog. rpt. on radiation effects of ion bombardment, final, 6/15/68--8/31/70, 25:3190 (COO-1053-15)
Relationship between ion impacts and clusters in gold crystal foils. Final progress report, June 15, 1969--August 31, 1970, 25:3189 (COO-1053-14)

NUCLEAR FUEL SERVICES, INC., WEST VALLEY, N.Y.
West Valley Reprocessing Plant. Conversion of existing emergency generator to diesel drive, 25:2309 (DOCKET-50201-55)

O

OAK RIDGE ASSOCIATED UNIVERSITIES, INC., TENN.
Conference on use of small accelerators for teaching and research, Oak Ridge, Tenn., 3/70, 25:3463 (CONF-700322)
Radiation safety in the operation of a low-energy accelerator, 25:3475 (CONF-700322-, pp 441-8)

OAK RIDGE NATIONAL LAB., TENN.
Absorber materials for sulfur dioxide from flue gas, 25:2820 (ORNL-4570, pp 213)
Addendum: experimental and analytical investigations of the structural behavior of nozzle-to-shell attachments, 25:2386 (ORNL-TM-2526(Add.))
Advanced LMFBR fuels development, 25:2769 (ORNL-4570, pp 62-7)
Alkali-metal corrosion of refractory metals, 25:2607 (CRNL-4570, pp 103-5)
Alloy development for Army Pulsed Radiation Facility Reactor, 25:2645 (ORNL-4570, pp 214)
Aluminum irradiation damage, 25:2759 (ORNL-4570, pp 152-6)
Approximate high-energy alpha-particle-nucleus-collision model, 25:3716 (ORNL-TM-3153)
Atomic physics of fast ion beams: fine structure experiments, 25:2889 (CONF-700322-, pp 289-95)
Bibliography of atomic and molecular processes, 1--12/69, 25:2901 (ORNL-AMPIC-13)
Chemical applications of nuclear explosions, 25:2380 (CRNL-4572, pp 196-8)
Chemical engineering research, 25:2195 (ORNL-4572, pp 251-7)
Chemical Technology Division annual progress report for period ending 5/31/70, 25:2312 (ORNL-4572)
Cladding and structural materials, 25:2758 (CRNL-4570, pp 76-84)
Comparison of calculated and measured lower critical field for some Nb--Ti alloys, 25:3020 (ORNL-TM-3206)
Conference on continuum aspects of graphite design, Gatlinburg, Tenn., 11/70, 25:2793 (ORNL-TM-3191)
Consideration of nuclear power expansion for Puerto Rico, including surplus capacity penalties, 25:3798 (ORNL-TM-3142)
Conversion studies in the LMFBR fuel cycle, 25:2317 (ORNL-4572, pp 170-3)
Corrosion of advanced steam generator alloys, 25:2608 (ORNL-4570, pp 124-6)
Crystal physics, 25:2727 (ORNL-4570, pp 1-4)
Deformation of crystalline solids, 25:2668 (CRNL-4570, pp 10-12)
Deformation, annealing, and interfaces in metallurgical phenomena, 25:2728 (ORNL-4570, pp 5-9)
Desalination, 25:2644 (ORNL-4570, pp 157-60)
Development of aqueous processes for fast reactor fuels, 25:2314 (ORNL-4572, pp 37-84)
Development of methods for reprocessing HTGR fuels, 25:2315 (ORNL-4572, pp 85-97)
Development of the thorium fuel cycle, 25:2773 (ORNL-4572, pp 135-48)
Diffusion in solids, 25:2786 (ORNL-4570, pp 13-15)
Electron microscopy, 25:2816 (ORNL-4570, pp 16-19)
Fabrication of fast breeder reactor cladding, 25:2641 (ORNL-4570, pp 85-7)
Fabrication voids in aluminum-base fuel dispersions, 25:2806 (ORNL-4611)
FASEII: a computer program for the stress analysis of thin cylindrical shells and flat plates, 25:3949 (GA-9203)
Fast breeder neutron absorber materials, 25:2790 (ORNL-4570, pp 98-102)
Fast reactor oxide fuels, 25:2768 (ORNL-4570, pp 47-61)
Fuel element fabrication development, 25:2770 (ORNL-4570, pp 127-35)
Fundamental ceramics research, 25:2729 (ORNL-4570, pp 20-2)
Gas-Cooled Reactor Program, 25:2771 (ORNL-4570, pp 161-9)
Hastelloy N improvement, 25:2674 (ORNL-4570, pp 136-42)
Heavy section steel technology, 25:2676 (ORNL-4570, pp 170-3)
Investigation of the need for variable orifices in multistage flash evaporators, 25:2387 (ORNL-TM-2746)
Ion channeling and blocking phenomena, 25:3188 (CONF-700322-, pp 141-53)
Irradiation effects on heterogeneous systems, 25:2295 (ORNL-4572, pp 225-30)
Joining research on nuclear materials, 25:2675 (ORNL-4570, pp 143-8)
LMFBR fuel element design and model development, 25:2789 (ORNL-4570, pp 68-75)
Materials development for isotopic power programs, 25:2643 (ORNL-4570, pp 106-11)
Measurement of residual stresses, 25:2410 (ORNL-TM-3113)
Metallography, 25:2731 (ORNL-4570, pp 215-23)
Metallurgy of refractory alloys, 25:2672 (ORNL-4570, pp 112-15)
Metals and ceramics division annual progress report for period ending June 30, 1970, 25:2601 (ORNL-4570)
Military reactor fuel element procurement assistance, 25:2772 (ORNL-4570, pp 174)
Miscellaneous programs, 25:2821 (ORNL-4572, pp 258-61)
Moessbauer studies of alloys, 25:2669 (ORNL-4570, pp 23)
Molten-salt reactor processing, 25:2313 (ORNL-4572, pp 1-36)
Molten-Salt Reactor Program, 25:2609 (ORNL-4570, pp 175-90)
NERVA Program metallurgical support, 25:2677 (ORNL-4570, pp 224-7)
Nitride fuels development, 25:2817 (ORNL-4570, pp 116-17)
Nondestructive test development, 25:2409 (CRNL-4570, pp 149-51)
Nondestructive testing techniques for LMFBR, 25:2408 (ORNL-4570, pp 96-7)
Physical ceramics studies, 25:2787 (ORNL-4570, pp 24-6)
Physical property research, 25:2788 (ORNL-4570, pp 27-30)
Preparation and properties of actinide oxides, 25:2775 (ORNL-4572, pp 242-50)
Preparation of $^{233}UO_2$ for Light Water Breeder Reactors, 25:2318 (ORNL-4572, pp 174-80)
Prog. rpt. on thorium fuel cycle development, 10/70, 25:2320 (ORNL-TM-3204)
Radiation safety in the operation of a low-energy accelerator, 25:3475 (CONF-700322-, pp 441-8)
Radiative capture of deuterons by protons at 20 and 30 MeV, 25:3546 (ORNL-TM-3168)
Reactor evaluation studies, 25:3797 (ORNL-4572, pp 236-41)
Reactor evaluation, 25:2602 (ORNL-4570, pp 191-4)
Savannah River Americium--Curium Slug Carrier, 25:2421 (ORNL-TM-3110)

Separations chemistry research, 25:2319 (ORNL-4572, pp 181-95)
SHELL5: SHELL-3D Version 5, a computer program for the structural analysis of arbitrary three-dimensional thin shells, 25:3950 (GA-9952)
Sodium corrosion in LMFBR systems, 25:2606 (ORNL-4570, pp 92-5)
Sol-gel processes for the uranium fuel cycle, 25:2774 (ORNL-4572, pp 149-69)
Spectrophotometric studies of solutions of lanthanides and actinides, 25:2152 (ORNL-4572, pp 231-5)
Spectroscopy of ionic media, 25:2805 (ORNL-4570, pp 31-4)
Stainless steel welding development, 25:2642 (ORNL-4570, pp 88-91)
Superconducting materials, 25:2670 (ORNL-4570, pp 35-6)
Surface reactions of metals, 25:2605 (ORNL-4570, pp 37-9)
Theoretical research, 25:2671 (ORNL-4570, pp 40-3)
Thorium utilization, 25:2791 (ORNL-4570, pp 195-200)
Title-author-company index to reports published by the U. S. Department of the Interior, Office of Saline Water, 25:3913 (ORNL-NDIC-8)
Transuranium program, 25:2792 (ORNL-4570, pp 201-4)
Transuranium-element processing, 25:2294 (ORNL-4572, pp 109-34)
Tungsten metallurgy, 25:2673 (ORNL-4570, pp 118-23)
Turbulent heat in mirror machines at ORNL, 25:3056 (ORO-1171-1, pp 78-97)
Vanadium neutron elastic- and inelastic-scattering cross sections from 4.19 to 8.56 MeV, 25:3595 (ORNL-4551)
Waste treatment and disposal, 25:2316 (ORNL-4572, pp 98-108)
Water reactor safety, 25:2610 (ORNL-4570, pp 205-12)
X-ray diffraction, 25:2730 (ORNL-4570, pp 44-6)

OHIO STATE UNIV., COLUMBUS.
Prog. rpt. on theoretical and experimental aspects of selection as applied to biological groups, 2--10/70, 25:3946 (COO-1761-13)
Prog. rpt. on theoretical and experimental aspects of selection as applied to biological groups, 1968--70, 25:3947 (COO-1761-14)

P

PACIFIC UNION COLL., ANGWIN, CALIF.
Charged particle excited x rays, 25:2862 (CONF-700322-, pp 113-24)

PADUA UNIV. (ITALY). ISTITUTO DI FISICA.
Annihilation anti pn → $\pi^+\pi^-\pi^-$ between 1.0 and 1.6 GeV/c and its comparison with Veneziano model, 25:3270 (INFN-PD-70/2)

PANAMETRICS, INC., WALTHAM, MASS.
Ultrasonic thermometry for LMFBR systems, 25:2503 (NYO-3906-4)

PARIS UNIV. (FRANCE).
Radiolysis of concentrated nitrate and formate solutions, 25:2257 (CEA-R-4046)

PARIS UNIV. (FRANCE). FACULTE DES SCIENCES.
Coalescence of organic solutions during the extraction of acids and metals by trialkylamines, 25:2308 (CEA-R-3845)

PARIS UNIV., ORSAY (FRANCE). FACULTE DES SCIENCES.
Distortion in reactions $^{12}C(p,2p)^{11}B$/sub 1P/ and $^{40}Ca(p,2p)^{39}K$/sub 2S/, 25:3565 (NP-18476)
Mechanism of the ($^3He,\alpha$) reaction at low energy, 25:3594 (NP-18464)

PENNSYLVANIA UNIV., PHILADELPHIA.
Self-adjoint algebras of unbounded operators, 25:3968 (NYO-2171-325)

PENNSYLVANIA UNIV., PHILADELPHIA. DEPT. OF PHYSICS.
Detection of the weak intermediate boson through its hadronic decay modes, 25:3333 (NYO-2171-323)

PHILADELPHIA ELECTRIC CO., PA.
Limerick Generating Station, Units 1 and 2. Preliminary safety analysis report, Amendment 2, Suppl. 2, 25:3846 (DOCKET-50352-9)
Peach Bottom Atomic Power Station, Unit 1. Monthly operations report No. 55, September 1970, 25:3784 (DOCKET-50171-58)

PHILIPPINE ATOMIC RESEARCH CENTER, DILIMAN, QUEZON CITY.
Neutron activation analysis in medical research in the Philippines, 25:2126 (IAEA-122, pp 37-40)

PRINCETON UNIV., N. J.
Lecture notes [on toroidal fusion reactors], 25:3132 (ORO-1171-1, pp 38-77)

PUBLIC SERVICE CO. OF COLORADO, DENVER.
Fort St. Vrain Nuclear Generating Station, Unit 1. Preliminary safety analysis report, Amendment 16, 25:3833 (DOCKET-50267-23)

PUBLIC SERVICE ELECTRIC AND GAS CO., NEWARK, N.J.
Newbold Island Nuclear Generating Station, Units 1 and 2. Preliminary safety analysis report, Amendment 3, 25:3847 (DOCKET-50354-9)

PURDUE UNIV., LAFAYETTE, IND. DEPT. OF PHYSICS.
Directional correlation and intensity studies of electromagnetic transitions in ^{181}Ta, 25:3647 (COO-1746-46)

Q

QUIRK, LAWLER AND MATUSKY ENGINEERS, NEW YORK.
Utility of radioisotope methodology in estuary pollution control studies. I, 25:2348 (NYO-3961-1)

R

REACTOR CENTRUM NEDERLAND, PETTEN.
CACES: an ALGOL program for solving diffusion type elliptic differential equations in plane involving arbitrary boundary conditions and shape, 25:3876 (RCN-123)

READING UNIV. (ENGLAND). DEPT. OF CHEMISTRY.
Neutron activation techniques in human metabolic studies, 25:2123 (IAEA-122, pp 1-13)
Use of activation analysis in the study of cystic fibrosis, 25:2127 (IAEA-122, pp 145-8)

RENSSELAER POLYTECHNIC INST., TROY, N.Y. DEPT. OF NUCLEAR SCIENCE.
Precision of tank capture cross section measurements, 25:2435 (RPI-328-202)

REYNOLDS ELECTRICAL AND ENGINEERING CO., INC., MERCURY, NEV. RADIOLOGICAL SCIENCES DEPT.
Carlsbad site roll-up program. On-site radiological safety report, 25:2420 (NVO-410-2)

ROANOKE COLL., SALEM, VA. DEPT. OF PHYSICS.
Wall erosion by sputtering in controlled thermonuclear fusion devices, 25:3135 (ORO-1171-1, pp 334-42)

ROCKEFELLER UNIV., NEW YORK.
Bjorken limit and Jin--Martin lower bound, 25:3294 (NYO-4204-5)
Deep inelastic e-p structure functions in a ladder model with spin $^1/_2$ nucleons, 25:3311 (NYO-4204-4)
Regge analysis of electroproduction and photoproduction, 25:3312 (NYO-4204-6)
Weak interactions at high energies, 25:3334 (NYO-4204-3)

RURAL COOPERATIVE POWER ASSOCIATION, ELK RIVER, MINN.
Elk River Reactor operations report, 8/69, 25:3782 (DOCKET-1151-3)

RUTHERFORD HIGH ENERGY LAB., CHILTON (ENGLAND).
Computer graphics patching of failed CYCLOPS events for spark chamber experiment, 25:2486 (RHEL/R-205)

S

SAN DIEGO GAS AND ELECTRIC CO., CALIF.
San Onofre Nuclear Generating Station, Units 2 and 3. Preliminary safety analysis report, Amendment 3, 25:3849 (DOCKET-50361-11)

SANDIA LABS., ALBUQUERQUE, N. MEX.
Application of neutron damage models to semiconductor device studies, 25:2514 (SC-R-70-4351)
Basic response phenomenology analytical techniques, 25:3974 (SC-R-68-1784)
Emission cross sections for H^+, Na^+, Ne^+, Rb^+, incident on molecular nitrogen, 25:2902 (SC-RR-70-695)
SMOPAS: Sandia matrix-oriented production assembly system, 25:3976 (SC-RR-70-645)
Stochastic approach to bioburden estimation and prediction, 25:3975 (SC-RR-70-561)
Studies in fast neutron activation analysis, 25:2120 (CONF-700322-, pp 231-48)

SASKATCHEWAN UNIV., SASKATOON. SASKATCHEWAN ACCELERATOR LAB.
Electrodisintegration of carbon, 25:3566 (SAL-14)
High-energy photoneutrons emitted from 1P-shell in ^{12}C, 25:3567 (SAL-15)

SOCIETE ANONYME DES ATELIERS DE SECHERON, GENEVA (SWITZERLAND).
Charge/discharge machine for Dragon reactor, 25:2385 (DP-Report-230)

SOUTH CAROLINA UNIV., COLUMBIA. DEPT. OF PHYSICS.
Directional correlation and intensity studies of electromagnetic transitions in ^{181}Ta, 25:3647 (COO-1746-46)

SOUTHERN CALIFORNIA EDISON CO., CAMP PENDLETON, CALIF.
San Onofre Nuclear Generating Station, Units 2 and 3. Preliminary safety analysis report, Amendment 3, 25:3849 (DOCKET-50361-11)

SOUTHERN CALIFORNIA EDISON CO., LOS ANGELES.
San Onofre Nuclear Generating Station, Unit 1. Malfunction of safety injection system valves, 25:3786 (DOCKET-50206-97)
San Onofre Nuclear Generating Station, Unit 1. Operation report, October 1970, 25:3785 (DOCKET-50206-94)
San Onofre Nuclear Generating Station, Unit 1. Preliminary safety analysis report, Amendment 20, 25:3809 (DOCKET-50206-95)

SOUTHWEST RESEARCH INST., SAN ANTONIO, TEX.
Connecticut Yankee Nuclear Power Plant. 1970 inservice inspection, 25:3812 (DOCKET-50213-85)

T

TENNESSEE TECHNOLOGICAL UNIV., COOKEVILLE. DEPT. OF PHYSICS.
Charged particle spectra from ^{9}Be + D reaction, 25:3560 (CONF-700322-, pp 89-94)
TENNESSEE UNIV., KNOXVILLE.
Study of the nuclei ^{61}Cu, ^{64}Cu, ^{67}Ga, and ^{68}Ga using the (p,n) reaction, 25:3596 (TID-25503)
TENNESSEE UNIV., OAK RIDGE. RESIDENT GRADUATE PROGRAM.
Programming techniques for PDP-8/I computer, 25:2501 (CONF-700322-, pp 105-11)
TENNESSEE VALLEY AUTHORITY, CHATTANOOGA. OFFICE OF POWER.
Browns Ferry Nuclear Plant, Units 1, 2, and 3. Preliminary safety analysis report, Amendment 10, 25:3827 (DOCKET-50259-20)
TEXAS AGRICULTURAL AND MECHANICAL UNIV., COLLEGE STATION. ACTIVATION ANALYSIS RESEARCH LAB.
Analysis of oceanographic samples by 14-MeV neutron activation, 25:2119 (CONF-700322-, pp 221-30)
TEXAS CHRISTIAN UNIV., FORT WORTH.
Inelastic electron--atom interactions in the 50 to 150 keV energy range, 25:3472 (CONF-700322-, pp 379-92)
TEXAS TECH UNIV., LUBBOCK. PLASMA LAB.
Conference on thermonuclear fusion reactor design, 6/70, Lubbock, Tex, 25:3130 (ORO-1171-1)
TOKYO UNIV. (JAPAN). INST. FOR NUCLEAR STUDY.
Device for observing the entry direction of air showers, 25:2484 (INS-TCA-26)
TOLEDO EDISON CO., OHIO.
Davis--Besse Nuclear Power Station. Safety evaluation, 25:3844 (DOCKET-50346-18)

U

UNION CARBIDE CORP., OAK RIDGE, TENN. Y-12 PLANT.
Automated quantometer data handling system, 25:2069 (Y-1740)
Radiation safety in the operation of a low-energy accelerator, 25:3475 (CONF-700322-, pp 441-8)
UNITED STATES STEEL CORP., MONROEVILLE, PA. APPLIED RESEARCH LAB.
Application of neutron generators in the steel industry, 25:2121 (CONF-700322-, pp 249-57)

V

VERMONT YANKEE NUCLEAR POWER CORP., RUTLAND.
Vermont Yankee Nuclear Power Station. Preliminary safety analysis report, Amendment 16 (includes additions and revisions to final safety analysis report, Vol. 4, App. I), 25:3835 (DOCKET-50271-34)

W

WADCO CORP., RICHLAND, WASH.
CCTL Mark I and Mark II prototype FFTF subassembly compression test development work, 25:3908 (WHAN-FR-18)
Creep rate correlation in solution-treated Type 304 and 316 stainless steels, 25:4007 (WHAN-FR-25)
WASHINGTON UNIV., ST. LOUIS, MO. DEPT. OF CHEMISTRY.
Structure of ^{51}Cr via $^{48}Ti(^{4}He, n\gamma)$ and $^{51}V(p,n\gamma)$ prompt γ-ray spectrometry, 25:3593 (COO-1530-21)
WASHINGTON UNIV., SEATTLE.
Energy dependence of quasifree scattering in the D(p,pn)p reaction, 25:3547 (RLO-1388-126)
WAYNE STATE UNIV., DETROIT, MICH. DEPT. OF PHYSICS.
Nuclear magnetic resonance study of the crystalline compounds of the NbBe/sub x/ system, 25:3220 (COO-1700-12)
WESTERN KENTUCKY UNIV., BOWLING GREEN.
Levels in ^{11}B by the $^{10}B(d,p)^{11}B$ reaction, 25:3561 (CONF-700322-, pp 133-40)
WESTERN WASHINGTON STATE COLL., BELLINGHAM.
Student experiments utilizing a neutron generator, 25:3526 (CONF-700322-, pp 33-47)
WESTINGHOUSE ELECTRIC CORP., PITTSBURGH, PA. ATOMIC POWER DIV.
Point Beach Nuclear Plant, Unit 1. Initial integrated leak rate test of the reactor containment building. Final report, 25:3829 (DOCKET-50266-32)
WISCONSIN UNIV., MADISON.
Fast neutron radiobiology and radiotherapy, 25:2582 (CONF-700322-, pp 393-406)
WISCONSIN UNIV., MADISON. DEPT. OF NUCLEAR ENGINEERING.
Engineering of a fusion plant-torch complex, 25:3136 (ORO-1171-1, pp 344-75)
Injector requirements for open ended fusion reactors, 25:3131 (ORO-1171-1, pp 3-37)
WISCONSIN UNIV., MADISON. DEPT. OF PHYSICS.
Detection of the weak intermediate boson through its hadronic decay modes, 25:3333 (NYO-2171-323)

Y

YANKEE ATOMIC ELECTRIC CO., WESTBORO, MASS.
Yankee Nuclear Power Station. Operation report No. 118, October 1970, 25:3783 (DOCKET-50029-140)

Z

ZENTRALSTELLE FUER ATOMKERNENERGIE-DOKUMENTATION, FRANKFURT AM MAIN (WEST GERMANY).
Bibliographies in nuclear science and technology, 25:2399 (AED-C-12-22)

PERSONAL AUTHOR INDEX

Authors' names are indexed in the form appearing in the abstracted publication. Each entry under an author's name gives the publication title and the *NSA* volume and abstract numbers. Report numbers, where applicable, are given in parentheses at the end of the entry.

Because of problems involved in the mechanical preparation of this index, all accent marks are omitted. The following changes in spelling have been introduced to reduce some of the confusion which might result from omitting the accents:

Germanic	ä	appears as ae
Germanic	ö	oe
Germanic	ü	ue
Scandinavian	ø	oe

A

AABERG, B., Whole-body measurements on distribution of ^{203}Hg in humans, 25:2533
ABDEL-GAWAD, A. S., Extraction of niobium from aqueous organic acid media by structurally related tert-amines, 25:2334
ABDEL-RASSOUL, A. A., Extraction of niobium from aqueous organic acid media by structurally related tert-amines, 25:2334
ABOOD, Karin A., Utility of radioisotope methodology in estuary pollution control studies. I, 25:2348 (NYO-3961-1)
ABOU-ELNASR, T. Z. A., Moessbauer spectrometer calibration, 25:3224
ABRAHAM, John, Thorium(VI) adducts of 8-quinolinol and derivatives, 25:2157
ABRAMOVICH, M., Spin--parity analysis of 3π system in reaction $\pi^-p \to p\pi^-\pi^+\pi^-$ at 3.9 GeV/c, 25:3276
ABRAMS, G. S., Reaction $\pi^+p \to \Delta^{++}A_2^0$ at 3.7 GeV/c, 25:3272 (UCRL-20050)
ABRAMYAN, E. A., Generator of short pulses of hard x-rays of high intensity, 25:2401
ABUL-MAGD, A. Y., Nuclear diffraction scattering, 25:3757
ACHARYA, R., Deser--Gilbert--Sudarshan representation and electroproduction structure functions, 25:3329
ACHMATOWICZ-SZMARJKE, Teresa, Radiation induced graft terpolymerization of poly(ethylene terephthalate). I, 25:2244
ACKER, Robert C., Experimental superconducting transformer for current step-up, 25:3509
ADACHI, Toshimi, Complex angular momentum and impact parameter amplitude, 25:3462
ADAM, G., Separation of overlapping decaying peaks, 25:2482
ADAM, J., Two ion collisional absorption of low frequency electromagnetic waves in a toroidal hard-core configuration, 25:3148 (CEA-CONF-1614)
ADAMS, J. B., Design studies for large proton synchrotron, 25:3501
ADAMSKI, J., Asymptotic stability by Liapunov's direct method in the case of circulating fuel reactor, 25:3857
ADIN, Anthony, Mixed-metal complexes between In(III) and U(VI) with malic, citric, and tartaric acids, 25:2206
AFANAS'EV, N. G., Electroproduction of pions on a proton at threshold and structure of the nucleon, 25:3244
Quasi-elastic scattering of 1115-MeV electrons by nucleons of ^{32}S nuclei, 25:3615
AGASYAN, P. K., Coulometric titration of Mn(VII), Ce(IV), Cr(VI), and V(V) by electrogenerated V(III), 25:2081
AGEEV, V. N., Interaction of water vapor with the surface of tungsten, 25:2722
AGRINIER, B., Optical spark chamber for the search of gamma-ray sources, 25:2841 (CEA-CONF-1633)
AGUILAR-BENITEZ, M., Branching ratios of the K(1420) meson, 25:3287
AHARONY, A., Time-reversal violation and the arrows of time, 25:3423
AHLSTROM, J. C., Space--time detector for cosmic ray showers, 25:2490
AHMED, M., Iron-54, $^{60}Ni(p,p)$ and $(p,p'\gamma)$, 25:3613
AHMED, M. A., Off-shell ππ Veneziano amplitude, 25:3373
Veneziano amplitudes for πA, scattering, 25:3374
AIHARA, Shuko, Effects of r.f. electric field on dispersion of ion waves, 25:3150 (IPPJ-93)
AIVAZYAN, Yu. M., Ionization-diffusion oscillations in a plasma, 25:3152
AIZU, Ko, Radio evolution of pulsars, 25:2842
AKIBA, Kenichi, Distribution of TTA and its Sc chelate into ether solvents, 25:2345
AKIYAMA, Hiromitsu, Device for observing the entry direction of air showers, 25:2484 (INS-TCA-26)
ALANAKYAN, Yu. R., Ionization-diffusion oscillations in a plasma, 25:3152
ALBRECHT, R. W., Calculations of neutron time-energy distributions in heavy moderators, 25:3541
ALBRIGHT, C. H., Weakly coupled neutral currents, 25:3302
ALBROW, M. G., Photoproduction of K^0 mesons from protons and from complex nuclei, 25:3248
Polarization in elastic proton--proton scattering between 0.86 and 2.74 GeV/c, 25:3262
ALDRIDGE, Ann Marshall, Beta decay of ^{52}Ti, 25:3640
ALEKSIN, V. F., Kinetics of magnetohydromagnetic waves. I, 25:3159
ALEKSYUK, M. M., Effect of temperature and deformation on mechanical characteristics of molybdenum and niobium, 25:2681
ALESSI, Victor Elliot, Reaction $^{11}B(p,3^4He)$ for proton-beam energies of 0.675, 1.00, and 1.388 MeV, 25:3589
ALEXANDER, G., General features of anti pp annihilation into six charged pions, 25:3263
ALEXANDER, W. K., Testing and surveillance of Hanford production reactor Zircaloy tubes, 25:3921 (DUN-SA-144)
ALEXANDROV, S., Study of the fixation of fluorine on antimony pentoxide in hydrochloric acid medium, 25:2332
ALEXEFF, I., Turbulent heat in mirror machines at ORNL, 25:3056 (ORO-1171-1, pp 78-97)
ALEY, R., Proton induced fission of ^{233}U and ^{238}U, 25:3660
ALFREDSON, P. G., Assessment of air-pulsing techniques for liquid extraction columns, 25:2383 (AAEC/TM-547)
ALI, Ahmad, Chiral-symmetry-breaking corrections to the K → 3π soft-pion theorem, 25:3347
ALIMARIN, I. P., New organic reagents for niobium, 25:2199
Radioactivation determination of impurities in yttrium and molybdenum by means of extraction displacement chromatography, 25:2138
ALLEN, G., Measurement of etarho/sub n/ versus T near T/sub lambda/ of dilute ^3He--^4He mixtures, 25:3016
ALLEN, J. E., Contribution to the co-rotating magnetic field model of the pulsar, 25:2850
ALLEN, J. S., Design of a 600-MeV microtron using a superconducting linac, 25:3506
ALLER, Margo Friedel, Model-atmosphere analysis of the peculiar A star Kappa Cancri, 25:2840
ALLMAN, M. B., Treatment of Rum Jungle U ore, 25:2336
ALPERT, N., Inelastic scattering of alpha particles from ^{64}Zn and ^{66}Zn, 25:3630
ALSMILLER, R. G. Jr., Approximate high-energy alpha-particle-nucleus-collision model, 25:3716 (ORNL-TM-3153)
ALSTER, Jonas, Inelastic scattering of alpha particles from ^{64}Zn and ^{66}Zn, 25:3630
ALTSTETTER, Carl, Ordered orthorhombic subnitride of vanadium, 25:2811
ALVAREZ DE TOLEDO, F., Two ion collisional absorption of low frequency electromagnetic waves in a toroidal hard-core configuration, 25:3148 (CEA-CONF-1614)
ALVENSLEBEN, H., Observation of coherent interference pattern between rho and ω decays, 25:3288
Photoproduction phase of rho^0 mesons, 25:3256
ALVI, Zahoor M., Modulation transfer function evaluation of scintillation camera and rectilinear scanner, 25:2447
AMANO, H., Target preparation, 25:2655
AMANO, Tsuneo, Decay instability of cyclotron harmonic

plasma waves, 25:3162
AMAVIS, R., Physico-chemical behavior of radioruthenium, 25:2362
AMAYA, C. B., Determination of traces of hafnium in aluminum--uranium alloys, 25:2063 (CNEA-276)
AMBARTSUMYAN, R. S., Dispersed precipitates in Zr--Nb alloys, 25:2742
AMIEL, S., Separation of fission produced iodine, 25:2342
AMMAR, R., Production of the anti K^{*0} (890) Δ^{-} (1236) final state in K-d interactions at 5.5 GeV/c, 25:3274
ANCARANI, A., Final safety analysis report on the use of plutonium in ZPR-6 and -9, 25:3901 (ANL-7442)
ANDERSON, D. W., Photoproduction of ^{28}Al and ^{29}Al from phosphorus, 25:3634
ANDERSON, Philip W., How Josephson discovered his effect, 25:3032
ANDERSON, Ralph R., Prog. rpt. on factors affecting thyroid hormone secretion rates and utilization rates in mammals using ^{131}I as a tracer, 1968--70, 25:3945 (COO-1758-27)
Prog. rpt. on factors affecting thyroid hormone secretion rates and utilization rates in mammals using ^{131}I as a tracer, annual, 1970, 25:3944 (COO-1758-26)
ANDERSSON, Myrna, Regulation of pyruvate kinase of an established rat liver cell line (RLC) in culture by insulin, glucose, and serum, 25:3984 (UCLA-12-794)
ANDERSSON/ALMEHED, S., Polarization in elastic proton--proton scattering between 0.86 and 2.74 GeV/c, 25:3262
ANDO, Masao, Introduction of nuclear reactors in iron manufacture industry, 25:3916
ANGELOVA, Veselka, Extraction of rhenium and molybdenum by dialkylmethylbenzylammonium salts, 25:2328
ANICIN, I. V., Finite solid-angle corrections for Ge(Li) detectors, 25:2454
ANIKINA, L. I., Increasing the sensitivity and accuracy of the luminescence determination of the rare earths by the method of the periodical scanning of the spectrum, 25:2066
ANNONI, H., Measurement of beam profile for high-intensity particles, 25:2434 (CERN-70-27)
ANSALDO, E. J., Hyperfine interactions on ^{237}Np and ^{239}Np implanted into copper and nickel, 25:3690
ANTONINI, B., Corrections to magnon dispersion relations, 25:3218
ANT-WUORINEN, O., Determination by x-ray fluorescence of chromium in cellulose, 25:2076
APIN, A. Ya., Determination of the decomposition time of hexogen under the effect of shock waves, 25:3964 (LA-4360-TR)
APPLETON, B. R., Ion channeling and blocking phenomena, 25:3188 (CONF-700322-, pp 141-53)
ARAFUNE, Jiro, Chiral symmetry in the unified fermion theory. II, 25:3428
ARAKAWA, E. T., Observed radiation from surface plasmons in aluminum, 25:2885
ARAKELYAN, M. A., Luminosity function and stellar density in neighborhood of the Sun, 25:2835
ARAVE, A. E., Ultrasonic void fraction detector using compressional stress waves in a wire helix, 25:3905 (IN-1441)
ARDAILLOU, N., Platelet lifespan, 25:2579
ARGIERO, L., Absorption of elements by clays, 25:2338
ARJUN, Tan Tung, Geometric representation of the uncertainty relation, 25:3297
Heuristic derivation of the perihelic precession, 25:3291
ARKATOV, I. M., Quasi-elastic scattering of 1115-MeV electrons by nucleons of ^{32}S nuclei, 25:3615
ARMSTRONG, D. A., Influence of alloying and temperature on the elastic constants of tantalum, 25:2721
ARNDT, U. W., Conference on accurate determination of x-ray intensities and structure factors, Cambridge, Eng., 6/68, 25:3216
ARNIKAR, H. J., Aquoluminescence: release of energy stored in γ-irradiated crystals, 25:2227
ARSENIJEVIC, Desanka, Determination of micro-quantities of carbon in metals, 25:2071
ARTAMONOVA, S. M., Reply to article of Spiridonov, 25:2807 (SC-T-70-4039)
ARTEM'EV, A. N., Investigation of suppressed nuclear absorption of resonant γ rays under Laue diffraction conditions, 25:3225
ARTYUKH, A. G., Neutron-rich isotopes of light elements produced in transfer reactions with heavy ions, 25:3648 (JINR-E7-5319)
ARWILL, T., Penetration of radioactive isotopes through enamel and dentine. II, 25:2532
ASADA, Hiroyuki, Carrier effects on anion-exchange and gel chromatographic behavior of ^{32}P recoil species produced in irradiated inorganic phosphates, 25:2298
ASANO, Hiroko, Distribution of TTA and its Sc chelate into ether solvents, 25:2345
ASCHER, E., Relativistic symmetry groups of uniform electromagnetic fields, 25:3432
ASFUR, F., Investigation of proton polarization in reaction $^{12}C(^{3}He,p_0)^{14}N$, 25:3563 (JINR-P15-5156)
ASHBAUGH, W. G., Stress corrosion cracking of process equipment, 25:2614
ASHCROFT, J., Gamma counting of ^{125}I using a metal-loaded liquid scintillator, 25:2116
ASHIROV, E. G., Polynomial approximation of the fast neutron spectrum measured by threshold detectors, 25:2442
ASHKALIEV, Ya. F., Influence of F2 layer on ionospheric scatter links, 25:2990
ASHLEY, W. H., Determination of Ti, Zr, Hf, Nb, Ta, Mo, and W in uranium alloys, 25:2065 (LA-4529)
ASHWORTH, F. P. O., Evaluation of data from first Dragon charge, 25:3796 (DP-Report-579)
ASINOVSKII, E. I., Calculation of the electrical conductivity of partially ionized plasma, 25:3093
ASLANYAN, A. M., Low-frequency spectra of extragalatic radio sources, 25:2845
ASMUSSEN, Keith Eugene, Detection of sodium boiling in fast sodium-cooled reactors by neutron measurements, 25:3864
ASTON, D., Photoproduction of K^{0} mesons from protons and from complex nuclei, 25:3248
ATEN, A. H. W. Jr., Decay of ^{169}Hf, 25:3676
ATHERTON, David L., Superconducting magnet suspension systems, 25:3038
ATKIN, Robert B., Sintering and ferroelectric properties of lead zirconate titanate ceramics, 25:3992 (UCRL-20309)
ATKINSON, D., Existence of functions that satisfy exactly both crossing and unitarity. IV, 25:3455
AUBERT, Henri, Kinetics of α--β phase change in U alloys, 25:2741
AUBERT, J. J., Large aperture Cherenkov counter, 25:2489
AUBERT, Jacques, Systems xenon hexafluoride--tantalum pentafluoride, xenon hexafluoride--manganese fluoride, xenon hexafluoride--uranium hexafluoride, 25:2156
AUERSPERG, N., Isoenzyme stability in human heteroploid cell lines, 25:2585
AULAGNIER, D., Study by triple labeling of reactions between tetraphenylstibonium and antimony trichloride, 25:2169
AUMUELLER, L., Post-irradiation gas release measurements on fuel elements from Dragon reactor, 25:3870 (DP-Report-497)
AUSLOOS, P., Carbonium ions in radiation chemistry. II. Isomerization process in protonated cyclopropane and cyclobutane ions, 25:2290
AVAKYAN, R. M., Polytropic models in the nonrelativistic generalized theory of gravitation, 25:2833
AVARBE, R. G., Rate of vaporization of congruently vaporizing compositions of NbC, 25:2802
AVDEICHIKOV, V. V., Neutron-rich isotopes of light elements produced in transfer reactions with heavy ions, 25:3648 (JINR-E7-5319)
AVIGNONE III, F. T., Directional correlation and intensity studies of electromagnetic transitions in ^{181}Ta, 25:3647 (COO-1746-46)
AVRAMENKO, M. I., Calculation of the phase focusing of intensive ion bunches, 25:3481
AWWAD, Z., Excited nuclear states in ^{125}Te, 25:3699
AXEL, P., Design of a 600-MeV microtron using a superconducting linac, 25:3506

B

BAARLI, J., Air pollution on the CERN site, 25:2562
BABA, S., Target preparation, 25:2655
BABAEV, Z. R., anti rho-Meson production in high energy pion-collisions with nuclei, 25:3406 (IFVE-STF-69-71)
BABAEVA, M. K., Activity of redoxy enzymes in beans and clover following γ irradiation, 25:2596
BABESHKIN, A. M., Determination of state of ^{129}I in β-/sup 129m/TeO_2 by nuclear gamma resonance, 25:2304
BACH, M., High-pressure pumps: solved sealing problems, 25:2392
BACON, R., Evidence for proton transfer concomitant with hydride expulsion from silanes, 25:2176
BADALYAN, A. M., Hyperspherical-expansion approach to nuclear bound states. I, 25:3730
BADRINARAYANAN, S., Impurity diffusion of rare earth metals in copper, 25:2680
BAGGERLY, L. L., Inelastic electron--atom interactions in the 50 to 150 keV energy range, 25:3472 (CONF-700322-, pp 379-92)
BAGNALL, Kenneth Winfield, UBr_4 and $UCBr_3$.2.5DMA, 25:2200
BAGYINSZKI, A., Calculation of resonance integrals: codes RIFFRAFF and RAD4, 25:3528 (KFKI-70-12-RPT)
BAHNSEN, R. M., Thick-target $^{16}O(d,n)^{17}F$ yield curves, 25:3586
BAINARD, W. D., Development of a waste disposal method for N reactor's decontamination wastes, 25:2426
BAISYA, H. L., Bhabha's equation and electromagnetic field, 25:3439
BAJARD, M., Distribution of ion densities in an arc discharge, 25:3085 (LYCEN-7061)
Production of multicharged ions in a reflex source with axial extraction, 25:3111 (LYCEN-7065)
BAKALDINA, V. D., Spaced sounding of the E/sub s/ layer, 25:2993
BAKER, R. B., CCTL Mark I and Mark II prototype FFTF subassembly compression test development work, 25:3908 (WHAN-FR-16)
BAKHRAKH, L. E., Effect of local heterogeneities of magnetic fields on pulsation of edges of electron beams, 25:3524
BAKHUROV, V. C., Migration and translocation of natural radioactive elements in water, 25:2547

BAKKER, A. M., I = 3/2 K+ elastic-scattering cross section from the reaction K-n → pK-π- at 3 GeV/c, 25:3278
BAKOWSKY, W., Reaction ^{28}Si(d,p)^{29}Si mechanism, 25:3606
BALANDIN, M. P., Electric discharge of gas bubbles in liquids, 25:2485 (JINR-P13-5277)
BALASHOV, V. V., anti rho-Meson production in high energy pion-collisions with nuclei, 25:3406 (IFVE-STF-69-71)
BALAUX, N., Lifetimes in ^{12}B, ^{16}N, and ^{16}O, 25:3569
BALDWIN, Jon M., Bibliography of laser publications of interest to emission spectroscopists. V, 25:3110 (IN-1425)
BALETSKAYA, M. V., Absolute measurements of the excitation functions for the KII line produced in collisions between K+ ions and Ne atoms, 25:2911
BALL, G. C., Rotational structure in ^{43}Sc, 25:3626
BALLANCE, Wilbur C., Hydraulic tests in hole UA-1 and water inflow into an underground chamber, Amchitka Island, Alaska, 25:2349 (USGS-474-72)
BANAIGS, J., Effective deuteron--proton elastic scattering cross section at 180°, 25:3264
BANERJEE, D., Analysis of nuclear separation energies, 25:3754
BANERJEE, Siddheswar, Cupferron in the analytical chemistry of rare earths and scandium, 25:2078
BANKS, P. H. T., Proton polarization measurements, 25:3500
BANSAL, Krishan M., Effect of ion and radical scavengers on the cyclohexyl radical yield in the radiolysis of cyclohexane, 25:2268
BARANGER, Michel, Definition of the single-nucleon potential, 25:3740
BARANOV, V. I., Natural radioisotope distribution in soils of USSR, 25:2371
BARAT, C., Influence of temperature on gain of electron multiplier, 25:2470
BARBASHOV, B. M., Poisson distribution of secondary particles in straight-line paths approximation, 25:3407 (JINR-E2-5329)
BARBER, D. P., Photoproduction of K° mesons from protons and from complex nuclei, 25:3248
BARCLAY, J. A., Radiative detection of single-passage nuclear magnetic resonance, 25:3223
BARGER, V., Empirical merger of geometrical and Regge pictures for elastic hadron scattering, 25:3354
New Regge models of asymptotic behavior, 25:3357
BARI, M. B., Factorization test for the Pomeranchukon in three-particle final states, 25:3395
BARNHAM, K. W. J., Reaction π+p → Δ++A2° at 3.7 GeV/c, 25:3272 (UCRL-20050)
BAR-NIR, I., General features of anti pp annihilation into six charged pions, 25:3263
BARR, P., Post-irradiation gas release measurements on fuel elements from Dragon reactor, 25:3870 (DP-Report-497)
BARRANCO, S. C., Time-specific effect of uv-irradiation on cells progressing from G2 into metaphase, 25:2558
BARRANDON, J. N., Study of the fixation of fluorine on antimony pentoxide in hydrochloric acid medium, 25:2332
BARRETT, R. C., Muonic atoms. I, 25:3661
BARTHOLOMEW, G. A., Study of the ^{207}Pb(d,p)^{208}Pb reaction, 25:3688
BARTLETT, A. C., Measurement of burn-up of Dragon first charge fuel elements, 25:3871 (DP-Report-538)
BARTLETT, Edwin S., Recent information on long-time creep data for columbium alloys, 25:2657 (AD-464715)
BARTLETT, Gerald L., Absence of thymic involvement in the inhibition of urethan lung adenomagenesis by x-radiation, 25:2589
BARTON, John P., Role of accelerators in neutron radiography, 25:3471 (CONF-700322-, pp 321-44)
BAR-TOUV, J., Generalized pairing in light nuclei. II, 25:3722
BARTSCH, J., Application of the Veneziano model with pion and Pomeron exchange to the reaction K- p → nc, 25:3386
BARUEL, J., Use of electrophoresis in thin films for control of the radiochemical purity of tracer compounds, 25:2062 (CNEA-271)
BARZON, G., Absorption of elements by clays, 25:2338
BASAR, I., Directional correlation studies in decay of /sup 177g/Lu, 25:3684
BASHKIN, S., Measurement of atomic lifetimes, 25:2888 (CONF-700322-, pp 281-8)
BASILE, M., Structure in the neutral A2 mass region, 25:3290
BASOV, V. N., Coulometric titration of Mn(VII), Ce(IV), Cr(VI), and V(V) by electrogenerated V(III), 25:2081
BASS, J. A., Mechanisms of recovery of radiation damaged silicate-treated zinc oxide thermal control coatings, 25:2815 (N-70-33138)
BASS, Jack, Prog. rpt. on transport and defect properties of thin metallic wires, annual, 9/69--9/70, 25:3939 (COO-1247-21)
BASS, R., Reaction ^{28}Si(^{3}He,p)^{30}P, 25:3602
BASS, William Thomas, Study of the nuclei ^{61}Cu, ^{64}Cu, ^{67}Ga, and ^{68}Ga using the (p,n) reaction, 25:3596 (TID-25503)
BASSANO, D., Branching ratios of the K(1420) meson, 25:3287
BASTIAN, C., Steady-state generation of rotating multipoles for plasma experiments in Mcs range, 25:3129 (JUL-667-PP)
BATALEVA, S. K., Phase diagram of niobium--cobalt system, 25:2749
BATENIN, V. M., Calculation of the electrical conductivity of partially ionized plasma, 25:3093
Plasma diagnostics of a weak-current arc discharge by means of a light probe, 25:3065
BATES, J. F., Creep rate correlation in solution-treated Type 304 and 316 stainless steels, 25:4007 (WHAN-FR-25)
BATRA, B. K., Effects of maternal x-irradiation of mice on the germ cells of their progeny, 25:2593
BAUD, G., Perovskite phases containing tetravalent uranium, 25:2210
BAUDOIN, Jean-Claude, Detachable head for a pneumatic system, 25:2427
BAUER, P., Thermal coupling between upper F2 region and magnetosphere, 25:2956
BAUER, R. S., Radiation-induced polymerization of isobutylene oxide, 25:2256
BAUGH, P. J., Radiation chemistry of carbohydrates. XVII, 25:2279
BAXTER, J. N., Positive ion scavenging in the radiolysis of liquid chloroform, 25:2264
BAYLY, M. G., Treatment of Rum Jungle U ore, 25:2336
BAYSDEN, J. N., Sodium corrosion of Westinghouse liquid metal fast breeder reactor (LMFBR) materials, 25:2619
BAZIN, M. J., Deuteron--deuteron scattering at 2.2 and 7.9 GeV/c, 25:3415
BEARD, David B., Self-consistent theory of the magnetotail, 25:2960
BEARPARK, K., Proton stripping to particle-hole states in ^{40}Ca and ^{42}Ca, 25:3627
BEBEL, D., Relativistic dispersion theory of the deuteron structure, 25:3409
BECKER, U., Observation of coherent interference pattern between rho and ω decays, 25:3288
Photoproduction phase of rho° mesons, 25:3256
BECKER, W. W., Segregation of impurities and the formation of particles in sodium systems, 25:2713
BEDA, A. G., Operation of large area silicon surface-barrier detectors at low temperatures, 25:2452
BEER, H., Hyperfine structure and Stark effect investigations in yttrium I spectrum, 25:2891
BEER, O., Spectroscopy of even tin isotopes by inelastic scattering of protons, 25:3668
BEERTEMA, H. E., Decay of ^{63}Ga, 25:3609
BEGHI, G., Formation of Al pearls on surface of SAP alloys, 25:2779
BEHRENS, H., Sensitivity of β-transitions to nuclear charge distribution, 25:3744
BEIGMAN, I. L., Calculation of effective scattering cross sections with atomic functions that take into account configuration interaction, 25:2918
Effective excitation and ionization cross sections of ions, 25:2914
BEJSOVEC, V., Polarized ion source for U-120 cyclotron. II, 25:3519
Polarized ion source for U-120 cyclotron. I, 25:3520
BELIAEV, I. N., Reply to article of Spiridonov, 25:2807 (SC-T-70-4039)
BELL, J. T., Near-infrared spectra of water and heavy water at temperature between 25 and 390°, 25:2165
BELL, R. A. I., Electromagnetic transitions in ^{19}Ne, 25:3575
BELL, S. B. M., Computer graphics patching of failed CYCLOPS events for spark chamber experiment, 25:2486 (RHEL/R-205)
BELOVA, T. Ya., New organic reagents for niobium, 25:2199
BELT, Bobby Dean, Radiative capture of deuterons by protons at 20 and 30 MeV, 25:3546 (ORNL-TM-3168)
BELYAEV, Yu. I., Increasing the sensitivity and accuracy of the luminescence determination of the rare earths by the method of the periodical scanning of the spectrum, 25:2086
BEM, P., Polarized ion source for U-120 cyclotron. II, 25:3519
Polarized ion source for U-120 cyclotron. I, 25:3520
BENEDETTI, G. R., Computer programs for irradiation planning in high-energy therapy, 25:2584
BENIN, S. D., Effect of local heterogeneities of magnetic fields on pulsation of edges of electron beams, 25:3524
BENINSON, D., Fission product fixation in fresh water species, 25:2548
BENNETT, Leslie R., Modulation transfer function evaluation of scintillation camera and rectilinear scanner, 25:2447
BENNETT, Robert A., Nuclear magnetic resonance study of the crystalline compounds of the NbBe/sub x/ system, 25:3220 (COO-1700-12)
BENZ, Robert, Crystal structure of the compounds U_2N_2X and Th_2N_2X with X = Sb, Te, and Bi, 25:2248
BENZI, V., Effects of the direct inelastic scattering anisotropy for fast neutrons in sodium, 25:3635
BERCAW, R. W., p-p and p-t interactions in ^{3}He(d,tp)p, 25:3552
BEREZHNOI, Yu. A., Scattering of fast deuterons at large angles, 25:3614
BERG, K. J., Influence of aggregation on V-band absorption in Ca-doped KCl, 25:3198
BERGER, C., Polarization of high-energy photons using highly oriented graphite, 25:3257
BERGER, J., Effective deuteron--proton elastic scattering

cross section at 180°, 25:3264
BERGER, James D., Radiation safety in the operation of a low-energy accelerator, 25:3475 (CONF-700322-, pp 441-8)
BERGER, W., Investigations of decontamination ability of paints, 25:2423
BERGQVIST, I., Study of the $^{207}Pb(d,p)^{208}Pb$ reaction, 25:3688
BERISHVILI, G. P., Relationship between geomagnetic and solar activities, 25:2998
BERKEY, Edgar, Oxidation-reduction reactions for chromium and 304 stainless steel in liquid sodium, 25:2710
BERLEC, I., Effects of impurities and heat treatment on the internal friction of tungsten at high temperatures, 25:2687
BERMAN, M. I., Heat transfer in the turbulent flow of an electrically conducting liquid in a circular tube in a longitudinal magnetic field, 25:2944
BERNDT, C. W., General description of Weapons Effects Display System, 25:2506 (UCRL-50922)
BERNOW, S., Muonic atoms. I, 25:3661
Muonic atoms. II, 25:3620
BERNSTEIN, G. J., Fuel cycle technology quarterly report, April, May, June 1970, 25:2306 (ANL-7735)
BERRY, H. G., Excitation of ionized helium states in a cooled hollow-cathode discharge, 25:2890
BERRY, J. W., Dissolution of plutonium in dilute nitric acid, 25:2153
Radiolysis of HNO_3 solutions: LET effects, 25:2284
BERSON, I. Ya., Electron in a quantized field of a plane electromagnetic wave, 25:3233
BERTHOU, P.-E., Densities of liquid In--Bi, Sn--In, Bi--Sb, and Bi--Cd--Tl alloys, 25:2692
BERTIN, M. C., Alpha-particle scattering from ^{204} ^{206} ^{208}Pb and ^{209}Bi, 25:3689
BERTRAM, W. K., Calculation of (n,2n) cross sections using Hauser--Feshbach theory, 25:3591 (AAEC/TM-542)
Use of Hauser--Feshbach theory for predicting inelastic scattering of neutrons by nuclei, 25:3712 (AAEC/TM-545)
BERTRAM, William K., Observation of coherent interference pattern between rho and w decays, 25:3288
BERTRAND, F., Proton hole states in 1f/sub 7/2/ nuclei, 25:3616
BERTSCHAT, H., Magnetic moment of level in ^{58}Co, 25:3618
BESPROZVANNAYA, A. S., Cyclic variations of latitude dependence of F2-layer ionization at noon, 25:2984
Relationship between F2-layer ionization in the northern and southern hemispheres during the solstices, 25:2972
BESSE, J. P., Perovskite phases containing tetravalent uranium, 25:2210
BETTEN, P. R., Operation of a 12-inch fast gate valve with a pressure cartridge, 25:3998 (UCRL-50930)
BETTINI, A., Annihilation anti pn + $\pi^+\pi^-\pi^-$ between 1.0 and 1.6 GeV/c and its comparison with Veneziano model, 25:3270 (INFN-PD-70/2)
BEVAN, P. L. T., Evidence for very early ionic effects in water radiolysis, 25:2274
BEZEL, V. S., DK-0.2 dosimeter for recording fast neutrons, 25:2493
BHAKAR, B. S., Correction to the nuclear-matter calculations, 25:3735
BHARGAVA, B. N., Statistical properties of world-wide fluctuations in the magnetic field, 25:2958
BHARUTH-RAM, K., Electromagnetic transitions in ^{19}Ne, 25:3575
BHAT, A. N., Pyridine-2-aldoxime and 6-methylpyridine-2-aldoxime as gravimetric reagents for estimation of Pd(II) and U(VI), 25:2072
BHATNAGAR, A. S., Closed circuit technique for measurement of Rn/thoron ratio in soil-gas, 25:2378
BHATTACHARYA, P., Alpha-particle model for nuclear matter, 25:3738
BHIDAY, M. R., Theoretical design of the experiment to study scattering of electrons and positrons by electrons, 25:3245
BHISE, V. M., Theoretical design of the experiment to study scattering of electrons and positrons by electrons, 25:3245
BIALAS, Andrzej, Polarization of Λ and Σ hyperons in two-body Y^* production processes and quark model, 25:3383 (TPJU-2/70)
BIANCASTELLI, R., Binary-to-decimal or decimal-to-binary converter, 25:2510
Printout system for analog-to-digital converters, 25:2511
BIBLER, N. E., Positive ion scavenging in the radiolysis of liquid chloroform, 25:2264
BIDEAU, Michele, Preparation and structure properties of a uranyl hydroxyformate, 25:2196
BIEBL, K. J., Relativistic dispersion theory of the deuteron structure, 25:3409
BIEDENHARN, L. C., 27-plet unitary symmetry operator, 25:3426
BIERZYNSKI, Andrzej, Gas-chromatographic analysis of C_1--C_6 hydrocarbons, products of radiolysis of gaseous ethylene, 25:2278
BIGGERSTAFF, J. A., Spectroscopy of ^{65} ^{67} ^{69}Ga by (d,n) reaction, 25:3625
BIGLIOCCA, C., Natural cesium in freshwater and fishes, 25:2517
BIGNAMI, A., Effects of the direct inelastic scattering anisotropy for fast neutrons in sodium, 25:3635
BIKIT, I. S., Finite solid-angle corrections for Ge(Li) detectors, 25:2454
BILPUCH, E. G., Analogue states in ^{59}Cu, ^{61}Cu, ^{63}Cu, and ^{65}Cu, 25:3628
BIN, Le Viet, Increasing the sensitivity and accuracy of the luminescence determination of the rare earths by the method of the periodical scanning of the spectrum, 25:2086
BIRD, Michael, Self-consistent theory of the magnetotail, 25:2960
BIRON, Didier Francois, Nonlinear transport of electrons and ions in a plasma diode, 25:2934
BISHOP, C. J., Proton induced fission of ^{233}U and ^{238}U, 25:3660
BISHOP, David M., Integral-transformation trial functions of the fractional-integral class, 25:2928
BISHOP, E. C., Effects of exposure to flowing sodium on vanadium alloys in stainless steel containment systems, 25:2621
BISHOP, J. M., Antiproton--neutron elastic scattering at 3.5 GeV/c, 25:3267
Associated production in K*p interactions at 3.5 GeV/c, 25:3277
BISSON, Andre, Acicular precipitates in irradiated austenitic steels using electron microscopy, 25:2756 (CEA-CONF-1638)
BIST, Hari D., Vibrational spectra of uranyl compounds in solutions, 25:2216
BISTIRLICH, James A., Radiative pion capture in ^{12}C, 25:3550
BITAR, Khalil M., Bjorken limit and Jin--Martin lower bound, 25:3294 (NYO-4204-5)
BITTEL, R., Distribution of ^{60}Co in fish, 25:2526
Physico-chemical processes of transfer of radioruthenium in continental medium, 25:2364
Transport of radiocobalt in artificial ecosystem, 25:2549
BIZZARRI, R., Upper limit on the w + 2π decay rate from anti pn annihilations at rest, 25:3269
BLACK, L. W., Non-contact gaging, 25:3966 (MHSMP-15)
BLACK, W. S. A., Thermal performance of the Dragon reactor, 25:3885 (DP-Report-546)
BLADA, J., Activation analysis in stomatology, 25:2135
BLAHA, Stephen, Deep inelastic e-p structure functions in a ladder model with spin $^1/_2$ nucleons, 25:3311 (NYO-4204-4)
BLAHNIK, D. E., CCTL Mark I and Mark II prototype FFTF subassembly compression test development work, 25:3908 (WHAN-FR-18)
BLAIN, Jean-Francois, Coalescence of organic solutions during the extraction of acids and metals by trialkylamines, 25:2308 (CEA-R-3845)
BLAKE, Martin I., Deuterium isotope effects in enzymatic transamination, 25:2168
BLANC, P., Drift waves in a collisionless plasma, 25:3147 (CEA-CONF-1612)
BLANC, Pierre, Drift waves due to a pressure gradient in a collisionless plasma, 25:3167
BLANCHARD, P., Uranium swelling under irradiation, 25:2762
BLANK, G. R., Direct reading spectrometric method using AgCl--LiF carrier to determine impurities in nuclear-grade U_3O_8 samples, 25:2068 (NLCO-1071)
BLOCH, M., Method to study events with two missing neutral particles, 25:3362
BLOCK, F. E., Kroll process beryllium, 25:2653
BLOCK, Robert C., Precision of tank capture cross section measurements, 25:2435 (RPI-328-202)
BLOMSTRAND, J. H., Fuel-cycle theory for on-load refuelled thermal converter reactors. I and II, 25:3887 (DP-Report-575)
Influence of fuel element heterogeneity on partly enriched U cycle, 25:3868 (DP-Report-477)
Thorium cycle in on-load refueled systems, 25:3873 (DP-Report-573)
BLOOM, D. W., Upper limit on electron--phonon interaction in vanadium carbide, 25:3034
BLOOM, E. E., Effect of helium on void formation in irradiated stainless steel, 25:2761
BLUM, B., Phenomenological approach for a π^- meson nucleus potential, 25:2897
BLUM, E. Ya., Mass exchange of a circular cylinder in presence of transverse magnetic field, 25:2941
BLUM, J. M., Physico-chemical processes of transfer of radioruthenium in continental medium, 25:2364
BLUMENFELD, H., Spin--parity analysis of 3π system in reaction $\pi^-p \rightarrow p\pi^-\pi^+\pi^-$ at 3.9 GeV/c, 25:3276
BLUMSTEIN, C., Prevention of alpha counter contamination by electrodeless discharge deposition of Si_3N_4, 25:2478
BOBROWSKA, A., Structure of the low lying levels of the ^{33}S nucleus, 25:3597
BOCK, E., Proton spin-lattice relaxation time of aniline-d_2 in deuterated benzene and deuterated aniline solution, 25:2182
BOCK, R., Mass-identification by time-of-flight methods, 25:2469
BODDENDIJK, J. C., Decay of ^{62}Co isomers, 25:3644
BODENSTEDT, E., Gamma--gamma angular correlation in ^{166}Er in different liquid sources, 25:3696
BODROV, D. P., Spherically shaped cartridges for extended sources in pilot and full-scale radiation-chemical

processors, 25:2404
BODYAGINA, V. V., Use of N-benzoyl-o-tolylhydroxylamine in method of amperometric titration. III, 25:2082
BOECK, H., Transient response of cobalt self-powered neutron detectors, 25:2467
BOECKEM, K., Isotope diagnosis of processes involving the posterior cerebral fossa, 25:2578
BOEHM, George Gustave Anton, Composition for measuring radiation, 25:2496
BOEHNING, M., Particle-hole states in equidistant-spacing model, 25:3760
BOELHOUWER, C., Relations between gas chromatographic behavior and chemical structure. III, 25:2167
BOELLA, G., Optical spark chamber for the search of gamma-ray sources, 25:2841 (CEA-CONF-1633)
BOGNER, G., Energy transport by cryogenic cables, 25:3050
BOGOLYUBOV, N. N. Jr., Obtaining the limiting relations for correlation averages, 25:3332 (ITF-70-59)
BOGOMOLOV, V. M., Determination of the decomposition time of hexogen under the effect of shock waves, 25:3964 (LA-4360-TR)
BOHM, G., Lifetime of the A-He^5 hypernucleus, 25:3259
BOHN, E. M., Final safety analysis report on the use of plutonium in ZPR-6 and -9, 25:3901 (ANL-7442)
BOHN, W. L., Radial pressure profile in an MPD hydrogen arc. I, 25:3104
Radial pressure profile in an MPD hydrogen arc. II, 25:3105
BOLDYREV, V. M., Working substance for single-component liquid-metal MHD units, 25:2937
BOLING, Maxon E., Ultraviolet action spectra for mutation in Escherichia coli, 25:2557
BOLLINGER, L. M., Rotational bands of ^{166}Ho, 25:3691
BOLTWOOD, C. M. Jr., Critical fluence needed to destroy thin metal films by laser deposition, 25:3997 (UCRL-50927)
BOLTZ, D. F., Ultraviolet spectrophotometric determination of gallium, 25:2100
BOMAL, R., Use of thin film solar cells in radiovoltaic generators, 25:2400 (CEA-CONF-1623)
BONAZZOLA, G. C., Backward scattering of 14 MeV neutrons, 25:2468
Excitation of states between 3 and 6 MeV in ^{31}P and ^{32}S, 25:3612
BONNELLE, Christiane, X-ray spectroscopic measurement of the temperature of atomic and ionic transfer in a plasma, 25:3073
BOOKBINDER, James Henry, Superfluidity of ^3He, 25:3017
BOONE, M. L. M., Fast neutron radiobiology and radiotherapy, 25:2582 (CONF-700322-, pp 393-406)
BOOTSMA, D., DNA repair replication in xeroderma pigmentosum cell strains, 25:2567
Repair of x-ray damage in DNA from patients having xeroderma pigmentosum, 25:2535
BORCHERS, R. R., Static and transient hyperfine magnetic fields at Ba isotopes recoiled in iron, 25:3686
BORCIC, Stanko, Thermodynamic and kinetic secondary isotope effects in the Cope rearrangement, 25:2188
BORG, R. J., Clustering and giant moments in Cu--Ni alloys, 25:4000 (UCRL-72587(Rev.1))
BORGARDT, A. A., Quantum mechanics of charged relativistic vector bosons. I, 25:3344
BORGOHAIN, P., Scattering by modified Gaussian potential, 25:3771
BORGONOVI, G. M., Calculation of the coherent neutron scattering from polycrystalline beryllium, 25:3533
BORN, H.-J., Reactor neutron-induced fission of ^{231}Pa, 25:3656
BOROK, A. M., Electrogasdynamic generator with neutralization of space charge, 25:2938
BOROVIK, E. S., Apparatus for the production and investigation of high-pressure heavy-current long arcs, 25:3112
BORREANI, G., Reaction $\pi^+p \to \Sigma^+K^+$ between 1850- and 2090-MeV cm energy, 25:3283
BORTLIK, Jiri, Power boundary limit between reactor heat output and process heat and electricity, 25:3914
BOSAMYKIN, V. S., Magnetic tracking of compensated electron beams in the acceleration region, 25:3486
BOSIO, C., Binary-to-decimal or decimal-to-binary converter, 25:2510
Printout system for analog-to-digital converters, 25:2511
BOSNJAKOVIC, B., Polarization in elastic proton--proton scattering between 0.86 and 2.74 GeV/c, 25:3262
BOSS, Gerald Ralph, Inelastic deuteron scattering from ^{151}Eu, 25:3653
BOSTIAN, Harry, Infrared and Raman spectra of trivalent lanthanide--Di-(2-ethylexyl) phosphoric acid solvent extraction organic equilibrium phases, 25:2193 (CONF-700403-8)
BOTKE, J. C., Reaction $\pi^-p \to \pi^0\pi^0n$ at 378 MeV, 25:3392
BOTTIGLIONI, F., Ion heating by beam plasma interaction, 25:3054 (CEA-CONF-1611)
Plasma formation by dissociation of an accelerated hydrogen cluster beam, 25:3109 (CEA-CONF-1610)
BOUDOURESQUES, B., Progress in fuel elements for gas--graphite reactors, 25:3877
BOULANGER, W., Standards agreement for IAEO reactor safety control, 25:3851
BOULESTEIX, C., Study of thin films of samarium by x rays and electron microscopy, 25:2734
BOURDEAU, P., Transport of radiocobalt in artificial ecosystem, 25:2549
BOURRELLY, I. N., Fixation of alkali metals on antimony pentoxide hydrate in strongly acid media, 25:2333
BOUSSOUKAYA, M., Radial motion of electrons and emittance from low-energy superconducting linear accelerator, 25:3518
BOUSTEAD, I., Thermoluminescence in n-heptane, 25:2291
BOUVIER, J. M., Use of an x-ray fluorescence spectrometer with a computer, 25:2105
BOVENKO, V. N., Stress relaxation in deformed U, 25:2699
BOWEN, A. W., Diffusion in bcc iron base alloys, 25:2691
BOWEN, H. J. M., Neutron activation techniques in human metabolic studies, 25:2123 (IAEA-122, pp 1-13)
Use of activation analysis in the study of cystic fibrosis, 25:2127 (IAEA-122, pp 145-8)
BOWERS, G. L., Automated quantometer data handling system, 25:2069 (Y-1740)
BOWMAN, H. R., Prompt de-excitation of fission fragments, 25:3673
Search for superheavy elements in nature by detection of events with large numbers of neutrons, 25:3652 (UCRL-19957)
BOWMAN, K. O., Tables for determining the statistical significance of mutation frequencies, 25:2559
BOYD, W. K., Stress corrosion cracking of Ti and Ti--6Al--4V in dinitrogen tetroxide, 25:2635
BRACCINI, P. L., Photoproduction of ω-mesons from nuclei, 25:3247
BRADASCHIA, C., Photoproduction of ω-mesons from nuclei, 25:3247
BRADLEY, D. T., Intensities of O_2^+ 1NG and N_2 1PG band systems in normal and type-B aurorae, 25:3002
BRADY, F. P., Nuclear interactions in Si(Li) detectors, 25:2451
BRAITHWAITE, W. J., Energy dependence of quasifree scattering in the D(p,pn)p reaction, 25:3547 (RLO-1388-126)
BRAND, G. F., Plasma diagnostics, 25:3069
BRAND, J. W. L. F., Internal cathodic protection of water cooled plant, 25:2634
BRANDOLINI, F., Spins and mean lives of ^{34}Cl levels, 25:3619
BRANDON, Eldon D., Gas coverage for PIGMA welding, 25:2646 (RFP-1550)
Parameters for pressurized inert gas metal arc welding of aluminum, 25:3973 (RFP-1515)
BRANDT, R. A., Universal light cone commutator, 25:3306
BRANKOWSKI, J., Vinca Nova: automatic unit for neutron spectrometer control, 25:2475 (INP-707)
BRAUN, Robert L., Quantitative phase analysis of rocks by x-ray diffractometry, 25:3995 (UCRL-50921)
BRAUNDMEIER, A. J. Jr., Observed radiation from surface plasmons in aluminum, 25:2885
BREDIKHIN, M. Yu., Investigation of dense plasma formation using electron beam injection into magnetic trap, 25:3113
BREGMAN, J. D., Quasi-elastic incoherent cold neutron scattering in liquid cyclohexanol, 25:3534
BREHM, W. F., Radioactive material transport in flowing sodium systems, 25:2706
BRESKMAN, D., Chemical shifts of the μ^+, 25:2899
BRESSANI, T., Backward scattering of 14 MeV neutrons, 25:2468
Excitation of states between 3 and 6 MeV in ^{31}P and ^{32}S, 25:3612
BRESSAT, Rene, Preparation and structure properties of a uranyl hydroxyformate, 25:2196
BRESSERS, J., Deformation properties of vanadium single crystals, 25:2718
BRINK, G., Infrared spectrum of HDO in aqueous solutions of perchlorates and tetrafluoroborates, 25:2183
BRINK, R. Alexander, Effects of x-irradiation and gamma irradiation on paramutation in R heterozygotes in maize, 25:2560
BRION, C. E., K-shell excitation of N_2 and CO by electron impact, 25:2910
BRISKMAN, B. A., Experimental study of the spatial absorbed-dose fields of reactor γ-radiation in a polyethylene sample, 25:2495
Spatial distribution of absorbed neutron dose in polyethylene, 25:2494
BRITT, H. C., Neutron fission cross sections for ^{231}Th, ^{233}Th, ^{235}U, ^{237}U, ^{239}U, ^{241}Pu, and ^{243}Pu from 0.5 to 2.25 MeV using (t,pf) reactions, 25:3679
BRITTON, R. B., Superconducting synchrotron magnets, 25:3512
BROCHU, Robert, Preparation and crystalline structure of UBa sulfide: $BaUS_3$, 25:2204
BROCK, J. C. F., Density of electronic states in α-phase In alloys containing Cd and Sn, 25:3205 (UCRL-19681)
BRODINE, John C., Electromagnetic final-state interactions and tests of time-reversal invariance in nuclear beta decay. II, 25:3424
BRODSKII, G. N., Electron-optical properties of two-potential two-dimensional lens, 25:3491
Two-potential lens with distorted focusing layer, 25:3490
BROGLIA, R. A., Coulomb excitation of ^{209}Bi, 25:3674
BRONCA, G., Application of pulsed superconducting magnets to synchrotrons, 25:3511

BROOMFIELD, A. M., Proton recoil counter techniques in ZEBRA, 25:2472 (AEEW-M-905)
BROSSIER, P., Drift waves in a collisionless plasma, 25:3147 (CEA-CONF-1612)
BROSSIER, Philippe, Drift waves due to a pressure gradient in a collisionless plasma, 25:3167
BROWN, A. K., Radiolysis of HNO_3 solutions: LET effects, 25:2284
BROWN, C. L., Thermal performance of the Dragon reactor, 25:3885 (DP-Report-546)
BROWN, J. T., One-boson-exchange potential model for the AN interaction, 25:3416
BROWN, P. E., Fission product distribution in Dragon after first 20 MW run, 25:3886 (DP-Report-571)
BROWN, W. D., Meson dynamics and the nuclear many-body problem. I, 25:3719
BROWNE, C. P., Isobaric spin doublets in ^{8}Be excited with the $^{10}B(d,\alpha)^8Be$ reaction, 25:3573
BROWNE, J. C., Analogue states in ^{59}Cu, ^{61}Cu, ^{63}Cu, and ^{65}Cu, 25:3628
BROZEK, V., Investigation of hydrolyzable carbides. III, 25:2782
BRUECKMANN, H., Polarized positively charged hydrogen ion beams, 25:3307
BRUNE, D., Studies of carbon content of steel by proton activation analysis, 25:2147
BRUNEDER, H., Complete core replacement and part reloaded systems in ^{235}U/Th and ^{235}U/ ^{238}U cycles, 25:3869 (DP-Report-478)
Influence of fuel element heterogeneity on partly enriched U cycle, 25:3868 (DP-Report-477)
BRUNORI, A., X-irradiation response of G_1 cells in dry seeds, 25:2555
BRUYANT, F., Spin--parity analysis of 3π system in reaction $\pi^-p \to p\pi^-\pi^+\pi^-$ at 3.9 GeV/c, 25:3276
BRUZZONE, G., Rare-earth intermediate phases with zinc, 25:2753
BRYANT, P. E. C., Corrosion and coolant chemistry interactions in pressurized water reactors, 25:2637
BUCCHERI, R., Optical spark chamber for the search of gamma-ray sources, 25:2841 (CEA-CONF-1633)
BUCHAU, J., Arctic ionosphere and aurora: airborne investigations, 25:2949 (AD-709359)
BUCKEE, J. W., Pulsar distances and emission, 25:2854
BUCKMASTER, John David, Some topics in magnetohydrodynamics, 25:2942
BUDZANOWSKI, A., Real part of the alpha--nucleus potential, 25:3755
BUEHRING, W., Sensitivity of β-transitions to nuclear charge distribution, 25:3744
BUKAU, F., High purity gas protective system for the use of high melting reactive metals at high temperatures, 25:2639 (LIB/Trans-309)
BULLOCK, J. I., Low frequency infrared and Raman spectroscopic studies of some uranyl complexes, 25:2212
BURGAN, C. E., Compatibility of Cu with Ta--10 wt. percent W alloy at elevated temperatures, 25:2720
BURGENER, C. S., Oxidation of neptunium(III) by oxygen and hydrogen peroxide, 25:2155
BURKE, P. G., Calculation of electron scattering and photoionization cross sections, 25:2903
BURKHOLDER, G. D., Uptake of isolated metaphase chromosomes by mammalian cells in vitro, 25:2515
BURLAK, L. F., Radiolysis of original and reinforced ED-5 type epoxy resin, 25:2273
BURMAN, R. R., Geodesics and Lyttleton--Bondi electrodynamics, 25:3431
BURN, Robert Daniel Jr., Computer studies of planar plasma configurations, 25:3094
BURNS, Robert Arthur, Surface studies of simple hydrocarbons on iridium by flash desorption, 25:3961 (IS-T-406)
BURNS, W. G., Effects of LET and temperature in radiolysis of cyclohexane. II, 25:2280
Effects of LET and temperature in radiolysis of cyclohexane. I, 25:2281
BURQ, J.-P., Elastic scattering $^{12}C(d,d)^{12}C$, $^{28}Si(d,d)^{28}Si$, and $^{40}Ca(d,d)^{40}Ca$, 25:3585
BUSCHHORN, G., Measurement of proton Compton scattering at 6 GeV and small momentum transfers, 25:3309 (DESY-70/46)
BUSCHMANN, J., Fission of heavy nuclei by helium ions and deuterons, 25:3710
BUSEV, A. I., Bismuthiols as analytical reagents, 25:2070
BUSH, D., Designation of persons working with unsealed radioactive substances, 25:2572
BUSH, Walter L., Gas coverage for PIGMA welding, 25:2646 (RFP-1550)
BUSSE, W., Reactions (d,n) on ^{11}B, ^{14}N, and ^{15}N, 25:3574
BUSSELL, Bertram, Instrumenting computer systems and their programs, 25:3981 (UCLA-10-P-14-94)
BUTLER, Hal M., Radiation safety in the operation of a low-energy accelerator, 25:3475 (CONF-700322-, pp 441-8)
BUTLER, W. R., Reaction $\pi^+p \to \Delta^{++}A_2^0$ at 3.7 GeV/c, 25:3272 (UCRL-20050)
BUTTERFIELD, A. W., Shape of thermoluminescence glow peaks in molecular solids, 25:2235
BUTTRAM, Malcolm T., Neutral branching ratios of the eta meson, 25:3258
BUZIN, V. I., Crystal structure of Mo containing ZrC, 25:2743
Substructure of cast Mo, 25:2744
BYALOBZHESKII, A. V., Radiation corrosion, 25:2603 (AEC-tr-7096)
BYCHKOV, Yu. F., Dispersed precipitates in Zr--Nb alloys, 25:2742
Superconducting Zr--Nb ribbon level indicator, 25:2394
BYLKIN, V. I., Resonance charge exchange between a molecular ion and diatomic molecule, 25:2912
BYSIEK, M., Cesium transport in fish-breeding pond, 25:2516
BYSTROV, L. N., State of carbon in martensite as influenced by electron bombardment, 25:2764

C

CABELL, M. J., Concerning the half-life of ^{144}Ce, 25:3645 (AERE-R-6529)
CADY, George H., Systems xenon hexafluoride--tantalum pentafluoride, xenon hexafluoride--manganese fluoride, xenon hexafluoride--uranium hexafluoride, 25:2156
CAFASSO, F. A., Grain boundary grooving of iron in liquid sodium, 25:2708
CAHILL, T. A., Nuclear interactions in Si(Li) detectors, 25:2451
CALARCO, J. R., Energy dependence of quasifree scattering in the D(p,pn)p reaction, 25:3547 (RLO-1388-126)
CALLENDER, W. D., Isobaric spin doublets in ^{8}Be excited with the $^{10}B(d,\alpha)^8Be$ reaction, 25:3573
CALOGERO, F., Hyperspherical-expansion approach to nuclear bound states. I, 25:3730
Positivity conditions for velocity-dependent and quadratic spin--orbit potentials, 25:3737
CAMERON, D. A., Fine structure of osteosarcomata in rats, 25:2594
CAMERON, J. M., Energy dependence of quasifree scattering in the D(p,pn)p reaction, 25:3547 (RLO-1388-126)
CAMP, D. C., Corrections to coaxial Ge(Li) detector solid angle correction factors, 25:2455
CAMPBELL, Thomas T., Kroll process beryllium, 25:2653
CANCIO, D., Fission product fixation in fresh water species, 25:2548
CANO, R., Change in the polarization of an electromagnetic wave in a sheared magnetic field, 25:3146 (CEA-CONF-1608)
Harmonic absorption of microwaves in magnetized low-density plasma, 25:3145 (CEA-CONF-1607)
CANONICO, D. A., Measurement of residual stresses, 25:2410 (ORNL-TM-3113)
CANTILLON, G., Radiomanganese and radiocobalt fixation by sediments, fauna, and flora, 25:2544
CAP, F. F., Applications of Lie series in atomic physics, 25:3236
CAPP, P. D., Removal and replacement of primary heat exchanger tube bundle and circulator on Dragon Reactor, 25:3863 (DP-Report-554)
CARBOTTE, J. P., Condensation energy of a superconductor, 25:3046
CARDINAL, C. U., Heavy-ion reactions as a technique for direct mass measurements of unknown Z > N nuclei, 25:3610
CARLETON, N. P., Time-of-arrival measurements of optical pulses from Crab pulsar, 25:2853
CARLSEN, F., Combination of an electron microscope and a heavy-ion accelerator, 25:2507
CARLSON, C. E., Evaluation of ππ scattering lengths using on-mass-shell pions, 25:3371
CARLSON, G. A., Thermal energy conversion system for a fusion reactor, 25:3133 (ORO-1171-1, pp 141-66)
CARLSSON, J.-O., Solution hardening of β-rhombohedral boron, 25:2801
CARLTON, Robert F., Experiments utilizing $D(^3He,p)^4He$ reaction, 25:3543 (CONF-700322-, pp 95-104)
CARNEVALE, E. H., Ultrasonic thermometry for LMFBR systems, 25:2503 (NYO-3906-4)
CAROLA, T. P. G., High spin states in ^{53}Fe, 25:3624
CAROLINE, D., Surface tension of liquid ^{4}He, 25:3010
CARPENTER, K. M., Green's paraparticles and the unified theory of identical particles, 25:3304
CARR, T. D., Very-long-baseline interferometry of Jupiter at 18 MHz, 25:2880
CARRERAS, B., K⁺p phase shift analysis, 25:3393
Regge-cut effects in pion--nucleon scattering, 25:3390
CARROLL, J. T., Difference in energy dependence for A_2^- and A_2^0 production, 25:3289
CARROLL, John T., Acid-catalyzed cyclization reactions. IX. The formation of oxazolinium and thiazolinium cations from N-allyl and substituted N-allylamides, -urethans, -ureas, and -thioureas, 25:2179
CARROTTE, John B., S-, P-, and D-wave low-energy pion--pion scattering, 25:3369
CARRUTHERS, J. R., Phase equilibria relations in the ternary system BaO--SrO--Nb_2O_5, 25:2808
CARSWELL, G. P., Magnetic domain structures of intermetallic compounds $SmCo_5$, $LaCo_5$, and $CeCo_5$, 25:3217
CARTER, H. K., Time-of-flight experiments for low-energy accelerators, 25:3468 (CONF-700322-, pp 125-32)
CARTER, M. D., Proton recoil counter techniques in ZEBRA, 25:2472 (AEEW-M-905)
CASPARI, A., Problems arising from nuclear blasting for oil

and gas production, 25:2382
CASTALDI, R., Photoproduction of ω-mesons from nuclei, 25:3247
CASTEL, B., Silicon-28 nucleus in projected Hartree--Fock model, 25:3605
CASTILHO ALCARAS, J. A., 27-plet unitary symmetry operator, 25:3426
CASTLEMAN, A. W. Jr., Importance of gravitational coagulation on the settling of high-mass density aerosols, 25:2369
Kinetics of γ-induced decomposition of methyl iodide in air, 25:2269
CASTO, Martin George, Separation of lanthanum from a rare earth chloride mixture using a multistage mixer-settler extractor, 25:2310 (IS-T-411)
CATELANI, D., Microbial degradation of aromatic hydrocarbons used as reactor coolants, 25:2327
CAWTHRON, E. R., Some phenomena produced by positive ion bombardment of metal surfaces at medium energies, 25:2884 (NP-18490)
CENACCHI, G., Effects of the direct inelastic scattering anisotropy for fast neutrons in sodium, 25:3635
CEPOLINA, A. G., Measurement of residual stresses, 25:2410 (ORNL-TM-3113)
CERCEK, B., Luminescence of aqueous Ti/sup I/-solutions after irradiation, 25:2233
CERF, V. G., Measurement of recursive programs, 25:3980 (UCLA-10-P-14-90)
CERNY, Joseph, Heavy-ion reactions as a technique for direct mass measurements of unknown Z > N nuclei, 25:3610
CETAS, Thomas Charles, Magnetic thermometry from 1 to 30 K, 25:3960 (IS-T-399)
CHABERT, A., Production of multicharged ions in a reflex source with axial extraction, 25:3111 (LYCEN-7065)
CHABRILLAC, Marcel, EL 600: fuel management studies, 25:3866 (CEA-N-1379)
CHAI, HI Dong, Impedance of parallel-plate capacitor in magnetoplasma, 25:3100
CHALABREYSSE, J., Inhalation of compounds of natural uranium. I, 25:2563
CHALLINOR, R. A., Neutral-air winds in ionospheric F region, 25:2954
CHAMAGNE, Francoise, Kinetics of α--β phase change in U alloys, 25:2741
CHAMBERS, E. E., Status and development of superconducting 2+ GeV accelerator at HEPL, 25:3496
CHAND, Ramesh, High-energy photoproduction of pseudoscalar mesons in a quark model, 25:3321
Vector-meson production in meson--nucleon collisions in a quark model, 25:3400
CHANDOLA, L., Spectroscopic analysis of uranium, 25:2074
CHANG, C. T. M., Dielectric loaded waveguides as particle separators, 25:3494
CHANMUGAM, G., Electromagnetic many-body forces, 25:3328
CHANNING, D. A., Liquid-nitrogen cryostat for keV heavy-ion irradiation experiments, 25:2388 (RD/B/M-1753)
CHAPLIN, D. H., Radiative detection of single-passage nuclear magnetic resonance, 25:3223
CHAPMAN, B. G., Dragon operations third quarterly progress report, December 1965--February 1966, 25:3790 (DP-Report-438)
First year at full power, 25:3791 (DP-Report-474)
Prog. rpt. on Dragon operations, 12/66--2/67, 25:3889 (DP-Report-582)
Prog. rpt. on Dragon operations, 3/67--5/67, 25:3890 (DP-Report-592)
Prog. rpt. on Dragon operations, 3--5/66, 25:3792 (DP-Report-483)
Prog. rpt. on Dragon operations, 6--8/66, 25:3793 (DP-Report-488)
Prog. rpt. on Dragon operations, 9-11/66, 25:3794 (DP-Report-531)
CHAPMAN, C., Measurement of plasma digoxin concentration by radioimmunoassay, 25:2522
CHAPMAN, N. G., Electromagnetic transitions in ^{19}Ne, 25:3575
CHAPPELL, W. R., Kinetic equations for autocorrelation functions in dilute gases, 25:3099
CHARAKHCH'YAN, A. N., Cosmic-ray energy spectrum in interstellar space, 25:2930
CHARAKHCH'YAN, T. N., Cosmic-ray energy spectrum in interstellar space, 25:2930
CHARMAN, W. N., Spaced-receiver observations of radio pulses, 25:2849
CHARVET, A., Decay scheme of 7 min ^{168}Lu, 25:3650 (LYCEN-7030)
CHARVILLAT, J. P., Perovskite phases containing tetravalent uranium, 25:2210
CHAUDHARY, Banvir, Comment on evidence for the H meson, 25:3286
CHAUDHURI, P. R., Weak interaction of photons and neutrino bremsstrahlung, 25:3335
CHAUDHURY, M. L., Non-local barrier and anisotropy of alpha emissions from oriented ^{237}Np nuclei, 25:3678
CHAURE, B. D., Aquoluminescence: release of energy stored in γ-irradiated crystals, 25:2227
CHAZAL, Guy, Hybrid simulation of the dynamics of a battery of mixer--settlers, 25:2384 (CEA-CONF-1579)
CHEEVER, C. L., Final safety analysis report on the use of plutonium in ZPR-6 and -9, 25:3901 (ANL-7442)
CHEIFETZ, E., Search for superheavy elements in nature by detection of events with large numbers of neutrons, 25:3652 (UCRL-19957)
CHEN, H., Crossing-symmetric amplitude for the Pomeranchuk trajectory, 25:3365
Equilibria and proton transfer in the bisulfate--sulfate system, 25:2173
CHEN, M., Photoproduction phase of rho^0 mesons, 25:3256
CHENG, Dah Yu, Plasma deflagration and the properties of a coaxial plasma deflagration gun, 25:3078
CHENG, Hung, Cross sections for two-pair production at infinite energy, 25:3325
CHENG, S. C., Muonic atoms. II, 25:3620
CHENG, Wen-kwei, Meson--nucleon scattering and asymptotic conservation of helicity, 25:3398
CHEN-TSAI, C. T., Shell-model structure of the p-shell hypernuclei, 25:3721
CHEREVATENKO, E. P., Attenuation of scattered synchrocyclotron radiation in a shield, 25:3480
CHERMETTE, H., Study by triple labeling of reactions between tetraphenylstibonium and antimony trichloride, 25:2169
CHERNYSHEV, A. S., Effect of spin-orbit and spin--spin forces on magnetic moments of deformed nuclei, 25:3692
CHERNYSHEVA, S. P., Influence of lower ionosphere on radio-wave reflections from E/sub s/ layer, 25:2994
CHERRY, J. T., Nuclear cratering on a digital computer, 25:2381 (UCRL-50898)
CHERY, R., Decay scheme of 7 min ^{168}Lu, 25:3650 (LYCEN-7030)
CHEUNG, T. H., Excitations in Bose gas at finite temperatures. I, 25:3044
CHHAJLANY, S. C., Axial-vector K/sub 14/-decay form factors based on current algebra, 25:3345
CHIAO, R. Y., Response of superconducting weak links to photons, 25:2444
CHIAVASSA, E., Backward scattering of 14 MeV neutrons, 25:2468
Excitation of states between 3 and 6 MeV in ^{31}P and ^{32}S, 25:3612
CHIMBULEV, Mincho, Recovery of tellurium from sulphate solutions by extraction, 25:2321
CHINNOV, V. F., Plasma diagnostics of a weak-current arc discharge by means of a light probe, 25:3065
CHINOWSKY, W., Reactions π-p at 456, 505, and 552 MeV/c, 25:3282
CHISTYAKOV, L. V., Neutron-induced ^{249}Bk fission, 25:3665
CHITNIS, V. D., Gamma-ray energy-absorption rates in Fe and Pb, 25:3169
CHOPPIN, Gregory R., Acetate complexing by trivalent actinide ions, 25:2208
CHOUDHURY, N. S., Steady-state chemical potential profiles in solid electrolytes, 25:2203
CHOW, G. Y., Crossing-symmetric amplitude for the Pomeranchuk trajectory, 25:3365
CHRISTALLER, G., Fission of heavy nuclei by helium ions and deuterons, 25:3710
CHRISTIAN, Gary D., Potentiometric studies with a liquid ion-exchange lead-selective electrode, 25:2104
CHRISTIANSEN, J., Magnetic moment of level in ^{58}Co, 25:3618
CHUBARYAN, E. V., Internal solution for stationary axially symmetric gravitational fields, 25:2828
CHUEV, V. I., Excited states (4p--3h) in reaction ^{13}C(^{6}Li,d)^{17}O and ^{13}C(^{7}Li,t)^{17}O, 25:3570
CHUNG, Jae Sun, Effective dielectric constant of cylindrical plasma at microwave regions, 25:3087
CHUPP, E. L., Beam-foil excitation using low-energy accelerators, 25:3465 (CONF-700322-, pp 21-31)
CHURIN, S. A., Reconstruction of the spectral and angular-distribution function of sources of γ radiation, 25:3168
CHYLA, K., Structure of the low lying levels of the ^{33}S nucleus, 25:3597
CIAPETTI, G., Upper limit on the ω → 2π decay rate from anti pn annihilations at rest, 25:3269
CIRBA, E., Analysis of pπ$^+$π$^-$ enhancements produced in reaction π$^+$p → π$^+$pπ$^+$π$^-$ at 5 GeV/c, 25:3275
CIRELLI, R., Study of a generalized optical potential, 25:3747
CLAAR, T. D., Evaluation of materials-compatibility problems in the EBR-II reactor, 25:2705
CLARK, Allan G., Fitting K-p → anti K^0 π-p with a generalized Veneziano model, 25:3391
CLARK, Hugh K., Calculation of relative reaction rates in interacting cylindrical cells, 25:3925 (DP-1238)
CLARKSON, T. W., Selective determination of inorganic mercury in the presence of organomercurial compounds in biological material, 25:2109
CLEMENTS, P. J., Some efficiency calculations for ^{6}Li suspended target semiconductor sandwich spectrometers, 25:2473 (AERE-R-6318)
CLEYRERGUE, C., Fixation of alkali metals on antimony pentoxide hydrate in strongly acid media, 25:2333
CLINE, D., Detection of the weak intermediate boson through its hadronic decay modes, 25:3333 (NYO-2171-323)
Empirical merger of geometrical and Regge pictures for elastic hadron scattering, 25:3354
First excited states of ^{58} ^{60} ^{62}Ni, 25:3642
CLOUGH, D. J., Record of programme and discussions at symposium of papers from Dragon contractors held at A.E.R.E., Harwell, 14--16 March 1966, 25:3774 (DP-

XUM

Report-439)
CLOUTIER, Roger J., Radiation safety in the operation of a low-energy accelerator, 25:3475 (CONF-700322-, pp 441-8)
COCHRAN, Andrew A., Boron and boron carbide coatings by vapor deposition, 25:2777
COCKE, W. J., Optical polarization of Crab Nebula pulsar, 25:2843
COFFEY, D. L., Compatibility of Cu with Ta--10 wt. percent W alloy at elevated temperatures, 25:2720
COHEN, E. Richard, Numerical calculation of the Milne problem extrapolation length, 25:3540
COHEN, J. A., DNA repair replication in xeroderma pigmentosum cell strains, 25:2567
COHN, C. M., Superconducting two tesla bending magnet, 25:3504
COLE, H. C., High-current Hall accelerator, 25:3141
COLE, Milton W., Width of the surface layer of liquid ^{4}He, 25:3008
COLES, R. E., Elastic and inelastic scattering of neutrons in energy range 2 to 5 MeV by ^{10}B and ^{11}B, 25:3559 (AWRE-O-45/70)
COLLATZ, S., Spectral function representation of time and energy dependent neutron density in fast media. I, 25:3535
COLLINS, P. V., Algebraic realization of chiral SU(2) x SU(2) symmetry, 25:3422
COLLINSON, A. J. L., Low temperature scintillation response of unactivated sodium iodide, 25:2436
COLONY, J. A., Mechanisms of recovery of radiation damaged silicate-treated zinc oxide thermal control coatings, 25:2815 (N-70-33138)
COLSON, James P., Polyoxymethylene crystals grown within irradiated trioxane crystals, 25:2252
COLTON, Eugene, Experimental comparison between on- and off-mass-shell inelasticities in π-p scattering. II, 25:3285
COMPRELLI, Frank, Evaluation of particulates deposited in flowing non-isothermal sodium systems, 25:2616
CONDON, P., Prog. rpt. on new heavy bosons in proton--antiproton interactions, 10/1/69--9/30/70, 25:3261 (UCI-34-P-149-1)
CONKLIN, Edward Kirkham, Anisotropy and inhomogeneity in the cosmic background radiation, 25:2876
CONNEELY, M. J., Calculation of electron scattering and photoionization cross sections, 25:2903
CONNER, William V., Anion exchange purification of Np by in situ conversion from nitrate to chloride system, 25:2339
CONNORS, D. C., Positron annihilation in quenched cadmium metal, 25:2898
COOK, B. C., Isospin splitting of the giant dipole resonance in ^{64}Zn, 25:3623
COOK, T. H., Infrared spectra and structure of beryllium borohydride, 25:2189
COOP, K. L., Angular correlation studies of the low-lying levels of ^{57}Co, 25:3622
COOPER, W. A., Production of strange particles in π^+p interactions at 5.5 GeV/c, 25:3279
COOPER, W. Charles, Corrosive action of selenium towards various materials in the temperature range 300 to 700°C, 25:2629
COOPER, W. S., High-frequency Stark effect in plasma diagnostics, 25:3062
COOTE, G. E., Reaction ^{56}Fe(p,γ)^{57}Co, 25:3601
CORBETT, S., Nuclear interactions in Si(Li) detectors, 25:2451
CORDAILLAT, A., Measurement of beam profile for high-intensity particles, 25:2434 (CERN-70-27)
COREY, B. E., p-p and p-t interactions in ^{3}He(d,tp)p, 25:3552
CORIO, P. L., Mathematical analysis of isotope exchange reactions, 25:2161
CORNWALL, John M., Mutually interacting instabilities in the magnetosphere, 25:2948 (AD-709200)
CORSINI, Alfio, Thorium(VI) adducts of 8-quinolinol and derivatives, 25:2157
CORTES, H., Evidence of a phase transition in an assembly of point contacts, 25:3035
COSSUTTA, D. D., Target technology for medium and high-power applications, 25:3474 (CONF-700322-, pp 431-9)
COTMAN, C., Subcellular fractionation of cultured glial cells, 25:3983 (UCLA-12-793)
COTTS, R. M., Self-diffusion in liquids: H_2O, D_2O, and Na, 25:2192
COUCH, R. G., Spectroscopy of ^{65} ^{67} ^{69}Ga by (d,n) reaction, 25:3625
COUSINS, J. A. R., Some efficiency calculations for ^{6}Li suspended target semiconductor sandwich spectrometers, 25:2473 (AERE-R-6318)
COUTANT, J., Plasma formation by dissociation of an accelerated hydrogen cluster beam, 25:3109 (CEA-CONF-1610)
COYNE, D. G., Reaction π^+p → $\Delta^{++}A_2^0$ at 3.7 GeV/c, 25:3272 (UCRL-20050)
COYNE, James E., Beta processing [forging] of Ti alloys, 25:2717
CRAGG, D. A., Proton polarization measurements, 25:3500
CRAMER, J. D., Neutron fission cross sections for ^{231}Th, ^{233}Th, ^{235}U, ^{237}U, ^{239}U, ^{241}Pu, and ^{243}Pu from 0.5 to 2.25 MeV using (t,pf) reactions, 25:3679
CRAMER, W. A., Radiation-induced isomerization of [2,2,1]bicycloheptadiene (norbornadiene) to [2,2,1,$0^{2,6}$,$0^{3,5}$]quadricycloheptane (quadricyclene) in cyclohexane solutions, 25:2239
CRAWFORD, Raymond Maxwell Jr., Analytical stability criteria for space-dependent systems, 25:3929
CRAWFORD, Richard W., Computerized fully automatic analytical mass spectrometer. I, 25:3999 (UCRL-50931(Pt.1))
CRAWLEY, D. J., UHV measurements by cold cathode gauges, 25:2430
CRESTI, M., Annihilation anti pn → $\pi^+\pi^-\pi^-$ between 1.0 and 1.6 GeV/c and its comparison with Veneziano model, 25:3270 (INFN-PD-70/2)
CREWTHER, R. J., Broken scale invariance and the width of a single dilaton, 25:3372
CRIEGEE, L., Measurement of proton Compton scattering at 6 GeV and small momentum transfers, 25:3309 (DESY-70/46)
CRISAN, I. Al., Complexometric determination of U with EDTA, 25:2088
CRISMAN, E. E., Effects of sub-threshold high-energy electrons on properties of Si photovoltaic cells, 25:2814 (N-70-27167)
CRISP, V. H. C., Positron annihilation in quenched cadmium metal, 25:2898
CROWE, Kenneth M., Radiative pion capture in ^{12}C, 25:3550
CSONKA, Paul L., Implications of full causality for neutrino and other particle production rates, 25:3301
CUE, N., Inhibited (^{3}He,d) transitions to 3s/sub $^1/_2$/ isobaric analog states, 25:3666
CURRAN, D. J., Voltammetric determination of europium(III) using the lanthanum hexaboride electrode, 25:2092
CURREN, E. F., Vibration testing of L-3 and L-10 shipping containers, 25:2415 (ARH-1819)
CZUBRYT, J., Proton spin-lattice relaxation time of aniline-d_2 in deuterated benzene and deuterated aniline solution, 25:2182

D

DADDI, L., Improved method in threshold neutron spectroscopy, 25:2439
DADIC, I., Inelastic processes and backward scattering in a model of multiple scattering, 25:3352 (IRB-TP-2-70)
DAGAN, S., General features of anti pp annihilation into six charged pions, 25:3263
DAGGS, V. M., Test measurements on scintillation Geiger--Mueller counters, 25:2432 (AD-706587)
DAHL, P. F., Superconducting synchrotron magnets, 25:3512
DAHMEN, Hans D., On-shell subtracted dispersion relations and low-energy theorems from current algebra, 25:3368
DAKE, Shyoji, Correspondence between ECC γ-ray and spark chamber shower, 25:2487
DALLA FINA, G. F., Study of a generalized optical potential, 25:3747
DALPIAZ, P., Structure in the neutral A_2 mass region, 25:3290
D'AMATO, F., X-irradiation response of G_1 cells in dry seeds, 25:2555
DAMGAARD, Joergen, Calculation of Coulomb energy differences, 25:3770
DAMLE, P. S., Aquoluminescence: release of energy stored in γ-irradiated crystals, 25:2227
DANBY, F. D., First year at full power, 25:3791 (DP-Report-474)
DANIEL, James M., Wall erosion by sputtering in controlled thermonuclear fusion devices, 25:3135 (ORO-1171-1, pp 334-42)
DANILOV, G. S., Some comments on parity-violating weak NNrho-vertex, 25:3338
DARCHIEVA, L. A., Development of a polar storm, 25:2977
DARIEL, M. P., Structure of $DyFe_3$ and Dy_6Fe_{23}, 25:2750
DARLING, A. S., Platinum and the refractory oxides. III, 25:2160
DARUGA, V. K., Spatial, energy, and angular distributions of neutrons in lithium, 25:3538
DAS, Ajit Kumar, Cupferron in the analytical chemistry of rare earths and scandium, 25:2078
DAS, G. B. L., Nuclear matter calculations with hard-core and long-range potentials, 25:3772
DATES, L. R., Final safety analysis report on the use of plutonium in ZPR-6 and -9, 25:3901 (ANL-7442)
D'AURIA, J., Cross sections for formation of compound nuclei in heavy-ion reactions, 25:3611
DAVID, Francois, Actinium polarography, 25:2159
DAVID, Georges, Influence of pulse length on the spatial echo in a collisionless plasma, 25:3154
DAVIES, P. C. W., Quantum theory of Wheeler--Feynman electrodynamics, 25:3446
DAVIS, A. I., Determination of lead by fast neutron inelastic scattering, 25:2137
DAVIS, B. E., Anisotropic thermal expansion of crystal lattice of α Hf, 25:2751
DAVIS, D. V., Inelastic electron--atom interactions in the 50 to 150 keV energy range, 25:3472 (CONF-700322-, pp 379-92)
DAVIS, I., Fission product distribution in Dragon after first 20 MW run, 25:3886 (DP-Report-571)
DAVIS, Owen H., Environmental aspects of nuclear energy, 25:2564
DAVIS, R., Production of the anti K^{*0} (890) Δ^- (1236) final

state in K-d interactions at 5.5 GeV/c, 25:3274
DAVYDOV, V. V., Excited states (4p--3h) in reaction $^{13}C(^{6}Li,d)^{17}O$ and $^{13}C(^{7}Li,t)^{17}O$, 25:3570
DAVYDOVA, T. A., Cyclotron instability of dense plasma, 25:3120
DAWSON, J. W., Dielectric loaded waveguides as particle separators, 25:3494
DAY, J. L., Proton--neutron elastic scattering on a deuterium target, 25:3266
DE AISENBERG, E. Y., Gamma--gamma coincidences in ^{140}Ce, 25:3646 (CNEA-275)
DEAN, P. N., Direct digital readout and computer calculation of amino acid analysis data, 25:3965 (LA-4507)
DE AZCARRAGA, J. A., Hard-pion calculation without current algebra, 25:3361
DE BORTOLI, M., Natural cesium in freshwater and fishes, 25:2517
DE CHERNATONY, L., UHV measurements by cold cathode gauges, 25:2430
DEDKOV, Yu. M., New reagent for the photometric determination of zirconium and hafnium, 25:2084
DEEV, Yu. C., Radiolysis of original and reinforced ED-5 type epoxy resin, 25:2273
DEEV, Yu. S., Electric breakdown in plastics irradiated with charged particles, 25:2225
DEGISI, S. L., Effects of amine catalysts on the physical properties of a rigid urethane foam system, 25:2818 (BDX-613-170)
DEGRAFF, Arthur C., Annual review of medicine. XX, 25:2575
DEGTYAREV, S. F., Exponential angular coefficients of neutrons for hydrogen-free media, 25:3171
Spatial, energy, and angular distributions of neutrons in lithium, 25:3538
DE LA CRUZ, B., Neutron activation analysis in medical research in the Philippines, 25:2126 (IAEA-122, pp 37-40)
DELALEX, Anne-Marie, Study of some nuclei of the 1p and 2s-1d shells using the Hartree--Fock method, 25:3545 (LYCEN-7047)
DE LANGE, J. C., Decay of ^{62}Co isomers, 25:3644
DELORME, J., Muon capture rate in ^{6}Li, 25:3748
DELSAUT, Romeo, Construction of semi-automatic device for measuring nuclear tracks, 25:2433 (CEA-R-4063)
DELUCCHI, A. A., Fission yields of iodine isotopes and ^{139}Te, 25:3663
DEMAUREX, P., Charge/discharge machine for Dragon reactor, 25:2385 (DP-Report-230)
DE MEESTER, P., Deformation properties of vanadium single crystals, 25:2718
DEMENTII, S. V., Quasi-elastic scattering of 1115-MeV electrons by nucleons of ^{32}S nuclei, 25:3615
DEMIKHOVSKII, D. A., Investigation of beam transversal characteristics at input of IHEP proton synchrotron, 25:3482
DE MORTON, M. E., Internal friction in In single crystals, 25:2667 (NP-18491)
DE MUL, F. F., Quasi-elastic incoherent cold neutron scattering in liquid cyclohexanol, 25:3534
DE NORDWALL, H. J., Fission product distribution in Dragon after first 20 MW run, 25:3886 (DP-Report-571)
DENOVION, Charles-Henri, Elastic constants of U and plutonium carbonitrides, 25:2798
DEREVSHCHIKOV, V. A., Measurement of radiative losses in pulsed plasma accelerator, 25:3084
DEROSSET, A. J., Benzene--deuteroxyl exchange over deuterated γ-alumina, 25:2164
DESAI, Bipin R., Complex Regge poles in the cut j plane, 25:3402
DESCHAMPS, J., Inverse Faraday effect in a plasma, 25:3082
DESCHAMPS, N., Fixation of alkali metals on antimony pentoxide hydrate in strongly acid media, 25:2333
DESCHAMPS, P., Drift waves in a collisionless plasma, 25:3147 (CEA-CONF-1612)
DESCHAMPS, Pierre, Drift waves due to a pressure gradient in a collisionless plasma, 25:3167
DESPORTES, H., Superconducting beam line, 25:3505
DE TOURREIL, Roland, Delayed neutron emission, 25:3713 (CEA-N-1333)
DEUTSCHMANN, M., Application of the Veneziano model with pion and Pomeron exchange to the reaction $K^- p \to nc$, 25:3386
DEVARE, H. G., g factor of the 114 keV state in ^{149}Pm, 25:3705
DEVARE, S. H., Half-lives of excited levels in ^{125}Te and ^{132}I, 25:3706
DEVONS, S., Muonic atoms. I, 25:3661
DE VRIES, E., Foldy--Wouthuysen transformations and related problems, 25:3231
DEVRIES, Gerrit, Corrosion of metals by molten lithium, 25:2626
DEWAN, John T., Submarine radioactivity logging technique, 25:2357
DEXTER, Richard John, Infrared absorption study of silicon implanted with high-energy nitrogen ions, 25:3203
DIAMOND, J. J., Bibliography on the high temperature chemistry and physics of materials, January--March 1970, 25:2665 (NBS-SPEC. PUBL-315-5)
DIBOBES, I. K., Norms for radiation protection, 25:2574
DICKINSON, R. E., Atmospheric response to heating within a stable auroral red arc, 25:2953
DICKSON, D. P. E., Surface tension of liquid ^{4}He, 25:3010
DICKSON, Howard, Radiation safety in the operation of a low-energy accelerator, 25:3475 (CONF-700322-, pp 441-8)
DIEDERIX, F., Decay of isomers of ^{102}Rh, 25:3671
DIETRICH, K., Nuclear Josephson effect in heavy ion scattering, 25:3752
DIETTRICH, O., Shielding calculations by means of the Monte Carlo method, 25:3170
DIKHTER, I. Ya., Heat capacity of tungsten near the melting point, 25:2726
DIKSIC, M., Directional correlation studies in decay of /sup 177g/Lu, 25:3684
DILLI, S., Radiation-induced reactions with cellulose. VIII, 25:2247
DIMIC, V., Cold neutron source efficiency in a tangential beam hole, 25:3904 (IJS-571)
DIN, G. U., Reaction Q values from near-threshold neutron spectra, 25:3608
DINCER, Targut, Nuclear techniques in hydrology, 25:2359
DINUNNO, Joseph J., Environmental aspects of nuclear energy, 25:2564
DISCO, Michael D., Utility of radioisotope methodology in estuary pollution control studies. I, 25:2348 (NYO-3961-1)
DISNEY, M. J., Optical polarization of Crab Nebula pulsar, 25:2843
DI TORO, M., Effect of short-range correlations and charge-dependent nuclear forces on the energy of the analog state, 25:3753
DITTER, W., Approximate methods for determining the structure of H_2O and HOD using near-infrared spectroscopy, 25:2171
DITTMER, David Louis, Direct reaction studies of vibrational nuclei in the mass-105 region, 25:3701
DIXON, A. F., Measurements of the shape of ionospheric irregularities using satellite transmissions, 25:3003
DMITRENKO, I. M., Superconductivity critical transition temperature in thin tin films, 25:3026
DNEPROVSKII, I. S., Radioactivation determination of Ta in minerals and rocks with a Ge(Li)-spectrometer, 25:2139
DOBO, J., Grafting of styrene on polyethylene. I, 25:2242
Grafting of styrene on polyethylene. II, 25:2241
DOBRY, H., Computer programs for irradiation planning in high-energy therapy, 25:2584
DOICHEVA, Rakhila, Extraction of rhenium and molybdenum by dialkylmethylbenzylammonium salts, 25:2328
DOKUTOVICH, V. A., Effect of tensor forces in residual pair nucleon interaction, 25:3766
DOLGUSHIN, V. M., Generator of short pulses of hard x-rays of high intensity, 25:2401
DOMRIN, V. I., Parametric instability of nonhomogeneous plasma, 25:3118
DON, C. G., Radiative detection of single-passage nuclear magnetic resonance, 25:3223
DONNACHIE, A., K^+p phase shift analysis, 25:3393
DONNE, M. Dalle, Considerations on coated particles, with oxide fuel, and graphite and Si carbide coating, for GCFR application, 25:3875 (EURFNR-834)
DONNELLY, M. F., Detection of a secondary isotope effect on partitioning of benzhydryl benzoate ion pairs, 25:2186
Dissection of α-isotope effects on the solvolysis of benzhydryl benzoate, 25:2185
DONNELLY, T. W., Quasielastic electron scattering, 25:3577
DORE, U., Upper limit on the $\omega \to 2\pi$ decay rate from anti pn annihilations at rest, 25:3269
DORLING, J., Energy-momentum conservation for collision, creation, and annihilation processes, 25:3243
DOTCHIN, L. W., Beam-foil excitation using low-energy accelerators, 25:3465 (CONF-700322-, pp 21-31)
DOWNEY, Daniel, Radiation damage studies with low-energy hydrogen isotopes, 25:3187 (CONF-700322-, pp 63-77)
DOWNS, B. W., One-boson-exchange potential model for the AN interaction, 25:3416
DRALEY, Joseph E., Corrosion by liquid metals. Proceedings of the sessions on corrosion by liquid metals of the 1969 fall meeting of the Metallurgical Society of AIME, October 13--16, 1969, Philadelphia, Pennsylvania, 25:2615
DRAWIN, H. W., Basic collision processes in plasmas; collision cross sections, 25:3075 (CEA-CONF-1627)
Spectroscopic diagnostics of nonequilibrium plasmas, 25:3061 (CEA-CONF-1628)
DRECHSLER, Wolfgang, Analysis of differential and total cross-section data for high-energy pp and p anti p interactions, 25:3411
DRESCH, C., Platelet lifespan, 25:2579
DREVERMANN, H., Analysis of $p\pi^+\pi^-$ enhancements produced in reaction $\pi^+p \to \pi^+p\pi^+\pi^-$ at 5 GeV/c, 25:3275
DRIATSKII, V. M., Meridional movement of auroral absorption bays, 25:2979
DRIEU, Fernand, Detachable head for a pneumatic system, 25:2427
DROC, M., Production of multicharged ions in a reflex source with axial extraction, 25:3111 (LYCEN-7065)
DROUIN, R., Aluminum oxide films and alpha stopping power, 25:2887
DROZDOV, V. E., Universal nomograms for calculating absorbed doses from plane radiators, 25:2566
DRUXES, H., Numerical calculations and description of

toroidal arcs by model theories, 25:3088
DUBAL, L., Measurement of proton Compton scattering at 6 GeV and small momentum transfers, 25:3309 (DESY-70/46)
DUBROVINA, S. M., Neutron-induced ^{249}Bk fission, 25:3665
DUDEK, A., Real part of the alpha--nucleus potential, 25:3755
DUDZIAK, Donald J., PHOXE: a FORTRAN-IV code to check format syntax, consistency, and physical realism of ENDF/B photon production data, 25:3531 (LA-4506)
DUEE, Emile D., Use of the Grenoble high flux reactor in biology, 25:3907 (NP-18462)
DUERDOTH, I., Muonic atoms. I, 25:3661
DUFF, C. E., Direct reading spectrometric method using AgCl--LiF carrier to determine impurities in nuclear-grade U_3O_8 samples, 25:2068 (NLCO-1071)
DUFFAIT, R., Decay scheme of 7 min ^{168}Lu, 25:3650 (LYCEN-7030)
DUFLO, J., Effective deuteron--proton elastic scattering cross section at 180°, 25:3264
DUGGAN, Jerome L., Conference on use of small accelerators for teaching and research, Oak Ridge, Tenn., 3/70, 25:3463 (CONF-700322)
DULFER, G. H., Decay of ^{63}Ga, 25:3609
DULK, George A., Very-long-baseline interferometry of decametric radiation from Jupiter, 25:2879
DUMBRAIS, O. V., Data on real parts of K^{+-} forward scattering amplitudes, 25:3379 (JINR-E1-5259)
DUMBRAIS, T. Yu., Data on real parts of K^{+-} forward scattering amplitudes, 25:3379 (JINR-E1-5259)
DUMITRESCU, O., Multi-step stripping on deformed nuclei, 25:3732
DUSHIN, L. A., Expansion of measurement limits of electron density in plasma, 25:3072
DUSSEL, G. G., T = 1 pairing Hamiltonian, 25:3758
DUTINA, Dragomir, Evaluation of particulates deposited in flowing non-isothermal sodium systems, 25:2616
DUTTA-ROY, Binayak, Meson--nucleon scattering and asymptotic conservation of helicity, 25:3398
DVORNIK, I., Grafting of styrene on polyethylene. I, 25:2242
Grafting of styrene on polyethylene. II, 25:2241
DYER, C. K., Beryllium and its alloys, 25:2654
DYRBYE, M. O., Determination of ^{3}HOH, ^{82}Br, ^{125}I-human albumin, and ^{51}Cr-red cell volumes, 25:2518
DZHAGATSPANYAN, R. V., Radiation chlorination of polymers, 25:2250
Spherically shaped cartridges for extended sources in pilot and full-scale radiation-chemical processors, 25:2404
DZHGARKAVA, M. I., Description of experimental data on πN and KN scattering in high-energy region on basis of complex angular momenta theory. I, 25:3381 (JINR-P2-5320)

E

EARLE, E. D., Study of the ^{207}Pb(d,p)^{208}Pb reaction, 25:3688
EARNSHAW, J. C., Space--time detector for cosmic ray showers, 25:2490
EBERHART, J. G., Grain boundary grooving of iron in liquid sodium, 25:2708
EBISAWA, H., Fluctuations of order parameter and Hall effect, 25:3036
ECKER, G., Consistency condition for the A_1 rhoπ system from unitarized current algebra, 25:3359
EDELSTEIN, N., Hyperfine structure anomaly of ^{241}Pu and ^{239}Pu, 25:2893
EDGE, R. D., Potassium-41 level structure from ^{40}Ar(^{3}He,d)^{41}K, 25:3632
EFKEN, B., Reactions (d,n) on ^{11}B, ^{14}N, and ^{15}N, 25:3574
EFRYUSHINA, N. P., Luminescence of neodymium and europium in cerium dioxide and its use in analysis, 25:2083
EGOROV, A. I., Charge radii of the nuclei of ^{124} ^{126} ^{128} ^{130}Te, 25:3551
EHMANN, William D., Determination of elements in lunar material by 14-MeV neutron activation, 25:2118 (CONF-700322-, pp 205-20)
EICHHOLZ, G. G., Spark counters as high-temperature neutron detectors, 25:2459
EICK, Harry A., Prog. rpt. on investigation of some lanthanide boron, carbon, nitrogen, silicon, chalcogen and halogen systems at elevated temperatures, annual, 2/70--1/71, 25:2803 (COO-716-66)
EISBERG, R., Proton hole states in 1f/sub 7/2/ nuclei, 25:3616
EISNER, A. M., Bound on virtual Compton scattering at 185 and 460 MeV/c^2, 25:3252
EISNER, R. L., Branching ratios of the K(1420) meson, 25:3287
EKMAN, L., Whole-body measurements on distribution of ^{203}Hg in humans, 25:2533
EL BEHAY, A., Spectroscopy of even tin isotopes by inelastic scattering of protons, 25:3668
ELER, G., Investigation of proton polarization in reaction ^{12}C(^{3}He,p_0)^{14}N, 25:3563 (JINR-P15-5156)
ELLERT, G. V., X ray studies of monoaquotetracarbamidouranyl halide nitrates, 25:2214
ELLIS, P. J., Bubble corrections to two-body matrix elements, 25:3759
EL-NESR, M. S., Low-energy gamma transitions in ^{171}Tm, 25:3659
EL-SHERBINI, Th. M., K-shell excitation of N_2 and CO by electron impact, 25:2910
ELY, John T. A., Satellite measurement of the relative abundance of relativistic cosmic-ray LH nuclei, 25:2931
ELZE, Th. W., Energy levels of ^{243}Am, 25:3669
EMEL'YANOV, V. S., Properties of uranium oxycarbides, 25:2809
EMSALLEM, A., Decay scheme of 7 min ^{168}Lu, 25:3650 (LYCEN-7030)
ENDEAN, V. G., Contribution to the co-rotating magnetic field model of the pulsar, 25:2850
ENGARDT, Ralph Duane, Nuclear magnetic resonance determination of the activation volume for self-diffusion in aluminum, 25:3962 (IS-T-410)
ENGEL, H., Industrial experience with fuel elements and activation, 25:3894
ENGELSTAFF, P. A., British high flux beam reactor, 25:3911
ENGLISH, Jerome J., Recent information on long-time creep data for columbium alloys, 25:2657 (AD-464715)
ENKOVSKI, L. L., Inelastic meson--baryon reactions in generalized Veneziano model, 25:3378 (ITF-70-77)
ENSSLEN, Benno, Bibliographies in nuclear science and technology, 25:2399 (AED-C-12-22)
EREMIN, Yu. G., Contemporary methods for determination of small quantities of cerium, 25:2061
EREZ, G., Structure of $DyFe_3$ and Dy_6Fe_{23}, 25:2750
ERICSON, L. G., Shape of thermoluminescence glow peaks in molecular solids, 25:2235
ERICSON, M., Muon capture rate in ^{6}Li, 25:3748
ERMAGAMBETOV, S. B., Fragment angular distributions and channel analysis of fission of ^{232}Th by neutrons, 25:3680
ERMAKOV, A. N., New reagent for the photometric determination of zirconium and hafnium, 25:2084
EROE, J., Neutron-rich isotopes of light elements produced in transfer reactions with heavy ions, 25:3648 (JINR-E7-5319)
ERSHOV, V. G., Magnetization of the superconducting alloy Ti--22 at. percent Nb, 25:3027
ERTEK, Cetin, Nordheim equation according to P_1-approximation, 25:3924 (CNAEM-73)
ERWIN, A. R., Associated production in K+p interactions at 3.5 GeV/c, 25:3277
ESTABROOK, K., Turbulent heat in mirror machines at ORNL, 25:3056 (ORO-1171-1, pp 78-97)
ETIEVANT, C., Change in the polarization of an electromagnetic wave in a sheared magnetic field, 25:3146 (CEA-CONF-1608)
ETTINGER, Harry J., Calibration of two-stage air samplers, 25:2446
EULER, H. C., Solar indices, 1/55--12/69, 25:2858 (N-70-32003)
EVANS, A. E., Use of small accelerators in nuclear safeguards research, 25:2416 (CONF-700322-, pp 357-78)
EVANS, E. P., Induction of translocations in mouse spermatogonia. III, 25:2553
EVERED, D. C., Measurement of plasma digoxin concentration by radioimmunoassay, 25:2522
EVERETT, M. R., Carbon transport studies for helium cooled high temperature reactors. project dragon, 25:3860 (DP-Report-491)
EVLANOV, M. V., Scattering of fast deuterons at large angles, 25:3614
EVSTYUKHIN, A. I., Dispersed precipitates in Zr--Nb alloys, 25:2742
Distribution of C in cast Mo, 25:2702
Effect of C on Mo and Mo alloys, 25:2745
Properties of extruded Mo, 25:2697
Properties of hydroextruded Mo, 25:2698
Properties of uranium oxycarbides, 25:2809
Recrystallization of extruded Mo, 25:2747
EXEROWA, D., Destruction of foam by α particles, 25:2223
EYRE, J. A., Primary yields in γ-radiolysis of ammonia, 25:2283
EZELL, C. R., Double-Regge pole analysis of $\pi^+p \to \pi^+\pi^-\Delta^{++}$ at 13.1 GeV/c, 25:3273
EZELL, R. D., Relation between mass spectra and reaction products of electron-irradiated aromatic ketones, 25:2266

F

FABIAN, H. U., Determination of the energy spectrum of a gamma-ray flash, 25:3183
FABREY, James D., Exponential representations of the canonical commutation relations, 25:3442
FACCHINI, A., Isolation of cerium from a mixture of rare earths with the production of a nitric mother liquor, 25:2326
FACIUS, H., Ten years of Kahl nuclear power plant, 25:3801
FAGES, Denis, Natural-convection irradiation device ''Esther'', 25:3903 (CEA-N-1348)
FALK, M., Infrared spectrum of HDO in aqueous solutions of perchlorates and tetrafluoroborates, 25:2183
FALK, R., Whole-body measurements on distribution of ^{203}Hg in humans, 25:2533
FAM, S. S., Ultrasonic thermometry for LMFBR systems, 25:2503 (NYO-3906-4)

FANE, A. G., Assessment of air-pulsing techniques for liquid extraction columns, 25:2383 (AAEC/TM-547)
FANG, Sen-maw, Deuterium isotope effects in enzymatic transamination, 25:2168
FARRELL, K., Effect of gas bubbles on recrystallization of tungsten, 25:2736
FAST, R. W., Superconducting two tesla bending magnet, 25:3504
FATIEVA, N. L., Determination of state of ^{129}I in β-/sup 129m/TeO_3 by nuclear gamma resonance, 25:2304
FATKULLIN, M. N., Plasma scale height in the upper F2 region, 25:2973
FAULK, J., Inelastic electron--atom interactions in the 50 to 150 keV energy range, 25:3472 (CONF-700322-, pp 379-92)
FAUSSAT, A., Limits in the use of tubular graphite core and annular fuel elements, 25:3878
FAUSSAT, Armand, Solution of two important problems in the nuclear industry by flame metal spraying, 25:2638 (CEA-CONF-1625)
FAYYAZUDDIN, Chiral-symmetry-breaking corrections to the K + 3π soft-pion theorem, 25:3347
FEDER, H. M., Grain boundary grooving of iron in liquid sodium, 25:2708
FEDIN, A. G., Mass exchange of a circular cylinder in presence of transverse magnetic field, 25:2941
FEDOROFF, Michel, Sulfur determination in Mo by activation analysis by thermal neutrons, 25:2136
FEDOROV, G. A., Investigation of fission product deposition in the Moscow region during 1962--1966, 25:2550
FEDOROV, G. B., Diffusion in W and Nb, 25:2703
Diffusion of Mo and Nb in Zr, 25:2704
Self-diffusion in binary systems, 25:2701
FEDOSEEV, I. A., Realization of representations of the quaternion group, 25:3420 (IFVE-STF-69-102)
FEESE, K., Stored energy measurements in electron-irradiated Pt, 25:3197
FEIST, H., Direct electron--positron pair production in copper by electrons of 5.8 MeV, 25:3250
FELDMAN, G. J., Bound on virtual Compton scattering at 185 and 460 MeV/c^2, 25:3252
FELICI, Noel, Constant electrical field surfaces, 25:3934 (ANL-Trans-862)
FELLINGER, M., Measurements of π-p elastic scattering from 1.71 to 5.53 GeV/c, 25:3280
FELTIN, D., Two ion collisional absorption of low frequency electromagnetic waves in a toroidal hard-core configuration, 25:3148 (CEA-CONF-1614)
FERGUSON, A. J., Study of the $^{207}Pb(d,p)^{208}Pb$ reaction, 25:3688
FETISOV, V. N., Dipole sum rule for three-particle nuclei, 25:3768
FEUZ, P., Swiss nuclear industry: traditional quality and world-wide effectiveness, 25:3781
FICENEC, J. R., Elastic electron--nickel scattering, 25:3687
FIDLERIS, V., Stress-dependence of in-reactor creep rate of Zr--2.5 wt percent Nb and Zy-2, 25:2760
FIDONE, I., Change in the polarization of an electromagnetic wave in a sheared magnetic field, 25:3146 (CEA-CONF-1608)
Harmonic absorption of microwaves in magnetized low-density plasma, 25:3145 (CEA-CONF-1607)
FIFE, Thomas H., Hydrolysis of bis(4-nitrophenyl) carbonate and the general base catalyzed hydrolysis of o-(4-nitrophenylene) carbonate, 25:2181
FIKHTENGOL'TS, I. G., Gravitational pressure in Friedman--Lobachevskii space, 25:3449
FILBY, R. H., Determination of lead by fast neutron inelastic scattering, 25:2137
FILIMONOVA, E. A., Investigation of charge exchange of a dense plasma current in a magnesium target, 25:3079
FILIPPOV, A. F., Corrosive behavior of alloys of the titanium--molybdenum--chromium system, 25:2613
FILISETTI, O., Grain counting in nuclear emulsions, 25:2457
FILONOVA, L. D., Relationship between the geomagnetic field and the sporadic E layer, 25:2995
FILOSOFO, I., Spins and mean lives of ^{34}Cl levels, 25:3619
FINCKH, E., Investigation of ^{65}Zn by (p,n) and (p,nγ) experiments, 25:3631
FINEGOLD, L., Upper limit on electron--phonon interaction in vanadium carbide, 25:3034
FINFGELD, C. R., Wall erosion by sputtering in controlled thermonuclear fusion devices, 25:3135 (ORO-1171-1, pp 334-42)
FINKEN, D., Polarized positively charged hydrogen ion beams, 25:3307
FINTZ, P., γ transitions in ^{16}O, 25:3584
FIREBAUGH, M. W., Difference in energy dependence for A_2^- and A_2^0 production, 25:3289
FIRSAKOV, A. S., Measurement of ionospheric parameters from Doppler and Faraday effects of coherent signals, 25:2971
FISCHER, H., Prevention of stress rupture formation of thermoplastics by radiation cross-linking, 25:2249
FISCHER, Konrad, Adsorption of oxygen and nitrogen on tantalum films. I, 25:2686
FISER, M., Gamma-ray spectrum of ^{192}Au, 25:3654
Transition multipolarities in decay of /sup 197m/Hg, 25:3682
FISHMAN, Steven Gerald, Isotope effect and diffusivity measurements in equi-atomic iron--cobalt alloys, 25:2178
FITAIRE, M., Inverse Faraday effect in a plasma, 25:3082
FITCH, Lewis Thomas, Survey between 0 and 20° N declination using Ohio State Univ. radio telescope, 25:2855
FITZGERALD, Maurice Edward, NMR studies of spontaneous polarization in Rochelle salt, 25:3221
FLEITMAN, A. H., Corrosion and mass transfer of pure iron, nickel, chromium, and cobalt in 660° to 760°C sodium, 25:2631
Measurements of the solubility of iron and chromium in sodium, 25:2712
FLEMING, S. J., Thermoluminescent dating: refinement of the quartz inclusion method, 25:2355
FLESHER, G. I., Statistical analysis of the information transfer process in radiometric betatron defectoscopy, 25:2412
FLETCHER, B., External collector gauge for ultrahigh vacuum measurement, 25:2431
FLETCHER III, K. S., Voltammetric determination of europium(III) using the lanthanum hexaboride electrode, 25:2092
FLID, B. D., Laws governing operation of metallic electrodes of MHD generator, 25:2940
FLIPOT, A. J., Electrodynamic vibrocompaction of sintered nodules of uranium oxide, 25:2778
FLORESTAN, J., Use of an x-ray fluorescence spectrometer with a computer, 25:2105
FLUENDY, M. A. D., Elastic scattering of alkali atoms from iodine atoms and molecules at thermal energies, 25:2922
FOELDIAK, G., Radiolysis of saturated and unsaturated binary hydrocarbon systems, 25:2270
FOIS, M., Plasma formation by dissociation of an accelerated hydrogen cluster beam, 25:3109 (CEA-CONF-1610)
FOJTIK, A., Pulse radiolytic investigation of short-lived hydrates of aromatic nitroso compounds, 25:2272
FOLOMESHKIN, V. N., Generalization of Tolman equality, 25:3447 (IFVE-SEF-69-59)
FONTAINE, G., Method to study events with two missing neutral particles, 25:3362
FORD, C. E., Induction of translocations in mouse spermatogonia. III, 25:2553
FORD, W. T., Search for violation of CP invariance in tau+- decay, 25:3427
Wire-spark-chamber system with on-line computers, 25:2491
FORICHON, M., Optical spark chamber for the search of gamma-ray sources, 25:2841 (CEA-CONF-1633)
FORKER, M., Gamma--gamma angular correlation in ^{166}Er in different liquid sources, 25:3696
FORNASINI, M. L., Rare-earth intermediate phases with zinc, 25:2753
FORSEN, Harold K., Injector requirements for open ended fusion reactors, 25:3131 (ORO-1171-1, pp 3-37)
FORSTER, J. S., Proton stripping to particle-hole states in ^{40}Ca and ^{42}Ca, 25:3627
Rotational structure in ^{43}Sc, 25:3626
FORSYTH, P. A., Measurements of the shape of ionospheric irregularities using satellite transmissions, 25:3003
FORT, E., Multiple diffusion of neutrons in ^6Li-loaded scintillators, 25:2456
FORTI, P., Excitation functions and differential cross sections for $^9Be(n,\alpha)$ reaction with 8 to 30 MeV neutrons, 25:3564 (KFK-1190)
FORTOV, V. E., Possibilities of a shock tube in obtaining and investigating a dense low-temperature plasma, 25:3116
FORTUNE, H. T., Distorted-wave analysis of stripping to unbound states, 25:3764
FOULQUIER, L., Contamination of anodonta cygnea by ^{137}Cs, 25:2525
FOX, J. D., Direct reaction in production of fission isomers, 25:3709
FRABETTI, P. L., Structure in the neutral A_2 mass region, 25:3290
FRANA, J., Gamma-ray spectrum of ^{192}Au, 25:3654
Transition multipolarities in decay of /sup 197m/Hg, 25:3682
FRANCIS, William Porter, Ground state of liquid helium four, 25:3013
FRATIELLO, Anthony, Direct proton magnetic resonance cation hydration study of uranyl perchlorate, nitrate, chloride, and bromide in water--acetone mixtures, 25:2209
FRAZER, Jack W., Computerized fully automatic analytical mass spectrometer. I, 25:3999 (UCRL-50931(Pt.1))
FRENCH, Walter R. Jr., Educational applications of nuclear electronics, 25:3467 (CONF-700322-, pp 79-88)
FREY, Jean Pierre, Nonlinear frequency shift in whistler and hydrodynamic propagation, 25:3004
FRIDLENDER, Bertold R., Distribution of polysomes in mouse brain tissue, 25:3986 (UCLA-12-796)
FRIEDLANDER, Gordon D., Power, pollution, and the imperiled environment. I, 25:3852
FRIEDMAN, H., Effects of RES blockade on antibody formation. III, 25:2538
FRIEDMAN, Harold L., Enthalpies of alkylammonium ions in water, heavy water propylene carbonate, and dimethyl sulfoxide, 25:2162

XUM

FRIEDRICH, L., Polarized positively charged hydrogen ion beams, 25:3307
FRISCH, W., Inherent stability of steam-cooled breeder reactors, 25:3856 (KFK-851)
FRISSEL, M. J., Migration of ^{90}Sr in soil, 25:2366
FRITZSCH, H., Angular-momentum distribution in dual-resonance models, 25:3366
FROEHLICH, F., Influence of aggregation on V-band absorption in Ca-doped KCl, 25:3198
FROLOV, V. V., Determination of Cl and V in graphite by activation method, 25:2142
FROLOV, Yu. G., Salting out at solvent extraction of acids and some radioactive elements. IV, 25:2335
FROMM, Eckehard, Adsorption of oxygen and nitrogen on tantalum films. I, 25:2686
FRUIN, J. H., Spaced-receiver observations of radio pulses, 25:2849
FU, Chumin, Resonance productions in K⁺p interactions at 4.6 GeV/c and 9 GeV/c, 25:3271 (UCRL-19809)
FUJII, Kanji, Universality of weak bilinear transitions and its relation to the fundamental weak interactions, 25:3348
FUJIMOTO, M., Free radicals in γ-irradiated disodium succinate. II, 25:2230
Free radicals in γ-irradiated disodium succinate. I, 25:2229
FUJIMURA, T., Creep and creep-rupture tests of stainless steel as structural material of fast breeding reactor, 25:2660 (JAERI-Memo-4097)
FUJIOKA, Manabu, Deexcitation of 931.1-keV 2_2^+ state of ^{152}Gd, 25:3681
FUKUDA, Toru, Analysis of JMTR flux variation during operation, 25:3906 (JAERI-Memo-4130)
FUKUSHIMA, Masao, Thermal conductivity of VIPAC UO_2 fuel. II, 25:2813 (JAERI-Memo-4128)
FUKUYAMA, H., Fluctuations of order parameter and Hall effect, 25:3036
FULCO, Armand J., Temperature-mediated hyper-induction of fatty acid desaturating enzyme, 25:3985 (UCLA-12-795)
FULFORD, Phillip James, Analysis of nuclear fuel management techniques for utilities, 25:3803
FULLER, E. L. Jr., Infrared studies of thorium oxide surfaces: hydroxyl spectra, 25:2207
FULLER, Robin Walter Ellecker, Improvements in cathodes, 25:3523
FULLWOOD, R. R., Versatile mercury film pulser, 25:2513
FURMAN, V. I., Optical potentials and elastic scattering of t and ^3He, 25:3769
FURNICA, G., Anion exchange between bentonites and ^{131}I ions, 25:2337
Retention of radioactive ions by suspensions and earths, 25:2363
FURUTA, Teruo, Effect of cold working on creep properties of stainless steel, 25:2661 (JAERI-Memo-4125)
FUSE, T., Optimum arrangement of laminated iron--water shields, 25:3174
FUSHCHICH, V. I., Additional invariance of relativistic equations of motion, 25:3292 (ITF-70-32)

G

GABRAKOV, S. I., States I/sup π/ = 1⁺ in even--even deformed nuclei, 25:3727
GABRIEL, L., Handling of radioactive wastes in Poland, 25:2422
GABRIEL, T. A., Approximate high-energy alpha-particle-nucleus-collision model, 25:3716 (ORNL-TM-3153)
GAGLIONE, P., Concentration factors for fallout ^{90}Sr and ^{137}Cs in fishes, 25:2527
GAIDOS, J. A., Double-Regge pole analysis of π⁺p → π⁺π⁻Δ⁺⁺ at 13.1 GeV/c, 25:3273
GAILLARD, R., Use of a Van de Graaff generator to simulate the transient effects due to radiation in semiconductors, 25:3477 (LYCEN-7063)
GAL, J., Charge states of Np recoil atoms, 25:2305
GALLAGHER, Edward V., Water decompression experiments and analysis for blowdown of nuclear reactors. final report, 25:3893 (IITRI-578-P-21-39)
GALLAI, Z. A., Use of N-benzoyl-o-tolylhydroxylamine in method of amperometric titration. III, 25:2082
GALLMANN, A., γ transitions in ^{14}O, 25:3584
Lifetimes in ^{12}B, ^{14}N, and ^{16}O, 25:3569
GAMMAGE, R. B., Infrared studies of thorium oxide surfaces: hydroxyl spectra, 25:2207
GANOPOL'SKII, V. I., Value of the reciprocal slope of the calibration graph and methods of calculating it in the indirect spectrophotometric determination of yttrium in rare-earth metals, 25:2091
GARDINER, C. W., Effect of a transverse momentum distribution in the Parton model, 25:3323
GARDINER, S. N., Non-intercepting beam current integrator, 25:3517
GARDNER, R. D., Determination of Ti, Zr, Hf, Nb, Ta, Mo, and W in uranium alloys, 25:2065 (LA-4529)
GARFINKEL, A., Difference in energy dependence for A_2^- and A_2^0 production, 25:3289
GARNETT, J. L., Radiation-induced reactions with cellulose. VIII, 25:2247
GARRETTSON, Garrett Aquila, Green's functions for multidimensional neutron transport in a slab, 25:3184
GARSIDE, L., Random-phase-approximation treatment of nucleon--nucleus scattering, 25:3718
GARTLER, S. M., Isoenzyme stability in human heteroploid cell lines, 25:2585
GASGNIER, M., Study of thin films of samarium by x rays and electron microscopy, 25:2734
GASPAR, Peter P., Reactions of recoiling Si atoms with phosphine, silane, and disilane, 25:2299
GASPAROVIC, Richard Francis, Superconducting penetration depth in lead, 25:3041
GAUR, S. C., Variation of attenuation of acoustic waves through plasma with ion--plasma frequency, 25:3155
GAUTHIER, Cl., Characteristics of two /sup 113m/In generators, 25:2296
GAVRILOV, N. V., Salting out at solvent extraction of acids and some radioactive elements. IV, 25:2335
GAWLOWSKI, Janusz, Gas-chromatographic analysis of C_1--C_4 hydrocarbons, products of radiolysis of gaseous ethylene, 25:2278
GEHRELS, T., Optical polarization of Crab Nebula pulsar, 25:2843
GEHRKE, E., Influence of aggregation on V-band absorption in Ca-doped KCl, 25:3198
GELLERI, A., Pyridine-N-oxide: vibrational assignment and thermodynamic quantities, 25:2163
GENCAY, Sarman, Nordheim equation according to P_1-approximation, 25:3924 (CNAEM-73)
GENRE, R., Use of a Van de Graaff generator to simulate the transient effects due to radiation in semiconductors, 25:3477 (LYCEN-7063)
GEORGE, Cl., Identity concerning the projection operators in nonequilibrium statistical mechanics, 25:3234
GEORGIEVA, Jordanka, X-irradiation response of G_1 cells in dry seeds, 25:2555
GERMAI, G., Addition of naphthalene to liquid scintillators, 25:2450
Degassing at low temperature of titanium targets impregnated with hydrogen isotopes, 25:3542
GERSCHENSON, L. E., Regulation of pyruvate kinase of an established rat liver cell line (RLC) in culture by insulin, glucose, and serum, 25:3984 (UCLA-12-794)
GHIORSO, A., Tracer chemical studies of Lr, 25:2197
GHOLAMREZA, Djalali-Behzad, Behavior of normal and irradiated bone marrow, 25:2595
GHOSH, P. C., Closed circuit technique for measurement of Rn/thoron ratio in soil-gas, 25:2378
GHOSH MAZUMDAR, A. S., Decomposition of brown peroxy complex of Pu(IV) in $HClO_4$, 25:2154
GIACOMELLI, G., Total cross-section measurements, 25:3268
GIBALO, I. M., Extraction--photometric determination of Nb(V) with benzohydroxamic acid, 25:2085
GIBSON, J. A., Record of programme and discussions at symposium of papers from Dragon contractors held at A.E.R.E., Harwell, 14--16 March 1966, 25:3774 (DP-Report-439)
GIFTCIOGLU, O., Moving-source soil density gauge, 25:2498
GILAR, Oldrich, Corona counters for nuclear radiation detection, 25:2440
GILBERT, E. R., Creep rate correlation in solution-treated Type 304 and 316 stainless steels, 25:4007 (WHAN-FR-25)
GILBERT, W. S., Superconductivity for high energy physics at LRL-Berkeley, 25:3510
GILL, R. D., Electromagnetic transitions in ^{19}Ne, 25:3575
GILLBRO, Thomas, Relative signs of principal elements of the α-proton hyperfine coupling tensor in NH_2CONHO, 25:2219 (NP-18449)
GINDLER, J., Fission of heavy nuclei by helium ions and deuterons, 25:3710
GINZBURG, S. S., Distribution of C in cast Mo, 25:2702
GIRAUD-HERAUD, F., Continuous and discontinuous precipitation reactions in U--1.5 percent Mo alloys, 25:2738
GIRIJA, M., Absorption spectrum of ammonium uranyl sulfate, 25:2211
GIROUX, J., Oxygen determination in silicon by means of alpha particles, 25:2128 (LYCEN-7060)
GIUSTI, E. R., Search for superheavy elements in nature by detection of events with large numbers of neutrons, 25:3652 (UCRL-19957)
GIZBERT-STUDNICKI, P., Ambiguities in the experimental determination of resonance production amplitudes, 25:3382 (TPJU-1/70)
Regge pole model with Veneziano residues for reactions $0^- \frac{1}{2}^+ \rightarrow 0^- \frac{3}{2}^+$, 25:3384 (TPJU-3/70)
GLASCOCK, R. B., Direct digital readout and computer calculation of amino acid analysis data, 25:3965 (LA-4507)
GLAZKOVA, I. N., Influence of radioactive radiation on the heterogeneous equilibrium in the system solid--solution, 25:2222
GLOYNA, E. F., Transport of radionuclides in aquatic system, 25:2542
GLUSHCHENKO, V. M., Effect of nuclear radiation on the physicomechanical properties of lacquer coatings, 25:2822
GMITRO, M., Brueckner reaction matrix and separable potentials, 25:3548
GOETZMANN, O., Compatibility tests with UC of differing stoichiometries and Fe--Ni--Cr alloys and the influence of stabilizers, 25:2765 (KFK-1213)
GOKHBERG, M. B., Pulsating auroras at conjugate points,

25:2999
GOL'DBERG, V. Z., Excited states (4p--3h) in reaction $^{13}C(^{6}Li,d)^{17}O$ and $^{13}C(^{7}Li,t)^{17}O$, 25:3570
GOLDEN, J. M., Bethe--Salpeter equation. Ward--Takahashi identity and the ladder approximation, 25:3436
GOLDEN, K. I., Nonlinear conductivity--ternary correlation relations in nonrelativistic plasmas, 25:3090
GOLDHABER, G., Reaction $\pi^{+}p \rightarrow \Delta^{++}A_2^{0}$ at 3.7 GeV/c, 25:3272 (UCRL-20050)
GOLDRING, G., Alpha-particle scattering from ^{204} ^{206} ^{208}Pb and ^{209}Bi, 25:3689
GOL'DSHTEIN, V. A., Quasi-elastic scattering of 1115-MeV electrons by nucleons of ^{32}S nuclei, 25:3615
GOLDSMITH, George J., Radiation damage studies with low-energy hydrogen isotopes, 25:3187 (CONF-700322-, pp 63-77)
GOLDSTEIN, Stephen, EL 600: fuel management studies, 25:3866 (CEA-N-1379)
GOLEMO, A., Ambiguities in the experimental determination of resonance production amplitudes, 25:3382 (TPJU-1/70)
Regge pole model with Veneziano residues for reactions $0^{-}\frac{1}{2}^{+} \rightarrow 0^{-}\frac{3}{2}^{+}$, 25:3384 (TPJU-3/70)
GOLESTANEH, A. A., Evaluation of $\pi\pi$ scattering lengths using on-mass-shell pions, 25:3371
GOLOVANOV, Yu. N., Stress relaxation in deformed U, 25:2699
GOLUBYATNIKOV, A. N., Model of the neutrino in the general theory of relativity with velocity groups G_3 on V_2, 25:3343
GONO, Yasuyuki, Deexcitation of 931.1-keV 2_2^{+} state of ^{152}Gd, 25:3681
GOODMAN, A. L., Generalized pairing in light nuclei. II, 25:3722
GOODWIN, G. L., E/sub s/ layer characteristics determined from spaced ionosondes, 25:2957
GOPAL, K., Production of external bremsstrahlung in different materials, 25:3249
GOPAL, S., Production of external bremsstrahlung in different materials, 25:3249
GOPALA RAO, G., Colorimetric determination of traces of Se, Te, Mn, and Ce, 25:2073
GOPINATHAN, Chakrapani, Hydrogen abstraction by primary species in the radiolysis of frozen aqueous system, 25:2293
GORBACHEV, I. I., Measurement of total electron content in the polar ionosphere from the recorded signals of the 3d satellite, 25:2983
GORBATSKII, V. G., Radiation from a gas heated by a shock wave and its role in the emission of stellar envelopes of close binary systems, 25:2830
GORBUKOV, V. I., Statistical analysis of the information transfer process in radiometric betatron defectoscopy, 25:2412
GORDEEV, A. V., Stability of a plasma contained by a strongly non-uniform magnetic field, 25:3122
GORDON, G. E., Decay of Zn and Zn to levels of ^{71}Ga, 25:3638
GORDON, I., Measurement of sub vpm levels of water and hydrogen under plant conditions, 25:3882 (DP-Report-487)
GORMAN, Michael, Radiation damage studies with low-energy hydrogen isotopes, 25:3187 (CONF-700322-, pp 63-77)
GOSHAW, A. T., Associated production in K+p interactions at 3.5 GeV/c, 25:3277
Deuteron--deuteron scattering at 2.2 and 7.9 GeV/c, 25:3415
GOSWAMI, A., Generalized pairing in light nuclei. II, 25:3722
GOTO, Takeshi, Spectrochemical analysis of Ti and its alloy. IV, 25:2097
GOTOVTSEV, A. V., Breakaway parameter of the turbulent magnetohydrodynamic boundary layer, 25:2947
GOTTIKH, R. P., Isotopic composition of uranium in ground waters, 25:2356
GOTTSCHALK, Alexander, Technetium-99m in clinical nuclear medicine, 25:2580
GOTTSCHALK, B., Quasi-elastic scattering of 160-MeV protons by alpha clusters in light nuclei. I. Carbon, 25:3581
GOUGH, W. C., Selected bibliography for fusion reactor design studies, 25:3139 (ORO-1171-1, pp 425-39)
GOUGH, William C., Why fusion, 25:3134 (ORO-1171-1, pp 256-331)
GOULDING, F. S., Performance of a pulsed-light feedback preamplifier, 25:2462
GOW, H. B. F., Helium utilization on Dragon during approach to power and first charge irradiation, 25:3861 (DP-Report-552)
GOZA, E. R., Energy estimation of 20-GeV/c pion interactions in photographic emulsion, 25:3284
GRABOWSKI, Z. W., Directional correlation and intensity studies of electromagnetic transitions in ^{181}Ta, 25:3647 (COO-1746-46)
GRAEDEL, T. E., Penetration of solar particles to ionospheric heights at low latitudes, 25:2965
GRAHAM, I. G., Angular correlation studies of the low-lying levels of ^{57}Co, 25:3622
GRAHMANN, H., Determination of traces of hafnium in aluminum--uranium alloys, 25:2063 (CNEA-276)
GRANDJEAN, Daniel, Preparation and crystalline structure of UBa sulfide: $BaUS_3$, 25:2204
GRANT III, Walter Henry, Investigation of the 5.96-MeV doublet in ^{10}Be, 25:3588
GRASSO, M., Phase equilibria relations in the ternary system BaO--SrO--Nb_2O_5, 25:2808
GRATTON, F., Heuristic approach to Landau damping, 25:3166
GRATTON, J., Heuristic approach to Landau damping, 25:3166
GRAUBY, A., Contamination of anodonta cygnea by ^{137}Cs, 25:2525
Liberation of radionuclides from forest bed, 25:2528
Radiocontamination of irrigation canals fed by Rhone, 25:2543
GRAVIER, R., Drift waves in a collisionless plasma, 25:3147 (CEA-CONF-1612)
GRAY, Lawrence J., Mass absorption coefficients of refractory metal carbides, 25:2095
GRAY, P. S., Helium utilization on Dragon during approach to power and first charge irradiation, 25:3861 (DP-Report-552)
Impurity removal from Dragon reactor during initial commissioning, 25:3862 (DP-Report-553)
Measurement of sub vpm levels of water and hydrogen under plant conditions, 25:3882 (DP-Report-487)
Removal and replacement of primary heat exchanger tube bundle and circulator on Dragon Reactor, 25:3863 (DP-Report-554)
GRECHIKHIN, L. I., Effect of nonhomogeneous interatomic electrical fields on a radiating atom in a low-temperature plasma, 25:3108
GREEN, B. J., Effect of inertia on losses from a plasma in toroidal equilibrium, 25:3060
GREEN, G. L., Relation between mass spectra and reaction products of electron-irradiated aromatic ketones, 25:2266
GREEN, I. S., Thermal performance of the Dragon reactor, 25:3885 (DP-Report-546)
GREEN, Michael A., Refrigeration of superconducting magnets, 25:3508
GREEN, W. K., 10-decade wide range neutron monitoring system. Final test report, 25:2502 (GEAP-11094)
GREENBERG, J. S., Photoproduction of Y* resonances above 1800 MeV, 25:3251
GREENDALE, A. E., Fission yields of iodine isotopes and ^{135}Te, 25:3663
GREENHUT, Gary K., Phases and forward cross sections in vector-meson photoproduction, 25:3319
GREENLEES, G. W., Elastic scattering of polarized protons from ^{58}Ni, ^{120}Sn, and ^{208}Pb, 25:3636
GREENSTOCK, C. L., Radiation chemistry of orotic acid as studied by pulse radiolysis, 25:2275
GREENSTREET, W. L., Addendum: experimental and analytical investigations of the structural behavior of nozzle-to-shell attachments, 25:2386 (ORNL-TM-2526(Add.))
GREENWOOD, M. R., Selective determination of inorganic mercury in the presence of organomercurial compounds in biological material, 25:2109
GREGORY, B. L., Application of neutron damage models to semiconductor device studies, 25:2514 (SC-R-70-4351)
GREGORY, P. C., Impedance measurements of a loop antenna in the topside ionosphere, 25:2967
GREISEN, K., Space--time detector for cosmic ray showers, 25:2490
GREITZ, U., Whole-body measurements on distribution of ^{203}Hg in humans, 25:2533
GRIDNEV, G. F., Neutron-rich isotopes of light elements produced in transfer reactions with heavy ions, 25:3648 (JINR-E7-5319)
GRIFFIN, Allan, Excitations in Bose gas at finite temperatures. I, 25:3044
GRIFFITHS, R. J., Angular distributions of $^{4}He(p,d)^{3}He$, $^{4}He(p,t)2p$, $^{4}He(p,^{3}He)pn$, and $^{3}He(p,d)2p$, 25:3555
System p-^{3}He at 30 and 50 MeV, 25:3556
GRODZINS, L., Hyperfine interactions on ^{237}Np and ^{239}Np implanted into copper and nickel, 25:3690
GROENEVELD, D. C., Heat transfer measurements on trefoil fuel bundles in the post-dryout regime-with data tabulation, 25:3865 (AECL-3414)
GROENEVELD, K. O., Reaction $^{28}Si(^{3}He,p)^{30}P$, 25:3602
GROFF, Alain, Elastic constants of U and plutonium carbonitrides, 25:2798
GROSS, David J., Basic operators of the dual-resonance model, 25:3353
GROSSE, Gottfried, Experiences with cryopumps in calibration devices, 25:2429
GROTOWSKI, K., Real part of the alpha--nucleus potential, 25:3755
GRUENBEIN, W., Pulse radiolytic investigation of short-lived hydrates of aromatic nitroso compounds, 25:2272
GRUSS, Leonard, Spectroscopic properties of solid solutions of erbium and ytterbium oxides, 25:3211
GRZYBOWSKA, D., Cesium transport in fish-breeding pond, 25:2516
GUAZZONI, Guido E., Spectral emittance of Nd, Sm, Er, and Yb oxides at high temperatures, 25:3204 (AD-708547)
GUERSU, Yurtcan, Nordheim equation according to P_1-approximation, 25:3924 (CNAEM-73)
GUGEL, E., Investigations on cermets of ThO_2--Ni and ZrC_2--Mo, 25:2796
GUIDO, O. O., Determination of traces of hafnium in aluminum--uranium alloys, 25:2063 (CNEA-276)
GUILLAUME, M., Degassing at low temperature of titanium targets impregnated with hydrogen isotopes, 25:3542

GUILLAUMIN, J., Continuous and discontinuous precipitation reactions in U--1.5 percent Mo alloys, 25:2738
GUILLEMOT, M., Amplitude and damping of plasma wave echoes, 25:3144 (CEA-CONF-1601)
GUINET, Philippe, Nuclear fuel having a UC base, 25:2776
GUL'EL'MI, A. V., Spectrum of Alfven oscillations of the magnetosphere, 25:2970
GUNSON, J. Russell, Sum rules and symmetries, 25:3387
GUPTA, S. P., Irregularities in night-time equatorial E region, 25:2963
GUTMAN, E., Measurements of π^-p elastic scattering from 1.71 to 5.53 GeV/c, 25:3280
GUYON, J., Use of a Van de Graaff generator to simulate the transient effects due to radiation in semiconductors, 25:3477 (LYCEN-7063)
GWALTNEY, R. C., Addendum: experimental and analytical investigations of the structural behavior of nozzle-to-shell attachments, 25:2386 (ORNL-TM-2526(Add.))
GWYN, C. W., Application of neutron damage models to semiconductor device studies, 25:2514 (SC-R-70-4351)

H

HAAS, F., Lifetimes in ^{12}B, ^{14}N, and ^{16}O, 25:3569
HABERER, K., Rapid methods for estimation of content of radioactive cations in water, 25:2117
HADARI, Z., Charge states of Np recoil atoms, 25:2305
HADINGER, G., Distribution of ion densities in an arc discharge, 25:3085 (LYCEN-7061)
Distribution of ion densities in an arc discharge, 25:3085 (LYCEN-7061)
Elastic scattering $^{12}C(d,d)^{12}C$, $^{28}Si(d,d)^{28}Si$, and $^{40}Ca(d,d)^{40}Ca$, 25:3585
Production of multicharged ions in a reflex source with axial extraction, 25:3111 (LYCEN-7065)
HAEGGLUND, S. E., Excited nuclear states in ^{125}Te, 25:3699
HAEMERS, J., Purification and single-crystal growth of V_2O_3, 25:2783
HAFTEL, Michael I., Mesons in nuclear saturation, 25:3763
HAGAN, P. G., Radiolysis of HNO_3 solutions: LET effects, 25:2284
HAGEDORN, R., Remarks on the thermodynamical model of strong interactions, 25:3355
HAGEMANN, K. A., Low-lying high-spin states in ^{155}Gd, 25:3700
HAGLER, M. O., Conference on thermonuclear fusion reactor design, 6/70, Lubbock, Tex, 25:3130 (ORO-1171-1)
HAHN, H., Design of dielectric-loaded rectangular deflectors, 25:3502
HAHN, Paul B., Ion exchange beads as calibrated microscopic radioactivity sources, 25:2406
HAHN, Yukap, Impact-parameter amplitudes for large-angle potential scattering. II, 25:3761
HAJEK, B., Investigation of hydrolyzable carbides. III, 25:2782
HALL, B. H., Reaction $\pi^+p \rightarrow \Delta^{++}A_2^0$ at 3.7 GeV/c, 25:3272 (UCRL-20050)
HALLOCK, Robert Bruce, Studies of ^4He by x-ray scattering, 25:3018
HALPERN, I., Proton induced fission of ^{233}U and ^{238}U, 25:3660
HAMBLING, P. G., Stabilization of Pu β phase in Pu--Ti alloys, 25:2739
HAMILL, W. H., Evidence for very early ionic effects in water radiolysis, 25:2274
HAMILL, William H., Evidence for very early effects in the radiolysis of water, 25:2267
HAMILTON, J. D., Helium utilization on Dragon during approach to power and first charge irradiation, 25:3861 (DP-Report-552)
HAMMOND, Joseph P., Corrosion of advanced steam generator alloy weldments in steam, 25:2636
HANKIEWICZ, Ewa, Achievements of the pure and applied radiation chemistry in Poland, 25:2217
HANLEY, Peter Ronald, Thermally stimulated conductivity of irradiated alkali halides, 25:3202
HANSEN, P. G., Unique first-forbidden beta transitions in deformed nuclei, 25:3672
HANSON, A. O., Design of a 600-MeV microtron using a superconducting linac, 25:3506
HARBISON, S. A., Angular distributions of $^4He(p,d)^3He$, $^4He(p,t)2p$, $^4He(p,^3He)pn$, and $^3He(p,d)2p$, 25:3555
System $p-^3He$ at 30 and 50 MeV, 25:3556
HARDER, Carroll Ross, Crossed-field experiment to study plasma formation processes, 25:3115
HARDIE, R. W., User's manual for the 1DX--2DB--3DB--PERT-V code package, 25:3923 (BNWL-1412)
HARLEY, John H., Manual of standard procedures, third issuance, 1970, 25:2059 (NYO-4700(3rd Ed.))
HARMS, A. A., Minimal-error few-group critical mass determination, 25:3930
HARMS, Archie Arkadius, Variable phase-space neutron transport analysis, 25:3532
HARMS, Klaus-Dieter, Calculation of anisotropy of H/sub c2/ in cubic single crystals, 25:3047
HARNEY, H. L., Number of degrees of freedom in fluctuation analysis, 25:3717
HARRIS, F. R., Intensities of O_2^+ 1NG and N_2 1PG band systems in normal and type-B aurorae, 25:3002
Nuclear wet-steam turbines, 25:3859
HARRIS, J. A., Treatment of Rum Jungle U ore, 25:2336
HARRISON, A. W., Altitude profile of airglow hydroxyl emission, 25:3001
HARRISON, J. L., Compatibility of Cu with Ta--10 wt. percent W alloy at elevated temperatures, 25:2720
HARRISON, Robert W., Corrosion of oxygen contaminated tantalum in NaK, 25:2623
Effects of welding atmosphere purity on the lithium corrosion resistance of refractory alloys, 25:2625
HARUYAMA, Masahiro, Pion electromagnetic form factor with dipion unitarity, 25:3330
HARWIT, M. O., Upper limits to electromagnetic energy radiated by normal galaxies, 25:2868
HASEGAWA, Akira, Group structure and accuracy of group constants in vicinity of 2.85-keV resonance scattering of Na, 25:3928 (JAERI-Memo-4110)
HASEGAWA, Ryusuke, Simple model for amorphous antiferromagnets, 25:3936 (CALT-822-16)
HATTA, Yoshisuke, Electrostatic low-frequency oscillations in an inhomogeneous magnetoplasma, 25:3163
HAUBERT, P., Fuel-cycle theory for on-load refuelled thermal converter reactors. I and II, 25:3887 (DP-Report-575)
HAUG, H., Equations of motion for complex order parameter of helium II, 25:3014
HAUGHTON, Geoffrey, Transplantation antigens and viral carcinogenesis, 25:2537
HAWTHORNE, J. Russell, Improved radiation embrittlement resistance of steel, 25:2757 (NRL-7121)
HAYAKAWA, Mizuaki, Gauge, renormalization, and the Goto--Imamura--Schwinger term in quantum electrodynamics, 25:3444
HAYTER, C. J., Measurement of plasma digoxin concentration by radioimmunoassay, 25:2522
HAYWARD, Evans, Photonuclear reactions, 25:3715 (NBS-MCN-118)
HAYWOOD, Fred F., Radiation safety in the operation of a low-energy accelerator, 25:3475 (CONF-700322-, pp 441-8)
HAZAMA, Michio, Correspondence between ECC γ-ray and spark chamber shower, 25:2487
HEAP, C. R., Fission product distribution in Dragon after first 20 MW run, 25:3886 (DP-Report-571)
HECHT, K. T., 27-plet unitary symmetry operator, 25:3426
HEEB, C. M., Analysis of the Phoenix fuel experiments, 25:3902 (BNWL-1514)
HEERSCHAP, M., Deformation properties of vanadium single crystals, 25:2718
HEHEMANN, R. F., Athermal omega transformation in Zr--Nb alloys, 25:2735
HEIM, J. R., Superconducting two tesla bending magnet, 25:3504
HEIN, D., Hydrodynamic stimulation of vibrations and their stabilization in the core of the Grenoble high flux reactor, 25:3909
Thermohydraulic displays of reflector space in the Grenoble high flux reactor, 25:3910
HEISENBERG, J., Elastic electron--nickel scattering, 25:3687
HELLBORG, R., Studies of carbon content of steel by proton activation analysis, 25:2147
HELMS, T. E., Levels in ^{11}B by the $^{10}B(d,p)^{11}B$ reaction, 25:3561 (CONF-700322-, pp 133-40)
HENDERSON, David Courtland, Preparation and some high temperature properties of rare earth trifluorides, 25:3957 (IS-T-384)
HENDERSON, W. R., Measurement of atomic oxygen height profiles in upper atmosphere, 25:2968
HENGLEIN, A., Pulse radiolytic investigation of short-lived hydrates of aromatic nitroso compounds, 25:2272
HENICKSMAN, A. L., Determination of Ti, Zr, Hf, Nb, Ta, Mo, and W in uranium alloys, 25:2065 (LA-4529)
HENISCH, H. K., Chemically stimulated luminescence in rare earth oxides, 25:3213
HENMI, Zenzo, Recrystallization process in Nb--Ag permalloy, 25:2679
HENNEBERGER, Walter C., Quantization of interacting fields, 25:3440
HENRIKSEN, L., Combination of an electron microscope and a heavy-ion accelerator, 25:2507
HENRY, R. J. W., Calculation of electron scattering and photoionization cross sections, 25:2903
HENSEL, John C., Proceedings of the Tenth International Conference on the Physics of Semiconductors, Cambridge, Mass., 8/17--21/70, 25:3185 (CONF-700801)
HENYEY, F. S., Structure of high-energy two-body non-diffractive reactions, 25:3454
HEPP, H., Investigations of decontamination ability of paints, 25:2423
HERAK, J. N., Radiation-induced conformation changes of pyrimidine ring in dihydrothymine, 25:2282
HERING, W. R., Inhibited (^3He,d) transitions to Js/sub $^1/_2$/ isobaric analog states, 25:3666
HERLINGER, Albert W., Laser Raman and infared spectra of amino acids and their metal complexes. III. Proline and bisprolinato complexes, 25:2190
HERMENT, Jacques, Separation of technetium from fission products, 25:2307 (CEA-N-1316)
HERMOCH, V., Schlieren method and its application for plasma diagnostics, 25:3067
HEROY, D., Inelastic electron--atom interactions in the 50 to 150 keV energy range, 25:3472 (CONF-700322-, pp

379-92)
HERRING, D. F., Neutron sources for radiotherapy, 25:3473 (CONF-700322-, pp 407-29)
HERRMANN, Walter, Basic response phenomenology analytical techniques, 25:3974 (SC-R-68-1784)
HERSCHMAN, H., Subcellular fractionation of cultured glial cells, 25:3983 (UCLA-12-793)
HERSCHMAN, Harvey R., Distribution of polysomes in mouse brain tissue, 25:3986 (UCLA-12-796)
HERTEL, P., Transition temperature of superconductors, 25:3023
HERZ, A. J., Measurement of beam profile for high-intensity particles, 25:2434 (CERN-70-27)
HEUCK, F., Densitometric and scintigraphic investigations of brain tissue during reduced blood flow, 25:2577
HEUSCH, B., Lifetimes in ^{12}B, ^{14}N, and ^{16}O, 25:3569
HEUSCH, C. A., Recoil proton polarization in eta photoproduction, 25:3255
HEVEZI, J. M., Fast neutron radiobiology and radiotherapy, 25:2582 (CONF-700322-, pp 393-406)
HIBBERT, A., Calculating angular momentum integrals in atomic structure, 25:2923
HIBLER III, William David, Electrical conductivity in pure type-II superconductors near H/sub c2/, 25:3043
HIBOU, F., γ transitions in ^{16}O, 25:3584
HICKEL, Bernard, Radiolysis of concentrated nitrate and formate solutions, 25:2257 (CEA-R-4046)
HICKS, W. W., High-frequency Stark effect in plasma diagnostics, 25:3062
HIDDLESTON, H. R., Isobaric analog resonances in N approximately equals 82 nuclei, 25:3685
HIEBERT, R. D., Direct digital readout and computer calculation of amino acid analysis data, 25:3965 (LA-4507)
HIGASHIONNA, R., Lumped-parameter analysis for shear failure in the end slab of cylindrical PCRV, 25:2411 (TID-25573)
HIIDA, Kichiro, Chiral symmetry in the unified fermion theory. II, 25:3428
HILL, John C., Decay of ^{55}Cr, 25:3607
HILLE, Peter, Reaction cross sections of medium weight nuclei for 14.5-MeV neutrons, 25:3643
HILPERT, H. G., Photoproduction of rho^0 mesons on deuterons between 1 and 5 GeV, 25:3246
HILSCHER, D., Reactions (d,n) on ^{11}B, ^{14}N, and ^{15}N, 25:3574
HILTON, D. A., Determination of Gd in irradiated gadolinia/magnesia mixtures, 25:2089
HILTZ, R. H., Corrosion of stainless steel in oxygen-contaminated sodium at 1200 F and 1400 F, 25:2620
HIMES, F. L., Movement of ^{90}Sr in soils, 25:2365
HINES, R. L., Prog. rpt. on radiation effects of ion bombardment, final, 6/15/68--8/31/70, 25:3190 (COO-1053-15)
Relationship between ion impacts and clusters in gold crystal foils. Final progress report, June 15, 1969--August 31, 1970, 25:3189 (COO-1053-14)
HINK, W., Apparatus for delivery of gas for flowthrough proportional counter, 25:2453
HIRAKI, Akio, Understanding of defects induced in n-type Ge by electron bombardment, 25:3200
HIRANO, Masanobu, Decay widths of resonances and composite model, 25:3405
HIRKO, R. G., Reactions $^{21}Ne(p,d)^{20}Ne$ and $^{21}Ne(d,p)^{22}Ne$, 25:3633
HIROSE, A., Turbulent heat in mirror machines at ORNL, 25:3056 (ORO-1171-1, pp 78-97)
HIROSE, Kazutoyo, Radiation curing of coating, 25:2243
HIRSCHBIEGEL, H., Isotope diagnosis of processes involving the posterior cerebral fossa, 25:2578
HISATAKE, K., Level structure of ^{105}Pd, 25:3670
HITLIN, D., Muonic atoms. I, 25:3661
HJORTH, S. A., Low-lying high-spin states in ^{155}Gd, 25:3700
HNIZDO, V., Elastic scattering of polarized protons from ^{58}Ni, ^{120}Sn, and ^{208}Pb, 25:3636
HOCKENBURY, Robert W., Precision of tank capture cross section measurements, 25:2435 (RPI-328-202)
HOCLET, Odette, Hybrid simulation of the dynamics of a battery of mixer--settlers, 25:2384 (CEA-CONF-1579)
HODGE, R. I., 5000-hr test of a eutectic lead--bismuth circuit constructed in steel and niobium, 25:2627
HODGINS, J. W., Temperature effects in the gamma-initiated polymerization of styrene, 25:2245
HODISAN, T., Complexometric determination of U with EDTA, 25:2088
HOFFMAN, B. W., Analysis of oceanographic samples by 14-MeV neutron activation, 25:2119 (CONF-700322-, pp 221-30)
HOFFMAN, James M., Emission cross sections for H^+, Na^+, Ne^+, Rb^+, incident on molecular nitrogen, 25:2902 (SC-RR-70-695)
HOFFMANN, D., Stored energy measurements in electron-irradiated Pt, 25:3197
HOHL, Frank, Simulation of the evolution of stellar systems, 25:2864
HOLL, P. M., Operation of a 12-inch fast gate valve with a pressure cartridge, 25:3998 (UCRL-50930)
HOLLAR, E. L., Composite film metallizing for ceramics, 25:2652
HOLLIDAY, R. J., Nuclear orientation studies of local moments in noble metal hosts, 25:3942 (COO-1569-67)
HOLLIS, J. C., Weapons Effects Display System: Maintenance Manual. Pt. 5, 25:2505 (UCRL-50892(Vol.4)(Pt.5))
HOLMES, H. F., Infrared studies of thorium oxide surfaces: hydroxyl spectra, 25:2207
HOLMES, J. M., Consideration of nuclear power expansion for Puerto Rico, including surplus capacity penalties, 25:3798 (ORNL-TM-3142)
HOLMES, R. L., Boilers for nuclear plant, 25:3900
HOLMGREN, Paul Robert, High-resolution autoradiography with ^{33}P, 25:2521
HOLT, S. S., Pulsar distributions without magnetic decay, 25:2851
HONECKER, R., Application of the Veneziano model with pion and Pomeron exchange to the reaction $K^- p \to nc$, 25:3386
HONERKAMP, J., Electromagnetic meson decays, 25:3316
HOOGLAND, W., $I = 3/2$ Kπ elastic-scattering cross section from the reaction $K^-n \to pK^-\pi^-$ at 3 GeV/c, 25:3278
HOOPER, H. O., Nuclear magnetic resonance study of the crystalline compounds of the NbBe/sub x/ system, 25:3220 (COO-1700-12)
HOPENFELD, J., Corrosion of Type 316 stainless steel with surface heat flux in 1200^{0}F flowing sodium, 25:2618
HOPPER, M. J., Effects of LET and temperature in radiolysis of cyclohexane. II, 25:2280
HORAK, Z., Classical and relativistic forces of inertia, 25:2871
HORAN, P. K., Role of hydrogen atoms in free radical site migration, 25:2246
HORN, D., Distributions of charged pions, 25:3370
HORNAK, R. J., Effects of exposure to flowing sodium on vanadium alloys in stainless steel containment systems, 25:2621
HORNE, D. S., Elastic scattering of alkali atoms from iodine atoms and molecules at thermal energies, 25:2922
HOROWITZ, P., Time-of-arrival measurements of optical pulses from Crab pulsar, 25:2853
HORVITZ, E. Philip, Spin--lattice relaxation of liquid ^3He and ^3He--^4He mixtures, 25:3051
HORWITZ, L. P., Analysis of the Serpukhov total cross section data with the algebra of vertex strengths, 25:3385
HOSANGDI, R. R., Half-lives of excited levels in ^{125}Te and ^{132}I, 25:3706
HOSODA, Masataka, Existence of μ^* and duality in weak processes, 25:3350
HOUCK, J. R., Upper limits to electromagnetic energy radiated by normal galaxies, 25:2868
HOUGHTON, Arthur V., SMCPAS: Sandia matrix-oriented production assembly system, 25:3976 (SC-RR-70-645)
HOURANY, Eid, Distortion in reactions $^{12}C(p,2p)^{11}B$/sub 1P/ and $^{40}Ca(p,2p)^{39}K$/sub 2S/, 25:3565 (NP-18476)
HOUSTON, J. T., Effect of gas bubbles on recrystallization of tungsten, 25:2736
HOWARD, A. J., Reactions $^{21}Ne(p,d)^{20}Ne$ and $^{21}Ne(d,p)^{22}Ne$, 25:3633
HRADIL, J., Kinetic model of stem-cells and proerythroblasts populations in the postirradiation bone marrow injury, 25:2590
HRASTNIK, B., Directional correlation studies in decay of /sup 177g/Lu, 25:3684
HRUSKA, A., Dependence of geomagnetic activity on the polarity of the interplanetary magnetic field, 25:2860
HRUSKOVA, J., Dependence of geomagnetic activity on the polarity of the interplanetary magnetic field, 25:2860
HSIEH, S. T., Shell-model structure of the p-shell hypernuclei, 25:3721
HSU, Chu Chung, Relation between the 2I + 1 rule and channel correlation, 25:3762
HUANG, Yao Hui, Self-consistent theory of the magnetotail, 25:2960
HUBBARD, Ward N., Enthalpy of formation of ThF_4 by fluorine bomb calorimetry, 25:2213
HUBERT, B., Reaction $^{28}Si(^3He,p)^{30}P$, 25:3602
HUEBSCHMANN, W., Inherent stability of steam-cooled breeder reactors, 25:3856 (KFK-851)
HUEGEL, Helmut, Flow of compressible plasmas in inherent fields of arc discharges, 25:3103
HUGHES, D., Designation of persons working with unsealed radioactive substances, 25:2573
HUGHES, V. W., Photoproduction of Y* resonances above 1800 MeV, 25:3251
HUIZENGA, J. R., Energy levels of ^{243}Am, 25:3669
HULL, J. R., Interpretation of small-angle π^-p elastic scattering from 1.71 to 3.01 GeV/c, 25:3281
HUMMEL, A., Slow electrons and negative ions in organic liquids, 25:2260 (IRI-133-70-2)
HUMPERT, B., Nonstrong amplitudes in a Veneziano-type model, 25:3342
HUMPHREY, D. L., Levels in ^{11}B by the $^{10}B(d,p)^{11}B$ reaction, 25:3561 (CONF-700322-, pp 133-40)
HUMPHREY, R. M., Time-specific effect of uv-irradiation on cells progressing from G_2 into metaphase, 25:2558
HUMSKI, Kresimir, Thermodynamic and kinetic secondary isotope effects in the Cope rearrangement, 25:2188
HUNT, C., Operational data for charge I, 25:3795 (DP-Report-561)
HUNT, Carolyn R., ISOP: a three-dimensional isometric plotting subroutine, 25:3987 (UCRL-14248(Rev.1))
HUNTER, J. B., Search for superheavy elements in nature by detection of events with large numbers of neutrons,

25:3652 (UCRL-19957)
HUTTON, J. L., Proton stripping to particle-hole states in ^{40}Ca and ^{42}Ca, 25:3627
HUWE, D. O., Antiproton--neutron elastic scattering at 3.5 GeV/c, 25:3267
HUYSER, Earl S., Primary isotope effects in hydrogen atom transfer reactions from α-hydroxyalkyl and monohydropyridyl radicals, 25:2180
HVIDT, Aase, Effect of hydrogen--deuterium substitution on the association of N-methylacetamide, 25:2174

I

IANOVICI, Eugenia, Chemical state of radiorhenium formed in some inorganic Ir compounds irradiated with 660-MeV protons, 25:2300
ICHIKAWA, Riei, Supercooling in the solidification of Al--Cr, Al--Mn, and Al--Zr binary alloys, 25:2733
IDA, Masakuni, Factorization and duality of multiloop diagrams, 25:3443
IDDINGS, C. K., One-boson-exchange potential model for the AN interaction, 25:3416
IDEDA, Tetsuyuki, Supercooling in the solidification of Al--Cr, Al--Mn, and Al--Zr binary alloys, 25:2733
IGNATYUK, A. V., Spin dependence of density of excited nuclear states, 25:3765
IINUMA, Takamasa, Extremely long period fuel cycle. II, 25:3881
IKEGAMI, H., Nonlinear effect of large-amplitude ion acoustic waves, 25:3151 (IPPJ-94)
ILAKOVAC, K., Directional correlation studies in decay of /sup 177g/Lu, 25:3684
IL'CHENKO, A. M., Investigation of dense plasma formation using electron beam injection into magnetic trap, 25:3113
IL'INA, V. A., State of carbon in martensite as influenced by electron bombardment, 25:2764
IMAHASHI, Masayuki, Titanium and Zr in hydrothermally altered rocks, 25:2098
INGEBRETSEN, F., Rotational structure in ^{43}Sc, 25:3626
INGHAM, D., Proton hole states in 1f/sub 7/2/ nuclei, 25:3616
IOANNOU, Tom Kyriacou, Prediction of equilibrium data for solvent extraction system $SmCl_3$--$NdCl_3$--$CeCl_3$--HCl--H_2O with extractant D2EHPA-Amsco, 25:2311 (IS-T-412)
IONOV, N. I., Interaction of water vapor with the surface of tungsten, 25:2722
IRISH, D. E., Equilibria and proton transfer in the bisulfate--sulfate system, 25:2173
ISAACS, H. S., Corrosion and mass transfer of pure iron, nickel, chromium, and cobalt in 660° to 760°C sodium, 25:2631
Determination of oxygen concentration and mass transfer coefficients in sodium using uranium, 25:2694
Measurements of the solubility of iron and chromium in sodium, 25:2712
Segregation of impurities and the formation of particles in sodium systems, 25:2713
ISAMUKHAMEDOVA, D. K., Effect of γ radiation on the volt--ampere characteristics of diodes, 25:3192
ISHII, Tamotsu, Electrical conductivity and defect structures in non-stoichiometric UO/sub 2 + x/, 25:3210
ISHIKAWA, Hiroaki, Determination of ^{14}N(n,2n)^{13}N reaction cross section for 14.7 MeV neutrons, 25:3576
ISHIMARU, Hajime, Energy-mass analysis for highly ionized steady-state plasma, 25:3063
ISHIZUKA, Yasuhiro, Making of Ge(Li) detector and its application, 25:2437
ISKRA, A. A., Migration and translocation of natural radioactive elements in water, 25:2547
ISMAIL, F. T., Prog. rpt. on exchange of interlayer cations in micaceous minerals, annual, 9/30/69--9/30/70, 25:3943 (COO-1680-10)
ISO, Yasuhiko, Optimum planning for radiation facilities, 25:2390
ISRAEL, W., Transport coefficients of a relativistic quantum gas, 25:2673
ITAHASHI, Takahisa, High excited levels of ^{27}Al, 25:3600
ITO, Akihiro, Decay widths of resonances and composite model, 25:3405
ITOH, N., Effects of radiation damage on channeling of MeV protons in KBr, 25:3201
IVANOV, D., Destruction of foam by α particles, 25:2223
IVANOV, G. A., Charge radii of the nuclei of ^{124} ^{126} ^{128} ^{130}Te, 25:3551
IVANOV, K. G., Interplanetary magnetic field flux and the K/sub p/ index of magnetic activity, 25:2981
Magnetic field of the neutral sheet in the tail of the magnetosphere, 25:2982
IVLEV, B. I., Simulated superconductivity in thin films, 25:3031
IVLIEV, D. Ya., Development of an elementary magnetic disturbance, 25:2978
IWASAKI, T., Tracer technique for behavior of dusts in animal lungs, 25:2523
IWATA, Kenzo, Decay widths of resonances and composite model, 25:3405
IYER, H. Parasurama, Spectrophotometric study of UO_2^{2+}--SCN- system in aqueous and water--methanol media, 25:2215
IZOTOV, G. T., Effect of nuclear radiation on the physicomechanical properties of lacquer coatings, 25:2822
IZUMI, A., Analysis of neutron correlation with shift registers, 25:3931

J

JACH, J., Clustering and giant moments in Cu--Ni alloys, 25:4000 (UCRL-72587(Rev.1))
JACKSON, Daphne F., Two-nucleon density functions and correlation functions, 25:3733
JACKSON, K. P., Electromagnetic transitions in ^{19}Ne, 25:3575
Heavy-ion reactions as a technique for direct mass measurements of unknown Z > N nuclei, 25:3610
JACKSON, Ross J., Homogenization of uranium-base niobium alloys, 25:2732 (RFP-1582)
JACKSON, W. D., Tenth symposium on engineering aspects of magnetohydrodynamics, Cambridge, Massachusetts, March 26--28, 1969, 25:2945
JACOB, Gerhard, Commutators and Lorentz covariance, 25:3298
JACOBS, J. A., Dependence of geomagnetic activity on the polarity of the interplanetary magnetic field, 25:2860
JACOBS, Matthew A., Improved upper bound on the imaginary part of elastic scattering amplitudes, 25:3460
JACOBSON, Melvin J., Statistics of a random plus constant vector with application to acoustic and electromagnetic-wave scattering, 25:3239
JACQUET, G., Production of multicharged ions in a reflex source with axial extraction, 25:3111 (LYCEN-7065)
JAENICKE, L., Regulating factor in methionine biosynthesis, 25:4002 (UCRL-Trans-10487)
JAHNKE, U., Investigation of ^{65}Zn by (p,n) and (p,nγ) experiments, 25:3631
JAIN, B. D., Pyridine-2-aldoxime and 6-methylpyridine-2-aldoxime as gravimetric reagents for estimation of Pd(II) and U(VI), 25:2072
JAKLEVIC, J. M., Performance of a pulsed-light feedback preamplifier, 25:2462
JANECKA, J., Free radicals in γ-irradiated disodium succinate. I, 25:2229
JANGG, G., Investigations on cermets of ThO_2--Ni and ZrO_2--Mo, 25:2796
JANJUA, M. B. I., Corrosive action of selenium towards various materials in the temperature range 300 to 700°C, 25:2629
JANNER, A., Relativistic symmetry groups of uniform electromagnetic fields, 25:3432
JANOS, W. A., Control-theoretic approach to the plasma confinement problem, 25:3057
JANSEN, J. F. W., Energy of gamma rays from ^{7}Be, ^{40}K, and ^{113}Sn, and decay of ^{113}Sn, 25:3694
JANSSON, Sven A., Oxidation-reduction reactions for chromium and 304 stainless steel in liquid sodium, 25:2710
Thermochemistry and solution chemistry in the sodium--oxygen--hydrogen system, 25:2205
JARED, R. C., Prompt de-excitation of fission fragments, 25:3673
Search for superheavy elements in nature by detection of events with large numbers of neutrons, 25:3652 (UCRL-19957)
JARKOVSKY, Jaroslav, Preparation of wood-plastic combinations on the basis of unsaturated polyester resins. II, 25:2254
JASSELETTE, P., Many pi--meson systems, 25:3364
JASTRAM, P. S., Search for double-photon decay in ^{90}Zr, 25:3658
JAUMIER, J. J., Physico-chemical processes of transfer of radioruthenium in continental medium, 25:2364
JEDRYCHOWSKI, Lucjan, Decontamination of milk from radioactive Cs and Sr by means of ion exchangers of Polish manufacture, 25:2329
JEFFERSON, T. C., Relation between mass spectra and reaction products of electron-irradiated aromatic ketones, 25:2266
JELLEY, J. V., Spaced-receiver observations of radio pulses, 25:2849
JENKINS, D. A., Pionic transition in ^{138}Ba, ^{140}Ce, and ^{142}Ce, 25:2896
JENSEN, A. S., Coulomb distortion in heavy-ion reactions, 25:3720
JICINSKY, G., Investigations on cermets of ThO_2--Ni and ZrO_2--Mo, 25:2796
JITSUNO, Kunihisa, Correspondence between ECC γ-ray and spark chamber events, 25:2488
Correspondence between ECC γ-ray and spark chamber shower, 25:2487
JNANANANDA, Swami, Lifetimes of 321- and 113-keV levels of ^{177}Hf, 25:3707
Photoelectric cross sections of 662-keV gamma rays in Ta and Pd, 25:2904
JODOGNE, J.-C., Cross sections for formation of compound nuclei in heavy-ion reactions, 25:3611
JOHANSON, A. E., Effect of magnetically conjugate photoelectrons on O I, 25:2959
JOHNSON, D. J., Study of ^{6}Li + ^{12}C reactions, 25:3578
JOHNSON, F. A., Source-dependent contributions to

photomultiplier noise, 25:2461
JOHNSON, G. D., Corrosion studies of liquid metal heat pipe systems at 1000° to 1800°C, 25:2628
JOHNSON, R. D., Minimal-error few-group critical mass determination, 25:3930
JOHNSON, R. T., Application of compressional cooling to study of nuclear ordering in solid ^{3}He, 25:4005 (UCSD-34-P-143-23)
JOHNSON, Robert C., Consistency of a model for pion--pion scattering, 25:3457
Derivation of the KSRF relation, 25:3363
S-, P-, and D-wave low-energy pion--pion scattering, 25:3369
JOHNSON, W. S., Unique 150-keV ion accelerator, 25:3469 (CONF-700322--, pp 173-84)
JOHNSSON, K. O., Title-author-company index to reports published by the U. S. Department of the Interior, Office of Saline Water, 25:3913 (ORNL-NDIC-8)
JOHNSTON, A. R., Angular distributions of ^{4}He(p,d)^{3}He, ^{4}He(p,t)2p, ^{4}He(p,^{3}He)pn, and ^{3}He(p,d)2p, 25:3555
System p-^{3}He at 30 and 50 MeV, 25:3556
JOHNSTONE, James Keith, Erbia--hafnia system, 25:2804 (IS-T-401)
JOLLY, R. K., Semiconductor position sensitive detectors in magnetic spectrographs, 25:2463
JONES, H. D., Two-quasiparticle states in ^{166}Ho, 25:3711
JONGSMA, H. W., Decay of ^{62}Co isomers, 25:3644
JONKE, A. A., Fuel cycle technology quarterly report, April, May, June 1970, 25:2306 (ANL-7735)
JORDAN, Thomas M., Advanced Monte Carlo concepts in radiation shielding calculations, 25:3177
JOSEPH, Anthony, Improved upper bound on the imaginary part of elastic scattering amplitudes, 25:3460
JOSEPH, C., D(p,d*)p cross section, 25:3553
JOSOVIC, M., Transition multipolarities in decay of /sup 197m/Hg, 25:3682
JOYCE, M. D., Operational data for charge I, 25:3795 (DP-Report-561)
JUCYS, A. A., Isoscalar factors of Clebsch--Gordan coefficients of unitary groups, 25:3305
JUILLERAT, T., CORONA: program for two-group control rod calculations in reflected reactor, 25:3926 (EIR-166)
JUN, Jae Shik, Counting efficiency for environmental samples, 25:2448

K

KADMENSKII, S. G., Alpha decay and nuclear interactions, 25:3725
Optical potentials and elastic scattering of t and ^{3}He, 25:3769
KADOI, Hajime, Electrical conductivity of γ-irradiated solid monomers at low temperature, 25:2221
KADUKHIN, G. F., Finding N(h) profile by computer techniques, 25:2974
KAGANOV, M. I., Transformation of first (second) sound into fourth sound in superfluid He, 25:3007
KAHL, Allan A., Primary isotope effects in hydrogen atom transfer reactions from α-hydroxyalkyl and monohydropyridyl radicals, 25:2180
KAI, Takaaki, Simulator for BWR type Tsuruga nuclear power station, 25:3933
KAIEDA, K., Thermal conductivity of VIPAC UO_2 fuel. II, 25:2813 (JAERI-Memo-4128)
KAISER, Walther, Level scheme of ^{152}Eu with conversion electrons from neutron capture, 25:3698
KAKKAR, L. R., Microdetermination of rhenium, 25:2102
KALECHITS, V. E., Alpha decay and nuclear interactions, 25:3725
Optical potentials and elastic scattering of t and ^{3}He, 25:3769
KALISH, R., Static and transient hyperfine magnetic fields at Ba isotopes recoiled in iron, 25:3686
KALMUS, G. E., Reaction $\pi^+p \to \Sigma^+K^+$ between 1850- and 2090-MeV cm energy, 25:3283
KALNINA, Z. K., Concentration of ^{90}Sr and U in hydrobionts, 25:2546
KALOS, Malvin H., Practical aspects of multi-dimensional Monte Carlo shielding calculations, 25:3176
KALTENBACH, V., Probe for precise magnetic field measurements, 25:2512
KAMAL, A. N., Gilbert-like dispersion relations for the form-factors, 25:3461
Soluble two-channel problems in potential scattering, 25:3458
KAMERMANS, R., Decay of ^{62}Co isomers, 25:3644
KANAZAWA, Akira, Pion electromagnetic form factor with dipion unitarity, 25:3330
KANE, G. L., Structure of high-energy two-body non-diffractive reactions, 25:3454
KANE, John William Jr., Decay of ^{185}Os, ^{74}As, and ^{51}Cr, 25:3704
KANEKO, Yoshihiko, Pulsed neutron research in Japan, 1965--70, 25:3927 (JAERI-Memo-4109)
KANG, H. D., One phonon excitation in titanium hydride by low energy neutrons, 25:3536
KANGAS, Clifford V., Homogenization of uranium-base niobium alloys, 25:2732 (RFP-1582)
KANNENBERG, S. L., Quasi-elastic scattering of 160-MeV protons by alpha clusters in light nuclei. I. Carbon, 25:3581
KANOFSKY, A., Chemical shifts of the μ^+, 25:2899
KANTSEDAL, V. P., Apparatus for the production and investigation of high-pressure heavy-current long arcs, 25:3112
KAPLAN, S. A., Application of the method of characteristics to the solution of the transfer equation for a nonstationary radiation field, 25:2829
KAPTEYN, Johanna C., Decay of ^{169}Hf, 25:3676
KARASIK, V. R., Magnetization of the superconducting alloy Ti--22 at. percent Nb, 25:3027
KARBAN, O., Elastic scattering of polarized protons from ^{58}Ni, ^{120}Sn, and ^{208}Pb, 25:3636
Iron-54, ^{60}Ni(p,p) and (p,p'γ), 25:3613
KARIMOV, S. N., IR-spectroscopy studies of γ-radiation effects on the crystallinity of poly(vinyl alcohol), 25:2220
KARPENKO, D. Ya., Quantum mechanics of charged relativistic vector bosons. I, 25:3344
KARPENKO, I. K., Poloidal fields and the minimum mean magnetic fields in a two-path stellarator, 25:3142
KARPENKO, N. K., Possibility of the existence of magnetic wells in the combined field of one- and two-path stellarators, 25:3143
KARPLUS, M., Comparison of 3D classical trajectory and transition-state theory reaction cross sections, 25:3951 (HUX-3780-29)
KARPLUS, Martin, Prog. rpt. on theoretical studies in chemical kinetics, annual, 1970, 25:3952 (HUX-3780-33)
KARTASHEV, K. B., Investigation of charge exchange of a dense plasma current in a magnesium target, 25:3079
KARYAKIN, A. V., Increasing the sensitivity and accuracy of the luminescence determination of the rare earths by the method of the periodical scanning of the spectrum, 25:2086
KASHIN, A. A., Drift of small-scale inhomogeneities in ionospheric F2 layer, 25:2986
KASHY, E., Semiconductor position sensitive detectors in magnetic spectrographs, 25:2463
KASPAREC, I., Activation analysis at the Institute of Applied Geophysics, Brno, 25:2131
KASSNER, T. F., Application of thermodynamic and kinetic parameters of the V--O--Na system to the sodium corrosion of vanadium-base alloys, 25:2622
KAST, J. W., Muonic atoms. I, 25:3661
KASTENBAUM, Marvin A., Tables for determining the statistical significance of mutation frequencies, 25:2559
KATAOKA, Shoei, Pinching processes in semiconductor plasmas, 25:3206
KATO, Akihiko, Studies of spectrochemical analysis of rare earth elements. V, 25:2096
KATO, Toyoaki, Photon-activation analysis for I using Cs as internal-reference, 25:2150
KATO, W. Y., Final safety analysis report on the use of plutonium in ZPR-6 and -9, 25:3901 (ANL-7442)
KATRIEL, J., Separation of overlapping decaying peaks, 25:2482
KATS, M. E., Acceleration of charged particles in a cosmic plasma, 25:2929
KATTENBORN, H., J-dependence in l = 2 (^{3}He,α) reactions on ^{24}Mg, ^{28}Si, and ^{30}Si, 25:3637
KATUYA, Mituaki, Universality of weak bilinear transitions and its relation to the fundamental weak interactions, 25:3348
KATZ, J., Meson--baryon interactions with broken SU(3) and the baryon spectrum in relativistic quantum mechanics, 25:3397
KATZ, Ludwig, Quiescent and disturbed proton and electron distributions, 25:2950 (AD-709363)
KATZ, O. M., Tetragonal hydride in low H content Zircaloy, 25:2740
KAUS, Peter, Complex Regge poles in the cut j plane, 25:3402
KAWAHARA, Hiromichi, Abnormal microstructure formed in hot rolled plates and sheets of α + β titanium alloys, 25:2752
KAWAI, Y., Nonlinear effect of large-amplitude ion acoustic waves, 25:3151 (IPPJ-94)
KAWAI, Yoshinobu, Ion-acoustic waves in streaming-ion plasma, 25:3161
KAWAKAMI, H., Level structure of ^{105}Pd, 25:3670
KAWAMURA, Takaichi, Stochastic model of electron cyclotron heating in a magnetic mirror, 25:3055 (IPPJ-100)
KAWASAKI, Mamoru, Energy dependence of the slope of the forward peak in elastic proton--proton scattering, 25:3417
KAWASE, Y., Level structure of ^{88}Sr, 25:3621
KAZAK, B. N., Pulsating auroras at conjugate points, 25:2999
KAZANJIAN, A. R., Radiolysis of HNO_3 solutions: LET effects, 25:2284
KAZANSKII, V. B., EPR studies of stable hydrogen atoms on γ-irradiated clinoptilolites containing La, Mg, and K ions, 25:2224
KAZARINOV, Yu. M., Description of experimental data on πN and KN scattering in high-energy region on basis of complex angular momenta theory. I, 25:3381 (JINR-P2-5320)
KAZ'MIN, G. S., Current confinement by space charge in sectioned electron accelerator tubes, 25:3489
KEEN, N. J., Extracting uranium from sea water, 25:2323

XU

KEIZER, Joel E., New approach for the justification of ensembles in quantum statistical mechanics. II, 25:3237
New approach for the justification of ensembles in quantum statistical mechanics. I, 25:3238
KELLER, Charles F. Jr., Hydrodynamic atmospheres of a Cepheid variable, 25:2838
KELLER, David Anthony, Electronic heat capacity of ReO_3, 25:3956 (IS-T-383)
KELLER, Donald L., Progress on LMFBR cladding, structural, and component materials studies during July 1969--June 1970. Annual report, 25:2754 (BMI-1889)
KELLER, George Earl, Band-mixing effects in the even--even deformed nuclei ^{154}Gd, ^{160}Dy, and ^{166}Er, 25:3677
KELLER, Seymour P., Proceedings of the Tenth International Conference on the Physics of Semiconductors, Cambridge, Mass., 8/17--21/70, 25:3185 (CONF-700801)
KEMMER, J., Reactor neutron-induced fission of ^{231}Pa, 25:3656
KEMPTER, C. P., Debye--Scherrer camera filter attachment for use with radioactive specimens, 25:2508
KENNA, Bernard T., Studies in fast neutron activation analysis, 25:2120 (CONF-700322-, pp 231-48)
KERESZTURY, G., Pyridine-N-oxide: vibrational assignment and thermodynamic quantities, 25:2163
KERNOHAN, R. H., Comparison of calculated and measured lower critical field for some Nb--Ti alloys, 25:3020 (ORNL-TM-3206)
KERSHAW, K., Radiation chemistry of carbohydrates. XVII, 25:2279
KHABIBULLIN, B. M., Resonant absorption of ultrasound by nuclei in an intermediate state superconductor, 25:3028
KHACHIKYAN, E. E., Spectral observations of Markaryan galaxies with ultraviolet continuum. I, 25:2865
KHADZHI, B. A., Phase of VLF signals during solar eclipse on Sept. 22, 1968, 25:2997
KHAIKIN, A. S., Investigation of transitions between excited states of neon atoms in collisions with electrons, 25:2920
KHANNA, K. M., Alpha-particle model for nuclear matter, 25:3738
Critical temperature of transition of nuclear matter, 25:3773
Effective mass of alpha particles in superfluid nuclear matter, 25:3728
Nuclear matter calculations with hard-core and long-range potentials, 25:3772
Phenomenological ^{4}He--^{4}He potential and properties of liquid ^{4}He, 25:3009
KHANTADZE, A. G., Theory of periodic wind currents in the lower ionosphere, 25:2991
KHARCHENKO, I. F., Transformation of the distribution function of an electron beam during cyclotron interaction with a plasma, 25:3080
KHIZHNYAK, N. A., Electron plasma induced oscillations in a magnetic field, 25:3160
KHODUSOV, V. D., Kinetics of magnetohydromagnetic waves. I, 25:3159
KHOROSHEVA, O. V., Development of a polar storm, 25:2977
KHRAPAK, A. G., Phase transition and negative clusters in an imperfect plasma of metal vapor, 25:3086
KHRUSTALEV, O. A., Solution of unitarity condition for the elastic scattering amplitude for high energies, 25:3451 (ITF-70-49)
KHURGIN, B., Recoilless absorption measurements of 25.6-keV gamma rays of ^{161}Dy, 25:3222
KHURI, N. N., Bjorken limit and Jin--Martin lower bound, 25:3294 (NYO-4204-5)
KIANG, D., Muon--proton scattering and possible anomalous interaction of the muon, 25:3324
KIEFER, H., Prog. rpt. of the Radiation Protection and Safety Department, annual, 1969, 25:2570 (KFK-1158)
KIEFFER, R., Investigations on cermets of ThO_2--Ni and ZrO_2--Mo, 25:2796
KIM, C. O., Energy estimation of 20-GeV/c pion interactions in photographic emulsion, 25:3284
KIM, C. Y., Solar neutron flux in energy range 20 to 160 MeV, 25:2861
KIM, J. I., Reactor neutron-induced fission of ^{231}Pa, 25:3656
KIM, Sung Sam, Environmental contaminations due to Chinese nuclear explosion tests Oct. 1964 to Jan. 1969, 25:2366
KIM, Sung Wun, Effective dielectric constant of cylindrical plasma at microwave regions, 25:3087
KIMEL, I., S-wave non-leptonic decays and gauge fields, 25:3341
KIMEL, L. R., Attenuation of scattered synchrocyclotron radiation in a shield, 25:3480
KINGDON, J., Monitoring fluidised beds by pressure measurements, 25:2767 (DP-Report-378)
KINNEY, W. E., Vanadium neutron elastic- and inelastic-scattering cross sections from 4.19 to 8.56 MeV, 25:3595 (ORNL-4551)
KINSEY, D. V., Carbon transport studies for helium cooled high temperature reactors. project dragon, 25:3860 (DP-Report-491)
KIRBY, R. D., Low lying even parity resonances in KI:Ag^+, 25:3969 (NYO-2391-121)
KIRCHMANN, R., Radiomanganese and radiocobalt fixation by sediments, fauna, and flora, 25:2544
KIRILLOV, V. V., Laws governing operation of metallic electrodes of MHD generator, 25:2940
KIRKPATRICK, Ronald Crecelius, Inhomogeneities in planetary nebulae, 25:2837
KIRMAN, I., Precipitation of Ni_3Nb phases in a Ni--Fe--Cr--Nb alloy, 25:2689
KISSEL, G., Solubility and reactions of oxygen in sodium, 25:2711
KITAHARA, Tanemichi, Thermal conductivity of VIPAC UO_2 fuel. II, 25:2813 (JAERI-Memo-4128)
KITANI, Kohei, Possible CPT nonconservation in K^0 decay, 25:3429
KLAASSE, A. A. C., Decay of isomers of ^{102}Rh, 25:3671
KLABUHN, J., Lifetime of the A-He^5 hypernucleus, 25:3259
KLAMUT, C. J., Interaction effects between dissimilar metals in high velocity sodium at temperatures up to 760°C. I. Mass transfer of vanadium onto type 321 stainless steel, 25:2617
KLEIBELER, Hans-Juergen, Tube materials in nuclear reactor construction, 25:2678
KLEIJER, W. J., Repair of x-ray damage in DNA from patients having xeroderma pigmentosum, 25:2535
KLEIN, Elias, Sample preparation for neutron activation analysis, 25:2146
KLEINFELDER, W. J., Unique 150-keV ion accelerator, 25:3469 (CONF-700322-, pp 173-84)
KLEMENT'EVA, V. V., Deformed Mo recovery, 25:2746
KLEPEIS, J. E., Tenth symposium on engineering aspects of magnetohydrodynamics, Cambridge, Massachusetts, March 26--28, 1969, 25:2945
KLIMA, B. B., Savannah River Americium--Curium Slug Carrier, 25:2421 (ORNL-TM-3110)
KLINGELHOEFER, R., Ion density from Stark broadening of H/sub β/, 25:3068
KLOEPPER, H., Hydrodynamic stimulation of vibrations and their stabilization in the core of the Grenoble high flux reactor, 25:3909
Thermohydraulic displays of reflector space in the Grenoble high flux reactor, 25:3910
KLOPOVSKII, K. S., Cyclotron instability in a plasma cylinder, 25:3124
KLOSE, W., Transition temperature of superconductors, 25:3023
KLOTZ, Paul, Mixed-metal complexes between In(III) and U(VI) with malic, citric, and tartaric acids, 25:2206
KLUEH, R. L., Penetration of refractory metals by alkali metals, 25:2707
KLUYVER, J. C., I = $^3/_2$ Kπ elastic-scattering cross section from the reaction K-n → pK-π- at 3 GeV/c, 25:3278
KNECHT, O., Determinism and statistics in reactor safety, 25:3895
KNEFF, D. W., Reaction Q values from near-threshold neutron spectra, 25:3608
KNEISSL, U., Sensitive profile and position monitor for electron and positron beams, 25:3497
KNIGHT, J. A., Arylation of nitrobenzene induced by γ-radiation, 25:2255
KNUDSON, A. R., Reaction ^{14}N(^{3}He,α)^{13}N, 25:3590
KNUSELMAN, A. R., Pionic transition in ^{138}Ba, ^{140}Ce, and ^{142}Ce, 25:2896
KNYAZEV, V. K., Effect of nuclear radiation on the physicomechanical properties of lacquer coatings, 25:2822
KNYAZEV, Yu. R., Apparatus for the production and investigation of high-pressure heavy-current long arcs, 25:3112
KOBAYASHI, Keinosuke, Paracrystalline structure of polymer-crystal lattice distortion induced by electron irradiation, 25:2234
KOBAYASHI, Masanori, Energy dependence of the slope of the forward peak in elastic proton--proton scattering, 25:3417
KOCBACH, L., Branching ratios for E1 transitions deexciting the octupole states in even--even deformed nuclei, 25:3751
KODAIRA, T., Creep and creep-rupture tests of stainless steel as structural material of fast breeding reactor, 25:2660 (JAERI-Memo-4097)
KODAMA, Tatsuro, Zircaloy tubes for nuclear cladding, 25:2695
KOEHLER, P., CORONA: program for two-group control rod calculations in reflected reactor, 25:3926 (EIR-166)
KOEHMSTEDT, P. L., Radioactive material transport in flowing sodium systems, 25:2706
KOELZER, W., Prog. rpt. of the Radiation Protection and Safety Department, annual, 1969, 25:2570 (KFK-1158)
KOEPPL, G. W., Comparison of 3D classical trajectory and transition-state theory reaction cross sections, 25:3951 (HUX-3780-29)
KOHLMEYER, B., Mass-identification by time-of-flight methods, 25:2469
KOIKE, Yoshiyasu, Local atomic arrangement in In--Pb alloys, 25:3207
KOKKE, R., Accumulation of radionuclides by bacteria and yeasts, 25:2530
KOLATA, J. J., Rapid emittance scanner, 25:3498
KOLDEWIJN, P., Decay of isomers of ^{102}Rh, 25:3671
Energy of gamma rays from ^{7}Be, ^{40}K, and ^{113}Sn, and decay of ^{113}Sn, 25:3694
KOLESNIKOVA, T. V., Relationship between the geomagnetic field and the sporadic E layer, 25:2995

KOLLWENTZ, W., Investigations on cermets of ThO_2--Ni and ZrO_2--Mo, 25:2796
KOMISSAROVA, L. N., System HfO_2--Er_2O_3, 25:3978 (SC-T-70-4043)
KOMNIK, Yu. F., Superconductivity critical transition temperature in thin tin films, 25:3026
KOMOCHKOV, M. M., Attenuation of scattered synchrocyclotron radiation in a shield, 25:3480
KONDO, K., Isomeric transition-activated ^{80}Br reactions in CH_4--/sup 80m/BrBr and CH_4--/sup 80m/Br systems, 25:2226
KONDO, Kenjiro, Solubility of xenon in carbon tetrachloride and in chloroform, 25:2201
KONDO, Yutaka, Zircaloy tubes for nuclear cladding, 25:2695
KONETSCHNY, W., Nuclear form factors from the Veneziano model, 25:3394
KONIJN, J., Decay of isomers of ^{102}Rh, 25:3671
KONISHI, Takao, Zircaloy tubes for nuclear cladding, 25:2695
KONONENKO, S. G., Studies of resonances of nonlinear synchrotron oscillations, 25:3488
KONOROVA, E. A., Semiconductor layers and structural changes produced in diamond by ion implantation, 25:3199
KONOROVA, Elena Alexandrovna, Nuclear radiation detector, 25:2441
KONSTANTINOV, I. E., Investigation of fission product deposition in the Moscow region during 1962--1966, 25:2550
KOPPANG, Hanna Stromme, Further studies on the radiosensitivity of the rat incisor, 25:2592
KORENMAN, G. Ya., anti rho-Meson production in high energy pion-collisions with nuclei, 25:3406 (IFVE-STF-69-71)
KORKISCH, J., Ion-exchange separation of uranium and thorium from ore pulps and clear solutions, 25:2330
KORNACKI, Kazimierz, Decontamination of milk from radioactive Cs and Sr by means of ion exchangers of Polish manufacture, 25:2329
KOROBKOV, I. I., Hardness of Zr--O alloys, 25:2700
KORODENKO, G. D., IR-spectroscopy studies of γ-radiation effects on the crystallinity of poly(vinyl alcohol), 25:2220
KOROLEV, B. M., Radiation chlorination of polymers, 25:2250
KOROTKICH, V. L., anti rho-Meson production in high energy pion-collisions with nuclei, 25:3406 (IFVE-STF-69-71)
KORSAKOVA, N. V., New reagent for the photometric determination of zirconium and hafnium, 25:2084
KOS, V., Directional correlation studies in decay of /sup 177g/Lu, 25:3684
KOSCIUKOVA, B., Estimation of the amount of exogenous inclusions in steel by means of neutron-activation analysis, 25:2132
KOSE, V. E., Generation of harmonics and subharmonics of Josephson oscillation, 25:3037
KOSEL, T., High-voltage electron microscopy study of slip band growth in copper, 25:3988 (UCRL-19601)
KOSHELEV, V. V., Diurnal variations of ionic structure in F1 region, 25:2987
KOSIANCIC, Eugene Joseph, Improvements in and relating to the preparation of nuclear fuel materials, 25:2784
KOSMOWSKI, A., Increasing tasks of radiation protection, 25:2571
KOSTER, Robert, Instrumenting computer systems and their programs, 25:3981 (UCLA-10-P-14-94)
KOSTROMIN, A. I., Coulometric titration of Mn(VII), Ce(IV), Cr(VI), and V(V) by electrogenerated V(III), 25:2081
KOSTYGOV, K. I., Complete functions in analysis and representation of distant atmospherics, 25:2975
KOSTYUKOVA, Yu. S., Ion-acoustic instability in current-carrying plasma, 25:3125
KOSYAKOV, V. N., Neutron-induced ^{249}Bk fission, 25:3665
KOTANI, Naomi, Spectrochemical analysis of Ti and its alloy. IV, 25:2097
KOTANSKI, A., Physical bounds for the components of statistical tensors, 25:3296
Physical bounds for the components of statistical tensors, 25:3295 (TPJU-12/70)
KOTANSKI, Andrzej, Polarization of Λ and Σ hyperons in two-body Y* production processes and quark model, 25:3383 (TPJU-2/70)
KOULOUMDJIAN, J., Elastic scattering $^{12}C(d,d)^{12}C$, $^{28}Si(d,d)^{28}Si$, and $^{40}Ca(d,d)^{40}Ca$, 25:3585
KOVACEVICH, E. A., Radioactive material transport in flowing sodium systems, 25:2706
KOVAL, A. N., Asymmetry of moustaches, 25:2863
KOVBASYUK, V. I., Analysis of a scheme of power plant with an MHD generator and thermocompressor, 25:2936
KOWALSKI, L., Cross sections for formation of compound nuclei in heavy-ion reactions, 25:3611
KOZLOV, I. G., Calculations of electrostatic energy analyzer for solid and hollow cylindrical beams of charged particles, 25:3487
KOZLOV, M. I., Dipole sum rule for three-particle nuclei, 25:3768
KOZLOV, Stanislav Fedorovich, Nuclear radiation detector, 25:2441
KOZLOVSKII, L. V., Mechanical properties and corrosion resistance of steel coated with titanium and zirconium carbonitrides, 25:2612
KOZLOVSKII, S. A., Determination of fast neutron flux, 25:2443
KRAGELUND, E., Determination of ^{3}HOH, ^{82}Br, ^{125}I-human albumin, and ^{51}Cr-red cell volumes, 25:2518
KRAKHMAL'NIKOV, E. B., Measurement of ionospheric parameters from Doppler and Faraday effects of coherent signals, 25:2971
KRAMER, Lorenz, Stability of superflow and ion mobility in ^{3}He--^{4}He mixtures, 25:3012
KRATZER, K., Radiochemical determination of traces of Sb, 25:2106
KRATZER, W. K., Development of a waste disposal method for N reactor's decontamination wastes, 25:2426
KREBS, A. T., Test measurements on scintillation Geiger--Mueller counters, 25:2432 (AD-706587)
KRECKER, U., Lifetime of the Λ-He^5 hypernucleus, 25:3259
KREISLER, Michael N., Neutral branching ratios of the eta meson, 25:3258
KREMSNER, W., Grain boundary grooving of iron in liquid sodium, 25:2708
KRESNIN, A. A., Distribution of radiation widths from (p,γ) reactions, 25:3767
KREUZER, H. J., Soluble two-channel problems in potential scattering, 25:3458
KRISHNAN, C. V., Enthalpies of alkylammonium ions in water, heavy water propylene carbonate, and dimethyl sulfoxide, 25:2162
KRISTIANSEN, M., Conference on thermonuclear fusion reactor design, 6/70, Lubbock, Tex, 25:3130 (ORO-1171-1)
KRITSKAYA, V. K., State of carbon in martensite as influenced by electron bombardment, 25:2764
KRIVOPUSTOV, M. I., Investigation of proton polarization in reaction $^{12}C(^{3}He,p_0)^{14}N$, 25:3563 (JINR-P15-5156)
KRIVSKII, I. Yu., Absolute measurements of the excitation functions for the KII line produced in collisions between K^+ ions and Ne atoms, 25:2911
KRLIN, L., Stochastic heating of particles in magnetic mirror systems, 25:3058
KROH, Jerzy, Achievements of the pure and applied radiation chemistry in Poland, 25:2217
KROHN, N. A., Near-infrared spectra of water and heavy water at temperature between 25 and 390°, 25:2165
KROPP, L., Excitation functions and differential cross sections for $^{9}Be(n,\alpha)$ reaction with 8 to 30 MeV neutrons, 25:3564 (KFK-1190)
KRORI, K. D., Scattering by modified Gaussian potential, 25:3771
KRUEGER, F. W., Gamma-ray shielding by high-density concretes with densities from 3.2 up to 3.8 g/cm³, 25:3172
KRUG, Marion P., Anisotropic thermal expansion of crystal lattice of α Hf, 25:2751
KRUGLYI, M. S., Electric breakdown in plastics irradiated with charged particles, 25:2225
KRZYWDZINSKI, S., Energy estimation of 20-GeV/c pion interactions in photographic emulsion, 25:3284
KSCHWENDT, H., Shielding calculations by means of the Monte Carlo method, 25:3170
KUBICEK, Petr, Application of absorption method using the gamma radiation with two different energies for continual analysis, 25:2111
KUBO, Vicki, Direct proton magnetic resonance cation hydration study of uranyl perchlorate, nitrate, chloride, and bromide in water--acetone mixtures, 25:2209
KUBOTA, Hisashi, In-field behavior of and cumulative effects on certain electrodes in a gamma field, 25:2231
KUBOTA, Narinobu, Simulator for BWR type Tsuruga nuclear power station, 25:3933
KUCHAR, Lumir, Solidus and liquidus curves of binary alloys of U with C, Mn, and V, 25:2737
KUCHOWICZ, Br., Equation for nonstatic matter distributions of spherical symmetry in general relativity, 25:3448
KUDO, Tsutomu, Decontamination of materials, 25:2346
KUGEL, H. W., Static and transient hyperfine magnetic fields at Ba isotopes recoiled in iron, 25:3686
KUGLER, Alfred A., Bounds for some equilibrium properties of an electron gas, 25:3232
KUHL, G., Sensitive profile and position monitor for electron and positron beams, 25:3497
KUHLMANN, Ugine, Process for decontaminating liquid radioactive effluents containing radium, 25:2340
KUHLMANN, W. R., Probe for precise magnetic field measurements, 25:2512
KUKHTEVICH, V. I., Spatial, energy, and angular distributions of neutrons in lithium, 25:3538
KUKHTIN, V. V., Inelastic meson--baryon reactions in generalized Veneziano model, 25:3378 (ITF-70-77)
KULESHOV, S. P., Poisson distribution of secondary particles in straight-line paths approximation, 25:3407 (JINR-E2-5329)
KULIEV, A. A., States I/sup π/ = 1⁺ in even--even deformed nuclei, 25:3727
KULIK, I. O., Fluctuation resistance of a tunnel junction at temperatures exceeding the critical, 25:3029
KULIKOV, N. V., Migration and translocation of natural radioactive elements in water, 25:2547
KULIS, P. B., Mass exchange of a circular cylinder in presence of transverse magnetic field, 25:2941
KUMAGAI, Katsuaki, Thermal conductivity of VIPAC UO_2 fuel. II, 25:2813 (JAERI-Memo-4128)

KUMAR, Narayan, Pyridine-2-aldoxime and 6-methylpyridine-2-aldoxime as gravimetric reagents for estimation of Pd(II) and U(VI), 25:2072

KUMAR, Rajendra, Covariant phase-space calculations of n-body decay and production processes. II, 25:3303

KUNDIG, K. J. A., Anodic treatment to improve the liquid zinc corrosion resistance of tantalum, 25:2630

KUNEV, Dinko, Recovery of tellurium from sulphate solutions by extraction, 25:2321

KUNZ, C., Optical absorption of metals in the X--UV range, 25:3948 (DESY-70/48)

KUNZENDORF, H., Determination of rare-earth elements in rocks, 25:2094

KUPLENNIKOV, E. L., Quasi-elastic scattering of 1115-MeV electrons by nucleons of ^{32}S nuclei, 25:3615

KUPRINA, V. V., Phase diagram of niobium--cobalt system, 25:2749

KUPSCH, J., Estimates of the unitarity integral, 25:3300

KUROCHKA, L. N., Last resolved line in Balmer series, 25:2892

KURODA, K., Impulse approximation in $^{2}H(p,2p)n$ reaction, 25:3554

KUSTOM, R. L., Dielectric loaded waveguides as particle separators, 25:3494

KUYKENDALL, W. E. Jr., Analysis of oceanographic samples by 14-MeV neutron activation, 25:2119 (CONF-700322-, pp 221-30)

KUZIN, A. M., Activity of redoxy enzymes in beans and clover following γ irradiation, 25:2596

KUZNETSOV, S. N., Relationship between outer-belt electron intensity and geomagnetic activity indexes, 25:2969

KUZNETSOV, V. G., X ray studies of monoaquotetracarbamidouranyl halide nitrates, 25:2214

KUZNETSOV, V. S., Calculation of the phase focusing of intensive ion bunches, 25:3481

KUZNETSOVA, T. I., Anomalous hydrogen line intensities in the spectrum of HD 152107, 25:2834

KWA, T. L., Relations between gas chromatographic behavior and chemical structure. III, 25:2167

KWUN, Sook-Il, Infrared absorption in gamma-ray irradiated single crystal of sodium nitrite, 25:3191

KYZ'YUROV, V. S., Determination of fast neutron flux, 25:2443

L

LA BLANCHETAIS, Ch. Henry, Study of thin films of samarium by x rays and electron microscopy, 25:2734

LACAZE, Rose-Marie, X-ray spectroscopic measurement of the temperature of atomic and ionic transfer in a plasma, 25:3073

LACEK, H., Reaction $^{28}Si(d,p)^{29}Si$ mechanism, 25:3606

LAGOUTTE, M., Inverse Faraday effect in a plasma, 25:3082

LAI, D. Y. F., Clustering and giant moments in Cu--Ni alloys, 25:4000 (UCRL-72587(Rev.1))

LAKSHMINARAYANA, V., Half-life of 181-keV level of ^{99}Tc, 25:3708

LAL, A., Bromine isomers under (n,γ) process, 25:2301

LAL, Sudarshan, Potentiometric studies with a liquid ion-exchange lead-selective electrode, 25:2104

LAMB, R. C., Measurements of π^-p elastic scattering from 1.71 to 5.53 GeV/c, 25:3280

LAMBERT, James M., Charged particle nuclear physics experiments for a teaching laboratory, 25:3464 (CONF-700322-, pp 1-19)

LAMBERT, Marcel H., Density of electronic states in α-phase In alloys containing Cd and Sn, 25:3205 (UCRL-19681)

LAMBERT, R. J., Use of man-computer interaction in root-finding and numerical problem-solving, 25:3955 (IS-2416)

LAMSA, J. W., Double-Regge pole analysis of $\pi^+p \to \pi^+\pi^-\Delta^{++}$ at 13.1 GeV/c, 25:3273

LANDIS, D. A., Performance of a pulsed-light feedback preamplifier, 25:2462

LANDT, D. L., Reflection and absorption of electrostatic waves in an inhomogeneous plasma, 25:3153

LANGBEIN, W., Prevention of stress rupture formation of thermoplastics by radiation cross-linking, 25:2249

LANGE, G., Behavior of solid fission products in pyrolytic carbon and graphite, 25:2797

LANGER, M., Problems arising from nuclear blasting for oil and gas production, 25:2382

LANKFORD, W. F., Potassium-41 level structure from $^{40}Ar(^{3}He,d)^{41}K$, 25:3632

LANZEROTTI, L. J., Penetration of solar particles to ionospheric heights at low latitudes, 25:2965

LAPTEV, V. G., Radioactivation determination of Ta in minerals and rocks with a Ge(Li)-spectrometer, 25:2139

LARNER, D., Intermediate coupling in the N = 29 and Z = 29 nuclei, 25:3592 (COO-1120-106)

LARSSON, S., Method of obtaining Brueckner orbitals for atoms and molecules, 25:2926

LASSEN, Hans, Effect of hydrogen--deuterium substitution on the association of N-methylacetamide, 25:2174

LAU, Bong Whan, Effective dielectric constant of cylindrical plasma at microwave regions, 25:3087

LAUNOIS, D., Bounce effects in the negative mass instability, 25:3117 (CEA-CONF-1598)
Plasma containment in a circularized quadrupolar magnetic well: DECA II B, 25:3053 (CEA-CONF-1597)

LAUSCHER, P., Photoproduction of rho^0 mesons on deuterons between 1 and 5 GeV, 25:3246

LAUTHIER, Jean-Claude, Natural-convection irradiation device ''Esther'', 25:3903 (CEA-N-1348)

LAVAL, G., Bounce effects in the negative mass instability, 25:3117 (CEA-CONF-1598)

LAWLER, John P., Utility of radioisotope methodology in estuary pollution control studies. I, 25:2348 (NYO-3961-1)

LAWLEY, K. P., Elastic scattering of alkali atoms from iodine atoms and molecules at thermal energies, 25:2922

LAWSON, A. C., Electrical resistivity of UPt, 25:3215

LAWSON, J. D., Some attributes of real and virtual photons, 25:3331

LAZORENKO, V. M., Effect of C on Mo and Mo alloys, 25:2745

LEACOCK, R. A., Interpretation of small-angle π^-p elastic scattering from 1.71 to 3.01 GeV/c, 25:3281

LEAK, G. M., Diffusion in bcc iron base alloys, 25:2691

LEARY, J. A., Mechanical properties of carbide and nitride reactor fuels, 25:2785 (LA-4452)

LEBEDEV, R. A., Determination of state of ^{129}I in β-/sup 129m/TeO_3 by nuclear gamma resonance, 25:2304

LEBEDEV, S. N., Application of the Monte-Carlo method to the solution of kinetic problems of low-temperature plasma, 25:3098

LEBEDEV, S. V., Heat capacity of tungsten near the melting point, 25:2726

LECK, J. H., Measurement of total pressure in range 10^{-8} to 10^{-12} torr, 25:2428

LECKRONE, David Stanley, Neutral He lines in normal B-type spectra, 25:2839

LECLERE, Jacques, Natural-convection irradiation device ''Esther'', 25:3903 (CEA-N-1348)

LECOUSTEY, P., Plasma containment in a circularized quadrupolar magnetic well: DECA II B, 25:3053 (CEA-CONF-1597)

L'ECUYER, J., Electromagnetic transitions in ^{19}Ne, 25:3575

LEDERER, M., Paper chromatographic data for inorganic substances, 25:2075

LEE, B. K., Neutron activation study of ancient pigments from murals of cholula and teotihuacan, 25:2133

LEE, L. L. Jr., Inhibited (^{3}He,d) transitions to 3s/sub $^{1}/_{2}$/ isobaric analog states, 25:3666

LEE, Moon Nam, Infrared absorption in gamma-ray irradiated single crystal of sodium nitrite, 25:3191

LEE, Robert E., Direct proton magnetic resonance cation hydration study of uranyl perchlorate, nitrate, chloride, and bromide in water--acetone mixtures, 25:2209

LEE, T. Y., Shell-model structure of the p-shell hypernuclei, 25:3721

LEE, Y. J., One phonon excitation in titanium hydride by low energy neutrons, 25:3536

LEECH, William Dale, Weight optimization of reactor shielding using transmission-matrix methods, 25:3859

LEFEVRE, H. W., Reaction Q values from near-threshold neutron spectra, 25:3608
Thick-target $^{18}O(d,n)^{17}F$ yield curves, 25:3586

LE GO, Roland, Behavior of normal and irradiated bone marrow, 25:2595

LEHMANN, J., Uranium swelling under irradiation, 25:2762

LEHNERT, B., Plasma motion and equilibrium in unsymmetric magnetic fields, 25:3097

LEJEUNE, G., Thermal coupling between upper F2 region and magnetosphere, 25:2956

LELONG, Claude, Kinetics of α--β phase change in U alloys, 25:2741

LENCIONI, Donald Eugene, Effects of time-varying fields on plasma contained in a toroidal octupole magnetic field, 25:3059

LENDEL, A. I., Dispersion--theoretic model of πN-scattering backward peaks, 25:3377 (ITF-70-65)

LEND'EL, V. I., Dispersion--theoretic model of πN-scattering backward peaks, 25:3377 (ITF-70-65)

LEONARD, J. W., Reaction $^{12}C(d,p_0)^{13}C$, 25:3572

LEONT'EV, N. I., Nonlinear stabilization of beam instability, 25:3126

LERAY, J. P., Optical spark chamber for the search of gamma-ray sources, 25:2841 (CEA-CONF-1633)

LERCH, C., CORONA: program for two-group control rod calculations in reflected reactor, 25:3926 (EIR-166)

LERNER, Michael P., Distribution of polysomes in mouse brain tissue, 25:3986 (UCLA-12-796)

LESSER, P. M. S., First excited states of ^{58} ^{60} ^{62}Ni, 25:3642

LETAVET, A. A., Norms for radiation protection, 25:2574

LEUNG, Charles Chi-hei, Three-body bound-state calculations for some light nuclei, 25:3579

LEUNG, P. S., Graphitization by neutron inelastic scattering, 25:2810

LEVAN, Hoa, Effect of administration of magnesium pemoline on radioresistance, 25:2576

LEVIN, Saul, Environmental aspects of nuclear energy, 25:2564

LEVINSON, Lionel M., Resolving power of coincidence Moessbauer spectroscopy, 25:2483

LEVITZ, N. M., Fuel cycle technology quarterly report, April, May, June 1970, 25:2306 (ANL-7735)

LEVY, Therese, Perturbation of Stokes flow past a hollow sphere in magnetohydrodynamics, 25:2946

LEVY-MANDEL, R., Application of pulsed superconducting

magnets to synchrotrons, 25:3511
LEWIN, J. D., Superconducting energy transfer systems, 25:3513
LEWIS, Paul Spurgeon Jr., Elastic and inelastic scattering of 28-MeV protons from iron, cobalt, nickel, and zinc, 25:3599
LEWIS, Trevor James, Coulomb excitation of ^{151}Eu and ^{153}Eu, 25:3703
LEZNOV, A. N., Realization of representations of the quaternion group, 25:3420 (IFVE-STF-69-102)
LHERMENIER, Andre, Natural-convection irradiation device ''Esther'', 25:3903 (CEA-N-1348)
LIAS, S. G., Carbonium ions in radiation chemistry. II. Isomerization process in protonated cyclopropane and cyclobutane ions, 25:2290
LICHTENSTEIN, Pearl R., Mid-latitude magnetic bays and auroral absorption, 25:2964
LICHTER, B. D., Hall coefficients for Hg--Tl and Hg--In systems, 25:3209
LIEBERMAN, David S., Martensitic transformations in ferrous and non-ferrous systems: some heuristic comparisons, 25:3938 (COO-1198-753)
LIEBLER, B. L., Inhibited (^{3}He,d) transitions to 3s/sub $^{1}/_{2}$/ isobaric analog states, 25:3666
LIERS, Henry Soehlke, Elastic scattering of 39.6-MeV protons by the nickel isotopes, 25:3598
LIKHACHEV, M. A., Longitudinal distribution of mean annual characteristic of F2-layer ionization, 25:2985
LIKUSSAR, W., Ultraviolet spectrophotometric determination of gallium, 25:2100
LILJENZIN, J. O., Stability constants for Pa(V)--acetylacetone complexes, 25:2202
LILLESTOEL, E., Method to study events with two missing neutral particles, 25:3362
LILLEY, J. S., Coulomb excitation of ^{209}Bi, 25:3674
LIN, Jung, Charged particle spectra from ^{9}Be + D reaction, 25:3560 (CONF-700322-, pp 89-94)
LINDAUER, G. C., Importance of gravitational coagulation on the settling of high-mass density aerosols, 25:2369
LINDGARD, P. A., Magnetic anisotropy in rare-earth metals, 25:3208
LINDSAY, R. H., Student experiments utilizing a neutron generator, 25:3526 (CONF-700322-, pp 33-47)
LINDSKOG, J., Excited nuclear states in ^{125}Te, 25:3699
LINGEMAN, E. W. A., Decay of isomers of ^{102}Rh, 25:3671
LINHART, J. G., Very-high-density plasmas for thermonuclear fusion, 25:3114
LINKE, Volkard, Leptonic decays of polarized baryons. II, 25:3339
LIOU, M. K., Low-energy theorem for nucleon--nucleon bremsstrahlung, 25:3756
LIPES, Richard G., Application of multi-Regge theory to production processes, 25:3389
LIPSKY, L., Calculation of electron scattering and photoionization cross sections, 25:2903
LISCHKE, B., Single magnetic flux quanta in superconducting tubes. III, 25:3024
LISOVSKAYA, S. I., Mass exchange of a circular cylinder in presence of transverse magnetic field, 25:2941
LITTLE, W. W. Jr., User's manual for the 1DX--2DB--3DB--PERT-V code package, 25:3923 (BNWL-1412)
LIU, D. C., EPR study of isothermal annealing kinetics of Cr ions in x-irradiated ruby, 25:3195
LIVSHITS, M. A., Spectra of magnetohydrodynamic turbulence in collisionless plasma, 25:3096
LJUBICIC, A., Directional correlation studies in decay of /sup 177g/Lu, 25:3684
LLOYD, Robert C., Infrared and Raman spectra of trivalent lanthanide--Di-(2-ethylexyl) phosphoric acid solvent extraction organic equilibrium phases, 25:2193 (CONF-700403-8)
LOBANOV, E. M., Activation analysis for determining the content of Ta and Cs in rocks, 25:2145
LOBANOV, F. I., Extraction--photometric determination of Nb(V) with benzohydroxamic acid, 25:2085
LOBASTOV, Yu. S., Multiwave studies of relaxation phenomena in argon plasma, 25:3064
LOBB, D. E., First-order effects of misalignments in beam transport system, 25:3495
LOCHER, M. P., dpn and tdn coupling constants from forward neutron--deuteron dispersion relations, 25:3408
LOCKHART, L. B. Jr., Filtration of particles of atomic dimensions, 25:2414 (AD-707709)
LOCKWOOD, Grant J., Emission cross sections for H^+, Na^+, Ne^+, Rb^+, incident on molecular nitrogen, 25:2902 (SC-RR-70-695)
LODGE, J. D., N-reactor hybrid simulation, 25:3920 (BNWL-B-8)
LOEVHOEIDEN, G., Low-lying high-spin states in ^{155}Gd, 25:3700
LOEW, G. A., Superconducting accelerator research and development at SLAC, 25:3507
LOEWENSTEIN, Henning, Effect of hydrogen--deuterium substitution on the association of N-methylacetamide, 25:2174
LOFERSKI, J. J., Effects of sub-threshold high-energy electrons on properties of Si photovoltaic cells, 25:2814 (N-70-27167)
LOGSDAIL, D. H., Record of programme and discussions at symposium of papers from Dragon contractors held at A.E.R.E., Harwell, 14--16 March 1966, 25:3774 (DP-Report-439)
LOHMAN, P. H. M., Repair of x-ray damage in DNA from patients having xeroderma pigmentosum, 25:2535
LOHR, D. E., Sodium corrosion of Westinghouse liquid metal fast breeder reactor (LMFBR) materials, 25:2619
LOMAKIN, B. N., Possibilities of a shock tube in obtaining and investigating a dense low-temperature plasma, 25:3116
LOMON, Earle L., Field-theoretical nucleon--nucleon potential, 25:3414
LONG, Thomas Veach, Laser Raman and infared spectra of amino acids and their metal complexes. III. Proline and bisprolinato complexes, 25:2190
LONGO, W. P., Work softening in polycrystalline metals, 25:2724
LONNGREN, K. E., Reflection and absorption of electrostatic waves in an inhomogeneous plasma, 25:3153
LOOS, W., Temperature variations produced by heat currents in liquid He II, 25:3006
LOPATINA, G. B., Relationship between outer-belt electron intensity and geomagnetic activity indexes, 25:2969
LOPATO, P., Spectroscopy of even tin isotopes by inelastic scattering of protons, 25:3668
LORD, E. A., Some efficiency calculations for ^{6}Li suspended target semiconductor sandwich spectrometers, 25:2473 (AERE-R-6318)
LORENZ, Jerry J., Carlsbad site roll-up program. On-site radiological safety report, 25:2420 (NVO-410-2)
LOUIE, J., Reaction $\pi^+p \to \Sigma^+K^+$ between 1850- and 2090-MeV cm energy, 25:3283
LOVELL, A. J., Creep rate correlation in solution-treated Type 304 and 316 stainless steels, 25:4007 (WHAN-FR-25)
LOVERA, G., Grain counting in nuclear emulsions, 25:2457
LOW, F. J., Narrow-band infrared photometry of α Ori, 25:2826
LOWE, J., Elastic scattering of polarized protons from ^{58}Ni, ^{120}Sn, and ^{208}Pb, 25:3636
Iron-54, ^{60}Ni(p,p) and (p,p'γ), 25:3613
LOWE, R. A., Internal cathodic protection of water cooled plant, 25:2634
LU, D. C., Photoproduction of Y* resonances above 1800 MeV, 25:3251
LU, Pao, Derivation of Sommerfeld--Dirac fine structure formula by WKB method, 25:2924
LUBELL, M. S., Comparison of calculated and measured lower critical field for some Nb--Ti alloys, 25:3020 (ORNL-TM-3206)
LUBENETS, V. P., Deformed Mo recovery, 25:2746
LUCK, W. A. P., Approximate methods for determining the structure of H_2O and HOD using near-infrared spectroscopy, 25:2171
LUKYANOV, V. K., Multi-step stripping on deformed nuclei, 25:3732
LUND, Anders, Relative signs of principal elements of the α-proton hyperfine coupling tensor in NH_2CONHO, 25:2219 (NP-18449)
LUNDE, Gulbrand, Improvement of wood by plastic impregnation, 25:2238
LUNDSTROEM, T., Solution hardening of β-rhombohedral boron, 25:2801
LUR'E, K. A., Optimum distribution of specific resistance tensors of working substances in MHD channels, 25:2933
LUTZ, G. J., Bibliography on neutron generators in activation analysis, 25:2130 (NBS-TN-533)
Pollution analysis: bibliography of the literature of activation analysis, 25:2129 (NBS-TN-532)
LUUKKO, A., Levels in ^{55}Fe from the decay of ^{55}Co, 25:3604
LUX, Franz, UBr_3 and $UOBr_3$.2.5DMA, 25:2200
LUXTON, G., Production processes and Regge-pole hypothesis, 25:3399
LYAPIDEVSKII, V. K., Electric breakdown in plastics irradiated with charged particles, 25:2225
LYE, R. G., Upper limit on electron--phonon interaction in vanadium carbide, 25:3034
LYNCH, M. A., Very-long-baseline interferometry of Jupiter at 18 MHz, 25:2880
LYNNWORTH, L. C., Ultrasonic thermometry for LMFBR systems, 25:2503 (NYO-3906-4)
LYONS, L., Fitting K-p $\to$ anti K^0 π-p with a generalized Veneziano model, 25:3391
LYTKIN, L. K., Electric discharge of gas bubbles in liquids, 25:2485 (JINR-P13-5277)

M

MA, Z. Ming, Experimental comparison between on- and off-mass-shell inelasticities in π-p scattering. II, 25:3285
MACAGNO, E. R., Muonic atoms. I, 25:3661
Muonic atoms. II, 25:3620
MACDONALD, R. R., Preparation and acetolysis of 5-deuteriated exo-norbornyl brosylates, 25:2172
MACKENZIE, G. H., Median surface of AVF cyclotron magnet, 25:3516
MACKINTOSH, A. R., Magnetic anisotropy in rare-earth metals, 25:3208
MACNAUGHTON, J., Reaction $\pi^+p \to \Delta^{++}A_2^0$ at 3.7 GeV/c, 25:3272 (UCRL-20050)
MAEKAWA, Akiji, Design of an electron linear accelerator for industrial use, 25:3483

MAERKER, R. E., Gamma-ray spectra arising from thermal-neutron capture in elements found in soils, concretes, and structural materials, 25:3181
MAERZ, K.-D, Densitometric and scintigraphic investigations of brain tissue during reduced blood flow, 25:2577
MAGHRAWI, H. B., Extraction of niobium from aqueous organic acid media by structurally related tert-amines, 25:2334
MAHLMAN, H. A., Kinetic evidence that G/sub OH/ in the radiolysis of aqueous sulfuric and nitric acid solutions is proportional to electron fraction water, 25:2277
MAHNKE, H.-E., Magnetic moment of level in ^{58}Co, 25:3618
MAI, Trinh Thi Hoang, Aluminum oxide films and alpha stopping power, 25:2887
MAIER, M. R., Constant fraction trigger, 25:2458
MAJANI, C., Paper chromatographic data for inorganic substances, 25:2075
MAJEROTTO, W., Nuclear form factors from the Veneziano model, 25:3394
MAJUMDAR, D. P., Effect of a transverse momentum distribution in the Parton model, 25:3323
MAKINO, M., Proton hole states in 1f/sub 7/2/ nuclei, 25:3616
MAKOFSKE, W., Elastic scattering of polarized protons from ^{58}Ni, ^{120}Sn, and ^{208}Pb, 25:3636
MALAMA, Yu. G., Application of the Monte-Carlo method to the solution of kinetic problems of low-temperature plasma, 25:3098
MALKO, J. A., Antiproton--neutron elastic scattering at 3.5 GeV/c, 25:3267
MALOCH, J., Velocity relations in the rail accelerator without an external magnetic field, 25:3077
MALOJCIC, Rajko, Thermodynamic and kinetic secondary isotope effects in the Cope rearrangement, 25:2188
MALUMYAN, V. G., Low-frequency spectra of extragalatic radio sources, 25:2845
MANCINI, G., Parametric survey of the low enriched uranium cycle in a high temperature reactor. project dragon, 25:3883 (DP-Report-466)
MANGAN, J., uv-sensitive mutant of Neurospora defective for photoreactivation, 25:2556
MANIN, A., Use of thin film solar cells in radiovoltaic generators, 25:2400 (CEA-CONF-1623)
MAN'KO, P. A., Production of marine reactors and steam generators, 25:3918
MAN'KOVSKII, K. K., Superconductivity critical transition temperature in thin tin films, 25:3026
MANKU, G. S., Pyridine-2-aldoxime and 6-methylpyridine-2-aldoxime as gravimetric reagents for estimation of Pd(II) and U(VI), 25:2072
MANN, A. K., Detection of the weak intermediate boson through its hadronic decay modes, 25:3333 (NYO-2171-323)
MANNER, W., Production of strange particles in π^+p interactions at 5.5 GeV/c, 25:3279
MANNHEIM, P. D., rho-meson mass shift in photoproduction processes, 25:3326
MANSON, N., Ocular hazard of CW lasers, 25:2591
MAOR, U., rho-meson mass shift in photoproduction processes, 25:3326
MAOR, Uri, Photoproduction at high energies, 25:3315
MAQUEDA, E., T = 1 pairing Hamiltonian, 25:3758
MARASCHI, L., Optical spark chamber for the search of gamma-ray sources, 25:2841 (CEA-CONF-1633)
MARCHIONNI, V., Establishment of laboratory for determination of Pu in biological samples, 25:2108 (RT/PROT-(70)14)
MARCKWORDT, U., Radiocesium in soils, 25:2529
MARELIUS, A., Excited nuclear states in ^{125}Te, 25:3699
MARES, J., Polarized ion source for U-120 cyclotron. II, 25:3519
Polarized ion source for U-120 cyclotron. I, 25:3520
MARGAZIOTIS, D. J., Modified impulse approximation calculation of the N--N quasi-free scattering and the Chew--Low extrapolation in the D(p,NN)N reaction, 25:3750
MARGOLIN, A. D., Determination of the decomposition time of hexogen under the effect of shock waves, 25:3964 (LA-4360-TR)
MARIEN, P., Utilisation of fuel resources in different reactor types. project dragon, 25:3867 (DP-Report-476)
MARINGELLI, M., Excitation of states between 3 and 6 MeV in ^{31}P and ^{32}S, 25:3612
MARIPUU, S., Properties of low-lying ^{53}Mn levels, 25:3617
MARKEZICH, R. L., Base-catalyzed hydrogen--deuterium exchange in diene--iron tricarbonyl complexes, 25:2187
MARKIV, V. Ya., Phase diagram of niobium--cobalt system, 25:2749
MARKS, Maria H., Determination of niobium and tantalum by chromatographic method, 25:2066 (NIM-834)
MARKUSCH, Peter, Reactions of recoiling Si atoms with phosphine, silane, and disilane, 25:2299
MARLIN, Henri, Detachable head for a pneumatic system, 25:2427
MARQUES, R. O., Use of electrophoresis in thin films for control of the radiochemical purity of tracer compounds, 25:2062 (CNEA-271)
MARQUIT, Erwin, Comment on evidence for the H meson, 25:3286
MARSHAK, M. L., Proton--neutron elastic scattering on a deuterium target, 25:3266
MARSHALL, J., Ocular hazard of CW lasers, 25:2591
MARSHALL, T. O., Attenuation of 14 MeV neutrons in water, 25:3537
MARSIK, Stanley J., Radiation-induced preparation of metals from their aqueous salt solutions, 25:2237 (N-70-32826)
MARTELET, C., Study by triple labeling of reactions between tetraphenylstibonium and antimony trichloride, 25:2169
MARTENS, E. J., Inelastic scattering of alpha particles from ^{66}Zn and ^{68}Zn, 25:3630
MARTIN, Edward, Radiation damage studies with low-energy hydrogen isotopes, 25:3187 (CONF-700322-, pp 63-77)
MARTIN, Leslie Leon, Crystal and molecular structures of selected organometallic compounds, 25:3959 (IS-T-390)
MARTIN, M. M., Fabrication voids in aluminum-base fuel dispersions, 25:2806 (ORNL-4611)
MARTIN, W. R., Fabrication voids in aluminum-base fuel dispersions, 25:2806 (ORNL-4611)
MARTINA, E. Frank, Proton energy distributions from 0.060 to 3.3 MeV at 6.6 earth radii, 25:2951 (AD-709723)
MARTINIS, M., Inelastic processes and backward scattering in a model of multiple scattering, 25:3352 (IRB-TP-2-70)
MARTYSHOVA, T. I., Contemporary methods for determination of small quantities of cerium, 25:2061
MARUPOV, R., Studies on thermal degradation of γ-irradiated polycaproamide by means of mass spectrometry, 25:2288
MARUSHENKO, V. I., Charge radii of the nuclei of ^{124} ^{126} ^{128} ^{130}Te, 25:3551
MASATO, Kazuo, Reaction of carbon with nickel-base solid solution alloy containing carbide-forming element, 25:2716
MASI, G., Establishment of laboratory for determination of Pu in biological samples, 25:2108 (RT/PROT-(70)14)
MASKEWITZ, Betty F., Computer codes for shielding calculations: 1970, 25:3179
MASKORNICK, Michael John, Proton exchange kinetics of olefins in cyclohexylamine, 25:2184
MASLOV, A. I., Investigation of dense plasma formation using electron beam injection into magnetic trap, 25:3113
MASON, E. A., Thermal separation of ortho and para forms of H_2 and D_2, 25:2405
MASSELOT, Yves, Sintering furnace, 25:2391
MASUJIMA, Michio, Production cross section of $\gamma\gamma$ + $e^+e^-\mu^+\mu^-$, 25:3314
MATHIESON, A. McL, Conference on accurate determination of x-ray intensities and structure factors, Cambridge, Eng., 6/68, 25:3216
MATHUR, H. B., Impurity diffusion of rare earth metals in copper, 25:2680
MATHUR, P. K., Solid state isotopic exchange in radiocobalt doped trisdripyridyl Co(III) perchlorate, 25:2191
MATOLCSI, Tamas, Application of the hard-pion method to the baryon--meson four-point functions, 25:3401
MATSUDA, Hiroyoshi, Simulator for BWR type Tsuruga nuclear power station, 25:3933
MATSUI, Isao, Design of an electron linear accelerator for industrial use, 25:3483
MATSUMOTO, Hideki, Factorization and duality of multiloop diagrams, 25:3443
MATSUMURA, Tetsuo, Spectrochemical analysis of Ti and its alloy. IV, 25:2097
MATSUSHIMA, Ryoka, Photochemical reactions of uranyl ions with organic compounds. II, 25:2158
MATTHEWS, J. L., Non-intercepting beam current integrator, 25:3517
MATTHEWS, R. W., Kinetic evidence that G/sub OH/ in the radiolysis of aqueous sulfuric and nitric acid solutions is proportional to electron fraction water, 25:2277
MATTHIEUSSENT, G., Amplitude and damping of plasma wave echoes, 25:3144 (CEA-CONF-1601)
MATTOX, D. M., Composite film metallizing for ceramics, 25:2652
MATUSSEK, P., Studies of radiative neutron capture and delayed fission gamma-ray spectra from uranium and plutonium as a basis for new nondestructive safeguards techniques, 25:3649 (KFK-1214)
MATVEEV, V. A., Poisson distribution of secondary particles in straight-line paths approximation, 25:3407 (JINR-E2-5329)
MATZIOLIS, M., Photoproduction of rho^0 sesons on deuterons between 1 and 5 GeV, 25:3246
MAVLYANOV, A. M., Studies on thermal degradation of γ-irradiated polycaproamide by means of mass spectrometry, 25:2288
MAXSON, R. C., Automated quantometer data handling system, 25:2069 (Y-1740)
MAXWELL, W. A., Corrosion of advanced steam generator alloy weldments in steam, 25:2636
MAYER-BOERICKE, C., J-dependence in 1 + 2 (^{3}He,a) reactions on ^{24}Mg, ^{28}Si, and ^{30}Si, 25:3637
MAYINGER, F., Hydrodynamic stimulation of vibrations and their stabilization in the core of the Grenoble high flux reactor, 25:3909
Thermohydraulic displays of reflector space in the Grenoble high flux reactor, 25:3910
MAZZUCATO, M., Annihilation anti pn + $\pi^+\pi^-\pi^-$ between 1.0 and 1.6 GeV/c and its comparison with Veneziano model,

25:3270 (INFN-PD-70/2)
MCCANN, John David, Improvements in cathodes, 25:3523
MCCANN, T. E., Radial pressure profile in an MPD hydrogen arc. I, 25:3104
Radial pressure profile in an MPD hydrogen arc. II, 25:3105
MCCARTHY, J. S., Electron scattering from ^{12}C and ^{16}O, 25:3587
MCCAVERT, P., Approximation in scattering theory, 25:2895
MCCLELLAN, G., Polarization of high-energy photons using highly oriented graphite, 25:3257
MCCONNELL, L. G., Canadian forsee $^{1}/_{2}$ mill nuclear fuel cost, 25:3802
MCCOY, G. A., Calibration of an infrared pyrometer, 25:3989 (UCRL-19665)
MCCURIE, R. A., Magnetic domain structures of intermetallic compounds $SmCo_5$, $LaCo_5$, and $CeCo_5$, 25:3217
MCDOUGAL, J. R., Compatibility of ^{238}Pu dioxide with platinum and platinum--rhodium alloys, 25:2663 (MLM-1684)
MCDOWELL, J. D., Programming techniques for PDP-8/I computer, 25:2501 (CONF-700322-, pp 105-11)
MCGILL, William Fleming, Proton total reaction cross sections for light nuclei between 24 and 46 MeV, 25:3568
MCGIMSEY, L. S., Levels in ^{11}B by the $^{10}B(d,p)^{11}B$ reaction, 25:3561 (CONF-700322-, pp 133-40)
MCGOWAN, F. K., Multiple Coulomb excitation of ^{152}Sm, ^{166}Er, and ^{172} ^{174} ^{176}Yb, 25:3662
MCGRATH, R. L., Inhibited (^{3}He,d) transitions to 3s/sub $^{1}/_{2}$/ isobaric analog states, 25:3666
MCMAHON, Diane M., Hydrolysis of bis(4-nitrophenyl) carbonate and the general base catalyzed hydrolysis of o-(4-nitrophenylene) carbonate, 25:2181
MCMANUS, Samuel P., Acid-catalyzed cyclization reactions. IX. The formation of oxazclinium and thiazolinium cations from N-allyl and substituted N-allylamides, -urethans, -ureas, and -thioureas, 25:2179
MCMURRY, H. L., Application of Solbrig's cell-dipole method to molecular crystals, 25:3953 (IN-1410)
Electron ground states in molecular and valence-bonded crystals, 25:3226 (IN-1420)
MCNULTY, P. J., Scattering of high-energy pions on electrons, 25:3253
MCPHERSON, G. D., Heat transfer measurements on trefoil fuel bundles in the post-dryout regime-with data tabulation, 25:3865 (AECL-3414)
MCWENNY, R., Methods of molecular quantum mechanics, 25:2927
MECKLENBURG, E., Rhenium and its alloys as construction material, 25:2647
MEDIN, S. A., Analysis of a scheme of power plant with an MHD generator and thermocompressor, 25:2936
MEDINA, R., Corrections to magnon dispersion relations, 25:3218
MEIJER, B. J., Decay of isomers of ^{102}Rh, 25:3671
Energy of gamma rays from ^{7}Be, ^{40}K, and ^{113}Sn, and decay of ^{113}Sn, 25:3694
MEININGHAUS, H.-R., Behavior of solid fission products in pyrolytic carbon and graphite, 25:2797
MEJDAHL, V., Measurement of environmental radiation at archaeological excavation sites, 25:2352
MELESE-D'HOSPITAL, Gilbert, Status report on fast breeder reactors, 25:3891 (ORO-1171-1, pp 206-55)
MELGARD, R., Prevention of alpha counter contamination by electrodeless discharge deposition of Si_3N_4, 25:2478
MELIK-ALAVERDYAN, Yu. K., Some properties of radio galaxies, 25:2867
MELLERIO, J., Ocular hazard of CW lasers, 25:2591
MELNIKOVA, S. A., Catalytic amalgam method for determining small amounts of Cr, V, and Mo in brine, 25:2080
MENDOLA, D., Measurement of beam profile for high-intensity particles, 25:2434 (CERN-70-27)
MENDOZA, E., Surface tension of liquid ^{4}He, 25:3010
MENON, M. N., Hall coefficients for Hg--Tl and Hg--In systems, 25:3209
MENOSSI, C., Fission product fixation in fresh water species, 25:2548
MENTZEN, Bernard, Preparation and structure properties of a uranyl hydroxyformate, 25:2196
MENZINGER, F., Corrections to magnon dispersion relations, 25:3218
MERCIER, C., Space--time evolution of Tokamak-type plasma, 25:3052 (CEA-CONF-1595)
MERLINI, M., Transport of radiocobalt in artificial ecosystem, 25:2549
MERLINI, Margaret, Distribution of ^{60}Co in fish, 25:2526
MERLO, F., Rare-earth intermediate phases with zinc, 25:2753
MERRIAM, M. F., Density of electronic states in α-phase In alloys containing Cd and Sn, 25:3205 (UCRL-19681)
MERTENS, B., J-dependence in $1 = 2$ (^{3}He,α) reactions on ^{24}Mg, ^{28}Si, and ^{30}Si, 25:3637
MERZ, L., Comments on determinism and statistics in reactor safety, 25:3896
MESHCHERYAKOV, V. A., Static model of s waves in πN scattering and t-channel peculiarities, 25:3380 (JINR-P2-5263)
MESSER, Guenter, Experiences with cryopumps in calibration devices, 25:2429
METAG, V., Direct reaction in production of fission isomers, 25:3709
MEUSER, R., Superconductivity for high energy physics at LRL-Berkeley, 25:3510
MEYER, J., Elastic scattering $^{12}C(d,d)^{12}C$, $^{28}Si(d,d)^{28}Si$, and $^{40}Ca(d,d)^{40}Ca$, 25:3585
MEYERS, C., Exchange degeneracy with SU(2) symmetry and absorptive corrections in hypercharge-exchange reactions, 25:3388
MEZENTSEV, A. F., Charge radii of the nuclei of ^{124} ^{126} ^{128} ^{130}Te, 25:3551
MICHAELIS, W., Studies of radiative neutron capture and delayed fission gamma-ray spectra from uranium and plutonium as a basis for new nondestructive safeguards techniques, 25:3649 (KFK-1214)
MICHEL, F., Fission of heavy nuclei by helium ions and deuterons, 25:3710
MIGUNOV, V. M., Measurement of total electron content in the polar ionosphere from the recorded signals of the 3d satellite, 25:2983
MIKERINA, N. V., Interplanetary magnetic field flux and the K/sub p/ index of magnetic activity, 25:2981
MIKHAILOV, Yu. N., X ray studies of monoaquotetracarbamidouranyl halide nitrates, 25:2214
MIKHALKIN, V. S., Oxidation of tantalum in the oxygen plasma of a high-frequency discharge, 25:2632
MIKHEEV, V. L., Neutron-rich isotopes of light elements produced in transfer reactions with heavy ions, 25:3648 (JINR-E7-5319)
MIKHEIKIN, I. D., EPR studies of stable hydrogen atoms on γ-irradiated clinoptilolites containing La, Mg, and K ions, 25:2224
MIKKOLA, D. E., Size distributions of antiphase domains in Cu_3Au, 25:3941 (COO-1431-10)
MILEY, George H., Experience teaching a fusion design seminar, 25:3137 (ORO-1171-1, pp 376-86)
MILLAR, D. D., Plasma diagnostics, 25:3069
MILLER, D. A., Corrosion and coolant chemistry interactions in pressurized water reactors, 25:2637
MILLER, Glenn H., Emission cross sections for H^+, Na^+, Ne^+, Rb^+, incident on molecular nitrogen, 25:2902 (SC-RR-70-695)
MILLER, H. G., High-energy photoneutrons emitted from 1P-shell in ^{12}C, 25:3567 (SAL-15)
MILLER, J. M., Cross sections for formation of compound nuclei in heavy-ion reactions, 25:3611
MILLER, O. A., Radiation chemistry of carbon monoxide at very high dose rates, 25:2287
MILLER, R. L., Sodium corrosion of Westinghouse liquid metal fast breeder reactor (LMFBR) materials, 25:2619
MILLER, William E., Transmission and backscatter coefficients of 1.0 to 3.0 MeV electrons incident on some metals and alloys, 25:2883 (N-70-25499)
MILLS, R. G., Lecture notes [on toroidal fusion reactors], 25:3132 (ORO-1171-1, pp 38-77)
MILNER, W. T., Multiple Coulomb excitation of ^{152}Sm, ^{166}Er, and ^{172} ^{174} ^{176}Yb, 25:3662
MILYUKOVA, M. S., Reaction of trivalent Am and Cm with Arsenazo III, 25:2079
MIN, Suk Ki., Effective dielectric constant of cylindrical plasma at microwave regions, 25:3087
MINAMI, S., Conspiracy, duality, and π^{+-}, Δ photoproduction, 25:3318
MINC, Stefan, Energy transfer in the Al/Al_2O_3 system. II, 25:2276
MINER, F. J., Dissolution of plutonium in dilute nitric acid, 25:2153
Radiolysis of HNO_3 solutions: LET effects, 25:2284
MINETTI MEZZETTI, E., Grain counting in nuclear emulsions, 25:2457
MINUSHKIN, B., Solubility and reactions of oxygen in sodium, 25:2711
MIRSAGATOV, Sh. A., Effect of γ radiation on the volt--ampere characteristics of diodes, 25:3192
MISCHKE, Richard E., Neutral branching ratios of the eta meson, 25:3258
MISHIMA, J., Some observations on noble gas partitioning in dynamic air-water systems, 25:3892 (BNWL-SA-3360)
MISTRY, N., Polarization of high-energy photons using highly oriented graphite, 25:3257
MISTRY, V., Inelastic electron--atom interactions in the 50 to 150 keV energy range, 25:3472 (CONF-700322-, pp 379-92)
MISYURA, V. A., Measurement of ionospheric parameters from Doppler and Faraday effects of coherent signals, 25:2971
Measurement of total electron content in the polar ionosphere from the recorded signals of the 3d satellite, 25:2983
MITAKE, S., Experimental studies on 20 per cent enriched U-light water assembly. III, 25:3912
MITCHELL, G. E., Analogue states in ^{59}Cu, ^{61}Cu, ^{63}Cu, and ^{65}Cu, 25:3628
MITENKOV, F. M., Non-stationary operation of marine nuclear steam-producing installations, 25:3919
MITIN, R. V., Apparatus for the production and investigation of high-pressure heavy-current long arcs, 25:3112
MITTELMAN, Phillip S., Practical aspects of multi-dimensional Monte Carlo shielding calculations, 25:3176
MIURA, T., Optimum arrangement of laminated iron--water shields, 25:3174

MIYAGAWA, Masayoshi, Rate constants of exchange reaction of the type RI + I*- reversible RI* + I- in acetone--water solution, 25:2177
MIYAKE, Yoshizo, Studies of spectrochemical analysis of rare earth elements. V, 25:2096
MIYAMOTO, Kenro, Magnetic and drift surfaces, current configuration of stellarator field, 25:3128 (IPPJ-95)
MIYAWAKI, Y., Experimental studies on 20 per cent enriched U-light water assembly. III, 25:3912
MNATSAKANYAN, M. A., Polytropic models in the nonrelativistic generalized theory of gravitation, 25:2833
Relativistic generalized theory of gravitation. I, 25:2870
MOCHALOV, G. A., Properties of extruded Mo, 25:2697
Properties of hydroextruded Mo, 25:2698
Recrystallization of extruded Mo, 25:2747
MOCHIZUKI, Hiroji, Study concerning the analysis and evaluation of a gas cooled fast breeder, 25:3854
MOELLER, F., Concentration factors for fallout ^{90}Sr and ^{137}Cs in fishes, 25:2527
MOELLER, H. Bjerrum, Magnetic anisotropy in rare-earth metals, 25:3208
MOHANTY, S. R., Kinetics of isothermal annealing of gamma-irradiation damage in crystalline lead nitrate, 25:2236
MOLOKHIA, Mohamed M., Neutron activation analysis of trace elements in skin. V, 25:2134
MOMO, E., Spectrophotometric determination of Sc with 4-(2-thiazolylazo)resorcinol, 25:2093
MOMOTA, Hiromu, Stochastic model of electron cyclotron heating in a magnetic mirror, 25:3055 (IPPJ-100)
MONAHAN, C. F., Rotational structure in ^{43}Sc, 25:3626
MONMA, Y., Creep and creep-rupture tests of stainless steel as structural material of fast breeding reactor, 25:2660 (JAERI-Memo-4097)
MONSON, William Albert, Measurement of charge form factors for ^{6}Li and ^{7}Li by electron scattering, 25:3558 (AD-7C4484)
MONTALVO, Joseph G. Jr., Sample preparation for neutron activation analysis, 25:2146
MONTET, G. L., Optical density and thickness of $NbSe_2$ and $Nb_{1.0}Se_2$ lamellae, 25:3214
MOOKERJEE, A., Effect of x-irradiation on hydra in the presence of arginine and citrulline and study of the radiolytic products, 25:2588
MOON, P. B., Moessbauer spectrometer calibration, 25:3224
MOORHOUSE, R. G., Single pion photoproduction in second resonance region, 25:3313
MOORTHY, P. N., Hydrogen abstraction by primary species in the radiolysis of frozen aqueous system, 25:2293
MORAIT, Margareta, Determination of neodymium and praseodymium in misch metal, 25:2077
MORAN, J. M., Very-long-baseline interferometry of galactic OH sources, 25:2844
MORANDO, M., Spins and mean lives of ^{34}Cl levels, 25:3619
MORDIKE, B. L., Influence of alloying and temperature on the elastic constants of tantalum, 25:2721
MORELAND, P. J., Stress corrosion cracking of Ti and Ti--6Al--4V in dinitrogen tetroxide, 25:2635
MORGAN, G. L., Infrared spectra and structure of beryllium borohydride, 25:2189
MORGAN, John W., Determination of elements in lunar material by 14-MeV neutron activation, 25:2118 (CONF-700322-, pp 205-20)
MORGAN, M., Superconducting beam line, 25:3505
MORGAN II, Millett Granger, Laboratory model for radio star scintillation and other diffraction phenomena, 25:2856
MORIMITSU, Wataru, Making of Ge(Li) detector and its application, 25:2437
MORITA, K., Effects of radiation damage on channeling of MeV protons in KBr, 25:3201
MORITZ, Barry Kyler, General-relativistic dynamics of Klein--Alfven cosmology, 25:2872
MORKIN, L. A., Generator of short pulses of hard x-rays of high intensity, 25:2401
MOROZOV, S. F., Application of the method of characteristics to the solution of the transfer equation for a nonstationary radiation field, 25:2829
MOROZOVA, N. G., Natural radioisotope distribution in soils of USSR, 25:2371
MORPURGO, M., Design of superconduction magnet for Omega project, 25:2492
MORRIS, A. W., Elastic scattering of alkali atoms from iodine atoms and molecules at thermal energies, 25:2922
MORRISON, R. C., Isospin splitting of the giant dipole resonance in ^{66}Zn, 25:3623
MORRISSON, W. E., Energy forecasts need new approaches, 25:2393
MOSEL, Ulrich, Structure of the potential energy surface at large deformations, 25:3734
MOSER, H., Ion density from Stark broadening of H/sub β/, 25:3068
MOSER, Z., Thermodynamic properties of zinc--indium dilute liquid solutions, 25:2685
MOSES, R. W. Jr., Impossibility of a defocusing quadrupole-lens system, 25:3450
MOSSELMANS, G., Microbial degradation of aromatic hydrocarbons used as reactor coolants, 25:2327
MOSTINSKII, I. L., Use of turbulent washer for removal of ionizing additive in MHD generators, 25:2939
MOTOI, S., Effect of additives on the sintering of zircon, 25:2766 (CSIRO-Trans-9924)
MOTOROV, B. I., Non-stationary operation of marine nuclear steam-producing installations, 25:3919
MOURLAM, Louis Jr., Lock-in detector, 25:3954 (IS-2389)
MOUSNY, J. M., Radiocesium in soils, 25:2529
MOWATT, R. S., Effective neutron capture cross section and half-life of ^{155}Eu, 25:3667
MRAZ, J., Kinetic model of stem-cells and proerythroblasts populations in the postirradiation bone marrow injury, 25:2590
MRAZEK, Libor, Application of absorption method using the gamma radiation with two different energies for continual analysis, 25:2111
MUCKENTHALER, F. J., Gamma-ray spectra arising from thermal-neutron capture in elements found in soils, concretes, and structural materials, 25:3181
MUELLER, A., Simple methods for evaluating zero-power experiments, 25:3777
MUENZEL, H., Fission of heavy nuclei by helium ions and deuterons, 25:3710
MUINOV, T. M., Studies on thermal degradation of γ-irradiated polycaproamide by means of mass spectrometry, 25:2288
MUKHERJEE, B. B., Uptake of isolated metaphase chromosomes by mammalian cells in vitro, 25:2515
MULDER, M. P., DNA repair replication in xeroderma pigmentosum cell strains, 25:2567
Repair of x-ray damage in DNA from patients having xeroderma pigmentosum, 25:2535
MULVEY, J. H., Reactions π⁻p at 456, 505, and 552 MeV/c, 25:3282
MUNCASTER, G. W., Optical polarization of Crab Nebula pulsar, 25:2843
MUNERA, H. A., Application of Compton-scattering techniques to activation analysis: a short evaluation, 25:2140
MUNRO, G. H., Seasonal changes in the ionosphere, 25:2966
MURATA, Hideo, Thermal conductivity of VIPAC UO_2 fuel. II, 25:2813 (JAERI-Memo-4128)
MURATA, Y., Analysis of neutron correlation with shift registers, 25:3931
MURDAY, J. S., Self-diffusion in liquids: H_2O, D_2O, and Na, 25:2192
MURDOCH, R. N., Oxidative and glycolytic activity of ejaculated ram spermatozoa in the presence of steroid hormones, 25:2519
MURR, B. L., Detection of a secondary isotope effect on partitioning of benzhydryl benzoate ion pairs, 25:2186
Dissection of α-isotope effects on the solvolysis of benzhydryl benzoate, 25:2185
MURUGESU, S., Two-nucleon density functions and correlation functions, 25:3733
MURZIN, V. V., Effect of local heterogeneities of magnetic fields on pulsation of edges of electron beams, 25:3524
MUSGRAVE, B., Production of strange particles in π⁺p interactions at 5.5 GeV/c, 25:3279
MUSSLER, R. E., Kroll process beryllium, 25:2653
MUSTACESCU, Erica, Determination of neodymium and praseodymium in misch metal, 25:2077
MUTKE, R., Examples of differences between steam generators for conventional and nuclear power plants, 25:3898
MYAE, E. A., Investigation of beam transversal characteristics at input of IHEP proton synchrotron, 25:3482
MYASOEDOV, B. F., Reaction of trivalent Am and Cm with Arsenazo III, 25:2079
MYERS, G. E., Optical density and thickness of $NbSe_2$ and $Nb_{1.0}Se_2$ lamellae, 25:3214
MYRBERG, N., Penetration of radioactive isotopes through enamel and dentine. II, 25:2532
MYRONUK, Donald Joseph, Properties of free jets of ionized nitrogen, 25:3070
MYTTENAERE, C., Transport of radiocobalt in artificial ecosystem, 25:2549

N

NAGAI, Masayuki, Prediction of the burnout heat flux for rod clusters, 25:3680
NAGAI, Takeshi, Recrystallization process in Nb--Ag permalloy, 25:2679
NAGASAKI, Rukichi, Effect of cold working on creep properties of stainless steel, 25:2661 (JAERI-Memo-4125)
NAGASAWA, Toshio, Paracrystalline structure of polymer-crystal lattice distortion induced by electron irradiation, 25:2234
NAGLI, L. E., Quick-response energy transfer in KBr:Tl crystals. II, 25:3194
Quick-response energy transfer in KBr:Tl crystals. I, 25:3193
NAIDU, P. P., Colorimetric determination of traces of Se, Te, Mn, and Ce, 25:2073
Titrimetric determination of U(IV) alone and in mixtures with V(IV), Mn(II), Ce(III), and Fe(II), 25:2099
NAIR, S. M. K., Kinetics of isothermal annealing of gamma-irradiation damage in crystalline lead nitrate, 25:2236
NAIRN, J. H., Dissolution of plutonium in dilute nitric

acid, 25:2153
NAITO, Keiji, Electrical conductivity and defect structures in non-stoichiometric UO/sub 2 + x/, 25:3210
NAJEAN, Y., Platelet lifespan, 25:2579
NAKAMURA, Terumasa, Carrier effects on anion-exchange and gel chromatographic behavior of ^{32}P recoil species produced in irradiated inorganic phosphates, 25:2298
Hot atom chemistry of solid inorganic phosphorus compounds: alkali and ammonium orthophosphates, 25:2302
NAKANO, Hideo, Preliminary design on the prototype fast reactor, 25:3855
NAMATAME, H., Creep and creep-rupture tests of stainless steel as structural material of fast breeding reactor, 25:2660 (JAERI-Memo-4097)
NAMBA, Chusei, Stochastic model of electron cyclotron heating in a magnetic mirror, 25:3055 (IPPJ-100)
NANN, H., Reaction $^{28}Si(^{3}He,p)^{30}P$, 25:3602
NARA, Shigeru, Lead shield in the first nuclear-powered ship Mutsu, 25:2683
NARASIMHAM, K. V., Absorption spectrum of ammonium uranyl sulfate, 25:2211
NARDOZZI, M. J., Application of neutron generators in the steel industry, 25:2121 (CONF-700322-, pp 249-57)
NARGOLWALLA, S. S., Application of neutron generators to activation analysis, 25:3527 (CONF-700322-, pp 185-204)
NARODETSKII, I. M., Gilbert--Schmidt expansion for potentials with hard core, 25:3724
NARZULLAEV, B. N., IR-spectroscopy studies of γ-radiation effects on the crystallinity of poly(vinyl alcohol), 25:2220
NASH, Donald R., Transplantation antigens and viral carcinogenesis, 25:2537
NASONOVA, G. I., Salting out at solvent extraction of acids and some radioactive elements. IV, 25:2335
NATARAJAN, P. R., Decomposition of brown peroxy complex of Pu(IV) in $HClO_4$, 25:2154
NAUDET, Roger, EL 600: fuel management studies, 25:3866 (CEA-N-1379)
NAVARRO, Alain, Preparation and structure properties of a uranyl hydroxyformate, 25:2196
NEAL, R. B., Superconducting accelerator research and development at SLAC, 25:3507
NEEDHAM, Paul B. Jr., Application of high-velocity ions to metallurgy research, 25:2604 (CONF-700322-, pp 155-71)
NEELY, G., 27-plet unitary symmetry operator, 25:3426
NE'EMAN, Y., Analysis of the Serpukhov total cross section data with the algebra of vertex strengths, 25:3385
Time-reversal violation and the arrows of time, 25:3423
NEET, T. E., Effects of amine catalysts on the physical properties of a rigid urethane foam system, 25:2818 (BDX-613-170)
NEIMARK, B. E., Thermal conductivity, specific electrical resistivity, and total emissivity of refractory metals at high temperatures, 25:2715
NEJEDLY, Z., Enzymic synthesis of radioactive nucleocides, 25:2520
NEKHOROSHEV, R. S., Use of turbulent washer for removal of ionizing additive in MHD generators, 25:2939
NEKRASOV, F. M., Ion-acoustic instability in current-carrying plasma, 25:3125
NELSON, A. H., Development of the MHD electrothermal instability with boundary effects, 25:3127
NEMASHKALO, B. A., Distribution of radiation widths from (p,γ) reactions, 25:3767
NEMBACH, Eckhard, Defect structure and critical current density in high field superconductors V_3Ga, $(VZr)_3Ga$, and $(VHf)_3Ga$, 25:3039
NEMSMANN, U., Determination of the energy spectrum of a gamma-ray flash, 25:3183
NENCINI, G., X-ray irradiation of helium containing gaseous impurities. project dragon, 25:2258 (DP-Report-447)
NESET, K. M., Impurity removal from Dragon reactor during initial commissioning, 25:3862 (DP-Report-553)
NESMEYANOV, A. N., Determination of state of ^{129}I in β-/sup 129m/TeO_3 by nuclear gamma resonance, 25:2304
NEUBACHER, H., Electron spin resonance studies of radiation-induced radicals, 25:2286
NEVEU, A., Sign of Regge-pole residues in Veneziano model, 25:3453
NEWMAN, Leonard, Mixed-metal complexes between In(III) and U(VI) with malic, citric, and tartaric acids, 25:2206
NEWMEYER, Jeff, Approximations involved in the theory of the interactions of particles and nuclei at high energies, 25:3317
NEWSON, H. W., Analogue states in ^{59}Cu, ^{61}Cu, ^{63}Cu, and ^{65}Cu, 25:3628
NEYRET, G., Application of pulsed superconducting magnets to synchrotrons, 25:3511
NG, S. H., Muon--proton scattering and possible anomalous interaction of the muon, 25:3324
NGUYEN-VAN-CHONG, Contribution to the theory of echo phenomena in a plasma, 25:3164
NICHOL, D. G., Pre-dawn enhancement of lambda6300 A airglow, 25:2961
NICHOLAS, D. J., Proton polarization measurements, 25:3500
NICKS, R., Attenuation of moncenergetic source neutrons in different shielding materials, 25:3173
NICOLAS, M., Plasma containment in a circularized quadrupolar magnetic well: DECA II B, 25:3053 (CEA-CONF-1597)
NIEBERGALL, F., Large aperture Cherenkov counter, 25:2489
NIEDERLE, Jiri, Validity of quantum electrodynamics, 25:3438
NIEDZIELSKI, Jan, Gas-chromatographic analysis of C_1--C_6 hydrocarbons, products of radiolysis of gaseous ethylene, 25:2278
NIELSEN, H. L., Unique first-forbidden beta transitions in deformed nuclei, 25:3672
NIELSEN, M., Magnetic anisotropy in rare-earth metals, 25:3208
NIENHAUS, J., Microbial degradation of aromatic hydrocarbons used as reactor coolants, 25:2327
NIEUWDORP, P. J., Accumulation of radionuclides by bacteria and yeasts, 25:2530
NIFONTOVA, N. V., Use of N-benzoyl-o-tolylhydroxylamine in method of amperometric titration. III, 25:2082
NIILER, A., D(p,d*)p cross section, 25:3553
Neutron--neutron interactions in $^{2}H(d,pp)2n$, 25:3549
NIKI, Eiji, Reaction of carbon with nickel-base solid solution alloy containing carbide-forming element, 25:2716
NIKISHANOV, V. V., Crystal structure of Mo containing ZrC, 25:2743
Distribution of C in cast Mo, 25:2702
Effect of C on Mo and Mo alloys, 25:2745
NIKOLAEV, A. N., Spatial, energy, and angular distributions of neutrons in lithium, 25:3538
NIKOLOV, N., Low-frequency resonances and averaged potential in non-isothermal plasma, taking account of ion collisions, 25:3165
NIKOL'SKAYA, T. A., Rate of vaporization of congruently vaporizing compositions of NbC, 25:2802
NILSSON, L. H., Retention of oral ^{47}Ca in patients with intestinal malabsorption, 25:2531
NISHIDA, Yasushi, Electrostatic low-frequency oscillations in an inhomogeneous magnetoplasma, 25:3163
NISHIKAWA, Kiyoshi, Correspondence between ECC γ-ray and spark chamber shower, 25:2487
NOCENTINI, A., Collisional drift instability in a Q-machine, 25:3119
NODA, Tomohiko, Separation and detection of ^{181}W and ^{185}W from radioactive fallout, 25:2110
NOIROT, Y., Exchange degeneracy with SU(2) symmetry and absorptive corrections in hypercharge-exchange reactions, 25:3388
NOMURA, Akio, State of constructions on Fukushima atomic power station, 25:3780
NORDEMANN, Daniel, Origin of pallasites, 25:2824
NORRIS, John A., Computers in analytical chemistry. 1968 Eastern analytical symposium, New York, N. Y., November 13--15, 1968, 25:2060
NOVAK, J., Impact of heat on a straight tube, 25:2684
NOVIKOV, S. M., Diffusion of Mo and Nb in Zr, 25:2704
NOVIKOV, V. S., Effect of nuclear radiation on the physicomechanical properties of lacquer coatings, 25:2822
NOXON, J. F., Effect of magnetically conjugate photoelectrons on O I, 25:2959
NUNBERG, P., Effect of short-range correlations and charge-dependent nuclear forces on the energy of the analog state, 25:3753
NUNEZ, Paul L., Electron plasma wave growth, 25:3157
NURMATOV, D., Activation analysis for determining the content of Ta and Cs in rocks, 25:2145
NURMINA, M., Tracer chemical studies of Lr, 25:2197
NUSSINOV, Shmuel, Improved upper bound on the imaginary part of elastic scattering amplitudes, 25:3460
NUTT, A. W., Mechanical properties of carbide and nitride reactor fuels, 25:2785 (LA-4452)
NYBERG, Jan Anders, Morphological and clinico-chemical studies of thyroid function in lactating cattle, 25:2524
NYMAN, Ebbe M., Form factors of the nucleon, 25:3745

O

OAKES, R. J., Weakly coupled neutral currents, 25:3302
O'BRIEN, B. J., Reaction $^{56}Fe(p,\gamma)^{57}Co$, 25:3601
ODDONE, P. J., Deuteron--deuteron scattering at 2.2 and 7.9 GeV/c, 25:3415
ODINTSOVA, I. N., Geophysical activity of solar flares as function of brightness emission of metals, 25:2859
ODYNETS, L. L., Oxidation of tantalum in the oxygen plasma of a high-frequency discharge, 25:2632
OEHMAN, Yngve, Conference on mass motions in solar flares and related phenomena, Anacapri, Italy, 6/68, 25:2862
OESTGAARD, E., Neutron matter: binding energy and magnetic susceptibility, 25:3746
OFER, S., Recoilless absorption measurements of 25.6-keV gamma rays of ^{161}Dy, 25:3222
OGAWA, Yutaka, Effect of cold working on creep properties of stainless steel, 25:2661 (JAERI-Memo-4125)
OGER, Robert, Detachable head for a pneumatic system, 25:2427
OGLOBLIN, A. A., Excited states (4p--3h) in reaction $^{13}C(^{6}Li,d)^{17}O$ and $^{13}C(^{7}Li,t)^{17}O$, 25:3570
OHASHI, Shigeru, Hot atom chemistry of solid inorganic phosphorus compounds: alkali and ammonium orthophosphates, 25:2302
OHASHI, Teruo, Supercooling in the solidification of Al--

Cr, Al--Mn, and Al--Zr binary alloys, 25:2733
OHTA, Masahisa, Reactions (^{3}He,^{7}Be) and (^{3}He,^{6}Li) on ^{16}O and ^{12}C at 24.5 and 28.0 MeV, 25:3583
OHTA, Tadayuki, Chiral symmetry in the unified fermion theory. II, 25:3428
OHYA, Katsuhiko, Nonleptonic hyperon decays and breaking of chiral SU(3) x SU(3), 25:3349
OITMAA, J., Expansions for Griffiths' model of ^{3}He--^{4}He mixtures, 25:3015
OJEDA, M., D_0 acidity function in deuterium sulphate solutions at 25°C, 25:2175
OKA, Yoshinaga, Photon-activation analysis for I using Cs as internal-reference, 25:2150
OKAMOTO, Masao, Decay instability of cyclotron harmonic plasma waves, 25:3162
OKANO, Shigeo, State of constructions on Mihama atomic power station, 25:3779
OKHANOVA, L. A., New organic reagents for niobium, 25:2199
OLANDER, D. R., Calibration of an infrared pyrometer, 25:3989 (UCRL-19665)
Investigation of the convective-diffusion limited oxidation of molybdenum by the rotating disk method, 25:2688
OLEJARCZYK, W., Vinca Nova: automatic unit for neutron spectrometer control, 25:2475 (INP-707)
OLIVAIN, J., Amplitude and damping of plasma wave echoes, 25:3144 (CEA-CONF-1601)
OLLIER, H., Reliability and safety of fuel elements for gas--graphite reactors, 25:3879
OLSEN, C. E., Debye--Scherrer camera filter attachment for use with radioactive specimens, 25:2508
OLSEN, W. C., High spin states in ^{55}Fe, 25:3624
OLSON, Clifford Gerald, Infrared spectra of substitutional H^- and D^- impurities in CsBr and CsI, 25:3958 (IS-T-388)
OLSON, Dale G., Sources and prevention of recoil contamination of solid-state alpha detectors, 25:2479
OLSON, W. P., Variations in Earth's surface magnetic field from magnetopause current system, 25:2955
OLSTAD, R. A., Calibration of an infrared pyrometer, 25:3989 (UCRL-19665)
OMORI, T., Chemical behavior of ^{60}Co in aqueous solutions of neutron-irradiated Na ethylenediaminetetraacetatocobaltate/III/ tetrahydrate, 25:2297
OMURA, Tatsuro, Analysis of JMTR flux variation during operation, 25:3906 (JAERI-Memo-4130)
OPLESNIN, B. A., Deformed Mo recovery, 25:2746
OPPEL, R., Measurement of beam profile for high-intensity particles, 25:2434 (CERN-70-27)
ORDWAY III, Frederick I., Advances in space science and technology. X, 25:2396
ORLENKO, P. A., Universal nomograms for calculating absorbed doses from plane radiators, 25:2566
ORR, Charles H., Computers in analytical chemistry. 1968 Eastern analytical symposium, New York, N. Y., November 13--15, 1968, 25:2060
ORREN, M. J., Determination of ^{210}Po and ^{210}Pb in seawater, 25:2112
ORTEGA, R. F., Neutron activation study of ancient pigments from murals of cholula and teotihuacan, 25:2133
OSHIMA, Keichi, Electrical conductivity and defect structures in non-stoichiometric UO/sub 2 + x/, 25:3210
Electrical conductivity of γ-irradiated solid monomers at low temperature, 25:2221
OSIPOV, V. B., Spherically shaped cartridges for extended sources in pilot and full-scale radiation-chemical processors, 25:2404
OSMAN, A., Short-range correlations in the three-body problem, 25:3731
OSNES, E., Calculation of Coulomb energy differences, 25:3770
OSUMI, Yasuaki, Studies of spectrochemical analysis of rare earth elements. V, 25:2096
OTTAVIANI, P. L., Proton scattering from ^{23}Na and ^{25}Mg, 25:3603
OUWEHAND, R. W., Preparation and acetolysis of 5-deuteriated exo-norbornyl brosylates, 25:2172
OVEZGEL'DEV, O., Spaced sounding of the E/sub s/ layer, 25:2993
OVSEPYAN, A. V., Effect of neutronization of the critical parameters of isothermal white dwarfs, 25:2832
OWCZARCZYK, Andrzej, Energy transfer in the Al/Al_2O_3 system. II, 25:2276
OWENS, R. O., Non-intercepting beam current integrator, 25:3517
OXENIUS, J., Optically thin hydrogen plasma with self-consistent electron velocity distribution, 25:3102

P

PACHE, B., Activities of the Pechiney group in the nuclear fuel cycle, 25:2379
PADEL, Andre, Elastic constants of U and plutonium carbonitrides, 25:2798
Mechanical properties of ceramics based on uranium and plutonium, 25:2794 (ORNL-tr-2388)
PADJEN, R., Theory of a self-consistent static field, 25:3739
PADMAVATHI, G., Influence of deuterons on proton relaxation times in paramagnetic solutions, 25:2166
PADRTA, F. G., Benzene--deuteroxyl exchange over deuterated γ-alumina, 25:2164
PAGELS, Heinz, Regge analysis of electroproduction and photoproduction, 25:3312 (NYO-4204-6)
PAIC, G., Modified impulse approximation calculation of the N--N quasi-free scattering and the Chew--Low extrapolation in the D(p,NN)N reaction, 25:3750
PAIS, A., Weak interactions at high energies, 25:3334 (NYO-4204-3)
PALAIS, C. J., Detection of beta-emitting nuclides, 25:2565
PALAYOOR, Thomas, Effects of maternal x-irradiation of mice on the germ cells of their progeny, 25:2593
PALIT, R., Effect of x-irradiation on hydra in the presence of arginine and citrulline and study of the radiolytic products, 25:2588
PALKINA, A. A., Resonance charge exchange between a molecular ion and diatomic molecule, 25:2912
PALMER, David R., Inelastic neutrino--nucleon scattering and the q^2 dependence of Regge residue functions, 25:3336
PANDIT, L. K., Axial-vector K/sub 14/-decay form factors based on current algebra, 25:3345
PANT, D. D., Role of impurities and D_2O substitution on fluorescence lifetimes of uranyl salts, 25:2198
PANT, H. C., Role of impurities and D_2O substitution on fluorescence lifetimes of uranyl salts, 25:2198
PAPALIOLIOS, C., Time-of-arrival measurements of optical pulses from Crab pulsar, 25:2853
PAPELEUX, P., Electrodynamic vibrocompaction of sintered nodules of uranium oxide, 25:2778
PAPP, Ya., EPR studies of stable hydrogen atoms on γ-irradiated clinoptilolites containing La, Mg, and K ions, 25:2224
PARAIN, J., Application of pulsed superconducting magnets to synchrotrons, 25:3511
PARDI, A. J., Direct reading spectrometric method using AgCl--LiF carrier to determine impurities in nuclear-grade U_3O_8 samples, 25:2068 (NLCO-1071)
PARIKH, J. C., Silicon-28 nucleus in projected Hartree--Fock model, 25:3605
PARK, J. N., Energy estimation of 20-GeV/c pion interactions in photographic emulsion, 25:3284
PARK, Robert T., Complex Regge poles in the cut j plane, 25:3402
PARLIER, B., Optical spark chamber for the search of gamma-ray sources, 25:2841 (CEA-CONF-1633)
PARR, R. M., Medical activation analysis research program of IAEA Laboratory, 25:2124 (IAEA-122, pp 15-26)
Photopeak count-rates in Ge(Li) and NaI(Tl) detectors, 25:2474 (IAEA-122, pp 150-63)
PARR, W. H., Test measurements on scintillation Geiger--Mueller counters, 25:2432 (AD-706587)
PARRETT, F. W., Low frequency infrared and Raman spectroscopic studies of some uranyl complexes, 25:2212
PARSONS, Anthony S. L., Radiative pion capture in ^{12}C, 25:3550
PARTHASARADHI, K., Effective atomic numbers in alloys for gamma-ray interactions at 100 to 662 keV, 25:2906
Incoherent scattering cross sections of γ rays by electrons in Al, Cu, Sn, Pb, and U, 25:2921
Photoelectric cross sections of 662-keV gamma rays in Ta and Pd, 25:2904
Photoelectric cross sections of gamma rays in La, Gd, Hf, and Th, 25:2907
Photoelectric cross-sections of gamma rays in Cu, Ag, and Pt, 25:2905
Total to subshell photoelectric cross section ratios, 25:2908
PARTOVI, M. Hossein, Field-theoretical nucleon--nucleon potential, 25:3414
PARTRIDGE, Jennings E., Calibration of two-stage air samplers, 25:2446
PASICHNYI, A. A., Electrodisintegration of light nuclei, 25:3714 (ITF-70-35)
PATEL, A. R., Fission tracks on (001) cleavages of topaz, 25:2351
PATEL, M. M., Fission tracks on (001) cleavages of topaz, 25:2351
PATI, Jogesh C., Nonelectromagnetic violation of isospin, charge-conjugation, and time-reversal invariance, 25:3425
PATRIARCA, P., Corrosion of advanced steam generator alloy weldments in steam, 25:2636
PATTERSON, J. W., Steady-state chemical potential profiles in solid electrolytes, 25:2203
PATTERSON, R. L. Jr., Filtration of particles of atomic dimensions, 25:2414 (AD-707709)
PATTISON, J., Record of programme and discussions at symposium of papers from Dragon contractors held at A.E.R.E., Harwell, 14--16 March 1966, 25:3774 (DP-Report-439)
PAUKKU, P., Levels in ^{59}Fe from the decay of ^{59}Co, 25:3604
PAUL, H., Coupling constants in β-decay, 25:3741
PAUL, J., Optical spark chamber for the search of gamma-ray sources, 25:2841 (CEA-CONF-1633)
PAUL, M. P., Very-long-baseline interferometry of Jupiter at 18 MHz, 25:2880
PAULIN, A., Injection, extraction, or splitting of a beam,

25:3522
PAVLENKO, V. N., Contribution to the theory of echo phenomena in a plasma, 25:3164
PAVLICEK, Zdenek, Corona counters for nuclear radiation detection, 25:2440
PAVLOV, P. V., Crystallization of amorphous films of silicon dioxide during ionic bombardment and subsequent annealing, 25:2823
PAYNE, Bryan R., Nuclear techniques in hydrology, 25:2359
PAZDZERSKII, V. I., Simple model for wide-angle, high-energy, elastic, proton--deuteron scattering, 25:3419
PECHERSKII, O. P., Generator of short pulses of hard x-rays of high intensity, 25:2401
Water-dielectric generator for producting intensive fast-electron and hard decelerated x-ray pulses, 25:3478
PECQUEUR, Michel, Separation of uranium isotopes, 25:2402
PEEVA, A., Self-quenching GM counters with heated anode, 25:2460
PEGG, D. J., Beam-foil excitation using low-energy accelerators, 25:3465 (CONF-700322-, pp 21-31)
PEKARSKII, G. Sh., Calculating the optimum thickness of the front screen in the transfer method of neutron radiography, 25:2413
PEKRUL, P. J., Prog. rpt. on Transit Time Flowmeter, 7--9/70, 25:2500 (AI-AEC-12981)
PELLAN, P., Evidence of a phase transition in an assembly of point contacts, 25:3035
PELLAT, R., Bounce effects in the negative mass instability, 25:3117 (CEA-CONF-1598)
PENKUHN, H., Attenuation of monoenergetic source neutrons in different shielding materials, 25:3173
Time optimization for gamma transport codes BIGGI 3/4, 25:3180
PENNINCQ, Alex, Detachable head for a pneumatic system, 25:2427
PENTTINEN, S., Levels in ^{55}Fe from the decay of ^{55}Co, 25:3604
PEPPER, C. E., Direct reading spectrometric method using AgCl--LiF carrier to determine impurities in nuclear-grade U_3O_8 samples, 25:2068 (NLCO-1071)
PERAZZO, R., Coulomb excitation of ^{209}Bi, 25:3674
PERAZZO, R. P. J., T = 1 pairing Hamiltonian, 25:3758
PERCEVAL, F., Amplitude and damping of plasma wave echoes, 25:3144 (CEA-CONF-1601)
PERES, Asher, Bogolyubov causality in S-matrix theory, 25:3452
PEREY, F. G., Spectroscopy of ^{65} ^{67} ^{69}Ga by (d,n) reaction, 25:3625
Vanadium neutron elastic- and inelastic-scattering cross sections from 4.19 to 8.56 MeV, 25:3595 (ORNL-4551)
PERKINS, A. J., Athermal omega transformation in Zr--Nb alloys, 25:2735
PERLINI, G., Attenuation of monoenergetic source neutrons in different shielding materials, 25:3173
PERSSON, Jan, Visualization of organs by means of radionuclides, 25:2581
PERVUSHIN, V. N., Poisson distribution of secondary particles in straight-line paths approximation, 25:3407 (JINR-E2-5329)
PESCHEL, D. J., Weapons Effects Display System: Maintenance Manual. Pt. 5, 25:2505 (UCRL-50892(Vol.4)(Pt.5))
Weapons Effects Display System: Operator's Manual, 25:2504 (UCRL-50892(Vol.2))
PESEK, Miroslav, Preparation of wood-plastic combinations on the basis of unsaturated polyester resins. II, 25:2254
PETERMANN, Juergen, Precipitates and flux line pinning in superconducting Pb--Na alloy, 25:3033
PETERS, J. M., Degassing at low temperature of titanium targets impregnated with hydrogen isotopes, 25:3542
PETERSEN, E. L., p-p and p-t interactions in ^{3}He(d,tp)p, 25:3552
PETERSON, F. C., Pulse radiolysis studies of aqueous solutions of aminothiols and compounds related to nucleic acid, 25:2259 (GA-10208)
PETERSON, R. N., Intensities of O_2^+ 1NG and N_2 1PG band systems in normal and type-B aurorae, 25:3002
PETERSON, Robert L., Generation of harmonics and subharmonics of Josephson oscillation, 25:3037
PETERSON, Sigfred, Metals and ceramics division annual progress report for period ending June 30, 1970, 25:2601 (ORNL-4570)
PETIT, M., Thermal coupling between upper F2 region and magnetosphere, 25:2956
PETKOV, I. Z., Multi-step stripping on deformed nuclei, 25:3732
PETKOVSEK, J., Cold neutron source efficiency in a tangential beam hole, 25:3904 (IJS-571)
PETRENKO, V. I., Apparatus for the production and investigation of high-pressure heavy-current long arcs, 25:3112
PETRINA, D. Ya., Hamiltonians of quantum statistics and theory of superconductivity, 25:3040
PETROV, G. D., Accuracy of probe measurements of the velocity of plasma flows, 25:3074
Laser methods of measurement of plasma density, 25:3066
PEYRAUD, Nelly, Deviations from the thermodynamic equilibrium in an atomic hydrogen plasma, 25:3106
PFEFFER, Robert, Meson--nucleon scattering and asymptotic conservation of helicity, 25:3398
PHILIPP, Warren H., Radiation-induced preparation of metals from their aqueous salt solutions, 25:2237 (N-70-32826)
PHILLIPS, G. C., D(p,d*)p cross section, 25:3553
Neutron--neutron interactions in ^{2}H(d,pp)2n, 25:3549
PHILLIPS, G. O., Radiation chemistry of carbohydrates. XVII, 25:2279
PHILLIPS, Norman E., Density of electronic states in a-phase In alloys containing Cd and Sn, 25:3205 (UCRL-19681)
Low-temperature heat capacities of dilute solutions of Fe and Cr in Cu, 25:3990 (UCRL-19686)
PHILLIPS, R. J. N., New Regge models of asymptotic behavior, 25:3357
PHILLIPS, R. S., Resistance of mice and rats to challenge by Babesia rodhaini after inoculation with irradiated red cells infected with B. rodhaini, 25:2539
PHILLIPS, W. R., Coulomb excitation of ^{209}Bi, 25:3674
PHILLIPS, Wayne M., Some alkali metal corrosion effects in a Rankine cycle test loop, 25:2624
PIATTI, G., Formation of Al pearls on surface of SAP alloys, 25:2779
PICAT, P., Radiocontamination of irrigation canals fed by Rhone, 25:2543
PIEPGRAS, U., Densitometric and scintigraphic investigations of brain tissue during reduced blood flow, 25:2577
PIERCE, Edward L., Equipment and technique for forming sensitized photographic film to a spherical shape, 25:3996 (UCRL-50926)
PIERCE, R. D., Fuel cycle technology quarterly report, April, May, June 1970, 25:2306 (ANL-7735)
PIGEON, Jacques, Elastic α scattering by ^{4}He, 25:3544 (LYCEN-7041)
PIHL, J., Excited nuclear states in ^{125}Te, 25:3699
PILIPENKO, V. V., Superconductivity critical transition temperature in thin tin films, 25:3026
PILT, A. A., High spin states in ^{55}Fe, 25:3624
PINDOR, Andrzej, Pseudopotentials and model potentials in solid state physics, 25:3227
PINGOT, O., Gamma rays from ^{124}Sb, ^{134}Cs, and /sup 110m/Ag, 25:3697
PINKERTON, D. M., Effects of gamma radiation on gas yields and crystallinity of PTFE, 25:2261 (NP-18518)
PIONTELLI, R., Morphological effects of relative movement between solid and liquid in electrochemical processes, 25:2648
PIROUE, P. A., Search for violation of CP invariance in tau^{+-} decay, 25:3427
Wire-spark-chamber system with on-line computers, 25:2491
PISAREV, A. F., Electric discharge of gas bubbles in liquids, 25:2485 (JINR-P13-5277)
PISK, K., Inelastic processes and backward scattering in a model of multiple scattering, 25:3352 (IRB-TP-2-70)
PISKUNOV, L. I., DK-0.2 dosimeter for recording fast neutrons, 25:2493
PISKUNOVA, L. V., Application of the method of characteristics to the solution of the transfer equation for a nonstationary radiation field, 25:2829
PISTUNOVICH, V. I., Investigation of charge exchange of a dense plasma current in a magnesium target, 25:3079
PITTENGER, E. W., Arctic ionosphere and aurora: airborne investigations, 25:2949 (AD-709359)
PITTMAN, Charles U. Jr., Acid-catalyzed cyclization reactions. IX. The formation of oxazolinium and thiazolinium cations from N-allyl and substituted N-allylamides, -urethans, -ureas, and -thioureas, 25:2179
PIZZIGONI, M., Study of a generalized optical potential, 25:3747
PLAJNER, Z., Gamma-ray spectrum of ^{192}Au, 25:3654
Transition multipolarities in decay of /sup 197m/Hg, 25:3682
PLATONOV, V. V., Investigation of charge exchange of a dense plasma current in a magnesium target, 25:3079
PLATTEN, J. L., 5000-hr test of a eutectic lead--bismuth circuit constructed in steel and niobium, 25:2627
POBEREZHSKII, L. P., Method of measuring electrical conductivity of plasma with a high time resolution, 25:3081
PODDER, N. G., Effect of x-irradiation on hydra in the presence of arginine and citrulline and study of the radiolytic products, 25:2588
POELSTRA, P., Migration of ^{90}Sr in soil, 25:2366
POKROVSKII, A. V., Statistical analysis of the information transfer process in radiometric betatron defectoscopy, 25:2412
POLETAVKIN, P. G., Thermal cycle for a direct flow, supersonic, compressorless MHD generator, 25:2935
POLGA, T., Static and transient hyperfine magnetic fields at Ba isotopes recoiled in iron, 25:3686
POLIKARPOV, G. G., Concentration of ^{90}Sr and U in hydrobionts, 25:2546
POLIVANSKII, V. P., Spatial, energy, and angular distributions of neutrons in lithium, 25:3538
POLLARD, D., Production of strange particles in π$^+$p interactions at 5.5 GeV/c, 25:3279
POLLITT, N., Post-irradiation gas release measurements on fuel elements from Dragon reactor, 25:3870 (DP-Report-497)
POLUEKTOV, I. A., Charge exchange at medium collision

XUM

energies, 25:2919
POLUEKTOV, N. S., Luminescence of neodymium and europium in cerium dioxide and its use in analysis, 25:2083
POLVANI, C., Concentration factors for fallout ^{90}Sr and ^{137}Cs in fishes, 25:2527
Natural cesium in freshwater and fishes, 25:2517
PONOMARENKO, V. G., Magneto-acoustic wave propagation in lamellar media, 25:3158
POP, S. S., Absolute measurements of the excitation functions for the KII line produced in collisions between K$^+$ ions and Ne atoms, 25:2911
POPL, M., Investigation of hydrolyzable carbides. III, 25:2782
POPOVA, G. M., Charge radii of the nuclei of ^{124} ^{126} ^{128} ^{130}Te, 25:3551
POPOVICH, V. P., Transformation of the distribution function of an electron beam during cyclotron interaction with a plasma, 25:3080
POQUETTE, G. E., Size distributions of antiphase domains in Cu_3Au, 25:3941 (COO-1431-10)
PORTER, D., Elastic and inelastic scattering of neutrons in energy range 2 to 5 MeV by ^{10}B and ^{11}B, 25:3559 (AWRE-O-45/70)
PORTER, L. G., Space--time detector for cosmic ray showers, 25:2490
PORTNOY, Benjamin, Neutron activation analysis of trace elements in skin. V, 25:2134
POSTNIKOVA, I. N., Working substance for single-component liquid-metal MHD units, 25:2937
POT, F., DNA repair replication in xeroderma pigmentosum cell strains, 25:2567
POTASHEV, P. I., DK-0.2 dosimeter for recording fast neutrons, 25:2493
POTASHNIKOVA, I. K., Description of experimental data on πN and KN scattering in high-energy region on basis of complex angular momenta theory. I, 25:3381 (JINR-P2-5320)
POTH, J. E., p-p and p-t interactions in ^{3}He(d,tp)p, 25:3552
POTTER, Donald, Ordered orthorhombic subnitride of vanadium, 25:2811
POUJOL, Georges, Sintering furnace, 25:2391
POWELL, J. E., Fast neutron spectrum measurements, 25:2481
POWERS, R. J., Pionic transition in ^{138}Ba, ^{140}Ce, and ^{142}Ce, 25:2896
POWERS, Robert T., Self-adjoint algebras of unbounded operators, 25:3968 (NYO-2171-325)
POZNANSKI, Stefan, Decontamination of milk from radioactive Cs and Sr by means of ion exchangers of Polish manufacture, 25:2329
PRAKASH, Satya, Irregularities in night-time equatorial E region, 25:2963
PRANTL, F. A., Air pollution on the CERN site, 25:2562
PREINREICH, G., Qualification of fission product release, 25:3775 (DP-Report-539)
PREINREICH, G. F. F. J., Evaluation of data from first Dragon charge, 25:3796 (DP-Report-579)
PRENTICE, A. J. R., Pulsar distances and emission, 25:2854
PRESCOTT, C. Y., Recoil proton polarization in eta photoproduction, 25:3255
PRESNYAKOV, L. P., Charge exchange at medium collision energies, 25:2919
Inseparable variables in the problem of excitation of atoms by electron impact, 25:2915
Role of intermediate states in excitation of atoms by electron impact, 25:2916
PRIDACHINA, N. N., Radiolysis of original and reinforced ED-5 type epoxy resin, 25:2273
PRIMAK-MIROLYUBOV, V. N., Output calculation for cylindrical irradiator with additional axial source, 25:2403
PRINCE, N., FASEII: a computer program for the stress analysis of thin cylindrical shells and flat plates, 25:3949 (GA-9203)
SHELL5: SHELL-3D Version 5, a computer program for the structural analysis of arbitrary three-dimensional thin shells, 25:3950 (GA-9952)
PRIVEZENTSEV, V. I., Expansion of measurement limits of electron density in plasma, 25:3072
PROCTOR, Stephen G., Anion exchange purification of Np by in situ conversion from nitrate to chloride system, 25:2339
PROKOPOV, Theodore S., Non-sulfide scheme of inorganic qualitative microanalysis, 25:2101
PRONKO, J. G., Reactions ^{21}Ne(p,d)^{20}Ne and ^{21}Ne(d,p)^{22}Ne, 25:3633
PROTO-OTERO, A. N., Gamma--gamma coincidences in ^{140}Ce, 25:3646 (CNEA-275)
PROTOPOPOV, L. A., Phase of VLF signals during solar eclipse on Sept. 22, 1968, 25:2997
PSHENITSYNA, V. P., Radiolysis of original and reinforced ED-5 type epoxy resin, 25:2273
PUDOVKIN, M. I., Development of an elementary magnetic disturbance, 25:2978
PUEHLHOFER, F., Reaction (^{3}He,p) on the Ca isotopes, 25:3629
PUFF, R. D., Meson dynamics and the nuclear many-body problem. I, 25:3719
PUGH, R. E., Gauge invariance and charge operator in the Heisenberg picture, 25:3437
PULTAR, Frantisek, Preparation of wood-plastic combinations on the basis of unsaturated polyester resins. II, 25:2254
PUMPLIN, Jon, Diffraction dissociation and the reaction $\gamma p \to \pi^+\pi^- p$, 25:3320
PURCELL, J., Superconducting beam line, 25:3505
PURI, B. K., Polarographic determination of Te(IV), 25:2090
PURVIS, J. D., First excited states of ^{58} ^{60} ^{62}Ni, 25:3642
PYATOV, N. I., States I/sup π/ = 1$^+$ in even--even deformed nuclei, 25:3727

Q

QAIM, S. M., Investigations of thermal and 14-MeV neutron activation analysis in Pakistan, 25:2125 (IAEA-122, pp 27-36)
QUAGLIA, L., Behavior of surfaces under bombardment using nuclear reactions, 25:2763
QUAGLIANO, James V., Structural studies of metal coordination compounds, 25:3979 (TID-25562)
QUARLES, C. A., Inelastic electron--atom interactions in the 50 to 150 keV energy range, 25:3472 (CONF-700322-, pp 379-92)
QUATAERT, D., X-ray microprobe studies of irradiated fuel particles, 25:2812 (DP-Report-320)
QUEEN, N. M., Data on real parts of K^{+-} forward scattering amplitudes, 25:3379 (JINR-E1-5259)
QUEMENEUR, A., Amplitude and damping of plasma wave echoes, 25:3144 (CEA-CONF-1601)
QUINTON, A. R., Reaction (p,α) with a 400-keV Van de Graaff accelerator, 25:3466 (CONF-700322-, pp 49-61)

R

RAAB, G. J., Operating experience using silver reactors for radioiodine removal in the Hanford Purex Plant, 25:2416 (ARH-SA-67)
RABRENOVIC, R., Ionic flotation of uranium from diluted solutions, 25:2331
RACHINSKAS, V. S., Electrodeposition of cobalt--tungsten magnetic alloys, 25:2649
RADEBAUGH, R., Upper limit on electron--phonon interaction in vanadium carbide, 25:3034
RADIOU, Jean, Preparation and crystalline structure of UBa sulfide: $BaUS_3$, 25:2204
RADOSAVLJEVIC, R., Capture of ^{60}Co by suspended particles in Danube, 25:2361
RADWAN, M., Estimation of the amount of exogenous inclusions in steel by means of neutron-activation analysis, 25:2132
RADZHYUNENE, B. S., Electrodeposition of cobalt--tungsten magnetic alloys, 25:2649
RADZIEVSKII, V. N., Wave radiation by a charge in nonequilibrium plasma, 25:3092
RAFFO, Peter L., Thermomechanical processing of a molybdenum alloy using hydrostatic extrusion, 25:2651
RAI, Rama Shanker, Separation of ^{234}Th from inactive Th, U, and Fe by adsorption on $Bi(IO_3)_3$, $Bi(IO_4)_3$, or $Pb(IO_3)_2$, 25:2341
RAINWATER, J., Muonic atoms. I, 25:3661
RAJA RAO, M., Photoelectric cross sections of 662-keV gamma rays in Ta and Pd, 25:2904
RAJASEKARAN, G., Axial-vector K/sub 14/-decay form factors based on current algebra, 25:3345
RAKAVY, M., Recoilless absorption measurements of 25.6-keV gamma rays of ^{161}Dy, 25:3222
RAM, Rishi, New approach to the equilibrium configuration of stellar envelopes, 25:2827
RAMAMOORTHY, A. N., Recoil studies of fission products, 25:3702
RAMAMURTY, V. V., Half-life of 181-keV level of ^{99}Tc, 25:3708
RAMAN, S., Spectroscopy of ^{65} ^{67} ^{69}Ga by (d,n) reaction, 25:3625
RAMANI, S. V., Work-hardening parameters of polycrystalline materials, 25:2723
RAMA RAO, M. T., Half-life of 181-keV level of ^{99}Tc, 25:3708
RAMAZASHVILI, R. R., Parametric instability of nonhomogeneous plasma, 25:3118
RAM MOHAN, L. R., Baryon pole model for S-wave hyperon decay, 25:3346
RAMSPOTT, Lawrence D., Quantitative phase analysis of rocks by x-ray diffractometry, 25:3995 (UCRL-50921)
RANDOLPH, J. K., Bound on virtual Compton scattering at 185 and 460 MeV/c^2, 25:3252
RANGWALA, Abbas A., Improved upper bound on the imaginary part of elastic scattering amplitudes, 25:3460
RANKIN, W. A., Single pion photoproduction in second resonance region, 25:3313
RANOGAJEC, F., Grafting of styrene on polyethylene. I, 25:2242
Grafting of styrene on polyethylene. II, 25:2241
RAO, A. L. J., Polarographic determination of Te(IV), 25:2090
RAO, B. V. Narasimha, Lifetimes of 321- and 113-keV levels of ^{177}Hf, 25:3707
RAO, D. R. K., Statistical properties of world-wide fluctuations in the magnetic field, 25:2958
RAO, G. G., Titrimetric determination of U(IV) alone and in

mixtures with V(IV), Mn(II), Ce(III), and Fe(II), 25:2099
RAO, K. N., Hydrogen abstraction by primary species in the radiolysis of frozen aqueous system, 25:2293
Radiation-induced polymerization of trioxane, 25:2253
RAO, M. H., Radiation-induced polymerization of trioxane, 25:2253
RASK-MADSEN, J., Absorption of ^{51}Cr-EDTA in ulcerative colitis, 25:2534
RASMUSSEN, J. O., Prompt de-excitation of fission fragments, 25:3673
RASPOPOV, O. M., Pulsating auroras at conjugate points, 25:2999
RASTEGAR, B., γ transitions in ^{160}, 25:3584
RAUB, Christoph Julius, Superconductivity of ternary β-titanium alloys, 25:3021 (UCRL-Trans-1409)
RAYHRER, Benno, Very-long-baseline interferometry of decametric radiation from Jupiter, 25:2879
RAYNAL, J., Transformation coefficients in the hyperspherical approach to the three-body problem, 25:3729
RAYSKI, Jerzy, Examples of quantum field theories without divergences, 25:3435 (TPJU-13/70)
RAZMI, M. S. K., Factorization test for the Pomeranchukon in three-particle final states, 25:3395
RAZZINI, G. C., Morphological effects of relative movement between solid and liquid in electrochemical processes, 25:2648
REBAGAY, Teofilo Velasco, Determination of zirconium and hafnium in meteorites and terrestrial materials by activation analysis, 25:2148
REBARCHIK, F. N., Composite film metallizing for ceramics, 25:2652
REBBERT, R. E., Carbonium ions in radiation chemistry. II. Isomerization process in protonated cyclopropane and cyclobutane ions, 25:2290
RECKNAGEL, E., Magnetic moment of level in ^{58}Co, 25:3618
REDDINGIUS, Ewout Roelof, Neutron-capture gamma-ray spectra from aligned Nd and Sm nuclei, 25:3651 (NP-18485)
REDI, Martha Harper, Fluctuations in superconductive films in a magnetic field, 25:3042
REED, C. R. V., Effects of LET and temperature in radiolysis of cyclohexane. II, 25:2280
Effects of LET and temperature in radiolysis of cyclohexane. I, 25:2281
REED, D. L., Comparison of carbon-atom displacement rate in graphite in Dragon reactor, Petten HTR and low enrichment HTR, 25:3672 (DP-Report-559)
Evaluation of data from first Dragon charge, 25:3796 (DP-Report-579)
Measurement of burn-up of Dragon first charge fuel elements, 25:3871 (DP-Report-538)
REED-HILL, R. E., Work softening in polycrystalline metals, 25:2724
REICH, C. R., Base-catalyzed hydrogen--deuterium exchange in diene--iron tricarbonyl complexes, 25:2187
REICH, H., Direct electron--positron pair production in copper by electrons of 5.8 MeV, 25:3250
REID, C. N., Moessbauer spectrometer calibration, 25:3224
REIFF, J., Coherent, incoherent, and inelastic cross sections for W-meson production by muons and neutrinos, 25:3340
REINIGER, P., Migration of ^{90}Sr in soil, 25:2366
REKALO, M. P., Propagation of cosmic rays in neutrino sea. II, 25:2875
Propagation of cosmic rays in neutrino sea. I, 25:2874
REMMEL, R. S., Search for violation of CP invariance in tau^{+-} decay, 25:3427
Wire-spark-chamber system with on-line computers, 25:2491
RENEKER, Darrell H., Polyoxymethylene crystals grown within irradiated trioxane crystals, 25:2252
RENNER, B., Algebraic realization of chiral SU(2) x SU(2) symmetry, 25:3422
Hard-pion calculation without current algebra, 25:3361
RENNIE, C. A., Self-sustaining mixed fast and thermal reactor systems, 25:3888 (DP-Report-581)
RENNINGER, George, Meson--nucleon scattering and asymptotic conservation of helicity, 25:3398
RENTLER, R. M., Effect of HNO_3--HF pickling on stress corrosion cracking of Ni--Cr--Fe Alloy 600 in high-purity water at 660F, 25:4006 (WAPD-TM-944)
REPACHOLI, M. H., Electrophoretic mobility of tumour cells exposed to ultrasound and ionising radiation, 25:2586
REPALOV, N. S., Electron plasma induced oscillations in a magnetic field, 25:3160
REPNOW, R., Direct reaction in production of fission isomers, 25:3709
REPRINTSEV, L. V., Studies of resonances of nonlinear synchrotron oscillations, 25:3488
RERIKH, K. V., Static model of s waves in πN scattering and t-channel peculiarities, 25:3380 (JINR-P2-5263)
RESHETOV, E. P., Laws governing operation of metallic electrodes of MHD generator, 25:2940
RESNICK, L., Rescattering, Omnes equation, and zeros in resonance peaks, 25:3459
RESTER, Alfred Carl Jr., Energy levels in ^{72}Ge from radioactive decay studies of ^{72}Ga and ^{72}As, 25:3639
RESTER, D. H., Electron backscatter measurements at 1.0 MeV, 25:2886
REVAI, J., Transformation coefficients in the hyperspherical approach to the three-body problem, 25:3729
REYNOLDS, B. G., Antiproton--neutron elastic scattering at 3.5 GeV/c, 25:3267
REYNOLDS, D. A., Measurement of average electron density between 75 and 80 kilometers, 25:2952 (N-70-33955)
REZANKA, I., Transition multipolarities in decay of /sup 197m/Hg, 25:3682
RHINEHART, Wayne A., Lock-in detector, 25:3954 (IS-2389)
RHO, Chae-shik, Environmental contaminations due to Chinese nuclear explosion tests Oct. 1964 to Jan. 1969, 25:2368
RHODES, Harold J., Deuterium isotope effects in enzymatic transamination, 25:2168
RIAZUDDIN, Chiral-symmetry-breaking corrections to the K + 3π soft-pion theorem, 25:3347
RIBAUX, P., Charge/discharge machine for Dragon reactor, 25:2385 (DP-Report-230)
RICCI, Robert W., Deuterium-isotope effect on indole derivatives, 25:2536
RICHARDS, Keith C., Mesons in nuclear saturation, 25:3763
RICHARDS, L. M., Critical fluence needed to destroy thin metal films by laser deposition, 25:3997 (UCRL-50927)
RICHARDSON, J. Reginald, Median surface of AVF cyclotron magnet, 25:3516
RICHTER, A., Number of degrees of freedom in fluctuation analysis, 25:3717
RICHTER, Herbert, Tube materials in nuclear reactor construction, 25:2678
RIIHIMAEKI, E. J., Effect of short-range correlations and charge-dependent nuclear forces on the energy of the analog state, 25:3753
RIJHIKOV, St., Self-quenching GM counters with heated anode, 25:2460
RILEY, P. J., Isobaric analog resonances in N approximately equals 82 nuclei, 25:3685
RIMPAULT, M., Exchange degeneracy with SU(2) symmetry and absorptive corrections in hypercharge-exchange reactions, 25:3388
RIPKA, G., Theory of a self-consistent static field, 25:3739
RIPLEY, Gerald David, Use of man-computer interaction in root-finding and numerical problem-solving, 25:3955 (IS-2416)
RISIK, N. S., Concentration of ^{90}Sr and U in hydrobionts, 25:2546
RISTOW, D., Interpreting curvature in extragalactic radio source spectrum, 25:2847
RIVOLTA, B., Morphological effects of relative movement between solid and liquid in electrochemical processes, 25:2648
RIZZI, Arthur W., Solar wind flow past nonmagnetic planets: Venus and Mars, 25:2878
ROARK, A. L., Stochastic approach to bioburden estimation and prediction, 25:3975 (SC-RR-70-561)
ROBALEWSKI, Andrzej M., Gamma-rays induced graft copolymerization of poly(ethylene terephthalate) with acrylic and methacrylic acids. I, 25:2240
ROBEL, Wolfgang, Complex compounds of hexavalent actinides with pyridine carboxylic acids, 25:2194 (KFK-1070)
ROBERTS, C. N., Direct digital readout and computer calculation of amino acid analysis data, 25:3965 (LA-4507)
ROBERTS, Edmond Jr., Radiation safety in the operation of a low-energy accelerator, 25:3475 (CONF-700322-, pp 441-8)
ROBERTS, Paul A., Screening for x-ray-induced crossover suppressors in Drosophila melanogaster: prevalence and effectiveness of translocations, 25:2561
ROBERTS, T. A., Recovering spores damaged by heat, ionizing radiations, or ethylene oxide, 25:2599
ROBERTSON, B. C., Electromagnetic transitions in ^{19}Ne, 25:3575
ROBINS, I. H., Determination of Gd in irradiated gadolinia/magnesia mixtures, 25:2089
ROBINSON, L. C., Cyclotron resonance experiments of Los Alamos group, 25:3235
ROBINSON, Peter D., Appraisal of an iterative method for bound states, 25:2925
ROBINSON, R. L., Multiple Coulomb excitation of ^{152}Sm, ^{166}Er, and ^{172} ^{174} ^{176}Yb, 25:3662
ROBLE, R. G., Atmospheric response to heating within a stable auroral red arc, 25:2953
ROCHESTER, L. S., Recoil proton polarization in eta photoproduction, 25:3255
RODRIGUEZ, P., Work-hardening parameters of polycrystalline materials, 25:2723
ROEHL, H., Ion density from Stark broadening of H/sub β/, 25:3068
ROEMBERG, E., Carbon transport studies for helium cooled high temperature reactors. project dragon, 25:3860 (DP-Report-491)
ROESLER, F. L., Excitation of ionized helium states in a cooled hollow-cathode discharge, 25:2890
ROGERS, J. W., Fast neutron spectrum measurements, 25:2481
ROHDE, G., Fission of heavy nuclei by helium ions and deuterons, 25:3710
ROLPH, P. M., Iron-54, ^{60}Ni(p,p) and (p,p'γ), 25:3613
ROMABY, R., Pulsar distributions without magnetic decay, 25:2851
ROMANO, A. J., Interaction effects between dissimilar metals in high velocity sodium at temperatures up to

760°C. I. Mass transfer of vanadium onto type 321 stainless steel, 25:2617
RONNANG, B. O., Very-long-baseline interferometry of galactic OH sources, 25:2844
ROOK, Harry L., Determination of oxygen in silicon in the sub-part-per million range by charged-particle activation analysis, 25:2143
ROSE, H. J., Electromagnetic transitions in ^{19}Ne, 25:3575
ROSE, K. S. B., Record of programme and discussions at symposium of papers from Dragon contractors held at A.E.R.E., Harwell, 14--16 March 1966, 25:3774 (DP-Report-439)
ROSENBLATT, G., Solubilities of several transition metals in liquid lead--bismuth eutectic, 25:2709
ROSENBLATT, J., Evidence of a phase transition in an assembly of point contacts, 25:3035
ROSENBLUTH, M. N., Synchrotron radiation in Tokamaks, 25:3095
ROSS, M., Structure of high-energy two-body non-diffractive reactions, 25:3454
ROT, M. L., Quick-response energy transfer in KBr:Tl crystals. I, 25:3193
Quick-response energy transfer in KBr:Tl crystals. II, 25:3194
ROTBARD, Georges, Mechanism of the (^{3}He,α) reaction at low energy, 25:3594 (NP-18464)
ROTHE, Klaus D., On-shell subtracted dispersion relations and low-energy theorems from current algebra, 25:3368
ROTHWELL, Paul L., Quiescent and disturbed proton and electron distributions, 25:2950 (AD-709363)
ROUSSELIN, R. J., Characteristics of two /sup 113m/In generators, 25:2296
ROUX, Alain, Nonlinear frequency shift in whistler and hydrodynamic propagation, 25:3004
ROUYER, Hubert, Hybrid simulation of the dynamics of a battery of mixer--settlers, 25:2384 (CEA-CONF-1579)
ROY, J. C., Mounting an anode wire in 4π proportional counter, 25:2464
ROY, Prodyot, Evaluation of particulates deposited in flowing non-isothermal sodium systems, 25:2616
ROY, R., Chemically stimulated luminescence in rare earth oxides, 25:3213
Proton-recoil spectrometer, 25:2480
ROYER, George W., Calibration of two-stage air samplers, 25:2446
ROZANOV, A. N., Superconducting Zr--Nb ribbon level indicator, 25:2394
RUBBIA, C., Detection of the weak intermediate boson through its hadronic decay modes, 25:3333 (NYO-2171-323)
RUBIN, Edward Stephen, Effects of electrode size on performance of MHD generator, 25:2398
RUDAK, E. A., Effect of tensor forces in residual pair nucleon interaction, 25:3766
RUDD, M. E., Electron spectroscopy with heavy ions, 25:2900 (CONF-700322-, pp 305-19)
RUDENKO, V. N., Effect of temperature and deformation on mechanical characteristics of molybdenum and niobium, 25:2681
Strength of niobium--molybdenum alloys in vacuum at high temperatures, 25:2682
RUDGE, M. R. H., Approximation in scattering theory, 25:2895
RUDIGER, H., Regulating factor in methionine biosynthesis, 25:4002 (UCRL-Trans-10487)
RUDIN, Robert A., Shadow correction in deuterium, 25:3412
RUDNEVA, N. M., Dependence of distance to magnetosphere boundary on longitude, 25:2980
RUDORF, G., Preparation and etching of microsections of zirconium and zirconium--niobium alloys, 25:2656
RUDZITIS, Edgars, Enthalpy of formation of ThF_4 by fluorine bomb calorimetry, 25:2213
RUGGE, C., Prompt de-excitation of fission fragments, 25:3673
RUMBALL, W. M., X-ray line broadening of a quenched Zr--1.25 wt. percent Cr alloy, 25:2719
RUNYAN, J. E., Debye--Scherrer camera filter attachment for use with radioactive specimens, 25:2508
RUPPE, Harry O., Astronautics: an outline of utility, 25:2397
RUSAKOV, A. A., Crystal structure of Mo containing ZrC, 25:2743
Substructure of cast Mo, 25:2744
RUSAKOV, N. V., Measurement of radiative losses in pulsed plasma accelerator, 25:3084
RUSCH, G. K., Final safety analysis report on the use of plutonium in ZPR-6 and -9, 25:3901 (ANL-7442)
RUSHFORTH, R., Platinum and the refractory oxides. III, 25:2160
RUSKOL, Yu. S., Corrosive behavior of alloys of the titanium--molybdenum--chromium system, 25:2613
RUSSELL, R. D., γ-radiolysis of carbon monoxide in presence of γ-alumina, 25:2262 (RD/B/N-1279)
RUTHER, W. E., Evaluation of materials-compatibility problems in the EBR-II reactor, 25:2705
RYBACHENKO, V. F., Spectrum of even-parity low-lying levels for ^{17}O nucleus, 25:3582
RYDBECK, O. E. H., Very-long-baseline interferometry of galactic OH sources, 25:2844
RYDE, H., Low-lying high-spin states in ^{155}Gd, 25:3700
RYDING, G., Atomic physics with a low-voltage tandem, 25:3470 (CONF-700322-, pp 259-79)
RYL'NIKOV, A. S., Charge radii of the nuclei of ^{124} ^{126} ^{128} ^{130}Te, 25:3551
RYSS, I. K., Influence of lower ionosphere on radio-wave reflections from E/sub s/ layer, 25:2994
RYZHOVA, L. V., Reaction of trivalent Am and Cm with Arsenazo III, 25:2079

S

SAAKYAN, G. S., Relativistic generalized theory of gravitation. I, 25:2870
SAAS, A., Liberation of radionuclides from forest bed, 25:2528
SAAVEDRA, I., Foldy--Wouthuysen, Lorentz, and Lorentz-Tachyon transformations, 25:3441
SABET, T. Y., Effects of RES blockade on antibody formation. III, 25:2538
SABRI, Zeinab A., Engineering of a fusion plant-torch complex, 25:3136 (ORO-1171-1, pp 344-75)
SACH, B. T., Effects of gamma radiation on gas yields and crystallinity of PTFE, 25:2261 (NP-18518)
SACH, R. S., Apparatus for the study of radiolytic carbon deposition from the gas phase, 25:2263 (RD/B/N-1748)
SACKMANN, Inga-Juliana, Structure and evolution of rapidly rotating B-type stars, 25:2836
SADOVOI, A. A., Spectrum of even-parity low-lying levels for ^{17}O nucleus, 25:3582
SAEKI, Bunzaburo, Reactions (^{3}He,^{7}Be) and (^{3}He,^{6}Li) on ^{16}O and ^{12}C at 24.5 and 28.0 MeV, 25:3583
SAFFORD, G. J., Graphitization by neutron inelastic scattering, 25:2810
SAGAN, C., Ultraviolet spectrophotometric determination of gallium, 25:2100
SAHA, G. B., Recoil studies of fission products, 25:3702
SAHA, N. N., Effect of x-irradiation on hydra in the presence of arginine and citrulline and study of the radiolytic products, 25:2588
SAIGUSA, T., Calculation of spectra of energy deposited by recoil heavy particles, 25:2568
SAITO, Ryusei, Design of an electron linear accelerator for industrial use, 25:3483
SAITO, T., Densities of pure Fe, Co, and Ni in molten state, 25:4003 (UCRL-Trans-10496)
SAITO, Takesi, Existence of μ^* and duality in weak processes, 25:3350
SAKAI, M., Size distributions of antiphase domains in Cu_3Au, 25:3941 (COO-1431-10)
SAKAMOTO, Y., Impulse approximation in ^{2}H(p,2p)n reaction, 25:3554
SAKANOUE, Masanobu, Nuclear track methods in solids and its development. II, 25:2438
SAKATA, Michinori, Correspondence between ECC γ-ray and spark chamber shower, 25:2487
SAKUMA, Y., Densities of pure Fe, Co, and Ni in molten state, 25:4003 (UCRL-Trans-10496)
SAKURABA, Shukichi, Photochemical reactions of uranyl ions with organic compounds. II, 25:2158
SAKUTA, S. B., Excited states (4p--3h) in reaction ^{13}C(^{6}Li,d)^{17}O and ^{13}C(^{7}Li,t)^{17}O, 25:3570
SALIN, Ph., Exchange degeneracy with SU(2) symmetry and absorptive corrections in hypercharge-exchange reactions, 25:3388
SALMENKOVA, M. A., Isotopic composition of uranium in ground waters, 25:2356
SALOMON, Robert E., Spectroscopic properties of solid solutions of erbium and ytterbium oxides, 25:3211
SAMAIN, A., Dynamic stabilization of a confined plasma, 25:3123
Influence of trapped particles on the drift waves, 25:3149 (CEA-CONF-1616)
SAMARAS, Demetrios George, Some thoughts on the design of a thermonuclear space power system, 25:3138 (ORO-1171-1, pp 387-411)
SAMOSVAT, G. S., Angular distributions of 1 to 40 keV neutron scattering, 25:3695
SAMPSON, C. F., Low temperature cryostat for single crystal and powder x-ray diffraction, 25:3048 (AERE-R-6532)
SAMPSON, W. B., Superconducting synchrotron magnets, 25:3512
SAMUEL, M., Alpha-particle scattering from ^{204} ^{206} ^{208}Pb and ^{209}Bi, 25:3689
SAMUELI, J. J., Use of a Van de Graaff generator to simulate the transient effects due to radiation in semiconductors, 25:3477 (LYCEN-7063)
SANAMYAN, V. A., Low-frequency spectra of extragalatic radio sources, 25:2845
SANDER, Stanley I., Thermal separation of ortho and para forms of H_2 and D_2, 25:2405
SANDERS, R., Angular correlation of 460 keV-27.7 keV gamma--gamma cascade in ^{129}I, 25:3675
SANDLER, J., Neutron--neutron interactions in ^{2}H(d,pp)2n, 25:3549
SANDOR, L. V., Anodic treatment to improve the liquid zinc corrosion resistance of tantalum, 25:2630
SANIKIDZE, D. G., Transformation of first (second) sound into fourth sound in superfluid He, 25:3007
SANJEEVAIAH, B., Production of external bremsstrahlung in different materials, 25:3249
SANJEEVAIAH, H., Production of external bremsstrahlung in different materials, 25:3249

SANTO, R., Reaction (^{3}He,p) on the Ca isotopes, 25:3629
SANTORO, R. T., Approximate high-energy alpha-particle-nucleus-collision model, 25:3716 (ORNL-TM-3153)
SAPIR, Joseph, Twenty-five group cross sections used in Los Alamos Rover program, 25:3530 (LA-4484)
SAPRAGONENE, M. S., Use of chelating reagents in the extraction--photometric determination of elements with basic dyes, 25:2087
SARANTITES, Demetrios G., Structure of ^{51}Cr via ^{48}Ti(^{4}He, nγ) and ^{51}V(p,nγ) prompt γ-ray spectrometry, 25:3593 (COO-1530-21)
SARANTSEV, V. P., Recent work on Dubna collective ion accelerator, 25:3515
SARGA, T., Vinca Nova: automatic unit for neutron spectrometer control, 25:2475 (INP-707)
SASSE, Ronald A., New procedure for purifying H_2O for radiation chemistry, 25:2228
SATO, Sukeyo, High-energy proton--proton scattering, 25:3418
SAUER, P. U., Reaction matrix in finite nuclei, 25:3742
SAUERMANN, P. F., Investigations of decontamination ability of paints, 25:2423
SAUNDERS, A. W. Jr., Filtration of particles of atomic dimensions, 25:2414 (AD-707709)
SAVINA, V. P., Experimental study of the spatial absorbed-dose fields of reactor γ-radiation in a polyethylene sample, 25:2495
  Spatial distribution of absorbed neutron dose in polyethylene, 25:2494
SAVRIN, V. I., Solution of unitarity condition for the elastic scattering amplitude for high energies, 25:3451 (ITF-70-49)
SAVVIN, S. B., New organic reagents for niobium, 25:2199
SAWAI, Takeshi, Evidence for very early effects in the radiolysis of water, 25:2267
SAXENA, A. P., Variation of attenuation of acoustic waves through plasma with ion--plasma frequency, 25:3155
SAXENA, R. P., Deser--Gilbert--Sudarshan representation and electroproduction structure functions, 25:3329
SAXL, I., Interaction between slip dislocations and twins in α-U. II, 25:2696
SAXON, Allan G., Fitting K⁻p → anti K⁰ π⁻p with a generalized Veneziano model, 25:3391
SAXON, D. H., Reactions π⁻p at 456, 505, and 552 MeV/c, 25:3282
SAYER, R. O., Multiple Coulomb excitation of ^{152}Sm, ^{166}Er, and ^{172} ^{174} ^{176}Yb, 25:3662
SCARSI, L., Optical spark chamber for the search of gamma-ray sources, 25:2841 (CEA-CONF-1633)
SCHAEFER, L., Relation between mass spectra and reaction products of electron-irradiated aromatic ketones, 25:2266
SCHAEFER, Robert Anthony, Scattering of laser light by high-density plasmas, 25:3101
SCHAEFFER, D. R., Compatibility of ^{238}Pu dioxide with platinum and platinum--rhodium alloys, 25:2663 (MLM-1684)
SCHAFFHAUSER, A. C., Effect of gas bubbles on recrystallization of tungsten, 25:2736
SCHAMBER, F. H., Isospin splitting of the giant dipole resonance in ^{64}Zn, 25:3623
SCHARNWEBER, Dieter, Structure of the potential energy surface at large deformations, 25:3734
SCHATZ, G., Magnetic moment of level in ^{58}Co, 25:3618
SCHEER, J. A., Reactions (d,n) on ^{11}B, ^{14}N, and ^{15}N, 25:3574
SCHEER, K. E., Radiologic side-effects, 25:2583
SCHEID, W., Partial and total sex-chromosome loss induced by x-rays in mature spermatozoa, 25:2554
SCHEIL, Erich, Magnetic measurements in the copper--manganese system, 25:3972 (ORNL-tr-2398)
SCHEIT, A. N., Apparatus for delivery of gas for flowthrough proportional counter, 25:2453
SCHENLEY, R. L., Control of respiration by DNA in ultraviolet-irradiated Escherichia coli B/r cells, 25:2598
SCHERBL, D., Compatibility tests with UC of differing stoichiometries and Fe--Ni--Cr alloys and the influence of stabilizers, 25:2765 (KFK-1213)
SCHERK, J., Sign of Regge-pole residues in Veneziano model, 25:3453
SCHIERHOLZ, G., Calculation of N anti N bound states from relativistic OBE model and meson spectrum, 25:3358 (DESY-70/49)
SCHIFF, H. I., Measurement of atomic oxygen height profiles in upper atmosphere, 25:2968
SCHIFFERSTEIN, K., Behavior of solid fission products in pyrolytic carbon and graphite, 25:2797
SCHIRBER, J. E., Effect of pressure on the Fermi surface of Zr, 25:3212
SCHIRRA, M., Creep and creep strength of V--Ti and V--Ti--Nb alloys with additions of Si and Ge, 25:2662 (KFK-1193)
SCHLEGEL, W., Reaction (^{3}He,p) on the Ca isotopes, 25:3629
SCHLEICHER, H. W., Formation of Al pearls on surface of SAP alloys, 25:2779
  X-ray microprobe studies of irradiated fuel particles, 25:2812 (DP-Report-320)
SCHLEIN, Peter E., Experimental comparison between on- and off-mass-shell inelasticities in π⁻p scattering. II, 25:3285
SCHLOESSER, J., Parametric survey of the low enriched uranium cycle in a high temperature reactor. project dragon, 25:3883 (DP-Report-466)
SCHMADEBECK, R., Neutron radiative capture methods for surface elemental analysis, 25:2144
SCHMIDT, F., Energy transport by cryogenic cables, 25:3050
SCHMITT, D., Reaction (^{3}He,p) on the Ca isotopes, 25:3629
SCHMITZ, G., Numerical calculations and description of toroidal arcs by model theories, 25:3088
SCHMUESER, P., Proton--neutron elastic scattering on a deuterium target, 25:3266
SCHNEIDER, H., Loading capacity of the Rhine for radioactive nuclides. VI, 25:2350
SCHNEIDER, Joan K., Acetate complexing by trivalent actinide ions, 25:2208
SCHNEIDER, R. A., Properties of the Pu estimate based on weighted Pu/U values, 25:2417 (BNWL-SA-3287)
SCHNEIDER, W. F. W., Mass-identification by time-of-flight methods, 25:2469
SCHNEPEL, Gerd Henning, Electron spin resonance spectroscopy of free radicals, 25:2289
SCHNOBRICH, W. C., Lumped-parameter analysis for shear failure in the end slab of cylindrical PCRV, 25:2411 (TID-25573)
SCHOFILL, J. L. Jr., Investigation of the convective-diffusion limited oxidation of molybdenum by the rotating disk method, 25:2688
SCHOLEFIELD, E. H., Superconducting two tesla bending magnet, 25:3504
SCHOLZ, H., Creep and creep strength of V--Ti and V--Ti--Nb alloys with additions of Si and Ge, 25:2662 (KFK-1193)
SCHOWEN, R. L., Evidence for proton transfer concomitant with hydride expulsion from silanes, 25:2176
SCHREIBER, B., Investigation of ^{65}Zn by (p,n) and (p,nγ) experiments, 25:3631
SCHREINER, Philip A., Fitting K⁻p → anti K⁰ π⁻p with a generalized Veneziano model, 25:3391
SCHROCK, S. L., Effects of exposure to flowing sodium on vanadium alloys in stainless steel containment systems, 25:2621
  Sodium corrosion of Westinghouse liquid metal fast breeder reactor (LMFBR) materials, 25:2619
SCHROEDER, E., Fuel cycles and reactor physics feed/breed and other Th cycles, 25:3884 (DP-Report-469)
SCHROEDER, John, Variational solution of the Schroedinger equation of finite fermion systems. II, 25:3242
  Variational solution of the Schroedinger equation of finite fermion systems. I, 25:3241
SCHULER, Robert H., Effect of ion and radical scavengers on the cyclohexyl radical yield in the radiolysis of cyclohexane, 25:2268
SCHULTZ, J., Prog. rpt. on new heavy bosons in proton--antiproton interactions, 10/1/69--9/30/70, 25:3261 (UCI-34-P-149-1)
SCHULZ, H., Multi-step stripping on deformed nuclei, 25:3732
SCHULZ, R. J., Values of C /sub lambda/ for polystyrene and lucite, 25:2569
SCHUMACHER, G., Considerations on coated particles, with oxide fuel, and graphite and Si carbide coating, for GCFR application, 25:3875 (EURFNR-834)
SCHUNK, Robert W., Minor-ion diffusion in F2 region, 25:2962
SCHUNN, R. A., Interaction of transition metal hydride complexes with deuterium, ethylene-d_4, and 1-butene, 25:2170
SCHUSTER, Ronald E., Direct proton magnetic resonance cation hydration study of uranyl perchlorate, nitrate, chloride, and bromide in water--acetone mixtures, 25:2209
SCHWARTZ, M., Absorption of ^{51}Cr-EDTA in ulcerative colitis, 25:2534
  Harmonic absorption of microwaves in magnetized low-density plasma, 25:3145 (CEA-CONF-1607)
SCHWARZ, John H., Basic operators of the dual-resonance model, 25:3353
SCHWEBER, S. S., Electromagnetic many-body forces, 25:3328
SCHWEIKERT, Emile A., Determination of oxygen in silicon in the sub-part-per million range by charged-particle activation analysis, 25:2143
SCHWENDIMAN, L. C., Some observations on noble gas partitioning in dynamic air-water systems, 25:3892 (BNWL-SA-3360)
SCHWENN, R., Radial distribution of electric field strength in hydrogen arcs, 25:3083
SCIESINSKI, J., Vinca Nova: automatic unit for neutron spectrometer control, 25:2475 (INP-707)
SCOTT, A. D., Prog. rpt. on exchange of interlayer cations in micaceous minerals, annual, 9/30/69--9/30/70, 25:3943 (COO-1680-10)
SCOTT, C. K., Calculation of Coulomb energy differences, 25:3770
SCOTT, D. K., Heavy-ion reactions as a technique for direct mass measurements of unknown Z > N nuclei, 25:3610
SEAMARK, R. F., Oxidative and glycolytic activity of ejaculated ram spermatozoa in the presence of steroid hormones, 25:2519
SEARLE, A. G., Induction of translocations in mouse spermatogonia. III, 25:2553
SEARS, V. F., High-energy neutron scattering from liquid ^{4}He. II, 25:3049
SECHRIST, C. F. Jr., Measurement of average electron

XUM

density between 75 and 80 kilometers, 25:2952 (N-70-33955)
SEDDON, W. A., Free radicals in γ-irradiated disodium succinate. II, 25:2230
SEDRAKYAN, D. M., Internal solution for stationary axially symmetric gravitational fields, 25:2828
SEEGER, Alfred, Superconductivity and physical metallurgy, 25:3025
SEIFER, Arnold D., Statistics of a random plus constant vector with application to acoustic and electromagnetic-wave scattering, 25:3239
SEISEBAEV, A. T., Activity of redoxy enzymes in beans and clover following γ irradiation, 25:2596
SEL'DYAKOV, Yu. I., Isotopic composition of uranium in ground waters, 25:2356
SELIVANOV, G. I., Electric discharge of gas bubbles in liquids, 25:2485 (JINR-P13-5277)
SELLE, J. E., Compatibility of ^{238}Pu dioxide with platinum and platinum--rhodium alloys, 25:2663 (MLM-1684)
SELLIN, I. A., Atomic physics of fast ion beams: fine structure experiments, 25:2889 (CONF-700322-, pp 289-95)
SELMAN, G. L., Platinum and the refractory oxides. III, 25:2160
SENFTLE, F., Neutron radiative capture methods for surface elemental analysis, 25:2144
SEN GUPTA, N. D., Solution of Dirac equation in magnetic field, 25:3230
SENGUPTA, S., Solid state isotopic exchange in radiocobalt doped trisdripyridyl Co(III) perchlorate, 25:2191
SEPTIER, A., Radial motion of electrons and emittance from low-energy superconducting linear accelerator, 25:3518
SEREGINA, G. P., Effect of nuclear radiation on the physicomechanical properties of lacquer coatings, 25:2822
SERENKOV, V. I., Electric breakdown in plastics irradiated with charged particles, 25:2225
Radiolysis of original and reinforced ED-5 type epoxy resin, 25:2273
SERGEEV, V. I., Electric breakdown in plastics irradiated with charged particles, 25:2225
SERGIENKO, V. F., Semiconductor layers and structural changes produced in diamond by ion implantation, 25:3199
SERYAKOVA, I. V., Use of chelating reagents in the extraction--photometric determination of elements with basic dyes, 25:2087
SESSIONS, C. E., Influence of titanium on the high-temperature deformation and fracture behavior of some nickel-based alloys, 25:2725
SESTAK, B., Velocity relations in the rail accelerator without an external magnetic field, 25:3077
SETH, Kamal K., Spectroscopy of $^{65\ 67\ 69}$Ga by (d,n) reaction, 25:3625
Spectroscopy of even tin isotopes by inelastic scattering of protons, 25:3668
SETH, V. P., Exotic exchange state and new sum rules, 25:3404
SETHI, Suman, Separation of ^{234}Th from inactive Th, U, and Fe by adsorption on $Bi(IO_3)_3$, $Bi(IO_4)_3$, or $Pb(IO_3)_2$, 25:2341
SETLOW, Jane K., Ultraviolet action spectra for mutation in Escherichia coli, 25:2557
SEVERIN, N. F., Electroproduction of pions on a proton at threshold and structure of the nucleon, 25:3244
SEVERNY, A. B., Asymmetry of moustaches, 25:2863
SEVRYUGIN, V. V., Properties of extruded Mo, 25:2697
SEWERYNSKI, M., Gauge invariance and helicity conservation in high-energy meson--baryon scattering, 25:3403
SHAH, K. R., Determination of lead by fast neutron inelastic scattering, 25:2137
SHANNON, D. W., Radioactive material transport in flowing sodium systems, 25:2706
SHANNON, L. V., Determination of ^{210}Po and ^{210}Pb in seawater, 25:2112
SHAPIRA, A., Δ^{++}(1236) Δ^{-}(1236) production in pn collisions, 25:3265
SHAPIRO, B. S., Parameters of F2 and F1-layers and prediction of diurnal N(h)-profiles, 25:2988
SHAPIRO, Charles Stephen, M1 gamma-ray strength functions for deformed nuclei, 25:3683
SHAPIRO, I. S., Regge trajectories and nuclear structure, 25:3723
SHAPIRO, Stuart J., Spectral emittance of Nd, Sm, Er, and Yb oxides at high temperatures, 25:3204 (AD-708547)
SHAPPERT, L. B., Savannah River Americium--Curium Slug Carrier, 25:2421 (ORNL-TM-3110)
SHARADZE, Z. S., Drift of small-scale inhomogeneities in ionospheric F2 layer, 25:2986
SHARMA, R. P., Unique first-forbidden beta transitions in deformed nuclei, 25:3672
SHARPEY-SCHAFER, J. F., Proton stripping to particle-hole states in ^{40}Ca and ^{42}Ca, 25:3627
SHASTRI, A. G., Theoretical design of the experiment to study scattering of electrons and positrons by electrons, 25:3245
SHAW, John Graham, Thermomigration in metal-interstitial solid solutions, 25:2666 (NP-18468)
SHAW, R. W. Jr., Proton induced fission of ^{233}U and ^{238}U, 25:3660
SHCHEKOTOV, O. E., Possibilities of a shock tube in obtaining and investigating a dense low-temperature plasma, 25:3116
SHCHEPKIN, L. A., Diurnal variations of ionic structure in F1 region, 25:2987
SHEINA, N. M., Use of N-benzoyl-o-tolylhydroxylamine in method of amperometric titration. III, 25:2082
SHEKHTMAN, A. Z., Role of boundary singularities in superconductivity, 25:3030
SHELINE, R. K., Two-quasiparticle states in ^{164}Ho, 25:3711
SHENDEROVICH, A. M., Studies of resonances of nonlinear synchrotron oscillations, 25:3488
SHEPHERD, G. R., Direct digital readout and computer calculation of amino acid analysis data, 25:3965 (LA-4507)
SHEPPARD, D. M., High spin states in ^{55}Fe, 25:3624
SHERIF, Sh. A., Extraction of niobium from aqueous organic acid media by structurally related tert-amines, 25:2334
SHERMAN, Nevin W., Systematic development of difference formulae, to arbitrary order, for the numerical differentiation and integration of a Taylor-expansible function, 25:3993 (UCRL-50874)
SHERWOOD, Harold Frank, Radiation sensitive materials, 25:2471
SHIGEMATSU, A., Tracer technique for behavior of dusts in animal lungs, 25:2523
SHIGEMATSU, Tomomichi, Optimum planning for radiation facilities, 25:2389
SHIGIN, V. A., Neutron-induced ^{249}Bk fission, 25:3665
SHIH, Katherine Lu, Effects of x-irradiation and gamma irradiation on paramutation in R heterozygotes in maize, 25:2560
SHILOVA, N. S., Geophysical activity of solar flares as function of brightness emission of metals, 25:2859
SHIMIZU, T., Spectrophotometric determination of Sc with 4-(2-thiazolylazo)resorcinol, 25:2093
SHIMOURA, Kazukuni, De-watering of radioactive sludge by super-decanter centrifuge, 25:2344
SHIOKAWA, T., Chemical behavior of ^{60}Co in aqueous solutions of neutron-irradiated Na ethylenediaminetetraacetatocobaltate/III/ tetrahydrate, 25:2297
SHIRAI, Eiji, Thermal conductivity of VIPAC UO_2 fuel. II, 25:2813 (JAERI-Memo-4128)
SHIRMER, G., Investigation of proton polarization in reaction $^{12}C(^3He,p_0)^{14}N$, 25:3563 (JINR-P15-5156)
SHITOVA, E. V., Crystallization of amorphous films of silicon dioxide during ionic bombardment and subsequent annealing, 25:2823
SHIVAROVA, A., Low-frequency resonances and averaged potential in non-isothermal plasma, taking account of ion collisions, 25:3165
SHLEIEN, Bernard, Ion exchange beads as calibrated microscopic radioactivity sources, 25:2406
SHLIONSKII, Sh. G., Finding N(h) profile by computer techniques, 25:2974
SHORT, R. D., New approach to the Reggeon calculus. II, 25:3456
SHOTTER, A. C., Heavy-ion reactions as a technique for direct mass measurements of unknown Z > N nuclei, 25:3610
SHPIL'RAIN, E. E., Working substance for single-component liquid-metal MHD units, 25:2937
SHTRIKMAN, S., Resolving power of coincidence Moessbauer spectroscopy, 25:2483
SHUBKO, V. M., Neutron-induced ^{249}Bk fission, 25:3665
SHUFELDT, R., Movement of ^{90}Sr in soils, 25:2365
SHULEPOV, V. I., Crystal structure of Mo containing ZrC, 25:2743
Distribution of C in cast Mo, 25:2702
Effect of C on Mo and Mo alloys, 25:2745
SHUMILOV, O. I., Meridional movement of auroral absorption bays, 25:2979
SHUSTIN, E. G., Transformation of the distribution function of an electron beam during cyclotron interaction with a plasma, 25:3080
SICHEV, B. S., Attenuation of scattered synchrocyclotron radiation in a shield, 25:3480
SICK, I., Elastic electron--nickel scattering, 25:3687
Electron scattering from ^{12}C and ^{16}O, 25:3587
SIDDAL, R. E., Determination of total C in SiC coated Dragon fuel particles, 25:2064 (DP-Report-494)
SIDORENKO, O. N., Properties of extruded Mo, 25:2697
Properties of hydroextruded Mo, 25:2698
SIDORIN, V. P., Attenuation of scattered synchrocyclotron radiation in a shield, 25:3480
SIDOROV, V. P., Low-frequency instabilities of the high-frequency skin layer in a plasma with non-uniform parameters, 25:3121
SIDORUK, A. M., Water-dielectric generator for producting intensive fast-electron and hard decelerated x-ray pulses, 25:3478
SIEGEL, S., Bubble corrections to two-body matrix elements, 25:3759
SIEGWARTH, J. D., Upper limit on electron--phonon interaction in vanadium carbide, 25:3034
SIEJKA, Juliusz, Energy transfer in the Al/Al_2O_3 system. II, 25:2276
SIELEMANN, R., Magnetic moment of level in ^{58}Co, 25:3618
SIERRA, J., D_0 acidity function in deuterium sulphate solutions at 25°C, 25:2175
SIFFERLEN, R., Continuous and discontinuous precipitation

reactions in U--1.5 percent Mo alloys, 25:2738
SIGNELL, Peter, Fixed-u finite-energy-sum-rule calculations and the CERN π-N amplitudes, 25:3396
SIGNORINI, C., Spins and mean lives of ^{34}Cl levels, 25:3619
SIGOV, Yu. S., Nonlinear problem on collision of antiparallel flows of a rarefied plasma, 25:3089
SIKAND, M. S., Effective mass of alpha particles in superfluid nuclear matter, 25:3728
SIKKELAND, T., Tracer chemical studies of Lr, 25:2197
SILBAR, R. R., Beam ellipse matching, 25:3521
SILCOX, J., Prog. rpt. on hard superconducting materials, annual, 12/69--11/70, 25:3019 (NYO-3029-48)
SILEVITCH, M. B., Nonlinear conductivity--ternary correlation relations in nonrelativistic plasmas, 25:3090
SILIN, I. N., Description of experimental data on πN and KN scattering in high-energy region on basis of complex angular moments theory. I, 25:3381 (JINR-P2-5320)
SILK, M. G., Some efficiency calculations for ^{6}Li suspended target semiconductor sandwich spectrometers, 25:2473 (AERE-R-6318)
SILL, Claude W., Sources and prevention of recoil contamination of solid-state alpha detectors, 25:2479
SILVA, R., Tracer chemical studies of Lr, 25:2197
SILVER, R., Distributions of charged pions, 25:3370
SIMBEL, M. H., Nuclear diffraction scattering, 25:3757
SIMON, Michel, Program IGOR, 25:3525 (CEA-N-1312)
SIMONINI, R., Effects of the direct inelastic scattering anisotropy for fast neutrons in sodium, 25:3635
SIMONOV, V. M., Spherically shaped cartridges for extended sources in pilot and full-scale radiation-chemical processors, 25:2404
SIMONOV, Yu. A., Hyperspherical-expansion approach to nuclear bound states. I, 25:3730
Positivity conditions for velocity-dependent and quadratic spin--orbit potentials, 25:3737
SIMONOVA, L. N., Bismuthiols as analytical reagents, 25:2070
SINGER, R. M., Measurements of the solubility of iron and chromium in sodium, 25:2712
Segregation of impurities and the formation of particles in sodium systems, 25:2713
SINGH, Bijai, New approach to the equilibrium configuration of stellar envelopes, 25:2827
SINGH, M., Incoherent scattering of gamma rays by K electrons, 25:2909
SINGH, S. K., Possible effects of lepton non-locality in the decays K → πe^{+}e^{-} and K → π ν anti ν, 25:3337
SINGH, S. R., Comparison of two perturbation methods, 25:3229
SINGH, Vikram, g-factor of 1127.8 keV, 2^{++} second excited state in ^{106}Pd, 25:3664
SINGH NAGI, A. D., Depression in order parameter of a superconductor with Kondo effect, 25:3022
SINHA, A. K., Model lead and radiometric ages from Churchill Province, Canadian Shield, 25:2353
SINHA, S. K., Effect of x irradiation on ferroelectric properties of barium titanate single crystal, 25:3196
SINITSYN, B. I., Spatial, energy, and angular distributions of neutrons in lithium, 25:3538
SINKEVICH, O. A., Existence of Newtonian-velocity sound in plasma, 25:3156
SINTSOVA, I. T., Mechanical properties and corrosion resistance of steel coated with titanium and zirconium carbonitrides, 25:2612
SISAKYAN, A. N., Poisson distribution of secondary particles in straight-line paths approximation, 25:3407 (JINR-E2-5329)
SISTEK, I., Radiation oxidation of liquid dodecane, 25:2292
SITENKO, A. G., Contribution to the theory of echo phenomena in a plasma, 25:3164
Electrodisintegration of light nuclei, 25:3714 (ITF-70-35)
SITTIG, Marshall, Pure chemical elements for semiconductors, 1969, 25:3219
SIVAKOVA, E. V., Effect of oxidation on the emissivity of molybdenum disilicide coatings, 25:2799
SIVERS, Dennis, Possible binding of a magnetic monopole to a particle with electric charge and a magnetic dipole moment, 25:3322
SIVERTSEN, John M., Local atomic arrangement in In--Pb alloys, 25:3207
SIZIKOV, V. S., Model of the mass distribution in M 31. I, 25:2866
SIZOO, A. H., Arctic ionosphere and aurora: airborne investigations, 25:2949 (AD-709359)
SIZOV, I. V., Investigation of proton polarization in reaction ^{12}C(^{3}He,p$_{0}$)^{14}N, 25:3563 (JINR-P15-5156)
SJOEBERG, H. E., Retention of oral ^{47}Ca in patients with intestinal malabsorption, 25:2531
SKAREK, P., Radiative pion capture in ^{12}C, 25:3550
SKINNER, R. F., Apparatus for the study of radiolytic carbon deposition from the gas phase, 25:2263 (RD/B/N-1748)
SKLYAREVSKII, V. V., Investigation of suppressed nuclear absorption of resonant γ rays under Laue diffraction conditions, 25:3225
SLATTER, D. De L., Oxidation of zirconium alloy in liquid sodium at different oxygen levels, 25:2611 (PEL-201)
SLAUGHTER, G. M., Corrosion of advanced steam generator alloy weldments in steam, 25:2636
SLOBODRIAN, R. J., Proton-recoil spectrometer, 25:2480
SLUTSKER, S. M., Measurement of ionospheric parameters from Doppler and Faraday effects of coherent signals, 25:2971
SMART, D., Ocular hazard of CW lasers, 25:2591
SMETANIN, A. A., Determination of fast neutron flux, 25:2443
SMID, A., Kinetic model of stem-cells and proerythroblasts populations in the postirradiation bone marrow injury, 25:2590
SMIRDOVA, N. I., Luminescence of neodymium and europium in cerium dioxide and its use in analysis, 25:2083
SMIRENKIN, G. N., Fragment angular distributions and channel analysis of fission of ^{232}Th by neutrons, 25:3680
SMIRNOV, B. M., Resonance charge exchange between a molecular ion and diatomic molecule, 25:2912
SMIRNOV, E. A., Diffusion in W and Nb, 25:2703
Diffusion of Mo and Nb in Zr, 25:2704
Self-diffusion in binary systems, 25:2701
SMIRNOV, G. V., Investigation of suppressed nuclear absorption of resonant γ rays under Laue diffraction conditions, 25:3225
SMITH, A. J. S., Search for violation of CP invariance in tau^{+-} decay, 25:3427
Wire-spark-chamber system with on-line computers, 25:2491
SMITH, D. L., Application of thermodynamic and kinetic parameters of the V--O--Na system to the sodium corrosion of vanadium-base alloys, 25:2622
SMITH, D. L. G., Determination of total C in SiC coated Dragon fuel particles, 25:2064 (DP-Report-494)
SMITH, F. G., Frequencies for radio astronomy, 25:2852
SMITH, Gerald A., Experimental comparison between on- and off-mass-shell inelasticities in π-p scattering. II, 25:3285
SMITH, K., Calculation of electron scattering and photoionization cross sections, 25:2903
SMITH, P. F., Rutherford Laboratory superconducting synchrotron program, 25:3514
Superconducting energy transfer systems, 25:3513
SMITH, V. H. Jr., Comparison of two perturbation methods, 25:3229
SMITHERS, D., Primary yields in γ-radiolysis of ammonia, 25:2283
SMITHWICK, Grover, Radiation safety in the operation of a low-energy accelerator, 25:3475 (CONF-700322-, pp 441-8)
SNEDKOV, B. A., Role of instabilities of monoenergetic electron beams, 25:3479
SNIHS, J. O., Whole-body measurements on distribution of ^{203}Hg in humans, 25:2533
SNIPES, W., Role of hydrogen atoms in free radical site migration, 25:2246
SNOWDEN, K. U., Effect of temperature on logarithmic creep of Zy-2, 25:2693
SOBKOWSKI, Jerzy, Radiolysis of aqueous sulphuric acid solutions, 25:2265
SOBOLEV, V. G., Statistical patterns of auroral hydrogen emission, 25:2976
SOBRA, K., Velocity relations in the rail accelerator without an external magnetic field, 25:3077
SOLODIKHINA, L. D., Spherically shaped cartridges for extended sources in pilot and full-scale radiation-chemical processors, 25:2404
SOLODOVNIKOV, G. K., Measurement of total electron content in the polar ionosphere from the recorded signals of the 3d satellite, 25:2983
SOLOIMSKII, B. E., Production of marine reactors and steam generators, 25:3918
SOLOV'EV, G. I., Properties of uranium oxycarbides, 25:2809
SOMLYAY, Z., Problems of gamma--gamma logging in ore mining in Mecsek, 25:2347 (CSIRO-Trans-10140)
SOMMERMEYER, K., Chemiluminescences of aqueous Tl/sup I/ solutions produced by irradiation, 25:2232
SOMORJAI, R. L., Integral-transformation trial functions of the fractional-integral class, 25:2928
SON, Hyeongjin, Environmental contaminations due to Chinese nuclear explosion tests Oct. 1964 to Jan. 1969, 25:2368
SOOD, S. P., Temperature effects in the gamma-initiated polymerization of styrene, 25:2245
SOREMARK, R., Penetration of radioactive isotopes through enamel and dentine. II, 25:2532
SORLINI, C., Microbial degradation of aromatic hydrocarbons used as reactor coolants, 25:2327
SOTOBAYASHI, Takeshi, Separation and detection of ^{181}W and ^{185}W from radioactive fallout, 25:2110
SOTONA, M., Brueckner reaction matrix and separable potentials, 25:3548
Realistic forces and deformed state admixtures in ^{18}O, 25:3580
SOTSKOV, Yu. P., Radioactivation determination of Ta in minerals and rocks with a Ge(Li)-spectrometer, 25:2139
SOUBBARAMAYER, Space--time evolution of Tokamak-type plasma, 25:3052 (CEA-CONF-1595)
SOUDER, P. A., Search for violation of CP invariance in tau^{+-} decay, 25:3427
Wire-spark-chamber system with on-line computers,

XUM

25:2491
SOUSSELIER, Yves, Handling and transport of irradiated fuels, 25:2424
SOUTHERN, J. F., Relation between mass spectra and reaction products of electron-irradiated aromatic ketones, 25:2266
SOUTHWOOD, J. R. M., Boilers for nuclear plant, 25:3900
SOWASH, Laurence J., Fixed-u finite-energy-sum-rule calculations and the CERN π-N amplitudes, 25:3396
SPALEK, A., Gamma-ray spectrum of ^{192}Au, 25:3654
Transition multipolarities in decay of /sup 197m/Hg, 25:3682
SPALEK, G., Scattering of 7.8-MeV polarized neutrons from ^{4}He, 25:3557
SPAULDING, J. D., Charged particle excited x rays, 25:2882 (CONF-700322-, pp 113-24)
SPELLMEYER, B., Magnetic moment of level in ^{58}Co, 25:3618
SPERR, P., Constant fraction trigger, 25:2458
SPICER, B. R., Stabilization of Pu β phase in Pu--Ti alloys, 25:2739
SPIGER, R. J., Neutron--neutron interactions in ^{2}H(d,pp)2n, 25:3549
SPIRIDONOV, A. I., Isotopic composition of uranium in ground waters, 25:2356
SPIRIDONOV, F. M., Physico-chemical properties of coprecipitated holmium and zirconium hydroxides and holmium, and hafnium hydroxides, 25:3977 (SC-T-70-4041)
System HfO_2--Er_2O_3, 25:3978 (SC-T-70-4043)
SPITSYN, V. I., Influence of radioactive radiation on the heterogeneous equilibrium in the system solid--solution, 25:2222
SPOONCER, W. W., Radiation-induced polymerization of isobutylene oxide, 25:2256
SPREITER, John R., Solar wind flow past nonmagnetic planets: Venus and Mars, 25:2878
SPREVAK, D., Calculation of the coherent neutron scattering from polycrystalline beryllium, 25:3533
SPYROU, N. M., Application of Compton-scattering techniques to activation analysis: a short evaluation, 25:2140
SQUIER, G. T. A., Angular distributions of ^{4}He(p,d)^{3}He, ^{4}He(p,t)2p, ^{4}He(p,^{3}He)pn, and ^{3}He(p,d)2p, 25:3555
System p-^{3}He at 30 and 50 MeV, 25:3556
SREDNIAWA, B., Physical bounds for the components of statistical tensors, 25:3296
Physical bounds for the components of statistical tensors, 25:3295 (TPJU-12/70)
STAFFORD, W., Prevention of alpha counter contamination by electrodeless discharge deposition of Si_3N_4, 25:2478
STAMMBACH, Th., Scattering of 7.8-MeV polarized neutrons from ^{4}He, 25:3557
STANEK, Z., Velocity relations in the rail accelerator without an external magnetic field, 25:3077
STANKEVICH, Yu. L., Possibility of induced amplification of characteristic x radiation, 25:2894
STANNARD, Kent M., Very-long-baseline interferometry of decametric radiation from Jupiter, 25:2879
STANNETT, V., Applications of accelerators in the radiation chemistry of polymers, 25:2218 (CONF-700322-, pp 345-56)
STARODUBTSEV, S. V., Polynomial approximation of the fast neutron spectrum measured by threshold detectors, 25:2442
STAROVATOV, A. A., Relationship between the geomagnetic field and the sporadic E layer, 25:2995
STAROVEROV, V. B., Exponential angular coefficients of neutrons for hydrogen-free media, 25:3171
STARTSEV, V. I., Quasi-elastic scattering of 1115-MeV electrons by nucleons of ^{32}S nuclei, 25:3615
STAVINSKII, V. S., Spin dependence of density of excited nuclear states, 25:3765
STECH, Berthold, Commutators and Lorentz covariance, 25:3298
Local current commutators, 25:3299
STECURA, Stephan, Solubilities of molybdenum, tungsten, vanadium, titanium, and zirconium in liquid potassium, 25:2714
STECURA, Stephen, Apparent solubilities of commercially pure and oxygen-doped tantalum and niobium in liquid potassium, 25:2664 (N-70-32146)
STEELE, T. W., Determination of niobium and tantalum by chromatographic method, 25:2066 (NIM-834)
Determination of uranium in ore samples by liquid--liquid extraction and spectrophotcmetric determination, 25:2067 (NIM-906)
STEFFEN, G., Chemiluminescences of aqueous Tl/sup I/ solutions produced by irradiation, 25:2232
Luminescence of aqueous Tl/sup I/-solutions after irradiation, 25:2233
STEIGMAN, M., Charge/discharge machine for Dragon reactor, 25:2385 (DP-Report-230)
STEINDLER, M. J., Fuel cycle technology quarterly report, April, May, June 1970, 25:2306 (ANL-7735)
STEINSCHADEN, K., Use of thin film solar cells in radiovoltaic generators, 25:2400 (CEA-CONF-1623)
STELSON, P. H., Multiple Coulomb excitation of ^{152}Sm, ^{166}Er, and $^{172\ 174\ 176}$Yb, 25:3662
STEPANETS, O. V., Radioactivation determination of impurities in yttrium and molybdenum by means of extraction displacement chromatography, 25:2138
STEPHENSON, James B., Boron and boron carbide coatings by vapor deposition, 25:2777
STERLIN, Ya. M., Metallurgy of plutonium, 25:2658 (AEC-tr-7095)
STERN, Frank, Proceedings of the Tenth International Conference on the Physics of Semiconductors, Cambridge, Mass., 8/17--21/70, 25:3185 (CONF-700801)
STEVENS, Jack G., Distribution of polysomes in mouse brain tissue, 25:3986 (UCLA-12-796)
STEVENS, John R., Proton energy distributions from 0.060 to 3.3 MeV at 6.6 earth radii, 25:2951 (AD-709723)
STEVENS, P. N., Use of discrete ordinates S/sub n/ method in radiation shielding calculations, 25:3175
STEWART, Jack D., Shear spinning rewards designer with automatically precise parts, 25:2650
STEWART, K. B., Properties of the Pu estimate based on weighted Pu/U values, 25:2417 (BNWL-SA-3287)
STEWART, N. M., Angular distributions of ^{4}He(p,d)^{3}He, ^{4}He(p,t)2p, ^{4}He(p,^{3}He)pn, and ^{3}He(p,d)2p, 25:3555
System p-^{3}He at 30 and 50 MeV, 25:3556
STIEGLER, J. O., Effect of helium on void formation in irradiated stainless steel, 25:2761
STIMLER, M., Transient response of cobalt self-powered neutron detectors, 25:2467
STOCH, H., Determination of niobium and tantalum by chromatographic method, 25:2066 (NIM-834)
Determination of uranium in ore samples by liquid--liquid extraction and spectrophotometric determination, 25:2067 (NIM-906)
STOKKE, Torvald, Further studies on the radiosensitivity of the rat incisor, 25:2592
STOLARCZYK, Lech W., Gamma-rays induced graft copolymerization of poly(ethylene terephthalate) with acrylic and methacrylic acids. I, 25:2240
Radiation induced graft terpolymerization of poly(ethylene terephthalate). I, 25:2244
STOLPOVSKII, V. G., Relationship between outer-belt electron intensity and geomagnetic activity indexes, 25:2969
STOLT, Kaj Gunnar, Atom probe field ion microscope, 25:3991 (UCRL-20303)
STONIER, D. R., Impurity removal from Dragon reactor during initial commissioning, 25:3862 (DP-Report-553)
STORIZHKO, V. E., Distribution of radiation widths from (p,γ) reactions, 25:3767
STORK, Donald H., Fitting K^{-}p → anti K^{0} π^{-}p with a generalized Veneziano model, 25:3391
STORM, Derek W., Energy dependence of quasifree scattering in the D(p,pn)p reaction, 25:3547 (RLO-1388-126)
STOW, G., Post-irradiation gas release measurements on fuel elements from Dragon reactor, 25:3870 (DP-Report-497)
STRAIN, R. V., Evaluation of materials-compatibility problems in the EBR-II reactor, 25:2705
STRAUSS, B. P., Superconducting two tesla bending magnet, 25:3504
STREL'TSOV, V. N., Invariance of nonrelativistic Hamiltonian--Jacobi equation in presence of electromagnetic field, 25:3430 (JINR-P2-5373)
Invariants in the nonrelativistic approximation, 25:3434 (JINR-P2-5363)
Limiting transition from nonrelativistic quantum mechanics to classical mechanics, 25:3935 (BNL-tr-354)
STRINDEHAG, O., Transient response of cobalt self-powered neutron detectors, 25:2467
STRIZHENKO, V. S., Calculations of electrostatic energy analyzer for solid and hollow cylindrical beams of charged particles, 25:3487
STROHBUSCH, U., Reaction ^{28}Si(d,p)^{29}Si mechanism, 25:3606
STRUBLE, G. L., Generalized pairing in light nuclei. II, 25:3722
STRZALKOWSKI, A., Real part of the alpha--nucleus potential, 25:3755
Structure of the low lying levels of the ^{33}S nucleus, 25:3597
STUBBS, T. F., Nuclear cratering on a digital computer, 25:2381 (UCRL-50898)
STUERZER, U., Rapid methods for estimation of content of radioactive cations in water, 25:2117
STUMP, Ronald K., Computerized fully automatic analytical mass spectrometer. I, 25:3999 (UCRL-50931(Pt.1))
SUAYA, Roberto, Analysis of differential and total cross-section data for high-energy pp and p anti p interactions, 25:3411
SUBBARAYA, B. H., Irregularities in night-time equatorial E region, 25:2963
SUBOTOWICZ, Mieczyslaw, Isotopic analysis of moon soil and rocks, 25:2881
SUD, S. P., Decay of ^{124}Sb, 25:3657
SUGIMOTO, Daiichiro, Mixing between stellar envelope and core in advanced phases of evolution. I, 25:2825
SUGIYAMA, Sakae, Simulator for BWR type Tsuruga nuclear power station, 25:3933
SUH, I. H., One phonon excitation in titanium hydride by low energy neutrons, 25:3536
SULC, Petr, EL 600: fuel management studies, 25:3866 (CEA-N-1379)
SULLIVAN, D. B., Generation of harmonics and subharmonics of Josephson oscillation, 25:3037
SULLIVAN, J. C., Oxidation of neptunium(III) by oxygen and hydrogen peroxide, 25:2155
SUMBAEV, O. I., Charge radii of the nuclei of $^{124\ 126\ 128\ 130}$Te, 25:3551
SUMITA, Kenji, Pulsed neutron research in Japan, 1965--70,

25:3927 (JAERI-Memo-4109)
Reactor neutron fluctuation simulator using pulsed neutron source, 25:3932
SUMMERS, Audrey L., Solar wind flow past nonmagnetic planets: Venus and Mars, 25:2878
SUMMERS, R. N., E/sub s/ layer characteristics determined from spaced ionosondes, 25:2957
SUMMERSON, Colleen D., Determination of uranium in ore samples by liquid--liquid extraction and spectrophotometric determination, 25:2067 (NIM-906)
SUN, C. R., Deuteron--deuteron scattering at 2.2 and 7.9 GeV/c, 25:3415
SUNDARAM, A., High-energy photoproduction of pseudoscalar mesons in a quark model, 25:3321
SUNKO, Dionis E., Thermodynamic and kinetic secondary isotope effects in the Cope rearrangement, 25:2188
SUROEGIN, L. M., Universal nomograms for calculating absorbed doses from plane radiators, 25:2566
SURRATT, R. E., Rapid emittance scanner, 25:3498
SUTCLIFFE, B. T., Methods of molecular quantum mechanics, 25:2927
SUVOROV, A. P., Spatial, energy, and angular distributions of neutrons in lithium, 25:3538
SUZUKI, Isamu, Design of an electron linear accelerator for industrial use, 25:3483
SUZUKI, Katsumichi, High excited levels of ^{27}Al, 25:3600
SUZUKI, Nobuo, Distribution of TTA and its Sc chelate into ether solvents, 25:2345
SUZUKI, T., Target preparation, 25:2655
SUZUKI, Toshio, Separation and detection of ^{181}W and ^{185}W from radioactive fallout, 25:2110
SWAMY, K. S. K., Narrow-band infrared photometry of α Ori, 25:2826
SWANN, C. P., Widths of the 6.92 MeV and 7.12 MeV levels of ^{16}O, 25:3571
SWEET, J. R., Chemically stimulated luminescence in rare earth oxides, 25:3213
SWENSON, D. A., Control of respiration by DNA in ultraviolet-irradiated Escherichia coli B/r cells, 25:2598
SWIFT, S. C., Photoproduction of ^{28}Al and ^{29}Al from phosphorus, 25:3634
SWORSKI, T. J., Kinetic evidence that G/sub OH/ in the radiolysis of aqueous sulfuric and nitric acid solutions is proportional to electron fraction water, 25:2277
SYAURUKAITE, L. M., Electrodeposition of cobalt--tungsten magnetic alloys, 25:2649
SYMON, K. R., Impossibility of a defocusing quadrupole-lens system, 25:3450
SYUNYAEV, R. S., Background radiation of the universe and difficulties with Lemaitre's cosmological model with plateau at Z = 1.95, 25:2869 (CSIRO-Trans-10207)
SZABO, G. Levente, α spectrometry of low-activity specimens, 25:2476
SZABO, J., Problems of gamma--gamma logging in ore mining in Mecsek, 25:2347 (CSIRO-Trans-10140)
SZASZ, Levente, Variational solution of the Schroedinger equation of finite fermion systems. I, 25:3241
Variational solution of the Schroedinger equation of finite fermion systems. II, 25:3242
SZATMARY, Z., Calculation of resonance integrals: codes RIFFRAFF and RAD4, 25:3528 (KFKI-70-12-RPT)
GRACE: multigroup fast neutron spectrum code, 25:3529 (KFKI-70-14-RPT)
SZEGO, K., SL(2,C) representations in explicitly energy dependent basis. II, 25:3421 (KFKI-70-19-HEP)
SZEKELY, E., Problems of gamma--gamma logging in ore mining in Mecsek, 25:2347 (CSIRO-Trans-10140)
SZOKE, S., Pyridine-N-oxide: vibrational assignment and thermodynamic quantities, 25:2163

T

TABAKIN, Frank, Mesons in nuclear saturation, 25:3763
TABATA, Yoneho, Electrical conductivity of γ-irradiated solid monomers at low temperature, 25:2221
TABOR, S. L., Alpha-particle scattering from ^{204} ^{206} ^{208}Pb and ^{209}Bi, 25:3689
TACANO, Munecazu, Pinching processes in semiconductor plasmas, 25:3206
TACHIBANA, Akira, Simulator for BWR type Tsuruga nuclear power station, 25:3933
TACHIBANA, K., Effects of radiation damage on channeling of MeV protons in KBr, 25:3201
TACHON, J., Bounce effects in the negative mass instability, 25:3117 (CEA-CONF-1598)
Plasma containment in a circularized quadrupolar magnetic well: DECA II B, 25:3053 (CEA-CONF-1597)
TAGGART, Keith, Asymmetry and background in eta + 3π, 25:3254
TAHA, M. O., Off-shell ππ Veneziano amplitude, 25:3373
Veneziano amplitudes for πA_1 scattering, 25:3374
TAKAHASHI, Noriaki, High excited levels of ^{27}Al, 25:3600
TAKAI, Nobuharu, Separation of uranium from sea water by precipitation method, 25:2325
TAKAMURA, Shuichi, Effects of r.f. electric field on dispersion of ion waves, 25:3150 (IPPJ-93)
TAKAYAMA, Kazuo, Effects of r.f. electric field on dispersion of ion waves, 25:3150 (IPPJ-93)
TAKEDA, E., Experimental studies on 20 per cent enriched U-light water assembly. III, 25:3912
TAKEDA, Keiji, Reversibility between the electron-excess center, e$^-$ $(CH_3CN)_2$, and methyl radicals in γ-irradiated acetonitrile-h_3, 25:2271
TAKEDA, Yasutsugu, Design of an electron linear accelerator for industrial use, 25:3483
TAKEI, Mitsuo, Optimization of nuclear power system, 25:3804
TAKETANI, Mituo, Radio evolution of pulsars, 25:2842
TAKEUTCHI, F., Impulse approximation in ^{2}H(p,2p)n reaction, 25:3554
TAKI, Ko, Reactions of recoil ^{35}S atoms with organic compounds. I, 25:2303
TALVAT, M., Oxygen determination in silicon by means of alpha particles, 25:2128 (LYCEN-7060)
TANAKA, Masatoshi, High-speed plasma flow in a cusped magnetic field, 25:3091
TANAKA, Toshiyuki, Analysis of JMTR flux variation during operation, 25:3906 (JAERI-Memo-4130)
TANDON, P. N., g factor of the 114 keV state in ^{149}Pm, 25:3705
Half-lives of excited levels in ^{125}Te and ^{132}I, 25:3706
TANG, I. N., Kinetics of γ-induced decomposition of methyl iodide in air, 25:2269
TANIGUCHI, Mitsuo, Abnormal microstructure formed in hot rolled plates and sheets of α + β titanium alloys, 25:2752
TAPPAN, John T., Carlsbad site roll-up program. On-site radiological safety report, 25:2420 (NVO-410-2)
TARASOV, A. V., Quasielastic scattering of particles on deuterons, 25:3293 (JINR-P2-5343)
TARASOV, V. D., Water-dielectric generator for producting intensive fast-electron and hard decelerated x-ray pulses, 25:3478
TARASOV, V. V., Exponential angular coefficients of neutrons for hydrogen-free media, 25:3171
Spatial, energy, and angular distributions of neutrons in lithium, 25:3538
TARTAKOVSKII, V. K., Electrodisintegration of light nuclei, 25:3714 (ITF-70-35)
TASOVAC, T., Capture of ^{60}Co by suspended particles in Danube, 25:2361
TAUTH, Th., Distribution of ion densities in an arc discharge, 25:3085 (LYCEN-7061)
Production of multicharged ions in a reflex source with axial extraction, 25:3111 (LYCEN-7065)
TAYLOR, D., Moving-source soil density gauge, 25:2498
Subcellular fractionation of cultured glial cells, 25:3983 (UCLA-12-793)
TAYLOR, J., Scattering of 7.8-MeV polarized neutrons from ^{4}He, 25:3557
TEATINI, A., Isolation of cerium from a mixture of rare earths with the production of a nitric mother liquor, 25:2326
TECKU, B., anti rho-Meson production in high energy pion-collisions with nuclei, 25:3406 (IFVE-STF-69-71)
TEDDE, P. G., Grain counting in nuclear emulsions, 25:2457
TERASHIMA, Yoshinosuke, Stochastic model of electron cyclotron heating in a magnetic mirror, 25:3055 (IPPJ-100)
TERAZAWA, Hidezumi, Model for failure of the Pomeranchuk theorem, 25:3356
TERDAL, J. Edward, Elastic scattering of 1.33 MeV gamma rays from tin, 25:3655
TER HAAR, D., Pulsar distances and emission, 25:2854
TERHUNE, R. W., Nuclear cratering on a digital computer, 25:2381 (UCRL-50898)
TERMAN, A. V., Norms for radiation protection, 25:2574
TERRIEN, Y., Spectroscopy of even tin isotopes by inelastic scattering of protons, 25:3668
TERRIER, Marc, X-ray spectroscopic measurement of the temperature of atomic and ionic transfer in a plasma, 25:3073
TESTA, C., Establishment of laboratory for determination of Pu in biological samples, 25:2108 (RT/PROT-(70)14)
TESTOV, V. G., Multiwave studies of relaxation phenomena in argon plasma, 25:3064
TEVEROVSKII, E. N., Norms for radiation protection, 25:2574
TEWARI, S. G., Closed circuit technique for measurement of Rn/thoron ratio in soil-gas, 25:2378
THATCHER, L. L., Principles of the application of nuclear techniques to hydrologic investigations, 25:2360
THAXTON, Charles Burton, Technique for cooling single crystals below 90°K for X-ray diffraction, and crystal structures of $H_2Ta_4Cl_{18}.6H_2O$, and photodimer of 1,1-dimethyl-2,5-diphenyl-1-silacyclopentadiene, 25:3963 (IS-T-423)
THEARD, L. M., Pulse radiolysis studies of aqueous solutions of aminothiols and compounds related to nucleic acid, 25:2259 (GA-10208)
THIBODEAU, M., Heat transfer measurements on trefoil fuel bundles in the post-dryout regime-with data tabulation, 25:3865 (AECL-3414)
THIBODEAUX, Devron P., Sample preparation for neutron activation analysis, 25:2146
THIEL, Manfred A. F., Polarization and transformation theory of quasi-monochromatic radiation fields, 25:2846
THIELHEIM, K. O., Influence of primary mass on structure of extensive air showers, 25:2932

XUM

THIMMEL, Hermann Michael, Realization of magnetic guide field in isochron--cyclotron at Juelich, 25:3493
THOMAS, G. E., Rotational bands of ^{165}Ho, 25:3691
THOMAS, J. M., Reactivity of carbon: some current problems and trends, 25:2800
THOMAS, J-P., Oxygen determination in silicon by means of alpha particles, 25:2128 (LYCEN-7060)
THOMPSON, S. G., Prompt de-excitation of fission fragments, 25:3673
Search for superheavy elements in nature by detection of events with large numbers of neutrons, 25:3652 (UCRL-19957)
THOMSON, William Joseph, Nonisothermal MHD duct flow, 25:2943
THONNARD, N., Simple holding scaler, 25:2466
THWAITES, T. T., Energy levels of ^{37}K, 25:3641
TIELSCH-CASSEL, E., Space--time detector for cosmic ray showers, 25:2490
TIKHONOV, V. K., Exponential angular coefficients of neutrons for hydrogen-free media, 25:3171
Spatial, energy, and angular distributions of neutrons in lithium, 25:3538
TIKHONOV, V. P., Universal nomograms for calculating absorbed doses from plane radiators, 25:2566
TILL, C. E., Final safety analysis report on the use of plutonium in ZPR-6 and -9, 25:3901 (ANL-7442)
TILLEY, D. R., Superradiance in arrays of superconducting weak links, 25:3045
TIMOKHIN, V. V., Inelastic meson--baryon reactions in generalized Veneziano model, 25:3378 (ITF-70-77)
TIMOSHENKO, A. P., Nonlinear stabilization of beam instability, 25:3126
TIRKALA, F., Problems of gamma--gamma logging in ore mining in Mecsek, 25:2347 (CSIRC-Trans-10140)
TISHECHKIN, A. S., Computer for processing γ-spectra, 25:2477
TITE, M. S., Impact of the natural sciences on archaeology, 25:2354
TITOV, Yu. I., Electroproduction of pions on a proton at threshold and structure of the nucleon, 25:3244
TITTERTON, E. W., Angular correlation studies of the low-lying levels of ^{57}Co, 25:3622
TKESHELASHVILI, O. G., Transformation of first (second) sound into fourth sound in superfluid He, 25:3007
TOBAILEM, Jacques, Origin of pallasites, 25:2824
TOELGYESSY, J., Activation analysis in stomatology, 25:2135
TOKAR, M., Mechanical properties of carbide and nitride reactor fuels, 25:2785 (LA-4452)
TOKUDA, Shoichi, Abnormal microstructure formed in hot rolled plates and sheets of α + β titanium alloys, 25:2752
TOLAR, Jiri, Validity of quantum electrodynamics, 25:3438
TOMASEVIC, Magdalena, Determination of micro-quantities of carbon in metals, 25:2071
TOMASHOV, N. D., Corrosive behavior of alloys of the titanium--molybdenum--chromium system, 25:2613
TOMBRELLO, T. A., Capture of alpha particles by ^{12}C, 25:3562 (CONF-700322-, pp 297-304)
TOMCHUK E., Proton spin-lattice relaxation time of aniline-d_2 in deuterated benzene and deuterated aniline sclution, 25:2182
TOMZA, U., Structure of the low lying levels of the ^{33}S nucleus, 25:3597
TONE, Tatsuzo, Group structure and accuracy of group constants in vicinity of 2.85-keV resonance scattering of Na, 25:3928 (JAERI-Memo-4110)
TORCHENKOVA, E. A., Influence of radioactive radiation on the heterogeneous equilibrium in the system solid--solution, 25:2222
TORIYAMA, Tamotsu, Deexcitation of 931.1-keV 2_2^+ state of ^{152}Gd, 25:3681
TOTH, K., SL(2,C) representations in explicitly energy dependent basis. II, 25:3421 (KFKI-76-19-HEP)
TOUGAS, R., Densities of liquid In--Bi, Sn--In, Bi--Sb, and Bi--Cd--Tl alloys, 25:2692
TOULEMONDE, M., Lifetimes in ^{12}B, ^{14}N, and ^{16}O, 25:3569
TOUSSET, J., Oxygen determination in silicon by means of alpha particles, 25:2128 (LYCEN-7060)
Study by triple labeling of reactions between tetraphenylstibonium and antimony trichloride, 25:2169
TOYOHARA, M., Tracer technique for behavior of dusts in animal lungs, 25:2523
TOYOSHIMA, N., Thermal conductivity of VIPAC UO_2 fuel. II, 25:2813 (JAERI-Memo-4128)
TRAPP, J. H., Pressurized low temperature reduction of green salt, 25:2640 (NLCO-1058)
TRAUT, H., Partial and total sex-chromosome loss induced by x-rays in mature spermatozoa, 25:2554
TREADO, Paul A., Charged particle nuclear physics experiments for a teaching laboratory, 25:3464 (CONF-700322-, pp 1-19)
TRECCANI, V., Microbial degradation of aromatic hydrocarbons used as reactor coolants, 25:2327
TREFIL, J. S., Approximations involved in the theory of the interactions of particles and nuclei at high energies, 25:3317
TREHAN, P. N., Decay of ^{124}Sb, 25:3657
TREJBAL, Z., Polarized ion source for U-120 cyclotron. I, 25:3520
Polarized ion source for U-120 cyclotron. II, 25:3519
TREKHOV, E. S., Physics of gas-discharge plasma. I, 25:3076
TRENTELMAN, G. F., Semiconductor position sensitive detectors in magnetic spectrographs, 25:2463
TREVES, A., Optical spark chamber for the search of gamma-ray sources, 25:2841 (CEA-CONF-1633)
TRIGGIANI, Leonard Vincent, Sol for making particles of actinide carbide, 25:2780
TRILLING, G. H., Reaction $\pi^+p \rightarrow \Delta^{++}A_2^0$ at 3.7 GeV/c, 25:3272 (UCRL-20050)
TRIPLETT, B. B., Low-temperature heat capacities of dilute solutions of Fe and Cr in Cu, 25:3990 (UCRL-19686)
TRLIFAJ, L., Realistic forces and deformed state admixtures in ^{18}O, 25:3580
TROMBKA, J. I., Neutron radiative capture methods for surface elemental analysis, 25:2144
TROUTMAN, Paul H., Absorption curve matching circuit in nucleonic measuring system, 25:2499
TROWER, W. P., Elastic electron--nickel scattering, 25:3687
TROYANOV, E. F., Investigation of beam transversal characteristics at input of IHEP proton synchrotron, 25:3482
TRUBEY, D. K., Computer codes for shielding calculations: 1970, 25:3179
Kernel methods for radiation shielding calculations, 25:3178
TRUEBLOOD, J. H., Directional correlation and intensity studies of electromagnetic transitions in ^{181}Ta, 25:3647 (COO-1746-46)
TRUOEL, P., Radiative pion capture in ^{12}C, 25:3550
TSAI, Hui-tuh, Photon-activation analysis for I using Cs as internal-reference, 25:2150
TSAI, S. Y., Principle of universality, 25:3351
TSANG, W., Determination of trace amounts of contaminants in water by isotope dilution gas chromatography, 25:2107
TSAP, T. T., Photospheric and chromospheric magnetic fields and the brightness of faculae and flocculi, 25:2857 (AD-707256)
TSAPKINA, I. V., X ray studies of monoaquotetracarbamidouranyl halide nitrates, 25:2214
TSEREN, Ch., Quasielastic scattering of particles on deuterons, 25:3293 (JINR-P2-5343)
TSUJII, Junro, Multi-purpose utilization of nuclear reactors in chemical industry, 25:3915
TSUKERMAN, V. A., Generator of short pulses of hard x-rays of high intensity, 25:2401
Water-dielectric generator for producting intensive fast-electron and hard decelerated x-ray pulses, 25:3478
TSUMORI, Yoshikatsu, Abnormal microstructure formed in hot rolled plates and sheets of α + β titanium alloys, 25:2752
TSUTSUI, Tenson, De-watering of radioactive sludge by super-decanter centrifuge, 25:2344
TSUZUKI, T., Fluctuations of order parameter and Hall effect, 25:3036
TSVETAEV, A. A., Stress relaxation in deformed U, 25:2699
TSYPIN, S. G., Exponential angular coefficients of neutrons for hydrogen-free media, 25:3171
Spatial, energy, and angular distributions of neutrons in lithium, 25:3538
TSYPIN, V. S., Low-frequency instabilities of the high-frequency skin layer in a plasma with non-uniform parameters, 25:3121
TSYTOVICH, V. N., Spectra of magnetohydrodynamic turbulence in collisionless plasma, 25:3096
TUFTS, Charles F., Application of transmission electron microscopy and electron diffraction to analysis for materials science, 25:2748
TUITE, P. T., Disposing of nuclear plant solid wastes, 25:2425
TURNER, C. E. Jr., Numerical correction of multichannel analyzer data, 25:2509
TURNER, R. B., 5000-hr test of a eutectic lead--bismuth circuit constructed in steel and niobium, 25:2627
TUTTLE, E. R., Hartree--Fock theory and Λ transformation in quantum statistical mechanics. II, 25:3228
TUVESON, R. W., uv-sensitive mutant of Neurospora defective for photoreactivation, 25:2556
TWIN, P. J., High spin states in ^{58}Fe, 25:3624
TYMINSKII, V. G., Isotopic composition of uranium in ground waters, 25:2356
TYURIN, N. E., Solution of unitarity condition for the elastic scattering amplitude for high energies, 25:3451 (ITF-70-49)

U

UDOVICHENKO, Yu. K., Nonlinear stabilization of beam instability, 25:3126
UEDA, Tamotsu, High-energy proton--proton scattering, 25:3418
UJIMOTO, Kikujiro, Carrier effects on anion-exchange and gel chromatographic behavior of ^{32}P recoil species produced in irradiated inorganic phosphates, 25:2298
Hot atom chemistry of solid inorganic phosphorus compounds: alkali and ammonium orthophosphates, 25:2302
ULITIN, O. A., Attenuation of scattered synchrocyclotron radiation in a shield, 25:3480

UL'YANOV, K. N., Theory of a plasma cathode, 25:3107
UMEZAWA, H., Target preparation, 25:2655
USTINOV, Yu. K., Interaction of water vapor with the surface of tungsten, 25:2722
UTKINA, L. A., Low-frequency instabilities of the high-frequency skin layer in a plasma with non-uniform parameters, 25:3121

V

VAELIVAARA, K. G., Excited nuclear states in ^{125}Te, 25:3699
VAGER, Z., Inhibited (^{3}He,d) transitions to 3s/sub $^{1}/_{2}$/ isobaric analog states, 25:3666
VAIDYANATHAN, S., Decomposition of brown peroxy complex of Pu(IV) in $HClO_4$, 25:2154
VAINSHTEIN, L. A., Approximate methods of calculation of excitation cross sections of atoms and ions, 25:2913
Effective excitation and ionization cross sections of ions, 25:2914
Role of intermediate states in excitation of atoms by electron impact, 25:2916
VAL'DBERG, A. Yu., Use of turbulent washer for removal of ionizing additive in MHD generators, 25:2939
VALENTIN, Pierre, X-ray spectroscopic measurement of the temperature of atomic and ionic transfer in a plasma, 25:3073
VALIERGUE, L., Study of thin films of samarium by x rays and electron microscopy, 25:2734
VALKO, J., GRACE: multigroup fast neutron spectrum code, 25:3529 (KFKI-70-14-RPT)
VALKOVIC, V., D(p,d*)p cross section, 25:3553
VALLOIS, G., Spectroscopy of even tin isotopes by inelastic scattering of protons, 25:3668
VANDENBOSCH, R., Proton induced fission of ^{233}U and ^{238}U, 25:3660
VAN DER BORGHT, O., Radiomanganese and radiocobalt fixation by sediments, fauna, and flora, 25:2544
VAN DER COOK, R. E., Operating experience using silver reactors for radioiodine removal in the Hanford Purex Plant, 25:2416 (ARH-SA-67)
VANDERGRAAF, Tjalle Thys, Neutron-activation analysis of silicate rocks, 25:2149
VANDERHAGHEN, R., Analysis of $\pi^+\pi^-$ enhancements produced in reaction $\pi^+p \to \pi^+p\pi^+\pi^-$ at 5 GeV/c, 25:3275
VANDERLEEDEN, J. C., Search for double-photon decay in ^{90}Zr, 25:3658
VAN DER WIEL, M. J., K-shell excitation of N_2 and CO by electron impact, 25:2910
VAN DEVENTER, Erven H., Enthalpy of formation of ThF_4 by fluorine bomb calorimetry, 25:2213
VAN DOORNINCK, J., Final safety analysis report on the use of plutonium in ZPR-6 and -9, 25:3901 (ANL-7442)
VAN GEEL, J. N. C., Technological aspects of reprocessing nuclear fuel at Eurochemic, 25:2324
VAN INGEN, J. W. F., Radiation-induced isomerization of [2,2,1]bicycloheptadiene (norbornadiene) to [2,2,1,$0^{2,6}$,$0^{3,5}$]quadricycloheptane (quadricyclene) in cyclohexane solutions, 25:2239
VAN KLEEFF, B. H. A., Accumulation of radionuclides by bacteria and yeasts, 25:2530
VAN KLINKEN, J., Double-beta decay, 25:3693
VAN LEHN, A. L., Corrections to coaxial Ge(Li) detector solid angle correction factors, 25:2455
VAN MIDDELKOOP, G., Study of the ^{207}Pb(d,p)^{208}Pb reaction, 25:3688
VAN TIEGHEM, C. H. C., Radiation-induced isomerization of [2,2,1]bicycloheptadiene (norbornadiene) to [2,2,1,$0^{2,6}$,$0^{3,5}$]quadricycloheptane (quadricyclene) in cyclohexane solutions, 25:2239
VAN WINKLE, R., Investigation of the need for variable orifices in multistage flash evaporators, 25:2387 (ORNL-TM-2746)
VAN ZUILEKOM, Jeannine T., Accumulation of radionuclides by bacteria and yeasts, 25:2530
VARDALAS, J. N., Transport coefficients of a relativistic quantum gas, 25:2873
VARDANYAN, R. A., Some properties of radio galaxies, 25:2867
VARSANYI, Gy., Pyridine-N-oxide: vibrational assignment and thermodynamic quantities, 25:2163
VARSHALOVICH, D. A., Dynamic particle-spin orientation in a cosmic medium, 25:2831
VARTANYAN, Yu. L., Effect of neutronization of the critical parameters of isothermal white dwarfs, 25:2832
VASAVADA, Kashyap V., Continuous-moment sum rules and pion photoproduction data, 25:3327
VASHISHTA, P., Condensation energy of a superconductor, 25:3046
VASIL'EV, A. A., Conference on particle accelerators, Moscow, 10/68. II, 25:3485
Conference on particle accelerators, Moscow, 10/68. I, 25:3484
VASILEV, Khristo, Recovery of tellurium from sulphate solutions by extraction, 25:2321
VASIL'EV, N. G., Magnetization of the superconducting alloy Ti--22 at. percent Nb, 25:3027
VASSERMAN, S. B., Generator of short pulses of hard x-rays of high intensity, 25:2401
VASSEUR, J., Optical spark chamber for the search of gamma-ray sources, 25:2841 (CEA-CONF-1633)
VATAZHIN, A. B., Breakaway parameter of the turbulent magnetohydrodynamic boundary layer, 25:2947
VAUGOYEAU, Henri, Nuclear fuel having a UC base, 25:2776
VAVILOV, V. S., Semiconductor layers and structural changes produced in diamond by ion implantation, 25:3199
VEIT, J. J., Student experiments utilizing a neutron generator, 25:3526 (CONF-700322-, pp 33-47)
VENEZIA, A., Separation of fission produced iodine, 25:2342
VENKATESWARLU, Ch., Spectrophotometric study of UO_2^{2+}--SCN-system in aqueous and water--methanol media, 25:2215
VENTURELLO, G., Backward scattering of 14 MeV neutrons, 25:2468
VERGANTI, G., Isolation of cerium from a mixture of rare earths with the production of a nitric mother liquor, 25:2326
VERHEUL, H., Decay of ^{62}Co isomers, 25:3644
Decay of ^{63}Ga, 25:3609
VERNOV, S. N., Relationship between outer-belt electron intensity and geomagnetic activity indexes, 25:2969
VEROT, J. L., Physico-chemical processes of transfer of radioruthenium in continental medium, 25:2364
VERVISCH, Pierre, X-ray spectroscopic measurement of the temperature of atomic and ionic transfer in a plasma, 25:3073
VIALATTE, B., Study of the fixation of fluorine on antimony pentoxide in hydrochloric acid medium, 25:2332
VIL'K, Yu. N., Rate of vaporization of congruently vaporizing compositions of NbC, 25:2802
VIL'KOVISKII, E. Ya., Synthesis of differently charged nuclei in plasma with strong electric current, 25:3140
VINCENT, C. M., Distorted-wave analysis of stripping to unbound states, 25:3764
VINCENT, Dietrich H., Plutonium--Be neutron source spectrum measured by ^{6}Li semiconductor spectrometer, 25:2407
VINNIKOVA-GULYAEVA, T. L., Influence of the depth of the interlayer ionization valley on F-region heights, 25:2989
VINOGRADOV, A. V., Quasi-classical method in theory of collisions of atoms with heavy particles and electrons, 25:2917
VINOGRADOVA, V. N., Classification of short-period pulsations of Earth's electromagnetic field, 25:3000
VIRAG, P., Problems of gamma--gamma logging in ore mining in Mecsek, 25:2347 (CSIRO-Trans-10140)
VISAKORPI, R., Effect of whole body x irradiation on hypersensitivity in rats, 25:2540
VISAPAEAE, A., Determination by x-ray fluorescence of chromium in cellulose, 25:2076
VISWESWARA RAO, V., Photoelectric cross sections of gamma rays in La, Gd, Hf, and Th, 25:2907
VIVANTE, C., Post-irradiation gas release measurements on fuel elements from Dragon reactor, 25:3870 (DP-Report-497)
VLADIMIROV, V. S., Representation of the Jost--Lehmann--Dyson type, 25:3433 (ITF-70-33)
VLASENKO, V. G., Quasi-elastic scattering of 1115-MeV electrons by nucleons of ^{32}S nuclei, 25:3615
VOBECKY, M., Gamma-ray spectrum of ^{192}Au, 25:3654
VOEHRINGER, O., Deformation behavior of polycrystalline metals, 25:2690
VOELKER, Ferd, Experimental superconducting transformer for current step-up, 25:3509
Resistance in small, twisted, multicore superconducting wires, 25:3499
VOGEL, P., Branching ratios for E1 transitions deexciting the octupole states in even--even deformed nuclei, 25:3751
VOGEL, R. C., Fuel cycle technology quarterly report, April, May, June 1970, 25:2306 (ANL-7735)
VOICE, Eric, Pyrolysis of methane in bed of particles, 25:2151 (DP-Report-569)
VOIGT, R. L., Pulse radiolysis studies of aqueous solutions of aminothiols and compounds related to nucleic acid, 25:2259 (GA-10208)
VOLKOV, G. I., Catalytic amalgam method for determining small amounts of Cr, V, and Mo in brine, 25:2080
VOLKOV, V. V., Neutron-rich isotopes of light elements produced in transfer reactions with heavy ions, 25:3648 (JINR-E7-5319)
VOLLBRECHT, W., Preparation and etching of microsections of zirconium and zirconium--niobium alloys, 25:2656
VOL'SKII, A. N., Metallurgy of plutonium, 25:2658 (AEC-tr-7095)
VON BRENTANO, P., Direct reaction in production of fission isomers, 25:3709
VONKA, V., CACES: an ALGOL program for solving diffusion type elliptic differential equations in plane involving arbitrary boundary conditions and shape, 25:3876 (RCN-123)
VON WITSCH, W., D(p,d*)p cross section, 25:3553
Neutron--neutron interactions in ^{2}H(d,pp)2n, 25:3549
VOROB'EV, A. A., Statistical analysis of the information transfer process in radiometric betatron defectoscopy, 25:2412
VOROB'EV, V. A., Statistical analysis of the information transfer process in radiometric betatron defectoscopy, 25:2412
VOROB'EVA, G. A., Use of chelating reagents in the extraction--photometric determination of elements with

basic dyes, 25:2087
VORONIN, L. K., Thermal conductivity, specific electrical resistivity, and total emissivity of refractory metals at high temperatures, 25:2715
VORONOVA, G. D., Action of plant hormones on dynamics of nucleic acids in growing spikes of irradiated barley plants, 25:2597
VOROTNIKOV, P. E., Neutron-induced ^{249}Bk fission, 25:3665
VOSKAN'YANTS, V. I., Radiolysis of original and reinforced ED-5 type epoxy resin, 25:2273
VOSKOBOINIKOV, I. M., Determination of the decomposition time of hexogen under the effect of shock waves, 25:3964 (LA-4360-TR)
VOSKOV, V. S., Extraction--photometric determination of Nb(V) with benzohydroxamic acid, 25:2085
VOUILLON, Michel, Acicular precipitates in irradiated austenitic steels using electron microscopy, 25:2756 (CEA-CONF-1638)
VOYVODIC, L., Production of strange particles in π^+p interactions at 5.5 GeV/c, 25:3279
VUL'FSON, N. D., Dieckmann reaction, 25:4001 (UCRL-Trans-1417)
VYAS, H. M., Free radicals in γ-irradiated disodium succinate. I, 25:2229

W

WACHTEL, Ernst, Magnetic measurements in the copper--manganese system, 25:3972 (ORNL-tr-2398)
WACHTEL, S. J., Interaction effects between dissimilar metals in high velocity sodium at temperatures up to 760°C. I. Mass transfer of vanadium onto type 321 stainless steel, 25:2617
WADA, T., Nuclear interactions by accelerator and cosmic-ray muons, 25:3260
WADDELL, C., Proton hole states in 1f/sub 7/2/ nuclei, 25:3616
WADDINGTON, J. C., Low-lying high-spin states in ^{155}Gd, 25:3700
WAGGONER, M. A., Study of ^{6}Li + ^{12}C reactions, 25:3578
WAGNER, H. F., Gamma--gamma angular correlation in ^{166}Er in different liquid sources, 25:3696
WAGNER, R. V., Upper limits to electromagnetic energy radiated by normal galaxies, 25:2868
WAGNER, S., Calculation of N anti N bound states from relativistic OBE model and meson spectrum, 25:3358 (DESY-70/49)
Meson--baryon interactions with broken SU(3) and the baryon spectrum in relativistic quantum mechanics, 25:3397
WAHI, Bhupinder N., Mobility and coefficients of slip of polystyrene latex particles, 25:3940 (COO-1248-22)
WAINERDI, R. E., Analysis of oceanographic samples by 14-MeV neutron activation, 25:2119 (CONF-700322-, pp 221-30)
WAKATSUKI, Tetsuo, High excited levels of ^{27}Al, 25:3600
WALKER, James C. G., Minor-ion diffusion in F2 region, 25:2962
WALKER, W. D., Associated production in K$^+$p interactions at 3.5 GeV/c, 25:3277
WALLACE, W. D., Electromagnetic generation of ultrasound in metals, 25:3967 (NYO-2150-63)
WALTER, K.-H., Behavior of solid fission products in pyrolytic carbon and graphite, 25:2797
WALTER, R. L., Scattering of 7.8-MeV polarized neutrons from ^{4}He, 25:3557
WALTERS, W. B., Decay of Zn and Zn to levels of ^{71}Ga, 25:3638
WALTHER, H., Calculation of the release of fission products from coated particles, 25:3874 (DP-Report-595)
WANDERER, E., Selfcleaning capacity on radionuclides of small river, 25:2545
WANG, P. K. C., Control-theoretic approach to the plasma confinement problem, 25:3057
WARD, B. J., Stabilization of Pu β phase in Pu--Ti alloys, 25:2739
WARNER, R. E., p-p and p-t interactions in ^{3}He(d,tp)p, 25:3552
WARNOCK, Tony T., Appraisal of an iterative method for bound states, 25:2925
WARRINGTON, D. H., Precipitation of Ni_3Nb phases in a Ni--Fe--Cr--Nb alloy, 25:2689
WASHBURN, J., High-voltage electron microscopy study of slip band growth in copper, 25:3988 (UCRL-19601)
WASIK, S. P., Determination of trace amounts of contaminants in water by isotope dilution gas chromatography, 25:2107
WATARUMI, C., Experimental studies on 20 per cent enriched U-light water assembly. III, 25:3912
WATERMAN, F. M., Scattering of high-energy pions on electrons, 25:3253
WATSON, B. A., Alpha-particle scattering from ^{204} ^{206} ^{208}Pb and ^{209}Bi, 25:3689
WATSON, Evelyn E., Radiation safety in the operation of a low-energy accelerator, 25:3475 (CONF-700322-, pp 441-8)
WATSON, Gary Ernest, Densities and solubility of ^{3}He in liquid ^{4}He under pressure, 25:3011
WATSON, R. L., Prompt de-excitation of fission fragments, 25:3673
WATTS, C., Removal and replacement of primary heat exchanger tube bundle and circulator on Dragon Reactor, 25:3863 (DP-Report-554)
WEAVER, K. E., Antiproton--neutron elastic scattering at 3.5 GeV/c, 25:3267
WEBB, Virgil H., Quiescent and disturbed proton and electron distributions, 25:2950 (AD-709363)
WEBB, W. W., Prog. rpt. on hard superconducting materials, annual, 12/69--11/70, 25:3019 (NYO-3029-48)
WEBELER, R. W. H., Measurement of etarho/sub n/ versus T near T/sub lambda/ of dilute ^{3}He--^{4}He mixtures, 25:3016
WEBER, G., Behavior of surfaces under bombardment using nuclear reactions, 25:2763
WEBER, H., Pocket radiometer with optic and acoustic signal, 25:2445
WEBER, H. J., Roper resonance and the short-range structure of the deuteron, 25:3410
WEBSTER, D. S., Fuel cycle technology quarterly report, April, May, June 1970, 25:2306 (ANL-7735)
WECHSELBERGER, E., Energy distribution of singly scattered and multiply scattered gamma radiation. II, 25:3182
WEEDMAN, D. W., Spectral observations of Markaryan galaxies with ultraviolet continuum. I, 25:2865
WEEKS, J. R., Measurements of the solubility of iron and chromium in sodium, 25:2712
WEEKS, John R., Corrosion by liquid metals. Proceedings of the sessions on corrosion by liquid metals of the 1969 fall meeting of the Metallurgical Society of AIME, October 13--16, 1969, Philadelphia, Pennsylvania, 25:2615
WEICHT, U., Parametric survey of the low enriched uranium cycle in a high temperature reactor. project dragon, 25:3883 (DP-Report-466)
WEIDINGER, A., Investigation of ^{65}Zn by (p,n) and (p,nγ) experiments, 25:3631
WEIGEL, M., Random-phase-approximation treatment of nucleon--nucleus scattering, 25:3718
WEIGL, Frederic, Mach--Zehnder and holographic interferometry for plasma diagnostics, 25:3071
WEIL, J. W., Applications of Lie series in atomic physics, 25:3236
WEINBERG, A., Associated production in K$^+$p interactions at 3.5 GeV/c, 25:3277
WEINGARTEN, Donald, Optical model of elastic proton--proton scattering, 25:3413
WEISS, K., Equations of motion for complex order parameter of helium II, 25:3014
WEISSKOPF, Victor F., Simple interpretation of inelastic electron-nucleon scattering, 25:3310 (DESY-70/50)
WEITKAMP, C., Studies of radiative neutron capture and delayed fission gamma-ray spectra from uranium and plutonium as a basis for new nondestructive safeguards techniques, 25:3649 (KFK-1214)
WELINSKY, I. H., Effect of HNO_3--HF pickling on stress corrosion cracking of Ni--Cr--Fe Alloy 600 in high-purity water at 660F, 25:4006 (WAPD-TM-944)
WELLS, D. O., Reaction ^{12}C(d,p$_0$)^{13}C, 25:3572
WENNING, W., Reactions (d,n) on ^{11}B, ^{14}N, and ^{15}N, 25:3574
WERNER, B., Production of the anti K^{*0} (890) Δ^- (1236) final state in K$^-$d interactions at 5.5 GeV/c, 25:3274
WERSTIUK, N. H., Preparation and acetolysis of 5-deuteriated exo-norbornyl brosylates, 25:2172
WERT, C. A., Mass absorption coefficients of refractory metal carbides, 25:2095
WEST, B. J., Induction of translocations in mouse spermatogonia. III, 25:2553
WEST, J. B., Low temperature scintillation response of unactivated sodium iodide, 25:2436
WEST, R. N., Positron annihilation in quenched cadmium metal, 25:2898
WETTSTEIN, Felix O., Distribution of polysomes in mouse brain tissue, 25:3986 (UCLA-12-796)
WEYHMANN, W., Nuclear orientation studies of local moments in noble metal hosts, 25:3942 (COO-1569-67)
WEZRANOWSKI, E., Estimation of the amount of exogenous inclusions in steel by means of neutron-activation analysis, 25:2132
WHIPP, A. T., Application of distribution theory to Martin's method in potential scattering, 25:3240
WHITE, I. G., Oxidative and glycolytic activity of ejaculated ram spermatozoa in the presence of steroid hormones, 25:2519
WHITE, J. N. J., Regge-cut effects in pion--nucleon scattering, 25:3390
WHITE, R. Stephen, Proton energy distributions from 0.060 to 3.3 MeV at 6.6 earth radii, 25:2951 (AD-709723)
WHITE, W. B., Chemically stimulated luminescence in rare earth oxides, 25:3213
WHITEHOUSE, P. R., Boilers for nuclear plant, 25:3900
WHITLOCK, Howard W. Jr., Base-catalyzed hydrogen--deuterium exchange in diene--iron tricarbonyl complexes, 25:2187
WHITLOW, G. A., Effects of exposure to flowing sodium on vanadium alloys in stainless steel containment systems, 25:2621
WHITTAKER, Brian, Improvements in cathodes, 25:3523
WIBLIN, E. R., Record of programme and discussions at symposium of papers from Dragon contractors held at A.E.R.E., Harwell, 14--16 March 1966, 25:3774 (DP-Report-439)
WICKER, E. E., Application of neutron generators in the steel industry, 25:2121 (CONF-700322-, pp 249-57)

WIEBICKE, H. J., Multi-step stripping on deformed nuclei, 25:3732
WIEBICKE, H.-J., Investigation of proton polarization in reaction $^{12}C(^3He,p_0)^{14}N$, 25:3563 (JINR-P15-5156)
WIESE, H.-W., Critical and safe dimensions of containers for storage and mixing of plutonium-containing nuclear fuel, 25:2419 (KFK-1192)
WIKTOR, S., Structure of the low lying levels of the ^{33}S nucleus, 25:3597
WILCZYNSKI, J., Neutron-rich isotopes of light elements produced in transfer reactions with heavy ions, 25:3648 (JINR-E7-5319)
WILETS, L., Meson dynamics and the nuclear many-body problem. I, 25:3719
WILHELMY, J. B., Prompt de-excitation of fission fragments, 25:3673
WILKINS, M., Concerning the half-life of ^{144}Ce, 25:3645 (AERE-R-6529)
WILKINSON, D. H., Allowed β-decay for light elements, 25:3743
WILLIAMS, Ffrancon, Reversibility between the electron-excess center, e^- $(CH_3CN)_2$, and methyl radicals in γ-irradiated acetonitrile-h_3, 25:2271
WILLIAMS, M. M. R., Neutron diffusion length experiment, 25:3539
WILLIAMS, W. G., Proton polarization measurements, 25:3500
WILLIAMSON, T. J., Calculations of neutron time-energy distributions in heavy moderators, 25:3541
WILLIS, C., Radiation chemistry of carbon monoxide at very high dose rates, 25:2287
WILLITTS, T. R., Large aperture Cherenkov counter, 25:2489
WILLMANN, R. B., Double-Regge pole analysis of $\pi^+p \to \pi^+\pi^-\Delta^{++}$ at 13.1 GeV/c, 25:3273
WILSON, E. J. N., Design studies for large proton synchrotron, 25:3501
WILSON, G. V. H., Radiative detection of single-passage nuclear magnetic resonance, 25:3223
WILSON, J. R., Solubilities of several transition metals in liquid lead--bismuth eutectic, 25:2709
WILSON, P. B., Superconducting accelerator research and development at SLAC, 25:3507
WIND, H., Partial and total sex-chromosome loss induced by x-rays in mature spermatozoa, 25:2554
WINN, Willard G., Structure of ^{51}Cr via $^{48}Ti(^3He,n\gamma)$ and $^{51}V(p,n\gamma)$ prompt γ-ray spectrometry, 25:3593 (COO-1530-21)
WINSTEIN, B. D., Recoil proton polarization in eta photoproduction, 25:3255
WIRTH, Gernoth, UBr_5 and $UOBr_3$.2.5DMA, 25:2200
WISE, Michael Louis, Phenomenological current algebra vertex, 25:3376
WIT, R., Lower bound for $\pi^0\pi^0$ scattering length, 25:3360
WITRIOL, Norman M., Point transforms and the hard-core Fermi system, 25:3005
WITTERN, H. W., Break-up of ^6Li in the Coulomb-field, 25:3749
WITTHUHN, W., Magnetic moment of level in ^{58}Co, 25:3618
WLODEK, S., Cesium transport in fish-breeding pond, 25:2516
WODA, H., Studies of radiative neutron capture and delayed fission gamma-ray spectra from uranium and plutonium as a basis for new nondestructive safeguards techniques, 25:3649 (KFK-1214)
WOHLENBERG, T., Combination of an electron microscope and a heavy-ion accelerator, 25:2507
WOJNAROVITS, L., Radiolysis of saturated and unsaturated binary hydrocarbon systems, 25:2270
WOLF, Guenter, Inelastic diffractive rho-photoproduction and Compton scattering, 25:3308 (DESY-70/45)
WOLFENSTEIN, L., Possible effects of lepton non-locality in the decays $K \to \pi e^+e^-$ and $K \to \pi \nu$ anti ν, 25:3337
WOLLENBERG, H. A., Determination of rare-earth elements in rocks, 25:2094
WOLLENBERGER, H., Stored energy measurements in electron-irradiated Pt, 25:3197
WONG, C. Y., Coulomb distortion in heavy-ion reactions, 25:3720
WONG, Cho Fai, Electrodisintegration of carbon, 25:3566 (SAL-14)
WOODCOCK, J. P., Ultrasonic absorption, 25:2285
WOODLEY, H. J., Pressure drop measurements made on a dragon heat exchanger fitted with various designs of water catch-pot. project dragon, 25:3897 (DP-Report-591)
Seizure tests on Dragon articulated control rod, 25:3858 (DP-Report-486)
WOODRUFF, William L., Some improvements in variational flux synthesis methods, 25:3922 (ANL-7696)
WOZNIAKOVA, Blanka, Solidus and liquidus curves of binary alloys of U with C, Mn, and V, 25:2737
WRIGHT, J. H., Environmental aspects of nuclear energy, 25:2564
WU, C. S., Muonic atoms. I, 25:3661
WU, Tai Tsun, Cross sections for two-pair production at infinite energy, 25:3325
WUESTENHAGEN, K., Problems arising from nuclear blasting for oil and gas production, 25:2382
WYATT, P. A. H., D_0 acidity function in deuterium sulphate solutions at 25°C, 25:2175
WYLD, K., Elastic and inelastic scattering of neutrons in energy range 2 to 5 MeV by ^{10}B and ^{11}B, 25:3559 (AWRE-O-45/70)
WYLIE, W. R., Thick-target $^{16}O(d,n)^{17}F$ yield curves, 25:3586
WYNANDS, A., Numerical calculations and description of toroidal arcs by model theories, 25:3088
WYNCHANK, S., Uniform tension in a plane array of thin parallel wires, 25:2465

Y

YADAV, Basudeo P., Method to calculate gravitational waves, 25:2877
YAFFE, D., $\Delta^{++}(1236)$ $\Delta^-(1236)$ production in pn collisions, 25:3265
YAFFE, L., Recoil studies of fission products, 25:3702
YAFFE, P. E., Athermal omega transformation in Zr--Nb alloys, 25:2735
YAGI, M., Isomeric transition-activated ^{80}Br reactions in CH_4--/sup 80m/BrBr and CH_4--/sup 80m/Br systems, 25:2226
YAGI, Masuo, Solubility of xenon in carbon tetrachloride and in chloroform, 25:2201
YAKOVLEV, Yu. V., Radioactivation determination of impurities in yttrium and molybdenum by means of extraction displacement chromatography, 25:2138
YAKUBOV, I. T., Phase transition and negative clusters in an imperfect plasma of metal vapor, 25:3086
YAL'TSEV, V. N., Substructure of cast Mo, 25:2744
YAMABE, Takeo, Separation of uranium from sea water by precipitation method, 25:2325
YAMADA, T., Thermal conductivity of VIPAC UO_2 fuel. II, 25:2813 (JAERI-Memo-4128)
YAMAJI, A., Optimum arrangement of laminated iron--water shields, 25:3174
YAMAMOTO, Jiro, Rate constants of exchange reaction of the type RI + I^{*-} reversible RI* + I^- in acetone--water solution, 25:2177
YAMPOL'SKII, V. A., Transformation of first (second) sound into fourth sound in superfluid He, 25:3007
YAMPOL'SKII, V. S., Lower ionosphere during solar eclipse of Sept. 22, 1968, 25:2996
YANG, Teh Li, Plutonium--Be neutron source spectrum measured by ^6Li semiconductor spectrometer, 25:2407
YANIR, E., Charge states of Np recoil atoms, 25:2305
YANNOPOULOS, J. C., Corrosive action of selenium towards various materials in the temperature range 300 to 700°C, 25:2629
YAP, C. T., Charge asymmetry of the internucleon potential, 25:3736
YASTREBKOV, A. A., Deformed Mo recovery, 25:2746
YASUDA, Hideshi, Reactor neutron fluctuation simulator using pulsed neutron source, 25:3932
YATIRAJAM, V., Microdetermination of rhenium, 25:2102
YAVOR, S. Ya., Electron-optical properties of two-potential two-dimensional lens, 25:3491
Two-potential lens with distorted focusing layer, 25:3490
YAZAKI, Shigeo, Factorization and duality of multiloop diagrams, 25:3443
YEKUTIELI, G., $\Delta^{++}(1236)$ $\Delta^-(1236)$ production in pn collisions, 25:3265
YEN, Yu-liang, Plutonium--Be neutron source spectrum measured by ^6Li semiconductor spectrometer, 25:2407
YOKOI, S., Creep and creep-rupture tests of stainless steel as structural material of fast breeding reactor, 25:2660 (JAERI-Memo-4097)
YOKOYAMA, Kan-ichi, Gauge, renormalization, and the Goto--Imamura--Schwinger term in quantum electrodynamics, 25:3444
YONEZAWA, Minoru, Energy dependence of the slope of the forward peak in elastic proton--proton scattering, 25:3417
YOSHIDA, Toshihiro, Non-duality of Pomeranchon term and quark line picture, 25:3375
YOSHIKURA, H., Radiological studies on murine sarcoma virus infection and cell cycle, 25:2587
YOSHIMURA, Tetz, Comments on Nishijima and Sato's paper on the HNZ construction, 25:3445
YOUNG, J. C., Modified impulse approximation calculation of the N--N quasi-free scattering and the Chew--Low extrapolation in the D(p,NN)N reaction, 25:3750
YOUNG, Jonathan D., Smoothing and differential analysis of magnetic field and gradient measurement, 25:3503
YOZA, Norimasa, Hot atom chemistry of solid inorganic phosphorus compounds: alkali and ammonium orthophosphates, 25:2302
YUASA, T., Impulse approximation in $^2H(p,2p)n$ reaction, 25:3554
YUDIN, V. M., Crystal structure of Mo containing ZrC, 25:2743
Substructure of cast Mo, 25:2744
YUDKOVSKII, S. I., Distribution of C in cast Mo, 25:2702
YUDOVICH, L. A., Cyclic variations of latitude dependence of F2-layer ionization at noon, 25:2984
YUKHIMUK, A. K., Acceleration of charged particles in a cosmic plasma, 25:2929
YUNUSOV, M. S., Effect of γ radiation on the volt--ampere characteristics of diodes, 25:3192

XUM

Z

ZABLOTNY, Wladyslaw, Review of isotopic methods applied in distillation and rectification, 25:2343

ZABOLOTSKII, N. N., Action of plant hormones on dynamics of nucleic acids in growing spikes of irradiated barley plants, 25:2597

ZACHARIASEN, F., Complex Regge poles in the cut j plane, 25:3402

ZACHARIASEN, W. H., Crystal structure of the compounds U_2N_2X and Th_2N_2X with X = Sb, Te, and Bi, 25:2248

ZAGULYAEVA, V. A., Drift of small-scale inhomogeneities in ionospheric F2 layer, 25:2986

ZAITSEV, E. I., Radioactivation determination of Ta in minerals and rocks with a Ge(Li)-spectrometer, 25:2139

ZAITSEV, L. N., Attenuation of scattered synchrocyclotron radiation in a shield, 25:3480

ZAITSEVA, Natalia, Chemical state of radiorhenium formed in some inorganic Ir compounds irradiated with 660-MeV protons, 25:2300

ZAITSEVA, S. A., Development of an elementary magnetic disturbance, 25:2978

ZAKHARCHUK, A. V., IR-spectroscopy studies of γ-radiation effects on the crystallinity of poly(vinyl alcohol), 25:2220

ZAKREVSKII, N. V., Description of M1 transitions between rotational states of deformed nuclei, 25:3726

ZALESKI, T., Vinca Nova: automatic unit for neutron spectrometer control, 25:2475 (INP-707)

ZALEWSKI, K., Ambiguities in the experimental determination of resonance production amplitudes, 25:3382 (TPJU-1/70)

Physical bounds for the components of statistical tensors, 25:3296

Physical bounds for the components of statistical tensors, 25:3295 (TPJU-12/70)

Regge pole model with Veneziano residues for reactions $0^- \frac{1}{2}^+ \to 0^- \frac{3}{2}^+$, 25:3384 (TPJU-3/70)

ZAMOLODCHIKOV, O. G., Superconducting Zr--Nb ribbon level indicator, 25:2394

ZANFAGNA, B., Change in the polarization of an electromagnetic wave in a sheared magnetic field, 25:3146 (CEA-CONF-1608)

Harmonic absorption of microwaves in magnetized low-density plasma, 25:3145 (CEA-CONF-1607)

ZAPESOCHNYI, I. P., Absolute measurements of the excitation functions for the KII line produced in collisions between K^+ ions and Ne atoms, 25:2911

ZARETSKII, V. I., Dieckmann reaction, 25:4001 (UCRL-Trans-1417)

ZARZECKA, E., Estimation of the amount of exogenous inclusions in steel by means of neutron-activation analysis, 25:2132

ZASLAWSKY, Maurice, Multiaxial stress studies on rigid polyurethane foam, 25:3994 (UCRL-50909)

ZAYUKOVA, N. D., Bismuthiols as analytical reagents, 25:2070

ZEHRFELD, H.-P., Effect of inertia on losses from a plasma in toroidal equilibrium, 25:3060

ZELIKSON, Yu. M., Laws governing operation of metallic electrodes of MHD generator, 25:2940

ZHALKOVSKAYA, L. V., Inhomogeneities in lower ionosphere, 25:2992

ZHARINOV, V. V., Representation of the Jost--Lehmann--Dyson type, 25:3433 (ITF-70-33)

ZHDANOV, A. I., Electron plasma induced oscillations in a magnetic field, 25:3160

ZHILEIKO, G. I., Role of instabilities of monoenergetic electron beams, 25:3479

ZHILIN, V. G., Heat transfer in the turbulent flow of an electrically conducting liquid in a circular tube in a longitudinal magnetic field, 25:2944

ZHOMOV, F. I., Diffusion in W and Nb, 25:2703

ZHOROV, G. A., Effect of oxidation on the emissivity of molybdenum disilicide coatings, 25:2799

ZIEGLER, A., Apparatus for delivery of gas for flowthrough proportional counter, 25:2453

ZIMA, V. G., Interference phenomena in decays rho → $e^+ + e^-$ and ω → $e^+ + e^-$, 25:3367

ZIMMERMAN, J. E., Generation of harmonics and subharmonics of Josephson oscillation, 25:3037

ZIMMERMANN, P., Measurements of radio sources at 10.69 GHz, 25:2848

ZINCHENKO, G. N., Measurement of ionospheric parameters from Doppler and Faraday effects of coherent signals, 25:2971

ZINDLER, H., Fission products of nuclear explosions detected on territory of the GDR. II, 25:2370

ZINOV'EV, N. V., Polynomial approximation of the fast neutron spectrum measured by threshold detectors, 25:2442

ZOLLER, W. H., Decay of Zn and Zn to levels of ^{71}Ga, 25:3638

ZOLOTOV, Yu. A., Use of chelating reagents in the extraction--photometric determination of elements with basic dyes, 25:2087

ZORIN, E. I., Crystallization of amorphous films of silicon dioxide during ionic bombardment and subsequent annealing, 25:2823

ZORIN, V. A., Complete functions in analysis and representation of distant atmospherics, 25:2975

ZUCAL, R., Determination of traces of hafnium in aluminum--uranium alloys, 25:2063 (CNEA-276)

ZUFFI, L., Proton scattering from ^{23}Na and ^{25}Mg, 25:3603

SUBJECT INDEX

Cross references are included in cumulative subject indexes and in *Subject Headings Used by the USAEC Division of Technical Information* (USAEC report TID-5001).

The reader is also referred to *Guide to Abstracting and Indexing for Nuclear Science Abstracts* (USAEC report TID-4576).

Most headings in the subject index are specific materials, things, and processes. The headings are followed by modifiers that describe the properties of, or processes applied to, the headings.

All index entries cite *NSA* volume and abstract numbers; volume number precedes the colon and the abstract number follows it. The designation (R) following the abstract number indicates a progress report; (P) indicates a patent; and (T) indicates a translation. Abstracts for reports other than progress reports carry no letter designation. Report numbers, where applicable, are included in parentheses after the abstract number of the citation. Published literature (journal article or book) can be identified by the absence of a report number.

Ideas presented in the original literature, rather than key words, have been indexed. The indexers have selected what seemed the most probable and logical place to look for typical information. Since it is not always possible to anticipate where a user would look for information, the cumulative indexes include numerous cross references. Consideration of synonymous or closely related terms will prove valuable.

Information is indexed for the greatest use to the greatest number of users. This requires that a topic be indexed to headings that most specifically describe it and not ordinarily to the headings that describe its ultimate use or to the general class headings that include the specific headings. For example, information on boiler design for the Fermi Fast Breeder Reactor would be indexed under the headings BOILERS and FERMI FAST BREEDER REACTOR but not necessarily under the headings REACTORS, FAST or REACTORS, BREEDER.

General or broad headings are reserved for general summaries, reviews, comprehensive reports, and similar literature.

Subject Heading Styles

Generally, the direct form of subject entry is used rather than inverted headings; e.g., AMINO ACIDS rather than ACIDS, AMINO; HELIUM ISOTOPES He-4 rather than HELIUM—ISOTOPES He-4 or HELIUM—He-4 ISOTOPES. Note, however, that in some cases parenthetic modifying terms or inverted headings such as NEUTRONS, FAST, are used where the alphabetical arrangement of a direct entry would cause information to be scattered. In addition, organic compounds are usually entered in the index in the inverted form to facilitate grouping like or related compounds with the parent compounds; e.g., BENZENE, BROMO- rather than BROMOBENZENE. In general, the nomenclature used is that of the subject indexes to *Chemical Abstracts*.

Alphabetization

Subject headings are alphabetized word by word. Parenthetic qualifiers, numbers, and Greek letters within subject headings are disregarded in alphabetizing unless there are two or more headings that are otherwise identical, in which case the qualifier, numerical progression, or spelled names for the Greek letters determine the order.

Examples:

M-Capture
  see ELECTRON CAPTURE
MAGNESIUM
MAGNESIUM ALLOYS AND SYSTEMS
MANGANESE FLUORIDES
MANGANESE FLUORIDES MnF_2
MESONS
MESONS (π)
MESONS (ρ)
1-PENTANOL
2-PENTANOL

Modifying Phrases

The modifiers appearing under a subject heading are written specifically to show the relation between the item being indexed and the heading. The modifier therefore contains a maximum of useful information. Although the modifier begins with the word judged to be of greatest use to the greatest number of users, there is still need for the searcher to consider all modifiers under the heading(s) of interest.

Modifiers usually form meaningful phrases when combined with the subject heading. Some are intended to be read following the subject heading, e.g., the entry HYDROGEN—sorption by charcoal should be read "hydrogen sorption by charcoal." As a result of placing the important word first, however, many modifiers must be rearranged for smooth reading, e.g., FORMALDEHYDE—yields in radiolysis of ethyl ether, effects of deuterium on, should be read "effects of deuterium on formaldehyde yields in radiolysis of ethyl ether" and URANIUM—crystal structure of, effect of cooling rate on allotropic transformations in, should be read "effect of cooling rate on allotropic transformations in crystal structure of uranium."

Special characters are added to modifiers in the fields of physics and reactor technology; if the modifier does not establish the experimental or theoretical character of a reference, a symbol (E), (T), or (E/T) is placed immediately after the modifying phrase and before the abstract number.

Physical States and Configurations of Materials

The specific physical state, if other than normal, or the geometric configuration of the material is included in the modifying phrase; e.g., information on liquid metals is indexed under the specific metal with "liquid" in the modifier and carbon crucibles is indexed under CARBON with "crucibles" appropriately placed in the modifier. The information on carbon crucibles is also indexed under CRUCIBLES.

Nomenclature of Inorganic Compounds

Inorganic compounds are indexed to subject headings in the direct form. Cations are listed in the order of increasing valence for polycationic salts of varying valence and in alphabetic order for polycationic salts in which all cations have the same valence; e.g., SODIUM ALUMINUM SILICATES and POTASSIUM SODIUM SULFATES. If more than one anionic species is presented in a compound, the anions are arranged alphabetically, e.g., BERYLLIUM FLUORIDE HYDROXIDES.

Nomenclature of Organic Compounds

Organic compounds are indexed by subject headings based on the indexes to *Chemical Abstracts* except in the area of enzymes, in which specific enzymes, named according to the 1964 recommendations of the International Union of Biochemistry, are used. In many cases nonproprietary names for drugs are used as subject headings, and cross references are made from the systematic chemical names. Subject headings for hormones appear in the inverted style at HORMONES.

Nomenclature of Life Sciences

Subject headings for plants are names of phyla with one exception: members of the Phylum Tracheophyta are indexed under class or subclass names. Scientific names (genus and species) are used as the initial, or file, word in the modifying phrase. Scientific names are omitted only when the name is not available in the literature or cannot be found in available references.

Subject headings for animals are the names of phyla with the following exceptions: (1) members of Phylum Arthropoda and Phylum Chordata are indexed under appropriate class name, and (2) common names are used for members of Class Mammalia.

Subject headings are entered for various classes of commodities, and specific products are identified in the file-word position of the modifier. In the following examples, approved subject headings are capitalized and typical modifier file words are listed in lower case.

Example 1	Example 2
CEREALS	MEATS
bread	beef
flour	fish
oats	mutton
rice	pork
rye	poultry
wheat	seafood

Diseases, pathological conditions, and in vitro studies of atypical cells and tissues are indexed under subject headings for the organism affected, under the appropriate anatomical structure of physiological phenomenon affected, and under the appropriate disease heading. Subject headings for diseases (defined as any deviation from the norm) are DISEASES; DISEASES, INFECTIOUS; DISEASES, NEOPLASTIC; DISEASES, PHYSIOLOGICAL; DISEASES, PLANT; and DISEASES, TRAUMATIC.

Diseases of mixed etiology are treated in the following manner: neoplastic diseases that are also classified as infectious or physiological are indexed under DISEASES, NEOPLASTIC; diseases in which a microorganism is the etiologic agent are classified under DISEASES, INFECTIOUS; physiological anomalies that are neither neoplastic nor infectious are indexed under DISEASES, PHYSIOLOGICAL; the acute radiation syndrome, nonspecific radiation injuries, trauma, and wounds or incisions inflicted mechanically are indexed under DISEASES, TRAUMATIC.

Specific diseases or pathological conditions are named in the file-word position of the modifier, in the author's terminology, and are set off from the remainder of the modifier by commas. Neoplasms are designated as benign or malignant in the file-word position when more specific information is not available.

Multicomponent Alloys and Other Systems

Multicomponent alloys and systems, except well-known trade names, are indexed under a subject heading for each component in the form "element systems" for nonmetals or "element alloys and systems" for metals. The modifier begins with element symbols for each component arranged alphabetically. In addition, if significance is placed on the base metal of the alloy, this is indicated by adding "-base" to the element symbol.

Example: A 1.5C, 12Cr, 0.25V, 0.8Mo, bal Fe alloy is indexed as

```
CARBON SYSTEMS
  C--Cr--Fe-base--Mo--V, ...
CHROMIUM ALLOYS AND SYSTEMS
  C--Cr--Fe-base--Mo--V,...
IRON ALLOYS AND SYSTEMS
  C--Cr--Fe-base--Mo--V, ...
MOLYBDENUM ALLOYS AND SYSTEMS
  C--Cr--Fe-base--Mo--V, ...
VANADIUM ALLOYS AND SYSTEMS
  C--Cr--Fe-base--Mo--V, ...
```

Well-known alloys, such as ZIRCALOY-2, are indexed under the trade name; cross references from each component of the alloy to the trade name appear in cumulative indexes.

Multicomponent systems in which nonmetallic elements are present in large percentage and which are commonly referred to as systems or mixtures are indexed in a manner similar to alloys.

Example: A tungsten–silicon preparation is indexed as

```
TUNGSTEN ALLOYS AND SYSTEMS
  Si--W, ...
SILICON SYSTEMS
  Si--W, ...
```

Multicompound systems and mixtures of inorganic compounds are indexed under the subject heading for each component compound; the modifiers begin with an alphabetical listing of compound formulas.

Example: A lead titanate–lead zirconate mixture is indexed as

```
LEAD TITANATES
  PbTiO3--PbZrO3
LEAD ZIRCONATES
  PbTiO3--PbZrO3
```

A mixed system of compounds and elements is indexed by a combined form of the preceding conventions; e.g., a dispersion of copper and alumina would be indexed as

ALUMINUM OXIDES
  Al_2O_3--Cu, ...
COPPER ALLOYS AND SYSTEMS
  Al_2O_3--Cu, ...

Mixtures of organic compounds are indexed under subject headings for each component of the mixture; the modifiers begin with an alphabetical listing of compound names.

Example:

ACETIC ACID
  acetic acid--BF_3, ...
BORON FLUORIDES
  acetic acid--BF_3, ...

Example:

BENZENE, CHLORO-
  bromophenol--chlorobenzene, ...
PHENOL, BROMO-
  bromophenol--chlorobenzene, ...

If modifiers for alloys and systems are included with other modifiers under the same subject heading, they are filed last.

Example:

CARBON SYSTEMS
  deposition on nuclear fuel particles
  molecular structure of
  neutron total cross section for
  sorptive properties for xenon
  Young's modulus for
  Al--C--Cr, superconductivity in
  B--C, phase studies for
  C--U--Zr, fabrication and physical properties of

Nomenclature of High Energy Physics

Information on particle-particle events is indexed under subject headings for the specific particles involved. The modifier file word *interactions* is followed by the specific interaction written in symbolic form. Particle nomenclature and symbols follow that of Rosenfeld, et al. *Data on Particles and Resonant States*, UCRL-8030 (latest revision). For consistency the incident particle is always written first. The mass (in MeV) of a resonance state is included in parentheses after the symbol to avoid ambiguity. Hyperfragments are indicated in modifiers as in the following examples: Λ-He^5, Σ-H^3, $\Lambda\Lambda$-Be^{10}. The superscript on the right indicates the total number of baryons in the composite system.

Examples:

MESONS (π^-)
  interactions $\pi^- + p \rightarrow \Lambda + K^+ + \pi^-$ at 6 GeV/c in hydrogen bubble chamber, ΛK(1700) enhancement in, (E)
BARYONS, RESONANCE (N^*)
  production of $\Delta^{++}(1236)$ and $\Delta^0(1236)$ from $K^- + p \rightarrow K^- + p + \pi^+ + \pi^-$ interactions at 2.63 and 2.70 GeV/c, (E)
HYPERFRAGMENTS
  binding energy of $\Lambda\Lambda$-He^6, three-body o--Λ--Λ model for

Subject headings are also provided for specific models and theories.

Examples:

ELEMENTARY PARTICLE MODELS (TRIPLET)
  hadron total cross sections in quark, numerical analysis of
CURRENT ALGEBRA
  PCAC hypothesis for A_1 and rho dominance in $\pi \rightarrow e + \nu + \gamma$ decay
REGGE POLE THEORY
  predictions for polarization in $K^- + p \rightarrow$ anti $K^0 + n$, $\pi^- + p \rightarrow \pi^0 + n$, and $\pi^- + p \rightarrow$ eta + n interactions at high energies
SYMMETRY GROUPS
  SU(2) × SU(4) intermediate-coupling model for nucleon and hyperon isobars

Nomenclature of Reactor Technology

Subject headings for reactors are of three types:

(1) Specific reactors, e.g., ARGONNE RESEARCH REACTOR, SAXTON POWER REACTOR

(2) Reactors having a common physics or engineering characteristic, e.g., REACTORS, FAST; REACTORS, ORGANIC-COOLED; REACTORS, PRESSURIZED-WATER

(3) Reactors having a common purpose, e.g., REACTORS, POWER; REACTORS, RESEARCH

Information on specific reactors, type (1), is indexed under the one specific subject heading. Information on classes or types of reactors, types (2) (characteristics) and (3) (purpose), is indexed under all applicable headings. For example, information on a heavy-water-moderated organic-cooled power reactor is indexed under REACTORS, HEAVY WATER-MODERATED; REACTORS, ORGANIC-COOLED; and REACTORS, POWER.

Subject headings exist for selected reactor components, e.g., REACTOR FUEL ELEMENTS. When applicable, headings for components are indexed even though they may have been included in a modifier under a type (1) or (2) heading. The materials in reactor components are indexed when the information is peculiar to the material.

Modifier file words under reactor headings are of two primary types: one type expresses reactor characteristics, e.g., reactivity; the other, components, e.g., control rod. If no subject heading appears for a reactor component, the heading REACTORS is used, and the component is used as the modifier file word.

A

ABERDEEN FAST PULSE REACTOR FACILITY
materials for, development of, 25:2645 (ORNL-4570, pp 214)
ACCELERATORS
beam injection, extraction, or splitting for, high current septum magnets for, 25:3522
conference on, 25:3484
conference on, 25:3485
conference on use of small, for teaching and research, 25:3463 (CONF-700322)
description of low-voltage tandem, for atomic physics experiments, 25:3470 (CONF-700322-, pp 259-79)
design and operation of heavy-ion 150-keV, for ion implantation, 25:3469 (CONF-700322-, pp 173-84)
experimental facilities for activation analysis, neutron source, 25:2120 (CONF-700322-, pp 231-48)
experimental facilities for low-energy, for educational purposes, time-of-flight, 25:3468 (CONF-700322-, pp 125-32)
experimental facilities for neutron radiography, review on, 25:3471 (CONF-700322-, pp 321-44)
experimental facilities for neutron therapy, review on development of, 25:3473 (CONF-700322-, pp 407-29)
experimental facilities for small, for educational purposes, 25:3464 (CONF-700322-, pp 1-19)
experimental facilities for, helium refrigeration systems for superconducting magnets in, 25:3508
radiation dosimetry and shielding at, conference on, 25:3476 (JINR-16-4888)
radiation safety at low-energy, 25:3475 (CONF-700322-, pp 441-8)
shielding measurements for, gamma dose rate distributions and neutron attenuation, 25:3480
uses in radiation facilities, design of equipment for, 25:2389
uses of small, in nuclear safeguards research, 25:2418 (CONF-700322-, pp 357-78)
ACETAMIDE, N,N-DIMETHYL-
complexes with uranium pentabromide in acetone, spectra of, 25:2200
ACETAMIDE, N-METHYL-
association in carbon tetrachloride, effects of deuterium on self-, 25:2174
ACETIC ACID
effects on γ-radioinduced graft polymerization of cellulose with styrene in methanol solutions, 25:2247
ACETIC ACID, ETHYL ESTER
effects on γ-radioinduced graft polymerization of cellulose with styrene in methanol solutions, 25:2247
ACETIC ACID, (ETHYLENEDINITRILO)TETRA-
effects on uv spectrophotometric determination of gallium in aqueous solutions, 25:2100
sodium salt, complexes with cobalt, radiation effects on aqueous solutions of tetrahydrated, chemistry of cobalt-60 recoils produced by neutron, 25:2297
sorption of chromium-51-labeled, in patient with ulcerative colitis, 25:2534
uses in complexometric determination of uranium, 25:2088
ACETIC ACID, VINYL ESTER
radiation effects on electric conductivity of solid, at -196°C, γ, 25:2221
ACETONE
effects on γ-radioinduced graft polymerization of cellulose with styrene in methanol solutions, 25:2247
effects on radiolysis of water, 25:2267
ACETONITRILE
radiation effects on electric conductivity of solid, at -196°C, γ, 25:2221
radiolysis of, reversibility of electron-excess center in γ, 25:2271
ACETOPHENONE
effects on radioinduced isomerization of norbornadiene, 25:2239
radiolysis of, yields from electron, 25:2266
ACETYLENE
determination in products from radiolysis of gaseous ethylene, gas chromatographic method for, 25:2278
ACIDS
effects on hydrogen abstraction by primary species from frozen γ-irradiated aqueous solutions of alcohols, 25:2293
separation from aqueous solutions by solvent extraction using trialkylamines, coalescence of organic solutions in, 25:2308 (CEA-R-3845)
ACRIDINE
effects on γ-radioinduced graft polymerization of cellulose with styrene in methanol solutions, 25:2247
ACRYLAMIDE
radiation effects on electric conductivity of solid, at -196°C, γ, 25:2221
radioinduced graft polymerization with poly(ethylene terephthalate) in presence of fumaric acid, maleic acid, and methylenesuccinic acid, 25:2244
ACRYLIC ACID
radioinduced polymerization with polyethylene terephthalate, effects of dose and temperature on mechanism of γ, 25:2240
ACRYLONITRILE
radiation effects on electric conductivity of solid, at -196°C, γ, 25:2221
ACTINIDE CARBIDES
preparation of microspheres of, method for, 25:2795(P)
preparation of particulate, sol process for, 25:2780(P)
ACTINIDE OXIDES
preparation of fuels of, method for, 25:2784(P)
preparation of microspheres of, method for, 25:2795(P)
properties of sols of, 25:2775 (ORNL-4572, pp 242-50)
ACTINIDES
chemistry of, research progress on, 25:2294 (ORNL-4572, pp 109-34)
complexes with acetates, thermodynamic properties of, 25:2208
separation by elution chromatography, 25:2294 (ORNL-4572, pp 109-34)
ACTINIUM
electric potential of divalent-trivalent couple of, 25:2159
polarographic behavior of, 25:2159
separation from thorium and/or radium and radioactive decay products by halogenation and sublimation, 25:2322(P)
ACTIVATION ANALYSIS
bibliography on 14-MeV neutron generators in, 25:2130 (NBS-TN-533)
bibliography on, of pollution samples, 25:2129 (NBS-TN-532)
Compton scattering methods applied to, 25:2140
conference on studies of mineral metabolism in man using, 25:2122 (IAEA-122)
conference on, Poznan, Poland, November 1968, 25:2141
equipment for, at Institute of Applied Geophysics, Brno, Czechoslovakia, 25:2131
equipment for, review on development of neutron generator, 25:3527 (CONF-700322-, pp 185-204)
neutron generators for, use of accelerators for, 25:2120 (CONF-700322-, pp 231-48)
research program for medical, at IAEA, 25:2124 (IAEA-122, pp 15-26)
research program on thermal and 14-MeV neutron, in Pakistan, 25:2125 (IAEA-122, pp 27-36)
sample preparation for neutron, by deposition on plastic matrix, 25:2146
ADENINE
radiolysis of aqueous chloride solutions of, rate constants for electron pulse and γ, 25:2259 (GA-10208)
ADENOSINE MONOPHOSPHATES
radiolysis of aqueous chloride solutions of, rate constants for electron pulse and γ, 25:2259 (GA-10208)
AEROSOLS
coagulation and settling of high-mass density, effects of Brownian motion and gravitation on, 25:2369
AIR
analysis of ambient, for molybdenum using thiocyanate, tentative spectrophotometric method for, 25:2103
analysis of ambient, for plutonium and plutonium isotopes, tentative radiochemical method for, 25:2113
analysis of ambient, for strontium-89, tentative radiochemical method for, 25:2114
analysis of ambient, for strontium-90, tentative radiochemical method for, 25:2115
properties for use as cover gas for pressurized gas metal-arc welding, 25:2646 (RFP-1550)
separation of radon from streams of, filter efficiency for, 25:2414 (AD-707709)
AIR FORCE ENGINEERING TEST REACTOR
fuels for, specifications and procurement of, 25:2772 (ORNL-4570, pp 174)
AIR SAMPLERS
calibration of two-stage, method for, 25:2446
AIRGLOW
enhancement of 6300-A predawn, at higher midlatitudes, (E), 25:2961
hydroxyl emission in, altitude profile of, (E), 25:3001
ALASKA
hydrology and lithology of Drill Hole UA-1 from 5000 to 6500 ft on Amchitka Island, 25:2349 (USGS-474-72)
ALIQUAT-336
solvent properties for niobium, 25:2334
ALKALI METALS
corrosive effects on refractory metals in space power systems, research program on, 25:2607 (ORNL-4570, pp 103-5)
nuclear magnetic resonance of, model for Knight shifts in, 25:2671 (ORNL-4570, pp 40-3)
ALKALINE EARTH METALS
separation of cerium, gadolinium, lanthanum, and neodymium from, by precipitation using cupferron, 25:2078
ALKENES
complexes with iron tricarbonyl, deuterium exchange in, 25:2187
ALKYL HALIDES
effects on γ radiolysis of cyclohexane, 25:2268
ALKYL IODIDES
iodine-131 exchange between iodide ions and, in acetone--water solution, 25:2177
ALLENE
determination in products from radiolysis of gaseous ethylene, gas chromatographic method for, 25:2278

ALLOYS
book: Radiation Corrosion, 25:2603(T) (AEC-tr-7096)
phase transformations in ferrous and nonferrous, heuristic comparisons of martensitic, 25:3938 (COO-1198-753)
properties of tubes of, for use in nuclear reactor construction, 25:2678
x-ray scattering from disordered binary, intensity distribution of, 25:2730 (ORNL-4570, pp 44-6)
ALPHA DECAY
theory for, alpha--daughter nucleus interaction in, 25:3725
ALPHA PARTICLES
effects on aqueous solutions of nitric acid, 25:2284
effects on destruction of foam, 25:2223
effects on trioxane crystals, production of polyoxymethylene crystals by, 25:2252
effects on void formation in aluminum subjected to preinjection of hydrogen, 25:2816 (ORNL-4570, pp 16-19)
energy loss in aluminum oxide at 5.5, 6.6, and 8.8 MeV, 25:2887
mass in superfluid nuclear matter, (T), 25:3728
reactions (α,3n) at 34 MeV, gamma energy and angular distributions for, (E), 25:3700
reactions (α,f) with gold-197, bismuth-209, and uranium isotopes at 103 MeV, cross sections and fragment angular distributions from, (E), 25:3710
reactions (α,γ) with carbon-12, survey of research on, 25:3562 (CONF-700322-, pp 297-304)
reactions (α,nγ) and (α,pγ) with titanium-48 at 12 to 15 MeV, γ singles and n-γ coincidence spectra from, (E), 25:3593 (COO-1530-21)
reactions (α,pγ) with calcium-40 at 7.0 to 12.0 MeV, gamma angular distributions from, (E), 25:3626
reactions with nuclei, model for analysis of, (T), 25:3716 (ORNL-TM-3153)
scattering by aluminum-27 at 22.2 MeV, α angular distributions and α-γ coincidence spectra from inelastic, (E), 25:3600
scattering by bismuth-209 and lead-204, -206, and -208 at 14 to 24 MeV, optical-model analysis of elastic, (E), 25:3689
scattering by europium-151 and europium-153 at 5 to 12 MeV with Coulomb excitation, γ spectra from inelastic, (E), 25:3703
scattering by nuclei at 27.5 MeV, optical-model analysis using real potentials from double-folding procedure of elastic, (T), 25:3755
scattering by zinc-64 and -66 at 31 MeV, angular distributions for, (E), 25:3630
scattering elastically by helium-4, analysis using separable nonlocal potential, (T), 25:3544 (LYCEN-7041)
ALPHA SOURCES
preparation for reduced recoil-nuclei and gaseous contamination of detectors, 25:2478
ALPHA SPECTROMETERS
contamination of semiconductor, sources and prevention of recoil, 25:2479
design and performance of low-level double-grid ionization, 25:2476
performance of time-of-flight, for nuclear reaction studies, 25:2469
sample preparation for reduced recoil-nuclei and gaseous contamination in, 25:2478
ALUMINUM
analysis by spark method, automated quantometer data handling system for, 25:2069 (Y-1740)
beta particle penetration in, intensity variation with thickness for external bremsstrahlung production from, (E), 25:3249
determination following nonsulfide separation from elements, qualitative, 25:2101
determination in lunar materials by 14-MeV neutron activation and γ spectrometry, 25:2118 (CONF-700322-, pp 205-20)
determination in oceanographic samples by 14-MeV neutron activation and γ spectrometry, 25:2119 (CONF-700322-, pp 221-30)
determination in pigments from ancient murals by neutron activation, 25:2133
determination in titanium alloys, x-ray fluorescence method for, 25:2097
determination of trace amounts of, in lanthanum oxide, neodymium oxide, and yttrium oxide by direct reading emission spectrometry, 25:2096
determination of trace amounts of, in nuclear-grade uranium oxide (U_3O_8) by direct reading spectrometric method, 25:2068 (NLCO-1071)
diffusion in, activation volume for self-, 25:3962 (IS-T-410)
effects on determination of trace amounts of antimony by isotopic exchange in organic phase, 25:2106
effects on photometric determination of hafnium and zirconium in geological specimens, 25:2084
effects on uv spectrophotometric determination of gallium in aqueous solutions, 25:2100
electron backscattering at 1 MeV, angular distribution and energy spectra for, 25:2886
electron reactions at 1 to 3 MeV with, backscatter and transmission coefficients for, (E), 25:2883 (N-70-25499)
electronic states in, theory of, 25:2671 (ORNL-4570, pp 40-3)
gamma reflection and transmission by, spectral and angular-distribution function for, 25:3168
gamma scattering by electrons in, incoherent cross sections for 30-keV to 2.62 MeV, (T), 25:2921
grain--boundary migration in zone-refined, relations with driving forces, 25:2728 (ORNL-4570, pp 5-9)
microstructure of recrystallized, 25:2728 (ORNL-4570, pp 5-9)
neutron attenuation by, monoenergetic-source fast-, (E/T), 25:3173
neutron capture by, gamma spectra from thermal, (E), 25:3181
neutron cross sections for, 25-group, (T), 25:3530 (LA-4484)
neutron reactions with, silicon production by, 25:2816 (ORNL-4570, pp 16-19)
neutron scattering by, exponential angular coefficients for fast, (E), 25:3171
photon reactions at 1.5 to 5 GeV, cross sections for K^0 production in, (E), 25:3248
photon reactions at 5.7 GeV, $\omega\gamma$ coupling constant and ωN cross section from ω production in, (E), 25:3247
plasmon excitation in electron-bombarded thin films of, radiative decay of volume and surface, 25:2885
radiation damage in monocrystals of, electron microsccpy of cesium-ion, 25:2507
radiation effects on porosity and swelling of, fast neutron, 25:2759 (ORNL-4570, pp 152-6)
radioinduced displacement damage in, electron, 25:2816 (ORNL-4570, pp 16-19)
radioinduced voids in, configuration of fast neutron, 25:2816 (ORNL-4570, pp 16-19)
radioinduced voids in, effects of preinjected hydrogen on alpha particle, fast neutron, and proton, 25:2816 (ORNL-4570, pp 16-19)
reactions with platinum, 25:2160
release to soil from organic debris in forest as function of decomposition mode and time, 25:2528
separation of cerium, gadolinium, lanthanum, and neodymium from, by precipitation using cupferron, 25:2078
welding of Type 1100, performance of air and argon as cover gases in pressurized gas metal-arc, 25:2646 (RFP-1550)
welding of, parameters for pressurized inert gas arc, 25:3973 (RFP-1515)
work softening in polycrystalline, 25:2724
ALUMINUM ALLOYS AND SYSTEMS
work softening in polycrystalline, 25:2724
Al--Al_2O_3, energy transfer in, during γ radiolysis of chrysoidine adsorbed on oxide surface, mechanism of, 25:2276
Al--Al_2O_3, thermal conductivity of dispersions of, at 280 to 400°K, 25:2770 (ORNL-4570, pp 127-35)
Al--Cr, crystal structure of supercooled solid solutions of, 25:2733
Al--Cr--Fe--Ti-base, microstructure of hot-rolled plates and sheets of α + β, relations of mechanical properties with abnormal, 25:2752
Al--Mn, crystal structure of solid solutions of, 25:2733
Al--Mo--Sn--Zr-base, corrosion by sodium at 450°C, effects of oxygen on, 25:2611 (PEL-201)
Al--Mo--Ti-base--V, microstructure of hot-rolled plates and sheets of α + β, relations of mechanical properties with abnormal, 25:2752
Al--Ti-base--V, corrosion by aqueous dinitrogen tetroxide, stress, 25:2635
Al--Ti-base--V, electron reactions at 1 to 3 MeV with, backscatter and transmission coefficients for, (E), 25:2883 (N-70-25499)
Al--Ti-base--V, microstructure of hot-rolled plates and sheets of α + β, relations of mechanical properties with abnormal, 25:2752
Al--U, analysis for hafnium, spectrographic, 25:2063 (CNEA-276)
Al--U_3O_8, fabrication of dispersion-type fuel elements of, development of methods for, 25:2770 (ORNL-4570, pp 127-35)
Al--U_3O_8, radiation effects on swelling of dispersion-type fuels of, in-pile, 25:2770 (ORNL-4570, pp 127-35)
Al--Zr, crystal structure of supercooled solid solutions of, 25:2733
Al-base--U, void content of fuel of UAl dispersions in Al matrix, effects of cladding, cold-rolling, and composition on, 25:2806 (ORNL-4611)
Al-base--U_3O_8, void content in, effects of cladding, cold-rolling deformation, and composition on, 25:2806 (ORNL-4611)
ALUMINUM BROMIDES
$AlBr_3$--NaBr, electric conductivity and density of molten mixtures of, 25:2805 (ORNL-4570, pp 31-4)
ALUMINUM CHLORIDES
electric conductivity of liquid and vaporous, 25:2805 (ORNL-4570, pp 31-4)
$AlCl_3$--CsCl--$NiCl_2$, formation of $NiCl_3^-$ complex in, mechanisms of, 25:2805 (ORNL-4570, pp 31-4)
$AlCl_3$--KCl, electric conductivity of molten mixtures of, 25:2805 (ORNL-4570, pp 31-4)

$AlCl_3$--$NiCl_2$, phase studies of, 25:2805 (ORNL-4570, pp 31-4)
$AlCl_3$--$TiCl_3$, phase studies of, 25:2805 (ORNL-4570, pp 31-4)
ALUMINUM IONS
implantation in diamond crystals, semiconducting layers induced by, 25:3199
ALUMINUM ISOTOPES Al-26
abundance in three pallasites, (E), 25:2824
ALUMINUM ISOTOPES Al-27
alpha inelastic scattering at 22.2 MeV, α angular distributions and α-γ coincidence spectra from, (E), 25:3600
energy levels from alpha inelastic scattering, spin-parity assignments and branching ratios for, (E), 25:3600
neon-20 reactions with, mica-detector measurements of cross sections for compound nucleus formation in, 25:3611
oxygen-16 reactions with, mica-detector measurements of cross sections for compound nucleus formation in, 25:3611
proton reactions at 24 to 46 MeV, total cross sections for, (E), 25:3568
ALUMINUM OXIDES
alpha particle stopping power at 5.5, 6.6, and 8.8 MeV, 25:2887
effects on γ radiolysis of carbon monoxide, 25:2262 (RD/B/N-1279)
effects on properties of sintered zircons, 25:2766(T) (CSIRO-Trans-9924)
preparation of microspheres of, method for, 25:2795(P)
preparation of thin films of, 25:2887
reactions with platinum, 25:2160
Al_2O_3--SiO_2, compatibility with stainless steel at 370 to 700°C, 25:2606 (ORNL-4570, pp 92-5)
Al--Al_2O_3, energy transfer in, during γ radiolysis of chrysoidine adsorbed on oxide surface, mechanism of, 25:2276
Al--Al_2O_3, thermal conductivity of dispersions of, at 280 to 400°K, 25:2770 (ORNL-4570, pp 127-35)
AMERICIUM
alpha decay of, chemical states of recoil neptunium from, 25:2305
basicities of aqueous solutions of, 25:2319 (ORNL-4572, pp 181-95)
complexes with Arsenazo III, spectrophotometric studies on, 25:2079
complexes with nicotinic acid, picolinic acid, and picolinic acid 1-oxide, ir and NMR spectral and thermogravimetric studies on, 25:2194 (KFK-1070)
determination in aqueous alcohol solutions using Arsenazo III, spectrophotometric, 25:2079
spectra of trivalent, in aqueous solutions, 25:2152 (ORNL-4572, pp 231-5)
AMERICIUM ACETATES
stability of ions of, effects of inner sphere complexing on, 25:2208
AMERICIUM ISOTOPES Am-243
energy levels from plutonium-242 (He-3,d) and (α,t) reactions, properties of, (E), 25:3669
AMERICIUM OXIDES
americium alpha decay in, chemical states of recoil neptunium from, 25:2305
fabrication of HFIR targets of, 25:2792 (ORNL-4570, pp 201-4)
Am_2O_3--Cm_2O_2, preparation of microspheres of, 25:2294 (ORNL-4572, pp 109-34)
AMIDE POLYMERS
radiation effects on stress-rupture stability of, by cross linking, electron, 25:2249
AMINES
effects as catalyst on physical properties of rigid urethane foams, 25:2818 (BDX-613-170)
solvent properties for uranium and thorium, effects of salting-out agents on, 25:2335
solvent properties of tertiary, for niobium, 25:2334
solvent properties of, evaluation of, 25:2319 (ORNL-4572, pp 181-95)
AMINO ACIDS
analysis of, direct digital readout of data from, 25:3965 (LA-4507)
AMMONIA
effects on radiolysis of chloroform at 25°C, 25:2264
production from x-irradiated arginine and citrulline, 25:2588
radiolysis of, effects of dose, pressure, and temperature on γ, 25:2283
AMMONIUM ACID PHOSPHATES
radiation effects on solid, reactions of recoil phosphorus-32 from thermal-neutron, 25:2302
AMMONIUM COMPOUNDS, SUBSTITUTED
dialkylmethylbenzylammonium salts, solvent properties for molybdenum and rhenium, 25:2328
tetraethylammonium uranyl nitrate, spectra of, ir and Raman, 25:2212
AMMONIUM IONS
determination by potentiometric titration with sodium tetraphenylboron using Orion liquid ion exchange lead-selective electrode, 25:2104
effects on cesium-137 availability in mineral soils, 25:2529
AMMONIUM URANYL NITRATES
spectra of, ir and Raman, 25:2212
AMMONIUM URANYL SULFATES
spectra of, electronic and ir absorption, 25:2211
ANALYTICAL CHEMISTRY
book: Computers in Analytical Chemistry, 25:2060
standard procedures for health and safety laboratory, manual on, 25:2059 (NYO-4700(3rd Ed.))
ANGIOSPERMIDAE
Citrus sinensis, radioinduced mutations in, northward migration by means of, 25:2552(R) (ORO-2909-9)
Citrus sinensis, survival of radioinduced mutations of, in cold weather, 25:2552(R) (ORO-2909-9)
Helianthus annuus, radioinduced chromosome aberrations in dormant seeds of, x, 25:2555
Hordeum sp., radiation effects on growth of spikes of, protective effects of plant hormones against γ, 25:2597
Lactuca sativa, radioinduced chromosome aberrations in dormant seeds of, x, 25:2555
Phaseolus sp., radiation effects on enzyme activity in sprouts of, γ, 25:2596
Phragmites communis, cesium accumulation by, in pond ecosystem, neutron activation analysis of, 25:2516
Trifolium sp., radiation effects on enzyme activity in sprouts of, γ, 25:2596
Zea mays, radioinduced mutations in, for aleurone pigmenting potential, effects of seed exposure on γ and x, 25:2560
ANILINE
effects on γ-radioinduced graft polymerization of cellulose with styrene in methanol solutions, 25:2247
ANIMALS
populations of, research on development of, (E/T), 25:3946(R) (COO-1761-13)
populations of, research on development of, (E/T), 25:3947(R) (COO-1761-14)
radioisotope fixation by aquatic, in Meuse River, cobalt-60 and manganese-54, 25:2544
ANTENNAS
impedance in topside ionosphere, parameters affecting satellite-borne loop, (E), 25:2967
ANTIBODIES
radiation effects on formation of, in rats following immunization with bovine serum albumin, x, 25:2540
synthesis in mice, effects of carbon blockage of reticulo-endothelial system on, 25:2538
ANTIFERROMAGNETIC MATERIALS
model of amorphous, 25:3936 (CALT-822-16)
ANTIGENS
transplantation, in animals, review of incidence of, 25:2537
ANTIMONY
density at 635 to 745°C, 25:2692
determination following nonsulfide separation from elements, qualitative, 25:2101
determination of trace amounts of, in presence of other metals, by isotopic exchange in organic phase, 25:2106
effects on uv spectrophotometric determination of gallium in aqueous solutions, 25:2100
neutron elastic scattering at 1 to 40 keV, analysis of angular distributions from, (E/T), 25:3695
production of pure, review of techniques for, 25:3219
radioinduced preparation from aqueous salt solutions, electron, 25:2237 (N-70-32826)
separation from nitrate and sulfate solutions by solvent extraction using amines, 25:2319 (ORNL-4572, pp 181-95)
ANTIMONY ALLOYS AND SYSTEMS
Bi--Sb, density at 403 to 742°C, 25:2692
In--Sb, pinch in avalanche plasma in n-type InSb, dynamic processes in linear, (E/T), 25:3206
N--Sb--Th, crystal structure of Th_2N_2Sb formed in, 25:2248
N--Sb--U, crystal structure of U_2N_2Sb formed in, 25:2248
ANTIMONY ISOTOPES Sb-124
beta decay of, β-γ circular polarization correlations in, (E), 25:3697
beta decay of, γ-γ coincidence spectra and angular correlations from, (E), 25:3657
exchange between antimony triiodide and antimony diethyldithiocarbamate in carbon tetrachloride, 25:2106
ANTIMONY ISOTOPES Sb-125
exchange between antimony trichloride and tetraphenylstibonium hydroxide, 25:2169
ANTIMONY OXIDES
alkali metal fixation on hydrated, in hydrochloric, nitric, and perchloric acids, effects of acidity and time on, 25:2333
fluorine fixation on hydrated, in hydrochloric acid, effects of acidity and time on, 25:2332
ARCHAEOLOGICAL SPECIMENS
age of, review of methods for estimation of, 25:2354
location of buried, review of methods for determining, 25:2354
ARGININE
effects on x-radiosensitivity of hydra, 25:2588
ARGON
plasma jets of, use for detection of hydrocarbon

deposits, (T), 25:3098
plasma of, relaxation phenomena in shock tubes, (E), 25:3064
properties for use as cover gas for pressurized gas metal-arc welding, 25:2646 (RFP-1550)
properties for use as protective atmosphere for niobium and tantalum at high temperatures, 25:2639(T) (LIB/Trans-309)
ARGON IONS
effects on glass crystallization at 50 keV, relations with annealing, 25:2823
reactions with graphite and metal surfaces at 5 to 50 keV, apparent total ion scattering, secondary electron emission coefficients, and electron and ion energy distributions for, (E), 25:2884 (NP-18490)
ARGON ISOTOPES Ar-36
energy levels of, calculation using Hartree--Fock--Bogolyubov method with isospin pairing, (T), 25:3722
proton elastic and inelastic scattering at 2.1 to 5.3 MeV, angular distributions for, (E), 25:3641
ARGON ISOTOPES Ar-40
energy-level transitions from potassium-40 decay, (E), 25:3694
helium-3 reactions (He-3,d) at 10 MeV, deuteron spectra from, (E), 25:3632
ARGONNE SYNCHROTRON (ZGS)
experimental facility for, superconducting beam line, 25:3505
ARMY REACTORS (MH-1)
fuels for, specifications and procurement of, 25:2772 (ORNL-4570, pp 174)
ARMY REACTORS (PM-3)
fuels for, specifications and procurement of, 25:2772 (ORNL-4570, pp 174)
ARSENIC
determination following nonsulfide separation from elements, qualitative, 25:2101
determination in pigments from ancient murals by neutron activation, 25:2133
determination of trace amounts of, in nuclear-grade uranium oxide (U_3O_8) by direct reading spectrometric method, 25:2068 (NLCO-1071)
effects on determination of trace amounts of antimony by isotopic exchange in organic phase, 25:2106
effects on uv spectrophotometric determination of gallium in aqueous solutions, 25:2100
production of pure, review of techniques for, 25:3219
separation from nitrate and sulfate solutions by solvent extraction using amines, 25:2319 (ORNL-4572, pp 181-95)
ARSENIC ISOTOPES As-72
beta and electron-capture decay of, γ singles and coincidence and conversion electron spectra from, (E), 25:3639
ARSENIC ISOTOPES As-74
beta and electron-capture decay of, γ spectra from, (E), 25:3704
ARSENIC OXIDES
proton reactions at 350 keV with, characteristic x-ray spectra from, (E), 25:2882 (CONF-700322-, pp 113-24)
ARSINE OXIDE, TRIPHENYL-
complexes with uranyl nitrate, spectra of, ir and Raman, 25:2212
ASTRONAUTICS
book: Advances in Space Science and Technology, Vol. 10, 25:2396
developments in, review of, 25:2397
ATMOSPHERE
fallout content of East German low-level, 1968 and 1969, 25:2370
oxygen height profile above 70 km in, sensor for atomic, (E), 25:2968
radioactive contamination of, at CERN accelerator site, extent and nature of, 25:2562
radioactivity in ground-level, at Seoul, Korea following Chinese nuclear explosion, effects of meteorological conditions on, (E), 25:2368
radioactivity of ground-level, at archaeological excavation sites in Germany and Sweden, 25:2352
response of stable, to heating in stable auroral red arc, (E/T), 25:2953
ATMOSPHERE EXPOSURE CHAMBERS
design for studying behavior of dusts in animal lungs using tracer technique, 25:2523
ATMOSPHERIC PRECIPITATION
deuterium content of, from 1964 to 1966, worldwide survey of, 25:2367 (STI/DOC-10/117)
fallout content of East German, 1968 and 1969, 25:2370
oxygen-18 content of, from 1964 to 1966, worldwide survey of, 25:2367 (STI/DOC-10/117)
tritium content of, from 1964 to 1966, worldwide survey of, 25:2367 (STI/DOC-10/117)
ATOMIC ENERGY
development in Germany during 1971, proposed budget for, 25:3853
ATOMIC ENERGY, LEGAL ASPECTS
regulations for protection of environment against radioactivity, 25:2564
ATOMIC STRUCTURE
angular momentum integrals in configuration-interaction calculation of, computer program for determining coefficients of, 25:2923
ATOMS
eigenvalues for bound states, iterative method for calculation of, 25:2925
electron inelastic scattering by, having two valence electrons, configuration-interaction calculations of, 25:2918
electron radial distribution in, iterative method for calculation of, 25:2925
electron reactions at 50 to 150 keV, equipment and methods for studying inelastic, 25:3472 (CONF-700322-, pp 379-92)
electron reactions with, calculation of excitation cross sections for, 25:2915
electron reactions with, quasi-classical method for calculation of cross sections for, 25:2917
electron reactions with, role of intermediate states in excitation in, (T), 25:2916
electron scattering by, computer program for calculation of cross sections for, 25:2903
energy levels of, beam--foil study of Stark effect on, 25:2888 (CONF-700322-, pp 281-8)
energy levels of, induced amplification of characteristic x radiation from excited, 25:2894
energy levels of, use of electron spectroscopy in study of, 25:2900 (CONF-700322-, pp 305-19)
energy levels of, use of fast ion beams in production and study of excited, 25:2889 (CONF-700322-, pp 289-95)
energy levels of, uses of beam--foil data on lifetimes of, 25:2888 (CONF-700322-, pp 281-8)
energy of, calculation using Euler transforms of Slater and Gaussian 1s functions, 25:2928
energy-level formula for one-electron bound state, derivation of relativistic Sommerfeld--Dirac, using modified WKB expansion, 25:2924
energy-level transitions between excited states of, modulation method for measuring rates of, 25:2920
excitation cross sections for, review of approximate methods of calculation of, 25:2913
ion reactions at 1 to 100 keV with, charge exchange into excited and ground states in, (T), 25:2919
ion reactions with, examples and uses of electron spectra from, 25:2900 (CONF-700322-, pp 305-19)
photon incoherent scattering at 280 to 1002 keV by K electrons of, having Z = 50 to 82, integrated cross sections for, 25:2909
photon reactions with, computer program for calculation of ionization cross sections for, 25:2903
photon reactions with, ratios of total to subshell photoelectric cross sections for, 25:2908
reactions with atoms, charged particles, and molecules, bibliography for 1969 on, 25:2901 (ORNL-AMPIC-13)
wave functions for, method for obtaining Brueckner orbitals using pair correlation functions, 25:2926
AURORAE
intensity of pulsating, at conjugate points, Feb. to April, 1968, (E), 25:2999
position of visible, effect of magnetic activity on, (E), 25:2976
radio absorption in, effects of midlatitude bays on, (E), 25:2964
spectral intensities in normal and type-B, O_2^+ and N_2 band system, (E), 25:3002
AURORAL ZONE
observations of midday- and night-sector oval, aircraft, 25:2949 (AD-709359)
polar magnetic storm above entire oval of, simultaneous commencement and development of, (E/T), 25:2977
polar substorms in, meridional motion of magnetic, (E), 25:2979
AUTORADIOGRAPHY
methods using phosphorus-33, 25:2521
performance of alpha, for metallographic analysis of nuclear materials, 25:2731 (ORNL-4570, pp 215-23)

B

BARITE CONCRETES
gamma scattering by, energy distribution of single and multiple, (E), 25:3182
gamma-ray shielding by high-density, at 0.3 to 10 MeV, 25:3172
BARIUM
corrosive effects on niobium--zirconium and tantalum--tungsten alloys at 1000 to 1800°C, 25:2628
determination following nonsulfide separation from elements, qualitative, 25:2101
determination of trace amounts of, in nuclear-grade uranium oxide (U_3O_8) by direct reading spectrometric method, 25:2068 (NLCO-1071)
effects on determination of trace amounts of antimony by isotopic exchange in organic phase, 25:2106
effects on photometric determination of hafnium and zirconium in geological specimens, 25:2084
effects on uv spectrophotometric determination of gallium in aqueous solutions, 25:2100
neutron capture by, gamma spectra from thermal, (E), 25:3181
BARIUM CARBONATES
effects on properties of sintered zircons, 25:2766(T) (CSIRO-Trans-9924)

BARIUM ISOTOPES Ba-130
energy levels of, precession angles due to static and transient hyperfine magnetic fields in polarized iron, (E), 25:3686
BARIUM ISOTOPES Ba-132
energy levels of, precession angles due to static and transient hyperfine magnetic fields in polarized iron, (E), 25:3686
BARIUM ISOTOPES Ba-134
energy levels of, precession angles due to static and transient hyperfine magnetic fields in polarized iron, (E), 25:3686
BARIUM ISOTOPES Ba-136
energy levels of, precession angles due to static and transient hyperfine magnetic fields in polarized iron, (E), 25:3686
BARIUM ISOTOPES Ba-138
proton inelastic scattering at 10 MeV, fits to angular distributions with configuration missing, (T), 25:3685
x-ray spectra from π-mesic atoms of, 4f → 3d, (E), 25:2896
BARIUM ISOTOPES Ba-140
uptake by aquatic molluscs and plants, effects of concentration in water on concentration factor for fallout, 25:2548
BARIUM ISOTOPES Ba-144
decay and energy-level transitions following californium-252 fission, (E), 25:3673
BARIUM OXIDES
BaO--Nb_2O_5--SrO, phase studies of Nb_2O_5-rich region of, 25:2808
BARIUM SULFATES
radiation effects on electrokinetic potentials of solid, effects of sodium sulfate and sulfuric acid on sulfur-35 β, 25:2222
BARIUM TITANATES
radiation effects on ferroelectric properties of single crystal of, x-, 25:3196
BARIUM URANATES
crystal structure of Ba_3UO_6 in perovskites, 25:2210
Ba_3UO_6--Sr_3UO_6, crystal structure of, 25:2210
BARIUM URANIUM SULFIDES
preparation and crystal structure of $BaUS_3$, 25:2204
BARYONS
decay of, hard-pion method for four-point functions for leptonic and nonleptonic, 25:3401
decays of polarized, asymmetry coefficients of leptonic, (T), 25:3339
interactions with antibaryons, additive quark model for polarization of Λ and Σ in two-body Y* and anti Y* production in, (T), 25:3383 (TPJU-2/70)
interactions with mesons and baryons, algebra of vertex strengths for analysis of Serpukhov total cross section data for, 25:3385
interactions with mesons at high energies, γ_5 gauge invariance for helicity conservation in, (T), 25:3403
interactions with mesons in broken SU(3), baryon spectra from partial-wave amplitudes for, 25:3397
interactions with mesons, exchange degeneracy with SU(3) symmetry and absorptive corrections for hypercharge-exchange, 25:3388
interactions with mesons, hard-pion method for four-point functions for, (T), 25:3401
interactions with pseudoscalar mesons, additive quark model for polarization of Λ and Σ in two-body pseudoscalar meson and Y* production in, (T), 25:3383 (TPJU-2/70)
interactions with pseudoscalar mesons, additive quark model for polarization of Λ and Σ in two-body vector meson and Y* production in, (T), 25:3383 (TPJU-2/70)
interactions with pseudoscalar mesons, quark model for ambiguities in transversity amplitudes for vector meson and $^3/_2^+$ resonance production in, (T), 25:3382 (TPJU-1/70)
interactions with pseudoscalar mesons, quark model for ambiguities in transversity amplitudes for pseudoscalar meson and $^3/_2^+$ resonance production in, (T), 25:3382 (TPJU-1/70)
production of, analysis as rescattering effect, (T), 25:3459
BARYONS (ANTIPARTICLES)
interactions with baryons, additive quark model for polarization of Λ and Σ in two-body Y* and anti Y* production in, (T), 25:3383 (TPJU-2/70)
BARYONS, RESONANCE
decay widths of, composite model predictions of regularities among, 25:3405
mass spectra from partial-wave amplitudes for meson interactions with baryons in broken SU(3), 25:3397
production of $^3/_2^+$, in pseudoscalar meson interactions with $^1/_2^+$ baryons, quark model for ambiguities in, (T), 25:3382 (TPJU-1/70)
BARYONS, RESONANCE (N*)
decay $\Delta(1950) \rightarrow \Sigma^+ + K^+$ from $\pi^+ + p$ interactions at 1850 to 2090 MeV, branching fraction of, (E), 25:3283
existence of N(2210) and N(2220) from $\pi^- + p \rightarrow \pi^- + p$ interactions at 1.71 to 3.01 GeV/c, evidence for, (E/T), 25:3281
production and decay in $p + n \rightarrow \Delta^{++}(1236) + \Delta^-(1236)$ interactions at 6.98 GeV/c, (E), 25:3265
production in $\gamma + p \rightarrow p + eta^0$, $eta^0 \rightarrow 2\pi$ interactions at 0.8 to 1.1 GeV, (E), 25:3255
production in $\gamma + p \rightarrow rho^0 + N + m\pi$ interactions at 5 to 100 GeV, diffractive, (T), 25:3308 (DESY-70/45)
production of double resonances $K^{*0}(890)$ $\Delta^{++}(1236)$ and $K^{*0}(1420)$ $\Delta^{++}(1236)$ and enhancement $\Delta^{++}(1236)\pi^-$ in $K^+ + p \rightarrow K^+ + \pi^- + \pi^+ + p$ interactions at 4.6 and 9 GeV/c in hydrogen bubble chamber, (E), 25:3271 (UCRL-19809)
production of $\Delta(1236)$ in $\pi^+ + p$ interactions at 5.5 GeV/c, cross sections for, (E), 25:3279
production of Δ^- in $\gamma + N \rightarrow \pi^+ + \Delta^-$ interactions, conspiracy and duality in model for forward cross sections for, (T), 25:3318
production of $\Delta^-(1236)$ in $K^- + d \rightarrow K^- + \pi^+ + \pi^- + n + p$ interactions at 5.5 GeV/c, cross section for, (E), 25:3274
production of Δ^{++} in $\gamma + N \rightarrow \pi^- + \Delta^{++}$ interactions, conspiracy and duality in model for forward cross sections for, (T), 25:3318
production of Δ^{++} in $\pi^+ + p \rightarrow p + 2\pi^+ + \pi^- + \pi^0$ interactions at 3.7 GeV/c, $A_2{}^0$ production associated with, (E), 25:3272 (UCRL-20050)
production of $p\pi\pi(1710)$ enhancement in $\pi^+ + p \rightarrow \pi^+ + p + \pi^+ + \pi^-$ interaction at 5 GeV/c, (E), 25:3275
BARYONS, RESONANCE (Y*)
production in $\gamma + p \rightarrow Y^* + K^+$ interactions at 1800 to 2600 MeV, widths and cross sections for, (E), 25:3251
production of $\Sigma(1385)$ in $\pi^+ + p$ interactions at 5.5 GeV/c, cross sections for, (E), 25:3279
production of Y* and anti Y* in baryon interactions with pseudoscalar mesons and baryon interactions with antibaryons, additive quark model for polarization of Λ and Σ in two-body, (T), 25:3383 (TPJU-2/70)
BASALT
analysis for hafnium and zirconium by neutron activation and radiochemical separation, 25:2148
BEAM SEPARATORS
deflectors for rf, design of dielectric-loaded rectangular, 25:3502
properties of dielectric-loaded rf waveguide, 25:3494
BEARINGS
development of liquid-metal, review of, 25:2600 (BNL-50258)
BELGIUM
radioisotope fixation in Meuse River in, cobalt-60 and manganese-54, 25:2544
BENTONITES
sorptive properties for iodide anions, 25:2337
BENZALDEHYDE
effects on γ-radioinduced graft polymerization of cellulose with styrene in methanol solutions, 25:2247
BENZENE
determination in water by isotope dilution gas--liquid chromatography, 25:2107
effects on γ-radioinduced graft polymerization of cellulose with styrene in methanol solutions, 25:2247
effects on radioinduced isomerization of norbornadiene, 25:2239
effects on radiolysis of ammonia, 25:2283
benzene--octane, radiolysis of, kinetics of production of ethane, hydrogen, and methane from γ, 25:2270
BENZENE, BROMO-
effects on γ-radioinduced graft polymerization of cellulose with styrene in methanol solutions, 25:2247
radiation effects on, electrolytic collection of recoil bromine-80 and bromine-80m from thermal-neutron, 25:2301
BENZENE, CHLORO-
effects on γ-radioinduced graft polymerization of cellulose with styrene in methanol solutions, 25:2247
BENZENE, FLUORO-
effects on γ-radioinduced graft polymerization of cellulose with styrene in methanol solutions, 25:2247
BENZENE, HEXAMETHYL-
effects on γ-radioinduced graft polymerization of cellulose with styrene in methanol solutions, 25:2247
BENZENE, NITRO-
radioinduced arylation of, effects of diphenylpicrylhydrazyl on γ, 25:2255
BENZENE, NITROSO-
radiolysis of hydrated, mechanism of electron pulse, 25:2272
BENZENE, 1,2,4,5-TETRAMETHYL-
effects on γ-radioinduced graft polymerization of cellulose with styrene in methanol solutions, 25:2247
BENZENEARSONIC ACID, 2,2'-[(1,8-DIHYDROXY-3,6-DISULFO-2,7-NAPHTHYLENE)BIS(AZO)]DI-
complexes with americium and curium, spectrophotometric studies on, 25:2079
BENZOTHIAZOLE, 2-(METHYLTHIO)-
reactions of sulfur-35 recoil atoms with, distribution and yields from, 25:2303
BENZOTHIAZOLETHIOL
reactions of sulfur-35 recoil atoms with, distribution and yields from, 25:2303
BENZOYL PEROXIDE
effects on graft polymerization of polyethylene with styrene, 25:2241
BERKELIUM
determination by alpha counting, 25:2294 (ORNL-4572, pp 109-34)
electric potential of tetravalent--trivalent couples of, in aqueous solutions, 25:2319 (ORNL-4572, pp 181-95)

purification by solvent extraction, 25:2319 (ORNL-4572, pp 181-95)
BERKELIUM ACETATES
stability of ions of, effects of inner sphere complexing on, 25:2208
BERKELIUM ISOTOPES Bk-249
neutron fission at 0.6 to 4.6 MeV, cross section and fragment angular distributions for, (E), 25:3665
production at HFIR and TRU, 25:2294 (ORNL-4572, pp 109-34)
BERYLLIUM
determination of trace amounts of, in nuclear-grade uranium oxide (U_3O_8) by direct reading spectrometric method, 25:2068 (NLCO-1071)
effects on determination of trace amounts of antimony by isotopic exchange in organic phase, 25:2106
effects on photometric determination of hafnium and zirconium in geological specimens, 25:2084
mechanical properties of Krcil-prepared high-purity, 25:2653
neutron cross sections for, 25-group, (T), 25:3530 (LA-4484)
neutron scattering law for polycrystalline, calculation of coherent one-phonon, 25:3533
photon reactions at 1.5 to 5 GeV, cross sections for K^0 production in, (E), 25:3248
photon reactions at 4.1 to 6.1 GeV, real-to-imaginary amplitude ratio for rho + N interactions from phase of rho production amplitude in, (E), 25:3256
photon reactions at 5.1 GeV, structure of e^+e^- mass spectrum for coherent interference between rho and ω decays from, (E), 25:3288
preparation of high-purity, by sodium reduction of beryllium chloride, Kroll method for, 25:2653
preparation of nuclear-grade, 25:2654
properties at 80 to 400°K, electric and thermal, 25:2677 (ORNL-4570, pp 224-7)
separation of cerium, gadolinium, lanthanum, and neodymium from, by precipitation using cupferron, 25:2078
testing of reflector components of, development of nondestructive methods for, 25:2677 (ORNL-4570, pp 224-7)
uses in nuclear technology, 25:2654
BERYLLIUM ALLOYS AND SYSTEMS
Be--Cu, corrosion of wear bushings of, by high-temperature sodium coolant, 25:2705
Be--Cu, uses in nuclear technology, 25:2654
Be--Nb, niobium-93 NMR in $NbBe_2$, $NbBe_3$, Nb_2Be_{17}, and $NbBe_{12}$, 25:3220 (COO-1700-12)
Be--Ni, uses in nuclear technology, 25:2654
BERYLLIUM BOROHYDRIDES
spectra and structure of, effects of boron-10 and deuterium on ir, 25:2189
BERYLLIUM CARBIDES
preparation of microspheres of, method for, 25:2795(P)
BERYLLIUM CHLORIDES
reduction by sodium in Kroll method to prepare beryllium, 25:2653
BERYLLIUM FLUORIDES
BeF_2--LiF--ThF_4--UF_4--ZrF_4, corrosive effects on Hastelloy N, stainless steel, and steel for MSRE, 25:2609 (ORNL-4570, pp 175-90)
BERYLLIUM IONS
energy of Be^{2+}, calculation using Euler transforms of Slater and Gaussian 1s functions, 25:2928
BERYLLIUM ISOTOPES Be-7
electron-capture decay of, (E), 25:3694
BERYLLIUM ISOTOPES Be-8
energy levels from boron-10 (d,α) reactions, isobaric-spin-doublet, (E), 25:3573
energy levels of, Hartree--Fock calculations for, (T), 25:3545 (LYCEN-7047)
BERYLLIUM ISOTOPES Be-9
deuteron reactions (d,p) at 2.9 MeV, p-γ angular correlations for, (E), 25:3588
deuteron reactions at 350 keV, charged-particle spectra from, 25:3560 (CONF-700322-, pp 89-94)
energy levels in, three-body bound-state calculations of, (T), 25:3579
neutron reactions (n,α) at 8 to 30 MeV, angular distributions and excitation functions for, (E), 25:3564 (KFK-1190)
proton reactions at 24 to 46 MeV, total cross sections for, (E), 25:3568
BERYLLIUM ISOTOPES Be-10
energy levels from beryllium-9 (d,p) reactions, spin assignments for 5.96-MeV doublet, (E), 25:3588
BERYLLIUM OXIDES
neutron scattering by, exponential angular coefficients for fast-, (E), 25:3171
preparation of microspheres of, method for, 25:2795(P)
BETA DECAY
charge asymmetry of internucleon potential in, 25:3736
coupling constants in, least-squares adjustment of, (T), 25:3741
electromagnetic final-state interactions in, test of T invariance in, (T), 25:3424
screening correction to allowed, evaluation for light nuclides, (T), 25:3743
sensitivity to the shape of the nuclear charge distribution, (T), 25:3744
BETA PARTICLES
dose to human tissues from fallout in Moscow region during 1962 to 1966, 25:2550
effects of sulfur-35, on electrokinetic potential of solid barium sulfate, effects of sodium sulfate and sulfuric acid on, 25:2222
effects on aqueous solutions of nitric acid, 25:2284
penetration in aluminum, copper, lead, and silver, intensity variation with thickness for external bremsstrahlung production from, (E), 25:3249
BETA SOURCES
monitoring of environmental, efficiency of G--M and proportional detectors for, 25:2448
BEVATRON
magnetic field measurements in, smoothing and differential analysis of, 25:3503
BIBLIOGRAPHIES
on 14-MeV neutron generators in activation analysis, 25:2130 (NBS-TN-533)
on activation analysis of pollution samples, 25:2129 (NBS-TN-532)
on atomic and molecular processes, 1969, 25:2901 (ORNL-AMPIC-13)
on high-temperature chemistry and physics of materials, 25:2665 (NBS-SPEC. PUBL-315-5)
on laser uses in emission spectroscopy, 25:3110 (IN-1425)
on radioisotope uses in industry and research in eastern countries, 1967 to 1969, 25:2399 (AED-C-12-22)
on thermonuclear reactor design, 25:3139 (ORO-1171-1, pp 425-39)
on U. S. desalination reactors, 25:3913 (ORNL-NDIC-8)
BINDING ENERGY
hyperspherical-expansion approach to nuclear bound states, 25:3730
role of mesons in nuclear saturation, 25:3763
BIOCHEMISTRY
research progress on, 25:2312(R) (ORNL-4572)
BIOLOGICAL MATERIALS
analysis for lead by potentiometric titration using Orion liquid ion-exchange lead-selective electrode, 25:2104
analysis for plutonium, establishment of laboratory for, 25:2108 (RT/PROT-(70)14)
analysis for trace elements by fast and thermal neutron activation, sensitivities of, 25:2125 (IAEA-122, pp 27-36)
analysis for trace elements by neutron activation, 25:2126 (IAEA-122, pp 37-40)
radioisotope uptake by aquatic, effects of lake type on concentration factors for strontium-90 and uranium-238, 25:2546
BIOLOGICAL MODELS
development for bioburden, 25:3975 (SC-RR-70-561)
development for determining radiation effects of populations of stem cells in bone marrow of rats, 25:2590
development for radioisotope transport in aquatic systems, 25:2542
BIOTITES
sorptive properties of Rhine River, for radioisotopes, (E), 25:2350
BISMUTH
density at 271 to 414°C, 25:2692
determination following nonsulfide separation from elements, qualitative, 25:2101
determination of trace amounts of, in nuclear-grade uranium oxide (U_3O_8) by direct reading spectrometric method, 25:2068 (NLCO-1071)
determination of, properties of derivatives of 2-mercapto-Δ^2-1,3,4-thiadiazoline-5-thione for use in extraction--photometric, 25:2070
effects on determination of trace amounts of antimony by isotopic exchange in organic phase, 25:2106
effects on determination of trace amounts of rhenium by thiocyanate--stannous chloride method, 25:2102
effects on photometric determination of hafnium and zirconium in geological specimens, 25:2084
effects on uv spectrophotometric determination of gallium in aqueous solutions, 25:2100
production of pure, review of techniques for, 25:3219
separation from nitrate and sulfate solutions by solvent extraction using amines, 25:2319 (ORNL-4572, pp 181-95)
spectra of bismuth tribromide-dissolved species of, absorption, 25:2805 (ORNL-4570, pp 31-4)
superconducting condensation energy calculation, 25:3046
BISMUTH ALLOYS AND SYSTEMS
Bi--Cd--Tl, density at 124 to 440°C, 25:2692
Bi--In, density at 73 to 660°C, 25:2692
Bi--N--Th, crystal structure of Th_2N_2Bi formed in, 25:2248
Bi--N--U, crystal structure of U_2 Bi formed in, 25:2248
Bi--Pb, corrosive effects on niot -coated steel tubing at 375 to 500°C, relations wit' nesium and zirconium additions, 25:2627
Bi--Pb, solvent properties of eutectic of, for chromium, cobalt, and nickel at 400 to 500°C, 25:2709
Bi--Sb, density at 403 to 742°C, 25:2692
BISMUTH IODATES
sorptive properties for thorium-234, 25:2341

BISMUTH ISOTOPES Bi-209
alpha elastic scattering at 14 to 24 MeV, optical-model analysis of, (E), 25:3689
alpha fission at 103 MeV, cross sections and fragment angular distributions for, (E), 25:3710
deuteron fission at 51.5 MeV, cross sections and fragment angular distributions for, (E), 25:3710
energy levels and transitions from Coulomb excitation in He weak-coupling model, (E/T), 25:3674
BISMUTH PERIODATES
sorptive properties for thorium-234, 25:2341
BLACK BODY RADIATION
cosmic background, anisotropy and inhomogeneity in, (T), 25:2876
BLOOD
circulation in human brain, effectiveness of technetium-99 scanning in combination with serial angiography for studies of, 25:2577
scanning of circulation of, in man, use of metastable technetium-99 for, 25:2580
BLOOD PLASMA
digoxin radioimmunoassay in, method for, 25:2522
BLOOD PLATELETS
life span of, in animals and man, radioisotope tracer methods for measurement of, 25:2579
BLOOD SERUM
analysis for copper and zinc in psoriatic patients by neutron activation and radiochemical separation, 25:2134
protein-bound iodine content of cattle, 25:2524
BODY FLUIDS
compartments of human, use of radioisotopes for simultaneous determination of, 25:2518
BOILERS
construction aspects for marine reactors, 25:3918
design characteristics of power reactor, 25:3898
design of liquid metal-heated, review of feasibility, 25:2600 (BNL-50258)
development of gas cooled power reactor, 25:3899
flow patterns in mercury, review of x-ray evaluations of, 25:2600 (BNL-50258)
BOILING
detection in liquid sodium cooled fast breeder reactors, methods for, 25:3864
BONE MARROW
radiation effects on populations of stem cells in, of rats, development of computer model for, 25:2590
transplantation of irradiated in anterior chamber of eye of rats, study of growth following, 25:2595
BONES
radioinduced sarcomas in, of rats, fine structure of phosphorus-32 β, 25:2594
BORON
deposition on graphite, mullite, fused silica, and tungsten at 1300°C, method for vapor, 25:2777
determination of trace amounts of, in lanthanum oxide, neodymium oxide, and yttrium oxide by direct reading emission spectrometry, 25:2096
determination of trace amounts of, in nuclear-grade uranium oxide (U_3O_8) by direct reading spectrometric method, 25:2068 (NLCO-1071)
hardness of transition metal-containing β-rhombohedral, 25:2801
neutron cross sections for, 25-group, (T), 25:3530 (LA-4484)
production of pure, review of techniques for, 25:3219
BORON CARBIDES
crystal structure of, 25:2790 (ORNL-4570, pp 98-102)
deposition on graphite, mullite, and tungsten at 1300°C, method for vapor, 25:2777
neutron scattering by, exponential angular coefficients for fast-, (E), 25:3171
properties for use as reactor control material, 25:2790 (ORNL-4570, pp 98-102)
radiation effects on properties and structure of, in-pile, 25:2790 (ORNL-4570, pp 98-102)
BORON IONS
effects on glass crystallization at 50 keV, relations with annealing, 25:2823
implantation in diamond crystals, semiconducting layers induced by, 25:3199
BORON ISOTOPES B-10
deuteron reactions (d,α) at 4.0 to 12.0 MeV, alpha spectra and differential cross sections for, (E), 25:3573
deuteron reactions (d,p) at 350 keV, energy levels of boron-11 from, (E), 25:3561 (CONF-700322-, pp 133-40)
effects on ir spectra of beryllium borohydride, 25:2189
neutron elastic and inelastic scattering at 2 to 4.8 MeV, angular distributions for, (E), 25:3559 (AWRE-O-45/70)
BORON ISOTOPES B-11
deuteron reactions (d,n) at 5.5 MeV, angular distribution and polarization for, (E), 25:3574
energy levels from boron-10 (d,p) reactions, (E), 25:3561 (CONF-700322-, pp 133-40)
neutron elastic and inelastic scattering at 2 to 4.8 MeV, angular distributions for, (E), 25:3559 (AWRE-O-45/70)
proton reactions (p,3α) at 0.7, 1.0, and 1.4 MeV, analysis for reaction mechanism in, (E), 25:3589
reactions with thorium-232, yields of light neutron-rich nuclei in, (E), 25:3648 (JINR-E7-5319)
BORON ISOTOPES B-12
energy level at 953 keV from boron-11 (d,p) reactions, lifetime of, (E), 25:3569
energy levels from carbon-12 (π^-,γ) reactions at 40 MeV, (E), 25:3550
BOSONS
excitations at finite temperatures in gas of, shielded potential in Hartree approximation, 25:3044
field interactions in three space--time dimensions for, exponential representations of canonical commutation relations for phi⁴, (T), 25:3442
Hartree--Fock theory and lambda transformation in quantum statistical mechanics for degenerate, 25:3228
motion of spinless zero-mass, additional invariance of relativistic equations for free, (T), 25:3292 (ITF-70-32)
production rates for spinless massless, implications of causality for, 25:3301
spin of, physical bounds for components of statistical tensors for, (T), 25:3295 (TPJU-12/70)
BOSONS, INTERMEDIATE-VECTOR
decay of, detection of W in neutrino reactions at 50 to 200 GeV from hadronic modes of, (E/T), 25:3333 (NYO-2171-323)
detection in neutrino reactions with lead-208 at 50 to 200 GeV, W hadronic decay modes for, (E/T), 25:3333 (NYO-2171-323)
energy levels and wave functions of charged relativistic, in external electromagnetic fields, (T), 25:3344
production in meson (μ) and neutrino reactions with nuclei at 50 to 100 GeV, coherent, incoherent, and inelastic cross sections for, (T), 25:3340
production in neutrino reactions with lead-208 at 50 to 200 GeV, W hadronic decay modes for detection of, (E/T), 25:3333 (NYO-2171-323)
BRAIN
blood circulation in human, effectiveness of metastable technetium-99 scanning in combination with serial angiography for studies of, 25:2577
mercury-203 concentration in human, after oral intake of labeled methyl nitrate, 25:2533
polysome distribution in rat, 25:3986 (UCLA-12-796)
scanning of, use of radioisotopes and scintillation camera in γ, 25:2581
scanning using metastable technetium-99, 25:2580
BRAZING ALLOYS
development of bismuth-resistant, 25:2609 (ORNL-4570, pp 175-90)
BREMSSTRAHLUNG
production in nucleon--nucleon interactions at low energies, (T), 25:3756
production of external, in beta particle penetration of aluminum, copper, lead, and silver, intensity variation with thickness for, (E), 25:3249
reactions (γ,2p) and (γ,2pn) at 23 to 62 MeV, cross sections for, (E), 25:3634
reactions (γ,n), (γ,2n), and (γ,np) with zinc-64 at 10 to 40 MeV, relative cross sections for, (E), 25:3623
reactions with carbon-12 at 64 to 128 MeV, photoneutron spectra from, (E), 25:3567 (SAL-15)
BROMINE
determination in human liver by neutron activation and γ spectrometry, 25:2124 (IAEA-122, pp 15-26)
determination in human tissues by thermal neutron activation, sensitivity of, 25:2123 (IAEA-122, pp 1-13)
determination in pigments from ancient murals by neutron activation, 25:2133
BROMINE ISOTOPES Br-80
collection of recoil, from thermal-neutron-irradiated alkyl bromides, electrolytic, 25:2301
isomeric transition in bromine--methane and hydrobromic acid--methane systems, yields of labeled bromomethane from, 25:2226
BROMINE ISOTOPES Br-82
use for determination of human body fluid compartments, 25:2518
BROMINE SYSTEMS
Br--methane, bromine-80m isomeric transition in, yields of labeled bromomethane from, 25:2226
BROOKHAVEN ALTERNATING-GRADIENT SYNCHROTRON (AGS)
beam separator for, design of dielectric-loaded rectangular deflectors for rf, 25:3502
BROWNS FERRY POWER REACTOR, UNIT 1
design parameters of, revised and additional data on, 25:3827 (DOCKET-50259-20)
operations aspects of, revised and additional data on, 25:3827 (DOCKET-50259-20)
technical specifications for, proposed, 25:3827 (DOCKET-50259-20)
BROWNS FERRY POWER REACTOR, UNIT 2
design parameters of, revised and additional data on, 25:3827 (DOCKET-50259-20)
operations aspects of, revised and additional data on, 25:3827 (DOCKET-50259-20)
technical specifications for, proposed, 25:3827 (DOCKET-50259-20)
BROWNS FERRY POWER REACTOR, UNIT 3
design parameters of, revised and additional data on, 25:3827 (DOCKET-50259-20)
operations aspects of, revised and additional data on, 25:3827 (DOCKET-50259-20)

technical specifications for, proposed, 25:3827 (DOCKET-50259-20)
BRUNSWICK POWER REACTOR, UNIT 1
containment structures for, seismic stress analysis of primary and secondary, 25:3839 (DOCKET-50324-17)
site for, preparation and testing of backfill for, 25:3839 (DOCKET-50324-17)
BRUNSWICK POWER REACTOR, UNIT 2
containment structures for, seismic stress analysis of primary and secondary, 25:3839 (DOCKET-50324-17)
site for, preparation and testing of backfill for, 25:3839 (DOCKET-50324-17)
BRYOPHYTA
radioisotope fixation by aquatic, in Meuse River, cobalt-60 and manganese-54, 25:2544
BUBBLES
formation in bubble chambers, calculation of electric field intensities for, 25:2485 (JINR-P13-5277)
BUGEY REACTORS (EDF-5)
fuel elements for, metal spraying method for clad bonding of, 25:2638 (CEA-CONF-1625)
1,3-BUTADIENE
determination in products from radiolysis of gaseous ethylene, gas chromatographic method for, 25:2278
BUTANE
determination in products from radiolysis of gaseous ethylene, gas chromatographic method for, 25:2278
radiolysis of gaseous, isomerization of propyl ions in γ, 25:2290
BUTANE, 2,2-DIMETHYL-
determination in products from radiolysis of gaseous ethylene, gas chromatographic method for, 25:2278
BUTANE, 2,3-DIMETHYL-
determination in products from radiolysis of gaseous ethylene, gas chromatographic method for, 25:2278
BUTANE, 2-METHYL-
determination in products from radiolysis of gaseous ethylene, gas chromatographic method for, 25:2278
radiolysis of gaseous, isomerization of butyl ions in γ, 25:2290
1,3-BUTANEDIONE, 4,4,4-TRIFLUORO-1-(2-THIENYL)-
complexes with scandium, distribution in series of ether solvents of, 25:2345
4-methyl-2-pentanone--4,4,4-trifluoro-1-(2-thienyl)-1,3-butanedine, solvent properties for lawrencium, 25:2197
1-BUTANOL
effects on radiolysis of chloroform at 25°C, 25:2264
oxidation by tert-butyl peroxide, effects of deuterium on, 25:2180
photooxidation by uranyl ions in aqueous solutions, mechanism of, 25:2158
2-BUTANOL
photooxidation by uranyl ions in aqueous solutions, mechanism of, 25:2158
1-BUTENE
determination in products from radiolysis of gaseous ethylene, gas chromatographic method for, 25:2278
2-BUTENE
determination in products from radiolysis of gaseous ethylene, gas chromatographic method for, 25:2278
1-BUTENE, 3-METHYL-
determination in products from radiolysis of gaseous ethylene, gas chromatographic method for, 25:2278
BUTENYNE
determination in products from radiolysis of gaseous ethylene, gas chromatographic method for, 25:2278
BUTYL RADICALS
structure of ionized, produced in gas-phase radiolysis of alkanes, 25:2290
BUTYROPHENONE
radiolysis of, yields from electron, 25:2266

C

C-129 (NIOBIUM ALLOY)
creep rupture at 980 to 1205°C, 25:2672 (ORNL-4570, pp 112-15)
CABLES
energy transport by cryogenic, 25:3050
radiation effects on, 1.3 MeV gamma and 6.0 MeV electron, 25:2819 (LCIE-342)
CADARACHE REACTORS
fuel elements of, cladding failure of, 25:3879
CADMIUM
coating with cadmium, copper, or zinc, surface morphology in electrochemical, 25:2648
deposition on rotating discs and cylindrical cathodes, surface morphology in electrochemical, 25:2648
determination following nonsulfide separation from elements, qualitative, 25:2101
determination in molybdenum or yttrium by neutron activation and extraction displacement chromatography, 25:2138
determination of trace amounts of, in lanthanum oxide, neodymium oxide, and yttrium oxide by direct reading emission spectrometry, 25:2096
determination of trace amounts of, in nuclear-grade uranium oxide (U_3O_8) by direct reading spectrometric method, 25:2068 (NLCO-1071)
effects on determination of trace amounts of antimony by isotopic exchange in organic phase, 25:2106
effects on radiolysis of water, 25:2267
effects on uv spectrophotometric determination of gallium in aqueous solutions, 25:2100
neutron elastic scattering at 1 to 40 keV, analysis of angular distributions from, (E/T), 25:3695
positron annihilation in quenched and annealed, temperature dependence of, 25:2898
radioinduced preparation from aqueous salt solutions, electron, 25:2237 (N-70-32826)
separation from nitrate and sulfate solutions by solvent extraction using amines, 25:2319 (ORNL-4572, pp 181-95)
CADMIUM ALLOYS AND SYSTEMS
Bi--Cd--Tl, density at 124 to 440°C, 25:2692
Cd--In--Sn, electron band structure of alpha-, effects of conduction electron/atom ratio on, 25:3205 (UCRL-19681)
CADMIUM SULFIDES
radiation effects on, educational program for studying low-energy deuteron, 25:3187 (CONF-700322-, pp 63-77)
CADMIUM TELLURIDES
use as radiovoltaic converter for tritium-decay-powered electric generators, 25:2400 (CEA-CONF-1623)
CALCIUM
abundance in Kappa Cancri, (E), 25:2840
corrosive effects on niobium--zirconium and tantalum--tungsten alloys at 1000 to 1800°C, 25:2628
determination following nonsulfide separation from elements, qualitative, 25:2101
determination in human tissues by thermal neutron activation, sensitivity of, 25:2123 (IAEA-122, pp 1-13)
determination of trace amounts of, in lanthanum oxide, neodymium oxide, and yttrium oxide by direct reading emission spectrometry, 25:2096
determination of trace amounts of, in nuclear-grade uranium oxide (U_3O_8) by direct reading spectrometric method, 25:2068 (NLCO-1071)
effects on determination of trace amounts of antimony by isotopic exchange in organic phase, 25:2106
effects on photometric determination of hafnium and zirconium in geological specimens, 25:2084
effects on uv spectrophotometric determination of gallium in aqueous solutions, 25:2100
electron reactions with, configuration-interaction calculations of cross sections for dielectronic transitions in, 25:2918
electron reactions with, quasi-classical calculation of cross section for excitation of $4s^2$--$4p^2$ transition in, 25:2917
neutron capture by, gamma spectra from thermal, (E), 25:3181
release to soil from organic debris in forest as function of decomposition mode and time, 25:2528
separation of cerium, gadolinium, lanthanum, and neodymium from, by precipitation using cupferron, 25:2078
structure of, calculation of electronic band, 25:2671 (ORNL-4570, pp 40-3)
CALCIUM FLUORIDE PHOSPHATES
microstructure of crystalline, electron microscopic study of, 25:2748
CALCIUM FLUORIDES
analysis for samarium, scanning method for improving accuracy of luminescence, 25:2086
CALCIUM ISOTOPES Ca-40
alpha reactions (α,pγ) at 7.0 to 12.0 MeV, gamma angular distributions from, (E), 25:3626
carbon-12 reactions (C-12,t) and (C-12,He-3) at 27.5 MeV, energy spectra from, (E), 25:3610
deuteron elastic scattering at 28 MeV, asymmetry in vector-polarized, (E), 25:3585
electron quasielastic scattering by, square-well shell model calculation of, (T), 25:3577
energy levels from potassium-39 (He-3,d) reactions, (E), 25:3627
energy levels of, Hartree--Fock calculations for, (T), 25:3545 (LYCEN-7047)
nuclear two-nucleon density function and Pauli correlation function for, (T), 25:3733
proton reactions (p,2p) at 156 MeV, analysis of angular distributions for distortion effects in, (E), 25:3565 (NP-18476)
spectra of, isotope shifts in muonic x-ray, (E), 25:3620
CALCIUM ISOTOPES Ca-42
energy levels from potassium-41 (He-3,d) reactions, (E), 25:3627
helium-3 reactions (He-3,p) at 15 and 18 MeV, angular distributions and Q-values for, (E), 25:3629
CALCIUM ISOTOPES Ca-43
helium-3 reactions (He-3,p) at 15 and 18 MeV, angular distributions and Q-values for, (E), 25:3629
CALCIUM ISOTOPES Ca-44
helium-3 reactions (He-3,p) at 15 and 18 MeV, angular distributions and Q-values for, (E), 25:3629
spectra of, isotope shifts in muonic x-ray, (E), 25:3620
CALCIUM ISOTOPES Ca-47
retention following ingestion by patients with intestinal malabsorption, whole-body counting of, 25:2531
CALCIUM ISOTOPES Ca-48
beta decay of, half-life for double, (E), 25:3693

XUM

helium-3 reactions (He-3,p) at 15 and 18 MeV, angular distributions and Q-values for, (E), 25:3629

CALCIUM OXIDES
performance as stainless steel welding electrode coating, 25:2642 (ORNL-4570, pp 88-91)

CALCIUM TUNGSTATES
preparation of high-purity and neodymium-doped, methods for, 25:2727 (ORNL-4570, pp 1-4)

CALIFORNIUM ACETATES
stability of ions of, effects of inner sphere complexing on, 25:2208

CALIFORNIUM ISOTOPES Cf-250
production at HFIR and TRU, 25:2294 (ORNL-4572, pp 109-34)

CALIFORNIUM ISOTOPES Cf-252
fission of, low-energy transitions from prompt de-excitation of fragments from spontaneous, (E), 25:3673
preparation of high-purity solutions of, ion exchange method for, 25:2792 (ORNL-4570, pp 201-4)
production at HFIR and TRU, 25:2294 (ORNL-4572, pp 109-34)

CALVERT CLIFFS POWER REACTOR, UNIT 1
effluents from, effects on environment of chemical, radioactive, and thermal, 25:3838 (DOCKET-50317-20)

CALVERT CLIFFS POWER REACTOR, UNIT 2
effluents from, effects on environment of chemical, radioactive, and thermal, 25:3838 (DOCKET-50317-20)

CANADA
lead deposits in Churchill Province of, lead-204/lead-208 ages of, 25:2353
rocks in Churchill Province of, rubidium/strontium ages of, 25:2353

CARBIDES
analysis of refractory metal, by x-ray microprobe method, 25:2095

CARBON
burning in advanced stellar evolution, (T), 25:2825
chemical reactivity of, model for, 25:2800
deposition of radiolytic, from gas phase, apparatus for studying, 25:2263 (RD/B/N-1748)
deposition on fuel particles in fluidized beds, theoretical study of pyrolytic, 25:2151 (DP-Report-569)
deposition on oxide fuel particles, 25:2320(R) (ORNL-TM-3204)
determination at various depths in steel by proton activation, 25:2147
determination in silicon carbide-coated Dragon fuel, gravimetric, 25:2064 (DP-Report-494)
determination in sodium, design of meter for, 25:2600 (BNL-50258)
determination in titanium carbide by x-ray microprobe method, 25:2095
determination of trace amounts of, in alloys and metals, conductometric method for, 25:2071
diffusion in cobalt, electronic mechanism in thermal, 25:2666 (NP-18468)
diffusion in iron, electronic mechanism in thermal, 25:2666 (NP-18468)
diffusion in nickel, electronic mechanisms in thermal, 25:2666 (NP-18468)
diffusion in palladium, electronic mechanisms in thermal, 25:2666 (NP-18468)
diffusion in titanium, electronic mechanisms in thermal, 25:2666 (NP-18468)
diffusion in vanadium, electronic mechanisms in thermal, 25:2666 (NP-18468)
effects of additions of, on tensile properties of molybdenum--niobium-base alloys, 25:2682
effects on crystal structure of molybdenum and dilute molybdenum-base alloys, 25:2745
effects on ductility of cast molybdenum, 25:2702
effects on reactions of uranium carbides with chromium--iron--nickel alloy at 900°C, 25:2765 (KFK-1213)
fission product distribution in fuel particle coating of pyrolytic, 25:2797
neutron cross sections for, 25-group, (T), 25:3530 (LA-4484)
photon reactions at 5.7 GeV, $w\gamma$ coupling constant and wN cross section from w production in, (E), 25:3247
photon reactions with, virtual Compton scattering in electron-pair production in, (E/T), 25:3252
proton reactions at 24 to 46 MeV, total cross sections for, (E), 25:3568
radiation effects on density and stability of, neutron, 25:2771 (ORNL-4570, pp 161-9)
reactions with oxygen, mechanisms of, 25:2800
reactions with yttrium oxide, preparation of yttrium carbide by, 25:2782

CARBON DIOXIDES
chemical properties of, 25:3774 (DP-Report-439)
effects on γ radiolysis of cyclohexane, 25:2268
reactions with graphite and metal surfaces at 5 to 50 keV of ions of, apparent total ion scattering, secondary electron emission coefficients, and electron and ion energy distributions for, (E), 25:2884 (NP-18490)
sorption by thorium dioxide sols, 25:2775 (ORNL-4572, pp 242-50)
yields from electron radiolysis of carbon monoxide, effects of propane or propene on, 25:2287
CO_2--He, radiolysis of, carbon-14 tracer study of x, 25:2258 (DP-Report-447)

CARBON IONS
implantation in diamond crystals, semiconducting layers induced by, 25:3199
reactions with graphite and metal surfaces at 5 to 50 keV, apparent total ion scattering, secondary electron emission coefficients, and electron and ion energy distributions for, (E), 25:2884 (NP-18490)

CARBON ISOTOPES C-12
alpha reactions (α,γ) with, survey of research on, 25:3562 (CONF-700322-, pp 297-304)
deuteron elastic scattering at 28 MeV, asymmetry in vector-polarized, (E), 25:3585
deuteron reactions (d,p) at 3.4 MeV, compound-nucleus direct interaction interference in angular distributions for, (E), 25:3572
electrodisintegration at 43 and 46 MeV, proton energy spectra and angular distributions from, (E), 25:3566 (SAL-14)
electrodisintegration of, cross-section calculation using Woods--Saxon potential, (T), 25:3714 (ITF-70-35)
electron elastic scattering at 375 and 750 MeV, cross sections and charge distributions from, (E), 25:3587
electron quasielastic scattering by, square-well shell model calculation of, (T), 25:3577
energy levels and rms radius of, three-body bound-state calculations for, (T), 25:3579
energy levels of, Hartree--Fock calculations for, (T), 25:3545 (LYCEN-7047)
helium-3 reactions (He-3, Be-7) with, strong-absorption model analysis of angular distributions from, (E/T), 25:3583
helium-3 reactions (He-3,p) at 2.4 to 3.6 MeV, proton polarization in, (E), 25:3563 (JINR-P15-5156)
lithium-6 elastic scattering at 13.0 MeV, optical-model analysis of angular distributions from, (E/T), 25:3578
lithium-6 reactions (Li-6,α), (Li-6,d), (Li-6,p), and (Li-6,t) at 5.6 to 14.0 MeV, direct-reaction and compound-nucleus analysis of energy spectra, excitation functions, and angular distributions from, (E/T), 25:3578
meson reactions (π^-,γ) at 40 MeV, gamma spectra from, (E), 25:3550
neutron backscattering differential cross sections at 14-MeV, time-of-flight arrangement for measurement of, 25:2468
nuclear two-nucleon density function and Pauli correlation function for, (T), 25:3733
photon reactions (γ,p) with, cross section for virtual, (E), 25:3566 (SAL-14)
photon reactions at 64 to 128 MeV, photoneutron spectra from, (E), 25:3567 (SAL-15)
proton reactions (p,2p) at 156 MeV, analysis of angular distributions for distortion effects in, (E), 25:3565 (NP-18476)
proton reactions (p,pα) at 160 MeV, plane-wave impulse-approximation analysis of triply differential cross sections from, (E/T), 25:3561
reactions (C-12,t) and (C-12,He-3) with calcium-40 at 27.5 MeV, energy spectra from, (E), 25:3610

CARBON ISOTOPES C-13
electrodisintegration at 43 and 46 MeV, proton energy spectra and angular distributions from, (E), 25:3566 (SAL-14)
lithium-6 reactions (Li-6,d) at 25.6 MeV, angular distributions for, (E), 25:3570
lithium-7 reactions (Li-7,t) at 30.1 MeV, angular distributions for, (E), 25:3570
photon reactions (γ,p) with, cross section for virtual, (E), 25:3566 (SAL-14)

CARBON ISOTOPES C-14
detection in radioecology studies, evaluation of liquid scintillation spectrometer for, 25:2565
use as tracer for determining protein synthesis in tobacco mosaic virus, 25:2551(R) (COO-873-26)
use for studying effects of steroid hormones on oxidative and glycolytic activity of ram spermatozoa, 25:2519

CARBON MONOXIDES
electron reactions at 10 keV with, K-shell excitation and ionization in, (E), 25:2910
radiolysis in presence of γ-alumina, chemisorption following γ, 25:2262 (RD/B/N-1279)
radiolysis of, apparatus for studying deposition of carbon from γ, 25:2263 (RD/B/N-1748)
radiolysis of, effects of propane or propene on yields from electron, 25:2287

CARBON SYSTEMS
C--steel, corrosion by aqueous sodium hydroxide, stress, 25:2614
C--U, phase studies of, using computers, 25:2737

CARBON TETRACHLORIDE
effects on radiolysis of ammonia, 25:2283
solvent properties for xenon isotopes in presence of iodine isotopes, 25:2201

CATALASE
radiation effects on activity of, in sprouts of beans and clover, γ, 25:2596

CATHODES
design of electron-emitting, for electron source, 25:3523(P)

CATIONS
exchange of interlayer, in micaceous minerals, 25:3943(R) (COO-1680-10)
CATTLE
thyroid function in lactating, iodine-131 uptake studies of, 25:2524
CAVITIES
water flow into underground, on Amchitka Island, Alaska, effects of hydraulic gradient on, 25:2349 (USGS-474-72)
CAVITY RESONATORS
superradiance in arrays of superconducting weak links, (T), 25:3045
CELLS
growth of antigen-reactive stem, from carbon-treated donors following transplantation to x-irradiated recipients, 25:2538
radiation effects on populations of stem, in bone marrow of rats, development of computer model for, 25:2590
CELLS, CULTURED
cell phase of, effects of, on infection by murine sarcoma virus, 25:2587
fractionation of glial, subcellular, 25:3983 (UCLA-12-753)
radiation effects on chromosome number and stability of isoenzymes in human carcinoma, x, 25:2585
radiation effects on DNA in xeroderma pigmentosum, repair synthesis following uv, 25:2567
radiation effects on DNA of human xeroderma pigmentosum, repair synthesis following uv and x, 25:2535
radiation effects on electrophoretic mobility of Ehrlich ascites tumor, combined ultrasonic and x, 25:2586
radioinduced delay in progression of Chinese hamster ovary, from G_2 into metaphase, uv, 25:2558
regulation of pyruvate kinase activity in rat liver, use of glucose, insulin, and serum for, 25:3984 (UCLA-12-754)
CELLS, HeLa
uptake of tritium-labeled chromosomes by, autoradiography of, 25:2515
CELLS, L
uptake of tritium-labeled chromosomes by, autoradiography of, 25:2515
CELLULOSE
analysis for trace amounts of chromium by x-ray fluorescence, 25:2076
radioinduced graft polymerization with styrene in methanol solutions, effects of additives on γ, 25:2247
CENTRIFUGES
development for plutonium separation from LMFBR fuels, 25:2306(R) (ANL-7735)
CERAMIC MATERIALS
research programs on, 25:2601(R) (ORNL-4570)
CERIUM
analysis for uranium using permanganate, potentiometric, 25:2099
complexes with cupferron, separation by solvent extraction using 2-methyl-1-propanol and 3-methyl-1-butanol, 25:2078
determination in phosphate and sulfate solutions by electrogeneration of trivalent vanadium, coulometric titration, 25:2081
determination in presence of chromium, iron, manganese, and vanadium by differential potentiometric titration, 25:2099
determination of trace amounts of, in lanthanum oxide, neodymium oxide, and yttrium oxide by direct reading emission spectrometry, 25:2096
determination of trace amounts of, using permanganate, colorimetric, 25:2073
determination of, review of methods for, 25:2061
distribution and ion exchange on clays, 25:2338
effects on determination of trace amounts of rhenium by thiocyanate--stannous chloride method, 25:2102
effects on polarographic determination of tellurium, 25:2090
effects on uv spectrophotometric determination of gallium in aqueous solutions, 25:2100
electric potential of tetravalent--trivalent couples of, in aqueous solutions, 25:2319 (ORNL-4572, pp 181-95)
separation from metals by precipitation using cupferron, 25:2078
separation from nitrate-containing rare earth mixtures in solution, comparison of crystallization, hydrolysis, and oxidation methods for, 25:2326
CERIUM ACETATES
stability of ions of, effects of inner sphere complexing on, 25:2208
CERIUM ALLOYS AND SYSTEMS
Ce--Co, magnetic properties of intermetallic $CeCo_5$, 25:3217
Ce--Gd, phase studies at high temperatures, electron microscopic and x-ray. 25:2670 (ORNL-4570, pp 35-6)
CERIUM CHLORIDES
bis(2-ethylhexyl) phosphate--$CeCl_3$--HCl--H_2O--$NdCl_3$--$SmCl_3$, equilibria in Amsco, 25:2311 (IS-T-412)
CERIUM ISOTOPES Ce-140
energy levels at 2.746 and 3.343 MeV from lanthanum-140 decay, (E), 25:3646 (CNEA-275)
proton inelastic scattering at 10 MeV, fits to angular distributions with configuration missing, (T), 25:3685
x-ray spectra from π-mesic atoms of, 4f → 3d, (E), 25:2896
CERIUM ISOTOPES Ce-141
diffusion in copper at 700 to 1010°C, tracer studies of, 25:2680
release to soil from organic debris in forest as function of decomposition mode and time, 25:2528
CERIUM ISOTOPES Ce-142
x-ray spectra from π-mesic atoms of, 4f → 3d, (E), 25:2896
CERIUM ISOTOPES Ce-144
detection in radioecology studies, use of Cherenkov counting for, 25:2565
determination in water by ion exchange or filtration and counting, 25:2117
half-life of, from evaluation of published data, 25:3645 (AERE-R-6529)
uptake by aquatic molluscs and plants, effects of concentration in water on concentration factor for fallout, 25:2548
CERIUM ISOTOPES Ce-148
decay and energy-level transitions following californium-252 fission, (E), 25:3673
CERIUM OXIDES
analysis for europium or neodymium by luminescence method, 25:2083
dysprosium-161 Moessbauer isomer shift in, (E), 25:3222
CERN SYNCHROTRON
experimental program at, review of, 25:3492
CESIUM
content of freshwater fishes and lakes, factors for natural, 25:2517
determination by potentiometric titration with sodium tetraphenylboron using Orion liquid ion exchange lead-selective electrode, 25:2104
determination in minerals and rocks by neutron activation and γ spectrometry, 25:2139
determination in rocks by neutron activation and γ spectrometry, 25:2145
distribution and ion exchange on clays, 25:2338
distribution in pond ecosystem, neutron activation analysis of, 25:2516
electron reactions with atomic, excitation cross sections for, (T), 25:2915
plasma of, production and properties in shock tubes, 25:3116
separation from other alkali metals by fixation on hydrated antimony pertoxide in hydrochloric, nitric, and perchloric acids, effects of acidity and time on, 25:2333
CESIUM ALLOYS AND SYSTEMS
Cs--I, analysis for iodine by photon activation using cesium as internal reference element, 25:2150
CESIUM BROMIDES
impurity centers in crystals of, ir spectra of H^- and D^-, 25:3958 (IS-T-388)
CESIUM CHLORIDES
$AlCl_3$--CsCl--$NiCl_2$, formation of $NiCl_3^-$ complex in, mechanisms of, 25:2805 (ORNL-4570, pp 31-4)
CsCl--$NiCl_2$--$ZnCl_2$, phase studies of, 25:2805 (ORNL-4570, pp 31-4)
CESIUM IODIDES
impurity centers in crystals of, ir spectra of H^- and D^-, 25:3958 (IS-T-388)
CESIUM ISOTOPES Cs-134
beta decay of, β-γ circular polarization correlations in, (E), 25:3697
retention by silts of Dimbovitza--Bucharest River, effects of chelating agents and pH on, 25:2363
separation from milk, performance of Polish-made ion exchangers for, 25:2329
CESIUM ISOTOPES Cs-137
accumulation in fish of northern Italy, statistical analysis of effects of location, sample date, season, and species on concentration factor for fallout, 25:2527
availability in mineral soils, effects of ammonium and potassium ions on, 25:2529
content in atmosphere and precipitation in East Germany, 1968 and 1969, 25:2370
determination in water by ion exchange or filtration and counting, 25:2117
energy levels from proton resonances in xenon-136, spins, partial widths, and spectroscopic factors for decay of isobaric analog, (T), 25:3685
monitoring in irrigation canal sediment and water downstream from nuclear power centers on Rhone River, 25:2543
sorption by Rhine River monomineralic fine sands, (E), 25:2350
uptake by Anodonta in model system, statistical study of effects of age, light, and temperature on, 25:2525
CESIUM ISOTOPES Cs-140
decay and energy-level transitions following californium-252 fission, (E), 25:3673
CESIUM URANYL BROMIDES
spectra of, ir and Raman, 25:2212
CESIUM URANYL CHLORIDES
spectra of, ir and Raman, 25:2212
CESIUM URANYL NITRATES
spectra of, ir and Raman, 25:2212

XUM

CHARGED-PARTICLE BEAMS
- bending magnet for, design of superconducting 2-tesla, 25:3504
- emittance measurements of, profile scanner for, 25:3498
- focusing in two-potential electromagnetic lenses, 25:3490
- monitoring of high-energy high-intensity, using dielectric track detectors, 25:2434 (CERN-70-27)
- transport in electromagnetic lenses, transformation matrix for beam ellipse matching in waist-to-waist, 25:3521

CHARGED PARTICLES
- acceleration in cosmic plasma, quasi-linear approximation of, (E/T), 25:2929
- effects on oxygen desorption from high-purity metal surfaces, 25:2763
- energy--momentum conservation for collision, creation, and annihilation processes, (T), 25:3243
- reactions with atoms, charged particles, and molecules, bibliography for 1969 on, 25:2901 (ORNL-AMPIC-13)
- trajectories in Lyttleton-Bondi electrodynamics, geodesics of affine connection for, (T), 25:3431
- trajectories of, analysis of first-order effects of misalignments in beam transport system on, 25:3495

CHEMICAL REACTIONS
- kinetics of Dieckmann, 25:4001(T) (UCRL-Trans-1417)
- kinetics of electron-attachment, 25:3937(R) (COO-958-19)
- kinetics of, Harvard Univ. studies of, (T), 25:3952(R) (HUX-3780-33)

CHEMISTRY
- bibliography on high-temperature materials, 25:2665 (NBS-SPEC. PUBL-315-5)
- research progress on, 25:2312(R) (ORNL-4572)

CHERENKOV RADIATION
- detection by liquid scintillation methods, use of, in radioecology studies, 25:2565

CHLORAMPHENICOL
- effects on uv-radioinduced inhibition of respiration in Escherichia coli, 25:2598

CHLORIDES
- effects on reactions in electron pulse and γ radiolysis of aqueous solutions of deoxynucleotides, purines, and pyrimidines, 25:2259 (GA-10208)

CHLORINE
- determination in graphite by neutron activation and gamma spectroscopy, 25:2142
- determination in human liver by neutron activation and γ spectrometry, 25:2124 (IAEA-122, pp 15-26)
- determination in human tissues by thermal neutron activation, sensitivity of, 25:2123 (IAEA-122, pp 1-13)
- neutron capture by, gamma spectra from thermal, (E), 25:3181

CHLORINE ISOTOPES Cl-34
- energy levels of, spins and mean lifetimes of, (E), 25:3619

CHLOROFORM
- effects on γ-radioinduced graft polymerization of cellulose with styrene in methanol solutions, 25:2247
- radiolysis of liquid, positive ion scavenging in, 25:2264
- solvent properties for xenon isotopes in presence of iodine isotopes, 25:2201

CHLOROPHYTA
- Cladophora sp., radioisotope content of, in drainage canal of reactor center in Austria, 25:2545

CHROMATOGRAPHY
- data tabulation for paper, 25:2075

CHROMIUM
- abundance in Kappa Cancri, (E), 25:2840
- corrosion and mass transfer by sodium at 660 and 760°C, effects of oxygen content on, 25:2631
- corrosion by selenium at 300 to 700°C, 25:2629
- corrosion resistance to lithium at 600 and 900°F, 25:2626
- determination following nonsulfide separation from elements, qualitative, 25:2101
- determination in biological materials by 14-MeV neutron and thermal neutron activation, sensitivity of, 25:2125 (IAEA-122, pp 27-36)
- determination in human tissues by thermal neutron activation sensitivity of, 25:2123 (IAEA-122, pp 1-13)
- determination in phosphate and sulfate solutions by electrogeneration of trivalent vanadium, coulometric titration, 25:2081
- determination in presence of cerium, iron, manganese, and vanadium by differential potentiometric titration, 25:2099
- determination in sodium chloride solutions by catalytic amalgam method, 25:2080
- determination in titanium alloys, x-ray fluorescence method for, 25:2097
- determination of trace amounts of, in cellulose by x-ray fluorescence, 25:2076
- determination of trace amounts of, in nuclear-grade uranium oxide (U_3O_8) by direct reading spectrometric method, 25:2068 (NLCO-1071)
- effects on corrosion of vanadium alloys by oxygen-containing sodium, 25:2622
- effects on corrosion resistance of chromium--molybdenum--titanium alloy, potentiometric studies of, 25:2613
- effects on determination of trace amounts of antimony by isotopic exchange in organic phase, 25:2106
- effects on determination of trace amounts of rhenium by thiocyanate--stannous chloride method, 25:2102
- effects on extraction--photometric determination of niobium in steel, 25:2085
- effects on mechanical properties and oxidation of molybdenum--zirconium dioxide cermets, 25:2796
- effects on photometric determination of hafnium and zirconium in geological specimens, 25:2084
- effects on polarographic determination of tellurium, 25:2090
- effects on uv spectrophotometric determination of gallium in aqueous solutions, 25:2100
- neutron cross sections for, 25-group, (T), 25:3530 (LA-4484)
- oxidation-reduction by oxygen-containing sodium at 300 to 500°C, electrochemical study of, 25:2710
- segregation on liquid sodium surface, 25:2713
- solubility in bismuth--lead eutectic at 400 to 500°C, 25:2709
- solubility in liquid sodium, effects of temperature on, 25:2712
- thermal conductivity of, electronic, 25:2788 (ORNL-4570, pp 27-30)

CHROMIUM ALLOYS AND SYSTEMS
- Al--Cr, crystal structure of supercooled solid solutions of, 25:2733
- Al--Cr--Fe--Ti-base, microstructure of hot-rolled plates and sheets of $\alpha + \beta$, relations of mechanical properties with abnormal, 25:2752
- Cr--Fe--Nb--Ni-base, hardening of, transmission electron microscopic study of age, 25:2689
- Cr--Fe--Ni, effects of hydrofluoric acid--nitric acid pickling on stress corrosion cracking in high purity water at 660°F, 25:4006 (WAPD-TM-944)
- Cr--Fe--Ni, reactions with uranium carbide at 900°C, effects of carbon content and metal stabilizers on, 25:2765 (KFK-1213)
- Cr--Fe-base, diffusion in bcc phases of, radioisotope tracer measurements of volume, 25:2691
- Cr--Fe-base--Mo, welding to Incoloy 800 using Inconel 82 filler metal, corrosion by steam at 1100 to 1200°F of welds produced by, 25:2636
- Cr--Mo--steel, creep at 900 to 1100°F and 8000 to 25,000 psi stress, 25:2755 (BMI-1889, Sect.B)
- Cr--Mo--Ti-base, corrosion resistance of, potentiometric method for studies of effects of chromium on, 25:2613
- Cr--Mo-base, crystal structure of dilute cast, effects of carbon additions on, 25:2745
- Cr--N--U, phase studies at 1600°C, 25:2769 (ORNL-4570, pp 62-7)
- Cr--Ni, diffusion in, thermodynamics of bond parameter changes in self-, 25:2701
- Cr--Pt, properties of intermetallic compounds of, for fuel capsule liners, 25:2643 (ORNL-4570, pp 106-11)
- Cr--ThO_2, mechanical properties of low-porosity corrosion-resistant cermets of, 25:2796
- Cr--Ti-base, corrosion resistance of, potentiometric studies of, 25:2613
- Cr--U-base, phase transformation in, kinetics of α--β, 25:2741
- Cr--V-base, corrosion by sodium at 600°C, effects of chromium content on, 25:2606 (ORNL-4570, pp 92-5)
- Cr--Zr-base, x-ray line broadening of β-quenched, effects of cooling rate, grain size, and lattice distortion on, 25:2719

CHROMIUM CHLORIDES
- proton reactions at 350 keV with, characteristic x-ray spectra from, (E), 25:2882 (CONF-700322--, pp 113-24)

CHROMIUM ISOTOPES Cr-50
- spectra of, isotope shifts in muonic x-ray, (E), 25:3620

CHROMIUM ISOTOPES Cr-51
- electron-capture decay of, γ and internal conversion spectra from, (E), 25:3704
- energy levels from titanium-48 (α,nγ) and vanadium-51 (p,nγ) reactions, spin-parity assignments for, (E), 25:3593 (COO-1530-21)
- sorption of EDTA-incorporated, by patients with ulcerative colitis, 25:2534
- transport and deposition of, in flowing sodium, 25:2706
- use for determination of human red cell volume, method for, 25:2518

CHROMIUM ISOTOPES Cr-52
- spectra of, isotope shifts in muonic x-ray, (E), 25:3620

CHROMIUM ISOTOPES Cr-53
- energy levels of, calculation using intermediate coupling model, (T), 25:3592 (COO-1120-106)
- spectra of, isotope shifts in muonic x-ray, (E), 25:3620

CHROMIUM ISOTOPES Cr-54
- spectra of, isotope shifts in muonic x-ray, (E), 25:3620

CHROMIUM ISOTOPES Cr-55
- beta decay scheme, (E), 25:3607

CHROMOSOMES
- radiation effects on number of, in human carcinoma cell cultures, x, 25:2585
- radioinduced aberrations of, in dormant seeds of Helianthus, Lactuca, and Pinus, x, 25:2555
- radioinduced aberrations of, in spermatocytes of mice following exposure of spermatogonia, frequency of x, 25:2553
- radioinduced translocation aberrations in, of Drosophila,

effects of, on crossover suppressors, x, 25:2561
uptake of tritium-labeled, by mammalian cells in vitro, autoradiography of, 25:2515
CHROMOSPHERE
brightness of faculae and flocculi in, magnetic field effects on, (E), 25:2857(T) (AD-707256)
CHRYSOIDINE
radiolysis of, adsorbed on surface of aluminum--aluminum oxide system, energy transfer during γ, 25:2276
CITRIC ACID
complexes with trivalent indium and hexavalent uranium, potentiometric, solvent extraction, and spectrophotometric studies on, 25:2206
CITRULLINE
effects on x-radiosensitivity of hydra, 25:2588
CLAYS
age of pottery, refinement of thermoluminescent method for estimation of, 25:2355
sorptive properties for cerium, cesium, and ruthenium, 25:2338
CLINOPTILOLITE
radiation effects on stability of hydrogen atoms in, containing lanthanum, magnesium, or potassium ions at 400 to 700°C, EPR spectra studies on γ, 25:2224
CNIDARIA
Hydra vulgaris, radiation effects on, protective effects of arginine and citrulline against x, 25:2588
COAL
determination in rocks by γ-γ method, 25:2111
COATINGS
radiation effects on, in air and water, gamma, 25:2821 (ORNL-4572, pp 258-61)
COBALT
complexes with sodium salt of EDTA, radiation effects on aqueous solutions of tetrahydrated, chemistry of cobalt-60 recoils produced by neutron, 25:2297
corrosion and mass transfer by sodium at 660 and 760°C, effects of oxygen content on, 25:2631
density of pure liquid, 25:4003(T) (UCRL-Trans-10496)
determination following nonsulfide separation from elements, qualitative, 25:2101
determination in human liver by neutron activation and γ spectrometry, 25:2124 (IAEA-122, pp 15-26)
determination in human tissues by thermal neutron activation sensitivity of, 25:2123 (IAEA-122, pp 1-13)
determination in minerals and rocks by neutron activation and γ spectrometry, 25:2139
determination in molybdenum or yttrium by neutron activation and extraction displacement chromatography, 25:2138
determination in titanium alloys, x-ray fluorescence method for, 25:2097
determination of trace amounts of, in nuclear-grade uranium oxide (U_3O_8) by direct reading spectrometric method, 25:2068 (NLCO-1071)
diffusion of carbon in, electronic mechanisms in thermal, 25:2666 (NP-18468)
effects on determination of trace amounts of antimony by isotopic exchange in organic phase, 25:2106
effects on determination of trace amounts of rhenium by thiocyanate--stannous chloride method, 25:2102
effects on extraction--photometric determination of niobium in steel, 25:2085
effects on uv spectrophotometric determination of gallium in aqueous solutions, 25:2100
radioinduced preparation from aqueous salt solutions, electron, 25:2237 (N-70-32826)
solubility in bismuth--lead eutectic at 400 to 500°C, 25:2709
COBALT ALLOYS AND SYSTEMS
Ce--Co, magnetic properties of intermetallic $CeCo_5$, 25:3217
Co--Fe, diffusion in, effects of crystal structure on effects of cobalt-57 and iron-59 on, 25:2178
Co--La, magnetic properties of intermetallic $LaCo_5$, 25:3217
Co--Nb, phase studies of, 25:2749
Co--Ni--V, mechanical properties of, effects of ordering on, 25:2643 (ORNL-4570, pp 106-11)
Co--Sm, magnetic properties of intermetallic $SmCo_5$, 25:3217
Co--W, properties of electrodeposited, effects of electrolyte composition and conditions on corrosion resistant and magnetic, 25:2649
COBALT ISOTOPES
effects on diffusion in cobalt--iron alloys, effects of crystal structure on, 25:2178
COBALT ISOTOPES Co-57
effects on diffusion in cobalt--iron alloys, effects of crystal structure on, 25:2178
energy levels and transitions from iron-54 (α,pγ) reactions, angular correlation studies of low-lying, (E), 25:3622
energy levels from iron-56 (p,γ) reactions, (E), 25:3601
COBALT ISOTOPES Co-58
energy level at 54 keV from iron-57 (d,n) reactions, g-factor for, (E), 25:3618
exchange in solid, doped trisdipyridyl cobalt(III) perchlorate, effects of prior heat treatment on, 25:2191
transport in artificial aquatic ecosystem, double tracer study of, 25:2549
COBALT ISOTOPES Co-59
alpha differential elastic scattering at 27.5 MeV, optical-model analysis of angular distributions using potentials obtained from double-folding procedure, (T), 25:3755
proton elastic and inelastic scattering at 28 MeV, cross sections for, (E), 25:3599
COBALT ISOTOPES Co-60
accumulation by suspended particles in Danube River, parameters affecting, 25:2361
capsules for radiation sources of, design, fabrication, and testing of spherical, 25:2404
chemistry of recoil atoms of, produced by neutron irradiation of cobalt complexes with sodium salt of EDTA in aqueous solutions, 25:2297
distribution in tissues of freshwater fish following uptake from water, 25:2526
fixation by aquatic fauna, flora, and sediments in Meuse River, 25:2544
nuclear magnetic resonance in iron, resonant destruction of gamma-ray anisotropy in single-passage, (E), 25:3223
transport and deposition of, in flowing sodium, 25:2706
transport in artificial aquatic ecosystem, double tracer study of, 25:2549
COBALT ISOTOPES Co-62
beta decay of isomeric, half-life, beta and gamma spectra, and log ft value for, (E), 25:3644
energy levels of, spins and parities of, (E), 25:3644
COCKCROFT-WALTON ACCELERATORS
experimental facility for 200-keV, for education, 25:3467 (CONF-700322-, pp 79-88)
COLCHICINE
effects on uv-radiosensitivity of cells infected with murine sarcoma virus, 25:2587
COLLISION PROCESSES
bibliography on atomic and molecular, 1969, 25:2901 (ORNL-AMPIC-13)
COMPLEXES
structure of coordination, Florida State Univ. research on, 25:3979 (TID-25562)
COMPOSITE PARTICLES
field operators for, HNZ construction of, 25:3445
Ward--Takahashi identity for, 25:3436
COMPTON EFFECT
uses in activation analysis, 25:2140
COMPUTER PROGRAMS
1DX, user manual and data files for, 25:3923 (BNWL-1412)
2DB, user manual and data files for, 25:3923 (BNWL-1412)
3DB, user manual and data files for, 25:3923 (BNWL-1412)
ATOMNP, for calculation of electron scattering and photoionization cross sections of atoms and ions, in FORTRAN IV for IBM 360, 25:2903
BABS, for fuel cycle analysis of on-load refueled high temperature reactors, FORTRAN II for IBM-709G, 25:3887 (DP-Report-575)
BASS, for fuel cycle analysis of on-load refueled high temperature reactors, FORTRAN II for IBM 709G, 25:3887 (DP-Report-575)
bibliography of discrete ordinates S/sub n/, available from Radiation Shielding Information Center, 25:3175
BIGGI $^3/_4$, gamma transport in shielding, time optimization for, 25:3180
CACES, for coolant mixing and heat transfer characteristics of power reactor fuel element assemblies, ALGOL, 25:3876 (RCN-123)
CORONA, for two-group control rod calculations in reflected reactors, ALGOL or FORTRAN, 25:3926 (EIR-166)
FASEII, for stress analysis of thin cylindrical shells and flat plates, 25:3949 (GA-9203)
FMODEL, for fuel performance calculations, 25:2789 (ORNL-4570, pp 68-75)
for graphic patching of failed CYCLOPS events for spark chamber experiment, 25:2486 (RHEL/R-205)
for shielding calculations, bibliography, 25:3179
GRACE, for multigroup fast neutron spectra, 25:3529 (KFKI-70-14-RPT)
IGOR, for neutron displacement cross sections, FORTRAN IV for IBM 360, 25:3525 (CEA-N-1312)
INCYCE, for neutron flux distribution in heterogeneous thermal reactors, FORTRAN 4 for IBM 360, 25:3925 (DP-1238)
ISOP, for three-dimensional isometric plotting, 25:3987 (UCRL-14248(Rev.1))
measurement of recursive, 25:3980 (UCLA-10-P-14-90)
PERT-V, user manual and data files for, 25:3923 (BNWL-1412)
PHOXE, for checking ENDF/B photon production data, in FORTRAN IV, 25:3531 (LA-4506)
RAO4, for calculation of resonance integrals and homogenized cross sections, 25:3528 (KFKI-70-12-RPT)
RIFFRAFF, for calculation of resonance integrals and homogenized cross sections, 25:3528 (KFKI-70-12-RPT)
SHELL 5, for structural analysis of arbitrary three-dimensional thin shells, 25:3950 (GA-9952)
SMOPAS, for manipulating matrices, 25:3976 (SC-RR-70-645)
SOC and TENSOR, for calculating effects of surrounding media on cratering by underground nuclear explosions, 25:2381 (UCRL-50898)

XUM

TRANS, for stress predictions in cylinders, 25:2789 (ORNL-4570, pp 68-75)
WEIGHTS, for calculating angular momentum integrals in atomic structure, in FORTRAN IV for ICL 1907, 25:2923
COMPUTERS
book: Computers in Analytical Chemistry, 25:2060
development at UCLA, summary of project for, 25:3982 (UCLA-10-P-14-X-56)
interactions with man in root finding and numerical problem solving, 25:3955 (IS-2416)
language for PDP-8, FOCAL, 25:2501 (CONF-700322-, pp 105-11)
programming for analysis of multistage mixer--settler performance, 25:2384 (CEA-CONF-1579)
programming for reactor fuel cost analysis, 25:2602 (ORNL-4570, pp 191-4)
system evaluation for, instrumentation for hardware and software, 25:3981 (UCLA-10-P-14-94)
use for determining populations of stem cells in bone marrow of irradiated rats, 25:2590
use for dose calculations for radiotherapy, survey of, 25:2584
CONCRETES
gamma dose rate distribution in hematite and ordinary, measurement of, 25:3480
gamma scattering by, energy distribution of single and multiple, (E), 25:3182
gamma-ray shielding by high-density iron-bearing, at 0.3 to 10 MeV, 25:3172
neutron attenuation in hematite and ordinary, measurement of, 25:3480
shear failure of prestressed pressure vessel end slabs of, lumped-parameter analysis of, 25:2411 (TID-25573)
CONNECTICUT YANKEE POWER REACTOR
inspection of, 1970 in-service, 25:3812 (DOCKET-50213-85)
operations history for October 1970, 25:3788 (DOCKET-50213-84)
operations incident of October 12, 1970, safety analysis of automatic plant trip and coolant cool down to 502°F, 25:3787 (DOCKET-50213-82)
operations of, administrative controls of, 25:3811 (DOCKET-50213-83)
personnel for, qualifications and responsibilities of, 25:3811 (DOCKET-50213-83)
CONTAMINATION
bibliography on activation analysis of pollution samples, 25:2129 (NBS-TN-532)
CONVEYERS
design for loading reactors, 25:2395(P)
COPPER
beta particle penetration in, intensity variation with thickness for external bremsstrahlung production from, (E), 25:3249
coating with cadmium, copper, or zinc, surface morphology in electrochemical, 25:2648
compatibility with T-111 and tantalum--tungsten alloys at 1100°C, 25:2720
complexes with 3,6-bisazo derivatives of chromotropic acid, spectrophotometric studies on, 25:2199
deformation behavior of polycrystalline, 25:2690
deposition on rotating discs and cylindrical cathodes, surface morphology in electrochemical, 25:2648
determination following nonsulfide separation from elements, qualitative, 25:2101
determination in biological materials by 14-MeV neutron and thermal neutron activation, sensitivity of, 25:2125 (IAEA-122, pp 27-36)
determination in blood serum and skin of psoriatic patients by neutron activation and radiochemical separation, 25:2134
determination in human tissues by thermal neutron activation, sensitivity of, 25:2123 (IAEA-122, pp 1-13)
determination in pigments from ancient murals by neutron activation, 25:2133
determination in titanium alloys, x-ray fluorescence method for, 25:2097
determination of trace amounts of, in lanthanum oxide, neodymium oxide, and yttrium oxide by direct reading emission spectrometry, 25:2096
determination of trace amounts of, in nuclear-grade uranium oxide (U_3O_8) by direct reading spectrometric method, 25:2068 (NLCO-1071)
determination of trace amounts of, in silicate rocks by neutron activation and radiochemical group separation, 25:2149
diffusion of rare earths in, at 700 to 1010°C, tracer studies of, 25:2680
effects on determination of trace amounts of antimony by isotopic exchange in organic phase, 25:2106
effects on determination of trace amounts of rhenium by thiocyanate--stannous chloride method, 25:2102
effects on photometric determination of hafnium and zirconium in geological specimens, 25:2084
effects on radioinduced brittleness of heavy-section Type A533B steel, 25:2757 (NRL-7121)
effects on uv spectrophotometric determination of gallium in aqueous solutions, 25:2100
electron reactions at 1 to 3 MeV with, backscatter and transmission coefficients for, (E), 25:2883 (N-70-25499)
electron reactions at 5.8 MeV, cross sectons for direct electron pair production in, (E), 25:3250
electronic states in, theory of, 25:2671 (ORNL-4570, pp 40-3)
gamma scattering by electrons in, incoherent cross sections for 30-keV to 2.62 MeV, (T), 25:2921
neutron capture by, gamma spectra from thermal, (E), 25:3181
photon reactions at 1.5 to 5 GeV, cross sections for K° production in, (E), 25:3248
photon reactions at 50 to 412 keV with, total photoelectric cross sections for, 25:2905
radiation effects on laminated, 1.3 MeV gamma and 6.0 MeV electron, 25:2819 (LCIE-342)
radioinduced preparation from aqueous salt solutions, electron, 25:2237 (N-70-32826)
slip band growth in pure single crystals of, high voltage electron microscopy of, 25:3988 (UCRL-19601)
solubility in high-temperature sodium coolant, 25:2705
work softening in polycrystalline, 25:2724
COPPER ALLOYS AND SYSTEMS
Ag--Cu, deposition of braze of, on silicon oxide composite film, method using molybdenum, niobium, tantalum, and tungsten for, 25:2652
Ag-base--Cu, photon reactions at 100 to 662 keV with sterling silver, effective atomic numbers for photoelectric, scattering, and total interaction processes in, 25:2906
Au--Cu, crystal orientation in rolled intermetallic Cu_3Au specimens, 25:2728 (ORNL-4570, pp 5-9)
Au--Cu, electron reactions at 1 to 3 MeV with, backscatter and transmission coefficients for, (E), 25:2883 (N-70-25499)
Au--Cu, size distribution of antiphase domains in intermetallic $AuCu_3$, 25:3941 (COO-1431-10)
Be--Cu, corrosion of wear bushings of, by high-temperature sodium coolant, 25:2705
Be--Cu, uses in nuclear technology, 25:2654
Cr--Cu, heat capacity at low temperatures, 25:3990 (UCRL-19686)
Cu--Fe, heat capacity at low temperatures, 25:3990 (UCRL-19686)
Cu--Mn, magnetic susceptibility with 20 to 25 atomic percent manganese, 25:3972(T) (ORNL-tr-2398)
Cu--Ni, magnetic clustering and giant moments in, 25:4000 (UCRL-72587(Rev.1))
Cu--Sn, deformation behavior of polycrystalline, 25:2690
Cu-base--Sn, photon reactions at 100 to 662 keV with bell metal, effective atomic numbers for photoelectric, scattering, and total interaction processes in, 25:2906
COPPER ISOTOPES Cu-59
energy levels from proton elastic scattering by nickel-58, isobaric analog, (E), 25:3628
COPPER ISOTOPES Cu-61
energy levels from nickel-61 (p,n) reactions, (E), 25:3596 (TID-25503)
energy levels from proton elastic scattering by nickel-60, isobaric analog, (E), 25:3628
energy levels of, calculation using intermediate coupling model, (T), 25:3592 (COO-1120-106)
COPPER ISOTOPES Cu-63
energy levels from proton elastic scattering by nickel-62, isobaric analog, (E), 25:3628
energy levels of, calculation using intermediate coupling model, (T), 25:3592 (COO-1120-106)
neutron reactions (n,2n) below (n,3n) threshold, cross-section calculations using Hauser--Feshback theory, (T), 25:3591 (AAEC/TM-542)
spectra of, isotope shifts in muonic x-ray, (E), 25:3620
COPPER ISOTOPES Cu-64
energy levels from nickel-64 (p,n) reactions, spins of, (E), 25:3596 (TID-25503)
COPPER ISOTOPES Cu-65
energy levels from proton elastic scattering by nickel-64, isobaric analog, (E), 25:3628
energy levels of, calculation using intermediate coupling model, (T), 25:3592 (COO-1120-106)
proton reactions (p,n) at 2.80 to 4.50 MeV, angular distributions, cross sections, and gamma spectra from, (E), 25:3631
spectra of, isotope shifts in muonic x-ray, (E), 25:3620
COPPER ORES
fracture by nuclear explosions for copper recovery, 25:2380 (ORNL-4572, pp 196-8)
CORROSION
book: Corrosion by Liquid Metals, 25:2615
book: Radiation Corrosion, 25:2603(T) (AEC-tr-7096)
conference on, Philadelphia, March 2 to 6, 1970, 25:2633
CORROSION LOOPS
deposits in flowing non-isothermal sodium, composition and structure of, 25:2616
design of sodium thermal, for studies of mass transfer between stainless steel and vanadium alloys, 25:2606 (ORNL-4570, pp 92-5)
mass transfer in high velocity sodium, at 710 to 760°C, dissimilar metal, 25:2617
COSMIC PARTICLES
abundance of relativistic Z = 9 to 17 nuclei, (E), 25:2931
acceleration in plasma of, quasi-linear approximation of,

(E/T), 25:2929
energy estimation from angular distribution of secondaries in high-energy interactions, 25:3284
mass of primary, effects on extensive air shower development, (T), 25:2932
meson (μ) reactions with nuclei, cloud chamber study of structure functions for, (E), 25:3260
COSMIC RADIATION
energy spectrum in interstellar space, effects of sunspots on 11-year variations of primary, (E/T), 25:2930
COSMIC RADIO SOURCES
flux densities at 10.69 GHz of 74, (E), 25:2848
flux densities for, between 0 and 20° north declination, (E), 25:2855
scintillation of, laboratory model for, (E/T), 25:2856
spectra of, between 0 and 20° north declination, (E), 25:2855
structure in W43 and W49, very-long-baseline interferometry of, (E), 25:2844
COSMIC RAY TELESCOPES
description of spark chamber, for detection of cosmic showers, 25:2488
development for observing entry direction of air showers, 25:2484 (INS-TCA-26)
development of spark chamber, for detection of cosmic showers, 25:2487
COSMIC SHOWERS
detection of atmospheric, light signals from extensive, photomultiplier arrays for, 25:2490
detection of, spark chamber system for, 25:2487
detection of, spark chamber system for, 25:2488
entry direction of, telescope for observing, 25:2484 (INS-TCA-26)
structure of extensive air, effect of primary mass on, (T), 25:2932
COSMOLOGY
dynamics of Klein--Alfven, general relativistic, (T), 25:2872
forces of inertia in, classical and relativistic, (T), 25:2871
models of, electron--neutrino effects in cosmic-ray penetration, (T), 25:2875
models of, relation of proton energy spectrum and degenerate neutrino gas in, 25:2874
time-reversal violation and the arrows of time in, (T), 25:3423
transport coefficients of a relativistic quantum gas in big-bang, (T), 25:2873
CRATERS
formation by underground nuclear explosions, computer calculations of effects of surrounding media on, 25:2381 (UCRL-50898)
CRITICAL ASSEMBLIES
design parameters of plutonium fueled ZPR-6 and ZPR-9, final safety analysis of, 25:3901 (ANL-7442)
operations aspects of plutonium fueled ZPR-6 and ZPR-9, final safety analysis of, 25:3901 (ANL-7442)
safety analysis of plutonium fueled ZPR-6 and ZPR-9, 25:3901 (ANL-7442)
CRITICALITY STUDIES
calculation of water moderated enriched uranium fueled assemblies, (E/T), 25:3912
calculation technique for, performance of minimum error few group programming, 25:3930
CROSS SECTIONS
book: Total Cross Section Measurements, 25:3268
charge-exchange and excitation, for proton reactions with helium and neon at 1 to 100 keV, (T), 25:2919
charge-exchange, between molecules and molecular ions, (T), 25:2912
charge-exchange, for proton reactions with helium at 1 to 100 keV, (T), 25:2919
comparison of 3D classical trajectory and transition-state, for atomic and molecular reactions, 25:3951 (HUX-3780-29)
excitation, for atoms and ions, review of approximate methods of calculation of, 25:2913
excitation, for electron reactions with alkali metal and hydrogen atoms, (T), 25:2915
excitation, for electron reactions with calcium and neon, quasi-classical calculation of, 25:2917
excitation, for electron reactions with calcium atoms and oxygen ions (OV), configuration-interaction calculations of dielectronic, 25:2918
excitation, for emission lines from ion reactions with nitrogen molecules at 30 to 100 keV, (E), 25:2902 (SC-RR-70-695)
excitation, for hydrogen atoms, lithium, potassium, and sodium, calculation using approximation based on regional trial functions, 25:2895
excitation, for ions by electron impact, formulas for, 25:2914
excitation, for potassium ions in collisions with neon atoms up to 30 keV, (E), 25:2911
ionization, for ions by electron impact, formulas for, 25:2914
ionization, for photon reactions with atoms and ions, computer program for calculation of, 25:2903
photoelectric, for gamma radiation in copper, platinum, and silver at 50 to 412 keV, total, 25:2905
photoelectric, for gamma radiation in gadolinium, hafnium, lanthanum, and thorium at 30 to 100 keV, 25:2907
photoelectric, for gamma radiation in palladium and tantalum at 662 keV, (E), 25:2904
photoelectric, for gamma radiation, ratios of total to subshell, 25:2908
scattering, for electrons by atoms and ions, computer program for calculation of, 25:2903
scattering, for gamma radiation by K electrons at 280 to 1002 keV, 25:2909
scattering, for γ radiation by aluminum, copper, lead, tin, and uranium at 30 keV to 2.62 MeV, incoherent, (T), 25:2921
scattering, for potassium atoms by iodine atoms and molecules at thermal energies and small angles, differential elastic, (E), 25:2922
CRUSTACEA
Gammarus pulex, radioisotope content of, in drainage canal of reactor center in Austria, 25:2545
CRYOSTATS
design and fabrication of low-temperature, for single-crystal and power x-ray diffraction, 25:3048 (AERE-R-6532)
design of liquid nitrogen, for use in annealing and heavy ion irradiation, 25:2388 (RD/B/M-1753)
CRYSTALLOGRAPHY
conference on accurate determination of x-ray intensities and structure factors, Cambridge, Eng., 6/68, 25:3216
CRYSTALS
dislocations in anisotropic, elastic characteristics of, 25:2668 (ORNL-4570, pp 10-12)
electron band structure of molecular, method for calculating ground states in, 25:3226 (IN-1420)
forces in molecular, Solbrig cell dipole description of, 25:3953 (IN-1410)
CUPFERRON
complexes with rare earths, composition and thermal stability of, 25:2078
CURIUM
basicities of aqueous solutions of, 25:2319 (ORNL-4572, pp 181-95)
complexes with Arsenazo III, spectrophotometric studies on, 25:2079
determination in aqueous alcohol solutions using Arsenazo III, spectrophotometric, 25:2079
CURIUM ACETATES
stability of ions of, effects of inner sphere complexing on, 25:2208
CURIUM ISOTOPES Cm-248
production at TRU, 25:2294 (ORNL-4572, pp 109-34)
CURIUM OXIDES
fabrication of HFIR targets of, incorporating curium-244, 25:2792 (ORNL-4570, pp 201-4)
Am_2O_3--Cm_2O_3, preparation of microspheres of, 25:2294 (ORNL-4572, pp 109-34)
CURRENT ALGEBRA
commutators in, Lorentz covariance for, 25:3298
commutators in, spectral functions for local, 25:3299
current commutator in, operator generalization of universal light cone, 25:3306
dispersion relations for ν + ν, ν + N, and e + N → ν + N interactions in, on-shell subtracted, 25:3368
hard-pion calculation in pole models, relation to, 25:3361
hard-pion method for Arhoν system in unitarized, consistency condition in, 25:3359
low-energy theorems and sum rules for ν + ν, ν + N, and e + N → ν + N interactions in, 25:3368
PCAC hypothesis for pseudoscalar form factor from muon capture rate in lithium-6, (T), 25:3748
soft-pion theorem for K → 3π decay, chiral-symmetry-breaking corrections to, 25:3347
vertex function for πrhoA$_1$ system and A$_1$ → rho + π and rho → 2π decays in phenomenological, 25:3376
CYCLOBUTANE
determination in products from radiolysis of gaseous ethylene, gas chromatographic method for, 25:2278
cyclobutane--methane, radiolysis of, isomerization of butyl ions in γ, 25:2290
CYCLOHEXANE
effects on radiolysis of ammonia, 25:2283
radiolysis of liquid, effects of LET and temperature on γ, helium-4, neon-20, and nitrogen-14, 25:2281
radiolysis of, diffusion model for effects of LET and temperature on, 25:2280
radiolysis of, effects of ion and radical scavengers on yields of cyclohexyl radicals from γ, 25:2268
CYCLOHEXANOL
neutron quasi-elastic scattering in liquid, incoherent cold, 25:3534
1,3-CYCLOOCTADIENE
1,3-cyclooctadiene--octane, radiolysis of, kinetics of production of ethane, hydrogen, and methane from γ, 25:2270
CYCLOOCTATETRAENE
cyclooctatetraene--octane, radiolysis of, kinetics of production of ethane, hydrogen, and methane from γ, 25:2270
CYCLOPENTANE
determination in products from radiolysis of gaseous ethylene, gas chromatographic method for, 25:2278

XUM

CYCLOPENTANE, METHYL-
determination in products from radiolysis of gaseous ethylene, gas chromatographic method for, 25:2278
CYCLOPROPANE
determination in products from radiolysis of gaseous ethylene, gas chromatographic method for, 25:2278
CYCLOTRONS
beam injection in U-120, performance of system for polarized deuteron radial, 25:3519
beam injection in U-120, system for polarized ion radial, 25:3520
design of 600-MeV microtron using superconducting linac, 25:3506
magnetic guide field for Juelich isochronous, design of, 25:3493
magnetic median surface in AVF, Hall probe for locating, 25:3516
CYLINDERS
mass exchange of circular, in transverse MHD flow, (T), 25:2941
CYTIDINE MONOPHOSPHATES
radiolysis of aqueous chloride solutions of, rate constants for electron pulse and γ, 25:2259 (GA-10208)
CYTOCHROME OXIDASE
radiation effects on activity of, in sprouts of beans and clover, γ, 25:2596
CYTOSINE
radiolysis of aqueous chloride solutions of, rate constants for electron pulse and γ, 25:2259 (GA-10208)

D

DACTINOMYCIN
effects on mitotic progression of cultured Chinese hamster ovary cells from G_2 into metaphase in comparison with uv, 25:2558
DATA ACQUISITION SYSTEMS
performance of high temperature gas cooled reactor, 25:3795 (DP-Report-561)
DATA DISPLAY SYSTEMS
description of Weapons Effects Display System, for fallout mapping, 25:2506 (UCRL-50922)
logic interfaces for Weapons Effects Display System, wiring tables for, 25:2505 (UCRL-50892(Vol.4)(Pt.5))
operation manual for Weapons Effects Display System, 25:2504 (UCRL-50892(Vol.2))
DATA PROCESSING SYSTEMS
design of computer-based, for scintillation gamma spectrometers, 25:2477
DAVIS-BESSE POWER REACTOR
safety evaluation of, Division of Reactor Licensing, 25:3844 (DOCKET-50346-18)
DECONTAMINATION
equipment and methods for Carlsbad Site, New Mexico, 25:2420 (NVO-410-2)
DENSIMETERS
circuit for radiometric, for automatic absorption curve matching, 25:2499(P)
design of gamma-backscatter moving-source, for soils, 25:2498
design of ultrasonic, for steam--water mixtures, 25:3905 (IN-1441)
DESALTING
bibliography on U. S. projects for, 25:3913 (ORNL-NDIC-8)
evaporators for, evaluation of variable orifices in flash, 25:2387 (ORNL-TM-2746)
DEUTERIUM
content in worldwide atmospheric precipitation, 1964 to 1966, data tabulations on, 25:2367 (STI/DOC-10/117)
deuteron reactions (d,2p) at 12 MeV, neutron--neutron final-state interactions in, (E), 25:3549
effects on acidity function of sulfuric acid, 25:2175
effects on Cope rearrangement of 1,5-hexadiene and 3,3-dicyano-2-ethyl-1-methyl-1,5-hexadiene, 25:2188
effects on enthalpies of alkylammonium ions in water, 25:2162
effects on fluorescence lifetimes of uranyl compounds, 25:2198
effects on fluorescence yields and lifetimes of indole derivatives, 25:2536
effects on gas chromatographic behavior of methylbenzene compounds, 25:2167
effects on hydrolysis of bis(4-nitrophenyl) carbonate and o-(4-nitrophenylene) carbonate, 25:2181
effects on ir and Raman spectra of proline, 25:2190
effects on ir spectra and structure of water, 25:2171
effects on ir spectra of beryllium borohydride, 25:2189
effects on ir spectra of pyridine-1-oxide, 25:2163
effects on ir spectra of water at 25 to 390°C, 25:2165
effects on ir spectra of water-d in aqueous solutions of perchlorates and tetrafluoroborates, 25:2183
effects on kinetics of enzymatic transamination, 25:2168
effects on oxidation of 2-butanol and 3,5-dicarbethoxy-1,4-dihydro-2,6-lutidine by tert-butyl peroxide, 25:2180
effects on proton relaxation times in aqueous solutions, 25:2166
effects on Raman spectra of potassium acid sulfate--water systems, 25:2173
effects on reaction rate of methoxide-catalyzed methanolysis of triphenylsilane, 25:2176
effects on self-association of N-methylacetamide in carbon tetrachloride, 25:2174
effects on self-diffusion in water, 25:2192
effects on solvolysis of benzhydryl benzoate, 25:2185
effects on solvolysis of norbornyl brosylates, 25:2172
effects on spin--lattice relaxation time of aniline, 25:2182
exchange between alkenes and cesium cyclohexylamide in cyclohexylamine at 25°C, kinetics of, 25:2184
exchange between benzene and deuterated γ-alumina, 25:2164
exchange in cyclization of allylic amides in deuterated sulfuric acid, 25:2179
exchange in electronegatively substituted diene--iron tricarbonyl complexes, base-catalyzed, 25:2187
exchange reactions in hydrocarbons, 25:2161
exchange with hydrogen in reactions of transition metal hydride complexes with 1-butene, deuterated ethylene, and deuterium, 25:2170
exchange with hydrogen in water adsorbed on thorium dioxide surfaces, ir spectral studies on, 25:2207
helium-3 reactions (helium-3,p) at 350 keV, educational experiments utilizing, 25:3543 (CONF-700322-, pp 95-104)
proton reactions (p,2p) at 156 MeV, angular distributions and differential cross sections as test of impulse approximation, (E), 25:3554
proton reactions (p,2p) at 9 to 13 MeV, spectra from, (E), 25:3553
proton reactions (p,2p) with, modified impulse approximation and Chew--Low extrapolation for, (E/T), 25:3750
proton reactions (p,d*)p at 9 to 13 MeV, excitation function of, (E), 25:3553
proton reactions (p,np) with, modified impulse approximation and Chew--Low extrapolation for, (E/T), 25:3750
proton reactions (p,pn) at 14 to 23 MeV, energy dependence of quasifree scattering in, (E), 25:3547 (RLO-1388-126)
reactions with helium-3, lithium-6 and -7 in plasma admixtures, 25:3140
separation of ortho- and para-, by thermal diffusion, 25:2405
DEUTERIUM IONS
reactions with graphite and metal surfaces at 5 to 50 keV, apparent total ion scattering, secondary electron emission coefficients, and electron and ion energy distributions for, (E), 25:2884 (NP-18490)
DEUTERIUM SYSTEMS
D--H, hydromagnetic wave absorption by plasma in Levitron-type device, (E/T), 25:3148 (CEA-CONF-1614)
DEUTERON SOURCES
development of polarized, from charge exchange collisions between metastable H(2S) atoms and halogens, 25:3307
performance of polarized, for radial injection into U-120 cyclotron, 25:3519
DEUTERONS
effects on cadmium sulfide, educational program for studying, 25:3187 (CONF-700322-, pp 63-77)
interactions d + d at 2.2 and 7.9 GeV/c, differential cross sections for elastic, (T), 25:3415
interactions d + p at 3.76 GeV/c, differential cross sections for elastic, (E), 25:3264
interactions γ + d → d(p + n) + π^+ + π^- at 1 to 5 GeV in bubble chamber, differential and total cross sections for rho^0 production in, (E), 25:3246
interactions K$^-$ + d → K$^-$ + π^+ + π^- + n + p at 5.5 GeV/c, cross section for anti K*^{0}(890) and Δ$^-$(1236) production in, (E), 25:3274
interactions n + d below 20 MeV, dpn and tdn coupling constants from forward dispersion relations for, (T), 25:3408
interactions p + d → p + d above 1 GeV, model for wide-angle, (T), 25:3419
interactions π + d → N + N, relativistic dispersion theory of deuteron structure from amplitudes for, (T), 25:3409
interactions π^+ + d → p + p + π^+ + π^- + π^0 at 3.65 GeV/c, evidence for H enhancement in, (E), 25:3286
interactions π^+ + d at 7 GeV/c in bubble chamber, difference in energy dependence for A_2^- and A_2^0 production in, (E), 25:3289
interactions with elementary particles, cross sections for quasielastic, (T), 25:3293 (JINR-P2-5343)
interactions with hadrons at high energies, Glauber shadow correction for calculation of cross-section defect in, (T), 25:3412
reactions (d,2p) with deuterium at 12 MeV, neutron--neutron final-state interactions in, (E), 25:3549
reactions (d,α) with boron-10 at 4.0 to 12.0 MeV, alpha spectra and differential cross sections for, (E), 25:3573
reactions (d,f) with gold-197, bismuth-209, and uranium isotopes at 51.5 MeV, cross sections and angular distributions from, (E), 25:3710
reactions (d,γ) with hydrogen at 19.8 and 29.6 MeV, helium-3 energy spectra, gamma angular distributions, and total cross sections for, (E), 25:3546 (ORNL-TM-3168)

reactions (d,n) and (d,p) with deformed nuclei with nonrotational states involved, (T), 25:3732
reactions (d,n) with boron-11, nitrogen-14, and nitrogen-15 at 5.5 MeV, angular distributions and polarizations for, (E), 25:3574
reactions (d,n) with oxygen-16 at 2.0 to 4.2 MeV, cross-section measurement by a thick-target method, (E), 25:3586
reactions (d,n) with zinc-64, -66, and -68 at 10 MeV, DWBA analysis of differential cross sections from, (E), 25:3625
reactions (d,p) and (d,t) with palladium-105 at 17 MeV, angular distributions for, (E), 25:3701
reactions (d,p) with beryllium-9 at 2.9 MeV, p-γ angular correlations for, (E), 25:3588
reactions (d,p) with boron-10 at 350 keV, energy levels of boron-11 from, (E), 25:3561 (CONF-700322-, pp 133-40)
reactions (d,p) with carbon-12 at 3.4 MeV, compound-nucleus direct interaction interference in angular distributions for, (E), 25:3572
reactions (d,p) with lead-207, γ-ray branching ratios for, (E), 25:3688
reactions (d,p) with neon-21 at 10.2 MeV, angular distributions for, (E), 25:3633
reactions (d,p) with nuclei, BWBA analysis for stripping to unbound states, (T), 25:3764
reactions (d,p) with oxygen-18 at 5.0 MeV, gamma and proton spectra from, (E), 25:3584
reactions (d,p) with silicon-28 at 2.00 to 6.12 MeV, angular distributions for, (E), 25:3606
reactions (d,p) with sulfur-32 at 12.3 MeV, proton spectra and angular distributions for, (E), 25:3597
reactions (d,p) with uranium-235 at 13 to 20 MeV, cross section for delayed fission in, (E), 25:3709
reactions (d,pn) with uranium-238 and -236 at 11 to 20 MeV, cross sections for delayed fission in, (E), 25:3709
reactions (d,t) with holmium-165 at 12 MeV, angular distributions for, (E), 25:3711
reactions (d,tp) with helium-3 at 20.7 MeV, p-p and p-t final-state interactions in, (E), 25:3552
reactions in lithium-drifted silicon detectors at 15 to 80 MeV, effects on pulse-height distributions of, 25:2451
reactions with beryllium-9 at 350 keV, charged particle spectra from, 25:3560 (CONF-700322-, pp 89-94)
reactions with graphite and metal surfaces at 5 to 50 keV, apparent total ion scattering, secondary electron emission coefficients, and electron and ion energy distributions for, (E), 25:2884 (NP-18490)
reactions with nickel at 50 MeV, analysis using adiabatic approximation for breakup, (T), 25:3614
scattering by europium-151 at 12 MeV, angular distributions and cross sections for inelastic, (E), 25:3653
scattering by nickel at 50 MeV, analysis using adiabatic approximation, (T), 25:3614
scattering of vector-polarized, by carbon-12, silicon-28, and calcium-40 at 28 MeV, asymmetries in, (E), 25:3585
structure of, short range, 25:3410

DIAMONDS
ion implantation in, semiconducting layers induced by, 25:3199
structure of, numerical-variational calculation of electronic band, 25:2671 (ORNL-4570, pp 40-3)

DIDO REACTORS
moderator for, comparison fast neutron dose scale for radiation effects on graphite, 25:3872 (DP-Report-559)

DIFFERENTIAL EQUATIONS
difference formulae for Taylor expansible function, 25:3993 (UCRL-50874)

DIGOXIN
radioimmunoassay in blood plasma, method for, 25:2522

DIODES
radiation damage to silicon, hybrid recombination model for neutron, 25:2514 (SC-R-70-4351)
radiation effects on voltage-current characteristic of silicon-carbide, gamma, 25:3192

DISEASES, NEOPLASTIC
adenomas, radioinduced inhibition of urethan-induced, in lungs of mice, role of thymus in x, 25:2589
leukemia, extracts from cells of mouse, catalytic effect of, 25:2520
osteosarcomas, radioinduced, in rats, ultrastructure of phosphorus-32 β, 25:2594
tumors, radiodiagnosis of human brain, in posterior fossa, comparison of effectiveness of iodine-131, technetium-99, mercury-197, or mercury-203 for, 25:2578
tumors, radioinduced, in animals, role of transplantation antigens in, 25:2537
tumors, radiotherapy of human, effectiveness of fast neutron, 25:2582 (CONF-700322-, pp 393-406)
tumors, radiotherapy of malignant, diagnosis and treatment of complications following combined cytostatic therapy, surgery, and, 25:2583

DISEASES, PHYSIOLOGICAL
colitis, sorption of chromium-51-labeled EDTA by patients with ulcerative, 25:2534
enteritis, effects on calcium-47 retention in patients, 25:2531
thrombocytopenia, radiodiagnosis in man, tracer method for, 25:2579

DISEASES, TRAUMATIC
radiation injuries, treatment of latent, in man following use of Thorotrast for diagnosis, 25:2583

DISILANE
reactions with recoil silicon-31 atoms, 25:2299
PH_3--Si_2H_6, radiation effects on, reactions of silicon-31 recoils from fast neutron, 25:2299

DISPERSION RELATIONS
derivation of on-shell subtracted, for π + π, π + N, and e + N → e + N interactions, 25:3368
form factors for scattering amplitudes, 25:3461
interactions π^- + N and π^+ + N, structure of backward differential cross sections for, 25:3377 (ITF-70-65)
sum rule for rms radius for scattering, 25:3461

DISTILLATION
efficiency of, tracer studies on, 25:2343

DODECANE
radiolysis of, effects of oxygen on yields from, 25:2292

DRESDEN POWER REACTOR, UNIT 1
site for, guide to environmental monitoring and recording requirements for, 25:3807 (DOCKET-50010-70)

DRESDEN POWER REACTOR, UNIT 2
design parameters of, revised and additional data on, 25:3815 (DOCKET-50237-85)
operations aspects of, revised and additional data on, 25:3815 (DOCKET-50237-85)
safety evaluation of, Division of Reactor Licensing, 25:3817 (DOCKET-50237-87)
site for, safety analysis of, 25:3816 (DOCKET-50237-86)

DRESDEN POWER REACTOR, UNIT 3
operation of, proposed license for, 25:3821 (DOCKET-50249-43)
safety evaluation of, Division of Reactor Licensing, 25:3821 (DOCKET-50249-43)

DRILL HOLES
testing of UA-1, to determine mining chamber location, results of hydraulic, 25:2349 (USGS-474-72)

DYES
evaluation of fluorescent, as tracers for pollution control studies of diffusion and flow conditions in estuaries, 25:2348 (NYO-3961-1)

DYSPROSIUM ALLOYS AND SYSTEMS
Dy--Fe, crystal structure of intermetallic $DyFe_3$ and Dy_6Fe_{23}, 25:2750

DYSPROSIUM ISOTOPES Dy-159
beta decay of, hindrance factors for unique first-forbidden, (E), 25:3672

DYSPROSIUM ISOTOPES Dy-160
energy-level transitions from octupole states in, branching ratios from E1, (T), 25:3751
energy-level transitions from terbium-160 beta decay, reduced transition probabilities and band-mixing parameters for, (E/T), 25:3677

DYSPROSIUM ISOTOPES Dy-161
Moessbauer isomer shift of 25.6-keV gamma ray from trivalent and tetravalent dysprosium ions in cerium dioxide, (E), 25:3222
nuclear magnetic moment of, effects of spin--orbit and spin--spin forces on, (T), 25:3692

DYSPROSIUM ISOTOPES Dy-162
spectra of muonic, dynamic hyperfine structure in x-ray, (E), 25:3661

DYSPROSIUM ISOTOPES Dy-163
nuclear magnetic moment of, effects of spin--orbit and spin--spin forces on, (T), 25:3692

DYSPROSIUM ISOTOPES Dy-164
spectra of muonic, dynamic hyperfine structure in x-ray, (E), 25:3661

E

ECOSYSTEMS
cesium distribution in pond, neutron activation analysis of, 25:2516
radiocobalt transport in artificial aquatic, double tracer study of, 25:2549
radioisotope transport in aquatic, development of mathematical model for, 25:2542
radioisotope transport in freshwater, 25:2541

EDDY CURRENT TESTING
methods for LMFBR materials, development of, 25:2408 (ORNL-4570, pp 96-7)
methods for reactor materials, development of, 25:2409 (ORNL-4570, pp 149-51)

EINSTEINIUM ISOTOPES Es-253
production at HFIR and TRU, 25:2294 (ORNL-4572, pp 109-34)

ELECTRIC ARCS
book: Physics of Gas Discharge Plasma, 25:3076
design of high-pressure and high-current long, for plasma production, (E), 25:3112
design of reflex, for plasma production, 25:3111 (LYCEN-7065)
electric field distribution in hydrogen, with axial magnetic field, (E), 25:3083
ion density distribution of xenon in, (T), 25:3085 (LYCEN-7061)
model of wall-stabilized toroidal, 25:3088

XUM

plasma diagnostics in, optical probing for, 25:3065
plasma flow in inherent fields of, compressible, (T), 25:3103
theory for radial pressure profile in hydrogen, 13-moments approximation, 25:3105
theory for radial pressure profile in hydrogen, 5-moments approximation, 25:3104
ELECTRIC CAPACITORS
impedance calculations for parallel-plate, in plasmas, 25:3100
ELECTRIC DISCHARGE
book: Physics of Gas Discharge Plasma, 25:3076
excitation processes in helium hollow-cathode, (E), 25:2890
plasma ion density measurement using Stark broadening, molecular hydrogen, 25:3068
ELECTRIC FIELDS
calculation method for constant, on surfaces, 25:3934(T) (ANL-Trans-862)
ELECTRIC INSULATORS
radiation effects on, 1.3 MeV gamma and 6.0 MeV electron, 25:2819 (LCIE-342)
ELECTRIC POWER
generation of, legal aspects of environmental effects of, 25:2564
requirements in US to 2000, prediction of total, 25:2393
ELECTRODES
effects of size of, on performance of combustion-driven MHD generator, 25:2398
immersion in plasma, volt--ampere characteristics of cathode, (T), 25:3107
operation in magnetohydrodynamic generators, performance of, 25:2940
radiation effects on calomel, fluoride specific, glass, and nitrate specific, γ, 25:2231
ELECTRODYNAMICS
charged-particle trajectories in Lyttleton-Bondi, geodesics of affine connection for, 25:3431
ELECTROHYDRODYNAMIC GENERATORS
development possibilities for, 25:2938
ELECTROJETS
auroral, occurrence of daytime polar cap magnetic disturbances preceding nighttime, (E), 25:2978
ELECTROLYTIC CELLS
development for use in reprocessing of MSBR fuel, 25:2313 (ORNL-4572, pp 1-36)
ELECTROMAGNETIC FIELDS
boson energy levels and wave functions in external, charged relativistic intermediate-vector, (T), 25:3344
electron system interactions with external, electromagnetic many-body forces for, (T), 25:3328
interactions with spin-$^3/_2$ particles in Bhabha theory, quantization of, 25:3439
particles in, invariance of nonrelativistic Hamiltonian--Jacobi equation for, (T), 25:3430 (JINR-P2-5373)
quantization of interacting, 25:3440
symmetry groups for uniform, relativistic, (T), 25:3432
ELECTROMAGNETIC LENSES
charged-particle beam transport in, transformation matrix for beam ellipse matching in waist-to-waist, 25:3521
charged-particle motion in two-potential, with distorted focusing layer, 25:3490
charged-particle trajectories in misaligned, analysis of first-order effects in, 25:3495
electron-optical properties of two-potential two-dimensional, 25:3491
ELECTROMAGNETIC PUMPS
design for space power systems, review of, 25:2600 (BNL-50258)
ELECTROMAGNETIC WAVES
analysis of distant concentrated spectrum-signal atmospherics, complete functions in, (E/T), 25:2975
interactions with nonisothermal plasma, if resonances and averaged potential in, (T), 25:3165
propagation in plasma in sheared magnetic field, polarization change in, (E), 25:3146 (CEA-CONF-1608)
propagation in plasma, decay instability of cyclotron harmonic, (T), 25:3162
scattering of, random walk approximation for analyzing, 25:3239
ELECTRON BEAMS
current integrator for pulsed, 25:3517
focusing by magnetic fields, effect of local inhomogeneities on pulsations at edges, (E/T), 25:3524
interactions with hydrogen-ion clusters, dissociation in, 25:3109 (CEA-CONF-1610)
interactions with magnetoplasma in waveguide, transformation of longitudinal into transverse energy in cyclotron, 25:3080
interactions with molecular hydrogen plasma, ion heating in, (E), 25:3054 (CEA-CONF-1611)
interactions with neutral gas streams, plasma production in, 25:3113
interactions with plasma, wave growth from, (T), 25:3157
interactions with preformed decay plasma, nonlinear stabilization of beam instability in, (E), 25:3126
monitoring of low-intensity, rotating plastic scintillation detector for, 25:3497
motion in electric and magnetic fields, equations for, 25:3486
ELECTRON GAS
equilibrium properties of, upper and lower bounds for, (T), 25:3232
ELECTRON MICROSCOPES
use with heavy-ion accelerator for radiation damage studies, 25:2507
ELECTRON MICROSCOPY
methods for use in materials science, 25:2748
ELECTRON MULTIPLIER TUBES
gain of channel, effects of temperature on, 25:2470
ELECTRON PAIRS
photoproduction on carbon, production of virtual photons in, (E/T), 25:3252
production in electron reactions with copper at 5.8 MeV, cross sections for direct, (E), 25:3250
ELECTRON PROBE MICROANALYSIS
method for reactor materials, 25:2731 (ORNL-4570, pp 215-23)
ELECTRON-RING ACCELERATORS
development at Dubna, 25:3515
ELECTRON SOURCES
cathode for gun-type, 25:3523(P)
ELECTRONIC FILTERS
design of lock-in detector, 25:3954 (IS-2389)
ELECTRONS
effect of magnetically conjugate photo-, on predawn enhancement of 6300-A line, (E/T), 25:2959
effects of fast, on properties of methyl methacrylate polymers, 25:2225
effects of pulsed, on aqueous chloride solutions of deoxynucleotides, purines, and pyrimidines, 25:2259 (GA-10208)
effects of pulsed, on aqueous thymine solutions, spectral studies on, 25:2259 (GA-10208)
effects of pulsed, on hydrated nitrosobenzene, mechanism of, 25:2272
effects of pulsed, on luminescence of aqueous solutions of thallium sulfate at 10 MeV, 25:2233
effects on aluminum films at 80 keV, radiative decay of volume and surface plasmons excited in, 25:2885
effects on aromatic ketones, 25:2266
effects on carbon monoxide, effects of propane or propene on yields from, 25:2287
effects on curing of paints, developments in, 25:2243
effects on hexachloroethane, effects of hydrogen atoms on site migration of free radicals produced from, 25:2246
effects on insulating materials at 6.0 MeV, 25:2819 (LCIE-342)
effects on lattice displacements in aluminum at 175 to 750 kV, 25:2816 (ORNL-4570, pp 16-19)
effects on n-type germanium at 30 and 77°K, model of defects induced in, 25:3200
effects on organic liquids, model for, 25:2260 (IRI-133-70-2)
effects on platinum at 3 MeV, stored-energy-release study of Frenkel defects induced in, (E), 25:3197
effects on polyethylene crystals, 25:2234
effects on preparation of metals from their aqueous salt solutions, 25:2237 (N-70-32826)
effects on properties of lithium-doped silicon photovoltaic cells, 25:2814 (N-70-27167)
effects on stress-rupture stability of thermoplastics by cross linking, 25:2249
effects on structure of amine-reinforced ED-5-type resins, 25:2273
effects on structure of martensite lattice in steel--uranium alloy, 25:2764
energy spectra of disturbed and quiescent magnetospheric, differential, (E), 25:2950 (AD-709363)
intensity of outer-zone E greater than or equal to 150 keV, correlation with geomagnetic indexes, 25:2969
interactions e + e, design of experiment for studying cross sections of, (E/T), 25:3245
interactions e + N + ν + N, on-shell subtracted dispersion relations and low-energy theorems and sum rules from current algebra for, (T), 25:3368
interactions e + N, Deser--Gilbert--Sudarshan representation for structure functions for particle production in, (T), 25:3329
interactions e + n, parton and quark models for deep inelastic, (T), 25:3310 (DESY-70/50)
interactions e + p → π^0 + n at threshold, neutron electromagnetic form factor from, (E), 25:3244
interactions e + p at high energies, effect of transverse momentum distribution in parton model for inelastic, (T), 25:3323
interactions e + p, Bjorken limit and Jin--Martin lower bound for, (T), 25:3294 (NYO-4204-5)
interactions e + p, parton and quark models for deep inelastic, (T), 25:3310 (DESY-70/50)
interactions e + p, Regge residues for extrapolation of γ + p total cross sections at high energies to deep inelastic region of, (T), 25:3312 (NYO-4204-6)
interactions e + p, structure functions in ladder model with spin-$^1/_2$ nucleons for deep inelastic, (T), 25:3311 (NYO-4204-4)
interactions e^+ + e^-, design of experiment for studying cross sections of, (E/T), 25:3245
interactions π^- + e at 16.2 GeV/c in nuclear emulsion, absolute cross sections for, (E), 25:3253
interactions with external field, electromagnetic many-body forces for, (T), 25:3328
motion in magnetic fields from helix, cyclotron

resonance, 25:3235
motion in quantized field of flat electromagnetic wave, 25:3233
production of intense fast, design of water-dielectric generator for, 25:3478
propagation of cosmic primary, in the neutrino sea, (T), 25:2875
reactions with alloys and metals at 1 to 3 MeV, backscatter and transmission coefficients for, (E), 25:2883 (N-70-25499)
reactions with aluminum, gold, iron, and tin at 1 MeV, angular distributions and energy spectra for backscattering, 25:2886
reactions with atoms and ions, calculation of excitation cross sections for, (T), 25:2915
reactions with atoms at 50 to 150 keV, equipment and methods for studying inelastic, 25:3472 (CONF-700322-, pp 379-92)
reactions with atoms, quasi-classical method for calculation of cross sections for, 25:2917
reactions with atoms, role of intermediate states in excitation in, (T), 25:2916
reactions with calcium and neon, quasi-classical calculation of excitation cross sections for, 25:2917
reactions with calcium atoms and oxygen ions (OV), configuration-interaction calculations of cross sections for dielectronic transitions in, 25:2918
reactions with carbon monoxide and nitrogen molecules at 10 keV, K-shell excitation and ionization in, (E), 25:2910
reactions with carbon-12 and -13 at 43 and 46 MeV with proton knockout, proton energy spectra and angular distributions from, (E), 25:3566 (SAL-14)
reactions with carbon-12 with nucleon knockout, cross-section calculations using Woods--Saxon potential, (T), 25:3714 (ITF-70-35)
reactions with copper at 5.8 MeV, cross sections for direct electron pair production in, (E), 25:3250
reactions with ions, formulas for excitation and ionization cross sections for, 25:2914
reactions with light nuclei, analysis of knockout in, (T), 25:3714 (ITF-70-35)
reactions with neon, rates of energy-level transitions in, (T), 25:2920
reactions with nuclei, cross sections of ν + anti ν pair production in, (T), 25:3335
scattering by atoms and ions having two valence electrons, configuration-interaction calculations of, 25:2918
scattering by atoms and ions, computer program for calculation of cross sections for, 25:2903
scattering by carbon-12 and calcium-40 in a square-well shell model, quasielastic, (T), 25:3577
scattering by carbon-12 and oxygen-16 at 375 and 750 MeV, cross sections and charge distribution from elastic, (E), 25:3587
scattering by lithium-6 and -7, charge form factors from elastic, (E), 25:3558 (AD-704484)
scattering by nickel-58, -60, -61, -62, and -64 at 300 MeV, charge parameters and K transition energies for elastic, (E), 25:3687
scattering by sulfur-32 at 1115 MeV, quasi-elastic, 25:3615
symmetry wih mesons (μ) in two-component neutrino theory, 25:3351
yields of solvated, from radiolysis of water, 25:2257 (CEA-R-4046)

ELECTROSTATIC ANALYZERS
calculations for hollow and cylindrical charged-particle beams, 25:3487

ELECTROSTATIC GENERATORS
design of water-dielectric, for production of intense fast electron and hard decelerated x-ray pulses, 25:3478

ELEMENTARY PARTICLE MODELS
composite, regularities among baryon resonance decay widths from, 25:3405
diffraction, for elastic p + p interactions above 20 GeV/c, 25:3417
dual resonance, factorization of multiloop diagrams in, 25:3443
dual-resonance, operators for constructing Feynman diagrams in, 25:3353
Glauber multiple scattering, meson (π^-,rho$^-$) and (π^-,rho^0) reactions with A = 20 to 208 nuclei at 30 GeV in, coherent and incoherent, 25:3406 (IFVE-STF-69-71)
ladder, interactions e + p in, deep inelastic, 25:3311 (NYO-4204-4)
one-boson-exchange potential, for Λ + N interactions, 25:3416
one-boson-exchange, meson spectrum in bound states of anti N + N interactions, 25:3358 (DESY-70/49)
optical, for differential cross sections for elastic p + p scattering, 25:3413
parton, for inelastic lepton-nucleon interactions, effect of transverse momentum distribution in, 25:3323
parton, interactions e + p and e + p in, deep inelastic, 25:3310 (DESY-70/50)
thermodynamic, of strong interactions, 25:3355
Veneziano, current amplitudes for lepton interactions with hadrons in, 25:3342
Veneziano, fits to $K^- + p \to K^0 + \pi^- + p$ interactions at 3.3 GeV/c in generalized, 25:3391
Veneziano, five-point amplitude for cross sections and effective-mass and angular distributions for $\pi^- + p$ interactions in, 25:3378 (ITF-70-77)
Veneziano, for 3π Dalitz plot structure in anti p + n + $2\pi^- + \pi^+$ interactions at 1.0 to 1.6 GeV/c in deuterium bubble chamber, (E/T), 25:3270 (INFN-PD-70/2)
Veneziano, for nucleon form factors, 25:3394
Veneziano, off-shell extension of amplitude for $\pi + \pi$ interaction in, 25:3373
Veneziano, residues in Regge pole model for $0^- + 1/2^+ \to 0^- + 3/2^+$ interactions, 25:3384 (TPJU-3/70)
Veneziano, sign of Regge-pole residues in, 25:3453
Veneziano, with π and Pomeron exchange interactions $K^- + p \to n + K^- + \pi^+$ at 10 GeV/c in, 25:3386

ELEMENTARY PARTICLE MODELS (TRIPLET)
coupling strength of quarks, universal, 25:3405
interactions e + p and e + n in quark, deep inelastic, 25:3310 (DESY-70/50)
polarization of Λ and Σ in two-body Y* and anti Y* production in baryon interactions with pseudoscalar mesons and baryon interactions with antibaryons in additive quark, 25:3383 (TPJU-2/70)
production amplitudes for vector and pseudoscalar mesons and $3/2^+$ baryon resonances in pseudoscalar meson interactions with $1/2^+$ baryons in quark, ambiguities in, 25:3382 (TPJU-1/70)

ELEMENTARY PARTICLES
decay of, covariant phase-space calculations of n-body, 25:3303
field operator for composite, HNZ construction of, 25:3445
interactions at high energies, models for energy and angular dependence of particle exchange in nondiffractive, 25:3454
interactions of identical, theorem for, 25:3304
interactions of scalar and pseudoscalar unit-mass identical, estimates of unitarity integral for elastic, 25:3300
interactions of, asymptotic behavior of cross sections for, 25:3455
interactions of, dispersion relations for form factors for amplitudes of, (T), 25:3461
interactions of, rescattering effects in resonance production, (T), 25:3459
interactions of, sum rule for rms radius for, (T), 25:3461
interactions of, weakly coupled neutral currents in, 25:3302
interactions with deuterons, cross sections for quasielastic,(T), 25:3293 (JINR-P2-5343)
interactions with two missing neutral particles, method for study of, 25:3362
motion of spinless zero-mass, additional invariance of relativistic equations for free, (T), 25:3292 (ITF-70-32)
production in e + N interactions, Deser--Gilbert--Sudarshan representation for structure functions for, (T), 25:3329
production of, covariant phase-space calculations of n-body, 25:3303
production rates for spinless massless, implications of causality for, 25:3301
reactions with nuclei at high energies, optical limit of Glauber theory for, 25:3317
scale invariance for massless scalar (dilaton), 25:3372
spin of, physical bounds for components of statistical tensors for, (T), 25:3296
spin of, physical bounds for components of statistical tensors for, (T), 25:3295 (TPJU-12/70)
strong interactions of, book on review of total cross sections for, (E), 25:3268
strong interactions of, thermodynamic model of, 25:3355
symmetry for, 27-plet unitary symmetry operator in SU(3), (T), 25:3426
theory for, geometric representation of uncertainty relation in, 25:3297
theory of identical particles for Green paraparticles in, unified, 25:3304
weak interactions in pole model, relation of fundamental to bilinear, 25:3348
weak interactions of, limiting relations for correlation averages for four-fermion, (T), 25:3332 (ITF-70-59)

ELEMENTS
determination in lunar soils, equipment and method for in situ neutron activation, 25:2144
determination in solution using x-ray fluorescence spectrometer with computer, 25:2105
determination of trace amounts of, in teeth, review on activation method for, 25:2135
determination of, paper chromatographic data for, 25:2075

ELK RIVER POWER REACTOR
operations history for August 1969, 25:3782 (DOCKET-1151-3)

ENVIRONMENT
radiation effects on, in vicinity of nuclear power plants, legal aspects of, 25:2564
radioisotope contamination in, of Moscow area during 1962 to 1966, fallout, 25:2550

XUM

ENZYMES
induction of fatty acid desaturating, temperature-mediated, 25:3985 (UCLA-12-795)
Moessbauer spectra of iron-containing, 25:3971(R) (NYO-3798-9)
EPOXY RESINS
radiolysis of amine-reinforced ED-5-type, electron or γ, 25:2273
ERBIUM ISOTOPES Er-166
energy levels from multiple Coulomb excitation, (E), 25:3662
energy-level transitions from octupole states in, branching ratios from E1, (T), 25:3751
energy-level transitions in, statistical perturbation of γ--γ angular correlations in different liquid sources, (E), 25:3696
ERBIUM ISOTOPES Er-167
nuclear magnetic moment of, effects of spin--orbit and spin--spin forces on, (T), 25:3692
ERBIUM ISOTOPES Er-168
energy-level transitions from thulium-168 electron-capture decay, reduced transition probabilities for, (E/T), 25:3677
energy-level transitions in, strength functions for M1, (T), 25:3683
spectra of muonic, dynamic hyperfine structure in x-ray, (E), 25:3661
ERBIUM ISOTOPES Er-169
beta decay of, hindrance factors for unique first-forbidden, (E), 25:3672
ERBIUM ISOTOPES Er-170
spectra of muonic, dynamic hyperfine structure in x-ray, (E), 25:3661
ERBIUM OXIDES
emittance at high temperatures of solid, spectral, 25:3204 (AD-708547)
Er_2O_3--HfO_2, phase studies, 25:3978(T) (SC-T-70-4043)
Er_2O_3--HfO_2, phase studies of, 25:2804 (IS-T-401)
Er_2O_3--Yb_2O_3, preparation, magnetic susceptibility, and spectra of solid solutions of, 25:3211
ERYTHROCYTES
radiolysis of aqueous solutions of, ultrasonic absorption studies on γ, 25:2285
ESTERS
cyclization of, kinetics of Dieckmann, 25:4001(T) (UCRL-Trans-1417)
radioinduced polymerization in wood, 25:2254
ESTUARIES
diffusion and flow conditions in, evaluation of fluorescent dye and radioisotope tracer techniques for pollution control studies of, 25:2348 (NYO-3961-1)
ETHANE
determination in products from radiolysis of gaseous ethylene, gas chromatographic method for, 25:2278
yields from γ radiolysis of mixtures of octane with benzene, 1,3-cyclooctadiene, or cyclooctatetraene, kinetics of production of, 25:2270
ETHANE, BROMO-
radiation effects on, electrolytic collection of recoil bromine-80 and bromine-80m from thermal-neutron, 25:2301
ETHANE, DIBROMO-
radiation effects on, electrolytic collection of recoil bromine-80 and bromine-80m from thermal-neutron, 25:2301
ETHANE, HEXACHLORO-
radiation effects on, effects of hydrogen atoms on site migration of free radicals produced from electron, 25:2246
ETHANOL
photooxidation by uranyl ions in aqueous solutions, mechanism of, 25:2158
radiolysis of frozen aqueous solutions of, effects of acids on hydrogen abstraction by primary species from γ, 25:2293
ETHYL SULFATES
effects on aleurone pigmenting potential in maize, mutagenic, 25:2560
ETHYLENE
effects on gaseous yields from γ radiolysis of poly(tetrafluoroethylene), 25:2261 (NP-18518)
effects on γ radiolysis of cyclohexane, 25:2268
radiolysis of gaseous, chromatographic method for determination of products from, 25:2278
ETHYLENE, CHLORO-, POLYMERS
radiation effects on stress-rupture stability of, by cross linking, electron, 25:2249
ETHYLENE GLYCOL
effects on γ-radioinduced graft polymerization of cellulose with styrene in methanol solutions, 25:2247
ETHYLENE OXIDE
effects on spores of Clostridium botulinum, review of effects of chemicals on recovery from, 25:2599
ETHYLENE POLYMERS
gamma dose distribution in, measurement of absorbed, 25:2495
neutron dose distribution in, measurement of absorbed, 25:2494
polymerization with styrene, mechanism of graft, induced by 2,2'-azobis[2-methylpropionitrile] and benzoyl peroxide, 25:2241
radiation effects on crystals of, electron, 25:2234
radiation effects on stress-rupture stability of, by cross linking, electron, 25:2249
radioinduced chlorination of, kinetics of, 25:2250
radioinduced graft polymerization with styrene, effects of crystallinity, pre-irradiation, temperature, and thickness on γ, 25:2242
radioinduced graft polymerization with styrene, mechanism of γ, 25:2241
ETHYLENE, TETRAFLUORO-, POLYMERS
radiation effects on crystallinity of, effects of gaseous additives on γ, 25:2261 (NP-18518)
radiolysis of, effects of gases on yields from γ, 25:2261 (NP-18518)
EUMYCOTA
Neurospora crassa, radiosensitivity of photoreactivation defective mutants of, uv, 25:2556
yeasts, radioisotope uptake by cultured, use of autoradiography to determine, 25:2530
EUROPIUM
determination by voltammetry using lanthanum hexaboride electrode, 25:2092
determination in cerium dioxide by luminescence method, 25:2083
determination in yttrium vanadates, scanning method for improving accuracy of luminescence, 25:2086
determination of trace amounts of, in lanthanum oxide, neodymium oxide, and yttrium oxide by direct reading emission spectrometry, 25:2096
EUROPIUM ACETATES
stability of ions of, effects of inner sphere complexing on, 25:2208
EUROPIUM CHLORIDES
vaporization at 1240 to 1705°K, kinetics of, 25:2803(R) (COO-716-66)
EUROPIUM ISOTOPES Eu-151
alpha inelastic scattering at 5 to 12 MeV with Coulomb excitation, γ spectra from, (E), 25:3703
deuteron inelastic scattering at 12 MeV, angular distributions and cross section for, (E), 25:3653
energy levels and transitions from alpha and proton Coulomb excitation, (E), 25:3703
energy levels from deuteron inelastic scattering, (E), 25:3653
neutron capture by, conversion electron spectrum from thermal, (E), 25:3698
EUROPIUM ISOTOPES Eu-152
diffusion in copper at 700 to 1010°C, tracer studies of, 25:2680
energy levels from thermal neutron capture by europium-151, spin--parity assignments for, (E), 25:3698
energy-level transitions from thermal neutron capture by europium-151, multipolarities of, (E), 25:3698
EUROPIUM ISOTOPES Eu-153
alpha inelastic scattering at 5 to 12 MeV with Coulomb excitation, γ spectra from, (E), 25:3703
energy levels and transitions from alpha and proton Coulomb excitation, (E), 25:3703
nuclear magnetic moment of, effects of spin--orbit and spin--spin forces on, (T), 25:3692
EUROPIUM ISOTOPES Eu-154
beta decay of, gamma spectra from, (E/T), 25:3677
diffusion in copper at 700 to 1010°C, tracer studies of, 25:2680
EUROPIUM ISOTOPES Eu-155
half-life, (E), 25:3667
neutron capture in reactor, cross section for, (E), 25:3667
EVAPORATORS
corrosion by seawater, cathodic protection from, 25:2634
orifices in multistage flash, evaluation of brine-flow controlling variable, 25:2387 (ORNL-TM-2746)
EXPERIMENTAL BREEDER REACTOR-II
coolant for, review of chemistry of, 25:2600 (BNL-50258)
materials for, compatibility of high-temperature sodium coolant with, 25:2705
EXPONENTIAL PILES
physics measurements for water moderated enriched uranium fueled, (E/T), 25:3912
EYES
radiation hazards to retina of rabbit, during mode locking, laser, 25:2591

F

FALLOUT
monitoring in East German low-level atmosphere, following 7th and 8th Chinese nuclear explosions, 25:2370
monitoring in Moscow region during 1962 to 1966, 25:2550
monitoring of, operator manual for Weapons Effects Display System for, 25:2504 (UCRL-50892(Vol.2))
monitoring of, Weapons Effects Display System for, 25:2506 (UCRL-50922)
monitoring of, wiring tables for logic interfaces for Weapons Effects Display System for, 25:2505 (UCRL-50892(Vol.4)(Pt.5))
separation of tungsten from radioactive, method for, 25:2110
FAST TEST REACTOR
fuel element assemblies for, compression testing of Mark 1 and Mark 2, (E), 25:3908 (WHAN-FR-18)

FEDERAL REPUBLIC OF GERMANY
archaeological excavation sites in, radioactivity of soils and ground-level atmosphere at, (E), 25:2352
radiation protection programs for personnel at Karlsruhe Nuclear Research Center in, 25:2970(R) (KFK-1158)
FELDSPARS
age of Churchill Province, Canada, rubidium/strontium method for estimation of, 25:2353
FERMI POWER REACTOR, UNIT 2
design parameters of, revised and additional data on, 25:3842 (DOCKET-50341-21)
electrical systems for, additional data on, 25:3842 (DOCKET-50341-21)
operations aspects of, revised and additional data on, 25:3842 (DOCKET-50341-21)
radioactive waste handling systems for, additional data on, 25:3842 (DOCKET-50341-21)
FERMIONS
field theory of, chiral U(n) x U(n) transformations in, 25:3428
point transforms and hard-core system of, (T), 25:3005
Schroedinger equation for finite systems of, variational solution of, 25:3242
Schroedinger equation for finite systems of, variational solution of, 25:3241
spin of, physical bounds for components of statistical tensors for, (T), 25:3295 (TPJU-12/70)
FERMIUM ISOTOPES Fm-257
production at HFIR and TRU, 25:2294 (ORNL-4572, pp 109-34)
FERROMAGNETIC MATERIALS
magnon dispersion relations from neutron scattering in, corrections to, 25:3218
FILTERS
efficiency for separation of atomic size particles from gas streams, 25:2414 (AD-707709)
FISSION FRAGMENTS
angular distributions from neutron fission of thorium-232 at 0.95 to 2.3 MeV, channel analysis of, (E), 25:3680
mass identification of, time-of-flight detector for, 25:2469
tracks in topaz from, morphology of, 25:2351
FISSION PRODUCTS
determination of, paper chromatographic data for, 25:2075
distribution in graphite and pyrolytic carbon fuel particle coatings, 25:2797
encapsulation of, recovered from radioactive waste, 25:2316 (ORNL-4572, pp 98-108)
release from Dragon Reactor, post 20 MW run survey of, 25:3886 (DP-Report-571)
release from gas cooled thorium carbide (ThC_2)--uranium carbide (UC_2) coated particle fuel elements, (E/T), 25:3775 (DP-Report-539)
release from gas cooled thorium carbide (ThC_2)--uranium carbide (UC_2) coated particle fuel elements, 25:3796 (DP-Report-579)
release from pyrolytic carbon and silicon carbide coated fuel particles, (T), 25:3874 (DP-Report-595)
release in high temperature gas cooled reactor systems, 25:3774 (DP-Report-439)
release of gaseous, from high temperature gas cooled thorium carbide (ThC_2)--uranium carbide (UC_2), 25:3870 (DP-Report-497)
release of noble gas, by dynamic air--water systems following reactor coolant loss accidents, (E), 25:3892 (BNWL-SA-3360)
separation from MSBR fuels, 25:2313 (ORNL-4572, pp 1-36)
separation of iodine from, by surface ionization, 25:2342
separation of technetium from, by ion exchange and solvent extraction, 25:2307 (CEA-N-1316)
separation of volatile, from LMFBR fuels, 25:2314 (ORNL-4572, pp 37-84)
shipping of mixed, with transuranium elements, design of container for, 25:2421 (ORNL-TM-3110)
transport in aquatic molluscs and plants, quantitative model for, 25:2548
FISSIONABLE MATERIAL
analysis of, delayed neutron method for, 25:2418 (CONF-700322-, pp 357-78)
sintering of pellets of, design of furnace for, 25:2391(P)
FLOWMETERS
development of transit time, for liquid metals, 25:2500(R) (AI-AEC-12981)
FLUID FLOW
magnetohydrodynamic duct, nonisothermal, 25:2943
magnetohydrodynamic, mass exchange of cylinder in transverse magnetic field, (T), 25:2941
magnetohydrodynamic, perturbation of Stokes flow past hollow sphere, 25:2946
magnetohydrodynamic, problems in, (T), 25:2942
FLUIDIZED BEDS
characteristics for coating reactor fuel particles, gas pressure measurements for monitoring steady-state and transient, 25:2767 (DP-Report-378)
FLUORESCENCE
deuterium effects on intensity of, of indole derivatives, 25:2536
FLUORIDES
effects on uv spectrophotometric determination of gallium in aqueous solutions, 25:2100
FLUORINATION
equipment for molten salt, frozen-wall, 25:2313 (ORNL-4572, pp 1-36)
FLUORINE
determination in oceanographic samples by 14-MeV neutron activation and γ spectrometry, 25:2119 (CONF-700322-, pp 221-30)
separation by fixation on hydrated antimony pentoxide in hydrochloric acid, effects of acidity and time on, 25:2332
FLUORINE ISOTOPES F-17
energy level at 0.5 MeV from oxygen-16 (d,n) reactions, (E), 25:3586
FLUORINE ISOTOPES F-19
proton reactions at 24 to 46 MeV, total cross sections for, (E), 25:3568
FLUORINE ISOTOPES F-20
beta decay of, charge asymmetry of the internucleon potential in, (T), 25:3736
FLUORINE SYSTEMS
F--Mn--Xe, reactions in, compounds produced by, 25:2156
FOAMS
radiation effects on stability of, effects of electrolyte, surfactant, and temperature on α, 25:2223
FORESTS
radioisotope release to soil from organic debris in, as function of decomposition mode and time, 25:2528
release of inorganic elements to soil from organic debris in, as function of decomposition mode and time, 25:2528
FORMALDEHYDE
production from x-irradiated arginine and citrulline, 25:2588
FORMIC ACID, (PHENYLAZO)THIO-, 2-PHENYLHYDRAZIDE
mercury salt, deposition on plastic matrix for neutron activation analysis, 25:2146
FORT ST. VRAIN POWER REACTOR, UNIT 1
design parameters of, requested additional information on, 25:3833 (DOCKET-50267-23)
operations aspects of, requested additional information on, 25:3833 (DOCKET-50267-23)
site for, environmental survey during April to June 1970, 25:3833 (DOCKET-50267-23)
FRANCE
radioisotope monitoring of irrigation canals in Rhone-Languedoc region of, 25:2543
reactor fuel element handling and storage in, methods and regulations for irradiated, 25:2424
FREE RADICALS
radioinduced in hexachloroethane, effects of hydrogen atoms on site migration of electron, 25:2246
radioinduced in monoclinic crystals of sodium succinate, ESR studies on γ, 25:2229
radioinduced in triclinic crystals of sodium succinate, ESR studies on γ, 25:2230
spectra of, produced in γ-irradiated hydroxyurea crystals, 25:2219 (NP-18449)
FS-85 (NIOBIUM ALLOY)
corrosion by lithium at 1000 and 1400°F, effects of welding atmosphere purity on, 25:2625
FUEL CAPSULES
design, fabrication, and testing of spherical cobalt-60, for use in radiation processing, 25:2404
fabrication for curium-244 oxide fuels, method of, 25:2643 (ORNL-4570, pp 106-11)
FUELS
electric power generation from fossil, in US to 2000, predictions for, 25:2393
FUKUSHIMA POWER REACTOR, UNIT 1
construction of, review of, 25:3780
FUKUSHIMA POWER REACTOR, UNIT 2
construction of, review of, 25:3780
FUKUSHIMA POWER REACTOR, UNIT 3
construction of, review of, 25:3780
FUMARIC ACID
effects on mechanism of γ-radioinduced graft polymerization of poly(ethylene terephthalate), 25:2244
FURNACES
design for sintering fissionable material pellets, 25:2391(P)

G

GADOLINIUM
complexes with cupferron, separation by solvent extraction using 2-methyl-1-propanol and 3-methyl-1-butanol, 25:2078
determination in irradiated gadolinia--magnesia mixtures by titration using gadolinium-153 as internal indicator, 25:2089
determination in silicate rocks using cupferron, spectrographic, 25:2078
determination of trace amounts of, in lanthanum oxide, neodymium oxide, and yttrium oxide by direct reading emission spectrometry, 25:2096
photon reactions at 30 to 100 keV with, photoelectric cross sections for, 25:2907
separation from metals by precipitation using cupferron,

XUM

25:2078
GADOLINIUM ALLOYS AND SYSTEMS
Ce--Gd, phase studies at high temperatures, electron microscopic and x-ray, 25:2670 (ORNL-4570, pp 35-6)
GADOLINIUM ISOTOPES Gd-152
energy levels from terbium-152 decay, spin--parity assignments for, (E), 25:3681
energy-level transitions from terbium-152 decay, conversion coefficients and mixing and branching ratios for, (E), 25:3681
GADOLINIUM ISOTOPES Gd-154
energy-level transitions from europium-154 beta decay, reduced transition probabilities and band-mixing parameters for, (E/T), 25:3677
GADOLINIUM ISOTOPES Gd-155
energy levels from samarium-154 (α,3n) reactions, (E), 25:3700
nuclear magnetic moment of, effects of spin--orbit and spin--spin forces on, (T), 25:3692
GADOLINIUM ISOTOPES Gd-157
nuclear magnetic moment of, effects of spin--orbit and spin--spin forces on, (T), 25:3692
GADOLINIUM ISOTOPES Gd-158
energy-level transitions from octupole states in, branching ratios from E1, (T), 25:3751
GADOLINIUM OXIDES
Gd_2O_3--MgO, analysis of irradiated, for gadolinium by titration using gadolinium-153 as internal indicator, 25:2089
GALAXIES
electromagnetic-wave emission from normal, upper limits for, (T), 25:2868
evolution of, computer simulation of, (T), 25:2864
formation of clusters of, (T), 25:2876
luminosity of M31, (T), 25:2866
mass distribution in M31, model of, (T), 25:2866
spectra of 17 Markaryan, (E), 25:2865
GALENAS
age of Churchill Province, Canada, lead-204/lead-208 method for estimation of, 25:2353
GALLIUM
abundance in Kappa Cancri, (E), 25:2840
determination in aqueous solutions by reactions with ammonium 1-pyrrolidinecarbodithioate and uv spectrophotometry, effects of impurities on, 25:2100
effects on determination of trace amounts of antimony by isotopic exchange in organic phase, 25:2106
production of pure, review of techniques for, 25:3219
separation from nitrate and sulfate solutions by solvent extraction using amines, 25:2319 (ORNL-4572, pp 181-95)
superconducting condensation energy calculation, 25:3046
GALLIUM ALLOYS AND SYSTEMS
Ga--Hf--V, critical current density and defect structure in high-fluid superconducting intermetallic $(VHf)_3Ga$, (E), 25:3039
Ga--V, critical current density and defect structure in high-field superconducting intermetallic V_3Ga, (E), 25:3039
Ga--V--Zr, critical current density and defect structure in high-field superconducting intermetallic $(VZr)_3Ga$, (E), 25:3039
GALLIUM ISOTOPES Ga-63
beta decay of, half-life, gamma spectra, and log ft value of, (E), 25:3609
GALLIUM ISOTOPES Ga-65
energy levels from zinc-64 (d,n) reactions at 10 MeV, spin--parity assignments and spectroscopic strengths for, (E), 25:3625
GALLIUM ISOTOPES Ga-67
energy levels from zinc-66 (d,n) reactions at 10 MeV, spin--parity assignments and spectroscopic strengths for, (E), 25:3625
energy levels from zinc-67 (p,n) reactions, spins of, (E), 25:3596 (TID-25503)
GALLIUM ISOTOPES Ga-68
energy levels from zinc-68 (p,n) reactions, spins of, (E), 25:3596 (TID-25503)
GALLIUM ISOTOPES Ga-69
energy levels from zinc-68 (d,n) reactions at 10 MeV, spin--parity assignments and spectroscopic strengths for, (E), 25:3625
GALLIUM ISOTOPES Ga-71
energy levels from zinc-71g and -71m decay, spins and parities of, (E), 25:3638
GALLIUM ISOTOPES Ga-72
beta decay of, γ singles and coincidence and conversion electron spectra from, (E), 25:3639
GAMMA-ABSORPTION ANALYSIS
development for continual analyses, 25:2111
GAMMA RADIATION
detection at 30 keV to 1 MeV, response of unactivated sodium iodide detector for, 25:2436
diffraction of iron-57 14.4-keV, under Laue conditions, suppressed absorption by resonant nuclei in, (E), 25:3225
dose conversion coefficients for Lucite and polystyrene, 25:2569
dose distribution in polyethylene, 25:2495
dose from plane γ sources, nomograms for calculation of absorbed, 25:2566
dose from plane γ sources, universal nomograms for calculating absorbed, 25:2566
dose rate distribution in hematite and ordinary concrete, measurement of, 25:3480
dose rate distributions in laminated iron/water shielding, (E/T), 25:3174
dose to human tissues from fallout in Moscow region during 1962 to 1966, 25:2550
effects on 5-methylhydrouracil monocrystals, 25:2282
effects on acetonitrile, 25:2271
effects on aleurone pigmenting potential in maize in comparison to effects of diethyl sulfate, 25:2560
effects on ammonia, effects of dose, pressure, and temperature on, 25:2283
effects on aqueous chloride solutions of deoxynucleotides, purines, and pyrimidines, 25:2259 (GA-10208)
effects on aqueous solutions of erythrocytes, glucose, and sodium salt of DNA, 25:2285
effects on aqueous solutions of nitric acid, 25:2284
effects on aqueous solutions of nitric and sulfuric acids, 25:2277
effects on aqueous sulfuric acid solutions, yields of hydrogen peroxide and persulfate from, 25:2265
effects on calomel, fluoride specific, glass, and nitrate specific electrodes, 25:2231
effects on carbon monoxide in presence of γ-alumina, 25:2262 (RD/B/N-1279)
effects on carbon monoxide, inert gas, or methane, apparatus for studying deposition of carbon from, 25:2263 (RD/B/N-1748)
effects on chrysoidine adsorbed on surface of aluminum--aluminum oxide system, energy transfer during, 25:2276
effects on coatings in air and water, 25:2821 (ORNL-4572, pp 258-61)
effects on crystalline lead nitrates, kinetics of annealing of damage from, 25:2236
effects on crystallinity of poly(tetrafluoroethylene), effects of gaseous additives on, 25:2261 (NP-18518)
effects on cyclohexane, yields of cyclohexyl radicals from, 25:2268
effects on electric conductivity of solid monomers at -196°C, 25:2221
effects on erythrocytes infected with Babesia rodhaini, use for protective immunization of mice and rats, 25:2539
effects on frozen aqueous solutions of alcohols, effects of acids on hydrogen abstraction following, 25:2293
effects on frozen solutions of glucose and sucrose at 77°K, ESR spectral studies on radical processes produced by, 25:2279
effects on gaseous alkenes, isomerization of butyl and propyl ions from, 25:2290
effects on graft polymerization of cellulose with styrene in methanol solutions, effects of additives on, 25:2247
effects on graft polymerization of poly(ethylene terephthalate) with acrylamide or methacrylamide, effects of dicarboxylic acids on, 25:2244
effects on graft polymerization of polyethylene terephthalate with acrylic acid or methacrylic acid, effects of dose and temperature on mechanism of, 25:2240
effects on graft polymerization of polyethylene with styrene, effects of crystallinity, pre-irradiation, temperature and thickness on, 25:2242
effects on graft polymerization of polyethylene with styrene, 25:2241
effects on growth of barley spikes, protective effects of plant hormones against, 25:2597
effects on hydroxyurea crystals, relative signs of proton coupling tensor of free radical from, 25:2219 (NP-18449)
effects on induction of arylation of nitrobenzene, effects of diphenylpicrylhydrazyl on, 25:2255
effects on insulating materials at 1.3 MeV, 25:2819 (LCIE-342)
effects on iodomethane in air at 15°C, 25:2269
effects on liquid cyclohexane, 25:2281
effects on mixtures of octane with benzene, 1,3-cyclooctadiene, or cyclooctatetraene, kinetics of production of ethane, hydrogen, and methane from, 25:2270
effects on monoclinic crystals of sodium succinate, ESR studies on free radicals produced from, 25:2229
effects on physicomechanical properties of lacquer coatings, 25:2822
effects on polarization in ferroelectric and nonferroelectric Rochelle salt, 25:3221
effects on poly(ethylene terephthalate), hydrogen yields from, 25:2244
effects on poly(tetrafluoroethylene), effects of gases on yields from, 25:2261 (NP-18518)
effects on polycrystalline heptane, thermoluminescence studies on, 25:2291
effects on polymerization of styrene, effects of temperature on, 25:2245
effects on polymerization of trioxane, effects of impurities on, 25:2253
effects on potassium and sodium salts, luminescence from aqueous release of stored energy produced by, 25:2227
effects on properties and structure of poly(vinyl

alcohol), ir spectral studies on, 25:2220
effects on purification of water for use in radiation chemistry, 25:2228
effects on seeds of bean and clover, effects of, on enzyme activity in sprouts, 25:2596
effects on sodium nitrite single crystals, free radicals induced in, 25:3191
effects on spores of Clostridium botulinum, review of effects of chemicals on recovery from, 25:2599
effects on stability of hydrogen atoms in clinoptilolites containing lanthanum, magnesium, or potassium ions at 400 to 700°C, EPR spectral studies on, 25:2224
effects on structure of amine-reinforced ED-5-type resins, 25:2273
effects on thermal decomposition of polyhexanamide, mass spectrometric studies on, 25:2288
effects on thermally stimulated conductivity in alkali metal halide single crystals, 25:3202
effects on triclinic crystals of sodium succinate, ESR studies on free radicals produced from, 25:2230
effects on voltage-current characteristic of silicon carbide diodes, 25:3192
effects on water, 25:2267
effects on water, effects of oxygen, potassium nitrate, and sodium formate on, 25:2257 (CEA-R-4046)
energy absorption rates in iron/lead laminated shielding, (T), 25:3169
energy distribution of singly and multiply scattered, (E), 25:3182
energy spectra of, determination of, 25:3183
reactions with alloys at 100 to 662 keV, effective atomic numbers for photoelectric, scattering, and total interaction processes in, 25:2906
reactions with atoms, ratios of total to subshell pnotoelectric cross sections for, 25:2908
reactions with copper, platinum, and silver at 50 to 412 keV, total photoelectric cross sections for, 25:2905
reactions with gadolinium, hafnium, lanthanum, and thorium at 30 to 100 keV, photoelectric cross sections for, 25:2907
reactions with palladium and tantalum at 662 keV, photoelectric cross sections for, (E), 25:2904
scattering by electron in metals, incoherent cross sections for 30-keV to 2.62-MeV, (T), 25:2921
scattering by K electrons at 280 to 1002 keV, integrated cross sections for incoherent, 25:2909
scattering by nuclei, analysis of elastic and inelastic, (T), 25:3655
scattering by shielding, spectral and angular-distribution function for, 25:3168
scattering by tin at 1.33 MeV, cross section for elastic, (E), 25:3655
shielding by high-density barite and iron-bearing concretes at 0.3 to 10 MeV, 25:3172
spectra from thermal neutron capture by shielding materials, (E), 25:3181

GAMMA SOURCES
dose rates from, in complex cylindrical irradiators, method for calculation of, 25:2403
photopeak count-rates from thermal neutron-activated, in scintillation and semiconductor detectors, 25:2474 (IAEA-122, pp 150-63)
preparation of high-energy, using transuranium elements, 25:2294 (ORNL-4572, pp 109-34)

GAMMA SPECTROMETERS
data processing system for scintillation, computer, 25:2477
photopeak count-rates from gamma sources formed by thermal neutron activation, tables of calculated, 25:2474 (IAEA-122, pp 150-63)

GAMMA SPECTROSCOPY
peak separation in, method for overlapping decaying, 25:2482

GAS CENTRIFUGES
evaluation for uranium enrichment in France, 25:2402

GAS FLOW
magnetohydrodynamic, breakaway parameter of turbulent boundary layer, (T), 25:2947

GASEOUS DIFFUSION PROCESS
evaluation for uranium enrichment in France, 25:2402

GASES
excitations at finite temperatures in Bose, shielded potential in Hartree approximation, 25:3044
kinetic equations for autocorrelation functions for, 25:3099
properties at high temperatures, bibliography on, 25:2665 (NBS-SPEC. PUBL-315-5)
radon-220/radon-222 ratio in soil, closed circuit method for measurement of, 25:2378
transport coefficients in relativistic quantum, (T), 25:2873
transport phenomena in, bibliography for 1969 on, 25:2901 (ORNL-AMPIC-13)

GEOMAGNETIC FIELDS
activity index of, correlation with outer-zone E greater than or equal to 150 keV electron intensity, (E), 25:2969
activity indexes of, solar effects on, Jan. 1, 1955 to Dec. 31, 1969, (E), 25:2858 (N-70-32003)
boundary of magnetospheric, geographic longitude-dependent, (E/T), 25:2980
disturbances of, effects of interplanetary magnetic field polarity on, (E), 25:2860
effect on longitudinal distribution of mean annual F2-layer ionization, (E/T), 25:2985
effects on auroral hydrogen emission intensity and visible aurorae positions, 1959 to 1966, (E), 25:2976
effects on plasma scale height in outer F2 layer, (E), 25:2973
intensity variations in, magnetopause current system production of, (E/T), 25:2955
parameters of, relation to ionospheric sporadic-E layer, 1964 to 1966, (E), 25:2995
pulsations in, accompanying pulsating aurorae at conjugate points, (E), 25:2999
pulsations in, classification of short-period, (E), 25:3000
relation of K/sub p/ index to interplanetary magnetic field flux, (E/T), 25:2981

GEOPHYSICS
activation analysis in, Brno, Czechoslovakia, 25:2131

GERMANIUM
effects on determination of trace amounts of antimony by isotopic exchange in organic phase, 25:2106
production of pure, review of techniques for, 25:3219
radioinduced defects in antimony-doped n-type, model of 30 and 77°K electron-, 25:3200
separation from nitrate and sulfate solutions by solvent extraction using amines, 25:2319 (ORNL-4572, pp 181-95)

GERMANIUM ALLOYS AND SYSTEMS
Ge--Ti--V-base, creep to 850°C, 25:2662 (KFK-1193)

GERMANIUM ISOTOPES Ge-72
energy levels from arsenic-72 and gallium-72 decays, (E), 25:3639

GERMANIUM ISOTOPES Ge-74
energy levels from arsenic-74 decay, spin-parity assignments for, (E), 25:3704

GLASS
corrosion of Pyrex and Vycor, by selenium at 300 to 700°C, 25:2629
radioinduced crystallization of amorphous, effects of annealing on 50-keV argon, boron, or phosphorus ion, 25:2823

GLUCOSE
radiolysis of aqueous solutions of, ultrasonic absorption studies on γ, 25:2285
radiolysis of crystals of, ESR studies on free radicals from x, 25:2286
radiolysis of frozen solutions of, at 77°K, ESR spectral studies on radical processes produced by γ, 25:2279

GLUCOSE 6-PHOSPHATE DEHYDROGENASE
radiation effects on stability of, in human carcinoma cell cultures, x, 25:2585

GLUCURONIC ACID
radiolysis of crystals of, ESR studies on free radicals from x, 25:2286

GLYCEROL
glycerol--H_2O, proton polarization measurements at high magnetic fields and low temperatures in porphyrexide-doped, 25:3500

GOLD
corrosion by selenium at 300 to 700°C, 25:2629
determination in biological materials by 14-MeV neutron and thermal neutron activation, sensitivity of, 25:2125 (IAEA-122, pp 27-36)
determination in pigments from ancient murals by neutron activation, 25:2133
effects on uv spectrophotometric determination of gallium in aqueous solutions, 25:2100
electron backscattering at 1 MeV, angular distribution and energy spectra for, 25:2886
electron reactions at 1 to 3 MeV with, backscatter and transmission coefficients for, (E), 25:2883 (N-70-25499)
microstructure of deposited layers of, electron microscopic study of, 25:2748
radioinduced imperfection clusters in foils of, xenon-ion-, (E), 25:3189(R) (COO-1053-14)
separation from nitrate and sulfate solutions by solvent extraction using amines, 25:2319 (ORNL-4572, pp 181-95)

GOLD ALLOYS AND SYSTEMS
Au--Cu, crystal orientation in rolled intermetallic Cu_3Au specimens, 25:2728 (ORNL-4570, pp 5-9)
Au--Cu, electron reactions at 1 to 3 MeV with, backscatter and transmission coefficients for, (E), 25:2883 (N-70-25499)

GOLD ISOTOPES Au-192
beta and electron-capture decay of, γ spectra from, (E), 25:3654

GOLD ISOTOPES Au-197
alpha fission at 103 MeV, cross sections and fragment angular distributions for, (E), 25:3710
energy-level transitions from mercury-197 decay, multipolarities of, (E), 25:3682
neutron reactions (n,2n) below (n,3n) threshold, cross-section calculations using Hauser--Feshback theory, (T), 25:3591 (AAEC/TM-542)

GRAPHITE
analysis for chlorine and vanadium by neutron activation and gamma spectroscopy, 25:2142
coating with boron and boron carbide at 1300°C, vapor

XUM

deposition method for, 25:2777
corrosion by selenium at 300 to 700°C, 25:2629
corrosion of, effects of high temperature helium cooled reactor environment on, 25:3860 (DP-Report-491)
crystallographic ordering in, neutron inelastic scattering studies of, 25:2810
design of shapes of, for nuclear uses, abstracts on continuum aspects of, 25:2793 (ORNL-TM-3191)
fission product distribution in fuel particle coating of, 25:2797
ion reactions at 5 to 50 keV with reactor-grade, apparent total ion scattering, secondary electron emission coefficients, and electron and ion energy distributions for, (E), 25:2884 (NP-18490)
mechanical properties of, 25:3774 (DP-Report-439)
mechanical properties of gas cooled reactor fuel element coatings of, calculation of operating limits from, 25:3875 (EURFNR-834)
neutron attenuation by, monoenergetic-source, (E/T), 25:3173
neutron scattering properties of, 25:3904 (IJS-571)
preparation of impermeable, method for, 25:2609 (ORNL-4570, pp 175-90)
properties for use in breeder reactors, research on, 25:2609 (ORNL-4570, pp 175-90)
properties of, abstracts on, 25:2793 (ORNL-TM-3191)
radiation effects on highly oriented, neutron, 25:2730 (ORNL-4570, pp 44-6)
radiation effects on microstructure of, neutron, 25:2609 (ORNL-4570, pp 175-90)
radiation effects on, comparison dose scale for fast neutron, 25:3872 (DP-Report-559)
structure of, variational calculation of electronic, 25:2671 (ORNL-4570, pp 40-3)
thermal conductivity at 30 to 120°C, effects of crystal orientation on, 25:2677 (ORNL-4570, pp 224-7)
use of highly oriented, for high-energy photon polarization, (E), 25:3257
x-ray diffraction from highly oriented, 25:2730 (ORNL-4570, pp 44-6)

GRAPHITE COUPLES
cold welding under static loads, 25:2677 (ORNL-4570, pp 224-7)

GRAVITATION
field equations in, nonstatic case in exact solutions of, 25:3448
field from neutrino in vacuum, constants for, (T), 25:3343
relativistic generalized theory of, (T), 25:2870

GRAVITATIONAL FIELDS
light wave propagation in, theorem for quadrupole-lens system defocusing for, 25:3450
solution for stationary axially symmetric, internal, (T), 25:2828
symmetry of, Tolman equality for spherical, (T), 25:3447 (IFVE-SEF-69-59)

GRAVITATIONAL RADIATION
pressure in Friedman--Lobachevshi space, 25:3449
radio-wave emission in association with, (T), 25:2849
wave fronts in, method for calculating, (T), 25:2877

GRAVITY WAVES
propagation of traveling, effect on plasma drift inhomogeneities in ionospheric F2 layer of, (E/T), 25:2986

GRENOBLE REACTORS (SILOE)
radiation target cans for, design parameters of natural convection cooled Esther, 25:3903 (CEA-N-1348)

GROUND WATERS
age of, review of principles of nuclear methods for estimation of, 25:2360
flow into underground cavities on Amchitka Island, Alaska, effects of hydraulic gradient on, 25:2349 (USGS-474-72)
radioisotope transport in, 25:2541
uranium-234/-238 ratio in USSR, alpha spectrometric method for measurement of, 25:2356

GROUP THEORY
representations of quaternion group in, realization of, 25:3420 (IFVE-STF-69-102)

GUANINE
radiolysis of aqueous chloride solutions of, rate constants for electron pulse and γ, 25:2259 (GA-10208)

GUANOSINE MONOPHOSPHATES
radiolysis of aqueous chloride solutions of, rate constants for electron pulse and γ, 25:2259 (GA-10208)

GYMNOSPERMIDAE
Pinus pinea, radioinduced chromosome aberrations in dormant seeds of, x, 25:2555

H

H.B. ROBINSON POWER REACTOR, UNIT 2
personnel for, request for respiratory protective equipment for, 25:3828 (DOCKET-50261-46)

HADRONS
interactions at high energies, inelastic processes and backward scattering in model for multiple, (T), 25:3352 (IRB-TP-2-70)
interactions of, geometrical and Regge pictures for elastic, 25:3354
interactions of, thermodynamic model of strong, 25:3355
interactions with deuterons at high energies, Glauber shadow correction for calculation of cross-section defect in, (T), 25:3412
interactions with hadrons, book on review of total cross sections of, (E), 25:3268
interactions with leptons, Veneziano model for current amplitudes of, (T), 25:3342

HAFNIUM
determination in aluminum--uranium alloys, spectrographic, 25:2063 (CNEA-276)
determination in geological specimens using 8-hydroxy-7-[(2-hydroxy-3,5-dinitrophenyl)-azo]-1,6-naphthalenedisulfonic acid, photometric, 25:2084
determination in meteorites and terrestrial materials by neutron activation and radiochemical separation, 25:2148
determination in minerals and rocks by neutron activation and γ spectrometry, 25:2139
determination in uranium alloys by atomic absorption spectrophotometry, 25:2065 (LA-4529)
photon reactions at 30 to 100 keV with, photoelectric cross sections for, 25:2907

HAFNIUM ALLOYS AND SYSTEMS
Ga--Hf--V, critical current density and defect structure in high-fluid superconducting intermetallic $(VHf)_3Ga$, (E), 25:3039
Hf--Nb, phase studies of, 25:2668 (ORNL-4570, pp 10-12)
Hf--Ta, hardness of, effects of aging on, 25:2672 (ORNL-4570, pp 112-15)
Hf--Ta, phase studies of, 25:2668 (ORNL-4570, pp 10-12)
Hf-base--Nb, phase studies of, 25:2735
Hf-base--Zr, crystal structure of α, at 23 to 1600°C, 25:2751
Hf-base--Zr, thermal expansion of α, at 23 to 1600°C, 25:2751

HAFNIUM ISOTOPES Hf-169
beta and electron-capture decay of, half-life for, (E), 25:3676

HAFNIUM ISOTOPES Hf-177
energy levels at 113 and 321 keV, lifetimes of, (E), 25:3707
energy-level transitions from lutetium-177 beta decay, correlation coefficients, multipole mixing ratios, partial widths, and hindrance factors for, (E), 25:3684

HAFNIUM OXIDES
Er_2O_3--HfO_2, phase studies, 25:3978(T) (SC-T-70-4043)
Er_2O_3--HfO_2, phase studies of, 25:2804 (IS-T-401)
HfO_2--Ho_2O_3--ZrO_2, crystal structure of $Ho_2O_3 \cdot 2ZrO_2(HfO_2)$ phase in, 25:2807(T) (SC-T-70-4039)

HAFNIUM SILICATES
preparation of high-purity and rare earth-doped monocrystalline, 25:2727 (ORNL-4570, pp 1-4)

HANDBOOKS AND MANUALS
on standard procedures for health and safety laboratory, 25:2059 (NYO-4700(3rd Ed.))

HANFORD PRODUCTION REACTORS
process tubes for K, inspection and testing of Zircaloy, 25:3921 (DUN-SA-144)

HANFORD PRODUCTION REACTORS (N)
process tubes for, inspection and testing of Zircaloy, 25:3921 (DUN-SA-144)
radioactive wastes from, disposal and processing methods for, 25:2426
simulator for, operation and programming procedures for hybrid computer, 25:3920 (BNWL-B-8)

HASTELLOY B
corrosion by selenium at 300 to 700°C, 25:2629

HASTELLOY C
compatibility with strontium titanate at 900 to 1100°C, 25:2643 (ORNL-4570, pp 106-11)
corrosion by selenium at 300 to 700°C, 25:2629

HASTELLOY F
corrosion by selenium at 300 to 700°C, 25:2629

HASTELLOY N
corrosion by sodium fluoride--sodium fluoroborate mixtures at 605°C, 25:2609 (ORNL-4570, pp 175-90)
corrosion by steam at 538°C, 25:2609 (ORNL-4570, pp 175-90)
corrosion of maraging, by MSRE coolant at 663°C, 25:2609 (ORNL-4570, pp 175-90)
deformation and fracture at high temperatures, effects of titanium additions on, 25:2674 (ORNL-4570, pp 136-42)
deformation and fracture behavior of, effects of titanium on high-temperature, 25:2725
evaporation rate at 1050°C and 10^{-9} torr, 25:2643 (ORNL-4570, pp 106-11)
mechanical properties of titanium-modified, 25:2609 (ORNL-4570, pp 175-90)
microstructure of, electron microscopy studies of, 25:2674 (ORNL-4570, pp 136-42)
performance in MSRE, 25:2609 (ORNL-4570, pp 175-90)
radiation effects on creep of, relations of temperature with neutron, 25:2674 (ORNL-4570, pp 136-42)
radiation effects on creep rupture of modified, relations of hafnium, niobium, or titanium additions with neutron, 25:2674 (ORNL-4570, pp 136-42)
stresses in welded, method for measuring residual, 25:2410 (ORNL-TM-3113)

HASTELLOY X
corrosion of similar metal welds of, by steam at 1100 to

1200°F, 25:2636
corrosion of similar metal welds of, by steam at 595 to 650°C, 25:2608 (ORNL-4570, pp 124-6)
welding to Incoloy 800 using Hastelloy X filler metal, corrosion by steam at 1100 to 1200°F of welds produced by, 25:2636
HAYNES 25 ALLOY
compatibility with strontium titanate at 900 to 1100°C, 25:2643 (ORNL-4570, pp 106-11)
HAYNES 188 ALLOY
evaporation rate at 1050°C and 10^{-9} torr, 25:2643 (ORNL-4570, pp 106-11)
HEAT
effects on spores of Clostridium botulinum, review of effects of chemicals on recovery from, 25:2599
HEAT-RESISTING ALLOYS AND METALS
corrosion by alkali metals in space power systems, research program on, 25:2607 (ORNL-4570, pp 103-5)
machining of, shear spinning method for automatic, 25:2650
HEAT TRANSFER
burnout in fuel rod clusters, equations for calculation of, 25:3880
HEAT TRANSFER SYSTEMS
protection of seawater-cooled, methods for cathodic, 25:2634
HELIUM
abundance in Kappa Cancri, (E), 25:2840
abundance in main-sequence B-Type stars, (E), 25:2839
analysis for hydrogen and water, pressurized electrolytic hygrometer for, 25:3882 (DP-Report-487)
effects of preinjected, on void formation in neutron irradiated Type 304 stainless steel, 25:2761
electric discharges in, excitation of ionized states in, (E), 25:2890
energy of, calculation using Euler transforms of Slater and Gaussian 1s functions, 25:2928
plasma jets of, use for detection of hydrocarbon deposits, (T), 25:3098
plasma of, electrostatic lf oscillations in inhomogeneous magnetized, (E/T), 25:3163
properties for use as protective atmosphere for niobium and tantalum at high temperatures, 25:2639(T) (LIB/Trans-309)
proton reactions at 1 to 100 keV with, cross sections for charge exchange into excited and ground states in, (T), 25:2919
radiation effects on, containing gaseous impurities, x, 25:2258 (DP-Report-447)
Stark effect in, use in plasma diagnostics of high-frequency, 25:3062
CO_2--He, radiolysis of, carbon-14 tracer study of x, 25:2258 (DP-Report-447)
HELIUM IONS
diffusion coefficients of He^+, in ionospheric F2 layer, (T), 25:2962
effects on liquid cyclohexane at 1.53 to 58 MeV, 25:2281
reactions in lithium-drifted silicon detectors at 15 to 80 MeV, effects on pulse-height distributions of, 25:2451
reactions with graphite and metal surfaces at 5 to 50 keV, apparent total ion scattering, secondary electron emission coefficients, and electron and ion energy distributions for, (E), 25:2884 (NP-18490)
spectra of, fine structure of 4686-Å line of, (E), 25:2890
HELIUM ISOTOPES He-3
deuteron reactions (d,tp) at 20.7 MeV, p-p and p-t final-state interactions in, (E), 25:3552
nuclear ordering in solid, use of compressional cooling in studies of, 25:4005 (UCSD-34-P-143-23)
parameters of liquid, using point transforms and hard-core Fermi system, (T), 25:3005
proton elastic scattering at 30 and 50 MeV, differential cross sections and polarizations of, (E), 25:3556
proton reactions (p,d) at 30.5 and 49.5 MeV, angular distributions from, (E/T), 25:3555
reactions (He-3, Be-7) with carbon-12, strong-absorption model analysis of angular distributions from, (E/T), 25:3583
reactions (He-3, Li-6) and (He-3, Be-7) with oxygen-16, strong-absorption model analysis of angular distributions from, (E/T), 25:3583
reactions (He-3,α) with magnesium-24 and silicon-28 and -30 at 18 to 20 MeV, j dependence of l = 2 angular distributions from, (E), 25:3637
reactions (He-3,α) with nitrogen-14 at 2.5 to 8.5 MeV, differential cross sections for, (E), 25:3590
reactions (He-3,α) with silicon-28 and sulfur-32 at 7.6 to 20 MeV, α angular distributions from, (E), 25:3594 (NP-18464)
reactions (He-3,d) with argon-40 at 10 MeV, deuteron spectra from, (E), 25:3632
reactions (He-3,d) with molybdenum-92, -94, -96, and -98 and zirconium-90, -92, and -94 at 24 MeV, energy spectra at 30° and cross sections for analog states from, (E), 25:3666
reactions (He-3,d) with potassium-39 and -41 at 11.0 MeV, angular distributions for, (E), 25:3627
reactions (He-3,d) with ruthenium-104 at 18 MeV, angular distributions for, (E), 25:3701
reactions (He-3,p) with calcium-40, -42, -43, -44, and -48 at 15 and 18 MeV, angular distributions and Q-values for, (E), 25:3629
reactions (He-3,p) with carbon-12 at 2.4 to 3.6 MeV, proton polarization in, (E), 25:3563 (JINR-P15-5156)
reactions (He-3,p) with deuterium at 350 keV, educational experiments utilizing, 25:3543 (CONF-700322-, pp 95-104)
reactions (He-3,p) with silicon-28 at 4.3 to 11.0 MeV, angular distributions for, (E), 25:3602
reactions with deuterium in plasma admixtures, 25:3140
scattering by nitrogen-14 at 4.5 and 7.0 MeV, differential cross sections for elastic, (E), 25:3590
scattering by potassium-39 at 11.0 MeV, angular distributions for elastic, (E), 25:3627
scattering elastically by A = 12 to 207 nuclei, analysis using optical potential, (T), 25:3769
solubility in helium-4 under pressure and low-temperature densities of, (E), 25:3011
spin--lattice relaxation of liquid, 25:3051
superfluidity of, possibility of, (T), 25:3017
He-3--He-4, molar volumes and dielectric constants down to 50 mK and pressures of 22 atm, (E), 25:3011
He-3--He-4, sound transformation in superfluid, first(second)-into-fourth, (T), 25:3007
He-3--He-4, spin--lattice relaxation of liquid mixtures of, 25:3051
He-3--He-4, superflow stability and ion mobility in mixtures of, (T), 25:3012
He-3--He-4, tricritical point in phase diagram of, high-temperature series expansion of Griffiths' lattice model of, 25:3015
He-3--He-4-base, viscosity--density product near lambda point, (E), 25:3016
HELIUM ISOTOPES He-4
alpha elastic scattering by, analysis using separable nonlocal potential, (T), 25:3544 (LYCEN-7041)
binding energy of, calculation using Brueckner reaction matrix and Tabakin potential, (T), 25:3548
energy levels of, ground-state, (T), 25:3013
energy levels of, Hartree--Fock calculations for, (T), 25:3545 (LYCEN-7047)
equations of motion of complex order parameter of liquid II, 25:3014
helium-3 solubility in, under pressure, (E), 25:3011
neutron scattering by liquid, interference and temperature effects in high-energy, (T), 25:3049
properties of liquid and phenomenological ^4He--^4He potential, 25:3009
proton elastic scattering at 3.38 and 7.80 MeV, polarization analyzing power and phase-shift analysis for, (E), 25:3557
proton reactions (p,d) and (p,t) at 49.5 MeV, angular distributions from, (E/T), 25:3555
proton reactions (p,He-3) at 49.5 MeV, angular distributions from, (E/T), 25:3555
sound transformation in superfluid, first(second)-into-fourth, (T), 25:3007
structure factors for gas and liquid, from x-ray scattering, 25:3018
superfluid, temperature variations produced by heat currents in, (T), 25:3006
surface layer thickness of liquid, (T), 25:3008
surface tension of liquid, 25:3010
viscosity--density product near lambda point, (E), 25:3016
He-3--He-4, molar volumes and dielectric constants down to 50 mK and pressures of 22 atm, (E), 25:3011
He-3--He-4, sound transformation in superfluid, first(second)-into-fourth, (T), 25:3007
He-3--He-4, spin--lattice relaxation of liquid mixtures of, 25:3051
He-3--He-4, superflow stability and ion mobility in mixtures of, (T), 25:3012
He-3--He-4, tricritical point in phase diagram of, high-temperature series expansion of Griffiths' lattice model of, 25:3015
He-3--He-4-base, viscosity--density product near lambda point, (E), 25:3016
HEPTANE
determination in products from radiolysis of gaseous ethylene, gas chromatographic method for, 25:2278
radiolysis of polycrystalline, thermoluminescence studies on γ, 25:2291
1-HEPTENE
determination in products from radiolysis of gaseous ethylene, gas chromatographic method for, 25:2278
1,5-HEXADIENE
Cope rearrangement of, effects of deuterium on, 25:2188
HEXAMETHYLENETETRAMINE
radiation effects on defects in, thermoluminescence glow peaks from x, 25:2235
HEXANAMIDE
polymers, radiation effects on thermal decomposition of, mass spectrometric studies on γ, 25:2288
HEXANE
determination in products from radiolysis of gaseous ethylene, gas chromatographic method for, 25:2278
radiolysis of gaseous, isomerization of butyl ions in γ, 25:2290
1-HEXANOL, 2-ETHYL-
recycle in thorium dioxide--uranium dioxide microsphere-

XUM

forming column, 25:2773 (ORNL-4572, pp 135-48)
1-HEXENE
determination in products from radiolysis of gaseous ethylene, gas chromatographic method for, 25:2278
2-HEXENE
determination in products from radiolysis of gaseous ethylene, gas chromatographic method for, 25:2278
HIGH-TEMPERATURE GAS-COOLED REACTOR EXPERIMENT
control elements of, effects of operating conditions on seizure of, (E), 25:3858 (DP-Report-486)
coolant circulator for, replacement of gas bearing, 25:3863 (DP-Report-554)
coolant losses during first core operation, 25:3861 (DP-Report-552)
coolant of, characteristics of carbon dioxide, 25:3774 (DP-Report-439)
cooling system for, impurity removal during hot testing of, 25:3862 (DP-Report-553)
cooling system of, fission product activity during first charge operation in primary, 25:3796 (DP-Report-579)
core components for, corrosion of graphite, 25:3860 (DP-Report-491)
core components of, development of graphite, 25:3774 (DP-Report-439)
data acquisition system for, 25:3795 (DP-Report-561)
fission product distribution in, post 20 MW run survey of, 25:3886 (DP-Report-571)
fuel cycle for, effects of fuel element heterogeneity on, 25:3868 (DP-Report-477)
fuel cycle management for on-load refueled, calculation of optimum thorium, 25:3873 (DP-Report-573)
fuel element cycle management for, calculation of optimum, 25:3869 (DP-Report-478)
fuel elements for, burnup measurements for first charge, (E/T), 25:3871 (DP-Report-538)
fuel elements for, calculation of fission product release from pyrolytic carbon and silicon carbide coated particle, (T), 25:3874 (DP-Report-595)
fuel elements for, measurement of gaseous fission product release of 20 MW operation of thorium carbide (ThC_2)--uranium carbide (UC_2), 25:3870 (DP-Report-497)
fuel elements of, burnup and fission product release of first charge, 25:3796 (DP-Report-579)
fuel elements of, development of coated particle, 25:3774 (DP-Report-439)
fuel elements of, fission product release from thorium carbide (ThC_2)--uranium carbide (UC_2) coated particle, (E/T), 25:3775 (DP-Report-539)
heat exchangers for, plugging of leaking tubes in, 25:3890(R) (DP-Report-592)
heat exchangers for, replacement of tube bundle in, 25:3863 (DP-Report-554)
heat exchangers for, tube leakage in primary, 25:3889(R) (DP-Report-582)
heat exchangers for, water catch-pot effects on pressure drop in, (E), 25:3897 (DP-Report-591)
loading machine for, design of, 25:2385 (DP-Report-230)
maintenance during December 1965 to February 1966, 25:3790(R) (DP-Report-438)
maintenance during December 1966 to February 1967, 25:3889(R) (DP-Report-582)
maintenance during June to August 1966, 25:3793(R) (DP-Report-488)
maintenance during March to May 1966, 25:3792(R) (DP-Report-483)
maintenance during March to May 1967, 25:3890(R) (DP-Report-592)
maintenance during September to November 1966, 25:3794(R) (DP-Report-531)
maintenance requirements during full power operation, 25:3791 (DP-Report-474)
moderator for, comparison fast neutron dose scale for radiation effects on graphite, 25:3872 (DP-Report-559)
operation of, recorded data for Charge I, 25:3795 (DP-Report-561)
operations during December 1965 to February 1966, 25:3790(R) (DP-Report-438)
operations during June to August 1966, 25:3793(R) (DP-Report-488)
operations during March to May 1966, 25:3792(R) (DP-Report-483)
operations during September to November 1966, 25:3794(R) (DP-Report-531)
operations for, review of full power, 25:3791 (DP-Report-474)
operations summary for December 1966 to February 1967, 25:3889(R) (DP-Report-582)
operations summary for March to May 1967, 25:3890(R) (DP-Report-592)
performance during first core operation, thermal, (E), 25:3885 (DP-Report-546)
HOLMIUM ALLOYS AND SYSTEMS
Ho--Tb, magnetic properties of monocrystalline, 25:2671 (ORNL-4570, pp 40-3)
Ho--Tb-base, magnetic anisotropy of, inelastic neutron scattering study of, 25:3208
HOLMIUM ISOTOPES Ho-164
energy levels from holmium-165 (d,t) reactions, spins and parities of two-quasiparticle, (E), 25:3711
HOLMIUM ISOTOPES Ho-165
deuteron reactions (d,t) at 12 MeV, angular distributions for, (E), 25:3711
neutron capture by, thermal, (E), 25:3691
nuclear magnetic moment of, effects of spin--orbit and spin--spin forces on, (T), 25:3692
HOLMIUM ISOTOPES Ho-166
beta decay of, hindrance factors for unique first-forbidden, (E), 25:3672
energy levels from thermal neutron capture by holmium-165, spin--parity assignments for, (E), 25:3691
HOLMIUM OXIDES
properties of mixed, prepared from coprecipitated hydroxides, 25:3977(T) (SC-T-70-4041)
HfO_2--Ho_2O_3--ZrO_2, crystal structure of $Ho_2O_3 \cdot 2ZrO_2$(HfO_2) phase in, 25:2807(T) (SC-T-70-4039)
HORMONES, PLANT
gibberellic acid, radioprotective effects of, on growth of barley spikes in relation to DNA synthesis, γ, 25:2597
indole-3-acetic acid, radioprotective effects of, on growth of barley spikes in relation to DNA synthesis, γ, 25:2597
HORMONES, SEX
20α-hydroxy-pregn-4-en-3-one, effects on metabolism in ram spermatozoa, carbon-14 tracer study of, 25:2519
20β-hydroxy-pregn-4-en-3-one, effects on metabolism in ram spermatozoa, carbon-14 tracer study of, 25:2519
3α-hydroxy-5β-pregnan-20-one, effects on metabolism in ram spermatozoa, carbon-14 tracer study of, 25:2519
5β androstane-3,17-dione, effects on metabolism in ram spermatozoa, carbon-14 tracer study of, 25:2519
5β-pregnane-3,20-dione, effects on metabolism in ram spermatozoa, carbon-14 tracer study of, 25:2519
androst-4-ene-3,17-dione, effects on metabolism in ram spermatozoa, carbon-14 tracer study of, 25:2519
oestra-1,3,5(10)-triene-3,16α,17β-triol, effects on metabolism in ram spermatozoa, carbon-14 tracer study of, 25:2519
oestra-1,3,5(10)-triene-3,17β-diol, effects on metabolism in ram spermatozoa, carbon-14 tracer study of, 25:2519
progesterone, effects on metabolism in ram spermatozoa, carbon-14 tracer study of, 25:2519
testosterone, effects on metabolism in ram spermatozoa, carbon-14 tracer study of, 25:2519
HORMONES, THYROID
thyroxine, secretion by lactating cattle, iodine-131 measurement of, 25:2524
HUMBOLDT BAY POWER REACTOR
radioisotopes for, authorized possession and use limits for, 25:3808 (DOCKET-50133-42)
HUNGARY
ore deposits in Mecsek region of, gamma--gamma logging method for prospecting for, 25:2347(T) (CSIRO-Trans-10140)
HYDRAZINE
effects on radiolysis of ammonia, 25:2283
HYDRAZYL, DIPHENYLPICRYL-
effects on γ-radioinduced arylation of nitrobenzene, 25:2255
HYDROBROMIC ACID
HBr--methane, bromine-80m isomeric transition in, yields of labeled bromomethane from, 25:2226
HYDROCARBONS
desorption of simple, from iridium, mass spectrometric analysis of products of flash, 25:3961 (IS-T-406)
determination of C_1--C_4, products from radiolysis of gaseous ethylene, gas chromatographic method for, 25:2278
HYDROCHLORIC ACID
effects on fixation of alkali metals on hydrated antimony pentoxide, 25:2333
effects on radiolysis of water, 25:2267
bis(2-ethylhexyl) phosphate--$CeCl_3$--HCl--H_2O--$NdCl_3$--$SmCl_3$, equilibria in Amsco, 25:2311 (IS-T-412)
HYDROFLUORIC ACID
effects on solubility of plutonium in dilute nitric acid, 25:2153
HYDROGEN
abstraction by primary species in γ-irradiated frozen aqueous solution of alcohols, 25:2293
determination in helium, pressurized electrolytic hygrometer for, 25:3882 (DP-Report-487)
deuteron reactions (d,γ) at 19.8 and 29.6 MeV, helium-3 energy spectra, gamma angular distributions, and total cross sectons for, (E), 25:3546 (ORNL-TM-3168)
diffusion in palladium, electronic mechanisms in thermal, 25:2666 (NP-18468)
effects on cathodic embrittlement of steel, 25:2816 (ORNL-4570, pp 16-19)
electron reactions with atomic, excitation cross sections for, (T), 25:2915
energy of molecular, calculation using integral-transformation trial functions, 25:2928
excitation cross sections for atomic, calculation using approximation based on regional trial functions, 25:2895
neutron cross sections for natural, ortho, and para, (T), 25:3530 (LA-4484)
plasma of, 13-moments approximation for radial pressure profile, 25:3105
plasma of, 5-moments approximation for radial pressure profile in, (T), 25:3104
plasma of, confinement in DECA II B, (E), 25:3053 (CEA-

CONF-1597)
plasma of, deviations from thermodynamic equilibrium of hydrogen, (T), 25:3106
plasma of, drift-wave propagation in collisionless, (E/T), 25:3167
plasma of, effects of time-varying fields on confinement in toroidal octupoles, (E/T), 25:3059
plasma of, electric field distribution in arcs with axial magnetic fields, (E), 25:3083
plasma of, electron velocity distribution in optically thin, (T), 25:3102
plasma of, ion heating by interacting electron beams, (E), 25:3054 (CEA-CONF-1611)
plasma of, Stark broadening measurement of ion density in discharge, 25:3068
radiation effects on stability of atomic, in clinoptilolites containing lanthanum, magnesium, or potassium ions at 400 to 700°C, EPR spectral studies on γ, 25:2224
reactions with gas phase substrate molecules, elementary rate constants for, 25:3970(R) (NYO-3794-11)
reactions with hydrogen ions (H_2^+), cross sections for charge exchange in, (T), 25:2912
reactions with niobium and tantalum at high temperatures, effects of argon or helium protective atmosphere on, 25:2639(T) (LIB/Trans-309)
reactions with steam and uranium hexafluoride in fluidized bed to produce ceramic-grade uranium dioxide, 25:2781(P)
separation of ortho- and para-, by thermal diffusion, 25:2405
spectra of, last resolved line in Balmer series, (T), 25:2892
spectral emission of auroral, effect of magnetic activity on intensity of, 1959 to 1966, (E), 25:2976
yields from γ radiolysis of mixtures of octane with benzene, 1,3-cyclooctadiene, or cyclooctatetraene, kinetics of production of, 25:2270
yields from γ radiolysis of poly(tetrafluoroethylene), effects of gaseous additives on, 25:2261 (NP-18518)
yields from radiolysis of water, 25:2257 (CEA-R-4046)

HYDROGEN IONS
dissociation of molecular clusters of, by electron beams, 25:3109 (CEA-CONF-1610)

HYDROGEN IONS (H^-)
energy of, calculation using Euler transforms of Slater and Gaussian 1s functions, 25:2928

HYDROGEN IONS (H_2^+)
reactions with graphite and metal surfaces at 5 to 50 keV, apparent total ion scattering, secondary electron emission coefficients, and electron and ion energy distributions for, (E), 25:2884 (NP-18490)
reactions with hydrogen molecules, cross sections for charge exchange in, (T), 25:2912

HYDROGEN PEROXIDES
reactions with trivalent neptunium, mechanism and products of oxidation, 25:2155
yields from γ radiolysis of aqueous sulfuric acid solutions, 25:2265
yields from radiolysis of water, 25:2257 (CEA-R-4046)

HYDROGEN SYSTEMS
D--H, hydromagnetic wave absorption by plasma in Levitron-type device, (E/T), 25:3148 (CEA-CONF-1614)
Fe--H--Rb--Si, phase studies of, 25:2727 (ORNL-4570, pp 1-4)
H--Na--O, phase studies of condensed phases in, at 400 to 1000°K, thermochemical, 25:2205
H--Na--O, vapor pressure of gaseous species over condensed phases in, at 400 to 1000°K, 25:2205

HYDROLOGY
conference on new developments in, Urbana, Ill., July 13 to 25, 1969, 25:2358
isotopic and nuclear methods in, review of, 25:2359
isotopic and nuclear methods in, review of principles of, 25:2360

HYDROMAGNETIC WAVES
absorption in Levitron-type device, (E/T), 25:3148 (CEA-CONF-1614)
propagation in magnetosphere, nonlinear frequency shift of, (T), 25:3004
propagation in magnetosphere, spectrum of one-dimensional Alfven, (T), 25:2970

HYDROQUINONE
effects on γ-radioinduced graft polymerization of cellulose with styrene in methanol solutions, 25:2247

HYDROURACIL, 5-METHYL-
radioinduced conformation changes of pyrimidine ring in monocrystals of, γ, 25:2282

HYDROXYL (HO)
radio interferometry of galactic, very-long-baseline, (E), 25:2844
spectral emission in airglow, altitude profile of, (E), 25:3001
yields from radiolysis of aqueous solutions of nitric and sulfuric acids, 25:2277
yields from radiolysis of water, 25:2257 (CEA-R-4046)

HYGROMETERS
development of electrolytic, for measurement of water and hydrogen in helium, 25:3882 (DP-Report-487)

HYPERFRAGMENTS
binding energy of Λ--p-shell nuclei, calculation using intermediate coupling shell model with two-body Λ-N interaction, 25:3721
lifetime of Λ-He^5 from Λ-He^5 + π^- + p + ^{4}He decay in nuclear emulsion, (E), 25:3259

HYPERONS
decay amplitudes in gauge-field model, S-wave nonleptonic, 25:3341
decay of, baryon pole model for S-wave, 25:3346
decays of polarized, asymmetry coefficients of leptonic, (T), 25:3339
decays of, chiral SU(3) x SU(3) symmetry breaking for nonleptonic, 25:3349
interactions with nucleons, geometrical and Regge pictures for elastic, 25:3354

HYPERONS (Λ)
interactions Λ + N; one-boson-exchange potential model for, (T), 25:3416
interactions Λ + p at low energies, one-boson-exchange potential model for, (T), 25:3416
polarization in two-body Y* and anti Y* production in baryon interactions with pseudoscalar mesons and baryon interactions with baryons, additive quark model for, (T), 25:3383 (TPJU-2/70)

HYPERONS (Σ)
polarization in two-body Y* and anti Y* production in baryon interactions with pseudoscalar mesons and baryon interactions with baryons, additive quark model for, (T), 25:3383 (TPJU-2/70)

HYPERONS (Σ^-)
interactions $\pi^+ + \Sigma^- + \pi^- + \Sigma^+$ with exotic crossed state, sum rules for, 25:3404

I

IMMUNE REACTIONS
radiation effects on, in rats, whole-body x, 25:2540

INCOLOY 800
corrosion of Inconel 82-filler weldments of, by steam at 595 to 650°C, 25:2608 (ORNL-4570, pp 124-6)
corrosion of sodium loops of Type 304 stainless steel and, at 900 to 1325°F, 25:2619
ductility of, effects of minor elemental additions on hot, 25:2675 (ORNL-4570, pp 143-8)
fatigue at 800 to 1400°F, measurement of low-cycle, 25:2659 (BMI-1889, Sect.A)
mechanical properties of, effects of thermal aging on, 25:2756 (ORNL-4570, pp 76-84)
radiation effects on mechanical properties of, in-pile, 25:2758 (ORNL-4570, pp 76-84)
welding to Hastelloy X using Hastelloy W or Inconel 82 filler metal, corrosion by steam at 1100 to 1200°F of welds produced by, 25:2636
welding to IN 102 alloy using IN 102 or Inconel 82 filler metal, corrosion by steam at 1100 to 1200°F of welds produced by, 25:2636
welding to Incoloy 800 using Inconel 82 filler metal, corrosion by steam at 1100 to 1200°F of welds produced by, 25:2636
welding to Inconel 625 using Inconel 82 filler metal, corrosion by steam at 1100 to 1200°F of welds produced by, 25:2636

INCONEL
corrosion of ceramic-coated, by selenium at 300 to 700°C, 25:2629

INCONEL 600
corrosion by ammoniated and lithiated PWR coolants, effects on reactor operation, 25:2637
corrosion of Inconel 82-filler weldments of, by steam at 595 to 650°C, 25:2608 (ORNL-4570, pp 124-6)
ductility of, effects of minor elemental additions on hot, 25:2675 (ORNL-4570, pp 143-8)
neutron cross sections for, 25-group, (T), 25:3530 (LA-4484)
welding to Inconel 600 using Inconel 82 filler metal, corrosion by steam at 1100 to 1200°F of welds produced by, 25:2636

INCONEL 625
corrosion of similar metal welds of, by steam at 1100 to 1200°F, 25:2636
corrosion of similar metal welds of, by steam at 595 to 650°C, 25:2608 (ORNL-4570, pp 124-6)
welding to Incoloy 800 using Inconel 625 filler metal, corrosion by steam at 1100 to 1200°F of welds processed by, 25:2636

INCONEL 718
bonding to gold-plated Type 302 stainless steel under static loads, 25:2677 (ORNL-4570, pp 224-7)
neutron cross sections for, 25-group, (T), 25:3530 (LA-4484)

INDIAN POINT POWER REACTOR, UNIT 1
site for, environmental survey during August 1969 to March 1970, 25:3806 (DOCKET-50003-59)

INDIAN POINT POWER REACTOR, UNIT 2
cooling system for, ultrasonic inspection of pressurizer for, 25:3818 (DOCKET-50247-42)
design parameters of, revised and additional data on, 25:3819 (DOCKET-50247-43)
operations aspects of, revised and additional data on, 25:3819 (DOCKET-50247-43)
safety evaluation of, Division of Reactor Licensing,

XUM

25:3820 (DOCKET-50247-44)
INDIUM
complexes of trivalent, with citric, malic, tartaric acids and hexavalent uranium, potentiometric, solvent extraction, and spectrophotometric studies on, 25:2206
corrosive effects on tantalum--tungsten and TZM alloys at 1000 to 1800°C, 25:2628
density at 160 to 532°C, 25:2692
effects on determination of trace amounts of antimony by isotopic exchange in organic phase, 25:2106
effects on photometric determination of hafnium and zirconium in geological specimens, 25:2084
internal friction spectra of single crystals of, 25:2667 (NP-18491)
production of pure, review of techniques for, 25:3219
separation from nitrate and sulfate solutions by solvent extraction using amines, 25:2319 (ORNL-4572, pp 181-95)
superconducting condensation energy calculation, 25:3046
INDIUM ALLOYS AND SYSTEMS
Bi--In, density at 73 to 660°C, 25:2692
Cd--In--Sn, electron band structure of alpha-, effects of conduction electron/atom ratio on, 25:3205 (UCRL-19681)
Hg--In, Hall coefficients of liquid, comparison with fluctuation scattering model, 25:3209
In--Pb, local order and size effect in solid solutions, 25:3207
In--Pb, magnetic flux quanta in superconducting tubes, direct observation of, 25:3024
In--Sb, pinch in avalanche plasma in n-type InSb, dynamic processes in linear, (E/T), 25:3206
In--Sn, density at 122 to 440°C, 25:2692
In-base--Zn, thermodynamic properties of dilute liquid solutions of, 25:2685
INDIUM ISOTOPES In-113
energy-level transitions from tin-113 electron-capture decay, (E), 25:3694
production of isomeric, tin-113 generator for, 25:2296
INDOLE
deuterium effects on fluorescence yields and lifetimes of, 25:2536
INFRARED RADIATION
effects on silicate-treated zinc oxide coatings, relations with oxygen loss, 25:2815 (N-70-33138)
emission from pulsars of pulsed, (T), 25:2854
INORGANIC COMPOUNDS
purity of radioisotope-labeled, use of thin-layer electrophoresis for control of, 25:2062 (CNEA-271)
INSECTA
Drosophila melanogaster, radioinduced sex chromosome loss in sperm of, x, 25:2554
Drosophila melanogaster, radioinduced translocation aberrations in chromosomes of, effects of, on crossover suppressors, 25:2561
INSTRUMENTS
development of radiometric, 25:2497(R) (INR-1180)
uses of radiometric, in hydrology, review of, 25:2359
INTERFEROMETERS
use of Mach--Zehnder and holographic, for plasma diagnostics, (E), 25:3071
use of Mercereau ring, in radiation detectors using superconducting weak links, 25:2444
INTERSTELLAR MATERIAL
particle--spin orientation in, dynamic, (T), 25:2831
INVARIANCE PRINCIPLES
C, CP, isospin, and T violation in elementary-particle interactions, nonelectromagnetic, (T), 25:3425
charge conjugation violation from asymmetry and background in eta → $\pi^+ + \pi^- + \pi^0$ decay, (E/T), 25:3254
CP violation in $K^+ \rightarrow 2\pi^+ + \pi^-$ and $K^- \rightarrow 2\pi^- + \pi^+$ decays, search for, (E), 25:3427
CPT violation in $K_2^0 \rightarrow 2\pi$ decay, field theory model for, 25:3429
time reversal invariance in nuclear beta decay, (T), 25:3424
time reversal violation in K^0 decay, relation to arrows of time, (T), 25:3423
IODIDES
iodine-131 exchange between alkyl iodides and, in acetone--water solution, 25:2177
sorption on bentonites, 25:2337
IODINE
content of milk of cattle, 25:2524
determination by photon activation and γ spectrometry using cesium as internal reference element, 25:2150
determination in biological materials by 14-MeV neutron and thermal neutron activation, sensitivity of, 25:2125 (IAEA-122, pp 27-36)
determination in human tissues by thermal neutron activation, sensitivity of, 25:2123 (IAEA-122, pp 1-13)
determination in milk and natural waters by neutron activation and γ spectrometry, 25:2124 (IAEA-122, pp 15-26)
effects on γ radiolysis of cyclohexane, 25:2268
neutron elastic scattering at 1 to 40 keV, analysis of angular distributions from, (E/T), 25:3695
potassium-atom elastic scattering at thermal energies by atomic and molecular, differential cross sections at small angles for, (E), 25:2922
separation from aqueous solutions by anion exchange, 25:2337
separation from fission products by surface ionization, 25:2342
separation from spent LMFBR fuels, 25:2314 (CRNL-4572, pp 37-84)
trapping with solid sorbents in fuel reprocessing plants, 25:2314 (ORNL-4572, pp 37-84)
IODINE ISOTOPES I-125
content of albumin-incorporated, of human body fluids, method for determination of, 25:2518
determination by γ counting using metal-loaded liquid scintillator, 25:2116
IODINE ISOTOPES I-129
chemical state of, from β decay of tellurium-129 in β-tellurium trioxide, nuclear γ resonance spectral studies on, 25:2304
energy levels and transitions from tellurium-129 decay, (E), 25:3675
IODINE ISOTOPES I-131
effectiveness of macroaggregate-incorporated, or RISA-incorporated, for localization of brain tumors in posterior fossa, computer evaluation of, 25:2578
energy levels from proton resonances in tellurium-130, spins, partial widths, and spectroscopic factors for decay of isobaric analog, (T), 25:3685
exchange between alkyl iodides and iodide ion in acetone--water solution, 25:2177
retention by silts of Dimbovitza--Bucharest River, effects of chelating agents and pH on, 25:2363
separation from Purex Plant gaseous wastes, performance of silver reactors for, 25:2416 (ARH-SA-67)
uptake by aquatic molluscs and plants, effects of concentration in water on concentration factor for fallout, 25:2548
uptake of L-triiodothyronine-incorporated, by blood of cattle, 25:2524
yield in thermal fission of uranium-235, (E), 25:3663
IODINE ISOTOPES I-132
energy levels at 49.7 and 277.9 keV, half-lives of, (E), 25:3706
yield in thermal fission of uranium-235, (E), 25:3663
IODINE ISOTOPES I-133
yield in thermal fission of uranium-235, (E), 25:3663
IODINE ISOTOPES I-134
yield in thermal fission of uranium-235, (E), 25:3663
IODINE ISOTOPES I-135
yield in thermal fission of uranium-235, (E), 25:3663
IODINE SYSTEMS
Cs--I, analysis for iodine by photon activation using cesium as internal reference element, 25:2150
ION-ACOUSTIC WAVES
attenuation in plasma, dispersion relations for, (T), 25:3155
propagation in plasma, nonlinear effects of large-amplitude, (E), 25:3151 (IPPJ-94)
propagation in streaming-ion plasma, (E/T), 25:3161
ION BEAMS
phase focusing of intensive, calculation of parameters for, 25:3481
ION EXCHANGE MATERIALS
use as calibrated microscopic radiation source, 25:2406
ION SOURCES
design of polarized, for radial injection into U-120 cyclotron, 25:3520
design of reflex, with axial extraction, 25:3111 (LYCEN-7065)
development for open-ended fusion reactors, requirements for, 25:3131 (ORO-1171-1, pp 3-37)
IONOSPHERE
airglow enhancement at higher midlatitudes in, 6300-A predawn, (E), 25:2961
antenna impedance in topside, parameters affecting loop, (E), 25:2967
D region, effect on radio-wave reflection from sporadic E, (E/T), 25:2994
D region, ionization from auroral-oval particle precipitation, aircraft observations of, 25:2949 (AD-709359)
D region, wind current patterns in lower, periodic, (E/T), 25:2991
E region, ionization from auroral-oval particle precipitation, aircraft observations of, 25:2949 (AD-709359)
E region, irregularities in equatorial nighttime, Langmuir- and plasma-noise-probe data for studying, (E), 25:2963
E region, wind current patterns in lower, periodic, (E/T), 25:2991
effect of lower, on appearance of sporadic-E radio-wave reflections, (E/T), 25:2994
effects of Sept. 22, 1968 sun eclipse on lower, (E), 25:2996
effects on scintillation of cosmic radio sources, (E/T), 25:2856
electron content in northern and southern polar, 3d satellite signal data during high solar activity for total, (E), 25:2983
electron density at 75 to 80 km in, instrumentation measurement of, (E), 25:2952 (N-70-33955)
electron density N(h) profiles from vertical radio sounding data, analog method for, (E/T), 25:2974

F region, height of, effect of depth of interlayer ionization valley on, (E/T), 25:2989
F region, ion recombination in midlatitude, predawn enhancement of 6300-A line from, (E/T), 25:2959
F region, neutral-air winds for asymmetric global pressure system in, (T), 25:2954
F region, relation between parameters of F1 and F2 layers and prediction of diurnal N(h)-profiles and h'f characteristics, (E/T), 25:2988
F region, shape of irregularities in, (E), 25:3003
F1 layer, appearance and size-shape factors of, relation of critical frequencies ratio of F1 and F2 layers, (E/T), 25:2988
F1 layer, ion structure at 140 to 210 km, effect of atmospheric variability on diurnal variations of, (E/T), 25:2987
F2 layer, diffusion coefficients for atomic helium, hydrogen, nitrogen, and oxygen ions in, (T), 25:2962
F2 layer, effect on ionospheric scatter links at 2000 km in short-wave frequency range, (E/T), 25:2990
F2 layer, ionization in northern and southern hemispheres during solstices, comparison of, (T), 25:2972
F2 layer, ionization of noontime, cyclic variations of A_0 and n variations of latitude-dependent, (E/T), 25:2984
F2 layer, ionization of, effect of magnetic field on longitudinal distribution of mean annual, (E/T), 25:2985
F2 layer, plasma drift inhomogeneities in, effect of traveling disturbances on small-scale, (E/T), 25:2986
F2 layer, plasma scale height in outer, magnetic activity-dependent, (E), 25:2973
F2 layer, thermal coupling to magnetosphere, relation of heat fluxes and energy production to upper, (E), 25:2956
heating in stable red arc, effect on steady-state neutral atmosphere, (E/T), 25:2953
magnetic storms in polar cap, development of elementary, (E), 25:2978
oxygen ion dissociative recombination in 6300-A predawn airglow, molecular, (E), 25:2961
parameters of midlatitude, measurements by Doppler and Faraday effects of coherent signals, (E), 25:2971
plasma drift variations of, seasonal, (E/T), 25:2966
plasma inhomogeneities in lower, along magnetic meridian, (E/T), 25:2992
proton penetration in equatorial, high-energy solar and flare-associated, (E), 25:2965
radio-wave propagation in, phase measurement during solar eclipse of Sept. 22, 1968, vlf, (E), 25:2997
sporadic E, characteristics of, effect of ionization irregularities and structural variations on, (E), 25:2957
sporadic E, parameters of, relation to geomagnetic field, 1964 to 1966, (E), 25:2995
sporadic E, radio-wave reflections from, effect of lower ionosphere on appearance of, (E/T), 25:2994
sporadic E, structure of, simultaneous measurements at two stations for study of spatial, 25:2993

IONS
channeling in solids, use in research and teaching, 25:3188 (CONF-700322-, pp 141-53)
effects on solids, research program on, 25:3190(R) (COO-1053-15)
electron inelastic scattering by, having two valence electrons, configuration-interaction calculations of, 25:2918
electron reactions with, calculation of excitation cross sections for, 25:2915
electron reactions with, formulas for excitation and ionization cross sections for, 25:2914
electron scattering by, computer program for calculation of cross sections for, 25:2903
energy levels of, use of fast ion beams in production and study of excited, 25:2889 (CONF-700322-, pp 289-95)
energy of, calculation using Euler transforms of Slater and Gaussian 1s functions, 25:2928
excitation cross sections for, review of approximate methods of calculation of, 25:2913
photon reactions with, computer program for calculation of ionization cross sections for, 25:2903
reactions of molecules with molecular, cross sections for resonance charge exchange in, (T), 25:2912
reactions with atoms at 1 to 100 keV, charge exchange into excited and ground states in, (T), 25:2919
reactions with atoms, examples and uses of electron spectra from, 25:2900 (CONF-700322-, pp 305-19)
uses of high-velocity, in metallurgy research, 25:2604 (CONF-700322-, pp 155-71)

IRIDIUM
proton reactions with, in inorganic compounds at 660 MeV, production of rhenium by, 25:2300

IRON
abundance in Kappa Cancri, (E), 25:2840
analysis for uranium using permanganate, potentiometric, 25:2099
cobalt-60 nuclear magnetic resonance in, resonant destruction of gamma-ray anisotropy in single-passage, (E), 25:3223
corrosion and mass transfer by sodium at 660 and 760°C, effects of oxygen content on, 25:2631
deformation behavior of polycrystalline, 25:2690
density of pure liquid, 25:4003(T) (UCRL-Trans-10496)
determination following nonsulfide separation from elements, qualitative, 25:2101
determination in biological materials by 14-MeV neutron and thermal neutron activation, sensitivity of, 25:2125 (IAEA-122, pp 27-36)
determination in human liver by neutron activation and γ spectrometry, 25:2124 (IAEA-122, pp 15-26)
determination in human tissues by thermal neutron activation, sensitivity of, 25:2123 (IAEA-122, pp 1-13)
determination in lunar materials by 14-MeV neutron activation and γ spectrometry, 25:2118 (CONF-700322-, pp 205-20)
determination in oceanographic samples by 14-MeV neutron activation and γ spectrometry, 25:2119 (CONF-700322-, pp 221-30)
determination in presence of cerium, chromium, manganese, and vanadium by differential potentiometric titration, 25:2099
determination in titanium alloys, x-ray fluorescence method for, 25:2097
determination of trace amounts of, in lanthanum oxide, neodymium oxide, and yttrium oxide by direct reading emission spectrometry, 25:2096
determination of trace amounts of, in nuclear-grade uranium oxide (U_3O_8) by direct reading spectrometric method, 25:2068 (NLCO-1071)
diffusion of α-, in liquid sodium, grain boundary grooving studies of surface self-, 25:2708
diffusion of carbon in, electronic mechanisms in thermal, 25:2666 (NP-18468)
effects on determination of trace amounts of antimony by isotopic exchange in organic phase, 25:2106
effects on determination of trace amounts of rhenium by thiocyanate--stannous chloride method, 25:2102
effects on extraction--photometric determination of niobium in steel, 25:2085
effects on photometric determination of hafnium and zirconium in geological specimens, 25:2084
effects on polarographic determination of tellurium, 25:2090
effects on uv spectrophotometric determination of gallium in aqueous solutions, 25:2100
electron backscattering at 1 MeV, angular distribution and energy spectra for, 25:2886
gamma dose-rate distributions in laminated iron/water shielding, (E/T), 25:3174
gamma energy absorption rates in laminated shields of lead and, (T), 25:3169
gamma reflection and transmission by, spectral and angular-distribution function for, 25:3168
gamma scattering by, energy distribution of single and multiple, (E), 25:3182
neutron attenuation by, monoenergetic-source fast-, (E/T), 25:3173
neutron capture by, gamma spectra from thermal, (E), 25:3181
neutron cross sections for, 25-group, (T), 25:3530 (LA-4484)
neutron flux-density distributions in laminated iron/water shielding, (E/T), 25:3174
oxidation of high-purity, at moderate temperatures, x-ray spectra studies of kinetics of, 25:2604 (CONF-700322-, pp 155-71)
production of, economics of process heat reactors for, 25:3916
proton elastic and inelastic scattering at 28 MeV, cross sections for, (E), 25:3599
radioinduced preparation from aqueous salt solutions, electron, 25:2237 (N-70-32826)
radioinduced voids in, distribution of fast neutron, 25:2816 (ORNL-4570, pp 16-19)
reactions with oxygen in sodium, 25:2711
segregation on liquid sodium surface, 25:2713
separation from thorium-234 by sorption on iodates and periodates, 25:2341
separation of cerium, gadolinium, lanthanum, and neodymium from, by precipitation using cupferron, 25:2078
solubility in liquid sodium, effects of temperature on, 25:2712
spectral lines in solar-disc flares effect on geophysical activity of solar flares, (E/T), 25:2859
work-hardening parameters for polycrystalline, 25:2723

IRON ALLOYS AND SYSTEMS
Ag--Fe--Nb--Ni-base, crystallization of, relations with magnetic properties, 25:2679
Al--Cr--Fe--Ti-base, microstructure of hot-rolled plates and sheets of α + β, relations of mechanical properties with abnormal, 25:2752
Co--Fe, diffusion in, effects of crystal structure on cobalt-57 and iron-59, 25:2178
Cr--Fe--Nb--Ni-base, hardening of, transmission electron microscopic study of age, 25:2689
Cr--Fe--Ni, reactions with uranium carbide at 900°C, effects of carbon content and metal stabilizers on, 25:2765 (KFK-1213)
Cr--Fe-base, diffusion in bcc phases of, radioisotope tracer measurements of volume, 25:2691
Cr--Fe-base--Mo, welding to Incoloy 800 using Inconel 82 filler metal, corrosion by steam at 1100 to 1200°F of

welds produced by, 25:2636
Dy--Fe, crystal structure of intermetallic $DyFe_3$ and Dy_6Fe_{23}, 25:2750
Fe--H--Rb--Si, phase studies of, 25:2727 (ORNL-4570, pp 1-4)
Fe--Mo, analysis for trace amounts of carbon, conductometric method for, 25:2071
Fe--Ni, neutron cross sections for invar, (T), 25:3530 (LA-4484)
Fe--Ni, thermal capacity and conductivity of intermetallic Ni_3Fe, 25:2788 (ORNL-4570, pp 27-30)
Fe--W, analysis for trace amounts of carbon, conductometric method for, 25:2071
Fe-base--Ti, diffusion in bcc phases of, radioisotope tracer measurements of volume, 25:2691
Fe-base--V, diffusion in bcc phases of, radioisotope tracer measurements of volume, 25:2691

IRON CARBONYLS
complexes with electronegatively substituted dienes, deuterium exchange in, 25:2187

IRON ISOTOPES
effects on diffusion in cobalt--iron alloys, effects of crystal structure on, 25:2178

IRON ISOTOPES Fe-54
energy levels of, binding energies and orbital spin assignments of proton-hole, (E), 25:3616
proton elastic and inelastic scattering at 10 MEV, differential cross sections, polarizations, and p--γ angular correlations for, (E), 25:3613

IRON ISOTOPES Fe-55
energy levels and transitions from manganese-55 (p,n) reactions, high-spin, (E), 25:3624
energy levels from cobalt-55 decay, (E), 25:3604
energy levels of, calculation using intermediate coupling model, (T), 25:3592 (COO-1120-106)

IRON ISOTOPES Fe-56
energy levels of, binding energies and orbital spin assignments of proton-hole, (E), 25:3616
proton reactions (p,γ) at 1.21 to 2.57 MeV, angular distributions, gamma spectra, cross sections, and Q-value for, (E), 25:3601

IRON ISOTOPES Fe-57
Mossbauer effect of, investigation of suppressed nuclear absorption of resonant γ rays using, (E), 25:3225
proton reactions (p,n) near threshold, Q-value for, (E), 25:3608

IRON ISOTOPES Fe-59
effects on diffusion in cobalt--iron alloys, effects of crystal structure on, 25:2178
retention by silts of Dimbovitza--Bucharest River, effects of chelating agents and pH on, 25:2363

IRON SULFATES $FeSO_4$
proton reactions at 350 keV with, characteristic x-ray spectra from, (E), 25:2882 (CONF-700322-, pp 113-24)

IRRADIATION FACILITIES
cryostat for heavy ion, design of, 25:2388 (RD/B/M-1753)
design of industrial and research, 25:2389
gamma sources for complex cylindrical, method for calculation of dose rates from, 25:2403

ISOBUTYROPHENONE
radiolysis of, yields from electron, 25:2266

ISOTOPE EXCHANGE
kinetics of, mathematical analysis of, 25:2161

ISOTOPES
determination of, paper chromatographic data for, 25:2075
production by Campbell reactions using alpha or neutron beams and molecular sieve, 25:2295 (ORNL-4572, pp 225-30)
uses at Inst. of Nuclear Research, Warsaw, 1969, 25:2497(R) (INR-1180)

ITALY
radioisotope accumulation in fish of northern, factors affecting concentration factors for fallout cesium-137 and strontium-90, 25:2527

J

JAPANESE EXPERIMENTAL FAST REACTOR
fuel cladding for, testing of Type 316 stainless steel, 25:2661 (JAERI-Memo-4125)

JAPANESE MATERIALS TESTING REACTOR
neutron flux variations in irradiation channels of, (E/T), 25:3906 (JAERI-Memo-4130)

JOSEPH M. FARLEY POWER REACTOR, UNIT 1
design parameters of, revised and additional data on, 25:3845 (DOCKET-50348-14)
operation aspects of, revised and additional data on, 25:3845 (DOCKET-50348-14)

JOSEPH M. FARLEY POWER REACTOR, UNIT 2
design parameters of, revised and additional data on, 25:3845 (DOCKET-50348-14)
operation aspects of, revised and additional data on, 25:3845 (DOCKET-50348-14)

JUPITER (PLANET)
radio emission at 18 MHz from, very-long-baseline interferometry of, 25:2880
radio emission at decametric wavelengths from, very-long-baseline interferometry of, 25:2879

K

KAOLINITES
sorptive properties of Rhine River, for radioisotopes, (E), 25:2350

KETONES
radiolysis of aromatic, yields from electron, 25:2266

KIDNEYS
phosphorus-33 uptake by, 25:2521
scanning of, use of radioisotopes and scintillation camera in γ, 25:2581
scanning using metastable technetium-99, 25:2580

KRYPTON
separation from spent LMFBR fuels, 25:2314 (ORNL-4572, pp 37-84)

KRYPTON ISOTOPES Kr-85
release by dynamic air--water systems, effects of agitation, temperature, and geometry on, (E), 25:3892 (BNWL-SA-3360)

L

LA CROSSE BOILING-WATER REACTOR
instrumentation for, automatic gain control system for, 25:3805 (DOCKET-1155-84)

LA SALLE COUNTY POWER REACTOR, UNIT 1
design parameters of, preliminary safety analysis of, 25:3850 (DOCKET-50373-6)
operations aspects of, preliminary safety analysis of, 25:3850 (DOCKET-50373-6)
quality assurance program for, 25:3850 (DOCKET-50373-6)
technical specifications for, proposed, 25:3850 (DOCKET-50373-6)

LA SALLE COUNTY POWER REACTOR, UNIT 2
design parameters of, preliminary safety analysis of, 25:3850 (DOCKET-50373-6)
operations aspects of, preliminary safety analysis of, 25:3850 (DOCKET-50373-6)
quality assurance program for, 25:3850 (DOCKET-50373-6)
technical specifications for, proposed, 25:3850 (DOCKET-50373-6)

LABORATORIES
design for radioisotope tracer studies, 25:2390

LACQUERS
radiation effects on physicomechanical properties of, gamma, 25:2822

LAKES
cesium content of freshwater, neutron activation analysis of natural, 25:2517
radioisotope concentration factors for organisms in, effects of nutritional state on strontium-90 and uranium-238, 25:2546

LANTHANUM
complexes with cupferron, separation by solvent extraction using 2-methyl-1-propanol and 3-methyl-1-butanol, 25:2078
determination in silicate rocks using cupferron, spectrographic, 25:2078
determination of trace amounts of, in silicate rocks by neutron activation and radiochemical group separation, 25:2149
effects on determination of trace amounts of antimony by isotopic exchange in organic phase, 25:2106
neutron elastic scattering at 1 to 40 keV, analysis of angular distributions from, (E/T), 25:3695
photon reactions at 30 to 100 keV with, photoelectric cross sections for, 25:2907
separation from metals by precipitation using cupferron, 25:2078
separation from rare earth chlorides by solvent extraction using D2EHPA and multistage mixer--settler extractor, 25:2310 (IS-T-411)

LANTHANUM ALLOYS AND SYSTEMS
Co--La, magnetic properties of intermetallic $LaCo_5$, 25:3217

LANTHANUM ISOTOPES La-139
energy levels from proton resonances in barium-138, spins, partial widths, and spectroscopic factors for decay of isobaric analog, (T), 25:3685

LANTHANUM ISOTOPES La-146
decay and energy-level transitions following californium-252 fission, (E), 25:3673

LANTHANUM NITRATES
complexes with bis(2-ethylhexyl) phosphate, spectra of, ir and Raman, 25:2193 (CONF-700403-8)

LANTHANUM OXIDES
analysis for trace amounts of rare earths and other elements by direct reading emission spectrometry, 25:2096

LASER RADIATION
effects on thin metal films, critical flux required for destructive, 25:3997 (UCRL-50927)
hazards to retina of rabbits during mode locking, CW, 25:2591
scattering by dense plasmas, cross sections for, (T), 25:3101

LASERS
bibliography on uses of, in emission spectroscopy, 25:3110 (IN-1425)
performance for plasma density measurements, (E), 25:3066
performance for plasma diagnostics, 25:3069
use with interferometers for plasma electron density measurements, limits of, 25:3072
use with Mach--Zehnder and holographic interferometry for plasma diagnostics, (E), 25:3071
LAWRENCIUM
chemical properties in aqueous solutions, 25:2197
separation from aqueous solutions by solvent extraction using 4-methyl-2-pentanone and TTA, 25:2197
LEAD
beta particle penetration in, intensity variation with thickness for external bremsstrahlung production from, (E), 25:3249
coating with cadmium, copper, or zinc, surface morphology in electrochemical, 25:2648
compounds, analysis for lead by fast-neutron activation and γ spectrometry, 25:2137
corrosive effects on niobium--zirconium and tantalum--tungsten alloys at 1000 to 1800°C, 25:2628
design requirements for shielding of, for Japanese nuclear-powered ship Mutsu, 25:2683
determination following nonsulfide separation from elements, qualitative, 25:2101
determination in biological fluids by potentiometric titration using Orion liquid ion-exchange lead-selective electrode, 25:2104
determination in lead compounds and ores by fast-neutron activation and γ spectrometry, 25:2137
determination of trace amounts of, in nuclear-grade uranium oxide (U_3O_8) by direct reading spectrometric method, 25:2068 (NLCO-1071)
effects on determination of trace amounts of antimony by isotopic exchange in organic phase, 25:2106
effects on photometric determination of hafnium and zirconium in geological specimens, 25:2084
effects on uv spectrophotometric determination of gallium in aqueous solutions, 25:2100
gamma energy absorption rates in laminated shields of iron and, (T), 25:3169
gamma scattering by electrons in, incoherent cross sections for 30-keV to 2.62 MeV, (T), 25:2921
gamma scattering by, energy distribution of single and multiple, (E), 25:3182
neutron attenuation by, monoenergetic-source fast-, (E/T), 25:3173
neutron scattering by, exponential angular coefficients for fast, (E), 25:3171
neutron time--energy distributions in, (T), 25:3541
photon reactions at 5.7 GeV, $\omega\gamma$ coupling constant and ωN cross section from ω production in, (E), 25:3247
radioinduced preparation from aqueous salt solutions, electron, 25:2237 (N-70-32826)
separation from nitrate and sulfate solutions by solvent extraction using amines, 25:2319 (ORNL-4572, pp 181-95)
superconducting condensation energy calculation, 25:3046
superconducting magnetic flux quanta in tubes of, observation of single, 25:3024
superconducting penetration depth in, (E), 25:3041
work softening in polycrystalline, 25:2724
LEAD ALLOYS AND SYSTEMS
Bi--Pb, corrosive effects on niobium-coated steel tubing at 375 to 500°C, relations with magnesium and zirconium additions, 25:2627
Bi--Pb, solvent properties of eutectic of, for chromium, cobalt, and nickel at 400 to 500°C, 25:2709
In--Pb, local order and size effect in solid solutions, 25:3207
In--Pb, magnetic flux quanta in superconducting tubes, direct observation of, 25:3024
Na--Pb, magnetic flux line pinning and precipitates in superconducting, (E/T), 25:3033
LEAD IODATES
sorptive properties for thorium-234, 25:2341
LEAD ISOTOPES Pb-198
potential-energy surface at large deformations from two-center shell model, (T), 25:3734
LEAD ISOTOPES Pb-204
alpha elastic scattering at 14 to 24 MeV, energy dependence of, (E), 25:3689
alpha elastic scattering at 14 to 24 MeV, optical-model analysis of, (E), 25:3689
LEAD ISOTOPES Pb-206
alpha elastic scattering at 14 to 24 MeV, optical-model analysis of, (E), 25:3689
LEAD ISOTOPES Pb-207
deuteron reactions (d,p) with, γ-ray branching ratios for, (E), 25:3688
LEAD ISOTOPES Pb-208
alpha elastic scattering at 14 to 24 MeV, energy dependence of, (E), 25:3689
alpha elastic scattering at 14 to 24 MeV, optical-model analysis of, (E), 25:3689
energy levels from lead-207 (d,p) reactions, spin--parity assignments for, (E), 25:3688
lithium-6 reactions (Li-6,αd) at 26 MeV, angular distributions for Coulomb-breakup, (T), 25:3749
neutrino reactions at 50 to 200 GeV, detection of W production from hadronic decay modes in, (E/T), 25:3333 (NYO-2171-323)
proton elastic scattering at 30.3 MeV, angular distributions, polarizations, and optical-model analysis of, (E), 25:3636
LEAD ISOTOPES Pb-210
determination in seawater by solvent extraction and α counting or α spectrometry, 25:2112
LEAD NITRATES
radiation effects on crystalline, kinetics of annealing of damage from γ, 25:2236
LEAD ORES
analysis for lead by fast-neutron activation and γ spectrometry, 25:2137
LEAD TITANATE ZIRCONATES
properties of, ferroelectric and sintering, 25:3992 (UCRL-20309)
LEPTONS
conservation law in two-component neutrino theory, 25:3351
interactions with hadrons, Veneziano model for current amplitudes of, (T), 25:3342
LEVEL INDICATORS
development for cryogenic helium systems, 25:2394
LIGHT
propagation in gravitational fields, theorem for quadrupole-lens system defocusing for, (T), 25:3450
LIMERICK POWER REACTOR, UNIT 1
design parameters of, revised and additional data on, 25:3846 (DOCKET-50352-9)
operations aspects of, revised and additional data on, 25:3846 (DOCKET-50352-9)
LIMERICK POWER REACTOR, UNIT 2
design parameters of, revised and additional data on, 25:3846 (DOCKET-50352-9)
operations aspects of, revised and additional data on, 25:3846 (DOCKET-50352-9)
LINEAR ACCELERATORS
beam current in sectioned tubes of electron, space charge limit of, 25:3489
beam current integrator for electron, 25:3517
beam emittance from low-energy superconducting electron, 25:3518
beam energy spread in electron, instability factors affecting, 25:3479
design of electron, for industrial use, 25:3483
development of Stanford superconducting 2-GeV electron, 25:3496
development of superconducting, survey on, 25:3507
particle motion in low-energy superconducting electron, radial, 25:3518
LIQUID FLOW
magnetohydrodynamic turbulent, heat transfer in circular tube in longitudinal magnetic field from, (T), 25:2944
LIQUID METAL FAST BREEDER REACTOR
coolant burnout limitations in, review of, 25:2600 (BNL-50258)
fuel cladding for, performance evaluation of, 25:2602 (ORNL-4570, pp 191-4)
fuel cycle for, criticality, radiation, and shielding studies on, 25:2314 (ORNL-4572, pp 37-84)
fuel element cladding for, development of, 25:2641 (ORNL-4570, pp 85-7)
fuel elements for, design of, 25:2789 (ORNL-4570, pp 68-75)
fuel reprocessing and recycle for, 25:2306(R) (ANL-7735)
fuel reprocessing for, 25:2317 (ORNL-4572, pp 170-3)
fuel reprocessing for, aqueous methods for, 25:2314 (ORNL-4572, pp 37-84)
fuels for, development and testing of, 25:2768 (ORNL-4570, pp 47-61)
materials for, development of, 25:2754(R) (BMI-1889)
materials for, radiation effects on mechanical properties of, 25:2755 (BMI-1889, Sect.B)
materials for, sodium corrosion of, 25:2619
materials for, sodium testing of, 25:2600 (BNL-50258)
thermometry system for, development of ultrasonic, 25:2503 (NYO-3906-4)
LIQUIDS
bubble formation in, calculation of electric field intensities for, 25:2485 (JINR-P13-5277)
properties at high temperatures, bibliography on, 25:2665 (NBS-SPEC. PUBL-315-5)
LITHIUM
corrosive effects on chromium, molybdenum, alloy steels, stainless steels, titanium, and tungsten, 25:2626
corrosive effects on FS-85, niobium--zirconium alloy, and T-111 alloys at 1000 and 1400°F, relations with welding atmosphere purity, 25:2625
corrosive effects on niobium--zirconium alloy in Rankine cycle test loop, effects of yttrium hot trap on, 25:2624
corrosive effects on T-111 alloy in loops at 1370°C, 25:2607 (ORNL-4570, pp 103-5)
deformation slip in monocrystalline, at high temperatures, 25:2728 (ORNL-4570, pp 5-9)
diffusion in oxygen-containing niobium and tantalum at 600°C, 25:2707
electron reactions with atomic, excitation cross sections for, (T), 25:2915

XUM

excitation cross sections for, calculation using approximation based on regional trial functions, 25:2895
neutron distributions in, angular, energy, and spatial, (E/T), 25:3538
neutron scattering by, exponential angular coefficients for fast, (E), 25:3171
properties for use as reactor coolant, review of, 25:2600 (BNL-50258)
structure of, variational calculation of electronic, 25:2671 (ORNL-4570, pp 40-3)
LITHIUM FLUORIDES
thermal conductivity of, electronic, 25:2788 (ORNL-4570, pp 27-30)
BeF_2--LiF--ThF_4--UF_4--ZrF_4, corrosive effects on Hastelloy N, stainless steel, and steel for MSRE, 25:2609 (ORNL-4570, pp 175-90)
LITHIUM IONS
energy of Li^+, calculation using Euler transforms of Slater and Gaussian 1s functions, 25:2928
implantation in diamond crystals, semiconducting layers induced by, 25:3199
LITHIUM ISOTOPES Li-6
electron elastic scattering by, charge form factors from, (E), 25:3558 (AD-704484)
energy levels in, three-body bound-state calculations of, (T), 25:3579
meson (μ^-) capture rate in, pseudoscalar form factor from PCAC hypothesis for, (T), 25:3748
nuclear two-nucleon density function and Pauli correlation function for, (T), 25:3733
reactions (Li-6,α), (Li-6,d), (Li-6,p), and (Li-6,t) with carbon-12 at 5.6 to 14.0 MeV, direct reaction and compound-nucleus analysis of energy spectra, excitation functions, and angular distributions from, (E/T), 25:3578
reactions (Li-6,αd) with lead-208 at 26 MeV, angular distributions for Coulomb-breakup, (T), 25:3749
reactions (Li-6,d) with carbon-13 at 25.6 MeV, angular distributions for, (E), 25:3570
reactions with deuterium in plasma admixtures, 25:3140
scattering by carbon-12 at 13.0 MeV, optical-model analysis of angular distributions from elastic, (E/T), 25:3578
LITHIUM ISOTOPES Li-7
electron elastic scattering by, charge form factors from, (E), 25:3558 (AD-704484)
energy-level transitions from beryllium-7 electron-capture decay, (E), 25:3694
reactions (Li-7,t) with carbon-13 at 30.1 MeV, angular distributions for, (E), 25:3570
reactions with deuterium in plasma admixtures, 25:3140
LIVER
analysis of human, for minerals by neutron activation and γ spectrometry, 25:2124 (IAEA-122, pp 15-26)
mercury-203 concentration in human, after oral intake of labeled methyl nitrate, 25:2533
phosphorus-33 uptake by, 25:2521
scanning of, use of radioisotopes and scintillation camera in γ, 25:2581
LOOPS
fluid flow in, design of permanent magnet probe-type sensor for measurement of, 25:2600 (BNL-50258)
LUNAR MATERIALS
age of surface fines, (T), 25:2881
analysis for aluminum, iron, oxygen, and silicon by 14-MeV neutron activation and γ spectrometry, 25:2118 (CONF-700322-, pp 205-20)
analysis of, equipment and method for in situ neutron activation, 25:2144
rare-gas abundance in surface, (T), 25:2881
LUNGS
anatomy of human, use of γ transmission scanning for determination of, 25:2580
radioinduced inhibition of urethan adenomagenesis in, of mice, role of thymus in x, 25:2589
scanning of, use of radioisotopes and scintillation camera in γ, 25:2581
scanning using metastable technetium-99, 25:2580
LUTETIUM ISOTOPES Lu-168
electron-capture decay scheme, (E), 25:3650 (LYCEN-7030)
energy levels, (E), 25:3650 (LYCEN-7030)
LUTETIUM ISOTOPES Lu-169
energy level at 492.3 keV from hafnium-169 decay, (E), 25:3676
energy-level transitions from hafnium-169 beta and electron-capture decay, intensities of, (E), 25:3676
LUTETIUM ISOTOPES Lu-175
nuclear magnetic moment of, effects of spin--orbit and spin--spin forces on, (T), 25:3692
LUTETIUM ISOTOPES Lu-177
beta decay of, gamma--gamma angular correlations in, (E), 25:3684
diffusion in copper at 700 to 1010°C, tracer studies of, 25:2680
nuclear magnetic moment of, effects of spin--orbit and spin--spin forces on, (T), 25:3692
LUTETIUM OXIDES
luminescence of terbium-doped, temperature effects on flame-excited, (E), 25:3213

M

MACHINING
shear spinning method for automatic, of precision parts, 25:2650
MAGNESIUM
abundance in Kappa Cancri, (E), 25:2840
analysis for trace amounts of carbon, conductometric method for, 25:2071
determination following nonsulfide separation from elements, qualitative, 25:2101
determination in human tissues by thermal neutron activation, sensitivity of, 25:2123 (IAEA-122, pp 1-13)
determination in oceanographic samples by 14-MeV neutron activation and γ spectrometry, 25:2119 (CONF-700322-, pp 221-30)
determination of trace amounts of, in lanthanum oxide, neodymium oxide, and yttrium oxide by direct reading emission spectrometry, 25:2096
determination of trace amounts of, in nuclear-grade uranium oxide (U_3O_8) by direct reading spectrometric method, 25:2068 (NLCO-1071)
effects on corrosion of niobium-coated steel tubing by bismuth--lead eutectic at 375 to 500°C, 25:2627
effects on determination of trace amounts of antimony by isotopic exchange in organic phase, 25:2106
effects on photometric determination of hafnium and zirconium in geological specimens, 25:2084
effects on uv spectrophotometric determination of gallium in aqueous solutions, 25:2100
plasma charge exchange in ultrasonic jet of, (E), 25:3079
reactions with platinum, 25:2160
reactions with uranium tetrafluoride at 2400°F and 75 psig to prepare high-purity uranium, reduction, 25:2640 (NLCO-1058)
release to soil from organic debris in forest as function of decomposition mode and time, 25:2528
spectral lines in solar-disc flares effect on geophysical activity of solar flares, (E/T), 25:2859
MAGNESIUM ISOTOPES Mg-23
energy levels from (He-3,α) reactions, (E), 25:3637
MAGNESIUM ISOTOPES Mg-24
energy levels of, calculation using Hartree--Fock--Bogolyubov method with isospin pairing, (T), 25:3722
helium-3 reactions (He-3,α) at 18 to 20 MeV, j dependence in l = 2 angular distributions from, (E), 25:3637
MAGNESIUM ISOTOPES Mg-25
proton inelastic scattering at 17.5 MeV, cross-section calculations for, (T), 25:3603
MAGNESIUM OXIDES
Gd_2O_3--MgO, analysis of irradiated, for gadolinium by titration using gadolinium-153 as internal indicator, 25:2089
MAGNESIUM SILICATES
preparation of monocrystalline, method for, 25:2727 (ORNL-4570, pp 1-4)
MAGNET COILS
resistance in small, twisted, multicore superconducting, 25:3499
MAGNETIC FIELDS
calculations in constant-radius cylindrical magnetotail, (T), 25:2960
distribution of neutral sheet in magnetospheric tail, (E/T), 25:2982
effect on ionospheric seasonal variations, (E/T), 25:2966
flux of interplanetary, relation to K/sub p/ index of geomagnetic fields, (E/T), 25:2981
measurement in Bevatron, smoothing and differential analysis of, 25:3503
polarity of interplanetary, effects on geomagnetic activity, (E), 25:2860
production of rotating multipole, for plasma studies, 25:3129 (JUL-667-PP)
relation of chromosphere and photosphere, to faculae and flocculi brightness in each, (E), 25:2857(T) (AD-707256)
variations in, statistics of world-wide, 25:2958
MAGNETIC MIRROR MACHINES
electron beam interactions with neutral gas streams in, plasma production in, 25:3113
plasma confinement in DECA II B, (E), 25:3053 (CEA-CONF-1597)
plasma heating by hf fields, stochastic, (T), 25:3058
plasma heating in, stochastic model of electron-cyclotron, (T), 25:3055 (IPPJ-100)
plasma injectors for, requirements of, 25:3131 (ORO-1171-1, pp 3-37)
plasma turbulent heating in, review of, 25:3056 (ORO-1171-1, pp 78-97)
MAGNETIC MONOPOLES
binding to naturally occurring free nuclei with magnetic dipole moment, 25:3322
MAGNETIC PROBES
performance of Hall plate, for locating magnetic median surface in AVF cyclotron, 25:3516

MAGNETIC SEPARATORS
detectors for, position-sensitive silicon surface-barrier, 25:2463
MAGNETIC STORMS
commencement and development of polar, above entire auroral oval, simultaneous, (E/T), 25:2977
development of elementary ionospheric polar cap, (E), 25:2978
effect on ionospheric seasonal variations, (E/T), 25:2966
effect on nighttime auroral electrojets, daytime polar cap, (E), 25:2978
effects of midlatitude bays on auroral absorption, (E), 25:2964
effects on 0.06 to 3.3 MeV proton distribution at 6.6 Earth radii, Oct. 2 and 13, 1968, (E), 25:2951 (AD-709723)
effects on flux distribution of 0.1- to 1.0-MeV magnetospheric electrons and protons, June 9, 1968, (E), 25:2950 (AD-709363)
intensity dependence on recurrence of, relation to solar activity, (E/T), 25:2998
polar sub--, meridional motion of auroral, (e), 25:2979
MAGNETOHYDRODYNAMIC GENERATORS
design for space vehicles, review of, 25:2600 (BNL-50258)
efficiency of condensation-type liquid-metal, effect of type working substance on, (E/T), 25:2937
electrode operation in, properties of, 25:2940
fluid resistivity in, optimum distribution of, (T), 25:2933
ionizing additive for, turbulent washer for recycle of potassium carbonate, 25:2939
performance of combustion-driven, effects of molybdenum electrode size on, 25:2398
plasma instability with boundary effects in, linear development of electrothermal, (T), 25:3127
power plant analysis using, and thermocompressor, 25:2936
thermal cycle for direct-flow supersonic compressorless, 25:2935
MAGNETOHYDRODYNAMICS
conference on engineering aspects of, tenth, Cambridge, Mass., 3/69, 25:2945
MAGNETOMETERS
equations for rotating-coil, 25:2512
MAGNETOPAUSE
current system of, production of variations in geomagnetic field from, (E/T), 25:2955
MAGNETOSPHERE
boundary of, geographic longitude dependence of distance to, (E/T), 25:2980
flux distribution of electrons and protons with energies between 0.1 and 1.0 MeV in, during magnetic storm, June 9, 1968, (E), 25:2950 (AD-709363)
hydromagnetic wave propagation in, spectrum of one-dimensional Alfven, (T), 25:2970
hydromagnetic-wave propagation in, nonlinear frequency shift of, (T), 25:3004
plasma instabilities in, mutually reacting drift-wave and high-frequency, (E/T), 25:2948 (AD-709200)
proton energy distribution of 0.06 to 3.3 MeV energies at 6.6 Earth radii, Oct. 2 to 13, 1968, (E), 25:2951 (AD-709723)
thermal coupling to upper ionospheric F2 layer, relation of heat fluxes and energy production to, (E), 25:2956
MAGNETOTAIL
effect on world-wide variations in magnetic field, statistics of, 25:2958
magnetic field calculations in constant-radius cylindrical, (T), 25:2960
magnetic fields in neutral sheet of, distribution of, (E/T), 25:2982
MAGNETS
design of high current septum, for beam injection, extraction, or splitting, 25:3522
design of superconducting 2-tesla, for beam bending, 25:3504
design of superconducting, for Omega spark chamber, 25:2492
design of superconducting, for synchrotrons, 25:3512
design of superconducting, for ZGS beam line, 25:3505
development and use of pulsed superconducting, in synchrotrons, 25:3511
development of superconducting dc, for beam transport, 25:3510
development of superconducting pulsed, for synchrotrons, 25:3510
development of superconducting, for synchrotrons, 25:3514
operation of superconducting, in persistent mode, lift force from, (T), 25:3038
power supply for superconducting synchrotron, 25:3513
power supply for superconducting, superconducting current step-up transformer for, 25:3509
refrigeration system for superconducting, helium, 25:3508
MAINE YANKEE POWER REACTOR
effluents from, effects on environment of chemical, radioactive, and thermal, 25:3837 (DOCKET-50309-25)
operations of, administrative controls of, 25:3836 (DOCKET-50309-24)
personnel for, qualifications and responsibilities of, 25:3836 (DOCKET-50309-24)
MALEIC ACID
effects on mechanism of γ-radioinduced graft polymerization of poly(ethylene terephthalate), 25:2244
MALIC ACID
complexes with trivalent indium and hexavalent uranium, potentiometric, solvent extraction, and spectrophotometric studies on, 25:2206
MAMMALIA
thyroid hormone secretion and utilization rates in, iodine-131 tracer study of factors effecting, 25:3945(R) (COO-1758-27)
thyroid hormone secretion and utilization rates in, iodine-131 tracer study of factors affecting, 25:3944(R) (COO-1758-26)
MAN
anatomy of lungs in, use of γ transmission scanning to determine, 25:2580
blood platelet life span in, tracer methods for measurement of, 25:2579
body fluid compartments of, use of bromine-82, chromium-51, iodine-125, and tritium for simultaneous determination of, technique for, 25:2518
calcium-47 retention in, with intestinal malabsorption, 25:2531
mercury-203 distribution in, after oral intake, whole-body counting of, 25:2533
mineral metabolism in, conference on activation analysis in studies on, 25:2122 (IAEA-122)
radiation dose to tissues of, in Moscow region during 1962 to 1966, fallout, 25:2550
radiation effects on DNA in xeroderma pigmentosum cells of, repair synthesis following uv, 25:2567
radiation effects on, following use of Thorotrast for diagnosis, 25:2583
radiotherapy of tumors in, effectiveness of fast neutron, 25:2582 (CONF-700322-, pp 393-406)
sorption of chromium-51-labeled EDTA by, with ulcerative colitis, 25:2534
transplantation antigens in, review of genetics of, 25:2537
MANGANESE
abundance in Kappa Cancri, (E), 25:2840
analysis for uranium using permanganate, potentiometric, 25:2099
determination following nonsulfide separation from elements, qualitative, 25:2101
determination in biological materials by 14-MeV neutron and thermal neutron activation, sensitivity of, 25:2125 (IAEA-122, pp 27-36)
determination in human liver by neutron activation and γ spectrometry, 25:2124 (IAEA-122, pp 15-26)
determination in human tissues by thermal neutron activation, sensitivity of, 25:2123 (IAEA-122, pp 1-13)
determination in molybdenum or yttrium by neutron activation and extraction displacement chromatography, 25:2138
determination in phosphate and sulfate solutions by electrogeneration of trivalent vanadium, coulometric titration, 25:2081
determination in presence of cerium, chromium, iron, and vanadium by differential potentiometric titration, 25:2099
determination in silicate rocks by neutron activation and radiochemical group separation, 25:2149
determination in soils in Pakistan by neutron activation and radiochemical separation, 25:2125 (IAEA-122, pp 27-36)
determination in titanium alloys, x-ray fluorescence method for, 25:2097
determination of trace amounts of, in nuclear-grade uranium oxide (U_3O_8) by direct reading spectrometric method, 25:2068 (NLCO-1071)
determination of trace amounts of, using permanganate, colorimetric, 25:2073
effects on determination of trace amounts of antimony by isotopic exchange in organic phase, 25:2106
effects on extraction--photometric determination of niobium in steel, 25:2085
effects on polarographic determination of tellurium, 25:2090
effects on uv spectrophotometric determination of gallium in aqueous solutions, 25:2100
release to soil from organic debris in forest as function of decomposition mode and time, 25:2528
MANGANESE ALLOYS AND SYSTEMS
Al--Mn, crystal structure of solid solutions of, 25:2733
F--Mn--Xe, reactions in, compounds produced by, 25:2156
Mn--Ti-base, microstructure of hot-rolled plates and sheets of α + β, relations of mechanical properties with abnormal, 25:2752
Mn--U, phase studies of, using computers, 25:2737
MANGANESE ISOTOPES Mn-53
energy levels and transitions from chromium-52 (p,γ) reactions, properties of low-lying, (E), 25:3617
MANGANESE ISOTOPES Mn-54
fixation by aquatic fauna, flora, and sediments in Meuse River, 25:2544

XUM

release to soil from organic debris in forest as function of decomposition mode and time, 25:2528
transport and deposition of, in flowing sodium, 25:2706
MANGANESE ISOTOPES Mn-55
energy levels from chromium-55 decay, (E), 25:3607
MANY BODY PROBLEM
field theory for nuclear, relativistic nucleon--meson, 25:3719
projection operators in nonequilibrium statistical mechanics, 25:3234
short-range correlations in three-body problem and Faddeev equations, 25:3731
MARITIME PRESSURIZED-WATER REACTOR
cooling system for, information on furnace sensitized stainless steel components of, 25:3917 (DOCKET-50238-74)
MARS (PLANET)
ionosphere of, boundary determination by solar wind flow past, (E/T), 25:2878
MASS SPECTROMETERS
design for diagnostics of highly-ionized steady-state plasma, 25:3063
design of computerized fully automatic analytical, 25:3999 (UCRL-50931(Pt.1))
performance of time-of-flight, for alpha particles and heavy ions, 25:2469
MATERIALS TESTING
methods for mechanical properties of irradiated fuel cladding materials, 25:2755 (BMI-1889, Sect.B)
MATERIALS TESTING ACCELERATORS
design of electron linac, 25:3483
MATERIALS TESTING REACTOR
core for, physics measurements for plutonium--aluminum alloy fueled Phoenix, (E/T), 25:3902 (BNWL-1514)
MATHEMATICAL PHYSICS
energy--momentum conservation for collision, creation, and annihilation processes, (T), 25:3243
Lie series in, applications of, 25:3236
MATHEMATICAL TABLES
designed for determination of frequencies of mutations, 25:2559
MATHEMATICS
self-adjoint algebras of unbounded operators, 25:3968 (NYO-2171-325)
MECHANICS
transition from nonrelativistic quantum to classical, 25:3935(T) (BNL-tr-354)
MEDICINE
book: Annual Review of Medicine, 25:2575
research program in Philippines using neutron activation analysis, 25:2126 (IAEA-122, pp 37-40)
MERCURY
abundance in Kappa Cancri, (E), 25:2840
compounds, analysis for mercury in presence of mercury-203-labeled organic compounds by reactions with stannous chloride and γ scintillation counting, 25:2109
determination by neutron activation, sample preparation by deposition on plastic matrix for, 25:2146
determination following nonsulfide separation from elements, qualitative, 25:2101
determination in inorganic compounds in presence of mercury-203-labeled organic compounds by reactions with stannous chloride and γ scintillation counting, 25:2109
determination in molybdenum or yttrium by neutron activation and extraction displacement chromatography, 25:2136
determination in pigments from ancient murals by neutron activation, 25:2133
effects on determination of trace amounts of antimony by isotopic exchange in organic phase, 25:2106
effects on uv spectrophotometric determination of gallium in aqueous solutions, 25:2100
flow in boilers, review of x-ray evaluation of, 25:2600 (BNL-50258)
plasma of, anti-drift waves in positive column, (E/T), 25:3163
superconducting condensation energy calculation, 25:3046
MERCURY (PLANET)
perihelion precession of, heuristic derivation of, (T), 25:3291
MERCURY ALLOYS AND SYSTEMS
Hg--In, Hall coefficients of liquid, comparison with fluctuation scattering model, 25:3209
Hg--Tl, Hall coefficients of liquid, comparison with fluctuation scattering model, 25:3209
MERCURY ISOTOPES Hg-197
effectiveness for localization of tumors in posterior fossa of human brain, computer evaluation of, 25:2578
electron-capture decay of isomeric, gamma spectra from, (E), 25:3682
MERCURY ISOTOPES Hg-203
distribution in man after oral intake, whole-body counting of, 25:2533
effectiveness for localization of tumors in posterior fossa of human brain, computer evaluation of, 25:2578
effects of organic compounds containing, on determination of inorganic mercury by reactions with stannous chloride and γ scintillation counting, 25:2109
MERCURY NITRATES
deposition on plastic matrix for neutron activation analysis, 25:2146
MERCURY OXIDES
deposition on plastic matrix for neutron activation analysis, 25:2146
MESIC ATOMS
energy-level shifts and widths of π⁻, optical potential for, 25:2897
x-ray spectra from barium-138, cerium-140, and cerium-142 π⁻, 4f - 3d, (E), 25:2896
MESIC MOLECULES
meson (μ⁺) chemical shifts in diatomic halide, 25:2899
MESONS
decay widths of, linear and nonlinear models in effective-Lagrangian approach for electromagnetic, 25:3316
interactions with $^1/_2^+$ baryons, quark model for ambiguities in transversity amplitudes for vector meson and $^3/_2^+$ resonance production in, (T), 25:3382 (TPJU-1/70)
interactions with $^1/_2^+$ baryons, quark model for ambiguities in transversity amplitudes for pseudoscalar meson and $^3/_2^+$ resonance production in, (T), 25:3382 (TPJU-1/70)
interactions with baryons at high energies, γ_5 gauge invariance for helicity conservation in, (T), 25:3403
interactions with baryons in broken SU(3), baryon spectra from partial-wave amplitudes for, (T), 25:3397
interactions with baryons, additive quark model for polarization of Λ and Σ in two-body pseudoscalar meson and Y* production in, (T), 25:3383 (TPJU-2/70)
interactions with baryons, additive quark model for polarization of Λ and Σ in two-body vector meson and Y* production in, (T), 25:3383 (TPJU-2/70)
interactions with baryons, algebra of vertex strengths for analysis of Serpukhov total cross section data for, 25:3385
interactions with baryons, exchange degeneracy with SU(3) symmetry and absorptive corrections for hypercharge-exchange, 25:3388
interactions with baryons, hard-pion method for four-point functions for, (T), 25:3401
interactions with mesons at high energies, γ_5 gauge invariance for helicity conservation in, (T), 25:3403
interactions with nucleons in SU(3) quark model, vector-meson production in, (T), 25:3400
interactions with nucleons, phenomenological model for violation of Pomeranchuk theorem for, 25:3356
photoproduction at high energies, review on, 25:3315
production in N + N interactions, Poisson distribution of secondary particles in straight-line approximation for, (T), 25:3407 (JINR-E2-5329)
production of heavy, in anti p + p interactions, research at Univ. of California Oct. 1, 1969 to Sept. 30, 1970 on, (E), 25:3261(R) (UCI-34-P-149-1)
production of pseudoscalar, in γ + N interactions, SU(3) quark model for, (T), 25:3321
production of vector, in meson interactions with nucleons, SU(3) quark model for, (T), 25:3400
scale invariance for scalar, 25:3372
MESONS (eta)
decay eta → 2γ, spark-chamber spectrometer study of branching ratio for, (E), 25:3258
decay eta → 3π, nonelectromagnetic violation of isospin, C, CP, and T invariance in, (T), 25:3425
decay eta → 3π⁰, spark-chamber spectrometer study of branching ratio for, (E), 25:3258
decay eta → π⁰ + 2γ, spark-chamber spectrometer study of branching ratio for, (E), 25:3258
decay eta → π⁺ + π⁻ + π⁰ evidence of C violation from asymmetry and background in, (E/T), 25:3254
production in γ + p → p + eta⁰, eta⁰ → 2π interactions at 0.8 to 1.1 GeV, (E), 25:3255
MESONS (K)
decay amplitudes in gauge-field model, S-wave nonleptonic, 25:3341
decay K → 3π in pole model, strength of bilinear weak transitions in, 25:3348
decay K → 3π, chiral-symmetry-breaking corrections to soft-pion theorem for, 25:3347
decay K → π + e⁺ + e⁻, effects of lepton nonlocality in, (T), 25:3337
decay K → π + l + ν, contribution of μ* to form factors of, 25:3350
decay K → π + l + ν, local current commutators for pole-type form factors of, (T), 25:3299
decay K → π + ν + anti ν, effects of lepton nonlocality in, (T), 25:3337
decay K → π + π + l + ν in current algebra, axial-vector form factors for, 25:3345
interactions K + N at 6 to 55 GeV, complex angular momenta theory for, (E/T), 25:3381 (JINR-P2-5320)
interactions K + N, asymptotic conservation of helicity for, 25:3398
interactions K + N, Regge models of asymptotic behavior of amplitudes for forward elastic, 25:3357
interactions K + p, upper bound on imaginary part of amplitude for elastic, 25:3460
interactions K + π, elastic cross section from K⁻ + n → p + K⁻ + π⁻ at 3 GeV/c, (E/T), 25:3278
MESONS (K⁻)
decay K⁻ → 2π⁻ + π⁺, search for CP violation in, (E),

25:3427
decay $K^- \to \pi^- + \pi^- + \pi^+$, wire spark chamber system with on-line computers for studying, 25:2491
interactions $K^- + d \to K^- + \pi^+ + \pi^- + n + p$ at 5.5 GeV/c, cross section for anti $K^{*0}(890)$ and $\Delta^-(1236)$ production in, (E), 25:3274
interactions $K^- + n \to p + K^- + \pi^-$ at 3 GeV/c, Chew--Low extrapolation of $K\pi$ elastic cross section from, (E/T), 25:3278
interactions K^- + N, Regge models of asymptotic behavior of amplitudes for forward elastic, 25:3357
interactions $K^- + p \to K^0 + \pi^- + p$ at 3.3 GeV/c, generalized Veneziano-model fits to, 25:3391
interactions $K^- + p \to n + K^- + \pi^+$ at 10 GeV/c, Veneziano model with π and Pomeron exchange for, (T), 25:3386
interactions K^- + p at 0.293 to 15.910 GeV/c, data compilation on real parts of forward amplitudes of, (E), 25:3379 (JINR-E1-5259)
interactions K^- + p at 3.9 to 5.0 GeV/c in hydrogen bubble chamber, $K^0(1420)$ production in, (E), 25:3287

MESONS (K^0)
decay $K^0 \to e + \pi + \nu$, performance of Cherenkov detector for studying time dependence of, 25:2489
decay $K_1^0 \to 2\pi$ in pole model, strength of bilinear weak transitions in, 25:3348
decay $K_2^0 \to 2\gamma$ in pole model, strength of bilinear weak transitions in, 25:3348
decay $K_2^0 \to 2\pi$, field theory model for CPT nonconservation in, 25:3429
decay of, arrows of time in time reversal violation in, (T), 25:3423
production in $\gamma + p \to \Sigma^+ + K^0$ interactions at 1.5 to 5 GeV, momentum spectra and cross sections for, (E), 25:3248
production in photon reactions with aluminum, beryllium, and copper at 1.5 to 5 GeV, momentum spectra and cross sections for, (E), 25:3248

MESONS (K^+)
decay $K^+ \to 2\pi^+ + \pi^-$, search for CP violation in, (E), 25:3427
decay $K^+ \to \pi^+ + \pi^+ + \pi^-$, wire spark chamber system with on-line computers for studying, 25:2491
interactions $K^+ + p \to K^0 + \Delta^{++}$, Regge pole model with Veneziano residues for, (T), 25:3384 (TPJU-3/70)
interactions $K^+ + p \to K^+ + \pi^- + \pi^+ + p$ at 4.6 and 9 GeV/c in hydrogen bubble chamber, $K^{*0}(890)$ $\Delta^{++}(1236)$ and $K^{*0}(1420)$ $\Delta^{++}(1236)$ double resonance and $\Delta^{++}(1236)\pi^-$ and $K^+\pi^-(1100)$ enhancement production in, (E), 25:3271 (UCRL-19809)
interactions K^+ + p at 0.140 to 14.800 GeV/c, data compilation on real parts of forward amplitudes of, (E), 25:3379 (JINR-E1-5259)
interactions K^+ + p at 3.5 GeV/c, associated production in, (E), 25:3277
interactions K^+ + p below 2.0 GeV/c, phase-shift analysis of elastic, 25:3393
theory for, local current commutators in, (T), 25:3299

MESONS (μ)
interactions μ + p, anomalous interaction for cross section ratio for e + p and, 25:3324
magnetic moment of, anomalous, 25:3324
reactions of cosmic, with nuclei, cloud chamber study of structure functions for, (E), 25:3260
reactions with nuclei at 50 to 100 GeV, coherent, incoherent, and inelastic cross sections for W-meson production in, (T), 25:3340
symmetry with electrons in two-component neutrino theory, 25:3351

MESONS (μ^-)
capture rate in lithium-6, pseudoscalar form factor from PCAC hypothesis, (T), 25:3748
reactions with nuclei at 15.9 GeV in emulsions, structure functions for, (E), 25:3260

MESONS (μ^+)
chemical shifts in diatomic halide molecules, 25:2899
reactions with nuclei at 10.3 GeV in emulsions, structure functions for, (E), 25:3260

MESONS (ω)
coupling constant ratio $\gamma\omega^2/\gamma\text{rho}^2$ from structure of e^+e^- mass spectrum in γ reactions with beryllium at 5.1 GeV, (E), 25:3288
decay $\omega \to e^+ + e^-$, interference with rho $\to e^+ + e^-$ decay, (T), 25:3367
decay $\omega \to e^+ + e^-$, rho--ω phase difference in coherent interference with rho $\to e^+ + e^-$ decay for, (E), 25:3288
decay $\omega \to \pi^+ + \pi^-$ in deuterium bubble chamber, upper limit for rate of, (E), 25:3269
interactions ω + N, cross sections from ω photoproduction on nuclei at 5.7 GeV, (E), 25:3247
interference rho--ω effects on cross sections for $\pi + p \to n + e^+ + e^-$ interactions, (T), 25:3367
production in anti p + n interactions at rest in deuterium bubble chamber, upper limit on $\omega \to \pi^+ + \pi^-$ decay rate from, (E), 25:3269
production in γ + N interactions, phases and forward cross sections for, (T), 25:3319
production in γ reactions with beryllium at 5.1 GeV, structure of e^+e^- mass spectrum for coherent interference between rho and ω decays for, (E), 25:3288
production in photon reactions with nuclei at 5.7 GeV, $\omega\gamma$ coupling constant and ωN cross sections from, (E), 25:3247

MESONS (phi)
production in γ + N interactions, phases and forward cross sections for, (T), 25:3319

MESONS (π)
exchange in diffractive $\gamma + p \to \text{rho}^0 + N + m\pi$ interactions at 5 to 100 GeV, (T), 25:3308 (DESY-70/45)
form factor with dipion unitarity, construction of electromagnetic, 25:3330
interactions K + π, elastic cross section from $K^- + n \to p + K^- + \pi^-$ at 3 GeV/c, (E/T), 25:3278
interactions $\pi + A_1 \to \pi + A_1$, Veneziano amplitudes for, 25:3374
interactions $\pi + A_1 \to \pi + \pi + \pi$, Veneziano amplitudes for, 25:3374
interactions $\pi + d \to N + N$, relativistic dispersion theory of deuteron structure from amplitudes for, (T), 25:3409
interactions $\pi + N \to \pi + \pi + N$ at high energies, Regge-pole model for, 25:3399
interactions $\pi + N \to \pi + \pi + N$, factorization test for Pomeranchukon in, 25:3395
interactions $\pi + N \to \pi + \text{rho} + N$ at high energies, Regge-pole model for, 25:3399
interactions π + N above 5 GeV/c, absorptive model corrections to Regge pole exchange in, 25:3390
interactions π + N at 6 to 55 GeV, complex angular momenta theory for, (E/T), 25:3381 (JINR-P2-5320)
interactions π + N at high energies, γ_5 gauge invariance for helicity conservation in, (T), 25:3403
interactions π + N, asymptotic conservation of helicity for, 25:3398
interactions π + N, complex Regge poles in cut j plane for charge exchange, (T), 25:3402
interactions π + N, duality concept for Pomeranchuk term for, 25:3375
interactions π + N, fixed-u finite-energy sum rule calculations of, 25:3396
interactions π + N, on-shell subtracted dispersion relations and low-energy theorems and sum rules from current algebra for, (T), 25:3368
interactions π + N, Regge models of asymptotic behavior of amplitudes for forward elastic, 25:3357
interactions π + N, sum rules and symmetries for, 25:3387
interactions π + N, t-channel peculiarities in static model of s waves in, (T), 25:3380 (JINR-P2-5263)
interactions $\pi + p \to n + e^+ + e^-$, rho--$\omega$ interference effects on cross sections for, (T), 25:3367
interactions $\pi + p \to \pi + \text{eta} + n$ at high energies, Regge-pole model for, 25:3399
interactions π + p, upper bound on imaginary part of amplitude for elastic, 25:3460
interactions $\pi + \pi$ at low energies, unitary and crossing-symmetric S-, P-, and D-wave, 25:3369
interactions $\pi + \pi$ on mass shell, current algebra evaluation of scattering lengths for, 25:3371
interactions $\pi + \pi$, consistency of model for subthreshold, 25:3457
interactions $\pi + \pi$, crossing-symmetric amplitude for Pomeranchuk trajectory, 25:3365
interactions $\pi + \pi$, duality concept for Pomeranchuk term for, 25:3375
interactions $\pi + \pi$, off-shell extension of Veneziano amplitude for, 25:3373
interactions $\pi + \pi$, on-shell subtracted dispersion relations and low-energy theorems and sum rules from current algebra for, (T), 25:3368
interactions $\pi + \pi$, P-wave phase shift for, 25:3330
interactions $\pi + \pi$, S-wave phase shift from $\pi^- + p \to \pi^0 + \pi^0 + n$ interactions at 378 MeV in isobar model, 25:3392
photoproduction of, continuous moment sum rules for, (T), 25:3327
production in $e + N \to \pi + N$ interactions, on-shell subtracted dispersion relations and low-energy theorems and sum rules from current algebra for, (T), 25:3368
production in γ + p interactions in second resonance region, isobar model analysis of single, 25:3313
production in inelastic interactions, statistical distribution of multiple, 25:3370
production of many-body system of, analysis of, 25:3364
vertex functions for $\pi\text{rho}A_1$ system phenomenological current algebra, 25:3376
vertex structure of $A_1\text{rho}\pi$, hard-pion calculation without current algebra for, 25:3361

MESONS (π^-)
interactions in nuclear emulsions at 20 GeV/c, energy estimations from angular distribution of secondaries in, (E), 25:3284
interactions π^- + e at 16.2 GeV/c in nuclear emulsion, absolute cross sections for, (E), 25:3253
interactions π^- + N, dispersion relations for structure of backward differential cross sections of, (T), 25:3377 (ITF-70-65)
interactions $\pi^- + p \to A_2^0 + n$ at 3.16 GeV, structure in A_2^0 mass spectrum in, (E), 25:3290
interactions $\pi^- + p \to \gamma + n$ and $\pi^- + p \to \pi^0 + n \to n + \gamma + \gamma$ at 40 MeV, gamma spectra for, (E), 25:3550

interactions $\pi^- + p \to \Lambda + K^+ + \pi^-$, five-point Veneziano amplitude for cross sections and effective-mass and angular distributions for, (T), 25:3378 (ITF-70-77)
interactions $\pi^- + p \to p + \pi^- + \pi^+ + \pi^-$ at 3.9 GeV/c, spin--parity analysis of 3π system in, (E), 25:3276
interactions $\pi^- + p \to p(n) + K^0 + K^-$(anti K^0), five-point Veneziano amplitude for cross sections and effective-mass and angular distributions for, (T), 25:3378 (ITF-70-77)
interactions $\pi^- + p \to \pi + \pi + N$ at 456 to 552 MeV/c, isobar analysis of, (E), 25:3282
interactions $\pi^- + p \to \pi^0 + \pi^0 + n$ at 378 MeV in isobar model, S-wave $\pi\pi$ phase shift from, 25:3392
interactions $\pi^- + p \to \pi^- + \Delta^+$, Regge pole model with Veneziano residues for, (T), 25:3384 (TPJU-3/70)
interactions $\pi^- + p \to \pi^- + p$ at 1.71 to 3.01 GeV/c, evidence for existence of N(2210) and N(2220) from, (E/T), 25:3281
interactions $\pi^- + p \to \pi^- + p$ at 1.71 to 5.53 GeV/c, differential cross sections for, (E), 25:3280
interactions $\pi^- + p \to \pi^- + rho + p$ at 25 GeV/c, multi-Regge theory for kinematics and dynamics of, 25:3389
interactions $\pi^- + p \to \Sigma^0 + K^+ + \pi^-$, five-point Veneziano amplitude for cross sections and effective-mass and angular distributions for, 25:3378 (ITF-70-77)
interactions $\pi^- + p \to \Sigma^0(A) + K^0 + \pi^0$, five-point Veneziano amplitude for cross sections and effective-mass and angular distributions for, (T), 25:3378 (ITF-70-77)
interactions $\pi^- + p$ above 5 GeV/c, absorptive model corrections to Regge pole exchanges in elastic and charge-exchange, 25:3390
interactions $\pi^- + p$ at 7 and 25 GeV/c in bubble chamber, difference in energy dependence for A_2^- and A_2^0 production in, (E), 25:3289
interactions $\pi^- + p$, experimental comparison between on- and off-mass-shell inelasticities in, 25:3285
production in $\gamma + N \to \pi^- + \Delta^{++}$ interactions, conspiracy and duality in model for forward cross sections of, (T), 25:3318
reactions (π^-,γ) with carbon-12 at 40 MeV, gamma spectra from, (E), 25:3550
reactions (π^-,rho$^-$) and (π^-,rho^0) with A = 20 to 208 nuclei at 30 GeV, Glauber multiple scattering calculations for coherent and incoherent, (T), 25:3406 (IFVE-STF-69-71)

MESONS (π^0)
interactions $\pi^0 + p \to \pi^0 + p$, Bjorken limit and Jin--Martin lower bound for, (T), 25:3294 (NYO-4204-5)
interactions $\pi^0 + \pi^0$, lower bound for scattering length for, (T), 25:3360
production in $e + p \to \pi^0 + n$ interactions at threshold, neutron electromagnetic form factors from, (E), 25:3244
theory for, local current commutators in, (T), 25:3299

MESONS (π^+)
interactions $\pi^+ + d \to p + p + \pi^+ + \pi^- + \pi^0$ at 3.65 GeV/c, evidence for H enhancement in, (E), 25:3286
interactions $\pi^+ + d$ at 7 GeV/c in bubble chamber, difference in energy dependence for A_2^- and A_2^0 production in, (E), 25:3289
interactions $\pi^+ + N$, dispersion relations for structure of backward differential cross sections of, (T), 25:3377 (ITF-70-65)
interactions $\pi^+ + p \to p + 2\pi^+ + \pi^- + \pi^0$ at 3.7 GeV/c, A_2^0 and Δ^{++} associated production in, (E), 25:3272 (UCRL-20050)
interactions $\pi^+ + p \to \pi^0$(eta) + Δ^{++}, Regge pole model with Veneziano residues for, (T), 25:3384 (TPJU-3/70)
interactions $\pi^+ + p \to \pi^+ + p + \pi^+ + \pi^-$ at 5 GeV/c, analysis of $p\pi\pi(1710)$ enhancement in, (E), 25:3275
interactions $\pi^+ + p \to \pi^+ + \pi^- + \Delta^{++}$ at 13.1 GeV/c, double-Regge pole analysis of, (E/T), 25:3273
interactions $\pi^+ + p \to \Sigma^+ + K^+$ at 1850 to 2090 MeV, angular distributions, polarization, and partial-wave analysis for, (E), 25:3283
interactions $\pi^+ + p$ at 5.5 GeV/c, production of Λ(1236), Σ(1385), and K^*(890) in, (E), 25:3279
interactions $\pi^+ + \Sigma^- \to \pi^- + \Sigma^+$ with exotic crossed state, sum rules for, 25:3404
production in $\gamma + N \to \pi^+ + \Delta^-$ interactions, conspiracy and duality in model for forward cross sections for, (T), 25:3318

MESONS (rho)
coupling constant ratio $\gamma\omega^2/\gamma\mathrm{rho}^2$ from structure of e^+e^- mass spectrum in γ reactions with beryllium at 5.1 GeV, (E), 25:3288
decay rho $\to 2\pi$, current algebra vertex function for, (T), 25:3376
decay rho $\to e^+ + e^-$, interference with $\omega \to e^+ + e^-$ decay, (T), 25:3367
decay rho $\to e^+ + e^-$, rho--ω phase difference in coherent interference with $\omega \to e^+ + e^-$ decay for, (E), 25:3288
decay width of, derivation of KSRF relation for rho$\pi\pi$ coupling constants and, 25:3363
interaction vertex for NNrho, Schwinger and sea-gull terms in parity-violating weak, 25:3338
interactions rho + N, cross sections from rho photoproduction on nuclei in Glauber theory, 25:3317
interactions rho + N, phase of rho production amplitude in γ reactions with beryllium at 4.1 to 6.1 GeV for real-to-imaginary amplitude ratio for, (E), 25:3256
interference rho--ω effects on cross sections for $\pi + p \to n + e^+ + e^-$ interactions, (T), 25:3367
production in $\gamma + N$ interactions, phases and forward cross sections for, (T), 25:3319
production in $\gamma + p \to$ rho$^0 + p$ interactions, rho mass shift in, 25:3326
production in γ reactions with beryllium at 4.1 to 6.1 GeV, real-to-imaginary amplitude ratio for rho + N interactions from phase of, (E), 25:3256
production in γ reactions with beryllium at 5.1 GeV, structure of e^+e^- mass spectrum for coherent interference between rho and ω decays for, (E), 25:3288
production in meson (π^-,rho$^-$) and (π^-,rho^0) reactions with A = 20 to 208 nuclei at 30 GeV, Glauber multiple scattering calculations for coherent and incoherent, (T), 25:3406 (IFVE-STF-69-71)
production of rho^0 in $\gamma + d \to d(p + n) + \pi^+ + \pi^-$ interactions at 1 to 5 GeV in bubble chamber, differential and total cross sections for, (E), 25:3246
production of rho^0 in $\gamma + p \to$ rho$^0 + N \to m\pi$ interactions at 5 to 100 GeV, double peripheral processes with Pomeron and π exchange in, (T), 25:3308 (DESY-70/45)
vertex functions for πrhoA_1 system phenomenological current algebra, 25:3376
vertex structure of A_1rhoπ, hard-pion calculation without current algebra for, 25:3361

MESONS, RESONANCE
angular-momentum structure in dual resonance models, Bose-gas theory for, (T), 25:3366
decay $A_1 \to$ rho $+ \pi$, consistency condition from uniterized current algebra for, 25:3359
decay $A_1 \to$ rho $+ \pi$, phenomenological current algebra vertex function for, (T), 25:3376
decay K^0(1420) $\to K + 2\pi$ in hydrogen bubble chamber, branching ratio for, (E), 25:3287
decay K^0(1420) $\to K +$ eta in hydrogen bubble chamber, branching ratio for, (E), 25:3287
decay K^0(1420) $\to K + \omega$ in hydrogen bubble chamber, branching ratio for, (E), 25:3287
decay K^0(1420) $\to K + \pi$ in hydrogen bubble chamber, branching ratio for, (E), 25:3287
decay K^0(1420) $\to K +$ rho in hydrogen bubble chamber, branching ratio for, (E), 25:3287
decay K^0(1420) $\to K$(890) $+ \pi$ in hydrogen bubble chamber, branching ratio for, (E), 25:3287
interactions $\pi + A_1 \to \pi + A_1$, Veneziano amplitudes for, 25:3374
interactions $\pi + A_1 \to \pi + \pi$, Veneziano amplitudes for, 25:3374
mass spectrum of A_2^0 in $\pi^- + p \to A_2^0 + n$ interactions at 3.16 GeV, structure in, (E), 25:3290
parity and spin of A_2 from $\pi^- + p \to p + \pi^- + \pi^+ + \pi^-$ interactions at 3.9 GeV/c, (E), 25:3276
production in anti $p + n \to 2\pi^- + \pi^+$ interactions at 1.0 to 1.6 GeV/c in deuterium bubble chamber, Veneziano model for 3π Dalitz plot structure in, (E/T), 25:3270 (INFN-PD-70/2)
production of A_2^0 in $\pi^+ + p \to p + 2\pi^+ + \pi^- + \pi^0$ interactions at 3.7 GeV/c, Δ^{++} production associated with, (E), 25:3272 (UCRL-20050)
production of A_2^- and A_2^0 in $\pi^- + p$ interactions at 7 and 25 GeV and $\pi^+ + d$ interactions at 7 GeV in bubble chamber, difference in energy dependence for, (E), 25:3289
production of anti K^{*0}(890) in $K^- + d \to K^- + \pi^+ + \pi^- + n + p$ interactions at 5.5 GeV/c, cross section for, (E), 25:3274
production of H enhancement in $\pi^+ + d \to p + p + \pi^+ + \pi^- + \pi^0$ at 3.65 GeV/c, (E), 25:3286
production of heavy, in anti $p + p$ interactions, research at Univ. of California Oct. 1, 1969 to Sept. 30, 1970 on, (E), 25:3261(R) (UCI-34-P-149-1)
production of K^*(890) in $\pi^+ + p$ interactions at 5.5 GeV/c, cross sections for, (E), 25:3279
production of K^{*0}(890) Δ^{++}(1236) and K^{*0}(1420) Δ^{++}(1236) double resonances and $K^+\pi^-$(1100) enhancement in $K^+ + p \to K^+ + \pi^- + \pi^+ + p$ interactions at 4.6 and 9 GeV/c in hydrogen bubble chamber, (E), 25:3271 (UCRL-19809)
production of K^0(1420) in $K^- + p$ interactions at 3.9 to 5.0 GeV/c in hydrogen bubble chamber, (E), 25:3287
production of, analysis as rescattering effect, (T), 25:3459
spectrum in bound states of anti N + N interactions, relativistic one-boson-exchange model for, (T), 25:3358 (DESY-70/49)
vertex functions for πrhoA_1 system phenomenological current algebra, 25:3376
vertex structure of A_1rhoπ, hard-pion calculation without current algebra for, 25:3361

METAL SPRAYING
method for Bugey reactor fuel element clad bonding, 25:2638 (CEA-CONF-1625)

METALLOGRAPHY
methods for reactor materials, 25:2731 (ORNL-4570, pp 215-23)
model for jogged screw dislocation glide, 25:2728 (ORNL-4570, pp 5-9)
use of topology in, 25:2787 (ORNL-4570, pp 24-6)

METALLURGICAL EQUIPMENT
design for studies of compressive creep in single crystals, 25:2728 (ORNL-4570, pp 5-9)
METALLURGY
research on, uses of high-velocity ions in, 25:2604 (CONF-700322-, pp 155-71)
superconductivity and physical, lecture on, 25:3025
METALS
book: Radiation Corrosion, 25:2603(T) (AEC-tr-7096)
conference on corrosion by liquid, Philadelphia, Oct. 13 to 16, 1969, 25:2615
electron energy at absolute zero, boundary singularities in, (T), 25:3030
electronic states in liquid, approximation for, 25:2671 (ORNL-4570, pp 40-3)
flow measurements of liquid, development of transit time flowmeter for, 25:2500(R) (AI-AEC-12981)
plasma of, formation of heavy negative charged clusters in, (T), 25:3086
proton reactions at 100 to 350 keV with, characteristic spectra and yields per proton of x rays from, (E), 25:2882 (CONF-700322-, pp 113-24)
radiation effects on oxygen desorption from surfaces of high-purity, charged particle, 25:2763
reactions with amines and ammonia, electrochemistry and spectral studies of, 25:3937(R) (COO-958-19)
research programs on, 25:2601(R) (ORNL-4570)
separation from aqueous solutions by solvent extraction using trialkylamines, coalescence of organic solutions in, 25:2308 (CEA-R-3845)
spectra in x--uv range, optical absorption, 25:3948 (DESY-70/48)
spectral emission in solar-disc flares, relation to solar-flare geophysical activity, (E/T), 25:2859
ultrasound generation in, electromagnetic, 25:3967 (NYO-2150-63)
METEORITES
aluminum-26 abundance in three pallasites, (E), 25:2824
analysis for hafnium and zirconium by neutron activation and radiochemical separation, 25:2148
origin of pallasites, (E), 25:2824
potassium-40 abundance in three pallasites, (E), 25:2824
METHACRYLAMIDE
radioinduced graft polymerization with poly(ethylene terephthalate) in presence of fumaric acid, maleic acid, and methylenesuccinic acid, 25:2244
METHACRYLIC ACID
radioinduced polymerization with polyethylene terephthalate, effects of dose and temperature on mechanism of γ, 25:2240
METHACRYLIC ACID, METHYL ESTER, POLYMERS
radiation dose conversion factor for, 25:2569
radiation effects on properties of, fast electron, 25:2225
METHACRYLONITRILE
radiation effects on electric conductivity of solid, at -196°C, γ, 25:2221
METHANE
determination in products from radiolysis of gaseous ethylene, gas chromatographic method for, 25:2278
effects on gaseous yields from γ radiolysis of poly(tetrafluoroethylene), 25:2261 (NP-18518)
neutron scattering properties of, 25:3904 (IJS-571)
pyrolysis in fluidized bed fuel particle coating furnace, 25:2151 (DP-Report-569)
radiolysis of, apparatus for studying deposition of carbon from γ, 25:2263 (RD/B/N-1748)
yields from γ radiolysis of mixtures of octane with benzene, 1,3-cyclooctadiene, or cyclooctatetraene, kinetics of production of, 25:2270
yields from γ radiolysis of poly(tetrafluoroethylene), effects of gaseous additives on, 25:2261 (NP-18518)
Br--methane, bromine-80m isomeric transition in, yields of labeled bromomethane from, 25:2226
cyclobutane--methane, radiolysis of, isomerization of butyl ions in γ, 25:2290
HBr--methane, bromine-80m isomeric transition in, yields of labeled bromomethane from, 25:2226
METHANE, BROMO-
yields of bromine-80-labeled, from bromine-80m isomeric transition in bromine--methane and hydrobromic acid--methane systems, 25:2226
METHANE, IODO-
radiolysis in air at 15°C, γ, 25:2269
METHANETHIOL
effects on gaseous yields from γ radiolysis of poly(tetrafluoroethylene), 25:2261 (NP-18518)
METHANOL
effects on radiolysis of ammonia, 25:2283
neutron scattering properties of, 25:3904 (IJS-571)
METHIONINE
synthesis by Escherichia coli, regulating factors in, 25:4002(T) (UCRL-Trans-10487)
MICE
dust inhalation by, tracer technique using air pollution reproducer for studying, 25:2523
immunization against Babesia rodhaini using γ-irradiated infected erythrocytes, 25:2539
radiation effects on antibody formation in, effects of carbon blockage of reticulo-endothelial system on, 25:2538
radiation effects on maternal, effects of, on germ cells of progeny in relation to age, x, 25:2593
radioinduced chromosome aberrations in spermatocytes of, following exposure of spermatogonia, frequency of x, 25:2553
radioinduced inhibition of urethan adenomagenesis in lungs of, role of thymus in x, 25:2589
transplantation antigens in, review of genetics of, 25:2537
MICROSCOPY
methods for televised, 25:2731 (ORNL-4570, pp 215-23)
MICROWAVES
absorption by magnetized low-density plasma, heating and ionization by harmonic cyclotron, (E), 25:3145 (CEA-CONF-1607)
cosmic background, and anomalies in Lemaitre model, (T), 25:2869(T) (CSIRO-Trans-10207)
cosmic background, anisotropy and inhomogeneity in, (T), 25:2876
cosmic background, relation to electromagnetic radiation from normal galaxies, (T), 25:2868
performance for plasma diagnostics, 25:3069
MIDLAND POWER REACTOR, UNIT 1
safety evaluation of, Division of Reactor Licensing, 25:3840 (DOCKET-50329-24)
MIDLAND POWER REACTOR, UNIT 2
safety evaluation of, Division of Reactor Licensing, 25:3840 (DOCKET-50329-24)
MIHAMA POWER REACTOR, UNIT 1
construction of, review of, 25:3779
seismic design of components of, review of, 25:3779
MIHAMA POWER REACTOR, UNIT 2
seismic design of components of, review of, 25:3779
MILK
analysis for iodine by neutron activation and γ spectrometry, 25:2124 (IAEA-122, pp 15-26)
decontamination of, performance of Polish-made ion exchangers for, 25:2329
separation of cesium-134, strontium-85, and strontium-89 from, performance of Polish-made ion exchangers for, 25:2329
separation of strontium-90 from, by sorption on alkali metal or alkaline earth salts of phytic acid, 25:2346(P)
MILLSTONE POINT POWER REACTOR, UNIT 1
operations incident of November 8, 1970, safety analysis of gas turbine generator test failure, 25:3789 (DOCKET-50245-42)
MINERAL DEPOSITS
prospecting for ocean floor, design of radiometric well logging equipment for, 25:2357(P)
MINERALS
analysis for cesium, cobalt, hafnium, scandium, and tantalum by neutron activation and γ spectrometry, 25:2139
analysis for hafnium and zirconium using 8-hydroxy-7-[(2-hydroxy-3,5-dinitrophenyl)-azo]-1,6-naphthalenedisulfonic acid, photometric, 25:2084
MISCH METAL
analysis for neodymium and praseodymium as chlorates, nitrates, or perchlorates, photometric, 25:2077
MITOSIS
radioinduced delay of, in cultured Chinese hamster ovary cells, uv, 25:2558
MIXER-SETTLERS
performance of multistage, computer analysis of, 25:2384 (CEA-CONF-1579)
MOESSBAUER EFFECT
line shift in metallic iron, correction by annealing, 25:3224
MOESSBAUER SPECTROMETERS
resolution of coincidence, 25:2483
MOLECULES
book: Methods of Molecular Quantum Mechanics, 25:2927
reactions with atoms, charged particles, and molecules, bibliography for 1969 on, 25:2901 (ORNL-AMPIC-13)
reactions with molecular ions, cross sections for resonance charge exchange in, (T), 25:2912
MOLLUSCA
Anodonta cygnea, cesium-137 uptake by, in model system, statistical analysis of effects of age, light, and temperature on, 25:2525
fission products transport in freshwater, quantitative model for, 25:2548
radioisotope uptake by aquatic, effects of concentration in water on concentration factor for fallout, 25:2548
MOLTEN SALT BREEDER REACTOR
fuel reprocessing for, flowsheets for, 25:2313 (ORNL-4572, pp 1-36)
performance of, computer program for determining effects of processing plant variables on, 25:2313 (ORNL-4572, pp 1-36)
MOLTEN SALT REACTOR EXPERIMENT
fuel reprocessing for, distillation for, 25:2313 (ORNL-4572, pp 1-36)
materials for, post operational evaluation of, 25:2609 (ORNL-4570, pp 175-90)
MOLYBDENUM
analysis for metallic impurities by neutron activation and extraction displacement chromatography, 25:2138
analysis for sulfur by thermal neutron activation and radiochemical separation, 25:2136

XUM

analysis for trace amounts of carbon, conductometric method for, 25:2071
corrosion resistance to lithium at 600 and 900°F, 25:2626
crystal structure of cast, effects of carbon additions on, 25:2745
crystal structure of cast, effects of zirconium carbide additions on, 25:2743
crystal structure of polycrystalline cast, 25:2744
crystallization of hydroextruded, effects of annealing on, 25:2747
deformation of monocrystalline, annealing recovery of, 25:2746
determination in ambient air using thiocyanate, tentative spectrophotometric method for, 25:2103
determination in human tissues by thermal neutron activation, sensitivity of, 25:2123 (IAEA-122, pp 1-13)
determination in sodium chloride solutions by catalytic amalgam method, 25:2080
determination in titanium alloys, x-ray fluorescence method for, 25:2097
determination in uranium alloys by atomic absorption spectrophotometry, 25:2065 (LA-4529)
determination of trace amounts of, in nuclear-grade uranium oxide (U_3O_8) by direct reading spectrometric method, 25:2068 (NLCO-1071)
effects on brazing of silicon oxide with copper--silver alloy using composite film method, 25:2652
effects on determination of trace amounts of antimony by isotopic exchange in organic phase, 25:2106
effects on determination of trace amounts of rhenium by thiocyanate--stannous chloride method, 25:2102
effects on extraction--photometric determination of niobium in steel, 25:2085
effects on photometric determination of hafnium and zirconium in geological specimens, 25:2084
effects on polarographic determination of tellurium, 25:2090
effects on uv spectrophotometric determination of gallium in aqueous solutions, 25:2100
elastic properties and internal friction of hydroextruded, effects of annealing on recovery of, 25:2698
elasticity and internal friction of hydroextruded, effects of impurities on, 25:2697
fabrication of packed columns of, for purification of molten salt mixtures, 25:2609 (ORNL-4570, pp 175-90)
ion reactions at 5 to 50 keV with, apparent total ion scattering, secondary electron emission coefficients, and electron and ion energy distributions for, (E), 25:2884 (NP-18490)
mechanical properties at 290 to 1870°K, effects of deformation rate on, 25:2681
neutron cross sections for, 25-group, (T), 25:3530 (LA-4484)
neutron elastic scattering at 1 to 40 keV, analysis of angular distributions from, (E/T), 25:3695
oxidation at 1100 to 2000°K, rotating disk method for studying convective-diffusion limited, 25:2686
plasticity of cast, effects of carbon and thermal treatments on, 25:2702
properties for use in curium-244 oxide fuel capsules, 25:2643 (ORNL-4570, pp 106-11)
separation by solvent extraction using dialkylmethylbenzylammonium salts, 25:2328
separation of cerium, gadolinium, lanthanum, and neodymium from, by precipitation using cupferron, 25:2078
solubility in potassium at 1012 to 1341°K, 25:2714
work softening in polycrystalline, 25:2724

MOLYBDENUM ALLOYS AND SYSTEMS
Al--Mo--Sn--Zr-base, corrosion by sodium at 450°C, effects of oxygen on, 25:2611 (PEL-201)
Al--Mo--Ti-base--V, microstructure of hot-rolled plates and sheets of $\alpha + \beta$, relations of mechanical properties with abnormal, 25:2752
Cr--Fe-base--Mo, welding to Incoloy 800 using Inconel 82 filler metal, corrosion by steam at 1100 to 1200°F of welds produced by, 25:2636
Cr--Mo--steel, creep at 900 to 1100°F and 8000 to 25,000 psi stress, 25:2755 (BMI-1889, Sect.B)
Cr--Mo--Ti-base, corrosion resistance of, potentiometric method for studies of effects of chromium on, 25:2613
Cr--Mo-base, crystal structure of dilute cast, effects of carbon additions on, 25:2745
Fe--Mo, analysis for trace amounts of carbon, conductometric method for, 25:2071
Mo--Nb--Zr, diffusion in, activation energy for, 25:2704
Mo--Nb-base, tensile properties at 20 to 1600°C and 10^{-5} torr, effects of traces of carbon and zirconium on, 25:2682
Mo--Ni-base, carburization of, relations with hardness, 25:2716
Mo--Re, properties for use in reactor components, review of, 25:2647
Mo--Ta-base, elastic properties of monocrystalline, at 80 to 1400°K, 25:2721
Mo--Ti-base, corrosion resistance of, potentiometric studies of, 25:2613
Mo--U-base, development and testing for Army Pulsed Radiation Facility Reactor fuel, 25:2645 (ORNL-4570, pp 214)
Mo--U-base, precipitation in, effects of cooling rate on continuous and discontinuous, 25:2738
Mo--V-base, corrosion by sodium at 600°C, effects of molybdenum content on, 25:2606 (ORNL-4570, pp 92-5)
Mo--W-base, creep rupture of arc-melted, stress--strain curves for, 25:2673 (ORNL-4570, pp 118-23)
Mo--Zr, diffusion in, activation energy for, 25:2704
Mo--ZrO_2, mechanical properties of low-porosity corrosion-resistant, effects of chromium on, 25:2796
Mo-base--Zr, crystal structure of dilute cast, effects of carbon additions on, 25:2745

MOLYBDENUM ISOTOPES Mo-92
helium-3 reactions (He-3,d) at 24 MeV, energy spectra at 30° and cross sections for analog states from, (E), 25:3666
spectra of, isotope shifts in muonic x-ray, (E), 25:3620

MOLYBDENUM ISOTOPES Mo-94
helium-3 reactions (He-3,d) at 24 MeV, energy spectra at 30° and cross sections for analog states from, (E), 25:3666

MOLYBDENUM ISOTOPES Mo-95
spectra of, isotope shifts in muonic x-ray, (E), 25:3620

MOLYBDENUM ISOTOPES Mo-96
helium-3 reactions (He-3,d) at 24 MeV, energy spectra at 30° and cross sections for analog states from, (E), 25:3666
spectra of, isotope shifts in muonic x-ray, (E), 25:3620

MOLYBDENUM ISOTOPES Mo-97
spectra of, isotope shifts in muonic x-ray, (E), 25:3620

MOLYBDENUM ISOTOPES Mo-98
helium-3 reactions (He-3,d) at 24 MeV, energy spectra at 30° and cross sections for analog states from, (E), 25:3666

MOLYBDENUM ISOTOPES Mo-106
decay and energy-level transitions following californium-252 fission, (E), 25:3673

MOLYBDENUM SILICIDES
emissivity of $MoSi_2$ coatings, effects of oxide film on total-radiation, 25:2799

MONEL
photon reactions at 100 to 662 keV with, effective atomic numbers for photoelectric, scattering, and total interaction processes in, 25:2906

MONOMERS
radiation effects on electric conductivity of solid, at -196°C, γ, 25:2221
radioinduced polymerization in wood, 25:2238
radioinduced polymerization of, use of accelerators in studying, 25:2218 (CONF-700322-, pp 345-56)

MONTE CARLO METHOD
use in shielding calculations, difficulties and solutions in, 25:3176
use in shielding calculations, methods and applications of advanced, 25:3177

MONTMORILLONITES
sorptive properties of Rhine River, for radioisotopes, (E), 25:2350

MOON
age of, (T), 25:2881

MULLITES
coating with boron and boron carbide at 1300°C, vapor deposition method for, 25:2777

MUSCLES
phosphorus-33 uptake by, 25:2521

MUSCOVITES
sorptive properties of Rhine River, for radioisotopes, (E), 25:2350

MUTATIONS
biochemistry of tobacco mosaic virus, progress report on, 25:2551(R) (COO-873-28)
radioinduced, in Escherichia coli in relation to nutrition requirements, action spectra for uv, 25:2557
radioinduced, in maize for aleurone pigmenting potential, effects of seed exposure on γ and x, 25:2560
radioinduced, in oranges for survival in cold weather, 25:2552(R) (ORO-2909-9)
radioinduced, in organisms, tables for determining statistical frequencies in comparisons of, 25:2559

N

NAILS
analysis for sodium in patients with cystic fibrosis by neutron activation and γ spectrometry, 25:2127 (IAEA-122, pp 145-8)

NAPHTHALENE
effects on γ-radioinduced graft polymerization of cellulose with styrene in methanol solutions, 25:2247

2,7-NAPHTHALENEDISULFONIC ACID, 4,5-DIHYDROXY-
bisazo derivatives, complexes with copper, niobium, and zirconium, spectrophotometric studies on, 25:2199

NATURAL BACKGROUND RADIATION
dosimetry of, calibration of ionization detector for, 25:2448

NATURAL GAS
production stimulation using underground nuclear explosions, problems resulting from, 25:2382

NATURAL WATERS
radioisotope contamination of, role of aquatic plants in,

25:2547
ruthenium radioisotope contamination of French, relations with chemical and physical properties, 25:2362
NEODYMIUM
complexes with cupferron, separation by solvent extraction using 2-methyl-1-propanol and 3-methyl-1-butanol, 25:2078
determination in cerium dioxide by luminescence method, 25:2083
determination in misch metal as chlorates, nitrates, or perchlorates, photometric, 25:2077
determination of trace amounts of, in lanthanum oxide and yttrium oxide by direct emission spectrometry, 25:2096
neutron capture by, gamma spectra from thermal, (E), 25:3651 (NP-18485)
separation from metals by precipitation using cupferron, 25:2078
NEODYMIUM CHLORIDES
bis(2-ethylhexyl) phosphate--$CeCl_3$--HCl--H_2O--$NdCl_3$--$SmCl_3$, equilibria in Amsco, 25:2311 (IS-T-412)
NEODYMIUM ISOTOPES Nd-142
proton inelastic scattering at 9 MeV, fits to angular distributions with configuration mixing, (T), 25:3685
spectra of, isotope shifts in muonic x-ray, (E), 25:3620
NEODYMIUM ISOTOPES Nd-143
neutron capture by, gamma spectra from thermal, (E), 25:3651 (NP-18485)
spectra of, isotope shifts in muonic x-ray, (E), 25:3620
NEODYMIUM ISOTOPES Nd-144
energy levels from thermal neutron capture by neodymium-143, spin and parity assignments for, (E), 25:3651 (NP-18485)
energy-level transitions from neutron capture by aligned neodymium-143, conversion coefficients and multipolarities for, (E), 25:3651 (NP-18485)
spectra of, isotope shifts in muonic x-ray, (E), 25:3620
NEODYMIUM ISOTOPES Nd-145
neutron capture by, gamma spectra from thermal, (E), 25:3651 (NP-18485)
spectra of, isotope shifts in muonic x-ray, (E), 25:3620
NEODYMIUM ISOTOPES Nd-146
energy levels from thermal neutron capture by neodymium-145, spin and parity assignments for, (E), 25:3651 (NP-18485)
spectra of, isotope shifts in muonic x-ray, (E), 25:3620
NEODYMIUM ISOTOPES Nd-148
spectra of, isotope shifts in muonic x-ray, (E), 25:3620
NEODYMIUM ISOTOPES Nd-150
spectra of muonic, dynamic hyperfine structure in x-ray, (E), 25:3661
spectra of, isotope shifts in muonic x-ray, (E), 25:3620
NEODYMIUM NITRATES
complexes with bis(2-ethylhexyl) phosphate, spectra of, ir and Raman, 25:2193 (CONF-700403-8)
NEODYMIUM OXIDES
analysis for trace amounts of rare earths and other elements by direct reading emission spectrometry, 25:2096
emittance at high temperatures of solid, spectral, 25:3204 (AD-708547)
NEON
electron reactions with, quasi-classical calculation of cross sections for excitation of 4p--4d transition in, 25:2917
electron reactions with, rates of energy-level transitions in, (T), 25:2920
potassium-ion reactions up to 30 keV, absolute excitation functions for K II spectra produced in, (E), 25:2911
proton reactions at 1 to 100 keV with, cross sections for charge exchange into excited states in, (T), 25:2919
NEON IONS
effects on liquid cyclohexane at 22 MeV, 25:2281
reactions with graphite and metal surfaces at 5 to 50 keV, apparent total ion scattering, secondary electron emission coefficients, and electron and ion energy distributions for, (E), 25:2884 (NP-18490)
reactions with nitrogen molecules at 30 to 100 keV, absolute emission cross sections for, (E), 25:2902 (SC-RR-70-695)
NEON ISOTOPES Ne-19
energy levels and transitions of, lifetimes, branching ratios, spins, and parities of, (E), 25:3575
NEON ISOTOPES Ne-20
energy levels from neon-21 (p,d) reactions, (E), 25:3633
reactions with aluminum-27, mica-detector measurements of cross sections for compound nucleus formation in, 25:3611
NEON ISOTOPES Ne-21
deuteron reactions (d,p) at 10.2 MeV, angular distributions for, (E), 25:3633
proton reactions (p,d) at 20.0 MeV, angular distributions for, (E), 25:3633
NEON ISOTOPES Ne-22
energy levels from neon-21 (d,p) reactions, (E), 25:3633
reactions with thorium-232, yields of light neutron-rich nuclei in, (E), 25:3648 (JINR-E7-5319)
NEPTUNIUM
complexes with nicotinic acid, picolinic acid, and picolinic acid 1-oxide, ir and NMR spectral and thermogravimetric studies on, 25:2194 (KFK-1070)
oxidation of trivalent, by hydrogen peroxide or oxygen, mechanism and products of, 25:2155
NEPTUNIUM ISOTOPES
chemical states of recoil, from americium decay, Moessbauer studies on, 25:2305
NEPTUNIUM ISOTOPES Np-237
alpha decay of oriented, anisotropy from nonlocal alpha--nucleus interaction potential, (T), 25:3678
magnetic hyperfine interactions after recoil implantation into copper, time-dependent anisotropy for, (E), 25:3690
NEPTUNIUM ISOTOPES Np-239
magnetic hyperfine interactions after recoil implantation into polarized nickel, α--γ correlations for, (E), 25:3690
magnetic hyperfine interactions after recoil implantation into copper, integral attenuation for, (E), 25:3690
NEPTUNIUM OXIDES
purification by in situ conversion from nitrate to chloride anion exchange system, 25:2339
NEUTRINOS
cosmic background, electron propagation in, (T), 25:2875
energy of cosmic, maximal, (T), 25:2875
flux effects on space geometry during universe expansion, (T), 25:3343
gravitational field in vacuum from, constants for, (T), 25:3343
interactions ν + N at high energies, review of, (T), 25:3334 (NYO-4204-3)
interactions ν + N in duality model, q^2 dependence of Regge residue functions for inelastic, 25:3336
interactions ν + p, Bjorken limit and Jin--Martin lower bound for, 25:3294 (NYO-4204-5)
interactions with protons in the Universe, (T), 25:2874
model in general relativity theory for, with velocity groups G_3 on V_2, (T), 25:3343
production of ν--anti ν pairs in electron reactions with nuclei, cross sections for, (T), 25:3335
production rate for, implications of full causality for, 25:3301
reactions with lead-208 at 50 to 200 GeV, detection of W production from hadronic decay modes in, (E/T), 25:3333 (NYO-2171-323)
reactions with nuclei at 50 to 100 GeV, coherent, incoherent, and inelastic cross sections for W-meson production in, (T), 25:3340
two-component theory of, lepton conservation and μ--e symmetry in, 25:3351
NEUTRINOS (ANTI ν)
production of ν--anti ν pairs in electron reactions with nuclei, cross sections for, (T), 25:3335
NEUTRON CROSS SECTIONS
calculations for nuclear reactor materials, (T), 25:3530 (LA-4484)
calculations of displacement, in spherical geometry, computer program for, 25:3525 (CEA-N-1312)
data file on photon production, computer program for checking ENDF/B, 25:3531 (LA-4506)
NEUTRON-DIFFRACTION ANALYSIS
use for studying protein structures, 25:3907 (NP-18462)
NEUTRON SOURCES
bibliography on use of 14-MeV, in activation analysis, 25:2130 (NBS-TN-533)
description and uses of 14-MeV, for education, 25:3526 (CONF-700322-, pp 33-47)
development for activation analysis, review on, 25:3527 (CONF-700322-, pp 185-204)
development of accelerator, for radiotherapy, review on, 25:3473 (CONF-700322-, pp 407-29)
fabrication of californium, 25:2294 (ORNL-4572, pp 109-34)
moderators for cold, performance of, 25:3904 (IJS-571)
neutron energy spectra from plutonium--beryllium, (E), 25:2407
targets for medium- and high-power accelerators, design of rotating and stationary, 25:3474 (CONF-700322-, pp 431-9)
targets for, tritium loss rates in titanium, 25:3542
NEUTRON SPECTROMETERS
control system for boron trifluoride proportional, automatic, 25:2475 (INP-707)
design and performance of proton recoil, using thin radiator and semiconductor detectors, 25:2480
design and performance of proton-recoil proportional, for in-core fast neutrons, 25:2472 (AEEW-M-905)
efficiency of lithium-6--semiconductor detector sandwich, calculation of geometric, 25:2473 (AERE-R-6318)
neutron time--energy distributions in lead slowing down, calculations of, 25:3541
performance of proton-recoil proportional, at 200 eV to 1 MeV, 25:2481
transport equations for fast media for slowing-down, 25:3535
NEUTRON STARS
transport coefficients of a relativistic quantum gas, (T), 25:2873
NEUTRONS
absorption in two-region cylindrical fuel cells, computer programs for calculation of resonance integrals and cross sections for, 25:3528 (KFKI-70-12-RPT)
attenuation in hematite and ordinary concrete, measurement of, 25:3480
capture by aligned neodymium-143 and samarium-149 at

XUM

0.047 eV, gamma energies and intensities from, (E), 25:3651 (NP-18485)
capture by nuclei, performance of liquid scintillation detectors for measurement of cross sections for, 25:2435 (RPI-328-202)
decay $n \rightarrow p + e^- + \nu$, limiting relations for correlation averages for, (T), 25:3332 (ITF-70-59)
detection at high temperatures, spark chamber for in-core, 25:2459
diffusion in heavy moderators, time-energy distributions of, (T), 25:3541
diffusion in infinite and finite media, approximations to energy-dependent Boltzmann equation for, (T), 25:3539
distributions in lithium, angular, energy, and spatial, (E/T), 25:3538
dose distribution in polyethylene, 25:2494
effects on creep of Hastelloy N, relations with temperature, 25:2674 (ORNL-4570, pp 136-42)
effects on density and stability of pyrolytic carbon, 25:2771 (ORNL-4570, pp 161-9)
effects on highly oriented graphite, 25:2730 (ORNL-4570, pp 44-6)
effects on microstructure of graphite, 25:2609 (ORNL-4570, pp 175-90)
effects on production of acicular precipitates in Type 316 stainless steel, 25:2756 (CEA-CONF-1638)
effects on silicon devices, hybrid recombination model for, 25:2514 (SC-R-70-4351)
effects on tetrahydrated cobalt complex with sodium salt of EDTA in aqueous solutions, chemistry of cobalt-60 recoils produced by, 25:2297
effects on thermally stimulated conductivity in alkali metal halide single crystals, 25:3202
flux characteristics in reactors, performance of pulsed neutron source simulator for, (E/T), 25:3932
flux distribution in water moderated enriched uranium fueled assemblies, (E/T), 25:3912
flux distributions in power reactors, comparison of variational synthesis methods for, (T), 25:3922 (ANL-7696)
flux noise in liquid sodium cooled fast breeder reactors, coolant boiling detection by, (T), 25:3864
form factor from $e + p \rightarrow \pi^0 + n$ interactions at threshold, electromagnetic, (E), 25:3244
interactions anti $p + n \rightarrow 2\pi^- + \pi^+$ at 1.0 to 1.6 GeV/c in deuterium bubble chamber, Veneziano model for 3π Dalitz plot structure in, (E/T), 25:3270 (INFN-PD-70/2)
interactions anti $p + n \rightarrow \omega + 2\pi^- + \pi^+$ at rest in deuterium bubble chamber, upper limit on $\omega \rightarrow \pi^+ + \pi^-$ decay rate from, (E), 25:3269
interactions anti $p + n \rightarrow \omega + \pi^- + \pi^0$ at rest in deuterium bubble chamber, upper limit on $\omega \rightarrow \pi^+ + \pi^-$ decay rate from, (E), 25:3269
interactions anti $p + n \rightarrow \omega + \pi^-$ at rest in deuterium bubble chamber, upper limit on $\omega \rightarrow \pi^+ + \pi^-$ decay rate from, (E), 25:3269
interactions anti p + n at 3.5 GeV/c, differential cross section for elastic, (E), 25:3267
interactions e + n, parton and quark models for deep inelastic, (T), 25:3310 (DESY-70/50)
interactions $K^- + n \rightarrow p + K^- + \pi^-$ at 3 GeV/c, Chew--Low extrapolation of $K\pi$ elastic cross section from, (E/T), 25:3278
interactions n + d below 20 MeV, dpn and tdn coupling constants from forward dispersion relations for, (T), 25:3408
interactions $p + n \rightarrow \Delta^{++}(1236) + \Delta^-(1236)$ at 6.98 GeV/c cross sections and decay correlations for, (E), 25:3265
interactions p + n and p + p at 12.4 GeV/c using liquid deuterium target, cross section ratio for elastic, (E), 25:3266
propagation in spherical geometry by straight line attenuation, computer program for study of, (T), 25:3525 (CEA-N-1312)
pulse propagation in reactors, 1965 to 1970 research in Japan on, 25:3927 (JAERI-Memo-4109)
reactions with aluminum, production of silicon by, 25:2816 (ORNL-4570, pp 16-19)
scattering by nuclei, Hauser--Feshbach analysis of inelastic, (T), 25:3712 (AAEC/TM-545)
scattering by single phonons of hydrogen in titanium hydride at 0.05 to 0.2 eV, cross sections for inelastic, 25:3536
scattering in ferromagnetic materials, corrections to magnon dispersion relations from, 25:3218
scattering in lithium-6-loaded scintillation detectors, Monte Carlo study of multiple, 25:2456
scattering law for polycrystalline beryllium, calculation of coherent one-phonon, 25:3533
scattering on graphite, determination of crystal ordering by inelastic, 25:2810
spectra measurements of, computer method for data analysis of threshold detectors for, 25:2439
spectra measurements of, semi-automatic system for analyzing nuclear emulsion particle tracks for, 25:2433 (CEA-R-4063)
transport equation in slab geometry, computer code for multigroup solution of, 25:3529 (KFKI-70-14-RPT)
transport in fast media, spectral functions for, 25:3535
transport in slab, Green's functions for multidimensional, 25:3184
transport in variable phase-space, analysis of, (T), 25:3532
transport of, numerical calculation of Milne problem extrapolation length for, (T), 25:3540

NEUTRONS, COLD
scattering in liquid cyclohexanol, incoherent quasi-elastic, 25:3534

NEUTRONS, DELAYED
emission of, energy spectra and probabilities for, (T), 25:3713 (CEA-N-1333)

NEUTRONS, FAST
attenuation by shielding materials, monoenergetic-source, (E/T), 25:3173
attenuation in water, relaxation length for 14-MeV, (E), 25:3537
detection of solar, in range 20 to 160 MeV, (E), 25:2861
dosimetry of, performance of DK-0.2 ionization detector for personnel, 25:2493
effects on configuration of voids in aluminum, 25:2816 (ORNL-4570, pp 16-19)
effects on disilane--phosphine mixtures, reactions of recoil silicon-31 atoms from, 25:2299
effects on graphite, comparison dose scale for, 25:3872 (DP-Report-559)
effects on mechanical properties of Types 347 and 348 stainless steel at 25 to 750°C, 25:2755 (BMI-1889, Sect.B)
effects on mechanical properties of Zircaloy tubes, 25:3921 (DUN-SA-144)
effects on porosity and swelling of aluminum, 25:2759 (ORNL-4570, pp 152-6)
effects on tensile properties of heavy-section Type A533 steel, 25:2676 (ORNL-4570, pp 170-3)
effects on void distribution in iron, 25:2816 (ORNL-4570, pp 16-19)
effects on void distribution in Type 304 stainless steel at 300 to 800°C, 25:2758 (ORNL-4570, pp 76-84)
effects on void distribution in vanadium, 25:2758 (ORNL-4570, pp 76-84)
effects on void formation in aluminum subjected to preinjection of hydrogen, 25:2816 (ORNL-4570, pp 16-19)
effects on void formation in Type 304 stainless steel, relations with preinjected helium, 25:2761
flux measurement of, sensitivity of silver-activated zinc sulfide scintillation detector in Plexiglas matrix for, 25:2443
reactions (n,2n) with copper-63, gold-197, thallium-203, thorium-232, and uranium-238 below (n,3n) thresholds, cross-section calculations using Hauser--Feshbach theory, (T), 25:3591 (AAEC/TM-542)
reactions (n,2n) with nitrogen-14 at 14.7 MeV, cross section for, (E), 25:3576
reactions (n,α) with beryllium-9 at 8 to 30 MeV, angular distributions and excitation functions for, (E), 25:3564 (KFK-1190)
reactions (n,α), (n,p), and (n,2n) with medium-weight nuclei at 14.5 MeV, systematics of cross sections for, (E/T), 25:3643
reactions (n,f) with berkelium-249 at 0.6 to 4.6 MeV, cross sections and fragment angular distributions for, (E), 25:3665
reactions (n,f) with thorium-232 at 0.95 to 2.3 MeV, channel analysis of fragment angular distributions and cross sections for, (E), 25:3680
reactions with tissues at 15.09 MeV, calculation of energy deposited by heavy recoil particles in, 25:2568
scattering by boron-10 and -11 at 2 to 4.8 MeV, angular distributions for elastic and inelastic, (E), 25:3559 (AWRE-O-45/70)
scattering by hydrogen-free plane shielding, (E), 25:3171
scattering by liquid ^{4}He, interference and temperature effects in, (T), 25:3049
scattering by phosphorus-31 and sulfur-32 at 14 MeV, differential cross sections for inelastic, (E), 25:3612
scattering by sodium-23 below 2 MeV, optical-model calculation of angular distributions for inelastic, (T), 25:3635
scattering by vanadium at 4.2 to 8.6 MeV, cross sections for elastic and inelastic, (E), 25:3595 (ORNL-4551)
scattering on carbon-12 at 14 MeV, time-of-flight arrangement for measurement of differential cross sections for backward, 25:2468
spectra measurements with activation detectors, polynomial approximation for, 25:2442
use for tumor therapy, effectiveness of, 25:2582 (CONF-700322-, pp 393-406)

NEUTRONS, INTERMEDIATE
flux measurements of, sensitivity of Basson detector containing boron oxide for, 25:2443
scattering by nuclei at 1 to 40 keV, analysis of angular distributions from elastic, (E/T), 25:3695
scattering in sodium at 2.85 keV, group structure and group constants for, (T), 25:3928 (JAERI-Memo-4110)

NEUTRONS, PILE
capture by europium-155, cross section for, (E), 25:3667
effects on brittleness of heavy-section Type A533B steel, relations with copper and phosphorus content, 25:2757 (NRL-7121)

effects on creep rate of heat treated niobium--zirconium alloy, relations with stress dependence, 25:2760
effects on mechanical properties of Incoloy 800, 25:2758 (ORNL-4570, pp 76-84)
effects on pyrocarbon-coated uranium carbide fuel particles, 25:2812 (DP-Report-320)
effects on swelling of uranium, 25:2762
effects on thermal conductivity of vibratory compacted uranium dioxide fuel pins at 200 to 1500°C, 25:2813 (JAERI-Memo-4128)
flux of, transient response of cobalt self-powered detectors for measurements of, 25:2467
flux-density distributions in laminated iron/water shielding, (E/T), 25:3174
reactions (n,f) with protactinium-231, mass and neutron yields for, (E), 25:3656

NEUTRONS, THERMAL
capture by europium-151, conversion electron spectrum from, (E), 25:3698
capture by holmium-165, (E), 25:3691
capture by neodymium-143, -145, natural neodymium, samarium-147, -152, and natural samarium, gamma spectra from, (E), 25:3651 (NP-18485)
capture by shielding materials, gamma spectra from, (E), 25:3181
effects on alkyl bromides, electrolytic collection of recoil bromine-80 and bromine-80m from, 25:2301
effects on solid inorganic phosphates, reactions of recoil phosphorus-32 from, 25:2302
flux distribution in heterogeneous reactors, computer program for, 25:3925 (DP-1238)
flux fluctuation in multiplying systems, shift registers for measurement of, 25:3931
flux monitoring of, 10-decade wide range fission detector system for in-core, 25:2502 (GEAP-11094)
reactions with plutonium-239 and uranium-235, separated γ spectra from, (E), 25:3649 (KFK-1214)

NEWBOLD ISLAND POWER REACTOR, UNIT 1
design parameters of, revised and additional data on, 25:3847 (DOCKET-50354-9)
operations aspects of, revised and additional data on, 25:3847 (DOCKET-50354-9)

NEWBOLD ISLAND POWER REACTOR, UNIT 2
design parameters of, revised and additional data on, 25:3847 (DOCKET-50354-9)
operations aspects of, revised and additional data on, 25:3847 (DOCKET-50354-9)

NICKEL
abundance in Kappa Cancri, (E), 25:2840
analysis for trace amounts of carbon, conductometric method for, 25:2071
coating with cadmium, copper, or zinc, surface morphology in electrochemical, 25:2648
corrosion and mass transfer by sodium at 660 and 760°C, effects of oxygen content on, 25:2631
deformation and fracture behavior of, effects of titanium on high-temperature, 25:2725
density of pure liquid, 25:4003(T) (UCRL-Trans-10496)
determination following nonsulfide separation from elements, qualitative, 25:2101
determination following solvent extraction using benzene, 8-quinolinol, and Rhodamine 6G, photometric, 25:2087
determination of trace amounts of, in nuclear-grade uranium oxide (U_3O_8) by direct reading spectrometric method, 25:2068 (NLCO-1071)
deuteron breakup at 50 MeV, analysis using adiabatic approximation, (T), 25:3614
deuteron elastic and inelastic scattering at 50 MeV, analysis using adiabatic approximation, (T), 25:3614
diffusion of carbon in, electronic mechanisms in thermal, 25:2666 (NP-18468)
effects on determination of trace amounts of antimony by isotopic exchange in organic phase, 25:2106
effects on determination of trace amounts of rhenium by thiocyanate--stannous chloride method, 25:2102
effects on extraction--photometric determination of niobium in steel, 25:2085
effects on photometric determination of hafnium and zirconium in geological specimens, 25:2084
effects on uv spectrophotometric determination of gallium in aqueous solutions, 25:2100
ion reactions at 5 to 50 keV with, apparent total ion scattering, secondary electron emission coefficients, and electron and ion energy distributions for, (E), 25:2884 (NP-18490)
neutron capture by, gamma spectra from thermal, (E), 25:3181
neutron cross sections for, 25-group, (T), 25:3530 (LA-4484)
proton elastic and inelastic scattering at 28 MeV, cross sections for, (E), 25:3599
radioinduced preparation from aqueous salt solutions, electron, 25:2237 (N-70-32826)
solubility in bismuth--lead eutectic at 400 to 500°C, 25:2709
solubility in liquid sodium, effects of temperature on, 25:2712
work softening in polycrystalline, 25:2724

NICKEL ALLOYS AND SYSTEMS
corrosion of similar metal welds in Type IN 102, by steam at 1100 to 1200°F, 25:2636
corrosion of similar metal welds of Type IN 102, by steam at 595 to 650°C, 25:2608 (ORNL-4570, pp 124-6)
Ag--Fe--Nb--Ni-base, crystallization of, relations with magnetic properties, 25:2679
Be--Ni, uses in nuclear technology, 25:2654
Co--Ni--V, mechanical properties of, effects of ordering on, 25:2643 (ORNL-4570, pp 106-11)
Cr--Fe--Nb--Ni-base, hardening of, transmission electron microscopic study of age, 25:2689
Cr--Fe--Ni, reactions with uranium carbide at 900°C, effects of carbon content and metal stabilizers on, 25:2765 (KFK-1213)
Cr--Ni, diffusion in, thermodynamics of bond parameter changes in self-, 25:2701
Fe--Ni, neutron cross sections for invar, (T), 25:3530 (LA-4484)
Fe--Ni, thermal capacity and conductivity of intermetallic Ni_3Fe, 25:2788 (ORNL-4570, pp 27-30)
Mo--Ni-base, carburization of, relations with hardness, 25:2716
Nb--Ni, precipitation of intermetallic phases of Ni_3Nb, during age hardening of chromium--iron--nickel--niobium alloy, 25:2689
Nb--Ni-base, carburization of, relations with hardness, 25:2716
Ni--Pd, magnetic hyperfine fields at nickel-61 nuclei in, Moessbauer studies of, 25:2669 (ORNL-4570, pp 23)
Ni-base--Ta, carburization of, relations with hardness, 25:2716
Ni-base--Ti, carburization of, relations with hardness, 25:2716
Ni-base--V, carburization of, relations with hardness, 25:2716
Ni-base--W, carburization of, relations with hardness, 25:2716
Ni-base--Zr, carburization of, relations with hardness, 25:2716

NICKEL CHLORIDES
spectra of $NiCl_4^{2-}$ in cesium magnesium chloride, electronic absorption, 25:2805 (ORNL-4570, pp 31-4)
$AlCl_3$--CsCl--$NiCl_2$, formation of $NiCl_3^-$ complex in, mechanisms of, 25:2805 (ORNL-4570, pp 31-4)
$AlCl_3$--$NiCl_2$, phase studies of, 25:2805 (ORNL-4570, pp 31-4)
CsCl--$NiCl_2$--$ZnCl_2$, phase studies of, 25:2805 (ORNL-4570, pp 31-4)

NICKEL ISOTOPES Ni-58
electron elastic scattering at 300 MeV, form factors, charge parameters, and K transition energies for, (E), 25:3687
energy levels from Coulomb excitation, static quadrupole moments and reduced transition probabilities of first-excited, (e), 25:3642
energy levels of, binding energies and orbital spin assignments of proton-hole, (E), 25:3616
proton elastic scattering at 1.8 to 3.3 MeV, differential cross sections for, (E), 25:3628
proton elastic scattering at 30.3 MeV, angular distributions, polarizations, and optical-model analysis of, (E), 25:3636
proton elastic scattering at 39.6 MeV, cross-section and polarization measurements for, (E), 25:3598

NICKEL ISOTOPES Ni-60
electron elastic scattering at 300 MeV, charge parameters and K transition energies for, (E), 25:3687
energy levels from Coulomb excitation, static quadrupole moments and reduced transition probabilities of first-excited, (e), 25:3642
energy levels of, binding energies and orbital spin assignments of proton-hole, (E), 25:3616
proton elastic and inelastic scattering at 10 MEV, differential cross sections, polarizations, and p--γ angular correlations for, (E), 25:3613
proton elastic scattering at 1.8 to 3.3 MeV, differential cross sections for, (E), 25:3628
proton elastic scattering at 39.6 MeV, cross-section and polarization measurements for, (E), 25:3598

NICKEL ISOTOPES Ni-61
electron elastic scattering at 300 MeV, charge parameters and K transition energies for, (E), 25:3687
proton reactions (p,n) at 3 to 6 MeV, neutron spectra from, (E), 25:3596 (TID-25503)

NICKEL ISOTOPES Ni-62
electron elastic scattering at 300 MeV, charge parameters and K transition energies for, (E), 25:3687
energy levels from cobalt-62 decay, spins and parities of, (E), 25:3644
energy levels from Coulomb excitation, static quadrupole moments and reduced transition probabilities of first-excited, (e), 25:3642
proton elastic scattering at 1.8 to 3.3 MeV, differential cross sections for, (E), 25:3628
proton elastic scattering at 39.6 MeV, cross-section and polarization measurements for, (E), 25:3598

NICKEL ISOTOPES Ni-64
electron elastic scattering at 300 MeV, charge parameters and K transition energies for, (E), 25:3687
proton elastic scattering at 1.8 to 3.3 MeV, differential cross sections for, (E), 25:3628
proton elastic scattering at 39.6 MeV, cross-section and polarization measurements for, (E), 25:3598
proton reactions (p,n) at 2.5 to 3.3 MeV, excitation

XUM

function for, (E), 25:3628
proton reactions (p,n) at 3 to 6 MeV, neutron spectra from, (E), 25:3596 (TID-25503)
NICKEL PHOSPHIDES
radiation effects on fuel cladding of, in-pile, 25:2770 (ORNL-4570, pp 127-35)
NICOTINIC ACID
complexes with americium, neptunium, plutonium, and uranium, ir and NMR spectral and thermogravimetric studies on, 25:2194 (KFK-1070)
NINE MILE POINT POWER REACTOR
operations aspects of, technical specifications for power increase, 25:3814 (DOCKET-50220-52)
NIOBIUM
complexes with 3,6-bisazo derivatives of chromotropic acid, spectrophotometric studies on, 25:2199
defects and dislocations in cold-rolled, anneal-induced recovery from, 25:2728 (ORNL-4570, pp 5-9)
deformation behavior of polycrystalline, 25:2690
determination in presence of tantalum by chromatographic and gravimetric methods, 25:2066 (NIM-834)
determination in steel using benzohydroxamic acid, extraction--photometric, 25:2085
determination in uranium alloys by atomic absorption spectrophotometry, 25:2065 (LA-4529)
determination of trace amounts of, in nuclear-grade uranium oxide (U_3O_8) by direct reading spectrometric method, 25:2068 (NLCO-1071)
determination using 3,6-bisazo derivatives of chromotropic acid, spectrophotometric, 25:2199
diffusion in tungsten, activation energy for, 25:2605 (ORNL-4570, pp 37-9)
diffusion in, niobium-95 tracer studies of mechanisms of self-, 25:2703
diffusion of lithium, potassium, and sodium in oxygen-containing, at 600°C, 25:2707
diffusion of tungsten in, tracer study of, 25:2703
effects of coating of, on corrosion of steel tubing by bismuth--lead eutectic containing magnesium and zirconium, 25:2627
effects on brazing of silicon oxide with copper--silver alloy using composite film method, 25:2652
electric conductivity at 100 to 1700°C, (E), 25:2715
emissivity at 100 to 1700°C, total, (E), 25:2715
mechanical properties at 290 to 1870°K, effects of deformation rate on, 25:2681
neutron cross sections for, 25-group, (T), 25:3530 (LA-4484)
properties of, effects of hydrogen, nitrogen, and oxygen on, 25:2639(T) (LIB/Trans-309)
protection of surfaces of, from gas reactions at high temperatures using argon or helium, 25:2639(T) (LIB/Trans-309)
separation from aqueous solutions of acetic, citric, or oxalic acids by solvent extraction using tertiary amines or Aliquat 336, 25:2334
solubility in potassium at 1055 to 1287°K, effects of oxygen doping on, 25:2664 (N-70-32146)
superconducting Josephson junction system in, transition to resistanceless state in, (E), 25:3035
thermal conductivity at 100 to 1700°C, (E), 25:2715
work-hardening parameters for polycrystalline, 25:2723
NIOBIUM ALLOYS AND SYSTEMS
creep of, review of recent data on long-time, 25:2657 (AD-464715)
Ag--Fe--Nb--Ni-base, crystallization of, relations with magnetic properties, 25:2679
Be--Nb, niobium-93 NMR in $NbBe_{22}$, $NbBe_3$, Nb_2Be_{17}, and $NbBe_{12}$, 25:3220 (COO-1700-12)
Co--Nb, phase studies of, 25:2749
Cr--Fe--Nb--Ni-base, hardening of, transmission electron microscopic study of age, 25:2689
Hf--Nb, phase studies of, 25:2668 (ORNL-4570, pp 10-12)
Hf-base--Nb, phase studies of, 25:2735
Mo--Nb--Zr, diffusion in, activation energy for, 25:2704
Mo--Nb-base, tensile properties at 20 to 1600°C and 10^{-5} torr, effects of traces of carbon and zirconium on, 25:2682
Nb--Ni, precipitation of intermetallic phases of Ni_3Nb, during age hardening of chromium--iron--nickel--niobium alloy, 25:2689
Nb--Ni-base, carburization of, relations with hardness, 25:2716
Nb--Si--Ti--V-base, creep to 850°C, 25:2662 (KFK-1193)
Nb--Ta-base, elastic properties of monocrystalline, at 80 to 1400°K, 25:2721
Nb--Ti, superconducting magnetic properties of, 25:3027
Nb--U-base, niobium segregation in, effects of casting, heat treatments, and melting on, 25:2732 (RFP-1582)
Nb--U-base, oxidation at 800°C, mechanisms and stresses in, 25:2605 (ORNL-4570, pp 37-9)
Nb--U-base--Zr, crystal structure of, effects of aging on, 25:2730 (ORNL-4570, pp 44-6)
Nb--U-base--Zr, oxidation at 800°C, mechanisms and stresses in, 25:2605 (ORNL-4570, pp 37-9)
Nb--Zr, diffusion in, activation energy for, 25:2704
Nb--Zr, phase studies of, 25:2668 (ORNL-4570, pp 10-12)
Nb--Zr, preparation and etching of microsections of, 25:2656
Nb--Zr, properties of superconducting ribbons of, for cryogenic level indicators, 25:2394
Nb--Zr-base, phase transformation in, studies of athermal omega, 25:2735
Nb--Zr-base, precipitates in alpha- and omega-phase, composition and volume of dispersed, 25:2742
Nb--Zr-base, radiation effects on creep rate of heat treated, relations of stress dependence with pile neutron, 25:2760
Nb-base--Ti, lower critical fields of superconducting, (E/T), 25:3020 (ORNL-TM-3206)
Nb-base--V, defects and dislocations in cold-rolled, anneal-induced recovery from, 25:2728 (ORNL-4570, pp 5-9)
Nb-base--Zr, corrosion by barium, calcium, and lead at 1000 to 1800°C, 25:2628
Nb-base--Zr, corrosion by boiling potassium in Rankine cycle test loop, effects of zirconium hot trap on, 25:2624
Nb-base--Zr, corrosion by lithium at 1000 and 1400°F, effects of welding atmosphere purity on, 25:2625
Nb-base--Zr, corrosion by lithium in Rankine cycle test loop, effects of yttrium hot trap on, 25:2624
NIOBIUM CARBIDES
vaporization of congruently vaporizing compositions of, rates of, 25:2802
NIOBIUM ISOTOPES Nb-93
nuclear magnetic resonance in niobium beryllides, 25:3220 (COO-1700-12)
NIOBIUM ISOTOPES Nb-95
uptake by aquatic molluscs and plants, effects of concentration in water on concentration factor for fallout, 25:2548
NIOBIUM OXIDES
effects on properties of sintered zircons, 25:2766(T) (CSIRO-Trans-9924)
BaO--Nb_2O_5--SrO, phase studies of Nb_2C_5-rich region of, 25:2808
Nb_2O_5--SrO, phase studies of, 25:2808
NIOBIUM SELENIDES
optical density of $NbSe_2$ lamellae, use for thickness determination, 25:3214
NITRATES
effects on radiolysis of water, 25:2267
NITRIC ACID
effects on fixation of alkali metals on hydrated antimony pentoxide, 25:2333
radiolysis of aqueous solutions of, γ, 25:2277
radiolysis of aqueous solutions of, LET effects on α, β, or γ, 25:2284
separation from aqueous solutions by solvent extraction using amines and TBP, effects of salting-out agents on, 25:2335
solvent properties of dilute, for plutonium, effects of hydrofluoric acid and temperature on, 25:2153
NITROGEN
electron reactions at 10 keV with molecular, K-shell excitation and ionization in, (E), 25:2910
ion reactions at 30 to 100 keV with molecular, absolute emission cross sections for, (E), 25:2902 (SC-RR-70-695)
plasma jets of, spectroscopic measurement of temperature and electron density in free, 25:3070
reactions with niobium and tantalum at high temperatures, effects of argon or helium protective atmosphere on, 25:2639(T) (LIB/Trans-309)
reactions with nitrogen ions (N_2^+), cross sections for charge exchange in, (T), 25:2912
sorption on tantalum films, method of determining, 25:2686
spectral intensity of molecular, in normal and type-B aurorae, (E), 25:3002
NITROGEN IONS
effects on liquid cyclohexane at 115 MeV, 25:2281
implantation in silicon at high energies, infrared spectral study of, (E), 25:3203
NITROGEN IONS (N^+)
diffusion coefficients of, in ionospheric F2 layer, (T), 25:2962
reactions with graphite and metal surfaces at 5 to 50 keV, apparent total ion scattering, secondary electron emission coefficients, and electron and ion energy distributions for, (E), 25:2884 (NP-18490)
NITROGEN IONS (N_2^+)
reactions with graphite and metal surfaces at 5 to 50 keV, apparent total ion scattering, secondary electron emission coefficients, and electron and ion energy distributions for, (E), 25:2884 (NP-18490)
reactions with nitrogen molecules, cross sections for charge exchange in, (T), 25:2912
NITROGEN ISOTOPES N-13
energy levels from nitrogen-14 (He-3,α) reactions, (E), 25:3590
NITROGEN ISOTOPES N-14
deuteron reactions (d,n) at 4.2 to 6.0 MeV differential cross sections and polarization for, (E), 25:3574
deuteron reactions (d,n) at 5.5 MeV angular distribution and polarization for, (E), 25:3574
energy level at 6.44 MeV from carbon-12 (He-3,p) reactions, lifetime of, (E), 25:3569
energy levels from carbon-12 (d,p) reactions, (E), 25:3572
helium-3 elastic scattering at 4.5 and 7.0 MeV, differential cross sections for, (E), 25:3590

helium-3 reactions (He-3,α) at 2.5 tc 8.5 MeV, differential cross sections for, (E), 25:3590
neutron reactions (n,2n) at 14.7 MeV, cross section for, (E), 25:3576
NITROGEN ISOTOPES N-15
deuteron reactions (d,n) at 8.5 MeV, angular distribution and optical model parameters for, (E), 25:3574
reactions with thorium-232, yields of light neutron-rich nuclei in, (E), 25:3648 (JINR-E7-5319)
NITROGEN OXIDES
abundance of ionized, in ionospheric F1 layer, diurnal variations of, (E/T), 25:2987
NITROGEN OXIDES NO
effects on radiolysis of ammonia, 25:2283
NITROGEN OXIDES NO_2 OR N_2O_4
corrosive effects of aqueous, on aluminum--titanium-base--vanadium alloys, 25:2635
NITROGEN OXIDES N_2O
effects on γ radiolysis of cyclohexane, 25:2268
NITROGEN SYSTEMS
Bi--N--Th, crystal structure of Th_2N_2Bi formed in, 25:2248
Bi--N--U, crystal structure of U_2N_2Bi formed in, 25:2248
Cr--N--U, phase studies at 1600°C, 25:2769 (ORNL-4570, pp 62-7)
N--Sb--Th, crystal structure of Th_2N_2Sb formed in, 25:2248
N--Sb--U, crystal structure of U_2N_2Sb formed in, 25:2248
N--V-base, crystal structures of quenched and aged, 25:2811
2,5-NORBORNADIENE
radioinduced isomerization of, in cyclohexane, effects of acetophenone, benzene, and toluene on, 25:2239
NORTH ANNA POWER REACTOR, UNIT 1
effluents from, effects on environment of chemical, radioactive, and thermal, 25:3841 (DOCKET-50338-26)
site for, safety aspects of, 25:3841 (DOCKET-50338-26)
NORTH ANNA POWER REACTOR, UNIT 2
effluents from, effects on environment of chemical, radioactive, and thermal, 25:3841 (DOCKET-50338-26)
site for, safety aspects of, 25:3841 (DOCKET-50338-26)
NOZZLES
junctions with cylindrical and spherical shells, stress analysis of region of, 25:2386 (ORNL-TM-2526(Add.))
NRL ISOCHRONOUS CYCLOTRON
beam monitoring at, design of rapid emittance scanner for, 25:3498
NUCLEAR BATTERIES
development of tritium-decay-powered, using cadmium telluride radiovoltaic converter, 25:2400 (CEA-CONF-1623)
NUCLEAR CHEMISTRY
research at Inst. of Nuclear Research, Warsaw, 1969, 25:2497(R) (INR-1180)
NUCLEAR EMULSIONS
grain counting for particle discrimination in, effect of mutual overlap on, 25:2457
meson (μ^+) reactions at 10.3 GeV in, structure functions for, (E), 25:3260
meson (μ^-) reactions at 15.9 GeV in, structure functions for, (E), 25:3260
meson (π^-) interactions at 20 GeV/c in, energy estimation from angular distribution of secondaries in, (E), 25:3284
particle track measurements in, for neutron spectroscopy, semi-automatic system for, 25:2433 (CEA-R-4063)
NUCLEAR EXPLOSIONS
effects of, operator manual for Weapons Effects Display System for mapping prompt, 25:2504 (UCRL-50892(Vol.2))
effects of, Weapons Effects Display System for mapping prompt, 25:2506 (UCRL-50922)
effects of, wiring tables for logic interfaces for Weapons Effects Display System for mapping prompt, 25:2505 (UCRL-50892(Vol.4)(Pt.5))
fallout from Chinese, effects of meteorological conditions on environmental contamination at Seoul, Korea from, (E), 25:2368
NUCLEAR EXPLOSIONS, ATMOSPHERIC
fallout monitoring in East Germany following 7th and 8th Chinese, 25:2370
NUCLEAR EXPLOSIONS, UNDERGROUND
crater formation by, computer calculations of effects of surrounding media on, 25:2381 (UCRL-50898)
uses for natural gas and oil production stimulation, problems resulting from, 25:2382
uses of, evaluation of chemical, 25:2380 (ORNL-4572, pp 196-8)
NUCLEAR MAGNETIC RESONANCE
radiative detection of single-passage, of cobalt-60 in iron, (E), 25:3223
NUCLEAR MATERIALS MANAGEMENT
plutonium/uranium ratio estimates for radiochemical processing plant solutions for, 25:2417 (BNWL-SA-3287)
safeguards research for, use of small accelerators in, 25:2418 (CONF-700322-, pp 357-78)
safeguards techniques for, 25:3649 (KFK-1214)
standards for IAEO, 25:3851
NUCLEAR MATTER
alpha-particle effective mass in superfluid, (T), 25:3728
alpha-particle model for, (T), 25:3738
binding energy and magnetic susceptibility of neutron matter, 25:3746
binding energy of, role of mesons in saturation of, 25:3763
binding-energy calculations for, corrections to second order v/c, (T), 25:3735
calculations with hard-core and long-range potentials, (T), 25:3772
transition temperature of, critical, (T), 25:3773
NUCLEAR MODELS
alpha-particle, for nuclear matter, 25:3738
equidistant-spacing, density of particle-hole states in, 25:3760
optical, generalized potential for, 25:3747
optical, Hauser--Feshbach analysis of neutron inelastic scattering using, (T), 25:3712 (AAEC/TM-545)
optical, real part of alpha--nucleus potential obtained by double-folding procedure, (T), 25:3755
shell, 27-plet unitary symmetry operator in SU(3) symmetry for, 25:3426
shell, analysis of separation energies, (T), 25:3754
shell, higher-order bubble corrections to two-body matrix elements in the 1s0d shell in, 25:3759
shell, potential-energy surface at large deformations for lead-198 and uranium-236 from two-center, (T), 25:3734
shell, quasielastic electron scattering in square-well, 25:3577
NUCLEAR PHYSICS
research at Inst. of Nuclear Research, Warsaw, 1969, 25:2497(R) (INR-1180)
NUCLEAR POWER PLANTS
component manufacturing in Switzerland for, capacity and quality of, 25:3781
development during 1970 to 1980, predictions for, 25:3776
development in Puerto Rico during 1970 to 2000, analysis of estimates of optimum economic, 25:3798 (ORNL-TM-3142)
development in U.S. of, calculational models for optimum economic, 25:3797 (ORNL-4572, pp 236-41)
effluents from, effects on environment in U. S. of chemical and thermal, 25:3852
electric power generation in, in US to 2000, predictions for, 25:2393
operation in U.S. of, calculational models for optimum economic, 25:3797 (ORNL-4572, pp 236-41)
piping for, U. S. standards code for, 25:3778
power production in Germany during 1969 from, 25:3800
radioactive wastes from, economic aspects of methods for disposal of solid, 25:2425
radioisotope release by, in relation to content of irrigation canal sediments and water downstream on Rhone River, 25:2543
NUCLEAR REACTIONS
calculation of the reaction matrix in finite nuclei, 25:3742
Coulomb distortion in heavy-ion, (T), 25:3720
cross-section fluctuations in, number of degrees of freedom in, (T), 25:3717
Josephson effect in nucleon-transfer heavy-ion, (T), 25:3752
neutron reactions (n,α), (n,p), and (n,2n) at 14.5 MeV with medium-weight nuclei, systematics of cross sections for, (E/T), 25:3643
photon-induced, review of experimental data and theory for, 25:3715 (NBS-MON-118)
relation between the 2I + 1 rule and channel correlation, 25:3762
NUCLEAR REACTIONS (DIRECT)
DWBA analysis of stripping to unbound states, (T), 25:3764
multi-step stripping on deformed nuclei with nonrotational states involved, (T), 25:3732
NUCLEAR STRUCTURE
calculations for 1^+ levels in deformed even-even nuclei, (T), 25:3727
calculations for light nuclei using Hartree--Fock--Bogolyubov method with isospin pairing, (T), 25:3722
description of M1 transitions between rotational levels of deformed even-even nuclei, (T), 25:3726
description using Regge trajectories in collective and shell models, 25:3723
energy-level transitions from octupole states in even--even deformed nuclei, branching ratios for E1, (T), 25:3751
nuclear level densities in, spin dependence of, (T), 25:3765
nucleon separation energies, shell-model analysis of, (T), 25:3754
nucleon--nucleon potential for, field-theoretic, 25:3414
self-consistent static field in the presence of two-particle-two-hole admixtures, 25:3739
sensitivity of β transitions to charge distribution, (T), 25:3744
NUCLEAR THEORY
calculation of Coulomb energy differences, 25:3770
calculation of the reaction matrix in finite nuclei, 25:3742
charge asymmetry of the internucleon potential in, 25:3736
definition of single-nucleon potential, 25:3740
density of particle-hole states in the equidistant-

XUM

spacing model, 25:3760
generalized optical potential in, 25:3747
higher-order bubble corrections to two-body matrix elements in the 1s0d shell, 25:3759
hyperspherical-expansion approach to nuclear bound states, 25:3730
Josephson effect in sub-Coulomb scattering of heavy ions, 25:3752
magnetic moments of deformed nuclei, effects of spin--orbit and spin--spin forces on, 25:3692
many-body problem in, relativistic nucleon--meson field theory for, 25:3719
nucleon residual interactions in, effect of tensor forces in, 25:3766
nucleon-nucleon potentials in, Gilbert--Schmitt expansion for hard-core, 25:3724
nucleon-nucleon potentials in, positivity conditions for velocity-dependent and quadratic spin-orbit, 25:3737
off-mass-shell form factors of the nucleon, 25:3745
relation between the 2I + 1 rule and channel correlation, 25:3762
role of mesons in nuclear saturation, 25:3763
self-consistent static field in the presence of two-particle-two-hole admixtures, 25:3739
short-range correlations in the three-body problem and the Faddeev equations, 25:3731
T = 1 pairing Hamiltonian in a two-level model, 25:3758
transformation coefficients in the hyperspherical approach to the three-body problem, 25:3729

NUCLEI
abundance of relativistic Z = 9 to 17, in primary cosmic radiation, (E), 25:2931
alpha elastic scattering from, optical-model analysis using real potentials obtained from double-folding procedure, (T), 25:3755
alpha reactions with, model for analysis of, (T), 25:3716 (ORNL-TM-3153)
beta decay of, electromagnetic final-state interactions and test of T invariance in, (T), 25:3424
binding to magnetic monopole, 25:3322
cosmic meson (μ) reactions with, cloud chamber study of structure functions for, (E), 25:3260
electrodisintegration of light, analysis of, (T), 25:3714 (ITF-70-35)
electron reactions, cross sections of ν + anti ν pair production in, (T), 25:3335
energy levels of deformed even-even, properties of 1^+, (T), 25:3727
energy levels of, effects of short-range correlations and charge-dependent nuclear forces on analog, (T), 25:3753
energy-level transitions in deformed, M1 strength functions for, (T), 25:3683
energy-level transitions in even-even deformed, description of M1 rotational, (T), 25:3726
helium-3 elastic scattering by A = 12 to 207, analysis using optical potential, (T), 25:3769
meson (μ) reactions with nuclei at 50 to 100 GeV, coherent, incoherent, and inelastic cross sections for W-meson production in, (T), 25:3340
meson (μ^+) reactions at 10.3 GeV in emulsions, structure functions for, (E), 25:3260
meson (μ^-) reactions at 15.9 GeV in emulsions, structure functions for, (E), 25:3260
meson reactions (π^-,rho$^-$) and (π^-,rho^0) with A = 20 to 208, at 30 GeV, Glauber multiple scattering calculations for coherent and incoherent, (T), 25:3406 (IFVE-STF-69-71)
neutrino reactions with nuclei at 50 to 100 GeV, coherent, incoherent, and inelastic cross sections for W-meson production in, (T), 25:3340
neutron capture by, performance of liquid scintillation detectors for measurement of cross sections for, 25:2435 (RPI-328-202)
neutron emission from, energy spectra and probabilities for delayed, (T), 25:3713 (CEA-N-1333)
neutron reactions (n,α), (n,p), and (n,2n) at 14.5 MeV with medium-weight, systematics of cross sections for, (E/T), 25:3643
nucleon scattering by, single-particle resonances in RPA treatment of, (T), 25:3718
particle reactions at high energies, optical limit of Glauber theory for, 25:3317
photodisintegration of A = 3, analysis using dipole sum rule and realistic potentials, (T), 25:3768
photon elastic and inelastic scattering by, analysis of, (T), 25:3655
photon reactions at high energies, Glauber theory approximation of rhoN cross sections from rho production in, 25:3317
photon reactions with, review on, 25:3715 (NBS-MON-118)
production of light neutron-rich, in heavy ion transfer reactions, (E), 25:3648 (JINR-E7-5319)
proton reactions (p,γ) with light and intermediate, distribution of radiation widths from, (T), 25:3767
triton elastic scattering by A = 24 to 116, analysis using optical potential, (T), 25:3769

NUCLEIC ACID
synthesis in γ-irradiated barley plants, role of plant hormones in, 25:2597

NUCLEIC ACID, DEOXYRIBO-
integration of extracellular chromosomal, into nuclei of recipient mammalian cells, autoradiography of, 25:2515
radiation effects on, of human xeroderma pigmentosum cells, repair synthesis following, uv and x, 25:2535
radiation effects on, of xeroderma pigmentosum cells, repair synthesis following uv, 25:2567
sodium salt, radiolysis of aqueous solutions of, ultrasonic absorption studies on γ, 25:2285

NUCLEIC ACID, RIBO-
synthesis in tobacco mosaic virus, double-stranded forms as intermediates in, 25:2551(R) (CCO-873-28)

NUCLEONS
form factors for, Veneziano model for, (T), 25:3394
form factors of, off-mass-shell, 25:3745
interaction vertex for NNrho, Schwinger and sea-gull terms in parity-violating weak, 25:3338
interactions anti N + N, relativistic one-boson-exchange model for meson spectrum in bound states of, (T), 25:3358 (DESY-70/49)
interactions e + N → e + N, on-shell subtracted dispersion relations and low-energy theorems and sum rules from current algebra for, (T), 25:3368
interactions e + N, Deser--Gilbert--Sudarshan representation for structure functions for particle production in, (T), 25:3329
interactions γ + N → $\pi^-(\pi^+)$ + $\Delta^{++}(\Delta^-)$, conspiracy and duality in model for forward cross sections of, (T), 25:3318
interactions γ + N in SU(3) quark model, pseudoscalar-meson production in, (T), 25:3321
interactions γ + N, phases and forward cross sections for rho^0, ω, and phi production in, (T), 25:3319
interactions K + N, asymptotic conservation of helicity for, 25:3398
interactions K + N, Regge models of asymptotic behavior of amplitudes for forward elastic, 25:3357
interactions K$^-$ + N, Regge models of asymptotic behavior of amplitudes for forward elastic, 25:3357
interactions Λ + N, one-boson-exchange potential model for, (T), 25:3416
interactions N + N → π + N + N, factorization test for Pomeranchukon in, 25:3395
interactions N + N at low energies, bremsstrahlung production in, (T), 25:3756
interactions N + N, duality concept for Pomeranchuk term for, 25:3375
interactions N + N, effect of tensor forces in residual, (T), 25:3766
interactions N + N, field-theoretic model of two-pion-exchange potential for, 25:3414
interactions N + N, Poisson distribution of secondary mesons in straight-line paths approximation for, (T), 25:3407 (JINR-E2-5329)
interactions N + N, Regge models of asymptotic behavior of amplitudes for forward elastic, 25:3357
interactions ν + N at high energies, review of, (T), 25:3334 (NYO-4204-3)
interactions ν + N in duality model, q^2 dependence of Regge residue functions for inelastic, 25:3336
interactions ω + N, cross sections from ω photoproduction on nuclei at 5.7 GeV, (E), 25:3247
interactions π + N → π + π + N at high energies, Regge-pole model for, 25:3399
interactions π + N → π + π + N, factorization test for Pomeranchukon in, 25:3395
interactions π + N → π + rho + N at high energies, Regge-pole model for, 25:3399
interactions π + N above 5 GeV/c, absorptive model corrections to Regge pole exchange in, 25:3390
interactions π + N at 6 to 55 GeV, complex angular momenta theory for, (E/T), 25:3381 (JINR-P2-5320)
interactions π + N at high energies, γ_5 gauge invariance for helicity conservation in, (T), 25:3403
interactions π + N, asymptotic conservation of helicity for, 25:3398
interactions π + N, complex Regge poles in cut j plane for charge exchange, (T), 25:3402
interactions π + N, duality concept for Pomeranchuk term for, 25:3375
interactions π + N, fixed-u finite-energy sum rule calculations of, 25:3396
interactions π + N, on-shell subtracted dispersion relations and low-energy theorems and sum rules from current algebra for, (T), 25:3368
interactions π + N, Regge models of asymptotic behavior of amplitudes for forward elastic, 25:3357
interactions π + N, sum rules and symmetries for, 25:3387
interactions π + N, t-channel peculiarities in static model of s waves in, (T), 25:3380 (JINR-P2-5263)
interactions π^- + N, dispersion relations for structure of backward differential cross sections of, (T), 25:3377 (ITF-70-65)
interactions π^+ + N, dispersion relations for structure of backward differential cross sections of, (T), 25:3377 (ITF-70-65)
interactions rho + N, cross sections from rho photoproduction on nuclei in Glauber theory, 25:3317
interactions rho + N, phase of rho production amplitude in γ reactions with beryllium at 4.1 to 6.1 GeV for real-to-imaginary amplitude ratio for, (E), 25:3256
interactions with hyperons, geometrical and Regge

pictures for elastic, 25:3354
interactions with mesons and nucleons, phenomenological model for violation of Pomeranchuk theorem for, 25:3356
interactions with mesons in SU(3) quark model, vector-meson production in, (T), 25:3400
scattering by nuclei, single-particle resonances in RPA treatment of, (T), 25:3718
transfer in heavy-ion scattering by nuclear Josephson effect, (T), 25:3752
NUCLEONS (anti N)
interactions anti N + N, relativistic one-boson-exchange model for meson spectrum in bound states of, (T), 25:3358 (DESY-70/49)
NUCLEOSIDES
labeling with radioisotopes, method for enzymatic, 25:2520

O

OCONEE POWER REACTOR, UNIT 1
emergency systems for, preliminary safety analysis of, 25:3834 (DOCKET-50269-28)
protection systems for, preliminary safety analysis of, 25:3834 (DOCKET-50269-28)
OCONEE POWER REACTOR, UNIT 2
emergency systems for, preliminary safety analysis of, 25:3834 (DOCKET-50269-28)
protection systems for, preliminary safety analysis of, 25:3834 (DOCKET-50269-28)
OCONEE POWER REACTOR, UNIT 3
emergency systems for, preliminary safety analysis of, 25:3834 (DOCKET-50269-28)
protection systems for, preliminary safety analysis of, 25:3834 (DOCKET-50269-28)
OCTANE
1,3-cyclooctadiene--octane, radiolysis of, kinetics of production of ethane, hydrogen, and methane from γ, 25:2270
benzene--octane, radiolysis of, kinetics of production of ethane, hydrogen, and methane from γ, 25:2270
cyclooctatetraene--octane, radiolysis of, kinetics of production of ethane, hydrogen, and methane from γ, 25:2270
OIL SHALES
fracture by nuclear explosions for oil recovery, 25:2380 (CRNL-4572, pp 196-8)
OLIVINES
effects on properties of sintered zircons, 25:2766(T) (CSIRO-Trans-9924)
OOCYTES
radiation effects on, of progeny of mice following maternal exposure, x, 25:2593
OPTICAL SYSTEMS
schlieren method and application to plasma diagnostics, (E/T), 25:3067
ORES
prospecting in Mecsek region of Hungary, gamma--gamma logging method for, 25:2347(T) (CSIRO-Trans-10140)
thermal treatment with plasma jets, Maxwellization of gas processes in, (T), 25:3098
ORGANIC COMPOUNDS
effects on photometric determination of hafnium and zirconium in geological specimens, 25:2084
effects on strontium-90 transport through soils, 25:2365
purity of radioisotope-labeled, use of thin-layer electrophoresis for control of, 25:2062 (CNEA-271)
radiolysis of, model for electron, 25:2260 (IRI-133-70-2)
ORGANIC COMPOUNDS, METALLO-
structure of, crystal and molecular, 25:3959 (IS-T-390)
ORGANIC COMPOUNDS, SILICO-
crystal structure of 1,1-dimethyl-2,5-diphenyl-1-silacyclopentadiene, 25:3963 (IS-T-423)
ORIFICES
brine flow control by variable, in multistage flash evaporators, 25:2387 (ORNL-TM-2746)
ORNL HIGH-FLUX ISOTOPE REACTOR
fuel plates for, fabrication and evaluation of, 25:2770 (ORNL-4570, pp 127-35)
OROTIC ACID
radiolysis of, spectral studies on kinetics of pulse, 25:2275
OROTIDINE MONOPHOSPHATES
synthesis of carbon-14-labeled, use of enzymes for, 25:2520
OSMIUM
effects on determination of trace amounts of rhenium by thiocyanate--stannous chloride method, 25:2102
separation from nitrate and sulfate solutions by solvent extraction using amines, 25:2319 (ORNL-4572, pp 181-95)
OSMIUM ISOTOPES Os-185
electron-capture decay of, γ and internal conversion spectra from, (E), 25:3704
OSTEICHTHYES
Cyprinus carpio, cesium accumulation by, in pond ecosystem, neutron activation analysis of, 25:2516
Lepomis gibbosus, cesium content of, neutron activation analysis of, 25:2517
Lepomis gibbosus, cobalt-60 distribution in tissues of, following uptake from water, 25:2526
Lepomis gibbosus, radioisotope accumulation in, of northern Italy, factors affecting concentration factors for fallout cesium-137 and strontium-90, 25:2527
Perca fluviatilis, cesium content of, neutron activation analysis of, 25:2517
Perca fluviatilis, radioisotope accumulation in, of northern Italy, factors affecting concentration factors for fallout cesium-137 and strontium-90, 25:2527
Scardinius erythrophtalmus, cesium content of, neutron activation analysis of, 25:2517
Scardinius erythrophtalmus, radioisotope accumulation in, of northern Italy, factors affecting concentration factors for fallout cesium-137 and strontium-90, 25:2527
OXYGEN
burning in advanced stellar evolution, (T), 25:2825
chemical potential profiles in electrolytes of pure and yttria-doped thoria, steady-state, 25:2203
determination in lunar materials by 14-MeV neutron activation and γ spectrometry, 25:2118 (CONF-700322-, pp 205-20)
determination in oceanographic samples by 14-MeV neutron activation and γ spectrometry, 25:2119 (CONF-700322-, pp 221-30)
determination in oxide fuels by x-ray diffraction measurements of lattice parameters, in-line, 25:2306(R) (ANL-7735)
determination in silicon by alpha activation, 25:2128 (LYCEN-7060)
determination in silicon by charged-particle activation method, 25:2143
determination in sodium using uranium, 25:2694
determination in steel by 14-MeV neutron activation, 25:2121 (CONF-700322-, pp 249-57)
effects on corrosion and mass transfer of chromium, cobalt, iron, and nickel by sodium at 660 and 760°C, 25:2631
effects on corrosion of zirconium and zirconium alloys by sodium at 450°C, 25:2611 (PEL-201)
effects on creep of tungsten at 1500 to 2000°C, 25:2673 (ORNL-4570, pp 118-23)
effects on gaseous yields from γ radiolysis of poly(tetrafluoroethylene), 25:2261 (NP-18518)
effects on radiolysis of water, 25:2257 (CEA-R-4046)
effects on solubility of tantalum and niobium in potassium at 1055 to 1287°K, 25:2664 (N-70-32146)
effects on yields from radiolysis of dodecane, 25:2292
enhancement of ionospheric F region 6300-A line of, effect of magnetically conjugate photoelectrons on predawn, (E/T), 25:2959
measurement of height profile in atmosphere above 70 km of atomic, sensor for, (E), 25:2968
proton reactions at 24 to 46 MeV, total cross sections for, (E), 25:3568
radiation effects on desorption of, from high-purity metal surfaces, charged particle, 25:2763
reactions of high-frequency plasmas of, with tantalum, 25:2632
reactions with carbon, mechanisms of, 25:2800
reactions with iron in sodium, 25:2711
reactions with molybdenum at 1100 to 2000°K, rotating disk method for studying convective-diffusion limited oxidation, 25:2688
reactions with niobium and tantalum at high temperatures, effects of argon or helium protective atmosphere on, 25:2639(T) (LIB/Trans-309)
reactions with oxygen ions (O_2^+), cross sections for charge exchange in, (T), 25:2912
reactions with trivalent neptunium, mechanism and products of oxidation, 25:2155
reactions with uranium in sodium 500 to 650°C, effects of oxygen concentration and mass transfer on oxidation, 25:2694
solubility in sodium at 350 to 550°C, electrochemical study of, 25:2711
sorption on tantalum films, method of determining, 25:2686
OXYGEN IONS
abundance of atomic and molecular, in ionospheric F1 layer, diurnal variations of, (E/T), 25:2987
electron reactions with OV, configuration-interaction calculations of cross sections for dielectronic transitions in, 25:2918
OXYGEN IONS (O^+)
diffusion coefficients of, in ionospheric F2 layer, (T), 25:2962
reactions with graphite and metal surfaces at 5 to 50 keV, apparent total ion scattering, secondary electron emission coefficients, and electron and ion energy distributions for, (E), 25:2884 (NP-18490)
OXYGEN IONS (O_2^+)
reactions with graphite and metal surfaces at 5 to 50 keV, apparent total ion scattering, secondary electron emission coefficients, and electron and ion energy distributions for, (E), 25:2884 (NP-18490)
reactions with oxygen molecules, cross sections for charge exchange in, (T), 25:2912
recombination in ionospheric 6300-A predawn airglow, dissociative, (E), 25:2961
spectral intensity in normal and type-B aurorae, (E),

XUM

25:3002
OXYGEN ISOTOPES O-16
binding energy of, calculation using Brueckner reaction matrix and Tabakin potential, (T), 25:3548
deuteron reactions (d,n) at 2.0 to 4.2 MeV, cross-section measurement by a thick-target method, (E), 25:3586
electron elastic scattering at 375 and 750 MeV, cross sections and charge distributions from, (E), 25:3587
energy level at 8.88 MeV from fluorine-19 (p,α) reactions, lifetime of, (E), 25:3569
energy levels at 6.92 and 7.12 MeV from gamma inelastic scattering, widths of, (E), 25:3571
energy levels of, Hartree--Fock calculations for, (T), 25:3545 (LYCEN-7047)
helium-3 reactions (He-3, Li-6) and (He-3, Be-7) with, strong-absorption model analysis of angular distributions from, (E/T), 25:3583
nuclear two-nucleon density function and Pauli correlation function for, (T), 25:3733
production in stars by carbon-12 (α,γ) reactions, 25:3562 (CONF-700322-, pp 297-304)
reactions with aluminum-27, mica-detector measurements of cross sections for compound nucleus formation in, 25:3611
OXYGEN ISOTOPES O-17
energy level at 7.56 MeV from carbon-13 (Li-6,d) and (Li-7,t) reactions, spin-parity assignment for, (E), 25:3570
energy levels of, calculation of even-parity low-lying, (T), 25:3582
OXYGEN ISOTOPES O-18
content in worldwide atmospheric precipitation, 1964 to 1966, data tabulations on, 25:2367 (STI/DOC-10/117)
deuteron reactions (d,p) and 5.0 MeV, proton and gamma and proton spectra from, (E), 25:3584
energy levels of, calculations using realistic forces and deformed-state admixtures, (T), 25:3580
reactions with thorium-232, yields of light neutron-rich nuclei in, (E), 25:3648 (JINR-E7-5319)
OXYGEN ISOTOPES O-19
energy levels and gamma branching ratios from oxygen-18 (d,p) reactions, (E), 25:3584
OXYGEN SYSTEMS
H--Na--O, phase studies of condensed phases in, at 400 to 1000°K, thermochemical, 25:2205
H--Na--O, vapor pressure of gaseous species over condensed phases in, at 400 to 1000°K, 25:2205
Na--O, electric potentials at 350 to 550°C, relations with composition, 25:2711
O--Zr, hardness of solid solutions of, effects of temperature on, 25:2700
OYSTER CREEK POWER REACTOR, UNIT 1
protection system for, scram circuit modifications for, 25:3813 (DOCKET-50219-115)

P

PACIFIC OCEAN
fish population and circulation in, 25:4004(R) (UCSD-34-P-127-5)
PACKED COLUMNS
dispersions in, axial, 25:2195 (ORNL-4572, pp 251-7)
fabrication for molten salt purification using molybdenum, 25:2609 (ORNL-4570, pp 175-90)
hydrodynamics of liquid bismuth--molten salts in, simulation of, 25:2313 (ORNL-4572, pp 1-36)
PAINTS
decontamination properties of, method for determination of, 25:2423
evaluation of commercial, for use in nuclear facilities, 25:2821 (ORNL-4572, pp 258-61)
radiation curing of, developments in, 25:2243
PAKISTAN
research programs in, on neutron activation analysis of biological materials, 25:2125 (IAEA-122, pp 27-36)
PALLADIUM
determination in titanium alloys, x-ray fluorescence method for, 25:2097
determination using pyridine-2-aldoxime, gravimetric, 25:2072
diffusion of carbon in, electronic mechanisms in thermal, 25:2666 (NP-18468)
diffusion of hydrogen in, electronic mechanisms in thermal, 25:2666 (NP-18468)
effects on determination of trace amounts of antimony by isotopic exchange in organic phase, 25:2106
effects on determination of trace amounts of rhenium by thiocyanate--stannous chloride method, 25:2102
photon reactions at 662 keV with, photoelectric cross sections for, (E), 25:2904
radioinduced preparation from aqueous salt solutions, electron, 25:2237 (N-70-32826)
PALLADIUM ALLOYS AND SYSTEMS
Ni--Pd, magnetic hyperfine fields at nickel-61 nuclei in, Moessbauer studies of, 25:2669 (ORNL-4570, pp 23)
PALLADIUM ISOTOPES Pd-102
energy levels from rhodium-102 decay, spins and parities of, (E), 25:3671
PALLADIUM ISOTOPES Pd-104
energy levels from palladium-105 (d,t) and silver-107 (p,α) reactions, spin-parity assignments and spectroscopic factors for, (E), 25:3701
PALLADIUM ISOTOPES Pd-105
deuteron reactions (d,p) and (d,t) at 17 MeV, angular distributions for, (E), 25:3701
energy levels from silver-105 decay, spins and parities of, (E), 25:3670
PALLADIUM ISOTOPES Pd-106
energy level at 1127.8 keV, g-factor for, (E), 25:3664
energy levels from palladium-105 (d,p) and silver-109 (p,α) reactions, spin-parity assignments and spectroscopic factors for, (E), 25:3701
PALLADIUM ISOTOPES Pd-108
proton reactions (p,α) and 12 and 15 MeV, angular distributions for, (E), 25:3701
PANCREAS
impairment of function of, effects on calcium-47 retention in patients, 25:2531
PARTICLE MICROSCOPES
design and performance of atom probe field ion, 25:3991 (UCRL-20303)
PARTICLE TRACKS
analysis of dielectric track detector, for particle discrimination and energy determination, 25:2438
analysis of nuclear emulsion, for neutron spectroscopy, semi-automatic system for, 25:2433 (CEA-R-4063)
analysis of spark chamber, computer graphics patching of failed CYCLOPS events in, 25:2486 (RHEL/R-205)
PARTICLE TRAJECTORIES
analysis of first-order effects of misalignments in beam transport system on, 25:3495
PEACH BOTTOM POWER REACTOR, UNIT 1
operations history for September 1970, 25:3784 (DOCKET-50171-58)
PEMOLINE
radioprotective effects of, on mice, effects of pre- and postexposure administration on x, 25:2576
PENTANE
determination in products from radiolysis of gaseous ethylene, gas chromatographic method for, 25:2278
PENTANE, 2-METHYL-
determination in products from radiolysis of gaseous ethylene, gas chromatographic method for, 25:2278
PENTANE, 3-METHYL-
determination in products from radiolysis of gaseous ethylene, gas chromatographic method for, 25:2278
radiation effects on electric conductivity of solid, at -196°C, γ, 25:2221
radiolysis of gaseous, isomerization of butyl ions in γ, 25:2290
2,4-PENTANEDIONE
complexes with protactinium, distribution and stability constants for, 25:2202
2-PENTANONE, 4-METHYL-
4-methyl-2-pentanone--4,4,4-trifluoro-1-(2-thienyl)-1,3-butanedine, solvent properties for lawrencium, 25:2197
1-PENTENE
determination in products from radiolysis of gaseous ethylene, gas chromatographic method for, 25:2278
2-PENTENE
determination in products from radiolysis of gaseous ethylene, gas chromatographic method for, 25:2278
1-PENTENE, 3-METHYL-
determination in products from radiolysis of gaseous ethylene, gas chromatographic method for, 25:2278
PEOPLE'S DEMOCRATIC REPUBLIC OF GERMANY
fallout monitoring in low-level atmosphere of, following 7th and 8th Chinese nuclear explosions, 25:2370
PERCHLORIC ACID
effects on fixation of alkali on hydrated antimony pentoxide, 25:2333
reactions with plutonium, formation and decomposition of peroxy complexes in, 25:2154
PEROXIDASE
radiation effects on activity of, in sprouts of beans and clover, γ, 25:2596
PEROXYSULFATES
yields from γ radiolysis of aqueous sulfuric acid solutions, 25:2265
PERSONNEL
radiation dose to radioactive materials handling, IRC recommendations for somatic, 25:2574
radiation hazards to radioactive materials handling, criteria for protection against, 25:2573
radiation hzards to radioactive materials handling, criteria for protection against, 25:2572
radiation protection programs for, at Karlsruhe Nuclear Research Center, 25:2570(R) (KFK-1158)
uranium excretion by, following accidental inhalation, 25:2563
PERTURBATION THEORY
Schroedinger solutions in, perturbation method for, 25:3229
PETROLEUM
production stimulation using underground nuclear explosions, problems resulting from, 25:2382
recovery from oil shales fractured by nuclear explosions, 25:2380 (ORNL-4572, pp 196-8)
PETTEN TEST REACTOR
moderator for, comparison fast neutron dose scale for radiation effects on graphite, 25:3872 (DP-Report-559)

PHENANTHRENE
effects on γ-radioinduced graft polymerization of cellulose with styrene in methanol solutions, 25:2247
PHENOL
effects on radiolysis of water, 25:2267
PHILIPPINE ISLANDS
research on neutron activation analysis in medicine in, 25:2126 (IAEA-122, pp 37-40)
PHOSPHATES
analysis of solutions of, for cerium, chromium, manganese, and vanadium by coulometric titration, 25:2081
radiation effects on, carrier effects on behavior of recoil phosphorus-32 from, 25:2298
PHOSPHINE
reactions with recoil silicon-31 atoms, 25:2299
PH_3--Si_2H_6, radiation effects on, reactions of silicon-31 recoils from fast neutron, 25:2299
PHOSPHINE OXIDE, TRIETHOXY-
complexes with uranyl nitrate, spectra of, ir and Raman, 25:2212
PHOSPHINE OXIDE, TRIOCTYL-
bis(2-ethyhexyl) phosphate--trioctylphosphine oxide, solvent properties for uranium, 25:2319 (ORNL-4572, pp 181-95)
PHOSPHINE OXIDE, TRIPHENYL-
complexes with uranyl nitrate, spectra of, ir and Raman, 25:2212
PHOSPHOGLUCOMUTASE
radiation effects on stability of, in human carcinoma cell cultures, x, 25:2585
PHOSPHORIC ACID
effects of anodizing electrolytes of, on tantalum corrosion by zinc at 1000°C, 25:2630
PHOSPHORIC ACID, BIS(2-ETHYLHEXYL) ESTER
complexes with lanthanum and neodymium nitrates, spectra of, ir and Raman, 25:2193 (CONF-700403-8)
solvent properties for tellurium in sulfate solutions, 25:2321
bis(2-ethyhexyl) phosphate--trioctylphosphine oxide, solvent properties for uranium, 25:2319 (ORNL-4572, pp 181-95)
bis(2-ethylhexyl) phosphate--$CeCl_3$--HCl--H_2O--$NdCl_3$--$SmCl_3$, equilibria in Amsco, 25:2311 (IS-T-412)
PHOSPHORIC ACID, TRIBUTYL ESTER
solvent properties for uranium and thorium, effects of salting-out agents on, 25:2335
PHOSPHORODITHIOIC ACID, ESTERS
solvent properties for tellurium in sulfate solutions, 25:2321
PHOSPHORUS
abundance in Kapps Cancri, (E), 25:2840
determination in human tissues by thermal neutron activation, sensitivity of, 25:2123 (IAEA-122, pp 1-13)
effects on radioinduced brittleness of heavy-section Type A533B steel, 25:2757 (NRL-7121)
production of pure, review of techniques for, 25:3219
PHOSPHORUS IONS
effects on glass crystallization at 50 keV, relations with annealing, 25:2823
implantation in diamond crystals, semiconducting layers induced by, 25:3199
PHOSPHORUS ISOTOPES P-30
energy levels from silicon-28 (He-3,p) reactions, (E), 25:3602
energy levels from silicon-29 (d,p) reactions, (E), 25:3606
PHOSPHORUS ISOTOPES P-31
neutron inelastic scattering at 14 MeV, differential cross sections, (E), 25:3612
photon reactions (γ,2p) and (γ,2pn) at 23 to 62 MeV, cross sections for, (E), 25:3634
PHOSPHORUS ISOTOPES P-32
detection in radioecology studies, use of Cherenkov counting for, 25:2565
effects on bones of rats, sarcomagenic β, 25:2594
reactions of recoil, in irradiated phosphates, anion-exchange and gel-chromatographic studies on, 25:2298
reactions of recoil, in thermal-neutron-irradiated solid inorganic phosphates, 25:2302
sorption by Rhine River monomineralic fine sands, (E), 25:2350
PHOSPHORUS ISOTOPES P-33
uptake in tissue following injection for autoradiography studies, 25:2521
PHOTOELECTRIC CELLS
radiation effects on lithium-doped silicon, electron, 25:2814 (N-70-27167)
PHOTOGRAPHIC FILM
forming to spherical shapes, equipment and technique for, 25:3996 (UCRL-50926)
PHOTOMULTIPLIER TUBES
design of arrays of, for detection of atmospheric light signals from cosmic showers, 25:2490
noise in, source-dependent, 25:2461
trigger circuit for, design of constant fraction of pulse height, 25:2458
PHOTONS
coupling constant ratio $\gamma\omega^2/\gamma rho^2$ from structure of e^+e^- mass spectrum in γ reactions with beryllium at 5.1 GeV, (E), 25:3288
interactions at high energies, review on meson production in, 25:3315
interactions γ + d → d(p + n) + π^+ + π^- at 1 to 5 GeV in bubble chamber, differential and total cross sections for rho^0 production in, (E), 25:3246
interactions γ + γ → e^+ + e^+ + e^- + e^-, total cross sections for, (T), 25:3325
interactions γ + γ → e^+ + e^- + μ^+ + μ^-, impact factor representation for calculation of cross section for, (T), 25:3314
interactions γ + γ → π^+ + π^- + e^+ + e^-, total cross sections for, (T), 25:3325
interactions γ + γ → π^+ + π^+ + π^- + π^-, total cross sections for, (T), 25:3325
interactions γ + γ, amplitudes for forward elastic, (T), 25:3325
interactions γ + N → $\pi^-(\pi^+)$ + $\Delta^{++}(\Delta^-)$, conspiracy and duality in model for forward cross sections of, (T), 25:3318
interactions γ + N in SU(3) quark model, pseudoscalar-meson production in, (T), 25:3321
interactions γ + N, phases and forward cross sections for rho^0, ω, and phi production in, (T), 25:3319
interactions γ + p → γ + p above 5 GeV, differential cross sections for inelastic diffractive Compton, (T), 25:3308 (DESY-70/45)
interactions γ + p → γ + p at 6 GeV and small momentum transfers, differential cross sections for, (E), 25:3309 (DESY-70/46)
interactions γ + p → p + eta^0, eta^0 → 2γ at 0.8 to 1.1 GeV, recoil proton polarization in, (E), 25:3255
interactions γ + p → π^+ + π^- + p, diffraction dissociation mechanism for, (T), 25:3320
interactions γ + p → rho^0 + N + mπ at 5 to 100 GeV, diffractive rho--N* production and double peripheral processes with Pomeron and π exchange in, (T), 25:3308 (DESY-70/45)
interactions γ + p → rho^0 + p, rho mass shift in, 25:3326
interactions γ + p → Σ^+ + K^0 at 1.5 to 5 GeV, momentum spectra and cross sections for, (E), 25:3248
interactions γ + p → Y* + K^+ at 1800 to 2600 MeV, resonance widths and cross sections for, (E), 25:3251
interactions γ + p at high energies, Regge residues for extrapolation to electroproduction region for total cross sections of, (T), 25:3312 (NYO-4204-6)
interactions γ + p in second resonance region, isobar model analysis of single π production in, 25:3313
interactions with hadrons, continuous moment sum rules for single π production in, (T), 25:3327
polarization of high-energy, method using highly oriented graphite for, (E), 25:3257
properties of real and virtual, (T), 25:3331
reactions (γ,p) with carbon-12 and -13, cross sections for virtual, (E), 25:3566 (SAL-14)
reactions with A = 3 nuclei, analysis using dipole sum rule and realistic potentials, 25:3768
reactions with aluminum, beryllium, and copper at 1.5 to 5 GeV, cross sections for K^0 production in, (E), 25:3248
reactions with aluminum, carbon, lead, silver, tantalum, and zinc at 5.7 GeV, ωγ coupling constant and ωN cross section from ω production in, (E), 25:3247
reactions with atoms and ions, computer program for calculation of ionization cross sections for, 25:2903
reactions with beryllium at 4.1 to 6.1 GeV, real-to-imaginary amplitude ratio for rho + N interactions from phase of rho production amplitude in, (E), 25:3256
reactions with beryllium at 5.1 GeV, structure of e^+e^- mass spectrum for coherent interference between rho and ω decays from, (E), 25:3288
reactions with carbon, virtual Compton scattering in electron-pair production in, (E/T), 25:3252
reactions with electrons, heavy particles, and photons, bibliography for 1969 on, 25:2901 (ORNL-AMPIC-13)
reactions with nuclei at high energies, Glauber theory approximation of rhoN cross sections from rho production in, 25:3317
reactions with nuclei, review on, 25:3715 (NBS-MON-118)
PHOTOSPHERE
brightness of faculae and flocculi in, magnetic field effects on, (E), 25:2857(T) (AD-707256)
PHYSICS
bibliography on high-temperature materials, 25:2665 (NBS-SPEC. PUBL-315-5)
formalism for justification of ensembles in quantum statistical mechanics, 25:3238
formalism for justification of ensembles in quantum statistical mechanics, 25:3237
PHYTIC ACID
alkali metal and alkaline earth salts of, sorptive properties for strontium-90 from milk, 25:2346(P)
PICKERING POWER REACTOR, UNIT 1
fuels for, estimates of economics of, 25:3802
PICKERING POWER REACTOR, UNIT 2
fuels for, estimates of economics of, 25:3802
PICOLINIC ACID
1-oxide, complexes with americium, neptunium, plutonium, and uranium, ir and NMR spectral and thermogravimetric studies on, 25:2194 (KFK-1070)
complexes with americium, neptunium, plutonium, and

XUM

uranium, ir and NMR spectral and thermogravimetric studies on, 25:2194 (KFK-1070)
PICOLINIC ACID, 6-METHYL-
complexes with plutonium and uranium, ir and NMR spectral and thermogravimetric studies on, 25:2194 (KFK-1070)
PIGMENTS
analysis of, from ancient murals by neutron activation, 25:2133
PINCH EFFECT
simulation of sheet, computer, 25:3094
PIPES
standards code for U. S. power reactors, 25:3778
PLANETARY NEBULAE
inhomogeneities in, (E/T), 25:2837
PLANETS
atmospheres of, dynamic particle--spin orientation in, (T), 25:2831
PLANTS
fission products transport in freshwater, quantitative model for, 25:2548
populations of, research on development of, (E/T), 25:3946(R) (COO-1761-13)
populations of, research on development of, (E/T), 25:3947(R) (COO-1761-14)
radioisotope accumulation by, in natural waters, 25:2547
radioisotope fixation by aquatic, in Meuse River, cobalt-60 and manganese-54, 25:2544
radioisotope uptake by aquatic, effects of concentration in water on concentration factor for fallout, 25:2548
role in distribution and transport of radioisotopes in natural waters, 25:2547
PLASMA
book: Physics of Gas Discharge Plasma, 25:3076
charge exchange of dense current in ultrasonic magnesium jet, (E), 25:3079
charged-particle drift surfaces and magnetic surfaces in stellarator field, (T), 25:3128 (IPPJ-95)
charged-particle motion in nonequilibrium, radiations from, (T), 25:3092
collisions in, cross sections for basic, (E/T), 25:3075 (CEA-CONF-1627)
conductivity measurement method for, high-time-resolution electric, (E), 25:3081
conductivity of magnetized nonrelativistic equilibrium, statistical mechanical perturbation theory of bilinear, 25:3090
conductivity of partially ionized, calculation of electric, (T), 25:3093
confinement in circular quadrupole magnetic well DECA II B, (E), 25:3053 (CEA-CONF-1597)
confinement in stellarator fields, effects of inertia on losses, (T), 25:3060
confinement in Tokamak devices, space--time evolution of, (T), 25:3052 (CEA-CONF-1595)
confinement in toroidal octupoles, effects of time-varying fields on, (E/T), 25:3059
confinement of collisionless, using external electromagnetic fields, (T), 25:3057
diagnostics of argon, relaxation phenomena in shock tubes, (E), 25:3064
diagnostics of molecular hydrogen discharges, ion density from Stark broadening, 25:3068
diagnostics of nonequilibrium, spectroscopic, (T), 25:3061 (CEA-CONF-1628)
diagnostics of weak-current arc discharges, using optical probing, 25:3065
diagnostics of, energy--mass analyzer for, (E), 25:3063
diagnostics of, parallel-plate capacitor impedance calculations for, 25:3100
diagnostics of, review of techniques for, 25:3069
diagnostics of, schlieren method for measuring density gradients, (E/T), 25:3067
diagnostics of, use of high-frequency Stark effect in, 25:3062
diagnostics of, using optical Mach--Zehnder and holographic interferometry, (E), 25:3071
diagnostics using laser interferometers, electron density measurement limits in, 25:3072
diagnostics using lasers, density, (E), 25:3066
diagnostics using x-ray spectroscopy, temperature, 25:3073
dielectric constant of cylindrical, at microwave regions, (T), 25:3087
electric discharges in, distribution of ion densities in, (T), 25:3085 (LYCEN-7061)
electric field distribution in hydrogen arcs, with axial magnetic fields, (E), 25:3083
electrode immersion in, volt--ampere properties of cathode, (T), 25:3107
electron beam interactions with hydrogen, ion heating in, (E), 25:3054 (CEA-CONF-1611)
electron beam interactions with mirror-confined neutral streams, ionization in, 25:3113
electron beam interactions with preformed decay, nonlinear stabilization of beam instability in, (E), 25:3126
electron beam interactions with waveguide, transformation of longitudinal into transverse energy in cyclotron, 25:3080
electron beam interactions with, wave growth from, (T), 25:3157
electron velocity distribution in optically thin hydrogen, (T), 25:3102
flow in inherent fields of arc discharges, compressible, (T), 25:3103
flow velocity of free-molecular, accuracy of probe measurements of, (T), 25:3074
heating and ionization by harmonic absorption of microwaves, (E), 25:3145 (CEA-CONF-1607)
heating by electron beam interactions with, ion, (E), 25:3054 (CEA-CONF-1611)
heating in magnetic mirrors, stochastic model of electron-cyclotron, (T), 25:3055 (IPPJ-100)
heating in magnetic mirrors, stochastic, (T), 25:3058
heating in mirror machines, review of turbulent, 25:3056 (ORO-1171-1, pp 78-97)
ionization and heating by harmonic absorption of microwaves, (E), 25:3145 (CEA-CONF-1607)
kinetic equations for autocorrelation functions for, 25:3099
kinetic theory of partially ionized hydrogen, deviations from thermodynamic equilibrium, (T), 25:3106
kinetics of argon--helium, Monte Carlo solution of Maxwellization process in, 25:3098
laser beam scattering by dense, cross sections for, (T), 25:3101
magnetic field production by electrons of, undergoing inverse Faraday effect, (E), 25:3082
motion and equilibrium in unsymmetric magnetic fields, (T), 25:3097
motion in cusped magnetic fields, flow velocity in, (T), 25:3091
oscillations from interacting rare gas flows, electrostatic, (T), 25:3089
oscillations in cold magnetized, nonlinear, (T), 25:3160
oscillations in current-carrying, Newtonian-velocity sound in, (T), 25:3156
oscillations in inhomogeneous magnetized, electrostatic low-frequency, (E/T), 25:3163
oscillations in partially ionized, low-frequency ionization--diffusion, (T), 25:3152
oscillations in turbulent cosmic, quasi-linear approximation of spectral energy density of, (E/T), 25:2929
particle--spin orientation in astrophysical, dynamic, (T), 25:2831
phase transition in imperfect metal-vapor, formation of heavy negative charged clusters in, (T), 25:3086
production and confinement in Tokamak devices, space--time evolution of, (T), 25:3052 (CEA-CONF-1595)
production by dissociation of accelerated hydrogen cluster beam, 25:3109 (CEA-CONF-1610)
production by laser irradiation, bibliographic references on, 25:3110 (IN-1425)
production for fusion research, review of, 25:3114
production in crossed-field devices, energy distribution in, 25:3115
production in high-pressure and high-current long arcs, (E), 25:3112
production in magnetic mirrors by electron beam injection, 25:3113
production of dense low-temperature, shock tubes for, 25:3116
production of, design of reflex source with axial extraction for, 25:3111 (LYCEN-7065)
radiations from Tokamak-confined, synchrotron, (T), 25:3095
reactions in current-carrying admixtures of, synthesis of differently charged nuclei in, 25:3140
research at Inst. of Nuclear Research, Warsaw, 1969, 25:2497(R) (INR-1180)
simulation of sheet pinch, computer, 25:3094
spectra of low-temperature, effect of nonhomogeneous interatomic electric fields on, (T), 25:3108
stability in constant magnetic and hf electric fields, .lf, (T), 25:3121
stability in Q machines, collisional drift, (T), 25:3119
stability in strongly nonuniform magnetic field, (T), 25:3122
stability of current-carrying, effect of hf field on ion--acoustic, (T), 25:3125
stability of cylindrical, ion cyclotron, (T), 25:3124
stability of dense, effects of stationary electric field on cyclotron, (T), 25:3120
stability of inhomogeneous, parametric, (T), 25:3118
stability of MHD nonequilibrium, boundary effects in linear development of electrothermal, (T), 25:3127
stability of, bounce effects on negative mass, (T), 25:3117 (CEA-CONF-1598)
stabilization of confined collisionless, using electromagnetic fields, (T), 25:3123
turbulence in collisionless, spectra of magnetohydrodynamic, (T), 25:3096
wave absorption by magnetized low-density, harmonic cyclotron, (E), 25:3145 (CEA-CONF-1607)
wave absorption in toroidal hard-core configuration, hydromagnetic, (E/T), 25:3148 (CEA-CONF-1614)
wave attenuation in, dispersion relations for acoustic, (T), 25:3155
wave damping in, Landau, (T), 25:3166
wave echoes in collisionless, effects of pulse length on spatial, (T), 25:3154
wave echoes in collisionless, theory for nondamping,

25:3164
wave echoes in, damping of, (T), 25:3144 (CEA-CONF-1601)
wave excitation and growth in electron beam--plasma system, (T), 25:3157
wave interactions in, theory of magnetohydrodynamic, 25:3159
wave interactions with nonisothermal, lf resonances and averaged potential in, (T), 25:3165
wave propagation in collisionless hydrogen, drift-, (E/T), 25:3167
wave propagation in collisionless magnetized, trapped-particle effect on drift-, (T), 25:3149 (CEA-CONF-1616)
wave propagation in collisionless, drift-, (E), 25:3147 (CEA-CONF-1612)
wave propagation in laminar, magneto-acoustic, (T), 25:3158
wave propagation in sheared magnetic field, polarization of electromagnetic, (E), 25:3146 (CEA-CONF-1608)
wave propagation in streaming-ion, ion--acoustic, (E/T), 25:3161
wave propagation in, decay instability of cyclotron harmonic, (T), 25:3162
wave propagation in, effects of rf electric field on dispersion of ion, (T), 25:3150 (IPPJ-93)
wave propagation in, nonlinear effects of large-amplitude ion--acoustic, (E), 25:3151 (IPPJ-94)
wave reflection and absorption in inhomogeneous, electrostatic, (E), 25:3163

PLASMA ACCELERATORS
development for open-ended fusion reactors, requirements for, 25:3131 (ORO-1171-1, pp 3-37)
development of deflagration, (E/T), 25:3076
jet velocity relations for rail-type, (E/T), 25:3077
performance of high-current Hall, for fusion research, 25:3141
radiative losses in pulsed, bolometric method for measuring, 25:3084

PLASMA JETS
diagnostics of free nitrogen, spectroscopic, 25:3070
interactions of rarefied, electrostatic oscillations from, (T), 25:3089
use for detection of hydrocarbon deposits, (T), 25:3098

PLASTICS
radiation effects on, 1.3 MeV gamma and 6.0 MeV electron, 25:2819 (LCIE-342)
plastics--wood, structural properties of, produced by radioinduced polymerization, 25:2238

PLATES
neutron diffusion in, (T), 25:3539

PLATINUM
bonding to tantalum--tungsten alloys, development of methods for, 25:2672 (ORNL-4570, pp 112-15)
compatibility with plutonium-238 dioxide powder and spheres at 1200°C, 25:2663 (MLM-1684)
compatibility with plutonium-238 dioxide powder at 1200°C in presence of tantalum--tungsten alloy, 25:2663 (MLM-1684)
compatibility with plutonium-238 dioxide spheres at 1200°C in helium--hydrogen atmosphere, 25:2663 (MLM-1684)
compatibility with plutonium-238 dioxide spheres at 1200°C in presence of molybdenum, tantalum, or TZM, 25:2663 (MLM-1684)
determination in pigments from ancient murals by neutron activation, 25:2133
effects on determination of trace amounts of rhenium by thiocyanate--stannous chloride method, 25:2102
effects on uv spectrophotometric determination of gallium in aqueous solutions, 25:2100
fabrication of filters of, for californium ion exchange assembly, 25:2792 (ORNL-4570, pp 201-4)
ion reactions at 5 to 50 keV with, apparent total ion scattering, secondary electron emission coefficients, and electron and ion energy distributions for, (E), 25:2884 (NP-18490)
photon reactions at 50 to 412 keV with, total photoelectric cross sections for, 25:2905
radioinduced Frenkel defects in, stored-energy-release study of 3-MeV electron-, (E), 25:3197
reactions with aluminum, magnesium, thorium, and zirconium and aluminum and zirconium oxides, 25:2160
separation from nitrate and sulfate solutions by solvent extraction using amines, 25:2319 (ORNL-4572, pp 181-95)

PLATINUM ALLOYS AND SYSTEMS
Cr--Pt, properties of intermetallic compounds of, for fuel capsule liners, 25:2643 (ORNL-4570, pp 106-11)
Pt--U, electric conductivity of ferromagnetic UPt, temperature dependence of, 25:3215
Pt-base--Rh, compatibility with plutonium-238 dioxide powder at 1200°C in presence of tantalum--tungsten alloy, 25:2663 (MLM-1684)
Pt-base--Rh, compatibility with plutonium-238 dioxide powder and spheres at 1200°C, 25:2663 (MLM-1684)
Pt-base--Rh, compatibility with plutonium-238 dioxide spheres in presence of molybdenum, tantalum, or TZM, 25:2663 (MLM-1684)

PLATINUM ISOTOPES Pt-192
energy levels from gold-192 decay, spin-parity assignments for, (E), 25:3654

PLATINUM METALS
magnetic moments in, nuclear orientation studies of local, 25:3942 (COO-1569-67)

PLOWSHARE PROJECT
decontamination of Carlsbad Site following Project Gnome in, equipment and methods for, 25:2420 (NVO-410-2)

PLUTONIUM
abundance relative to uranium in reprocessing plant solutions, mathematical evaluation of, 25:2417 (BNWL-SA-3287)
book: The Metallurgy of Plutonium, 25:2658(T) (AEC-tr-7095)
complexes with 6-methylpicolinic acid, nicotinic acid, picolinic acid, and picolinic acid 1-oxide, ir and NMR spectral and thermogravimetric studies on, 25:2194 (KFK-1070)
determination in ambient air, tentative radiochemical method for, 25:2113
determination in biological materials, establishment of laboratory for, 25:2108 (RT/PROT-(70)14)
determination relative to uranium in oxide fuels by x-ray fluorescence, in-line, 25:2306(R) (ANL-7735)
reactions in perchloric acid, formation and decomposition of peroxy complexes in, 25:2154
separation from aqueous solutions by solvent extraction using trialkylamines, coalescence of organic solutions in, 25:2308 (CEA-R-3845)
separation from LMFBR fuels by solvent extraction, centrifugal contactor for, 25:2306(R) (ANL-7735)
solubility in dilute nitric acid, effects of hydrofluoric acid and temperature on, 25:2153

PLUTONIUM ALLOYS AND SYSTEMS
Pu-base--Ti, stability of β phase in, effects of heat treatments on, 25:2739

PLUTONIUM CARBIDES
mechanical properties of, review of, 25:2785 (LA-4452)
PuC--UC, preparation of dense microspheres and shards of, 25:2775 (ORNL-4572, pp 242-50)

PLUTONIUM CARBONITRIDES
PuCN--UCN, elastic properties of, 25:2798
PuCN--UCN, preparation of dense microspheres and shards, 25:2775 (ORNL-4572, pp 242-50)

PLUTONIUM FLUORIDES PuF_3
capsules for plutonium-239-enriched, 25:2313 (ORNL-4572, pp 1-36)

PLUTONIUM IONS
spectra of, hyperfine structure anomaly of plutonium-239 and -241, 25:2893

PLUTONIUM ISOTOPES Pu-238
determination in ambient air, tentative method for α spectrometric, 25:2113

PLUTONIUM ISOTOPES Pu-239
determination in ambient air, tentative method for α spectrometric, 25:2113
hyperfine structure anomaly of, from s electron, 25:2893
neutron reactions with, separated γ spectra from thermal, (E), 25:3649 (KFK-1214)

PLUTONIUM ISOTOPES Pu-240
determination in ambient air, tentative method for α spectrometric, 25:2113
triton reactions (t,pf) at 18 MeV, fission probabilities for, (E), 25:3679

PLUTONIUM ISOTOPES Pu-241
hyperfine structure anomaly of, from s electron, 25:2893
neutron fission cross sections from plutonium-240 (t,pf) reactions at 18 MeV, (E), 25:3679
nuclear magnetic moment, 25:2893

PLUTONIUM ISOTOPES Pu-242
triton reactions (t,pf) at 18 MeV, fission probabilities for, (E), 25:3679

PLUTONIUM ISOTOPES Pu-243
neutron fission cross sections from plutonium-242 (t,pf) reactions at 18 MeV, (E), 25:3679

PLUTONIUM NITRATES
shipping of, vibration testing of containers for, 25:2415 (ARH-1819)

PLUTONIUM NITRIDES
mechanical properties of, review of, 25:2785 (LA-4452)
PuN--UN, fabrication of advanced fuels of, development of methods for, 25:2769 (ORNL-4570, pp 62-7)
PuN--UN, mechanical properties of nonstoichiometric, at 25 to 1300°C, 25:2794(T) (ORNL-tr-2388)
PuN--UN, mechanical properties of, review of, 25:2785 (LA-4452)
PuN--UN, properties of clad fuels of, methods for characterization of, 25:2769 (ORNL-4570, pp 62-7)
PuN--UN, radiation effects on fuel pellets of, in-pile, 25:2769 (ORNL-4570, pp 62-7)

PLUTONIUM OXIDES PuO_2
compatibility of plutonium-238-enriched, with platinum and platinum--rhodium alloys at 1200°C, 25:2663 (MLM-1684)
fabrication of HFIR targets of, incorporating plutonium-242, 25:2792 (ORNL-4570, pp 201-4)
preparation by sol-gel process, 25:2317 (ORNL-4572, pp 170-3)
PuO_2--UO_2, fabrication of fuel pins of, development of methods for, 25:2768 (ORNL-4570, pp 47-61)
PuO_2--UO_2, mechanical properties of nonstoichiometric, at 25 to 1300°C, 25:2794(T) (ORNL-tr-2388)
PuO_2--UO_2, performance of fuels of, development of prediction methods for, 25:2789 (ORNL-4570, pp 68-75)

XUM

PuO_2--UO_2, preparation of microspheres of, by sol-gel process, 25:2774 (ORNL-4572, pp 149-69)
PuO_2--UO_2, production from nitrates, plant for continuous, 25:2306(R) (ANL-7735)
PuO_2--UO_2, radiation effects on clad pellet-type fuels of, in-pile, 25:2771 (ORNL-4570, pp 161-9)
PuO_2--UO_2, radiation effects on sphere-pac fuels of, review of in-pile, 25:2768 (ORNL-4570, pp 47-61)

PLUTONIUM URANIUM CARBIDES
elastic properties of, 25:2798
mechanical properties of, 25:2785 (LA-4452)

PLUTONIUM URANIUM NITRIDES
elastic properties of, 25:2798

PNEUMATIC SYSTEMS
design of terminal head for conduit-type, for remote transfer of articles, 25:2427(P)

POINT BEACH POWER REACTOR, UNIT 1
containment structure for, integrated leak rate test of, 25:3829 (DOCKET-50266-32)
containment structure for, stress testing of, 25:3830 (DOCKET-50266-33)
containment structure for, surveillance requirements for tendons of prestressed concrete, 25:3831 (DOCKET-50266-34)
coolant for, revised activity limits for, 25:3832 (DOCKET-50266-35)
radioactive waste for, revised handling procedures for liquid, 25:3832 (DOCKET-50266-35)

POLAND
cesium distribution in pond ecosystem in, neutron activation analysis of, 25:2516
radiation chemistry in, review on, 25:2217
radioactive waste processing in, design and operation of plant for, 25:2422

POLONIUM ISOTOPES Po-210
determination in seawater by solvent extraction and α counting or α spectrometry, 25:2112

POLYMERS
conference on, 25:2251
radiation effects on, 1.3 MeV gamma and 6.0 MeV electron, 25:2819 (LCIE-342)
radiation effects on, use of accelerators in studying, 25:2218 (CONF-700322-, pp 345-56)

POLYOXYMETHYLENE
radioinduced production in trioxane crystals, α, 25:2252

POLYPHENYLS
decontamination of, bacteriological processes in, 25:2327

POPULATIONS
radiation dose to human, IRC recommendations for maximum permissible, 25:2574
radiation effects on genetics of human, expanding role of protective programs against, 25:2571

POSITRON BEAMS
monitoring of low-intensity, rotating plastic scintillation detector for, 25:3497

POSITRONS
annihilation in quenched and annealed cadmium, temperature dependence of, 25:2898
interactions $e^+ + e^-$, design of experiment for studying cross sections of, (E/T), 25:3245

POTASSIUM
corrosive effects of boiling, on niobium--zirconium alloy in Rankine cycle test loop, effects of zirconium hot trap on, 25:2624
determination by potentiometric titration with sodium tetraphenylboron using Orion liquid ion exchange lead-selective electrode, 25:2104
determination following nonsulfide separation from elements, qualitative, 25:2101
determination in human liver by neutron activation and γ spectrometry, 25:2124 (IAEA-122, pp 15-26)
determination in human tissues by thermal neutron activation, sensitivity of, 25:2123 (IAEA-122, pp 1-13)
determination in oceanographic samples by 14-MeV neutron activation and γ spectrometry, 25:2119 (CONF-700322-, pp 221-30)
determination of trace amounts of, in nuclear-grade uranium oxide (U_3O_8) by direct reading spectrometric method, 25:2068 (NLCO-1071)
diffusion in oxygen-containing niobium and tantalum at 600°C, 25:2707
electron reactions with atomic, excitation cross sections for, (T), 25:2915
excitation cross sections for, calculation using approximation based on regional trial functions, 25:2895
neutron capture by, gamma spectra from thermal, (E), 25:3181
plasma of, optical probing for diagnostics in arcs, 25:3065
release to soil from organic debris in forest as function of decomposition mode and time, 25:2528
scattering by iodine atoms and molecules at thermal energies, differential cross sections at small angles for elastic, (E), 25:2922
separation from other alkali metals by fixation on hydrated antimony pertoxide in hydrochloric, nitric, and perchloric acids, effects of acidity and time on, 25:2333
solvent properties for molybdenum, titanium, tungsten, vanadium, and zirconium at 1012 to 1341°K, 25:2714
solvent properties for niobium at 1055 to 1287°K, effects of oxygen on, 25:2664 (N-70-32146)
solvent properties for tantalum at 1055 to 1287°K, effects of oxygen on, 25:2664 (N-70-32146)

POTASSIUM ACID PHOSPHATES
radiation effects on solid, reactions of recoil phosphorus-32 from thermal-neutron, 25:2302

POTASSIUM ALLOYS AND SYSTEMS
K--Na, corrosive effects on oxygen-contaminated tantalum at 1200 and 1350°F, effects of exposure time and welding on, 25:2623

POTASSIUM BROMIDES
proton channeling in crystals of, effects of radiation damage on, 25:3201
radiation effects on thallium-activated crystals of, photoscintillations in x-, 25:3194
radioinduced energy storage in crystals of, luminescence from aqueous release of γ, 25:2227
radioinduced luminescence of thallium-activated crystals of, flash x-, (E), 25:3193
radioinduced thermally stimulated conductivity of single crystals of, gamma and neutron, 25:3202

POTASSIUM CHLORIDES
proton reactions at 350 keV with, characteristic x-ray spectra from, (E), 25:2882 (CONF-700322-, pp 113-24)
radioinduced energy storage in crystals of, luminescence from aqueous release of γ, irradiated crystals of, 25:2227
radioinduced V bands in calcium-doped crystals of, effects of aggregation processes on x-, (E/T), 25:3198
$AlCl_3$--KCl, electric conductivity of molten mixtures of, 25:2805 (ORNL-4570, pp 31-4)

POTASSIUM IODIDES
lattice resonances in silver doped crystals of, low-lying, 25:3969 (NYO-2391-121)

POTASSIUM IONS
effects on cesium-137 availability in mineral soils, 25:2529
reactions with neon up to 30 keV, absolute excitation functions for K II spectra produced in, (E), 25:2911

POTASSIUM ISOTOPES K-37
energy levels from proton elastic and inelastic scattering by argon-36, spins, parities, and widths of, (E), 25:3641

POTASSIUM ISOTOPES K-39
helium-3 elastic scattering at 11.0 MeV, angular distributions for, (E), 25:3627
helium-3 reactions (He-3,d) at 11.0 MeV, angular distributions for, (E), 25:3627

POTASSIUM ISOTOPES K-40
abundance in three pallasites, (E), 25:2824
decay of, gamma spectra from, (E), 25:3694

POTASSIUM ISOTOPES K-41
energy levels from argon-40 (He-3,d) reactions, (E), 25:3632
helium-3 reactions (He-3,d) at 11.0 MeV, angular distributions for, (E), 25:3627
proton reactions (p,n) near threshold, Q-value for, (E), 25:3608

POTASSIUM MAGNESIUM FLUORIDES
preparation of high-purity and rare earth-doped monocrystalline, 25:2727 (ORNL-4570, pp 1-4)

POTASSIUM NITRATES
effects on radiolysis of water, 25:2257 (CEA-R-4046)

POTASSIUM SODIUM TARTRATES
polarization in ferroelectric transition in, NMR study of spontaneous, 25:3221
radiation effects on polarization in ferroelectric and nonferroelectric, γ-, 25:3221

POTASSIUM URANYL NITRATES
spectra of, ir and Raman, 25:2212

POTASSIUM URANYL SULFATES
fluorescence lifetimes of, effects of heavy water and impurities on, 25:2198

POWER CYCLES
materials for Rankine space, development of, 25:2607 (ORNL-4570, pp 103-5)

POWER PLANTS
cooling system protection from seawater corrosion, methods for cathodic, 25:2634
electric power generation in hydroelectric, in US to 2000, predictions for, 25:2393
thermal cycle for direct-flow supersonic compressorless MHD generator, 25:2935
thermodynamic analysis of, using MHD generator and thermocompressor, 25:2936

POWER SUPPLIES
development for superconducting magnets for synchrotron, 25:3513

PRASEODYMIUM
determination in misch metal as chlorates, nitrates, or perchlorates, photometric, 25:2077
determination of trace amounts of, in lanthanum oxide, neodymium oxide, and yttrium oxide by direct reading emission spectrometry, 25:2096

PRASEODYMIUM ISOTOPES Pr-141
energy levels from proton resonances in cerium-140, spins, partial widths, and spectroscopic factors for decay of isobaric analog, (T), 25:3685

PRASEODYMIUM ISOTOPES Pr-144
detection in radioecology studies, use of Cherenkov counting for, 25:2565
PRASEODYMIUM ISOTOPES Pr-150
decay and energy-level transitions following californium-252 fission, (E), 25:3673
PREAMPLIFIERS
performance of pulsed-light feedback, with semiconductor detector for x-ray spectroscopy, 25:2462
PRESSURE VESSELS
failure of end slabs in prestressed concrete, lumped-parameter analysis of, 25:2411 (TID-25573)
nozzle-to-shell junctions in, stress analysis of region of, 25:2386 (ORNL-TM-2526(Add.))
PROLINE
spectra of, effects of deuterium on ir and Raman, 25:2190
PROMETHIUM ISOTOPES Pm-143
energy levels from proton resonances in neodymium-142, spins, partial widths, and spectroscopic factors for decay of isobaric analog, (T), 25:3685
PROMETHIUM ISOTOPES Pm-147
diffusion in copper at 700 to 1010°C, tracer studies of, 25:2680
PROMETHIUM ISOTOPES Pm-149
energy level at 114 keV, g factor for, (E), 25:3705
PROPANE
determination in products from radiolysis of gaseous ethylene, gas chromatographic method for, 25:2278
effects on radiolysis of ammonia, 25:2283
PROPANE, 2,2-DIMETHYL-
radiolysis of gaseous, isomerization of butyl ions in γ, 25:2290
PROPANE, 1,2-EPOXY-2-METHYL-
radioinduced polymerization of liquid, mechanism of x, 25:2256
PROPANE, 2-METHYL-
determination in products from radiolysis of gaseous ethylene, gas chromatographic method for, 25:2278
radiolysis of gaseous, isomerization of propyl ions in γ, 25:2290
2-PROPANOL
effects on radiolysis of ammonia, 25:2283
photooxidation by uranyl ions in aqueous solutions, mechanism of, 25:2158
radiolysis of frozen aqueous solutions of, effects of acids on hydrogen abstraction by primary species from γ, 25:2293
1-PROPANOL, 2-METHYL-
photooxidation by uranyl ions in aqueous solutions, mechanism of, 25:2158
2-PROPANOL, 2-METHYL-
photooxidation by uranyl ions in aqueous solutions, mechanism of, 25:2158
PROPENE
determination in products from radiolysis of gaseous ethylene, gas chromatographic method for, 25:2278
effects on radiolysis of ammonia, 25:2283
PROPENE POLYMERS
radiation effects on stress-rupture stability of isotactic, by cross linking, electron, 25:2249
radioinduced chlorination of, kinetics of, 25:2250
PROPIONITRILE, 2,2'-AZOBIS[2-METHYL-
effects on graft polymerization of polyethylene with styrene, 25:2241
PROPIOPHENONE
radiolysis of, yields from electron, 25:2266
PROPYL RADICALS
structure of ionized, produced in gas-phase radiolysis of alkanes, 25:2290
PROPYNE
determination in products from radiolysis of gaseous ethylene, gas chromatographic method for, 25:2278
PROTACTINIUM
complexes with 2,4-pentanedione, distribution and stability constants for, 25:2202
separation from MSBR fuel by fluorination--reductive extraction, 25:2313 (ORNL-4572, pp 1-36)
PROTACTINIUM ISOTOPES Pa-231
neutron fission in reactor spectrum, mass and neutron yields for, (E), 25:3656
PROTEINS
structure of, neutron diffraction techniques for study of, 25:3907 (NP-18462)
synthesis in tobacco mosaic virus, carbon-14 and tritium tracer study of, 25:2551(R) (COO-673-28)
PROTON BEAMS
monitoring of high-energy high-intensity, using dielectric track detectors, 25:2434 (CERN-70-27)
transport in electromagnetic lenses, transformation matrix for beam ellipse matching in waist-to-waist, 25:3521
PROTON SOURCES
development of polarized, from charge exchange collisions between metastable H(2S) atoms and halogens, 25:3307
PROTONS
channeling in potassium bromide crystals at 1.5 MeV, effects of radiation damage on, 25:3201
diffusion coefficients in ionospheric F2 layer, (T), 25:2962
effects on void formation in aluminum subjected to preinjection of hydrogen, 25:2816 (ORNL-4570, pp 16-19)
energy distribution of 0.06 to 3.3 MeV, at 6.6 Earth radii, Oct. 2 to 13, 1968, (E), 25:2951 (AD-709723)
energy spectra of disturbed and quiescent magnetospheric, differential, (E), 25:2980 (AD-709363)
interactions anti p + p → $2\omega^0 + 2\pi^+ + 2\pi^- + 2\pi^0$, method for study of, 25:3362
interactions anti p + p → $3\pi^+ + 3\pi^- + m\pi^0$, cross sections and angular and momentum distributions for, (E), 25:3263
interactions anti p + p at high energies, analysis of differential and total cross section data for, 25:3411
interactions anti p + p, research at Univ. of California Oct. 1, 1969 to Sept. 30, 1970 on heavy boson production in, (E), 25:3261(R) (UCI-34-P-149-1)
interactions anti p + p, upper bound on imaginary part of amplitude for, 25:3460
interactions d + p at 3.75 GeV/c, differential cross sections for elastic, (E), 25:3264
interactions e + p → π^0 + n at threshold, neutron electromagnetic form factor from, (E), 25:3244
interactions e + p at high energies, effect of transverse momentum distribution in parton model for inelastic, (T), 25:3323
interactions e + p, Bjorken limit and Jin--Martin lower bound for, (T), 25:3294 (NYO-4204-5)
interactions e + p, parton and quark models for deep inelastic, (T), 25:3310 (DESY-70/50)
interactions e + p, Regge residues for extrapolation of γ + p total cross sections at high energies to deep inelastic region of, (T), 25:3312 (NYO-4204-6)
interactions e + p, structure functions in ladder model with spin-$^1/_2$ nucleons for deep inelastic, (T), 25:3311 (NYO-4204-4)
interactions γ + p → γ + p above 5 GeV, differential cross sections for inelastic diffractive Compton, (T), 25:3308 (DESY-70/45)
interactions γ + p → γ + p at 6 GeV and small momentum transfers, differential cross sections for, (E), 25:3309 (DESY-70/46)
interactions γ + p → p + eta^0, eta^0 → 2γ at 0.8 to 1.1 GeV, recoil proton polarization in, (E), 25:3255
interactions γ + p → $\pi^+ + \pi^-$ + p, diffraction dissociation mechanism for, (T), 25:3320
interactions γ + p → rho^0 + N → mπ at 5 to 100 GeV, diffractive rho--N* production and double peripheral processes with Pomeron and π exchange in, (T), 25:3308 (DESY-70/45)
interactions γ + p → rho^0 + p, rho mass shift in, 25:3326
interactions γ + p → $\Lambda^+ + K^0$ at 1.5 to 5 GeV, momentum spectra and cross sections for, (E), 25:3248
interactions γ + p → $Y^* + K^+$ at 1800 to 2600 MeV, resonance widths and cross sections for, (E), 25:3251
interactions γ + p at high energies, Regge residues for extrapolation to electroproduction region for total cross sections of, (T), 25:3312 (NYO-4204-6)
interactions γ + p in second resonance region, isobar model analysis of single π production in, 25:3313
interactions K + p, upper bound on imaginary part of amplitude for elastic, 25:3460
interactions K^+ + p → K^0 + Δ^{++}, Regge pole model with Veneziano residues for, (T), 25:3384 (TPJU-3/70)
interactions K^- + p → K^0 + π^- + p at 3.3 GeV/c, generalized Veneziano-model fits to, 25:3391
interactions K^+ + p → $K^+ + \pi^- + \pi^+$ + p at 4.6 and 9 GeV/c in hydrogen bubble chamber, K^{*0}(890) Δ^{++}(1236) and K^{*0}(1420) Δ^{++}(1236) double resonance and Δ^{++}(1236)π^- and $K^+\pi^-$(1100) enhancement production in, (E), 25:3271 (UCRL-19809)
interactions K^- + p → n + K^- + π^+ at 10 GeV/c, Veneziano model with π and Pomeron exchange for, (T), 25:3386
interactions K^+ + p at 0.140 to 14.800 GeV/c, data compilation on real parts of forward amplitudes of, (E), 25:3379 (JINR-E1-5259)
interactions K^- + p at 0.293 to 15.910 GeV/c, data compilation on real parts of forward amplitudes of, (E), 25:3379 (JINR-E1-5259)
interactions K^+ + p at 3.5 GeV/c, associated production in, (E), 25:3277
interactions K^- + p at 3.9 to 5.0 GeV/c in hydrogen bubble chamber, K^0(1420) production in, (E), 25:3287
interactions K^+ + p below 2.0 GeV/c, phase-shift analysis of elastic, 25:3392
interactions Λ + p at low energies, one-boson-exchange potential model for, (T), 25:3416
interactions μ + p, anomalous interaction for cross section ratio for e + p and, 25:3324
interactions ν + p, Bjorken limit and Jin--Martin lower bound for, 25:3294 (NYO-4204-5)
interactions p + d → p + d above 1 GeV, model for wide-angle, (T), 25:3419
interactions p + n → Δ^{++}(1236) + Δ^-(1236) at 6.98 GeV/c cross sections and decay correlations for, (E), 25:3265
interactions p + n and p + p at 12.4 GeV/c using liquid deuterium target, cross section ratio for elastic, (E), 25:3266
interactions p + p → d + π^+ at threshold, nucleon and Roper-resonance pole analysis of, 25:3410
interactions p + p above 20 GeV/c, diffraction model for

forward peak in elastic, 25:3417
interactions p + p at 0.86 to 2.74 GeV/c, polarization and differential cross sections for elastic, (E), 25:3262
interactions p + p at 5 to 31 GeV in OBE model, differential cross section, polarization, and forward amplitude for, 25:3418
interactions p + p at high energies, analysis of differential and total cross section data for, 25:3411
interactions p + p, optical model for differential cross sections for elastic, (T), 25:3413
interactions p + p, upper bound on imaginary part of amplitude for elastic, 25:3460
interactions π + p → n + e+ + e−, rho--ω interference effects on cross sections for, (T), 25:3367
interactions π + p → π + eta + n at high energies, Regge-pole model for, 25:3399
interactions π + p, upper bound on imaginary part of amplitude for elastic, 25:3460
interactions π0 + p → π0 + p, Bjorken limit and Jin--Martin lower bound for, (T), 25:3294 (NYO-4204-5)
interactions π− + p → A2− + n at 3.16 GeV, structure in A2− mass spectrum in, (E), 25:3290
interactions π− + p → γ + n and π− + p → π0 + n → n + γ + γ at 40 MeV, gamma spectra for, (E), 25:3550
interactions π− + p → Λ + K+ + π−, five-point Veneziano amplitude for cross sections and effective-mass and angular distributions for, (T), 25:3378 (ITF-70-77)
interactions π+ + p → p + 2π+ + π− + π0 at 3.7 GeV/c, A2− and Δ++ associated production in, (E), 25:3272 (UCRL-20050)
interactions π− + p → p + π− + π+ + π− at 3.9 GeV/c, spin--parity analysis of 3π system in, (E), 25:3276
interactions π− + p → p(n) + K0 + K-(anti K0), five-point Veneziano amplitude for cross sections and effective-mass and angular distributions for, (T), 25:3378 (ITF-70-77)
interactions π− + p → π + π + N at 456 to 552 MeV/c, isobar analysis of, (E), 25:3282
interactions π− + p → π0 + π0 + n at 378 MeV in isobar model, S-wave ππ phase shift from, 25:3392
interactions π+ + p → π0(eta) + Δ++, Regge pole model with Veneziano residues for, (T), 25:3384 (TPJU-3/70)
interactions π− + p → π− + Δ+, Regge pole model with Veneziano residues for, (T), 25:3384 (TPJU-3/70)
interactions π+ + p → π+ + p + π− + π− at 5 GeV/c, analysis of pπ(1710) enhancement in, (E), 25:3275
interactions π− + p → π− + p at 1.71 to 3.01 GeV/c, evidence for existence of N(2210) and N(2220) from, (E/T), 25:3281
interactions π− + p → π− + p at 1.71 to 5.53 GeV/c, differential cross sections for, (E), 25:3280
interactions π+ + p → π+ + π− + Δ++ at 13.1 GeV/c, double-Regge pole analysis of, (E/T), 25:3273
interactions π− + p → π− + rho + p at 25 GeV/c, multi-Regge theory for kinematics and dynamics of, 25:3389
interactions π− + p → Σ0 + K+ + π−, five-point Veneziano amplitude for cross sections and effective-mass and angular distributions for, 25:3378 (ITF-70-77)
interactions π− + p → Σ0(Λ) + K0 + π0, five-point Veneziano amplitude for cross sections and effective-mass and angular distributions for, (T), 25:3378 (ITF-70-77)
interactions π+ + p → Σ+ + K+ at 1850 to 2090 MeV, angular distributions, polarization, and partial-wave analysis for, (E), 25:3283
interactions π− + p above 5 GeV/c, absorptive model corrections to Regge pole exchanges in elastic and charge-exchange, 25:3390
interactions π+ + p at 5.5 GeV/c, production of Δ(1236), Σ(1385), and K*(890) in, (E), 25:3279
interactions π− + p at 7 and 25 GeV/c in bubble chamber, difference in energy dependence for A2− and A20 production in, (E), 25:3289
interactions π− + p, experimental comparison between on- and off-mass-shell inelasticities in, 25:3285
interactions with charged conserved current, Bjorken limit and Jin--Martin lower bound for, (T), 25:3294 (NYO-4204-5)
interactions with neutrinos in the Universe, (T), 25:2874
penetration of high-energy solar and flare-associated, to equatorial ionosphere, (E), 25:2965
polarization measurements in porphyrexide-doped glycerol--water at low temperatures and high magnetic fields, 25:3500
polarization of recoil, in γ + p → p + eta0, eta0 → 2γ interactions at 0.8 to 1.1 GeV, (E), 25:3255
propagation of cosmic primary, in the neutrino sea, (T), 25:2874
reaction (p,d) with neon-21 at 20.0 MeV, angular distributions for, (E), 25:3633
reactions (p,2p) with calcium-40 and carbon-12 at 156 MeV, analysis of angular distributions for distortion effects in, (E), 25:3565 (NP-18476)
reactions (p,2p) with deuterium at 156 MeV, angular distributions and differential cross sections as test of impulse approximation, (E), 25:3554
reactions (p,2p) with deuterium at 9 to 13 MeV, spectra from, (E), 25:3553
reactions (p,3α) with boron-11 at 0.7, 1.0, and 1.4 MeV, analysis for reaction mechanism in, (E), 25:3589
reactions (p,α) with palladium-108, silver-107, and silver-109 at 12 and 15 MeV, angular distributions for, (E), 25:3701
reactions (p,d) with helium-3 at 30.5 and 49.5 MeV, angular distributions from, (E/T), 25:3555
reactions (p,d), (p,t), and (p,He-3) with helium-4 at 49.5 MeV, angular distributions from, (E/T), 25:3555
reactions (p,d*)p with deuterium at 9 to 13 MeV, excitation function for, (E), 25:3553
reactions (p,f) with uranium-233 at 25 to 85 MeV, fragment energy and angular distributions for, (E), 25:3702
reactions (p,f) with uranium-235 and -238 at 9.5 to 22 MeV, prompt-neutron energies and yields and fragment kinetic energy release in, (E), 25:3660
reactions (p,γ) with iron-56 at 1.21 to 2.57 MeV, angular distributions, gamma spectra, cross sections, and Q-value for, (E), 25:3601
reactions (p,γ) with light and intermediate nuclei, distribution of radiation widths from, (T), 25:3767
reactions (p,n) with copper-65 at 2.80 to 4.50 MeV, angular distributions, cross sections, and gamma spectra from, (E), 25:3631
reactions (p,n) with nickel-61, nickel-64, zinc-67, and zinc-68 at 3 to 6 MeV, neutron spectra from, (E), 25:3596 (TID-25503)
reactions (p,n) with nickel-64 at 2.5 to 3.3 MeV, excitation function for, (E), 25:3628
reactions (p,n) with potassium-41, scandium-45, vanadium-51, and iron-57 near threshold, Q-values for, (E), 25:3608
reactions (p,nγ) with vanadium-51 at 2.3 to 6 MeV, γ singles and coincidence and n-γ coincidence spectra from, (E), 25:3593 (COO-1530-21)
reactions (p,np) and (p,2p) with deuterium, modified impulse approximation and Chew--Low extrapolation for, (E/T)γ, 25:3750
reactions (p,pα) with carbon-12 at 160 MeV, plane-wave impulse-approximation analysis of triply differential cross sections from, (E/T), 25:3581
reactions (p,pn) with deuterium at 14 to 23 MeV, energy dependence of quasifree scattering in, (E), 25:3547 (RLO-1388-126)
reactions in lithium-drifted silicon detectors at 15 to 80 MeV, effects on pulse-height distributions of, 25:2451
reactions with aluminum-27, beryllium-9, carbon, fluorine-19, oxygen, and silicon at 24 to 46 MeV, total cross sections for, (E), 25:3568
reactions with graphite and metal surfaces at 5 to 50 keV, apparent total ion scattering, secondary electron emission coefficients, and electron and ion energy distributions for, (E), 25:2884 (NP-18490)
reactions with helium and neon at 1 to 100 keV, cross sections for charge exchange into excited and ground states in, (T), 25:2919
reactions with iridium in inorganic iridium compounds at 660 MeV, production of rhenium by, 25:2300
reactions with metals and nonmetals at 100 to 350 keV, characteristic spectra and yields per proton of x rays from, (E), 25:2862 (CONF-700322-, pp 113-24)
reactions with nitrogen molecules at 30 to 100 keV, absolute emission cross sections for, (E), 25:2902 (SC-RR-70-695)
scattering by argon-36 at 2.1 to 5.3 MeV, angular distributions for, (E), 25:3641
scattering by barium-138, cerium-140, neodymium-142, tellurium-130, and xenon-136 at 9 and 10 MeV, fits to angular distributions from resonance, (T), 25:3685
scattering by cobalt-59, iron, nickel, and zinc at 28 MeV, cross sections for elastic and inelastic, (E), 25:3599
scattering by europium-151 and europium-153 at 4.5 to 6 MeV with Coulomb excitation, γ spectra from inelastic, (E), 25:3703
scattering by even tin isotopes at 24.5 MeV, angular distributions for elastic and inelastic, (E), 25:3668
scattering by helium-3 at 30 and 50 MeV, differential cross sections and polarizations of elastic, (E), 25:3556
scattering by iron-54 and nickel-60 at 10 MeV, differential cross sections, polarizations, and p--γ angular correlations for elastic and inelastic, (E), 25:3613
scattering by nickel-58, -60, -62, and -64 and zinc-64, -66, and -68 at 39.6 MeV, cross-section and polarization measurements for elastic, (E), 25:3598
scattering by nickel-58, -60, -62, and F-64 at 1.8 to 3.3 MeV, differential cross sections for elastic, (E), 25:3628
scattering by nickel-58, tin-120, lead-208 at 30.3 MeV, angular distributions, polarizations, and optical-model analysis of elastic, (E), 25:3636
scattering by sodium-23 and magnesium-25 at 17.5 MeV, cross-section calculations for inelastic, (T), 25:3603
scattering by vanadium-51 at 23 to 6 MeV, γ spectra from inelastic, (E), 25:3593 (COO-1530-21)
scattering of polarized, by helium-4 at 3.38 and 7.80 MeV, polarization analyzing power and phase-shift analysis for elastic, (E), 25:3557

PROTONS (anti p)
interactions anti p + n → 2π⁻ + π⁺ at 1.0 to 1.6 GeV/c in deuterium bubble chamber, Veneziano model for 3π Dalitz plot structure in, (E/T), 25:3270 (INFN-PD-70/2)
interactions anti p + n → ω + 2π⁻ + π⁺ at rest in deuterium bubble chamber, upper limit on ω → π⁺ + π⁻ decay rate from, (E), 25:3269
interactions anti p + n → ω + π⁻ + π⁰ at rest in deuterium bubble chamber, upper limit on ω → π⁺ + π⁻ decay rate from, (E), 25:3269
interactions anti p + n → ω + π⁻ at rest in deuterium bubble chamber, upper limit on ω → π⁺ + π⁻ decay rate from, (E), 25:3269
interactions anti p + n at 3.5 GeV/c, differential cross section for elastic, (E), 25:3267
interactions anti p + p → 2ω⁰ + 2π⁺ + 2π⁻ + 2π⁰, method for study of, 25:3362
interactions anti p + p → 3π⁺ + 3π⁻ + mπ⁰, cross sections and angular and momentum distributions for, (E), 25:3263
interactions anti p + p at high energies, analysis of differential and total cross section data for, 25:3411
interactions anti p + p, research at Univ. of California Oct. 1, 1969 to Sept. 30, 1970 on heavy boson production in, (E), 25:3261(R) (UCI-34-P-149-1)
interactions anti p + p, upper bound on imaginary part of amplitude for, 25:3460
PULSARS
birth rate of, comparison to Type-II supernovae occurrence, (T), 25:2842
distances to, (T), 25:2854
evolution of, radio, (T), 25:2842
gravitational-wave emission from, (T), 25:2849
infrared pulses from, (T), 25:2854
magnetic fields of, decay of surface, (T), 25:2851
model of, co-rotating magnetic field, 25:2850
NP 0532, optical polarization of, (E), 25:2843
NP 0532, pulsed gamma emission from, (E), 25:2841 (CEA-CONF-1633)
NP 0532, time-of-arrival measurements of optical pulses from, 25:2853
radio luminosity of, (T), 25:2851
PULSE ANALYZERS
response of multichannel, numerical correction of nonlinear, 25:2509
PULSE COLUMNS
air-pulsing methods for, 25:2383 (AAEC/TM-547)
PULSE CONVERTERS
design of binary-to-decimal or decimal-to-binary, 25:2510
readout system for analog-to-digital, 25:2511
PULSE GENERATORS (ELECTRONICS)
design using mercury relay, 25:2513
PUMPS
seals for high-pressure nuclear power plant, design of, 25:2392
PYCNOMETERS
design for stabilization of gas pressure for flow-through proportional detectors, 25:2453
PYRENE
effects on γ-radioinduced graft polymerization of cellulose with styrene in methanol solutions, 25:2247
PYRIDINE
effects on γ-radioinduced graft polymerization of cellulose with styrene in methanol solutions, 25:2247
PYRIDINE-1-OXIDE
spectra of, effects of deuterium on ir, 25:2163
PYROMETERS
calibration of infrared, 25:3989 (UCRL-19665)

Q

Q DEVICES
plasma drift instabilities in, collisional, (T), 25:3119
QUAD CITIES POWER REACTOR, UNIT 1
design parameters of, requested additional information on, 25:3823 (DOCKET-50254-22)
effluents from, effects on environment of radioactive and thermal, 25:3826 (DOCKET-50254-25)
operations aspects of, requested additional information on, 25:3823 (DOCKET-50254-22)
operations aspects of, revised and additional data on, 25:3824 (DOCKET-50254-23)
pressure vessel for, design parameters and seismic stress analysis of, 25:3824 (DOCKET-50254-23)
site for, information on foundation grouting of, 25:3825 (DOCKET-50254-24)
QUAD CITIES POWER REACTOR, UNIT 2
design parameters of, requested additional information on, 25:3823 (DOCKET-50254-22)
effluents from, effects on environment of radioactive and thermal, 25:3826 (DOCKET-50254-25)
operations aspects of, requested additional information on, 25:3823 (DOCKET-50254-22)
operations aspects of, revised and additional data on, 25:3824 (DOCKET-50254-23)
pressure vessel for, design parameters and seismic stress analysis of, 25:3824 (DOCKET-50254-23)
site for, information on foundation grouting of, 25:3825 (DOCKET-50254-24)
QUANTUM ELECTRODYNAMICS
formulation of Wheeler--Feynman, S-matrix, 25:3446
formulations of relativistic and nonrelativistic, 25:3440
gauge formulation and renormalization in, Schwinger terms in, 25:3444
validity at low and high energies, tests of, (E), 25:3438
QUANTUM FIELD THEORY
Bethe--Salpeter equation, ladder approximation, and Ward--Takahashi identity for composite particles in, 25:3436
boson field phi⁴ interactions in three space--time dimensions in, exponential representations of canonical commutation relations for, 25:3442
Feynman-like diagram in harmonic oscillator formalism, factorization and duality of, 25:3443
field operators for composite particles, HNZ construction of, 25:3445
formulation of divergenceless, 25:3435 (TPJU-13/70)
formulations of relativistic and nonrelativistic, 25:3440
gauge invariance for charge operator for interpolating Heisenberg fields in, 25:3437
photon wave function in, gauge invariance and charge operator for interpolating Heisenberg fields for, 25:3437
quantization of Bhabha field with electromagnetic interaction, 25:3439
representation in, Jost--Lehmann-Dyson, 25:3433 (ITF-70-33)
QUANTUM MECHANICS
book: Methods of Molecular Quantum Mechanics, 25:2927
Dirac equation solutions in a magnetic field, 25:3230
electron motion in quantized field of flat electromagnetic wave, 25:3233
formalism for justification of ensembles in quantum statistical mechanics, 25:3237
formalism for justification of ensembles in quantum statistical mechanics, 25:3238
Fouldy--Wouthuysen transformations and related problems in, 25:3231
Hamiltonian of quantum statistics, 25:3040
Hartree--Fock theory and lambda transformation in statistical, for degenerate Bose system, 25:3228
scattering in, Martin's method for theory of potential, 25:3240
Schroedinger solutions in, perturbation method for, 25:3229
transformation coefficients in the hyperspherical approach to the three-body problem, 25:3729
variational solution of Schroedinger equation for finite fermion systems, 25:3241
variational solution of Schroedinger equation for finite fermion systems, 25:3242
QUARTZ
microstructure of, prepared using rubidium hydroxide solvent, 25:2727 (ORNL-4570, pp 1-4)
QUASARS
masses of, (T), 25:2876
radio spectra at 60 MHz, (E), 25:2845
radio spectra of, interpretation of curvature in, (E/T), 25:2847
8-QUINOLINOL
complexes with thorium(IV), structure of adduct from, 25:2157

R

RABBITS
radiation effects on retina of, laser, 25:2591
RADIATION
book: Radiation Corrosion, 25:2603(T) (AEC-tr-7096)
dose to personnel handling radioactive materials, IRC recommendations for somatic, 25:2574
effects of pulsed, on orotic acid, spectral studies on kinetics of, 25:2275
effects on bone marrow of rats, use of intraocular transplant technique for study of growth following, 25:2595
effects on curing of paints, developments in, 25:2243
effects on human population, expanding role of protective programs against genetic, 25:2571
effects on oranges in relation to cold weather survival, mutagenic, 25:2552(R) (ORO-2909-9)
effects on organisms, tables for determining statistical frequencies in comparisons of mutagenic, 25:2559
effects on stem cell populations in bone marrow of rats, development of computer model for, 25:2590
effects on water, ionic effects in, 25:2274
hazards to personnel handling radioactive materials, criteria for protection against, 25:2573
hazards to personnel handling radioactive materials, criteria for protection against, 25:2572
polarization and transformation theory of quasi-monochromatic, (T), 25:2846
RADIATION CHEMISTRY
developments in Poland in, review on, 25:2217
neutron generators for studies in, use of accelerators for, 25:2120 (CONF-700322-, pp 231-48)

RADIATION DETECTORS
design and operation of gas discharge, 25:2440
design of arrays of photomultipliers for detection of atmospheric light signals from cosmic showers, 25:2490
response of cobalt self-powered, for in-core neutron detection, 25:2467
theory of superconducting-weak-link, 25:2444
RADIATION DETECTORS, ACTIVATION
data analysis for neutron spectroscopy, computer method for, 25:2439
data processing of multiple, polynomial approximation of fast neutron spectrum in, 25:2442
RADIATION DETECTORS, BUBBLE CHAMBER
bubble formation in, calculation of electric field intensities for, 25:2485 (JINR-P13-5277)
RADIATION DETECTORS, CHERENKOV
design and performance of large aperture, 25:2489
RADIATION DETECTORS, CRYSTAL
design of diamond, 25:2441(P)
RADIATION DETECTORS, DIELECTRIC TRACK
particle tracks in, analysis for particle discrimination and energy determination, 25:2438
performance for profile measurements of high-intensity beams, 25:2434 (CERN-70-27)
RADIATION DETECTORS, FISSION CHAMBER
circuits for in-core thermal neutron flux monitoring, design and testing of 10-decade wide range, 25:2502 (GEAP-11094)
RADIATION DETECTORS, FISSION FOIL
data analysis for neutron spectroscopy, computer method for, 25:2439
RADIATION DETECTORS, GEIGER-MUELLER
efficiency for beta monitoring of environmental samples, 25:2448
operation of self-quenching, with heated anode, 25:2460
sensitivity measurements for radiobiological studies, 25:2432 (AD-706587)
RADIATION DETECTORS, IONIZATION CHAMBER
calibration for dosimetry of natural background radiation, 25:2448
design and performance of double-grid, for low-level alpha spectroscopy, 25:2476
design of pocket, with both optic and acoustic alarm, 25:2445
performance of DK-0.2, for fast neutron personnel dosimetry, 25:2493
RADIATION DETECTORS, PROPORTIONAL
control system for boron trifluoride, for neutron spectroscopy, automatic, 25:2475 (INP-707)
design and performance of proton-recoil, for in-core fast neutron spectroscopy, 25:2472 (AEEW-M-905)
development of multiwire position-sensitive, 25:2449
efficiency for beta monitoring of environmental samples, 25:2448
fabrication of 4π, method for mounting anode for, 25:2464
fabrication of Charpak multiwire, method for winding wires for, 25:2465
gas amplification factor for xenon-filled, equation for calculation of, 25:2730 (ORNL-4570, pp 44-6)
gas pressure stabilization in flowthrough, system for, 25:2453
performance of proton-recoil, for neutron spectroscopy at 200 eV to 1 MeV, 25:2481
RADIATION DETECTORS, SCINTILLATION
data processing for gamma spectroscopy, computer system for, 25:2477
design of rotating thin plastic, for monitoring electron and positron beams, 25:3497
energy transfer mechanism in naphthalene-containing liquid, 25:2450
neutron scattering in lithium-6-loaded, Monte Carlo study of multiple, 25:2456
performance of large liquid, for neutron capture cross section measurements, 25:2435 (RPI-328-202)
photopeak count-rates in thallium-activated sodium iodide, from gamma emitters formed by thermal neutron activation, table of calculated, 25:2474 (IAEA-122, pp 150-63)
response of unactivated sodium iodide, to gamma rays at 30 keV to 1 MeV at low temperatures, 25:2436
sensitivity measurements for radiobiological studies, 25:2432 (AD-706587)
sensitivity of Basson, containing boron oxide for intermediate neutron flux measurements, 25:2443
sensitivity of silver-activated zinc sulfide, in Plexiglas matrix for fast neutron flux measurements, 25:2443
use in radioecology studies of β emitters, 25:2565
RADIATION DETECTORS, SEMICONDUCTOR
contamination of surface-barrier, in alpha spectroscopy, sources and prevention of recoil, 25:2479
efficiency calculations for lithium-6 sandwich, for neutron spectroscopy, 25:2473 (AERE-R-6318)
performance for x-ray spectroscopy, using pulsed-light feedback preamplifier, 25:2462
performance of telescope, with thin radiator for proton-recoil neutron spectroscopy, 25:2480
RADIATION DETECTORS, SEMICONDUCTOR (GERMANIUM)
fabrication and performance of coaxial lithium-drifted, 25:2437
geometric corrections for coaxial lithium-drifted, finite solid-angle, 25:2455
geometric corrections for coaxial lithium-drifted, finite solid-angle, 25:2454
photopeak count-rates in lithium-drifted, from gamma emitters formed by thermal neutron activation, table of calculated, 25:2474 (IAEA-122, pp 150-63)
RADIATION DETECTORS, SEMICONDUCTOR (SILICON)
fabrication of large area surface-barrier, at low temperatures, 25:2452
operation of large area surface-barrier, at low temperatures, 25:2452
performance of position-sensitive surface-barrier, for magnetic spectrographs, 25:2463
pulse height distributions in lithium-drifted, due to nuclear reactions of charged-particle beams, 25:2451
RADIATION DETECTORS, SPARK CHAMBER
description of balloon-borne, for pulsed gamma emission from NP 0532, (E), 25:2841 (CEA-CONF-1633)
design of cylindrical, with boron nitride converters for in-core neutron detection at high temperature, 25:2459
magnet for Omega, design of superconducting, 25:2492
particle tracks in, computer graphics patching of failed CYCLOPS events in analysis of, 25:2486 (RHEL/R-205)
performance of wire, with on-line computers for studying meson (K^+) and meson (K^-) decay, 25:2491
RADIATION DOSE
maximum permissible, to human population, IRC recommendations for, 25:2574
RADIATION DOSIMETERS, CHEMICAL
design of vinyl film, 25:2496(P)
RADIATION DOSIMETERS, PHOTOGRAPHIC FILM
development of high-contrast, using selective development with thin film dielectric track detectors, 25:2471(P)
RADIATION DOSIMETRY
conference on, around accelerators, 25:3476 (JINR-16-4888)
RADIATION FILTERS
design for Debye--Scherrer camera for elimination of alpha and beta background, 25:2508
RADIATION MONITORING
programs at Karlsruhe Nuclear Research Center, 25:2570(R) (KFK-1158)
RADIATION PROTECTION
methods for environments, review of, 25:2571
programs for personnel at Karlsruhe Nuclear Research Center, 25:2570(R) (KFK-1158)
programs of nuclear power industry, legal aspects of environmental, 25:2564
standards for personnel handling radioactive materials, 25:2573
RADIATION SOURCES
preparation of spherical microscopic, using ion exchange resin beads, 25:2406
RADIATION TARGET CANS
design for HGTR recycle fuel tests, 25:2791 (ORNL-4570, pp 195-200)
design for in-pile testing of manifolded--vented fuel pins, 25:2771 (ORNL-4570, pp 161-9)
design parameters of liquid metal, for swimming pool type reactors, 25:3903 (CEA-N-1348)
RADIATION TARGET CHAMBERS
design for studying inelastic electron reactions with atoms at 50 to 150 keV, 25:3472 (CONF-700322-, pp 379-92)
RADIATION TARGETS
design of rotating and stationary, for medium- and high-power accelerators, 25:3474 (CONF-700322-, pp 431-9)
performance in HFIR, 25:2792 (ORNL-4570, pp 201-4)
preparation from powder by centrifugation in liquid paraffin, 25:2655
proton polarization measurements at high magnetic fields and low temperatures in porphyrexide-doped glycerol--water, 25:3500
tritium loss rates in tritiated titanium, for neutron production, 25:3542
RADIO ASTRONOMY
frequencies for, allocations of, (T), 25:2852
polarization and transformation theory of quasi-monochromatic radiation fields, (T), 25:2846
survey between 0 and 20° north declination, (E), 25:2855
RADIO GALAXIES
nuclei of, dependence of radio emission of ejected clouds on, (T), 25:2867
radio spectra at 60 MHz, (E), 25:2845
radio spectra of, interpretation of curvature in, (E/T), 25:2847
RADIO WAVES
absorption of, relation to midlatitude bays of auroral, (E), 25:2964
emission from Sun of 10.7-cm, indexes from Jan. 1, 1955 to Dec. 31, 1969, (E), 25:2858 (N-70-32003)
emission of, associated with gravitational waves, (T), 25:2849
ionospheric propagation, effect of F2 layer on scatter links in, (E/T), 25:2990
phase measurement of vlf, during solar eclipse Sept.22, 1968, (E), 25:2997
reflections from sporadic E, effect of lower ionosphere on appearance of, (E/T), 25:2994
RADIOACTIVE MATERIALS
handling of, criteria for protection of personnel during,

25:2573
handling of, response to criteria for protection of personnel during, 25:2572
RADIOACTIVE MINERALS
prospecting for, closed circuit method for measurement of radon-220/radon-222 ratio in soil gas for, 25:2378
RADIOACTIVE WASTE
calcination of high-level, 25:2316 (ORNL-4572, pp 98-108)
disposal in salt mines, 25:2316 (ORNL-4572, pp 98-108)
disposal into Rhine River, radioisotope sorption by sediment sands from, 25:2350
disposal of N Reactor, methods for, 25:2426
disposal of nuclear explosion-produced, at Carlsbad Site, New Mexico, equipment and methods for, 25:2420 (NVO-410-2)
disposal of solid, from nuclear power plants, economic aspects of methods for, 25:2425
handling and storage of liquid and solid, in Poland, equipment and method for, 25:2422
processing of Purex Plant gaseous, for iodine-131 separation, performance of silver reactors for, 25:2416 (ARH-SA-67)
processing of, from aqueous reprocessing of fuels, economics of, 25:2316 (ORNL-4572, pp 98-108)
processing of, from decontamination of organic coolants by bacteriological pretreatment, 25:2327
processing of, volume reduction by de-watering using super-decanter centrifuge in, 25:2344
RADIOACTIVITY
measurement of ocean floor, design of equipment for, 25:2357(P)
measurements in soils and ground-level atmosphere at archaeological excavation sites in Germany and Sweden, 25:2352
monitoring at CERN accelerator site, 25:2562
RADIOBIOLOGY
book: Annual Review of Medicine, 25:2575
RADIOCHEMICAL PROCESSING PLANTS
design and operation of, at Polish Nuclear Research Institute, 25:2422
iodine trapping by solid sorbents in, 25:2314 (ORNL-4572, pp 37-84)
maintenance of TURF, 25:2791 (ORNL-4570, pp 195-200)
operation of Eurochemic, 25:2324
plutonium/uranium ratio in solutions in, mathematical estimates of, 25:2417 (BNWL-SA-3287)
RADIOGRAPHY, BIOMEDICAL
equipment for neutron, review on accelerator, 25:3471 (CONF-700322-, pp 321-44)
RADIOGRAPHY, INDUSTRIAL
equipment for neutron, calculation of optimum thickness of image screen for, 25:2413
equipment for neutron, review on accelerator, 25:3471 (CONF-700322-, pp 321-44)
information transfer process in betatron bremsstrahlung, statistical analysis of, 25:2412
methods for testing HFIR fuel elements, 25:2770 (ORNL-4570, pp 127-35)
RADIOIMMUNOASSAY
methods for digoxin content of blood plasma, 25:2522
RADIOISOTOPE SCANNERS
modulation transfer function of, evaluation of, 25:2447
RADIOISOTOPE SCANNING
book: Annual Review of Medicine, 25:2575
RADIOISOTOPES
bibliography on uses in industry and research in eastern countries, 1967 to 1969, 25:2399 (AED-C-12-22)
conference on industrial uses of, Poznan, Poland, November 1968, 25:2141
contamination of natural waters, role of aquatic plants in, 25:2547
determination in water by ion exchange or filtration and counting, 25:2117
distribution of natural, in soils of USSR in relation to climatic zones, 25:2371
evaluation for use as tracers for pollution control studies of diffusion and flow conditions in estuaries, 25:2348 (NYO-3961-1)
transport in freshwater ecosystems, 25:2541
transport in freshwater ecosystems, development of mathematical model for, 25:2542
transport in soils and water, 25:2541
uptake by cultured bacteria and yeasts, use of autoradiography to determine, 25:2530
use for organ visualization by scanning, 25:2581
uses in radiation facilities, design of equipment for, 25:2389
uses in tracer studies, design of facilities for, 25:2390
uses of artificial and natural, in hydrology, review of, 25:2359
uses of artificial and natural, in hydrology, review of principles of, 25:2360
RADIOMETRIC ANALYSIS
conference on, Poznan, Poland, November 1968, 25:2141
RADIOMETRIC TESTING
methods for reactor materials, development of, 25:2409 (ORNL-4570, pp 149-51)
RADIOTHERAPY
computer programs for irradiation planning in betatron and cobalt, 25:2584
equipment for neutron, review on development of accelerator, 25:3473 (CONF-700322-, pp 407-29)
RADIUM
contamination of natural waters, role of aquatic plants in, 25:2547
removal from liquid radioactive effluents by ion exchange on zeolite containing alkali metal or alkaline earth metal ions, 25:2340(P)
separation from actinium and/or thorium and radioactive decay products by halogenation and sublimation, 25:2322(P)
RADON
separation from air streams, relations of air velocity with filter efficiency for, 25:2414 (AD-707709)
RADON ISOTOPES Rn-220
content ratio to radon-222 in soil gas, closed circuit method for measurement of, 25:2378
RADON ISOTOPES Rn-222
content ratio to radon-220 in soil gas, closed circuit method for measurement of, 25:2378
RARE EARTH ALLOYS AND SYSTEMS
rare earths--Zn-base, crystal structure of intermetallic compounds of, 25:2753
RARE EARTH CARBIDES
preparation of microspheres of, method for, 25:2795(F)
RARE EARTH CHLORIDES
separation of lanthanum from, by solvent extracton using D2EHPA and multistage mixer--settler extractor, 25:2310 (IS-T-411)
RARE EARTH FLUORIDES
preparation and high-temperature properties of, 25:3957 (IS-T-384)
RARE EARTH ISOTOPES
production by alpha or neutron bombardment of rare earths in molecular sieve, 25:2295 (ORNL-4572, pp 225-30)
RARE EARTH OXIDES
preparation of microspheres of, method for, 25:2795(F)
properties of sols of, 25:2775 (ORNL-4572, pp 242-50)
RARE EARTHS
analysis for yttrium by indirect spectrophotometric method, 25:2091
basicities of aqueous solutions of, 25:2319 (ORNL-4572, pp 181-95)
complexes with acetates, thermodynamic properties of, 25:2208
complexes with cupferron, composition and thermal stability of, 25:2078
determination in rocks, equipment and method for x-ray fluorescence, 25:2094
determination using cupferron, developments in, 25:2078
effects on photometric determination of hafnium and zirconium in geological specimens, 25:2084
preparation of thin targets of, by centrifuging powder suspended in liquid paraffin, 25:2655
separation by solvent extraction using bis(2-ethylhexyl) phosphate, 25:2311 (IS-T-412)
separation by solvent extraction using bis(2-ethylhexyl) phosphate, ir and Raman spectra of organic equilibrium phases in, 25:2193 (CONF-700403-8)
separation from MSBR fuel by fluorination--reductive extraction, 25:2313 (ORNL-4572, pp 1-36)
separation of cerium from nitrate-containing mixtures of, in solution, comparison of crystallization, hydrolysis, and oxidation methods for, 25:2326
RARE GASES
occurrence in lunar surface materials, isotopic, (T), 25:2881
RATS
immunization against Babesia rodhaini using γ-irradiated infected erythrocytes, 25:2539
radiation effects on bone marrow of, use of intraocular transplant technique for studying growth following, 25:2595
radiation effects on delayed hypersensitivity in, whole-body x, 25:2540
radiation effects on populations of stem cells in bone marrow of, development of computer model for, 25:2590
radioinduced lesions in dentine of incisors of, effects of dose on x, 25:2592
radioinduced osteosarcomas in, histological study of phosphorus-32 β, 25:2594
transplantation antigens in, review of genetics of, 25:2537
REACTIVITY
calculation for stable and transient periods, Nordheis equation in P_1-approximation for, 25:3924 (CNAEM-73)
measurement of power reactor, evaluation techniques for zero power, 25:3777
REACTOR CONTROL ELEMENTS
performance of helium cooled, effects of operating conditions on movement, (E), 25:3858 (DP-Report-486)
reactivity worth of, evaluation techniques for, 25:3777
REACTOR COOLANTS
decontamination of, bacteriological processes in, 25:2327
REACTOR EXPERIMENTAL FACILITIES
moderators for cold neutron source in tangential beam hole, performance of, 25:3904 (IJS-571)
REACTOR FUEL ELEMENTS
burnout heat flux for rod cluster, (E/T), 25:3880

burnup of gas cooled thorium carbide (ThC_2)--uranium carbide (UC_2) coated particle, 25:3796 (DP-Report-579)
burnup of heavy water cooled and moderated, calculation of cycle management procedures for optimum, 25:3866 (CEA-N-1379)
burnup of high temperature gas cooled, effects of heterogeneity on, 25:3868 (DP-Report-477)
burnup of high temperature gas cooled, nondestructive method for estimating, (E/T), 25:3871 (DP-Report-538)
burnup of, calculation of cycle management procedures for optimum, 25:3869 (DP-Report-478)
burnup of, calculation of cycle management procedures for optimum, 25:3803
clad bonding of, metal spraying method for, 25:2638 (CEA-CONF-1625)
cladding failure of gas cooled graphite moderated power, 25:3879
cladding for, radioinduced mechanical property changes in, 25:2755 (BMI-1889, Sect.B)
decladding of LMFBR, in molten zinc, 25:2306(R) (ANL-7735)
degasification behavior of NERVA, at low pressures, 25:2677 (ORNL-4570, pp 224-7)
design modifications for gas cooled graphite moderated power, in France, 25:3877
development of high temperature gas cooled coated particle, 25:3774 (DP-Report-439)
dismantling multitubular assemblies of LMFBR, 25:2314 (ORNL-4572, pp 37-84)
fabrication for recycle tests, 25:2791 (ORNL-4570, pp 195-200)
failure in water-cooled reactors, effects on safety, 25:2610 (ORNL-4570, pp 205-12)
fission product release from gas cooled thorium carbide (ThC_2)--uranium carbide (UC_2) coated particle, (E/T), 25:3775 (DP-Report-539)
fission product release from gas cooled thorium carbide (ThC_2)--uranium carbide (UC_2) coated particle, 25:3796 (DP-Report-579)
fission product release from high temperature gas cooled thorium carbide (ThC_2)--uranium carbide (UC_2), measurement of gaseous, 25:3870 (DP-Report-497)
fission product release from pyrolytic carbon and silicon carbide coated particle type, (T), 25:3874 (DP-Report-595)
handling and storage of irradiated, in France, methods and regulations for, 25:2424
heat transfer characteristics of assemblies of power, (T), 25:3876 (RCN-123)
heat transfer characteristics of water cooled Type 304L stainless steel clad uranium oxide (UO_2) bundle type, measurement of post-dryout, (E/T), 25:3865 (AECL-3414)
neutron absorption in two-region cylindrical, computer program for calculation of resonance integrals and cross sections for, 25:3528 (KFKI-70-12-RPT)
operating limits for gas cooled graphite and silicon carbide coated plutonium oxide (PuO_2)--uranium oxide (UO_2) particles, 25:3875 (EURFNR-834)
performance of gas cooled graphite moderated power, analysis in France of optimum economic, 25:3878
physics measurements for plutonium--aluminum alloy, (E/T), 25:3902 (BNWL-1514)
radiation hazards for boiling power, 25:3894
reprocessing of HTGR, head-end processes for, 25:2320(R) (ORNL-TM-3204)
reprocessing of HTGR, head-end processes in, 25:2315 (ORNL-4572, pp 85-97)
reprocessing of LMFBR, melt-decladding or shear-leach head-end processes in, 25:2314 (ORNL-4572, pp 37-84)
safety analysis of plutonium, 25:3901 (ANL-7442)
testing of hexagonal arranged pin type, compression, (E), 25:3908 (WHAN-FR-18)
vibrations in assemblies of water cooled, mockup testing for hydrodynamic, (E), 25:3909
welding of clad plate-type, electron-beam method for, 25:2770 (ORNL-4570, pp 127-35)

REACTOR FUELS
analysis of oxide, for oxygen by x-ray-diffraction measurements of lattice parameters, in-line, 25:2306(R) (ANL-7735)
analysis of oxide, for plutonium/uranium ratio, in-line x-ray fluorescence, 25:2306(R) (ANL-7735)
analysis using radiative neutron capture and fission γ-ray spectra, 25:3649 (KFK-1214)
burnup of, effects of reactor type on management procedures for optimum, 25:3867 (DP-Report-476)
coating of spherical particles of, gas pressure measurements in fluidized bed method for, 25:2767 (DP-Report-378)
cost of, computer analysis of factors affecting, 25:2602 (ORNL-4570, pp 191-4)
cycle economics for self-sustaining mixed fast and thermal systems, (T), 25:3888 (DP-Report-581)
cycle for power reactor, calculation of optimum 60 year, 25:3881
cycle parameters for on-load refueled thermal converters, (T), 25:3887 (DP-Report-575)
cycles for high temperature helium cooled reactors, comparison of various thorium, (T), 25:3884 (DP-Report-469)
cycles for high temperature helium cooled reactors, parametric analysis of low-enriched uranium, 25:3883 (DP-Report-466)
cycles for, activities of French Pechiney Group in, 25:2379
distillation of MSRE, 25:2313 (ORNL-4572, pp 1-36)
economics for heavy water moderated power reactors, estimates of, 25:3802
fabrication and preparation of coated-particle carbide, development of method for, 25:2771 (ORNL-4570, pp 161-9)
fabrication of graphite-base, development of remote methods for, 25:2791 (ORNL-4570, pp 195-200)
fabrication of oxide-loaded graphite, 25:2320(R) (ORNL-TM-3204)
fission gas release and swelling of, model for determination of, 25:2789 (ORNL-4570, pp 68-75)
handling and storage of plutonium-containing, design of criticality-safe containers for, 25:2419 (KFK-1192)
loading of particulate, design of conveyor for, 25:2395(P)
performance of, computer analysis of factors affecting, 25:2602 (ORNL-4570, pp 191-4)
preparation for military reactors, summary on, 25:2772 (ORNL-4570, pp 174)
preparation of coated-particle, by loading actinide ions on exchange resins and carbonizing, 25:2771 (ORNL-4570, pp 161-9)
preparation of oxide, method for, 25:2784(P)
radiation effects on clad cermet, in-pile, 25:2770 (ORNL-4570, pp 127-35)
reprocessing of HTGR, 25:2320(R) (ORNL-TM-3204)
reprocessing of LMFBR, 25:2317 (ORNL-4572, pp 170-3)
reprocessing of LMFBR, aqueous methods for, 25:2314 (ORNL-4572, pp 37-84)
reprocessing of MSBR, by fluorination--reductive extraction and metal transfer, 25:2313 (ORNL-4572, pp 1-36)
reprocessing of MSBR, flowsheet for, 25:2313 (ORNL-4572, pp 1-36)
reprocessing of, air-pulsing methods for extraction columns for, 25:2383 (AAEC/TM-547)
reprocessing of, operation of Eurochemic plant for, 25:2324
reprocessing of, processing and disposal of radioactive wastes from, 25:2316 (ORNL-4572, pp 98-108)
separation of plutonium from LMFBR, by solvent extraction, centrifugal contactor for, 25:2306(R) (ANL-7735)
shipping of spent LMFBR, liquid-sodium-cooled containers for, 25:2314 (ORNL-4572, pp 37-84)

REACTOR LOADING MACHINES
design for Dragon reactor, 25:2385 (DP-Report-230)
design for particulate fuel elements, 25:2395(P)

REACTOR SAFETY
accidents in reactors, comparison of determinism and probability analysis concepts for, 25:3895
accidents in reactors, comparison of determinism and probability analysis concepts for, 25:3896
analysis of plutonium fueled fast critical assemblies, final, 25:3901 (ANL-7442)
blowdown of water cooled reactors, pressure and time variations for, (E/T), 25:3893 (IITRI-578-P-21-39)
failure modes of Zircaloy-clad light water reactor fuel elements, 25:2610 (ORNL-4570, pp 205-12)
radiation hazards for fuel elements and turbines of boiling power reactors, 25:3894
review of LMFBR programs for, 25:2600 (BNL-50258)

REACTOR SAFETY EXPERIMENTS
steam--water density in LOFT, ultrasonic void fraction detector for measurement of, 25:3905 (IN-1441)

REACTOR SIMULATORS
operation procedures for hybrid computer, for production reactors, 25:3920 (BNWL-B-8)
performance of analog computer, for boiling water power reactors, 25:3933
performance of pulsed neutron source in non-multiplying medium, for neutron flux characteristics, (E/T), 25:3932

REACTORS
accidents in, comparison of determinism and probability analysis concepts for, 25:3896
accidents in, comparison of determinism and probability analysis concepts for, 25:3895
criticality of, performance of minimum error few group programming technique for, 25:3930
instrumentation for, design requirements for accident monitoring, 25:3895
kinetics of, review of pulsed neutron research in Japan on, 25:3927 (JAERI-Memo-4109)
multiplication factors in reflected, CORONA code for control rod position effects on, 25:3926 (EIR-166)
neutron flux in reflected, CORONA code for control rod position effects on, 25:3926 (EIR-166)
neutron flux monitoring in, 10-decade wide range fission detector system for thermal, 25:2502 (GEAP-11094)
noise in, shift registers for measurement of, 25:3931
research at Inst. of Nuclear Research, Warsaw, 1969, 25:2497(R) (INR-1180)
shielding for, transmission matrix methods for optimum weight of, 25:3859
stability criteria for space-dependent, analytical models for, 25:3929

tubes for, properties of alloys for, 25:2678
REACTORS, AGR-TYPE
boilers for, development of, 25:3899
REACTORS, BOILING
fuel elements for, measurement of post-dryout heat transfer characteristics of bundle type, (E/T), 25:3865 (AECL-3414)
fuel elements of power, radiation hazards for, 25:3894
power conversion system of power, radiation induced activation hazards for, 25:3894
simulator for power, performance of analog computer, 25:3933
REACTORS, BREEDER
control materials for, development of boron carbide, 25:2790 (ORNL-4570, pp 98-102)
coolant boiling in liquid sodium cooled fast, detection methods for, (T), 25:3864
design parameters in Japan of prototype liquid metal ccoled fast, 25:3855
design parameters of gas cooled fast power, 25:3854
development of, status report on, 25:3891 (ORO-1171-1, pp 206-55)
materials for, creep testing of Type 316 stainless steel, 25:2660 (JAERI-Memo-4097)
stability of steam cooled fast, calculation of inherent, 25:3856 (KFK-851)
REACTORS, CANDU-TYPE
fuel element cycle management for, calculation of optimum, 25:3866 (CEA-N-1379)
REACTORS, FAST
control materials for, development of boron carbide, 25:2790 (ORNL-4570, pp 98-102)
coolant boiling in liquid sodium cooled breeder, detection methods for, (T), 25:3864
design parameters in Japan of prototype liquid metal cooled breeder, 25:3855
design parameters of gas cooled breeder power, 25:3854
development of, status report on, 25:3891 (ORO-1171-1, pp 206-55)
economics of self-sustaining mixed fast and thermal systems, (T), 25:3888 (DP-Report-581)
fuel particles for gas cooled, operating limits for graphite and silicon carbide coated plutonium oxide (PuO_2)--uranium oxide (UO_2), 25:3875 (EURFNR-834)
stability of steam cooled breeder, calculation of inherent, 25:3856 (KFK-851)
REACTORS, FLUID-FUELED
stability of shutdown equilibrium state in, Krasovskii's functional method for asymptotic, (T), 25:3857
REACTORS, FRANCE
fuel elements for gas cooled graphite moderated power, design modifications for, 25:3877
fuel elements for gas cooled graphite moderated power, optimum economic operating limits for, 25:3878
fuel elements of gas cooled graphite moderated power, failure in France of cladding of, 25:3879
REACTORS, GAS-COOLED
boilers for power, design characteristics of, 25:3898
boilers for power, development of, 25:3899
coolant for high temperature, electrolytic hygrometer for measurement of water and hydrogen in, 25:3882 (DP-Report-487)
core components of, corrosion of graphite, 25:3860 (DP-Report-491)
design parameters of fast breeder power, 25:3854
fuel cycles for high temperature, comparison of various thorium, (T), 25:3884 (DP-Report-469)
fuel cycles for high temperature, parametric analysis of low enriched uranium, 25:3883 (DP-Report-466)
fuel elements for graphite moderated power, design modifications in France for, 25:3877
fuel elements for graphite moderated power, optimum economic operating limits in France for, 25:3878
fuel elements for, development of method for production of carbide, 25:2771 (ORNL-4570, pp 161-9)
fuel elements of graphite moderated power, failure in France of cladding of, 25:3879
fuel particles for fast, operating limits for graphite and silicon carbide coated plutonium oxide and silicon carbide coated plutonium oxide (PuO_2)--uranium oxide (UO_2), 25:3875 (EURFNR-834)
thorium fuel cycle development for, 25:2320(R) (ORNL-TM-3204)
REACTORS, GERMANY
development during 1971, proposed budget for, 25:3853
REACTORS, GRAPHITE-MODERATED
fuel elements for gas cooled power, design modification in France for, 25:3877
fuel elements for gas cooled power, optimum economic operating limits in France for, 25:3878
fuel elements of gas cooled power, failure in France of cladding of, 25:3879
REACTORS, HEAVY WATER-MODERATED
fuel element cycle management for power, calculation of optimum, 25:3866 (CEA-N-1379)
REACTORS, HETEROGENEOUS
neutron flux distribution in thermal, computer program for, 25:3925 (DP-1238)
REACTORS, JAPAN
design parameters of prototype liquid metal cooled fast breeder, 25:3855
development of power, analysis of optimum economic, 25:3804
REACTORS, LIQUID METAL-COOLED
boilers for power, design characteristics of, 25:3898
coolant boiling in fast breeder sodium, detection methods for, (T), 25:3864
design parameters in Japan of prototype fast breeder power, 25:3855
kinetics parameters of, effects of sodium 2.85 keV resonance scattering data on, (T), 25:3928 (JAERI-Memo-4110)
REACTORS, MAGNOX
boilers for, development of, 25:3899
REACTORS, MARITIME
book: Nonstationary Operation of Marine Nuclear Steam Producing Installations, in Russian, 25:3919
book: Production of Marine Reactors and Steam Generators, in Russian, 25:3918
operation of, mathematical models for transient, 25:3919
REACTORS, POWER
boilers for gas cooled, development of, 25:3899
boilers for, design characteristics of, 25:3898
core components of helium cooled, corrosion of graphite, 25:3860 (DP-Report-491)
design parameters in Japan of prototype liquid metal cooled fast breeder, 25:3855
design parameters of gas cooled fast breeder, 25:3854
development in Japan of, analysis of optimum economic, 25:3804
economics of dual purpose process heat and, (T), 25:3914
economics of self-sustaining mixed fast and thermal systems, (T), 25:3888 (DP-Report-581)
fuel cycle for, calculation of optimum 60 year, 25:3881
fuel cycle management procedures for, effects of reactor type on, 25:3867 (DP-Report-476)
fuel cycle parameters for on-load refueled thermal converters, (T), 25:3887 (DP-Report-575)
fuel element cycle management for heavy water cooled and moderated, calculation of optimum, 25:3866 (CEA-N-1379)
fuel element cycle management for, calculation of optimum, 25:3869 (DP-Report-478)
fuel element cycle management for, calculation of optimum, 25:3803
fuel elements assemblies for, calculation of coolant mixing and heat transfer characteristics of, (T), 25:3876 (RCN-123)
fuel elements for gas cooled graphite moderated, design modification in France for, 25:3877
fuel elements for gas cooled graphite moderated, optimum economic operating limits in France for, 25:3878
fuel elements of boiling, radiation hazards for, 25:3894
fuel elements of gas cooled graphite moderated, failure in France of cladding of, 25:3879
kinetics of, comparison of variational flux synthesis methods for, (T), 25:3922 (ANL-7696)
nuclear materials management standards for, IAEO, 25:3851
power conversion system of boiling, radiation induced activation hazards for, 25:3894
simulator for boiling, performance of analog computer, 25:3933
turbines for, design problems of wet steam, 25:3900
REACTORS, PROCESS HEAT
bibliography on U. S. desalination, 25:3913 (ORNL-NDIC-8)
development of multiple purpose, for chemical industry, 25:3915
economics for iron production, 25:3916
economics of dual purpose power and, (T), 25:3914
fuel elements for, development of, 25:2644 (ORNL-4570, pp 157-60)
REACTORS, RESEARCH
core of HFR (Grenoble), mockup testing for hydrodynamic vibrations in, (E), 25:3909
design parameters in U.K. of proposed heavy water cooled high flux, 25:3911
experimental facilities of HFR (Grenoble), for study of protein structure with neutron diffraction, 25:3907 (NP-18462)
experimental facilities of Triga Mark 2, performance of moderators for cold neutron source in tangential beam hole, 25:3904 (IJS-571)
nuclear materials management standards for, IAEO, 25:3851
reflector for HFR (Grenoble), hydraulic and thermal design requirements of, (E/T), 25:3910
REACTORS, SUPERHEATING
stability of steam cooled fast breeder, calculation of inherent, 25:3856 (KFK-851)
REACTORS, THERMAL
economics of self-sustaining mixed fast and thermal systems, (T), 25:3888 (DP-Report-581)
neutron flux distribution in heterogeneous, computer program for, 25:3925 (DP-1238)
REACTORS, WATER-COOLED
blowdown of, pressure and time variations for, (E/T), 25:3893 (IITRI-578-P-21-39)
boilers for power, design characteristics of, 25:3898
coolant loss accidents in, noble gas absorption and release by emergency core cooling water following, (E), 25:3892 (BNWL-SA-3360)

XUM

coolant pumps for, design of seals for, 25:2392
fuel rod failure in, effects on safety, 25:2610 (ORNL-4570, pp 205-12)
operation of, mathematical models for transient, 25:3919
RECOILS
energy deposition by heavy-particle, in fast neutron reactions in tissues, 25:2568
REFRIGERATION
equipment for superconducting magnets, helium, 25:3508
REGGE POLE THEORY
angular momenta for K + N and π + N interactions at 6 to 55 GeV in, complex, (E/T), 25:3381 (JINR-P2-5320)
conspiracy and duality in model for forward cross sections of γ + N + $\pi^-(\pi^+)$ + $\Delta^{++}(\Delta^-)$ interactions in, 25:3318
cut corrections to π + N elastic and charge-exchange interactions above 5 GeV/c, absorptive-model, 25:3390
diagrams with three-reggeon vertices, Polkinghorne method for, 25:3456
dual resonance models for angular momentum structure of resonances in, bose-gas theory for, 25:3366
model with Veneziano residues for $0^- + 1/2^+ \rightarrow 0^- + 3/2^+$ interactions in, 25:3384 (TPJU-3/70)
models of asymptotic behavior of amplitudes for hadrons interactions, 25:3357
poles in cut j plane for charge exchange π + N interactions, complex, 25:3402
Pomeranchuk trajectory for π + π interactions, crossing-symmetric amplitude for, 25:3365
Pomeranchukon in interactions with three-particle final states, factorization test, 25:3395
Pomeron exchange in diffractive γ + p + rho^0 + N + $m\pi$ interactions at 5 to 100 GeV, (T), 25:3308 (DESY-70/45)
production processes in multi-, kinematics and dynamics of, 25:3389
Regge symmetry of SU(2) group Wigner coefficients in, 25:3305
residues for extrapolation of γ + p total cross sections at high energies to deep inelastic e + p interactions, 25:3312 (NYO-4204-6)
residues in Veneziano model, sign of, 25:3453
RELATIVITY THEORY
forces of inertia in general, (T), 25:2871
gravitational field equations in general, nonstatic case in exact solutions of, 25:3448
invariants of special, in nonrelativistic and Galilean approximation, 25:3434 (JINR-P2-5363)
Lorentz and Lorentz-tachyon transformations in, 25:3441
matter distributions of spherical symmetry in general, equation for nonstatic, 25:3448
mercury perihelic precession in, heuristic derivation of, 25:3291
neutrino model in general, with velocity groups G_3 on V_2, 25:3343
REMOTE-HANDLING EQUIPMENT
design of terminal head for conduit-type pneumatic, 25:2427(P)
REPUBLIC OF KOREA
radioactivity in ground-level atmosphere at Seoul, following Chinese nuclear explosion, effects of meteorological conditions on, 25:2368
RETICULO-ENDOTHELIAL SYSTEM
scanning using metastable technetium-99, 25:2580
RHEINSBERG POWER REACTOR
physics measurements for, evaluation techniques for zero power, 25:3777
RHENIUM
chemical state of recoil, in proton-irradiated inorganic iridium compounds, 25:2300
determination of trace amounts of, by thiocyanate--stannous chloride method, effects of impurities on, 25:2102
effects on uv spectrophotometric determination of gallium in aqueous solutions, 25:2100
properties for use in reactor components, review of, 25:2647
separation by solvent extraction using dialkylmethylbenzylammonium salts, 25:2328
separation from nitrate and sulfate solutions by solvent extraction using amines, 25:2319 (ORNL-4572, pp 181-95)
RHENIUM ALLOYS AND SYSTEMS
Mo--Re, properties for use in reactor components, review of, 25:2647
Re--Ta-base, elastic properties of monocrystalline, at 80 to 1400°K, 25:2721
Re--W, properties for use in reactor components, review of, 25:2647
Re--W-base, creep rupture of arc-melted and chemical vapor deposited, stress--strain curves for, 25:2673 (CRNL-4570, pp 118-23)
Re--W-base, internal friction of doped, at 300 to 3000°K, 25:2687
Re--W-base, production by hexafluoride reduction and vapor deposition, 25:2673 (ORNL-4570, pp 118-23)
Re--W-base, properties for use in curium-244 oxide fuel capsules, 25:2643 (ORNL-4570, pp 106-11)
RHENIUM ISOTOPES Re-185
energy levels from osmium-185 decay, spin-parity assignments for, (E), 25:3704
energy-level transitions from osmium-185 decay, internal conversion coefficients for, (E), 25:3704
RHENIUM OXIDES
thermal capacity of ReO_3, electronic, 25:3956 (IS-T-383)
RHINE RIVER
sands of, sorption of radioisotopes by noncmineralic fine, (E), 25:2350
RHODIUM
neutron elastic scattering at 1 to 40 keV, analysis of angular distributions from, (E/T), 25:3695
RHODIUM ALLOYS AND SYSTEMS
Pt-base--Rh, compatibility with plutonium-238 dioxide powder and spheres at 1200°C, 25:2663 (MLM-1684)
Pt-base--Rh, compatibility with plutonium-238 dioxide powder at 1200°C in presence of tantalum--tungsten alloy, 25:2663 (MLM-1684)
Pt-base--Rh, compatibility with plutonium-238 dioxide spheres in presence of molybdenum, tantalum, or TZM, 25:2663 (MLM-1684)
Rh--Ti-base, superconductivity of ternary β-titanium, 25:3021(T) (UCRL-Trans-1409)
RHODIUM ISOTOPES Rh-105
energy levels from palladium-108 (p,α) and ruthenium-104 (He-3,d) reactions, spin-parity assignments and spectroscopic factors for, (E), 25:3701
RHODIUM ISOTOPES Rh-106
monitoring in irrigation canal sediment and water downstream from nuclear power centers on Rhone River, 25:2543
RHODIUM ISOTOPES Rh-116
decay and energy-level transitions following californium-252 fission, (E), 25:3673
RIVERS
cobalt-60 accumulation by suspended particles in Danube, parameters affecting, 25:2361
radioactivity in irrigation canal sediment and water from Rhone, downstream from nuclear power centers, cesium-137, rhodium-106, ruthenium-106, strontium-90, and yttrium-90 β, 25:2543
radioisotope contamination of Meuse, in relation to fixation by aquatic fauna, flora, and sediments, cobalt-60 and manganese-54, 25:2544
radioisotope decontamination of, near Austrian reactor center, self-cleaning capacity for, 25:2545
radioisotope transport in, development of mathematical model for, 25:2542
ROCKET REACTORS (NERVA)
materials for, bonding and shear behavior of, 25:2677 (ORNL-4570, pp 224-7)
ROCKS
age of Churchill Province, Canada, rubidium/strontium method for estimation of, 25:2353
analysis by 14-MeV neutron activation and γ spectrometry, 25:2119 (CONF-700322-, pp 221-30)
analysis by x-ray diffractometry, 25:3995 (UCRL-50921)
analysis for cesium and tantalum by neutron activation and γ spectrometry, 25:2145
analysis for cesium, cobalt, hafnium, scandium, and tantalum by neutron activation and γ spectrometry, 25:2139
analysis for coal by γ-γ method, 25:2111
analysis for hafnium and zirconium using 8-hydroxy-7-[(2-hydroxy-3,5-dinitrophenyl)-azo]-1,6-naphthalenedisulfonic acid, photometric, 25:2084
analysis for rare earth elements, equipment and method for x-ray fluorescence, 25:2094
analysis of hydrothermally altered, from Tateyama Jigokudani Hot Springs, Toyama, Japan for titanium and zirconium, colorimetric, 25:2098
RUBIDIUM
determination by potentiometric titration with sodium tetraphenylboron using Orion liquid ion exchange lead-selective electrode, 25:2104
determination in human liver by neutron activation and γ spectrometry, 25:2124 (IAEA-122, pp 15-26)
electron reactions with atomic, excitation cross sections for, (T), 25:2915
separation from other alkali metals by fixation on hydrated antimony pertoxide in hydrochloric, nitric, and perchloric acids, effects of acidity and time on, 25:2333
RUBIDIUM ALLOYS AND SYSTEMS
Fe--H--Rb--Si, phase studies of, 25:2727 (ORNL-4570, pp 1-4)
RUBIDIUM IONS
reactions with nitrogen molecules at 30 to 100 keV, absolute emission cross sections for, (E), 25:2902 (SC-RR-70-695)
RUBIDIUM URANYL NITRATES
spectra of, ir and Raman, 25:2212
RUBIES
radiation effects on chromium ions in, EPR study of annealing kinetics of x-, (E), 25:3195
RUTHENIUM
distribution and ion exchange on clays, 25:2338
effects on determination of trace amounts of rhenium by thiocyanate--stannous chloride method, 25:2102
separation from nitrate and sulfate solutions by solvent extraction using amines, 25:2319 (ORNL-4572, pp 181-95)
RUTHENIUM ISOTOPES
accumulation by silts, effects of physicochemical

properties on, 25:2362
physicochemical properties of radioactive, in radioactive waste, 25:2362
RUTHENIUM ISOTOPES Ru-102
energy levels from rhodium-102 decay, spins and parities of, (E), 25:3671
RUTHENIUM ISOTOPES Ru-103
detection in radioecology studies, use of Cherenkov counting for, 25:2565
release to soil from organic debris in forest as function of decomposition mode and time, 25:2528
transport in soils, effects of physicochemical processes on, 25:2364
uptake by aquatic molluscs and plants, effects of concentration in water on concentration factor for fallout, 25:2548
RUTHENIUM ISOTOPES Ru-104
helium-3 reactions (He-3,d) 18 MeV, angular distributions for, (E), 25:3701
RUTHENIUM ISOTOPES Ru-106
detection in radioecology studies, use of Cherenkov counting for, 25:2565
monitoring in irrigation canal sediment and water downstream from nuclear power centers on Rhone River, 25:2543
release to soil from organic debris in forest as function of decomposition mode and time, 25:2528
transport in soils, effects of physicochemical processes on, 25:2364
RUTHENIUM ISOTOPES Ru-110
decay and energy-level transitions following californium-252 fission, (E), 25:3673

S

S-MATRIX
causality condition for, Bogolyubov, 25:3452
SACLAY REACTORS (OSIRIS)
radiation target cans for, design parameters of natural convection cooled Esther, 25:3903 (CEA-N-1348)
SAMARIUM
crystal structure as function of temperature at 25 to 600°C, 25:2730 (ORNL-4579, pp 44-6)
determination in calcium fluorides, scanning method for improving accuracy of luminescence, 25:2086
determination of trace amounts of, in lanthanum oxide, neodymium oxide, and yttrium oxide by direct reading emission spectrometry, 25:2096
neutron capture by natural, gamma spectra from thermal, (E), 25:3651 (NP-18485)
phase studies of thin films of, by electron microscopy and x-ray diffraction, 25:2734
SAMARIUM ALLOYS AND SYSTEMS
Co--Sm, magnetic properties of intermetallic $SmCo_5$, 25:3217
SAMARIUM CHLORIDES
bis(2-ethylhexyl) phosphate--$CeCl_3$--HCl--H_2O--$NdCl_3$--$SmCl_3$, equilibria in Amsco, 25:2311 (IS-T-412)
SAMARIUM ISOTOPES Sm-147
neutron capture by, gamma spectra from thermal, (E), 25:3651 (NP-18485)
SAMARIUM ISOTOPES Sm-148
energy levels from thermal neutron capture by samarium-147, spins and parities for, (E), 25:3651 (NP-18485)
SAMARIUM ISOTOPES Sm-149
neutron cross sections for, 25-group, (T), 25:3530 (LA-4484)
SAMARIUM ISOTOPES Sm-150
energy levels from neutron capture at 0.047 eV by aligned samarium-149, spins and parities for, (E), 25:3651 (NP-18485)
energy-level transitions from neutron capture by aligned samarium-149, multipolarities and conversion coefficients of, (E), 25:3651 (NP-18485)
SAMARIUM ISOTOPES Sm-152
energy levels from multiple Coulomb excitation, (E), 25:3662
neutron capture by, gamma spectra from thermal, (E), 25:3651 (NP-18485)
spectra of muonic, dynamic hyperfine structure in x-ray, (E), 25:3661
SAMARIUM ISOTOPES Sm-153
energy levels from thermal neutron capture by samarium-152, spins and parities for, (E), 25:3651 (NP-18485)
SAMARIUM ISOTOPES Sm-154
alpha reactions (α,3n) at 34 MeV, gamma energy and angular distributions for, (E), 25:3700
SAMARIUM OXIDES
emittance at high temperatures of solid, spectral, 25:3204 (AD-708547)
SAMARIUM OXYBROMIDES
vaporization of, kinetics of, 25:2803(R) (COO-716-66)
SAN ONOFRE POWER REACTOR, UNIT 1
core for, authorization for checkerboard arranged Cycle 2, 25:3810 (DOCKET-50206-96)
design parameters of, requested additional information on, 25:3809 (DOCKET-50206-95)
fuel elements for, authorization for plutonium oxide (PuO_2)--uranium oxide (UO_2), 25:3810 (DOCKET-50206-96)
operations aspects of, requested additional information on, 25:3809 (DOCKET-50206-95)
operations history for October 1970, 25:3785 (DOCKET-50206-94)
operations incident of October 19, 1970, safety analysis of safety injection system valves malfunction, 25:3786 (DOCKET-50206-97)
SAN ONOFRE POWER REACTOR, UNIT 2
design parameters of, revised and additional data on, 25:3849 (DOCKET-50361-11)
operations aspects of, revised and additional data on, 25:3849 (DOCKET-50361-11)
SAN ONOFRE POWER REACTOR, UNIT 3
design parameters of, revised and additional data on, 25:3849 (DOCKET-50361-11)
operations aspects of, revised and additional data on, 25:3849 (DOCKET-50361-11)
SANDS
sorptive properties of Rhine River monomineralic fine, for radioisotopes, (E), 25:2350
SAP (SINTERED ALUMINUM POWDERS)
mechanical properties and microstructure of, relations with heat-induced aluminum surface pearls, 25:2779
SCALERS
design of holding, using neon lamps as indicators and memory units, 25:2466
SCANDIUM
abundance in Kappa Cancri, (E), 25:2840
complexes with cupferron, separation by solvent extraction using 2-methyl-1-propanol and 3-methyl-1-butanol, 25:2078
complexes with TTA, distribution in series of ether solvents of, 25:2345
determination as barium scandium cupferronate, gravimetric, 25:2078
determination in minerals and rocks by neutron activation and γ spectrometry, 25:2139
determination in silicate rocks by spectrophotometry using 4-(2-thiazolylazo)resorcinol, 25:2093
determination in silicate rocks using cupferron, spectrographic, 25:2076
determination using cupferron, developments in, 25:2078
SCANDIUM ISOTOPES Sc-43
energy levels from calcium-40 (α,pγ) reactions at 7.0 to 12.0 MeV, spin--parity assignments and lifetimes for, (E), 25:3626
energy-level transitions from calcium-40 (α,pγ) reactions at 7.0 to 12.0 MeV, branching and multipole mixing ratios for, (E), 25:3626
SCANDIUM ISOTOPES Sc-44
energy levels from calcium-42 (He-3,p) reactions, spins, parities, and L-values for, (E), 25:3629
SCANDIUM ISOTOPES Sc-45
energy levels from calcium-43 (He-3,p) reactions, spins, parities, and L-values for, (E), 25:3629
proton reactions (p,n) near threshold, Q-value for, (E), 25:3608
SCANDIUM ISOTOPES Sc-46
energy levels from calcium-44 (He-3,p) reactions, spins, parities, and L-values for, (E), 25:3629
SCANDIUM ISOTOPES Sc-50
energy levels from calcium-48 (He-3,p) reactions, spins, parities, and L-values for, (E), 25:3629
SCATTERING
amplitude of, contribution of singularities in complex l-plane to impact parameters, 25:3462
amplitudes at high energies, structure of nondiffractive two-body, 25:3454
amplitudes for elastic, upper bound on imaginary part of, 25:3460
amplitudes of high-energy elastic, solution of unitarity condition for, 25:3451 (ITF-70-49)
amplitudes of, dispersion relations for form factors for, 25:3461
amplitudes with unitarity and crossing symmetry, asymptotic behavior of, 25:3455
by modified Gaussian potential, (T), 25:3771
impact-parameter amplitudes for large-angle potential, (T), 25:3761
potential, models of two-channel, 25:3458
sum rule for rms radius in, 25:3461
theory for potential, Martin's method for, 25:3240
theory of nuclear diffraction, accuracy of the Inopin--Ericson, 25:3757
SCHIZOMYCOTA
Brevibacterium ammonigenes, enzyme preparation from cells of, 25:2520
Clostridium botulinum, radiation effects on spores of, factors affecting recovery following heat and γ, 25:2599
Escherichia coli, radioinduced inhibition of respiration in, uv, 25:2598
Escherichia coli, radioinduced mutations in, action spectra for uv, 25:2557
radioisotope uptake by cultured, use of autoradiography to determine, 25:2530
SCINTILLATION CAMERAS
modulation transfer function of, evaluation of, 25:2447
SEALS AND GLANDS
design for high-pressure nuclear power plant pumps, 25:2392
SEAWATER
analysis for lead-210 and polonium-210 by solvent

XUM

extraction and α counting or α spectrometry, 25:2112
corrosive effects on evaporator surfaces, cathodic protection from, 25:2634
separation of uranium from, economics and feasibility of methods for, 25:2323
separation of uranium from, precipitation method for, 25:2325

SELENIUM
corrosive effects on alloys, ceramics, glasses, graphite, and metals at 300 to 700°C, 25:2629
determination in biological materials by 14-MeV neutron and thermal neutron activation, sensitivity of, 25:2125 (IAEA-122, pp 27-36)
determination in human tissues by thermal neutron activation, sensitivity of, 25:2123 (IAEA-122, pp 1-13)
determination in soils in Pakistan by neutron activation and radiochemical separation, 25:2125 (IAEA-122, pp 27-36)
determination of trace amounts of, using permanganate, colorimetric, 25:2073
effects on determination of trace amounts of rhenium by thiocyanate--stannous chloride method, 25:2102
effects on polarographic determination of tellurium, 25:2090
effects on uv spectrophotometric determination of gallium in aqueous solutions, 25:2100
production of pure, review of techniques for, 25:3219
separation from nitrate and sulfate solutions by solvent extraction using amines, 25:2319 (ORNL-4572, pp 181-95)

SELENIUM ISOTOPES Se-74
energy levels from arsenic-74 decay, spin-parity assignments for, (E), 25:3704

SEMICONDUCTORS
conference on physics of, international, Cambridge, Mass., 7/70, 25:3185 (CONF-700801)
production of pure elements for, review of techniques for, 25:3219
radiation effects on, simulation of transient, 25:3477 (LYCEN-7063)

SERPUKHOV SYNCHROTRON
beam injection into, linac injector emittance and transversal characteristics for, 25:3482

SHEEP
metabolism in spermatozoa of, carbon-14 tracer study of effects of steroid hormones on, 25:2519

SHELLS (GEOMETRY)
nozzle junctions with cylindrical and spherical, stress analysis of region of, 25:2386 (ORNL-TM-2526(Add.))

SHIELDED CONTAINERS
design and testing of Savannah River Americium--Curium Slug, for shipping solid-form transuranium elements with mixed fission products, 25:2421 (ORNL-TM-3110)
development of liquid-sodium-cooled, for shipping spent LMFBR fuels, 25:2314 (ORNL-4572, pp 37-84)
testing of Types L-3 and L-10, for shipping plutonium nitrate, equipment and method for vibration, 25:2415 (ARH-1619)

SHIELDING
calculations for, problems in multi-dimensional Monte Carlo, 25:3176
calculations using Monte Carlo method, 25:3170
calculations, bibliography of computer codes for, 25:3179
calculations, development of discrete ordinates S/sub n/ method for, 25:3175
calculations, kernel methods for, 25:3178
calculations, methods and uses of advanced Monte Carlo concepts in, 25:3177
conference on accelerator, 25:3476 (JINR-16-4888)
gamma energy absorption rates in iron/lead laminated shielding, (T), 25:3169
gamma reflection and transmission by, spectral and angular-distribution function for, 25:3168
gamma scattering by, energy distribution of single and multiple, (E), 25:3182
gamma transport code for, time optimization for BIGGI $^3/_4$, 25:3180
gamma-dose rate distributions in laminated iron/water, (E/T), 25:3174
neutron flux density distributions in laminated iron/water, (E/T), 25:3174
physics measurements for reactor, transmission matrix methods for optimum, 25:3859
seismic design of Mihama Power Reactor, 25:3779

SHIELDING MATERIALS
neutron attenuation by, monoenergetic-source fast-, (E/T), 25:3173
neutron capture by, γ spectra from thermal-, (E), 25:3181

SHIPPINGPORT PRESSURIZED-WATER REACTOR
core for, physics measurements of Core 2, 25:3799(R) (WAPD-MRP-132)
maintenance during January 24 to April 25, 1970, 25:3799(R) (WAPD-MRP-132)
operations during January 24 to April 25, 1970, 25:3799(R) (WAPD-MRP-132)

SHIPS
shielding for Japanese nuclear-powered Mutsu, design requirements for lead, 25:2683

SHOCK TUBES
performance for dense low-temperature plasma production, 25:3116

SHOCK WAVES
propagation in solids, survey of equations for predicting, 25:3974 (SC-R-68-1784)

SILANE
reactions with recoil silicon-31 atoms, 25:2299

SILANE, TRIPHENYL-
methanolysis of, effects of deuterium on reaction rate of methoxide-catalyzed, 25:2176

SILICATE ROCKS
analysis for hafnium and zirconium by neutron activation and radiochemical separation, 25:2148
analysis for manganese and trace amounts of copper and lanthanum by neutron activation and radiochemical group separation, 25:2149
analysis for rare earths, scandium, and thorium using cupferron, spectrographic, 25:2078
analysis for scandium by spectrophotometry using 4-(2-thiazolylazo)resorcinol, 25:2093

SILICATES
effects of circumstellar, on infrared emission from α Ori, (E), 25:2826

SILICON
abundance in Kappa Cancri, (E), 25:2840
analysis for oxygen by alpha activation, 25:2128 (LYCEN-7060)
analysis for oxygen by charged-particle activation method, 25:2143
determination in lunar materials by 14-MeV neutron activation and γ spectrometry, 25:2118 (CONF-700322-, pp 205-20)
determination in oceanographic samples by 14-MeV neutron activation and γ spectrometry, 25:2119 (CONF-700322-, pp 221-30)
determination in steel by 14-MeV neutron activation, 25:2121 (CONF-700322-, pp 249-57)
determination of trace amounts of, in nuclear-grade uranium oxide (U_3O_8) by direct reading spectrometric method, 25:2068 (NLCO-1071)
effects on determination of trace amounts of rhenium by thiocyanate--stannous chloride method, 25:2102
microstructure of crystalline, electron microscopic study of, 25:2748
neutron capture by, gamma spectra from thermal, (E), 25:3181
nitrogen ion implantation in, infrared spectral study of high-energy, (E), 25:3203
production of pure, review of techniques for, 25:3219
proton reactions at 24 to 46 MeV, total cross sections for, (E), 25:3568
radiation damage to, hybrid recombination model for neutron, 25:2514 (SC-R-70-4351)
radiation effects on lithium-doped photovoltaic cells of, electron, 25:2814 (N-70-27167)
radioinduced production in aluminum, neutron, 25:2816 (ORNL-4570, pp 16-19)

SILICON CARBIDES
corrosion by selenium at 300 to 700°C, 25:2629
deposition on oxide fuel particles, 25:2320(R) (ORNL-TM-3204)
mechanical properties of gas cooled reactor fuel element coatings of, calculation of operating limits from, 25:3875 (EURFNR-834)
microstructure of crystalline, electron microscopic study of, 25:2748
radiation effects on voltage--current characteristic of diodes of, gamma, 25:3192

SILICON ISOTOPES Si-27
energy levels from (He-3,α) reactions, (E), 25:3637
energy levels from silicon-28 (He-3,α) reactions at 7.6 to 20 MeV, spins of, (E), 25:3594 (NP-18464)

SILICON ISOTOPES Si-28
deuteron elastic scattering at 28 MeV, asymmetry in vector-polarized, (E), 25:3585
deuteron reactions (d,p) at 2.00 to 6.12 MeV, angular distributions for, (E), 25:3606
energy levels and transitions of, in the projected Hartree--Fock model, (T), 25:3605
helium-3 reactions (He-3,α) at 18 to 20 MeV, j dependence in l = 2 angular distributions from, (E), 25:3637
helium-3 reactions (He-3,α) at 7.6 to 20 MeV, α angular distributions from, (E), 25:3594 (NP-18464)
helium-3 reactions (He-3,p) at 4.3 to 11.0 MeV, angular distributions for, (E), 25:3602

SILICON ISOTOPES Si-29
energy levels from (He-3,α) reactions, (E), 25:3637
energy levels from silicon-29 (d,p) reactions, (E), 25:3606

SILICON ISOTOPES Si-30
helium-3 reactions (He-3,α) at 18 to 20 MeV, j dependence in l = 2 angular distributions from, (E), 25:3637

SILICON ISOTOPES Si-31
reactions of recoil, with disilane, phosphine, and silane, 25:2299

SILICON NITRIDES
formation in high-energy nitrogen-implanted silicon, 25:3203

SILICON OXIDES
brazing with copper--silver alloy, composite film method using molybdenum, niobium, tantalum, and tungsten for,

25:2652
coating of fused, with boron at 1300°C, vapor deposition method for, 25:2777
effects on properties of sintered zircons, 25:2766(T) (CSIRO-Trans-9924)
Al_2O_3--SiO_2, compatibility with stainless steel at 370 to 700°C, 25:2606 (ORNL-4570, pp 92-5)
SILICON OXYNITRIDES
formation in high-energy nitrogen-implanted silicon, 25:3203
SILICON SYSTEMS
Fe--H--Rb--Si, phase studies of, 25:2727 (ORNL-4570, pp 1-4)
Nb--Si--Ti--V-base, creep to 850°C, 25:2662 (KFK-1193)
Si--Ti--V-base, creep to 850°C, 25:2662 (KFK-1193)
SILTS
analysis of ocean, by 14-MeV neutron activation and γ spectrometry, 25:2119 (CONF-700322-, pp 221-30)
cesium-137 affinity for, effects of particle size on, 25:2543
radioisotope accumulation by, in natural waters, 25:2547
radioisotope content of, in drainage canal of reactor center in Austria, 25:2545
radioisotope fixation by aquatic, in Meuse River, cobalt-60 and manganese-54, 25:2544
radioisotopes retention by Dimbovitza--Bucharest River, effects of chelating agents and pH on, 25:2363
ruthenium radioisotope accumulation by, in natural waters containing radioactive effluents, 25:2362
sorption of radioactive particles by aquatic, effects of grain size and suspension concentration on, 25:2545
SILVER
beta particle penetration in, intensity variation with thickness for external bremsstrahlung production from, (E), 25:3249
determination following nonsulfide separation from elements, qualitative, 25:2101
determination in molybdenum or yttrium by neutron activation and extraction displacement chromatography, 25:2138
determination in pigments from ancient murals by neutron activation, 25:2133
effects on determination of trace amounts of antimony by isotopic exchange in organic phase, 25:2106
effects on uv spectrophotometric determination of gallium in aqueous solutions, 25:2100
photon reactions at 5.7 GeV, $\omega\gamma$ coupling constant and ωN cross section from ω production in, (E), 25:3247
photon reactions at 50 to 412 keV with, total photoelectric cross sections for, 25:2905
work softening in polycrystalline, 25:2724
SILVER ALLOYS AND SYSTEMS
Ag--Cu, deposition of braze of, on silicon oxide composite film, method using molybdenum, niobium, tantalum, and tungsten for, 25:2652
Ag--Fe--Nb--Ni-base, crystallization of, relations with magnetic properties, 25:2679
Ag-base--Cu, photon reactions at 100 to 662 keV with sterling silver, effective atomic numbers for photoelectric, scattering, and total interaction processes in, 25:2906
SILVER ISOTOPES Ag-107
proton reactions (p,α) and 12 and 15 MeV, angular distributions for, (E), 25:3701
SILVER ISOTOPES Ag-109
proton reactions (p,α) and 12 and 15 MeV, angular distributions for, (E), 25:3701
SILVER ISOTOPES Ag-110
beta decay of metastable, β-γ circular polarization correlations in, (E), 25:3697
retention by silts of Dimbovitza--Bucharest River, effects of chelating agents and pH on, 25:2363
SINGLE CRYSTALS
conference on accurate determination of x-ray intensities and structure factors, Cambridge, Eng., 6/68, 25:3216
cooling below 90°K, technique for, 25:3963 (IS-T-423)
creep of, design of machine for study of compressive, 25:2728 (ORNL-4570, pp 5-9)
structure factors and x-ray intensities of, conference on, 25:3216
SINTERING
model for non-steady-state, 25:2787 (ORNL-4570, pp 24-6)
SKIN
analysis of psoriatic, for copper and zinc by neutron activation and radiochemical separation, 25:2134
phosphorus-33 uptake by, 25:2521
SODIUM
analysis for carbon, design of meter for, 25:2600 (BNL-50258)
analysis for oxygen using uranium, 25:2694
chromium segregation on surface of liquid, 25:2713
compatibility of high-temperature coolant of, with EBR-II construction materials, 25:2705
corrosion product transport in flowing, radioisotope transport loop for studies of activated, 25:2706
corrosive effects of flowing, on Type 316 stainless steel at 1200°F, 25:2618
corrosive effects of high velocity, on cobalt alloys, iron alloys, and refractory metal alloys at 710 to 760°C, 25:2617
corrosive effects of oxygen-containing, on vanadium and vanadium alloys, kinetic and thermodynamic properties of, 25:2622
corrosive effects of oxygen-contaminated, on Types 304 and 316 stainless steel at 1200 and 1400°F, 25:2620
corrosive effects on 3Z1 zirconium alloy at 450°C, effects of oxygen on, 25:2611 (PEL-201)
corrosive effects on chromium, cobalt, iron, and nickel at 660 and 760°C, 25:2631
corrosive effects on Incoloy 800 and Type 304 stainless steel and Type 304 and 316 stainless steel sodium loops at 900 to 1325°F, 25:2619
corrosive effects on reactor materials at high temperatures, review of, 25:2600 (BNL-50258)
corrosive effects on thorium and thorium--uranium alloys at 425°C, 25:2644 (ORNL-4570, pp 157-60)
corrosive effects on titanium--vanadium alloy, and Vanstar-7, -8, and -9, in Type 316 stainless steel loop system at 675 to 800°C, 25:2621
corrosive effects on vanadium-base alloys at 600°C, 25:2606 (ORNL-4570, pp 92-5)
corrosive effects on zirconium and zirconium alloys at 450°C, effects of oxygen on, 25:2611 (PEL-201)
determination following nonsulfide separation from elements, qualitative, 25:2101
determination in fingernails of patients with cystic fibrosis by neutron activation and γ spectrometry, 25:2127 (IAEA-122, pp 145-8)
determination in human liver by neutron activation and γ spectrometry, 25:2124 (IAEA-122, pp 15-26)
determination in human tissues by thermal neutron activation, sensitivity of, 25:2123 (IAEA-122, pp 1-13)
determination of trace amounts of, in nuclear-grade uranium oxide (U_3O_8) by direct reading spectrometric method, 25:2068 (NLCO-1071)
diffusion in oxygen-containing niobium and tantalum at 600°C, 25:2707
effects of liquid, on surface self-diffusion of α-iron, grain boundary grooving studies of, 25:2708
electron reactions with atomic, excitation cross sections for, (T), 25:2915
excitation cross sections for, calculation using approximation based on regional trial functions, 25:2895
formation of particles on surface of liquid, 25:2713
iron segregation on surface of liquid, 25:2713
neutron capture by, gamma spectra from thermal, (E), 25:3181
neutron resonance scattering at 2.85 keV in, group structure and group constants for, (T), 25:3928 (JAERI-Memo-4110)
reactions of oxygen-containing, with chromium and Type 304 stainless steel at 300 to 500°C, electrochemical study of oxidation-reduction, 25:2710
reactions with beryllium chloride to prepare beryllium by Kroll method, reduction, 25:2653
release to soil from organic debris in forest as function of decomposition mode and time, 25:2528
segregation of impurities on surface of liquid, 25:2713
separation from other alkali metals by fixation on hydrated antimony pertoxide in hydrochloric, nitric, and perchloric acids, effects of acidity and time on, 25:2333
solvent properties for chromium, iron, and nickel, effects of temperature on, 25:2712
solvent properties for oxygen at 350 to 550°C, electrochemical study of, 25:2711
SODIUM ACID CARBONATES
effects on recovery of γ-irradiated spores of Clostridium, 25:2599
SODIUM ALLOYS AND SYSTEMS
H--Na--O, phase studies of condensed phases in, at 400 to 1000°K, thermochemical, 25:2205
H--Na--O, vapor pressure of gaseous species over condensed phases in, at 400 to 1000°K, 25:2205
K--Na, corrosive effects on oxygen-contaminated tantalum at 1200 and 1350°F, effects of exposure time and welding on, 25:2623
Na--O, electric potentials at 350 to 550°C, relations with composition, 25:2711
Na--Pb, magnetic flux line pinning and precipitates in superconducting, (E/T), 25:3033
SODIUM ALUMINATES
sorptive properties for sulfur dioxide from flue gases, 25:2820 (ORNL-4570, pp 213)
SODIUM BROMIDES
radioinduced energy storage in crystals of, luminescence from aqueous release of γ, 25:2227
$AlBr_3$--NaBr, electric conductivity and density of molten mixtures of, 25:2805 (ORNL-4570, pp 31-4)
SODIUM CHLORIDES
analysis of solutions of, for chromium, molybdenum, and vanadium by catalytic amalgam method, 25:2080
effects on radioinduced luminescence of aqueous solutions of monovalent thallium, 25:2232
radioinduced energy storage in crystals of, luminescence from aqueous release of γ, 25:2227
radioinduced thermally stimulated conductivity of single crystals of, gamma and neutron, 25:3202
SODIUM CHLOROIRIDATES
radiation effects on, chemical states of recoil rhenium from proton, 25:2300

XUM

SODIUM FLUORIDES
effects on properties of sintered zircons, 25:2766(T) (CSIRO-Trans-9924)
radioinduced energy storage in crystals of, luminescence from aqueous release of γ, 25:2227
$NaBF_4$--NaF, corrosive effects on Hastelloy N at 605°C, 25:2609 (ORNL-4570, pp 175-90)
SODIUM FLUOROBORATES
$NaBF_4$--NaF, corrosive effects on Hastelloy N at 605°C, 25:2609 (ORNL-4570, pp 175-90)
SODIUM FORMATES
effects on radiolysis of water, 25:2257 (CEA-R-4046)
SODIUM HYDROXIDES
corrosive effects of aqueous, on carbon steel, 25:2614
SODIUM IONS
reactions with nitrogen molecules at 30 to 100 keV, absolute emission cross sections for, (E), 25:2902 (SC-RR-70-695)
SODIUM ISOTOPES Na-22
retention by silts of Dimbovitza--Bucharest River, effects of chelating agents and pH on, 25:2363
transfer through dentine and enamel of teeth, effects of chemicals on, 25:2532
SODIUM ISOTOPES Na-23
diffusion in liquid, self-, 25:2192
neutron inelastic scattering below 2 MeV, optical-model calculation of angular distributions for, (T), 25:3635
nuclear magnetic resonance quadrupole spectrum in Rochelle salt, 25:3221
proton inelastic scattering at 17.5 MeV, cross-section calculations for, (T), 25:3603
SODIUM NITRITES
radioinduced free radicals in single crystals of, infrared absorption and Faraday rotation of γ-, (E), 25:3191
SODIUM OXIDES
thermodynamic properties of, electrochemical study of, 25:2711
SODIUM SILICATES
effects on properties of sintered zircons, 25:2766(T) (CSIRO-Trans-9924)
SODIUM SULFATES
effects on sulfur-35 β radiation effects on electrokinetic potential of solid barium sulfate, 25:2222
SODIUM URANYL ACETATES
fluorescence lifetimes of, effects of heavy water and impurities on, 25:2198
SOILS
analysis for manganese, selenium, and zinc by neutron activation, 25:2125 (IAEA-122, pp 27-36)
cesium-137 availability in mineral, effects of ammonium and potassium ions on, 25:2529
density of, gamma-backscatter moving-source gage for measurements of, 25:2498
radioactive contamination by cerium, cesium, and ruthenium isotopes, 25:2338
radioactivity of archaeological excavation site, in Germany and Sweden, 25:2352
radioisotope distribution in, of USSR in relation to climatic zones, natural, 25:2371
radioisotope release to, from organic debris in forest as function of decomposition mode and time, 25:2528
radioisotope transport in, 25:2541
release of inorganic elements to, from organic debris in forest as function of decomposition mode and time, 25:2528
ruthenium-103 and -106 transport in, effects of physicochemical processes on, 25:2364
strontium-90 transport through, computer calculation of, 25:2366
strontium-90 transport through, effects of organic compounds on, 25:2365
SOL-GEL PROCESS
chemical engineering for, 25:2195 (ORNL-4572, pp 251-7)
microsphere production by, 25:2195 (ORNL-4572, pp 251-7)
SOLAR ACTIVE REGIONS
brightness distribution in, (E), 25:2857(T) (AD-707256)
SOLAR DISTURBANCES
relation to geomagnetic storms and on storm recurrence, (E/T), 25:2998
SOLAR FLARES
activity of solar-disc, relation to metal emission brightness of geophysical, (E/T), 25:2859
conference on mass motions in, Anacapri, Italy, 6/68, 25:2862
mass motions in, (T), 25:2862
SOLAR PARTICLES
emission of neutrons at 20 to 160 MeV, measurement of, 25:2861
SOLAR RADIATION
emission spectra of moustaches, asymmetry of, (E), 25:2863
SOLAR WIND
effect on world-wide variations in magnetic field, statistics of, 25:2958
effects on scintillation of cosmic radio sources, (E/T), 25:2856
flow past Mars and Venus, determination of ionospheric boundary from, (E/T), 25:2878
interactions with magnetosphere, production of variations in geomagnetic field from, (E/T), 25:2955
SOLDERS
photon reactions at 100 to 662 keV with, effective atomic numbers for photoelectric, scattering, and total interaction processes in, 25:2906
SOLID SOLUTIONS
atom arrangements in, computer simulation of, 25:2668 (ORNL-4570, pp 10-12)
SOLID STATE PHYSICS
pseudopotential and model potentials in, (T), 25:3227
SOLIDS
ion bombardment damage in, research program on, 25:3190(R) (COO-1053-15)
ion channeling in, use in research and teaching, 25:3188 (CONF-700322-, pp 141-53)
ion implantation in, 150-keV accelerator for, 25:3469 (CONF-700322-, pp 173-84)
particle reactions with, bibliography for 1969 on, 25:2901 (ORNL-AMPIC-13)
properties at high temperatures, bibliography on, 25:2665 (NBS-SPEC. PUBL-315-5)
radiation effects on defects in, thermoluminescence glow peaks from x, 25:2235
structure of disordered and ordered, development of methods for determining electronic, 25:2671 (ORNL-4570, pp 40-3)
SOLUTIONS
chemical properties of aqueous, spectrophotometric studies on, 25:2152 (ORNL-4572, pp 231-5)
SOLVENT EXTRACTION PROCESSES
enhancement by air-pulsing, review of methods for, 25:2383 (AAEC/TM-547)
solvent distribution in, 25:2345
SOUND
scattering of, random walk approximation for analyzing, 25:3239
SOVIET UNION
radioisotope contamination in Moscow area of, during 1962 to 1966, fallout, 25:2550
radioisotope distribution in soils of European regions of, in relation to climatic zones, natural, 25:2371
SPACE
cosmic radiation energy spectrum in interstellar, effects of sunspots on 11-year variations of primary, (E/T), 25:2930
SPECTROMETERS
data handling system for quantometer, 25:2069 (Y-1740)
detectors for magnetic, position-sensitive silicon surface-barrier, 25:2463
performance of x-ray fluorescence, with computer for determination of elements in solution, 25:2105
SPECTROSCOPY
bibliography on laser uses in emission, 25:3110 (IN-1425)
equipment and methods for electron, 25:2900 (CONF-700322-, pp 305-19)
SPERM
metabolism in ejaculated ram, carbon-14 tracer study of effects of steroid hormones on, 25:2519
radioinduced sex chromosome loss in, of Drosophila melanogaster, partial and total x, 25:2554
SPERMATOCYTES
radioinduced chromosome aberrations in, of mice following exposure of spermatogonia, incidence of x, 25:2553
SPERMATOGONIA
radiation effects on chromosomes in, of mice in relation to translocation frequency in spermatocytes, x, 25:2553
SPLEEN
scanning of, use of radioisotopes and scintillation camera in γ, 25:2581
SPORES
radiation effects on, of Clostridium botulinum, factors affecting recovery following heat and γ, 25:2599
SPUTTERING
method for sectioning metal diffusion specimens by radiofrequency, 25:2786 (ORNL-4570, pp 13-15)
STACK DISPOSAL
iodine release in, methods for minimizing, 25:2314 (ORNL-4572, pp 37-84)
STAINLESS STEEL
bonding of gold-plated Type 302, to Inconel 718 under static loads, 25:2677 (ORNL-4570, pp 224-7)
coating with cadmium, copper, or zinc, surface morphology in electrochemical, 25:2648
cold work in small-diameter tubes of, magnetic permeability measurements of, 25:2408 (ORNL-4570, pp 96-7)
compatibility of Types 304 and 316, with aluminum oxide--silicon oxide insulation at 370 to 700°C, 25:2606 (ORNL-4570, pp 92-5)
compatibility with strontium titanate at 900 to 1100°C, 25:2643 (ORNL-4570, pp 106-11)
corrosion by selenium at 300 to 700°C, 25:2629
corrosion by steam of weldments of Type 304, incorporating Type 308 stainless steel weld filler, 25:2608 (ORNL-4570, pp 124-6)
corrosion of austenitic, ferritic, and hardenable, by lithium at 600 and 900°F, 25:2626
corrosion of similar metal welds using Type 308 stainless steel filter metal, by steam at 1100 to 1200°F,

25:2636
corrosion of sodium loops of Incoloy 800 and Type 304, at 900 to 1325°F, 25:2619
corrosion of sodium loops of Type 304 and 316, at 900 to 1325°F, 25:2619
corrosion of Type 304 by gaseous chlorides, stress, 25:2614
corrosion of Type 304, by MSRE coolant at 663°C, 25:2609 (ORNL-4570, pp 175-90)
corrosion of Type 316, by flowing sodium at 1200°F, 25:2618
corrosion of Types 304 and 316, by oxygen-contaminated sodium at 1200 and 1400°F, 25:2620
corrosion of Types 304, 316, and 348, by ammoniated and lithiated PWR coolants, effects on reactor operation, 25:2637
creep and tensile properties of Types 304 and 316, effects of shock strengthening on, 25:2755 (BMI-1889, Sect.B)
creep of Type 316, at 650 to 750°C and 4 to 8 kg/mm² stress, effects of prior cold work on, 25:2661 (JAERI-Memo-4125)
creep rate correlation in solution treated Type 304 and 316, 25:4007 (WHAN-FR-25)
creep rupture of heavy-section plates of Type 316, at 500 to 600°C, 25:2660 (JAERI-Memo-4057)
fabrication of fuel cladding of Type 304, performance of planetary swaging process for, 25:2641 (ORNL-4570, pp 85-7)
fabrication of ultrafine grain tubes of Type 316, methods for, 25:2641 (ORNL-4570, pp 85-7)
mass transfer of carbon and nitrogen to vanadium from, by sodium carrier, 25:2606 (ORNL-4570, pp 92-5)
mechanical properties of Type 316, for LMFBR fuel cladding, 25:2789 (ORNL-4570, pp 68-75)
microstructure of ferritic phases in austenitic, effects of chemical composition on, 25:2675 (ORNL-4570, pp 143-8)
neutron capture by Type 321, gamma spectra from thermal-, (E), 25:3181
neutron cross sections for, 25-group, (T), 25:3530 (LA-4484)
oxidation-reduction of Type 304, by oxygen-containing sodium at 300 to 500°C, electrochemical study of, 25:2710
performance of welding electrodes of Type 308, effects of coating on, 25:2642 (ORNL-4570, pp 88-91)
radiation effects on mechanical properties of Types 347 and 348, at 25 to 750°C, fast neutron, 25:2755 (BMI-1889, Sect.B)
radiation effects on void distribution in Type-304, fast neutron, 25:2758 (ORNL-4570, pp 76-84)
radiation effects on void formation in Type 304, relations of preinjected helium with fast neutron, 25:2761
radioinduced acicular precipitates in Type 316, morphology of neutron, 25:2756 (CEA-CONF-1638)
stress rupture of ultrafine grain tubes of Type 316, at 650°C, 25:2641 (ORNL-4570, pp 85-7)
tensile properties of titanium-modified Type 304, at 550 to 650°C, 25:2758 (ORNL-4570, pp 76-84)
vanadium mass transfer to Type 321, by high velocity sodium at 710 to 760°C, 25:2617
weldments of, effects of electrode coating and arc process on properties of, 25:2642 (ORNL-4570, pp 88-91)

STAINLESS STEEL COUPLES
cold welding in Type 440°C, under static loads, effects of surface contamination on, 25:2677 (ORNL-4570, pp 224-7)

STANDARDS
piping for U. S. power reactors, 25:3778

STANFORD LINEAR ACCELERATOR
design modification proposal for 100-GeV superconducting, feasibility of, 25:3507

STARK EFFECT
use of high-frequency, in plasma diagnostics, 25:3062

STARS
atmospheres of Cepheid variable, hydrodynamic model, (T), 25:2838
atmospheres of, dynamic particle--spin orientation in, (T), 25:2831
atmospheres of, equilibrium configuration of, (T), 25:2827
critical parameters of isothermal white-dwarf, effect of neutronization on, (T), 25:2832
distribution in vicinity of Sun, (E), 25:2835
element abundances in, use of beam--foil data in determining, 25:2688 (CONF-700322-, pp 281-8)
energy loss from neutrino pair emission from electron reactions with nuclei in, (T), 25:3335
evolution of rapidly rotating B-type, (T), 25:2836
evolution of, mixing between envelope and core in advanced, (T), 25:2825
helium abundance in main-sequence B-Type, (E), 25:2839
interactions in galactic disks, computer simulation of, (T), 25:2864
luminosity function of, in vicinity of Sun, (E), 25:2835
model-atmosphere analysis of Kappa Cancri, (E), 25:2840
models in nonrelativistic generalized theory of gravitation, polytropic, (T), 25:2833
neutrino luminosity from ν--anti ν pair production from electron reactions with nuclei in, (T), 25:3335
oxygen-16 production in, by carbon-12 (α,γ) reactions, 25:3562 (CONF-700322-, pp 297-304)
photometry of α Ori, narrow-band infrared, (E), 25:2826
radiation emission from envelopes of close-binary, due to shock heating, (T), 25:2830
spectra of HD 152107, anomalous hydrogen line intensities in, (E), 25:2834
structure of rapidly rotating B-type, (T), 25:2836
transfer equation for nonstationary radiation field in atmospheres of, (T), 25:2829

STATISTICS
formalism for justification of ensembles in quantum statistical mechanics, 25:3238
formalism for justification of ensembles in quantum statistical mechanics, 25:3237
projection operators in nonequilibrium mechanics, identity concerning, 25:3234

STEAM
corrosive effects on advanced steam generator alloys, 25:2608 (ORNL-4570, pp 124-6)
corrosive effects on Hastelloy N at 538°C, 25:2609 (ORNL-4570, pp 175-90)
corrosive effects on steam generator alloy weldments at 1100 to 1200°F, 25:2636
reactions with hydrogen and uranium hexafluoride in fluidized bed to produce ceramic-grade uranium dioxide, 25:2781(P)
steam--water, density of, ultrasonic void fraction detector for measurement of, 25:3905 (IN-1441)

STEAM POWER PLANTS
development during 1970 to 1980, predictions for, 25:3776
effluents from, effects on environment in U. S. of chemical and thermal, 25:3852
power production in Germany during 1969 from, 25:3800

STEEL
analysis for carbon at various depths by proton activation, 25:2147
analysis for exogenous inclusions by neutron activation, 25:2132
analysis for niobium using benzohydroxamic acid, extraction--photometric, 25:2085
analysis for oxygen and silicon by 14-MeV neutron activation, 25:2121 (CONF-700322-, pp 249-57)
corrosion of alloy, by lithium at 600 and 900°F, effects of tempering at 1100°F on, 25:2626
corrosion of maraging, by MSRE coolant at 663°C, 25:2609 (ORNL-4570, pp 175-90)
corrosion of niobium-coated tubing of, by bismuth--lead eutectic containing magnesium and zirconium at 375 to 500°C, 25:2627
corrosion resistance and mechanical properties of titanium carbonitride-coated, 25:2612
corrosion resistance and mechanical properties of zirconium carbonitride-coated, 25:2612
embrittlement by hydrogen, mechanisms of cathodic, 25:2816 (ORNL-4570, pp 16-19)
mechanical properties of heavy-section Type A533, research on characteristic, 25:2676 (ORNL-4570, pp 170-3)
photon reactions at 100 to 662 keV with tungsten, effective atomic numbers for photoelectric, scattering, and total interaction processes in, 25:2906
radiation effects on brittleness of heavy-section specimens of Type A533B, relations of copper and phosphorus content with in-pile, 25:2757 (NRL-7121)
radiation effects on heavy-section plates and welds of Type A533, fast neutron, 25:2676 (ORNL-4570, pp 170-3)
radiation effects on structure of martensite lattice in U-10, electron, 25:2764
tensile properties of weldments of heavy-section, 25:2676 (ORNL-4570, pp 170-3)
thermal expansion of straight tubes of, for Czechoslovak nuclear power plant, 25:2684
work-hardening parameters for polycrystalline mild, 25:2723
C--steel, corrosion by aqueous sodium hydroxide, stress, 25:2614
Cr--Mo--steel, creep at 900 to 1100°F and 8000 to 25,000 psi stress, 25:2755 (BMI-1889, Sect.B)

STELLARATORS
magnetic fields in two-path, poloidal fields and minimum mean, (T), 25:3142
magnetic surfaces and drift surfaces of charged particles in, (T), 25:3128 (IPPJ-95)
magnetic wells in combined fields of one- and two-path, possibility of existence of, (T), 25:3143
plasma confinement in, effects of inertia on losses, (T), 25:3060

STILBENE
effects on γ-radioinduced graft polymerization of cellulose with styrene in methanol solutions, 25:2247

STRANGE PARTICLES
production in $\pi^+ + p$ interactions at 5.5 GeV/c, cross sections for, (E), 25:3279

STRESS
measurement of residual, in welded structures, method for, 25:2410 (ORNL-TM-3113)

STRONTIUM
determination following nonsulfide separation from

XUM

elements, qualitative, 25:2101
determination of trace amounts of, in nuclear-grade uranium oxide (U_3O_8) by direct reading spectrometric method, 25:2068 (NLCO-1071)
effects on determination of trace amounts of antimony by isotopic exchange in organic phase, 25:2106
effects on uv spectrophotometric determination of gallium in aqueous solutions, 25:2100
neutron elastic scattering at 1 to 40 keV, analysis of angular distributions from, (E/T), 25:3695
STRONTIUM CHLORIDES
proton reactions at 350 keV with, characteristic x-ray spectra from, (E), 25:2882 (CONF-700522-, pp 113-24)
STRONTIUM ISOTOPES Sr-85
retention by silts of Dimbovitza--Bucharest River, effects of chelating agents and pH on, 25:2363
separation from milk, performance of Polish-made ion exchangers for, 25:2329
STRONTIUM ISOTOPES Sr-88
energy levels and transitions from rubidium-88 decay, (E), 25:3621
STRONTIUM ISOTOPES Sr-89
determination in ambient air, tentative radiochemical method for, 25:2114
separation from milk, performance of Polish-made ion exchangers for, 25:2329
STRONTIUM ISOTOPES Sr-90
accumulation in fish of northern Italy, statistical analysis of effects of location, sample date, season, and species on concentration factor for fallout, 25:2527
concentration by hydrobionts, effects of nutritional type of lake on, 25:2546
content in atmosphere and precipitation in East Germany, 1968 and 1969, 25:2370
detection in radioecology studies, use of Cherenkov counting for, 25:2565
determination in ambient air, tentative radiochemical method for, 25:2115
determination in water by ion exchange or filtration and counting, 25:2117
monitoring in irrigation canal sediment and water downstream from nuclear power centers on Rhone River, 25:2543
separation from milk by sorption on alkali metal or alkaline earth salts of phytic acid, 25:2346(P)
sorption by Rhine River monomineralic fine sands, (E), 25:2350
transport through soils, computer calculation of, 25:2366
transport through soils, effects of organic compounds on, 25:2365
STRONTIUM OXIDES
BaO--Nb_2O_5--SrO, phase studies of Nb_2O_5-rich region of, 25:2808
Nb_2O_5--SrO, phase studies of, 25:2808
STRONTIUM TITANATES
compatibility with refractory fuel capsule materials at 900 to 1100°C, 25:2643 (ORNL-4570, pp 106-11)
STRONTIUM URANATES
Ba_3UO_6--Sr_3UO_6, crystal structure of, 25:2210
STYRENE
polymerization with polyethylene, mechanism of graft, induced by 2,2'-azobis[2-methylpropionitrile] and benzoyl peroxide, 25:2241
radioinduced graft polymerization with cellulose in methanol solutions, effects of additives on γ, 25:2247
radioinduced graft polymerization with polyethylene, mechanism of γ, 25:2241
radioinduced graft polymerization with polyethylene, effects of crystallinity, pre-irradiation, temperature, and thickness on γ, 25:2242
radioinduced polymerization in wood, 25:2254
radioinduced polymerization of, effects of temperature on γ, 25:2245
STYRENE POLYMERS
mobility of particles of, in aerosols, 25:3940 (COO-1248-22)
radiation dose conversion factor for, 25:2569
radiation effects on stress-rupture stability of, by cross linking, electron, 25:2249
SUCCINIC ACID
sodium salt, radiation effects on monoclinic crystals of, ESR studies on free radicals produced from γ, 25:2229
sodium salt, radiation effects on triclinic crystals of, ESR studies on free radicals produced from γ, 25:2230
SUCCINIC ACID, METHYLENE-
effects on mechanism of γ-radioinduced graft polymerization of poly(ethylene terephthalate), 25:2244
SUCCINIC ACID, METHYLENE-, DIMETHYL ESTER
radiation effects on electric conductivity of solid, at -196°C, γ, 25:2221
SUCROSE
radiolysis of frozen solutions of, at 77°K, ESR spectral studies on radical processes produced by γ, 25:2279
SULFATES
analysis of solutions of, for cerium, chromium, manganese, and vanadium by coulometric titration, 25:2081
separation of tellurium from solutions of, by solvent extraction using dialkyl phosphorodithioate or D2EHPA, 25:2321
SULFUR
determination in human tissues by thermal neutron activation, sensitivity of, 25:2123 (IAEA-122, pp 1-13)
determination in molybdenum by thermal neutron activation and radiochemical separation, 25:2136
neutron capture by, gamma spectra from thermal, (E), 25:3181
SULFUR FLUORIDES
effects on γ radiolysis of cyclohexane, 25:2268
SULFUR ISOTOPES S-31
energy levels from sulfur-32 (He-3,α) reactions at 7.6 to 20 MeV, spins of, (E), 25:3594 (NP-18464)
SULFUR ISOTOPES S-32
deuteron reactions (d,p) at 12.3 MeV, proton spectra and angular distributions for, (E), 25:3597
electron quasi-elastic scattering at 1115 MeV, 25:3615
energy levels of, calculation using Hartree--Fock--Bogolyubov method with isospin pairing, (T), 25:3722
helium-3 reactions (He-3,α) at 7.6 to 20 MeV, α angular distributions from, (E), 25:3594 (NP-18464)
neutron inelastic scattering at 14 MeV, differential cross sections, (E), 25:3612
nuclear charge radius from electron quasi-elastic scattering, 25:3615
SULFUR ISOTOPES S-33
energy levels from sulfur-32 (d,p) reactions, spectroscopic factors for low-lying, (E), 25:3597
SULFUR ISOTOPES S-35
reactions of recoil atoms of, with benzothiazolethiol and 2-(methylthio)benzothiazole, distribution and yields from, 25:2303
SULFUR OXIDES
sorption of flue-gas, development of materials for, 25:2820 (ORNL-4570, pp 213)
SULFURIC ACID
acidity function in, effects of deuterium on, 25:2175
effects on sulfur-35 β radiation effects on electrokinetic potential of solid barium sulfate, 25:2222
radiolysis of aqueous solutions of, γ, 25:2277
radiolysis of aqueous solutions of, mechanism and yields of hydrogen peroxide and persulfate from γ, 25:2265
SUN
eclipse of Sept. 22, 1968, effect on lower ionosphere, (E), 25:2996
eclipse of Sept. 22, 1968, vlf radio-wave phase measurement during, (E), 25:2997
photometry of moustaches to reveal asymmetry of their emission, 25:2863
SUNSPOTS
activity indexes of 27-, 54-, and 81-day data, Jan. 1, 1955 to Dec. 31, 1969, (E), 25:2858 (N-70-32003)
effects on 11-year variations of primary cosmic radiation energy spectrum in interstellar space, (E/T), 25:2930
SUPERCONDUCTIVITY
electron energy at absolute zero, boundary singularities in, (T), 25:3030
Josephson effect in, history of discovery of, 25:3032
Kondo effects on, (T), 25:3022
physical metallurgy and, lecture on, 25:3025
theory of, Hamiltonians of quantum statistics and model Hamiltonian of, 25:3040
SUPERCONDUCTORS
cavity resonance in arrays of weak links of, superradiance in, (T), 25:3045
condensation energy calculations for seven metals, 25:3046
critical current density and defect structure in high-field, (E), 25:3039
critical field of cubic monocrystals, correlation function calculations of upper, 25:3047
critical fields of niobium--titanium alloys, lower, (E/T), 25:3020 (ORNL-TM-3206)
critical state in hysteretic, 25:2670 (ORNL-4570, pp 35-6)
critical temperature of thin tin films, (E/T), 25:3026
electric conductivity in pure Type-II, near H/sub c2/, (T), 25:3043
Hall effect in, effects of order parameter fluctuations on, (T), 25:3036
Josephson junction system, transition to resistanceless state in, (E), 25:3035
Josephson oscillation in, generation of harmonics and subharmonics of, 25:3037
Josephson tunnel junctions in, fluctuations above critical temperature, (T), 25:3029
losses in, model for moving fluxoid-induced, 25:2670 (ORNL-4570, pp 35-6)
magnetic flux line pinning and precipitates in alloys, (E/T), 25:3033
magnetic flux quanta in tubes of, direct observation of single, 25:3024
magnetic properties of titanium--22 at. per cent niobium alloy, 25:3027
order parameter depression with Kondo effect, (T), 25:3022
order parameter fluctuations in film, in magnetic field, (T), 25:3042
penetration depth in bulk polycrystalline lead, (E),

25:3041
properties of β-titanium alloys as, 25:3021(T) (UCRL-Trans-1409)
properties of thin films containing paramagnetic impurities in uhf field, (T), 25:3031
research on hard, 25:3019(R) (NYO-3029-48)
transition temperature of, iteration procedure for, (T), 25:3023
ultrasound absorption by nuclei in intermediate state, resonant, (T), 25:3028
use in radiation detectors, 25:2444
SUPERFLUIDITY
equations of motion of complex order parameter of helium II, 25:3014
heat currents in helium II, temperature variations from, (T), 25:3006
occurrence in helium-3, possibility of, (T), 25:3017
properties of nonideal boson gas with particles interacting through Gaussian potential, 25:3009
stability of, and ion mobility in He-3--He-4 mixtures, (T), 25:3012
SURVIVAL
radiation effects on bacterial, mechanism of uv, 25:2598
SWEDEN
archaeological excavation sites in, radioactivity of soils and ground-level atmosphere at, (E), 25:2352
SWITZERLAND
nuclear power engineering in, capacity and quality of, 25:3781
SYMMETRY GROUPS
electromagnetic fields in relativistic, uniform, 25:3432
G_3 on V_2 velocity groups, neutrino model in general relativity theory with, 25:3343
interactions π + N in, 25:3387
SL(2,C), representations in explicitly energy-dependent basis for, 25:3421 (KFKI-70-19-HEP)
SU(2) x SU(2) chiral saturation of Adler--Weiskerger relations in, 25:3422
SU(2), Regge symmetry of Wigner coefficients in, 25:3305
SU(3) x SU(3) chiral symmetry breaking corrections to soft-pion theorem for K → 3π decay, 25:3347
SU(3) x SU(3) chiral symmetry breaking for hyperon nonleptonic decays, 25:3349
U(n) x U(n) chiral transformations in unified fermion theory, 25:3428
unitary groups, isoscalar factors of Clebsch--Gordan coefficients of, 25:3305
SYMMETRY GROUPS SU(3)
operator for particles and nuclear shell model in, 27-plet, 25:3426
SYNCHROCYCLOTRONS
shielding measurements for, gamma dose rate distributions and neutron attenuation, 25:3480
SYNCHROTRONS
beam oscillations in, study of resonances of nonlinear, 25:3488
design studies for CERN 300-GeV proton, 25:3501
development of superconducting, at Rutherford Lab, review on, 25:3514
magnet power supply for superconducting, development of, 25:3513
magnets for, design of superconducting, 25:3512
magnets for, development and use of pulsed superconducting, 25:3511
magnets for, development of superconducting, 25:3510

T

T-111 (TANTALUM ALLOY)
compatibility with copper at 1100°C, 25:2720
corrosion by flowing lithium at 1370°C, 25:2607 (ORNL-4570, pp 103-5)
corrosion by lithium at 1000 and 1400°F, effects of welding atmosphere purity on, 25:2625
mechanical properties of, effects of fabrication variables on, 25:2672 (ORNL-4570, pp 112-15)
oxidation at 600°C, mechanisms of, 25:2605 (ORNL-4570, pp 37-9)
TACHYONS
Lorentz-tachyon transformations for Dirac, (T), 25:3441
TANTALUM
corrosion by high-temperature sodium coolant, 25:2705
corrosion by zinc at 1000°C, effects of anodization in phosphoric acid on, 25:2630
corrosion of oxygen-contaminated, by potassium--sodium alloy at 1200 and 1350°F, effects of exposure time and welding on, 25:2623
determination in minerals and rocks by neutron activation and γ spectrometry, 25:2139
determination in presence of niobium by chromatographic and gravimetric methods, 25:2066 (NIM-834)
determination in rocks by neutron activation and γ spectrometry, 25:2145
determination in titanium alloys, x-ray fluorescence method for, 25:2097
determination in uranium alloys by atomic absorption spectrophotometry, 25:2065 (LA-4529)
diffusion in tungsten, activation energy for, 25:2605 (ORNL-4570, pp 37-9)
diffusion of lithium, potassium, and sodium in oxygen-containing, at 600°C, 25:2707
effects on brazing of silicon oxide with copper--silver alloy using composite film method, 25:2652
effects on extraction--photometric determination of niobium in steel, 25:2085
electric conductivity at 100 to 1700°C, (E), 25:2715
emissivity at 100 to 1700°C, total, (E), 25:2715
ion reactions at 5 to 50 keV with, apparent total ion scattering, secondary electron emission coefficients, and electron and ion energy distributions for, (E), 25:2884 (NP-18490)
neutron cross sections for, 25-group, (T), 25:3530 (LA-4484)
oxidation by high-frequency oxygen plasma, kinetics of, 25:2632
oxidation by oxygen at 550 to 800°C, flexure measurements during, 25:2605 (ORNL-4570, pp 37-9)
photon reactions at 5.7 GeV, $\omega\gamma$ coupling constant and ωN cross section from ω production in, (E), 25:3247
photon reactions at 662 keV with, photoelectric cross sections for, (E), 25:2904
properties of, effects of hydrogen, nitrogen, and oxygen on, 25:2639(T) (LIB/Trans-309)
separation from nitrate and sulfate solutions by solvent extraction using amines, 25:2319 (ORNL-4572, pp 181-95)
solubility in potassium at 1055 to 1287°K, effects of oxygen doping on, 25:2664 (N-70-32146)
sorptive properties for nitrogen and oxygen, method for determining, 25:2686
superconducting Josephson junction system in, transition to resistanceless state in, (E), 25:3035
thermal conductivity at 100 to 1700°C, (E), 25:2715
thermal conductivity at 80 to 400°K, 25:2672 (ORNL-4570, pp 112-15)
thermal conductivity of, electronic, 25:2788 (ORNL-4570, pp 27-30)
work-hardening parameters for polycrystalline, 25:2723
TANTALUM ALLOYS AND SYSTEMS
Hf--Ta, hardness of, effects of aging on, 25:2672 (ORNL-4570, pp 112-15)
Hf--Ta, phase studies of, 25:2668 (ORNL-4570, pp 10-12)
Mo--Ta-base, elastic properties of monocrystalline, at 80 to 1400°K, 25:2721
Nb--Ta-base, elastic properties of monocrystalline, at 80 to 1400°K, 25:2721
Ni-base--Ta, carburization of, relations with hardness, 25:2716
Re--Ta-base, elastic properties of monocrystalline, at 80 to 1400°K, 25:2721
Ta-base--W, bonding to platinum, development of methods for, 25:2672 (ORNL-4570, pp 112-15)
Ta-base--W, compatibility with copper at 1100°C, 25:2720
Ta-base--W, corrosion by barium, calcium, indium, lead, and thallium at 1000 to 1800°C, 25:2628
Ta-base--W, elastic properties of monocrystalline, at 80 to 1400°K, 25:2721
TANTALUM CHLORIDES
crystal structure of $H_2Ta_6Cl_{18} \cdot 6H_2O$, 25:3963 (IS-T-423)
TANTALUM FLUORIDES
TaF_5--XeF_6, reactions in, properties and structure of products produced by, 25:2156
TANTALUM ISOTOPES Ta-181
energy-level transitions in, γ--γ directional correlations for γ cascade, (E), 25:3647 (COO-1746-46)
TANTALUM OXIDES
effects on properties of sintered zircons, 25:2766(T) (CSIRO-Trans-9924)
TARTARIC ACID
complexes with trivalent indium and hexavalent uranium, potentiometric, solvent extraction, and spectrophotometric studies on, 25:2206
TD-NICKEL
mechanical properties of low-porosity corrosion-resistant, 25:2796
TECHNETIUM
elastic properties at cryogenic temperatures, 25:2670 (ORNL-4570, pp 35-6)
separation from fission products by ion exchange and solvent extraction, 25:2307 (CEA-N-1316)
TECHNETIUM ISOTOPES Tc-99
chemical and physical properties of metastable, 25:2580
effectiveness of metastable, for localization of tumors in posterior fossa of human brain, computer evaluation of, 25:2578
effectiveness of metastable, for scanning of cerebral blood flow in combination with serial angiography, 25:2577
energy level at 181 keV, half-life of, (E), 25:3708
use of metastable, as γ source for transmission scanning of anatomy of human lungs, 25:2580
use of metastable, for organ scanning, 25:2581
use of metastable, for scanning human blood circulation, brain, kidneys, lungs, reticulo-endothelial system, and thyroid gland, 25:2580
TECHNETIUM ISOTOPES Tc-108
decay and energy-level transitions following californium-252 fission, (E), 25:3673
TECHNETIUM ISOTOPES Tc-109
decay and energy-level transitions following californium-252 fission, (E), 25:3673

XUM

TEETH
analysis for trace elements, review on activation method for, 25:2135
radiosensitivity of incisor, of rats, x, 25:2592
sodium-22 transfer through dentine and enamel of, effects of chemicals on, 25:2532
TELLURIUM
determination of trace amounts of, using permanganate, colorimetric, 25:2073
determination of, properties of derivatives of 2-mercapto-Δ^2-1,3,4-thiadiazoline-5-thione for use in extraction--photometric, 25:2070
determination using monoethanolamine, polarographic, 25:2090
effects on determination of trace amounts of rhenium by thiocyanate--stannous chloride method, 25:2102
effects on uv spectrophotometric determination of gallium in aqueous solutions, 25:2100
neutron elastic scattering at 1 to 40 keV, analysis of angular distributions from, (E/T), 25:3695
production of pure, review of techniques for, 25:3219
separation from nitrate and sulfate solutions by solvent extraction using amines, 25:2319 (ORNL-4572, pp 181-95)
separation from sulfate solutions by solvent extraction using dialkyl phosphorodithioate or D2EHPA, 25:2321
TELLURIUM ISOTOPES Te-124
energy levels from antimony-124 decay, spin-parity assignments for, (E), 25:3657
nuclear charge radius from measurement of K-shell energy-level transitions, (E), 25:3551
TELLURIUM ISOTOPES Te-125
energy level at 321 keV, half-life of, (E), 25:3706
energy levels of, lifetimes and M1 and E2 transition probabilities for, (E), 25:3699
TELLURIUM ISOTOPES Te-126
nuclear charge radius from measurement of K-shell energy-level transitions, (E), 25:3551
TELLURIUM ISOTOPES Te-128
nuclear charge radius from measurement of K-shell energy-level transitions, (E), 25:3551
TELLURIUM ISOTOPES Te-129
beta decay of, in β-tellurium trioxide, nuclear γ resonance spectral studies on chemical states of iodine-129 from, 25:2304
TELLURIUM ISOTOPES Te-130
beta decay of, half-life for double, (E), 25:3693
nuclear charge radius from measurement of K-shell energy-level transitions, (E), 25:3551
proton inelastic scattering at 10 MeV, fits to angular distributions with configuration missing, (T), 25:3685
TELLURIUM ISOTOPES Te-135
half-life, (E), 25:3663
yield in thermal fission of uranium-235, (E), 25:3663
TELLURIUM OXIDES
tellurium-129 decay in β-, nuclear γ resonance spectra of chemical state of iodine-129 produced by, 25:2304
TEMPERATURE
effects on recovery of γ-irradiated spores of Clostridium, 25:2599
measurement between 1 and 30°K using chromic methylammonium alum and ammonium sulfates, 25:3960 (IS-T-399)
TERBIUM
complexes with cupferron, separation by solvent extraction using 2-methyl-1-propanol and 3-methyl-1-butanol, 25:2078
determination in yttrium oxide, scanning method for improving accuracy of luminescence, 25:2086
TERBIUM ALLOYS AND SYSTEMS
Ho--Tb, magnetic properties of monocrystalline, 25:2671 (ORNL-4570, pp 40-3)
Ho--Tb-base, magnetic anisotropy of, inelastic neutron scattering study of, 25:3208
TERBIUM IONS
effects on luminescence in yttrium and lutetium oxides, temperature influence on, (E), 25:3213
TERBIUM ISOTOPES Tb-152
beta and electron-capture decay of, gamma and conversion-electron spectra from, (E), 25:3681
TERBIUM ISOTOPES Tb-159
nuclear magnetic moment of, effects of spin--orbit and spin--spin forces on, (T), 25:3692
TERBIUM ISOTOPES Tb-160
beta decay of, gamma spectra from, (E/T), 25:3677
diffusion in copper at 700 to 1010°C, tracer studies of, 25:2680
TEREPHTHALIC ACID, POLYETHYLENE ESTERS
radioinduced graft polymerization with acrylamide or methacrylamide, effects of dicarboxylic acids on mechanism of, 25:2244
radioinduced graft polymerization with acrylic acid or methacrylic acid, effects of dose and temperature on mechanism of γ, 25:2240
radiolysis of, hydrogen yield and mechanism of γ, 25:2244
TERPHENYL
neutron attenuation by, monoenergetic-source fast-, (E/T), 25:3173
THALLIUM
corrosive effects on tantalum--tungsten alloys at 1000 to 1800°C, 25:2628
determination by potentiometric titration with sodium tetraphenylboron using Orion liquid ion exchange lead-selective electrode, 25:2104
determination in biological materials by 14-MeV neutron and thermal neutron activation, sensitivity of, 25:2125 (IAEA-122, pp 27-36)
effects on determination of trace amounts of antimony by isotopic exchange in organic phase, 25:2106
effects on uv spectrophotometric determination of gallium in aqueous solutions, 25:2100
production of pure, review of techniques for, 25:3219
radiation effects on potassium bromide crystals doped with, photoscintillations in x-, 25:3194
radioinduced luminescence of aqueous solutions of monovalent, electron pulse, 25:2233
radioinduced luminescence of aqueous solutions of monovalent, 25:2232
radioinduced luminescence of potassium bromide crystals doped with, flash x-, (E), 25:3193
radioinduced preparation from aqueous salt solutions, electron, 25:2237 (N-70-32826)
separation from nitrate and sulfate solutions by solvent extraction using amines, 25:2319 (ORNL-4572, pp 181-95)
superconducting condensation energy calculation, 25:3046
THALLIUM ALLOYS AND SYSTEMS
Bi--Cd--Tl, density at 124 to 440°C, 25:2692
Hg--Tl, Hall coefficients of liquid, comparison with fluctuation scattering model, 25:3209
THALLIUM ISOTOPES Tl-203
neutron reactions (n,2n) below (n,3n) threshold, cross-section calculations using Hauser--Feshback theory, (T), 25:3591 (AAEC/TM-542)
THALLIUM SULFATES
radioinduced luminescence of aqueous solutions of, effects of pH on electron pulse, 25:2233
THERMAL CONDUCTIVITY CELLS
calibration of, interlaboratory, 25:2788 (ORNL-4570, pp 27-30)
design for graphite measurements, 25:2609 (ORNL-4570, pp 175-90)
THERMIONIC CONVERTERS
plasma transport theory for, 25:2934
THERMOLUMINESCENCE
measurements for age estimation of pottery, refinement of quartz inclusion method for, 25:2355
THERMOMETRY
development of instruments for ultrasonic, for LMFBR, 25:2503 (NYO-3906-4)
development of ultrasonic, for LMFBR systems, 25:2600 (BNL-50258)
THERMONUCLEAR REACTORS
bibliography on design of, 25:3139 (ORO-1171-1, pp 425-39)
design for space uses, 25:3138 (ORO-1171-1, pp 387-411)
design of, 25:3137 (ORO-1171-1, pp 376-86)
design of fusion plant--torch complex, 25:3136 (ORO-1171-1, pp 344-75)
design of, bibliography on, 25:3139 (ORO-1171-1, pp 425-39)
design of, conference on, 25:3130 (ORO-1171-1)
energy conversion system for, design of thermal, 25:3133 (ORO-1171-1, pp 141-66)
hydromagnetic wave absorption in Levitron-type, (E/T), 25:3148 (CEA-CONF-1614)
operational fundamentals for toroidal, 25:3132 (ORO-1171-1, pp 38-77)
plasma confinement in toroidal octupoles, effects of time-varying fields on, (E/t), 25:3059
plasma flow velocities in cusped magnetic fields, (T), 25:3091
use for power generation, future prospects for, 25:3134 (ORO-1171-1, pp 256-331)
wall erosion by sputtering in, 25:3135 (ORO-1171-1, pp 334-42)
Δ^2-1,3,4-THIADIAZOLINE-5-THIONE, 2-MERCAPTO-
properties for use in analytical chemistry, 25:2070
properties of derivatives of, for use in extraction--photometric determination of bismuth and tellurium, 25:2070
Δ^2-1,3,4-THIADIAZOLINE-5-THIONE, 2-MERCAPTO-4-PHENYL-
properties for use in analytical chemistry, 25:2070
THICKNESS GAGES
circuit for radiometric, for automatic absorption curve matching, 25:2499(P)
design of non-contact, for soft materials, 25:3966 (MHSMP-15)
THIOCYANATES
complexes with uranyl ions in water and methanol--water media, spectrophotometric studies on, 25:2215
THIOPHENE
effects on γ-radioinduced graft polymerization of cellulose with styrene in methanol solutions, 25:2247
THORIUM
complexes with 8-quinolinol and derivatives, structure of adduct from, 25:2157
contamination of natural waters, role of aquatic plants in, 25:2547
corrosion by sodium at 425°C, 25:2644 (ORNL-4570, pp 157-60)
determination in silicate rocks using cupferron,

spectrographic, 25:2078
effects on determination of trace amounts of antimony by isotopic exchange in organic phase, 25:2106
effects on photometric determination of hafnium and zirconium in geological specimens, 25:2084
effects on polarographic determination of tellurium, 25:2090
effects on uv spectrophotometric determination of gallium in aqueous solutions, 25:2100
neutron elastic scattering at 1 to 40 keV, analysis of angular distributions from, (E/T), 25:3695
photon reactions at 30 to 100 keV with, photoelectric cross sections for, 25:2907
reactions with platinum, 25:2160
separation from actinium and/or thorium and radioactive decay products by halogenation and sublimation, 25:2322(P)
separation from aqueous solutions by solvent extraction using amines and TBP, effects of salting-out agents on, 25:2335
separation from aqueous solutions by solvent extraction using trialkylamines, coalescence of organic solutions in, 25:2308 (CEA-R-3845)
separation from MSBR fuels, 25:2313 (ORNL-4572, pp 1-36)
separation from nitrate and sulfate solutions by solvent extraction using amines, 25:2319 (ORNL-4572, pp 181-95)
separation from solutions by ion exchange, review on, 25:2330
separation from thorium-234 by sorption on iodates and periodates, 25:2341
separation of cerium, gadolinium, lanthanum, and neodymium from, by precipitation using cupferron, 25:2078

THORIUM ALLOYS AND SYSTEMS
Bi--N--Th, crystal structure of Th_2N_2Bi formed in, 25:2248
N--Sb--Th, crystal structure of Th_2N_2Sb formed in, 25:2248
Th-base--U, corrosion by sodium at 425°C, 25:2644 (ORNL-4570, pp 157-60)
Th-base--U, fabrication of fuel elements of, method for, 25:2644 (ORNL-4570, pp 157-60)

THORIUM CARBIDES
properties of, compilation of data on chemical, mechanical, and physical, 25:2791 (ORNL-4570, pp 195-200)
ThC--UC, analysis of silicon carbide-coated fuels particles of, for total carbon, gravimetric, 25:2064 (DP-Report-494)

THORIUM FLUORIDES ThF_4
entnalpy of formation of, 25:2213
BeF_2--LiF--ThF_4--UF_4--ZrF, corrosive effects on Hastelloy N, stainless steel, and steel for MSRE, 25:2609 (ORNL-4570, pp 175-90)

THORIUM ISOTOPES Th-230
triton reactions (t,pf) at 18 MeV, fission probabilities for, (E), 25:3679

THORIUM ISOTOPES Th-231
neutron fission cross sections from thorium-230 (t,pf) reactions at 18 MeV, (E), 25:3679

THORIUM ISOTOPES Th-232
boron-11 reactions with, yields of light neutron-rich nuclei in, (E), 25:3648 (JINR-E7-5319)
neon-22 reactions with, yields of light neutron-rich nuclei in, (E), 25:3648 (JINR-E7-5319)
neutron fission at 0.95 to 2.3 MeV, channel analysis of angular distributions of fragments and cross sections for, (E), 25:3680
neutron reactions (n,2n) below (n,3n) threshold, cross-section calculations using Hauser--Feshback theory, (T), 25:3591 (AAEC/TM-542)
nitrogen-15 reactions with, yields of light neutron-rich nuclei in, (E), 25:3648 (JINR-E7-5319)
oxygen-18 reactions with, yields of light neutron-rich nuclei in, (E), 25:3648 (JINR-E7-5319)
triton reactions (t,pf) at 18 MeV, fission probabilities for, (E), 25:3679

THORIUM ISOTOPES Th-233
neutron fission cross sections from thorium-232 (t,pf) reactions at 18 MeV, (E), 25:3679

THORIUM ISOTOPES Th-234
separation from iron, uranium, and inactive thorium by sorption on iodates and periodates, 25:2341

THORIUM NITRATES
separation from aqueous solutions by solvent extraction using amines and TBP, effects of salting-out agents on, 25:2335

THORIUM NITRIDE TELLURIDES
crystal structure of Th_2N_2Te formed in, 25:2248

THORIUM NITRIDES
properties of, compilation of data on chemical, mechanical, and physical, 25:2791 (ORNL-4570, pp 195-200)
properties of, thermal and thermoelectric, 25:2788 (ORNL-4570, pp 27-30)

THORIUM OXIDES
sorptive properties of sols of, for carbon dioxide, 25:2775 (ORNL-4572, pp 242-50)

THORIUM OXIDES ThO_2
chemical potential profiles of oxygen in pure and yttria-doped electrolytes of, steady-state, 25:2203
density of sintered compacts of, effects of heating at 1400 to 1800°C on, 25:2787 (ORNL-4570, pp 24-6)
effects on man following use for diagnosis, latent, 25:2583
microstructure of crystalline, electron microscopic study of, 25:2748
preparation of crystals of, method for, 25:2727 (ORNL-4570, pp 1-4)
preparation of curium oxide- and thulium oxide-doped monocrystalline, 25:2727 (ORNL-4570, pp 1-4)
preparation of plutonium dioxide-doped monocrystalline, incorporating plutonium-239, 25:2727 (ORNL-4570, pp 1-4)
properties of, compilation of data on chemical, mechanical, and physical, 25:2791 (ORNL-4570, pp 195-200)
spectra of water bound to surfaces of, ir, 25:2207
Cr--ThO_2, mechanical properties of low-porosity corrosion-resistant cermets of, 25:2796
ThO_2--UO_2, preparation of microspheres of, alcohol recycle and drying techniques for, 25:2773 (ORNL-4572, pp 135-48)
ThO_2--UO_2, preparation of microspheres of, by sol-gel process, 25:2320(R) (ORNL-TM-3204)
ThO_2--UO_2, preparation of microspheres of, nonfluidized-bed columns for, 25:2773 (ORNL-4572, pp 135-48)
ThO_2--UO_2--W, preparation of eutectics of, method for, 25:2727 (ORNL-4570, pp 1-4)
ThO_2--W-base, internal friction at 300 to 3000°K, 25:2687

THORIUM SILICATES
preparation of high-purity and rare earth-doped monocrystalline, 25:2727 (ORNL-4570, pp 1-4)

THULIUM CARBIDES
preparation of monocrystals of, 25:2803(R) (COO-716-66)
structure of monocrystals of, 25:2803(R) (COO-716-66)

THULIUM ISOTOPES Tm-168
electron-capture decay of, gamma spectra from, (E/T), 25:3677

THULIUM ISOTOPES Tm-169
beta decay of, hindrance factors for unique first-forbidden, (E), 25:3672

THULIUM ISOTOPES Tm-170
diffusion in copper at 700 to 1010°C, tracer studies of, 25:2680

THULIUM ISOTOPES Tm-171
energy levels at 636, 676, 738, and 913 keV from erbium-171 decay, (E), 25:3659

THYMIDINE MONOPHOSPHATES
radiolysis of aqueous chloride solutions of, rate constants for electron pulse and γ, 25:2259 (GA-10208)

THYMINE
radiolysis of aqueous chloride solutions of, rate constants for electron pulse and γ, 25:2259 (GA-10208)
radiolysis of aqueous solutions of, spectral studies on mechanism of electron pulse, 25:2259 (GA-10208)

THYMUS GLAND
effects on x-radioinduced inhibition of urethan adenomagenesis in lungs of mice, 25:2589

THYROID GLAND
function in lactating cattle, morphological and clinico-chemical studies of, 25:2524
scanning of, use of radioisotopes and scintillation camera in γ, 25:2581
scanning using metastable technetium-99, 25:2580

TIMING CIRCUITS
design of fast constant fraction trigger, for photomultiplier tubes, 25:2458

TIN
density at 232 to 438°C, 25:2692
determination following nonsulfide separation from elements, qualitative, 25:2101
determination in titanium alloys, x-ray fluorescence method for, 25:2097
determination of trace amounts of, in nuclear-grade uranium oxide (U_3O_8) by direct reading spectrometric method, 25:2068 (NLCO-1071)
effects on uv spectrophotometric determination of gallium in aqueous solutions, 25:2100
electron backscattering at 1 MeV, angular distribution and energy spectra for, 25:2886
gamma scattering by electrons in, incoherent cross sections for 30-keV to 2.62 MeV, (T), 25:2921
neutron elastic scattering at 1 to 40 keV, analysis of angular distributions from, (E/T), 25:3695
photon elastic scattering at 1.33 MeV, cross section for, (E), 25:3655
radioinduced preparation from aqueous salt solutions, electron, 25:2237 (N-70-32826)
separation from nitrate and sulfate solutions by solvent extraction using amines, 25:2319 (ORNL-4572, pp 181-95)
superconducting condensation energy calculation, 25:3046
superconducting critical temperature in thin films of, (E/T), 25:3026

TIN ALLOYS AND SYSTEMS
Al--Mo--Sn--Zr-base, corrosion by sodium at 450°C, effects of oxygen on, 25:2611 (PEL-201)
Cd--In--Sn, electron band structure of alpha-, effects of conduction electron/atom ratio on, 25:3205 (UCRL-

XUM

19681)
Cu--Sn, deformation behavior of polycrystalline, 25:2690
Cu-base--Sn, photon reactions at 100 to 662 keV with bell metal, effective atomic numbers for photoelectric, scattering, and total interaction processes in, 25:2906
In--Sn, density at 122 to 440°C, 25:2692
TIN ISOTOPES Sn-113
decay of, production of indium-113m by, 25:2296
electron-capture decay of, gamma spectra from, (E), 25:3694
TIN ISOTOPES Sn-116
energy levels from proton inelastic scattering, (E), 25:3668
proton elastic and inelastic scattering at 24.5 MeV, angular distributions for, (E), 25:3668
spectra of, isotope shifts in muonic x-ray, (E), 25:3620
TIN ISOTOPES Sn-117
spectra of, isotope shifts in muonic x-ray, (E), 25:3620
TIN ISOTOPES Sn-118
energy levels from proton inelastic scattering, (E), 25:3668
proton elastic and inelastic scattering at 24.5 MeV, angular distributions for, (E), 25:3668
spectra of, isotope shifts in muonic x-ray, (E), 25:3620
TIN ISOTOPES Sn-119
spectra of, isotope shifts in muonic x-ray, (E), 25:3620
TIN ISOTOPES Sn-120
energy levels from proton inelastic scattering, (E), 25:3668
proton elastic and inelastic scattering at 24.5 MeV, angular distributions for, (E), 25:3668
proton elastic scattering at 30.3 MeV, angular distributions, polarizations, and optical-model analysis of, (E), 25:3636
spectra of, isotope shifts in muonic x-ray, (E), 25:3620
TIN ISOTOPES Sn-122
energy levels from proton inelastic scattering, (E), 25:3668
proton elastic and inelastic scattering at 24.5 MeV, angular distributions for, (E), 25:3668
spectra of, isotope shifts in muonic x-ray, (E), 25:3620
TIN ISOTOPES Sn-124
energy levels from proton inelastic scattering, (E), 25:3668
proton elastic and inelastic scattering at 24.5 MeV, angular distributions for, (E), 25:3668
spectra of, isotope shifts in muonic x-ray, (E), 25:3620
TISSUES
analysis for trace elements by neutron activation, 25:2124 (IAEA-122, pp 15-26)
analysis of human, evaluation of sensitivity of thermal neutron activation, 25:2123 (IAEA-122, pp 1-13)
cobalt-60 uptake by, of freshwater fish in relation to contamination of human food chain, 25:2526
neutron reactions with, calculation of energy deposited by heavy recoil particles in 15.09 MeV, 25:2568
sodium-22 transfer through dentine and enamel of dental, effects of chemicals on, 25:2532
TITANIUM
abundance in Kappa Cancri, (E), 25:2840
analysis for trace amounts of carbon, conductometric method for, 25:2071
corrosion resistance to lithium at 600 and 900°F, 25:2626
determination by amperometric titration using N-o-tolylbenzohydroxamic acid, 25:2082
determination in biological materials by 14-MeV neutron and thermal neutron activation, sensitivity of, 25:2125 (IAEA-122, pp 27-36)
determination in hydrothermally altered rocks from Tateyama Jigokudani Hot Springs, Toyama, Japan, colorimetric, 25:2098
determination in pigments from ancient murals by neutron activation, 25:2133
determination in uranium alloys by atomic absorption spectrophotometry, 25:2065 (LA-4529)
determination of trace amounts of, in nuclear-grade uranium oxide (U_3O_8) by direct reading spectrometric method, 25:2068 (NLCO-1071)
diffusion of carbon in, electronic mechanisms in thermal, 25:2666 (NP-18468)
effects on extraction--photometric determination of niobium in steel, 25:2085
effects on high-temperature deformation and fracture behavior of Hastelloy N and nickel, 25:2725
effects on photometric determination of hafnium and zirconium in geological specimens, 25:2084
effects on uv spectrophotometric determination of gallium in aqueous solutions, 25:2100
electron reactions at 1 to 3 MeV with, backscatter and transmission coefficients for, (E), 25:2883 (N-70-25499)
neutron capture by, gamma spectra from thermal, (E), 25:3181
solubility in potassium at 1012 to 1341°K, 25:2714
spectral lines in solar-disc flares effect on geophysical activity of solar flares, (E/T), 25:2859
TITANIUM ALLOYS AND SYSTEMS
analysis of, x-ray fluorescence method for, 25:2097
mechanical properties of, effects of beta forging on, 25:2717
Al--Cr--Fe--Ti-base, microstructure of hot-rolled plates and sheets of α + β, relations of mechanical properties with abnormal, 25:2752
Al--Mo--Ti-base--V, microstructure of hot-rolled plates and sheets of α + β, relations of mechanical properties with abnormal, 25:2752
Al--Ti-base--V, corrosion by aqueous dinitrogen tetroxide, stress, 25:2635
Al--Ti-base--V, electron reactions at 1 to 3 MeV with, backscatter and transmission coefficients for, (E), 25:2883 (N-70-25499)
Al--Ti-base--V, microstructure of hot-rolled plates and sheets of α + β, relations of mechanical properties with abnormal, 25:2752
Cr--Mo--Ti-base, corrosion resistance of, potentiometric method for studies of effects of chromium on, 25:2613
Cr--Ti-base, corrosion resistance of, potentiometric studies of, 25:2613
Fe-base--Ti, diffusion in bcc phases of, radioisotope tracer measurements of volume, 25:2691
Ge--Ti--V-base, creep to 850°C, 25:2662 (KFK-1193)
Mn--Ti-base, microstructure of hot-rolled plates and sheets of α + β, relations of mechanical properties with abnormal, 25:2752
Mo--Ti-base, corrosion resistance of, potentiometric studies of, 25:2613
Nb--Si--Ti--V-base, creep to 850°C, 25:2662 (KFK-1193)
Nb--Ti, superconducting magnetic properties of, 25:3027
Nb-base--Ti, lower critical fields of superconducting, (E/T), 25:3020 (ORNL-TM-3206)
Ni-base--Ti, carburization of, relations with hardness, 25:2716
Pu-base--Ti, stability of β phase in, effects of heat treatments on, 25:2739
Rh--Ti-base, superconductivity of ternary β-titanium, 25:3021(T) (UCRL-Trans-1409)
Si--Ti--V-base, creep to 850°C, 25:2662 (KFK-1193)
Ti--V-base, corrosion by sodium at 600°C, effects of titanium content on, 25:2606 (ORNL-4570, pp 92-5)
Ti--V-base, corrosion by sodium in Type 316 stainless steel loop system at 675 to 800°C, 25:2621
Ti--V-base, creep to 850°C, 25:2662 (KFK-1193)
Ti--V-base, mechanical properties of, at 25 and 800°C, effects of interstitial absorption on, 25:2621
Ti-base--V, phase studies of, 25:2735
TITANIUM CARBIDES
analysis for carbon by x-ray microprobe method, 25:2095
TITANIUM CARBONITRIDES
effects of coating of, on corrosion resistance and mechanical properties of steel, 25:2612
TITANIUM CHLORIDES
$AlCl_3$--$TiCl_3$, phase studies of, 25:2805 (ORNL-4570, pp 31-4)
TITANIUM HYDRIDES
neutron inelastic scattering by single phonons of hydrogen in TiH_2 0.05 to 0.2 eV, cross sections for, (E), 25:3536
TITANIUM ISOTOPES Ti-42
beta decay of, branching ratios, γ spectra, and half-life for, (E), 25:3640
TITANIUM ISOTOPES Ti-46
energy levels of, binding energies and orbital spin assignments of proton-hole, (E), 25:3616
TITANIUM ISOTOPES Ti-48
alpha reactions (α,nγ) and (α,pγ) at 12 to 15 MeV, γ singles and n-γ coincidence spectra from, (E), 25:3593 (COO-1530-21)
TITANIUM ISOTOPES Ti-51
energy levels of, calculation using intermediate coupling model, (T), 25:3592 (COO-1120-106)
TITANIUM OXIDES
diffusion in, titanium-44 tracer study of cation self-, 25:2786 (ORNL-4570, pp 13-15)
performance as stainless steel welding electrode coating, 25:2642 (ORNL-4570, pp 88-91)
proton reactions at 350 keV with, characteristic x-ray spectra from, (E), 25:2882 (CONF-700322-, pp 113-24)
TOKAMAK DEVICES
plasma evolution in, space--time, (T), 25:3052 (CEA-CONF-1595)
synchrotron radiations from, (T), 25:3095
TOLUENE
effects on radioinduced isomerization of norbornadiene, 25:2239
TOPAZ
fission tracks in Nigerian, morphology of, 25:2351
TRACE ELEMENTS
determination in biological materials by neutron activation, 25:2126 (IAEA-122, pp 37-40)
determination in biological materials, sensitivities of fast and thermal activation methods for, 25:2125 (IAEA-122, pp 27-36)
TRACER TECHNIQUES
conference on industrial uses of, Poznan, Poland, November 1968, 25:2141
development for distillation and rectification studies, 25:2343
development for measurement of blood platelet life span in animals and man, 25:2579
equipment and facilities for radioisotope, design of, 25:2390

method for comparison of penetration plots using alpha emitters, 25:2786 (ORNL-4570, pp 13-15)
use of radioisotope, in hydrology, review of, 25:2359
uses of radioisotope, in hydrology, review of principles of, 25:2360
TRANSACTINIDE ELEMENTS
search for superheavy, in nature, 25:3652 (UCRL-19957)
TRANSFORMERS
design and testing of superconducting current step-up, 25:3509
TRANSISTORS
radiation damage to silicon, hybrid recombination model for neutron, 25:2514 (SC-R-70-4351)
radiation effects on, simulation of transient, 25:3477 (LYCEN-7063)
TRANSITION METAL CARBIDES
preparation of microspheres of, method for, 25:2795(P)
TRANSITION METAL OXIDES
preparation of microspheres of, method for, 25:2795(P)
TRANSITION METALS
effects on hardness of β-rhombohedral boron, 25:2801
TRANSPLANTS
use of technique of intraocular, to study behavior of irradiated bone marrow in rats, 25:2595
TRANSPORT THEORY
radiative, solution for nonstationary field, (T), 25:2829
TRANSURANIUM ELEMENTS
production of, operation of HFIR facility for, 25:2792 (ORNL-4570, pp 201-4)
separation by displacement elution from ion exchange resins, 25:2319 (ORNL-4572, pp 181-95)
shipping of solid, with associated fission products, design and testing of container for, 25:2421 (ORNL-TM-3110)
TRANSURANIUM PROCESSING PLANT
radioisotope production in, 25:2294 (ORNL-4572, pp 109-34)
TRIALKYLAMINES
solvent properties for acids and metals, effects of coalescence of organic solutions on, 25:2308 (CEA-R-3645)
s-TRIAZINE, HEXAHYDRO-1,3,5-TRINITRO-
decomposition time under effect of shock waves, 25:3964(T) (LA-4360-TR)
TRIMETHYLAMINE
x-ray diffraction by hydrated liquid, at 5°C, 25:2730 (ORNL-4570, pp 44-6)
s-TRIOXANE
radioinduced polymerization of crystals of, production of polyoxymethylene crystals from α, 25:2252
TRIOXANES
radioinduced polymerization of, effects of impurities on γ, 25:2253
TRITIUM
content in worldwide atmospheric precipitation, 1964 to 1966, data tabulations on, 25:2367 (STI/DOC-10/117)
detection in radioecology studies, evaluation of liquid scintillation spectrometer for, 25:2565
effects on partitioning of benzhydryl benzoate ion pairs, 25:2186
effects on solvolysis of benzhydryl benzoate, 25:2185
exchange between alkenes and lithium cyclohexylamide in cyclohexylamine at 50°C, kinetics of, 25:2184
separation from spent LMFBR fuels, 25:2314 (ORNL-4572, pp 37-84)
use as tracer for determining protein synthesis in tobacco mosaic virus, 25:2551(R) (COO-873-28)
use as tracer for determining uptake of chromosomes by mammalian cells in vitro, 25:2515
use for human body fluid determination, method for, 25:2518
TRITONS
reactions (t,pf) with plutonium-240, -242, thorium-230, 232, and uranium-234, -236, and -238 at 18 MeV, cross sections and fission probabilities for, (E), 25:3679
scattering elastically by A = 24 to 116 nuclei, analysis using optical potential, (T), 25:3769
TROJAN POWER REACTOR, UNIT 1
effluents from, effects on environment of chemical, radioactive, and thermal, 25:3843 (DOCKET-50344-18)
TRYPTAMINE
deuterium effects on fluorescence yields and lifetimes of, 25:2536
TRYPTOPHAN
deuterium effects on fluorescence yields and lifetimes of, 25:2536
TUNGSTEN
coating with boron and boron carbide at 1300°C, vapor deposition method for, 25:2777
corrosion resistance to lithium at 600 and 900°F, 25:2626
creep at 1500 to 2000°C, effects of oxygen on, 25:2673 (ORNL-4570, pp 118-23)
creep rupture of arc-melted and chemical vapor deposited, stress--strain curves for, 25:2673 (ORNL-4570, pp 118-23)
crystallization of sheets of, effects of gas bubbles on, 25:2736
determination in uranium alloys by atomic absorption spectrophotometry, 25:2065 (LA-4529)
diffusion in niobium, tracer studies of, 25:2703
diffusion in, tungsten-185 tracer studies of mechanisms of self-, 25:2703
diffusion of niobium and tantalum in, activation energy for, 25:2605 (ORNL-4570, pp 37-9)
effects on brazing of silicon oxide with copper--silver alloy using composite film method, 25:2652
effects on determination of trace amounts of rhenium by thiocyanate--stannous chloride method, 25:2102
effects on extraction--photometric determination of niobium in steel, 25:2085
effects on polarographic determination of tellurium, 25:2090
effects on uv spectrophotometric determination of gallium in aqueous solutions, 25:2100
electric conductivity at 100 to 1700°C, (E), 25:2715
emissivity at 100 to 1700°C, total, (E), 25:2715
internal friction of recrystallized and worked, at 300 to 3000°K, effects of alloying additions and impurities on, 25:2687
mechanical properties of powder metallurgy-produced tubes of, 25:2673 (ORNL-4570, pp 118-23)
microstructure of wires of, electron microscopic study of, 25:2748
neutron cross sections for, 25-group, (T), 25:3530 (LA-4484)
neutron scattering by, exponential angular coefficients for fast, (E), 25:3171
production by hexafluoride reduction and vapor deposition, 25:2673 (ORNL-4570, pp 118-23)
properties for use as protective coating on MSBR core materials, 25:2609 (ORNL-4570, pp 175-90)
separation from nitrate and sulfate solutions by solvent extraction using amines, 25:2319 (ORNL-4572, pp 181-95)
separation from radioactive fallout, method for, 25:2110
solubility in potassium at 1012 to 1341°K, 25:2714
sorptive properties of surfaces of, for water vapor, 25:2722
thermal capacity at 2600 to 4500°K, 25:2726
thermal conductivity at 100 to 1700°C, (E), 25:2715
TUNGSTEN ALLOYS AND SYSTEMS
joining methods for, development of, 25:2673 (ORNL-4570, pp 118-23)
Co--W, properties of electrodeposited, effects of electrolyte composition and conditions on corrosion resistant and magnetic, 25:2649
Fe--W, analysis for trace amounts of carbon, conductometric method for, 25:2071
Mo--W-base, creep rupture of arc-melted, stress--strain curves for, 25:2673 (ORNL-4570, pp 118-23)
Ni-base--W, carburization of, relations with hardness, 25:2716
Re--W, properties for use in reactor components, review of, 25:2647
Re--W-base, creep rupture of arc-melted and chemical vapor deposited, stress--strain curves for, 25:2673 (ORNL-4570, pp 118-23)
Re--W-base, internal friction of doped, at 300 to 3000°K, 25:2687
Re--W-base, production by hexafluoride reduction and vapor deposition, 25:2673 (ORNL-4570, pp 118-23)
Re--W-base, properties for use in curium-244 oxide fuel capsules, 25:2643 (ORNL-4570, pp 106-11)
Ta-base--W, bonding to platinum, development of methods for, 25:2672 (ORNL-4570, pp 112-15)
Ta-base--W, compatibility with copper at 1100°C, 25:2720
Ta-base--W, corrosion by barium, calcium, indium, lead, and thallium at 1000 to 1800°C, 25:2628
Ta-base--W, elastic properties of monocrystalline, at 80 to 1400°K, 25:2721
ThO_2--UO_2--W, preparation of eutectics of, method for, 25:2727 (ORNL-4570, pp 1-4)
ThO_2--W-base, internal friction at 300 to 3000°K, 25:2687
UO_2--W, microstructure of composites of, incorporating tungsten fibers, 25:2727 (ORNL-4570, pp 1-4)
UO_2--W, preparation of eutectics of, method for, 25:2727 (ORNL-4570, pp 1-4)
TUNGSTEN ISOTOPES W-181
determination in rainwater in Niigata, Japan by γ counting, 25:2110
TUNGSTEN ISOTOPES W-182
spectra of muonic, dynamic hyperfine structure in x-ray, (E), 25:3661
TUNGSTEN ISOTOPES W-184
spectra of muonic, dynamic hyperfine structure in x-ray, (E), 25:3661
TUNGSTEN ISOTOPES W-185
beta decay of, hindrance factors for unique first-forbidden, (E), 25:3672
determination in rainwater in Niigata, Japan by γ counting, 25:2110
TUNGSTEN ISOTOPES W-186
spectra of muonic, dynamic hyperfine structure in x-ray, (E), 25:3661
TURBINES
design problems wet steam, for power reactors, 25:3900
radiation induced activation hazards for boiling power reactor, 25:3894
TURKEY POINT POWER REACTOR, UNIT 3
design parameters of, revised and additional data on,

XUM

25:3822 (DOCKET-50250-35)
operations aspects of, revised and additional data on, 25:3822 (DOCKET-50250-35)
TURKEY POINT POWER REACTOR, UNIT 4
design parameters of, revised and additional data on, 25:3822 (DOCKET-50250-35)
operations aspects of, revised and additional data on, 25:3822 (DOCKET-50250-35)
TZC (MOLYBDENUM ALLOY)
preparation of high-temperature strength, room-temperature hydrostatic extrusion method for, 25:2651
TZM (MOLYBDENUM ALLOY)
corrosion by indium at 1000 to 1800°C, 25:2628
mechanical properties of, effects of fabrication variables on, 25:2672 (ORNL-4570, pp 112-15)
properties for use in curium-244 oxide fuel capsules, 25:2643 (ORNL-4570, pp 106-11)

U

ULTRASONIC TESTING
methods for LMFBR materials, development of, 25:2408 (ORNL-4570, pp 96-7)
methods for reactor materials, development of, 25:2409 (ORNL-4570, pp 149-51)
ULTRASOUND
absorption by intermediate-state superconductor, (T), 25:3028
effects on electrophoretic mobility of Ehrlich ascites tumor cells, 25:2586
ULTRAVIOLET RADIATION
effects on cell cultures infected with murine sarcoma virus, effects of cell phase on, 25:2587
effects on DNA in human xeroderma pigmentosum cells, repair synthesis following, 25:2567
effects on DNA of human xeroderma pigmentosum cells, repair synthesis following, 25:2535
effects on Escherichia coli in relation to nutrition requirements, action spectra for mutagenic, 25:2557
effects on photosensitive defective mutant of Neurospora crassa, 25:2556
effects on progression of cultured Chinese hamster ovary cells from G_2 into metaphase, 25:2558
effects on respiration in Escherichia coli, effects of chloramphenical, 5-fluorouracil, and T_4 phage mutants on inhibitory, 25:2598
UNIVERSE
expansion of, completely polarized neutrino flux effects on space geometry during, (T), 25:3343
models of Lemaitre, background radiation anomalies in, (T), 25:2669(T) (CSIRO-Trans-10207)
URACIL
radiolysis of aqueous chloride solutions of, rate constants for electron pulse and γ, 25:2259 (GA-10208)
URACIL, 5-FLUORO-
effects on uv-radioinduced inhibition of respiration in Escherichia coli, 25:2598
URANIUM
abundance relative to plutonium in reprocessing plant solutions, mathematical evaluation of, 25:2417 (BNWL-SA-3287)
analysis by carrier distillation method, automated quantometer data handling system for, 25:2069 (Y-1740)
analysis for trace amounts of carbon, conductometric method for, 25:2071
analysis of fuels of, for impurities, spectroscopic, 25:2074
complexes of hexavalent, with citric, malic, or tartaric acids and trivalent indium, potentiometric, solvent extraction, and spectrophotometric studies on, 25:2206
complexes with 6-methylpicolinic acid, nicotinic acid, picolinic acid, and picolinic acid 1-oxide, ir and NMR spectral and thermogravimetric studies on, 25:2194 (KFK-1070)
complexes with cupferron, separation by solvent extraction using 2-methyl-1-propanol and 3-methyl-1-butanol, 25:2078
contamination of natural waters, role of aquatic plants in, 25:2547
determination alone and in presence of cerium, iron, manganese, and vanadium using permanganate, potentiometric, 25:2099
determination following solvent extraction using benzene, 8-quinolinol, and Rhodamine 6G, photometric, 25:2087
determination in ores by TBP extraction and spectrophotometry, 25:2067 (NIM-906)
determination in solution using x-ray fluorescence spectrometer with computer, 25:2105
determination relative to plutonium in oxide fuels by x-ray fluorescence, in-line, 25:2306(R) (ANL-7735)
determination using 6-methylpyridine-2-aldoxime and pyridine-2-aldoxime, gravimetric, 25:2072
determination using EDTA, complexometric, 25:2088
effects on determination of trace amounts of antimony by isotopic exchange in organic phase, 25:2106
effects on determination of trace amounts of rhenium by thiocyanate--stannous chloride method, 25:2102
effects on uv spectrophotometric determination of gallium in aqueous solutions, 25:2100
enrichment by gaseous diffusion and ultracentrifugation, industrial prospects in France for, 25:2402
gamma scattering by electrons in, incoherent cross sections for 30-keV to 2.62 MeV, (T), 25:2921
metallurgy of fuels of, 25:2074
oxidation by oxygen in sodium at 500 to 650°C, effects of oxygen concentration and mass transfer on, 25:2694
preparation by magnesium reduction of uranium tetrafluoride at 2400°F and 75 psig, 25:2640 (NLCO-1058)
preparation of thin targets of, by centrifuging powder suspended in liquid paraffin, 25:2655
properties of fuels of, 25:2074
radioinduced swelling of, in-pile, 25:2762
separation from aqueous solutions by solvent extraction using amines and TBP, effects of salting-out agents on, 25:2335
separation from aqueous solutions by solvent extraction using trialkylamines, coalescence of organic solutions in, 25:2308 (CEA-R-3845)
separation from dilute uranium ore leach solutions by ionic flotation, 25:2331
separation from MSBR fuel, frozen-wall fluorinator for, 25:2313 (ORNL-4572, pp 1-36)
separation from ore pulps and solutions by ion exchange, review on, 25:2330
separation from seawater, economics and feasibility of methods for, 25:2323
separation from seawater, precipitation method for, 25:2325
separation from thorium-234 by sorption on iodates and periodates, 25:2341
separation from wet-process phosphoric acid by solvent extraction using DEHPA and TOPO, 25:2319 (ORNL-4572, pp 181-95)
separation of cerium, gadolinium, lanthanum, and neodymium from, by precipitation using cupferron, 25:2078
slip dislocation propagation through twins in alpha-, calculation of forces on, 25:2696
stress relaxation in tempered and deformed, effects of bending on, 25:2699
URANIUM ALLOYS AND SYSTEMS
analysis for hafnium, molybdenum, niobium, tantalum, titanium, tungsten, and zirconium by atomic absorption spectrophotometry, 25:2065 (LA-4529)
Al--U, analysis for hafnium, spectrographic, 25:2063 (CNEA-276)
Al-base--U, void content of fuel of UAl dispersions in Al matrix, effects of cladding, cold-rolling, and composition on, 25:2806 (ORNL-4611)
Bi--N--U, crystal structure of U_2N_2Bi formed in, 25:2248
C--U, phase studies of, using computers, 25:2737
Cr--N--U, phase studies at 1600°C, 25:2769 (ORNL-4570, pp 62-7)
Cr--U-base, phase transformation in, kinetics of α--β, 25:2741
Mn--U, phase studies of, using computers, 25:2737
Mo--U-base, development and testing for Army Pulsed Radiation Facility Reactor fuel, 25:2645 (ORNL-4570, pp 214)
Mo--U-base, precipitation in, effects of cooling rate on continuous and discontinuous, 25:2738
N--Sb--U, crystal structure of U_2N_2Sb formed in, 25:2248
Nb--U-base, niobium segregation in, effects of casting, heat treatments, and melting on, 25:2732 (RFP-1582)
Nb--U-base, oxidation at 800°C, mechanisms and stresses in, 25:2605 (ORNL-4570, pp 37-9)
Nb--U-base--Zr, crystal structure of, effects of aging on, 25:2730 (ORNL-4570, pp 44-6)
Nb--U-base--Zr, oxidation at 800°C, mechanisms and stresses in, 25:2605 (ORNL-4570, pp 37-9)
Pt--U, electric conductivity of ferromagnetic UPt, temperature dependence of, 25:3215
Th-base--U, corrosion by sodium at 425°C, 25:2644 (ORNL-4570, pp 157-60)
Th-base--U, fabrication of fuel elements of, method for, 25:2644 (ORNL-4570, pp 157-60)
U--V, phase studies of, using computers, 25:2737
U--Zr, diffusion in, thermodynamics of bond changes in self-, 25:2701
URANIUM ARSENIDES
structure of, calculation of electronic band, 25:2729 (ORNL-4570, pp 20-2)
URANIUM BROMIDES UBr_5
complexes with N,N-dimethylacetamide in acetone, spectra of, 25:2200
preparation, properties, and structure of, 25:2200
URANIUM CARBIDES
analysis of silicon carbide-coated fuel particles of, for total carbon, gravimetric, 25:2064 (DP-Report-494)
elastic properties of, 25:2798
mechanical properties of, at 25 to 1300°C, effects of porosity on, 25:2794(T) (ORNL-tr-2388)
mechanical properties of, review of, 25:2785 (LA-4452)
preparation of beryllium carbide-coated fuels of, method for, 25:2776(P)
radiation effects on pyrocarbon-coated fuel particles of, pile neutron, 25:2812 (DP-Report-320)
reactions with chromium--iron--nickel alloy at 900°C, effects of carbon content and metal stabilizers on, 25:2765 (KFK-1213)
structure of, calculation of electronic band, 25:2729

(ORNL-4570, pp 20-2)
PuC--UC, preparation of dense microspheres and shards of, 25:2775 (ORNL-4572, pp 242-50)
ThC--UC, analysis of silicon carbide-coated fuels particles of, for total carbon, gravimetric, 25:2064 (DP-Report-494)
UC--UN, elastic properties of, effects of porosity on, 25:2794(T) (ORNL-tr-2388)
URANIUM CARBONITRIDES
crystal lattice parameters of, effects of composition on, 25:2769 (ORNL-4570, pp 62-7)
elastic properties of, 25:2798
PuCN--UCN, elastic properties of, 25:2798
PuCN--UCN, preparation of dense microspheres and shards, 25:2775 (ORNL-4572, pp 242-50)
URANIUM DEPOSITS
prospecting for, in France, activities of Pechiney Group in, 25:2379
prospecting in Apache and Cochise Counties, Arizona, during 1950 to 1957, preliminary reconnaissance data for, 25:2373 (RME-154)
prospecting in Coconino County, Arizona, during 1951 to 1955, preliminary reconnaissance data for, 25:2374 (RME-155)
prospecting in Gila County, Arizona, during 1951 to 1956, preliminary reconnaissance data for, 25:2375 (RME-156)
prospecting in Mohave County, Arizona, during 1952 to 1956, preliminary reconnaissance data for, 25:2376 (RME-158)
prospecting in Pima and Pinal Counties, Arizona, during 1950 to 1957, preliminary reconnaissance data for, 25:2377 (RME-159)
prospecting in Texas during 1951 to 1957, preliminary reconnaissance data for, 25:2372 (RME-153)
URANIUM FLUORIDES UF_4
reduction by magnesium at 2400°F and 75 psig to prepare high-purity uranium, 25:2640 (NLCO-1058)
BeF_2--LiF--ThF_4--UF_4--ZrF_4, corrosive effects on Hastelloy N, stainless steel, and steel for MSRE, 25:2609 (ORNL-4570, pp 175-90)
URANIUM FLUORIDES UF_6
reactions with hydrogen and steam in fluidized bed to produce ceramic-grade uranium dioxide, 25:2781(P)
UF_6--XeF_6, reactions in, compounds produced by, 25:2156
URANIUM ISOTOPES U-232
energy-level transitions from octupole states in, branching ratios from E1, (T), 25:3751
URANIUM ISOTOPES U-233
alpha fission at 103 MeV, cross sections and fragment angular distributions for, (E), 25:3710
deuteron fission at 51.5 MeV, cross sections and fragment angular distributions for, (E), 25:3710
proton fission at 25 to 85 MeV, fragment energy and angular distribution for, (E), 25:3702
proton fission at 9.5 to 22 MeV, prompt-neutron energies and yields and fragment kinetic energy release in, (E), 25:3660
purification and storage of, 25:2773 (ORNL-4572, pp 135-48)
purification of, process development for, 25:2318 (ORNL-4572, pp 174-80)
URANIUM ISOTOPES U-234
alpha fission at 103 MeV, cross sections and fragment angular distributions for, (E), 25:3710
content ratio to uranium-238 in USSR ground waters, alpha spectrometric measurements of, 25:2356
deuteron fission at 51.5 MeV, cross sections and fragment angular distributions for, (E), 25:3710
triton reactions (t,pf) at 18 MeV, fission probabilities for, (E), 25:3679
URANIUM ISOTOPES U-235
alpha fission at 103 MeV, cross sections and fragment angular distributions for, (E), 25:3710
concentration in uranium by gaseous diffusion and ultracentrifugation, industrial prospects in France for, 25:2402
deuteron fission at 51.5 MeV, cross sections and fragment angular distributions for, (E), 25:3710
deuteron reactions (d,p) at 13 to 20 MeV, cross section for delayed fission in, (E), 25:3709
neutron cross sections for, 25-group, (T), 25:3530 (LA-4484)
neutron fission cross sections from uranium-234 (t,pf) reactions at 18 MeV, (E), 25:3679
neutron fission of, iodine isotope and tellurium-135 yields from thermal, (E), 25:3663
neutron reactions with, separated γ spectra from thermal, (E), 25:3649 (KFK-1214)
URANIUM ISOTOPES U-236
deuteron reactions (d,pn) at 11 to 20 MeV, cross section for delayed fission in, (E), 25:3709
half-life of fission isomer of, (E), 25:3709
potential-energy surface at large deformations from two-center shell model, (T), 25:3734
triton reactions (t,pf) at 18 MeV, fission probabilities for, (E), 25:3679
URANIUM ISOTOPES U-237
neutron fission cross sections from uranium-236 (t,pf) reactions at 18 MeV, (E), 25:3679
URANIUM ISOTOPES U-238
alpha fission at 103 MeV, cross sections and fragment angular distributions for, (E), 25:3710
concentration by hydrobionts, effects of nutritional type of lake on, 25:2546
content ratio to uranium-234 in ground water, alpha spectrometric measurements of, 25:2356
deuteron fission at 51.5 MeV, cross sections and fragment angular distributions for, (E), 25:3710
deuteron reactions (d,pn) at 11 to 20 MeV, cross section for delayed fission in, (E), 25:3709
half-life of fission isomer of, (E), 25:3709
neutron cross sections for, 25-group, (T), 25:3530 (LA-4484)
neutron reactions (n,2n) below (n,3n) threshold, cross-section calculations using Hauser--Feshback theory, (T), 25:3591 (AAEC/TM-542)
proton fission at 9.5 to 22 MeV, prompt-neutron energies and yields and fragment kinetic energy release in, (E), 25:3660
triton reactions (t,pf) at 18 MeV, cross sections and fission probabilities for, (E), 25:3679
URANIUM ISOTOPES U-239
energy-level transitions in, strength functions for M1, (T), 25:3683
neutron fission cross sections from uranium-238 (t,pf) reactions at 18 MeV, (E), 25:3679
URANIUM LEACH SOLUTIONS
decontamination of radium-containing, by ion exchange on zeolite containing alkali metal or alkaline earth metal ions, 25:2340(P)
separation of uranium from dilute, by ionic flotation, 25:2331
URANIUM NITRIDE TELLURIDES
crystal structure of U_2N_2Te formed in, 25:2248
URANIUM NITRIDES
creep of, mechanisms of compressive, 25:2787 (ORNL-4570, pp 24-6)
diffusion in UN, uranium-233 tracer study of cation self-, 25:2786 (ORNL-4570, pp 13-15)
elastic properties of, 25:2798
electric properties of UN, at 4.2 to 400°K, 25:2729 (ORNL-4570, pp 20-2)
heat transfer at metal interfaces from, correlations for, 25:2769 (ORNL-4570, pp 62-7)
mechanical properties of, at 25 to 1300°C, effects of porosity on, 25:2794(T) (ORNL-tr-2388)
mechanical properties of, review of, 25:2785 (LA-4452)
optical properties of paramagnetic UN, 25:2729 (ORNL-4570, pp 20-2)
preparation of fuels of, 25:2817 (ORNL-4570, pp 116-17)
properties of, thermal and thermoelectric, 25:2788 (ORNL-4570, pp 27-30)
radiation effects on clad fuel elements of, at 900 to 1400°C, 25:2817 (ORNL-4570, pp 116-17)
structure of, calculation of electronic band, 25:2729 (ORNL-4570, pp 20-2)
thermal capacity of UN, at 1.6 to 10°K, 25:2729 (ORNL-4570, pp 20-2)
PuN--UN, fabrication of advanced fuels of, development of methods for, 25:2769 (ORNL-4570, pp 62-7)
PuN--UN, mechanical properties of nonstoichiometric, at 25 to 1300°C, 25:2794(T) (ORNL-tr-2388)
PuN--UN, mechanical properties of, review of, 25:2785 (LA-4452)
PuN--UN, properties of clad fuels of, methods for characterization of, 25:2769 (ORNL-4570, pp 62-7)
PuN--UN, radiation effects on fuel pellets of, in-pile, 25:2769 (ORNL-4570, pp 62-7)
UC--UN, elastic properties of, effects of porosity on, 25:2794(T) (ORNL-tr-2388)
URANIUM ORE PROCESSING PLANTS
operation of Australian, 25:2336
URANIUM ORES
analysis for uranium by TBP extraction and spectrophotometry, 25:2067 (NIM-906)
processing of Rum Jungle, Australia, methods for, 25:2336
URANIUM OXIDES UO_2
compaction of sintered nodules and powders of, method for electrodynamic vibro-, 25:2778
defect structures in hyperstoichiometric, effects of temperature on, 25:3210
deformation of monocrystalline, mechanisms of, 25:2787 (ORNL-4570, pp 24-6)
electric conductivity of hyperstoichiometric, at 500 to 1400°C, 25:3210
mechanical properties of, at 25 to 1300°C, effects of porosity on, 25:2794(T) (ORNL-tr-2388)
preparation by sol-gel process, 25:2317 (ORNL-4572, pp 170-3)
preparation of sols of, 25:2774 (ORNL-4572, pp 149-69)
preparation of uranium-233-enriched, process development for, 25:2318 (ORNL-4572, pp 174-80)
production by reactions of uranium hexafluoride with hydrogen and steam in fluidized bed, 25:2781(P)
production of nuclear grade, from uranium ores in Rum Jungle, Australia, methods for, 25:2336
radiation effects on thermal conductivity of compacted pins of, at 200 to 1500°C, in-pile, 25:2813 (JAERI-Memo-4128)
structure of monocrystalline, 25:2727 (ORNL-4570, pp 1-4)

thermal conductivity of, electronic, 25:2788 (ORNL-4570, pp 27-30)
PuO_2--UO_2, fabrication of fuel pins of, development of methods for, 25:2768 (ORNL-4570, pp 47-61)
PuO_2--UO_2, mechanical properties of nonstoichiometric, at 25 to 1300°C, 25:2794(T) (ORNL-tr-2388)
PuO_2--UO_2, performance of fuels of, development of prediction methods for, 25:2789 (ORNL-4570, pp 68-75)
PuO_2--UO_2, preparation of microspheres of, by sol-gel process, 25:2774 (ORNL-4572, pp 149-69)
PuO_2--UO_2, production from nitrates, plant for continuous, 25:2306(R) (ANL-7735)
PuO_2--UO_2, radiation effects on clad pellet-type fuels of, in-pile, 25:2771 (ORNL-4570, pp 161-9)
PuO_2--UO_2, radiation effects on sphere-pac fuels of, review of in-pile, 25:2768 (ORNL-4570, pp 47-61)
ThO_2--UO_2, preparation of microspheres of, alcohol recycle and drying techniques for, 25:2773 (ORNL-4572, pp 135-48)
ThO_2--UO_2, preparation of microspheres of, by sol-gel process, 25:2320(R) (ORNL-TM-3204)
ThO_2--UO_2, preparation of microspheres of, nonfluidized-bed columns for, 25:2773 (ORNL-4572, pp 135-48)
ThO_2--UO_2--W, preparation of eutectics of, method for, 25:2727 (ORNL-4570, pp 1-4)
UO_2--W, microstructure of composites of, incorporating tungsten fibers, 25:2727 (ORNL-4570, pp 1-4)
UO_2--W, preparation of eutectics of, method for, 25:2727 (ORNL-4570, pp 1-4)

URANIUM OXIDES U_3O_8
analysis of nuclear-grade, for trace amounts of impurities by direct reading spectrometric method, 25:2068 (NLCO-1071)
production of nuclear grade, from uranium ores in Rum Jungle, Australia, methods for, 25:2336
Al--U_3O_8, fabrication of dispersion-type fuel elements of, development of methods for, 25:2770 (ORNL-4570, pp 127-35)
Al--U_3O_8, radiation effects on swelling of dispersion-type fuels of, in-pile, 25:2770 (ORNL-4570, pp 127-35)
Al-base--U_3O_8, void content in, effects of cladding, cold-rolling deformation, and composition on, 25:2806 (ORNL-4611)

URANIUM OXYCARBIDES
phase studies at 1450 to 1850°C, 25:2809

URANIUM PHOSPHIDES
structure of, calculation of electronic band, 25:2729 (ORNL-4570, pp 20-2)

URANIUM SELENIDES
structure of, calculation of electronic band, 25:2729 (ORNL-4570, pp 20-2)

URANIUM SULFIDES
structure of, calculation of electronic band, 25:2729 (ORNL-4570, pp 20-2)

URANIUM VANADIUM CARBIDES
phase studies at 1900°C, 25:2769 (ORNL-4570, pp 62-7)

URANIUM VANADIUM NITRIDES
phase studies at 1400 to 2000°C, 25:2769 (ORNL-4570, pp 62-7)

URANYL BROMIDES
hydration study of, in acetone--water mixture, PMR cation, 25:2209

URANYL CHLORIDES
fluorescence lifetimes of, effects of heavy water and impurities on, 25:2198
hydration study of, in acetone--water mixture, PMR cation, 25:2209
spectra of sclutions of, vibrational, 25:2216

URANYL COMPOUNDS
effects on photometric determination of hafnium and zirconium in geological specimens, 25:2084
fluorescence lifetimes of, effects of heavy water and impurities on, 25:2198
spectra of, ir and Raman, 25:2212

URANYL FORMATE HYDROXIDES
preparation and structure of, 25:2196

URANYL HALIDES
complexes with uranyl nitrates and urea, composition of, 25:2214

URANYL IONS
complexes with thiocyanate in water and methanol--water media, spectrophotometers studies on, 25:2215
reactions with alcohols in aqueous solutions, mechanism of photooxidation, 25:2158

URANYL NITRATES
complexes with triethoxyphosphine oxide, spectra of, ir and Raman, 25:2212
complexes with triphenylarsine oxide, spectra of, ir and Raman, 25:2212
complexes with triphenylphosphine oxide, spectra of, ir and Raman, 25:2212
complexes with uranyl halides and urea, composition of, 25:2214
hydration study of, in acetone--water mixture, PMR cation, 25:2209
separation from aqueous solutions by solvent extraction using amines and TBP, effects of salting-out agents on, 25:2335
spectra of hexahydrated, ir and Raman, 25:2212
spectra of hexahydrates of, in acidic, alkaline, and neutral solutions, vibrational, 25:2216

URANYL PERCHLORATES
hydration study of, in acetone--water mixture, PMR cation, 25:2209
spectra of solutions of, vibrational, 25:2216

URANYL SULFATES
fluorescence lifetimes of, effects of heavy water and impurities on, 25:2198
spectra of solutions of, vibrational, 25:2216

UREA
complexes with uranyl halides and nitrates, composition of, 25:2214

UREA, HYDROXY-
radiation effects on, relative signs of proton coupling tensor of free radical from γ, 25:2219 (NP-18449)

UREA, THIO-
effects on γ-radioinduced graft polymerization of cellulose with styrene in methanol solutions, 25:2247

URETHAN POLYMERS
properties of rigid foams of, effects of amine catalysts on, 25:2818 (BDX-613-170)
stress properties of rigid foams of, multiaxial, 25:3994 (UCRL-50909)

URINE
radioactivity in human, following rectal instillation of chromium-51-labeled EDTA, γ, 25:2534

V

VACUUM GAGES
design and operation of external collector, for ultrahigh vacuum measurement, 25:2431
modification of ionization, for measurements below 10^{-9} torr, 25:2428
performance of cold cathode, for ultrahigh vacuum measurements, 25:2430

VACUUM PUMPS
design and performance of helium evaporator cryo-, in ultrahigh vacuum room-temperature calibration system, 25:2429

VAK REACTOR
operations history during 1960 to 1970, 25:3801

VALEROPHENONE
radiolysis of, yields from electron, 25:2266

VALINE
radiolysis of polycrystalline, ESR studies on free radicals from x, 25:2289

VALINE, N-ACETYL-
radiolysis of polycrystalline, ESR studies on free radicals from x, 25:2289

VALINE, N-GLYCYL-
radiolysis of polycrystalline, ESR studies on free radicals from x, 25:2289

VALVES
operation of 12-inch gate, with pressure cartridges, 25:3998 (UCRL-50930)

VAN ALLEN RADIATION BELTS
electron intensity of E greater than or equal to 150 keV in outer, relation with geomagnetic indexes, (E), 25:2969
flux distribution of electrons and protons with energies between 0.1 and 1.0 MeV in, during magnetic storm, June 9, 1968, (E), 25:2950 (AD-709363)

VAN DE GRAAFF ACCELERATORS
experimental facilities for 400-keV, for beam--foil spectroscopy, 25:3465 (CONF-700322-, pp 21-31)
experimental facility for 150-keV, for studying inelastic electron reactions with atoms, 25:3472 (CONF-700322-, pp 379-92)
experimental facility for studying transient radiation effects in semiconductor devices, 25:3477 (LYCEN-7063)
uses for education experiments in nuclear physics, 25:3466 (CONF-700322-, pp 49-61)

VANADIUM
analysis for uranium using permanganate, potentiometric, 25:2099
corrosion by oxygen-containing sodium, kinetic and thermodynamic properties of, 25:2622
creep at 600°C and 11,000 psi, effects of oxygen on, 25:2606 (ORNL-4570, pp 92-5)
determination in biological materials by 14-MeV neutron and thermal neutron activation, sensitivity of, 25:2125 (IAEA-122, pp 27-36)
determination in graphite by neutron activation and gamma spectroscopy, 25:2142
determination in pigments from ancient murals by neutron activation, 25:2133
determination in presence of cerium, chromium, iron, and manganese by differential potentiometric titration, 25:2099
determination in sodium chloride solutions by catalytic amalgam method, 25:2080
determination in titanium alloys, x-ray fluorescence method for, 25:2097
determination of pentavalent, in phosphate and sulfate solutions by electrogeneration of trivalent vanadium, coulometric titration, 25:2081
determination of trace amounts of, in nuclear-grade uranium oxide (U_3O_8) by direct reading spectrometric method, 25:2068 (NLCO-1071)
diffusion of carbon in, electronic mechanisms in thermal, 25:2666 (NP-18468)

effects on determination of trace amounts of antimony by isotopic exchange in organic phase, 25:2106
effects on determination of trace amounts of rhenium by thiocyanate--stannous chloride method, 25:2102
effects on photometric determination of hafnium and zirconium in geological specimens, 25:2084
effects on polarographic determination of tellurium, 25:2090
effects on uv spectrophotometric determination of gallium in aqueous solutions, 25:2100
electron reactions at 1 to 3 MeV with, backscatter and transmission coefficients for, (E), 25:2883 (N-70-25499)
hardening and yield stresses in monocrystalline, effects of orientation, strain rate, and temperature on, 25:2718
neutron elastic and elastic scattering at 4.2 to 8.6 MeV, cross sections for, (E), 25:3595 (ORNL-4551)
production by pentachloride or pentafluoride reduction and vapor deposition, 25:2673 (ORNL-4570, pp 118-23)
radiation effects on void distribution in, fast neutron, 25:2758 (ORNL-4570, pp 76-84)
solubility in potassium at 1012 to 1341°K, 25:2714

VANADIUM ALLOYS AND SYSTEMS
corrosion by oxygen-containing sodium, effects of chromium additions on, 25:2622
mass transfer to Type 321 stainless steel by high velocity sodium at 710 to 760°C, 25:2617
Ti--V-base, creep to 850°C, 25:2662 (KFK-1193)
Al--Mo--Ti-base--V, microstructure of hot-rolled plates and sheets of α + β, relations of mechanical properties with abnormal, 25:2752
Al--Ti-base--V, corrosion by aqueous dinitrogen tetroxide, stress, 25:2635
Al--Ti-base--V, electron reactions at 1 to 3 MeV with, backscatter and transmission coefficients for, (E), 25:2883 (N-70-25499)
Al--Ti-base--V, microstructure of hot-rolled plates and sheets of α + β, relations of mechanical properties with abnormal, 25:2752
Co--Ni--V, mechanical properties of, effects of ordering on, 25:2643 (ORNL-4570, pp 106-11)
Cr--V-base, corrosion by sodium at 600°C, effects of chromium content on, 25:2606 (ORNL-4570, pp 92-5)
Fe-base--V, diffusion in bcc phases of, radioisotope tracer measurements of volume, 25:2691
Ga--Hf--V, critical current density and defect structure in high-fluid superconducting intermetallic $(VHf)_3Ga$, (E), 25:3039
Ga--V, critical current density and defect structure in high-field superconducting intermetallic V_3Ga, (E), 25:3039
Ga--V--Zr, critical current density and defect structure in high-field superconducting intermetallic $(VZr)_3Ga$, (E), 25:3039
Ge--Ti--V-base, creep to 850°C, 25:2662 (KFK-1193)
Mo--V-base, corrosion by sodium at 600°C, effects of molybdenum content on, 25:2606 (ORNL-4570, pp 92-5)
N--V-base, crystal structures of quenched and aged, 25:2811
Nb--Si--Ti--V-base, creep to 850°C, 25:2662 (KFK-1193)
Nb-base--V, defects and dislocations in cold-rolled, anneal-induced recovery from, 25:2728 (ORNL-4570, pp 5-9)
Ni-base--V, carburization of, relations with hardness, 25:2716
Si--Ti--V-base, creep to 850°C, 25:2662 (KFK-1193)
Ti--V-base, corrosion by sodium at 600°C, effects of titanium content on, 25:2606 (ORNL-4570, pp 92-5)
Ti--V-base, corrosion by sodium in Type 316 stainless steel loop system at 675 to 800°C, 25:2621
Ti--V-base, mechanical properties of, at 25 and 800°C, effects of interstitial absorption on, 25:2621
Ti-base--V, phase studies of, 25:2735
U--V, phase studies of, using computers, 25:2737
V-base--Zr, corrosion by sodium at 600°C, effects of zirconium content on, 25:2606 (ORNL-4570, pp 92-5)

VANADIUM CARBIDE NITRIDES
crystal lattice parameters of, effects of composition on, 25:2769 (ORNL-4570, pp 62-7)

VANADIUM CARBIDES
electron--phonon interaction in, upper limit of, 25:3034
superconductivity of single crystals of, search for, 25:3034

VANADIUM ISOTOPES V-51
energy levels from chromium-51 decay, spin-parity assignments for, (E), 25:3704
energy levels from proton inelastic scattering and titanium-48 (α,pγ) reactions, spin-parity assignments for, (E), 25:3593 (COO-1530-21)
energy-level transitions from chromium-51 decay, internal conversion coefficients for, (E), 25:3704
proton inelastic scattering at 2.3 to 6 MeV, γ spectra from, (E), 25:3593 (COO-1530-21)
proton reactions (p,n) near threshold, Q-value for, (E), 25:3608
proton reactions (p,nγ) at 2.3 to 6 MeV, γ singles and coincidence and n-γ coincidence spectra from, (E), 25:3593 (COO-1530-21)

VANADIUM OXIDES
effects on photometric determination of hafnium and zirconium in geological specimens, 25:2084
effects on properties of sintered zircons, 25:2766(T) (CSIRO-Trans-9924)
preparation and purification of monocrystalline V_2O_5, 25:2783

VANSTAR-7
corrosion by sodium at 600°C, 25:2606 (ORNL-4570, pp 92-5)
corrosion by sodium in Type 316 stainless steel loop system at 675 to 800°C, 25:2621
mechanical properties of, at 25 and 800°C, effects of interstitial absorption on, 25:2621

VANSTAR-8
corrosion by sodium at 600°C, 25:2606 (ORNL-4570, pp 92-5)
corrosion by sodium in Type 316 stainless steel loop system at 675 to 800°C, 25:2621
mechanical properties of, at 25 and 800°C, effects of interstitial absorption on, 25:2621

VANSTAR-9
corrosion by sodium at 600°C, 25:2606 (ORNL-4570, pp 92-5)
corrosion by sodium in Type 316 stainless steel loop system at 675 to 800°C, 25:2621
mechanical properties of, at 25 and 800°C, effects of interstitial absorption on, 25:2621

VENUS (PLANET)
ionosphere of, boundary determination by solar wind flow past, (E/T), 25:2878

VERMONT YANKEE POWER REACTOR
design parameters of, revised and additional data on, 25:3835 (DOCKET-50271-34)
operations aspects of, revised and additional data on, 25:3835 (DOCKET-50271-34)

VESSELS
design of criticality-safe, for mixing and storage of plutonium-containing fuel materials, 25:2419 (KFK-1192)
development of stacked-clone contactor, 25:2195 (ORNL-4572, pp 251-7)
performance of silver reaction, for separation of iodine-131 from gaseous Purex Plant wastes, 25:2416 (ARH-SA-67)

VINYL ALCOHOL POLYMERS
radiation effects on properties and structure of, ir spectral studies on γ, 25:2220

VIRUSES
effects on tumor induction in mice, incidence of transplantation antigens following, 25:2537
murine sarcoma, infectivity in cells, effects of cell phase on, 25:2587
TMV, biochemistry of mutations in, 25:2551(R) (COO-873-28)

VOID FRACTION
measurement in LOFT reactor vessel and piping, development of ultrasonic detector for, 25:3905 (IN-1441)

W

WATER
analysis for contaminants by isotope dilution gas--liquid chromatography, 25:2107
analysis for iodine by neutron activation and γ spectrometry, 25:2124 (IAEA-122, pp 15-26)
analysis for radioisotopes by ion exchange or filtration and counting, 25:2117
analysis for tungsten-181 and tungsten-185 by γ counting, 25:2110
corrosive effects of ammoniated and lithiated PWR coolant, on Inconel 600, stainless steel, and Zircaloy-4, 25:2637
determination in helium, pressurized electrolytic hygrometer for, 25:3882 (DP-Report-487)
diffusion in, self-, 25:2192
gamma dose-rate distributions in laminated iron/water shielding, (E/T), 25:3174
mass transfer from soils, 25:2195 (ORNL-4572, pp 251-7)
neutron attenuation by normal and deuterated, monoenergetic-source fast-, (E/T), 25:3173
neutron attenuation in, relaxation length for 14-MeV, (E), 25:3537
neutron flux-density distributions in laminated iron/water shielding, (E/T), 25:3174
radioinduced purification of, for use in radiation chemistry, γ, 25:2228
radiolysis of, effects of oxygen, potassium nitrate, and sodium formate on γ, 25:2257 (CEA-R-4046)
radiolysis of, evidence for very early effects in, 25:2267
radiolysis of, ionic effects in, 25:2274
spectra at 25 to 390°C, ir, 25:2165
spectra of bound, on thorium dioxide surfaces, ir, 25:2207
spectra of, compared with heavy water spectra, 25:2152 (ORNL-4572, pp 231-5)
steam--water, density of, ultrasonic void fraction detector for measurement of, 25:3905 (IN-1441)
structure of, ir studies on, 25:2171
bis(2-ethylhexyl) phosphate--$CeCl_3$--HCl--H_2O--$NdCl_3$--

XUM

$SmCl_3$, equilibria in Amsco, 25:2311 (IS-T-412)
glycerol--H_2O, proton polarization measurements at high magnetic fields and low temperatures in porphyrexide-doped, 25:3500
WATER-d
structure of, ir studies on, 25:2171
WATER-d_2
diffusion in, self-, 25:2192
effects on fluorescence lifetimes of uranyl compounds, 25:2198
spectra at 25 to 390°C, ir, 25:2165
spectra of, compared with water spectra, 25:2152 (ORNL-4572, pp 231-5)
WATER VAPOR
sorption and desorption on tungsten surfaces, 25:2722
WELDING
method for pressurized gas metal-arc, performance of air and argon as cover gases in, 25:2646 (RFP-1550)
WELDS
stresses in, method of measuring residual, 25:2410 (CRNL-TM-3113)
WELL LOGGING
equipment for radiometric, of ocean floor, design of, 25:2357(P)
method for gamma--gamma, for measuring rock density in ore mining area of Mecsek Mountains, Hungary, 25:2347(T) (CSIRO-Trans-10140)
WEST VALLEY PROCESSING PLANT
emergency power system for, diesel drive for, 25:2309 (DOCKET-50201-55)
WHISTLERS
propagation in magnetosphere, nonlinear frequency shift of, (T), 25:3004
WILLIAM H. ZIMMER POWER REACTOR, UNIT 1
site for, revised and additional data on hydrology of, 25:3848 (DOCKET-50358-8)
WILLIAM H. ZIMMER POWER REACTOR, UNIT 2
site for, revised and additional data on hydrology of, 25:3848 (DOCKET-50358-8)
WIND
effect of neutral-air, on ionospheric F region, (T), 25:2954
WIRES
properties of thin, defect and transport, 25:3939(R) (COO-1247-21)
radiation effects on, 1.3 MeV gamma and 6.0 MeV electron, 25:2819 (LCIE-342)
resistance in small, twisted, multicore superconducting, 25:3499
WOOD
radioinduced polymerization of esters in, 25:2254
radioinduced polymerization of monomers in, 25:2238
plastics--wood, structural properties of, produced by radioinduced polymerization, 25:2238

X

X RADIATION
dose conversion coefficients for Lucite and polystyrene, 25:2569
effects on aleurone pigmenting potential in maize, in comparison to effects of diethyl sulfate, effects of seed exposure on mutagenic, 25:2560
effects on calcium-doped potassium chloride crystals, effects of aggregation processes on V bands induced in, (E/T), 25:3198
effects on chromosome number and stability of isoenzymes in human carcinoma cell cultures, 100 to 1500 rad, 25:2585
effects on chromosomes in dormant seeds of Helianthus, Lactuca, and Pinus, aberrant, 25:2555
effects on chromosomes of Drosophila, effects of aberrant, on crossover suppressors, 25:2561
effects on chromosomes of spermatocytes in mice following exposure of spermatogonia, frequency of aberrant, 25:2553
effects on crystals of glucose and glucuronic acid, 25:2286
effects on delayed hypersensitivity in rats, whole-body, 25:2540
effects on DNA of human xeroderma pigmentosum cells, repair synthesis following, 25:2535
effects on electrophoretic mobility of Ehrlich ascites tumor cells, 25:2586
effects on ferroelectric properties of barium titanate single crystal, 25:3196
effects on helium containing gaseous impurities, 25:2258 (DP-Report-447)
effects on hydra, protective effects of arginine and citrulline against, 25:2588
effects on incisor teeth of rats, effects of dose on, 25:2592
effects on luminescence of aqueous solutions of monovalent thallium, 25:2232
effects on mice, injection of spleen cells from carbon-treated donors following, 25:2538
effects on partial and total sex chromosome loss in spermatozoa of Drosophila melanogaster, 25:2554
effects on polycrystals of acetylvaline, glycylvaline, and valine, ESR studies on free radicals from, 25:2289
effects on polymerization of liquid 1,2-epoxy-2-methylpropane, mechanism of, 25:2256
effects on rubies, EPR study of annealing kinetics of chromium ions in, (E), 25:3195
effects on silicate-treated zinc oxide coatings, relations with oxygen loss, 25:2815 (N-70-33138)
effects on solids, thermoluminescence glow peaks from, 25:2235
effects on thallium-activated potassium bromide crystals, photoscintillations induced in, 25:3194
effects on thallium-activated potassium bromide crystals, flash luminescence induced in, 25:3193
effects on tumor cells, immunization of hosts following, 25:2537
effects on urethan adenomagenesis in lungs of mice, role of thymus in inhibitory, 25:2589
emission from envelopes of close-binary systems due to shock heating, (T), 25:2830
production of hard decelerated, design of water-dielectric generator for, 25:3478
scattering by helium-4, at 5°K and below, 25:3018
scattering of, intensity measurements in small-angle, 25:2730 (ORNL-4570, pp 44-6)
X-RAY CAMERAS
design modification of Kratky small-angle, 25:2730 (ORNL-4570, pp 44-6)
filter for Debye--Scherrer, for radioactive samples, background alpha--beta, 25:2508
X-RAY-DIFFRACTION ANALYSIS
conference on accurate determination of x-ray intensities and structure factors, Cambridge, Eng., 6/68, 25:3216
X-RAY EQUIPMENT
design of pulsed high-intensity tube, 25:2401
X-RAY SOURCES
design of pulsed high-intensity tube-type, 25:2401
X-RAY SPECTROMETERS
design and construction of low-temperature, 25:3018
performance of semiconductor, using pulsed-light feedback preamplifier, 25:2462
XENON
abundance in Kappa Cancri, (E), 25:2840
plasma of, distribution of ion densities in arc discharges, (T), 25:3085 (LYCEN-7061)
separation from spent LMFBR fuels, 25:2314 (ORNL-4572, pp 37-84)
XENON FLUORIDES
TaF_5--XeF_6, reactions in, properties and structure of products produced by, 25:2156
UF_6--XeF_6, reactions in, compounds produced by, 25:2156
XENON IONS
effects on gold foils, imperfection clusters induced in, (E), 25:3169(R) (COO-1053-14)
XENON ISOTOPES
solubility in carbon tetrachloride and chloroform for solvent extraction separation from iodine isotopes, 25:2201
XENON ISOTOPES Xe-135
neutron cross sections for, 25-group, (T), 25:3530 (LA-4484)
XENON ISOTOPES Xe-136
proton inelastic scattering at 10 MeV, fits to angular distributions with configuration missing, (T), 25:3685
XENON SYSTEMS
F--Mn--Xe, reactions in, compounds produced by, 25:2156

Y

YANKEE POWER REACTOR
operations history for October 1970, 25:3783 (DOCKET-50029-140)
YTTERBIUM
complexes with cupferron, separation by solvent extraction using 2-methyl-1-propanol and 3-methyl-1-butanol, 25:2078
determination in silicate rocks using cupferron, spectrographic, 25:2078
YTTERBIUM BROMIDES
preparation of, 25:2803(R) (COO-716-66)
structure of, 25:2803(R) (COO-716-66)
YTTERBIUM ISOTOPES Yb-168
energy levels from lutetium-168 decay, (E), 25:3650 (LYCEN-7030)
YTTERBIUM ISOTOPES Yb-172
energy levels from multiple Coulomb excitation, (E), 25:3662
YTTERBIUM ISOTOPES Yb-173
nuclear magnetic moment of, effects of spin--orbit and spin--spin forces on, (T), 25:3692
YTTERBIUM ISOTOPES Yb-174
energy levels from multiple Coulomb excitation, (E), 25:3662
YTTERBIUM ISOTOPES Yb-176
energy levels from multiple Coulomb excitation, (E), 25:3662
YTTERBIUM OXIDES
emittance at high temperatures of solid, spectral, 25:3204 (AD-708547)
Er_2O_3--Yb_2O_3, preparation, magnetic susceptibility, and spectra of solid solutions of, 25:3211
YTTRIUM
analysis for metallic impurities by neutron activation

and extraction displacement chromatography, 25:2138
complexes with cupferron, separation by solvent extraction using 2-methyl-1-propanol and 3-methyl-1-butanol, 25:2078
determination in rare earth metals by indirect spectrophotometric method, 25:2091
determination in silicate rocks using cupferron, spectrographic, 25:2078
determination of trace amounts of, in lanthanum oxide and neodymium oxide by direct reading emission spectrometry, 25:2096
effects of hot trap of, on lithium corrosion of niobium--zirconium alloy in Rankine cycle test loop, 25:2624
energy levels of, lifetimes and magnetic splitting factors for, (E), 25:2891
spectra of, level-crossing measurements of hyperfine structure and Stark effect in, 25:2891

YTTRIUM CARBIDES
hydrolysis of, analysis of products from, 25:2782
preparation by reactions of carbon with yttrium oxide, 25:2782
preparation of microspheres of, method for, 25:2795(P)

YTTRIUM ISOTOPES Y-90
detection in radioecology studies, use of Cherenkov counting for, 25:2565
determination in water by ion exchange or filtration and counting, 25:2117
monitoring in irrigation canal sediment and water downstream from nuclear power centers on Rhone River, 25:2543

YTTRIUM OXIDES
analysis for terbium, scanning method for improving accuracy of luminescence, 25:2086
analysis for trace amounts of rare earths and other elements by direct reading emission spectrometry, 25:2096
effects on properties of sintered zircons, 25:2766(T) (CSIRO-Trans-9924)
luminescence of terbium-doped, temperature effects on flame-excited, (E), 25:3213
preparation of microspheres of, method for, 25:2795(P)
proton reactions at 350 keV with, characteristic x-ray spectra from, (E), 25:2882 (CONF-700322-, pp 113-24)
reactions with carbon, preparation of yttrium carbide by, 25:2782

YTTRIUM VANADATES
analysis for europium, scanning method for improving accuracy of luminescence, 25:2086

Z

ZINC
corrosive effects on tantalum at 1000°C, effects of anodization in phosphoric acid on, 25:2630
deposition on rotating discs and cylindrical cathodes, surface morphology in electrochemical, 25:2648
determination following nonsulfide separation from elements, qualitative, 25:2101
determination following solvent extraction using benzene, 8-quinolinol, and Rhodamine 6G, photometric, 25:2087
determination in biological materials by 14-MeV neutron and thermal neutron activation, sensitivity of, 25:2125 (IAEA-122, pp 27-36)
determination in blood serum and skin of psoriatic patients by neutron activation and radiochemical separation, 25:2134
determination in human liver by neutron activation and γ spectrometry, 25:2124 (IAEA-122, pp 15-26)
determination in human tissues by thermal neutron activation, sensitivity of, 25:2123 (IAEA-122, pp 1-13)
determination in molybdenum or yttrium by neutron activation and extraction displacement chromatography, 25:2138
determination in soils in Pakistan by neutron activation and radiochemical separation, 25:2125 (IAEA-122, pp 27-36)
determination of trace amounts of, in nuclear-grade uranium oxide (U_3O_8) by direct reading spectrometric method, 25:2068 (NLCO-1071)
effects on determination of trace amounts of antimony by isotopic exchange in organic phase, 25:2106
effects on extraction--photometric determination of niobium in steel, 25:2085
effects on photometric determination of hafnium and zirconium in geological specimens, 25:2084
neutron capture by, gamma spectra from thermal, (E), 25:3181
photon reactions at 5.7 GeV, $w\gamma$ coupling constant and wN cross section from w production in, (E), 25:3247
production of pure, review of techniques for, 25:3219
proton elastic and inelastic scattering at 28 MeV, cross sections for, (E), 25:3599
radioinduced preparation from aqueous salt solutions, electron, 25:2237 (N-70-32826)

ZINC ALLOYS AND SYSTEMS
In-base--Zn, thermodynamic properties of dilute liquid solutions of, 25:2685
rare earths--Zn-base, crystal structure of intermetallic compounds of, 25:2753

ZINC CHLORIDES
CsCl--$NiCl_2$--$ZnCl_2$, phase studies of, 25:2805 (ORNL-4570, pp 31-4)

ZINC ISOTOPES Zn-63
energy levels from gallium-63 decay, (E), 25:3609

ZINC ISOTOPES Zn-64
alpha inelastic scattering at 31 MeV, angular distributions for, (E), 25:3630
deuteron reactions (d,n) at 10 MeV, DWBA analysis of differential cross sections from, (E), 25:3625
energy levels from alpha inelastic scattering, (E), 25:3630
photon reactions (γ,n), (γ,2n), and (γ,np) at 10 to 40 MeV, relative cross sections for, (E), 25:3623
proton elastic scattering at 39.6 MeV, cross-section and polarization measurements for, (E), 25:3598

ZINC ISOTOPES Zn-65
energy levels from copper-65 (p,n) reactions, spins and parities of, (E), 25:3631
release to soil from organic debris in forest as function of decomposition mode and time, 25:2528
retention by silts of Dimbovitza--Bucharest River, effects of chelating agents and pH on, 25:2363
sorption by Rhine River monomineralic fine sands, (E), 25:2350

ZINC ISOTOPES Zn-66
alpha inelastic scattering at 31 MeV, angular distributions for, (E), 25:3630
deuteron reactions (d,n) at 10 MeV, DWBA analysis of differential cross sections from, (E), 25:3625
energy levels from alpha inelastic scattering, (E), 25:3630
proton elastic scattering at 39.6 MeV, cross-section and polarization measurements for, (E), 25:3598

ZINC ISOTOPES Zn-67
proton reactions (p,n) at 3 to 6 MeV, neutron spectra from, (E), 25:3596 (TID-25503)

ZINC ISOTOPES Zn-68
deuteron reactions (d,n) at 10 MeV, DWBA analysis of differential cross sections from, (E), 25:3625
proton elastic scattering at 39.6 MeV, cross-section and polarization measurements for, (E), 25:3598
proton reactions (p,n) at 3 to 6 MeV, neutron spectra from, (E), 25:3596 (TID-25503)

ZINC ISOTOPES Zn-71
beta decay of ground-state and metastable, (E), 25:3638

ZINC OXIDES
radiation effects on silicate-treated coatings of, recovery from ir and x, 25:2815 (N-70-33138)

ZINC SULFIDES
microstructure of crystals of, electron microscopic study of, 25:2748

ZIRCALOY
burst testing of multitube assemblies of, for loss of coolant accident research, 25:2610 (ORNL-4570, pp 205-12)
fabrication of fuel cladding tubes of, method for, 25:2695
properties of fuel cladding of, mechanical and physical, 25:2695
radiation effects on mechanical properties of tubes of, fast neutron, 25:3921 (DUN-SA-144)
rupture of tubes of, analysis of mechanisms of, 25:2610 (ORNL-4570, pp 205-12)

ZIRCALOY-2
creep at 25 to 428°C, 25:2693

ZIRCALOY-4
corrosion by ammoniated and lithiated PWR coolants, effects on reactor operation, 25:2637
crystal structure of hydrides in low hydrogen content, 25:2740

ZIRCONIUM
analysis for trace amounts of carbon, conductometric method for, 25:2071
complexes with 3,6-bisazo derivatives of chromotropic acid, spectrophotometric studies on, 25:2199
corrosion by selenium at 300 to 700°C, 25:2629
corrosion by sodium at 450°C, effects of oxygen on, 25:2611 (PEL-201)
determination by amperometric titration using N-o-tolylbenzohydroxamic acid, 25:2082
determination in geological specimens using 8-hydroxy-7-[(2-hydroxy-3,5-dinitrophenyl)-azo]-1,6-naphthalenedisulfonic acid, photometric, 25:2084
determination in hydrothermally altered rocks from Tateyama Jigokudani Hot Springs, Toyama, Japan, colorimetric, 25:2098
determination in meteorites and terrestrial materials by neutron activation and radiochemical separation, 25:2148
determination in titanium alloys, x-ray fluorescence method for, 25:2097
determination in uranium alloys by atomic absorption spectrophotometry, 25:2065 (LA-4529)
effects of additions of, on tensile properties of molybdenum--niobium-base alloys, 25:2682
effects of hot trap of, on boiling potassium corrosion of niobium--zirconium alloy in Rankine cycle test loop, 25:2624
effects on corrosion of niobium-coated steel tubing by bismuth--lead eutectic at 375 to 500°C, 25:2627
effects on determination of trace amounts of antimony by

XUM

isotopic exchange in organic phase, 25:2106
effects on extraction--photometric determination of niobium in steel, 25:2085
Fermi surface of, pressure dependence of cross sections of, (E), 25:3212
neutron cross sections for, 25-group, (T), 25:3530 (LA-4484)
preparation and etching of microsections of, 25:2656
reactions with platinum, 25:2160
release to soil from organic debris in forest as function of decomposition mode and time, 25:2528
separation from MSBR fuels, 25:2313 (ORNL-4572, pp 1-36)
solubility in potassium at 1012 to 1341°K, 25:2714

ZIRCONIUM ALLOYS AND SYSTEMS
corrosion of 3Zl, by sodium at 450°C, effects of oxygen on, 25:2611 (PEL-201)
determination of trace amounts of, in nuclear-grade uranium oxide (U_3O_8) by direct reading spectrometric method, 25:2068 (NLCO-1071)
Al--Mo--Sn--Zr-base, corrosion by sodium at 450°C, effects of oxygen on, 25:2611 (PEL-201)
Al--Zr, crystal structure of supercooled solid solutions of, 25:2733
Cr--Zr-base, x-ray line broadening of β-quenched, effects of cooling rate, grain size, and lattice distortion on, 25:2719
Ga--V--Zr, critical current density and defect structure in high-field superconducting intermetallic $(VZr)_3Ga$, (E), 25:3039
Hf-base--Zr, crystal structure of α, at 23 to 1600°C, 25:2751
Hf-base--Zr, thermal expansion of α, at 23 to 1600°C, 25:2751
Mo--Nb--Zr, diffusion in, activation energy for, 25:2704
Mo--Zr, diffusion in, activation energy for, 25:2704
Mo-base--Zr, crystal structure of dilute cast, effects of carbon additions on, 25:2745
Nb--U-base--Zr, crystal structure of, effects of aging on, 25:2730 (ORNL-4570, pp 44-6)
Nb--U-base--Zr, oxidation at 800°C, mechanisms and stresses in, 25:2605 (ORNL-4570, pp 37-9)
Nb--Zr, diffusion in, activation energy for, 25:2704
Nb--Zr, phase studies of, 25:2668 (ORNL-4570, pp 10-12)
Nb--Zr, preparation and etching of microsections of, 25:2656
Nb--Zr, properties of superconducting ribbons of, for cryogenic level indicators, 25:2394
Nb--Zr-base, phase transformation in, studies of athermal omega, 25:2735
Nb--Zr-base, precipitates in alpha- and omega-phase, composition and volume of dispersed, 25:2742
Nb--Zr-base, radiation effects on creep rate of heat treated, relations of stress dependence with pile neutron, 25:2760
Nb-base--Zr, corrosion by barium, calcium, and lead at 1000 to 1800°C, 25:2628
Nb-base--Zr, corrosion by boiling potassium in Rankine cycle test loop, effects of zirconium hot trap on, 25:2624
Nb-base--Zr, corrosion by lithium at 1000 and 1400°F, effects of welding atmosphere purity on, 25:2625
Nb-base--Zr, corrosion by lithium in Rankine cycle test loop, effects of yttrium hot trap on, 25:2624
Ni-base--Zr, carburization of, relations with hardness, 25:2716
O--Zr, hardness of solid solutions of, effects of temperature on, 25:2700
U--Zr, diffusion in, thermodynamics of bond changes in self-, 25:2701
V-base--Zr, corrosion by sodium at 600°C, effects of zirconium content on, 25:2606 (ORNL-4570, pp 92-5)

ZIRCONIUM CARBIDES
effects of additions of, on crystal structure of cast molybdenum, 25:2743

ZIRCONIUM CARBONITRIDES
effects of coating of, on corrosion resistance and mechanical properties of steel, 25:2612

ZIRCONIUM FLUORIDES
BeF_2--LiF--ThF_4--UF_4--ZrF_4, corrosive effects on Hastelloy N, stainless steel, and steel for MSRE, 25:2609 (ORNL-4570, pp 175-90)

ZIRCONIUM HYDRIDES
crystal structure in low hydrogen content Zircaloy-4, 25:2740

ZIRCONIUM ISOTOPES Zr-90
energy-level transitions in, search for double-photon, (E), 25:3658
helium-3 reactions (He-3,d) at 24 MeV, energy spectra at 30° and cross sections for analog states from, (E), 25:3666

ZIRCONIUM ISOTOPES Zr-92
helium-3 reactions (He-3,d) at 24 MeV, energy spectra at 30° and cross sections for analog states from, (E), 25:3666

ZIRCONIUM ISOTOPES Zr-94
helium-3 reactions (He-3,d) at 24 MeV, energy spectra at 30° and cross sections for analog states from, (E), 25:3666

ZIRCONIUM ISOTOPES Zr-95
uptake by aquatic molluscs and plants, effects of concentration in water on concentration factor for fallout, 25:2548

ZIRCONIUM ISOTOPES Zr-102
decay and energy-level transitions following californium-252 fission, (E), 25:3673

ZIRCONIUM OXIDES
corrosion by selenium at 300 to 700°C, 25:2629
reactions with platinum, 25:2160
HfO_2--Ho_2O_3--ZrO_2, crystal structure of $Ho_2O_3 \cdot 2ZrO_2(HfO_2)$ phase in, 25:2807(T) (SC-T-70-4039)
Mo--ZrO_2, mechanical properties of low-porosity corrosion-resistant, effects of chromium on, 25:2796

ZIRCONIUM SILICATES
preparation of rare earth-doped monocrystalline, 25:2727 (ORNL-4570, pp 1-4)

ZIRCONS
physical properties of sintered, effects of bonding agents and ceramic additives on, 25:2766(T) (CSIRO-Trans-9924)

REPORT NUMBER INDEX

Reports, conference papers and proceedings, numbered translations, and patents are included in this index. Each item is listed by report number; this is followed by the abstract number and a brief notation regarding public availability. The index entries show which reports are on file in the institutions listed on the back of the front cover (Dep.), which reports have been published in open-literature journals (journal citation), and which reports can be purchased (source and price). Whenever a report is identified by more than one number, the availability is given under the primary number, and a cross reference is given under the secondary report number.

The report number codes apply to USAEC reports unless designated otherwise. Non-USAEC reports are identified by parenthetical notes after the report codes; e.g., (non-AEC), (British), (Canadian), (French). The note (Misc.) identifies the codes used for both USAEC and non-USAEC reports. Patents are listed under the heading "PATENTS"; the country of origin is included in parentheses.

A comprehensive list of both USAEC and non-USAEC report codes is contained in the latest revision of TID-85, *Report Number Series Used by the Division of Technical Information in Cataloging Reports.* This information is also included in the Cumulative Report Number Index (issued annually).

Availability of USAEC Reports

All USAEC Reports abstracted in *Nuclear Science Abstracts* are available through one or more of the following sources:

(1) University and public libraries in the United States. A list of these organizations appears on the inside front cover of each issue of *NSA*.

(2) NCR Microcard Editions in Microcard and micronegative form. Orders and inquiries should be sent to: Order Processing Department, 365 South Oak Street, West Salem, Wisconsin 54669.

(3) National Technical Information Service, U. S. Department of Commerce, Springfield, Virginia 22151.

(4) Superintendent of Documents, U. S. Government Printing Office, Washington, D. C. 20402.

(5) National Cash Register Co., P. O. Box 3111, Oak Ridge, Tenn. 37830, in micronegative form. Purchase details available on request.

Availability of Non-USAEC Reports

U. S. Reports. Reports of U. S. Government agencies are available to the public from the National Technical Information Service (NTIS). If specific availability is not shown, inquiries may be directed to NTIS.

Non-U. S. Reports. Reports of atomic energy organizations of other countries are available from NTIS for U. S. sale only. Specific availability in the country of origin is shown, when known, at the report number entry. Otherwise, inquiries should be made to the organizations listed below:

AUSTRALIA

Australian Atomic Energy Commission Research Establishment. Available upon request from the Library, Australian Atomic Research Establishment, Private Mail Bag, Sutherland, New South Wales, Australia.

BELGIUM

Centre d'Étude de l'Energie Nucléaire. Available upon request to individuals and organizations from the Centre d'Etude de l'Energie Nucléaire (C.E.N.), Studiecentrum voor Kernenergie (S.C.K.), Technical Information Dept., MOL-DONK (Belgium).

CERN

CERN European Organization for Nuclear Research. Available without charge from CERN European Organization for Nuclear Research, Geneva 23, Switzerland. Copies are deposited in libraries throughout the world.

FRANCE

Commissariat à l'Energie Atomique. Inquiries for reports numbered 1-2199 should be addressed to Service Central de Documentation du C.E.A., Centre d'Etudes Nucléaires de Saclay, Boîte postale n° 2, 91. GIF-sur-YVETTE, FRANCE. Reports numbered 2200 and above are available from La Documentation Française, 31 quai Voltaire, 75, PARIS (7e), FRANCE.

Service Central de Protection contre les Rayonnements Ionisants. Copies are available from Ministère de la Santé Publique, Service Central de Protection contre les Rayonnements Ionisants, B.P. n° 78 Le Vesinet (France) Telex 25667.

GERMANY

Deutsches Elektronen-Synchrotron DESY. Copies are available from Deutsches Elektronen-Synchrotron DESY, Dokumentation, 2000 Hamburg 52, Notkestieg 1, Germany.

Gesellschaft für Kernforschung mbH (KFK). Copies are available from Gesellschaft für Kernforschung mbH, 75 Karlsruhe, Postfach 947, Germany. Copies are also deposited in many national nuclear centers in the world.

Kernforschungsanlage. Copies may be ordered from Zentralbibliothek der Kernforschungsanlage Jülich, Jülich, Bundesrepublik Deutschland.

Hahn-Meitner-Institute für Kernforschung. Available without charge from Hahn-Meitner-Institute für Kernforschung Ber-

XUM

lin, Bibliothek, Glienicker Strasse 100, 1 Berlin 39, Germany. Copies are deposited in many national nuclear centers in the world.

Johann-Wolfgang-Goethe Universität, Frankfurt Am Main, Institut für Kernphysik, (IKF). Copies are available from Gmelin Institut, 40–42 Varrentrappstrasse, Frankfurt (Main), West Germany.

ISRAEL

Israel Atomic Energy Commission. Available without charge from Israel Atomic Energy Commission, Soreq Nuclear Research Centre, Yavne, Israel.

ITALY

Centro Informazioni Studi Esperienze (CISE). For sale at CISE Press Office, Casella Postale 3986, Milano, Italy. Copies are deposited in the libraries of various nuclear centers in Italy and abroad.

Comitato Nazionale per l'Energia Nucleare. Copies are available from Comitato Nazionale p. Energia Nucleare, Divisione Affari Internazionali e Studi Economici, Ufficio Pubblicazioni, Via Belisario, 15, Roma, Italy.

JAPAN

Japan Atomic Energy Research Institute (JAERI). Available from the Staff Supply Cooperative of Japan Atomic Energy Research Institute (JAERI), Tokai-mura, Naka-gun, Ibaraki-ken, Japan. Copies are deposited in depositories in Tokyo, Nagoya, and Osaka.

Nagoya University. Copies are available from Research Information Center, Institute of Plasma Physics, Nagoya University, Nagoya, Japan.

University of Tokyo. Available free of charge from Institute for Nuclear Study, University of Tokyo, Tanashi-Machi, Kitatama-gun, Tokyo, Japan.

NETHERLANDS

Reactor Centrum Nederland. For sale by Reactor Centrum Nederland, 112 Scheveningseweg, 's-Gravenhage, The Netherlands. Copies are deposited in university libraries in Holland and in many national nuclear centers in the world.

NEW ZEALAND

Institute of Nuclear Sciences. Copies are available from Librarian, N. Z. Institute of Nuclear Sciences, D.S.I.R., Private Bag, Lower Hutt, New Zealand. Copies are deposited in other countries.

PAKISTAN

Atomic Energy Center. Copies are available from Atomic Energy Center, P. O. Box 658, Lahore, (West Pakistan).

POLAND

Reports of the Polish nuclear institutes are published by the Nuclear Energy Information Center of the Government Commissioner for Use of Nuclear Energy. Copies are available free of charge from Nuclear Energy Information Center, Palace of Culture and Science, Warsaw, Poland.

SPAIN

Junta de Energia Nuclear. "JEN" reports are available without charge from Servicio de Documentation, Junta de Energia Nuclear, Ciudad Universitaria, Madrid (3), España.

SWITZERLAND

Eidgenössisches Institut für Reaktorforschung. "EIR" reports are available from Eidgenössisches Institut für Reaktorforschung, c/o Bibliothek, 5303 Würenlingen/Switzerland.

TURKEY

Turkish Atomic Energy Commission. Copies are available free of charge from T.A.E.C., Çekmece Nuclear Research Center, P. O. Box 1, Airport, Istanbul, Turkey.

Conferences

Published conference proceedings as well as individual unpublished papers from conferences are included in this index. A CONF number is assigned to the conference if published proceedings are received and also if only a single paper is received. The base number used is year-month-sequence. Thus, the number CONF-650101 indicates that the conference was held in 1965, in January, and that this was the first January 1965 conference so received. This number would be assigned to complete published proceedings. If individual papers are received, the base number is extended to include a paper number, e.g., CONF-650101-1. As additional papers are received, they will be assigned consecutive numbers in the series, CONF-650101-1, CONF-650101-2, etc. This numbering system ensures that all papers received from a conference will be associated with that conference in this index.

If published proceedings are received after the receipt of individual papers, the complete proceedings will be abstracted and the abstract number will appear in this index with the base CONF number.

Abbreviations Used in Availability Column

AECL	Reports of the Atomic Energy of Canada Limited are for sale by the Scientific Document Distribution Office, Atomic Energy of Canada Limited, Chalk River, Ontario, Canada.
CFSTI	See NTIS
DENM	Reports of the Atomic Energy Commission Research Establishment, Risö, are available on exchange from the Library, Danish Atomic Energy Commission, Risö, Roskilde, Denmark. Also for sale at the price shown from Jul. Gjellerup, Booksellers, 87 Sölvgade, Kobenhavn K., Denmark. Reports of Danatom are available on loan from Research Establishment, Risö, Roskilde, Denmark. Copies are available from Danatom, Aurehojvej 2, Hellerup, Denmark.
Dep.	AEC reports so designated are maintained in the organizations listed on the inside front cover of *NSA*. Prior to July 1, 1965, reports were deposited either in printed copy form or in microform. After that time, all reports have been in the form of micronegatives. Reports from other countries so designated are available in the United States at the organizations listed on the inside front cover of *NSA*.

DTIE — Available from the U. S. Atomic Energy Commission, Division of Technical Information Extension, P. O. Box 62, Oak Ridge, Tennessee 37830. (Conference papers are available on loan only.)

EM — Blueprints of AEC engineering drawings are available from NTIS, U. S. Department of Commerce, Springfield, Virginia 22151. Current prices of the CAPE-packages may be obtained from this address. TID-4100, available from the Division of Technical Information Extension, P. O. Box 62, Oak Ridge, Tennessee 37830, contains information on all the CAPE-packages for sale.

EUR — For sale by Centrale de vente des publications des Communautés européennes 37, rue Glesener-Luxembourg.

GPO — For sale by the Superintendent of Documents, Government Printing Office, Washington, D. C. 20402.

IAEA — Available from the International Atomic Energy Agency, Vienna, Austria, and from its sales agencies in various countries throughout the world. A list of these agencies is found in each STI/DOC and STI/PUB publication.

NORW — Reports from Forsvarets Forskningsinstitutt are available from Norwegian Defense Research Establishment, Library, P. O. Box 25, Kjeller, Norway.
"KR" reports are available on an exchange basis from the Library, Institutt for Atomenergi, Box 40, Kjeller, Norway.
Reports of the Norwegian Reactor School are available from the Library, Institutt for Atomenergi, P. O. Box 40, Kjeller, Norway.

NRC — For sale by the National Research Council of Canada, Ottawa, Ontario, Canada.

NTIS — For sale by the National Technical Information Service (NTIS), U. S. Department of Commerce, Springfield, Virginia 22151 at the following prices for eye legible copy:

1–300 pages	$3.00
301–600 pages	$6.00
601–900 pages	$9.00

Documents over 900 pages have special prices which may be obtained from NTIS. Microfiche copy of each separately bound document can be purchased for $0.95.

Reports issued by organizations outside the United States will be sold by NTIS *only to purchasers within the United States.*
Purchasers outside the United States may acquire such reports from the sources described elsewhere in these columns.

OECD — Available from O. E. C. D., Publications 2, rue, André-Pascal, 75 Paris 16^{e}, France, and from its sales agencies in various countries throughout the world. A list of these agencies is found in each OECD publication.

SWED — "AE" reports are for sale from Aktiebolaget Atomenergi, Library Section, Box 43041, Stockholm 43, Sweden. Microcopy of these reports is available from the International Documentation Center, Turnba, Sweden.
Reports of the VDDIT-series may be obtained from Aktiebolaget Atomenergi, Information Office, Scientific and Technical Information, Box 43041, Stockholm 43, Sweden.
Other series are not generally available to the public. Organizations in the Atomic Energy field may obtain copies from Aktiebolaget Atomenergi.

UK — United Kingdom Atomic Energy Authority reports generally may be purchased from Her Majesty's Stationery Office, P. O. Box 569, London S.E.1. Copies of many UKAEA reports (particularly earlier ones) may be purchased in microcopy form from Micro Methods Ltd., East Ardsley, Wakefield, Yorkshire, England. Copies of UKAEA reports are deposited with the National Lending Library for Science and Technology and 10 public libraries in England; with the USAEC and (through USAEC) with NTIS; and in most national nuclear centers throughout the world. In the USA, UKAEA reports are available on a subscription basis, by subject category, from UNIPUB, Inc., P. O. Box 433, New York, N. Y. 10016, USA.

UN — Mail orders should be directed to the Sales Section, Room 1059, United Nations Headquarters, New York, New York 10017.

ZAED — Available from Zentralstelle für Atomkernenergie Dokumentation, 6000 Frankfurt/Main 90, P. O. Box 901069, Westendstr. 21, West Germany

XUM

Report No.	Abstract No.	Availability
AAEC/TM-	(Australian)	
542	25-3591	Dep. NTIS (U. S. Sales Only)
545	25-3712	Dep. NTIS (U. S. Sales Only)
547	25-2383	Dep. NTIS (U. S. Sales Only)
AD-	(Misc.)	
464715	25-2657	NTIS
704484	25-3558	CFSTI
706587	25-2432	NTIS
707256	25-2857	NTIS
707709	25-2414	NTIS
708547	25-3204	NTIS
709200	25-2948	NTIS
709359	25-2949	NTIS
709363	25-2950	NTIS
709723	25-2951	NTIS
AEC-tr-		
7095	25-2658	Dep. NTIS
7096	25-2603	Dep. NTIS
AECL-	(Canadian)	
3414	25-3865	Dep. NTIS (U. S. Sales Only). AECL $1.00
3633	25-3667	Can. J. Phys.; 48: 1933-5 (15 Aug 1970)
3648	25-2230	Can. J. Chem.; 48: 2809-13(15 Sep 1970)
3696	25-2287	Can. J. Chem.; 48: 3029-33(1 Oct 1970)
AED-C-	(Non-AEC)	
12-22	25-2399	Dep. NTIS (U. S. Sales Only)
AEEW-M-	(British)	
905	25-2472	Dep. NTIS (U. S. Sales Only). UK 4s. 6d
AERE-M-	(British)	
1862	25-3886	See DP-Report-571
AERE-R-	(British)	
5219	25-3774	See DP-Report-439
6318	25-2473	Dep. NTIS (U. S. Sales Only). UK 2s. 6d
6525	25-3645	Dep. NTIS (U. S. Sales Only). UK 1s. 2d
6532	25-3048	Dep. NTIS (U. S. Sales Only). UK 2s. 6d
AFCRL-	(Non-AEC)	
70-214	25-2857	See AD-707256
70-280	25-2949	See AD-709359
70-334	25-2950	See AD-709363
AFCRL-ERP-	(Non-AEC)	
322	25-2949	See AD-709359
324	25-2950	See AD-709363
AFCRL-Trans-	(Non-AEC)	
75	25-2857	See AD-707256
AI-AEC-		
12981	25-2500	Dep. NTIS
ANL-		
7442	25-3901	Dep. NTIS
7696	25-3922	Dep. NTIS
7735	25-2306	Dep. NTIS
ANL-Trans-		
862	25-3934	Dep. NTIS
ARH-		
1819	25-2415	Dep. NTIS
ARH-SA-		
67	25-2416	Dep. NTIS
AWRE-O-	(British)	
45/70	25-3559	Dep. NTIS (U. S. Sales Only). UK 7s
BDX-		
613-170	25-2818	Dep. NTIS
BMI-	(Misc.)	
1885	25-2754	Dep. NTIS
BNL-		
50258	25-2600	Dep. NTIS
BNL-tr-		
354	25-3935	Dep. CFSTI
BNWL-		
1412	25-3923	Dep. CFSTI
1514	25-3902	Dep. NTIS
BNWL-B-		
8	25-3920	Dep. NTIS
BNWL-SA-		
3287	25-2417	Dep. NTIS
3360	25-3892	Dep. NTIS
CALT-		
822-16	25-3936	Dep. NTIS
CEA-CONF-	(French)	
1579	25-2384	Dep. NTIS (U. S. Sales Only)
1595	25-3052	Dep. NTIS (U. S. Sales Only)
1597	25-3053	Dep. NTIS (U. S. Sales Only)
1598	25-3117	Dep. NTIS (U. S. Sales Only)
1601	25-3144	Dep. NTIS (U. S. Sales Only)
1607	25-3145	Dep. NTIS (U. S. Sales Only)
1608	25-3146	Dep. CFSTI (U. S. Sales Only)
1610	25-3109	Dep. NTIS (U. S. Sales Only)
1611	25-3054	Dep. NTIS (U. S. Sales Only)
1612	25-3147	Dep. NTIS (U. S. Sales Only)
1614	25-3148	Dep. NTIS (U. S. Sales Only)
1616	25-3149	Dep. NTIS (U. S. Sales Only)
1623	25-2400	Dep. NTIS (U. S. Sales Only)
1625	25-2638	Dep. NTIS (U. S. Sales Only)
1627	25-3075	Dep. NTIS (U. S. Sales Only)
1628	25-3061	Dep. NTIS (U. S. Sales Only)
1633	25-2841	Dep. NTIS (U. S. Sales Only)
1638	25-2756	Dep. NTIS (U. S. Sales Only)
CEA-N-	(French)	
1312	25-3525	Dep. CFSTI (U. S. Sales Only)
1316	25-2307	Dep. NTIS (U. S. Sales Only)
1333	25-3713	Dep. CFSTI (U. S. Sales Only)
1348	25-3903	Dep. NTIS (U. S. Sales Only)
1379	25-3866	Dep. NTIS (U. S. Sales Only)
CEA-R-	(French)	
3845	25-2308	Dep. NTIS (U. S. Sales Only)
3953	25-2794	For translation see CRNL-tr-2388
4046	25-2257	Dep. NTIS (U. S. Sales Only)
4063	25-2433	Dep. NTIS (U. S. Sales Only)
CERN-	(European Organization for Nuclear Research)	
70-27	25-2434	Dep. NTIS (U. S. Sales Only)
CNAEM-	(Turkish)	
73	25-3924	Dep. NTIS (U. S. Sales Only)
CNEA-	(Argentinean)	
271	25-2062	Dep. NTIS (U. S. Sales Only)
275	25-3646	Dep. NTIS (U. S. Sales Only)
276	25-2063	Dep. NTIS (U. S. Sales Only)
CONF-631012-	(Dragon Project Engineering Symposium, Bournemouth, England, Oct. 21-23, 1963)	
11	25-2385	See DP-Report-230
CONF-641031-	(Symposium on Basic Research, Harwell, England, Oct. 19-21, 1964)	
9	25-2812	See DP-Report-320
CONF-670723-	(Defense Atomic Support Agency Effects Conference, Columbus, Ohio, July 11-13, 1967)	
2	25-3974	See SC-R-68-1784
CONF-680619-	(Meeting on Accurate Determination of X-Ray Intensities and Structure Factors, Cambridge, England, June 24-26, 1968)	
	25-3216	Acta Crystallogr., Sect. A; 25: 1-276(1 Jan 1969)
CONF-680668-	(Meeting on Uses of Activation Analysis in Studies of Mineral Element Metabolism in Man, Teheran, Iran, June 3-7, 1968)	
	25-2122	See IAEA-122
CONF-680671-	(9th Symposium on Mass Motions in Solar Flares and Related Phenomena, Anacapri, Italy, June 10-12, 1968)	
	25-2862	New York; John Wiley and Sons, Inc. (1968). 245p. $22.00
CONF-681029-	(National Particle Accelerator Conference, Moscow, U.S.S.R., Oct. 9-16, 1968)	
(Vol.1)	25-3484	Moscow; Vsesoyuznyi Institut Nauchnoi i Tekhnicheskoi Informatsii (1970). 684p
(Vol.2)	25-3485	Moscow; Vsesoyuznyi Institut Nauchnoi i Tekhnicheskoi Informatsii (1970). 596p
CONF-681137-	(Symposium on Technological and Industrial Uses of Labeled Atoms and Applications of Nuclear-Physics Methods for Analysis of Materials, Poznan, Poland, Nov. 12--15, 1968)	
	25-2141	Warszawa; Osrodek Informacji o Energii Jadrowej (1969). 477p
CONF-681138-	(Symposium on Computers in Analytical Chemistry, New York, N. Y., Nov. 13-15,	

Report No.	Abstract No.	Availability
		1968)
	25-2060	New York; Plenum Publishing Corporation (1970). 113p. $12.50
CONF-690348-		(10th Symposium on Engineering Aspects of Magnetohydrodynamics, Cambridge, Mass., Mar. 26-28, 1969)
	25-2945	Cambridge, Mass.; Massachusetts Institute of Technology (1969). 209p
CONF-690445-		(Convention Arranged by The Steam Plant Group, London, England, Apr. 23-25, 1969)
	25-3776	Proc. Inst. Mech. Eng. (London); 183: 1-162(1968--69)
CONF-690726-		(1st International Seminar for Hydrology Professors, Urbana, Ill., July 13-25, 1969)
(Vol.1)	25-2358	Urbana, Ill.; University of Illinois (1969). 511p
CONF-690918-		(Conference on Radioecology, Cadarache, France, Sept. 8-11, 1969)
(Vol.1)	25-2541	
CONF-690966-		(3rd Bolton Landing Conference on Ordered Alloys, Bolton Landing, N. Y., Sept. 8-10, 1969)
1	25-3941	See COO-1431-10
CONF-691007-		(Corrosion by Liquid Metals Conference, Philadelphia, Pa., Oct. 13-16, 1969)
	25-2615	New York; Plenum Publishing Corporation (1970). 625p. $29.00
CONF-691049-		(Dosimetry and Physics of Accelerator Shielding Conference, Dubna, U.S.S.R., Oct. 7-10, 1969)
	25-3476	See JINR-16-4888
CONF-691222-		(Meeting of The American Physical Society, Los Angeles, Calif., Dec. 29-31, 1969)
	25-2251	J. Appl. Phys.; 41: 4248-4378(Oct 1970)
CONF-700322-		(2nd Conference on the Use of Small Accelerators for Teaching and Research, Oak Ridge, Tenn., Mar. 23-25, 1970)
	25-3463	Dep. CFSTI
CONF-700324-		(26th Annual National Association of Corrosion Engineers, Philadelphia, Pa., Mar. 2-6, 1970)
	25-2633	Houston, Tex.; National Association of Corrosion Engineers (1970). 651p. $30.00
CONF-700329-		(Meeting of the American Physical Society, Dallas, Tex., Mar. 23-26, 1970)
	25-2251	J. Appl. Phys.; 41: 4248-4378(Oct 1970)
CONF-700403-		(8th Rare Earth Conference, Reno, Nev., Apr. 19-22, 1970)
8	25-2193	
CONF-700610-		(4th International Congress of Radiation Research, Evian, France, June 29-July 4, 1970)
10	25-2260	See IRI-133-70-2
CONF-700614-		(Symposium on Thermonuclear Fusion Reactor Design, Lubbock, Tex., June 2-5, 1970)
	25-3130	See ORO-1171-1
CONF-700627-		(4th International Conference on Resonant Particles, Athens, Ohio, June 15-17, 1970)
1	25-3272	See UCRL-20050
CONF-700701-		(IAEA Symposium on Progress in Safeguards Techniques, Karlsruhe, Germany, July 6-10, 1970)
5	25-3649	See KFK-1214
6	25-2417	See BNWL-SA-3287
CONF-700703-		(22nd Congress of the Brazilian Society for Science Progress, Salvador, Brazil, July 1970)
	25-3186	Notas Fis., Cent. Brasil. Pesqui. Fis.; 16: 1-73(Jul 1970)
CONF-700706-		(5th Plasma Physics Symposium, Herceg-Novi, Yugoslavia, July 6-16, 1970)
1	25-3075	See CEA-CONF-1627
2	25-3061	See CEA-CONF-1628
CONF-700707-		(International Meeting on Solar Cells, Toulouse, France, July 6-10, 1970)
1	25-2400	See CEA-CONF-1623
CONF-700801-		(10th International Conference on the Physics of Semiconductors, Cambridge, Mass., Aug. 17-21, 1970)
	25-3185	Dep. NTIS
CONF-700806-		(15th International Conference on High Energy Physics, Kiev, U.S.S.R., Aug. 26-Sept. 4, 1970)
43	25-3272	See UCRL-20050
CONF-700815-		(Conference on the Properties of Nuclei Far from the Region of Beta-Stability, Leysin, Switzerland, Aug. 31-Sept. 4, 1970)
3	25-3652	See UCRL-19957
5	25-3648	See JINR-E7-5319
CONF-700816-		(11th AEC Air Cleaning Conference, Richland, Wash., Aug. 31-Sept. 3, 1970)
5	25-3892	See BNWL-SA-3360
CONF-700817-		(4th European Conference on Controlled Fusion and Plasma Physics, Rome, Italy, Aug. 31-Sept. 4-19, 1970)
2	25-3148	See CEA-CONF-1614
4	25-3147	See CEA-CONF-1612
5	25-3054	See CEA-CONF-1611
6	25-3109	See CEA-CONF-1610
10	25-3145	See CEA-CONF-1607
11	25-3146	See CEA-CONF-1608
16	25-3144	See CEA-CONF-1601
18	25-3053	See CEA-CONF-1597
19	25-3117	See CEA-CONF-1598
20	25-3052	See CEA-CONF-1595
22	25-3149	See CEA-CONF-1616
CONF-700819-		(2nd International Conference on the Strength of Metals and Alloys, Pacific Grove, Calif., Aug. 30-Sept. 4, 1970)
6	25-3988	See UCRL-19601
CONF-700825-		(Symposium I.A.U. on New Techniques in Space Astronomy, Garching, Germany, Aug. 10-14, 1970)
1	25-2841	See CEA-CONF-1633
CONF-700826-		(Conference on Hybrid Computation, Munich, Germany, Aug. 31-Sept. 4, 1970)
1	25-2384	See CEA-CONF-1579
CONF-700920-		(International Meeting on Fast Reactor Fuel and Fuel Elements, Karlsruhe, Germany, Sept. 28-30, 1970)
1	25-2756	See CEA-CONF-1638
CONF-700921-		(12th International Conference on Low Temperature Physics, Kyoto, Japan, Sept. 4-10, 1970)
1	25-3205	See UCRL-19681
2	25-3990	See UCRL-19686
CONF-700922-		(6th International Conference on Metal Spraying, Paris, France, Sept. 14-19, 1970)
1	25-2638	See CEA-CONF-1625
CONF-700923-		(International Conference on the Science and Technology of Steel, Tokyo, Japan, Sept. 7-11, 1970)
1	25-3938	See COO-1198-753
CONF-701002-		(EANDC Symposium on Neutron Standards and Flux Normalization, Argonne, Ill., Oct. 21-23, 1970)
1	25-2435	See RPI-328-202
CONF-701103-		(63rd National Meeting of the American Institute of Chemical Engineers, Chicago, Ill., Nov. 29--Dec. 3, 1970)
3	25-2416	See ARH-SA-67
CONF-701104-		(16th Annual Conference on Magnetism and Magnetic Materials, Miami Beach, Fla., Nov. 17-20, 1970)
2	25-4000	See UCRL-72587(Rev.1)
CONF-701105-		(Conference on Continuum Aspects of Graphite Design, Gatlinburg, Tenn., Nov. 9-12, 1970)
(Absts.)	25-2793	See ORNL-TM-3191
COO-		
651-78	25-3782	See DOCKET-1151-3
716-66	25-2803	Dep. NTIS
873-28	25-2551	Dep. CFSTI
958-19	25-3937	Dep. NTIS
1053-14	25-3189	Dep. NTIS
1053-15	25-3190	Dep. NTIS
1120-106	25-3592	Dep. NTIS
1190-580	25-2095	Advan. X-ray Anal.; 12: 563-80(1969)

XUM

Report No.	Abstract No.	Availability
1198-753	25-3938	Dep. NTIS
1247-21	25-3939	Dep. NTIS
1248-22	25-3940	Dep. NTIS
1265-88	25-3636	Phys. Rev., C; 2: 1063-70(Sep 1970)
1431-10	25-3941	Dep. NTIS
1530-21	25-3593	Dep. NTIS
1569-67	25-3942	Dep. NTIS
1680-10	25-3943	Dep. NTIS
1700-12	25-3220	Dep. NTIS
1746-46	25-3647	Dep. CFSTI
1758-26	25-3944	Dep. NTIS
1758-27	25-3945	Dep. NTIS
1761-13	25-3946	Dep. NTIS
1761-14	25-3947	Dep. NTIS
CSIRO-Trans-	(Australian)	
9924	25-2766	Dep. NTIS (U. S. Sales Only)
10140	25-2347	Dep. NTIS (U. S. Sales Only)
10207	25-2869	Dep. NTIS (U. S. Sales Only)
DESY-	(German)	
70/45	25-3308	Dep. NTIS (U. S. Sales Only)
70/46	25-3309	Dep. NTIS (U. S. Sales Only)
70/48	25-3948	Dep. NTIS (U. S. Sales Only)
70/49	25-3356	Dep. NTIS (U. S. Sales Only)
70/50	25-3310	Dep. NTIS (U. S. Sales Only)
DMIC-Memo-	(Non-AEC)	
203	25-2657	See AD-464715
DOCKET-1151-	(Elk River Reactor) (AEC)	
3	25-3782	Dep. CFSTI
DOCKET-1155-	(LaCrosse Boiling Water Reactor) (AEC)	
84	25-3805	Dep. NTIS
DOCKET-50003-	(Indian Point Station; See Also DOCKET-50247, DOCKET-50286) (Non-AEC)	
59	25-3806	Dep. NTIS
DOCKET-50010-	(Dresden Nuclear Power Station; See also DOCKET-50237 and DOCKET-50249) (Non-AEC)	
70	25-3807	Dep. NTIS
DOCKET-50029-	(Yankee Atomic Electric Co.) (Non-AEC)	
140	25-3783	Dep. NTIS
DOCKET-50133-	(Humboldt Bay Power Plant) (Non-AEC)	
42	25-3808	Dep. NTIS
DOCKET-50171-	(Peach Bottom Atomic Power Station; See also DOCKET-50277 and DOCKET-50278) (Non-AEC)	
58	25-3784	Dep. NTIS
DOCKET-50201-	(West Valley Reprocessing Plant--Formerly Spent Fuel Processing Plant) (Misc.)	
55	25-2309	Dep. NTIS
DOCKET-50206-	(San Onofre Nuclear Generating Station) (Non-AEC)	
94	25-3785	Dep. NTIS
95	25-3809	Dep. NTIS
96	25-3810	Dep. NTIS
97	25-3786	Dep. NTIS
DOCKET-50213-	(Connecticut Yankee Atomic Power Plant) (Misc.)	
82	25-3787	Dep. NTIS
83	25-3811	Dep. NTIS
84	25-3788	Dep. NTIS
85	25-3812	Dep. NTIS
DOCKET-50219-	(Oyster Creek Nuclear Power Plant) (Non-AEC)	
115	25-3813	Dep. NTIS
DOCKET-50220-	(Nine Mile Point Nuclear Station) (Non-AEC)	
52	25-3814	Dep. NTIS
DOCKET-50237-	(Dresden Nuclear Power Station, See also DOCKET-50249) (Non-AEC)	
85	25-3815	Dep. NTIS
86	25-3816	Dep. NTIS
87	25-3817	Dep. NTIS
DOCKET-50238-	(N.S. Savannah Safety Assessment) (Non-AEC)	
74	25-3917	Dep. NTIS
DOCKET-50245-	(Millstone Point Nuclear Power Station) (Non-AEC)	
42	25-3789	Dep. NTIS
DOCKET-50247-	(Indian Point Nuclear Generating; See also DOCKET-50286) (Non-AEC)	
42	25-3818	Dep. NTIS
43	25-3819	Dep. NTIS
44	25-3820	Dep. NTIS
DOCKET-50249-	(Dresden Nuclear Power Station; See also DOCKET-50237) (Non-AEC)	
43	25-3821	Dep. NTIS
DOCKET-50250-	(Turkey Point, See also DOCKET-50251) (Non-AEC)	
35	25-3822	Dep. NTIS
DOCKET-50251-	(Turkey Point, See also DOCKET-50250) (Non-AEC)	
33	25-3822	See DOCKET-50250-35
DOCKET-50254-	(Quad-Cities Station; See also DOCKET-50265) (Non-AEC)	
22	25-3823	Dep. NTIS
23	25-3824	Dep. NTIS
24	25-3825	Dep. NTIS
25	25-3826	Dep. NTIS
DOCKET-50259-	(Browns Ferry Nuclear Power Station. See also DOCKET-50260 and DOCKET-50296) (Non-AEC)	
20	25-3827	Dep. NTIS
DOCKET-50260-	(Browns Ferry Nuclear Power Station. See also DOCKET-50259 and DOCKET-50296) (Non-AEC)	
20	25-3827	See DOCKET-50259-20
DOCKET-50261-	(H. B. Robinson) (Non-AEC)	
46	25-3828	Dep. NTIS
DOCKET-50265-	(Quad-Cities Station; See also DOCKET-50254) (Non-AEC)	
18	25-3823	See DOCKET-50254-22
19	25-3824	See DOCKET-50254-23
20	25-3825	See DOCKET-50254-24
21	25-3826	See DOCKET-50254-25
DOCKET-50266-	(Point Beach Nuclear Plant) (Non-AEC)	
32	25-3829	Dep. NTIS
33	25-3830	Dep. NTIS
34	25-3831	Dep. NTIS
35	25-3832	Dep. NTIS
DOCKET-50267-	(Fort St. Vrain Nuclear Generating Station) (Non-AEC)	
23	25-3833	Dep. NTIS
DOCKET-50269-	(Oconee Nuclear Station, See also DOCKET-50270, and DOCKET-50287) (Non-AEC)	
28	25-3834	Dep. NTIS
DOCKET-50270-	(Oconee Nuclear Station, See also DOCKET-50269, and DOCKET-50287) (Non-AEC)	
28	25-3834	See DOCKET-50269-28
DOCKET-50271-	(Vermont Yankee Nuclear Power Station) (Non-AEC)	
34	25-3835	Dep. NTIS
DOCKET-50287-	(Oconee Nuclear Station; see also DOCKET-50269 and DOCKET-50270) (Non-AEC)	
25	25-3834	See DOCKET-50269-28
DOCKET-50296-	(Browns Ferry Nuclear Power Station. See also DOCKET-50259 and DOCKET-50260) (Non-AEC)	
19	25-3827	See DOCKET-50259-20
DOCKET-50309-	(Maine Yankee Atomic Power Company) (Non-AEC)	
24	25-3836	Dep. NTIS
25	25-3837	Dep. NTIS
DOCKET-50317-	(Calvert Cliffs Nuclear Power Plant, See also DOCKET-50318) (Non-AEC)	
20	25-3838	Dep. NTIS
DOCKET-50318-	(Calvert Cliffs Nuclear Power Plant, See also DOCKET-50317) (Non-AEC)	
20	25-3838	See DOCKET-50317-20
DOCKET-50324-	(Brunswick Steam Electric Plant, Units 1 and 2, See also DOCKET-50325) (Non-AEC)	
17	25-3839	Dep. NTIS
DOCKET-50325-	(Brunswick Steam Electric Plant, Units 1 and 2, See also DOCKET-50324) (Non-AEC)	
17	25-3839	See DOCKET-50324-17
DOCKET-50329-	(Midland Plant; see also DOCKET-50330) (Non-AEC)	
24	25-3840	Dep. NTIS
DOCKET-50330-	(Midland Plant; see also DOCKET-50329) (Non-AEC)	
23	25-3840	See DOCKET-50329-24
DOCKET-50338-	(North Anna Power Station; See also DOCKET-50339) (Non-AEC)	
26	25-3841	Dep. NTIS
DOCKET-50339-	(North Anna Power Station; See also DOCKET-50338) (Non-AEC)	
25	25-3841	See DOCKET-50338-26

Report No.	Abstract No.	Availability
DOCKET-50341-	(Enrico Fermi Atomic Power Plant) (Non-AEC)	
21	25-3842	Dep. NTIS
DOCKET-50344-	(Trojan Nuclear Plant) (Non-AEC)	
18	25-3843	Dep. NTIS
DOCKET-50346-	(Davis-Besse Nuclear Power Station) (Non-AEC)	
18	25-3844	Dep. NTIS
DOCKET-50348-	(Joseph M. Farley Nuclear Plant, Units 1 and 2, Formerly Seala Nuclear Plant, See also DOCKET-50364) (Non-AEC)	
14	25-3845	Dep. NTIS
DOCKET-50352-	(Limerick Generating Station) (See also DOCKET-50353) (Non-AEC)	
9	25-3846	Dep. NTIS
DOCKET-50353-	(Limerick Generating Station) (See also DOCKET-50352) (Non-AEC)	
9	25-3846	See DOCKET-50352-9
DOCKET-50354-	(Newbold Island Nuclear Generating Station) (See also DOCKET-50355) (Non-AEC)	
9	25-3847	Dep. NTIS
DOCKET-50355-	(Newbold Island Nuclear Generating Station) (See also DOCKET-50354) (Non-AEC)	
9	25-3847	See DOCKET-50354-9
DOCKET-50358-	(Wm. H. Zimmer Nuclear Power Station, Units 1 and 2) (See also DOCKET-50359) (Non-AEC)	
8	25-3848	Dep. NTIS
DOCKET-50359-	(Wm. H. Zimmer Nuclear Power Station, Units 1 and 2) (See also DOCKET-50358) (Non-AEC)	
7	25-3848	See DOCKET-50358-8
DOCKET-50361-	(San Onofre Nuclear Generating Station) (Units 2 and 3) (See also Docket-50362) (Docket-50206) (Unit 1) (Non-AEC)	
11	25-3849	Dep. NTIS
DOCKET-50362-	(San Onofre Nuclear Generating Station) (Units 2 and 3) (See also Docket-50361) (Docket-50206) (Unit 1) (Non-AEC)	
10	25-3849	See DOCKET-50361-11
DOCKET-50364-	(Joseph M. Farley Nuclear Plant, Units 1 and 2, See also DOCKET-50348) (Non-AEC)	
8	25-3845	See DOCKET-50348-14
DOCKET-50373-	(LaSalle County Station Units 1 and 2) (See also DOCKET-50374) (Non-AEC)	
6	25-3850	Dep. NTIS
DOCKET-50374-	(LaSalle County Station Units 1 and 2) (See also DOCKET-50373) (Non-AEC)	
6	25-3850	See DOCKET-50373-6
DP-		
1238	25-3925	Dep. NTIS
DP-Report-	(British)	
230	25-2385	Dep. NTIS
320	25-2812	Dep. NTIS
378	25-2767	Dep. CFSTI (U. S. Sales Only)
438	25-3790	Dep. NTIS
439	25-3774	Dep. NTIS
447	25-2258	Dep. NTIS
466	25-3883	Dep. NTIS
469	25-3884	Dep. NTIS
474	25-3791	Dep. NTIS
476	25-3867	Dep. NTIS
477	25-3868	Dep. NTIS
478	25-3869	Dep. NTIS
483	25-3792	Dep. NTIS
486	25-3858	Dep. NTIS
487	25-3882	Dep. NTIS
488	25-3793	Dep. NTIS
491	25-3860	Dep. NTIS
494	25-2064	Dep. NTIS
497	25-3870	Dep. NTIS
531	25-3794	Dep. NTIS
538	25-3871	Dep. NTIS
539	25-3775	Dep. NTIS
546	25-3885	Dep. NTIS
552	25-3861	Dep. NTIS
553	25-3862	Dep. NTIS
554	25-3863	Dep. NTIS
559	25-3872	Dep. NTIS
561	25-3795	Dep. NTIS
569	25-2151	Dep. NTIS
571	25-3886	Dep. NTIS
573	25-3873	Dep. NTIS
575	25-3887	Dep. NTIS
579	25-3796	Dep. NTIS
581	25-3888	Dep. NTIS
582	25-3889	Dep. NTIS
591	25-3897	Dep. NTIS
592	25-3890	Dep. NTIS
595	25-3874	Dep. NTIS
DUN-SA-		
144	25-3921	Dep. NTIS
E-	(Misc.)	
5615	25-2664	See N-70-32146
5623	25-2237	See N-70-32826
EANDC(UK)-	(European-American Nuclear Data Committee)	
130-AL	25-3645	See AERE-R-6529
ECOM-	(Non-AEC)	
3281	25-3204	See AD-708547
EIR-	(Swiss)	
166	25-3926	Dep. NTIS (U. S. Sales Only)
EUR-	(European Atomic Energy Community)	
4153	25-3856	See KFK-851
4318	25-3875	See EURFNR-834
EURFNR-	(European Atomic Energy Community)	
834	25-3875	Dep. NTIS (U. S. Sales Only)
GA-	(Misc.)	
9203	25-3949	Dep. NTIS
9952	25-3950	Dep. NTIS
10171	25-3891	See ORO-1171-1, pp 206-55
10208	25-2259	Dep. NTIS
GEAP-	(Misc.)	
11094	25-2502	Dep. NTIS
HUX-		
3780-29	25-3951	Dep. NTIS
3780-33	25-3952	Dep. NTIS
IAEA-	(International Atomic Energy Agency)	
122	25-2122	
IFVE-SEF-	(Russian)	
69-59	25-3447	Dep. NTIS (U. S. Sales Only)
IFVE-STF-	(Russian)	
69-71	25-3406	Dep. NTIS (U. S. Sales Only)
69-102	25-3420	Dep. NTIS (U. S. Sales Only)
IITRI-	(Misc.)	
578-P-21-39	25-3893	Dep. NTIS
IJS-	(Yugoslavian)	
571	25-3904	Dep. NTIS (U. S. Sales Only)
IN-		
1410	25-3953	Dep. NTIS
1420	25-3226	Dep. NTIS
1425	25-3110	Dep. NTIS
1441	25-3905	Dep. NTIS
INFN-PD-	(Italian)	
70/2	25-3270	Dep. NTIS (U. S. Sales Only)
INP-	(Polish)	
707	25-2475	Dep. NTIS (U. S. Sales Only)
INR-	(Non-AEC)	
1180	25-2497	Dep. CFSTI (U. S. Sales Only)
INS-TCA-	(Japanese)	
26	25-2484	Dep. NTIS (U. S. Sales Only)
IPPJ-	(Japanese)	
93	25-3150	Dep. NTIS (U. S. Sales Only)
94	25-3151	Dep. NTIS (U. S. Sales Only)
95	25-3128	Dep. NTIS (U. S. Sales Only)
100	25-3055	Dep. NTIS (U. S. Sales Only)
IPST-Cat.-	(Russian)	
5653	25-2658	See AEC-tr-7095
5655	25-2603	See AEC-tr-7096
IRB-TP-	(Yugoslavian)	
2-70	25-3352	Dep. NTIS (U. S. Sales Only)
IRI-	(Dutch)	
133-70-2	25-2260	Dep. NTIS (U. S. Sales Only)
IS-		
2389	25-3954	Dep. NTIS
2416	25-3955	Dep. NTIS
IS-T-		
383	25-3956	Dep. NTIS
384	25-3957	Dep. NTIS
388	25-3958	Dep. NTIS
390	25-3959	Dep. NTIS
399	25-3960	Dep. NTIS
401	25-2804	Dep. NTIS
406	25-3961	Dep. NTIS

XUM

Report No.	Abstract No.	Availability
410	25-3962	Dep. NTIS
411	25-2310	Dep. NTIS
412	25-2311	Dep. NTIS
423	25-3963	Dep. NTIS
ITF-	(Russian)	
70-32	25-3292	Dep. NTIS (U. S. Sales Only)
70-33	25-3433	Dep. NTIS (U. S. Sales Only)
70-35	25-3714	Dep. NTIS (U. S. Sales Only)
70-49	25-3451	Dep. NTIS (U. S. Sales Only)
70-59	25-3332	Dep. NTIS (U. S. Sales Only)
70-65	25-3377	Dep. NTIS (U. S. Sales Only)
70-77	25-3378	Dep. NTIS (U. S. Sales Only)
JAERI-Memo-	(Japanese)	
4097	25-2660	Dep. NTIS (U. S. Sales Only)
4109	25-3927	Dep. NTIS (U. S. Sales Only)
4110	25-3928	Dep. NTIS (U. S. Sales Only)
4125	25-2661	Dep. NTIS (U. S. Sales Only)
4128	25-2813	Dep. NTIS (U. S. Sales Only)
4130	25-3906	Dep. NTIS (U. S. Sales Only)
JINR-	(Russian)	
16-4888	25-3476	
E1-5259	25-3379	Dep. NTIS (U. S. Sales Only)
E2-5329	25-3407	Dep. NTIS (U. S. Sales Only)
E7-5319	25-3648	Dep. NTIS (U. S. Sales Only)
P2-4944	25-3935	For translation see BNL-tr-354
P2-5263	25-3380	Dep. NTIS (U. S. Sales Only)
P2-5320	25-3381	Dep. NTIS (U. S. Sales Only)
P2-5343	25-3293	Dep. NTIS (U. S. Sales Only)
P2-5363	25-3434	Dep. NTIS (U. S. Sales Only)
P2-5373	25-3430	Dep. NTIS (U. S. Sales Only)
P13-5277	25-2485	Dep. NTIS (U. S. Sales Only)
P15-5156	25-3563	Dep. NTIS (U. S. Sales Only)
JUL-	(German)	
667-PP	25-3129	Dep. NTIS (U. S. Sales Only)
KFK-	(German)	
851	25-3856	Dep. NTIS (U. S. Sales Only)
927	25-2639	For translation see LIB/Trans-309
1070	25-2194	Dep. NTIS (U. S. Sales Only)
1158	25-2570	Dep. CFSTI (U. S. Sales Only)
1190	25-3564	Dep. NTIS (U. S. Sales Only)
1192	25-2419	Dep. NTIS (U. S. Sales Only)
1193	25-2662	Dep. NTIS (U. S. Sales Only)
1213	25-2765	Dep. NTIS (U. S. Sales Only)
1214	25-3649	Dep. NTIS (U. S. Sales Only)
1254	25-3875	See EURFNR-834
KFKI-	(Hungarian)	
70-12-RPT	25-3528	Dep. NTIS (U. S. Sales Only)
70-14-RPT	25-3529	Dep. NTIS (U. S. Sales Only)
70-19-HEP	25-3421	Dep. NTIS (U. S. Sales Only)
L-	(Misc.)	
6776	25-2883	See N-70-25499
LA-		
4360-TR	25-3964	Dep. NTIS
4452	25-2785	Dep. NTIS
4484	25-3530	Dep. CFSTI
4506	25-3531	Dep. NTIS
4507	25-3965	Dep. NTIS
4529	25-2065	Dep. NTIS
LCIE-	(French)	
342	25-2819	Dep. NTIS (U. S. Sales Only)
LF-	(Misc.)	
28	25-2219	See NP-18449
LIB/Trans-	(Australian)	
309	25-2639	Dep. NTIS (U. S. Sales Only)
LYCEN-	(French)	
7030	25-3650	Dep. NTIS (U. S. Sales Only)
7041	25-3544	Dep. NTIS (U. S. Sales Only)
7047	25-3545	Dep. NTIS (U. S. Sales Only)
7060	25-2128	Dep. NTIS (U. S. Sales Only)
7061	25-3085	Dep. NTIS (U. S. Sales Only)
7063	25-3477	Dep. NTIS (U. S. Sales Only)
7065	25-3111	Dep. NTIS (U. S. Sales Only)
MHSMP-		
15	25-3966	Dep. NTIS
MLM-		
1684	25-2663	Dep. NTIS
N-	(Misc.)	
70-25499	25-2883	NTIS
70-27167	25-2814	NTIS
70-32003	25-2858	NTIS
70-32146	25-2664	NTIS
70-32826	25-2237	NTIS
70-33138	25-2815	NTIS
70-33955	25-2952	NTIS
NASA-CR-	(Misc.)	
109850	25-2952	See N-70-33955

Report No.	Abstract No.	Availability
109851	25-2814	See N-70-27167
NASA-TM-X-	(Misc.)	
63965	25-2815	See N-70-33138
64526	25-2858	See N-70-32003
NASA-TN-D-	(Misc.)	
5724	25-2883	See N-70-25499
5875	25-2664	See N-70-32146
5880	25-2237	See N-70-32826
NBS-MON-	(Misc.)	
118	25-3715	GPO $0.50
NBS-SPEC. PUBL-	(Non-AEC)	
315-5	25-2665	GPO $0.75
NBS-TN-	(Misc.)	
532	25-2129	GPO $0.45
533	25-2130	GPO $1.00
NIM-	(Non-AEC)	
834	25-2066	Dep. NTIS (U. S. Sales Only)
906	25-2067	Dep. NTIS (U. S. Sales Only)
NLCO-		
1058	25-2640	Dep. NTIS
1071	25-2068	Dep. NTIS
NP-	(AEC File No. for Non-AEC Reports)	
18449	25-2219	Dep. CFSTI (U. S. Sales Only). Almquist and Wiksell Gamla Brogatan 26 Stockholm, Sweden Sw Cr 10: --
18462	25-3907	Dep. NTIS (U. S. Sales Only)
18464	25-3594	Dep. NTIS (U. S. Sales Only)
18468	25-2666	Dep. NTIS (U. S. Sales Only)
18476	25-3565	Dep. NTIS (U. S. Sales Only)
18485	25-3651	Dep. NTIS (U. S. Sales Only)
18490	25-2884	Dep. NTIS (U. S. Sales Only)
18491	25-2667	Dep. NTIS (U. S. Sales Only)
18518	25-2261	Dep. NTIS (U. S. Sales Only)
NRL-	(Misc.)	
7047	25-2414	See AD-707709
7121	25-2757	
NVO-		
410-2	25-2420	Dep. NTIS
NYO-		
2150-63	25-3967	Dep. NTIS
2171-323	25-3333	Dep. NTIS
2171-325	25-3968	Dep. NTIS
2391-121	25-3969	Dep. NTIS
3029-48	25-3019	Dep. NTIS
3250-53	25-3788	See DOCKET-50213-84
3270-43	25-3785	See DOCKET-50206-94
3794-11	25-3970	Dep. NTIS
3798-9	25-3971	Dep. NTIS
3906-4	25-2503	Dep. NTIS
3961-1	25-2348	Dep. NTIS
4204-3	25-3334	Dep. CFSTI
4204-4	25-3311	Dep. NTIS
4204-5	25-3294	Dep. NTIS
4204-6	25-3312	Dep. NTIS
4700(3rd Ed.)	25-2059	Dep. NTIS
ORNL-		
4551	25-3595	Dep. NTIS
4570	25-2601	Dep. NTIS
4572	25-2312	Dep. NTIS
4611	25-2806	Dep. NTIS
ORNL-AMPIC-		
13	25-2901	Dep. NTIS
ORNL-NDIC-		
8	25-3913	Dep. NTIS
ORNL-TM-		
2526(Add.)	25-2386	Dep. NTIS
2746	25-2387	Dep. NTIS
3110	25-2421	Dep. NTIS
3113	25-2410	Dep. NTIS
3142	25-3798	Dep. NTIS
3153	25-3716	Dep. NTIS
3168	25-3546	Dep. NTIS
3191	25-2793	Dep. NTIS
3204	25-2320	Dep. NTIS
3206	25-3020	Dep. NTIS
ORNL-tr-		
2388	25-2794	Dep. NTIS
2398	25-3972	Dep NTIS
ORO-		

XUM

Report No.	Abstract No.	Availability
1171-1	25-3130	Dep. NTIS
2909-9	25-2552	Dep. CFSTI
2968-52	25-2271	J. Phys. Chem.; 74: 4007-8(29 Oct 1970)
3519-4	25-2255	Radiat. Res.; 44: 50-8(Oct 1970)
3557-11	25-3135	See ORO-1171-1, pp 334-42
3634-3	25-2537	Progr. Med. Virol.; 11: 248-306(1969)
PATENTS	(British)	
1,204,316	25-3523	
1,205,115	25-2441	
1,206,385	25-2496	
1,206,712	25-2322	
1,208,024	25-2471	
1,208,521	25-2346	
1,208,877	25-2335	
1,209,223	25-2780	
1,210,057	25-2781	
1,210,609	25-2795	
1,210,778	25-2391	
1,210,800	25-2776	
1,211,211	25-2784	
1,211,315	25-2427	
PATENTS	(French)	
1,569,793	25-2340	
PATENTS	(U. S.)	
3,529,162	25-2499	
3,532,881	25-2357	
PEL-	(South African)	
201	25-2611	Dep. NTIS (U. S. Sales Only)
RCN-	(Dutch)	
123	25-3876	Dep. NTIS (U. S. Sales Only)
RD/B/M-	(British)	
1753	25-2388	Dep. NTIS (U. S. Sales Only)
RD/B/N-	(British)	
1279	25-2262	Dep. NTIS (U. S. Sales Only)
1748	25-2263	Dep. NTIS (U. S. Sales Only)
RFP-		
1070	25-2153	Ind. Eng. Chem., Prod. Res. Develop.; 8: 402-5(Dec 1969)
1515	25-3973	Dep. NTIS
1550	25-2646	Dep. NTIS
1582	25-2732	Dep. NTIS
RHEL/R-	(British)	
205	25-2486	Dep. NTIS (U. S. Sales Only). UK 7s
RLO-		
1388-126	25-3547	Dep. NTIS
RME-		
153	25-2372	Dep. GPO $1.75
154	25-2373	
155	25-2374	Dep. GPO $1.00
156	25-2375	Dep. GPO $1.50
158	25-2376	Dep. GPO $1.75
159	25-2377	Dep. GPO $1.00
RPI-	(Misc.)	
328-202	25-2435	Dep. NTIS
RT/PROT-	(Italian)	
(70)14	25-2108	Dep. NTIS (U. S. Sales Only)
SAL-	(Canadian)	
14	25-3566	
15	25-3567	
SAMSO-TR-	(Non-AEC)	
70-233	25-2948	See AD-709200
70-262	25-2951	See AD-709723
SC-R-		
68-1784	25-3974	Dep. NTIS
70-4351	25-2514	Dep. NTIS
SC-RR-		
70-561	25-3975	Dep. NTIS
70-645	25-3976	Dep. NTIS
70-695	25-2902	Dep. NTIS
SC-T-		
70-4039	25-2807	Dep. NTIS
70-4041	25-3977	Dep. NTIS
70-4043	25-3978	Dep. NTIS
SM-	(Misc.)	
133/33	25-3649	See KFK-1214
133/55	25-2417	See BNWL-SA-3287
STI/DOC-	(International Atomic Energy Agency)	
10/117	25-2367	IAEA $8.00
TID-		
25503	25-3596	Dep. CFSTI
25562	25-3979	Dep. NTIS
25573	25-2411	Dep. NTIS
TPJU-	(Polish)	
1/70	25-3382	Dep. NTIS (U. S. Sales Only)
2/70	25-3383	Dep. NTIS (U. S. Sales Only)
3/70	25-3384	Dep. NTIS (U. S. Sales Only)
12/70	25-3295	Dep. NTIS (U. S. Sales Only)
13/70	25-3435	Dep. NTIS (U. S. Sales Only)
TR-	(Misc.)	
59(6260-20)-4	25-2951	See AD-709723
66(5260-20)-18	25-2948	See AD-709200
TT-	(Misc.)	
70-50004	25-2658	See AEC-tr-7095
70-50005	25-2603	See AEC-tr-7096
UCI-		
34-P-149-1	25-3261	Dep. NTIS
UCLA-		
10-P-14-90	25-3980	Dep. NTIS
10-P-14-94	25-3981	Dep. NTIS
10-P-14-X-56	25-3982	Dep. NTIS
12-793	25-3983	Dep. NTIS
12-794	25-3984	Dep. NTIS
12-795	25-3985	Dep. NTIS
12-796	25-3986	Dep. NTIS
UCRL-		
14248(Rev. 1)	25-3987	Dep. NTIS
19601	25-3988	Dep. NTIS
19665	25-3989	Dep. NTIS
19681	25-3205	Dep. NTIS
19686	25-3990	Dep. NTIS
19809	25-3271	Dep. NTIS
19957	25-3652	Dep. NTIS
20050	25-3272	Dep. NTIS
20303	25-3991	Dep. NTIS
20309	25-3992	Dep. NTIS
50874	25-3993	Dep. NTIS
50892(Vol. 2)	25-2504	Dep. NTIS
50892(Vol. 4)(Pt.5)	25-2505	Dep. NTIS
50898	25-2381	Dep. NTIS
50909	25-3994	Dep. NTIS
50921	25-3995	Dep. NTIS
50922	25-2506	Dep. NTIS
50926	25-3996	Dep. NTIS
50927	25-3997	Dep. NTIS
50930	25-3998	Dep. NTIS
50931(Pt.1)	25-3999	Dep. NTIS
72479	25-3133	See ORO-1171-1, pp 141-66
72587(Rev. 1)	25-4000	Dep. NTIS
UCRL-Trans-		
1409	25-3021	Dep. NTIS
1417	25-4001	Dep. NTIS
10487	25-4002	Dep. NTIS
10496	25-4003	Dep. NTIS
UCSD-		
34-P-127-5	25-4004	Dep. CFSTI
34-P-143-23	25-4005	Dep. NTIS
USGS-		
474-72	25-2349	Dep. NTIS
WAPD-MRP-		
132	25-3799	Dep. NTIS
WAPD-TM-	(Misc.)	
944	25-4006	Dep. NTIS
WHAN-FR-		
18	25-3908	Dep. NTIS
25	25-4007	Dep. NTIS
X-	(Misc.)	
713-70-251	25-2815	See N-70-33138
Y-		
1740	25-2069	Dep. NTIS

☆U. S. Government Printing Office: 1971—436-210/14

XUM

UNITED STATES
ATOMIC ENERGY COMMISSION
P. O. BOX 62
GOVEI OAK RIDGE, TENNESSEE 37830

OFFICIAL BUSINESS

POSTAGE AND FEES PAID
U. S. ATOMIC ENERGY COMMISSION

POSTAGE AND FEES PAID
U. S. GOVERNMENT PRINTING OFFICE

1

UNIVERSITY MICROFILMS
ATTN MRS. MARLENE HURST
MANAGER, PUBLISHER RELATIONS
ANN ARBOR MICHIGAN 48106

Recent USAEC publication of special interest

SYMPOSIUM ON ENGINEERING WITH NUCLEAR EXPLOSIVES

January 14-16, 1970
Las Vegas, Nevada

This symposium reports both national and international progress achieved since April 1964, the date of the Third Plowshare Symposium. The seven papers presented in the Plenary Session review the current status of the Plowshare Program from the technical, government, and industrial points of view. The 106 papers presented at 16 technical sessions cover all technical aspects of the Plowshare Program. The technical sessions were: underground nuclear effects (3 sessions), excavation (2 sessions), radioactivity (3 sessions), oil and gas, mineral recovery, nuclear operations, seismic effects, water-resources development, scientific applications, underground engineering applications, and nuclear-excavation effects.

A list of attendees and an author index are included.

Available in two volumes as CONF-700101(Vol. 1) and CONF-700101(Vol. 2) for $6.00 from

National Technical Information Service
U. S. Department of Commerce
Springfield, Virginia 22151

XUM

KUM